

Lecture Notes in Civil Engineering

M. V. L. R. Anjaneyulu

M. Harikrishna

Shriniwas S. Arkatkar

A. Veeraragavan *Editors*

Recent Advances in Transportation Systems Engineering and Management

Select Proceedings of CTSEM 2021

 Springer

Lecture Notes in Civil Engineering

Volume 261

Series Editors

Marco di Prisco, Politecnico di Milano, Milano, Italy

Sheng-Hong Chen, School of Water Resources and Hydropower Engineering,
Wuhan University, Wuhan, China

Ioannis Vayas, Institute of Steel Structures, National Technical University of
Athens, Athens, Greece

Sanjay Kumar Shukla, School of Engineering, Edith Cowan University, Joondalup,
WA, Australia

Anuj Sharma, Iowa State University, Ames, IA, USA

Nagesh Kumar, Department of Civil Engineering, Indian Institute of Science
Bangalore, Bengaluru, Karnataka, India

Chien Ming Wang, School of Civil Engineering, The University of Queensland,
Brisbane, QLD, Australia

Lecture Notes in Civil Engineering (LNCE) publishes the latest developments in Civil Engineering—quickly, informally and in top quality. Though original research reported in proceedings and post-proceedings represents the core of LNCE, edited volumes of exceptionally high quality and interest may also be considered for publication. Volumes published in LNCE embrace all aspects and subfields of, as well as new challenges in, Civil Engineering. Topics in the series include:

- Construction and Structural Mechanics
- Building Materials
- Concrete, Steel and Timber Structures
- Geotechnical Engineering
- Earthquake Engineering
- Coastal Engineering
- Ocean and Offshore Engineering; Ships and Floating Structures
- Hydraulics, Hydrology and Water Resources Engineering
- Environmental Engineering and Sustainability
- Structural Health and Monitoring
- Surveying and Geographical Information Systems
- Indoor Environments
- Transportation and Traffic
- Risk Analysis
- Safety and Security

To submit a proposal or request further information, please contact the appropriate Springer Editor:

- Pierpaolo Riva at pierpaolo.riva@springer.com (Europe and Americas);
- Swati Meherishi at swati.meherishi@springer.com (Asia—except China, Australia, and New Zealand);
- Wayne Hu at wayne.hu@springer.com (China).

All books in the series now indexed by Scopus and EI Compendex database!

M. V. L. R. Anjaneyulu · M. Harikrishna ·
Shriniwas S. Arkatkar · A. Veeraragavan
Editors

Recent Advances in Transportation Systems Engineering and Management

Select Proceedings of CTSEM 2021

 Springer

Editors

M. V. L. R. Anjaneyulu
Department of Civil Engineering
National Institute of Technology Calicut
Calicut, India

M. Harikrishna
Department of Civil Engineering
National Institute of Technology Calicut
Calicut, India

Shriniwas S. Arkatkar
Department of Civil Engineering
Sardar Vallabhbhai National Institute
of Technology
Surat, India

A. Veeraragavan
Department of Civil Engineering
Indian Institute of Technology Madras
Chennai, India

ISSN 2366-2557

ISSN 2366-2565 (electronic)

Lecture Notes in Civil Engineering

ISBN 978-981-19-2272-5

ISBN 978-981-19-2273-2 (eBook)

<https://doi.org/10.1007/978-981-19-2273-2>

© The Editor(s) (if applicable) and The Author(s), under exclusive license to Springer Nature Singapore Pte Ltd. 2023

This work is subject to copyright. All rights are solely and exclusively licensed by the Publisher, whether the whole or part of the material is concerned, specifically the rights of translation, reprinting, reuse of illustrations, recitation, broadcasting, reproduction on microfilms or in any other physical way, and transmission or information storage and retrieval, electronic adaptation, computer software, or by similar or dissimilar methodology now known or hereafter developed.

The use of general descriptive names, registered names, trademarks, service marks, etc. in this publication does not imply, even in the absence of a specific statement, that such names are exempt from the relevant protective laws and regulations and therefore free for general use.

The publisher, the authors, and the editors are safe to assume that the advice and information in this book are believed to be true and accurate at the date of publication. Neither the publisher nor the authors or the editors give a warranty, expressed or implied, with respect to the material contained herein or for any errors or omissions that may have been made. The publisher remains neutral with regard to jurisdictional claims in published maps and institutional affiliations.

This Springer imprint is published by the registered company Springer Nature Singapore Pte Ltd.

The registered company address is: 152 Beach Road, #21-01/04 Gateway East, Singapore 189721, Singapore

Preface

Transportation systems play a vital role in the day-to-day life of people around the world. Whatever be the purpose for which travel is undertaken, the use of a mode of transport for movement and using a transportation facility is inevitable. Hence, the provision of a safe, convenient and efficient transportation system is the need of the hour. Moreover, in the context of the challenges associated with climate change, sustainable use of energy and resources for creating and operating transportation systems, synergy between academicians, researchers and engineers becomes important for evolving solutions for the same. It is in this context that opportunity was given for academicians, researchers and engineers to pool in their ideas for evolving optimal and sustainable solutions for the problems. Conferences provide the ideal platform for mutually beneficial interaction between the stakeholders of the transportation sector, which could pave way for apt solutions for particular problems.

The 8th International Conference on Transportation Systems Engineering and Management (CTSEM 2021), organised Online by the Centre for Transportation Research, Department of Civil Engineering, National Institute of Technology Calicut, Kerala, India, during 26–27 August 2021, aimed to bring together researchers, academicians and engineers in different areas of transportation engineering and management. The objectives of the CTSEM were to provide an opportunity for students, research scholars, academicians, scientists and practising professionals to present their research works, exchange ideas, learn about advancements and applications in their respective fields and thus arrive at future directions for research.

A total of 247 technical papers were received for the conference. After an initial screening of the papers, 218 papers were identified for a double-blind review process. After the double-blind review process, 175 papers were accepted for presentation in the conference. Out of the 175 papers, 38 were in the transportation planning track, 45 in the traffic engineering track, 55 in the pavement technology track and 37 in the ITS track. Researchers from 67 institutes/organisations contributed to the technical papers.

The research papers were subjected to a double-blind review scrutiny for their technical and presentation content. The expertise of reviewers from research organisations from around the world was efficiently utilised for the double-blind review

process. The research papers were evaluated, and the authors were given the opportunity to revise the contents, based on the reviewers' comments. The revised papers were scrutinised for their compliance to the suggestions put forth by the reviewers. The consent of the authors was sought for the publication of their research papers in "Recent Advances in Transportation Systems Engineering and Management—Select Proceedings of CTSEM 2021".

The editorial team places on record the heartfelt thanks and appreciation to the expert team of reviewers for their meticulous and time-bound scrutiny of the research papers and for giving constructive suggestions for improving the quality of the research papers. The authors are congratulated for their efforts and for their contributions towards solving the problems associated with transportation systems.

As George Bernard Shaw rightly said, "Progress is impossible without change; and those who cannot change their minds cannot change anything", it is hoped that this attempt to highlight the contributions in the field of transportation systems engineering and management would provide further impetus for researchers to work with greater zeal for finding sustainable solutions to the problems in this field.

Calicut, India
Calicut, India
Surat, India
Chennai, India

M. V. L. R. Anjaneyulu
M. Harikrishna
Shriniwas S. Arkatkar
A. Veeraragavan

Contents

Air Pollution

Effect of Fog on Traffic Parameters in Mixed Traffic Condition	3
Angshuman Pandit and Anuj Kishor Budhkar	

Capacity and LOS Analysis

Analyzing Traffic Performance of Toll Plazas Using Performance Box: A Case Study	17
Chintaman Bari, Yogeshwar V. Navandar, and Ashish Dhamaniya	

Capacity Analysis for Electronically Operated Toll Plaza Under Mixed Traffic Condition	35
Meet D. Ajudiya, Pradip J. Gundaliya, and Yogeshwar V. Navandar	

Comparison of Dynamic Passenger Car Values Estimated at Signalised Intersections Under Heterogeneous Traffic Conditions	51
P. N. Salini, B. Anish Kini, and Gopika Mohan	

Dynamic Passenger Car Equivalency Values for Multilane Roundabouts Under Mixed Traffic Conditions—A Case Study	67
Vaibhav Negi, Hari Krishna Gaddam, and K. Ramachandra Rao	

Impact of Implementing Two-Wheeler Boxes at Signalized T-Intersections Under Mixed Traffic Conditions	81
V. H. Ardra, B. Anish Kini, and S. Moses Santhakumar	

Optimisation

Combined Passenger and Cargo Transport: A Hybrid Simulation and Optimization Approach Focusing on the Transshipment of Cargo Between Tram Vehicles	99
Ralf Elbert, Jessica Schwarz, and Johannes Rentschler	

GIS-Based Model for Optimum Location of Electric Vehicle Charging Stations	113
Binal Vansola, Minal, and Rena N. Shukla	
Optimizing Points of Intersection for Highway and Railway Alignment—Using Path Planner Method and Ant Algorithm-Based Approach	127
M. B. Sushma, Sandeepan Roy, and Avijit Maji	
Pavement Analysis	
Comparison of Dynamic Loads Generated by Truck with Dual Tires and Wide Base Tires	147
Suraparaju Venkata Sai Tharun, Kakara Srikanth, and Venkaiah Chowdary	
Impact of Choice of Lane on Multilane Flexible Pavement	159
J. Priscilla Ponmani and M. R. Nivitha	
Pavement Evaluation and Management	
Establishing an Optimum Maintenance Strategy for a National Highway Using HDM-4: A Case Study of NH 66 Section in Kerala, India	175
Sangeetha Jayamohan, V. S. Sanjay Kumar, and T. Sreelatha	
Delineation of Pavement Stretches into Homogeneous Sections Using Pavement Condition Data: An Optimization Approach	189
Soumyarup Biswas and Kranthi K. Kuna	
Simplified Methodology for Optimal Maintenance Management of Highway Pavement Network	205
M. R. Archana, V. Anjaneyappa, M. S. Amarnath, and A. Veeraragavan	
Pavement Materials	
Evaluation of Performance of Reclaimed Asphalt Pavement Mixtures Using Acetone as Rejuvenator	219
Lekhaz Devulapalli, Goutham Sarang, and Saravanan Kothadaraman	
Investigating the Effect of Aggregate Size and Binder Material Proportion on Strength and Permeability of Pervious Concrete by Statistical Modeling	235
Sudhir Kumar Boddu	
Investigations on Stone Matrix Asphalt Mixes by Utilizing Slag and Cellulose Fiber	253
Shriram Marathe, P. K. Akarsh, Arun Kumar Bhat, and Mahesh Kumar	

Laboratory Evaluation on the Use of Natural Fibre in Gap-Graded Asphalt Mixtures 261
 Raghuram K. Chinnabhandar, A. U. Ravi Shankar, V. Sai Ganesh, Arnet Cleetus, and Shubham Chourasia

Linear Viscoelastic Limits for Aged and Unaged Bitumen 275
 T. Srikanth and A. Padmarekha

Evaluation of Mechanical Properties of Rigid Pavement with High RAP Content 285
 M. K. Diptikanta Rout, Sabyasachi Biswas, and Abdhesh Kumar Sinha

Public Transport

Analysis of Bus Stop Delay Variability Using Public Transit GPS Data 301
 H. Ayana, Raviraj H. Mulangi, and M. M. Harsha

Effectiveness of Passenger Attraction Policies: A Pre-COVID-19 and Post-lockdown Comparison 317
 Sandra Kamar, S. Shaheem, B. Vinayaka, and Samson Mathew

Evaluation of Transit Accessibility by Geoprocessing Techniques for Surat City 331
 Rohit B. Rathod, Gaurang J. Joshi, and Shriniwas S. Arkatkar

Evaluation of Users Approbation Indicators of Delhi Metro 349
 Salman Khursheed and Farhan Ahmed Kidwai

“Multi-criteria Approach for Identification of Suitable Land Parcels to Develop Intermodal Transit Hubs: A Case Study of Bengaluru, India” 367
 Krishna Saw and Priyanka Kataria

Identifying User Preference Criteria for Selecting Public Transportation System as a Mode of Transport: A State-of-the-Art Review 391
 Kanika and Chetan R. Patel

Urban Metrorail Funding and Financing in India: Empirical Analysis of Potential Innovative Options 411
 Anjula Negi and Sanjay Gupta

Visualisation of Transit Passenger’s Mobility from Automatic Fare Collection Data (AFC): Case Study of Hubli–Dharwad BRTS 431
 Shivaraj Halyal, Raviraj H. Mulangi, and M. M. Harsha

Stabilisation

Chemically Stabilized Laterite Soil Using Rice Husk Ash	451
Somnath Paul and Dipankar Sarkar	
Effect of Stabilized Subgrade on Rutting Resistance of Asphalt Concrete Pavement	465
Polukonda Gopalam, Barnali Debnath, and Partha Pratim Sarkar	
Modal Studies on the Performance of Geosynthetic Reinforced Soil Walls Under Static Local Loading	477
M. K. Hudha and Renjitha Mary Varghese	
Performance Evaluation of Cement-Treated Recycled Concrete Aggregate Bases	489
Sarella Chakravarthi, Matta Devendra Vara Prasad, and S. Shankar	
Performance Evaluation of Low-Volume Road Sections Consisting of Enzyme Stabilized Inverted Base	503
Kakara Srikanth, Attada Haresh, B. Raj Kumar, Mahammad Sameer, Matta Devendra Vara Prasad, Satyaveer Singh, Shubham Ghosh, S. Shankar, Venkaiah Chowdary, C. S. R. K. Prasad, and Apoorva Modi	
Performance Evaluation of Scrap Rubber-Sand Mixture Reinforced with Geogrids	519
K. P. Anjali and Renjitha Mary Varghese	
Traffic Flow Modelling	
A Review of Real-Time Traffic Data Extraction Based on Spatio-Temporal Inference for Traffic Analysis Using UAV	535
K. Prathibaa and K. Gunasekaran	
Analysis of Effect of Crossing Pedestrians on Traffic Characteristics at Urban Midblock Sections Using Support Vector Regression	553
Sreechitra, Yogeshwar V. Navandar, Hareshkumar D. Golakiya, and M. V. L. R. Anjaneyulu	
Analysis of the Impact of Pedestrian Crossing Activity on the Traffic Characteristics at Urban Midblock Sections Using Simulation Technique	569
C. M. Prakash, Yogeshwar V. Navandar, Hareshkumar D. Golakiya, and Ashish Dhamaniya	
Analysis of Vehicle Time Headway Distributions for Passenger Car and Commercial Vehicles Interaction	585
Sandeep Singh and S. Moses Santhakumar	

Deep Bi-LSTM Neural Network for Short-Term Traffic Flow Prediction Under Heterogeneous Traffic Conditions 597
 Kranti Kumar and Bharti

Delay Variability Analysis at Intersections Using Public Transit GPS Data 613
 Arathy Lal, Raviraj H. Mulangi, and M. M. Harsha

Influence of Roadside Friction on Speed and Lateral Clearance for Different Types of Vehicles 629
 S. K. Santosh, S. Geethanjali, M. R. Archana, and V. Anjaneyappa

Study of Lane Adherence of Heterogeneous Traffic on Intercity Roads 645
 S. Satheesh, V. Guruprasath, and K. Gunasekaran

Traffic Analysis and Forecast for Meghalaya Road Network 657
 Manmeet Singh and Ravindra Kumar

Traffic Impact Assessment of a Proposed Shopping Mall in a Medium-Sized Town 673
 Neelu Mammen, K. C. Wilson, and Vincy Verghese

Traffic Management

Effectiveness of Speed Calming Measures Along Arterial Roads 691
 Akshata Badiger, Kuldeep, M. R. Archana, and V. Anjaneyappa

Traffic Management in Forest and Ecosystem Conservation. A Study on NH 766 Through Bandipore National Park and Proposing a Traffic Management Plan with Alternate Route Consideration 703
 Arun Baby M. Wilson and M. A. Naseer

Traffic Safety

Accident Blackspot Ranking: An Alternative Approach in the Presence of Limited Data 721
 Sivakumar Balakrishnan and Krishnamurthy Karuppanagounder

Accident Prediction Modeling for Collision Types Using Machine Learning Tools 737
 T. C. Harsha Jasni, S. Moses Santhakumar, and S. Ebin Sam

Operating Speed Prediction of Vehicles at Combined Curves Using Mixed Effect Modeling Approach 751
 Neena M. Joseph, M. Harikrishna, M. V. L. R. Anjaneyulu, and IceyElzen Mathew

Pedestrians Safety Analysis at Uncontrolled Midblock Crosswalks	763
Siddharth Jain, Mukti Advani, and Lalit Kumar Yadav	
Two Wheeler Rider Support System	775
Gunendra Mahore, Sonam Solanki, Ritik Barua, and Rupesh Mahore	
User Preferences and Behaviour	
Determinants of Mobile Phone Use and Seat Belt Non-compliance Among Vehicle Drivers in Nigeria: An Observational Study	789
Yingigba Chioma Akinyemi	
Determinants of Ride-Hailing Applications Adoption: How Travelers' Characteristics and Attitudes Affect the Adoption of New Online Mobility Platforms in Bangkok?	805
Wattana Laosinwattana, Phathinan Thaitatkul, and Saksith Chalermpong	
Genealogy of Shared Mobility in India	821
Nidhi Kathait and Amit Agarwal	
Investigating the Barriers for Electric Vehicle Adoption Using Analytical Hierarchy Process Approach	837
Manivel Murugan, Sankaran Marisamynathan, and Preetha Nair	
Investigating the Influencing Factors to Adopt Public Electric Vehicle Charging Facility at Existing Fueling Station: A Study Based on Users Perceptive	851
Manivel Murugan, Sankaran Marisamynathan, and Tejas Panjwani	
Public Bicycle Sharing System: A Global Synthesis of Literature and Future Research Directions	869
Samir J. Patel and Chetan R. Patel	
Travelers' Response to Network Disruptions in Ernakulam City	885
Navitha Valsalan, P. C. Haritha, and M. V. L. R. Anjaneyulu	
User Perceived Service Quality of Indian Railway Platform Using Structural Equation Modeling and Importance-Performance Map Analysis: A Case Study of Tiruchirappalli Railway Junction	901
Rameshwar Metage and Darshana Othayoth	
Which Factors Affect Lane Choice Behavior at Toll Plaza? An Analytical Hierarchical Process (AHP) Approach	915
Rohit Chopade, Chintaman Bari, and Ashish Dhamaniya	

Editors and Contributors

About the Editors

Dr. M. V. L. R. Anjaneyulu is currently working as Professor in the Department of Civil Engineering, National Institute of Technology Calicut. He is having more than 30 years of teaching, research and consultancy experience in Transportation Engineering. His areas of research interest include urban transportation planning, travel behavior studies, traffic flow analysis and modeling, traffic safety analysis and evaluation and applications of GIS in transportation. He has guided seven Ph.D. works and presently guiding eight Ph.D. scholars. He has guided nearly 160 postgraduate dissertation works. He has published more than 180 research papers in various journals and conferences. He is a recipient of IRC Best Research Paper award in 1998 and 2014. He is the coordinator of the Centre for Transportation Research, a Centre of Excellence set up under FAST scheme, with support from MoE, GoI. He is also coordinator of 'State Technical Agency' for implementation of PMGSY scheme in northern districts of Kerala under NRIDA, MoRD. He has successfully completed seven research projects sponsored by different agencies. He organised more than 20 training programs for field engineers and engineering faculty.

Dr. M. Harikrishna is working as Assistant professor in the Department of Civil Engineering, National Institute of Technology Calicut. He has completed his bachelor's degree in Civil Engineering from College of Engineering Trivandrum, Kerala University and master's degree from College of Engineering Guindy, Anna University. He completed his doctoral studies from the Indian Institute of Technology Roorkee in the year 2013. He joined NIT Calicut in 2005. His research interests include 'Travel behavior modeling'; 'Stated and Revealed Preference Survey planning and design' and 'Capacity and Level of Service Estimation of Transport Facilities'. He has published several research papers in international and national journals and conferences. He has guided 16 projects at the undergraduate level and 50 projects at the postgraduate level and is currently guiding four research scholars. He is a team member of the Centre for Transportation Research, a Centre of Excellence

set up under FAST scheme, with support from MoE, GoI. He has conducted faculty development programs in the areas of Urban Transport Systems Planning, Traffic Engineering and Advanced Surveying. He is also a member in professional bodies such as the Indian Roads Congress and the Indian Society for Technical Education. He is the Reviewer of journals such as *ASCE Journal of Transportation Engineering, Part A: Systems and Transportation Research Interdisciplinary Perspectives*.

Dr. Shrinivas S. Arkatkar is currently working as 'Associate Professor' in the Civil Engineering Department at SVNIT Surat. Recently, he was appointed as 'Adjunct Professor' at the Department of Civil Engineering, Ryerson University, Ontario, Canada. Prior to joining SVNIT Surat, he worked in the Department of Civil Engineering at BITS, Pilani, Rajasthan. Presently, he holds more than 15 years of experience in teaching, research, and consultancy with a specialization in different areas of transportation engineering. Before joining BITS, he pursued his Ph.D. research in the Transportation Engineering Division, Department of Civil Engineering, IIT Madras. His research interests are: traffic flow modelling and simulation, Intelligent transportation systems (ITS), public transportation and sustainable transportation, and road safety and simulation. He has guided eight doctoral students and more than fifty postgraduate students on their dissertation topics from his research interests. He has coordinated over 8 major research projects with a budget over Rs. 5 crores. Currently, he is guiding eight doctoral students on different topics of traffic and transportation engineering. He has published over 100 research papers in journals and over 200 papers in national and international conference proceedings. He is currently member of Indian Roads Congress (IRC), Institute of Urban Transport (IUT), and Transportation Research Group of India (TRG). Presently, he is serving as the Vice President, Transportation Research Group India (TRG). He is also serving as Associate Editor for the journals, *Transportation letters*, *The International Journal of Transportation Research* (Taylor and Francis), *IET Intelligent Transportation Systems (ITS)*, Wiley Publications and *Journal of Advanced Transportation*, Hindawi/Wiley Publications.

Dr. A. Veeraragavan is a Professor in the Department of Civil Engineering at IIT Madras. He has over four decades of experience in teaching, research and industrial consultancy. Prof. Veeraragavan received the Indian Roads Congress (IRC) Pandit Jawaharlal Nehru Birth Centenary Award for his outstanding contributions in the field of highway engineering, IRC Medals for his best papers, IRC Commendation certificates, UGC Career Award, National Award for Promising Engineering College Teacher in India from the Indian Society for Technical Education, Vishwakarma Award under the category—Outstanding Academician/Technologist/Scientist/Innovator from the Construction Industry Development Council and the Award for Distinguished Services to the Institute from the IIT Madras Alumni Association. Prof. Veeraragavan has published over 100 research papers in national and international journals and over 150 papers in national and international conference proceedings. He has coordinated several major research projects sponsored by the DST, MoRTH, AICTE, NRIDA etc. Currently, he is coordinating (networking with ten academic institutions) two major research projects sponsored by NRIDA on

performance evaluation of rural roads constructed with waste plastics in premixed carpet wearing course and performance evaluation of rural roads constructed with cold bituminous mixes in wearing courses. He has co-authored four books on: *Surveying*, *Highway Engineering* (11th edition under print), *Highway Materials and Pavement Testing* (5th edition) by M/s Nem Chand & Bros. and *Pavement Drainage—Theory and Practice*, by CRC Press, Taylor & Francis Group, UK. He is an Independent Director in L&T-IDPL Board and also serves as an Independent Director in three SPVs of L&T-IDPL.

Contributors

Advani Mukti Transport Planning Division, Central Road Research Institute, New Delhi, India

Agarwal Amit Indian Institute of Technology Roorkee, Roorkee, India

Ajudiya Meet D. Civil Engineering Department, L. D. College of Engineering, Ahmedabad, India

Akarsh P. K. National Institute of Technology Karnataka, Surathkal, India

Akinyemi Yingigba Chioma Department of Geography, University of Ibadan, Ibadan, Nigeria

Amarnath M. S. UVCE (Retd.), Bengaluru, India

Anjali K. P. Department of Civil Engineering, NIT Calicut, Kerala, India

Anjaneyappa V. R.V. College of Engineering, Bengaluru, India

Anjaneyulu M. V. L. R. Department of Civil Engineering, National Institute of Technology Calicut, Calicut, India

Archana M. R. R.V. College of Engineering, Bengaluru, India

Ardra V. H. Department of Civil Engineering, NIT Tiruchirappalli, Tiruchirappalli, India

Arkatkar Shriniwas S. Sardar Vallabhbhai National Institute of Technology, Surat, India

Ayana H. Department of Civil Engineering, National Institute of Technology Karnataka, Surathkal, India

Badiger Akshata R.V. College of Engineering, Bengaluru, India

Balakrishnan Sivakumar Research Scholar, Department of Civil Engineering, NIT Calicut, Calicut, India

Bari Chintaman Sardar Vallabhbhai National Institute of Technology, Surat, India

- Barua Ritik** Madhav Institute of Technology and Science, Gwalior, India
- Bharti** School of Liberal Studies, Dr. B. R. Ambedkar University Delhi, Delhi, India
- Bhat Arun Kumar** NMAM Institute of Technology, Nitte, Karkala, India
- Biswas Sabyasachi** Department of Civil Engineering, NIT Jamshedpur, Jamshedpur, India
- Biswas Soumyarup** Indian Institute of Technology, Kharagpur, India
- Budhkar Anuj Kishor** Department of Civil Engineering, Indian Institute of Engineering Science and Technology, Shibpur, Howrah, India
- Chakravarthi Sarella** NIT Warangal, Warangal, India
- Chalermpong Saksith** Department of Civil Engineering, Chulalongkorn University, Bangkok, Thailand;
Transportation Institute, Chulalongkorn University, Bangkok, Thailand
- Chinnabhandar Raghuram K.** Department of Civil Engineering, National Institute of Technology Karnataka, Surathkal, India
- Chopade Rohit** Sardar Vallabhbhai National Institute of Technology, Surat, India
- Chourasia Shubham** Department of Civil Engineering, National Institute of Technology Karnataka, Surathkal, India
- Chowdary Venkaiah** Civil Engineering Department, Transportation Division, National Institute of Technology Warangal, Warangal, India
- Cleetus Arnet** Department of Civil Engineering, National Institute of Technology Karnataka, Surathkal, India
- Debnath Barnali** National Institute of Technology Agartala, Agartala, India
- Devendra Vara Prasad Matta** Civil Engineering Department, Transportation Division, National Institute of Technology Warangal, Warangal, India
- Devulapalli Lekhaz** Vellore Institute of Technology Chennai, Chennai, India
- Dhamaniya Ashish** Department of Civil Engineering, Sardar Vallabhbhai National Institute of Technology Surat, Surat, India
- Diptikanta Rout M. K.** Department of Civil Engineering, NIT Jamshedpur, Jamshedpur, India
- Ebin Sam S.** KSCSTE-National Transportation Planning and Research Centre, Thiruvananthapuram, India
- Elbert Ralf** Chair of Management and Logistics, Technical University of Darmstadt, Darmstadt, Germany

Gaddam Hari Krishna School of Transport Planning and Design, National Rail and Transportation Institute, Vadodara, Gujarat, India

Geethanjali S. R.V. College of Engineering, Bengaluru, India

Ghosh Shubham Civil Engineering Department, Transportation Division, National Institute of Technology Warangal, Warangal, India

Golakiya Hareshkumar D. Dr. S. and S. S. Gandhi Government College of Engineering, Surat, Gujarat, India

Gopalam Polukonda National Institute of Technology Agartala, Agartala, India

Gunasekaran K. Division of Transportation Engineering, Anna University, Kotturpuram, Chennai, India;
Professor, Division of Transportation Engineering, College of Engineering Guindy, Anna University, Chennai, India

Gundaliya Pradip J. Civil Engineering Department, L. D. College of Engineering, Ahmedabad, India

Gupta Sanjay School of Planning and Architecture, New Delhi, India

Guruprasath V. Division of Transportation Engineering, Anna University, Kotturpuram, Chennai, India

Halyal Shivaraj Department of Civil Engineering, National Institute of Technology, Surathkal, India

Haresh Attada Civil Engineering Department, Transportation Division, National Institute of Technology Warangal, Warangal, India

Harikrishna M. NIT, Calicut, India

Haritha P. C. Department of Civil Engineering, National Institute of Technology Calicut, Calicut, India

Harsha M. M. Department of Civil Engineering, Siddaganga Institute of Technology, Tumakuru, India;
Department of Civil Engineering, National Institute of Technology, Surathkal, India

Harsha Jasni T. C. NIT Tiruchirappalli, Tiruchirappalli, India;
KSCSTE-National Transportation Planning and Research Centre, Thiruvananthapuram, India

Hudha M. K. Department of Civil Engineering, NIT Calicut, Calicut, India

Jain Siddharth Department of Civil Engineering, Amity University, Noida, India

Jayamohan Sangeetha RIT, Kottayam, India

Joseph Neena M. Viswajyothi College of Engineering and Technology, Vazhakulam, India

Joshi Gaurang J. Sardar Vallabhbhai National Institute of Technology, Surat, India

Kamar Sandra REVA University, Bengaluru, India

Kanika Department of Civil Engineering, National Institute of Technology, Surat, India

Karuppanagounder Krishnamurthy Department of Civil Engineering, NIT Calicut, Calicut, India

Kataria Priyanka RITES Limited, Gurgaon, India

Kathait Nidhi Indian Institute of Technology Roorkee, Roorkee, India

Khursheed Salman Department of Civil Engineering, Faculty of Engineering and Technology, Jamia Millia Islamia, New Delhi, India

Kidwai Farhan Ahmed Department of Civil Engineering, Faculty of Engineering and Technology, Jamia Millia Islamia, New Delhi, India

Kini B. Anish KSCSTE-NATPAC, Thiruvananthapuram, India

Kothadaraman Saravanan Vellore Institute of Technology Chennai, Chennai, India

Kuldeep R.V. College of Engineering, Bengaluru, India

Kumar Mahesh Nitte Meenakshi Institute of Technology, Yelahanka, Bangalore, India

Kumar Ravindra TPE Division, CSIR-CRRI, ACSIR, New Delhi, India

Kumar Kranti School of Liberal Studies, Dr. B. R. Ambedkar University Delhi, Delhi, India

Kuna Kranthi K. Indian Institute of Technology, Kharagpur, India

Lal Arathy Department of Civil Engineering, National Institute of Technology Karnataka, Surathkal, India

Laosinwattana Wattana Department of Civil Engineering, Chulalongkorn University, Bangkok, Thailand

Mahore Gunendra Madhav Institute of Technology and Science, Gwalior, India

Mahore Rupesh National Institute of Technology, Rourkela, India

Maji Avijit Department of Civil Engineering, Indian Institute of Technology Bombay, Mumbai, India

Mammen Neelu Jyothi Engineering College, Thrissur, India

Marathe Shriram NMAM Institute of Technology, Nitte, Karkala, India

Marisamynathan Sankaran Department of Civil Engineering, National Institute of Technology, Tiruchirappalli, Tamil Nadu, India

Mathew IceyElzen WSP Consultants, Bengaluru, India

Mathew Samson KSCSTE-NATPAC, Thiruvananthapuram, India

Metage Rameshwar NIT Tiruchirappalli, Tiruchirappalli, India

Modi Apoorva Avijeet Agencies (P) Ltd, Chennai, India

Mohan Gopika KSCSTE-NATPAC, Thiruvananthapuram, India

Mulangi Raviraj H. Department of Civil Engineering, National Institute of Technology Karnataka, Surathkal, India

Murugan Manivel Department of Civil Engineering, National Institute of Technology Tiruchirappalli, Tiruchirappalli, Tamil Nadu, India

Nair Preetha Department of Civil Engineering, Pandit Deendayal Energy University, Gandhinagar, India

Naseer M. A. Department of Architecture and Planning, National Institute of Technology-Calicut, Kozhikode, India

Navandar Yogeshwar V. Department of Civil Engineering, National Institute of Technology Calicut, Calicut, India

Negi Anjula School of Planning and Architecture, New Delhi, India

Negi Vaibhav Department of Civil Engineering, Indian Institute of Technology Delhi, New Delhi, India

Nivitha M. R. PSG College of Technology, Coimbatore, India

Othayoth Darshana NIT Tiruchirappalli, Tiruchirappalli, India

Padmarekha A. Department of Civil Engineering, SRM IST, Chennai, India

Pandit Angshuman Department of Civil Engineering, Indian Institute of Engineering Science and Technology, Shibpur, Howrah, India

Panjwani Tejas Department of Civil Engineering, Pandit Deendayal Energy University, Gandhinagar, Gujarat, India

Patel Chetan R. SVNIT, Surat, India;
Department of Civil Engineering, National Institute of Technology, Surat, India

Patel Samir J. Department of Civil Engineering, IITE, Indus University, Rancharda, Ahmedabad, Gujarat, India

Paul Somnath Graduate Engineer, NIT Agartala, Agartala, India

Prakash C. M. NIT Calicut, Calicut, Kerala, India

Prasad C. S. R. K. Civil Engineering Department, Transportation Division, National Institute of Technology Warangal, Warangal, India

Prathibaa K. Research Scholar, Division of Transportation Engineering, College of Engineering Guindy, Anna University, Chennai, India

Priscilla Ponmani J. PSG College of Technology, Coimbatore, India

Raj Kumar B. Civil Engineering Department, Transportation Division, National Institute of Technology Warangal, Warangal, India

Ramachandra Rao K. Department of Civil Engineering and Centre for Transportation Research and Injury Prevention (CTRI), Indian Institute of Technology Delhi, New Delhi, India

Rathod Rohit B. Sardar Vallabhbhai National Institute of Technology, Surat, India

Ravi Shankar A. U. Department of Civil Engineering, National Institute of Technology Karnataka, Surathkal, India

Rentschler Johannes Chair of Management and Logistics, Technical University of Darmstadt, Darmstadt, Germany

Roy Sandeepan Department of Civil Engineering, Indian Institute of Technology Bombay, Mumbai, India

Sai Ganesh V. Department of Civil Engineering, National Institute of Technology Karnataka, Surathkal, India

Salini P. N. KSCSTE-NATPAC, Thiruvananthapuram, India

Sameer Mahammad Civil Engineering Department, Transportation Division, National Institute of Technology Warangal, Warangal, India

Sanjay Kumar V. S. NATPAC, Trivandrum, India

Santhakumar S. Moses Transportation Engineering and Management, Department of Civil Engineering, National Institute of Technology Tiruchirappalli, Tiruchirappalli, India

Santosh S. K. R.V. College of Engineering, Bengaluru, India

Sarang Goutham Vellore Institute of Technology Chennai, Chennai, India

Sarkar Dipankar Assistant Professor, NIT Agartala, Agartala, India

Sarkar Partha Pratim National Institute of Technology Agartala, Agartala, India

Satheesh S. Division of Transportation Engineering, Anna University, Kotturpuram, Chennai, India

Saw Krishna RITES Limited, Gurgaon, India

Schwarz Jessica Chair of Management and Logistics, Technical University of Darmstadt, Darmstadt, Germany

Shaheem S. KSCSTE-NATPAC, Thiruvananthapuram, India

Shankar S. NIT Warangal, Warangal, India;
Civil Engineering Department, Transportation Division, National Institute of Technology Warangal, Warangal, India

Shukla Rena N. Civil Engineering Department, L. D. College of Engineering, Ahmedabad, India

Singh Manmeet TPE Division, CSIR-CRRI, ACSIR, New Delhi, India

Singh Sandeep Transportation Engineering and Management, Department of Civil Engineering, National Institute of Technology Tiruchirappalli, Tiruchirappalli, India

Singh Satyaveer Civil Engineering Department, Transportation Division, National Institute of Technology Warangal, Warangal, India

Sinha Abdhesh Kumar Department of Civil Engineering, NIT Jamshedpur, Jamshedpur, India

Solanki Sonam Madhav Institute of Technology and Science, Gwalior, India

Sreechitra National Institute of Technology Calicut, Calicut, India

Sreelatha T. RIT, Kottayam, India

Srikanth Kakara Civil Engineering Department, Transportation Division, National Institute of Technology Warangal, Warangal, India

Srikanth T. Department of Civil Engineering, SRM IST, Chennai, India

Sushma M. B. Department of Civil Engineering, Kakatiya Institute of Technology and Science, Warangal, India

Thaithatkul Phathinan Transportation Institute, Chulalongkorn University, Bangkok, Thailand

Tharun Suraparaju Venkata Sai Civil Engineering Department, National Institute of Technology Warangal, Warangal, Telangana, India

Valsalan Navitha Department of Civil Engineering, National Institute of Technology Calicut, Calicut, India

Vansola Binal Civil Engineering Department, L. D. College of Engineering, Ahmedabad, India

Varghese Renjitha Mary Department of Civil Engineering, NIT Calicut, Kerala, India

Veeraragavan A. IITM, Chennai, India

Verghese Vincy Jyothi Engineering College, Thrissur, India

Vinayaka B. REVA University, Bengaluru, India

Wilson K. C. KSCSTE-NATPAC, Trivandrum, India

Wilson Arun Baby M. School of Architecture, Christ (Deemed to be University),
Kengeri, Bangalore, India

Yadav Lalit Kumar UITP India, Gurgaon, India

Air Pollution

Effect of Fog on Traffic Parameters in Mixed Traffic Condition



Angshuman Pandit and Anuj Kishor Budhkar

Abstract One of the adverse weathers affecting traffic movement is reduced visibility in the form of fog, which compromises traffic operations as well as safety. Research on fog effects over traffic parameters is mostly simulation-based, and a robust conclusion about fog effects is not arrived at. Furthermore, there is no study on effect of fog on mixed traffic conditions observed in developing economies. This paper compares macroscopic (speed and flow) and microscopic (headway) traffic parameters between foggy and non-foggy conditions in an inter-urban highway in mixed traffic conditions. Flow, speed and headways were obtained from the collected videos of traffic in foggy and non-foggy conditions and compared. Headway values for various car interactions are fitted in distribution functions. The findings of this paper estimate a lower speed value at capacity conditions for traffic in foggy weather. Further, there is a compromise in safety as overall headways are observed to be unsafe. Cars tend to follow leading car in case of fog but overtake truck and LCV more compared to non-foggy section. Truck-car headways are less in foggy weather. The results of this study can be used in various traffic applications like capacity estimation and safety analysis for foggy weather.

Keywords Adverse weather · Fog · Headway · Mixed traffic · Safety

1 Introduction

Generally, traffic engineering involves the study of traffic parameters, viz. speed, flow, density, headway, etc. In a traffic study, we assume some factors to be unaffacting like road surface condition (cracks and potholes), land use characteristics, altitude of the place, etc., as these factors have negligible effect on traffic parameters. However, bad weather is a reason of several traffic disruptions and even accidents. Traffic movement and safety are adversely affected due to bad weather such as fog, rain or

A. Pandit (✉) · A. K. Budhkar
Department of Civil Engineering, Indian Institute of Engineering Science and Technology,
Shibpur, Howrah, India
e-mail: pandit.angshuman333@gmail.com

© The Author(s), under exclusive license to Springer Nature Singapore Pte Ltd. 2023
M. V. L. R. Anjaneyulu et al. (eds.), *Recent Advances in Transportation Systems Engineering and Management*, Lecture Notes in Civil Engineering 261,
https://doi.org/10.1007/978-981-19-2273-2_1

snow. Fog ahead of the windshield scatters light, reduces visibility which increases crash risk significantly. Road Weather Management Program of the Federal Highway Administration reports that roughly 1.3 million road accidents occur due to adverse weather condition globally. Visibility is the most affecting factor of bad weather.

Response of drivers in poor visibility conditions is different: Some slow down; others do not. Many drivers find it easy to follow the taillights of the vehicle ahead [1]. Although drivers may realize consequence of lack of visibility, they may or may not drive safely. Due to a reduced visibility, drivers cannot perceive scenarios at greater distances, and therefore, the interaction range decreases severely. The drivers may need to drive safely (such as driving at lower speeds or maintaining larger time headways) so that enough time is available to respond to hazards, and steer or stop the vehicle. Perception of safer driving may result in deterioration of highway operational parameters, such as section capacity or travel time.

Limited research has been hitherto conducted to explore the changes in driver behavior due to the impact of foggy weather. The results are not consistent. For an instance, several studies have found headway decreases with visibility, but other studies had conflicting interpretations [2]. Moreover, none of these studies were conducted for mixed traffic conditions and weak lane discipline, commonly observed in developing countries like India. Consequently, it is necessary to study effect of fog on various traffic parameters such as speed, sight distance and vehicle maneuvering in these conditions, in order to improve the operations and ensure safety in this weather conditions. Based on real-time traffic data and fog data, this paper attempts to evaluate the effect of fog on macroscopic (speed and flow) and microscopic (headway) traffic parameters. The next section describes the literature review on fog effects on traffic and safety. Section 4 describes traffic data collection on foggy and non-foggy site located on inter-urban highway. Section 5 obtains microscopic parameters, viz. speed and headway, macroscopic parameters, viz. flow and compares them in foggy and non-foggy conditions. Hence, the impact of fog on driver's behavioral characteristics such as time headway, desired speed and flow is analyzed.

2 Literature Review

2.1 Behavioral Effect of Fog

Fog ahead of windshield scatters light and reduces visibility. Broughton et al. [3] studied car-following behavior in reduced visibility and concluded that the average headway distance reduces with poor visibility conditions. In foggy conditions, Ni et al. [4] investigated the impact of drivers' car-following behavior. In the highest fog density condition, the most significant reduction in car-following performance was recorded at moderate speeds. When compared to young drivers, elderly drivers maintain a substantially lower headway distance, making them more dangerous. Caro et al. [5] found that headways are reduced in foggy conditions. Peng et al. [2]

found that the mean headway and headway variation are significantly higher in fog. Recent literatures mostly suggest that headways are lower in foggy condition and the reason could be the misconception of relative motion by the drivers. Mueller et al. [6] have simulated driving on foggy and non-foggy condition and concluded that drivers reduce speed in fog. But based on their simulation experiment, Snowden et al. [7] claimed that in foggy conditions, drivers unconsciously increase their speed.

2.2 Operational Effect of Fog

Fog reduces overall traffic density. Al-Ghamdi et al. [1] have studied traffic behavior in foggy condition and found average speed was reduced by 6.5 km/h and 85th percentile speed was reduced by 5 km/h. Flow and density were low for foggy case. Peng et al. [2] found that mean speed and volume are significantly lower for foggy traffic.

2.3 Measurement of Fog

During the daytime, the further away a dark object is from an observer, the brighter it appears to be. At far distances, it becomes indistinguishable from the horizon sky. This limiting distance is the daytime visibility, and it can be determined by the visual contrast threshold of the observer's eye. From this theory, Koschmieder [8] has derived visibility in daytime (V) in Eq. (1).

$$V = 3.91/\bar{\sigma} \quad V = 3.91R/\ln C' \quad (1)$$

From Eq. (1), daytime visibility can be determined by measuring either the atmospheric extinction coefficient ($\bar{\sigma}$) or the apparent brightness contrast (C') of one or more targets at a known distance R . There are several fog measurement devices developed by researchers, such as Secchi disk, visibility meter of Visiometer, optical sensors [9] or photovoltaic cells [10]. Most devices are either very costly or very bulky for regular mobility or inaccurate and inconsistent. Sutter et al. [11] have proposed a model based on Koschmieder's law to estimate visibility. Lee et al. [12] have tried to evaluate accuracy of Koschmieder's law for visibility estimation and found that it is very inaccurate for harsh weather conditions like rain or fog. Therefore, a robust and indigenous technique is necessary for estimating visibility.

2.4 Some Incidents Due to Fog

In winter season, various places face moderate to heavy fog more often. On December 19, 2017, several people were injured after 10 cars rammed into each other on the Lucknow-Agra expressway due to fog-induced poor visibility. More recently on February 3, 2020, more than 50 vehicles piled up on National Highway 1 between Sirhind and Mandi Gobindgarh on Monday morning after a canter loaded with a chemical hit an Army truck [13]. In the past four years, fog-related road fatalities in India have risen almost 100%. There is very few research on real-life crashes due to fog. Lynn et al. [14] have studied two major multivehicle crashes that occurred in 1998 in Virginia. Total 86 vehicles crashed within just three weeks due to fog. Extensive investigation of these crashes suggested to install variable message signs (VMS) to warn drivers of fog-related vehicle stops or slowdowns.

Thus, the following outcome can be concluded from the peer review of literature:

- Although there has been considerable amount of research effort so far, results are very haphazard, and proper relation between visibility and traffic parameters is not properly understood.
- One of the most typical limitations in these fog research is that they rely on simulation data. Therefore, more research is needed to understand the driving behavior and traffic parameter changes in foggy situation on the basis of real-world data.
- Moreover, there is no study of effect of fog in traffic in mixed traffic condition. Lane discipline is very poor in mixed traffic scenario which makes traffic movement very complex compared to other countries.

Therefore, this paper focuses on investigating the effect of fog on macroscopic (speed and flow) and microscopic (headway) traffic parameters using real-world traffic data.

3 Data Collection

For the purpose of accurate data, video graphic technique is used to record microscopic and macroscopic traffic data. Preliminary weather forecasts from Meteorological Department of India were studied to finalize data collection date and locations in Punjab state of northern India. Videos were recorded from two locations—one with and another without foggy conditions, on a six lane inter-urban road (Asia Highway 1, or AH 1) from Amritsar to Ambala commonly called as Grand Trunk Road. Data were collected simultaneously from the two locations, located about 200 km apart from each other. Video camera was fitted at a high vantage point to capture the traffic in entire width of road for both directions. The site with foggy conditions (hereafter referred as Site 1) is located at Kharajpur, in Patiala district of Punjab, whereas the site with non-foggy conditions (hereafter referred as site 2) is located at Daburji,

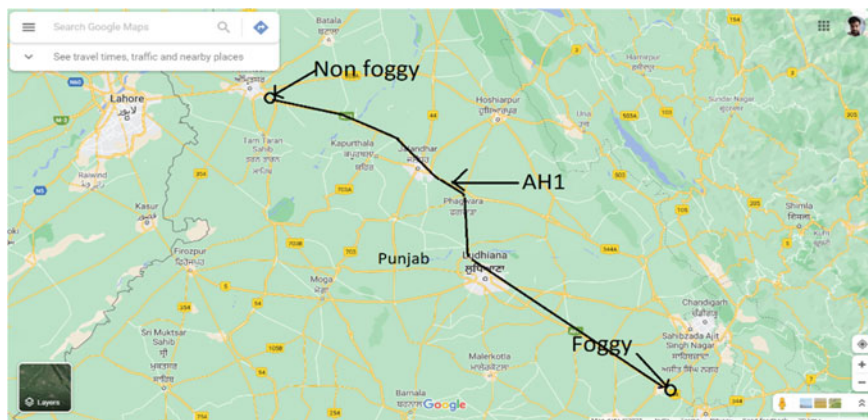


Fig. 1 Location of foggy and non-foggy section. *Source* google.com/maps



(a). Foggy section

(b). Non-foggy section

Fig. 2 Snapshot of video data of both sections **a** Foggy section, **b** Non-foggy section

near Daburji State Bank of India branch, in Amritsar district of Punjab. At both the locations, 90 min of traffic data were recorded for both the carriageways. A corridor length of 100 m is easily visible on both these locations, since recording is conducted from a montage point, i.e., foot over bridge or a tall tripod in the median. Figure 1 shows location of these corridors in Punjab state, whereas Fig. 2a, b shows video snapshot of the site 1 and 2, respectively.

4 Data Extraction

4.1 Traffic Parameters

Total 90 min video data was extracted with manual method for speed and flow values in per minute basis for both sections. The flow was made in the form of classified vehicle count and converted into relevant passenger car units (PCU) as per

Indian Roads Congress Manual for capacity in urban areas (IRC 106:1990), since the sections were located in the outskirts of urban areas. A trap length of 30 m was taken to calculate speed and flow for both lanes of the sections using in-time out-time manual method. The vehicle-to-vehicle headways are calculated manually using a screen marker, and the leader–follower vehicle type is also noted. 25 frames per second video was used for data extraction in higher accuracy.

4.2 Visibility Measurement

According to the definition of visibility, it is the distance up to which a non-reflective black object can be identified against a uniform background. This definition is used to mark the image coordinate of the point, where road marking ceases to appear. Using camera calibration, distance of this point is calculated from the camera. This procedure is conducted every minute, and it is observed that the visibility remains in a constant range of 140–180 m in the 90 min duration of video recording. It is therefore assumed that within this (limited) range of visibility, the overall effect of fog will remain the same.

5 Data Analysis and Results

5.1 Speed–Flow Analysis

In this study, two fundamental macro-traffic parameters have analyzed: speed and flow. Speed–flow diagram has been plotted for both foggy and non-foggy videos and shown in Fig. 3.

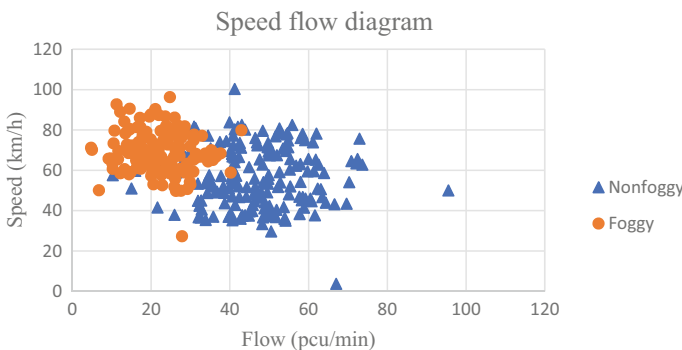


Fig. 3 Speed–flow diagram for both sections

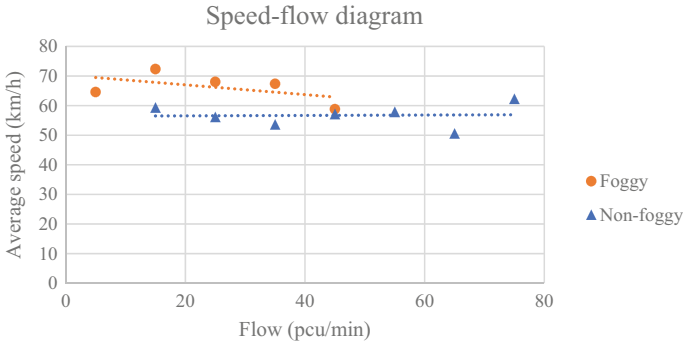


Fig. 4 Speed–flow diagram based on flow range

The speed–flow diagram shows that the non-foggy section had higher flow levels whereas foggy section had lower flow levels during data collection. It is assumed the adverse weather conditions are unfavorable for trip makers, and thereby overall flow reduces. Ideally the speed comparison needs to be conducted on traffic with equal flow levels. For better understanding the difference between foggy and non-foggy conditions in speed–flow relationship, flow interval is made as groups of every 10 PCU/min interval. Then, normalization is done by calculating mean of vehicle speed, and the speed vs flow trends are observed (Refer Fig. 4).

From the trend lines in Fig. 4, it can be observed that speed tends to decrease in an early range of flow for foggy case compared to non-foggy condition. Hence, at higher flow levels, it is expected that average speed for foggy conditions would be less (based on the slopes of regression lines).

5.2 Headway Distribution

Flow level on foggy data is on lower side, and time headway data for that same flow level in non-foggy data are separated and fitted to the probability distribution functions. The goodness of fit test for each probability function is conducted by Kolmogorov Smirnov method. Time headway data sample size is taken more than 80 for better accuracy of fitting. Several common distributions (normal, lognormal, gamma, log-logistic, etc.) are fitted against the headway data for both sections (foggy and non-foggy). Same type of distribution is fitted for each vehicle interaction category, in which car is the following vehicle in all cases, whereas leading vehicles change as per car, truck or light commercial vehicle (LCV). The headways of foggy and non-foggy conditions are compared based on distribution parameters (Table 1).

General expression for each distribution is described as

Table 1 Estimated parameters of fitted distribution for headway

Section	Vehicular interaction	Type of distribution	Parameters	Critical value (K-S)	Statistics value	P-value	Average headway
Foggy	Car–Car	Burr	$k = 4.131$ $\alpha = 2.629$ $\beta = 2.525$	0.15	0.10	0.32	1.401
	Truck–Car	Gamma	$\alpha = 2.774$ $\beta = 0.522$	0.15	0.07	0.79	1.448
	LCV–Car	Lognormal	$\sigma = 0.771$ $\mu = 0.096$	0.21	0.74	0.96	1.445
Non-foggy	Car–Car	Burr	$k = 5.129$ $\alpha = 2.147$ $\beta = 2.560$	0.09	0.10	0.02	1.138
	Truck–Car	Gamma	$\alpha = 2.369$ $\beta = 0.682$	0.15	0.11	0.33	1.618
	LCV–Car	Lognormal	$\sigma = 0.754$ $\mu = -0.068$	0.14	0.16	0.01	1.178

Burr Distribution

$$f(x) = \frac{\alpha k \left(\frac{x}{\beta}\right)^{\alpha-1}}{\beta \left(1 + \left(\frac{x}{\beta}\right)^\alpha\right)^{k+1}} \tag{2}$$

where $f(x)$ stands for the frequency distribution function of Burr distribution. Burr distribution is determined by three parameters: k and α are the shape parameters, and β is the scale parameter. For car–car vehicular interaction, Burr distribution is fitted. Scale parameter k is higher in non-foggy case which means that standard deviation of headway data is more for non-foggy case.

Gamma Distribution

$$f(x) = \frac{x^{\alpha-1}}{\beta^\alpha \Gamma(\alpha)} \exp\left(-\frac{x}{\beta}\right) \tag{3}$$

where $f(x)$ stands for the frequency distribution function of gamma distribution. Gamma distribution is determined by two parameters: α being the shape parameter, β is the scale parameter. Plotting gamma distribution for truck–car headways, it can be conferred that scale parameter is higher for non-foggy condition. This indicates that median value is higher for non-foggy case.

Lognormal Distribution

$$f(x) = \frac{\exp\left(-\frac{1}{2}\left(\frac{\ln x - \mu}{\sigma}\right)^2\right)}{x\sigma\sqrt{2\pi}} \tag{3}$$

where $f(x)$ stands for the frequency distribution function of lognormal distribution. Lognormal distribution is determined by two parameters: σ , shape parameter, and μ , scale parameter. For light commercial vehicle (LCV)–car interaction, lognormal distribution is fitted. In case of non-foggy weather, the value of the scale parameter is reduced, indicating that the median value of headway is less for bad weather.

5.3 Staggering Behavior

The vehicles in mixed traffic do not assume full leadership to the front leader but travel in a staggered manner. To understand this kind of car-following behavior, headways are classified based on three zones:

- Zone 1: More than 50% overlap between following and leading car.
- Zone 2: 25–50% overlap between following and leading car.
- Zone 3: Less than 25% overlap between following and leading car.

Zone 1 suggests that the following car is following the leading vehicle by watching taillight and there is no intention of overtaking. Zone 2 suggests that the car may overtake the leading vehicle but undecided. Zone 3 suggests that the car is most likely to overtake the leading vehicle and the car is trying to see the traffic ahead of leading vehicle. Headways for different vehicular interaction are filtered out based on these three zones and shown in Table 2.

From the count of headways for different zones, it can be concluded that,

- In case of non-foggy condition, headway count of car–car interaction in all zones is almost similar, but for foggy case, there is a significant reduction in interaction

Table 2 Headway count and average headway (seconds) per zone for both sections

Section	Interaction	Zone 1		Zone 2		Zone 3	
		Count	Average	Count	Average	Count	Average
Non-foggy	Car–car	60	1.851	81	1.123	66	0.509
	Truck–car	40	2.58	21	1.051	18	0.536
	LCV–car	26	2.37	34	1.112	34	0.441
Foggy	Car–car	39	1.918	26	1.117	15	0.549
	Truck–car	37	2.192	24	1.068	19	0.479
	LCV–car	17	2.488	12	1.012	13	0.481

in zones 2 and 3. Cars tend to follow leading car in foggy weather as visibility gets low and drivers try to drive by following the taillight of leading car. Average values of headways are very similar for both foggy and non-foggy condition.

- In case of truck–car interaction, there is not much difference in foggy and non-foggy condition. Staggering behavior is more in case of fog which suggests mostly cars try to overtake trucks more compared to non-foggy condition. But average headway is moderately less in foggy case. Cars get much closer to leading truck in foggy case which is very unsafe in case of emergency braking. The authors assume that this phenomenon maybe happening, since speed reduction of trucks is higher than cars.
- There is very less LCV–car interaction in foggy compared to non-foggy condition.
- Observing the average values of headways for different interactions, it can be observed that car–car and LCV–car headways are more in foggy case, which is safe, but truck–car headway gets reduced in foggy case which is unsafe.
- In foggy case, average headways for different interaction are almost similar. This may happen due to the following car tries to follow leading vehicle's taillight in similar way regardless the vehicle type.

6 Conclusion

Real-world video data were collected on a six lane inter-urban road (AH1) from Amritsar to Ambala commonly called as Grand Trunk Road, simultaneously from two locations Rajpura (foggy video) and Daburji (non-foggy) and traffic parameters like speed, flow and headway were compared. Further headways were filtered based on same flow level and vehicular interaction type: car–car, truck–car and LCV–car headways and compared based on fitted distributions for each case. Staggering behavior of following cars are also categorized on three zones for each of three vehicular interaction, and car-following behavior of cars behind truck and LCV is compared for foggy and non-foggy conditions. Following conclusions can be drawn from the study:

1. The slope of speed–flow plot is more for foggy case which indicates that speed will be less in higher flow level. Flow level on non-foggy section is higher than foggy section on same time of the day. This may be happening due to low visibility in adverse weather condition.
2. Car–car headways are fitted to Burr distribution for both foggy and non-foggy section, and distribution parameters are compared. The shape parameter is higher in non-foggy case. Scale parameter k is higher in non-foggy case which means that standard deviation of headway data is more for non-foggy case. In case of truck–car interaction, the scale parameter is higher in Gamma distribution in non-foggy section which implies that median of headway is more in non-foggy case. LCV–car headways are fitted to lognormal distribution, and in case of non-foggy weather, scale parameter is less meaning the median value of headway is less for bad weather.

3. In case of car–car interaction, headway count on all zones is almost similar for non-foggy section, but for foggy case, there is a significant reduction in interaction with higher amount of staggering, which suggests cars try to follow the leading car when visibility is low. Though average headway is almost similar, it is unsafe to follow leading car with that less headway in foggy condition.
4. Average of non-staggered car-following headways are less in case of foggy case for truck–car interaction which suggests unsafe car following. Car–car and LCV–car headways are more in foggy case, but truck–car headways are less in foggy case which is unsafe.
5. It is observed that, in foggy case, cars may follow leading car but avoids following truck and LCV. But average headway of different interactions is almost similar in foggy case which suggests when cars try to follow leading vehicle in foggy case, following behavior is very similar. Which is unsafe in case of emergency braking especially for truck.

This paper compares real-world data to estimate the effect of foggy weather on various traffic parameters. The results of this study can be used in various traffic applications like capacity estimation, safety analysis for foggy weather.

Future scope of this work includes estimation of surrogate safety measures in the foggy conditions. Current data are limited to only one roadway and less time duration; however, more roadways and fog intensities can be covered in order to estimate whether the findings in this paper remain consistent with the increase or decrease in fog levels.

References

1. Al-Ghamdi AS (2007) Experimental evaluation of fog warning system. *Accid Anal Prev* 39(6):1065–1072
2. Peng Y, Mohamed A, Jaeyoung L, Yajie Z (2018) Analysis of the impact of fog-related reduced visibility on traffic parameters. *J Transp Eng Part A Syst* 144(2):04017077
3. Broughton KLM, Fred S, Don S (2007) Car following decisions under three visibility conditions and two speeds tested with a driving simulator. *Accid Anal Prev* 39(1):106–116
4. Ni R, Julie JK, George JA (2010) Age-related declines in car following performance under simulated fog conditions. *Accid Anal Prev* 42(3):818–826
5. Caro S, Viola C, Christian M, Erwin RB, Fabrice V (2009) Can headway reduction in fog be explained by impaired perception of relative motion? *Hum Factors* 51(3):378–392
6. Mueller AS, Trick LM (2012) Driving in fog: the effects of driving experience and visibility on speed compensation and hazard avoidance. *Accid Anal Prev* 48:472–479
7. Snowden RJ, Nicola S, Roy AR (1998) Speed perception fogs up as visibility drops. *Nature* 392(6675):450–450
8. Koschmieder H (1924) Theorie der horizontalen Sichtweite. *Beitrage zur Physik der freien Atmosphäre*, pp 33–53
9. Ovsenik L, Jan T, Pavol M, Janos B, Laszlo C (2012) Fog density measuring system. *Acta Electrotechnica et Informatica* 12(2):67
10. Dumont E, Viola C (2004) Extended photometric model of fog effects on road vision. *Transp Res Rec* 1862(1):77–81

11. Sutter T, Fabian N, Christian S (2016) Camera based visibility estimation. In Proceedings TECO–2016 (technical conference on meteorological and environmental instruments and methods of observation) P, vol 2
12. Lee Z, Shaoling S (2016) Visibility: how applicable is the century-old Koschmieder model? *J Atmos Sci* 73(11):4573–4581
13. <https://timesofindia.indiatimes.com/city/ludhiana/punjab-over-a-dozen-vehicles-collide-amid-dense-fog-no-casualties/articleshow/73913113.cms>
14. Lynn C, Christopher S, Ross C (2002) Virginia commonwealth transportation board: reducing fog-related crashes on the afton and fancy gap mountain sections of I-64 and I-77 in Virginia. No. VTRC-03-CR2, Virginia transportation research council

Capacity and LOS Analysis

Analyzing Traffic Performance of Toll Plazas Using Performance Box: A Case Study



Chintaman Bari, Yogeshwar V. Navandar, and Ashish Dhamaniya

Abstract The objective of the present study is to analyze the traffic characteristics at Ghoti Toll Plaza (GTP) under mixed traffic conditions using a performance-box (P-box), a Global Positioning System (GPS)-based instrument. P-box records the actual time taken by a vehicle to cross the toll plaza, its acceleration and deceleration values, zone of influence (ZOI) of the toll plaza, system delay, vehicle's cruising speed before approaching the toll plaza, number of the vehicles in the queue and control delay. Results show that the ZOI starts at 250 m upstream and downstream of the tollbooth. The control delay was measured between the instances when a vehicle starts to decelerate after joining the queue and regains its original speed after negotiating the tollbooth, the vehicle starts to accelerate. In comparison, the system delay includes the time elapsed between the moments when the vehicle joins the queue and leaves the tollbooth. The minimum and maximum control delays were found to be 15.01 s and 246.30 s, respectively. A linear relationship was established between the number of vehicles in the queue and the control delay. The delay ratio (the ratio of control delay to system delay) varies from 1.07 to 2.10. A negatively correlated linear relationship found between the number of vehicles in the queue and delay ratio. Control delay to system delay conversion factor is found to be 1.31 for the toll plazas. The outcome of the present study will help practitioners estimate the control delay that could be used to derive users' ideal waiting time cost and in the planning and designing of toll-plaza.

Keywords Toll plaza · P-box · Delay ratio

C. Bari · A. Dhamaniya (✉)
Sardar Vallabhbhai National Institute of Technology, Surat, India
e-mail: adhamaniya@gmail.com

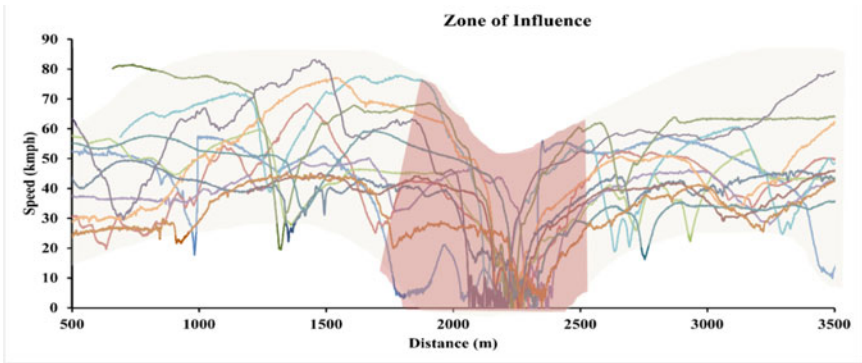
Y. V. Navandar
National Institute of Technology, Calicut, India

© The Author(s), under exclusive license to Springer Nature Singapore Pte Ltd. 2023
M. V. L. R. Anjaneyulu et al. (eds.), *Recent Advances in Transportation Systems Engineering and Management*, Lecture Notes in Civil Engineering 261,
https://doi.org/10.1007/978-981-19-2273-2_2

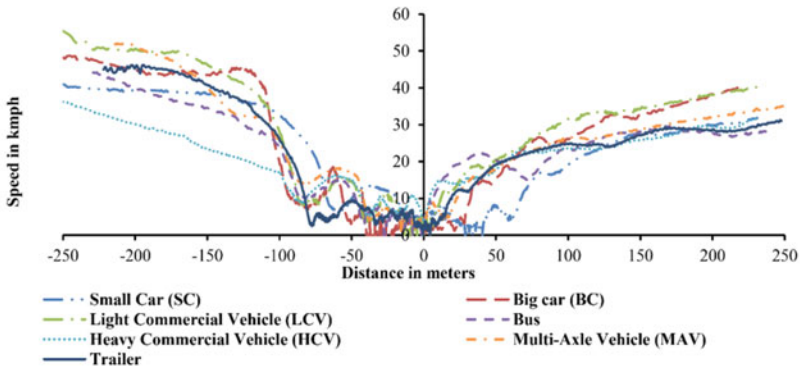
1 Introduction

In India, toll plazas are constructed on highway projects executed under the public–private partnership (PPP) to collect road users’ fees. Generally, separate tollbooths are allocated for different vehicle classes approaching the toll plaza, but it has been observed that drivers join the shortest queue at a toll plaza to avoid delay and thereby present mixed traffic conditions in each of the toll lanes. This causes variation in service time [1], causing detrimental effects on the capacity of the tollbooth. Further, in the case of manually operated tollbooths, vehicles approaching the toll plaza have to take a complete stop at the tollbooth for completing toll transactions, and hence delay occurs [2]. This involves the vehicle to decelerate first and then join the queue where stop and go cycles prevails, exchange the toll rate and then accelerate again to some distance to achieve their desired speed. Therefore, the procedure followed in the estimation of delay at a signalized intersection may not be a proper approach to estimate delay at toll plazas. Hence, considering this aspect, conventional control delay is measured in the present study.

The control delay is defined as the difference between the actual time taken to cross the toll plaza, which includes toll plaza operations, acceleration, and deceleration delay in the zone of influence (ZOI) of the toll plaza (Fig. 1), and the time to traverse the same road segment at the desired cruising speed. Thus, the control delay includes system delay (waiting time in the queue, inter-vehicle, and service time), as well as time lost because of the slow movement when a vehicle decelerates before the toll plaza and then accelerates and regains its original speed after clearing the tollbooth. Delay to road users is the key concern while passing through the toll plaza. Many previous studies [3–8] generally categorized the vehicle delay at the toll plaza into the waiting time while in the queue, move-up time, and service time. However, limited studies considered control delay that includes acceleration and deceleration delay. Hence, in the present study, an attempt has been made to find the control delay by conducting a performance box (P-box) survey at Ghoti Toll Plaza (GTP). Acceleration and deceleration rates are proposed for different vehicle categories at manually operated toll plaza under mixed traffic conditions. These values may be useful for the generation of vehicles in simulation models. Furthermore, the relationship between control delay and queue length (number of vehicles in the queue), delay ratio, and number of the vehicle in the queue are developed. The developed relationships will be useful for quick estimation of a control delay from observed field delay and queue length. Control delay estimation at toll plaza will be useful in planning the configuration of the toll plaza, emission studies [9], simulation modeling [10], and calculating users waiting cost at the toll plaza and in the dynamic tolling strategy [11].



(a)



(b)

Fig. 1 a Zone of influence observed, b Google Map image, and the variation of speed for ZOI at GTP for different vehicle classes

2 Literature Review

Many researchers in the past considered delay and waiting time as variables to assess the performance of toll plaza. In 1954, delay at toll plaza was first ever studied by Edie [12] to evaluate operational efficiency of toll plaza. During that period, the cash transactions were used for paying the toll and hence he observed that the transaction

time was the main factor for the delay at toll plazas. He developed the delay ratio for proper understanding of the occurrence of the delay at tollbooths. The study for the development of level of service (LOS) thresholds for toll plazas was carried out by Lin and Su [13] using the microsimulation model. Various types of delay occurring at toll plaza including approach and queue delay were considered. They developed the six different LOS thresholds based on two parameters, (a) the number of queued vehicles and (b) overall delay including service delay and queue delay. They concluded that the toll plaza is operating in LOS F condition for average delay time of more than 80 s. Al-Deek et al. [6] also used a simulation software for understanding the operations at toll plazas and thus determined the queue delay for further assessment of the facility. Study was conducted by Lin and Lin [14] for analyzing the overall delay occurring at the toll plaza starting from first deceleration till the point of regain of desired speed. They developed the delay equations for the acceleration and deceleration delay, the service time and queue delay. A new approach for defining LOS at toll plazas using 85th percentile delay was given by Klodzinski and Al-Deek [15]. However, the authors neglected the acceleration and deceleration delay occurring in departure and approach section, respectively. A theoretical approach was developed by Aycin [7] for the estimation of tollbooth capacity, queueing delay and service time delay considering the approach traffic and the composition of vehicles. Highway capacity manual [16] also gives the delay ratio as 1.30 at a signalized intersection. Shi and Liu [17] used GPS data from vehicles for real-time traffic monitoring in China. Delay at toll plaza was studied using microsimulation approach by Aksoy et al. [18] in 2014. They concluded that when the number of active tollbooths is reduced, total delay time (per vehicle) also decreases. Hasim et al. [19] used GPS data for optimizing the delay and emissions at the signalized intersections. Bari et al. [20] studied in detail the service time occurring at manually operated toll plazas (MTC) under mixed traffic conditions. It was observed that the service time shows large variation due to vehicular characteristics, drivers' behavior, tollbooth operators' behavior, and difference in toll rate. In another study by Bari et al. [21], the LOS thresholds were developed using the service time data. It was observed that normalized service time lower than 4 s illustrates the LOS A condition. A detailed overall delay study at MTC was carried by Bari et al. [22]. They considered the acceleration and deceleration delays, service time and waiting time in the queue. The acceleration and deceleration delay was considered with the variable acceleration and deceleration values considered from the study Bari et al. [23].

The review of existing literature reveals that several studies have attempted to estimate delay at the toll plaza in terms of waiting time in queue or system delay. There are limited studies that explicitly attempted to estimate control delay, which includes waiting time in queue, system delay, deceleration delay before toll plaza, and acceleration delay after clearing the toll booth. Vehicles start to decelerate from their mainstream speed at a particular distance ahead of the toll plaza to join queues, and after toll payment, the vehicle accelerates through some distance to attain its original speed. This ZOI (Fig. 1) before and after the toll plaza may cause delays to vehicles negotiating through toll plazas. In many previous studies, researchers have not considered delay due to the speed reduction in a ZOI at the toll plaza as part of

the control delay. Hence, the present study attempts to find the ZOI at the toll plaza, control delay, system delay, and finally, the delay ratio using the P-box data.

3 Field Data Collection

Traffic flow data were collected at Ghoti Toll Plaza (GTP), having latitude 19° 42' 31.33" N and longitude 73° 36' 52.97" E located on the National Highway (NH-3) in the western region of India, as illustrated in Fig. 2. The videographic data was collected for a whole day.

Traffic at the toll plaza was observed as mixed in nature, and even within the same category of cars, there are several models of cars that vary in their operating conditions. All vehicles, therefore, are divided into seven categories based on their physical and operational characteristics as small car (SC), big car (BC), light commercial vehicle (LCV), bus, heavy commercial vehicle (HCV), multi-axle vehicle (MAV), and trailer [1]. The pictorial representation for different vehicle categories and their average length is shown in Fig. 3.

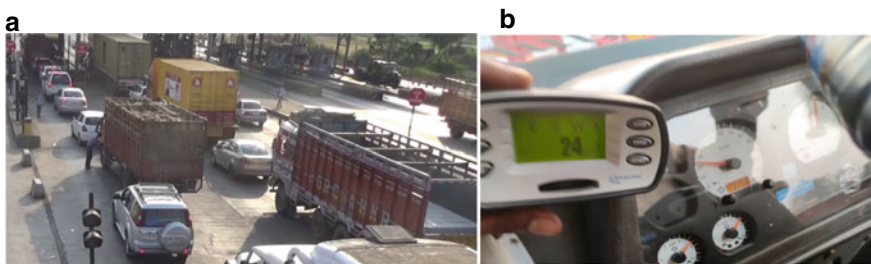


Fig. 2 a Mixed traffic condition at Ghoti Toll Plaza (GTP), b P-Box data collection

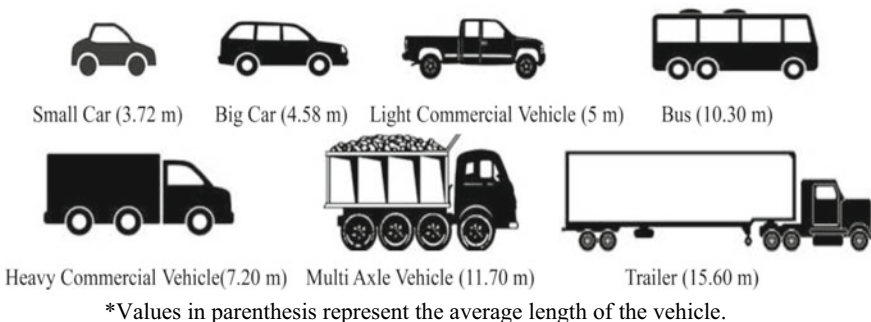
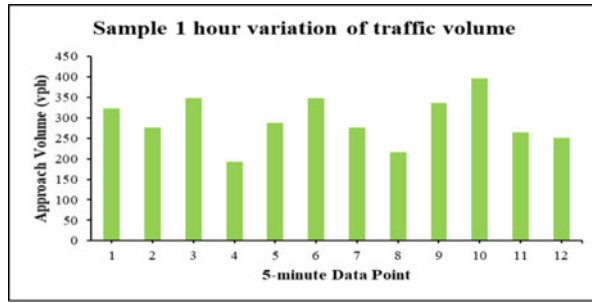


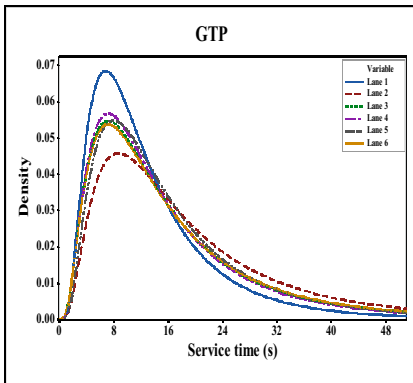
Fig. 3 Vehicle class considered for the present study

The traffic volume at the Ghoti Toll Plaza (GTP) varies between 90 and 450vph. The sample 1 h graph of traffic variation is shown in Fig. 4a. The traffic composition between different lanes also varies, which causes the difference in the service time of each lane. Figure 4b shows the probability density function (PDF) of the service time variation in different lanes at GTP. Further, Fig. 4c shows the vehicle class-wise service time variation at GTP. The average service time of small car (SC) was found to be lower than the other class of vehicles. The maximum service time was found for the trailers with a maximum of 45.76 s. The service time varies due to traffic composition, vehicle class, drivers, and tollbooth operator’s behavior, and toll rate [20].

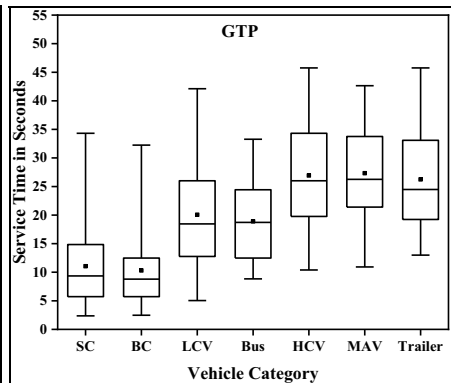
The data were collected using GPS based P-box device (approximate cost \$650), which was mounted on a vehicle. It gives precise data of instantaneous speed, acceleration, and deceleration [24–26]. The performance box (P-box) data were collected in varying time period for the whole day to get the data of peak and off-peak hours. A number of runs were conducted in the different classes of vehicles to find the trajectories of such vehicles traversing the ZOI. P-box software was used for data analysis,



(a)



(b)



(c)

Fig. 4 Preliminary results **a** sample 1 h variation of traffic volume, **b** lane-wise service time variation, **c** vehicle class-wise service time variation

and per second interval data was used for analysis. P-box data were collected for approximately 2–3 km stretch before and after the toll plaza for each of the runs. A total of 220 runs were completed (Table 1) at GTP, and kinematic data were recorded at 1 s interval. From Fig. 1, it is observed that the speed of the approaching vehicle gets affected as it gets closer to the facility (tollbooth). This close proximity is called a zone of influence (ZOI) in the present study, which is shown in Fig. 1a (light red color). Table 1 shows the descriptive statistics for the ZOI at the GTP. Field observation shows that vehicles start to decelerate from their mainstream speed in the range of 40–240 m distance before the toll plaza and achieve its mainstream desired speed after crossing toll plaza in the range of 40–240 m distance, depending upon vehicle category as shown in Table 1. Hence, for the analysis purpose, ZOI is set at 500 m distance (250 m before and after toll plaza) (Fig. 1).

Figure 1b clearly depicts the effect of vehicle size on the cursing speed. It was observed that the cruising speed has inverse relation with the vehicle size, i.e., lower the vehicle length, higher the cruising speed. Also, the average distance for deceleration found to vary with vehicle class, i.e., lower for SC and maximum for trailer. The same variation is observed in the departure zone (region after the tollbooth in downstream side). The average distance for trailer to regain the desired speed is about 1.56 times that of SC. It is also concluded from Table 1 that the distance required for acceleration is more as compared to the deceleration distance. Figure 5 depicts the deceleration delay, system delay (waiting time, inter-vehicle time, and service time), and acceleration delay, which comprises the control delay.

4 Analysis of Field Data

4.1 Acceleration and Deceleration Characteristics at GTP

Table 2 includes a class-wise descriptive analysis of vehicles for acceleration and deceleration at the toll plaza. It may be observed from Table 2 that the average acceleration for SC is 2.83 m/s^2 , whereas that for HCV and trailer is 1.21 m/s^2 and 1.33 m/s^2 , respectively. The minimum and maximum acceleration for the trailer is observed as 0.02 m/s^2 and 4.33 m/s^2 , respectively. Similarly, average deceleration for BC is 1.49 m/s^2 , whereas for bus and trailer it is 1.35 and 1.56 m/s^2 . The maximum average acceleration was found for SC, and the minimum was observed in the case of buses. On the other hand, the maximum average deceleration was observed for LCV, and the minimum average deceleration was for MAV.

Russo et al. [27] suggested the acceleration and deceleration values for passenger cars as 2.97 m/s^2 and 1.20 m/s^2 for a truck for toll plaza model calibration. These values are nearer to the finding of the present studies, as shown in Table 2. Zarrillo and Radwan [28] attempted to model toll plaza simulation using the SHAKER queuing

Table 1 Descriptive statistics for ZOI

Vehicle class	No. of observation	Distance before toll plaza			Distance after toll plaza				
		Min. (m)	Max. (m)	Avg. (m)	Std. Dev	Min. (m)	Max. (m)	Avg. (m)	Std. Dev. (m)
SC	33	60.00	160.00	90.00	28.90	60.00	140.00	85.00	33.60
BC	32	50.00	240.00	130.00	26.70	60.00	180.00	126.00	55.00
LCV	31	100.00	206.50	167.00	31.68	40.00	240.00	185.00	52.00
Bus	31	40.00	220.00	175.00	57.66	120.00	230.00	206.00	35.00
HCV	31	100.00	208.00	161.80	31.58	120.00	240.00	212.00	32.60
MAV	31	40.00	180.00	143.20	37.06	60.00	240.00	192.00	51.50
Trailer	31	143.80	200.00	175.40	19.75	100.00	240.00	195.00	47.70

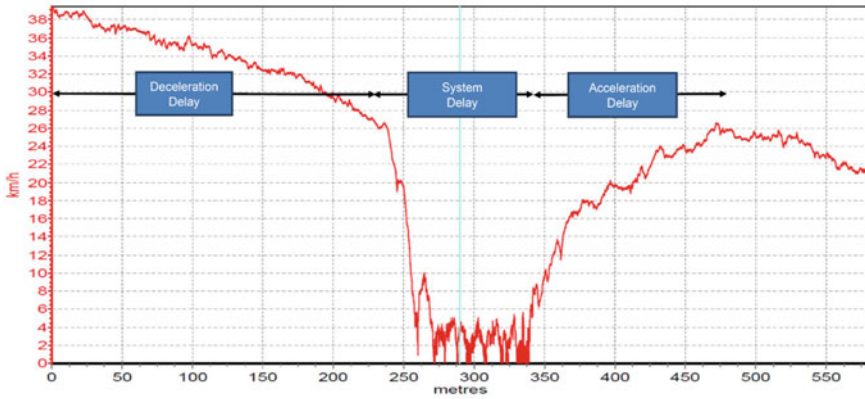


Fig. 5 Illustration of various types of delay

model that computes maximum hourly throughput by combining the vehicle occurrence probability and the physics-motion equations. Researchers considered acceleration values as 2.00 and 0.25 m/s² for passenger cars and trucks, respectively. Similarly, deceleration for passenger cars and trucks is 2.00 and 0.25 m/s², respectively. In comparison with the outcome of the present study, values proposed by Zarrillo and Radwan [28] are very less except for the average deceleration value. The graphical representation of the comparison between acceleration and deceleration values as obtained in the present study, with previous literature, is shown in Fig. 6. The minimum, maximum, and average acceleration and deceleration values for different vehicle classes at toll plaza under mixed traffic conditions are proposed in Table 2. These values will be useful for toll plaza simulation models under mixed traffic conditions.

4.2 Estimation of Control Delay and Delay Ratio

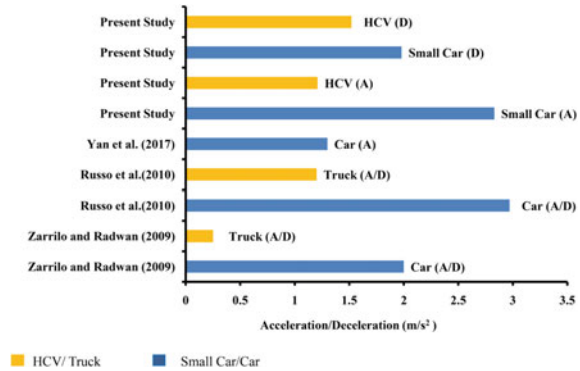
Control delay (D_o) includes acceleration and deceleration delay in ZOI before and after toll plaza and system delay (D_s), which includes waiting time in queue, inter-vehicle time, and service time. In the present study, the control delay is calculated by taking the difference between the actual time taken by a vehicle to cross the toll plaza (t_a) and time that the same vehicle might need to traverse the road section at its desired speed (t_d) if toll plaza was absent. Here, the desired speed is the average speed of the vehicle before approaching the ZOI of the toll plaza. Using this desired speed and considering 500 m distance as ZOI of the toll plaza, the t_d is calculated. The following expression (Eq. 1) shows the calculation for the control delay.

$$D_o = t_a - t_d \tag{1}$$

Table 2 Vehicle category-wise acceleration and deceleration values at GTP

Vehicle class	No. of observation	Acceleration in m/s^2				Deceleration in m/s^2			
		Min.	Max.	Avg.	Standard deviation	Min.	Max.	Avg.	Standard deviation
SC	33	0.02	4.97	2.83	0.67	0.02	5.77	1.98	1.20
BC	32	0.02	4.66	2.53	0.55	0.02	5.47	1.49	0.63
LCV	31	0.02	5.25	1.56	0.10	0.02	5.55	2.02	0.46
Bus	31	0.02	2.91	1.10	0.42	0.02	3.89	1.35	0.50
HCV	31	0.02	3.00	1.21	0.68	0.02	4.22	1.52	0.78
MAV	31	0.02	3.44	1.11	0.49	0.02	2.72	1.31	0.61
Trailer	31	0.02	4.33	1.33	0.49	0.02	4.08	1.56	1.03

Fig. 6 Comparison of acceleration and deceleration with literature



(Note: A = Acceleration in m/s²; D = Deceleration in m/s²)

Delay ratio (D_r) calculated as shown in Eq. (2)

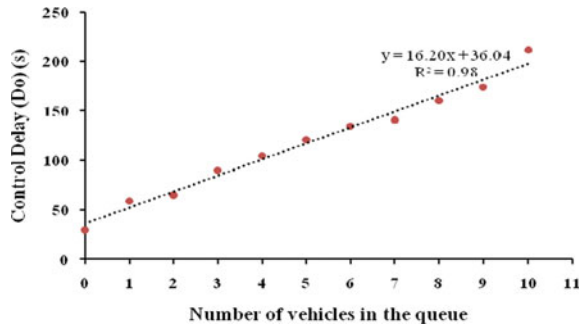
$$D_r = D_o / D_s \tag{2}$$

The minimum and maximum field observed control delay was obtained as 15.01 s and 246.30 s, respectively, as shown in Table 3. It is found that a linear relationship exists between the numbers of vehicles in the queue and control delay (Fig. 7), with a good R^2 value (0.98). In the absence of a queue, there is a control delay of 36.04 s (Table 3), and this may be due to acceleration, deceleration delay before and after the toll plaza, and system delay. A maximum of 10 vehicles was observed in queue during the observation period, and the control delay was observed as 246.30 s. From Table 3, it is concluded that as the number of vehicles in the queue increases, the control delay will increase. Further, the delay ratio (D_r) defined as the ratio of control delay to system delay is estimated. The D_r was estimated in the range of 1.07–2.10. A negatively correlated linear relationship was found between D_r and the number of vehicles in the queue (Fig. 8), with a good compromise with the available dataset replicates by model R^2 value (0.92). It means that if the number of the vehicle in queue increases the D_r will decrease. It can be explained on the basis of the fact that as the vehicle in queue increases at tollbooth the system, the delay will also increase, and hence, D_r decreases respectively. The relationship between D_r and number of vehicle shows that if there is no queuing of vehicles, the average delay ratio is 1.70, which indicates 70% additional delay occurs to the vehicle as compared to system delay on account of deceleration and acceleration of the vehicle in the ZOI of the toll plaza. In the field, it is easy to estimate system delay as compared to the control delay. Hence, many previous studies used system delay as a performance indicator instead of the control delay. Some of the studies [7, 18] calculated control delay but did not consider the acceleration delay after the vehicle clears the tollbooth. It is important to estimate control delay, which includes system delay, as well as acceleration and deceleration delays for better planning of toll plaza, estimation of emission at the toll plaza, estimation of users' waiting time cost, and for simulation studies. The

Table 3 Analysis of control delay and delay ratio (data from the peak and off-peak hours)

Number of vehicle in queue	Control delay			Ratio of control delay to system delay (D_r)		
	Min. (s)	Max. (s)	Avg. (s)	Min.	Max.	Avg.
0	15.01	59.22	29.80	1.32	2.10	1.70
1	25.24	75.24	59.12	1.58	2.10	1.67
2	33.94	95.00	65.23	1.50	1.88	1.59
3	51.22	117.23	89.60	1.29	1.79	1.53
4	68.00	135.55	104.30	1.21	1.62	1.46
5	87.54	157.35	120.45	1.41	1.41	1.41
6	96.23	175.26	134.30	1.18	1.65	1.41
7	102.30	186.33	140.20	1.02	1.41	1.36
8	114.23	199.00	160.20	1.31	1.54	1.41
9	130.01	215.89	173.91	1.20	1.62	1.39
10	142.36	246.30	211.23	1.23	1.38	1.27

Fig. 7 Relationship between D_o and number of vehicle in queue

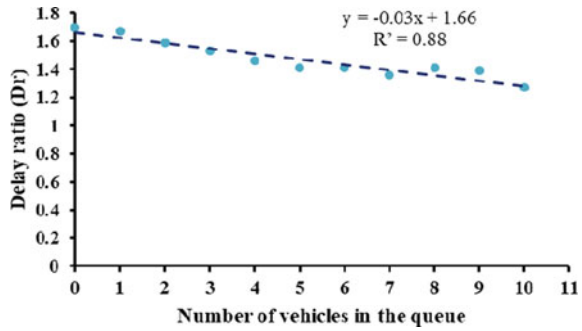


relationship developed in the present study will assist in the estimation of the control delay by using the number of vehicles present in the queue at the instant when a vehicle is likely to join the queue and from system delay information. Further, the delay ratio (D_r) will be helpful to field engineers and planners to easily estimate the control delay in the field.

4.3 Relationship Between Stopped Delay and Control Delay

Mean values for the particular delay component are not relevant when there are huge variations in the observed delay entities (system delay, control delay, etc.) [29]. Hence in the present study, the relationship between system delay and control delay is established using regression analysis. The regression coefficient gives the

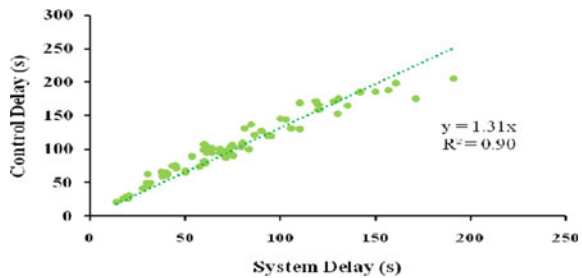
Fig. 8 Relationship between the ratio of D_r and the number of the vehicle in a queue



conversion factor between the system delay and control delay. Figure 9 shows the plot for the control delay versus system delay. From the regression analysis, the conversion factor is found to be 1.31, which clarifies that the system delay is about 76% of the control delay. Furthermore, the model is found statistically significant at a 5% level of significance as the t-statistics value of 64.11 is more than the t-critical of 1.98. Moreover, the coefficient of determination (R^2) is found to be 0.90 for the developed model, thus indicating the reliability of the model. The conversion coefficient is found to be more than the coefficient given by the Indo-HCM [30] (given as 1.19) at the signalized intersection. This is due to the fact that drivers' behavior is entirely different at the toll plaza in comparison with a signalized intersection, where the driver is required to come to a complete halt at tollbooth for toll exchange. Further on approaching the toll plaza, the driver tries to join the shortest queue, which affects the acceleration-deceleration characteristics of the approaching vehicles, which is absent in the case of signalized intersections. Thus, the field engineer could predict the control delay just by calculating the system delay.

Though the system delay to control delay conversion factor is used for approximate estimation, the drivers' behavior while driving and varying acceleration and deceleration patterns at toll plazas make the relationship complicated (same as seen in the case of signalized intersection) [31]. Thus, in order to determine the value of control delay in addition to system delay, an attempt is made to study the exact relationship between the system delay and control delay for varied behavior of drivers at the toll plaza. Figure 10 illustrates the exact relationship between the system delay

Fig. 9 Relationship between control delay and system delay



(Y-axis) and the control delay (X-axis). Regression analysis was performed, and it was found that the developed equation follows a linear relationship. The relationship shows an intercept of 12.42 (on X-axis), illustrating this as the minimum value of acceleration-deceleration delay for any vehicle approaching the toll plaza; that is, the control delay is 12.42 s more than the system delay, and this additional time is due to the deceleration and acceleration of vehicle before and after the tollbooth, respectively. The developed equation is further compared with the equations given in available studies [16, 30–33], which is as shown in Fig. 11.

Figure 11 shows that the developed equation underestimates the system delay values compared with the Indo-HCM [30], Othayoth and Rao [31], Quiroga and Bullock [33]. But it overestimates in comparison to Mousa [32]. This may be because the values presented by these authors are for signalized intersections, where there is a fixed red time for each cycle, which is not the case with toll plazas. Delay at toll plazas varies mostly due to service time and service headway, which depends on the vehicle class, the composition of the mix, drivers' and tollbooth operator's behavior [1]. In comparison with the study carried out by Mousa [32], the values were lower than in the present study after the control delay of 50 s. This may be due to the fact that Mousa [32] reported the values for stopped and non-stopped vehicles both at a signalized intersection. In comparison with delay values given in HCM [16] for

Fig. 10 Exact relationship between system delay and control delay

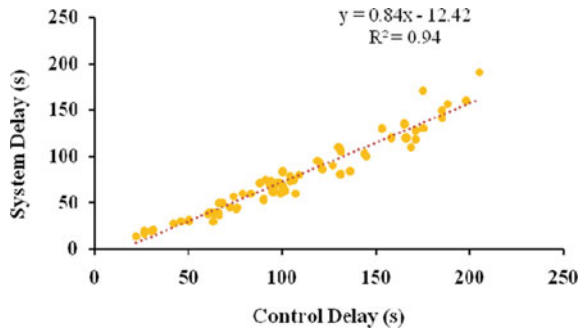
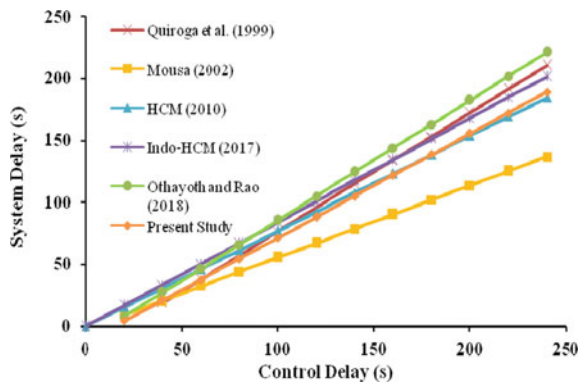


Fig. 11 Comparison with the literature values



signalized intersection, the present study delay ratio value underestimates before the values of control delay of 160 s and after that overestimates over the value of 180 s of control delay. The delay values obtained in the study are also useful to provide information to the road users approaching toll plaza through variable message signs in order to enhance safety [34].

5 Conclusions

The present study attempted to analyze the traffic characteristics at toll plaza using P-box. Traffic characteristics include control delay, system delay (waiting time in queue, inter-vehicle, and service time), number of vehicles in the queue, acceleration and deceleration rate, the distance of ZOI before and after the toll plaza, and cruising speed of the vehicle before approaching the toll plaza. Many previous researchers had attempted to consider delay at toll plaza as a variable for measuring the operational efficiency of the toll plaza in terms such as waiting time in queue, move up time, and service time. There are limited studies available that considered acceleration and deceleration delay at the toll plaza, along with system delay, as the control delay. Hence, the present study was performed to find the control delay and delay ratio at a toll plaza. The study shows that ZOI before and after toll plaza ranges from 40 to 240 m, within which the vehicle started to decelerate from its mainstream speed and regained its original speed after passing the toll plaza. In the present study, it is observed that the control delay varies from 15.00 s to 246.30. This is due to the fact that control delay depends upon many factors such as the number of vehicles in the queue, the distance before the toll plaza where vehicles start to decelerate, the distance after the toll plaza where vehicles regain its original speed and vehicle characteristics. The linear relationship was obtained between control delay and the number of the vehicle in the queue. This shows that as vehicles in queue increase, their control delay also increases linearly. Delay ratio is also calculated in the present study by dividing control delay to system delay, and field observed values for that were in the range of 1.07–2.10. The average value for the delay ratio is 1.70 when there is no queue at the tollbooths. This shows that, compared with system delay, more than 70% additional delay time is experienced by the users' at a toll plaza, which may be due to acceleration and deceleration delay before and after the toll plaza. In the present work, the relationship between the delay ratio and the number of the vehicle in the queue is also developed. It is found that both variables are negatively correlated with a linear relationship. Further, models were developed for approximate and exact estimation of the system delay and the control delay. The conversion factor of 1.31 was found to be statistically significant for control and system delay at toll plazas. Moreover, the developed model is compared with values from previous studies. The mathematical relationships developed in the present study may be useful to field engineers for easily estimating the control delay at toll plaza with less cost and effort. The outcomes of the present study may be useful for the designing of toll plaza configuration, estimation of emission, calculating road users'

ideal waiting time cost, in the simulation studies, defining LOS thresholds values at the toll plaza, and deciding dynamic toll strategies based on control delay at a toll plaza.

Acknowledgements The authors would like to thank TEQIP-III, a Government of India initiative, for sponsoring this project. The project is entitled “Development of Warrants for Automation of Toll Plazas in India.” (Project number SVNIT/CED/AD/TEQIPIII/144/2019). The present study is a part of the project.

References

1. Navandar YV, Dhamaniya A, Patel DA, Chandra S (2019) Traffic flow analysis at manual tollbooth operation under mixed traffic conditions. *J Transp Eng Part A Syst ASCE* 145:1–17. <https://doi.org/10.1061/JTEPBS.0000247>
2. Ozbay K, Cochran AM (2008) Safety assessment of barrier toll plazas. *Adv Transp Stud* 15:85–96
3. Wanisubut S (1989) Toll plaza simulation model and level of service criteria. Dr Diss Polytech Univ Michigan, USA
4. Al-Deek HM, Radwan AE, Mohammed AA, Klodzinski JG (1996) Evaluating the improvements in traffic operations at a real-life toll plaza with electronic toll collection. *ITS J Intell Transp Syst* 3:37–41. <https://doi.org/10.1080/10248079608903720>
5. Gulewicz V, Danko J (1995) Simulation-based approach to evaluating optimal lane staffing requirements for toll plazas. *Transp Res Rec J Transp Res Board* 1484:33–39
6. Al-Deek HM, Mohamed AA, Radwan AE (1997) Operational benefits of electronic toll collection: case study. *J Transp Eng* 123:467–477
7. Aycin MF (2006) Simple methodology for evaluating toll plaza operations. In: 85th Annual Meet Transportation Research Board, Washington, DC pp 92–101
8. Bari CS, Kumawat A, Dhamaniya A (2021) Effectiveness of FASTag system for toll payment in India. In: 7th international IEEE conference on model and technologies for intelligent transportation system pp 16–17
9. Bari CS, Navandar YV, Dhamaniya A (2020) Vehicular emission modeling at toll plaza using performance box data. *J Hazard, Toxic, Radioact Waste* 24. [https://doi.org/10.1061/\(ASCE\)HZ.2153-5515.0000550](https://doi.org/10.1061/(ASCE)HZ.2153-5515.0000550)
10. Bari CS, Gupta U, Chandra S, et al (2021) Examining effect of electronic toll collection (ETC) system on queue delay using microsimulation approach at toll plaza -a case study of Ghoti toll plaza, India. In: 7th international IEEE conference on model and technologies for intelligent transportation system, pp 16–17
11. Swami H, Bari C, Dhamaniya A (2021) Developing policy framework of dynamic toll pricing in India. *Transp Res Procedia* 52:605–612. <https://doi.org/10.1016/j.trpro.2021.01.072>
12. Edie LC (1954) Traffic delay at toll booths. *J Oper Res Soc Am* 2:107–138
13. Lin F-B, Su C-W (1994) Level of service analysis of toll plazas on freeway main lines. *J Transp Eng* 120:246–263
14. Lin FB, Lin MW (2001) Modeling traffic delays at northern New York border crossings. *J Transp Eng ASCE* 127:540–545
15. Klodzinski J, Al-Deek HM (2002) New methodology for defining level of service at toll plazas. *J Transp Eng* 128:173–181. <https://doi.org/10.3141/1802-11>
16. HCM Highway Capacity Manual (2010) Transportation Research Board, National Research Council, Washington, DC, pp 1–1207

17. Shi W, Liu Y (2010) Real-time urban traffic monitoring with global positioning system-equipped vehicles. *IET Intell Transp Syst* 4:113–120. <https://doi.org/10.1049/iet-its.2009.0053>
18. Aksoy G, Berk H, Gedizlioglu E (2014) Analysis of toll queues by micro-simulation: results from a case study in analysis of toll queues by micro-simulation: results from a case study in Istanbul. *Procedia Soc Behav Sci* 111:614–623. <https://doi.org/10.1016/j.sbspro.2014.01.095>
19. Hashim I, Ragab M, Asar G (2018) Optimization of vehicle delay and exhaust emissions at signalized intersections. *Adv Transp Stud* 15:5–18
20. Bari C, Navandar YV, Dhamaniya A (2019) Service time variation analysis at manually operated toll plazas under mixed traffic conditions in India
21. Bari CS, Chandra S, Dhamaniya A et al (2021) Service time variability at manual operated tollbooths under mixed traffic environment: Towards level-of-service thresholds. *Transp Policy* 106:11–24. <https://doi.org/10.1016/j.tranpol.2021.03.018>
22. Bari CS, Navandar YV, Dhamaniya A (2020) Delay modelling at manually operated toll plazas under mixed traffic conditions. *Int J Transp Sci Technol*. <https://doi.org/10.1016/j.ijst.2020.10.001>
23. Bari CS, Navandar YV, Dhamaniya A (2021) Analysis of vehicle specific acceleration and deceleration characteristics at toll plazas in India. *Transp Dev Econ* 7:1–19. <https://doi.org/10.1007/s40890-021-00115-6>
24. Molzahn SE, Kerner BS, Rehborn H et al (2017) Analysis of speed disturbances in empirical single vehicle probe data before traffic breakdown. *IET Intell Transp Syst* 11:604–612. <https://doi.org/10.1049/iet-its.2016.0315>
25. Tian D, Shan X, Sheng Z et al (2017) Break-taking behaviour pattern of long distance freight vehicles based on GPS trajectory data. *IET Intell Transp Syst* 11:340–348. <https://doi.org/10.1049/iet-its.2016.0195>
26. Yu L, Li XG, Zhou W (2006) A genetic algorithm-based calibration of VISSIM using GPS data. *Adv Transp Stud* 8:57–69
27. Russo C, Harb R, Radwan E (2010) Calibration and verification of SHAKER, a deterministic toll plaza simulation model. *J Transp Eng ASCE* 136:85–92. [https://doi.org/10.1061/\(ASCE\)TE.1943-5436.0000060](https://doi.org/10.1061/(ASCE)TE.1943-5436.0000060)
28. Zarrillo ML, Radwan AE (2009) Methodology SHAKER and the capacity analysis of five toll plazas. *J Transp Eng ASCE* 135:83–93. [https://doi.org/10.1061/\(asce\)0733-947x\(2009\)135:3\(83\)](https://doi.org/10.1061/(asce)0733-947x(2009)135:3(83))
29. Tenekeci G, Wainaina S, Askew I, Mohammad A (2014) Sustainable operational lane capacity for highways. *Proc Inst Civ Eng Transp* 167:36–47. <https://doi.org/10.1680/tran.9.00052>
30. Indo-HCM (2017) Indian highway capacity manual (Indo-HCM). New Delhi
31. Othayoth D, Rao KKV (2018) Estimation of stopped delay to control delay conversion factor and development of delay model for non-lane based heterogeneous traffic. *Eur Transp Trasp Eur*:1–21
32. Mousa RM (2002) Analysis and modeling of measured delays at isolated signalized intersections. *J Transp Eng ASCE* 128:347–354
33. Quiroga CA, Bullock D (1999) Measuring control delay at signalized intersections. *J Transp Eng ASCE* 125:271–280
34. Al-Deek H, Lochrane TWP, Chandra CVRS, Khattak A (2012) Diversion during unexpected congestion on toll roads: the role of traffic information displayed on dynamic message signs. *IET Intell Transp Syst* 6:97–106. <https://doi.org/10.1049/iet-its.2010.0163>

Capacity Analysis for Electronically Operated Toll Plaza Under Mixed Traffic Condition



Meet D. Ajudiya , Pradip J. Gundaliya , and Yogeshwar V. Navandar 

Abstract The service headway between two consecutive vehicles is more important factor for the operation of toll plaza. The service headway is mainly dependent on service time, traffic composition, vehicular characteristic, and driver's behavior. The wide variation in service headway is observed at different toll plaza, and also, at same toll plaza the service headway has wide variation. The aim of this study is to get variation in service headway in mixed traffic condition and to create a model to define capacity based on service headway. The leader and follower wise service headway variation is considered because service headway mainly differs with it. In this study, the capacity model is developed by using harmonic mean of traffic composition at toll booth with respect to capacity of different same leader and same follower pair of vehicles. The outcomes of this study will be useful for toll plaza management to evaluate capacity of toll plaza.

Keywords Service headway · Toll plaza · Mixed traffic · Capacity · Operation and management

1 Introduction

Most of the developing countries are in serious need of highway construction for economic development. The main objective of road development is to get the benefits to the road users such as convenience, cost saving, safety, and reduction in time of travel. Traditionally, the Indian highways are viewed as a public convenience

M. D. Ajudiya (✉) · P. J. Gundaliya
Department of Civil Engineering, L. D. College of Engineering, Ahmedabad, India
e-mail: ajudiyameet.mdusa@gmail.com

P. J. Gundaliya
e-mail: pjgundaliya@ldce.ac.in

Y. V. Navandar
Department of Civil Engineering, National Institute of Technology Calicut, Calicut, India
e-mail: navandar@nitc.ac.in

that finance and operated by the public sector. But to this, Government of India faced funding problems in later development because of budgetary problems. Then, public–private partnership model is used in highway development in 1990s and the NHAI (National Highway Authority of India) was set up in 1995 for supervising the functioning of the private parties in the highway development. After that, a number of highway projects have been constructed on the basis of PPP model, through BOT (Build, Operate, and Transfer) contract. Consequently, it has become increasingly accepted that all highways should be built, financed, and operated by private entities and the users of highways should pay toll tax for using them. Road users also accept the concept of toll tax because it owned by private sector that construct highway quickly and more efficiently than public sector. During the specified period in public–private partnership contract, the private firm operates and maintains the highway constructed by them; thereby, the road users get the adequate quality, safety, and security standards on the toll roads.

For collection of this toll tax, the toll plazas are built along the new developed highway stretch. There are mainly three methods of toll collection. These are manual, automatic, and electronic. The most widely used collection method was manual toll collection in India before some time but now it is mixed up of manual and electronic toll collection. In this manual method, the toll collector or attendant is required for collecting tax and gives receipt to the patron. Due to manual collection, the processing time is higher than other methods. In automatic toll collection, the tax is collected by Automated Coin Machine (ACM); this method is not widely used in India. In ETC (Electronic Toll Collection) vehicle automatically identifies with encoded tag like FASTag as it passes through the toll plaza. After that, the tax is debited from the account of patron. In these days, Government of India interested in making all toll plazas with ETC method and use of FASTag.

1.1 Objectives of the study

This study aims to create a methodology which gives the capacity of toll plazas in heterogeneous traffic condition with following objectives:

- To analyze the variation in service headway between various class of vehicle in different traffic condition.
- To determine the capacity of the toll plaza in mixed traffic condition in developing country like India.
- To compare the capacity data of this study of ETC facility with MTC facility.

2 Literature Review

Various studies were carried out related to capacity of toll plazas, which considered the service time, delay, v/c ratio, etc. [13] studied on toll plaza for capacity of toll

booth based on V/C ratio and traffic density. This study shows that the capacity may differ from lane to lane depending upon the traffic composition at that lane. Al-Deek [1], Woo and Hoel [13], Zarrillo, [14] provided different methods to evaluate capacity but there is no standard method available worldwide to estimate capacity at toll plaza. Obelherio [11] determine level of service at toll plaza based on road user's experience. The measure of effectiveness for this study was mean queue length and percentage of heavy vehicles available in traffic composition for LOS at toll plaza which directly affects the service headway between vehicles [5–9]. Navandar et al. [7] studied about level of service at manually operated toll booths under mixed traffic conditions. In this study, authors use v/c ratio to develop methodology for LOS at toll plaza in which they developed capacity model by usage of harmonic mean. Bari et al. [2] studied the service time variability at manually operated toll plaza and take 13 different leader–follower pair which shows that the service time follows the lognormal distribution.

From the literature review, it was found that the service headway between two consecutive vehicles at toll booth is dynamic in nature and varies with different factors like vehicular characteristic, payment method, toll booth operator's and driver's behavior, reaction time of driver, vehicle class, and traffic composition at approach of toll plaza [5–10]. All these studies are carried out for manually operated toll plaza but limited studies are carried out for electronic toll collection in mixed traffic condition. Hence, this study mainly focuses on toll plazas with electronic toll collection facility and variation of service headway with respect to different factors like class of vehicle, traffic composition, leader–follower pair for analysis of capacity at toll booth.

3 Methodology

The flow chart for detailed methodology for this study has been presented in Fig. 1. To meet the objectives of present study, video graphic survey was carried out at two different toll plazas to also ensure the variability of human characteristics and different environmental characteristic. To get maximum accuracy, the AVIDEMUX 2.7 player was used and the time was noted up to three decimals of seconds. MS Excel is used for data extraction, and the data like lane number, class of vehicle, and the entry and exit time of each vehicle from system were extracted. To get the variation in service headway, the box plot and Probability Density Function (PDF) were plotted with respect to class of vehicle, lane, and leader–follower pair.

4 Data Collection

For present study, the video graphic survey was conducted at two different locations in the western part of India. One was Bharthan Toll Plaza near Karjan, and second

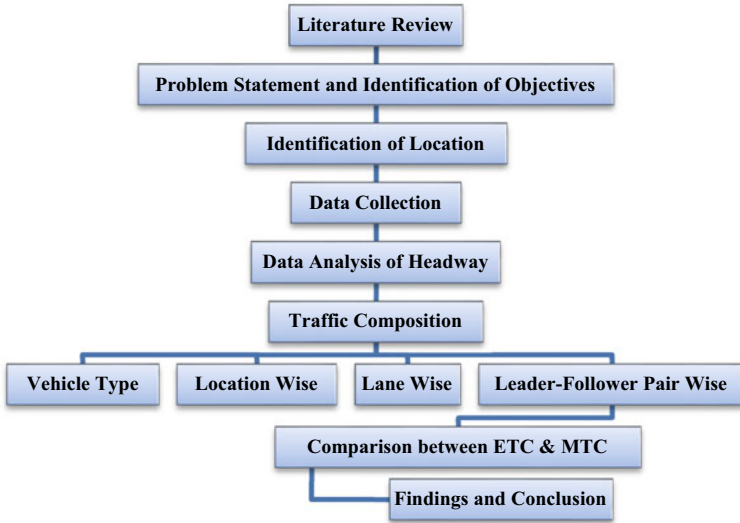


Fig. 1 Flow chart of methodology

Table 1 Survey details

Sr. No.	Name	City	Date and day	Timing	Number of lane
1	Bharthan toll plaza	Karjan	22/01/2021 Friday	10:00 AM–01:00 PM and 3:00 PM–07:00 PM	4
2	Narmada bridge toll plaza	Bharuch	29/01/2021 Friday		4

was Narmada Bridge Toll Plaza near Bharuch. Both the toll plazas are situated on NH-48. The details of traffic survey schedule are given in Table 1. Figure 2 shows the location of both toll plazas in Gujarat, state of India.

The vehicles were classified under seven categories to get the accurate variation in service headway for same vehicle and also for comparison to another vehicle. This classification is given in Table 2.

5 Analysis of Data

The field data show that the driver of any class of vehicle tends to go on the lane which has lesser queue length, so that mixed traffic condition occurs and all classes of vehicle are mostly available at all the lanes and this tends to various leader–follower pair. The share of different class of vehicles at toll plaza is shown in Figs. 3 and 4.



Fig. 2 Study location

Table 2 Classification of vehicle

Sr. No.	Vehicle class	Included vehicles	Length (m)
1	Small car (SC)	Car	3.72
2	Big car (BC)	Big utility vehicle, XUS, SUV	4.58
3	Large commercial vehicle (LCV)	Light motor vehicle	5.00
4	Bus	Standard bus	10.30
5	Heavy commercial Vehicle (HCV)	2 Axle truck	7.20
6	Multi axle vehicle	3 or more axle vehicle	11.70
7	Trailer	Trailer	15.60

Fig. 3 Traffic composition at Bharthan toll plaza

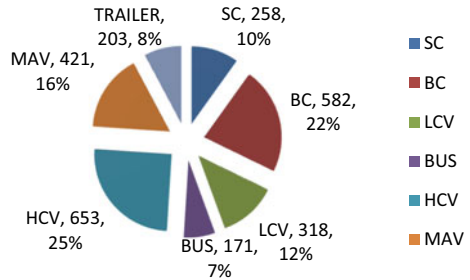
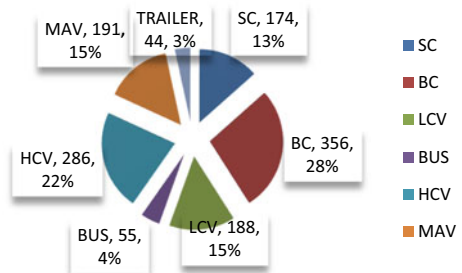


Fig. 4 Traffic composition at Narmada bridge toll plaza



The traffic data were manually extracted for all survey lane with Avidemux 2.7 to achieve desired degree of precision. In the spreadsheet, the data were extracted lane wise and type of vehicle, entry and exit of vehicle from system, and leader–follower pair are noted. The time difference between leader and follower vehicle to exit from the system is considered as service headway. The boom barrier is open for leader vehicle and for follower vehicle; this time is considered as service headway for follower vehicle.

6 Service Headway Variability

Service headway is the time that elapses between the arrival of the leading vehicle and the following vehicle at the designated test point. In this study, the exit from system of leading and following vehicle is taken as designated test point. The time difference between leader and follower vehicle starts their movement toward downstream after making payment is known as service headway, and it is measured front bumper of leading vehicle to front bumper of following vehicle.

According to various classes of vehicles, the below tables show the descriptive statistics of service headway at Bharthan toll plaza (BTP) and Narmada Bridge toll plaza (NBTP) (Fig. 5) (Table 3).

The mean service headway is higher for Trailer as 13.841 which is 80.5% more than SC. The Box plot shows that variation is more for the MAV. The Bus and HCV have approximately same mean service headway; it is due the same vehicle size. The graph of PDF shows that SC has more density with lesser mean service headway. The Trailer follows the normal distribution (Fig. 6) (Table 4).

The Box plot of service headway at NBTP shows that the Trailer has maximum mean service headway with higher variation. The PDF graph shows that SC has minimum service headway and BC has higher density.

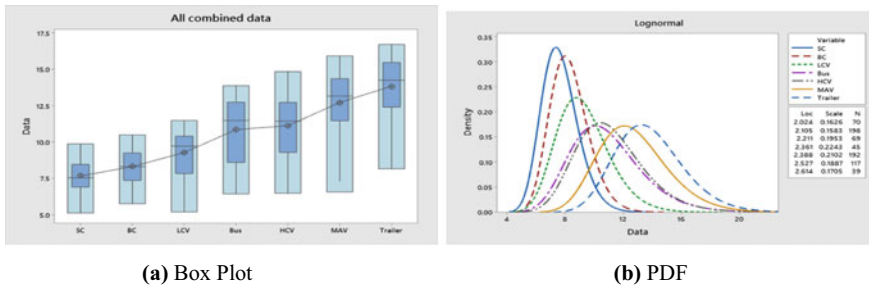


Fig. 5 Service headway variability at BTP

Table 3 Descriptive statistic for service headway at BTP

Vehicle class	Sample size	Minimum (s)	Maximum (s)	Mean (s)	Standard deviation
SC	70	5.12	9.88	7.67	1.22
BC	198	5.76	10.49	8.31	1.29
LCV	69	5.19	11.48	9.29	1.64
Bus	45	6.44	13.88	10.86	2.26
HCV	192	6.48	14.84	11.12	2.20
MAV	117	6.56	15.92	12.73	2.16
Trailer	39	8.16	16.72	13.84	2.18

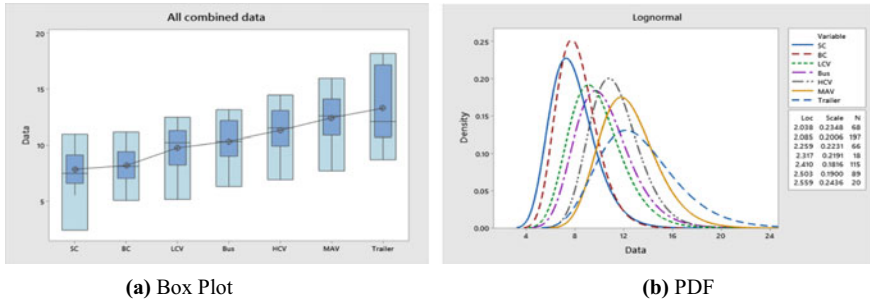


Fig. 6 Service headway variability at NBTP

Table 4 Descriptive statistic for service headway at NBTP

Vehicle class	Sample size	Minimum (s)	Maximum (s)	Mean (s)	Standard deviation
SC	68	2.40	10.96	7.87	1.64
BC	197	5.08	11.16	8.20	1.61
LCV	66	5.16	12.48	9.79	1.98
Bus	18	6.32	13.16	10.37	2.09
HCV	115	6.92	14.46	11.31	1.95
MAV	89	7.72	15.96	12.43	2.21
Trailer	20	8.72	18.20	13.29	3.25

The results of both the toll plazas show that the trailer has more service headway compared to other vehicles. It shows that service headway depended on service time and clearance time. The variation in service headway is due to vehicular characteristics, driver’s behavior, and speed of scanner to scan the FASTag.

7 Leader–Follower Wise Service Headway Variation

This section includes the study about variation in service headway with different leader to follower pair. There are mainly different 49 of leader–follower pair considered and 19 leader–follower pair out of them who gives the accurate result taken in this study (Fig. 7) (Table 5).

The above box plot of service headway at BTP shows that variation of service headway for pair SC to Trailer is higher as compared to others as it varies from 10.20 to 26.14 s. The minimum mean service headway is 7.73 s for pair of BC to SC. The PDF shows that BC to SC has minimum mean service time but with higher density (Fig. 8) (Table 6).

This is the important variation to take into consideration as which vehicle is leading and which vehicle is following. The pair of BC-SC has lower service headway as

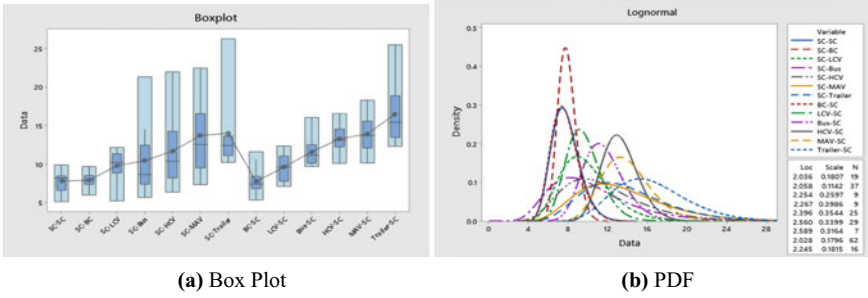


Fig. 7 Leader-follower wise service headway variability at BTP

Table 5 Descriptive statistic for leader-follower wise service headway at BTP

Vehicle class	Sample size	Minimum (s)	Maximum (s)	Mean (s)	Standard deviation
SC-SC	19	5.12	9.88	7.78	1.33
SC-BC	37	5.97	9.68	7.88	0.87
SC-LCV	9	5.19	12.16	9.78	2.12
SC-Bus	9	5.64	21.32	10.43	4.80
SC-HCV	25	6.36	21.96	11.69	4.36
SC-MAV	29	7.32	22.44	13.68	4.72
SC-Trailer	7	10.20	26.24	13.99	5.54
BC-SC	62	5.32	11.61	7.73	1.44
LCV-SC	16	7.11	12.35	9.59	1.72
Bus-SC	6	9.68	16.04	11.59	2.27
HCV-SC	21	10.08	16.57	13.26	1.78
MAV-SC	17	10.12	18.29	13.91	2.47
Trailer-SC	9	12.28	25.48	16.48	4.18

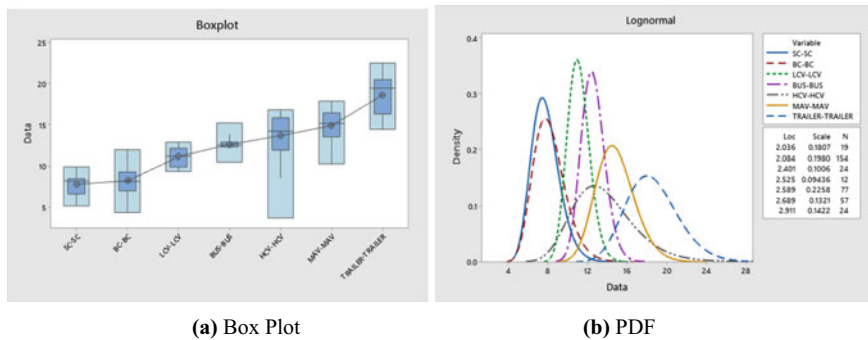


Fig. 8 Same leader-follower wise service headway variability at BTP

Table 6 Descriptive statistic for same leader–follower wise service headway at BTTP

Vehicle class	Sample size	Minimum (s)	Maximum (s)	Mean (s)	Standard deviation
SC-SC	19	5.12	9.88	7.78	1.33
BC-BC	154	4.34	11.91	8.19	1.60
LCV-LCV	24	9.34	12.85	11.09	1.10
Bus-Bus	12	10.44	15.16	12.54	1.19
HCV-HCV	77	3.65	16.75	13.60	2.50
MAV-MAV	57	10.24	17.80	14.83	1.89
Trailer-Trailer	24	14.36	22.44	18.55	2.58

7.725 s, and the Trailer–Trailer has maximum of 18.553 s. The PDF graph shows that all pairs have higher variation with no same results (Figs. 9 and 10) (Table 7).

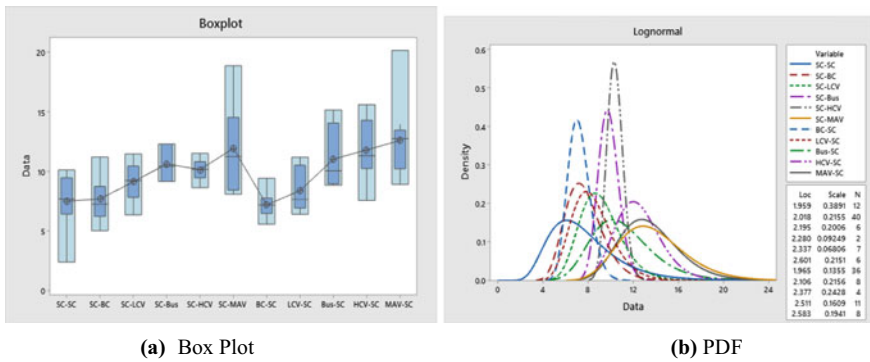


Fig. 9 Leader–follower wise service headway variability at NBTP

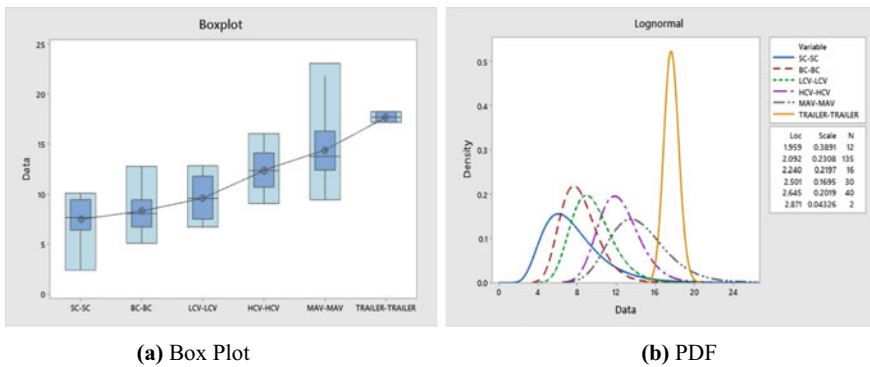


Fig. 10 Same leader–follower wise service headway variability at NBTP

Table 7 Descriptive statistic for leader–follower wise service headway at NBTP

Vehicle class	Sample size	Minimum (s)	Maximum (s)	Mean (s)	Standard deviation
SC-SC	12	2.4	10.12	7.50	2.17
SC-BC	40	5.02	11.22	7.70	1.71
SC-LCV	6	6.36	11.48	9.13	1.72
SC-Bus	2	9.16	10.44	9.80	0.91
SC-HCV	7	9.32	11.52	10.37	0.71
SC-MAV	6	10.84	18.88	13.75	3.11
B-SC	36	5.58	9.44	7.20	0.99
LCV-SC	8	6.4	11.2	8.39	1.87
Bus-SC	4	8.84	15.16	11.03	2.88
HCV-SC	11	10.16	15.6	12.46	2.03
MAV-SC	8	10.56	20.16	13.48	2.93

Table 8 Descriptive statistic for same leader–follower wise service headway at NBTP

Vehicle class	Sample size	Minimum (s)	Maximum (s)	Mean (s)	Standard deviation
SC-SC	12	2.40	10.12	7.50	2.17
BC-BC	135	5.08	12.72	8.32	1.94
LCV-LCV	16	6.72	12.80	9.61	2.08
HCV-HCV	30	9.08	16.00	12.36	2.04
MAV-MAV	40	9.44	23.04	14.37	3.07
Trailer-Trailer	2	17.12	18.20	17.66	0.76

The box plot says that the MAV-SC has more variation than other pairs. The pair of BC-SC has lower mean service headway as compared to other pairs same as of Bharthan Toll Plaza and also Trailer–Trailer has higher mean service headway.

The results show that there is a wide difference for every pair of leader–follower. The service headway is mainly dependent on the leader vehicle and follower vehicle. This variation of service headway is mainly due to driver's behavior in different situation of leader vehicle (Tables 8 and 9).

8 Capacity of Toll Booth

To get interaction between different classes of vehicles, the 30 min period is considered in survey time. Same pair of leader and follower such as the class of vehicle is same for leader and follower taken for the measurement of service headway between them for the calculation of capacity at toll booth. The mean service headway for all such leader–follower pair is calculated for the capacity of toll booth in homogenous

Table 9 Capacity for different leader–follower pair

Vehicle class	Sample size	Mean service headway (s)	Capacity (vehicle/hr)
SC-SC	31	7.67	469
BC-BC	289	8.25	436
LCV-LCV	40	10.50	342
Bus-Bus	12	12.54	287
HCV-HCV	107	13.26	271
MAV-MAV	97	14.64	245
Trailer-Trailer	26	18.48	194

traffic condition when one type of vehicle class is available in traffic stream. The capacity for each pair of leader–follower is calculated by equation given by Wardrop [12].

$$\text{Capacity}_y = \frac{3600}{\text{Average Service Headway}_{y-y}} \tag{1}$$

where

- $y - y$ vehicle combination (y class of vehicle as leader to y class of vehicle as follower)
- Capacity_y Capacity of toll booth when only y type of vehicle available at approach of toll booth

When only Small Car is available in traffic stream, the capacity of toll booth is 469 vehicle/hr. It changes with class of vehicle such as for Big car it is 436 vehicle/hr, for Light Commercial vehicle it is 342 vehicle/hr, for Bus it is 287 vehicle/hr, for Heavy Commercial Vehicle it is 271 vehicle/hr, for Multi Axle Vehicle it is 245 vehicle/hr, and for Trailer it is 194 vehicle/hr.

The IRC SP:84-2014 gives standard capacity as 240 vehicle/hr irrespective of class of vehicle whereas the equation is given by Wardrop for homogenous traffic condition when only same class of vehicle is available at toll booth the capacity increased for SC, BC, LCV, Bus, HCV, and MAV by 95.42%, 81.67%, 42.50%, 19.58%, 12.92%, and 2.08%, respectively, and reduced by 19.17% for Trailer.

These values of capacity for different pair of same leader–follower were used to develop the general equation for mixed traffic condition. The percentage share of different vehicle class is available at toll booth, and the capacity derived by mean service headway was used to develop the generalized equation.

$$\frac{100}{\text{Capacity}_{\text{mix}}} = \frac{P_{\text{SC}}}{469} + \frac{P_{\text{BC}}}{436} + \frac{P_{\text{LCV}}}{342} + \frac{P_{\text{Bus}}}{287} + \frac{P_{\text{HCV}}}{271} + \frac{P_{\text{MAV}}}{245} + \frac{P_{\text{Trailer}}}{194} \tag{2}$$

where

Capacity _{mix}	Capacity of toll booth in mixed traffic condition
P_{SC}	Percentage share of SC in traffic at toll booth approach
P_{BC}	Percentage share of BC in traffic at toll booth approach
P_{LCV}	Percentage share of LCV in traffic at toll booth approach
P_{Bus}	Percentage share of Bus in traffic at toll booth approach
P_{HCV}	Percentage share of HCV in traffic at toll booth approach
P_{MAV}	Percentage share of MAV in traffic at toll booth approach
$P_{Trailer}$	Percentage share of Trailer in traffic at toll booth approach

9 Comparison Between MTC and ETC

As per the previous section, the capacity is different for different pair of leader–follower. The capacity of toll booth decreases with increase in the size of vehicle. In MTC (Manual toll collection), the payment is made through cash; that is why, it requires more time as compared to ETC (Electronic Toll Collection) because the driver gives the cash to toll booth operator then toll booth operator makes a receipt after that he gives the receipt and change to the driver. No manual work is there in ETC facility because the payment is made through the FASTag by the use of scanner so that the time required for toll collection is less as compared to MTC.

The equation of capacity is given by the Wardrop use for the calculation of capacity for facility of toll collection like MTC and ETC (Table 10).

Table 10 Capacity comparison for MTC and ETC facility

Vehicle Class	MTC (Navandar et al. [7])		ETC	
	service headway	Capacity	Service headway	Capacity
SC	15.86	226	7.87	457
BC	15.18	237	8.31	433
LCV	19.62	183	9.79	367
Bus	24.45	147	10.86	331
HCV	25.06	143	11.31	318
MAV	31.70	113	12.73	282
Trailer	35.68	100	13.84	260
SC-SC	15.36	234	7.67	469
BC-BC	16.84	213	8.25	436
LCV-LCV	18.03	199	10.50	342
Bus-Bus	25.71	140	12.54	287
HCV-HCV	25.31	142	13.26	271
MAV-MAV	30.42	118	14.64	245
Trailer-Trailer	38.72	92	18.48	194

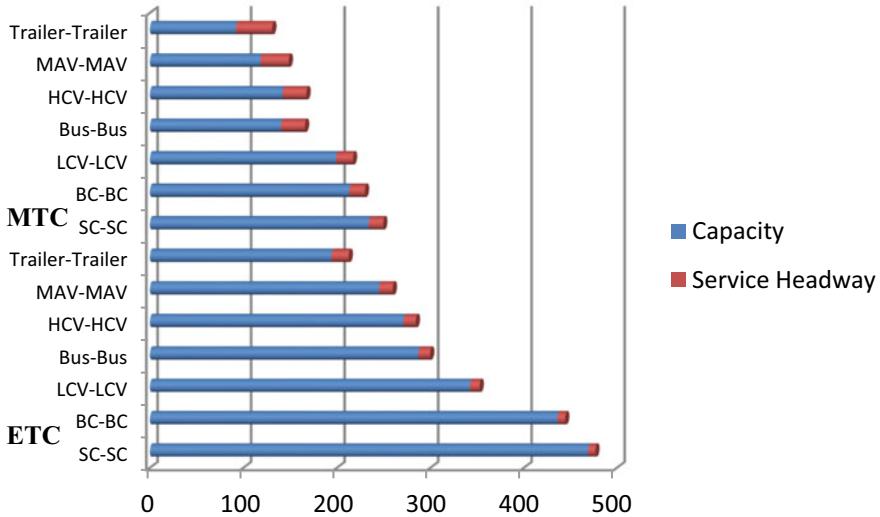


Fig. 11 Comparison of capacity for MTC and ETC facility

Result shows that as the size of vehicle increases the capacity decreases. The capacity of toll plaza with MTC facility for SC without considering the leader–follower is 226 vehicle/hr, and for ETC, it is 457 vehicle/hr which is increased by 102.21% from MTC. The size of trailer is more as compared to another class of vehicle and for that the capacity for MTC is 100 vehicle/hr and for ETC it is increased by 160% as 260 vehicle/hr. For the same leader–follower pair, the capacity for SC-SC with ETC is increased by 100.43% from MTC. For Trailer-Trailer, the capacity with ETC is 194 vehicle/hr increased by 110.87% from MTC. For all situation, the capacity for toll booth with ETC facility is approximately 100% more than toll booth with MTC facility (Fig. 11).

The capacity of toll booth with ETC facility for Trailer-Trailer is more than the capacity of toll booth with MTC facility for Bus-Bus, HCV-HCV, MAV-MAV, and Trailer-Trailer. The value of SC-SC for ETC facility is very high as compared Trailer-Trailer for MTC facility.

10 Conclusion

Service headway is an important element for operation of toll plaza. This study shows that the service headway is dynamic in nature which differ with various conditions. The study shows that the service headway in Electronic Toll Collection (ETC) is mainly depending upon vehicular characteristic, service time, speed of scanner to scan FASTag, location of FASTag on vehicle, traffic composition, and driver’s behavior in different situation.

The mean service headway for SC is 7.868 s and for Trailer is 13.841 s; this shows that as the size of vehicle increase, the service headway increases. The service headway is mainly affected by service time and clearance time. As the service time for ETC facility is lesser than MTC facility, the service headway also very much decreased for ETC facility from MTC facility. The capacity of toll booth is determined by the harmonic equation by considering the percentage share of different class of vehicle. This model gives the accurate result for the capacity of toll booth with ETC facility. If the same percentage of share is considered for both the facilities, then the MTC facility has capacity of 156 vehicle/hr and ETC facility has capacity of 310 vehicle/hr; this shows the wide variation in capacity.

References

1. Al-Deek H, Mohamed A, Radwan A (1997) Operational benefits of electronic toll collection: case study. *J Transp Eng ASCE* 123(December):467–477
2. Bari CS, Chandra S, Dhamaniya A, Arkatkar S, Navandar YV (2021) Service time variability at manual operated tollbooths under mixed traffic environment: towards level-of-service thresholds. *Transp Policy* 106:11–24
3. Highway Capacity Manual (HCM) (2000) Transportation research board. Washington, DC
4. Indian Highway Capacity Manual (Indo-HCM), CRRI-Central Road Research Institute, New Delhi
5. Lin FB, Su CW (1994) Level of service analysis of toll plazas on freeway main lines. *J Transp Eng* 120(2):246–263
6. Navandar YV, Dhamaniya, Patel DA (2017) Distribution of service time at toll plaza in India under mixed traffic condition. In: *Proceedings of the Eastern Asia society for transportation studies*, pp 1–15
7. Navandar YV, Bari C, Dhamaniya A, Patel DA (2019) Analysis of level of service for manually operated tollbooths under mixed traffic scenario. *J Eastern Asia Soc Transp Stud* 13:1648–1663
8. Navandar YV, Patel DA, Dhamaniya A (2018) Service time prediction models for manual toll booth operation under mixed traffic conditions. *European Transp* (68):1–21
9. Navandar YV, Dhamaniya A, Patel DA (2020) A Quick method for estimation of level of service at manually operated tollbooths under mixed traffic condition. *Transp Res Procedia* 48:3107–3120
10. Nonika N, Arundhathi MV, Rohith M (2017) Analysis of traffic behavior at the toll plazas around Bangalore. *Int Res J Eng Technol* 04(09)
11. Obelheiro MR, Cybis B, Ribeiro LD (2011) Level of service method for Brazilian toll plazas. *Procedia Soc Behav Sci* 16:120–130
12. Wardrop GJ (1952) Some theoretical aspects of road traffic research. In: *Proceedings of the Institution of Civil Engineers, Part II*, pp 325–378
13. Woo TH, Hoel LA (1991) Toll plaza capacity and level of service. *Transp Res Rec* 1320, 1987(7):119–127
14. Zarrillo ML, Radwan AE, Dowd JH (2002) Toll network capacity calculator: operations management and assessment tool for toll network operators. *Transp Res Rec* 1781(1):49–55

Comparison of Dynamic Passenger Car Values Estimated at Signalised Intersections Under Heterogeneous Traffic Conditions



P. N. Salini, B. Anish Kini, and Gopika Mohan

Abstract Passenger car units (PCU) play a pivotal role in the measurement of level of service (LOS) and capacity analysis of signalised intersections in developing countries where heterogeneous traffic conditions are prevalent. Literatures are available with different methods for estimating dynamic PCU values, but less of researches are done on their evaluation based on field measurements. This paper brings out a comparative analysis of estimated dynamic PCU values for signalised intersections having heterogeneous traffic conditions focusing on two methods—(1) dynamic PCU estimation using time headway ratio method and (2) dynamic PCU estimation using clearance time and projected area of vehicles. These two methods are compared with respect to the saturation flow at three signalised intersections to establish the suitability of these methods for dynamic PCU estimation for signalised intersections with heterogeneous traffic conditions. Results show that dynamic PCU estimation based on time headway ratio method and simulation model involving traffic volume and composition analysis goes in better conformity with the Indo-HCM method of saturation flow assessment for signalised intersections with heterogeneous traffic conditions.

Keywords Dynamic PCU · Heterogeneous traffic · Saturation flow · Signalised intersections

P. N. Salini (✉) · B. A. Kini · G. Mohan
KSCSTE-NATPAC, Thiruvananthapuram, India
e-mail: salini.jayaprakash@gmail.com

B. A. Kini
e-mail: anishkini85@gmail.com

G. Mohan
e-mail: gopikamohan14@gmail.com

1 Introduction

Intersections are major part of a road network which plays a vital role in safe and effective traffic movement. If not properly designed, they act as bottlenecks on a road network in urban areas. Proper design of intersections is a challenge under heterogeneous traffic as it has wide variety of vehicles with different size and manoeuvrability which utilises the same space without segregation. Thus, urban road intersections are the major critical points with respect to safety, capacity, delay and efficiency. Therefore, both from the safety perspective and the service perspective, the study of intersections is very important especially in the urban scenario. Signalised intersections though more disciplined with respect to unsignalised, still the heterogeneous traffic poses a great challenge in properly estimating the various parameters of traffic flow.

Indian Highway Capacity Manual (Indo-HCM) [1] presents the methodologies for estimating the capacity and level of service (LOS) for traffic facilities. Saturation flow is defined by Indo-HCM as the steady state discharge of queued vehicles from an approach at a signalised intersection with continuous green and an infinite queue. It is expressed in passenger car units (PCU)/hour of green time. Indo-HCM has adopted the method suggested by Transport Research Laboratory (UK) for the field measurement of saturation flow. The saturation flow and delay can be estimated for existing signalised intersections or for a newly planned intersection using the methodology in Indo-HCM. Furthermore, users are also given the option to either use the models developed or by field measurement procedures prescribed in this manual in the case of existing signalised intersections.

The traffic flow characteristics in developing countries will be entirely different from the developed countries. In most of the developed countries, the traffic will be homogeneous, and following lane discipline and a predominant share of the vehicle composition will be cars. However, in developing countries, the traffic will be heterogeneous comprising a wide range of vehicles without following lane discipline. Consequently, the vehicles tend to occupy any available road space especially the smaller size vehicles use the gaps among large vehicles. PCU is a metric used to solve the problem of measuring mixed traffic volume by converting the different types of vehicles into equivalent passenger cars.

Marfani and Dave [2] observed a variation in actual capacity at intersections, and they stated the need for more accurate formulation of saturation flow which plays a major role in signal timing design. Radhakrishnan and Mathew [3] used microscopic analysis for developing a saturation flow model based on dynamic PCUs, and it reduced the error in normal flow estimation methods. Chand et al. [4] estimated dynamic PCU values in the assumption that it depends on the space and clearance time of vehicles at a signalised intersection. Arkatkar and Arasan [5] studied the effect of magnitude of upgrade and its length on PCU values.

Hadiuzzaman et al. [6] studied the different methods available for saturation flow measurement and identification of suitable method to measure different parameters for traffic condition prevailing in developing countries. Savitha et al. [7] developed

a model for saturation flow estimation by incorporating the significant geometric factors. Prathapan and Rajamma [8] compared the PCU values of through and right turn moving vehicles in same phase with that of only through moving vehicles in a phase and concluded that the former had lower values than the latter. Arasan and Vedagiri [9] showed that there is road width which is directly proportional to saturation flow per unit width of road.

Alex and Issac [10] observed that dynamic PCU estimation increased with proportion of vehicles except for two wheelers. Majhi [11] developed a method based on optimisation, which gives saturation period, dynamic passenger car units and saturation flow values. They ignored side friction and turning movements due to time constraints and complexity in the analysis.

1.1 Need and Relevance of the Study

Most of the signalised intersections in Kerala have a lot of bus stop, parking and pedestrian activity which will be having a significant effect on the saturation flow. The vehicle composition observed in Kerala is also different from other parts of India. So, this study was intended to find the best method for dynamic PCU estimation which will go in better conformity with field traffic conditions in Kerala.

1.2 Objectives of the Study

This paper presents the comparative study between two dynamic PCU estimation methods (a) Method 1—by Asaithambi et al. [12] and (b) Method 2—by Mahidadiya and Juremalani [13] to identify the better method that is suitable for the typical intersections in Kerala, India.

1.3 Methods for Estimation of PCU

The review of literature reveals that PCU studies were carried out mostly for mid-blocks, and only limited studies on signalised intersections were done under mixed traffic conditions. Raj et al. [14] reviewed the dynamic PCU estimation methods for different facilities under homogeneous and mixed traffic conditions. Various methods of dynamic PCU estimation available for signalised intersections were reviewed and are discussed in this section.

Headway Method: Greenshields et al. [15] estimated PCU values based on basic headway using Eq. (1).

$$PCU_i = H_i/H_c \quad (1)$$

where,

PCU_i PCU of vehicle type i under homogeneous traffic condition,

H_i average headway of vehicle type i and

H_c average headway of passenger car

Based on Delay: Zhao [16] developed a delay-based passenger car equivalent method for heavy vehicles at signalised intersections. Mathematically, PCE for a heavy vehicle type i based on delay is expressed by Eq. (2).

$$D_PCE_i = 1 + \left(\frac{\Delta d_i}{d_0} \right) \quad (2)$$

where

D_PCE_i PCE for a heavy vehicle type i based on delay,

Δd_i additional delay caused by a vehicle type i and

d_0 average vehicle delay when the traffic is composed of passenger cars only.

Based on Queue Discharge Flow: Radhakrishnan and Mathew [3] optimised the difference between ideal flow profile and the observed flow profile for the computation of dynamic PCU at urban signalised intersections.

Based on Travel Time: Dynamic PCUs for signalised intersections were estimated by Mahidadiya and Juremalani [13] from Eq. (3).

$$PCU_i = (t_i/t_c)/(A_c/A_i) \quad (3)$$

where

A_c and A_i projected area of passenger car and vehicle type i , respectively

t_c and t_i travel time of passenger car and vehicle type i , respectively.

Multiple Linear Regression Method: For the formulation of dynamic PCU values, multiple linear regression analysis was used by Adams et al. [17] by considering the number of vehicles passing the intersection during saturated period as the independent variables and the saturated period as dependent variable. The ratio of regression coefficient of each vehicle to the regression coefficient of car was taken as the PCU factor of that group.

Simulation Method: Asaithambi et al. [12] developing a model for dynamic PCU estimation by considering the effect of vehicle composition, vehicles per hour and road width.

2 Study Area and Methodology

This work presents the comparative study between two dynamic PCU estimation methods Method 1 and Method 2 as explained in earlier sections. The methods

were compared with the Indo-HCM methods for estimation of saturation flow at signalised intersections. Field measurements for the present study are conducted at three intersections identified in Kerala State, India, namely Kowdiar (Intersection-A), LMS (Intersection-B) and Nilamel (Intersection-C). Intersections A and B are three arm intersections in urban area. Intersection-C is a four arm intersection in semi-urban area.

2.1 Field Measurement of Saturation Flow

After completing field data collection from the selected intersections, direction-wise classified traffic count during each green phase was extracted at 5 s interval. The field saturation flow was calculated for each movement group as per Indo-HCM. On each approach during green interval, the operation of movements may happen in a shared manner or in an exclusive manner. Indo-HCM considered movement group as anyone or combination of through or right turning or left turning movements at an intersection approach that were allowed in a shared operation in the same phase. It was treated as a separate entity by assigning appropriate effective width of the approach for capacity and LOS analysis.

2.2 Saturation Flow Using Static PCU

The static PCU values for signalised intersections provided in the Indo-HCM manual are shown in Table 1. The movement groups in each intersection were named using the direction of traffic flow and the turning movements in that movement group. For example, a movement group in the northbound direction which consists of left and through traffic was named as NBM-LT, where 'NBM' indicated the northbound approach, and 'LT' indicated the turning movements included. The movement groups identified for a typical intersection are shown in Fig. 1.

The field measured saturation flow using the static PCU values and saturation flow computed using the model provided in Indo-HCM for each movement group is shown in Table 2. For the computation of saturation flow for each movement group using the model provided in Indo-HCM, the effective approach width available for the corresponding movement group was used.

When field measured saturation flow was compared with the theoretical saturation flow estimated using Indo-HCM model, significant variation as high as 52% was observed at intersection-B. Since similar trend was also observed for other study intersections. Hence it was decided to adopt dynamic PCU was used for further studies.

Table 1 Passenger car unit values for signalised intersection

Vehicle type	Passenger car unit
Two wheelers (TW)	0.4
Auto rickshaws (Auto)	0.5
Passenger cars	1.0
Light commercial vehicle (LCV)	1.1
All heavy goods vehicles (HCV)	1.6
Bus	1.6
Bicycle	0.3
Cycle rickshaw	1.8
Hand/animal drawn cart	4.0

3 Dynamic PCU Estimation

The dynamic PCU calculation methods suggested by Asaithambi et al. [12] [Method 1], Mahidadiya and Juremalani [13] [Method 2] were compared, and the better method was identified for further studies. The dynamic PCU values estimated are plotted and compared with the dynamic PCU range provided in Indo-HCM (given in Table 3) and discussed in subsequent sections.

3.1 Estimation of Dynamic PCU Values—Method 1

In Method 1, microscopic simulation model was used to estimate the PCU for different vehicle types at signalised intersections in mixed traffic using the time headway ratio method. They developed a multiple linear regression model to predict the PCU values of each class of vehicle for known traffic volume, composition and road width (Table 4). They considered LCV, HCV and bus together as heavy vehicles due to lesser sample size.

3.2 Saturation Flow Estimation Using Dynamic PCU by Method 1

The dynamic PCU values were estimated using Method 1 for all the study locations. The saturation flow values thus calculated from field measurements were showing better conformity with the theoretically estimated values of saturation flow based on Indo-HCM model or expression. Also, the dynamic PCU values thus obtained were almost within the range for dynamic PCU values provided in Indo-HCM. The dynamic PCU values estimated for a typical intersection, intersection-B using the Method 1 are shown in Table 5.

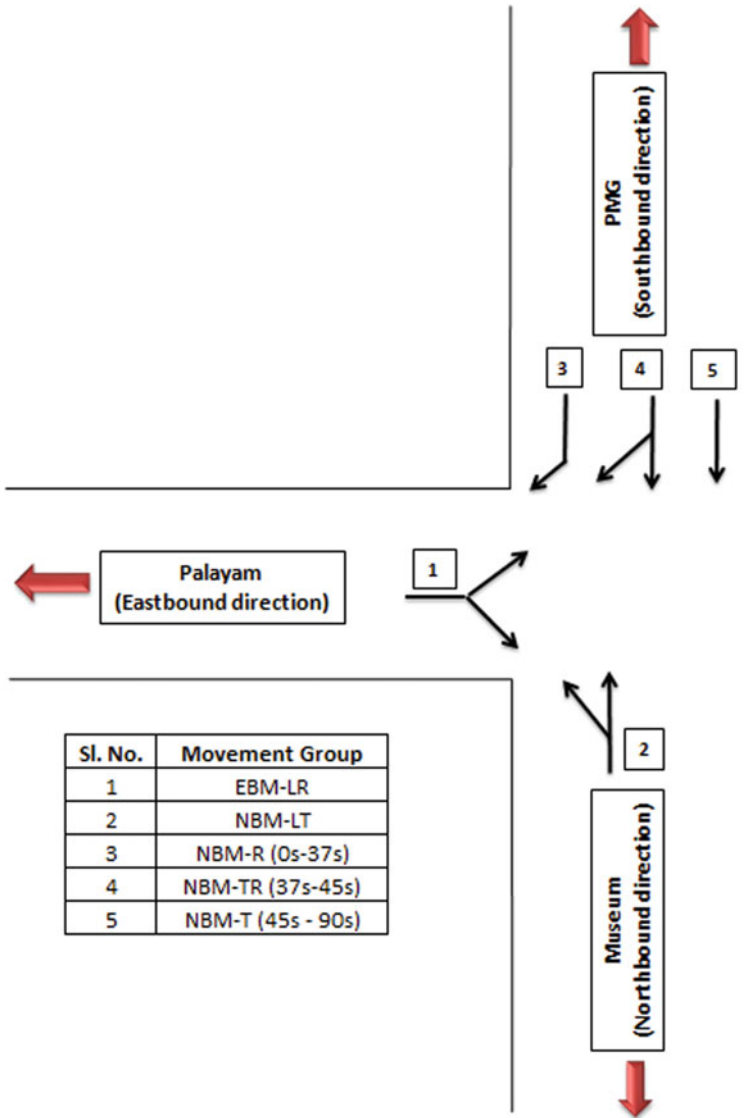


Fig. 1 Diagrammatic representation of movement groups observed at intersection-B

The field measured saturation flow computed for each movement group using these dynamic PCU values is given in Table 6. It can be seen that the percentage difference between field measured saturation flow and saturation flow (Indo-HCM [1]) is much lesser than that in Table 2 where static PCU was used. It is clearly visible from Fig. 2 that very close values for theoretically estimated values and field

Table 2 Saturation flow at intersection-B

Sl. No.	Movement group	Effective approach width (m)	Measured saturation flow (PCU/hr)	Saturation flow (PCU/hr) Indo-HCM [1]	Percentage difference (%)
1	EBM-LR	7.1	2824	4473	37
2	NBM-LT	8.3	2707	5323	49
3	SBM-R	3.5	1242	2205	44
4	SBM-TR	9.0	3599	5400	33
5	SBM-T	5.5	1196	2503	52

Table 3 Range of PCU value as per Indo-HCM [1]

PCU of vehicle type	Minimum value	Maximum value
TW	0.2	0.75
Auto	0.3	1.0
Passenger cars	1.0	1.0
LCV	1.0	2.0
Bus	1.5	4.0
Truck	1.5	4.0

Table 4 Regression model—dynamic PCU values

PCU value	Variables	Coefficients
Two wheeler	Constant	2.07
	Volume	-0.00002
	TW	-0.02
	AUTO	-0.02
	HV	-0.01
	Road width	0.03
Auto	Constant	1.77
	Volume	-0.00001
	TW	-0.02
	AUTO	-0.02
	HV	-0.02
	Road width	0.04
Heavy vehicles	Constant	2.20
	Volume	0.00007
	TW	-0.01
	Car	-0.01

Source Asaithambi et al. [12]

estimated saturation flow were obtained for movement groups EBM-LR, SBM-R, SBM-TR and SBM-T when dynamic PCU values were used.

Table 5 Dynamic PCU obtained at intersection-B based on method 1

Movement group	Approach width (m)	Traffic volume (veh/hr)	PCU-TW	PCU-Auto	PCU—LCV, HCV, bus
EBM-LR	7.1	3849	0.88	0.63	1.28
NBM-LT	8.3	3402	0.91	0.68	1.28
SBM-R	3.5	1837	0.79	0.49	1.33
SBM-TR	9	5220	0.94	0.71	1.32
SBM-T	5.5	1792	0.84	0.57	1.32

Table 6 Measured saturation flow at intersection-B based on method 1

Sl. No.	Movement group	Effective approach width (m)	Measured saturation flow (PCU/hr, method 1)	Saturation flow (Indo-HCM [1])	Percentage difference (%)
1	EBM-LR	7.1	3849	4473	14
2	NBM-LT	8.3	3402	5323	36
3	SBM-R	3.5	1837	2205	17
4	SBM-TR	9	5220	5400	3
5	SBM-T	5.5	1792	2503	28

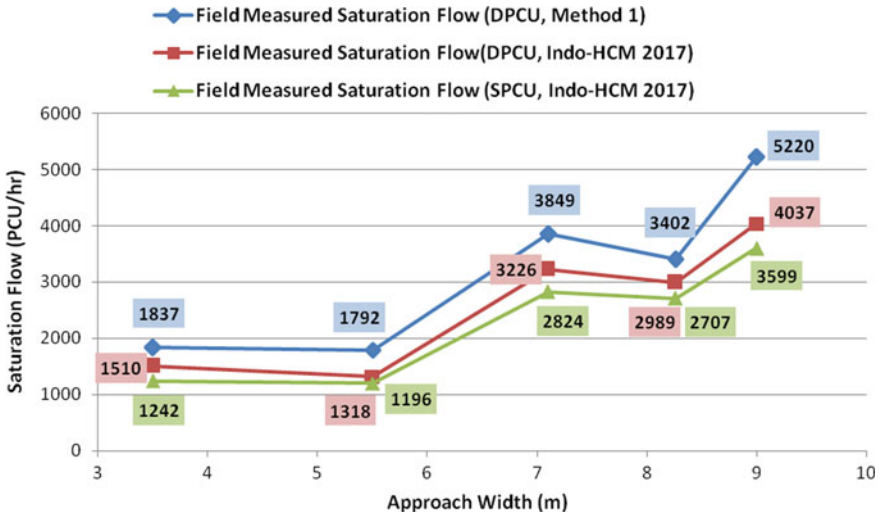


Fig. 2 Plot of saturation flow with respect to approach width for intersection-B (method 1)

3.3 Estimation of Dynamic PCU Values—Method 2

In Method 2, the dynamic PCU estimation method suggested by Chandra et al. [18] was modified to suit signalised intersections. The method proposed by Chandra et al. [18] was actually suggested for midblock sections.

The speed component in Chandra's method was replaced with the clearance time taken by the vehicles to clear the intersection area in Method 2. The PCU estimation as per Method 2 is given below:

$$PCU_i = \frac{t_i/t_c}{A_c/A_i} \quad (4)$$

where

A_c and A_i projected area of passenger car and vehicle type i , respectively, and t_{cv} and t_i travel time of passenger car and vehicle type i , respectively.

Project rectangular area of each vehicle type required for the estimation of dynamic PCU by this method was considered as provided in Indo-HCM.

3.4 Saturation Flow Estimation Using Dynamic PCU by Method 2

The dynamic PCU values estimated for intersection-B using the method 2 is shown in Table 7. Most of the dynamic PCU values estimated were falling within the range provided in Indo-HCM. The field measured saturation flow computed for each movement group using these dynamic PCU values are given in Table 8. There is not much difference in the percentage difference between field measured saturation flow and saturation flow (Indo-HCM [1]) when compared with Table 2 where static PCU was used (Fig. 3). There is not much difference when dynamic PCU developed using method 2 is used for saturation flow calculation.

Table 7 Dynamic PCU obtained at intersection-B based on method 2

Vehicle type	TW	Car	Auto	Bus	LCV	HCV	Bicycle
Projected area in m ² (Indo-HCM [1])	1.2	5.36	4.48	24.54	12.81	17.63	1.2
Average clearance time (s)	3.37	4.13	3.85	6.81	4.78	5.33	3.37
Dynamic PCU (method 2)	0.18	1.00	0.78	7.54	2.76	4.25	0.18

Table 8 Measured saturation flow at intersection-B-based DPCU by method 2

Sl. No.	Movement group	Effective approach width (m)	Measured saturation flow (PCU/hr, Method 2)	Saturation flow (Indo-HCM [1])	Percentage difference (%)
1	EBM-LR	7.1	3032	4473	32
2	NBM-LT	8.3	2735	5323	49
3	SBM-R	3.5	1968	2205	11
4	SBM-TR	9	3737	5400	31
5	SBM-T	5.5	1097	2503	56

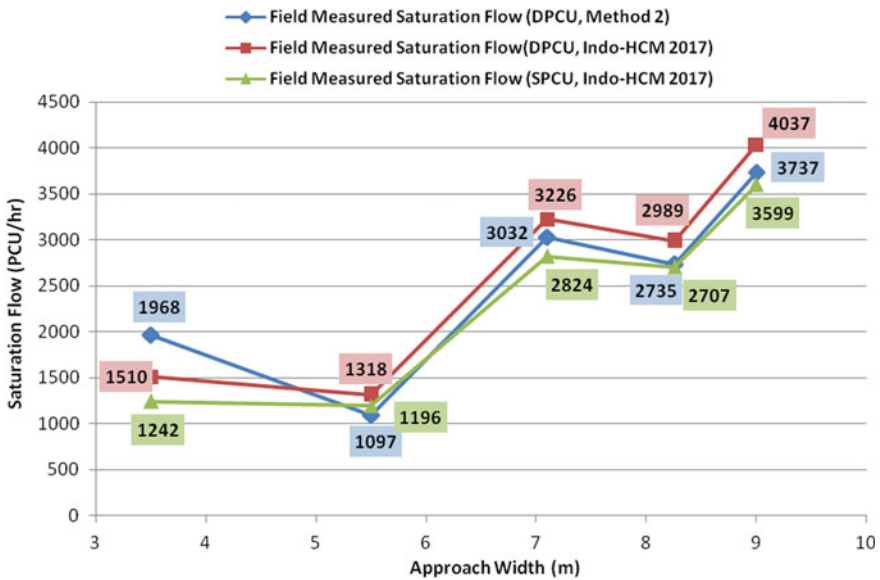


Fig. 3 Plot of saturation flow with respect to approach width for intersection-B (method 2)

4 Comparison Between Method 1 and Method 2

Both the methods were used for assessment of field measured saturation flow at the study intersections and compared and further compared with field saturation flow estimation based on static and dynamic PCU values given in Indo-HCM. The graphs showing comparison between the two methods for dynamic PCU estimation, static PCU (Indo-HCM) and dynamic PCU range as given Indo-HCM are shown in Figs. 4, 5 and 6 for intersections A, B and C, respectively.

When static PCU for signalised intersections provided in Indo-HCM was used for estimation of field measured saturation flow, very high deviation was observed from the values obtained using the model provided in Indo-HCM for estimation of

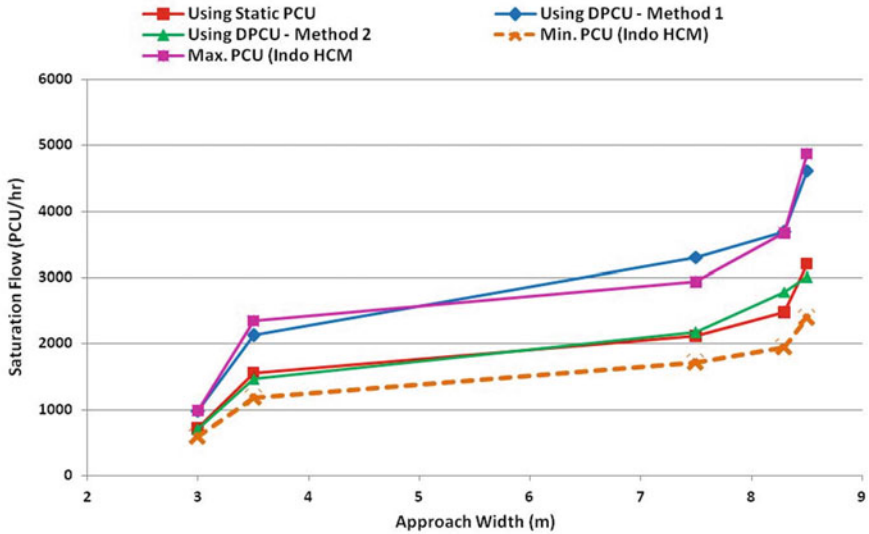


Fig. 4 Comparison between method 1 and method 2 (intersection-A)

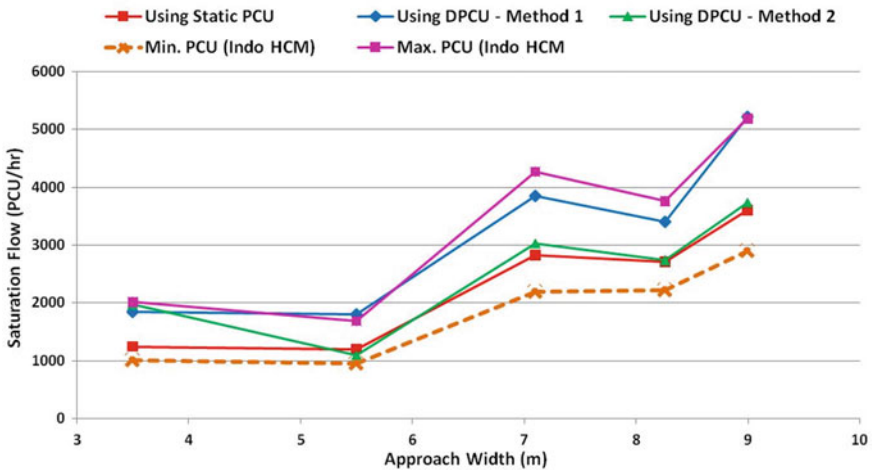


Fig. 5 Comparison between method 1 and method 2 (intersection-B)

saturation flow. Using dynamic PCU values in the literatures provided better results adhering to the model provided in Indo-HCM saturation flow estimation. Comparison between the estimated dynamic PCU values using Method 1, method 2 and the PCU value range provided in Indo-HCM is shown in Fig. 7.

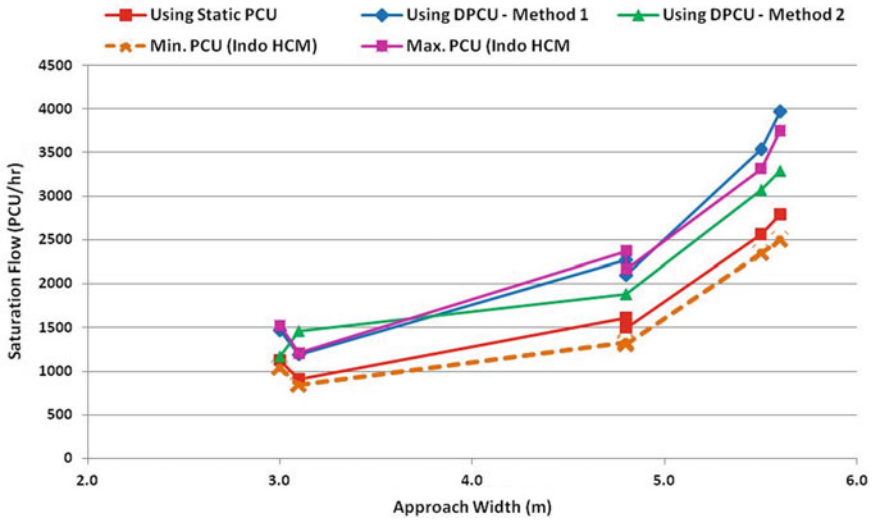


Fig. 6 Comparison between method 1 and method 2 (intersection-C)

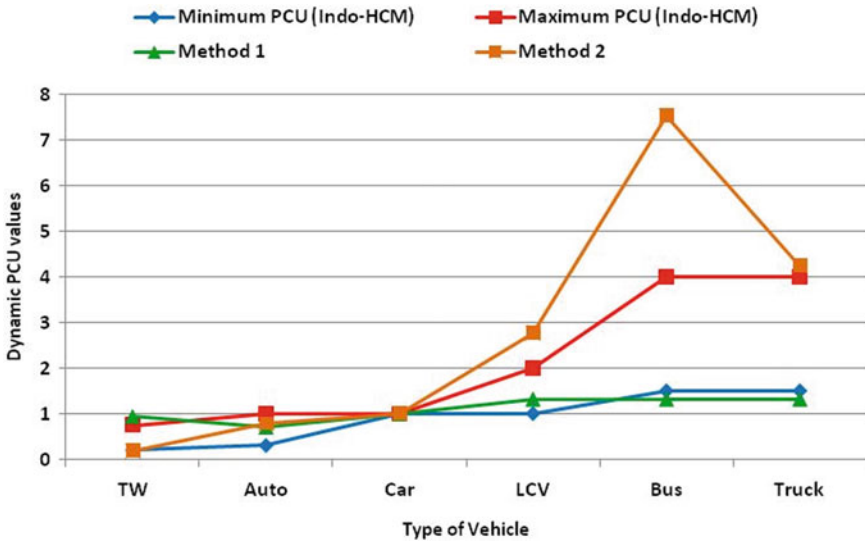


Fig. 7 Comparison between PCU values

The field measured saturation flow using Method 1 was almost similar to the saturation flow values obtained using the upper limit of the dynamic PCU range provided in Indo-HCM for signalised intersections. In the case of method 2, the dynamic PCU values were closer to static PCU values given in Indo-HCM. The field measured saturation flow using static PCU and method 2 was almost similar. Thus,

it was concluded that Method 1 is better suited for analysis of the heterogeneous traffic flow at signalised intersections in the state of Kerala in India. This is expected to hold good in other parts of the country also where heterogeneous traffic of same pattern and similar intersection characteristics as prevalent in Kerala exist.

5 Summary and Conclusions

The road traffic in India is heterogeneous in nature with extensively varying static and dynamic vehicle characteristics. At intersections, different vehicle types occupy road spaces without much segregation and have varying sizes, speed and acceleration capabilities. For addressing the difficulty of measuring volume of such mixed traffic, PCU was introduced for converting different vehicles categories into equivalent passenger cars. For the better operation and management of roadway facilities, accurate estimation of PCU values is essential. This work brings out a comparative study, thereby identifying the better suited method for estimating the dynamic PCU values for the traffic at signalised intersections in Indian conditions.

When the static PCU provided in Indo-HCM was used for determination of field saturation flow at signalised intersections, the field estimated values showed huge deviance from the saturation flow calculated using Indo-HCM model. The dynamic PCUs are given in Indo-HCM as a range of values; hence, an exact single value of dynamic PCU has to be determined for each vehicle category based on a better method of estimation and further conforming to Indo-HCM guidelines. Various methods available for dynamic PCU estimation were reviewed, and two methods were selected for detailed studies based on the practical easiness in data collection required for the PCU estimation. The dynamic PCU estimation methods suggested in Method 1 and Method 2 were compared based on better estimations of field saturation flows at signalised intersections. It was observed that the method suggested by Asaithambi et al. [12] was better suited for the estimation of dynamic PCU for signalised intersections with heterogeneous traffic conditions.

References

1. Indian Highway Capacity Manual. CSIR—Central Road Research Institute, New Delhi (2017)
2. Marfani SM, Dave HK (2016) Analysis of saturation flow at signalised intersection in urban area: Surat. *Int J Sci Technol Eng* 2(12):505–509
3. Radhakrishnan P, Mathew TV (2011) Passenger car units and saturation flow models for highly heterogeneous traffic at urban signalised intersections. *Transportmetrica* 7(2):141–162
4. Chand S, Gupta NJ, Velmurugan S (2017) Development of saturation flow model at signalised intersection for heterogeneous traffic. *Transp Res Procedia* 25:1662–1671
5. Arkatkar SS, Arasan VT (2010) Effect of gradient and its length on performance of vehicles under heterogeneous traffic conditions. *J Transp Eng* 136(12):1120–1136
6. Hadiuzzaman M, Rahman MM, Karim MA (2008) Saturation flow model at signalised intersection for non-lane based traffic. *Can J Transp* 2(1):77–90

7. Savitha BG, Murthy RS, Jagadeesh HS, Sathish HS, Sundararajan T (2017) Study on geometric factors influencing saturation flow rate at signalised intersections under heterogeneous traffic conditions. *J Transp Technol* 7:83–94
8. Prathapan P, Rajamma A (2016) Quantification of vehicular interaction during saturation flow at signalised intersections. *Int J Traffic Transp Eng* 6(4):453–473
9. Arasan VT, Vedagiri P (2006) Estimation of saturation flow of heterogeneous traffic using computer simulation. In: proceedings of the 20th European conference on modelling and simulation, ECMS, Bonn, Germany
10. Alex S, Issac KP (2014) Traffic simulation model and its application for estimating saturation flow at signalised intersection. *Int J Traffic Transp Eng* 4(3):320–338
11. Majhi RC (2017) Field saturation flow measurement using dynamic passenger car unit under mixed traffic condition. *Int J Traffic Transp Eng* 7(4):475–486
12. Asaithambi G, Mourie HS, Sivanandan R (2017) Passenger car unit estimation at signalised intersection for non-lane based mixed traffic using microscopic simulation model. *Periodica Polytech Transp Eng* 45(1):12–20
13. Mahidadiya AN, Juremalani J (2016) Estimation of passenger car unit value at signalised intersection. *IJSRSET* 2(2):1317–1324
14. Raj P, Sivagnanasundaram K, Asaithambi G, Shankar AUR (2019) Review of methods for estimation of passenger car unit values of vehicles. *J Transp Eng Part A Syst* 145(6):2473–2907
15. Greenshields BD, Schapiro D, Ericksen EL (1947) Traffic performance at urban intersections. Technical Rep. No. 1. New Haven, CT: Yale Univ.
16. Zhao W (1998) Delay-based passenger car equivalents for heavy vehicles at signalised intersections. In: proceedings traffic and transportation studies. Reston, VA: ASCE pp 691–700
17. Adams CA, Zambang MAM, Boahen RO (2015) Effects of motorcycles on saturation flow rates of mixed traffic at signalised intersections in Ghana. *Int J Traffic Transp Eng* 4(3):94–101
18. Chandra S, Kumar V, Sikdar PK (1995) Dynamic PCU and estimation of capacity of urban roads. *Indian Highways* 23(4):17–28

Dynamic Passenger Car Equivalency Values for Multilane Roundabouts Under Mixed Traffic Conditions—A Case Study



Vaibhav Negi, Hari Krishna Gaddam, and K. Ramachandra Rao

Abstract Passenger car equivalency (PCE) values provide a basis for estimating capacity of roadway and its elements such as signalized and unsignalized intersections. The present study aims to provide a novel framework to estimate dynamic PCE values for various vehicle classes under mixed traffic conditions for roundabouts. The data was collected and analyzed for the roundabout located in Chanakyapuri, New Delhi, India. In this study, PCE values of a particular vehicle class were estimated using entry versus circulating flow curves and a rational mathematical equation. Systematically calibrated VISSIM simulation tool helped in developing capacity curves for different vehicle proportions. With the help of entry capacity values for each approaching road, PCE values were obtained by comparing the car only flow with vehicle under consideration. Results show that PCE values are sensitive to traffic volume and composition. It is also observed that the PCE value increases with increase in opposing flow and vehicle proportion. For motorized three wheelers, PCE value exceeds one at high-circulating flow conditions as well as for larger proportion of motorized three wheelers in road traffic. The PCE value of motorized two wheelers varies from 0.34 in free flow condition to 0.7 in congested condition. It is noticed that the estimated PCE values of two wheelers do not differ much when compared to the past results. In heavy vehicles scenario, PCE values are inflated at high-circulating flow. This is due to their slow acceleration and deceleration characteristics.

V. Negi

Department of Civil Engineering, Indian Institute of Technology Delhi, Hauz Khas, New Delhi 110016, India

H. K. Gaddam (✉)

School of Transport Planning and Design, National Rail and Transportation Institute, Lalbaug, Vadodara, Gujarat 390004, India

e-mail: harikrishna.g@nrti.edu.in

K. Ramachandra Rao

Department of Civil Engineering and Centre for Transportation Research and Injury Prevention (CTRIIP), Indian Institute of Technology Delhi, Hauz Khas, New Delhi 110016, India

e-mail: rrkalaga@civil.iitd.ac.in

Keywords Multilane roundabouts · Passenger car equivalency · Mixed traffic environment · VISSIM simulation tool · Optimization

1 Introduction

The multilane roundabouts consist of unidirectional circulating roadway connected with approach roads in which importance is provided to vehicles moving around the circle. The vehicles approaching the roundabout entry point have to judge whether the sufficient gap size is available between the circulating vehicles to enter into the roundabout circulating section or not. In road safety point of view, roundabouts are safer in comparison with other types of unsignalized intersections as reduced vehicular speed and angular collision between vehicles at merging and diverging locations play a significant role. Besides number of conflict points at roundabouts are reduced from thirty-two to eight (4 merging and 4 diverging). Attributes such as geometric conditions, driver behavior, traffic composition, and environmental conditions considerably influence the performance of roundabouts. Mainly, circulating flow and entry flow characteristics of roundabout play a critical part in evaluating the functional characteristics and entry capacity. As different types of vehicles use the roundabout, capacity analysis is a bit complicated. The non-lane based mixed traffic for instance cars, motor two-wheelers (MTW), motor three-wheelers (MThW), and heavy vehicles (HV) (for instance buses and trucks) further makes it more complex. Thus, suitable conversion mechanism for passenger car equivalency (PCE) values is required to convert all the vehicles into a standard vehicle. This study proposes a novel methodology to estimate dynamic PCE values in mixed traffic flow environment where lane discipline is absent.

Lee et al. [1] suggested a framework for evaluating PCE values for different kinds of vehicles at modern small sized three-legged roundabouts. In this study, experimental and analytical methods for estimating PCE values on three-legged roundabouts were evaluated. Results in this study show that the PCE values were highly correlated with the field measurements. Lee and Eng [2] study presents a method for estimating PCE values for heavy vehicle, and it considers the variation in entry capacity of the mixed car and heavy vehicles. In addition, the estimated PCE value was utilized to estimate maximum entry flow using equivalent capacity equation. It has been noted that PCE value of light truck is smaller than the default value given in the HCM 2010 [3] and recommended that light trucks must be separated from heavy trucks in the traffic flow analysis. Another outcome from the study is that the estimated PCEs for roundabouts with various geometric configurations and various truck percentage with the help of micro-stimulation value obtained for 100% HV are twice that of suggested by HCM 2010 for roundabout.

A study by Pajecki et al. [4] researched on proposing a method to calculate PCE of HV at roundabouts with varying entry flow rates. The data collected from a roundabout with a single lane was used under heterogeneous traffic scenarios in VISSIM micro-simulation environment tool. The calculated PCE values for HV, single unit

truck, small semi-trailers, bus, and large semi-trailers in heterogeneous traffic flow conditions are 1.30, 1.40, 1.60, and 1.70, respectively. A general equation was also proposed to estimate HV reduction factors. Giuffrè et al. [5] presented the effect of HVs on functional characteristics of a turbo type of roundabout. Entry capacity of each lane of the turbo roundabout is obtained with the help of simulation with varying percentage of heavy vehicles where nonlinear regression analysis between entry flow and circulating flow at different percentage of heavy vehicles was carried out. Finally, the PCE values were obtained for heavy vehicles which varied with heavy vehicles percentage and circulating flow with the turbo roundabout. It is being noted that PCE value increases as the percentage of heavy vehicles increases. Giuffrè et al. [6] in another study estimate the PCEs for HVs on single-lane roundabouts. A calibration procedure based on genetic algorithm is applied to determine the parameters in AIMSUN simulator. In continuation using the calibrated model, the PCEs were estimated by drawing a comparison between cars with the different percentages of HVs. Similarly, few other studies [7, 8] used traffic simulation tools to estimate PCE values at two lane roundabouts and turbo type roundabouts. Macioszek [9] presents the passenger car equivalent factors for HVs including trucks, buses, trucks with trailers, articulated buses on turbo type roundabouts in Poland. Grana et al. [10] study reviewed the literature on methods of estimation to determine PCE values for heavy vehicles. The aim of this study is to present various methods available to calculate PCEs for heavy vehicles on roundabouts.

In developing countries, where non-lane-based mixed traffic conditions are prevalent, only few researchers attempted to estimate PCE values using different techniques. Sonu et al. [11] estimated the PCUs of different types of vehicles at a classic four-legged roundabout using time occupancy concept. A stream equivalency factors (k) were also determined using estimated PCU values which were used in converting the heterogeneous traffic mix into a homogenous stream equivalent. Sugiarto et al. [12] calculated PCU values for roundabouts using time occupancy data collected from drones in mixed traffic conditions. The data of this study was collected at one of the roundabouts in Aceh Besar, Aceh province, Indonesia. The results from this study show that the PCU values obtained are 0.16, 0.59, 1.07, 1.91, 3.76 for motorcycle, rickshaw, pickup, medium vehicle, and 'heavy vehicle, respectively. Ahmad and Rastogi [13] estimated the PCU values using lagging headway and width of the vehicle. Indo-HCM [14] proposed an equation to approximate PCU values for various vehicles types, based on five important inputs, namely traffic flow, headway, conflict angle of vehicles negotiating the roundabout, vehicular speed, and composition. The PCU values are available for different diameters of roundabouts ranging from 20 to 70 m.

The most important concern is identifying the appropriate framework to calculate the PCE values of the roundabouts. Several methods with different input parameters have been developed globally to identify suitable PCE values, however, they have not considered the interactions between the vehicles completely. In addition, the procedures used for estimating PCE values are only suitable for lane-based homogeneous traffic flow conditions. Conversely, the vehicular traffic in emerging nations such as India have many vehicle classes with variable physical and dynamic characteristics

including weak lane discipline. The PCE estimation methods available for developing countries perspective accounted only a few important parameters and have not considered the vehicle interaction in the absence of lane discipline explicitly. Moreover, they do not account for the effect of flow variation (entry as well as circulating flow) and the proportion of heterogeneous mix on the PCE value. The present study aims to overcome these limitations through a new methodology. Thus, the objective of this study is to propose a new simulation framework to estimate dynamic PCE values (PCE values at different flow conditions) for various vehicle classes for the given roundabout.

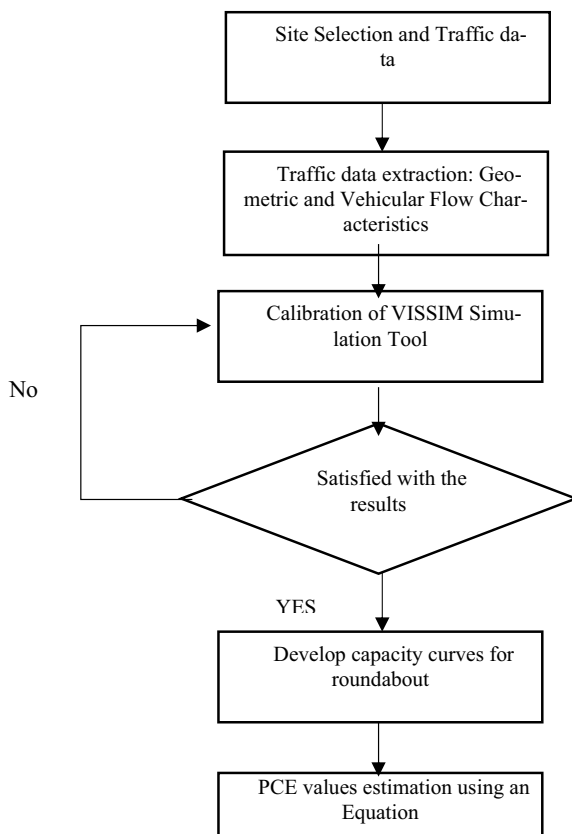
2 Methodology

The research method in this study involves calibration of a micro-simulation software system such as VISSIM for obtaining suitable entry capacity curves for the given roundabout to estimate PCE values for various types of vehicles using the roundabout. The data required for the analysis was collected by means of video cameras and field surveying techniques. From the video graphic data, several variables (such as entry flow and speeds of the vehicles before and at the entry of roundabout and so on.) have been extracted to calibrate the parameters. Based on the capacity curves obtained from the simulation runs, PCE values are estimated using Eq. 1. The methodology chosen for developing capacity curves and estimating PCE values is shown in Fig. 1.

2.1 Selection of Study Section and Data Pooling

With the purpose of estimating PCE values, roundabout located in Chanakyapuri area, New Delhi is selected as showed in Table 1, and the roundabout is carefully chosen from main road sections represent considerable traffic in Chanakyapuri.

The intersection has significant amount of traffic volume varying moderate to high. The google map image of roundabout 38 is shown in Fig. 2. Video cameras located on each leg of the roundabout were used to record the movement of vehicles. The position of one of the video cameras used in data collection is indicated in Fig. 3. The traffic data was recorded for 1 h 30 min at each leg of roundabout between 11:30 a.m. and 1:00 p.m. Various geometric characteristics of selected roundabout were noted (Given in Table 2), and in addition, other roundabout-related information for instance lane usage, composition of vehicles, types of vehicles using the facility, weather information, safety information, and geometric features and number of lanes were obtained using special add-on in a video player, i.e., 'time v-2.1' in VLC media player (Fig. 4). Observation from this roundabout revealed that vehicle classes such as cars, MTW, MThW, and HV were using the roundabout during peak and non-peak hours uninterruptedly. The percentage composition is 65, 18, 13 and 5 for cars, MTW, MThW, and HV, respectively. The maximum flow at entry point is

Fig. 1 Methodology for estimating PCE values**Table 1** Details of the study area

Intersection details	Roundabout number	Intersection name	Number of approaches	Location
Roundabout	38	Shantipath—Satya marg	4	Shantipath

observed on roundabout was 1740 veh/h. The information about traffic flow data at two different legs of the roundabout is provided in Tables 3 and 4. The traffic information obtained from the roundabout is used for the optimization of the VISSIM simulation parameters.

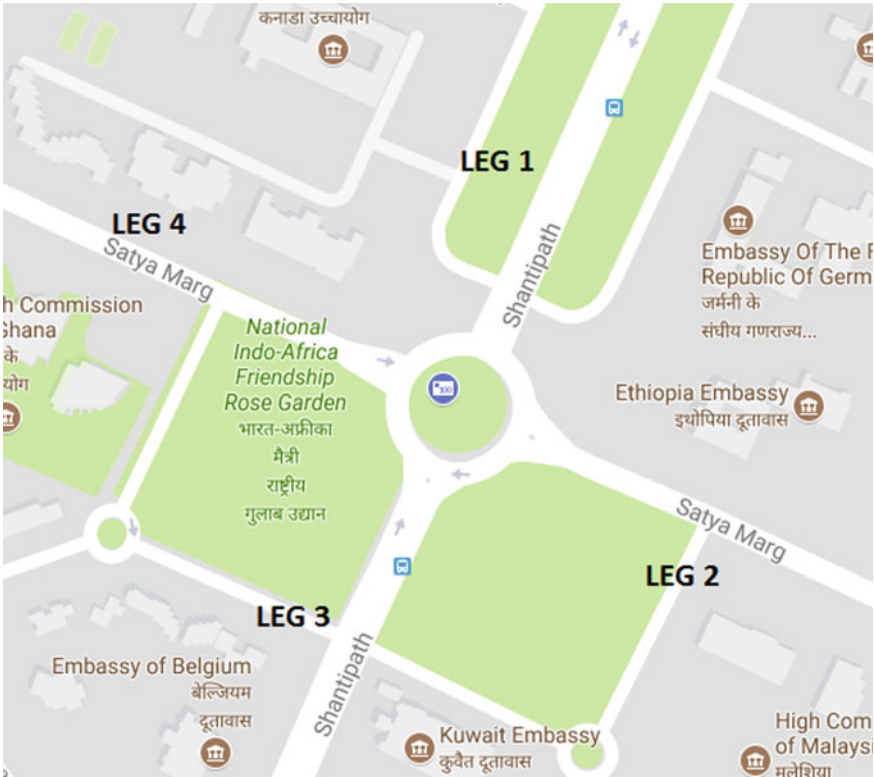


Fig. 2 Roundabouts (Shantipath—Satya marg roundabout-R38) location details. *Source* Google maps



Fig. 3 Image showing traffic survey at one of the roundabout legs

Table 2 Geometric features of roundabout 38

Parameter	Description	R 38
e	Entry width	10.93
v	Lane width	6.34
e'	Previous entry width	8.78
v'	Previous lane width	5.38
u	Circle width	8.99
l, l' ($l' = 1.6 * l$)	Flare mean length	17.85
r	Entry bend radius	63.56
φ	Entry angle	42
D	Inscribed circle diameter	78.5
W	Exchange section width	7.78
L	Exchange section length	56.96

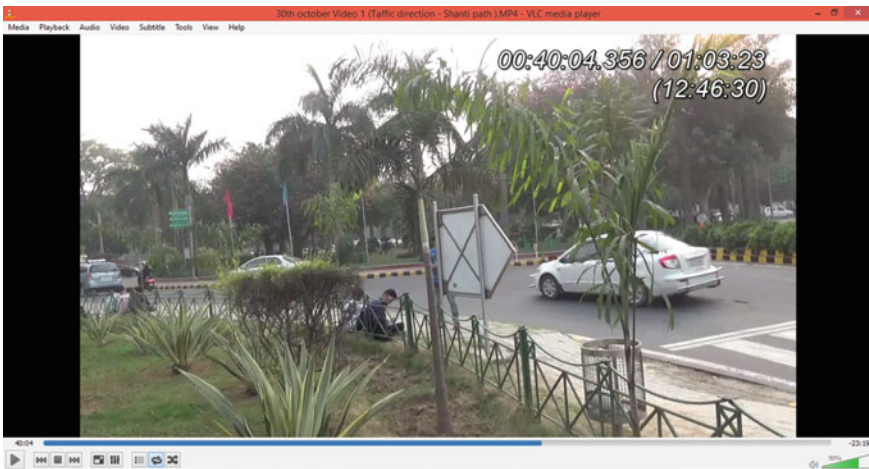


Fig. 4 Screenshot from the data extraction tool

3 PCE Estimation Using Simulation Framework

3.1 PCE Estimation Procedure

In this study, dynamic PCE values for various vehicle classes were calculated using the simulation method. We extended the simulation method suggested by Giuffrè et al. [6] for multilane non-lane-based heterogeneous traffic stream. The following are the steps suggested to calculate PCE values of a vehicles on a roundabout.

- a. Calibration and validation of VISSIM simulation tool using the data collected from the field.

Table 3 Traffic flow data at leg 1 of roundabout 38

Observed 5 min count of entry flow (veh/5 min) at leg 1	Observed rate flow of entry flow (veh/h) at leg 1	Vehicle composition (in percentage)			
		Car	MTW	MThW	Heavy vehicle
145	1740	65	17	13	5
111	1332				
128	1536				
137	1644				
101	1212				
106	1272				
84	1008				
125	1500				
98	1176				
85	1020				

Table 4 Traffic flow data at leg 2 of roundabout 38

Observed 5-min count of entry flow (veh/5 min) at leg 2	Observed rate flow of entry flow (veh/h) at leg 2	Vehicle composition (in percentage)			
		Car	MTW	MThW	Heavy vehicle
106	1272	69	15	13	3
127	1524				
106	1272				
127	1524				
134	1608				
94	1128				
93	1116				
99	1188				
90	1080				
130	1560				

- b. Generate entry versus circulating flow curve for passenger car only condition using simulations. Since passenger car is the base vehicle, this curve is also known as base curve.
- c. Generate entry versus circulating flow curves for different percentage of motorized two wheelers (i.e., 20, 40, 60, and 80%). Estimate the passenger car equivalent for given percentage of motorized two wheelers at a particular circulating flow using the Eq. 1.
- d. Repeat the procedure for each category of vehicle plying in heterogeneous traffic stream.

$$\text{PCE} = \frac{1}{P} \times \left(\frac{C_{\text{car}}}{C_p} - 1 \right) + 1 \quad (1)$$

where P = the percentage of vehicles, C_{car} = entering traffic flows only comprising passenger cars, C_p = capacity confirming to vehicular demand characterized by a proportion p of other vehicles. Based on the method described in the previous chapter, entry versus circulating flow curve has generated at various percentage for the following category of vehicle.

4 VISSIM Roundabout Model and Calibration Procedure

Microscopic simulation tools allow the researchers to produce various alternative situations with increasing complexity in the functioning of traffic networks and atypical road establishments. In the present study, VISSIM microscopic simulation tool (PTV Germany) was helpful in deriving capacity curves for the roundabout. In comparison with similar tools, VISSIM is effective in producing capacity curves using geometric, vehicle, and driver characteristics of roundabout, and it is able to mimic non-lane-based heterogeneous traffic behavior close to the real-world behavior. The heterogeneous traffic mix is presented by exporting various vehicle three-dimensional models into the VISSIM. Both geometry and driver gap acceptance behavior at the roundabout were incorporated in the VISSIM roundabout model. Thus, it is comparatively accurate in estimating capacity compared to rest other methods available. In addition, capacity curves were derived after optimizing the VISSIM simulation parameters meant for the roundabout. To achieve this, the simulation parameters are calibrated using genetic algorithm (GA) [4–7, 15–17]. Component object model (COM) interface developed in MATLAB® based is used to control VISSIM parameters [15]. The method proposed by Tettamanti et al. [18] was implemented for setting up COM interface. The model considered the single objective optimization function. Mean absolute percentage error (MAPE) calculated for observed data and estimated data using VISSIM simulations for vehicle speeds is used as optimization function. The parameter values are selected by minimizing this optimization function.

In VISSIM, Weidmann 74 psycho-physical car following rule is used for simulating driver and vehicle characteristics including longitudinal vehicle movements and sideway vehicle movements in vehicular flow where it uses three parameters such as average stand still distance (ax), additive part (bx_add), and multiplicative part of safety distances (bx_mult) to represent the driver behavior in urban setting. According to the Weidmann 74 rule, vehicle acceleration changes with respect to minimum distance between leader and follower. Speed is a governing factor in developing VISSIM simulation model for mixed traffic and also aids in optimizing the parameters of the simulation tool. Spot speed values with respect to various vehicles categories are gathered using radar speed guns at the entrance and weaving sections of the of the roundabout. Using the spot speed data, speed distribution curves are

Table 5 Physical dimensions and speeds of vehicles using the roundabout

Vehicle type	Length (m)	Width (m)	Percentile speeds (km/h)				Acceleration (m/s ²)		Deceleration (m/s ²)	
			15th	50th	85th	98th	Max	Desired	Max	Desired
Car	4.2	2	33	42	51	60	1.7	1.2	1.2	1
MTW	2	0.84	27	35	43	52	2.5	1.7	1.7	1.2
MThW	2.36	1.17	22	31	38	43	1.2	0.9	1.1	0.8
HV	11.54	2.69	19	30	36	42	1.2	1.0	1.0	0.9

Table 6 Calibration result

S. No.	VISSIM parameter set (ax, bx_add, bx_mult)	MAPE (%)
1	2.2928, 4.2479, 3.8297	10.14

obtained for all types of vehicles using the roundabout which will be act as a input for VISSIM. Physical measurements and speeds of the vehicles created for VISSIM are given in Table 5. Initial inputs considered for simulating VISSIM with MATLAB interface are GA population size = 50; no. of generations in GA = 10; target of optimization = minimizing speed; and to represent the driver behavior following parameters were considered: average standstill distance (ax), additive part of safety distance (bx_add), and multiplicative part of safety distance, (bx_mult); The result obtained with optimization procedure is given in Table 6.

5 Results and Discussion

The mechanism through which the vehicle under consideration is converted into the passenger car is using the capacity curves obtained from the calibrated simulation model and the proposed equation (Eq. 1). Capacity curves obtained from the VISSIM simulation run for different vehicle classes such as MTWs, MThWs, and HVs with varying proportions are presented from Figs. 5, 6 and 7. The PCE value for a vehicle under consideration was calculated as a function of different percentages of other vehicles that characterized the traffic demand. PCE values of various vehicle classes obtained for different flow conditions and changing percentages are given in Table 7. The results show that the PCEs vary with the vehicles percentage in consideration and the circulating flows on the roundabout.

The PCE value of motorized two-wheeler ranges from 0.34 (in free flow condition) to 0.7 (in congested condition). However, these values are higher than the values predicted by other researchers in similar conditions [11, 13, 14]. A comparison has been made in Table 7 among PCE values reported by different researchers in India. Similarly, analysis is also carried out for other combinations such as car vs motorized three wheelers and car vs heavy vehicles. From the analysis, it is observed that the

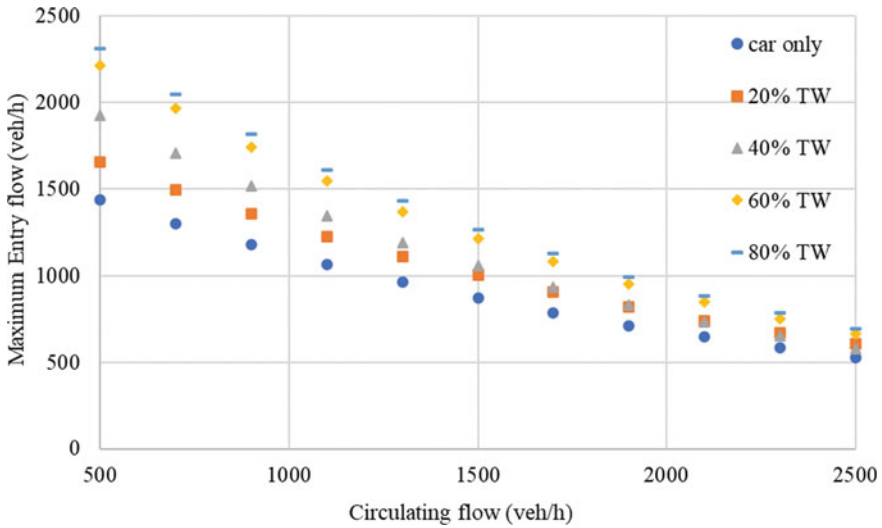


Fig. 5 Entry flow versus circulating flow for MTWs at different proportion

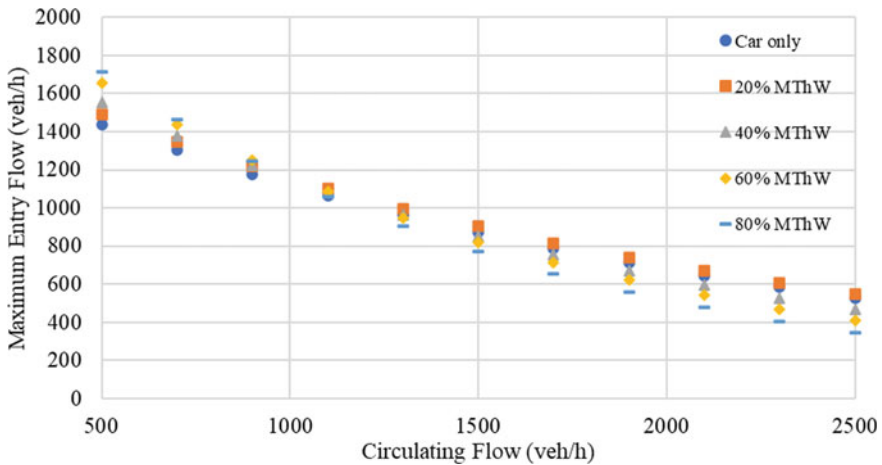


Fig. 6 Entry flow versus circulating flow for MThWs at different proportion

behavior of motorized three wheelers is similar to that of the car and the PCE value of motorized three-wheeler varies from 0.83 (in free flow condition) to 1.66 (in congested conditions). One reason that can be attributed is due their low acceleration and deceleration capability, they take longer time to enter in to the circulating stream.

It is also further noticed that the PCE values of heavy vehicles are very high at high circulating flows. This may be due to the difficulty in acceleration and deceleration of heavy vehicle (i.e., heavy vehicle accelerate/decelerate slowly). Sometimes, fully

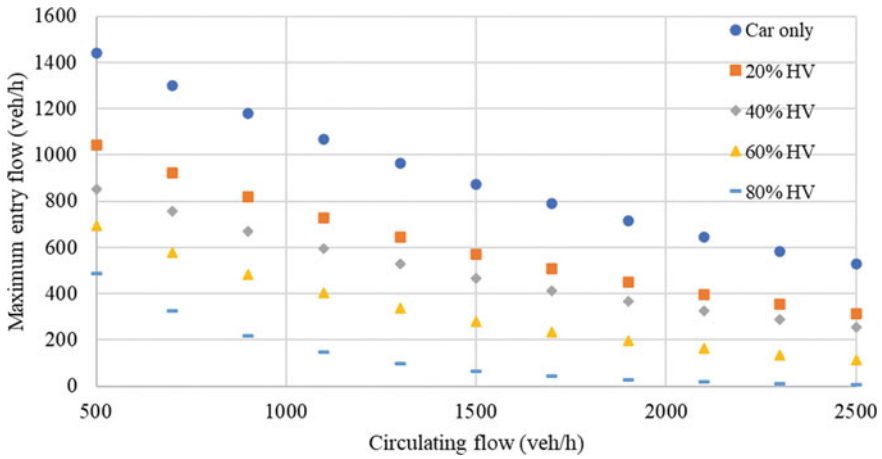


Fig. 7 Entry flow versus circulating flow for HVs at different proportion

Table 7 PCE value of various vehicle classes

Circulating flow (veh/h)	Percent of <i>i</i> th vehicle class	PCE of MTW	PCE of MThW	PCE of HV
Qc < 1100	20	0.34	0.83	2.91–3.33
	40	0.36–0.48	0.81–0.96	2.72–2.98
	60	0.41–0.48	0.78–0.96	2.78–3.72
	80	0.52–0.57	0.80–1.00	3.45–8.85
1100 < Qc < 1900	20	0.34	0.83	3.33–3.94
	40	0.48–0.64	0.96–1.16	2.98–3.35
	60	0.48–0.57	0.97–1.25	3.72–5.37
	80	0.57–0.64	1.00–1.35	–
1900 < Qc < 2500	20	0.34	0.83	3.94–4.44
	40	0.69–0.78	1.16–1.33	3.35–3.65
	60	0.6–0.65	1.25–1.49	5.37–7.01
	80	0.66–0.7	1.35–1.66	–

loaded heavy vehicles are responsible for the reduction of traffic flow and hence the capacity of the traffic streams.

A comparison among the different PCE estimation methods in Indian context is also presented in Table 8. The observation between different studies shows that values predicted by simulation framework are close to the Indo-HCM [14] values for free flow condition. However, PCE values at capacity and congested traffic flow conditions are higher than the values obtained by other researchers. The variations could also be attributed to the varied geometries of the roundabouts besides the traffic conditions.

Table 8 PCE values comparison in mixed traffic environment context

Vehicle type	Research study			
	Present study	Sonu et al. [11]	Ahmad and Rastogi [13]	Indo-HCM [14]
Car	1	1	1	1
MThW	0.34–0.7	0.21–0.23	0.34	0.32
MThW	0.83–1.345	0.63–0.7	1	0.83
HV	2.9–8.85	4.37–4.5	2.91	3.05–3.65

6 Conclusions and Future Scope

In this study, PCE value for different vehicle types is estimated with the help of systematically calibrated microscopic simulation tool such as VISSIM. The effect of variables like percentage of vehicle and circulating flow on PCE is investigated. The following conclusions can be drawn from this study:

- Results from the analysis show that PCE value increases with increase in opposing flow and percentage of vehicle under consideration. It is also observed that the PCE value is sensitive to traffic volume and composition.
- For motorized three wheelers, PCE value is greater than one for high-circulating flow as well as for greater percentage of motorized three wheelers, respectively. This may be due to slow acceleration and deceleration characteristics of motorized three wheelers at high-flow conditions.
- The PCE value of motorized two wheelers varies from 0.34 in free flow condition to 0.7 in congested condition.
- In case of heavy vehicles, PCE values are very high at high-circulating flow. This is due to the difficulty in acceleration and deceleration of heavy vehicle (i.e., heavy vehicle accelerates and decelerates very slowly).
- Comparison with other studies in Indian context shows that PCE values for two wheelers do not differ much with the past studies. However, MThWs and HVs differ at high-flow conditions.
- This research is carried out with limited data collected in Delhi. To validate the outcomes, the study can be further extended to roundabouts exist in Delhi and other cities in India. In future, the proposed methodology needs to be applied for roundabouts with varying geometry and traffic flow conditions.

References

1. Lee YJ, Lee IG, Lee DM (2010) Determination of passenger car equivalents when estimating capacity at small 3-leg roundabouts. *J Korean Soc Transp* 28(6):65–74
2. Lee C, Ph D, Eng P (2015) Developing passenger-car equivalents for heavy vehicles in entry flow at roundabouts. *J Transp Eng* 141(8):1–7. [https://doi.org/10.1061/\(ASCE\)TE.1943-5436.0000775](https://doi.org/10.1061/(ASCE)TE.1943-5436.0000775)
3. Highway Capacity Manual (2010) Transportation research board, USA
4. Pajeccki R, Ahmed F, Qu X, Zheng X, Yang Y, Easa SM (2019) Estimating passenger car equivalent of heavy vehicles at roundabout entry using micro-traffic simulation. *Front Built Environ* 5:77
5. Giuffrè O, Granà A, Marino S, Galatioto F (2016) Microsimulation-based passenger car equivalents for heavy vehicles driving turbo-roundabouts. *Transport* 31(2):295–303
6. Giuffrè O, Grana A, Tumminello ML, Sferlazza A (2017) Estimation of passenger car equivalents for single-lane roundabouts using a microsimulation-based procedure. *Expert Syst Appl* 79:333–347. <https://doi.org/10.1016/j.eswa.2017.03.003>
7. Giuffrè O, Granà A, Tumminello ML, Sferlazza A (2018) Capacity-based calculation of passenger car equivalents using traffic simulation at double-lane roundabouts. *Simul Model Pract Theory* 81:11–30
8. Macioszek E (2019) The passenger car equivalent factors for heavy vehicles on turbo roundabouts. *Front Built Environ* 5:68
9. Grana AG, Giuffrè O, Giuffrè T, Tumminello ML, Acuto F (2019) Passenger Car Equivalents for heavy vehicles at roundabouts. A synthesis review. *Front Built Environ* 5:80
10. Granà A, Giuffrè T, Macioszek E, Acuto F (2020) Estimation of passenger car equivalents for two-lane and turbo roundabouts using AIMSUN. *Front Built Environ* 6:86
11. Sonu M, Dhamaniya A, Arkatkar S, Joshi G (2016) Time occupancy as measure of PCU at four legged roundabouts. *Transp Lett*:1–12. <https://doi.org/10.1080/19427867.2016.1154685>.
12. Sugiarto S, Apriandy F, Faisal R, Saleh SM (2018) Measuring passenger car unit at four-legged roundabout using time occupancy data collected from drone. *Aceh Int J Sci Technol* 7(2):77–84
13. Ahmad A, Rastogi R (2019) Calibrating HCM model for roundabout entry capacity under heterogeneous traffic. *J Mod Transp* 27:293–305. <https://doi.org/10.1007/s40534-019-00194-7>
14. Indo-HCM (2017) Roundabouts. In: Development of Indian highway capacity manual
15. Arroju R, Gaddam HK, Vanumu LD, Ramachandra RK (2015) Comparative evaluation of roundabout capacities under heterogeneous traffic conditions'. *J Mod Transp* 35(6):310–324. <https://doi.org/10.1007/s40534-015-0089-8>
16. Li Z, DeAmico M, Chitturi MV, Bill AR, Noyce DA (2013) Calibrating VISSIM roundabout model using a critical gap and follow-up headway approach. In: 16th international conference road safety on four continents. Beijing, China (RS4C 2013). 15–17. Statens väg-och transportforskningsinstitut
17. Giuffrè O, Granà A, Tumminello ML, Sferlazza A (2018) Calibrating a microscopic traffic simulation model for roundabouts using genetic algorithms. *J Intell Fuzzy Syst* 35(2):1791–1806
18. Tettamanti T, Csikós A, Varga I, Eleőd A (2015) Iterative calibration of VISSIM simulator based on genetic algorithm. *Acta Technica Jaurinensis* 8(2):145–215

Impact of Implementing Two-Wheeler Boxes at Signalized T-Intersections Under Mixed Traffic Conditions



V. H. Ardra , B. Anish Kini , and S. Moses Santhakumar 

Abstract Cities in Kerala, like many other Indian cities, account for a high percentage of two-wheelers (about 65% of new vehicle registrations in a year are two-wheelers) but adequate measures to ensure their safety are seldom undertaken. This results in higher involvement of two-wheelers in crashes (approximately 42.5% of crashes involved two-wheelers as per Kerala Police records, 2020). The two-wheelers are at high risks on the road especially so at the intersections. T-intersections account for about 9.76% of crashes as per MoRTH 2019. Through this study, a novel approach, developed abroad, was applied to T-intersections whose implementation can ensure better safety and priority to two-wheeler users. This study presents the impact of implementing two-wheeler boxes at T-intersections and evaluates its effectiveness using micro-simulation tool and Surrogate Safety Assessment Model. The study area chosen is Kowdiar, a signalized T-intersection, situated in Thiruvananthapuram, Kerala, India. Video analysis was used to extract the traffic parameters at the junction which was employed for the calibration and validation of the base model in VISSIM software. Modified model, with inclusion of two-wheeler box giving priority to two-wheelers, was developed and compared with the base model. The comparative analysis showed that the modified model was beneficial over the base model due to about 25.6% reduction in number of possible conflicts, higher values of surrogate safety measures, 22.1% reduction in average queue length and improved saturation flow. Therefore, this study makes a case for the implementation of two-wheeler boxes at signalized T-intersections with mixed traffic conditions.

Keywords Two-wheeler box · Signalized T-intersection · Mixed traffic condition · Surrogate safety assessment

V. H. Ardra (✉) · S. M. Santhakumar
Department of Civil Engineering, NIT Tiruchirappalli, Tiruchirappalli, India
e-mail: ardrachess@gmail.com

S. M. Santhakumar
e-mail: moses@nitt.edu

B. A. Kini
KSCSTE—National Transportation Planning and Research Centre, Thiruvananthapuram, India

1 Introduction

The burgeoning vehicular population in cities has resulted in issues such as traffic congestion, pollution, fuel wastage and crashes. Due to poor public transport facilities, rapid urbanization and faster availability of loans along with the advantage of door-to-door connectivity, the number of two-wheelers has been increasing manifold. The COVID-19 pandemic has made this transition all the more likely due to the perception that public transport usage would entail an increased risk of infection as reported by Hörcher et al. [9]. As per Economic Review 2020 [15], about 65% of newly registered vehicles were two-wheelers in Kerala. However, these two-wheeler users are forced to intermingle with other vehicle types including heavy vehicles inviting a higher risk of crashes and related severity. As per Kerala Police records [16], about 42.5% of crashes involved two-wheelers in 2020. Ministry of Road Transport and Highways (MoRTH) in its report on Road Accidents in India—2019 [19] presented that T-intersections account for about 9.76% of accidents in the country. All these point toward the significance of countermeasures for enhancing the safety of two-wheeler users at intersections and particularly T-intersections.

Bike boxes, also known as advanced stop boxes or advanced stop lines (ASLs), are a novel treatment sought to reduce the conflicts between bicycles and other vehicles by partially segregating them in critical zones of a road network, i.e., at intersections. A typical bike box design is shown in Fig. 1 which was prepared by National Association of City Transportation Officials (NACTO), USA. Though used primarily for bicycles abroad, the concept has been modified in this study for providing priority to two-wheelers at intersections and is henceforth referred to as ‘two-wheeler boxes.’ Bike boxes are designed with the intention to put two-wheelers at the front of the line during a red signal phase, increasing their visibility and in turn their safety.

Fig. 1 Typical bike box design [22]



2 Literature Review

Hunter [11] presented an experiment of providing a right-angled extension to the bike lane at the signal with signs at Eugene, Oregon in 1998. The bike box's goal was to make it easier for bicyclists to shift from a left-sided bike lane before a 2-way intersection to a bike lane, which is on the right side. The findings revealed that bike boxes are widely used, with 22% of the bicyclists for whom they were created using them. Due to the substantial amount of motor vehicle intrusion into the bike box, usage was minimal. It was also reported that the conflicts between motor vehicles and bicycles changed little in the before-after analysis. James et al. [12] carried out a research at two crossroads in Minneapolis, Minnesota. In the north westbound direction, the test crossing featured a bike box, whereas the controlled crossing did not. In order to compare stated behavior with observed behavior of bicyclists utilizing the bike box, data was analyzed using both observation measures from field and an online questionnaire survey. According to a bicycle poll, 87% of bicyclists would stop inside the bike box for through moves and 83% would stop on the left side of the bike box for left moves. Only 40% of bicyclists stopped exactly inside the bike box, according to field observations. According to the poll, 54% of bicyclists would use the bike box for turning left on a red light; however, this number dropped to 7% when field observation was conducted. In the test junction, both bicycle's and motorist's crosswalk intrusion dropped from 33 to 10% and from 4 to 1%, respectively. Chen et al. [4] presented that on street, bicycle lanes were installed, and as a result, there was no increase in crashes even when the number of bicyclists increased. This was due to reduced speed and conflicts with other vehicles due to which bike boxes were recommended at intersections.

Dill et al. [6] conducted a study in Portland which focused at the impact of bike boxes at ten of the signalized junctions (seven with green color, three without green color) and two of the controlled intersections. At five of the crossroads, a survey of bicycles and cars was undertaken to assess and analyze the safety perceptions and estimate user knowledge. According to the video data, both colored and uncolored signalized intersections saw a significant reduction in motor vehicle and bike incursion into the crosswalk. In addition, the quantity of motor vehicle yielding behaviors has grown. According to the survey, 77% of the bicyclists felt safe and comfortable riding through an intersection with the addition of the box. According to a poll of drivers, 89% of respondents felt that green is the superior hue. Furthermore, the green hue reduced the amount of motor vehicles that encroached on the bike lane before reaching the intersection. Loskorn et al. [16] undertook a study in 2009 to determine the impact of three scenarios—existing, after bike box marking and after green color pavement marking—on the behavior of bicyclists and motorists. The study reported that there were no collisions observed during the study period and that about 90% of the bicyclists stopped in front of the motorists making them visible. Green pavement coloring also improved the bicyclist behavior. Sohail et al. [24] reported a study in

Montreal where longitudinal video data analysis was carried out for pre-post implementation of bike box at intersections. It showed that the presence of bike box had a significant impact on reducing the violations committed by cyclists.

Johnson et al. [13] reported the attitudes toward cyclists by other road users gathered through a survey in Australia. Drivers who were cyclists were more aware of the rules toward cycle infrastructure than other drivers and were 1.5 times more likely to show safe behavior toward cyclists than other drivers. This research showed the significance of increased education for drivers with respect to safe driving behavior, rules and attitudes toward cyclists. DiGioia et al. [5] studied safety literatures related to 22 bicycle-related treatments. It suggested that even when there are reasonable studies carried out on the safety and efficacy of certain treatments like on bike lanes, considerable research is still needed on other treatments to ascertain their safety and effectiveness. Al-Houz [1] compared two crash countermeasures related to bicycles—bike boxes and protected intersections—along with a survey to gauge the perception of the users. VISSIM micro-simulation was carried out, and surrogate safety measures were used for the analysis which showed that the introduction of bike boxes would increase the safety perception of the bicyclists at and near intersections.

Huang et al. [10] reported that the SSAM could provide reasonably good estimates for rear-end and total conflicts at signalized intersections. [2, 14, 18, 20, 23] researched various methodologies for modeling driving behavior in mixed traffic conditions without lane discipline and the application of trajectory data for analyzing driving behavior.

2.1 Research Gap

All the literatures have reported that bike boxes are effective and a safety enhancing countermeasure which could be implemented at signalized intersections to provide priority. They have been found to be effective in reducing the conflicts between bicyclists and other vehicles while bringing about a positive behavior in terms of reduced encroachments within the bike boxes. Even when research on bike boxes has been conducted, research on the safety and effectiveness of other bicycle-related treatments needs attention. However, it should be noted that these studies have been conducted where homogeneous traffic conditions along with a greater adherence to lane discipline are prevalent. The bike boxes have primarily focused on providing priority to bicycles.

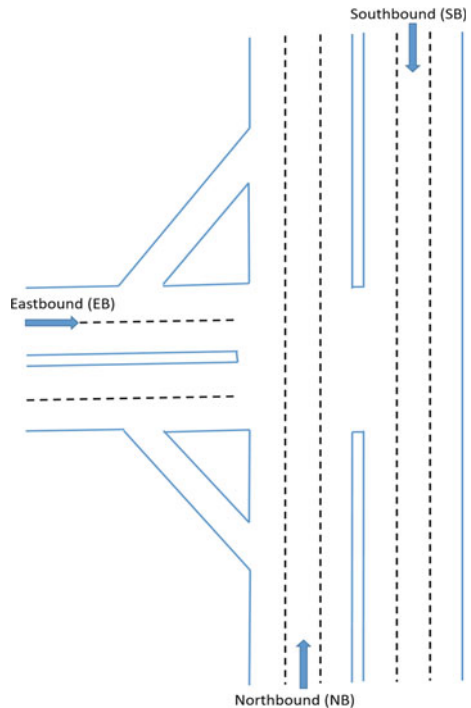
This presents an opportunity for research by testing the safety and effectiveness of the concept on bike boxes on Indian roads where mixed traffic conditions exist along with lane indiscipline. As the number of two-wheelers is high in Indian cities, would the provision of 'two-wheeler boxes' at signalized T-intersections be beneficial with respect to safety? Are the conflicts going to decrease? Even if it does, would the road users be keen for its implementation? These research questions have been addressed in this study.

3 Scope and Objectives

The scope of the study is limited to Kowdiar ('study intersection' shown in Fig. 2)—a signalized T-intersection in Thiruvananthapuram, Kerala, India, with an average lane width of 3.5 m. This intersection has been selected based on the favorable factors such as reasonably straight approaches on plain terrain, only one approach having conflicting movements in the form of straight and right turning movements, road surface with good riding quality, sufficient carriageway width for the implementation of two-wheeler boxes and absence of side access.

The objectives of the study are to (i) develop the design criteria for implementation of two-wheeler boxes at signalized T-intersection and (ii) investigate the effectiveness of two-wheeler boxes at signalized T-intersection with respect to traffic parameters like queue length and saturation flow, along with safety.

Fig. 2 Layout of the study intersection



4 Methodology

The methodology consists of various tasks as illustrated in Fig. 3.

Once the study intersection was finalized, data collection was initiated through videography to obtain classified traffic volume in each direction and queue length. The signal phase timing as well as road inventory details were also collected. Base model was created in VISSIM incorporating data obtained from video data processing for the study intersection. The base model thus created required to be calibrated and validated.

The universally accepted parameter GEH was used to compare the simulation output with that of observed traffic volume in the field. The GEH value is given by Eq. (1). A GEH of five or fewer is considered acceptable in the engineering industry.

$$GEH = \sqrt{\frac{2(m - c)^2}{m + c}} \tag{1}$$

where ‘*m*’ represents traffic volume from the model simulated (veh/h), and ‘*c*’ represents the field observed traffic volume (veh/h).

Wiedemann 99 car-following model parameters were adjusted for calibrating the queue length. Then, the calibrated model was also validated with another set of newly collected traffic volume data to check its robustness. Once validated, the micro-simulation model was considered as the final base model.

Base model was modified with the inclusion of two-wheeler box to obtain the modified model. Various versions of the modified model were tested with different values of design elements like (i) two-wheeler box length from the STOP line—8, 12, 16 and 20 m—it is to be noted that the width of the box is same as that of the carriageway width), (ii) two-wheeler lane width of 1.2 and 1.5 m, (iii) position and number of two-wheeler lanes—single/double side, (iv) length of two-wheeler lanes and (v) priority green time for two-wheelers waiting in the two-wheeler box. It is to be noted that the available carriageway width and green time for SB approach would

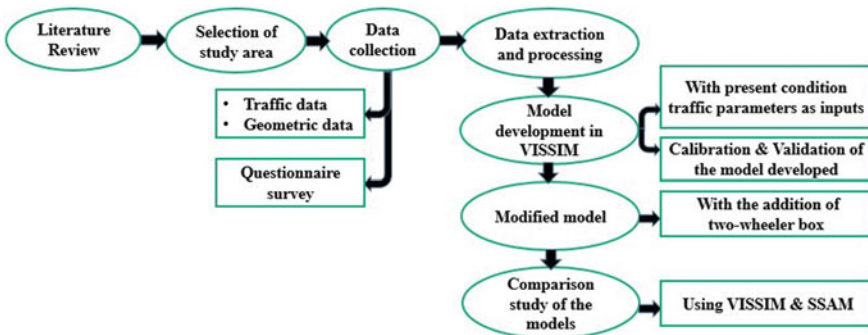


Fig. 3 Methodology adopted

be utilized. These trials were carried out to determine the optimal modified model that suits the study intersection which would actually present the specific values to be adopted for the design elements of the two-wheeler box.

Comparison of both the models (base and optimal modified model), with respect to average queue length, average saturation flow values, number of possible conflicts and values of surrogate safety measures, was carried out using VISSIM and Surrogate Safety Assessment Model (SSAM). In addition, an online survey was also conducted to gauge the knowledge and perception of road users toward the concept of two-wheeler boxes.

5 Data Collection and Analysis

5.1 Data Collection

In this study, videographic method was employed to collect the data at the study intersection. The video data for the study intersection along with many other junctions was collected for a total period of 3 h, as part of another research work [24], which comprised the peak hour. The study section was free from any kind of obstructions, and the weather was clear with good visibility. Road inventory data as well as signal phase timing was collected from the field.

Road user opinions were collected through an online survey for assessing the knowledge and perception regarding two-wheeler boxes. The survey mostly contained multiple choice questions, with questions 1–5 focused on obtaining the demographic details of the respondents; questions 6–10 focused on obtaining the respondent's purpose of travel and years of experience in riding two-wheelers; and questions 11–21 evinced the safety perceptions of respondents toward the concept of two-wheeler boxes and its associated factors.

5.2 Data Analysis

Questionnaire survey . The questionnaire survey was conducted online by circulating a Google form clearly explaining the details of two-wheeler boxes. The responses were collected from people belonging to different regions within Kerala including their age, gender, vehicle ownership, etc. The following observations were made from the questionnaire survey:

- More than 60% of the respondents responded positively toward the question on awareness about the purpose of two-wheeler boxes, while only less than 20% responded negatively to the same. The rest remained neutral.

- More than half of the respondents had positive perception toward the concept of two-wheeler boxes since they agreed to the ideas that safety of the two-wheeler users would increase due to the addition of two-wheeler boxes and that more aggregated space and improved signal timing would be available for two-wheeler users.

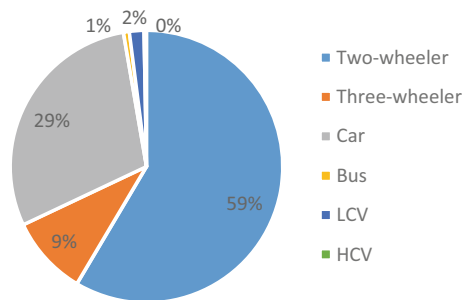
Videographic Survey . The video data collected was extracted [21] to obtain the classified traffic volume count corresponding to each direction of movement [SB-through (T) and right turn (R), NB-through (T) and left turn (L), EB-right turn (R) and left turn (L)] at the study intersection. The survey for the study intersection was conducted for a period of three hours in the morning, i.e., 8:30–11:30 am. The peak hour classified traffic volume for various directions of the study intersection is shown in Table 1, while the vehicle composition is illustrated in Fig. 4.

From the vehicle-wise traffic composition, it was observed that for the study intersection, two-wheelers accounted for 59% of the total traffic volume in the peak hour followed by cars and auto-rickshaws having a share of 29% and 9% of the total traffic volume, respectively. The vehicular composition at this intersection clearly indicates the requirement of measures to be undertaken to improve the safety and security of two-wheeler users.

Table 1 Peak hour classified traffic volume at the study intersection

Movement	Traffic volume (veh/h)						Total
	Two-wheeler	Auto	Car	Bus	LCV	HCV	
SB—T	1905	280	870	27	27	6	3115
SB—R	545	60	192	–	8	9	814
NB—T	825	197	477	29	55	2	1585
NB—L	661	94	340	–	18	2	1115
EB—R	604	91	386	–	16	4	1101
EB—L	183	40	100	–	15	1	339
Total	4723	762	2365	56	139	24	8069

Fig. 4 Vehicle composition in peak hour



6 Microscopic Simulation Model

6.1 Base Model Development

The study intersection was created in VISSIM from the scaled Google map image. The data collected from the surveys was input into the software. Data collection points and queue counters were used to extract data from the software. The average of three runs with varying random seeds was used as the result.

Calibration of the Base Model . The Wiedemann 99 (W-99) car-following model is one of the two implementations of car-following models available in VISSIM. W-99 is suitable for urban traffic and intersections, and so in this study, W-99 was adopted. W-99 car-following model has 10 user-defined driving behavior parameters: CC0 to CC9. The CC0 to CC9 values were varied to obtain the calibrated base model of the study intersection. The values of the parameters adopted in the calibrated base model are provided in Table 2.

Table 2 Parameter values of calibrated base model

Parameter	Calibrated value	Default value
<i>Car following</i>		
Standstill distance (m)—CC0	0.5	1.5
Gap time distribution (s)—CC1	0.9	1.5
<i>Lane changing</i>		
Overtake reduced speed area	Allowed	Not allowed
<i>Lateral</i>		
Desired position at free flow	Any	Middle of lane
Observed vehicles on next lane	Allowed	Not allowed
Diamond queuing	Allowed	Not allowed
Consider next turning direction	Allowed	Not allowed
<i>Minimum lateral distance (m)</i>		
Distance at 0 km/h	0.5	1.0
Distance at 50 km/h	0.8	1.0
<i>Overtake on same lane</i>		
On left	Allowed	Not allowed
On right	Allowed	Not allowed

Table 3 Comparison of queue length from field observation and simulation result

Queue length (m)	Approach		
	SB	NB	EB
Field observation	72.83	25.00	32.63
Simulation result	75.56	29.04	37.21

Table 4 GEH values for different approaches of the study intersection

Movement	Actual volume	Simulated volume	Difference	Percentage change	GEH
	(veh/h)	(veh/h)			
SB—T	3115	3083	32	1.03	0.57
SB—R	814	826	-12	-1.47	0.42
NB—T	1585	1564	21	1.32	0.53
NB—L	1115	1147	-32	-2.87	0.95
EB—R	1101	1089	12	1.09	0.36
EB—L	339	321	18	5.3	0.99
Total	8069	8030	39	4.4	3.82

Simulation results of calibrated base model. Data collection points and queue counters were used to obtain traffic volume and queue length as output from simulation. Queue length values were collected from the field for each approach during the same time of videographic data collection. The field observed queue length was compared to that obtained as simulation result which is shown in Table 3.

The queue length values obtained as simulation result showed less than 15% difference from field data. Analysis revealed that a GEH less than five was obtained as shown in Table 4. As a result, the simulated intersection was deemed to be a good fit, implying that the underlying model had been calibrated.

Then, the calibrated model was evaluated for the new set of data (input volumes, traffic composition, turning movement proportion, etc.) with the same driving behavior parameter values for validation. The results obtained from the simulation runs were compared with one-hour field data for which a reasonable fit was obtained. Through this process, the base model was validated as well.

6.2 Modified Model Development

Even though there were three approaches in the study intersection, only one approach required the implementation of two-wheeler box, i.e., SB approach as it catered to both through and right turning traffic. From SB approach, about 61.2% of through traffic and about 67% of right turning traffic constituted two-wheelers. Thus, the two-wheeler box was decided to be provided on SB approach of the intersection.



Fig. 5 Modified model with two-wheeler box **a** case 1 and **b** case 2. The box length, from STOP line, considered in this test cases is 20 m as indicated

The base model was modified by adding the two-wheeler box to obtain the modified model. However, different scenarios had to be analyzed for coming up with a two-wheeler box design for the study intersection. The two-wheeler box design elements included (i) box length, (ii) lane width, (iii) position and number of the two-wheeler lanes, i.e., single/double side, (iv) length of two-wheeler lane along the approach and (v) the priority green time allowable for two-wheelers. Case 1 considered two-wheeler lane on one side and Case 2 considered two-wheeler lanes on both sides which is depicted in Fig. 5a, b, respectively.

Case 1 with one side two-wheeler lane and varying other design elements like length of two-wheeler lane, two-wheeler box length, etc., did not give good results because the maneuvering portion of two-wheeler box was leading to more congestion and collisions and thus was not studied further.

Case 2 was tested with different values of design elements—length of two-wheeler lane was adjusted from 150 m and finally fixed at 250 m; the priority green time for two-wheelers was adjusted from 5 s and finally fixed at 10 s after several trial runs. After this, the length and priority green time were treated as fixed parameters and all other design elements like two-wheeler box length, number of lanes, width of two-wheeler lane, etc., were varied to estimate the optimal modified model to establish the design criteria for the study intersection. After several trial runs, the optimal modified model was determined as the one in which the average queue length was minimum.

Optimal Design Criteria . The values of the design variables for the optimal modified model for two-wheeler box at the study intersection are given below:

- Two-wheeler box length (at intersection): 20 m
- Number of two-wheeler lanes (on eastern side of SB approach): 2
- Number of two-wheeler lanes (on western side of SB approach): 1
- Two-wheeler lane width: 1.2 m
- Length of two-wheeler lane: 250 m

Table 5 Comparison of average queue length

Queue length (m)	Approach (SB)
Base model	75.56
Optimal modified model	58.88

- Priority green time for two-wheelers: 10 s

7 Comparison of Base and Modified Model

Eventually, a comparison of the optimal modified model against the base model was carried out to determine the effectiveness of providing two-wheeler box at a signalized T-intersection with mixed traffic conditions. The comparison was based on the change in average queue length and saturation flow using VISSIM along with change in possible conflicts and values of surrogate safety measures using Surrogate Safety Assessment Model [7, 7].

7.1 Queue Length

The average queue length outputs obtained from base model were compared with the average queue length outputs from the optimal modified model. Table 5 shows the results.

From Table 5, it was observed that the average queue length reduced by about 22.1% with the addition of two-wheeler box as against the base model.

7.2 Saturation Flow

The saturation flow, in Passenger Car Units (PCU) per hour, for the study intersection was calculated according to the procedure laid out in the Indian Highway Capacity Manual [3]. The average saturation flow was calculated for SB approach of the study intersection for the base model as well as for the optimal modified model to determine the effect of addition of two-wheeler box on saturation flow, the results of which are provided in Table 6.

It was observed that the addition of two-wheeler box led to an increase in the average saturation flow as shown in Table 6.

Table 6 Comparison of average saturation flow

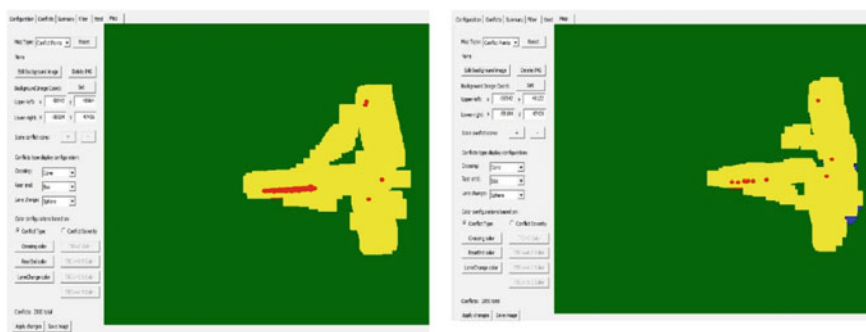
Approach	Saturation flow (PCU per hour)		Percentage change
	Base model	Optimal modified model	
SB—T	4512	5047	11.86
SB—R	1408	2098	49.00

7.3 Surrogate Safety Assessment

In this study, VISSIM trajectory files were imported into SSAM to measure the effectiveness of the studied treatment in terms of improvement in the safety of road users at the signalized intersection. Figure 6a represents the SSAM map for the base model, while Fig. 6b represents the SSAM map for the optimal modified model. In these figures, blue represents the region of possible lane change conflicts, yellow represents the region of possible rear-end conflicts, and red represents the region of possible crossing conflicts.

From Fig. 6, it was observed that the total number of possible collisions reduced in the optimal modified model as compared to the base model. The comparison of the number of possible conflicts and the values of the surrogate safety measures is shown in Tables 7 and 8, respectively.

It was observed from Table 7 that the number of possible conflicts got reduced by about 25.6% with the addition of two-wheeler box, and from Table 8, it was ascertained that the surrogate safety measure (TTC and PET) critical values for

**Fig. 6** SSAM map for **a** base model and **b** optimal modified model**Table 7** Comparison of the number of possible conflicts

Number of conflicts	Crossing	Rear-end	Lane change	Total
Base model	448	2015	87	2550
Optimal modified model	10	1780	106	1896

Table 8 Comparison of the surrogate safety measures

Surrogate safety measures	Time to collision (TTC)	Post encroachment time (PET)
Base model (s)	0.52	1.64
Optimal modified model (s)	0.61	1.79

optimal modified model were more than those for the base model indicating that the inclusion of the two-wheeler box has made the intersection safer.

8 Conclusion

Cities in Kerala, like many other cities in India, witness a large proportion of motorized two-wheelers on their road network due to multiple reasons. Higher adoption of two-wheelers has its pitfalls on account of the higher involvement in crashes. The crash records show that about 42.5% of crashes in Kerala involved two-wheelers. Crashes at intersections form a sizable proportion with T-intersections accounting for 9.76% on a national level. This calls for two-wheeler specific countermeasures which could be adopted for saving precious lives at these vulnerable locations.

This study used a modified version of bike box, adopted abroad for the safety of bicycles at intersections, to develop a two-wheeler box at signalized T-intersections for providing priority and safety to two-wheeler users. However, the impact of such a countermeasure was not studied in mixed traffic conditions which motivated this study. This research aimed at developing the design criteria for implementation of two-wheeler box at a signalized T-intersection and for assessing its effectiveness with respect to queue length, saturation flow and safety at the intersection.

Kowdiar was selected as the study intersection as its geometry favored two-wheeler box implementation. VISSIM micro-simulation software was used for developing the base model which after calibration and validation was used for developing the modified model with the addition of two-wheeler box. Various values of design elements were tested to establish the design criteria for the optimal modified model which provided the minimum queue length for the study intersection. Results from VISSIM and Surrogate Safety Assessment Model were used for comparing the base model and the optimal modified model. The major results of this comparison show that with the addition of the two-wheeler box, there was a reduction in the average queue length by about 22.1%, increase in the average saturation flow and reduction in the number of possible conflicts by 25.6% at a signalized T-intersection with mixed traffic conditions. This indicates that the inclusion of the two-wheeler box had made the intersection safer in addition to bettering the saturation flow and reducing the average queue length. An online survey conducted for assessing the perception toward two-wheeler boxes showed that more than half of the respondents favored two-wheeler boxes since they agreed to the notion that safety of two-wheeler users

would increase upon the addition of two-wheeler boxes and that more aggregated space and improved signal timing would be available for two-wheeler users.

The major limitations are that only one signalized T-intersection has been studied and the sensitivity analysis for determining the range of traffic volume for which the design criteria hold has not been worked out. The cost–benefit analysis for estimating the economic components associated with the two-wheeler box has not been covered. The impact of implementation in other types of signalized intersections needs to be researched. These aspects are intended to be included in future work. Field implementation to gauge the actual behavior of road users toward this novel concept can be studied in future only with its pilot implementation at a few junctions. The field implementation would have to consider its innate problem that it requires considerable length near the intersection without side access for providing hindrance-free path to two-wheelers. This pre-condition could play spoilsport as side accesses are seldom controlled/regulated in the India. Moreover, without physical segregation, two-wheeler lanes would more likely be encroached upon by other vehicles. The signal posts would also require alterations to display the priority green time applicable to the two-wheeler users.

This study, to the best of our knowledge, is the first one evaluating the two-wheeler box concept in India which shows positive signs for its adoption at signalized T-intersections. However, more research is required to strengthen this line of thought which, if found beneficial, could be used as an effective countermeasure for improving the safety of two-wheeler users, thereby addressing a large proportion of the crashes occurring in India. In addition to comprehensive research, its effective adoption would require setting up of design criteria based on intersection geometry, traffic characteristics and type of regulation; drafting rules and regulations to suit Indian conditions with inclusion in Motor Vehicles Act and other rules related to road transport; preparation of implementation guidelines; and awareness building campaigns and enforcement strategies.

References

1. Al-Houz O (2018) Evaluation of bike boxes and protected intersections with bicycle signal treatments for improving safety and multimodal mobility at urban signalized intersections. Master's Thesis 3810. Western Michigan University
2. Arasan VT, Koshy RZ (2005) Methodology for modeling highly heterogeneous traffic flow. *J Transp Eng* 131(7):544–551
3. Chandra S, Gangopadhyay S, Velmurugam S, Ravinder K (2017) Indian highway capacity manual. 1st edn. CSIR-Central Road Research Institute, New Delhi
4. Chen L, Chen C, Srinivasan R, McKnight CE, Ewing R, Roe M (2011) Evaluating the safety effects of bicycle lanes in New York city. *Am J Public Health* 102(6):1120–1127
5. DiGioia J, Watkins KE, Xu Y, Rodgers M, Guensler R (2017) Safety impacts of bicycle infrastructure: A critical review. *J Safety Res* 61:105–119
6. Dill J, Monsere CM, McNeil N (2012) Evaluation of bike boxes at signalized intersections. *Accid Anal Prev* 44(1):126–134
7. Gettman D, Head L (2003) Surrogate safety measures from traffic simulation models. Federal Highway Administration, US Department of Transportation, Washington, DC

8. Gettman D, Pu L, Sayed T, Shelby S (2008) Surrogate safety assessment model and validation—final report. Federal highway administration, US Department of Transportation, Washington, DC
9. Hörcher D, Singh R, Graham DJ (2021) Social distancing in public transport: mobilising new technologies for demand management under the Covid-19 crisis. *Transportation*. <https://doi.org/10.1007/s11116-021-10192-6>
10. Huang F, Liu P, Yu H, Wang W (2013) Identifying if VISSIM simulation model and SSAM provide reasonable estimates for field measured traffic conflicts at signalized intersections. *Accid Anal Prev* 50:1014–1024
11. Hunter W (2000) Evaluation of innovative bike-box application in Eugene. *Oregon Transp Res Rec* 1705:99–106
12. James E, Pederson K, Ryan C, Ryan R, Wascalus J (2011) Minneapolis bike boxes: an evaluation of bike boxes at signalized intersections designed to facilitate bicyclist left turns. Master's Thesis, The University of Minnesota
13. Johnson M, Oxley J, Newstead S, Charlton J (2014) Safety in numbers? investigating Australian driver behaviour, knowledge and attitudes towards cyclists. *Accid Anal Prev* 70:148–154
14. Kanagaraj V, Asaithambi G, Toledo T, Lee T (2015) Trajectory data and flow characteristics of mixed traffic. *J Transp Res Board* 2491(1):1–11
15. Kerala state planning board homepage. <https://spb.kerala.gov.in/economic-review/ER2020>. Accessed 2021/06/06
16. Loskorn J, Mills AF, Brady JF, Duthie JC, Machemehl RB (2013) Effects of bicycle boxes on bicyclist and motorist behavior at intersections in Austin. *Texas J Transp Eng* 139(10):1039–1046
17. Metkari M, Budhkar A, Maurya AK (2013) Development of simulation model for heterogeneous traffic with no lane discipline. *Procedia Soc Behav Sci* 104:360–369
18. Ministry of road transport and highways homepage. <https://www.morth.nic.in/road-accident-in-india>. Accessed 2021/06/06
19. Munigety CR, Mathew TV (2013) Towards behavioral modeling of drivers in mixed traffic conditions. *Transp Developing Econ* 2(6):1–20
20. Munigety CR, Vicraman V, Mathew TV (2014) Semiautomated tool for extraction of micro level traffic data from videographic survey. *J Transp Res Board* 2443(1):88–95
21. National association of city transportation officials homepage. <https://nacto.org/publication/urban-bikeway-design-guide/intersection-treatments/bike-boxes>. Accessed 2021/06/06
22. Raju N, Kumar P, Jain A, Arkatkar SS, Joshi G (2018) Application of trajectory data for investigating vehicle behavior in mixed traffic environment. *J Transp Res Board* 2672(43):122–133
23. Salini PN, Kini BA (2021) Studies on Indo-HCM adjustment factors for estimation of saturation flow at signalised intersections in Kerala. KSCSTE-National Transportation Planning and Research Centre, Thiruvananthapuram
24. Sohail Z, Luis M, Nicolas S (2013) Impact of bicycle boxes on safety of cyclists: a case study in Montreal. In: 92nd Annual meeting, 13–2909. Transportation research board, Washington DC (2013)

Optimisation

Combined Passenger and Cargo Transport: A Hybrid Simulation and Optimization Approach Focusing on the Transshipment of Cargo Between Tram Vehicles



Ralf Elbert , Jessica Schwarz , and Johannes Rentschler 

Abstract Offering a promising opportunity for cargo transport in urban areas, cargo is transported along with passengers sharing the same infrastructure and vehicle. Cargo must be routed efficiently through the network and assigned to vehicles. The resulting problem can be modeled as a network flow problem. Additionally, constraints such as varying capacities due to fluctuations in passenger numbers during the day must be considered. These numbers, as well as the demand for cargo transports, are assumed to be stochastic and therefore considered in a simulation study. To solve this problem, a hybrid simulation and optimization approach are presented. The deterministic network flow problem is solved to optimality with the help of a commercial solver. A simulator uses this solution to assign transport units to vehicles and determine a route through the network. As soon as the solution becomes infeasible, the deterministic problem is resolved with the current parameters. The new solution serves once again as an input for the simulation. This approach is expected to be more efficient compared to considering scenarios for every possible form of uncertainty.

Keywords Freight on transit · Public transport · Simulation · Optimization · Urban logistics

1 Introduction

The current COVID-19 pandemic has exacerbated the situation in e-commerce and for public transport providers. E-commerce has grown disproportionately across

R. Elbert · J. Schwarz · J. Rentschler (✉)
Chair of Management and Logistics, Technical University of Darmstadt, Darmstadt, Germany
e-mail: rentschler@log.tu-darmstadt.de

R. Elbert
e-mail: elbert@log.tu-darmstadt.de

J. Schwarz
e-mail: schwarz@log.tu-darmstadt.de

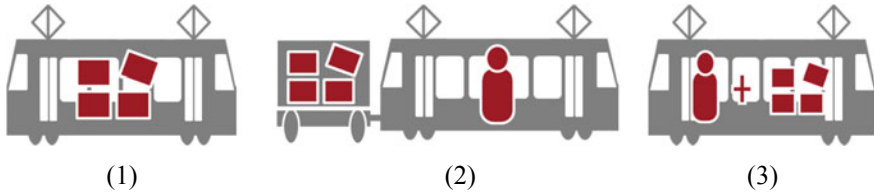


Fig. 1 Alternatives for an FOT

national borders, leading to increased deliveries [1, 2]. In contrast, public transport providers have to contend with stark challenges. Declining passenger numbers, hygiene regulations, and the necessity to maintain the network, operated mainly by the public sector, have led to high losses [3–6]. Cargo on public transport offers the chance to address both challenges. In this case, the existing infrastructure of public transport supports cargo delivery, which is also called freight on transit (FOT) [7].

FOT can be installed on different public transport infrastructures. One possible example is the usage of trams. There are several options for transport as shown in Fig. 1:

- (1) Shared track: Freight is transported in a separate vehicle, which only shares the infrastructure with public transportation vehicles. It must be ensured that freight vehicles do not interfere with the timetable of passenger vehicles. Example: [8]
- (2) Shared vehicle: Freight is transported inside a separate wagon (light railways) or an attached trailer (e.g., bus). Persons and freight share the same travel route, time, and distance. Dependencies exist in particular about loading/unloading and transshipment operations. Examples: [9, 10]
- (3) Shared Wagon: Freight is transported in the same wagon or compartment as persons. Passengers and freight do not only share travel routes, time, and distance but share space as well. In particular, peak periods of transportation demand for both persons and freight must be considered, as the available space must be split between the two. Furthermore, design and safety considerations must be addressed. Example [11]

This work focuses on the third category, where cargo is transported along with passengers in the same vehicle. An entire network is considered to ensure assumptions apply to every tramway, vehicle, and station. Current research of [12] shows that FOT usage can result in higher efficiency and sustainability. But as stated by Behiri et al. [10], Kelly and Marinov [11], there is still the following research gap: the transshipment of cargo between different vehicles. Another yet less researched field in FOT is uncertainties. Ghilas et al. [13] took uncertainties in demand into account but identified some remaining challenges like other sources of uncertainties and a re-design of the public transport network to make the routing of commodities possible. Mourad et al. [14] found that varying demands during the day should be considered. This is why this work deals with uncertainties in demands for transporting

commodities and uncertainties in transport demands of passengers, which both vary during the day. Therefore, this work answers the following research question (RQ):

RQ: How can cargo be efficiently routed through a public transport network considering the transshipment between different vehicles and facing uncertain demands and uncertain capacities in vehicles?

To answer this research question, a combined simulation and optimization approach are proposed. The uncertain demands and capacities in vehicles are considered in the simulation model. The transshipment, routing, and allocation of cargo to trams are modeled as a deterministic network flow problem solved by a commercial solver. Whenever a new commodity that needs to be transported occurs or the former deterministic solution becomes infeasible due to a lower capacity in trams, the optimizer is called and resolves the deterministic problem. Thanks to the consideration of uncertainties and fluctuations of capacities during the day, the results of this procedure are expected to represent real-world networks adequately.

Before describing the model or solution procedure, a summary of the relevant literature on FOT is given. Afterward, the combined passenger and cargo transport problem is introduced. For this model, a hybrid simulation and optimization procedure are proposed as methodology. This paper finishes with the expected results and a short conclusion.

2 Literature Review

A common situation in cities is that the public passenger transport network coexists alongside the cargo transport infrastructure due to its different characteristics [15]. As a result, significant capacities, both in local public transport and transport vehicles, remain unused [16, 17]. The success of combining the flow of goods and passengers has already been demonstrated on long-haul routes (e.g., belly freight, Hurtigruten mail ships) [8, 18]. The idea of combining last-mile cargo with passenger transport dates back to the last millennium and has been taken up several times since. In addition, several attempts have been made across European cities to integrate cargo into light railways over the last two decades [19–21].

Over the past few years, interest in cargo on public transport has grown steadily. Researchers have approached the topic from various angles so that a large and diverse body of literature has emerged. A comprehensive summary of the literature on FOT is provided in [22].

Thereby several terms are used for cargo transport on public transport. In addition to the terms FOT, cargo hitching, or passenger-and-package sharing, there is a multitude of other possible terms [7, 23–25]. Here, cargo on public transport is defined as the integrated and organized transport of passengers and goods within urban areas, which uses buses and trains that operate at regular times on fixed routes and are used by the public.

So far, a distinction can be made between the two areas of research. The first research area deals with the shared use of (rail) infrastructure by cargo and passenger transport, with the transport of cargo being carried out in separate vehicles [26]. Until the middle of the twentieth century, it was quite common to transport various types of goods by tram [27]. This approach is now enjoying new popularity. For example, [27] investigate in a case study the use of a cargo tram in Barcelona, [28] conduct a feasibility study for Newcastle upon Tyne, and [29] investigate the potential of a shared goods and passengers on-demand rapid transit system. The second research area investigates the sharing of vehicles between people and cargo [12]. Further, the research of this area can be divided into two subcategories.

The first one has a strong operational orientation and considers the modeling and mathematical optimization of single lines [10] or whole transport networks [14]. The second subcategory examines how public transport can be integrated into the overall system of urban logistics. For example, [14, 30] analysis how a pickup-and-delivery problem with scheduled lines affects an urban transport system. de Langhe et al. [31] investigates the conditions for a successful and viable implementation of urban cargo transport by tram.

Concerning the methodology, [22] divided the research into qualitative and quantitative. Mathematical programming, like the pickup-and-delivery or vehicle routing problem (VRP), is considered quantitative [13, 32]. In contrast to that, case studies like the one in [12] are part of the qualitative research field.

Cargo on public transport has not only been studied in theory. First pilot studies, which all belong to the qualitative research area of shared infrastructure, have been conducted so far and are briefly presented below.

- Amsterdam (Netherlands): In 2007, City Cargo Amsterdam launched the project CargoTram to reduce the number of trucks in the inner-city by 50% and reduce pollution by 20%. A pilot project consisting of two empty cargo trams running on the network for one month was successful. In 2009, City Cargo Amsterdam got bankrupt [33].
- Dresden (Germany): From 2001 to 2020, the Cargo Tram of DVB Dresden has been supplying the “transparent factory” of Volkswagen AG in Dresden city center with automotive components just in time. With up to eight rounds per day, up to 25 truck journeys can be avoided [34].
- Frankfurt (Germany): In 2019, Hermes, a Courier Express Parcel service provider, and the Frankfurt University of Applied Sciences conducted the pilot study “Last-MileTram” in Frankfurt. From a depot outside the city, customized transport boxes were taken by tram to the city center. From there, they were transported by special e-bikes to their final delivery location. According to the pilot study, transport by tram is possible in principle, but the costs are slightly higher than for the delivery by road [35, 36].
- Zurich (Switzerland): Since 2003, the Cargo Tram has enabled the disposal of electrical waste and bulky goods in Zurich. A regular timetable provides access to eleven stops where citizens can hand in their electrical or bulky waste free of

charge. Several hundred tons of bulky waste are thus removed each year, reducing traffic on the roads [37].

- Mumbai (India): So-called dabbawalas collect lunch boxes in specific geographical areas in Mumbai. At train stations, the boxes are sorted regarding their destinations. The lunch boxes are then transported to the central business district (CBD) of Mumbai by trains in dedicated compartments. Local dabbawalas transport the lunches to their final destinations, which are businessmen. After lunch, the empty boxes are collected by the dabbawalas and are transported back to their origin in the same way. Like this, and with the help of the public transport system, it is possible to supply people at work with home-cooked meals [38, 39].

In recent years, FOT became an emerging topic for researchers worldwide. Research can mainly be divided into qualitative and quantitative approaches but can also be differentiated by their transportation mode, shared instances, and the underlying network. Many papers focus on mathematical programming, especially on mixed-integer programming like the VRP, but also case studies are quite often chosen as topics. The underlying problems are solved mainly by metaheuristics.

Elbert and Rentschler [22] identifies four main fields future research should focus on the consideration of external effects, optimizing profit instead of costs, the need for data, and the usage of stochastic and real-time information. This work aims to contribute to the last research field by including stochastic demands and capacities in vehicles together with a network flow problem and a simulation model that should be solved by a combined simulation and optimization approach. To the best of the authors' knowledge, there has not yet been such a solution approach to solve FOT problems.

3 The Combined Passenger and Cargo Transport Problem

For efficient usage of spare capacity in public transport, the combined transport of passengers and cargo with stochastic demand of cargo and stochastic capacities in vehicles is investigated in this case. The deterministic problem can be modeled as a network flow problem. As a solution to the problem, an allocation of transport units, called commodities, to vehicles is determined. The uncertainties are considered in a simulation model. Therefore, the public transport network is modeled as a graph where tram stations serve as nodes and the links between them serve as arcs.

3.1 Deterministic Problem

Tram stations are modeled as nodes N in a graph. Tram services between two tram stations are modeled as arcs A . A defined number of periods T is considered in every model. In a so-called time-space graph, every arc and node in the physical network

are replicated in every considered period $t \in T$. An example of such a graph is displayed in Fig. 2. Arcs (i, j) in the time–space graph represent tram rides resulting from the timetable of the passenger transport. Capacities e_{ij}^t on arcs (i, j) show the available capacity for cargo in trams that is determined by the number of passengers traveling in a tram. If no tram is deployed on arc (i, j) in period t , $e_{ij}^t = 0$ is applied.

Transport units are modeled as commodities K . They occur at their origin node $o(k) \in N$ when they are available at time $\sigma(k) \in T$. Commodities must be transported to their destination $d(k) \in N$. They must be delivered until $\tau(k) \in T$. One commodity can contain multiple transport units. The number of transport units per commodity is noted as demand q^k .

Table 1 summarizes all notations necessary for the model.

The decision variable x_{ij}^{kt} determines the allocation of commodity k on arc (i, j) in period t . If the commodity k is allocated to arc (i, j) in period t , x_{ij}^{kt} must be 1.

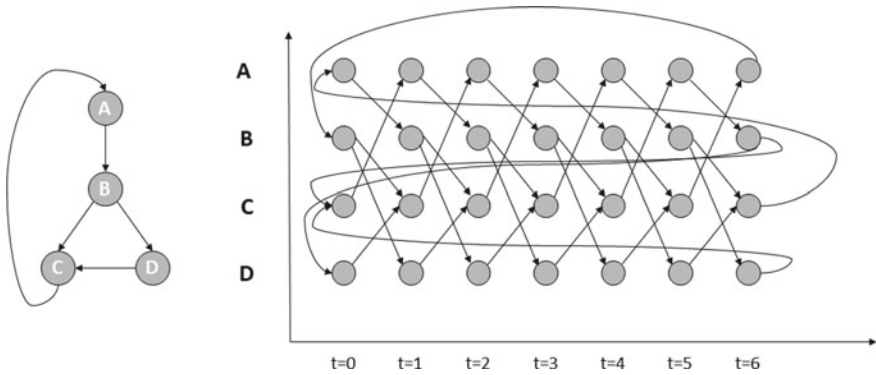


Fig. 2 Time–space graph

Table 1 Notation

Variable	Description
A	Set of arcs
N	Set of nodes
K	Set of commodities
T	Set of periods
$o(k) \in N$	Origin node of commodity k
$d(k) \in N$	Destination node of commodity k
$\sigma(k) \in T$	The earliest time of availability at origin node of commodity k
$\tau(k) \in T$	Latest delivery time at destination node of commodity k
q^k	The demand of commodity k
e_{ij}^t	Capacity on arc (i, j) in period t

Otherwise, $x_{ij}^{kt} = 0$ is applied. The variable t_i^k is depending on x_{ij}^{kt} and describes the period in which commodity k arrives at node i .

The deterministic FOT problem minimizes the transport time for each commodity. Constraints should ensure that the available capacity on each tram is not exceeded, and that commodities are transported correctly between their period of availability and delivery deadline. The problem can be modeled as follows:

$$\min \sum_{k \in K} (t_{d(k)}^k - t_{o(k)}^k) \quad (1)$$

Subject to

$$\sum_{k \in K} q^k x_{ij}^{kt} \leq e_{ij}^t \forall (i, j) \in A, \forall t \in T \quad (2)$$

$$\sum_{j \in N^+(i)} x_{ij}^{kt-1} - \sum_{j \in N^-(i)} x_{ji}^{kt} = \begin{cases} 1 & \text{if } i = o(k), t = \sigma(k) \\ -1 & \text{if } j = d(k), t = \tau(k) \forall i, j \in N, k \in K, \forall t \in T \\ 0 & \text{else} \end{cases} \quad (3)$$

$$x_{ij}^{kt} \in \{0, 1\} \forall (i, j) \in A, k \in K, t \in T \quad (4)$$

The objective function (1) minimizes the total transport time overall commodity $k \in K$. Therefore, the arrival time $t_{d(k)}^k$ at the destination $d(k)$ of commodity k is subtracted from the arrival or creation time $t_{o(k)}^k$ at the origin $o(k)$.

Constraint (2) ensures that the capacity e_{ij}^t of a tram running on arc (i, j) at period t is not exceeded. The volume of transport units per arc (i, j) at period t can be calculated by the objective variable x_{ij}^{kt} , which states if commodity k is transported on arc (i, j) at period t , and the number of transport units q^k for commodity k . The flow conservation is considered in constraints (3) which also forbid the transport outside the period of availability $\sigma(k)$ and the limit of the delivery time $\tau(k)$ of commodity k . Therefore, commodity k flows out of node $o(k)$ in period $\sigma(k)$ to any of the connected neighboring nodes. Vice-versa in period $\tau(k)$, commodity k arrives at node $d(k)$. Constraint (4) ensures that x_{ij}^{kt} is binary indicating that transport requests are transported in one and no division of demands on different vehicles occurs, which ensures that the model does not become too complex.

3.2 Simulation Model

The stochastic problem with uncertain demands and capacities in trams is considered in an agent-based simulation model that includes the following agents:

- Trams

- Tram stations
- Commodities

Trams operate between different tram stations. They have predefined and deterministic departure times that follow a given timetable. Trams run on a predefined tram line that includes a sequence of tram stations. Tram stations can be part of multiple tram lines what ensures the transshipment of transport units.

Passengers are modeled implicitly as the available capacity in trams for cargo. The capacity is modeled stochastically and varies between different stations where passengers can enter or get off a tram. The capacity also varies during the day with peaks during rush hours. The data for passengers is based on a real-life dataset.

Commodities originate as transport requests at tram stops at stochastic times and must be transported in a reasonable time. Their destination is another tram stop in the network that must not necessarily be part of the same tram line. Commodities are transshipped at tram stops where the tram stop is part of both tram lines. They include one or more transport units.

4 Methodology: Hybrid Simulation and Optimization

One possibility for modeling and solving FOP with uncertainties are two-staged-stochastic programs. Thereby, a scenario for every specification of the uncertain parameter with their reasonable probability of occurrence is considered. Ghilas et al. [13], Mourad [14] use this approach to model uncertainties in demand. They solve the problem with the help of an adaptive large neighborhood search heuristic embedded into a scenario-based sample average approximation method.

This work follows a different approach called hybrid simulation and optimization that has already been used for other types of problems like the service network design problem (SNDP). SNDP is quite similar to the considered FOT problem in this work as they consider service planning decisions for transport services and modes [40]. In some SNDP models like the one in [41], similar constraints like the flow conservation and capacity constraints as in the model of this work are used. Layeb et al. [42] faces an SNDP with stochastic demand and travel times and uses the hybrid simulation and optimization to solve this problem. Therefore, an optimizer sends a path to the simulator to test this path. The simulator returns the costs to the optimizer, which tries to enhance the solution further. Hrušovský et al. [43] uses a similar approach to handle uncertainties in the travel time. A deterministic version of the problem is solved optimally by a mathematical solver. This solution is used by a simulation model that considers stochastic travel times. Whenever the deterministic solution becomes infeasible because of a stochastic factor that occurs during the simulation, the updated deterministic problem is solved again by the mathematical solver.

In the context of dynamic VRP, this solution approach is also known as online optimization. VRP is used to determine routes for a fleet of vehicles and customers [44]. Problems are characterized as dynamic if the input varies and is continuously

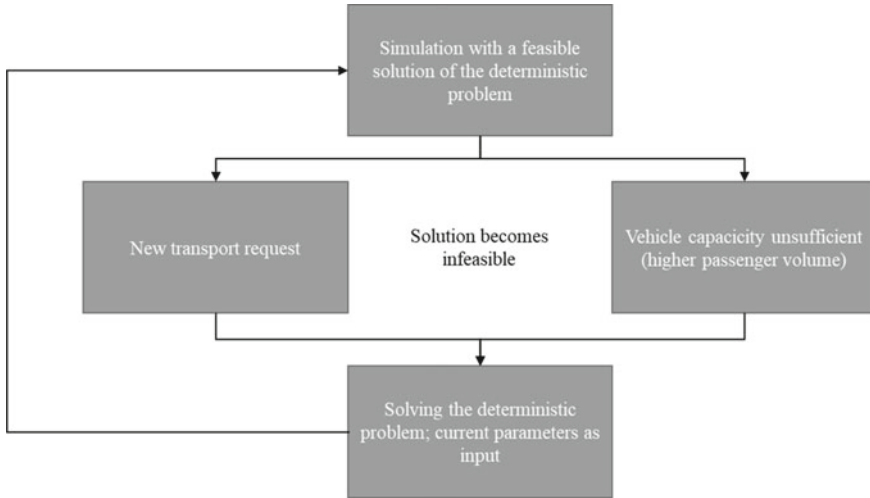


Fig. 3 Schematic solution procedure: hybrid simulation and optimization

updated while determining a route [45]. The resulting problem is considered deterministic and must be solved repeatedly with current dynamic events and the system state as inputs [46].

The solution approach for FOT in this work is shown in Fig. 3. A simulation starts that considers uncertainties in demand and the capacity in the vehicles. Therefore, transport demands occur at stochastic points in time. The number of passengers is implicitly considered by the capacity of the trams, which is determined by stochastic distributions. The simulation run starts with trams only transporting passengers but not yet cargo. When the first transport request occurs, the deterministic problem is solved by the mathematical solver. The current demand and capacity of the vehicles in the simulation are used as input for the optimizer.

The optimizer calculates the optimal solution for the FOT problem. All commodities currently in the system serve as input for the optimizer and are considered with their concrete origin, destination, time of availability, deadline for transport, and demand. The schedule of the trams, in addition to the stochastically determined capacity of each tram, serves as an input for the capacity e_{ij}^t on arc (i, j) in period t . If there is no tram running an arc (i, j) in period t , e_{ij}^t is zero.

The results of the optimizer are the binary values of x_{ij}^{kt} which are used to assign commodity k to a tram running on arc (i, j) in period t . They are returned to the simulation, which keeps running without interruptions until the solution becomes eventually infeasible. This can be the case if a new transport request occurs that must be routed through the network and allocated to vehicles. Another case is if the capacity in a vehicle is not sufficient to transport the commodities that have been allocated to this vehicle. This is because there are more passengers in the vehicle, which is determined stochastically for each arc. The number of passengers changes during the day. Rush hours are explicitly considered and result in higher passengers

and therefore, in a lower capacity for cargo in trams. Former solutions of optimization runs can become infeasible because they considered a higher capacity of the vehicles which changed during the rush hour.

The current parameters in the simulation serve as an input for a new optimization run that considers the updated parameters. During later calls of the optimizer, there are already commodities in the system for which a solution has been calculated in former optimization calls. In this case, the objective variable x_{ji}^{kt} for all passed periods t in the simulation time is fixed to their values assigned in former optimization calls. For future periods t , x_{ji}^{kt} is recalculated with the current demand of commodities and the capacity of trams.

The results are again returned to the simulation, which uses these results until the solution becomes once again infeasible. The procedure is repeated until the simulation time ends.

In scenario-based solution approaches like [13, 14], every possible uncertainty in demand and capacity fluctuations must be considered in different scenarios resulting in a high number of scenarios and therefore, a high-computational time. The advantage of the combined simulation and optimization compared to a scenario-based approach is that not all possible demands and capacities have to be considered in scenarios. This saves computational time regarding the optimizer. Another advantage is that fluctuations depending on the time of the day, like a higher passenger volume and lower cargo capacity during rush hours, are considered. As soon as formerly calculated solutions become infeasible because of a lower capacity or new commodity, the optimizer recalculates the solution for the current network. Like this, higher demands and lower capacities are considered immediately.

5 Expected Results

Modeling a network and transport demands should be as realistic as possible. This is why the usage of synthetic datasets is unusual in the research on FOT. A real-life dataset based on the tram network in Frankfurt is intended to be used as input for the underlying model and solution approach. The metropolis Frankfurt is one of the biggest cities in Germany [47]. Nearly, 200 million passengers are transported by public transport every year [48]. This is why Frankfurt serves as a case study for the model in the simulation. This network consists of 139 tram stops that are connected by ten tram lines [48]. For the case study, the tram network was limited to five lines that cover all parts of the city connected to the tram network.

Different capacities depending on the number of passengers traveling in trams varying during the day are considered, which are based on real-live data provided by the operator of the tram network. The demand is derived from [36]. Numbers like the capacities in trams and the transport demands are volatile. This is why a simulation combined with optimization and not a stand-alone mathematical optimization is conducted to answer the RQ. An agent-based simulation was chosen because agents

like trams, staff, and transport units are considered. The simulation is implemented with the software AnyLogic. The deterministic problem is solved by CPLEX.

The simulation studies are still ongoing. Therefore, no final results can be presented at this time. First results show that an efficient allocation of commodities to trams is crucial to serving all transport demands. Especially during rush hours, transport demands of passengers and for commodities are higher than the available capacity what underlines the necessity of an efficient algorithm. The final results will expectantly show that the hybrid simulation and optimization approach are efficient for solving the combined passenger and cargo transport problem. With the help of the implemented solution approach, cargo can be routed through the network and can be assigned to trams. The consideration of stochastic demands and capacities in trams and a real-life dataset shows how an FOT network can be designed. Transshipments will be an essential part of the model and solution to cover a whole transport network and city what is also the main contributor to this research area.

6 Conclusion

The combined passenger and cargo transport problem were introduced based on a network flow problem and considered transshipments between tramlines. Cargo is assumed to be transported in trams in the same vehicles as passengers. Transport demands for cargo and the capacity in trams are considered stochastic and varying depending on the time of the day. The deterministic problem is modeled mathematically. The uncertainties are considered in a simulation. The focus of this paper lies on the methodological part where a hybrid simulation and optimization approach are proposed. At first, the simulation is started and runs until the first commodity occurs. Then, the deterministic problem is solved by a commercial solver. The solution serves as an input for the allocation of commodities to trams in the simulation. The formerly calculated solution becomes eventually infeasible as soon as a new commodity occurs or the capacity for cargo in a vehicle is lower due to a higher number of passengers than considered in the last optimizer run. Every time the current solution becomes infeasible, it is resolved by the optimizer with the current parameters from the simulation as input. The output is once again used in the simulation.

The underlying model and solution procedure are to be tested with the help of the tram network of the city of Frankfurt. Even if the results and conclusions are based on one case study, they should be as general as possible to ensure transferability on other networks. Nevertheless, future works should consider different case studies of other cities or synthetic datasets to test the transferability and generalization of the proposed model and solution approach. Moreover, future research should design different solution approaches for the deterministic problem. In the underlying case, the deterministic problem was solved by a commercial solver. Other solution methods, like heuristics, can realize shorter computational times. In real life, tram networks often face delays or traffic disruptions. In the case of FOT, this

would also lead to a delay in the transportation time which is not considered in the underlying model. Therefore, these additional factors should be considered to ensure transferability to real-life networks and use cases.

References

1. OECD: E-commerce in the time of COVID-19. OECD policy responses to coronavirus (COVID-19) (2020). <http://www.oecd.org/coronavirus/policy-responses/e-commerce-in-the-time-of-covid-19-3a2b78e8/>
2. United Nations: COVID-19 and E-Commerce. A global review. New York (2021)
3. Gutiérrez A, Miravet D, Domènech A (2020) COVID-19 and urban public transport services: emerging challenges and research agenda. *Cities Health*:1–4
4. Schwarz S (2020) Public transit and COVID-19 pandemic. *Global research and best practices*
5. Tirachini A, Cats O (2020) COVID-19 and public transportation: current assessment, prospects, and research needs. *JPT* 22
6. Vitrano C (2021) COVID-19 and public transport. A review of the international academic literature. Lund, Sweden
7. Cochrane K, Saxe S, Roorda MJ, Shalaby A (2017) Moving freight on public transit: best practices, challenges, and opportunities. *Int J Sustain Transp* 11:120–132
8. Marinov M, Giubilei F, Gerhardt M, Özkan T, Stergiou E, Papadopol M, Cabecinha L (2013) Urban freight movement by rail. *J Transp Lit* 7:87–116. <https://doi.org/10.1590/S2238-10312013000300005>
9. Shen J, Qiu F, Li W, Feng P (2015) A new urban logistics transport system based on a public transit service. In: Zhang Y, Yan X, Yin Y (eds) CICTP 2015. Efficient, safe, and green multi-modal transportation: proceedings of the 15th COTA international conference of transportation professionals, July 24–27, 2015, Beijing, China, pp 650–661. American Society of Civil Engineers, Reston, Virginia (2015). <https://doi.org/10.1061/9780784479292.060>
10. Behiri W, Belmokhtar-Berraf S, Chu C (2018) Urban freight transport using passenger rail network: Scientific issues and quantitative analysis. *Transp Res Part E Logistics Transp Rev* 115:227–245. <https://doi.org/10.1016/j.tre.2018.05.002>
11. Kelly J, Marinov M (2017) Innovative interior designs for urban freight distribution using light rail systems. *Urban Rail Transit* 3:238–254. <https://doi.org/10.1007/s40864-017-0073-1>
12. Bruzzone F, Cavallaro F, Nocera S (2021) The integration of passenger and freight transport for first-last mile operations. *Transp Policy* 100:31–48. <https://doi.org/10.1016/j.tranpol.2020.10.009>
13. Ghilas V, Demir E, van Woensel T (2016) A scenario-based planning for the pickup and delivery problem with time windows, scheduled lines and stochastic demands. *Transp Res Part B Methodol* 91:34–51
14. Mourad A, Puchinger J, van Woensel T (2020) Integrating autonomous delivery service into a passenger transportation system. *Int J Prod Res*
15. Do PT, Nghiem NVD, Nguyen NQ, Nguyen DN (2016) A practical dynamic share-a-ride problem with speed windows for Tokyo city. In: 2016 8th international conference on knowledge and systems engineering (KSE), pp 55–60. IEEE. <https://doi.org/10.1109/KSE.2016.7758029>
16. Cheng G, Guo D, Shi J, Qin Y (2018) When packages ride a bus: towards efficient city-wide package distribution. In: 2018 IEEE 24th international conference on parallel and distributed systems (ICPADS 2018), pp 259–266
17. Pternea M, Lan CL, Haghani A, Chin SM (2018) A feasibility study for last-mile synergies between passenger and freight transport for an urban area. In: transportation research board 97th annual meeting

18. Hurtigruten (2021) The History of Hurtigruten—sailing in the wake of giants (2021). <https://www.hurtigruten.com/about-hurtigruten/history/>
19. Rien W, Roggenkamp M (1995) Can trams carry cargo? New logistics for urban areas. *World Transp Policy Practices* 1:32–36
20. Robinson M, Mortimer P (2004) Rail in urban freight. What future, if any? *logistics & transport focus. J Inst Logistics Transp* 6:33–39
21. Robinson M, Mortimer P (2004) Urban freight and rail. The state of the art. *logistics & transport focus. J Inst Logistics Transp* 6:46–51
22. Elbert R, Rentschler J Freight on urban public transportation: a systematic literature review. *Res Transp Bus Manage*. Accepted for publication
23. Ji Y, Zheng Y, Zhao J, Shen Y, Du Y (2020) A Multimodal passenger-and-package sharing network for urban logistics. *J Adv Transp* 2020:1–16. <https://doi.org/10.1155/2020/6039032>
24. Mazzarino M, Rubini L (2019) Smart urban planning: evaluating urban logistics performance of innovative solutions and sustainable policies in the Venice lagoon—the results of a case study. *Sustainability* 11. <https://doi.org/10.3390/su11174580>
25. Pimentel C, Alvelos F (2018) Integrated urban freight logistics combining passenger and freight flows—mathematical model proposal. *Transp Res Procedia* 30:80–89. <https://doi.org/10.1016/j.trpro.2018.09.010>
26. Xie C, Wang X, Fukuda D (2020) On the pricing of urban rail transit with track sharing freight service. *Sustainability* 12:2758. <https://doi.org/10.3390/su12072758>
27. Regué R, Bristow AL (2013) Appraising freight tram schemes: a case study of Barcelona. *European J Transp Infrastruct Res* 13(1). <https://doi.org/10.18757/EJTIR.2013.13.1.2988>
28. Dampier A, Marinov M (2015) A study of the feasibility and potential implementation of metro-based freight transportation in Newcastle upon Tyne. *Urban Rail Transit* 1:164–182. <https://doi.org/10.1007/s40864-015-0024-7>
29. Fatnassi E, Chaouachi J, Klihi W (2015) Planning and operating a shared goods and passengers on-demand rapid transit system for sustainable city-logistics. *Transp Res Part B Methodol* 81:440–460
30. Ghilas V, Demir E, van Woensel T (2016) The pickup and delivery problem with time windows and scheduled lines. *Infor* 54:147–167. <https://doi.org/10.1080/03155986.2016.1166793>
31. de Langhe K, Meersman H, Sys C, van de Voorde E, Vanelslander T (2019) How to make urban freight transport by tram successful? *J Shipp Trd* 4:9. <https://doi.org/10.1186/s41072-019-0055-4>
32. Zhao L, Wang X, Stoeter J, Sun Y, Li H, Hu Q, Li M (2019) Path optimization model for intra-city express delivery in combination with subway system and ground transportation. *Sustainability* 11:758. <https://doi.org/10.3390/su11030758>
33. Arvidsson N, Browne M (2013) A review of the success and failure of tram systems to carry urban freight: the implications for a low emission intermodal solution using electric vehicles on trams. *European Transp/Trasporti Europei*
34. Dresdner Verkehrsbetriebe AG (2020) Die Dresdner Güterstraßenbahn—Ein System für alle Fälle? (2020). <https://www.dvb.de/-/media/files/die-dvb/dvb-vortrag-cargotram.pdf>
35. Riemann H (2021) Logistiktram. <http://www.logistiktram.de/#ancor-partner>
36. Schocke KO, Schäfer P, Höhl S, Gilbert A (2020) LastMileTram. Empirische Forschung zum Einsatz einer Güterstraßenbahn am Beispiel Frankfurt am Main. Frankfurt am Main
37. Stadt Zürich (2021) Cargo-tram und e-tram. https://www.stadt-zuerich.ch/ted/de/index/entsorgung_recycling/sauberes_zuerich/wo_%2B_wann_entsorgen/cargo-tram_und_e-tram.html
38. Baidur D, Macário RM (2013) Mumbai lunch box delivery system: a transferable benchmark in urban logistics? *Res Transp Econ* 38:110–121. <https://doi.org/10.1016/j.retrec.2012.05.002>
39. Rai S (2007) In India, grandma cooks, they deliver. *The New York Times*
40. SteadieSeifi M, Dellaert NP, Nuijten W, van Woensel T, Raoufi R (2014) Multimodal freight transportation planning: a literature review. *Eur J Oper Res* 233:1–15. <https://doi.org/10.1016/j.ejor.2013.06.055>
41. Pedersen MB, Crainic TG, Madsen OBG (2009) Models and tabu search metaheuristics for service network design with asset-balance requirements. *Transp Sci* 43:158–177. <https://doi.org/10.1287/trsc.1080.0234>

42. Layeb SB, Jaoua A, Jbira A, Makhoulf Y (2018) A simulation-optimization approach for scheduling in stochastic freight transportation. *Comput Ind Eng* 126:99–110. <https://doi.org/10.1016/j.cie.2018.09.021>
43. Hrušovský M, Demir E, Jammerneegg W, van Woensel T (2018) Hybrid simulation and optimization approach for green intermodal transportation problem with travel time uncertainty. *Flex Serv Manuf J* 30:486–516. <https://doi.org/10.1007/s10696-016-9267-1>
44. Toth P, Vigo D (eds) (2002) *The vehicle routing problem*. In: *SIAM monographs on discrete mathematics and applications*. Society for Industrial and Applied Mathematics, Philadelphia, Pa. <https://doi.org/10.1137/1.9780898718515>
45. Psaraftis HN, Wen M, Kontovas CA (2016) Dynamic vehicle routing problems: three decades and counting. *Networks* 67:3–31. <https://doi.org/10.1002/net.21628>
46. Ferrucci F, Bock S (2014) Real-time control of express pickup and delivery processes in a dynamic environment. *Transp Res Part B Methodol* 63:1–14. <https://doi.org/10.1016/j.trb.2014.02.001>
47. Regionalstatistik: Statistische Ämter des Bundes und der Länder: Bevölkerung nach Geschlecht (2021). <https://www.regionalstatistik.de/genesis/online?operation=abruftabelleBearbeiten&levelindex=1&levelid=1613471717464&auswahloperation=abruftabelleAuspraegungAuswahlen&auswahlverzeichnis=ordnungsstruktur&auswahlziel=werteabruf&code=12411-01-01-4&auswahltext=&werteabruf=Werteabruf#abreadcrumb>
48. VGF: Geschäftsbericht 2020 (2021). <https://www.vgf-ffm.de/de/die-vgf/zahlen-berichte/geschftsberichte/>

GIS-Based Model for Optimum Location of Electric Vehicle Charging Stations



Binal Vansola , Minal , and Rena N. Shukla 

Abstract Many countries are adopting Electric vehicle (EV), as the best available alternative source of traditional Internal Combustion Engine (ICE) vehicles. EVs are environment friendly as they emit zero exhaust Carbon Dioxide (CO₂) in the atmosphere. To increase the adoption rate of EV, it is pertinent to boost and develop the charging infrastructure. Installing public EV charging stations will highly promote the EV usage. The public EV charging station location depends upon various factors like investment cost, expected profit, land use, drag distance, waiting time, charging demand, and available power supply. The objective of this study is to develop a model based on geographical information system (GIS) for level 2 chargers, i.e., to locate a slow charging station in a commercial and industrial land use zone in Indian capital city of New Delhi. The study considers mixed traffic flow, typical of Indian traffic condition. The scope of study is limited to private vehicles like two-wheelers (2w) and four-wheelers (4w) only. Three-wheeler and commercial vehicle are excluded in this study. Slow charging station takes approximately 5–6 h per vehicle for a full charge. Slow charging stations are suitable for private vehicles which remain in parking for working hours of approximately 7–8 h in commercial and industrial zones. The QGIS-based model, presented in this study, is implemented for mixed traffic conditions for the study area. Origin–Destination data of NCT-Delhi has been used for modeling the charging demand.

Keywords GIS · Charging station · Electric vehicle · Land use · Optimum location

B. Vansola (✉) · R. N. Shukla
Civil Engineering Department, L. D. College of Engineering, Ahmedabad, India
e-mail: binal.vansola@gmail.com

R. N. Shukla
e-mail: renashukla@ldce.ac.in

Minal
Council of Science and Industrial Research—Central Road Research Institute, Transportation Planning and Environmental Division, New Delhi, India
e-mail: minal.crii@nic.in

1 Introduction

The electric light vehicle sales are increasing from 0.6% to 2.5% globally from 2015 to 2019, respectively [1]. As India has mixed traffic flow condition, the rate of growth of vehicle ownership is different for different classes of vehicles. According to India Brand Equity Foundation, India was the 5th largest auto market with 3.9 million units combined sold in the passenger and commercial vehicle categories [2]. Domestic automobile sales increased at 1.29% Compound Annual Growth Rate (CAGR) between financial year 2016–2020 with 21.55 million vehicles being sold in 2020. Automobile export reached 4.77 million vehicles in 2020, growing at a CAGR of 6.94% during financial year 2016–2020 [2]. Two-wheelers made up 73.9% of the vehicles exported, followed by passenger vehicles at 14.2%, three-wheelers at 10.5%, and commercial vehicles at 1.3% [2]. With the increase in vehicle ownership, the consumption of oil has also increased. The transportation sector is accountable for 49% of total oil consumption making it the largest consumer of oil in the world [3]. Indian transport sector consumes 99.6% of petrol (2 million tons) and 70% of diesel (6 million tons) annually [4] making India the world's third-largest energy consumer and Green House Gases (GHG) emitter after the US [4] and China, costing a staggering Rs. 8 lakh crores in import bill [3].

According to International Energy Agency (IEA), globally 45.1% of CO₂ emission is done by passenger vehicles that run on the road (cars, motorcycles, and buses) [3]. While 29.4% of CO₂ emission is done by freight transporting vehicles like trucks and lorries [3]. Since oil being a nonrenewable source of energy, it is nearing depletion as well as its usage by ICE vehicles leads to emittance of large amount of CO₂ in the atmosphere. Hence, the world is transforming toward the usage of electric energy as an alternative in the form of EV. Electric vehicles consume less energy than traditional ICE vehicles with zero emission in the environment. Many countries have started adopting EV as seen in Fig. 1. Figure 1 shows global EV stocks and the types of chargers installed in different countries. According to Fig. 1, China has a maximum stock of EV and the highest number of charger types is installed in China which are slow chargers.

The Indian government is also fostering EV adoption by launching National Electric Mobility Mission Plan (2020). Several states like Karnataka, Delhi, Andhra Pradesh, Uttar Pradesh, and Maharashtra have launched the policies that promote the use of EVs.

This paper is organized as follows: Sect. 2 presents an overview of literature survey of related work. In Sect. 3, various technical specification provided to understanding charging station and electric vehicles is discussed; in Sect. 4, methodology flow chart is discussed for QGIS-based model. In Sect. 5, application of the model to the study area is done and results are obtained. In Sect. 6, the conclusions and future scope of the work are discussed.

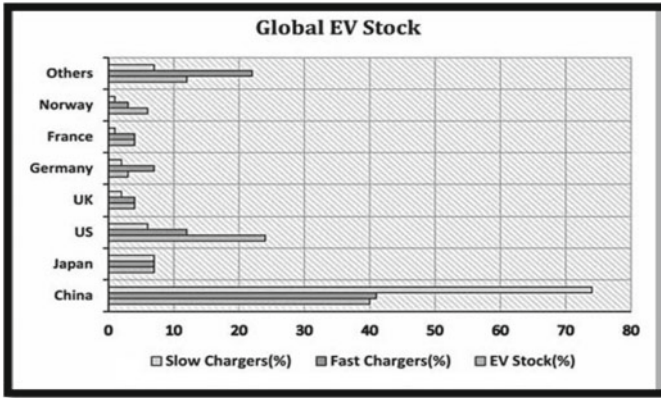


Fig. 1 Global EV and charging stock. *Source* Chandra and Minal [3]

2 Literature Review

The literature on the determination of the optimum location of EV charging stations can be classified into mainly two categories: first, finding charging station location for private vehicles and, second, determining the charging station location for autonomous electric vehicle (AEV). The method is further classified into three categories according to the types of chargers installed. The different types of chargers are level 1, level 2, and level 3 chargers.

The study by Braunl et al. [5] determines the optimum location and allocation of EV public charging stations in Western Australia [5]. The public Direct Current (DC) charging station is installed outside the urban area on the highway [5]. The study by Ngo et al. [6] proposed sequential two-level planning where the total system travel time and total system net energy consumption are considered [6]. The study by Quddus et al. [7] proposes long-term planning decisions and short-term operation decisions and developed a hedging algorithm to solve the location problem [7]. The study by Brandstatter et al. [8] is focused on the electric car-sharing system under stochastic demand and optimizing the problem by time-dependent integer linear program based on heuristic algorithm [8]. The study by Xu et al. [9] minimizes the accumulated range anxiety of concerned travelers to locate EV charging stations under minimum budget through a compact mixed-integer nonlinear programming model [9].

The study by Kaya et al. [10] used GIS to identify the most suitable location for a charging station by considering different parameters that affect the charging station location [10]. In this paper, they use multi-criteria decision-making (MCDM) methods to locate charging stations. The study by Iacobucci et al. [11] determines charging station location for shared autonomous electric vehicles [11]. Charging station location is optimized over longer time scales to minimize both approximate waiting times and electricity costs in Tokyo [11]. The study by Zhang et al. [12] is

also focused on locating a charging station for shared autonomous electric vehicles in urban areas by an agent-based simulation model, called BEAM [12]. Further, they use the output produced by the BEAM model in K means algorithm to locate the charging station. The study by Shen et al. [13] gives the detailed review on optimization of charging station location where literature is classified according to recurring themes, such as EV charging infrastructure planning, EV charging operations, and public policy and business models [13]. A study by Xiao-zhi [14] focuses on Nature-inspired Algorithm (NIO) and compared the method of different NIO [14]. A study by Morro-Mello et al. [15] determines the location for level 3 chargers in an urban area for taxis [15].

A study by Mohammad et al. [16] locates fast public charging stations for urban areas by the set cover method by using greedy algorithm and genetic algorithm [16]. They used pervasive mobility data which is collected by cell phone [17]. In a study by Bian et al. [17], the optimum charging station is determined by mixed-integer linear programming (MILP) model to maximize the profit of new charging station based on geographic information system (GIS) [17]. In a study by Efthymiou et al. [18], objective is to locate charging stations by genetic algorithm for the urban area [18]. They develop tools to locate charging stations which require input of the OD data, distance between zones and their latitude and longitude [18]. A study by Zhang et al. [12] focuses on multi-day data instead of single-day data to locate charging stations, and they compare the results generated by both multi-day data and single-day data [19]. A study by Chandra and Minal [3] focuses on the challenges of EV adoption in India, and they also provide the solution to different challenges [3].

There are several studies regarding EV charging station location for single traffic using fast charger. This leads to the motivation behind this study to develop a model for mixed traffic flow and charging stations with slow chargers. Many models are developed based on GA-genetic algorithm, set cover method, linear integer programming, and k means clustering but few studies are done on GIS-based model development. Thus, this study aims to develop a GIS-based model for optimum location of charging stations with slow chargers for mixed traffic condition of New Delhi.

3 Technical Specification

3.1 Charging Station Specification

According to Table 1, charging station is classified into three categories. Level 1 charger is a slow charger, and power requirement is low; therefore, it is installed in a residential area. Level 2 charger is installed at commercial and residential zone. The charging time of EV charge by level 2 charger is shorter than level 1 charger. Level 3 charger is a fast charger that requires a higher electric supply. Therefore, it is installed in a commercial zone. Level 2 charger can be installed at parking lots: office parking, shopping mall parking, etc.

Table 1 Charging station specifications

Type of charging station	Power supply required	Mounting	Where to install
Level 1	120 VAC, 15A/16 A	Wall pole, bollard	Residential area
Level 2	208/240 VAC, 30 A	Wall pole, bollard	Commercial zone/residential zone
Level 3	240–500 VDC, 125 A	Gas station	Commercial zone

3.2 EV Specification Electric 2W and 4W

Tables 2 and 3 describe the specification of electric 2W and 4W. Electric 2W and 4W take an average of 4–5 h and 7–8 h, respectively, to charge by level 2 chargers. Level 2 chargers can only be installed at the locations where people spend a higher amount of time, i.e., at industrial and commercial zone. The vehicles like 3W cannot charge during pick up and drop time. The commercial vehicles wait for uploading and downloading the goods which are limited to 15 min only and not sufficient for charging at level 2 charging station in study area; therefore, 3W and 4W are not considered in this study. As charging time is higher, hence max 3–4 vehicles can be charged through a single charging plug within 24 h in a day. Here, in calculation one charger per private vehicle is considered at study area during working hours.

Table 2 Electric 2w specification [20–22]

S. No.	Model name	Range (km)	Power requires	Charging time (h)
1	OPTIMA HS 500 ER	113	51.2 V/30 A h	4–5
2	NYX HX	127	51.2 V/30 A h	4–5
3	OPTIMA E5	80	48 V, 28 A h	4–5
4	RV 300	99	1500 W	4.2
5	ZEAL VX1	102	60 V 1200 W	5–6
6	iPraise+	139	72 V, 40 A h, 2500 W	4–5
7	SPOCK	107.4	72 V, 40A h, 2000 W	3

Table 3 Electric 4w specification [23, 24]

S. No.	Model name	Range	Charger	Charging time (h)
1	Tata Nexon	312	15 A	8.5
			Fast charging	1
2	Mahindra eVerito D2	181	288 A h—fast charging	1.5
			21.2 kwh	11.5
3	Tata Tigor	213	Fast charging	2

3.3 Segment Wise Analysis

EV take-up/penetration rate for 2W will increase by 7–10% by 2025, and it will rise to 25–35% by 2030 [25, 26]. The EV penetration rate for 4W will reach 1–3% by 2025, and it will increase to 10–15% by 2030 [25, 26].

4 GIS-Based Model

GIS-based model can be used to locate charging stations. Analysis was done by analyzing various maps related to the study area. For EV charging station location, useful maps are land use map, zone map, route map, and point of interest map. In this study, the analysis is carried out on a zone map, grid map, and land use map in QGIS open-source software.

For the analysis following tools are used:

- Vector tools
- Analysis tools
- Research tools
- Geometry tools
- Geoprocessing tools.

4.1 Methodology

Maps Creation in QGIS Create maps in QGIS, which are zone map, grid map, and land use map. The study area is divided into known overlapping traffic zones or wards to get the OD data. To locate the charging station at a certain distance, divide the study area into grids. Therefore, the dimension of the grid is according to the allowable distance between the charging stations. A land use map is a map that gives information about the type of land use available in the study area. Different land uses are industrial zone, commercial zone, recreation zone, institutional zone, and green areas.

Validity Checks Validity checks are done on maps by using a strict Open Geospatial Consortium (OGC) definition of polygon validity, where a polygon is marked as invalid if a self-intersecting ring causes an interior hole. If maps pass the validity check, then the next step will be performed in QGIS. If the map did not pass the validity checks, then we create a new map (Fig. 2).

Join Attributes of Maps The different maps can be joined by common attributes location in QGIS. The grid map and land use map are joined to know which grid contains industrial zone and commercial zone. Grids that cover industrial zones and residential zones are our charging station's location. When zone map, grid map,

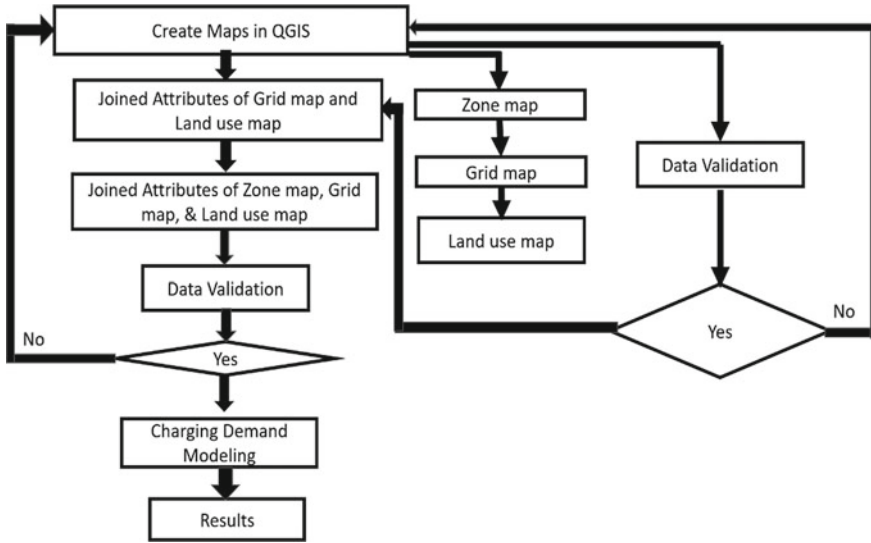


Fig. 2 Flow chart of methodology

and land use map are joined together by attributes' location, then we arrive at the approximate charging demand to analyze the charging plugs required to be installed.

Validation of Map : Perform validity checks on the joint attribute location maps. If the map passes the validity checks, then the next step will be performed.

Modeling Charging Demand To calculate charging demand, the EV penetration rate is set, considering the segment-wise average EV penetration rate by 2025 for private vehicles (2w and 4w) as presented in Table 4 [25, 26]. OD data of zones gives the value of the vehicle trips in respective zones throughout the day. According to the study done by Braunla et al., 60–80% of EV owners charge their electric vehicles at home; and 40–20% of EV users will use public charging stations [5]. Therefore, it is assumed that 60% EV owner will charge their vehicles at home and 40% will use the charging stations. We have OD data for all 360 traffic zones. To locate charging station at 3 km distance, 3 km × 3 km grid map is created. The location of CS will provide as centroid of each grid. Therefore, converted OD data from zone to grid by using below formulae where charging demand in zones is calculated by considering EV penetration rate, rate of EV user will use public charging station and rate of people will come into industrial and commercial zone. Charging demand in grids is calculated as:

$$Z = \{z_1, z_2, \dots, z_n\} \tag{1}$$

$$G = \{g_1, g_2, \dots, g_n\} \tag{2}$$

Table 4 Segment-wise analysis of Electric 2w and 4w [25, 26]

Segment	Sub-segment	EV penetration (%)	
		2025	2030
2w	Scooters	10–25	50–70
	–B2B	40–60	60–80
	–B2C	13–18	40–60
	Motorcycles	1–2	10–20
	Overall	7–10	25–35
4w—PV	Personal	1–3	10–15

Distribute zone demand in grids:

$$f_{ij}, j \in p_i = \frac{d_i}{m_i} \quad (3)$$

Total charging demand in grid:

$$c_j = \sum f_{ij}, i \in q_j \quad (4)$$

where

p_i Overlap grids in w. r. t zone i

m number of overlap grids in zone

f_{ij} Distribution factor of demand from zone to grid

q_j Zone corresponding to grids

c_j Total charging demand in grid j

z Set of zones

z_i Zone i

g_j grid j

i Zone number

j Grid number

d_i Charging demand or destine vehicles in zone i

m Number of grids overlap over zone i .

5 Case Study

The GIS-based model is implemented on NCT-Delhi, which has an area of 1484 km². Delhi is divided into 360 traffic zones, as shown in Fig. 3. OD data of 360 traffic zone of Delhi is collected. Grid map of Delhi is shown in Fig. 4. The grid map contains 204 grids, while the dimension of the grid is 3 km × 3 km which is taken as according to Delhi government EV policy 2020 [27]. Based on Delhi government EV policy 2020, distance between two charging stations should not be more than

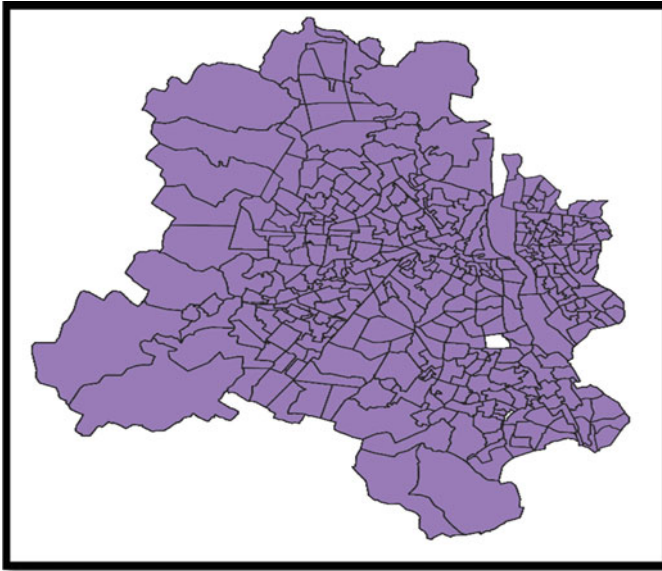


Fig. 3 Traffic zone map of Delhi created in QGIS

3 km. The land use map gives information about land use types which are residential, commercial, industrial, farmland, forest, grass, retail, cemetery, meadow, military, natural reserve, orchard, park, and recreation ground, as seen in Fig. 5. All three maps have been validated. Maps are created by joining attribute by location. First, taking the grid map and the land use map, a total 2550 combination is generated by joining two maps. 91 charging station location is identified for level 2 chargers. To calculate charging demand, we create a map by joining attributes of all three maps. A total of 30,516 combinations are generated after joining the three maps.

The EV penetration rate is set to calculate charging demand of EV for different classes of vehicles. By being not too pessimistic and optimistic, the average EV penetration rate is taken as per the segment-wise analysis. Assuming, 40% of EV users will use the public charging station to charge their vehicles. The two standard assumptions have been taken as shown in Table 5. Given the number of electric vehicles in grids, it did not indicate that every vehicle will come at commercial and industrial zones. There are other zones also available within the grid. Hence, we assume that 60% of total electric vehicle will come at commercial or industrial zone and 40% of total EV are in other than commercial and industrial zone.

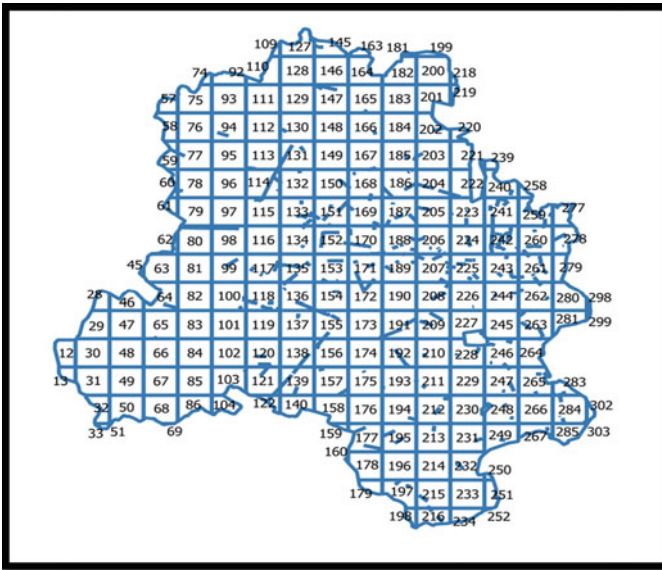


Fig. 4 Grid map of Delhi created in QGIS

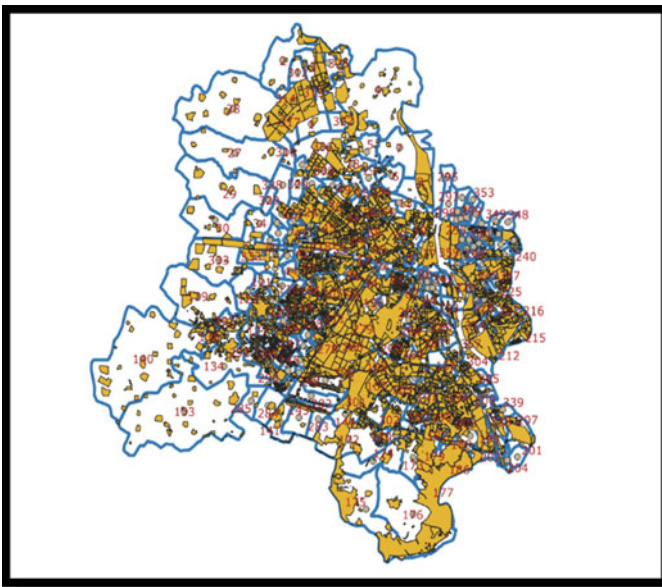


Fig. 5 Land use map of Delhi. Source Geofabric.de [28]

Table 5 Assumptions for demand modeling

Category of vehicles	Average EV penetration rate by 2025 (%) [25, 26]	Public charger users (%)	Percentage of EV user comes in industrial and commercial zone (%)
2w	8.5	40	60
4w	2	40	60

5.1 Result

The charging station locations are found by plotting 204 grids of size 3 km × 3 km. Out of 204 grids, 91 grids are found to have location for charging station as determined by QGIS-based model as shown in Fig. 6. All 91 grids consist of the industrial and/or commercial zone in addition to other zones. Remaining 113 grids have neither industrial nor commercial or both as land use. According to demand modeling, the approximate number of required charging plugs is calculated. As expected, with a decrease in grid dimension from 3 km × 3 km to 2 km × 2 km, the number of charging stations will increase from 91 to 136. The average distance between the charging stations for 3 km × 3 km is approximately 2.8 km. While the result generated for 2 km × 2 km grid, the average distance between charging station is 2 km.

When we change the grid dimension, the number of charging stations changes accordingly. However, the location will remain the same because the land use area will not change.

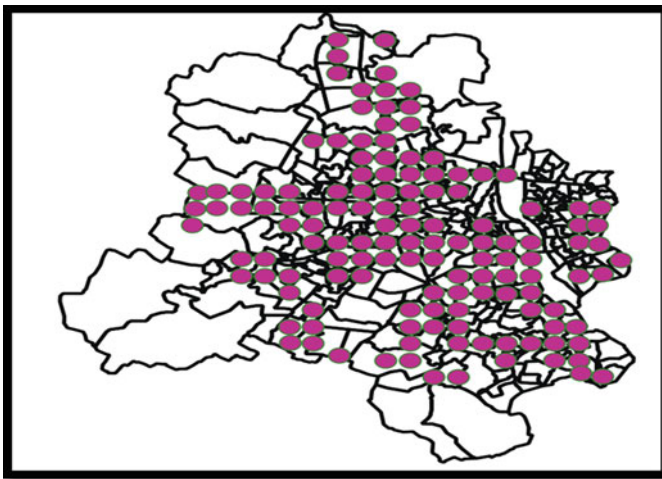
Table 6 shows the result generated from 3 km × 3 km grids for randomly selected 10 grid numbers as sample [27]. Table 6 consists of the selected 10 grids by its



Fig. 6 Charging station location for 3 km × 3 km grid for study area

Table 6 Charging station at grid number and respective charging plugs required to install for 2w and 4w

Grid No.	Charging plugs for 4w	Charging plugs for 2w
62	40	31
63	40	31
80	26	20
81	40	31
98	50	39
99	278	275
100	264	204
101	121	194

**Fig. 7** Charging station location for 2 km × 2 km grid for study area

number, which is the charging station location and charging plugs required to be installed in respective grids. The maximum charging plugs are 387, which needs to be installed at grid 262. Grid 262 has maximum charging demand. While, minimum 3 charging plugs are required to be installed at grid 103, which has minimum charging demand (Fig. 7).

6 Conclusions

The electric vehicle penetration rate for two-wheelers will be 7–10% by 2025, and it will increase to 25–35% by 2030. The EV penetration rate for 4w will reach 1–3% by

2025, and it will rise to 10–15% by 2030. The prevailing scenario says that only 40% of electric vehicle users will use public charging stations and rest 60% of electric vehicle users will charge their EV at home.

Level 2 charging station is located at a place by considering the land use data. If located level 2 charging station has commercial and/or industrial zone, then it has a wider usage. Charging a vehicle through a level 2 charger requires a longer time for a full charge. Generally, people spend a longer duration in commercial and residential zones compared to other zones. Therefore, a level 2 charging station is located in the commercial and industrial zones. The fast-charging station-level 3 is suitable for places like parking lot, gas station, and petrol station.

According to the Delhi government EV policy 2020, the distance between charging stations should be less than 3 km [27]. Thus, a 3 km × 3 km grid size has been taken in the study to locate the charging station in QGIS. The result shows, if a 3 km × 3 km grid map is used in the model, then the average distance between the charging stations is 2.8 km. To conclude the study, 91 location of level 2 charging station is found in Delhi for the commercial and industrial zone. All 91 locations are centroid of 3 km × 3 km grid.

The future scope of the study lies in expanding it to develop the model based on different criteria. To expand this study, various optimization methods can be integrated with QGIS. This study may prove useful for planning for future EV charging infrastructure development. The developed model can be used as a guide for other Indian cities to locate level 2 charging stations for mixed traffic flow conditions.

Acknowledgements Support from Project OLP-0624 sponsored by CSIR-Central Road Research Institute, New Delhi, India, was received to assist with the preparation of this manuscript.

References

1. Gersdorf T, Hertzke P, Schaufuss P, Schenk S (2020) McKinsey electric vehicle index: Europe cushions a global plunge in EV sales. [Online]
2. Ministry of Commerce & Industries and Government of India. Indian Automobile Industry Report. India brand equity foundation, New Delhi, India (2021)
3. Chandra S, Minal S (2019) Challenges of electric vehicle adoption in India. Research Gate
4. PIB (2014) 70% of diesel, 99.6% of petrol consumed by transport sector. Press Information Bureau, Government of India, Ministry of Petroleum & Natural Gas, New Delhi
5. Bräunla T, Harriesa D, McHenryb M, Wagera X (2020) Determining the optimal electric vehicle DC-charging infrastructure for Western Australia. *Transp Res Part D*:1–15
6. Ngo H, Kumar A, Mishra S (2020) Optimal positioning of dynamic wireless charging infrastructure in a road network for battery electric vehicles. *Transp Res Part D*:1–21
7. Quddus MA, Kabli M, Marufuzzaman M (2019) Modeling electric vehicle charging station expansion with an integration of renewable energy and vehicle-to-grid sources. *Transp Res Part E*:251–278
8. Brandstätter G, Kahr M, Leitner M (2017) Determining optimum locations for charging stations of electric car sharing systems under stochastic demand. *Transp Res Part B*:17–35
9. Xu M, Yang H, Wang S (2020) Mitigate the range anxiety: Siting battery charging stations for electric vehicle drivers. *Transp Res Part C Emerg Technol*:164–188

10. Kaya Ö, Tortum A, Alemdar KD, Çodur MY (2020) Site selection for EVCS in Istanbul by GIS and multi criteria decision making. *Transp Res Part D Transp Environ*:1–16
11. Lacobucci R, McLellan B, Tezuka T (2019) Optimization of shared autonomous electric vehicles operations with charge scheduling and vehicle-to-grid. *Transp Res Part C*:34–52
12. Zhang H, Sheppard CJ, Lipman TE, Zeng T, Moura SJ (2020) Charging infrastructure demands of shared-use autonomous electric vehicles in urban areas. *Transp Res Part D*:1–16
13. Shen ZJ, Feng B, Mao C, Ran L (2019) Optimization models for electric vehicle service operation: a literature review. *Transp Res Part B*:462–477
14. Gao XZ, Deb S, Tammi K, Kalita K, Mahanta P (2019) Nature-inspired optimization algorithms applied for solving. Springer Transportation
15. Morro-Mello I, Padilha-Feltrin A, Melo JD, Calvino A (2019) Fast charging stations placement methodology for electric taxis in urban zones. *Energy*
16. Vazifeh MM, Zhang H, Santi P, Ratti C (2019) Optimizing the deployment of electric vehicle charging station using pervasive mobility data. *Transp Res Part A*:75–90
17. Bian C, Li H, Wallin F, Avelin F, Finding the optimal location for public charging stations—GIS based—MLIP approach. Science Direct Energy Procedia, Hong kong, China
18. Efthymiou D, Chrysostomou K, Morfoulaki M, Aifantopoulou G (2017) Electric vehicles charging infrastructure location: a genetic algorithm approach. *Transportation*
19. Zhang A, Kang JE, Kwon C (2020) Multi-day scenario analysis for battery electric vehicle feasibility assessment and charging planning. *Transp Res Part C*:439–456
20. <https://ev.delhi.gov.in/>. (2020)
21. H. Electric, heroelectric.in, (2020). [Online]. <https://heroelectric.in/bike/optima-hx-dual-battery/>
22. Bikewale, www.bikewale.com, Heroelectric Bikes, (2020). [Online]. <https://www.bikewale.com/heroelectric-bikes/optima/>
23. <https://nexonev.tatamotors.com/>. (2020)
24. <https://www.mahindra.com/>. (2020)
25. Tomar D, Priya S (2020) auto.economictimes.indiatimes.com, 04 November 2020. [Online]. <https://auto.economictimes.indiatimes.com/news/passenger-vehicle/cars/only-10-15-penetration-of-electric-cars-is-expected-by-2030-in-india-report/79039710#:~:text=electric/20cars/20in/20India/3A/20Only,Report/2C/20Auto/20News/2C/20ET/20Auto>
26. Energy S (2020) Shifting gears: the evolving electric vehicle landscape in India. KPMG & CII Report 4(11):1–40
27. Jyoti Sheth DC transport.delhi.gov.in, [Online]. Available: https://transport.delhi.gov.in/sites/default/files/All-PDF/Delhi_Electric_Vehicles_Policy_2020.pdf
28. <https://geofabrik.html>. [Online]. <https://download.geofabrik.de/asia/india.html>
29. Hannah R (2020) Cars, planes, trains: where do CO₂ emissions from transport come from?, CO₂ and Greenhouse Gas Emission and Energy

Optimizing Points of Intersection for Highway and Railway Alignment—Using Path Planner Method and Ant Algorithm-Based Approach



M. B. Sushma, Sandeepan Roy, and Avijit Maji

Abstract The essential decision factors that govern the design of highway and railway alignment are the number of intermediate points (PIs), their locations, and the circular curve radius. The development of optimal alignment involves many challenges, such as evaluating an infinite number of potential solutions, complex terrain, environmental conditions, entwined complicated cost, and design constraints. The alignment development process is primarily manual, highly expensive, and time consuming and is also not practically feasible. So, many computer-aided optimization methods were developed to address the alignment optimization problem. However, most of these methods predefine the value of either one or more of these factors; thus, this approximation of values limits these models from obtaining an optimal solution. This paper proposes a heuristic-based path planner method (PPM) to address such issues. The model includes (a) exploration of non-convex high-dimensional space for obtaining a least-cost horizontal alignment, (b) sampling technique, along with PPM, is used to generate potential PIs and develop feasible alignments by finding a suitable number of intermediate PIs at feasible locations followed by curve fitting at each PIs, and (c) geographical information system (GIS) database is integrated with the method for estimation of right-of-way cost and environmental impact. The alignment is developed as per the standard geometric design guidelines of highway and railway alignment. The effectiveness of the model is verified by using it for a real-world case study. The proposed method is capable of automatizing the development of a green field horizontal alignment and can aid engineers in the process of planning and development.

M. B. Sushma (✉)

Department of Civil Engineering, Kakatiya Institute of Technology and Science,
Warangal 506015, India

e-mail: prustysushma618@gmail.com

S. Roy · A. Maji

Department of Civil Engineering, Indian Institute of Technology Bombay, Mumbai 400076, India

e-mail: sandeepan.roy1991@iitb.ac.in

A. Maji

e-mail: avimaji@iitb.ac.in

Keywords Highway and railway alignment · Ant algorithm · Path planner method (PPM) · Alignment optimization

1 Introduction

The challenge of obtaining an optimal highway and railway alignment is a cumbersome task and is highly topical in civil engineering. In general, the primary objective of any alignment optimization method is to obtain a permissible layout while minimizing the overall cost of the highway and/or railway project. The layout must meet the specified constraints provided by the design standards as well as intrinsic the physical attributes of the location, such as considering the regions from where alignment must pass and/or the prohibited regions.

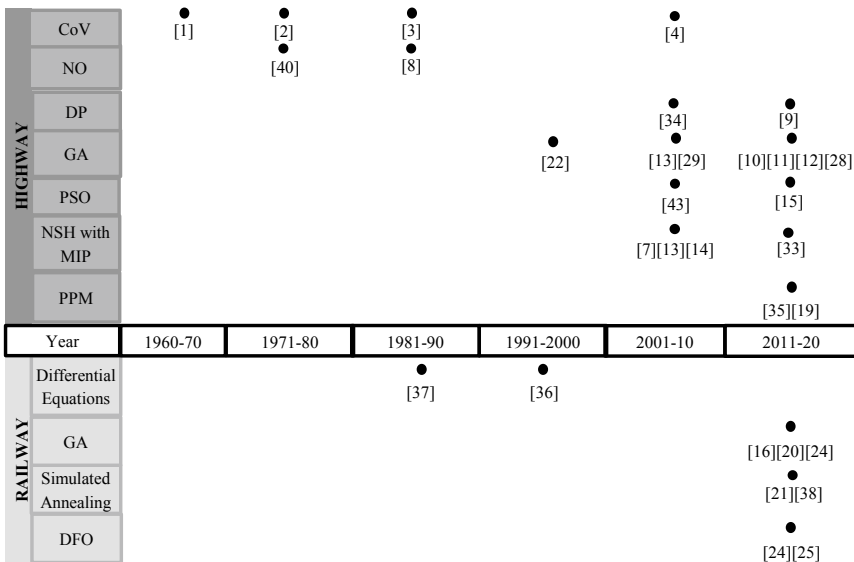
During the period of 1960s–1990s, the researchers mainly used the mathematical-oriented conventional methods to solve the alignment optimization problem, including the calculus of variation (CoV) [1–4], numerical search [5], linear programming [6], enumeration [7], network optimization (NO) [8], and dynamic programming (DP) [9]. In actual application, the objective functions considered for alignment optimization should comprise mathematical properties such as nonlinearity, non-differentiability, and non-convexity in cost functions. These aforementioned methods involved many unreasonable assumptions and were not capable to efficiently solve the alignment optimization problem and also not competent in dealing with complex constraints in real-world scenarios.

Mathematical-based optimization models along with heuristic algorithms blend into a powerful tool for resolving any optimization problem. These optimization methods were efficient in solving the alignment optimization problem. The aforementioned technique produced the alignment solutions at a reasonable computational time with fair memory usage. It did not require the derivatives and differentials of explicit functions, unlike the classic mathematical models. These algorithms are genetic algorithm (GA) [10–12], neighborhood search heuristics for mixed integer programming (NSH with MIP) [13, 14], particle swarm optimization (PSO) [15, 16], simulated annealing [17], grid adaptive direct search [18], path planner method (PPM) [19], and distance transform [20, 21].

Among all heuristic algorithms, GA is the most popular method that has been used to solve the alignment optimization problem. This method converted the alignment problem into similar techniques as in biological evolution, gene crossing and mutation are implemented. In this, the intersection points of the alignment, i.e., PIs, are considered as gene and various crossover mutation operators to solve the alignment optimization problem. It was further extended by integrating it with GIS applications to exploit the geospatial topographical data [22]. Model's efficiency was further extended by hierarchical optimization strategy [12, 23] and formulating the multi-objective optimization model [10, 11]. However, this model typically considers a predefined distribution of the PIs at specified orthogonal planes. Furthermore, there was no sufficient explanation defining the spacing or location of the planes, which

reduced the reliability of the obtained solution. Other heuristic methods tried to replace the orthogonal cutting planes with grids and angular bisector [18, 23, 24]. Still, the model required an initial set of PIs with predefined or specified location and its count. Instead of specified orthogonal sections, a butterfly-shaped region is used for PIs distribution in a PSO [25]. It produced a better solution than the one constrained with orthogonal sections [24]. However, the model limited the search in a single forward direction using a greedy search technique, in which the obtained solution may not be globally optimal. Figure 1 summarizes the relevant methods and their corresponding references for both highway and railway alignment.

The literature review establishes a need for an automated computer-aided model that can efficiently develop a greenfield highway and railway alignment without a predefined number of the PIs, confining the location of the PIs to any present grid, lattice, square, orthogonal sections, or any defined pattern, initial information of the existing alignment for cost optimization, and predefined constant radius for horizontal curves. The paper proposes a heuristic-based PPM that addresses these issues and develops the least-cost alignment even within a search space containing complex clustered environmental regions. This model increases the flexibility in alignment development and enhances the precision of alignment developed during the planning stage.



NL-MIP = Nonlinear Mixed Integer Programming

DFO = Derivative-free Optimization

Fig. 1 Methods to optimize horizontal highway and railway alignment

The highway and railway alignments design consists of line sections connected with circular and transition curves to provide a smooth transition. Primarily, horizontal alignment design considers the circular curves to prevent the lateral skid of the vehicle while retaining the centrifugal force, which is possible due to suitable curve sections and superelevation (for highways) or cant (for railways). The model exploits the search space to obtain a globally optimal alignment solution. It minimizes the objective cost for the standard geometric design constraints. Highway and railway alignment development problems have similarities. In both cases, the developed alignment is constrained by land use features, topology, and socio-environmental factors, incurs considerable investment, deals with vast amounts of geospatial information, and involves complex computational effort [26].

The model is integrated with a GIS database to exploit the spatial features of the region for obtaining a realistic alignment. It extensively explores the study region and ensures that horizontal alignment's objective function and standard design guidelines are fulfilled [19]. Ant algorithm (AA) is one of the most successful strands of swarm intelligence [27] and can generate promising results at faster convergence capability [28]. So, the efficacy of the proposed method is demonstrated by comparing it with the AA for developing a green field horizontal alignment for both highways and railways.

2 Horizontal Alignment Cost Model and Problem Formulation

The length-dependent costs, location-dependent costs, and environmental impact constitute the cost of horizontal alignment. Construction cost is associated with the alignment length. The overall alignment length, $L(\text{HA})$, can be evaluated as the summation of the length of all tangents and curves, as shown in Eq. (1) [10, 11, 29]. Length-dependent cost (TC_{LNC}) is the unit length cost associated with the alignment construction, as in Eq. (2).

$$L(\text{HA}) = |HPI_0, A_1| + \sum_{i=1}^N |B_i, A_{i+1}| + |B_N, HPI_{N+1}| + \sum_{i=1}^N R_i \theta_i \quad \forall i = 1, 2, 3, \dots, N \quad (1)$$

where, $\theta_i = \text{rcos} \left(\frac{(HPI_{i-1} - HPI_i) \cdot (HPI_{i+1} - HPI_i)}{HPI_{i-1} - HPI_i, HPI_{i+1} - HPI_i} \right)$

$$\text{TC}_{\text{LNC}} = L(\text{HA}) \times U_{\text{ld}} \quad (2)$$

where

- N total number of PIs
 U_{ld} unit length-dependent cost
 R_i radius of i th circular curve
 θ_i angle of intersection of i th circular curve

The costs associated with the land acquired for the development of highways and railways are known as location-dependent costs. It includes the cumulative cost of different land parcels acquired for constructing the highway, such as agricultural land, residential area, and built-up areas, depending highly on the project site. The portion of land parcels through which alignment passes is summed to evaluate the overall location-dependent cost. Let L_{CUM_i} and uc_i be the unit cost and the acquired portion of the i th land parcel, then, the ROW cost will be $L_{CUM_i} \times uc_i$. Thus, $uc_i = 0$ if the alignment avoids a specific land parcel. Let PL be the total count of the land parcels; thus, overall location-dependent cost, TC_{LOC} , can be evaluated by Eq. (3) [10]. The environmental impact is evaluating the impact on various environmentally sensitive regions, such as wetlands, forests, and marshes. Impact on these land features, TC_{ENV} , can be mathematically evaluated similar to the location-dependent cost, as in Eq. (4), where α is the penalty cost, e_j is the fractional area of j th environmental land parcel, and EPL is the total count of environmentally sensitive land parcels.

$$TC_{Loc} = \sum_{i=1}^{PL} L_{CUM_i} \times uc_i \quad (3)$$

$$TC_{ENV} = \sum_{i=1}^{EPL} \alpha \times e_j \quad (4)$$

The total alignment length depends on the length of the tangential sections (obtained as per the location of the PIs) and horizontal curve sections. An adequately designed horizontal curve can also minimize the impacts on environmentally sensitive areas. Thus, the objective is to minimize the overall horizontal alignment cost (C_{HA}) by minimizing the total length-dependent, location-dependent, and environmental impact cost, and mathematically, it is represented as Eq. (5).

$$\text{Minimize } C_{HA} = TC_{LNC} + TC_{LOC} + TC_{ENV} \quad (5)$$

3 Path Planner Method (PPM)

PPM is based on the rapidly exploring random tree (RRT) algorithm [30]. It has a wide application in robotics and biomedical science for determining the effective pathway for robots by avoiding the obstacles and steering a needle in the clustered environment, respectively. Thus, it is efficient in identifying the shortest path even

in the high-dimensional space configurations. However, in alignment design, apart from cost minimization, it needs to satisfy the environmental and design constraints [31]. Hence, RRT is improvised to attain the alignments requirements.

PPM incrementally propagates from a start point, S_{start} , by using a set of random points, S_{rand} generated in the search space [19, 32]. These points are generated using the low-dispersion sampling principle. The idea behind using this sampling technique is to have an equidistribution of the points in the search space to promote maximum exploration. Once a point is placed, the dispersion is checked. It uses a metric-based criterion that identifies the largest vacant space without any sample points. The dispersion (δ) measures the space coverage of a finite point set (R) and is presented in Eq. (6).

$$\delta(R, \emptyset) = \sup_{y \in S} \min_{r \in R} \emptyset(y, r) \quad (6)$$

where \emptyset represents the largest circular radius within the space S . To reduce dispersion, it is necessary to reduce the radius y , i.e., the metric. In this study, the metric that determines the distance between the generated points is defined as the step size. Its value is based on highway geometric standards. While progressing, the model iteratively expands in the form of a path tree, ω . Table 1 describes the PPM functions used for generating horizontal alignment. In a tree, the S_{rand} is considered as one of the potential PIs (PPIs). The line segment joining these PPIs is classified as the edge, ψ , of the path tree. Hence, it can be represented as $\omega(\text{PPI}, \psi)$, where $\text{PPI} \subset S$ and $\psi \in \text{PPI} \times \text{PPI}$. The subset of PPIs that ultimately connects the S_{rand} and the endpoint, S_{End} , is defined as the PIs of the developed alignment. So, the generation of each S_{rand} aids in the expansion of the path tree. All the PPIs of the path tree within the vicinity of S_{rand} are identified. The boundary of the neighborhood region (i.e., the circumference around the S_{rand}) is decided based on the adopted step size, whose range depends on the minimal tangent length. The process selects the nearest point ($\text{PPI}_{\text{nearest}}$) among all the identified points that yields the shortest distance between S_{start} and S_{rand} in ω . .. In obstacle overlap, if the developed path overlaps an area considered a soft constraint (i.e., where the alignment is permitted to pass with a penalty), then the respected land parcel cost is added to the cost of the path. But, if it is a prohibited area, then the point is discarded, and a new S_{rand} is developed at a different location using *Addpoint* function. Otherwise, P_{rand} is added as a new point to the path tree, PPI_{new} , the edge between PPI_{new} and $\text{PPI}_{\text{nearest}}$ becomes part of the path tree, and the $\text{PPI}_{\text{nearest}}$ is considered as the parent of PPI_{new} through *ChooseParent* function. After inducting a new point (PPI_{new}) in the path tree, the PPIs that can potentially connect with the PPI_{new} in the search space and are within the local vicinity of PPI_{new} are assessed, and the edges of the identified neighborhood points are optimized. The total path lengths from the S_{start} to these PPIs, through PPI_{new} , are estimated. For a specific PPI , if this length is less than the existing one, then the existing link between the PPI and its parent point is removed and reconnected with PPI_{new} using the *Reconnect function*. If S_{End} exists in the vicinity of the PPI_{new} , it develops a

connection with S_{End} and creates the initial horizontal alignment $HA[0, 1] = (PI, \psi)$. The developed solution may contain PIs with zero angles of deflection. For such a case, *SmoothTrajectory* function is used to eliminate those PIs and aid in developing a straighter alignment. This process continues until it connects the termini, thus developing an initial solution. After that, the algorithm searches the entire space for potentially feasible connections with minimum cost and reconnects to refine the alignment. The method progresses till it meets the termination criteria, i.e., either it has attained the maximum iterations, M , or improvement in the alignment cost is less than 5% of the obtained best solution for ten consecutive iterations. The algorithm for path tree development is shown in Fig. 2.

Table 1 Description of functions in PPM

Function	Description	Purpose
Sample	Maintains set of random point population defined in the obstacle-free region	Generates random point $S_{rand} \in S_{area}$, where S_{area} represent the search space
Neighbors	Set of points present within the neighborhood of the new point	Identifies all points present within the step size and selects an optimal point
Distance	Cost of each edge connected to the tree in S_{area}	Calculates the cost of an obstacle-free path in terms of Euclidean distance between the two points
Nearest	Searches for the possible nearest point $PPI_{nearest}$ in the study area that can be connected to form a path	Helps to add random points to the tree, and joins with the nearest point in the study area
Obstacle check	Checks whether the path connected by the steer function lies in the obstacle-free region	Helps the generated path to avoid environmentally sensitive areas
Choose-parent	Checks if the cost of the path from initial point to the newly added random point to the tree is reduced	Helps to select the optimal points to add in the tree
Add point	Adds a random point to the tree, which is removed by the forced removal. Also, adds point if it reduces the path cost	Helps to optimize the path after reaching the maximum number of random points
Reconnect	Removes connections that increases the cost of the path	An optimal connection to the cost function is selected
Total cost	Determines the total cost of the path	Reviews cost of generated path with the existing one to select an optimal path
Smooth trajectory	Incorporates smooth continuous curvature into the piecewise linear path	Avoids sharp ends of a path by adding curve in between the tangential sections

```

1.  $\omega(PPIs, \psi) \leftarrow PPM(S_{start}, M, I)$ 
2.  $\omega \leftarrow InsertPoint(P_{rand})$ ;
3. for  $i = 1$  to  $i = I$  do
4. if  $M < PointsAdded(\omega)$ , then  $\omega_{old} \leftarrow \omega$ ; end if
5. if  $M > PointsAdded(\alpha)$ , then  $Addpoint(S_{rand}) \leftarrow$   

    $Removepoint\ onlychild(Parent(PPI_{near}))$ ; end if
6.  $S_{rand} \leftarrow Rand\_Sample(i)$ ;
7.  $PPI_{nearest} \leftarrow Nearest(\omega, S_{rand})$ ;
8.  $(PPI_{new}, E_{new}) \leftarrow Connect(PPI_{nearest}, S_{rand})$ ;
9. if  $ObstacleFree(PPI_{new})$ , then
10.  $PHPI_{near} \leftarrow Neighbors(PHPI_{new}, )$ ;
11.  $PHPI_{min} \leftarrow ChooseParent(PPI_{near}, PPI_{nearest}, PPI_{new}, \psi)$ ;
12.  $\omega \leftarrow InsertPoint(PPI_{min}, PPI_{new}, \psi)$ ;
13.  $\omega \leftarrow Reconnect(\omega, PPI_{nearest}, PPI_{min}, PPI_{new})$ ;
14.  $\omega \leftarrow SmoothTrajectory(PPI, len\_|\psi|, deflection\_ang\_|\psi|)$ 
15. end if
16. end for
17. return  $\alpha$ 

```

Note: Notations used in the algorithm

M	= Predefined number of $PPIs$
α_{old}	= Existing path tree
$Neighbors$	= All $PPIs$ of a path tree within a local vicinity of S_{rand}
p_{near}	= One of the PPI that belongs to the class of $Neighbors$
$onlyChild$	= $PPIs$ with only single edge or connection

Fig. 2 Algorithm for path tree development

4 Ant Algorithm

It is inspired by ants' foraging behavior, developed by Dorigo, and also called ant colony optimization (ACO) [27]. It mimics the foraging behavior of ants, where they establish communication through the trails of chemical pheromones. In this, each ant observes the concentration of pheromone, which indicates the quality of their path. Higher pheromone concentration represents better path quality. Thus, this behavior emerges into finding the optimal path from the collection of alternative solutions. AA can efficiently solve optimization problems with a discrete search space. Therefore, it is considered a local search algorithm. It also aids the algorithm to process faster and obtain the best solution. AA has wide applications in solving the traveling salesman problem, job shop problem, and vehicle routing problem [27]. ACO was also used to solve the alignment optimization problem [28]. The PIs were randomly generated on each equidistant orthogonal sections between the two termini [28]. Since the number of PIs is prefixed, and their locations are known a priori, the distance between PIs can be computed and stored as a cost matrix. Then, AA is used where each ant starts traveling from a start point to the endpoint by connecting the PIs generated on N orthogonal cross sections. At every iteration, the ant executes a decision policy to determine the next point on the path, i.e., the transition probability. Transition probability or transition rule allows the ants to select the point

based on the pheromone's state and the ants' visibility and aids in constructing a complete solution to the problem. The ant decision on point selection is obtained by combining the visibility and pheromone trails, as shown in Eq. (7), where, P_{mn}^q = probability of ant q traveling from point m to n . The transition probability used by the ant algorithm provides a balance between the pheromone intensity, τ_{mn} , and the heuristic information, η_{mn} (which includes the inter-distance between the PIs from the cost matrix). It includes heuristic information. It effectively trades off between the exploration and exploitation. The best trade-off is achieved by selecting appropriate β (controls pheromone trail) and γ (rate of visibility) values. Adding heuristic information to AA makes it a problem-dependent function. It shows an explicit bias toward the most attractive solutions or the solution with the least objective value, as shown in Eq. (8). Once all the ants construct the alignments, each ant starts retracing its path back to the origin point effectively and deposits pheromone. The fitness of the obtained alignment is accomplished by calculating the pheromone deposition on each alignment using Eqs. (9) and (10).

$$P_{mn}^q(t) = \frac{\tau_{mn}^\beta(t)\eta_{mn}^\gamma(t)}{\sum_{c \in N_j} \tau_{mc}^\beta(t)\eta_{mc}^\gamma(t)} \text{ where, } n \in N_j \quad (7)$$

$$\eta_{mn} \propto \frac{1}{f(C_{HA})} \quad (8)$$

$$\tau_{mn}(t+1) = (1-\varphi) \cdot \tau_{mn}(t) + \varphi \cdot \Delta\tau_{mn}(t) \quad (9)$$

$$\Delta\tau_{mn}(t) = \sum_{q=1}^{n_q} \Delta\tau_{mn}^q(t) \quad (10)$$

$$\tau_{mn}(t) \leftarrow (1-\varphi)\tau_{mn}(t) \quad (11)$$

Initially, the pheromone count is initialized to a very small value $[0, \tau_0]$. To avoid premature convergence and promote exploration, pheromone intensities (τ) are allowed to evaporate with iterations (t), Eq. (11). The constant, φ , specifies the evaporation rate of pheromone, for each link (m, n), $\varphi \in [0, 1]$. A higher evaporation rate facilitates a better exploration of the search space. Thus, it helps to explore the maximum possible solution between the two termini. After generation of n_p alignments, the model starts shortlisting the alignments based on total pheromone deposition. The best few alignments are retained as output at the end of each iteration. Each ant chooses their respective path independently, i.e., there exists an alignment T^p for p th ant sent. Figure 3 shows the working AA used for developing alignment.

```

Initialize all parameters, i.e.,  $\gamma, \beta, \varphi$ 
Initialize  $\tau_0$  to a small random value,  $[0, \tau_0]$ ;
 $t = 0$ 
Place all the ants,  $n_p$  at the start point
for each link  $(m, n)$  do
     $\tau_{mn}(t) \sim \mathbb{Z}[0, 1]$ ;
end
repeat
    for each ant  $p = 1, 2, 3 \dots, n_p$  do
         $T^p(t) = \emptyset$ ;
        repeat
            From current node  $m$ , select next node  $n$  with probability as defined in Eq.(7);
             $T^p(t) = T^p(t) \cup \{(m, n)\}$ ;
            until a complete path is constructed;
            Compute  $f(T^p(t))$ ;
        end
        for each link  $(m, n)$  do
            Use evaporation, Eq.(11);
            Calculate  $\Delta\tau_{mn}(t)$  from Eq.(10);
            Update pheromone by Eq.(9);
        end
        for each link  $(m, n)$  do
             $\tau_{mn}(t + 1) = \tau_{mn}(t)$ ;
        end
         $t = t + 1$ 
    until stopping criteria is true;
Return  $T^p(t) : f(T^p(t)) = \min_{p=1,2,\dots,n_p}\{f(T^p(t))\}$ ;

```

Fig. 3 Algorithm for alignment optimization with ant algorithm

5 Case Studies

In this section, the application of PPM and AA is demonstrated. A comparative analysis was conducted between these two methods for solving the highway and railway alignment problem for two different case studies. A real-world test case was adopted for developing highway alignment between Bantiya ($21^\circ 32' 24''$ N, $70^\circ 17' 27.6''$ E) and Gadhvana ($21^\circ 31' 12''$ N, $69^\circ 58' 33.6''$ E) in Gujarat, India. The two locations are 31 km apart. This study region was taken from a different study, where authors compared AA and PPM's convergence rate [19]. The study area had 919 sensitive land parcels of forests, wetlands, and water bodies (used as environmentally sensitive regions) and historic and built-up areas (restricted zones). The alignment was prohibited in these zones. GIS was used to extract the land parcels in a shapefile, which was accessed in MATLAB. The land parcels cost is \$ 2.48 per m^2 [44], the area impact cost is \$ 80 per sq.m, and the construction cost is \$ 150 per m. The alignment was developed for a two-lane two-way highway 10 m wide for 100 km/hr design speed. Table 2 presents the input parameters of search algorithms (i.e., AA and PPM), respectively. Figure 4 shows the alignments generated by AA and PPM and

Table 2 AA and PPM input parameters for highway alignment

Input parameters	PPM	AA
Evaporation rate of pheromone (φ)	–	0.5
Trail factor (β)	–	0.1
Visibility factor (γ)	–	2.0
Population size	4000	4000
Total iteration count	42,000	42,000

the corresponding details in Table 3. In Fig. 4, it is visible that both alignments almost overlap, yet PPM yields a slightly better solution in terms of alignment cost. Both alignments avoided environmentally infeasible land parcels; thus, there is negligible impact. In this case, PPM developed the alignment faster than AA. The difference in computation time can be attributed to the additional time taken by AA in generating and evaluating infeasible solutions, which PPM pre-screened while generating the points in PPM.

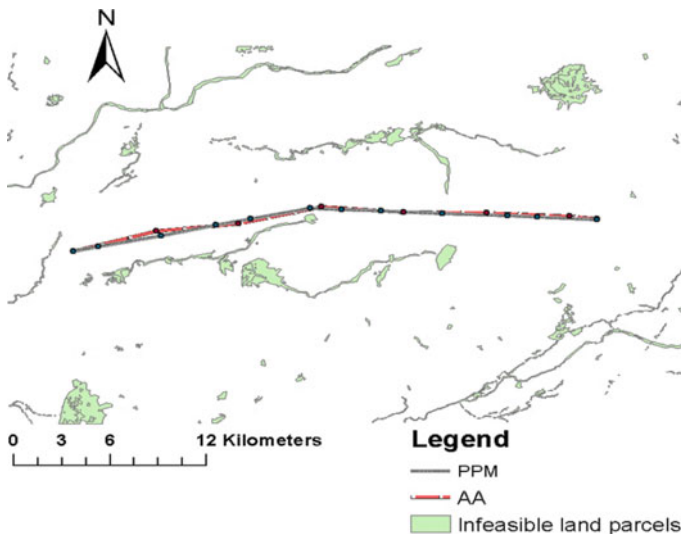


Fig. 4 Optimal highway alignments generated

Table 3 Objective values of highway alignments generated

Parameters	PPM alignment	AA alignment
Roadway length	33.1 km	34.9 km
Environmental impact	0 m ²	0 m ²
Total roadway cost	\$ 5.01 million	\$ 5.12 million
Computation time elapsed	6.5 h	8 h

Table 4 Design parameters for railway alignment

Parameters		Values
Design parameters	Cross-section width	29.1 m (2-tracks, formation width of 11.3 and 8.9 m embankment width on either side)
	Design speed	350 km/hr
Cost parameters	Track construction cost, per m	\$ 300
	ROW cost, per m ²	\$ 2.48
	Impact area cost, per m ²	\$ 80

Table 5 Input parameters of AA and PPM for railway alignment

Input parameters	AA	PPM
Evaporation rate of pheromone (φ)	0.5	–
Trail factor (β)	0.1	–
Visibility factor (γ)	2.0	–
Population size	4000	4000
Total iteration count	60,000	60,000

A real-world environment was considered for developing a railway alignment between two cities in Gujarat, India, i.e., Bilimora (20° 45' 52" N, 73° 0' 26" E) as the origin, and Surat (21° 10' 38" N, 72° 56' 9" E) as the destination. These cities are 46.3 km apart. 6605 sensitive land parcels were identified in the study area. The restricted or infeasible land parcels include the historic and built-up areas. Wetlands and forests were identified to estimate the environmental impact. The study considered a standard gauge double track (one-way) railway line for alignment design. Tables 4 and 5 represent the input parameters for the railway alignment design and search algorithms (i.e., AA and PPM), respectively. The alignments generated by AA and PPM are shown in Fig. 5, and the corresponding details are in Table 6.

In Fig. 5, it is visible that the alignments generated were almost similar. However, the alignments generated by AA (i.e., AA_Rail) deviated in certain locations, where it was unable to avoid infeasible land parcels. It can be observed that the PPM yielded alignment (i.e., PPM_Rail) with lower total cost. For this study, the length of AA_Rail was shorter, but the alignment had some impacts on the environmentally sensitive regions. Further, the computational time of PPM was lower than AA. The higher cost and computation time can be associated with the lack of flexibility in PI generation, as PIs on fixed orthogonal sections restrict the movement of AA in avoiding the infeasible land parcels. As the proposed PPM is heuristic in nature, the model was run for ten different instances. In each run, the results converged to the same solution. Thus, PPM is consistent in converging into an identical solution for the same input data.

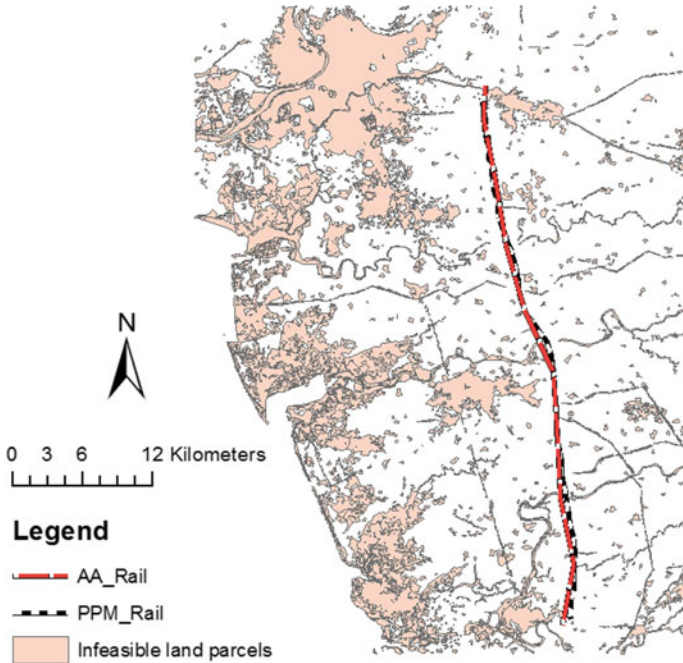


Fig. 5 Optimal railway alignments generated

Table 6 Objective values of railway alignments generate

Parameters	PPM alignment	AA alignment
Railway line length	46.6 km	45.8 km
Environmental impact	0 m ²	5072.687 m ²
Total railway line cost	\$ 14.64 million	\$ 15.52 million
Computation time elapsed	4 h	6 h

6 Summary

This paper presents a method for developing optimal horizontal highway and railway alignment. The method can efficiently search the entire space and find a suitable number of PIs at feasible locations by satisfying the geometric constraints required for developing the horizontal alignment. Unlike the existing methods, in PPM, the locations of the PIs are not confined to the grid, lattice, square, sections, or any defined pattern. Further, it does not require reference alignment. The locations of the PIs are defined based on the site of prohibited areas and high-cost land parcels. The proposed process automatically identifies a suitable number of *HPIs* at feasible locations for developing the horizontal highway alignment. The results show that

the proposed method is reliable and can be used to develop solutions with optimized cost and impact.

The efficiency of the proposed method was investigated by comparing it with AA, one of the existing evolutionary algorithms in the field of alignment optimization. The efficacy of the proposed and existing method was validated through two different real-world case scenarios: one for highway alignment and the other for railway alignment. The highway alignments obtained by PPM and AA are almost similar and have no impact on environmentally sensitive regions. However, the computational time for AA was more than the PPM for achieving similar results. Similarly, for railway alignment, the lengths of both the alignments were almost equal, but the alignment obtained by the AA shows some impact on the environmentally sensitive areas. It is due to a lack of flexibility in selecting the PIs locations. In AA, the PIs were confined to the fixed orthogonal sections, which in some instances could not avoid the infeasible land parcels.

The results obtained by both methods were comparable, although the discrete search spaces on orthogonal sections were required for the AA. As the test case study area was relatively small, the computation time of the algorithms is inconsequential. However, the AA uses a probabilistic search method and evaluates both feasible and infeasible solutions. It can sometimes get trapped in infeasible regions and increase the computation time, and it would be even significant for a larger region. However, for PPM, the solutions were evaluated in the feasible spaces only. The proposed method efficiently explored the search space without confining the location of the PIs, which increases the model's precision in obtaining an optimal solution. PPM efficiently maneuvers around the infeasible and high-cost land parcels, thus prevents from getting trapped in local optimum solutions. Table 7 summarizes the main differences observed between the AA and PPM.

This study can further be investigated in different directions. This work only discussed the generation of PIs; a curve fitting optimization model can aid in obtaining a reliable solution. This model can be integrated with other cost functions such as user cost, earthwork cost [33, 34], traffic flow [10], and accident cost [29] to make it comprehensive. It is also worth investigating the three-dimensional alignment using this method.

Table 7 Comparison between ant algorithm and path planner method

Feature	Ant algorithm	Path planner method
Search space	Suitable for discrete search space [28]. Some are developed for continuous search space but have very few applications	Suitable for both discrete and continuous search space
Population	Needs an initial point population generated over the equidistanced sections	Points are created progressively for the complete search space
PI flexibility	PIs are confined to the planes or sections	PIs are not confined by any preselected planes or sections
Termination criteria	Reached maximum iterations or all ants' convergences to a single solution	Reached maximum iterations or no change is results
Computation time	Significantly more for clustered environment	Comparatively less
Transition rule	Transition probabilistic rule is used to choose the next adjacent node from the set of viable nodes	Evaluates the costs of neighborhood nodes, along with endpoint and select accordingly
Optimality of solution	Possibly a local or global optimum solution	Expected a globally optimum solution

References

- Howard BE, Bramnick Z, Shaw JF (1968) Optimum curvature principle in highway routing. *J Highw Div* 94(1):61–82
- Nicholson AJ, Elms DG, Williman (1973) A variational approach to optimal route location. *Highw Eng* 23(3)
- Shaw JF, Howard BE (1982) Expressway route optimization by OCP. *J Transp Eng* 108(TE3)
- Wan F (2017) Introduction to the calculus of variations and its app. Routledge, CRC Press
- Chew E, Goh C, Fwa T (1989) Simultaneous optimization of horizontal and vertical alignments for highways. *Transp Res Part B* 22:315–329
- Kabongo Booto G, Run Vignisdottir H, Marinelli G, Brattebø H, Bohne RA (2020) Optimizing road gradients regarding earthwork cost, fuel cost, and tank-to-wheel emissions. *J Transp Eng Part A Syst* 146(3)04019079
- Easa SM, Strauss TR, Hassan Y, Souleyrette RR (2002) Three-dimensional transportation analysis: Planning and design. *J Transp Eng* 128(3):250–258
- Trietsch D (1987) A family of methods for preliminary highway alignment. *Transp Sci* 21(1):17–25
- Li W, Pu H, Zhao H, Liu W (2013) Approach for optimizing 3D highway alignments based on two-stage dynamic programming. *J Software* 8(11):2967–2973
- Maji A, Jha MK (2013) Highway alignment optimization using cost-benefit analysis under user equilibrium. In: *Optimizing, innovating, and capitalizing on information systems for operations*, pp 313–327, IGI Global
- Maji A, Jha MK Multi-objective evolutionary algorithm framework for highway route planning with case study. *Adv Transp Stud* 41
- Kang MW, Jha MK, Schonfeld P (2012) Applicability of highway alignment optimization models. *Transp Res Part C Emerg Technol* 21(1):257–286

13. Cheng JF, Lee Y (2006) Model for three-dimensional highway alignment. *J Transp Eng* 132(12):913–920
14. Lee Y, Tsou YR, Liu HL (2009) Optimization method for highway horizontal alignment design. *J Transp Eng* 135(4):217–224
15. Shafahi Y, Bagherian M (2013) A customized particle swarm method to solve highway alignment optimization problem. *Comput Aided Civ Infrastruct Eng* 28(1):52–67
16. Zhang H, Pu H, Schonfeld P, Song T, Li W, Wang J, Peng X, Hu J (2020) Multi-objective railway alignment optimization considering costs and environmental impacts. *Appl Soft Comput* 89:106105
17. Cruz-Chávez MA, Moreno-Bernal P, Rivera-López R, Ávila-Melgar EY, Martínez-Bahena B, Cruz-Rosales MH (2020) GIS spatial optimization for corridor alignment using simulated annealing. *Appl Sci* 10(18):6190
18. Pushak Y, Hare W, Lucet Y (2016) Multiple-path selection for new highway alignments using discrete algorithms. *Eur J Oper Res* 248(2):415–427
19. Sushma MB, Maji A (2020) A modified motion planning algorithm for horizontal highway alignment development. *Comput Aided Civ Infrastruct Eng* 35:818–831. <https://doi.org/10.1111/mice.12534>
20. Li W, Pu H, Schonfeld P, Zhang H, Zheng X (2016) Methodology for optimizing constrained 3-dimensional railway alignments in mountainous terrain. *Transp Res Part C Emerg Technol* 68:549–565. <https://doi.org/10.1016/j.trc.2016.05.010>
21. Pu H, Xie J, Schonfeld P, Song T, Li W, Wang J, Hu J (2021) Railway alignment optimization in mountainous regions considering spatial geological hazards: a sustainable safety perspective. *Sustainability* 13:1661
22. Jha MK, Schonfeld P (2000) Integrating genetic algorithms and geographic information system to optimize highway alignments. *Transp Res Rec* 1719(1):233–240
23. Mondal S, Lucet Y, Hare W (2015) Optimizing horizontal alignment of roads in a specified corridor. *Comput Oper Res* 64:130–138
24. Li W, Pu H, Schonfeld P, Yang J, Zhang H, Wang L (2017) Mountain railway alignment optimization with bidirectional distance transform and genetic algorithm. *Comput Aided Civ Infrastruct Eng* 32(8):691–709
25. Pu H, Song T, Schonfeld P, Li W, Zhang H, Wang J, Hu J, Peng X (2019) A three-dimensional distance transform for optimizing constrained mountain railway alignments. *Comput Aided Civ Infrastruct Eng* 34:972–990
26. Lai X, Schonfeld P (2012) Optimization of rail transit alignments considering vehicle dynamics. *Transp Res Rec* 2275(1):77–87
27. Dorigo M, Caro GD, Gambardella LM (1999) Ant algorithms for discrete optimization. *Artif Life* 5(2):137–172
28. Samanta S, Jha MK (2012) Applicability of genetic and ant algorithms in highway alignment and rail transit station location optimization. *Int J Oper Res Inf Syst (IJORIS)* 3(1):13–36
29. Jong JC, Jha MK, Schonfeld P (2000) Preliminary highway design with genetic algorithms and geographic information systems. *Comput Aided Civ Infrastruct Eng* 15(4):261–271
30. LaValle SM, Kuffner JJ (2001) Rapidly-exploring random trees: Progress and prospects. In: Peters AK (ed) *Algorithmic and computational robotics: new directions*
31. Transport. Officials. *A Policy on Geometric Design of Highways and Streets*. AASHTO (2011)
32. Maji AV (2017) Optimization of horizontal highway alignment using a path planner method. *WIT Trans Built Environ* 176, 81–92
33. Hare W, Koch VR, Lucet Y (2011) Models and algorithms to improve earth work operations in road design using mixed integer linear programming. *Eur J Oper Res* 215(2):470–480
34. Göktepe AB, Altun S, Ahmedzade P (2009) Optimization of vertical alignment of highways utilizing discrete dynamic programming and weighted ground line. *Turk J Eng Environ Sci* 33(2):105–116
35. Laporte G, Pascoal MM (2015) Path based algorithms for metro network design. *Comput Oper Res* 62:78–94

36. Chien S, Schonfeld P (1998) Joint optimization of a rail transit line and its feeder bus system. *J Adv Transp* 32(3):253–284
37. Wirasinghe SC, Seneviratne PN (1986) Rail line length in an urban transportation corridor. *Transp Sci* 20(4):237–245
38. Costa PA, Colaço A, Calçada R, Cardoso AS (2015) Critical speed of railway tracks detailed and simplified approaches. *Transp Geotech* 2:30–46
39. Wan FYM (1995) *Introduction to the calculus of variations and its applications*. Chapman & Hall, New York
40. Athanassoulis GC, Calogero V (1973) Optimal location of a new highway from A to B—A computer technique for route planning. In: PTRC seminar proceedings on cost models & optimization in highway, pp 9
41. Turner AK, Miles RD (1971) The GCARS system: a computer-assisted method of regional route location 348
42. Roise JP, Shear TH, Bianco JV (2004) Sensitivity analysis of transportation corridor location in wetland areas: a multi objective programming and GIS approach. *Wetlands Ecol Manage* 12(5):519–529
43. Yang WA, Guo Y, Liao WH (2010) A novel particle swarm optimization algorithm based on fuzzy velocity updating for multi-objective optimization. In: fourth international conference on genetic and evolutionary computing. IEEE, pp 22–26
44. Chakraborty S (2013) *The price of land*. Oxford University Press, New Delhi, India

Pavement Analysis

Comparison of Dynamic Loads Generated by Truck with Dual Tires and Wide Base Tires



Suraparaju Venkata Sai Tharun, Kakara Srikanth, and Venkaiah Chowdary

Abstract As per International Energy Agency (IEA), there will be about a 90% net increase in the fuel demand for the road freight transportation sector by 2050 in India. This results in increased environmental pollution caused by gas emissions from vehicles used for road freight transport. Therefore, it is necessary to take required measures for improved road freight transport with minimal damage to the environment. One such step in that direction is replacing conventional dual tire assembly with wide base tires, whose manufacturing started in the 1980s. Tire manufacturers modified the first-generation wide base tire to reduce the pavement damage caused by wide base tires and produced New Generation Wide Base (NGWB) tires. These NGWB tires must be studied thoroughly as their benefits are significant. In this study, an attempt has been made to compare the dynamic loads generated due to wide base tires and dual tires for a 3-axle truck. The dynamic loads generated are influenced by truck characteristics such as speed of the truck and load acting on the truck. In all the cases, the dynamic loads induced by trucks with NGWB tires are less than that caused by trucks with dual wheel tires.

Keywords Wide base tires · Dynamic loads · Roughness · Dynamic load coefficient

S. V. S. Tharun · K. Srikanth (✉) · V. Chowdary
Civil Engineering Department, National Institute of Technology Warangal, Warangal, Telangana, India

e-mail: sri717004@student.nitw.ac.in

S. V. S. Tharun
e-mail: Surapa_CE19314@student.nitw.ac.in

V. Chowdary
e-mail: vc@nitw.ac.in

1 Introduction

The overall development of nation largely depends on the road network. India is a country having the second largest road network with 5.89 million kilometers. The volume of freight transport by road increased by 7.4% since 2014 [1]. The advantage of road freight transport is attributed to the flexibility in operation with various routes between the origin and destination. This increase in freight demand will boost the country's economy, but result in allied problems such as premature failure of highway pavements, increased fuel consumption, and increased emissions. Because of premature failure of the pavements, there will be an increase in the pavement maintenance cost. As fuel is obtained from natural resources, increased fuel consumption may lead to scarcity of fuel, and increased emissions will pollute the environment. To address these issues, measures should be taken from the pavement design side and by altering the vehicle characteristics.

The pavements should be designed so that they sustain throughout the design period without any requirement for major rehabilitation. Design life plays a major role as a huge amount of money is being invested in the roadway sector. Thus, it is necessary to be aware of all the factors affecting the life of the pavement. The life of the pavement is significantly influenced by the magnitude of wheel load experienced by the pavement [2] throughout its service life. However, pavement surface and vehicle characteristics also contribute toward the magnitude of pavement surface loading [3].

The roughness of the pavement is responsible for creating vertical movements in the vehicle, which produces dynamic loads at the pavement tire interface [4]. Due to this dynamic nature of loads, the magnitude of load experienced by the pavement will be more than that of the static load. The dynamic loads thus result in an increased deterioration rate of the pavement [5]. The loads imparted by the vehicle onto the pavement will vary depending upon the oscillations in the moving vehicle induced by the pavement surface undulations [6]. In general, the frequency domain is used to characterize the dynamic loads generated by a moving vehicle. Dynamic loads corresponding to the frequency of 1–4 Hz produce pitch and bounce in the vehicle body. On the other hand, axle hop is produced for loads corresponding to the frequency range of 8–15 Hz [7]. Vehicle characteristics like vehicle speed, type of suspension, tires, axle, the distribution of vehicle body mass, and pavement characteristics like the roughness of pavement surface are proved to affect the magnitude of dynamic loads [8–10]. The dynamic loads generated under the vehicle axle follow a normal distribution with its mean as static load and standard deviation influenced by vehicle and pavement surface characteristics. Thus, these are the appropriate parameters to be considered while comparing the dynamic loading effect produced for different tire types.

The early deterioration of pavement is mostly affected by the factors such as vehicle loading and tire type. It is appropriate to consider the dynamic loading effects while designing a pavement such that the pavement sustains throughout the design period. Besides that, replacing dual tires with wide base tires is also a solution to

address the issues related to the increased freight traffic. In Canada and Europe, use of wide base tires for trucks started in the early 1980s. By 1997 in Germany, nearly 67% of tires for truck trailers and semi-trailers are wide base tires [11].

In the United States, by around 2002, usage of wide base tires is not even more than 5% of the trucks, even after legalizing the use of wide base tires for five-axle trucks [12]. But after realizing the benefits of using wide base tires, there is an increase in the use of wide base tires, and the trend will continue in the future as there will be an increase in the demand for freight transportation. Replacing standard dual tires with wide base single tires will improve fuel efficiency, reduce tire cost, and ease handling and monitoring [13]. The major issue regarding the use of wide base tires is that they cause more damage to the pavement than dual tires. In the early 1980s, there was no balance between the economic advantages of wide base tires and the cost incurred due to pavement damage. Thus, the earlier wide base tires commonly referred to as first-generation wide base tires were not successful. They are restricted to serve as steer axles for specific applications like mining and construction activities. New generation wide base (NGWB) tires were introduced because of nearly twenty years of research in both the trucking industry and transportation department agencies. The width of NGWB tires is 15–18% more than that of first-generation single tires. The special wall design of these tires avoids the need for high inflation tire pressures [14]. As these tires provide more contact area with uniform distribution of pressure at tire pavement interface, they are expected to decrease the pavement damage and improve safety, apart from other cost savings. New generation wide base tires need to be evaluated for the possible change in pavement damage resulting due to replacement of dual tires with wide base tires. It is also necessary to identify the suitable operating conditions of wide base single tires to maintain a proper balance between the economic advantage for the trucking industry and the costs accrued through road infrastructure damage.

The consequences of replacing the dual tires with wide base tires were analyzed in the earlier research works using analytical approaches such as modeling pavement and performing experiments in the field. However, the magnitude of dynamic loads resulting due to specific aspects of tires in combination with magnitude of vehicular load, speed of the vehicle, and pavement roughness is still lacking in the literature. Thus, the main objective of this study is to quantify the tandem axle dynamic loads generated at tire pavement interface for different pavement and vehicle characteristics apart from comparing the estimated Dynamic Load Coefficient (DLC) values for dual tires (11R22.5) and NGWB tires (495/80R22.5). The dynamic loads generated are quantified for three-axle trucks with two tire types including 11R22.5 and 495/80R22.5. The variation in the magnitude of dynamic loads for each tire and for different vehicle and pavement characteristics are compared using a DLC. DLC is the ratio of the standard deviation of all instantaneous loads acting on the pavement over a length to their mean value. DLC was used by most of the researchers. DLC shows a very good correlation with IRI, and it is stated that DLC is a good indicator to characterize the dynamic loads generated at the tire pavement interface [15–17]. The variables considered in this study include the roughness of the pavement, speed, and gross weight of the vehicle.

2 Methodology

To achieve the objective of this study, a commercial vehicle operating on Indian roads is considered, and a full truck model is simulated using TruckMaker software. The vehicle considered is a three-axle rigid truck consisting of a steering axle fitted with single wheel and a rear tandem axle fitted with dual wheels. Simulations are performed by replacing the dual tires with a single wide base tire for both axles of the rear tandem axle. To simulate various pavement roughness conditions, pavements with International Roughness Index (IRI) ranging from 1.5 to 4 m/km are considered in the study. The profile is obtained from the survey conducted on a flexible pavement section on National Highway (NH)—1, using network survey vehicle. The total length of profile obtained was 54 km, the profiles were further divided in 1000 m sub-profiles, and the IRI of each sub-profile was determined. The pavement model was created in the TruckMaker software by inputting 1000 m pavement profile data. The length of road model created is 2000 m, where the initial and final 500 m are considered to be smooth sections. The initial and final 500 m smooth sections are considered to avoid the effect of acceleration and deceleration. On the pavement thus created in the TruckMaker software, the vehicle model was simulated with varying vehicle characteristics such as the truck gross vehicle weight and speed with different tires on the rear axle including either the dual tires alone or the wide base tires alone. The generated load magnitudes acting on the pavement were recorded during simulation under each tire for each condition and analyzed subsequently using Dynamic Load Coefficient (DLC) values. The obtained DLC values for both dual tires and wide base tires are compared statistically.

3 Vehicle Simulation

TruckMaker is a computer software developed by IPG Automotive, a global solution for virtual test driving. Development of vehicles and systems in the automotive industry can be done by using this software. Besides creating a real test drive in the virtual world, it simulates the real environment and appropriate models. This software is mostly used in the automotive industry to study vehicle dynamics and powertrain. This software enables the partial or complete modeling of real test drives in simulation, which results in saving time and money with risk-free testing. The component of the virtual environment consists of virtual road, virtual vehicle, and virtual driver. The virtual road is a computer model, and it is a digital representation of a road for testing. TruckMaker allows simulating different surface conditions of the road.

A virtual vehicle is a model for the representation of an actual vehicle. In this software, differential and algebraic equations are used to simulate the motion of the vehicle models. The fundamental actions of the actual driver are simulated by the virtual driver, which is a computer driver. The different forces acting on the vehicle,

including internal, external forces, and torques, can be quantified using the developed programs in this software. The loads measured in the study are the instantaneous loads that act vertically at the point of contact of tire and pavement. The software provides the models of vehicles that are validated [18]. Thus, the factors related to the vehicle model are taken as default values in the software. The virtual road is created as per the requirement using the pavement profile data. Driver behavior is defined by giving required maneuvers for the simulation. In the software, the process starts by selecting the required vehicle model which best represents the vehicle to be simulated. The vehicle characteristics and other properties like axle configuration, number of tires, and tire types are selected. The axle configuration considered in this study is shown in Fig. 1. After truck generation, the roads of straight sections with required roughness are created using the profile data.

In the present study, simulations were carried out by varying the vehicle speed and gross vehicle weight with varying road roughness. The different load conditions considered vary from 0% payload to 150% payload, by considering 0% payload as empty truck, 100% payload as fully loaded truck, and 150% payload as a truck with 50% overloading. The payload conditions with different gross vehicle weight are shown in Table 1. To understand the impact of vehicle speed on dynamic loads generated, the speed is varied from 40 to 100 kmph.

4 Simulation Results

After simulation, the wheel load profile is obtained for the given road section with 0.01 s as the sampling interval over the entire run time of the simulation. The wheel load profile of the first and last 500 m length of the roads is not taken into account

Fig. 1 Axle configuration of the three-axle truck with dual tires on the rear axle

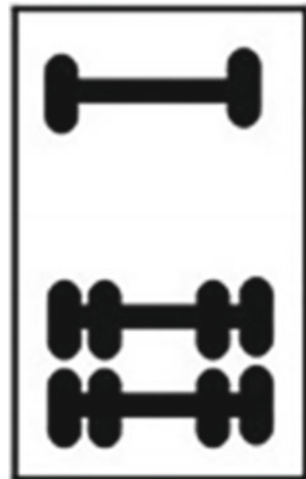


Table 1 Gross vehicle weight for different payload conditions

Payload (%)	Gross vehicle weight (kg) for three-axle truck
0	7500
25	11,875
50	16,250
75	20,625
100	25,000
125	29,375
150	33,750

for the analysis to avoid errors due to the effect of acceleration and deceleration of the truck. The rear axle of the vehicle causes more damage to the pavement [19, 20]. Thus, the dynamic loads generated under the rear axle are considered for the analysis. It is important to note here that the gross weight of the truck is distributed to the front axle and the rear axle group in the proportion of 29% and 71%, respectively. The proportion of gross weight distribution is specific to the vehicle type selected in the TruckMaker software. These dynamic loads are characterized using the DLC factor. DLC is ratio of standard deviation of dynamic loads to the average dynamic load. For instance, consider that the static load applied by rear tandem axle of truck is 175136 N. When the truck is moving at a speed of 80 kmph on a profile of roughness 2.23 m/km, the load applied by the rear axle of truck over a length of road is found to be 9344.341 N. Thus, DLC is ratio of 9344.341–175,136, which is equal to 0.053. The gross vehicle weight, speed, and roughness of pavement are the significant factors that influence the magnitude of dynamic loads [21]. Thus, in this study, the effect of these three factors on the DLC factor is analyzed for different characteristics related to the vehicle and the pavement.

4.1 Effect of Roughness

Roughness is one of the influencing factors which affect the magnitude of dynamic loads. In the present study, the impact of pavement roughness on the dynamic loads is quantified by analyzing the variation of DLC with pavement roughness. A three-axle fully loaded truck traveling at 80 kmph is simulated to get the variation of DLC, and generated dynamic loads are recorded. The variation of DLC with pavement roughness for a three-axle truck with standard dual tires and wide base single tire is shown in Fig. 2.

As DLC is the ratio of standard deviation to the mean of the wheel loads over a particular road length, high DLC indicates a higher standard deviation in wheel loads. Pavement roughness is the change in elevations in the pavement profile along the road length. While the vehicle is traveling on the road, the undulations induce vertical acceleration in the vehicle and cause the variation in the wheel loads applied on to the

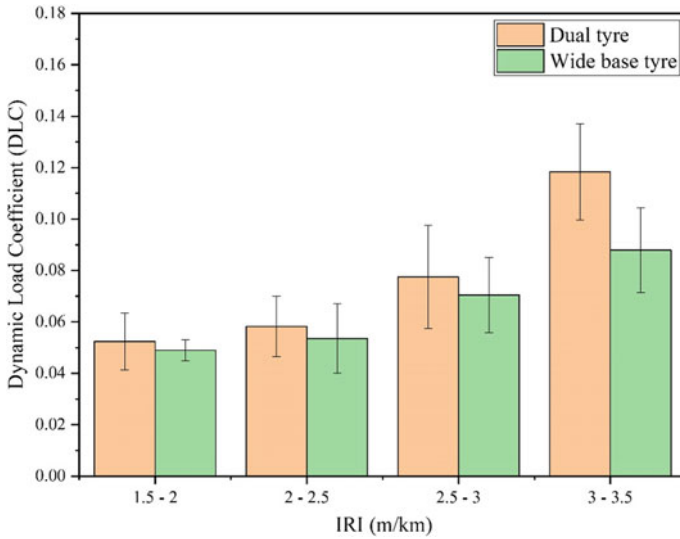


Fig. 2 Variation of DLC with pavement roughness

pavement. Pavement with high roughness creates more vertical vehicle displacement, which results in higher variation in the wheel loads, thereby increasing the DLC. As shown in Fig. 2, DLC increases with the increase in pavement roughness. It can be inferred that rougher pavement will experience more load than the static wheel load. Thus, rougher pavements will deteriorate at a faster rate due to the effect of dynamic loads. New generation wide base tires have fewer side walls than dual tires, which makes the wheel more flexible than that of standard dual tires [22]. Wide base tires with more tire width than dual tires can distribute the contact pressure uniformly [23]. Because of the uniform distribution of contact pressure and flexibility, wide base tires can absorb the vibrations caused due to the pavement roughness. Thus, as shown in Fig. 2, DLC values for trucks with wide base tires are less than that of standard dual tires. Even though the difference in DLC between standard dual tires and wide base single tires is less at lower pavement roughness, the difference tends to diverge with increase in pavement roughness. Thus, the wide base single tires are more effective in reducing the dynamic loads even on rough pavement surfaces which are most common on Indian roads.

4.2 Effect of Speed

In this study, to understand the influence of speed on dynamic loads, a fully loaded three-axle truck is simulated at varying speeds ranging from 40 to 100 kmph with an increment of 20 kmph. At each speed, the dynamic loads acting on the pavement

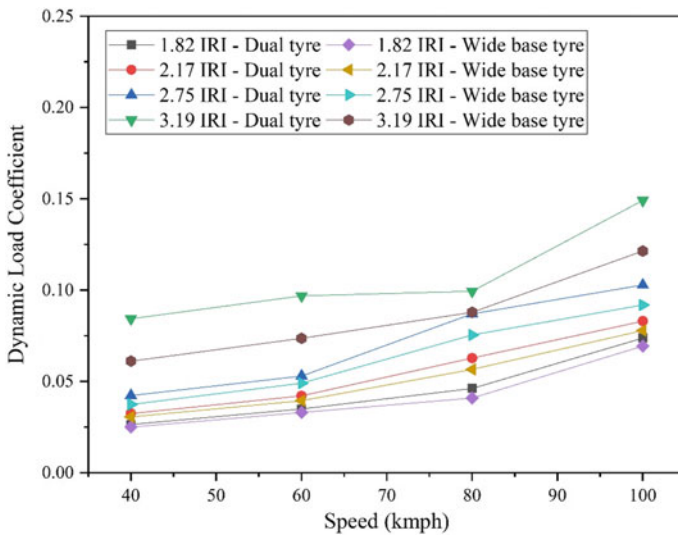


Fig. 3 Variation of DLC with speed: a standard dual tires, b wide base tires

through the truck’s rear axles are recorded for both tire types. An increase in vehicle speed causes an increase in the standard deviation of load profile, which increases the DLC values. DLC increases with the increased vehicle speed at constant pavement roughness [24]. Figure 3 shows the variation of DLC with speed for three-axle trucks with standard dual tires and wide base tires, and the results are consistent with the results of Wang et al. [25]. DLC values for a truck with wide base single tires are less than that of dual tires at a given speed, as shown in Fig. 3. It states that with the increase in pavement roughness, wide base tires cause less variation in the load profile than dual tires. Minor DLC represents less standard deviation for dynamic loads, which indicates that the magnitude of applied loads onto the road surface is relatively close to the static wheel load. Thus, damage caused to the pavement due to the dynamic loading effect is less for the truck with wide base tires on the rear axle.

4.3 Effect of Truckload

When a vehicle is traveling on the road, the magnitude of wheel load experienced by the road depends on the load carried by that vehicle. Truckload is considered as a significant factor influencing the magnitude of dynamic loads. A three-axle truck traveling at 80 kmph with different loading conditions is simulated to evaluate the influence of truckload on dynamic loads. The corresponding dynamic loads generated by the truck are recorded for both tire types.

The vertical displacement of the vehicle caused due to the undulations in the pavement profile creates the vehicle body bounce. A truck carrying less load bounces

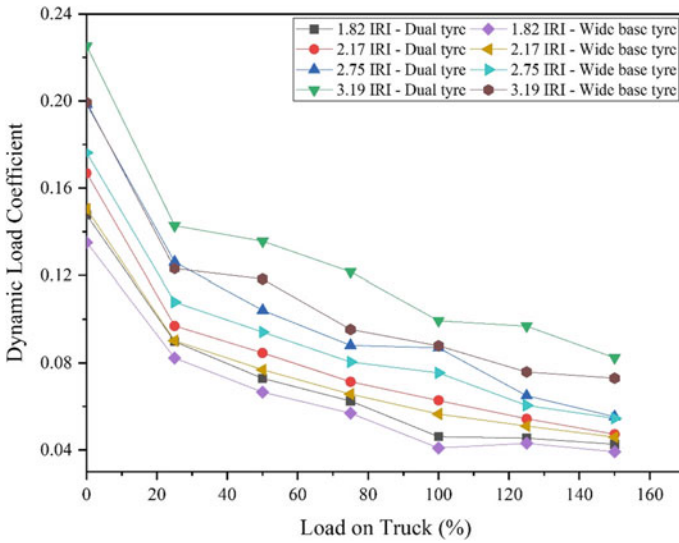


Fig. 4 Variation of DLC with truckload: **a** standard dual tires, **b** wide base tires

more than a fully loaded truck for a given road roughness as the gravity acting on the empty truck is less than a fully loaded truck. This body bounce is responsible for the variation in the load applied to the pavement. Higher the body bounce, the higher the difference between the applied load and static load. Thus, DLC for empty truck is more than that of a fully loaded truck. As shown in Fig. 4, with an increase in the payload, the DLC value decreases. This indicates that the partially loaded truck causes more damage to the pavement as it applies more load than its gross vehicle weight compared to a fully loaded truck. From Fig. 4, it is observed that the DLC values for a truck with wide base tires are less compared to that of standard dual tires.

5 Statistical Analysis

To check the significance of the difference between DLC values obtained for the truck with dual standard tires and wide base tires, a one-way analysis of variance (ANOVA) test is performed. Dynamic loads are recorded by simulating the three-axle truck by changing the tire type, keeping the speed and truckload as constants at 80 kmph and 100% gross weight, respectively. Individual DLC values are determined for dual tire and wide base tire over a pavement profile of 55 km length with varying roughness. 55 DLC values are obtained for each tire type, i.e., one DLC per km length of road. The results of the one-way ANOVA test are shown in Table 2.

Table 2 Results of one-way ANOVA test

ANOVA						
Source of variation	Sum of squares	Degrees of freedom	Mean square	<i>F</i>	<i>P</i> value	<i>F</i> -critical
Between groups	7.14E-05	1	7.14E-05	10.75	1.17E-06	3.9
Within groups	0.07	108	6.64E-06			
Total	0.07180	109				

The *F*-test of ANOVA results shows that the *F* value calculated is more than the *F*-critical value at a 5% significance level. It indicates that the difference between the DLC values of standard dual tires and wide base tires is significant, which means wide base tires cause significantly less damage to the pavement due to the dynamic loading effect than dual tires.

6 Conclusions

The current study is aimed to check the influence of vehicle and pavement characteristics on the generation of dynamic loads at the interface of tire and pavement. A three-axle truck with a rear tandem axle is simulated at various conditions of road roughness, speed, and the load of the vehicle, and dynamic loads generated are measured under the rear axle. For the measured load profiles, DLC values are determined. The conclusions drawn from the study are as follows:

- (1) For a three-axle truck, the difference between the dynamic load and the static load increases with increase in the pavement roughness. The increase is more for the truck with standard dual tires on the rear axle. The axle dynamic load on the pavement having dual tires is 12–31% more than that of wide base tires on the road having the roughness varying between 1.5 and 4 m/km at a constant speed and payload. Further, the DLC values for the wheel types tend to diverge with increase in pavement roughness indicating that the wide base single tires are more effective in reducing the dynamic loads even on rough pavement surfaces which are most common on Indian roads.
- (2) DLC value increases with the increase in speed at constant roughness, and this increase is less for a truck with wide base single tires on the rear axle. This is because wide base tires create less amplitude in the rear axle. The amplitudes of vibrations depend on the vehicle speed, and they are caused due to the undulations in the pavement profile.
- (3) As the payload on the vehicle increases, DLC decreases, and this decrease is more for the truck with wide base tires. Rear axles with standard dual tires are more rigid with more tire sidewalls compared with wide base single tires. The

body bounce in the vehicle for a given payload is more for a truck with dual tires. Thus, it results in more variation in the dynamic load profile, i.e., higher DLC.

- (4) The statistical analysis proves that there is a significant difference between the dynamic loads generated from dual tires and wide base tires. New generation wide base tires generate dynamic loads with less DLC values, indicating that the damage caused to the pavement due to the dynamic loading effect is significantly less for wide base tires.
- (5) First-generation wide base tires are proved to cause more damage to the pavement than dual tires as they decrease the contact area at the tire pavement interface. Considering only the effect of dynamic loads, new generation wide base tires cause less damage to the pavement than dual tires. However, further structural analysis of pavement cross-sections consisting various material types and thicknesses subjected to load applied by a dual tire and wide base tire is required to quantify the damage caused to the pavement by either tires.
- (6) As the new generation wide base tires are becoming more popular due to their added advantages over the conventional dual tires, the distresses occurring on the pavements are expected to be much different for the vehicles fitted with wide base tires. The present study differentiates the dynamic loads generated by a standard dual wheel assembly and wide base tires. The study reveals the range of dynamic loads generated by wide base tires due to variation in the pavement roughness, vehicle speed, and gross vehicle weight of the vehicle. Further the flexible pavement can be analyzed by applying the dynamic loads generated by wide base tires over given pavement cross-section with varied rigidity and tire pressure to determine the critical responses. Further, the study can be extended to develop a methodology to include the effects of dynamic loads in the design of flexible pavement.

References

1. Basic Road Statistics of India (2016–17). <https://morth.gov.in/sites/default/files/File3100.pdf>. Accessed 2021/06/01
2. Guidelines for the design of flexible pavements IRC: 37 (2018). Fourth revision. Indian Roads Congress, New Delhi, India
3. Cole DJ, Cebon D (1998) Influence of tractor-trailer interaction on assessment of road damaging performance. *Proc Inst Mech Eng Part D J Autom Eng* 212(1):1–10
4. Kim SM, Rhee SK, Park HB, Yun DJ (2009) Correlations among pavement surface roughness, moving dynamic vehicle loads, and concrete pavement performance. In: performance modeling and evaluation of pavement systems and materials. American Society of Civil Engineers, Reston, VA, pp 25–31
5. Sun BL, Deng X (1998) Predicting vertical dynamic loads caused by vehicle–pavement interaction. *J Transp Eng* 124:470–478
6. Liu C, Herman R, McCullough BF (1998) Pavement deterioration, rate of dynamic force, and ride quality. *Transp. Res Rec J Transp Res Board* 1643(1):14–19

7. Hassan R (2012) Highlighting dynamically loaded pavement sections with profile indices. *Transp. Res Rec J Transp Res Board* 2306(1):65–72
8. Sayers M, Gillespie TD (1983) Dynamic pavement/wheel loading for trucks with tandem suspensions. *Veh Syst Dyn Int J Veh Mech Mob* 12(1–3):171–172
9. Heath AN, Good MC (1985) Heavy vehicle design parameters and dynamic pavement loading. *Aust Road Res* 15:249–263
10. Cebon D (1989) Vehicle-generated road damage: a review. *Veh Syst Dyn* 18:107–150
11. Effects of Wide Single Tyres and Dual Tyres. Final Report of the Action (Version 29). COST 334. European Cooperation in the Field of Scientific and Technical Research, Brussels, Belgium, (2001)
12. Ang-Olson J, Schroeer W (2002) Energy efficiency strategies for freight trucking: potential impact on fuel use and greenhouse gas emissions. *Transp Res Rec* 1815:11–18, Transportation Research Board, Washington, D.C.
13. Al-Qad L, Mostafa AE (2007) New generation of wide-base tires impact on trucking operations, environment, and pavements. *Transp Res Rec J Transp Res Board* 2008:100–109
14. Al-Qadi IL, Yoo PJ, Elseifi MA, Janajreh I (2005) Effects of tire configurations on pavement damage. *J Assoc Asphalt Paving Technol* 74:921–962
15. Elischer M (2012) Dynamic wheel loads of heavy vehicles—preliminary analysis. Department of Transport and Main Roads, Queensland, Australia, pp 1–12
16. Můčka P (2016) Road roughness limit values based on measured vehicle vibration. *J Infrastruct Syst* 23(2):1–13
17. Bilodeau JP, Gagnon L, Doré G (2017) Assessment of the relationship between the international roughness index and dynamic loading of heavy vehicles. *Int J Pavement Eng* 18(8):693–701
18. IPG TruckMaker (2014) Reference Manual Version 4.5, IPG Automotive, Karlsruhe, Germany
19. Salama HK, Chatti K, Lyles RW (2006) Effect of heavy multiple axle trucks on flexible pavement damage using in-service pavement performance data. *J Transp Eng* 132(10):763–770
20. Gillespie TD (1993) Effects of heavy-vehicle characteristics on pavement response and performance. *Transp Res Board*, Washington, D.C.
21. Kakara S, Chandrasekhar C, Chowdary V (2020) Influence of commercial vehicle characteristics on the magnitude of dynamic wheel loads over asphalt pavement profiles with different roughness. *J Inst Eng (India) Ser A* 101:723–734
22. Grellet D, Doré G, Bilodeau JP, Gauliard T (2013) Wide-base single-tire and dual-tire assemblies—comparison based on experimental pavement response and predicted damage. *Transp Res Rec J Transp Res Board*
23. Al-Qadi IL, Yoo PJ (2007) Effect of surface tangential contact stress on flexible pavement response. *J Assoc Asphalt Paving Technol* 76:663–692
24. Goenaga B, Fuentes L, Mora O (2018) A practical approach to incorporate roughness-induced dynamic loads in pavement design and performance prediction. *Arab J Sci Eng* 44:4339–4348
25. Wang H, Zhao J, Hu X, Zhang X (2020) Flexible pavement response analysis under dynamic loading at different vehicle speeds and pavement surface roughness conditions. *J Transp Eng Part B Pavements* 146(3)

Impact of Choice of Lane on Multilane Flexible Pavement



J. Priscilla Ponmani and M. R. Nivitha

Abstract Traffic data is one of the key inputs in designing a pavement. The pavement design methods currently available use the defaulted traffic volume for design. The default parameters however vary with traffic volume, axle configuration, level of service and vehicle composition. The parameter under consideration here is the lane distribution factor (LDF) which is used in the design of pavements to identify and use the lane that experiences the maximum amount of vehicle flow as the design lane. While many agencies have specified default LDF values depending on the type of roads, studies have shown that it mainly depends on the traffic volume and speed. The extent of influence exerted by individual highways on the LDF values specified in IRC:37-2018 was estimated in this study. For this purpose, the traffic survey was conducted on two four-lane and one six-lane National Highways, and the corresponding LDF was calculated. It was seen that for the four-lane highways, the average LDF obtained was 0.4 and 0.41 which was closer to the values specified in IRC:37-2018. However, for the six-lane highway, the LDF obtained was only 0.32, whereas the specified value in IRC:37-2018 was 0.6. This shows that the characteristics of the highway play a significant role. It was also seen that the LDF values exhibited marginal differences depending on the spatial and temporal variation associated with the data collection.

Keywords Lane distribution factor · Vehicle type · Pavement design · Temporal and spatial variation

1 Introduction

Efficient transportation systems bring economic and social benefits such as improved market access, employment, education, services and increased investments [1]. They also reduce the transportation costs, optimize the travel duration and vehicle operation costs. The transportation network creates new commercial areas and better markets.

J. Priscilla Ponmani · M. R. Nivitha (✉)
PSG College of Technology, Coimbatore, India
e-mail: mrn.civil@psgtech.ac.in

© The Author(s), under exclusive license to Springer Nature Singapore Pte Ltd. 2023
M. V. L. R. Anjaneyulu et al. (eds.), *Recent Advances in Transportation Systems Engineering and Management*, Lecture Notes in Civil Engineering 261,
https://doi.org/10.1007/978-981-19-2273-2_11

159

Thus, it is necessary for a country's road sector to be developed and maintained at appropriate standards. However, many of the roads currently available do not serve their design life as they undergo premature failure before their design life. Among many factors that could be attributed to the premature failure, approximations in the input parameters used for design are considered as a significant factor. Traffic volume and traffic loading are key inputs in the design of pavements in addition to the environmental factors and the type and the quality of the materials used. The magnitude of influence exerted by these input parameters varies with the type of pavement. Three types of pavements, namely flexible pavements, rigid pavements and composite pavements are commonly suggested. In this paper, discussion is limited to the design of flexible pavements only.

In India, IRC:37-2018 provides the guidelines for the design of flexible pavements. The flexible pavements were designed using the California Bearing Ratio method (CBR method) developed by the California Highway Department to obtain the total thickness of the pavement using the CBR value [2]. Rutting and fatigue cracking are taken as the critical distresses. To evaluate rutting, the vertical compressive strain at the top of the subgrade is considered and to calculate fatigue cracking, the horizontal tensile strain at the bottom of the bituminous layers is taken into consideration [3]. The inputs required for this design are cumulative standard axle repetitions during design period (N) expressed in Million Standard Axles (MSA), initial traffic intensity expressed as Cumulative Vehicles per Day (CVPD), lane distribution factor (D), vehicle damage factor (F), design life (n) in years and annual rate of growth for commercial vehicles (r). The standard values for the inputs required for the design of pavements are given in IRC:37-2018. In this study, the focus is on the traffic-related input parameters used for design.

According to IRC:37-2018, the number of commercial vehicles having gross vehicle weight of 30 kN or more is considered for the pavement design. The present-day average traffic is based on seven-day 24-h count made in accordance with IRC:9-1972 "Traffic Census on Non-Urban Roads". The variations in commercial vehicle count (CVPD), vehicle damage factor (VDF), lane distribution factor (LDF) and vehicle growth rate (r) are the traffic volume related parameters. Studies have shown that variation in other traffic-related pavement design input parameters such as wheel spacing and tire pressure have negligible influence on pavement performance compared to layer thicknesses, layer moduli, CVPD, LDF and VDF [4]. One aspect that has received little attention is the distribution of vehicles by lane on multilane highways [5]. The clause 4.5 in IRC:37-2018 provides the default LDF values for single-lane roads, two-lane two-way roads, four-lane single carriageway roads and dual carriageway roads. This value is considered to be a constant for a given type of highway.

The distribution of total volume to individual lanes is an important component of the traffic analysis conducted in multilane highways. Usually, models describe traffic flow in one dimension (along the pavement axis), even though traffic flow over the highway width is generally not homogeneously distributed (e.g. trucks and slow-moving vehicles generally utilize the right lane) [6, 7]. Let us assume a divided highway with three lanes in each direction. For a divided dual carriageway, the default

LDF value according to IRC:37-2018 is 60%. Let us assume a scenario, wherein 80% of the vehicles are using the design lane. The pavement is now considered to be under designed and the design lane will reach failure sooner than the other lanes. If only 40% of the vehicles are using the design lane, then the pavement is over designed resulting in higher initial cost of construction. A variety of factors influence the traffic distribution across lanes, including vehicle composition, driver behaviour, the need for overtaking and lane width [8]. The above factors vary depending on the type and characteristics of any given highway. This influences the LDF values and therefore there is a need to recalculate the LDF values when designing individual highways [9].

Studies have shown that LDF varies significantly with traffic volume, time of day and driver population characteristics [9]. Speed also plays an important role. Heavy vehicles usually move at a speed less than normal commercial vehicles. They tend to use the outer lane or the left most lane. Fast moving cars usually occupy the inner lane. The middle lane is mostly used for the transition of one lane to the next. Only when the traffic flow is high, the middle lane is generally used. The climatic conditions also influence the choice of lane. During hard rains and winds, the drivers tend to slow down and move to the shoulder lane. Although these time periods are brief, they do influence (to varying degrees) the distribution of traffic by lane [5]. According to studies, heavy vehicles dominate the shoulder lane and rarely used the middle lane; when used, it was mostly for the transition of lanes [4]. LDF also depends on the type of highways and studies show that on expressways, the trucks used the outer lanes especially with the increase in traffic flow [10]. In India, the bus stops are provided on the left side of the carriageway. When the buses approach or exit a bus stop, they tend to use the left or the outer lane. Even during normal conditions, they tend to use the outer lane to reach the next stop especially when the buses travel within the city limits. They use the middle lane for transition between the lanes to approach or exit a bus stop. Previous studies have shown that in case of a six-lane highway, most of the trucks tend to use the outer lanes (by about 35%), while the median lane was also used by 35% of the truck traffic [5].

It is thus necessary to identify the volume and axle loads of truck traffic by lane when designing new pavement [4]. The lane that carries the heaviest vehicle traffic is known as the design lane, and it governs pavement design [11]. The design lane is subjected to repeated heavy loading, resulting in increased deflection compared to the other lanes [5]. Highway engineers are concerned about the performance of the design lane as it is likely to reach the end of its service life sooner than other lanes. To withstand the higher number of heavy vehicle traffic experienced by this lane, the pavement must be designed accordingly. For this purpose, the lane with the highest loading is selected as the design lane and then companion lanes are designed similar to it [12]. The lane distribution of mixed traffic flow is utmost necessary for design of flexible pavement and pavement maintenance management [13].

In this regard, the objectives of this study are (i) to analyse the choice of lane for vehicles of different category in a particular stretch of the chosen highway and (ii) to calculate the lane distribution factor (LDF) for at least two different types of highways and (iii) to evaluate the impact of LDF on the design life of a flexible

pavement. In this study, three highway sections comprising two four-lane stretches and one six-lane stretch were chosen, and the traffic volume on the selected ten points along these three stretches was recorded. The data was then processed to identify the choice of lane for different vehicle categories in the selected study area. On identifying the choice of lane, the LDFs for the selected stretches are calculated. Based on the analysis of traffic data, it was found that the LDF values obtained for the selected four-lane stretches were closer to the values recommended by IRC:37-2018, whereas for the six-lane stretch, the values obtained were almost half of the value recommended by IRC:37-2018. The variability in LDF depending on the time of the day and the choice of data collection point was also highlighted.

2 Data Collection

2.1 Site Selection

Different literatures were reviewed and the site selection for traffic survey was based on the below mentioned factors:

1. There is no influence of lateral restrictions such as ramps, traffic lights and/or rest stops. There is little or no influence of vehicles turning left and right, so entries and exits are located a considerable distance away. The traffic must be free flowing [5].
2. The data collection points chosen on a given highway should be located fairly close together so that the traffic observed at the locations are almost identical [14].
3. There should be a suitable viewing point at each data collection point with good visibility of the traffic operation while offering maximum concealment of the data collection operation [4].
4. There must be no significant up or downhill gradient [12].
5. No pavement defects should be present closer to the data collection point that can adversely affect traffic flow [13, 14].
6. Sections should be selected on roads that carry different types of traffic, mainly heavy vehicle traffic [15].
7. The physical condition of the shoulders and medians should be in an as-built condition [12].

Considering the criteria above, two four-lane sections and a six-lane section were chosen for the study. They are given in Table 1.

Table 1 Data collection stretches

Stretch	Highway	Points chosen	Type of highway
Stretch A	Coimbatore-Gundlupet highway (NH-181)	1. Kavundampalayam 2. Cheran nagar 3. Thekkupalayam Privu 4. Veerapandi Privu	4-lane undivided
Stretch B	Coimbatore-Nagapattinam highway (NH-83)	5. Chinthamanipudur 6. Sulusur 7. Karanampettai	4-lane undivided
Stretch C	Kochi-Salem highway (NH-544)	8. Thennampalayam 9. Neelambur 10. Sitra	Dual three-lane carriageway

2.2 Site Description

The first stretch A is NH-181 that connects Coimbatore in Tamil Nadu to Gundlupet in Karnataka. The stretch chosen for study is the Coimbatore-Mettupalayam stretch, which is a four-lane flexible pavement, having two lanes in each direction. Four points were taken along this stretch. The points located along this stretch were Kavundampalayam, Cheran nagar, Thekkupalayam Privu and Veerapandi Privu. The traffic flow in the first point (Kavundampalayam) was sometimes restricted due to the construction of a bridge few kilometres before the test site. The second stretch B is NH-83 connecting Coimbatore and Nagapattinam in Tamil Nadu. The selected area is between Coimbatore-Sulusur, which is also a four-lane flexible pavement. Three points, namely Chinthamanipudur, Sulusur and Karanampettai were taken in this stretch for data collection. The third stretch C, NH-544, connects Kochi in Kerala and Salem in Tamil Nadu. The study area taken along this highway is the Coimbatore-Neelambur stretch, which is a six-lane flexible pavement with three lanes in each direction. Three points, Thennampalayam, Neelambur and Sitra, were taken for the study. All the ten data collection points were chosen in accordance with the conditions mentioned in Sect. 2.1. There were no restrictions to traffic flow observed at any of the locations except for the third point in stretch B. There was a toll plaza nearby the third point resulting in the slowing down of the vehicles. Figure 1 shows the data collection points taken for the traffic survey.

2.3 Data Collection Procedure

Traffic surveys were carried out at each point along the sections chosen for the study. The surveys were conducted for a seven-day period. The dates for data collection were chosen such that there were no major changes in the traffic flow due to festivals or holidays. For this reason, the counts were not made on a holiday [5]. The procedure for lane distribution factor consisted essentially of monitoring lane use by vehicle type

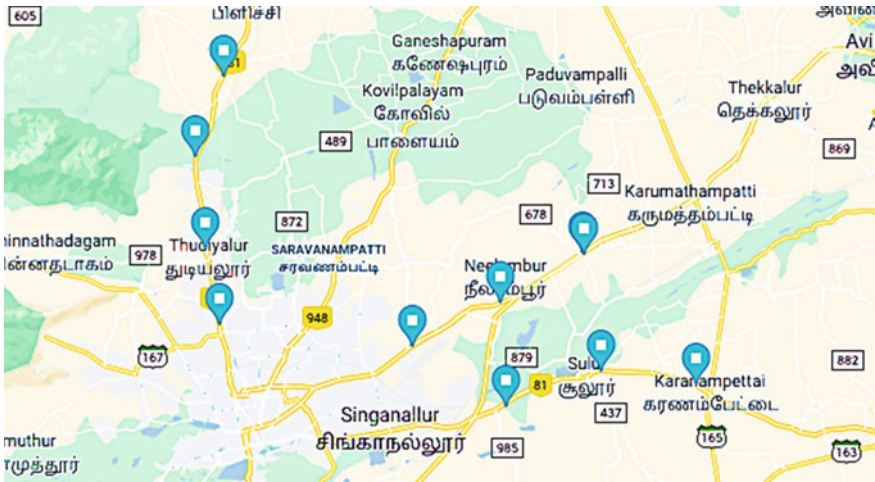


Fig. 1 Data collection points for traffic survey

for each vehicle passing through the test site. Lane distribution data was recorded for a specific test site, direction of travel and time interval using cameras. A camera was placed on the buildings near the selected points so as to capture all traffic movements. Data was collected for a period of 2 h in the morning (10 am to 12 pm) and 2 h in the afternoon (1:30 pm to 3:30 pm) totalling up to 4 h for the four points along stretch A. For stretches B and C, the data was collected for a period of 2 h in the morning (9 am to 11 am) and one hour in the afternoon (1 pm to 2 pm) for the three points in each stretch.

2.4 Data Extraction

The videos from the test sites were analysed to identify the vehicles using different lanes. The lane distribution data was obtained by observing lane use by vehicle type for each vehicle passing through the study location. The lanes are numbered from 1 to n , starting from the shoulder lane. If a vehicle occupies more than one lane at the time of observation, the lane in which a major portion of the vehicle is present is considered as the lane in which the vehicle is travelling.

3 Results and Discussion

3.1 Influence of Data Collection Points

Figure 2 shows the percentage of vehicles travelling on each lane for the seven points as indicated in Table 1. Only the heavy vehicles were considered here. Lane 1 and 2 represent the traffic towards the city, and lane 3 and 4 represent the traffic away from the city. Lane 1 and 4 are the outermost lanes in their respective directions. From Fig. 2, it can be observed that the lane distribution percentage of heavy vehicles varies marginally for all the chosen points along the selected four-lane stretch for study. From Fig. 2, it can be inferred that Lanes 2 and 3 are the most commonly used lanes followed by Lanes 1 and 4. At an average, about 13% of the heavy vehicles used lane 1; 39.4% used lane 2; 30.5% used lane 3 and 17.1% used lane 4. The outer lanes were rarely used, while the inner lanes were used at an average of 35% per lane by the heavy vehicles.

Table 2 gives the lane distribution for the six-lane highway. From Table 2, it can be observed that the lane distribution varies along the lanes for each point. Here also, it can be seen that the inner most lane, namely lanes 3 and 4 were highly used when compared to the other lanes. For points 8 and 10, lane 3 is the most commonly used lane, which represents the traffic towards the city. Along point 9, the most commonly used lane is lane 4, wherein traffic moves away from the city. The innermost lanes are the most used lanes, at an average of 31% for a given lane. In case of the six-lane stretch, the percentage of vehicles choosing the innermost lanes is relatively lower than the four-lane stretches. This reduction is due to the presence of the intermediate lanes which were used at an average of 18.5%. Lane 1 and lane 6 were used at an average of 1.5% and 0.4%, respectively, and therefore, the outer lanes were used at an average of 0.95%, mostly by the motorcyclists.

The LDF values were then computed for all the points. The lane distribution factor for a lane is the percentage of heavy vehicles choosing a particular lane along a particular highway. It is also known as lane usage, lane split or lane ratio. This is given by Eq. 1.

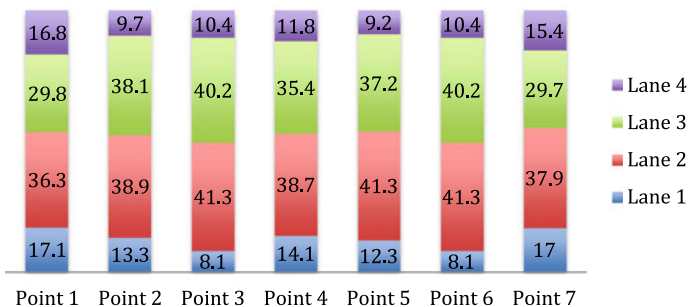


Fig. 2 Average heavy vehicle lane distribution for the four-lane stretches

Table 2 Average heavy vehicle lane distribution for the six-lane highway

	Lane 1	Lane 2	Lane 3	Lane 4	Lane 5	Lane 6
Point 8	0.8	19.8	30.4	29.8	18.7	0.5
Point 9	0.7	19.1	30.8	31.9	17.1	0.4
Point 10	1.5	17.2	32.7	29.5	18.8	0.3

$$LDF = \frac{\text{Total number of vehicles using a particular lane}}{\text{Total number of vehicles plying on that road}} \tag{1}$$

Using Eq. (1), the LDF values were calculated and averaged for all the seven days for a given point. The average values are given in Table 3. From Table 3, it can be observed as the heavy vehicle traffic distribution along the lanes varies at each of the points, the corresponding LDF values also change. For point 1 (0.37), the LDF is comparatively less than the recommended value since the traffic was diverted, and the point 3 is observed to have the highest LDF value (0.43), which is slightly higher than the standard value according to IRC:37-2018 which recommends a value of 0.4. The other values along the four-lane stretches are closer to the recommended values for the four-lane stretch. For a given highway, there is about 5% variability depending on the point of data collection. In case of the dual three-lane carriageway, the values vary significantly compared to the recommended values by IRC:37-2018. The values obtained are almost half of the recommended values in IRC:37-2018 for dual three-lane carriageway highway. The reason behind such variability is not clear at this juncture.

Table 3 Average LDF values

Points	Obtained average LDF value	LDF according to IRC
1. Kavundampalayam	0.37	0.4
2. Cheran nagar	0.41	
3. Thekkupalayam Pirivu	0.39	
4. Veerapandi Privu	0.42	
5. Chinthamanipudur	0.43	0.4
6. Sular	0.42	
7. Karanampettai	0.38	
8. Thennampalayam	0.31	0.6
9. Neelambur	0.32	
10. Sitra	0.33	

3.2 Influence of Time of Data Collection

Figure 3 represents vehicle composition for point 4 as an instance depending on the day in which the data was collected. This figure shows that the lane usage of the vehicles exhibits daily variation, and a similar variability was observed for the other locations also. The survey was started on a Monday and completed on a Monday excluding Sunday. Here, lane 2 is used at an average of 39% and lane 3 at an average of 35%. The outer lanes were the least used at an average of 12.3%. The variability was observed to be higher for lane 2, wherein it varied from 34.3% on day 5 to 42.6% on day 4. For lane 3, the variability was from 32.9% on day 7 to 38.7% on day 5. This shows that the LDF's could vary depending on the day and time of the survey collected. Table 4 gives the LDF values calculated for point 4. From Table 4, it can be observed that the LDF values vary from 0.38 to 0.44, which is about 6% variability. Based on the results given in Tables 3 and 4, it is seen that LDF is more sensitive to the temporal variation in comparison with the spatial variation for the conditions considered in this study.

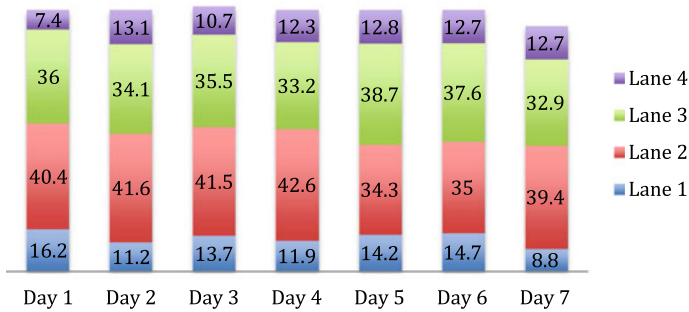


Fig. 3 Heavy vehicle lane distribution for point 4

Table 4 Calculated seven-day LDF values of point 4-Stretch A

Days of the week taken for survey	Obtained LDF values
Day 1-Monday	0.44
Day 2-Tuesday	0.44
Day 3-Wednesday	0.43
Day 4-Thursday	0.43
Day 5-Friday	0.40
Day 6-Saturday	0.38
Day 7-Monday	0.41

Table 5 Vehicle composition at selected points

Point	Type of vehicle	Lane 1	Lane 2	Lane 3	Lane 4	Obtained LDF
Point 1-(Kavundampalayam) Stretch A	Trucks	12.3	41.4	34.9	11.4	0.42
	Buses	29	24.3	18.1	28.6	0.33
	Cars	12.4	37.5	35.4	14.7	0.38
Point 6-(Sulur) Stretch B	Trucks	6.3	38.4	48.5	6.8	0.46
	Buses	24.4	29.8	33.3	12.5	0.35
	Cars	14.9	36.5	38.1	10.5	0.39

3.3 Influence of Vehicle Composition

Table 5 gives the vehicle composition along the dual three-lane carriageway highway (six-lane highway) for selected stretches. From Table 5, it can be observed that the lane usage depended on the type of vehicle also. The highest vehicle composition in a given lane was observed for trucks. For instance, for point 1, it is seen that 76.3% of the trucks use the inner lane and only the remaining 23.7% trucks use the outer lane. For buses and cars, the percentage of vehicles using the inner lane is 42.4% and 72.9%, respectively. A similar behaviour is also seen for point 6 given in Table 5. Trucks and cars used the inner lanes to traverse, while buses use both lanes. The above data indicates that the average lane distribution differs for each vehicle type. In this case, it was observed that the truck traffic was predominant and the LDF was observed to be high for trucks (an average of 0.44), higher than the value suggested by IRC:37-2018 (0.4). The volume of the buses was comparatively low and the calculated LDF value is also less (average of 0.34) than the value 0.4 recommended by IRC:37-2018.

3.4 Average Lane Distribution Factor (LDF)

The average LDF for the selected stretches are calculated as given in Table 6. From Table 6, the LDF for the chosen four-lane stretches is closer to the value recommended by IRC:37-2018, whereas the value obtained for the chosen six-lane stretch is less compared to the value recommended by IRC:37-2018.

Table 6 Calculated LDF values

Stretch	Calculated LDF	LDF according to IRC
Stretch A (NH181)	0.4	0.4
Stretch B (NH 84)	0.41	0.4
Stretch C (NH-544)	0.32	0.6

Table 7 LDF of chosen section

Stretches chosen	LDF	MSA obtained
Four-lane stretches A and B	0.37	25.8
	0.44	30.7
Six-lane stretch C	0.32	22.3
	0.60	41.9

4 Impact of LDF on Pavement Performance

The design traffic, in terms of the cumulative number of standard axles to be carried during the design period of the pavement, is estimated using Eq. (2). Here, a design period (*n*) of 20 years with the vehicle damage factor (*F*) as 5.2 and the annual growth rate (*r*) of commercial vehicles as 0.06, i.e. 6% is chosen as per the values suggested in IRC:37-2018, assuming an ADT of 1000 vehicles in one way direction. The LDF values chosen are based on the maximum LDF values obtained from the collected data and recommended values by IRC:37-2018.

$$N = \frac{365 \times [(1 + r)^n - 1]}{r} \times A \times D \times F \tag{2}$$

Table 7 shows that for the two 4-lane stretches, when LDF varied from 0.37 to 0.44, the design traffic is increased by about 5 MSA. Since a 30 MSA section is chosen for both the cases, one may not see any significant difference in the strain values when calculated for the four-lane stretches. For the six-lane stretch, however, the obtained LDF value is 0.32 while that mentioned in the IRC:37-2018 guideline is 0.6. From Table 7, it can be seen that the design traffic is reduced by about half in this case and the cross-sections to be chosen also differ. However, only one six-lane stretch was considered in this study. Data from additional stretches are required to comment about the LDF obtained from field for the six-lane highway. It was also seen that the influence of LDF values increased with increase in AADT values.

5 Conclusion

In this study, it was desired to estimate the LDF value obtained from field for different highway stretches and compare it with the values specified in IRC:37-2018. For this purpose, the video of the traffic flow was recorded for two four-lane and one six-lane highway for 7 days and one hour each day. The recorded video was analysed manually, and the lane distribution was estimated. The following are the conclusions obtained from this study.

1. The obtained LDF values for the selected four-lane stretches (Stretch A and B) are approximately equal to 0.4 and 0.41. This value is similar to the values given

- by IRC:37-2018, which recommends a value of 0.4 for four-lane highway. Hence, the obtained values are in line with the recommendations given by IRC:37-2018.
2. The obtained LDF value for the chosen dual three-lane carriageway (six-lane stretch) is approximately equal to 0.3. The values recommended by IRC:37-2018 is however 0.6. The LDF obtained here is only half of the value specified in IRC:37-2018. Additional data from six-lane highways has to be collected to probe onto this variability.
 3. Most of the trucks and cars used the inner lane. About 73–87% of trucks and 72–75% of the cars used the inner lanes. Buses mainly used the outer lanes for entry and exit. The percentage of buses using the inner lane is about 49–63%.
 4. The point of data collection along a given highway and the time of data collection exhibited a marginally significant effect on the LDF value obtained. The LDF varied from 0.37 to 0.44 considering both the cases. This is said to influence the design traffic capacity by about 5 MSA for an AADT of 1000 CV/day. This influence is significant in the case of dual three-lane carriageway (six-lane stretch) as the design traffic is reduced by about 50%.

References

1. Rodrigue JP (2016) The role of transport and communication infrastructure in realizing development outcomes. In: *The Palgrave handbook of international development*. Palgrave Macmillan, London, pp 595–614
2. Sanjay G (2012) Perpetual flexible pavements: pavements of future. *J Indian Road Cong* 73(1)
3. IRC:37-2018. Guidelines for the design of flexible pavements, Fourth revision. Indian Roads Congress, New Delhi
4. Pompigna A, Rupi JF (2017) Lane-distribution models and related effects on the capacity for a three-lane freeway section: case study in Italy. *J Transp Eng Part A Syst* 143(10)
5. Lynch I, Gary N (1969) Lateral distribution of traffic on a four-lane and six-lane section of I-75 south of Covington, Hamby. Research report submitted to the division of research, Department of Highways of the commonwealth of Kentucky
6. Laval L, Daganzo CF (2006) Lane-changing in traffic streams. *Transp Res Part B: Methodol* 40(3):251–264
7. Fisk C (1990) Traffic assignment and the lane choice problem. *Transportation Research Board* 24B(5), Washington DC
8. Albright D, Blewett C (1988) Volume-based model for forecasting truck lane use on the rural interstate. *Transportation Research Board (TRB)*, Washington DC
9. Asaithambi G, Kanagaraj V, Toledo T (2016) Driving behaviors: models and challenges for non-lane based mixed traffic. *Transp Dev Econ* 2(19)
10. Fwa TF, Li S (1995) Estimation of lane distribution of truck traffic for pavement design. *J Transp Eng* 121(3)
11. Yerneni LP (1996) Lane distribution behavior of mixed traffic flow. M. Tech. Dissertation, REC, Warangal
12. Golias J, Tsamboulas D (1995) Introduction to macro level estimation of highway lane usage. *J Transp Eng* 121(1)
13. Koganti SP, Raja KH, Sajja S, Narendra SM (2018) A study on volume, speed and lane distribution of mixed traffic flow by using video graphic technique. *Int J Eng Technol* 7(2.1):59–62

14. Reddy B (1993) Effect of lateral placement of vehicles on development of pavement distress. M. Tech. Dissertation, REC, Warangal
15. Chandra S, Kumar U (2003) Effect of lane width on capacity under mixed traffic condition in India. J Transp Eng 129(2):155–165

Pavement Evaluation and Management

Establishing an Optimum Maintenance Strategy for a National Highway Using HDM-4: A Case Study of NH 66 Section in Kerala, India



Sangeetha Jayamohan, V. S. Sanjay Kumar, and T. Sreelatha

Abstract Timely maintenance of pavements is an essential requirement for the efficiency of any road network. Roads which are inadequately maintained most often require major rehabilitation works to be performed much earlier than those which are maintained on a regular basis. This could result in huge financial burdens on the economy. The requirements for pavement maintenance and repair are continuously increasing, but the resources and funds are limited. Hence, a proper pavement management system is necessary to preserve the road assets in a good condition, to achieve a more efficient allocation of the available funds and a more accurate evaluation of future needs. This paper presents the use of the World Bank developed HDM-4 model for deriving optimum maintenance standards for flexible pavements. The portion of NH66 passing through Thrissur district of Kerala was considered for the study. Required data was collected, and analysis was carried out at the project level for determining the optimum maintenance strategy, based on the criteria of maximization of ratio of net present value to cost. It is hoped that the results of this study shall be of use to the highway agencies in better decision making and effective management of the highway network.

Keywords Pavement management system · Road assets · Maintenance · Serviceability · HDM-4

S. Jayamohan (✉) · T. Sreelatha
RIT, Kottayam, India
e-mail: sangeethajayamohan97@gmail.com

T. Sreelatha
e-mail: sreelatha@rit.ac.in

V. S. Sanjay Kumar
NATPAC, Trivandrum, India

1 Introduction

Transportation infrastructure is like a baseline that ensures continuous and smooth flow of people and goods. Effective transportation is an indispensable element to achieve economic progress. Among the various transportation systems, road transportation is crucial to economic development and growth. Roads are of great significance that makes a country grow and develop by providing access to employment, social, education and healthcare services. They help stimulate social and economic development. And, for these reasons, road infrastructure is considered to be the most important of all public assets.

The road infrastructure becomes aged due to continuous use and time, and it requires maintenance, renewal and upgradation. Construction of road infrastructure necessitates huge investments, and as a result, it is critical to maintain these assets in good order. Adequate maintenance of the road infrastructure is essential to preserve and enhance its serviceability. Inadequate maintenance can cause irreversible deterioration of the road network, which could spread across the road systems very quickly resulting in rising costs and major financial burdens. Also, delay of maintenance and rehabilitation activities can lead to a fall in the level of pavement performance [14]. The importance of maintenance thus needs to be recognized by decision-makers. A proper management system is necessary to help preserve the road assets in a good condition and to balance the long-term need, thereby benefiting the stakeholders.

The actual resources available are also much less than what is actually needed. The pavements are simply maintained rather than being properly managed [8]. In India, the road maintenance and rehabilitation techniques are currently determined entirely based on the subjective judgment and expertise of the field engineers. The life-cycle costs and other management requirements are not given any thought. The root causes of road deterioration, as well as the ineffectiveness of various maintenance measures, are frequently ignored. This is mostly due to the lack of objective databases needed for the study of different activities such as design, construction and maintenance of pavements [17].

As a result of this, there occurs a complex problem with respect to the matching of resources, equipment, time, labor, funds, design and decision making, which consequently leads to the accumulation of gap between the allocation of resources and the actual requirements over a period of time [17]. But in today's economic environment, a more systematic approach for the determination of maintenance and rehabilitation techniques and priorities is needed. Pavement management systems are now being used by highway administrations worldwide to make systematic decisions regarding all the activities related to pavement development and maintenance [18]. However, developing countries such as India still require a systematic strategy to PMS implementation. Today's highway administrators have a number of tools that help them make the best use of available resources for highway pavement maintenance and rehabilitation, but they are not universally accepted. As a result, there is a lack of global acceptance and implementation of these tools [19]. The Highway Development and Management System (HDM-4) was therefore designed by the World

Bank as a universally recognized instrument for making timely and cost-effective maintenance management choices for road networks.

2 Literature Review

Pavement maintenance management systems promote an improvement in the quality and performance of pavements as well as a reduction in the costs through effective management practices. They offer a systematic way for inspecting and assessing pavement conditions in order to assure timely maintenance and, as a result, eliminate all undetected pavement faults. It assists decision-makers in determining best strategies for existing pavement conditions through pavement evaluation and maintenance in order to maintain acceptable serviceability for a specified duration. Pavement management systems (PMS) can be simply defined as a 'set of tools or methods that assist the decision-makers in finding out the optimum strategies for providing and maintaining the pavement in a serviceable condition over a given period of time' [15]. It is a comprehensive package that is used to assess the condition of pavement, recommend the best M&R strategy, create road maintenance investment plans and conduct economic analysis of road projects [19].

Sudhakar [17] developed PMS for a network of urban roads in Chennai. The project analysis application module of HDM-4 was utilized for determining the optimum maintenance strategy for the pavement sections considered based on the criteria of maximization of NPV/cost ratio.

Odoki and Khan [9] used the HDM-4 model for establishing optimal pavement maintenance standards for Bangladesh.

Mathew and Issac [10] attempted an optimization of maintenance strategy for a rural road network in the state of Kerala. Prior to the use of the software, the HDM-4 deterioration models were calibrated to suit low volume conditions, and the optimized strategy for the network was developed using the HDM-4 strategy analysis.

Jain et al. [7] conducted a comparative study of scheduled versus condition responsive maintenance strategies which in turn could result in an optimum utilization of the maintenance funds. Economic analysis was conducted for the pavement sections, and it was found that the condition responsive maintenance was more advantageous over the analysis period than scheduled maintenance. For some pavements the resurfacing was done as per the renewal cycle even when the pavement condition was good, while for some other sections that deteriorated quickly, the renewal was urgently required but was not covered by the maintenance cycle.

Jain et al. [8] developed a PMS for selecting an optimum M&R strategy for multilane highways. The optimum strategy was chosen based on the highest value of NPV/cost ratio, and the section having a higher value of this ratio would be maintained at a higher priority than other sections.

Girimath et al. [4] determined the optimum maintenance treatment for urban road network of Bangalore city, using the HDM-4 Project Analysis.

Gupta et al. [5] used the HDM-4 Project Analysis application module for the optimization maintenance and rehabilitation strategies for three urban road sections in Punchkula district of Haryana.

Yogesh et al. [19] developed a pavement management system for a network of 21 urban roads of Noida. The aim of the study was to make use of the HDM-4 strategy analysis to determine the required funding levels for a set of user defined maintenance standards. The evaluation was done based on two criteria: maximization of the net present value (NPV) and also minimization of the cost required to achieve a target level International Roughness Index (IRI). The strategy analysis was performed, and the optimum M&R strategy under both the criteria was determined. The selection of an optimum maintenance alternative is based on the selection criteria which the planner adopts. It is for this reason that the HDM-4 strategic analysis is considered to be a customized economic evaluation tool which could be utilized in better management of urban roads.

Chopra et al. [1] developed a PMMS for an urban road network comprising four road sections in Patiala district of Punjab, using the Highway Development and Management model.

3 Objective of the Study

The study focuses on the development of a pavement maintenance management system for a selected stretch of NH66 passing through Trissur district of Kerala using the HDM-4 model. The objective of the study is to find an optimum maintenance strategy for the road sections based on the criteria of maximization of net present value to cost ratio.

4 Overview of the Highway Development and Management Model (HDM-4)

The Highway Development and Management (HDM-4) is a globally recognized decision-making tool developed by the World Bank for evaluating the engineering and economic feasibility of the of potential road investment alternatives. It is an international standard which helps predict the future economic, social and environmental and technical implications of investment decisions concerning maintenance and management of pavements. HDM-4 was created as a result of a number of investigations conducted in various parts of the world. Despite the fact that it was founded by the World Bank in the late 1960s, several of the world's major research institutions have made significant contributions to its development during the past three decades. The HDM-4 system could be used to make good investment decisions at all levels of management.

4.1 HDM-4 Applications

The three basic areas of analysis that can be undertaken in HDM-4 are project analysis, program analysis and strategy analysis [19].

The project analysis can be utilized to compare the physical, functional and economic feasibility of various project alternatives against a base alternative of 'do nothing'. This can be done for the evaluation of M&R options for existing roads, for geometric improvement or pavement upgradation schemes, construction of new roads and so on.

The program analysis is largely concerned with prioritizing a long list of candidate road projects into a one-year or multi-year work schedule that is constrained by a budget. This tool has been integrated into HDM-4 to allow for quick examination of the entire road network in order to identify candidate road sections for maintenance during a certain budget period. The maximization of the NPV/cost ratio is adopted as the economic criteria for selection of the candidate road for maintenance under the constrained budget.

Strategic analysis refers to the analysis of a certain road network as a whole. The preparation of estimates of investment needs for road network development and maintenance under various budget conditions is a typical application of strategy analysis. Estimates are made for medium to long-term expenditure requirements ranging from 5 to 40 years. The applicability of program and strategy analysis is determined by the size of the road network under consideration as well as the length of the analysis period. Program analysis is usually favored for a smaller highway network and a shorter period of analysis, but strategic analysis is more effective for a bigger highway network and long-term strategic planning [19].

5 Methodology

The methodology adopted for the study is illustrated in the flowchart shown in Fig. 1.

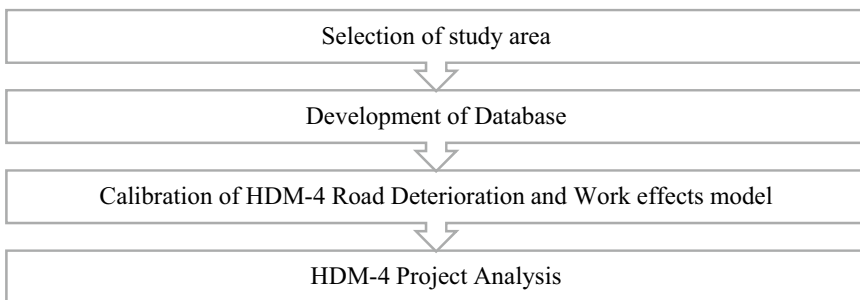


Fig. 1 Methodology of the study

Table 1 List of study sections

S. No.	Section ID	Section name	Length (m)
1	N1	Kottapuram–Chanthapura	800
2	N2	Chanthapura–Kottapuram	800
3	N3	Chanthapura–Mathilakam	1000
4	N4	Mathilakam–Moonupeedika	1000
5	N5	Moonupeedika–Thriprayar	1000
6	N6	Thriprayar–Vadanapally	1000
7	N7	Vadanapally–Chettuva	1000
8	N8	Chettuva–Chavakkad	1000

The first stage is the selection of the highway network for analysis. The second stage involves the collection of the required data. The third stage is to calibrate the road deterioration and work effects model of HDM-4 to suit the conditions of the study area. In the fourth stage, all the required data is given as input to the software, and project level analysis is carried out. The optimum maintenance strategy is selected based on the results of the economic analysis.

5.1 Selection of the Study Area

National Highway 66, commonly referred to as NH 66 is a 1608 km long busy National Highway running roughly north–south, parallel to the Western Ghats along the west coast of India. It connects Panvel in Maharashtra to Kanyakumari in Tamil Nadu and passes through the states of Maharashtra, Goa, Karnataka, Kerala and Tamil Nadu.

For the study, the portion of NH 66 passing through Thrissur district of Kerala, starting from Kottappuram and ending at Chavakkadu, is selected. The total length of the stretch of NH 66 selected for the study is 49.7 km. The total study stretch was then divided into homogenous sections from which 8 sections (6 sections of 1 km each and 2 sections of 800 m) were demarcated for further data collection. Table 1 shows the list of study sections. Figure 2 shows the study stretch.

5.2 Data Collection

The data requirements for analysis using HDM-4 can be categorized into the following four categories:

- Road network data
- Vehicle fleet data

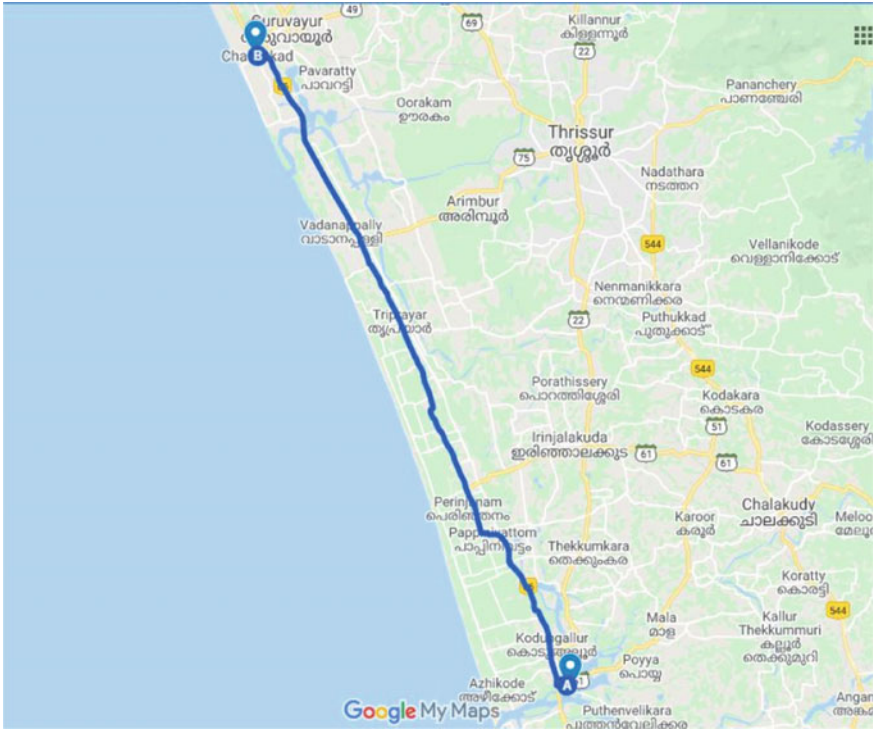


Fig. 2 Map view of the study stretch. Source Google Maps

- Maintenance and rehabilitation works data
- Cost data.

Road Network Data: The road network data collection involves the road inventory data and the pavement structural and functional condition data. Inventory data includes details like length and width of the sections, shoulder width, drainage conditions, details of maintenance and rehabilitation works, etc. The structural condition of the test sections was assessed in terms of their rebound deflection values by performing the Benkelman beam deflection survey. The functional condition was assessed in terms of pavement condition as well as roughness. The roughness survey was performed using ARRB Roughometer. Pavement condition survey was conducted to determine the extent and severity of different distresses present on the pavement. The predominant distresses that were observed on the test sections include longitudinal, transverse and edge cracking, alligator cracking, raveling, potholes and so on. The characteristics of the study sections are summarized in Table 2, and the pavement condition survey data is shown in Table 3.

Vehicle Fleet Data: This comprises the details like basic characteristics of vehicles, economic cost details of vehicles, vehicular compositions and growth rates.

Table 2 Road network data

S. No.	Section ID	Carriageway width (m)	Roughness IRI (m/km)	Characteristic deflection (mm)	Traffic volume (veh/day)
1	N1	7	3.45	0.639	17,638
2	N2	7	3.55	0.532	17,638
3	N3	7	3.15	0.380	34,576
4	N4	7	2.75	0.303	35,816
5	N5	7	3.55	0.328	41,755
6	N6	7	2.95	0.287	26,642
7	N7	7	2.60	0.305	26,970
8	N8	6	3.00	0.353	20,599

Table 3 Pavement condition data

Section ID	Cracking area (%)	Raveled area (%)	Potholes (%)	Depression (%)	Patchwork (%)
N1	13.76	0.126	0	0.073	0.82
N2	1.24	0.246	0	0.01	1.97
N3	0.1	0.187	0	0	0
N4	0	0.0025	0	0	0
N5	0	0.375	0	0	0
N6	0	0.005	0	0	0
N7	0.011	0	0	0	0
N8	0	0.013	0	0	0

The vehicle fleet for the present study consists of only motorized vehicles, as non-motorized transport is not very common in the study area.

Maintenance and Rehabilitation Works Data: *Maintenance Serviceability Levels:* The maintenance serviceability levels considered for the study are based on the recommendations of IRC: 82–2015 [6]. The serviceability levels and the allowable levels of defects in terms of roughness and distresses like cracking, raveling and pothole are shown in Table 4.

Cost Data: *Cost of Maintenance and Rehabilitation Works:* The costs of various maintenance items were obtained from the ‘Report of the Committee on Norms for Maintenance of Roads in India’, MoRTH 2001 [12]. These costs were updated to the base year 2020–2021 by using the mathematical model for updation of norms. The updated costs for the different maintenance activities are shown in Table 5.

Road User Cost: One of the most important components in the life-cycle cost analysis of pavements is road user cost, which is the expense incurred by vehicle operators and the traveling public. The vehicle operating cost, the time cost and the cost of a

Table 4 Serviceability levels for highways

Serviceability indicator	Level 1 (Good)	Level 2 (Fair)	Level 3 (Poor)
Cracking (%)	< 5	5–10	> 10
Raveling (%)	< 1	1–10	> 10
Potholes (%)	< 0.1	0.1–1	> 1
Roughness (max permissible)	1800 mm/km	2400 mm/km	3200 mm/km
Equivalent IRI	2.52 m/km	3.26 m/km	4.21 m/km

Source IRC: 82–2015 [6]

Table 5 Costs data for various maintenance activities

Type of maintenance activity	Unit costs for the base year 1999–2000 (Rs per sqm)	Updated costs for 2020–2021 (Rs per sqm)
<i>Routine maintenance</i>		
Crack repair	30	93.9
Pothole patching	37.8	118.3
<i>Periodic maintenance</i>		
25 mm DBSD	75.14	295.15
40 mm BC	171.44	672.0
50 mm DBM	172.01	674.31

road accident make up the road user cost. The price that has to be spent by the user in moving a vehicle per unit distance on the road is known as vehicle operating cost. The monetary worth of the time spent by people traveling and the time consumed by freight in transit is referred to as time cost. The cost of a traffic accident includes human life and property losses, which are difficult to quantify in monetary terms. Among these components, the VOC is the largest component and is considered in this study. The VOC components include cost of new vehicle, fuel cost, lubricating oil cost, tyre replacement costs and so on.

5.3 Calibration of HDM-4

The HDM-4 pavement deterioration models were developed as a result of a large number of field experiments carried out in various locations across the world. As a result of this, if the default equations are used without proper calibration, the predicted performance of the pavement may differ from what is actually observed on the road sections. So, in order to improve the accuracy of pavement performance predictions and vehicle resource consumption, proper calibration of HDM-4 is required. Prior to using HDM-4, it is assumed that the pavement performance models will be calibrated

Table 6 Calibration factors

Model	Calibration factors
Roughness progression	0.2
Cracking progression	0.7
Raveling progression	0.3
Pothole progression	0.7

to match the observed rates of deterioration on the pavement sections where the models will be applied [2].

Prior to the study, the deterioration models of HDM-4 were calibrated using secondary data collected from National Transportation Planning and Research Centre (NATPAC), Trivandrum [13]. Calibration was done for roughness progression model, cracking progression model, raveling progression model and pothole progression model, and the obtained calibration factors are shown in Table 6.

The calibration of HDM-4 models revealed that the progression of deterioration for the study stretch is at a slower rate than that predicted by the HDM-4 models. The obtained calibration factors were also compared with works carried out within and outside Kerala [2, 3, 11, 16], and it was observed that the values were comparable with the obtained results.

5.4 Maintenance Strategies Considered

The M&R alternatives considered for the study and the intervention criteria adopted are shown in Table 7. Four alternatives along with routine maintenance as the base alternative is considered. The intervention criteria were fixed based on the serviceability levels as per IRC: 82-2015 [6].

Table 7 M&R alternatives considered

Alternative	Works standard	Description of work	Intervention criteria
Base alternative	Routine maintenance	Crack sealing and patching	Scheduled annually
Alternative 1	Resealing	25 mm DBSD	Total damage area \geq 10%
Alternative 2	Resealing	25 mm DBSD	Total damage area \geq 10%
	Overlay	40 mm BC	IRI \geq 3.26 m/km
Alternative 3	Overlay	40 mm BC	IRI \geq 3.26 m/km
Alternative 4	Mill and Replace	Remove 90 mm surface and provide 50 mm DBM + 40 mm BC	Total carriageway cracked area \geq 10% IRI \geq 4.21 m/km

Routine maintenance activities like crack sealing and patching are to be performed on an annual basis. The resealing is to be done with 25 mm double bituminous surface dressing (DBSD). For triggering resealing of the pavement surface, the total damage area comprising cracking, raveling, and potholing area was considered as the controlling factor, while for overlays, roughness in terms of IRI was considered. For the study overlay using 40 mm bituminous concrete (BC) was considered. In case of the mill & replace alternative, total percentage of carriageway cracked was also considered along with the roughness criterion. Here, the top 90 mm of the surface will be removed and replaced with 50 mm Dense Bituminous Macadam (DBM) followed by 40 mm bituminous concrete.

5.5 Project Analysis

The project analysis was set up with routine maintenance as the base alternative with which all other alternatives were compared. Economic analysis was conducted at a discount rate of 12% and for a period of 10 years. The maintenance and rehabilitation work reports and the economic analysis summary reports were generated. A sample of M&R work report and the associated costs for section N1 are shown in Tables 8 and 9. The economic analysis summary for the entire project is shown in Table 10.

5.6 Selection of the Optimum Maintenance Strategy

Based on the results of the economic analysis, it is observed that Alternative 3, i.e., 40 mm BC overlay, has the maximum value of net present value/cost ratio. The internal rate of return is also higher for this alternative. So, overlay with 40 mm bituminous concrete is suggested as the optimum maintenance strategy for the pavement sections under study.

6 Conclusions

The objective of this paper was to overcome some of the limitations in the current maintenance and rehabilitation practices and to provide a better aid in decision making. The Highway Development and Management Model (HDM-4) developed by the World Bank can be used as a very powerful tool in this respect. In this paper, an attempt was made to optimize the maintenance strategies for the pavement section under study based on the criteria of maximization of net present value to cost ratio. The software was calibrated prior to the study so as to suit the conditions of the study area. Five different alternatives along with their intervention criteria were defined,

Table 8 Sample of M&R work report for section N1

Year	Base alternative	Alternative 1	Alternative 2	Alternative 3	Alternative 4
2021	Patchwork and crack sealing	25 mm DBSD	40 mm BC	40 mm BC	***
2022	Patchwork and crack sealing	***	***	***	***
2023	Patchwork and crack sealing	***	***	***	***
2024	Patchwork and crack sealing	25 mm DBSD	***	***	Mill and replace
2025	Patchwork and crack sealing	***	40 mm BC	40 mm BC	***
2026	Patchwork and crack sealing	25 mm DBSD	***	***	***
2027	Patchwork and crack sealing	***	***	***	***
2028	Patchwork and crack sealing	25 mm DBSD	25 mm DBSD	***	***
2029	Patchwork and crack sealing	25 mm DBSD	25 mm DBSD	***	***
2030	Patchwork and crack sealing	25 mm DBSD	40 mm BC	40 mm BC	***

*** indicates that 'no M&R work is assigned in that particular year'

Table 9 Sample of cost report for section N1

Year	Cost of works in Million Rupees				
	Base alternative	Alternative 1	Alternative 2	Alternative 3	Alternative 4
2021	0.0097	1.652	3.763	3.763	0.00
2022	0.0156	0.00	0.00	0.00	0.00
2023	0.0143	0.00	0.00	0.00	0.00
2024	0.0132	1.652	0.00	0.00	7.543
2025	0.0186	0.00	3.763	3.763	0.00
2026	0.0218	1.652	0.00	0.00	0.00
2027	0.0217	0.00	0.00	0.00	0.00
2028	0.0215	1.652	1.652	0.00	0.00
2029	0.0212	1.652	1.652	0.00	0.00
2030	0.0191	1.652	3.763	3.763	0.00
Total cost	0.1767	9.917	14.595	11.289	7.543

Table 10 Economic analysis summary for the pavement sections

Alternative	Increase in agency cost (C)	Decrease in user cost (B)	Net present value (NPV = B – C)	NPV/cost ratio	Internal rate of return (IRR)
Base alternative	0.00	0.00	0.00	0.00	0.00
Alternative 1	73.699	885.836	812.136	11.020	451.1
Alternative 2	95.200	1965.943	1870.743	19.651	559.9
Alternative 3	53.470	1673.138	1619.668	30.291	575.1
Alternative 4	33.900	881.456	847.556	25.001	421.9

and economic analysis at the project level was carried out using HDM-4. The alternative ‘40 mm BC overlay’ was obtained as the optimum maintenance strategy based on the results of economic analysis, and the intervals of application of the overlay were also obtained from the work reports.

References

1. Chopra T, Parida M, Kwatra N, Mandhani J (2017) Development of pavement maintenance management system (PMMS) of urban road network using HDM-4 model. *Int J Eng Appl Sci (IJEAS)* 9(1):14–31
2. Deori S, Choudhary R, Tiwari D, Gangopadhyay S (2019) HDM-4 deterioration modelling: validation and adoption for flexible pavements with modified bituminous road surfacing. *Int J Pavement Eng* 14(2):208–226
3. Geethu S, Sreelatha T, Sreedevi BG (2013) A case study on overlay design using HDM-4. *Int J Innov Res Sci Eng Technol* 2(Special Issue 1)
4. Girimath SB, Chilukuri V, Sitharam TG, Krishnamurthy (2014) Pavement management system for urban roads. *Int J Sci Res Dev* 2(3)
5. Gupta PK, Kumar R (2015) Development of optimum maintenance & rehabilitation strategies for urban bituminous concrete surfaced roads. *Int J Sci Technol Res* 4(2)
6. IRC: 82-2015 Code of practice for maintenance of bituminous road surfaces. Indian Road Congress, New Delhi
7. Jain K, Jain SS, Chauhan MPS (2012) Schedule and condition responsive maintenance strategies for optimum utilization of maintenance budget. *Int J Eng Res Dev* 1(8):47–53
8. Jain K, Jain SS, Chauhan MPS (2013) Selection of optimum maintenance and rehabilitation strategy for multilane highways. *Int J Traffic Transp Eng* 3(3):269–278
9. Khan MU, Odoki JB (2010) Establishing optimal pavement maintenance standards using the HDM-4 model for Bangladesh. *J Civ Eng (IEB)* 38(1):1–16
10. Mathew BS, Issac KP (2011) Optimization of maintenance strategy for rural road network using HDM-4. National Technological Congress, Kerala
11. Mathew BS, Rose S, Isaac KP, Chandrasekhar BP (2010) Pavement performance modelling and calibration of HDM-4 deterioration models for rural roads in India. *J Inst Eng (India)* 91
12. MoRTH (2001) Report of the Committee on norms for maintenance of roads in India. Ministry of Road Transport & Highways, Government of India, New Delhi
13. NATPAC (2020) Road asset management for National Highways and State Highways in Kerala. Study Report

14. Peterson DE (1981) Evaluation of pavement maintenance strategies. National Cooperative Highway Research Program—Synthesis of Highway Practice, Transportation Research Board
15. Sidess A, Ravina A, Oged E (2020) A model for predicting the deterioration of the pavement condition index. *Int J Pavement Eng*
16. Singh A, Chopra T (2018) Development of pavement maintenance management system for the urban road network by calibrating the HDM-4 distress models. In: International conference on pavements and computational approaches (ICOPAC-2018), vol 3284, pp 1–8
17. Sudhakar R (2009) Pavement maintenance management system for urban roads using HDM-4. Indian Geotechnical Society Proceeding, Chennai
18. Tavakoli A, Lapin MS, Figueroa JL (1992) PMSC: Pavement management system for small communities. *J Transp Eng* 118(2)
19. Yogesh SU, Jain SS, Devesh T (2016) Adaptation of HDM-4 tool for strategic analysis of urban roads network. *Transp Res Procedia* 17:71–80

Delineation of Pavement Stretches into Homogeneous Sections Using Pavement Condition Data: An Optimization Approach



Soumyarup Biswas and Kranthi K. Kuna

Abstract The paper illustrates a dynamic programming-based search algorithm known as the Pruned Exact Linear Time (PELT) algorithm to produce a solution for an optimization problem to identify change-points within the measurement series to delineate a pavement stretch into homogeneous sections. The data used in this paper was measured using a Falling Weight Deflectometer (FWD) in the runway stretch of an international airport with a length of 3220 m. This paper also comprehensively demonstrates two other existing methods, namely Cumulative Difference Approach (CDA) and Bayesian Segmentation Method, for delineating the same pavement stretch into homogeneous sections. Some of the shortcomings of both the methods have been discussed and the algorithms have been modified to overcome few of the drawbacks. This paper also formulated a comparative study between the three methods in terms of their sensitivity toward type of data, profound mathematical definition of homogeneity, computational complexity and ability for post-segmentation analysis for identification of homogeneous sections.

Keywords Pruned exact linear time (PELT) · Cumulative difference approach (CDA) · Homogeneous sections

1 Introduction

The pavement surface is characterized by a number of parameters such as Pavement Condition Index, International Roughness Index (IRI), skid resistance and central deflection to define its state or condition. Such data, when collected using advanced measuring devices, produces closely spaced measurements that are random in nature. As the pavement deteriorates with time, the condition of pavement at any time instant

S. Biswas (✉) · K. K. Kuna
Indian Institute of Technology, Kharagpur, India
e-mail: jewelbiswas57@gmail.com

K. K. Kuna
e-mail: kranthi@iitkgp.ac.in

is prominently reflected by these measurements. However, these parameters do not vary uniformly along the pavement stretch due to which the respective treatment for a section of pavement differs from another within the stretch. Therefore, the road agencies delineate the pavement stretches into homogeneous sections with respect to one or more of these parameter when the Pavement Management System (PMS) is implemented [1]. Further to the effective treatment selection, delineation of a pavement stretch into homogenous sections is also useful when developing the deterioration models as the measured characteristics of the homogenous section are required in model development. Thus, delineating of the pavement stretches into homogeneous sections is considered as one of the pre-requisites for setting up the PMS for pavement networks.

There has been a number of statistical methods recommended by various road agencies for performing the delineation of pavement segments into homogeneous sections. One of the first such method and widely used approach was proposed by the American Association of State Highway and Transportation Officials (AASHTO) in its 1993 design guide [2]. The approach requires delineating the road sections based on a Cumulative Difference Approach (CDA). Despite the simplistic framework of this method, a number of limitations were identified by various past studies [3, 4], specifically when handling the continuous and closely spaced condition data of large samples. One of the major limitations with this approach is that the method detects a change in the measurement series based on the sliding of absolute mean values and thus, in some cases, fails to capture the variability in the series. Further, the method does not offer a choice on the number of homogeneous sections the agency intends to delineate the stretch. Moreover, the framework by itself provides no guidance on how to limit the length of a homogeneous pavement section, so that very small and un-manageable sections are prevented. A minimum length criterion was incorporated into the CDA computational framework later by Cafiso and Graziano [5] so that the method does not result in sections that are too small to practically manage during the execution of the treatment. Another concern with regard to the 1993 CDA approach is that, as the method is sensitive to the local variation, due to the sensitivity to local variations in the data series, there may be cases of two consecutive sections with similar mean response identified as separate homogenous sections. Therefore, it is important to ascertain whether the two subsequent sections are statistically different or not. For this purpose, a student t test was also incorporated into the CDA approach by Cafiso and Graziano [5] to check statistical significance in the difference in mean between two subsequent segments of the entire pavement section. The initial aspects of the CDA approach are relatively simple but the limiting criteria, threshold criteria and the statistical difference criteria have made the computational procedures complex.

Researchers [6, 7] proposed delineating the pavement into homogeneous sections based on identifying a point in the road condition data series at which the sum of the squared differences determined for data on either side of the point is least. The method considers the point as a change-point and involves exhaustive searching of such change-points so as to divide the pavement into homogeneous sections using recursive binary splitting. To optimize the computational cost involved in such exhaustive

searching, the study adopted the Classification and Regression Tree (CART) algorithm [6, 7]. The CART algorithm adopts a binary splitting technique associated with an exhaustive search method for detecting multiple change-points. Therefore, it increases the CPU time for a large measurement series. Moreover, it is not capable of fitting any statistical distribution but is limited to fitting linear regression models in each segment. The deterministic nature of this method makes it quite rigid to test the uncertainty within the delineated series after segmentation. The exhaustive search terminates splitting the pavement stretch when it reaches the minimum segment length. This makes the approach extremely sensitive to small changes and returns a very microscopic segmented solution [5, 8].

More robust statistical methods based on the Bayesian statistical approach have been proposed by Thomas [3, 9, 10]. These methods delineate a long pavement segment by identifying the abrupt changes called change-points in the property of the road condition data series. These methods give a clear definition in terms of homogeneity compared to the CDA method [9]. A Bayesian change-point algorithm for road segmentation was very well put together by Thomas [9]. The approach fits an autoregressive (AR) model to each segmented length with different model parameters. The location of a single change-point is triggered where there is a significant change in model parameters. Thereafter based on the Bayes factor, it is decided whether a change-point is significant or not. This is a binary segmentation problem that is converted into a recursive framework with a high CPU time [5]. This computational framework was augmented initially to make it feasible for large condition measurement data series by using the at most one change-point (AMOC) algorithm, which is capable of delineating the pavement segment into two homogeneous sections. Looping the algorithm can convert it into a recursive process that can handle multiple change-point detection problems of a measurement series. One such improvement was proposed by Thomas [10], in which a binary segmentation search algorithm known as BINSEG was adopted and looped to form a recursive process for handling multiple change-point detection problem. The Bayesian approach is backed up by fitting AR models of order 1 [1, 10] in delineated sections and then conducting statistical tests based on the Bayes factors for the detection of a particular change-point or a set of change-points [9]. Though the Bayesian algorithm detects reasonable change-points, the delineation is based on the change of model parameters of the AR models. The Bayesian approach does not fit any statistical distribution to the segments but is only limited to fitting the AR model of order 1 which makes it less sensitive to the small but significant changes [5]. Thus, the Bayesian segmentation algorithm returns a more of a macroscopic segmentation. This evidence is reinforced in the present paper based on the results of this study.

2 Objectives and Methodology

Some of the above-discussed drawbacks associated with difference delineation approaches can be handled by using the optimal change-point detection methods.

In this method, an objective function or cost function is developed by fitting models to the piecewise stationary data of the measurement series fused with a well-defined penalty function [11, 12]. Then by minimizing the negative log-likelihood of the cost function, a solution is generated [12]. A dynamic programming method is known as the Pruned Exact Linear Time (PELT) search algorithm which can be used to generate exact solutions in very little CPU time [12]. Most of the criteria are fused into the optimization problem by setting them as constraints. Thus, multiple change-points in the condition data series can be identified simultaneously. Moreover, a set of optimal solutions for different criteria can be generated based on which the best judgments can be made with the help of diagnostic plots. Thus, no assumptions need to be made on the number of sections the pavement stretch to be delineated. Thus, the main objective of this paper to illustrate the adoption of optimal change-point detection technique on pavement condition data for homogeneous section delineation purposes. For this purpose, pavement deflection data collected on a runway of an international airport was used. The paper also attempts to demonstrate the ability of the proposed approach to overcome the limitations of the existing delineation methods in the literature. This is accomplished by inferring the strength of the PELT algorithm over the other algorithms by a comparative study.

The pavement surface deflection data for the study is of a runway of an international airport. The data was collected using a Falling Weight Deflectometer (FWD) at an interval of 20 m for a total runway length of 3220 m. For the analysis presented in the paper, the central deflection values of the deflection bowl are used. The deflection data corresponding to chainage of the runway after correcting for temperature is as in Fig. 1. The scope of the present study includes the exercise of three different approaches of delineation, i.e., CDA, Bayesian BINSEG algorithm and optimal change-point analysis on the deflection data. The AASHTO 1993 CDA algorithm was modified by incorporating the minimum length criteria and a statistical test for proving the significance of a potential change-point location. Later, the homogeneous sections were generated based on Bayesian AMOC and BINSEG algorithm. For this, the data series was divided using a binary segmentation technique. Then, each segment length was fitted with an AR model with unique model parameters. Thereafter, taking the ratio of the posterior probabilities of two scenarios (with and without change-point), a change-point was triggered based on the Bayes factors. The later part of the paper presents the adoption of the optimal change-point detection method. PELT was used as a search method to generate optimal solutions. A detailed diagnostic analysis was also carried out to identify potential change-points for different user-defined criteria. The necessary data analysis for the test of assumptions of the PELT algorithm was also carried out post-delineation. The necessary framework is coded in R-programming language, and the entire analysis was carried out using the same. Based on the results from all the methods, a detailed comparison of each approach adopted in the study is reported in later sections of the paper.

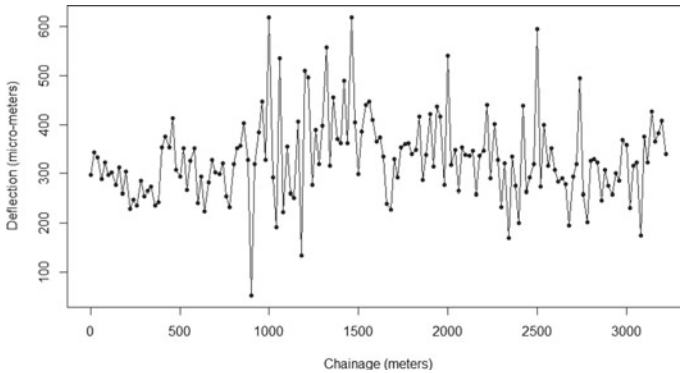


Fig. 1 Surface deflection versus chainage data used in the study

3 Modified AASHTO 1993 Cumulative Difference Approach (CDA)

The AASHTO (1993) CDA method is a special case of the CUSUM (Cumulative Sum) method that is used to detect shifts in the mean of a process. For the purpose of the pavement stretch delineation, cumulative differences are computed at each data point in the series, and then, the pavement stretch is delineated into homogeneous sections by triggering a change-point wherever there is an algebraic sign change in the slopes of the computed cumulative differences. Figure 2 shows the concept of the CDA using the assumption of a continuous and constant deflection within various intervals along the pavement stretch. If the constant value of the deflection is r_i and the respective length of the sections is L_s , then the cumulative area A_x is calculated as follows:

$$A_x = \int_0^{x_1} r_1 dx + \int_{x_1}^{x_2} r_2 dx \tag{1}$$

The mean of the response parameter, A_T , being the total cumulative area is calculated as:

$$\bar{r} = \frac{\int_0^{x_1} r_1 dx + \int_{x_1}^{x_2} r_2 dx + \int_{x_2}^{x_3} r_3 dx}{L_s} = \frac{A_T}{L_s} \tag{2}$$

The cumulative areas are calculated as:

$$\bar{A}_x = \int_0^x \bar{r} dx = \bar{r}x \tag{3}$$

In Fig. 2b, the dashed line represents the cumulative area values between the actual data (A_x) point and the mean of the data series (\bar{A}_x). The cumulative difference

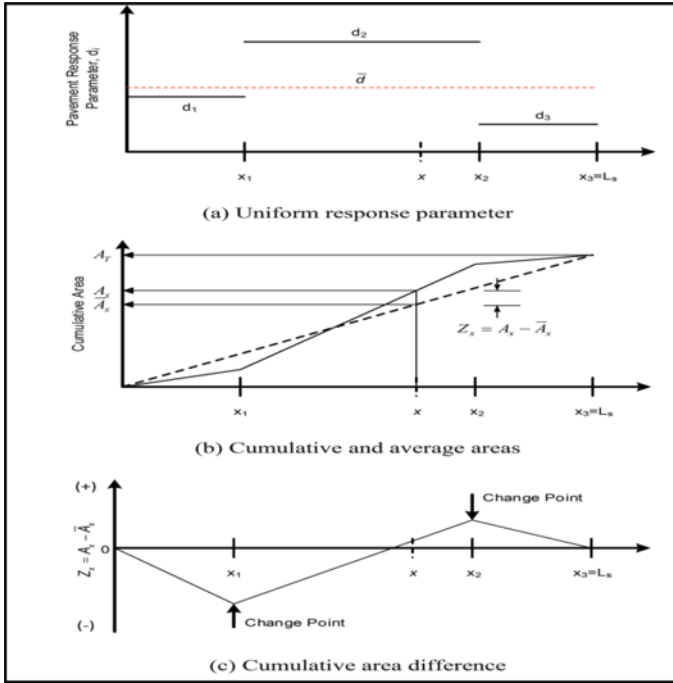


Fig. 2 Cumulative deflection approach for three homogeneous sections [2]

variable Z_x is simply the difference in cumulative area values ($Z_x = A_x - \bar{A}_x$) along the portion of measurement at a given x . In Fig. 2b, wherever there is a change in algebraic sign of the slope of the cumulative difference plot, a change-point is identified at that location.

For the method to be compatible with PMS with regard to associated maintenance activities, there should be a limit to the length of a homogeneous section where a particular treatment is applied. It should not be too short, say 50 m or less, for economic and practical consideration. Therefore, a minimum length criterion was incorporated into the computational framework. Whenever the length of a detected homogeneous section was less than the selected minimum length, the current section is merged with the subsequent section. Delineating a section based only on the minimum length criteria alone may sometimes result in two subsequent sections with a statistically similar mean response. For these two consecutive sections, similar treatment may be required, and hence, they both can be merged into a single section. To accommodate this, a student t test is incorporated into the algorithm such that, whenever the t test at the selected confidence level fails to track a significant difference in the properties, say mean, two subsequent sections are merged to a single homogeneous section.

Figure 3 shows a flowchart which describes the steps involved in developing the CDA algorithm. Using recursive techniques and some conditional statements,

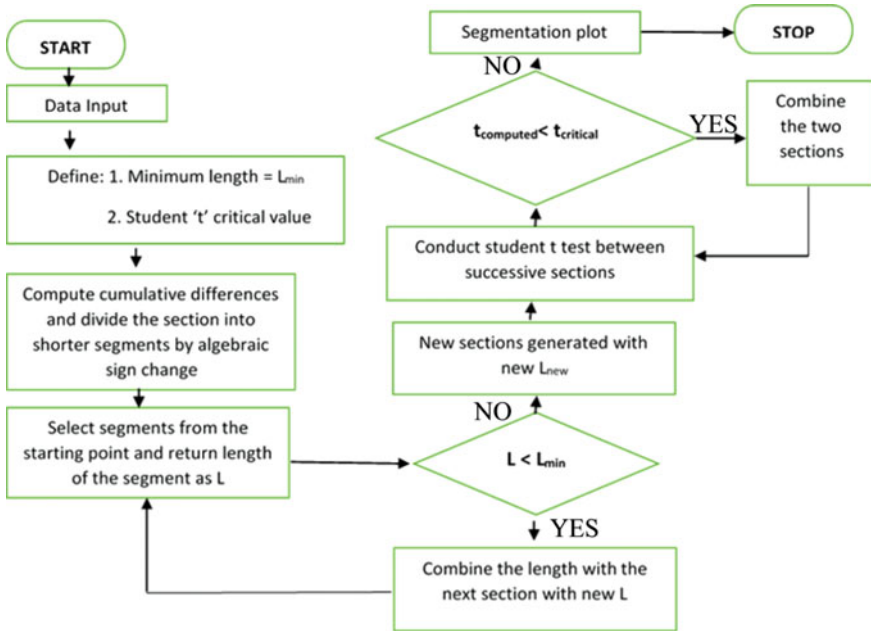


Fig. 3 Flowchart for CDA with necessary constraints

the constraints have been incorporated in the algorithm. The cumulative differences (Z_x) computed for the deflection data series along the chainage are presented in Fig. 4. The vertical lines in the figure are the location of the change-points that are identified by the algorithm within the constraints incorporated into the framework. By incorporating the two constraints, the pavement section is delineated into 17 homogeneous section when the statistical test is done at a 95% confidence level. These 17 sections with regard to the deflection data can be seen in Fig. 5. The vertical lines represent the location of the change-point, while the horizontal lines represent the mean of the response for each homogeneous section. The longest section by adopting these two constraints was found to be 280 m, while the shortest section is 100 m. Without the minimum length criteria, the number of change-points would have been 62, with sections as short as 20 m were obtained.

4 Offline Change-Point Detection Method: A Bayesian Approach

In this approach, the measurement series is assumed as piecewise stationary, which means, after delineation, each segment will have stationary time series data. Thus, the entire pavement stretch is comprised of autoregressive models of the first order,

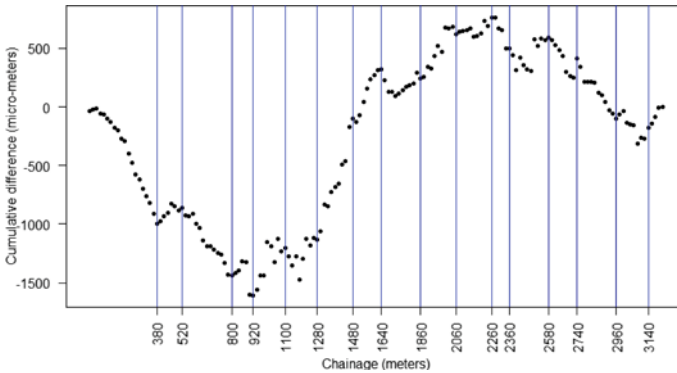


Fig. 4 Cumulative differences versus chainage plot and locations of change-points

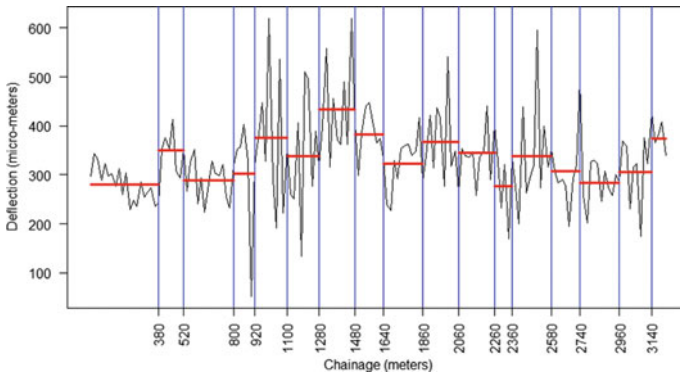


Fig. 5 Segmentation plot from CDA

and after delineation, each segment has varying model parameters [9, 13]. The AR model can be written as follows:

$$x_t = \alpha_1 + \beta_1 x_{t-1} + \varepsilon_t; \quad t = 1, \dots, n \tag{4}$$

where α_1, β_1 are unknown model parameters, ‘ t ’ is time instant, ‘ n ’ is total number of measurements, and ε_t is the error term. Here, the error term is assumed to be normally distributed with a mean of 0 and a common variance. If magnitude of β_1 is less than 1, the measurement series is assumed to be stationary for each homogeneous section. After first delineation, the measurement series splits into two fitted AR models having different model parameters. They can be written as:

$$x_t = \alpha_1 + \beta_1 x_{t-1} + \varepsilon_t; \quad t = 1, \dots, r \tag{5}$$

$$x_t = \alpha_2 + \beta_2 x_{t-1} + \varepsilon_t; \quad t = r + 1, \dots, n \tag{6}$$

where r is the change-point in the measurement series and α_2 and β_2 are the model parameters for the second delineated segment.

Then, the posterior probability distribution for a potential change-point which is triggered in the measurement series is obtained. In the Bayesian approach, the posterior probability is directly proportional to the prior probability multiplied by the likelihood of the measurement series. In this case, the posterior probabilities are calculated for two scenarios; one scenario is with a change-point, and the other is without a change-point. The ratios of the two are computed, and based on the Bayes factor, the change-point is triggered.

The BINSEG algorithm, which is a recursive process modified from the at most one change-point (AMOC) algorithm, was implemented in R . The segment was put in a loop, and a binary segmentation search was adopted to develop BINSEG. A cutoff value of the probability of 0.7 was adopted in this analysis as recommended in Thomas [9] for detecting a potential change-point. The upper plot in Fig. 6 shows the estimated posterior means after 5 iterations versus chainage. Whenever there is a significant change in the mean, a probability spike is observed in the plot below. The lower plot in Fig. 6 shows the posterior probability distributions for the change-points in the measurement series. Median was chosen as the parameter of choosing a change-point with a cutoff value of 0.7. Four potential change-points are detected in the measurement series, dividing the measurement into five homogeneous sections as shown in Fig. 7. The change-points detected for the chainages are 900, 1000, 1180 and 2500 m, as shown in Fig. 7.

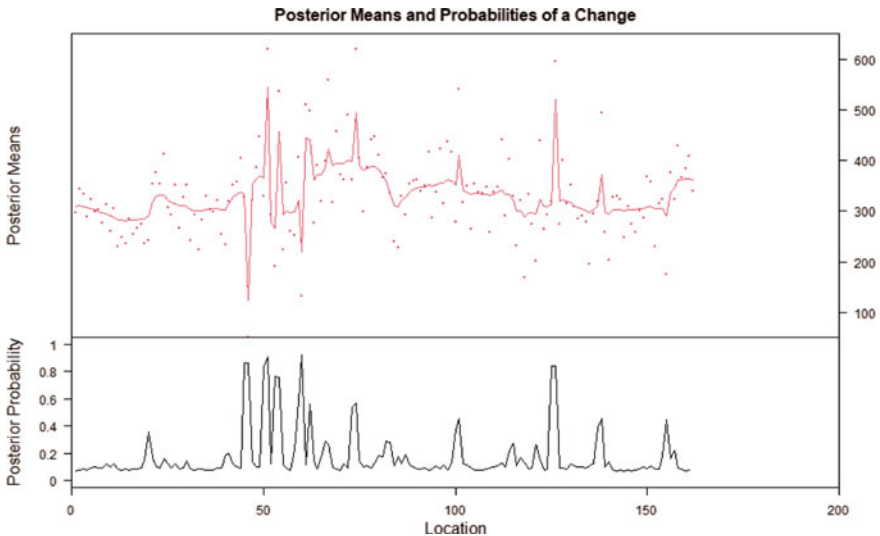


Fig. 6 Posterior probability distributions for change-point detection

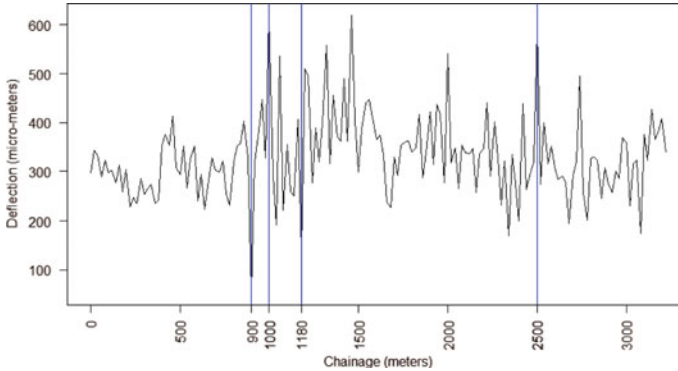


Fig. 7 Segmentation plot using Bayesian segmentation algorithm

5 Optimal Change-Point Detection

5.1 Methodological Framework

In this approach, the measurement series is considered as time series data. The change-points within the data series are identified by fitting models within the segments which are called as cost functions for each segment. The cost functions were summed up for the total measurement series for a pavement stretch. Each segmented measurement series is modeled by iid variables as a normal distribution [14] as shown in Eq. (7).

$$y_t \sim \sum_{k=0}^{K^*} N(\mu_k, \sigma_k^2) I(t_k^* < t < t_{k+1}^*) \quad (7)$$

where y_t is the iid random variable (deflection value) and assumed to follow a piecewise normal distribution with parameters, μ_k and σ_k for a section triggered after k th change-point. Here, I is an indicator function ranging between two successive change-points, with a total of $(K^* + 1)$ change-points that are unknown. The change-points are named as variable 't' in the measurement time series.

The likelihood of the one piecewise stationary segment with sample size as 'n' and parameters μ_k and σ_k^2 is written as in Eq. (8). Taking the negative log-likelihood of the piecewise cost function $V(1)$, the total cost function $V(t, K + 1)$ is computed by summing up the cost functions of the piecewise stationary data {Eq. (9)} for all the segments. Then, the objective function is to minimize the total cost function, as shown in Eq. (10).

$$L(k = 1) = \prod_{i=1}^n f(y_i/\mu_1, \sigma_1^2) \quad (8)$$

$$V(1) = - \sum_{i=1}^n \log\{f(y_i/\mu_1, \sigma_1^2)\} \quad (9)$$

$$\text{Min } V(t, K + 1) \quad (10)$$

The distribution of the test statistic is chosen as normal (z -statistic), and the likelihood ratio test is performed for tracking statistical difference between the subsequent sections based on the distribution parameters, i.e., mean and variance [14, 15]. This optimization problem was solved with the help of the PELT algorithm which is a dynamic programming search method with linear time complexity. The best locations of the change-points were detected whenever there was a significant change in both the means and variance of the distribution depending on the test statistic. To know the significant difference in the series between with zero change-point model fit and one or multiple change-point model fit, a penalty function was chosen, and a cutoff value was set for that. The optimal number of change-points was generated for a range of penalty values and select the number by generating a diagnostic plot for all the possible number of optimal change-points. The constraint for the minimum segment length was also incorporated into the computational framework.

The algorithm delineates the section based on the statistical difference of both the mean and variance. The analysis was carried out for an arbitrary range of 5–500 to find out at what penalty value the algorithm detects no change-points. For the minimum length criteria, a length of 100 m was chosen for the analysis, which is equivalent to 5 data points in the measurement series. The segmentation plot in Fig. 8 shows that, for a minimum penalty value of 5, 17 optimal change-point locations have been detected by the algorithm. Figure 8 shows the segmentation plot with the means highlighted for the same. Therefore, a more practical set of solutions have to be generated based on the penalty matrix in Table 1. As included inside the function, the range of the penalty value decides at what cutoff point the penalty value shows zero change-points [15]. Below that cutoff point, the number of location combinations for a chosen optimal solution is generated in the form of a matrix. From Table 1, it is evident that above the penalty value of 35.61, the algorithm does not detect any change-points. A diagnostic plot is presented in Fig. 9, which shows all the possible penalty values for the data series and the best locations of change-points corresponding to those penalty values. From this plot, the number of change-points is chosen, which show a significant difference in the test statistic. The diagnostic plot shows that below 5 number of change-points, the test statistic shows steep drops. After five change-points, the difference in the test statistic seems to be much flatter. The general rule is to take the number at the elbow of the plot as the optimal solution. Hence, five change-points with a penalty value of 9.67 are considered for the delineation of homogeneous sections. Figure 10 shows the final segmentation plot for the homogeneous sections. Although the plots have highlighted the means of the distribution, the segmentation is done based on both mean and variance.

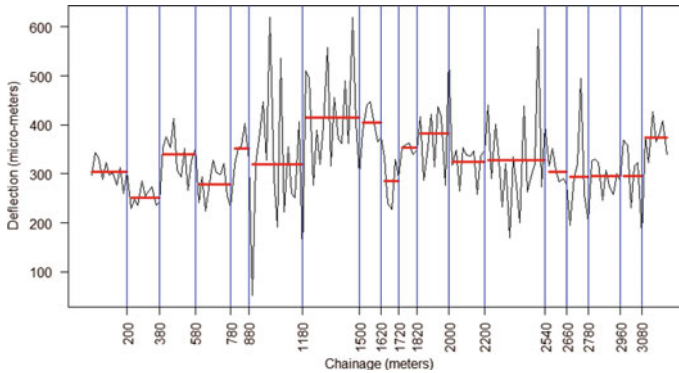


Fig. 8 Segmentation plot obtained for PELT algorithm for a penalty value of 5

6 Comparison of Methods

The main limitation with the CDA is that it fails to capture the variability in the measurement series, thereby making it difficult to specify any criteria to define homogeneity within a segment. It is also not evident enough to carry out the statistical tests to measure the difference in response mean of two segments, because there are chances of deviation from normality. It also suffers from a scalability issue, due to which some potential change-points might not be identified when the measurement series is large. On the other hand, the Bayesian algorithm, which built around statistical properties, is certainly clear about the definition of homogeneity. A segment is defined to be homogeneous if it follows a first-order autoregressive process with specific model parameters. Lastly, optimal change-point detection has a wide range of choices about how to define homogeneity. A number of parametric and non-parametric distributions and models can be fitted into the cost functions for the piecewise stationary data. Hence, the optimal change-point detection method sets a wide number of choices for the cost function, which can be decided based on the purpose of the delineation.

The basic CDA approach which was proposed initially by the AASHTO to delineate road stretches into homogeneous sections was computationally very simple. But, when some of the improvements were incorporated into the algorithm, such modifications lead to a complex computational framework. An attempt has been made in this work to develop the CDA using 'R' programming language. The time complexity and the number of arguments required were observed to be higher than the other algorithms. The Bayesian approach uses a BINSEG algorithm which is converted into a recursive process. Due to the recursive approach, the order of the CPU time is in the ' $n * \log(n)$ ' order of the measurement sample size. Though this algorithm is not computationally extremely slow, the solutions obtained are approximate. The PELT algorithm, on the other hand, is a pruned dynamic programming

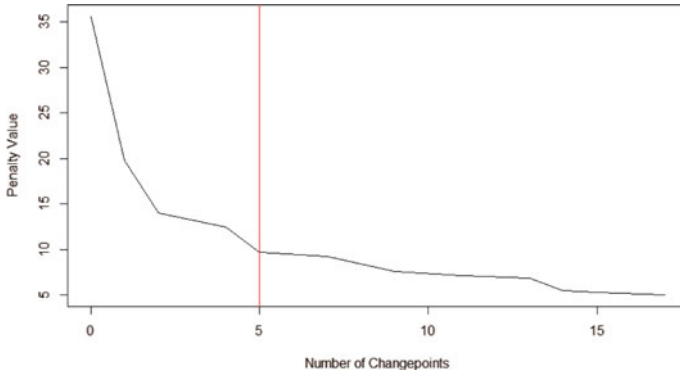


Fig. 9 Diagnostic plot to choose the number of change-points

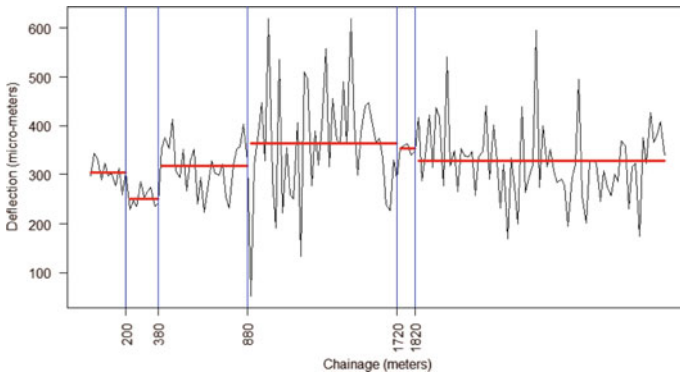


Fig. 10 Segmentation plot for five change-points (optimal change-point analysis)

search method that gives exact solutions in very little CPU time. The CPU time is in the linear order of the measurement sample size.

Though the CDA can be modified according to the pavement maintenance requirements, it still lacks the mathematical definition of homogeneity. On the other hand, even though the Bayesian algorithm has a profound mathematical definition of homogeneity, the flexibility to modify the algorithm for the identification of homogeneity is a very difficult task. The optimal change-point detection method provides an opportunity to choose and fit mathematical models into the cost functions by the user, which definitely suffices the need to define homogeneity for a segment. Moreover, it certainly provides a reasonable degree of flexibility for identifying homogeneous sections.

The algorithm developed for the CDA, when applied to the measurement series considered for this study, triggered 17 change-points. The number of change-points that was detected without the minimum length criteria was 62, which is very impractical in terms of applying treatments. The change-point, which possesses a very high

penalty value in the optimal change-point detection at a chainage of about 800 m, certainly matches with the change-point detected by the Bayesian algorithm, but the rest of the locations vary by some margin. This is probably because of the fact that the BINSEG algorithm generates an approximate solution. The above is true when the probability cutoff value was kept as 0.7. But when the probability cutoff value was reduced to 0.3, the algorithm detected 11 change-points, the locations of which also tend to significantly differ with the solutions produced by the other algorithms.

7 Conclusions

The existing methods for identifying homogeneous sections trigger a change-point that can delineate the pavement stretch. But, having reasonably meaningful inferences about a delineated segment closely correlated to the pavement asset management requirements and that can be executed in a simple, robust computational framework is the need of the hour. This work is an attempt to illustrate the optimal change-point detection method in detail to fulfill the above needs and to show its advantages over the other existing methods. For this purpose, the PELT algorithm was applied to surface deflection data collected on a runway pavement. The approach, which is based on a dynamic programming search method with linear time complexity, addresses the limitations of some of the existing techniques, such as CDA and Bayesian change-point detection methods. The proposed optimal method offers a choice of the number of homogeneous sections the road intends to delineate. Thus, the approach is more flexible compared to the CDA method. Unlike the Bayesian BINSEG algorithm, for which the change-point locations are approximate, the PELT algorithm gives the exact locations of change in the statistic of a given data series. Furthermore, as the CPU time is in the linear order of the measurement sample size, the proposed approach is computationally faster than both CDA and Bayesian BINSEG approaches.

References

1. Bennett C (2004) Sectioning of road data for pavement management. *Conf Manag Pavements*
2. AASHTO (1993) *Guide for design of pavement structures*
3. Thomas F, Weninger-Vycudil A, Simanek P (2004) Generating homogeneous road sections based on surface measurements: available methods. In: 6th International conference on management pavements, pp 21–23
4. Haide SW, Varm S (2015) Another look at delineation of uniform pavement sections based on falling weight deflectometer deflections data. *Can J Civ Eng* 43:40–50. <https://doi.org/10.1139/cjce-2015-0281>
5. Cafiso S, Di Graziano A (2012) Definition of homogenous sections in road pavement measurements. *Procedia Soc Behav Sci* 53:1069–1079. <https://doi.org/10.1016/j.sbspro.2012.09.956>

6. Gey S, Lebarbier E (2008) Using CART to detect multiple change points in the mean for large samples by using CART to detect multiple change points in the mean for large samples, pp 1–17
7. Misra R, Das A (2003) Identification of homogeneous sections from road data. *Int J Pavement Eng* 4:229–233. <https://doi.org/10.1080/10298430410001672237>
8. West RW (2014) Change point analysis. Wiley StatsRef: statistics reference online, pp 1–2. <https://doi.org/10.1002/9781118445112.stat03687>
9. Thomas F (2003) Statistical approach to road segmentation. *J Transp Eng* 129:300–308. [https://doi.org/10.1061/\(ASCE\)0733-947X\(2003\)129:3\(300\)](https://doi.org/10.1061/(ASCE)0733-947X(2003)129:3(300))
10. Thomas F (2005) Automated road segmentation using a Bayesian algorithm. *J Transp Eng* 131:591–598. [https://doi.org/10.1061/\(ASCE\)0733-947X\(2005\)131:8\(591\)](https://doi.org/10.1061/(ASCE)0733-947X(2005)131:8(591))
11. Taylor WA (2000) Change-point analysis: a powerful new tool for detecting changes. Taylor Enterp, pp 1–19. <http://www.variation.com/cpa/tech/changepoint.html>
12. Truong C, Oudre L, Vayatis N (2018) Ruptures: change point detection in Python, pp 1–5
13. Ruggieri E (2013) A Bayesian approach to detecting change points in climatic records. *Int J Climatol* 33:520–528. <https://doi.org/10.1002/joc.3447>
14. Ko SIM, Chong TTL, Ghosh P (2015) Dirichlet process hidden Markov multiple change-point model. *Bayesian Anal* 10. <https://doi.org/10.1214/14-BA910>
15. Keshavarz H, Scott C, Nguyen X (2018) Optimal change point detection in Gaussian processes. *J Stat Plan Infer* 193:151–178. <https://doi.org/10.1016/j.jspi.2017.09.003>

Simplified Methodology for Optimal Maintenance Management of Highway Pavement Network



M. R. Archana, V. Anjaneyappa, M. S. Amarnath, and A. Veeraragavan

Abstract The data pertaining to structural and functional performance for a highway pavement network of eight hundred and forty kilometres in the district of Ramana-gara near Bengaluru, Karnataka, India, were collected. Falling weight deflectometer (FWD) and road measurement and data acquisition system (ROMDAS) have been utilized for determination of structural and functional adequacy. The road network is segmented into homogeneous sections based on cumulative difference approach (AASHTO, 1995). The strength co-efficient of layers in the pavement expressed as layer moduli were computed using FWD data is used to compute critical stresses and strains of road network and for estimation of maintenance and rehabilitation treatments. The condition of the homogeneous sections in the network is assessed based on the pavement condition index (PCI) on a scale of 0–100. The pavement performance model for PCI is developed using Markovian approach. Different choices of maintenance and rehabilitation treatments are considered to improve the performance of the pavement sections in the network. A simplified methodology for the optimal timing for the pavement maintenance and management is developed so that the pavement network reaches a steady state in five years. The paper presents the importance of survey and a comprehensive discussion on key issues related to pavement maintenance and rehabilitation optimization. This study can form a window of reference for local highway agencies to determine budgetary needs, scientific basis for funding allocations and treatment policy. This paper provides useful findings for highway

M. R. Archana (✉) · V. Anjaneyappa
RV College of Engineering, Bengaluru, India
e-mail: archanamr@rvce.edu.in

V. Anjaneyappa
e-mail: anjaneyappa@rvce.edu.in

M. S. Amarnath
UVCE (Retd.), Bengaluru, India

A. Veeraragavan
IITM, Chennai, India
e-mail: av@iitm.ac.in

agencies, for promoting consideration of effective maintenance and rehabilitation alternatives and their funding options.

Keywords Optimization · Markovian deterioration model · Multi-year · Pavement maintenance and management

1 Introduction

Pavement evaluation studies involve the assessment of the structural and functional adequacies and its ability to carry the intended design traffic. This aids in timely planning of appropriate maintenance and measures to be undertaken. Due to increased magnitude of wheel loads, tyre pressure and traffic load repetitions, the pavement deterioration starts taking place, much earlier than the anticipated design life. Optimization is a systematic procedure of maximization of pavement serviceability with an objective to efficiently enhance repair, maintenance and rehabilitation activities. Many techniques for optimization are developed since mid1970s, which facilitates with analytical tools to help highway agencies for pavement management decisions.

The pavement maintenance management system delivers optimal strategies to decision makers at all levels of management, which are generated using a well-defined rational approach. A pavement maintenance management system evaluates all different strategies for defined period of analysis. This is based on estimated values of factors affecting pavement performance, which in turn are subjected to varying constraints and criteria. Hence, this necessitates a systematic and integrated working of different areas of pavement performance management. This is a continuous process requiring incorporation of evaluation of different factors affecting pavement performance, constraints and criteria. A total pavement maintenance management system consists of a coordinated set of activities aimed towards achieving the best value possible for the available public funds in providing and operating smooth, safe and economical pavements.

2 Literature Review

Most of the literatures report determination of structural capacity of flexible pavements and have expressed in the form of capacity/performance/distress indices. Structural capacity index may be used for determining the network-level decision. The sensitivity of this index with change in various input parameters indicating pavement performance is determined [1–8]. 3D—Move dynamic deflection basins are used to describe comprehensive sensitivity analysis to ascertain effect of pavement—layer configuration on critical responses of pavement. Effectiveness of a modified model in identifying structurally deficient pavement segments based on extracted cores of surveyed pavement structures, as well as a significant reduction in structural number,

is discussed [9, 10]. The results show that the developed model is a useful tool that can be utilized in a pavement management system at the network level to anticipate pavement structural conditions with an acceptable level of accuracy and to complement currently adopted functional indices.

Various pavement performance models from around the world are compared and one of them is used for Portuguese pavement management system [11]. Pavement-performance and prediction model based on the PCI and the age of the pavement is developed [12]. New optimization model for addressing the problem of planning pavement maintenance and rehabilitation for a large-scale road network is presented [13]. An optimized maintenance strategy for the rural road network of Kerala state, India, is worked out [14]. The model is capable of planning the maintenance activities over a multi-year planning period. Genetic algorithm is used to search huge solution spaces to find good solutions for pavement. Using efficient surfaces to break down the network problem into project sub-problems holds a great deal of promise to overcome some of the existing problems of optimization in pavement management. Formulation of a network-level pavement management system model, which includes the identification of specific network links in the optimization, is presented [15].

The use of approximate dynamic programming mitigates the curse of dimensionality that has haunted distinct Markov decision problem formulations of the maintenance optimization and limited their complexity [16]. Methodology based on robust optimization to estimate the future budget for optimal M&R programming of a pavement is presented [17–20].

Huge resources are devoted to the road construction and maintenance and hence the resultant road network has an asset value that represents a significant proportion of national wealth. India has the second largest road network system in the world; however, the usage of new technologies related to pavement maintenance and management needs to be explored. The complexity of problems is more in traditional or manual methods of optimization as the data is uncertain, ambiguous and sometimes incomplete. The process of optimization using manual method is laborious and time consuming. There is a need for developing multi-objective-oriented software which is user-friendly. Thus, there is a need of developing a scientific approach towards determining the maintenance and rehabilitation requirements of pavements. Also, there a need for research studies related to pavement maintenance and management system models for Indian pavement conditions, regional wise. In this study, an attempt is made to arrive at a simplified methodology for arriving at sequential decision making for pavement maintenance and management system at network level.

3 Objectives

The studies were carried out with following objectives.

- i. Development of simplified framework for multi-year pavement maintenance and management
- ii. Determination of penalties for deferred maintenance and management for in-service network pavements.

4 Study Area and Methodology

The methodology for the research study involves selection of road pavement network of about 840 km of State Highways (State Highway-03, State Highway-85, State Highway-92 and State Highway-94) in Ramanagara district. The road pavement network is subdivided into homogeneous sections based on cumulative deflection approach, in accordance with IRC: 115 [21]. The structural adequacy of the road network is measured using falling weight deflectometer (FWD). ROMDAS is used to evaluate the functional adequacy of the road network. The pavement distresses measured using ROMDAS include rut depth, fatigue cracking, patching, potholes, ravelling and roughness. These distresses are used to determine the pavement condition index in accordance with ASTM D 6477-03. The strain values in the pavement layers are determined; the remaining service life in terms of rutting and fatigue lives are calculated on the basis of FWD outputs.

Field data collected at network level indicated that most pavement sections required immediate attention. Treatment alternatives for the road network based on current pavement structural condition are determined. Treatments, which result in restricting the strains at critical locations within permissible limits, are chosen. The possible rehabilitation treatment alternatives are calculated based on pavement condition index in accordance with IRC 115-2014. The five base treatments/overlay treatments are determined for five different ranges of pavement condition index values varying from 0–20, 20–40, 40–60, 60–80 and 80–100. The budget required for maintenance and rehabilitation is estimated to ensure that all the road sections improve their structural and functional performance. The optimized solution for the maintenance and rehabilitation treatment under budget constraints for multi-year period is worked out.

5 Homogenization

The homogeneous sections are identified based on falling weight deflectometer data in accordance with IRC: 115-2014 [21]. A relation is plotted against cumulative deflection of $(D_0 - D_m)/D_m$ on y-axis and chain age in metres on x-axis. D_0 being the deflection measured directly under the load and D_m is the mean of all central deflections measured for the road network. The obtained homogeneous sections are compared with the trends for distress (type and severity), pavement condition index, roughness and strains at critical locations. The number of homogeneous sections

Table 1 Layer moduli and strains at critical locations determined for the road network

SH No.	E1, MPa		E2, MPa		E3, MPa		ϵ_r , μ strains		ϵ_z , μ strains		PCI	
	Min	Max	Min	Max	Min	Max	Min	Max	Min	Max	Max	Min
03	500	2422	100	135	22	99	602	950	171	298	66	22
85	587	2305	100	136	52	96	488	691	158	753	70	16
92	742	2456	102	304	60	99	420	760	180	500	68	46
94	564	2349	100	214	35	93	230	870	150	310	42	14

identified for the four State Highways (SH)—03, 85, 92 and 94 are 24, 18, 13 and 19, respectively.

6 Pavement Condition Evaluation

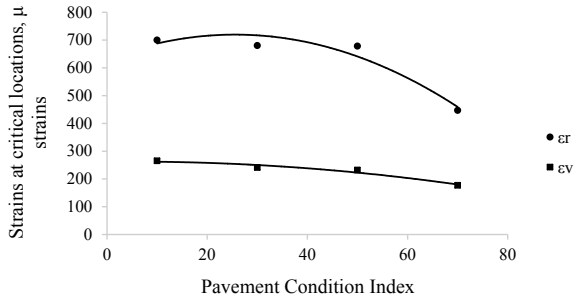
6.1 Determination of Pavement Condition Index

The pavement condition index values for homogeneous sections are determined as per ASTM 6433-07. The pavement condition index is a measurement of the current state of the pavement based on the distress observed on the surface, which also shows structural integrity and surface operating condition (localized roughness and safety). It provides a rational and objective basis for assessing the needs and priorities for maintenance and rehabilitation (M&R). Pavement condition index determined for the road network is as shown in Table 1. It was noted that none of the sections exhibited a PCI of 80–100 in the study network.

6.2 Structural Evaluation of Road Network

In the falling weight deflectometer test, the deflection bowl is described using six to nine deflection measurements per km. The elastic modulus of each layer can be calculated from the measured deflection bowl assuming the impact load to be elastic. The process of back calculation is cumbersome and time consuming if done manually for a large data. Many agencies use different software for back calculation process. IIT-KGP developed by IIT Kharagpur, India, is used to determine the layer moduli (IRC: 115-2014). Major inputs for the BACKGA software include FWD deflection values, wheel load, tyre pressure, tentative range of surface, granular and subgrade layer moduli, Poisson's ratio, the depths and radial distance at which the moduli values are required. This software provides us the back calculated layer moduli values. Major outputs from IITPAVE software are strain values at the lowest depth of the bituminous layer and on upper layer of the subgrade layer (HTS and

Fig. 1 Relationship between pavement condition index and strains at critical locations. ϵ_r —HTS at the lowest layer of bituminous layer and ϵ_v —VCS on upper layer of subgrade



VCS, respectively). Maximum and minimum values of layer moduli (surface (E1), granular (E2) and subgrade (E3)) and the strains (HTS at the bottom of bituminous layer (ϵ_r) and VCS on top of subgrade (ϵ_z)) obtained at critical locations, for all the roads in the network are as shown in Table 1. It was noted that most of the stretches yielded strains exceeding the permissible limits as per IRC: 37-2018 [22], which is also in consensus with the PCI determined for the homogeneous sections. Figure 1 presents the correlation of PCI with strains at critical locations (horizontal tensile strain at the bottom of bituminous layer (ϵ_r) and vertical compressive strain on top of subgrade (ϵ_z)). This figure indicates that critical strains are higher for pavements with lower PCI values and vice versa. This indicates a direct relationship between surface distresses and critical strains.

7 Maintenance Strategy

Based on the current condition of the road network, maintenance requirements to restore the pavement network to best condition, i.e. PCI value of 80–100 is worked out. Major rehabilitation treatment with hot mix asphalt (HMA) of 150, 115, 80, 40 and 30 mm is required when the PCI of the road sections is 0–20, 20–40, 40–60, 60–80 and 80–100, respectively. These rehabilitation requirements are decided to restrict critical strain values under allowable limits as per IRC-37-2018 [22]. The total cost estimated for the set of treatments is Rs. 2593 million (₹, 1 US\$ = ₹70 Indian rupees).

8 Optimization Technique

The optimization of pavement maintenance strategies for multi-year pavement maintenance and management based on the availability of budget is determined using the Java programming on eclipse platform. The algorithm adopted for optimization carried out to arrive at optimized solutions using computer-based optimization

technique is presented in Fig. 2. The possible optimized solutions for budget availability from 55 to 100% is explored for multi-constraint system. The deterioration of pavement condition during the time in between two consecutive M&R treatments is estimated based on the Markovian deterioration matrix.

A Markov transition matrix expresses the probability that a pavement network of similar condition for a given geographical location from one state of distress or serviceability to another within a specified time period. Hence, it describes “before and after” condition of the pavement network. Transition probability matrix to note the transition of pavement condition in terms of pavement condition index is developed for the chosen road network. The transition probability matrix for pavement condition index is as shown in Eq. 1.

$$\text{TPM} = \begin{pmatrix} 0.89 & 0.11 & 0 & 0 & 0 \\ 0 & 0.79 & 0.21 & 0 & 0 \\ 0 & 0 & 0.76 & 0.24 & 0 \\ 0 & 0 & 0 & 0.36 & 0.64 \\ 0 & 0 & 0 & 0 & 1 \end{pmatrix} \quad (1)$$

The existing length of roads (km) available for different ranges of pavement condition index is: 13 km in PCI value of 0–20, 351 km in PCI of 21–40, 205 km in PCI of 41–60, and 253 km in PCI 61–80 range, respectively. The effect of budget available for maintenance and rehabilitation, when the budget available is the range of 55–100%, is worked out. The requirement of budget for 1–10 years scheduling of pavement maintenance and management is worked out and the same is presented in Table 2. Once the pavement network attains the PCI values in the range 80–100, they require only preventive maintenance treatments till the end of the service life.

Relationship between the total cost for multi-year optimized scheduling of maintenance and management and annual budget availability is as presented in Fig. 3. It is evident that the total cost required for pavement maintenance and management increased with increased maintenance deferment. The benefits are found to reduce by about 34% on an average with an average annual budget availability deferment by about 7%.

9 Results and Conclusions

- i. The HTS and VCS varied in the range 230–950 μ strains and 150–753 μ strains respectively, for the pavement network.
- ii. Most of the stretches warranted rehabilitation as the strains exceeded the permissible limits. Major rehabilitation treatments to restrain the strain values in the pavement layers within permissible limits are worked out and the rehabilitation treatment (HMA) thickness varied between 150 mm for roads with 0–20 PCI to as low as 30 mm for roads with a PCI of 80–100.

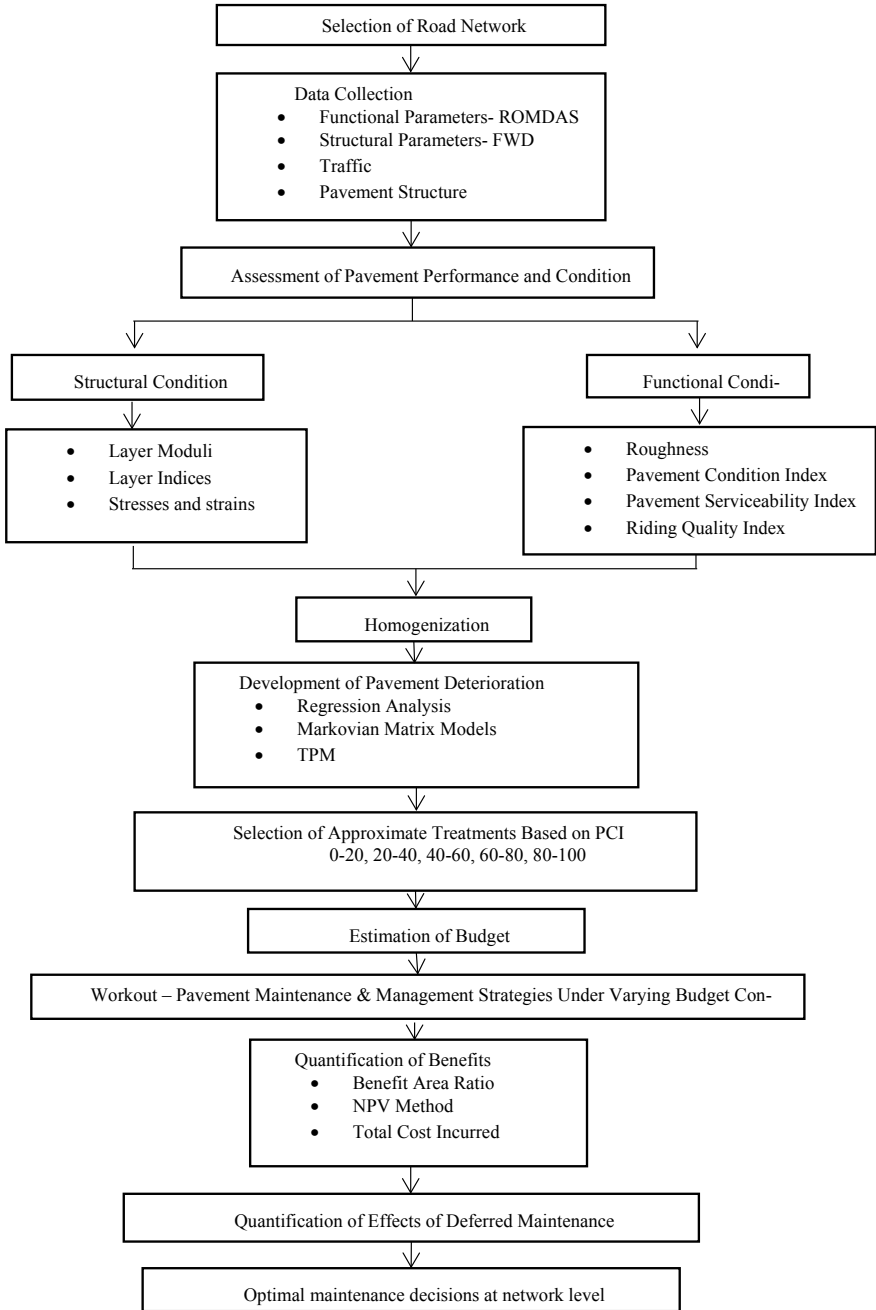


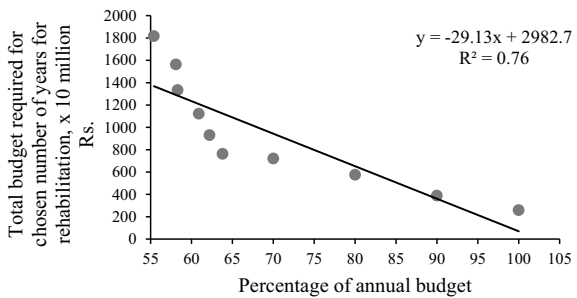
Fig. 2 Procedure adopted for optimization

Table 2 Multi-year budget requirements for the chosen pavement network

Number of years considered for rehabilitation/annual budget, × 10 million Rs									Number of years	Average annual budget availability, %
1/259.31	PM	PM	PM	PM	PM	PM	PM	PM	1	100
2/388.67	PM	PM	PM	PM	PM	PM	PM	PM	2	90
3/575.45		PM	PM	PM	PM	PM	PM	PM	3	80
4/720.65			PM	PM	PM	PM	PM	PM	4	70
5/762.6				PM	PM	PM	PM	PM	5	64.6
6/930.1					PM	PM	PM	PM	6	62.8
7/1122.2						PM	PM	PM	7	60.6
8/1334.4							PM	PM	8	58.9
9/1563.6								PM	9	58.2
10/1817.0									10	55.6

PM: Preventive maintenance

Fig. 3 Relation between percentage of total budget available and total budget required



- iii. The effect of partial budget availability on pavement network repair, maintenance and rehabilitation is worked out and the effect of the same on network condition is studied.
- iv. It is found that the total cost of rehabilitation over the years to restore the pavements to PCI values of 80–100 increased manifold with the reduction in annual budget available.
- v. The total estimated budget increased by about 34% due to deferment of annual budget availability by about 7% of the total amount of Rs. 2593 million required for rehabilitation in one year.
- vi. This work forms a window to all pavement maintenance and management projects under similar conditions, to estimate the budget requirement and penalties due to deferred maintenance.

Acknowledgements The authors gratefully acknowledge Project and Road Asset Management Centre, Public Works Department, Government of Karnataka, for sharing the data needed for the analysis.

References

1. Bryce J, Flintsch G, Katicha S, Diefenderfer B (2013) Developing a network-level structural capacity index for asphalt pavements. *J Transp Eng* 139(2)
2. Gharaibeh NG, Zou Y, Saliminejad S (2010) Assessing the agreement among pavement condition indexes. *J Transp Eng* 136(8):765–772
3. Setyawana A, Nainggolanb J, Budiarto A (2015) Predicting the remaining service life of road using pavement condition index. In: The 5th International conference of Euro Asia civil engineering forum (EACEF-5). *Procedia Engineering*, vol 125, pp. 417–423. Elsevier
4. Juang CH, Amirkhanian SN (1992) Unified pavement distress index for managing flexible pavements. *J Transp Eng* 118(5):686–699
5. Ahmed K, Abu-Lebdeh G, Lyles RW (2012) Prediction of pavement distress index with limited data on causal factors: an auto-regression approach. *Int J Pavement Eng* 7(1):23–35
6. Al-Suleiman T, Shiyad AMS (2003) Prediction of pavement remaining service life using roughness data-case study in Dubai. *Int J Pavement Eng* 4(2):121–129
7. Hall KT, Correa CE, Simpson AL (2003) Performance of flexible pavement rehabilitation treatments in the long-term pavement performance SPS-5 experiment. *Transp Res Rec* 1823(1):93–101
8. Horak E, Hefer A, Maina J, Emery S (2008) Structural number determined with the falling weight deflectometer and used as benchmark methodology. *Can J Civ Eng* 50(2):2–9
9. Elbagalati O, Elseifi MA, Gaspard K, Zhang Z (2016) Prediction of in-service pavement structural capacity based on traffic-speed deflection measurements. *J Transp Eng* 142(11):1–8
10. Shahnazari H, Tutunchian MA, Mashayekhi M, Amini AA (2012) Application of soft computing for prediction of pavement condition index. *J Transp Eng* 138(12):1495–1506
11. Ferreira A, Santos L, Wu Z, Flintsch G (2013) Selection of pavement performance models for use in the Portuguese PMS. *Int J Pavement Eng* 12(1):87–97
12. Burr AA, Shahin MY, Feighan KJ, Carpenter SH (1987) Pavement performance prediction model using the Markov process. *Transp Res Rec* 1123:12–19
13. Zhao J, Lu J, Xiang Q (2006) Some theoretical discussion on high-grade asphalt pavement maintenance quality evaluation method. *J Highw Transp Res Dev* 1(1):10–14
14. Mathew BS, Isaac KP (2013) Optimisation of maintenance strategy for rural road network using genetic algorithm. *Int J Pavement Eng* 15(4):352–360
15. Meikandaan TP, Hemapriya M (2018) Cost benefit analysis of accident prevention in construction industry. *Int J Pure Appl Math* 119(12):8831–8842. <http://www.ijpam.eu>
16. France-Mensah J, O'Brien WJ (2018) Budget allocation models for pavement maintenance and rehabilitation: comparative case study. *J Manag Eng* 34(2):05018002
17. Pulugurta H, Shao Q, Chou YJ (2013) Pavement condition prediction using Markov process. *J Stat Manag Syst* 12(5):853–871
18. Khaled AA (2017) Empirical-Markovian model for predicting the overlay design thickness for asphalt concrete pavement. *J Road Mater Pavement Des* 19(7):1617–1635
19. Mandiartha P, Duffield CF, Thompson RG, Wigan MR (2017) Measuring pavement maintenance effectiveness using Markov chains analysis. *Struct Infrastruct Eng Maintenance Manage Life-Cycle Des Perform* 13(7):844–854
20. Spencer BF Jr, Tang J (1988) Markov process model for fatigue crack growth. *J Eng Mech* 114(12):2134–2157

21. IRC (Indian Roads Congress) (2014) Guidelines for structural evaluation and strengthening of flexible road pavements using falling weight deflectometer (FWD) technique. IRC 115-2014, New Delhi
22. IRC (Indian Roads Congress) (2018) Tentative guidelines for the design of flexible pavements. IRC 37-2018, New Delhi

Pavement Materials

Evaluation of Performance of Reclaimed Asphalt Pavement Mixtures Using Acetone as Rejuvenator



Lek haz Devulapalli, Goutham Sarang, and Saravanan Kothadaraman

Abstract Reclaimed asphalt pavement (RAP) is the removed asphalt mixture, which has many advantages like economical, reduces landfills and greenhouse gases emission, and is sustainable. So, it is significant to use RAP in stone matrix asphalt (SMA) mixtures, whereas SMA mixture is proven to be rutting resistant mixture. In this study, acetone is used as a rejuvenator and that may improve the aged binder properties. From the test results, it is seen that acetone reacted with aged binder and improved the blending up to 20% RAP content and increased the fracture and moisture resistance. It is confirmed that acetone removed the aged binder from the RAP and enhanced blending process (mixing of RAP and virgin asphalt) up to 20% RAP content. However, acetone failed to improve the moisture and fracture resistance of 30 and 40% RAP content mixtures. About 9% acetone dosage is optimum dosage to enhance the performance of the RAP-incorporated SMA mixture. It is recommended that further detailed investigation is needed to understand the behaviour of Acetone on the RAP.

Keywords RAP · SMA · Acetone · Rejuvenators · Fracture energy · Moisture resistance

1 Introduction

The asphalt pavements required continuous maintenance during their service life. However, some asphalt pavements reach a stage where maintenance process does not fit to improve the conditions such pavements are milled using machinery [1]. The pavement material obtained from the milling process after completing its service life is known as RAP. The recycling of RAP has many benefits, such as it is economic

L. Devulapalli · G. Sarang (✉) · S. Kothadaraman
Vellore Institute of Technology Chennai, Chennai, India
e-mail: gouthamsarang@gmail.com; goutham.sarang@vit.ac.in

S. Kothadaraman
e-mail: saravanan@vit.ac.in

since it will save a lot of virgin aggregate and asphalt, removes disposal issues, thereby benefitting the environment [2–5]. In developed countries, RAP is being used as substitute to natural materials in the pavement construction and this has shown good results. It is estimated that approximately 75 and 76.2 million tons of RAP are used in the USA in 2015 and 2018, respectively [6]. According to NAPA, about USD 2.2 billion are saved in 2017 by using RAP in the asphalt mixture [7]. Unlikely, in India, large quantity of RAP is extracted, but the same is dumped as landfills and/or discarded as waste materials. The utilization of RAP is despised due to lack of proper specifications from the agencies. Currently, researchers have acknowledged the potential of the RAP and are trying to utilize its benefits utmost. Hence, the successful utilization of RAP will reduce the environmental pollution and lead towards sustainable development. The recent developments in mix design improved the incorporation of RAP in the asphalt mixtures. However, several problems related to production, durability, pavement performance, and blending restrict the RAP content up to 30% [1]. The usage of RAP in the dense graded mixtures is favourable, but the RAP incorporation in the gap-graded mixtures is intricate because of the unrealistic behaviour of the RAP and virgin materials [8].

Stone matrix asphalt (SMA) is a gap-graded asphalt mixture, that is made up of asphalt, fine aggregate, higher coarse aggregate and filler, and stabilizing additive [9, 10]. Dr. Zichner, a German engineer, invented SMA mixture in 1960s, to overcome the rutting, because of studded tires on the wearing course, and to improve service life of the pavement [11]. The USA State Transportation Departments (DOT's) studied this new technology closely and after the successful implication in Europe made the USA to adopt this technology. So, the research and development on the SMA mixtures are increasing, and that forced the incorporation of RAP in the SMA mixtures [12]. Therefore, a comprehensive study on the SMA mixtures with RAP is needed to be conducted.

A rejuvenator is an additive, which is added in RAP mixtures to increase the workability of the aged RAP binder. Several researchers stated that rejuvenators can improve the aged binder for another service life [1–4]. Recent studies on the effect of rejuvenator found that rejuvenators mainly improved the RAP-incorporated SMA mixtures performance [2, 4, 13]. Apart from these, the optimum rejuvenator dosage is must to develop a comprehensive mixture. So, it is important to determine the optimum rejuvenator dosage. According to Baghaee and Baaj [2], both the rejuvenator type and dosage are equally important and has to be selected carefully. Several researchers conducted experiments using different commercial and non-commercial materials as rejuvenators in the asphalt mixtures. Similarly, in this study, acetone is used as a rejuvenator and tests are conducted to analyse the effectiveness of acetone in the RAP-incorporated SMA mixtures. So, it is believed that usage of acetone may be beneficial in rejuvenating and reducing the stiffness of the RAP.

1.1 Objective

The research work is aimed to use acetone as a rejuvenator. In the present research study, the performance tests are conducted by varying the RAP content, and acetone dosage is conducted to achieve the objectives. The main objectives include: (i) to determine the effectiveness of acetone as a rejuvenator; (ii) to evaluate the moisture and fracture resistance of the prepared mixtures; (iii) to evaluate the optimum acetone dosage and the superior mixture combination among all.

2 Materials and Mix Preparation

2.1 Asphalt and Fibre

In this study, viscosity grade-30 asphalt is used as a virgin binder, and the physical properties are tested. To control the drain down phenomenon, a stabilizing agent is added and a pelletized cellulose fibre is chosen as per the Indian Road Congress (IRC) SP-79 specifications.

2.2 Aggregate and RAP

Crushed granite aggregate, which passed preliminary tests, is used as a virgin aggregate. RAP is brought from the nearby asphalt mixing plant, which is milled from various pavement sections in Chennai, India. Initial screening is conducted to remove the impurities. Both the virgin aggregate and RAP physical properties are tested as per ASTM standards and are within the specification limits.

2.3 Aggregate Gradation

In mix design of SMA mixtures, it is important to follow proper aggregates gradation. Several researcher studies confirm that accurately designed aggregate gradation will produce a superior and homogenous mixture. The designed gradation will have sufficient air voids and that permits the asphalt to flow freely between the aggregates and supports thermal expansion of asphalt. The incorporation of RAP into SMA mixtures is a sensitive issue, since the obtained RAP material is of dense graded, whereas, SMA is gap-graded mixture, so gradation process must be done carefully. The incorporation of the RAP should not disturb the stone-on-stone contact phenomenon. For that purpose, at each sieve size, the appropriate percentage of virgin aggregate is replaced with the same percentage of RAP. It is believed that the replacement at each

sieve size is pertaining with least variations in the gradation. In this study, the 13 mm nominal maximum aggregate size (NMAS) of SMA gradation is chosen (IRC SP 79-2008).

2.4 Acetone

Acetone, a polar compound that can breakdown the asphalt molecules, can be used as a rejuvenator to reduce the stiffness of the RAP. Acetone is a colourless liquid solvent, which is made up of three carbons, six hydrogens, and one oxygen atom. It is the smallest ketone and falls under the carbonyl group, where the carbon atom is double bonded with the oxygen atom. Acetone can dissolve fats, resins, and cellulose fibre, which makes it useful in thinning the oil-based paints and resins and the solvent in manufacturing polymers. Therefore, acetone reacts with the RAP and dilutes aged binder and may improve the blending process. Petersen [14] confirmed that ketones are formed during the oxidation of the asphalt, which is highly reactive and increases the volatility of asphalt.

2.5 Methodology

In order to evaluate acetone's effectiveness in the RAP-incorporated SMA mixtures, different acetone dosages are used to determine the optimum dosage required to enhance the properties of the mixture. In this study, acetone dosage and RAP content are varied in four levels, i.e., 0, 3, 6, and 9% (by weight of binder) and 10, 20, 30, and 40% (by weight of total mixture), respectively, and a control mixture (CM) without RAP or acetone (conventional SMA mixture) is prepared for reference purpose and total 17 different mixture combinations are obtained. In the test matrix, RAP-incorporated SMA mixtures with 0% acetone dosage are designated as non-rejuvenated mixture and mixtures with 3, 6, and 9% of acetone dosage are designated as rejuvenated mixtures. Table 1 presents the notation of each mixture combination. In this study, volumetric properties, moisture susceptibility tests such retained Marshall Stability (RMS) and tensile strength ratio (TSR) and fracture resistance test, i.e., semicircle bending test are conducted.

Table 1 Symbolization of each mixture

Symbol	RAP (%)	Rejuvenator (%)	No. of mixtures	Remarks
CM	0	0	1	Control mixture
R_j	$j = 10, 20, 30$ and 40	0	4	R = RAP content
R_jA_i	$j = 10, 20, 30$ and 40	$i = 3, 6,$ and 9	12	A = Acetone

2.6 Mixture Preparation

In this study, 100 mm diameter Marshall specimens are prepared as per the Marshall mix design procedure given by asphalt institute manual series-2. Primarily, virgin aggregates are taken and placed in the oven at 170–190 °C temperature for 2 h. To the heated virgin aggregates, corresponding RAP and cellulose fibre are added. To avoid premature oxidation, RAP is not heated in the oven. In case of acetone mixture, the requisite acetone dosage is added to the combined aggregates (Virgin and RAP) and mixed for 5 min evenly, and then heated up to 175–190 °C. Meanwhile, required binder content (BC) (percentage by weight of mixture) is heated and then added to the aggregates. All the ingredients are mixed at a temperature of 140–160 °C until a uniform colour and homogenous mixture are obtained (ASTM D6926). The loose mixture is transferred into the pre-heated standard moulds and compacted. In the case of non-rejuvenated mixtures, asphalt is added without any rejuvenator to the aggregates. The compacted specimens are cooled overnight and removed from the moulds using extrusion jack. The BC is varied in four levels, viz. 5.5, 6.0, 6.5, and 7.0% to determine the optimum binder content (OBC) and the same is used in the preparation of performance test specimens. Note: the addition of acetone should be done carefully, since it is highly flammable material and its addition to the heated aggregates should be avoided.

3 Experiments and Test Procedures

3.1 Drain Down Test

Drain down test is conducted using a drain down basket (ASTM D6390). The drain down basket with 6.3 mm sieve cloth and dimensions as follows: 108 mm diameter and 165 mm height. In this study, the drain down test is conducted at 7% BC and OBC to ensure that drain down is within acceptable limits. The drain down of the SMA mixtures should be less than 0.3% as per the IRC SP 79-2008 specification.

3.2 Marshall and Volumetric Properties

Volumetric properties such as maximum theoretical specific gravity (G_{mm}), bulk specific gravity (G_{mb}), air voids (V_a), voids in mineral aggregate (VMA), voids filled with asphalt (VFA), and stone-on-stone contact of the compacted specimen are determined. The OBC should be chosen at 4% V_a and VMA should be more 17% (IRC SP 78-2008). The Marshall properties, viz. Marshall stability (MS) and flow value (FV) are determined on the compacted specimens (ASTM D6927).

3.3 Retained Marshall Stability Test

The RMS test is conducted as per ASTM D 6926 specifications and six Marshall specimens are prepared. These specimens are divided into two sets: conditioned and unconditioned. The three Marshall specimens are conditioned at 60 ± 1 °C for 24 h and is kept for 2 h in water bath maintained at 25 ± 1 °C before testing. The other three Marshall specimens are unconditioned specimens. The Marshall testing is conducted on the six specimens at a constant loading rate of 50 ± 5 mm/min [15]. RMS is the ratio of MS value of conditioned and unconditioned specimens.

3.4 Tensile Strength Ratio

In this study, TSR is conducted as per AASHTO T283 specification. Accordingly, a minimum of six specimens are prepared and are divided into two sets: conditioned set and unconditioned set, where each set consist of three specimens [16, 17]. It is important to ensure that the two sets are alike in volumetric properties and are with $7 \pm 0.5\% V_a$. The condition set specimens and subjected to freeze at -18 ± 1 °C temperature for 16 h and then enforced to thaw in a water bath at 60 ± 1 °C for 24 h. Before testing, the specimens are placed in a water bath at 25 ± 1 °C for 2 h [18]. The unconditioned set specimens are placed in a water bath maintained at 25 ± 1 °C for 2 h and subjected to testing. According to IRC specification, for SMA mixture, the TSR should be greater than 85% (IRC SP 79-2008).

3.5 Semicircle Bending Test

For SCB test, Marshall specimens are cut into a semicircle and a notch is created at the centre. Arabani et al. [19] and Dai et al. [20] recommended a notch length of 10 ± 1 mm, and the same is considered in this study. Prior to testing, the specimens are kept in a temperature-controlled water bath for 2 h at 25 ± 1 °C. The specimen is placed on the two steel supports, having a span length of 0.8 times the diameter, and monotonic load is applied at a rate of 20 mm/min [21]. Three replicates are prepared and tested for each mixture. From the SCB test, three fracture characteristics such as maximum tensile strength (TS), fracture energy (FE), and flexibility index (FI) are analysed [20–23].

4 Results and Discussion

4.1 Drain Down Test Results

It is evident that the drain down values of the all SMA mixtures at 7% BC are less than 0.3%, which confirms that the pelletized fibre content is sufficient to control the drain down within the permissible limit. For CM at OBC, the drain down value is 0.19%, and for non-rejuvenated mixture, it is in between 0.18 and 0.15% that shows drain down is decreased with increase in RAP content. Drain down at 7% BC is less sensitive to RAP content however still less than CM.

The drain down at OBC of the 10–40% RAP content with 3% acetone mixtures is almost equal that of non-rejuvenated mixtures and the similar trend is followed for the 6 and 9% acetone mixtures. Because boiling point of acetone is low, hence, major portion of acetone gets removed from mixture during elevated mixing temperature and does not show much variation in the drain down. However, during the mixing process, the asphalt in RAP is dissolved in acetone and gets removed from aggregate. Because of this, polarity compounds present in the asphalt and their ability to mutually interaction are increases and this play an important role in the asphalt physical behaviour.

4.2 Volumetric Properties Analysis

Table 2 indicates the volumetric properties of the non-rejuvenated SMA mixtures. This shows that incorporation of RAP decreased the OBC value. The aged binder in the RAP is liquified under the action of heat, that mixes with the virgin materials and reduced the OBC value [25]. It is also observed that the increase in RAP content considerably decreased the OBC value. On the other hand, at OBC, the G_{mb} of the 40% RAP content mixtures is 2.420 g/cm³, whereas, for the CM, it is 2.375 g/cm³, which shows that G_{mb} value increased and that is due to the existence of the RAP. For all the mixture combinations, VFA value is less than 80% and is within the specification limit. The VCA_{mix} of the non-rejuvenated SMA mixtures is less than the VCA_{dry} , that confirms that stone-on-stone exists between the coarse aggregate [18] and gradation followed in this study is proved to be valid.

The OBC value of the $R_{10-40}A_3$ mixtures is in the range of 6.12–5.81%, and the values are identical to the non-rejuvenated mixtures. This confirms that the 3% acetone did not activate the aged binder. The OBC values of the 6% acetone mixtures are in between 6.06 and 5.80, and for 9% acetone mixtures, it is in between 5.96 and 5.79%. This shows that acetone showed a very negligible reduction in the OBC value. For the $R_{10}A_9$ mixture, the OBC value is lesser than the non-rejuvenated mixtures. Table 2 summarizes the volumetric properties of acetone mixture. The VMA is in the range of 17.40–17.15% for all the acetone-rejuvenated SMA mixture. The G_{mb} of the acetone mixtures is in between 2.302 and 2.365 g/cm³, which are lesser than

Table 2 Volumetric properties of acetone-rejuvenated SMA mixtures

Mixture	OBC (%)	VMA (%)	G_{mb} (g/cm ³)	VCA _{mix} /VCA _{dry}	VFA (%)	MS (kN)	FV (mm)
CM	6.24	17.70	2.375	0.77	78.50	13.23	3.45
R ₁₀	6.13	17.65	2.392	0.79	78.00	13.50	3.25
R ₂₀	6.05	17.40	2.407	0.78	77.00	14.20	2.86
R ₃₀	5.98	17.35	2.412	0.79	76.50	15.40	2.70
R ₄₀	5.83	17.10	2.420	0.79	76.50	14.25	2.45
R ₁₀ A ₃	6.12	17.40	2.302	0.82	75.13	13.9	3.30
R ₂₀ A ₃	6.03	17.38	2.321	0.85	73.44	14.75	2.92
R ₃₀ A ₃	5.96	17.25	2.344	0.80	77.33	15.60	2.73
R ₄₀ A ₃	5.81	17.20	2.333	0.81	76.24	15.10	2.61
R ₁₀ A ₆	6.06	17.36	2.324	0.84	77.34	14.06	3.32
R ₂₀ A ₆	5.99	17.28	2.346	0.82	76.46	14.96	2.95
R ₃₀ A ₆	5.93	17.23	2.347	0.79	75.32	15.82	2.69
R ₄₀ A ₆	5.80	17.20	2.367	0.78	77.45	15.17	2.62
R ₁₀ A ₉	5.96	17.35	2.310	0.82	75.23	14.40	3.33
R ₂₀ A ₉	5.99	17.25	2.324	0.83	76.24	15.19	2.95
R ₃₀ A ₉	5.93	17.20	2.353	0.79	77.24	16.04	2.75
R ₄₀ A ₉	5.79	17.15	2.365	0.84	78.35	15.38	2.65

the non-rejuvenated mixtures and that indicates lesser stability. The G_{mb} value is decreased because of improper blending and inhomogeneity. Test results indicate that the presence of stone-on-stone contact. For all acetone mixtures, the VFA value is less than 80% and are within the specification limit.

4.3 Marshall Stability

The MS value of the CM is 13.23 kN, and for non-rejuvenated SMA mixtures of 10, 20, 30, and 40% RAP content, it is 13.50, 14.20, 15.40, and 14.25 kN, respectively. The MS value is increased up to 30% RAP content, but decreased for the 40% RAP content mixture. The MS value is increased since the RAP consists of stiffer aged binder and that may increase the same [1]. However, the reduction of MS value at 40% RAP content is due to improper blending between the virgin materials and aged binder.

The acetone mixtures showed higher the MS value and that shows the increase in the acetone dosage improved the stability, because the acetone reacted with the aged binder and that removed the aged binder from the RAP and increased the homogeneity. It may be also due to the proper blending between the RAP and virgin material. Overall, the 40% RAP content with 9% acetone mixture showed highest MS

value, i.e. 16.04 kN. It is seen that higher RAP content may require higher acetone dosage to improve the blending process.

4.4 Flow Value

The FV of the CM is 3.45 mm, and for the R₁₀, R₂₀, R₃₀, and R₄₀ mixture, it is 3.25, 2.86, 2.70, and 2.45 mm, respectively. The FV is decreased because of the aged binder in the RAP. The increase in the stiffness will lead to fatigue and flexural failure [1].

The FV of the 3% acetone dosage is in the range of 3.30–2.61 mm, and for the 6 and 9% acetone dosage, it is in the range of 3.32–2.62 mm and 3.33–2.65 mm, respectively. The FV of the acetone mixtures and the non-rejuvenated SMA mixtures is similar, indicating that the addition of the acetone did not increase the FV, and that specifies that the mixtures are stiffer. From FV results, it can be concluded that acetone failed to improve activation of the aged binder.

4.5 Retained Marshall Stability

The RMS value of non-rejuvenated SMA mixture is increased with the increase RAP content up to 30% and then decreased slightly for the 40%. Since RAP contains aged binder and that is resistant to the moisture. However, it is decreased for the 40%, due to improper blending and that reduces the bonding between the aggregate and asphalt [26].

The RMS values of the acetone-rejuvenated SMA mixtures shown in Fig. 1. indicates that the acetone increased moisture resistance. The RMS of the 3% acetone mixtures is in the range of 94.24–95.26%, which is increased up to 30% RAP content. For 6 and 9% acetone dosage mixtures is in between the 94.59–95.45% and 95.83–96.12%, respectively. The RMS value increased as the acetone dosage increases, since acetone reacted with the aged binder and removed it from the RAP aggregate. This improved the blending process, providing better moisture resistance to the mixtures.

4.6 Tensile Strength Ratio

The TSR value marginally improved up to 20% RAP content and reduced beyond that and indicating higher moisture resistance [26]. On the other hand, the TSR value of 40% RAP is less than 85%, this is due to higher stiffness and less adhesion between the aggregates, which ultimately reduced the moisture resistance. Figure 2 shows the TSR values of the acetone-rejuvenated SMA mixtures. It is seen that the TSR values

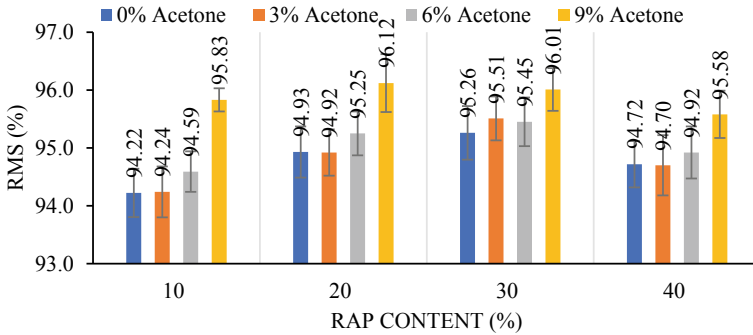


Fig. 1 RMS of acetone-rejuvenated SMA mixtures

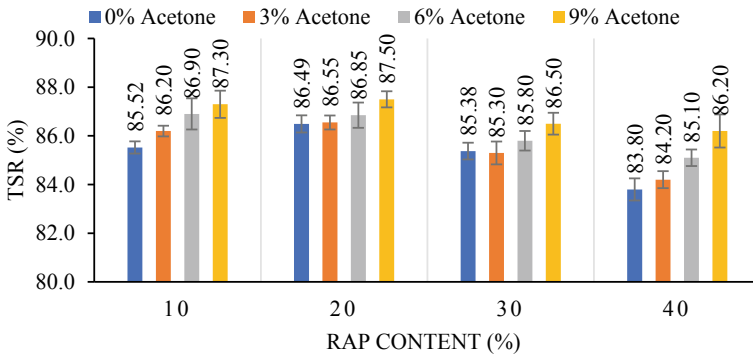


Fig. 2 TSR of RAP-incorporated SMA mixture with acetone

of the acetone-rejuvenated SMA mixtures are higher than remaining mixtures. Apart from this, the increase in the acetone dosage increased the TSR value, since acetone reacted with RAP and that removed the binder from that aggregate and blended in the virgin material. The maximum TSR value is seen for the R₂₀A₉ mixture (87.50%).

4.7 Semicircle Bending Test

4.7.1 Maximum Tensile Stress

Mixtures with higher tensile stress can take a higher load before damage, and they have higher fracture resistance. The TS is increased up to 20% RAP content because of the aged binder, whereas the TS of higher RAP content mixture is decreased since RAP decreased the blending process and that decreased the homogeneity.

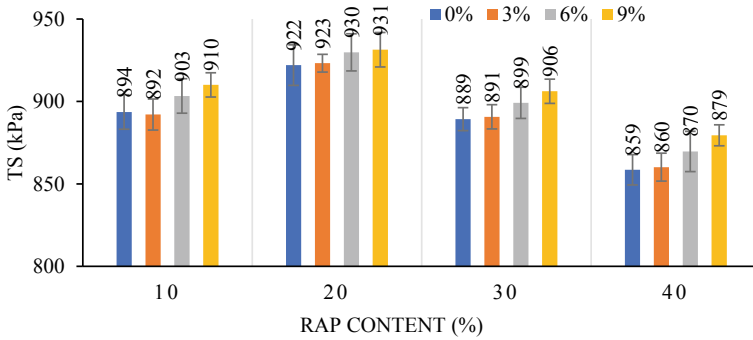


Fig. 3 TS value of acetone-rejuvenated SMA mixtures

The results presented in Fig. 3 shows that TS value of mixtures with of the 3% acetone is similar to the non-rejuvenated SMA mixtures. Increasing the acetone dosage slightly increased the TS value, which is due to the removal of the aged binder. The TS value of the R₂₀A₉ showed the highest TS value. It is observed that the high acetone dosage is required to improve the TS value. For all the acetone dosages, the TS value is increased up to 20% RAP. However, TS is decreased for 30% RAP content, this is due to the improper blending, since the acetone failed to lubricate the aged binder.

4.7.2 Fracture Energy

The higher FE value illustrates higher fracture resistance. The FE is decreased as the RAP content increased above 10%. Because the incorporation of RAP increases the stiffness and that leads to fracture failure. The higher FE value is observed for 20 and 30% RAP content. While 40% RAP content, the FE is lesser than the CM. The decrease is due to the inhomogeneity and improper blending of the mixture.

The addition of acetone as rejuvenator showed some interesting results in the FE values, as presented in Fig. 4. The FE value is increased for the acetone-rejuvenated SMA mixtures. It is increased because the acetone has reacted with the aged binder and removed the binder from the aggregate and that has enhanced the blending process. On the other hand, the higher RAP content showed lesser FE value, since the acetone dosage is insufficient to improve the blending process. However, FE value is increased as the acetone dosage increases, and the maximum FE value (1735 N.mm⁻¹) is observed for the 20% RAP content mixture with 9% acetone. This indicates that higher acetone dosage is required to improve the FE value of the RAP mixture.

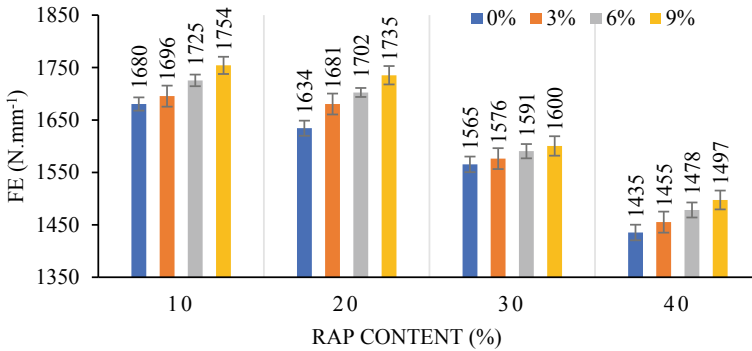


Fig. 4 FE value of acetone-rejuvenated SMA mixtures

4.7.3 Flexibility Index

Results showed that RAP mixtures have lesser the FI, that indicating resistance of RAP mixtures towards permanent deformation. Because aged binder increased the stiffness and decreased the FI value. The FI value of 10–40% RAP content mixture is in between 3.44 and 2.79, and for the CM, it is 3.44. While the 40% of RAP content has decreased the FI by 19% when compared to that of CM. The higher decrease in the FI value leads to fatigue and cracking failure. Therefore, it is important to decrease stiffness of RAP-incorporated SMA mixtures.

FI results of the acetone mixtures are seen in Fig. 5. The FI values of the 3% acetone mixtures are in between 3.46 and 2.83, which indicates the of FI value is decreased with the increase in the RAP. The FI values of the 6% acetone mixtures are in the range of 3.42–2.52, and for 9% of acetone mixtures, it is in between 3.02 and 2.38. The higher acetone dosage mixtures showed higher FI value, because acetone has acted on the RAP and improved the blending. It is observed that the acetone did not alter the rheology of the RAP-incorporated SMA mixture, and that confirms that the mixtures are stiffer.

5 Conclusion

The RAP is waste material, and its successful utilization in the SMA mixtures will reduce environmental pollution and landfills. Based on the experimental results, the following conclusions are drawn:

- Unlike other rejuvenators, which usually improve the workability of the asphalt mixtures acetone did not lubricate the RAP, however, it has removed the aged binder from the RAP and blended with the virgin materials.

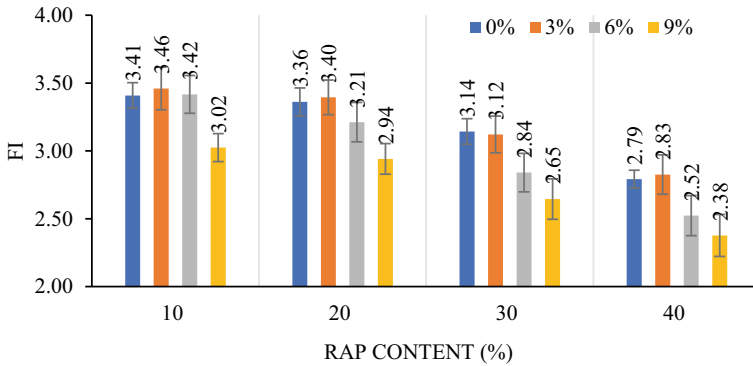


Fig. 5 FI results of acetone mixtures

- The integration of RAP into SMA did not change stone-on-stone contact, and this indicates that the combined gradation followed in this study can be recommended to incorporate RAP in SMA mixtures.
- The addition of acetone and RAP significantly reduced the OBC value, and for 9% POS and 40% RAP content mixtures, the OBC value is decreased by 7% when compared to the CM. All the mixture combinations have achieved the mix design specifications limits for volumetric all properties.
- Acetone has moderately improved the MS value and FV, which indicates that the acetone reacted with RAP and slightly reduced the stiffness. However, reduction is negligible.
- The RMS and TSR tests results showed that 9% acetone dosage has increased the moisture resistance. This is may be due to removal of the aged binder from the RAP and proper blending between with the RAP and virgin aggregate.
- From the experimental results, it is concluded that 30% RAP content with 9% acetone dosage is the best mixture combination, whereas, 9% acetone dosage is an optimum dosage.
- Finally, it is recommended that 30% RAP can be possible to integrated into SMA mixtures with acetone, but care should be taken by considering all the pertaining factors such as acetone dosage, mixing time, and temperature.

To have a consistency in the test results, the source of acetone and RAP is unchanged and conclusions are drawn accordingly. Therefore, it is suggested using acetone and RAP from different sources to check the variabilities in the test results. The acetone used in this study is a new product as a rejuvenator in asphalt mixtures and never been reported before. It is recommended to conduct the comprehensive studies to analyse the behaviour of acetone on the RAP.

References

1. Al-Qadi IL, Elseifi M, Carpenter SH (2007) Reclaimed asphalt pavement—a literature review. FHWA-ICT-07-001
2. Moghaddam TB, Baaj H (2016) The use of rejuvenating agents in production of recycled hot mix asphalt: a systematic review. *Constr Build Mater* 114:805–816
3. Copeland A (2011) Reclaimed asphalt pavement in asphalt mixtures: state of the practice (No. FHWA-HRT-11-021). United States. Federal Highway Administration. Office of Research, Development, and Technology
4. Kennedy TW, Tam WO, Solaimanian M (1998) *Effect of reclaimed asphalt pavement on binder properties using the superpave system* (No. FHWA/TX-98/1250–1). University of Texas at Austin. Center for Transportation Research
5. Kandhal PS, Mallick RB (1998) Pavement recycling guidelines for state and local governments: participant's reference book (No. FHWA-SA-98-042)
6. Hansen KR, Copeland A (2015) Asphalt pavement industry survey on recycled materials and warm-mix asphalt usage: 2014 (No. information series 138)
7. West RC, Copeland A (2015) High RAP asphalt pavements: Japan practice-lesson learned, (No. IS 139)
8. McDaniel RS, Anderson RM (2001) Recommended use of reclaimed asphalt pavement in the Superpave mix design method: technician's manual (No. Project D9-12 FY'97). National Research Council (US). Transportation Research Board
9. Brown ER, Manglorkar H (1993) Evaluation of laboratory properties of SMA mixtures. National Center for Asphalt Technology, Auburn, AL
10. Sarang G, Lekha BM, Krishna G, Ravi Shankar AU (2016) Comparison of stone matrix asphalt mixtures with polymer-modified bitumen and shredded waste plastics. *Road Mater Pavement Des* 17(4):933–945
11. Brown ER, Mallick RB (1995) Evaluation of stone-on-stone contact in stone-matrix asphalt. *Transp Res Rec* 208–219
12. Van Thanh D, Feng CP (2013) Study on Marshall and Rutting test of SMA at abnormally high temperature. *Constr Build Mater* 47:1337–1341
13. Devulapalli L, Kothandaraman S, Sarang G (2020) Effect of rejuvenating agents on stone matrix asphalt mixtures incorporating RAP. *Constr Build Mater* 254:119298
14. Petersen JC (2000) Chemical composition of asphalt as related to asphalt durability. In: *Developments in petroleum science*, vol. 40. Elsevier, pp 363–399
15. Panda M, Mazumdar M (2002) Utilization of reclaimed polyethylene in bituminous paving mixes. *J Mater Civ Eng* 14(6):527–530
16. Xiao F, Su N, Yao S, Amirkhanian S, Wang J (2019) Performance grades, environmental and economic investigations of reclaimed asphalt pavement materials. *J Clean Prod* 211:1299–1312
17. Devulapalli L, Kothandaraman S, Sarang G (2019) Evaluation of rejuvenator's effectiveness on the reclaimed asphalt pavement incorporated stone matrix asphalt mixtures. *Constr Build Mater* 224:909–919
18. Sarang G, Lekha BM, Geethu JS, Shankar AR (2015) Laboratory performance of stone matrix asphalt mixtures with two aggregate gradations. *J Mod Transp* 23(2):130–136
19. Arabani M, Ferdowsi B (2009) Evaluating the semi-circular bending test for HMA mixtures. *Int J Eng* 22(1):47–58
20. Dai LX (2016) Evaluation of warm mix asphalt performance incorporating high reclaimed asphalt pavement content. A thesis submitted to Partial Fulfilment Requirement Degree Master Engineering Transportation
21. AASHTO TP 105-13 (2013) Standard method of test for determining the fracture energy of asphalt mixtures using the semicircular bend geometry (SCB). American Association of State and Highway Transportation Officials
22. Ozer H, Al-Qadi IL, Singhvi P, Khan T, Rivera-Perez J, El-Khatib A (2016) Fracture characterization of asphalt mixtures with high recycled content using Illinois semicircular bending test method and flexibility index. *Transp Res Rec* 2575(1):130–137

23. Li XJ, Marasteanu MO (2010) Using semi circular bending test to evaluate low temperature fracture resistance for asphalt concrete. *Exp Mech* 50(7):867–876
24. Zaumanis M, Mallick RB, Poulidakos L, Frank R (2014) Influence of six rejuvenators on the performance properties of reclaimed asphalt pavement (RAP) binder and 100% recycled asphalt mixtures. *Constr Build Mater* 71:538–550
25. Shirodkar P, Mehta Y, Nolan A, Sonpal K, Norton A, Tomlinson C, Dubois E, Sullivan P, Sauber R (2011) A study to determine the degree of partial blending of reclaimed asphalt pavement (RAP) binder for high RAP hot mix asphalt. *Constr Build Mater* 25(1):150–155
26. Watson DE, Vargas-Nordbeck A, Moore J, Jared D, Wu P (2008) Evaluation of the use of reclaimed asphalt pavement in stone matrix asphalt mixtures. *Transp Res Rec* 2051(1):64–70

Investigating the Effect of Aggregate Size and Binder Material Proportion on Strength and Permeability of Pervious Concrete by Statistical Modeling



Sudhir Kumar Boddu 

Abstract The application of pervious concrete in highway pavements is restricted due to its less compressive strength. Several techniques were identified to increase the strength of the pervious concrete by altering cement to aggregate ratio, utilizing extra cementitious material, changing aggregate size and gradation. The present work is focused on the study of the relationship between variation in fly ash content and aggregate size on strength and permeability. This study adopts a different test setup for casting the specimen and measuring the coefficient of permeability. Statistical analysis was performed for the collected data to test whether the applied technique is significantly influencing the compressive strength and permeability. Results revealed that changes in aggregate sizes had less effect in increasing the concrete strength. By reducing the aggregate size from 26.5 to 10 mm, there is an average strength reduction of 3.3 MPa, but there is an increase in permeability of 0.21 cm/s. The effect of fly ash addition in partial replacement of cement had increased the strength of pervious concrete and also improved the concrete specimen workability and surface finishing characteristics. The addition of binder material at a certain proportion played a vital role in increasing the strength of pervious concrete.

Keywords Pervious concrete · Coefficient of permeability · Compressive strength · Fly ash · Aggregate size

1 Introduction

Due to rapid urbanization, the naturally formed pervious earth's surface is being converted into an impervious land cover. The major reason for the formation of this impervious surface layer is the construction of high-raised buildings and asphalt roads [1, 2]. This impervious layer blocks the storm water to percolate through the inter-granular earth's surface pores and causes a reduction in groundwater recharge

S. K. Boddu (✉)

Department of Civil Engineering, National Institute of Technology, Warangal, Telangana, India
e-mail: sudhir23@student.nitw.ac.in

conditions [3]. Due to this phenomenon, large cities are turning to be “hot-islands”, which release heat into the atmosphere during the night times [4].

Problems such as increased earth’s surface temperature decreased groundwater level, and unpredictable climate changes are consequences of the impervious pavement surface. All these environmental issues are due to the lack of air and water exchange from the top surface of the pavement to the soil lying under it [5].

To solve this urban environmental issue, research has focused on the implementation of eco-friendly sustainable materials, one among them is the pervious concrete. This type of concrete was first used in the 1800’s European countries as load-bearing walls and for surfacing the pavements [6, 7]. It is a type of concrete, which intentionally allows stormwater to pass through it, as the internal void occupancy is about 15–20% of the total volume [8]. The limited usage of fine aggregate creates a large volume of voids to help the runoff water to percolate into the earth. Porous concrete pavements also absorb the noise from road traffic, do not glitter light while driving at night, and improve skid resistance [9].

The serviceability life of pervious concrete is lesser than its design life as its compressive strength varies between 3.5 and 28 MPa [10]. The high volume of void content is responsible for high-permeability and low-compressive strength [11]. The application of pervious concrete as a construction material is limited due to its less compressive strength and is mostly used in the parking lots, pedestrian sidewalks, running or jogging tracks, dedicated cycle bays, etc. [12]. On the other hand, highway pavements require more compressive strength as well as permeability, this type of concrete cannot be used. The technical challenges associated with pervious concrete are [13–15]:

- During the construction phase, high skill is required to have the appropriate amount of voids to maintain hydrology.
- Proper maintenance is required to clear the clogged debris or dust particles that were decomposing the surface layer.

The interfacial layer between the cement paste and aggregates is observed to be the weakest link for all types of concrete. So, increasing the bond strength between matrix (cement) and filler (aggregates) is the key aspect to increase the strength [16].

Using this concept, research was conducted to increase the compressive strength of pervious concrete by increasing cement to aggregate ratio, including admixtures, altering the water-cement ratio, utilizing extra cementitious materials, changing aggregate size, and gradation. Studies conducted by Hesami et al. [17] used rice husk ash (RHA), glass (0.2%), steel (0.5%), and poly-phenylene sulfide (PPS) (0.3%) in partial replacement of cement to strengthen the cement paste of pervious concrete. RHA was replaced with cement in the percentage of 0, 2, 4, 6, 8, 10, and 12%. The results revealed that 8% is the optimal replacement of RHA, and the addition of fiber materials could not show much effect on the optimal amount. The compressive strength increased by 30–40% for glass, 34–37% for steel, and 41–47% for PPS. The permeability values first decreased by increasing RHA to 8–10% and increased for more RHA content. A study by Borhan [18] used various proportions

of styrene-butadiene rubber (SBR) in partial replacement of cement and investigated the physical and mechanical properties. Results revealed that there is a positive response in the mixes containing SBR when compared to mixes without SBR. Another study by Li [19] performed an investigation on the utilization of fly ash as a supplementary cementitious material in replacement of cement at optimum cement-aggregate ratio. Results revealed that high-strength pervious concrete was produced at a cement-aggregate ratio of 0.2–0.4 and 20% replacement of fly ash content.

Another technique was applied by changing the aggregate size in pervious concrete content. Sun Daquan et al. [20] used aggregates of sizes 2.36, 4.75, 6, 8, 9.5, 10, 12.5, and 15 mm. Results revealed that compressive strength increased till the aggregate size of 8 mm and still increasing the size of aggregate did not have any effect on strength.

2 Research Objective and Methodology

Several studies have been conducted to increase the bond strength by blending cement with several pozzolanic materials. In the present work, two techniques were used to check whether the strength is increasing or not.

- (a) **Blending cement with fly ash:** The function of supplementary cementitious material (SCM) is to provide sufficient bond strength by coating around the aggregates. Past research indicated that the influence of fly ash addition as an SCM is not similar as observed in normal conventional concrete [21].
- (b) **Changing the size of aggregate:** At a particular aggregate size, the concrete attains maximum strength. By simply increasing the size of aggregate to increase the concrete strength is a wrong perception. By increasing the maximum size of aggregate from 20 to 63 mm, there is a reduction in tensile strength of concrete by 35–50%, when compared with concrete having an aggregate size of 20 mm [22].

As the primary objective of the work is to find whether there is an increase in strength of pervious concrete by using fly ash as the pozzolanic material at three different proportions (20, 35, and 50%). Also to test the effect of different aggregate sizes (26.5–20, 20–12.5, and 12.5–10 mm) in combination with fly ash addition. The properties of pervious concrete are tested through compressive strength test, porosity test, and permeability test.

The significance of this research is to reduce the usage of environmentally unfriendly Portland cement in making pervious concrete and finding whether there is an increase in strength by using fly ash as the supplementary pozzolanic material. All the tests were performed by meeting all the specification requirements of pavement applications. The detailed methodology of the present work is shown in Fig. 1.

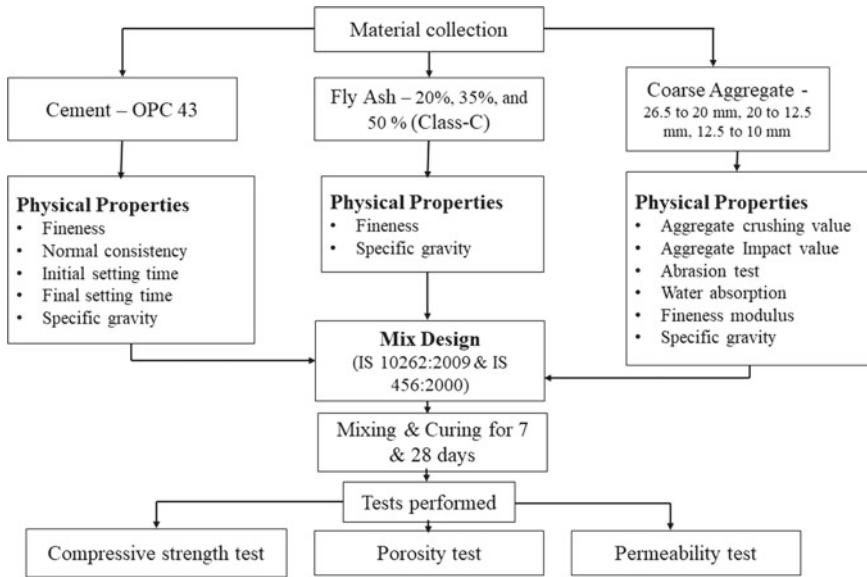


Fig. 1 Flowchart showing methodology of the research work

3 Materials and Test Method

The materials used in the present study are ordinary Portland cement (OPC) of 43 grade and were tested as per IS: 4031-1968, Class-c fly ash having specific gravity 2.51, the coarse aggregate of three different sizes passing through 26.5–20, 20–12.5 and 12.5–10 mm, which was obtained from a local quarry.

3.1 Fly Ash Properties

In the present study, fly ash was taken in three proportions of 20, 35, and 50% in partial replacement with cement. Past literature had classified the proportion of fly ash replacement as shown in Table 1. Past research identified the usage of fly ash as a replacement for cement in the proportion ranging from 25 to 50% based upon its practical application and its chemical properties [23]. The chemical composition of fly ash and cement is shown in Table 2. So, the present study tests the fly ash replacement in all three categories of low, medium, and high. The physical properties of fly ash and cement used in this study are presented in Table 3.

Table 1 Classification of fly ash replacement with cement

The proportion of fly ash replacement (%)	Classification
0–20	Low
20–35	Medium
35–50	High
Greater than 50	Very high

Table 2 Chemical composition of fly ash and cement

Chemical composition (%)	SiO ₂ Silicon dioxide	Al ₂ O ₃ Aluminum oxide	Fe ₂ O ₃ Hematite	CaO Calcium oxide	MgO Magnesium oxide	SO ₃ Sulfur trioxide	K ₂ O Potassium oxide	Na ₂ O Sodium oxide
Fly ash (class-c)	30.7	15.7	6.5	34.7	1	6.6	0.3	1.8
Cement	21.2	4.3	1.8	64.3	1.8	3.7	0.7	0.17

Table 3 Physical properties of fly ash and cement

Properties	Cement	Fly ash
Fineness (%)	4.4	3.4
Normal consistency (%)	28	–
Initial setting time (min)	158	–
Final setting time (min)	280	–
Specific gravity	3.13	2.51

3.2 Aggregate Properties

To maintain sufficient voids in the concrete, the size of the aggregates should be in the range of 9.5 to 26.5 mm [24]. The aggregates taken in this study had satisfied the properties like a limited amount of deleterious materials such as clay and other minerals, which affect the bonding between cement paste and aggregates. The aggregate sizes were taken based on the suggestion from the past study which is used in combination with fly ash. Larger aggregate sizes would give better strength than small-sized aggregates (< 4.75 mm), and the bond strength is taken care of by pozzolanic material [25]. The aggregates used are of single-sized and round-shaped which became easy while mixing. On the other hand, we did not compromise in maintaining the required mix proportion throughout the analysis. The physical properties of the aggregates are tested as per IS: 383-1970 and listed in Table 4.

Table 4 Physical properties of coarse aggregate

Property	Observed value	Requirement as per IS: 383
Aggregate crushing value	25%	Should be less than 45%
Aggregate impact value	22%	Should be less than 45%
Aggregate abrasion value	18%	Should be less than 30%
Water absorption	0.7%	Should be less than 2%
Fineness modulus	6.6	6.0–6.9
Specific gravity	2.8	2.5–3.0

3.3 Mix Design

The mix proportions, in the present study, were calculated based on the design guidelines proposed by IS 10262:2009 along with the aid of IS 456:2000.

Mix design for M30 grade of concrete was prepared by taking w/c ratio as 0.37. A small amount of fine aggregate (7% weight of coarse aggregate) is added to maintain minimum bond strength between coarse aggregate and binder (cement and fly ash). The mix proportion for several aggregate sizes is mentioned in Table 5.

Table 5 Mix proportion for 1m³ volume samples

Fly ash replacement	Coarse aggregate (kg)	Fine aggregate (kg)	Water (kg)	Cement (kg)	Replaced material (kg)
<i>Aggregate of size 10 mm</i>					
20%	1248	87	148	449	112
35%	1220	85	148	365	196
50%	1209	84	148	281	281
<i>Aggregate of size 12.5 mm</i>					
20%	1307	91	130	396	99
35%	1298	90	130	321	173
50%	1287	89	130	247	247
<i>Aggregate of size 20 mm</i>					
20%	1441	100	117	256	64
35%	1434	99	117	208	112
50%	1426	98	117	160	160

3.4 Specimen Preparation

To test the influence of fly ash replacement and change in aggregate size on permeability and compressive strength of pervious concrete, three specimens were prepared in each fly ash proportion and aggregate size. So, a total of 60 specimens (30 for compression test and 30 for permeability) were prepared and tested. The specimen size for the cube compression test is $150 \times 150 \times 150$ cm and for permeability test cylinders of size 150×300 cm. A compressive strength test was conducted as per ASTM C 39 [26]. All these specimens were prepared using M30 grade of concrete by varying proportions of fly ash and aggregate sizes.

3.5 Porosity Test

The functional and structural properties of permeable concrete are majorly influenced by the connected and disconnected pores. The pores present in the specimen are measured by the porosity test, which is the ratio of the volume of pores to the volume of the specimen [27]. Equation (1) shows the formula for porosity.

$$\tilde{\eta} = 1 - \frac{(w_2 - w_1)}{\gamma v} \quad (1)$$

where $\tilde{\eta}$ = porosity (%), W_1 = Sample weight taken in water (gm), W_2 = Sample weight when oven dried (gm), γ = Water density (gm/cc), V = Volume of sample (cm^3).

3.6 Permeability Test

The constant head permeability test is used to calculate the coefficient of permeability (k). Sidewall leakage is the biggest problem for the conventional test procedure. A different test procedure is used in casting the pervious concrete. In the present study, PVC pipes are used as a mold to give the cylindrical shape to the concrete specimen. The inner surface of the pipe is lubricated to easily remove the concrete while demolding. The two open ends are closed with PVC caps to give a closed structure. The caps are pierced, and valves are introduced into the hole so that the discharged water can be collected through these valves. The detailed procedure is shown in (Fig. 2, 3, and 4). The coefficient of permeability (k) is calculated using the formula shown in Eq. (2).

$$k = \frac{Q * L}{A * h * t} \quad (2)$$

where k = Coefficient of permeability (cm/sec), Q = Amount of water discharge (cm^3), L = Length of concrete specimen (cm), A = Area of concrete specimen (cm^2), h = Height of water (cm), t = Time (sec).



Fig. 2 Casting pervious concrete in PVC pipes

Fig. 3 Closing both sides with PVC caps

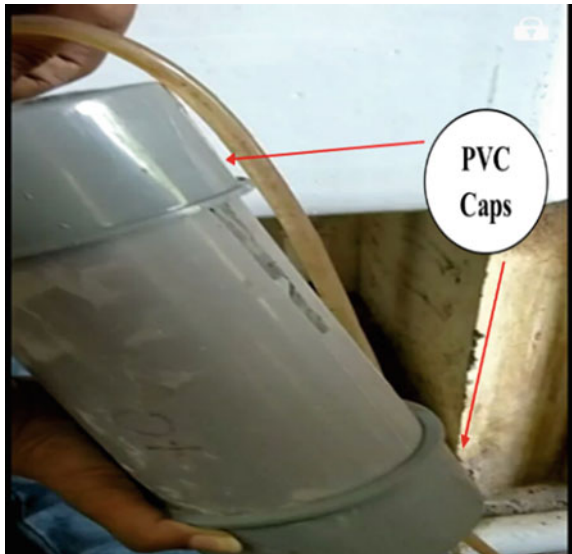
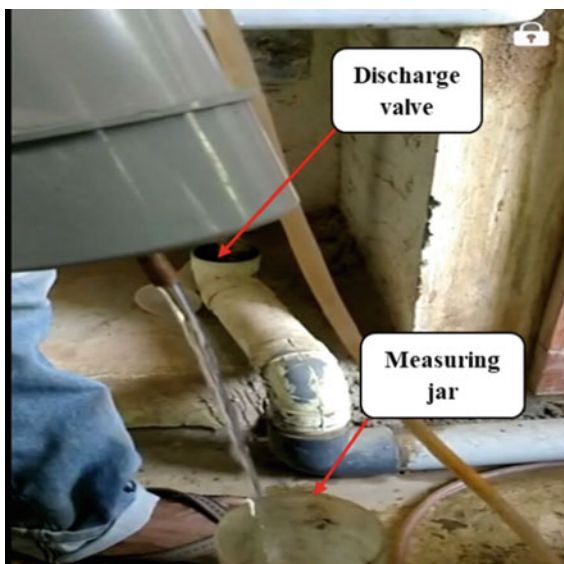


Fig. 4 Collecting water into the measuring jar



4 Results and Discussion

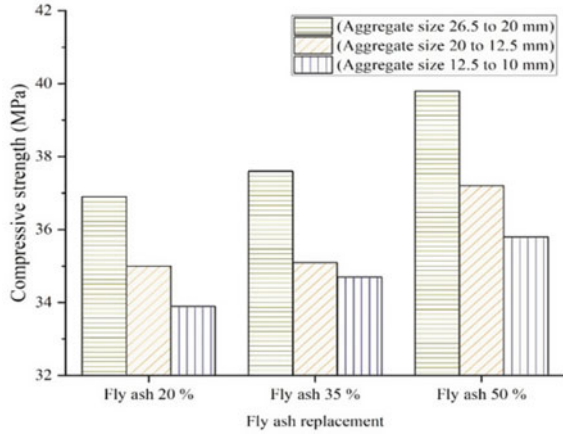
4.1 Influence of Fly Ash Addition in Replacement of Cement

Compressive Strength: The strength values of pervious concrete are relatively low due to high porosity when compared to conventional concrete. The pervious concrete specimens which were cast without any usage of fly ash as SCM had achieved 34.5 MPa. But when fly ash is used as SCM for cement, the compressive strength has improved from 33.9 to 39.8 MPa. Without considering the effect of aggregate size, increasing the fly ash replacement from 20 to 50% resulted in higher compressive strength values. On the further increase of fly ash content, the strength values were observed to decrease drastically. From Fig. 5, we can see that, by increasing the fly ash replacement in the concrete, the compressive strength has increased, irrespective of the aggregate size.

The reason for higher strength achievement is due to the mixing of fly ash with the cement during the hydration process, the calcium hydroxide is released to form calcium-silicate and calcium-aluminate hydrates. These bonds are observed to be strong, and thereby higher strength is obtained by increasing the fly ash content in replacement of cement.

Permeability: In a normal pervious concrete, the coefficient of permeability ranges from 0.007 to 4 cm/s, but in the present study as fly ash is used as SCM, the obtained “*k*” values ranged from 1.20 to 1.61 cm/s. The pervious concrete specimens which were cast without any usage of fly ash as SCM had achieved “*k*” value of 1.4 cm/s.

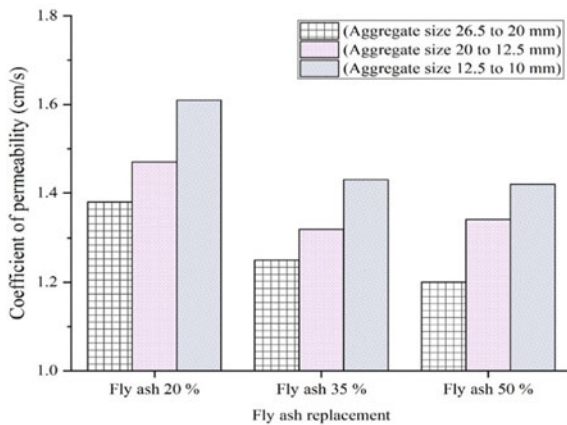
Fig. 5 Variation of strength by changing aggregate size and binder content



It was observed that the “*k*” values had decreased as the fly ash replacement had increased from 20 to 50%. A higher “*k*” value is obtained when fly ash is replaced at 20% and aggregates used are of 12.5–10 mm. The lowest “*k*” value is obtained as 1.20 cm/s when cement is replaced with 50% fly ash and aggregate size as 26.5–20 mm. The overall obtained “*k*” value is sufficient enough to act as a porous medium for draining out the runoff water. From Fig. 6, we can see the variation of “*k*” values with change in fly ash content and aggregate size.

The reason for decreased permeability is due to the replacement of cement with a certain proportion of binder material (fly ash) reduces the water demand for concrete and improves workability. If fly ash is replaced by 20% of cement in weight, the water demand is reduced by nearly 10%. Further replacing the cement with fly ash, up to 50%, will result in high water reduction. As there is a reduction in demand

Fig. 6 Variation of permeability by changing aggregate size and binder content



for water and increased cementitious material in the concrete, the inter-connectivity pores have reduced, leading to reduced permeability.

4.2 Influence of Change in Aggregate Size

Compressive strength: The load-carrying capability of a concrete specimen is taken care by the aggregates, thereby changing its gradation may result in strength variation.

It was observed that by reducing the aggregate size from 26.5 to 10 mm, there is an average strength reduction of 3.3 MPa. The highest strength was obtained when the aggregate size of 26.5–20 mm was used, and the lowest strength when 12.5–10 mm was used. The reason for strength enhancement by increasing the aggregate size is the homogeneity of the concrete is being disturbed due to the presence of large size aggregates. Due to the absence of fine aggregates, there exists a weaker bond between binder content and aggregates. For small size aggregates, the binder paste can easily spread over its entire surface area. But still increasing the size, the binder paste could not spread the entire surface area which leads to a weaker bond.

Permeability: The inter-granular pore size of a pervious concrete specimen changes due to the change in aggregate size, which leads to permeability variation. From Fig. 7 considering the variation of porosity (%) with change in aggregate size, 12.5–10 mm aggregates produce larger porosity rather than 26.5–20 mm. As the inter-connectivity pores (porosity) present in the previous concrete specimens with small aggregates are high, the permeability values are also observed to be high.

In the present study, by changing the aggregate size from 26.5–10 mm, there is an increase of “k” value by 0.21 cm/s. The highest “k” value is observed when

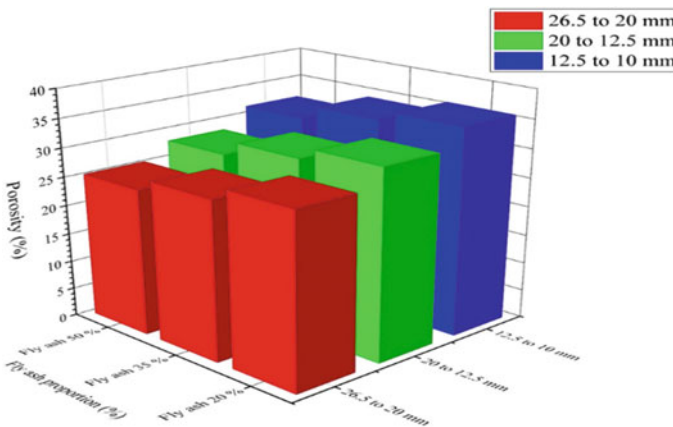


Fig. 7 Variation of porosity by changing aggregate size and fly ash proportion

aggregates of size 12.5–10 mm were used, and the lowest was observed when 26.5–20 mm were used. Thereby decreasing the size of aggregates in pervious concrete production, the porosity and permeability had increased.

5 Statistical Analysis

Statistical analysis was performed for the collected data to develop an empirical model for predicting the variation in strength and permeability, by changing the SCM proportion and aggregate size. In the present study, the dependent variables are compressive strength (σ), coefficient of permeability (k), and porosity (%), and the independent variables are different proportions of fly ash prepared with different aggregate sizes. The significance of each parameter is discussed in Table 6.

The inference of each test is detailed below:

- (1) The mean or average value of the entire data set represents the central tendency or the center value. The maximum strength is obtained when fly ash is replaced at 50%, and aggregate size is 26.5–20 mm. The minimum strength is obtained at 20% replacement, and aggregates are 12.5–10 mm. In the case of permeability, the maximum value is obtained at 20% fly ash and the minimum value at 50% replacement.
- (2) The standard deviation tells how far the data is dispersed concerning the mean value. For all the obtained values, there is a very less dispersion rate which is ranging from 1.23 to 2.12 MPa in the case of strength and 0.13–0.42 cm/s

Table 6 Statistical characteristics of each parameter

Variables	Mean		Standard deviation		Skewness		Kurtosis	
	σ^*	K^*	σ	K	σ	K	σ	K
<i>20% fly ash</i>								
26.5–20 mm	36.9	1.38	1.18	0.23	+ 0.25	+ 0.32	1.82	2.03
20–12.5 mm	35	1.47	2.03	0.15	+ 0.22	+ 0.31	1.93	2.24
12.5–10 mm	33.9	1.61	2.01	0.34	+ 0.31	+ 0.34	2.35	2.56
<i>35% fly ash</i>								
26.5–20 mm	37.6	1.25	2.12	0.13	+ 0.21	+ 0.29	1.52	1.75
20–12.5 mm	35.1	1.32	1.34	0.42	+ 0.18	+ 0.26	2.32	2.35
12.5–10 mm	34.7	1.43	1.32	0.24	+ 0.23	+ 0.30	2.45	2.57
<i>50% fly ash</i>								
26.5–20 mm	39.8	1.20	1.51	0.21	+ 0.16	+ 0.32	2.54	2.23
20–12.5 mm	37.2	1.34	1.65	0.34	+ 0.21	+ 0.38	2.36	2.39
12.5–10 mm	35.8	1.42	1.75	0.15	+ 0.24	+ 0.42	2.47	2.56
Normal pervious concrete	34.5	1.40	1.23	0.17	+ 0.22	+ 0.31	2.25	2.51

σ^* = compressive strength (MPa), K^* = coefficient of permeability (cm/s)

in the case of permeability. From these values, we can infer that uniformity is maintained throughout the data set.

- (3) Skewness explains how this data distribution leans concerning the center axis. All the values in the present study are positively skewed, and the shape of the curve is inferred by kurtosis. If the value is less than 3, then the curve is of platykurtic shape. In the present study, all the values are less than 3, and so the shape of the distribution curve is Platykurtic.

5.1 Correlation Matrix

In the present study, there are nine independent variables and three dependent variables (porosity, strength, and permeability). The interdependency of these variables is studied using a correlation matrix. Almost all the values are observed to be greater than 0.5 except in a few cases. This tells us that there is a strong correlation between the dependent and independent variables. The strongest relationship is observed between permeability and porosity (0.91), and the least relation is observed between porosity and strength (−0.25). A conclusion is drawn that, by changing binder content and aggregate size, there is a significant change in strength and permeability. But we need to know among all the parameters, which one is the best fitting in terms of strength and permeability. To get the best fit, we try to assume that there exists a completely linear relationship between the independent and dependent variables. Multiple linear regression analysis is performed to draw the best outcome. Table 7 shows the correlation matrix for dependent and independent variables.

5.2 Multiple Linear Regression Analysis (MLR)

The purpose of doing this analysis is to test whether the taken independent variables can predict the changes in strength and permeability. Equation 3 is the basic form for MLR, and “Y” is the dependent variable (strength and permeability).

$$\begin{aligned}
 Y = & \beta_0 + \beta_1 X_1 + \beta_2 X_2 + \beta_3 X_3 + \beta_4 X_4 + \beta_5 X_5 + \beta_6 X_6 \\
 & + \beta_7 X_7 \dots + \beta_{10} X_{10} + \varepsilon.
 \end{aligned}
 \tag{3}$$

Y is the dependent variable (strength or permeability).

β_0 is the intercept. $\beta_1, \beta_2, \beta_3, \dots, \beta_{10}$ are influencing coefficients, ε is error.

X_1 is porosity, X_2 is 20% fly ash–aggregates 26.5–20 mm, X_3 is 20% fly ash–aggregates 20–12.5 mm, X_4 is 20% fly ash–aggregates 12.5–10 mm, X_5 is 35% fly ash–aggregates 26.5–20 mm, X_6 is 35% fly ash–aggregates 20–12.5 mm, X_7 is 35% fly ash–aggregates 12.5–10 mm, X_8 is 50% fly ash–aggregates 26.5–20 mm, X_9 is 50% fly ash–aggregates 20–12.5 mm, X_{10} is 50% fly ash–aggregates 12.5–10 mm. The influencing parameters or regression coefficients signify if there is a unit change

Table 7 Correlation matrix

R values	Strength (MPa)	Porosity (%)	Permeability (cm/s)	20% fly ash			35% fly ash			50% fly ash					
				26.5–20 mm	20–12.5 mm	12.5–10 mm	26.5–20 mm	20–12.5 mm	12.5–10 mm	26.5–20 mm	20–12.5 mm	12.5–10 mm			
Strength (MPa)	1														
Porosity (%)	-0.25	1													
Permeability (cm/s)	-0.75	0.91	1												
20% fly ash	26.5–20 mm	0.65	0.58	1											
	20–12.5 mm	0.55	0.64	0.67	1										
	12.5–10 mm	0.45	0.75	0.78	0.86	0.92	1								
35% Fly ash	26.5–20 mm	0.56	0.38	0.40	0.75	0.67	0.54	1							
	20–12.5 mm	0.48	0.45	0.46	0.66	0.62	0.58	0.83	1						
	12.5–10 mm	0.42	0.52	0.54	0.54	0.50	0.48	0.78	0.86	1					
50% fly ash	26.5–20 mm	0.52	0.36	0.38	0.67	0.61	0.54	0.56	0.68	0.62	1				
	20–12.5 mm	0.5	0.40	0.43	0.56	0.59	0.48	0.54	0.65	0.60	0.82	1			
	12.5–10 mm	0.38	0.52	0.56	0.52	0.48	0.45	0.48	0.55	0.52	0.75	0.86	1		

Table 8 Influencing coefficients

Independent variables	Dependent variables	
	Strength (MPa)	Permeability (cm/s)
	Influencing coefficients	
Intercept	23.64	19.52
Porosity	-0.34	1.62
20% fly ash–aggregates 26.5–20 mm	1.21	0.97
20% fly ash–aggregates 20–12.5 mm	0.98	1.25
20% fly ash–aggregates 12.5–10 mm	0.82	1.34
35% fly ash–aggregates 26.5–20 mm	0.96	0.72
35% fly ash–aggregates 20–12.5 mm	0.78	0.83
35% fly ash–aggregates 12.5–10 mm	0.57	0.94
50% fly ash–aggregates 26.5–20 mm	0.42	0.34
50% fly ash–aggregates 20–12.5 mm	0.38	0.52
50% fly ash–aggregates 12.5–10 mm	0.25	0.63
Error	10.34	12.42

in the independent variable, then there will be a “ β ” change in the dependent variable. For example, if we take the influencing coefficient between porosity and permeability, the obtained value is 1.62 (Table 8). This tells that if the porosity is increased by a value of “1”, then permeability will increase to a value of “1.62”. In the same way, the entire set of coefficient values behaves with dependent and independent variables.

From Table 8, the maximum value is obtained for 20% fly ash–aggregates 26.5–20 mm in case of strength and 20% fly ash–aggregates 12.5–10 mm in case of permeability. We can conclude that a 20% replacement of binder content is most preferable for strength and permeability. When it comes to aggregate size, there is no exact solution from the table. But it is preferable to use lesser aggregate size than the larger aggregates to provide better strength and permeability.

6 Conclusions

The following are the major conclusions drawn from the study:

1. The influence of adding fly ash as supplementary cementitious material (SCM) in pervious concrete production had a significant effect on variation in strength and permeability. Statistical analysis revealed that 20% replacement of fly ash with cement in the manufacturing pervious concrete resulted in optimal strength and permeability.

2. Varying the fly ash content from 20 to 50%, the permeability of the concrete is observed to decrease. As the fly ash content is increased, the water demand is reduced which leads to a decrease in inter-connectivity pores.
3. The compressive strength increased by varying the fly ash content from 20 to 50%. When fly ash is mixed with the cement during the hydration process, calcium hydroxide is released to form calcium-silicate and calcium-aluminate hydrates. These bonds are observed to be strong, and thereby higher strength is obtained by increasing the fly ash content in replacement of cement.
4. The change in aggregate size had very little significance on the strength and permeability variation. Increasing the aggregate size from 10 to 26.5 mm, there is an increase in porosity and water permeability as the inter-connectivity pores are high in the case of large size aggregates and low in small size aggregates.
5. From the statistical analysis, the usage of different aggregate sizes has less effect in increasing the strength. It was observed that by reducing the aggregate size from 26.5 to 10 mm, there is an average strength reduction of 3.3 MPa.
6. The developed multiple regression model yielded excellent regression coefficients for predicting the strength and permeability by varying the fly ash content and aggregate size.

References

1. Cree D, Green M, Noumowe A (2013) Residual strength of concrete containing recycled materials after exposure to fire: a review. *Constr Build Mater* 45:208–223. <https://doi.org/10.1016/j.conbuildmat.2013.04.005>
2. Volder A, Watson T, Viswanathan B (2009) Potential use of pervious concrete for maintaining existing mature trees during and after urban development. *Urban For Urban Green* 8:249–256. <https://doi.org/10.1016/j.ufug.2009.08.006>
3. Takebayashi H, Moriyama M (2012) Study on surface heat budget of various pavements for urban heat island mitigation. *Adv Mater Sci Eng* 2012. <https://doi.org/10.1155/2012/523051>
4. Tan K, Fwa T, Lim E (2013) Effect of mix proportion on strength and permeability of pervious concrete for use in pavement. *J East Asia Soc Transp Stud* 10:1565–1575. <https://doi.org/10.11175/easts.10.1565>
5. Luck JD, Workman SR, Coyne MS, Higgins SF (2008) Solid material retention and nutrient reduction properties of pervious concrete mixtures. *Biosyst Eng* 100:401–408. <https://doi.org/10.1016/j.biosystemseng.2008.03.011>
6. Kolokotroni M, Ren X, Davies M, Mavrogianni A (2012) London's urban heat island: impact on current and future energy consumption in office buildings. *Energy Build* 47:302–311. <https://doi.org/10.1016/j.enbuild.2011.12.019>
7. Nguyen DH, Sebaibi N, Boutouil M, Leleyter L, Baraud F (2014) A modified method for the design of pervious concrete mix. *Constr Build Mater* 73:271–282. <https://doi.org/10.1016/j.conbuildmat.2014.09.088>
8. Yahia A, Kabagire KD (2014) New approach to proportion pervious concrete. *Constr Build Mater* 62:38–46. <https://doi.org/10.1016/j.conbuildmat.2014.03.025>
9. Jing Yang GJ (2002) Department: Experimental study on properties of pervious concrete pavement materials. *Cem Concr Res* 33:381–386. https://doi.org/10.1007/978-981-13-6717-5_36

10. Tariq Al-Shafi'i N, Falih Al-Busaltan S, Adnan Abdulwahid A (2018) Experimental study on properties of pervious concrete pavement comprising sustainable materials. *J Eng Sustain Dev* 22:94–106. <https://doi.org/10.31272/jeasd.2018.2.71>
11. Kevern JT, Schaefer VR, Wang K (2009) Evaluation of Pervious concrete workability using gyratory compaction. *J Mater Civ Eng* 21:764–770. [https://doi.org/10.1061/\(asce\)0899-1561\(2009\)21:12\(764\)](https://doi.org/10.1061/(asce)0899-1561(2009)21:12(764))
12. Deo O, Neithalath N (2011) Compressive response of pervious concretes proportioned for desired porosities. *Constr Build Mater* 25:4181–4189. <https://doi.org/10.1016/j.conbuildmat.2011.04.055>
13. Nguyen DH, Boutouil M, Sebaibi N, Baraud F, Leleyter L (2017) Durability of pervious concrete using crushed seashells. *Constr Build Mater* 135:137–150. <https://doi.org/10.1016/j.conbuildmat.2016.12.219>
14. Paula Junior AC, Jacinto C, Oliveira TM, Polisseni AE, Brum FM, Teixeira ER, Mateus R (2021) Characterisation and life cycle assessment of pervious concrete with recycled concrete aggregates. *Crystals* 11(2):1–30. <https://doi.org/10.3390/cryst11020209>
15. Xie N, Akin M, Shi X (2019) Permeable concrete pavements: a review of environmental benefits and durability. *J Clean Prod* 210:1605–1621. <https://doi.org/10.1016/j.jclepro.2018.11.134>
16. Marolf A, Neithalath N, Sell E, Wegner K, Weiss J, Olek J (2004) Influence of aggregate size and gradation on acoustic absorption of enhanced porosity concrete. *ACI Mater J* 101:82–91. <https://doi.org/10.14359/12991>
17. Hesami S, Ahmadi S, Nematzadeh M (2014) Effects of rice husk ash and fiber on mechanical properties of pervious concrete pavement. *Constr Build Mater* 53:680–691. <https://doi.org/10.1016/j.conbuildmat.2013.11.070>
18. Borhan TM, Al Karawi RJ (2020) Experimental investigations on polymer modified pervious concrete. *Case Stud Constr Mater* 12. <https://doi.org/10.1016/j.cscm.2020.e00335>
19. Wang H, Li H, Liang X, Zhou H, Xie N, Dai Z (2019) Investigation on the mechanical properties and environmental impacts of pervious concrete containing fly ash based on the cement-aggregate ratio. *Constr Build Mater* 202:387–395. <https://doi.org/10.1016/j.conbuildmat.2019.01.044>
20. Yu F, Sun D, Wang J, Hu M (2019) Influence of aggregate size on compressive strength of pervious concrete. *Constr Build Mater* 209:463–475. <https://doi.org/10.1016/j.conbuildmat.2019.03.140>
21. Chen X, Wang H, Najm H, Venkateela G, Hencken J (2019) Evaluating engineering properties and environmental impact of pervious concrete with fly ash and slag. *J Clean Prod* 237:117714. <https://doi.org/10.1016/j.jclepro.2019.117714>
22. Liu H, Luo G, Wei H, Yu H (2018) Strength, permeability, and freeze-thaw durability of pervious concrete with different aggregate sizes, porosities, and water-binder ratios. *Appl Sci* 8. <https://doi.org/10.3390/app8081217>
23. Hemalatha T, Ramaswamy A (2017) A review on fly ash characteristics—towards promoting high volume utilization in developing sustainable concrete. *J Clean Prod* 147:546–559. <https://doi.org/10.1016/j.jclepro.2017.01.114>
24. Zhong R, Wille K (2016) Compression response of normal and high strength pervious concrete. *Constr Build Mater* 109:177–187. <https://doi.org/10.1016/j.conbuildmat.2016.01.051>
25. Tijani MA, Ajagbe WO, Ganiyu AA (2019) Effect of aggregate type on properties of pervious concrete. *J Mod Technol Eng* 4:37–46
26. Shu X, Huang B, Wu H, Dong Q, Burdette EG (2011) Performance comparison of laboratory and field produced pervious concrete mixtures. *Constr Build Mater* 25:3187–3192. <https://doi.org/10.1016/j.conbuildmat.2011.03.002>
27. Dong Q, Wu H, Huang B, Shu X, Wang K (2013) Investigation into laboratory Abrasion test methods for pervious concrete. *J Mater Civ Eng* 25:886–892. [https://doi.org/10.1061/\(asce\)mt.1943-5533.0000683](https://doi.org/10.1061/(asce)mt.1943-5533.0000683)

Investigations on Stone Matrix Asphalt Mixes by Utilizing Slag and Cellulose Fiber



Shriram Marathe, P. K. Akarsh, Arun Kumar Bhat, and Mahesh Kumar

Abstract Stone Matrix Asphalt (SMA) has become one of the most admired Asphalt Pavement layers due to its superior deformation-resistant capacity through a coarse stone skeleton providing more stone-on-stone contact than the other Dense Graded Asphalt (DGA) mixes. SMA has proved superior on heavily trafficked roads and in industrial applications. SMA has distinct advantages as a Surfacing, due to its potential for high resistance to fatigue and rutting. In the present study, the SMA specimens were prepared by incorporating Ground Granulated Blast Furnace Slag (GGBS) as filler and the Marshall properties were studied. Further, for the optimum Marshall mix (containing 2.5% of GGBS), the cellulose fiber was added. The results have shown that the maximum strength was obtained for the SMA mix containing 7% of bitumen content with 2.5% of GGBFS and 0.3% of cellulose fiber.

Keywords Stone matrix asphalt (SMA) · Marshall stability · Ground granulated blast furnace slag (GGBS) · Cellulose fiber

1 Introduction

Due to increased heavy traffic volume and extreme environmental conditions, there is increased distress in the conventional bituminous pavements. These increased distresses will lead to the reduced design life of the pavements. Hence, there is

S. Marathe (✉) · A. K. Bhat
NMAM Institute of Technology, Nitte, Karkala, India
e-mail: ram.nmamit@gmail.com

A. K. Bhat
e-mail: arun.bhat@nitte.edu.in

P. K. Akarsh
National Institute of Technology Karnataka, Surathkal, India

M. Kumar
Nitte Meenakshi Institute of Technology, Yelahanka, Bangalore, India
e-mail: maheshkumar.cl@nmit.ac.in

a continuous search for better construction techniques that would encounter the existing problems and ensures the satisfactory performance of resulting pavements. Surface course (combined wearing and following binder course) will always be considered as most important layers which are responsible to sustain most stresses developed in the pavements [15]. In most parts of India, the commonly used surface course in flexible pavements is conventional dense-graded Hot Mix Asphalt (HMA) mixes. The HMA may be dense-graded, gap-graded, or open-graded. The dense-graded HMA are more likely susceptible to fatigue and rutting action due to repeated heavy wheel loads and moisture damages. There is a need for better, durable, and efficient pavements with minimized pavement distresses, which may further lead to a reduction in other related costs such as travel costs, vehicle operation cost, traffic delay costs, and accident costs. The use of Stone Mastic/Matrix Asphalt (SMA), Open Graded Frictional Course (OGFC), and modified bituminous mixes (MB) would be effective to use instead of conventional asphaltic mixes [14]. SMA is one of the new generation asphaltic concrete mix with a gap-graded rut-resistant skeleton. Several experimental-preliminary studies and the field performance investigations carried out in recent past have proven that SMA mixes can be considered as one of the durable alternative to the conventional superior quality HMA mixes. This engineered HMA mix is defined with a strong aggregate skeleton with high-binder mastic mortar content (bitumen, fine aggregate, filler passing $75\ \mu$, and stabilizing agent). Typically, SMA consists of “70–80% of coarse aggregate, 6.0–7.0% of binder, 8–12% of filler, and 0.2–0.5% of stabilizing additives.” The higher percentage of coarse aggregate skeleton provides stone-on-stone interlock to induce resistance against permanent deformation and vehicular skidding, while the superior binder mastic adds to the durability and stability of SMA against pavement distresses by adhering along with the coarse aggregate [9, 10, 20]. In the gap-graded SMA, the mutually interlocked coarse aggregate will rest against each other, forming a primary component in the configuration of the skeleton, which in turn resists the heavier traffic loads. These aggregates are called active aggregates, and those which fill the voids between aggregates are called passive grains. Stabilizing additives are added to prevent the drain down of SMA, which usually occurs in gap-graded asphaltic mixes with high binder and filler content and to reduce the chances of the separation and flow down of asphalt during higher temperatures of production, transportation, and placement [7, 18]. A potential problem associated with SMA is drained down and bleeding. High bitumen content in the SMA Mix can cause the drain down the issue, and it remains a major problem with SMA [12, 16]. As per the standards, the drain down in any type of superior bituminous mixes must be less than 0.3% [2]. Therefore, it is very much essential to use a fewer portion of stabilizing additives such as fibers, rubber, and polymers which will stiffen the matrix, thereby reducing the drain down and bleeding problems significantly in SMA mixes [3, 6]. Since these stabilizing additives are generally costly, hence there exists a need to obtain an alternative, low-cost stabilizer which will essentially serve the same purpose, in a similar way as obtained by using other commonly used stabilizing additives. From the literature, the use of cellulose in the SMA matrix has shown very superior results with negligible drain down performances even at $170\ ^\circ\text{C}$; the study also revealed clearly that the incorporation of fibers

would help better in enhancing the resistance to drain down while compared with that of the polymer-based additives [8]. Incorporation of different types of slags in the laboratory SMA mixes was studied by several researchers; Pasetto and Baldo [17] have reported the laboratory performance of SMA mixes with “electric arc furnace steel (EAF) slag,” where they revealed satisfactory performances; also, a study by Behnood and Ameri [5] reported the satisfactory incorporation of steel slag in SMA mixes, where the improvements in engineering performances such as Marshall properties, resilient modulus, moisture damage resistance, and tensile strength performances were reported. Few recent studies have shown that the use of GGBS in the pavement quality mixes is beneficial to improve the engineering performance in long run due to its cementing and stiffness abilities even in highly humid conditions [11]. Hence under the present research scope, an attempt was made to use an unconventional natural cellulose fiber, and the performance of the SMA mix was investigated. In the current scope of research, the SMA mixes were designed with varied “ground granulated furnace slag” (i.e., GGBS) mineral filler and varied natural “cellulose fiber” stabilizing additives and the strength characteristics were investigated. The tested properties involve the Marshall performance, indirect tensile strength, and the drain down performances. All the preparations of mixes, specifications, and testing were made as per the IRC guidelines [13].

2 Materials and Methodology

2.1 Materials

The bituminous binder used for the study is conforming to VG-30. The aggregate mixture is of the classification satisfying “19 mm SMA” with Nominal Aggregate size, i.e., NMA of 19 mm as per IRC-SP-79. The GGBS is used in the study as the mineral filler was supplied by JSW cements, which had the specific gravity of 2.88. Locally available crushed stone aggregates were used for the investigation. The properties of the aggregates are presented in Table 1. The mechanical tests carried as per relevant parts of BIS:2386 on aggregates have shown that they possess Aggregate Impact Value of 10.99%, LA Abrasion value of 22.64%, and Aggregate Crushing Value of 17.06%. The bituminous binder used for this study is taken from local supplier which is having the specific gravity of 1.03 and the other properties satisfying the requirements for VG-30 grade.

2.2 Methodology

After conducting the preliminary tests on the materials, the sieving of the aggregates was carried out and the required amount of aggregates was separately collected. The

Table 1 Properties of aggregates

Sieve sizes (mm)	Target gradation (% Finer)	Design gradation (% Finer)	Specific gravity
25.0	100	100	2.71
19.0	90–100	95	2.70
13.2	45–70	95	2.69
9.5	25–60	62.5	2.66
4.75	20–28	24	2.65
2.36	16–24	20	2.57
1.18	13–21	17	2.63
0.60	12–18	15	2.60
0.30	10–15	15	2.52
0.075	8–12	10	2.45

sequence of the sieving and the different aggregate mixes are typically presented in Fig. 1. The entire mixtures consisting of a binder, and aggregates were heated separately to the prescribed mixing temperature, mixed properly and compacted using a Compactive effort of 50 blows on each side using the standard rammer. Then, the optimum bituminous binder content (OBC) is obtained using the standard Marshall Stability test as per the relevant standards (shown in Fig. 1). The trials were made by varying the bituminous binders in the SMA mix from 5 to 8%, at an increment of 0.5%. The OBC is obtained through density void analysis and stability flow tests. Further, by using the obtained OBC, the investigations were continued to obtain the optimum dosage of mineral filler (GGBS) and cellulose fiber content. Then, the other tests to study the behavior of Indirect tensile strength (ITS) and the drain down performances of the developed SMA mixes were carried out. The ITS test is measured by the application of diametrical planar load on the bituminous cylindrical specimen, and the “drain down” test is carried out in a wired basket of opening size of 6.3 mm. These tests were carried out as per the standard method available in the literature [1, 4, 19].

3 Results and Discussions

The preliminary Marshall Stability test results show that the OBC of the VG-30 binder for the given design aggregate mix was obtained as 7.0%. At this OBC, the SMA mix has shown a maximum Marshall stability value of 12.28 kN, flow value of 3.55 mm; Specific gravity of 2.37; Air voids of 4.818%; Voids in Mineral Aggregates (VMA) of 18.66%, and Voids filled with Bitumen (VFB) of 84.89%. The same mix is taken as the reference mix. The ITS and drain down performance results indicated, respectively, 1.025 MPa and 0.75%. For the SMA mix with this OBC, the GGBS



Fig. 1 Sieving and collection of aggregates, Marshall stability testing of SMA mix

filler is added in various intervals from 1 to 3%, and the results of Marshall Stability, flow, and ITS are shown in Table 2. The results showcase that the Marshall Stability value increases as the % of GGBS increases in the SMA mix reaches optimum and then reduces. At 2.5% of GGBS content, the maximum stability of 18.18 kN is approximately 48% more than the reference mix. At this GGBS dosage, a flow value of 2.89 mm was obtained, which is 18.5% less than the reference mix. The ITS results reveal that at 2.5% GGBS content, a maximum value of 1.312 MPa was achieved which is 28% greater than that of the reference mix. The improved strength performance of the SMA mix in the presence of GGBS may be due to the reactivity and improved binding behavior of the asphalt up to certain limits in the asphalt concrete mixes. The strength enhancements may be due to the stiffening of the binder mastic in the presence of GGBS. It may be also due to the improvement of strength and stiffness behavior of the asphaltic mix by the incorporation of slags as reported by various researchers in the works of literature [5, 11, 17].

Further investigations were continued to study the effect of cellulose fiber in the SMA mix containing 7% bituminous binder and 2.5% of the GGBS filler. The dosage of fiber is varied from 0.2 to 0.5% at an increment of 0.1% in the SMA mix. The results of the various test results were indicated in Table 3. Since there is only a

Table 2 Effect of GGBS mineral filler in the SMA mix

% GGBS	Marshall stability (kN)	Marshall flow (mm)	Indirect tensile strength (MPa)
0	12.28	3.55	1.025
1.0	13.87	3.48	1.078
1.5	15.87	3.38	1.128
2.0	17.73	3.04	1.274
2.5	18.18	2.89	1.312
3.0	16.28	3.12	1.289

Table 3 Effect of cellulose fiber in the SMA mix containing 2.5% GGBS Filler

% Fiber	Indirect tensile strength (MPa)	Drain down (%)
0	1.312	3.85
0.2	1.321	1.40
0.3	1.322	1.25
0.4	1.315	1.35
0.5	1.316	1.55

marginal improvement in the Marshall Properties, they were not presented in the results. The results reveal that however there is a marginal increment in the ITS results due to incorporation of fibers in the optimum SMA mix with 7% binder and 2.5% GGBS, which cannot be considered significant. Remarkable improvements in the drain down properties were indicated by the addition of fibers up to certain limits. The results reveal that there is a 65% reduction in the drain down property of the optimum reference mix when small dosages of 0.3% of the cellulose fibers were used in the SMA mix. The improvement in the engineering performance with the fiber may be due to the provision of high level of binder reinforcement with higher surface area in the mastic asphalt up to a certain limit as reported in the literature [14]. Hence, the use of cellulose fibers will help in providing better stiffness to the mastic asphalt mixes, which would help in enhancing the stability of the freshly prepared mix while compared with that of the mix without the usage of these fibers. Hence, the usages of the fibers are highly recommended in SMA mixes.

4 Conclusions and Future Scope

Under the present scope of the study, limited experimental investigations are carried out on the Stone Matrix Asphalt mixes. After the preliminary investigations, the Marshall Stability tests were performed on the prepared SMA with 19 mm nominal maximum-sized aggregates designed using IRC specifications to obtain the Optimum Bitumen Content (OBC) and was attained as 7.0% by weight of the mix. By keeping the OBC content at 7.0%, further investigations are carried out. Initially, the effect of GGBS mineral filler on the mechanical properties of the asphalt mix was investigated, which revealed that a better performance in terms of Marshall Stability, Flow, and Indirect Tensile Strength could be achieved at a dosage of 2.5% GGBS. Further, in the test by addition of 0.3% of cellulose fibers, the drain down characteristics were improved to a value greater than 65% while compared it with the optimum SMA mix. From the test results, it can be concluded that the usage of the fibers would help in providing better stiffness to the mastic asphalt mixes, which would help in enhancing the stability of the freshly prepared mix while compared with that of the mix without the usage of these fibers.

The test results have shown a satisfactory and improved performance of the SMA mix with GGBS and cellulose fibers; hence, the usage of both would be recommended while designing SMA mixes. However, the investigations could be extended to study further performance characteristics such as rutting studies, repeated loading studies, long-term aging studies, moisture susceptibility, and retained strength so as to gain more confidence in applying this SMA improvement technique in the field applications.

References

1. AASHTO-T283 (2003) Resistance of compacted asphalt mixtures to moisture-induced damage
2. AASHTO (2000) Determination of draindown characteristics in uncompacted asphalt mixtures
3. Al-Hdabi A et al (2019) Laboratory investigation on the properties of asphalt concrete mixture with GGBFS as filler. *IOP Conf Ser Mater Sci Eng* 557(1):1–12. <https://doi.org/10.1088/1757-899X/557/1/012063>
4. ASTM D-6390 (2011) Standard test method for determination of draindown characteristics in uncompacted asphalt mixtures
5. Behnood A, Ameri M (2012) Experimental investigation of stone matrix asphalt mixtures containing steel slag. *Sci Iran* 19(5):1214–1219. <https://doi.org/10.1016/j.scient.2012.07.007>
6. Bindu CS, Beana KS (2014) Influence of additives on the characteristics of stone matrix asphalt. *Int J Res Eng Technol* 03(07):83–88
7. Blazejowski K (2010) Stone matrix asphalt: theory and practice. CRC Press, Taylor and Francis Group, Florida. <https://doi.org/10.1201/b10285>
8. Brown ER et al (1997) Development of a mixture design procedure for stone matrix asphalt (SMA). *J Assoc Asphalt Paving Technol* 66:1–19
9. Brown ER et al (1997) Development of a mixture design procedure for stone matrix asphalt (SMA). *J Assoc Asphalt Paving Technol* 66:1–65
10. Brown ER, Manglorkar H (1993) Evaluation of properties of SMA mixtures. Auburn University
11. Ellis C et al (2011) Properties of GGBS-bitumen emulsion systems with recycled aggregates. *Road Mater Pavement Des* 5(3):373–383. <https://doi.org/10.1080/14680629.2004.9689977>
12. Ferreira da Costa L et al (2020) Asphalt mixture reinforced with banana fibres. *Road Mater Pavement Des* 1–13. <https://doi.org/10.1080/14680629.2020.1713866>
13. IRC:SP-79 (2008) Tentative specifications for stone matrix asphalt
14. Kamaraj C et al (2013) Design, construction and performance of stone matrix asphalt (SMA)—field test section. *Highw Res J* 12–25
15. Khanna SK, Justo CEG (2011) Highway engineering. Nem Chand & Bros., Roorkee, India
16. Mithanthaya IR et al (2018) Effect of gradation and waste plastic on performance of stone matrix asphalt (SMA). *Int J Civ Eng Technol* 9(9):1645–1656
17. Pasetto M, Baldo N (2012) Performance comparative analysis of stone mastic asphalts with electric arc furnace steel slag: a laboratory evaluation. *Mater Struct Constr* 45(3):411–424. <https://doi.org/10.1617/s11527-011-9773-2>
18. Qiu YF, Lum KM (2006) Design and performance of stone mastic asphalt. *J Transp Eng* 132(12):956–963
19. Sarang G et al (2016) Comparison of stone matrix asphalt mixtures with polymer-modified bitumen and shredded waste plastics. *Road Mater Pavement Des* 17(4):933–945. <https://doi.org/10.1080/14680629.2015.1124799>
20. Sarang G (2015) Experimental investigation of stone matrix asphalt mixture. NITK Surathkal

Laboratory Evaluation on the Use of Natural Fibre in Gap-Graded Asphalt Mixtures



Raghuram K. Chinnabhandar, A. U. Ravi Shankar, V. Sai Ganesh, Arnet Cleetus, and Shubham Chourasia

Abstract Stone Matrix Asphalt (SMA) is a gap-graded mixture that consists of a high concentration of coarse aggregates, which imparts strength and rut resistance and a high binder content, making the mixture durable. The high binder content mortar consists of fine aggregates, filler, bitumen and stabilising additive. One of the limitations of SMA is it suffers from draindown of binder mortar which can be reduced by adding a mineral fibre, natural fibre or synthetic fibre. The addition of a stabilising additive not only controls the draindown but also improves the tensile strength because of the network of fibres in the mixture. In the present study, an attempt is made to determine the effect of Areca fibre, a natural fibre abundantly available in the southern Indian region. A comparison between two SMA mixtures prepared with and without stabilising additive is made. The Superpave mix design method was adopted, and tests such as draindown, fatigue, rutting and moisture-induced damage properties such as tensile strength ratio (TSR) were evaluated. The results indicate that the mixture with Areca fibre effectively controls the draindown and satisfies the volumetric and mix design criteria as per IRC SP 79. However, the performance of SMA without stabilising additive was better than the mixture with the stabilising additive with respect to resistance to rutting, fatigue and moisture-induced damage.

Keywords Stone matrix asphalt · Areca fibre · Tensile strength ratio · Rutting · Superpave mix design

1 Introduction

The primary reason for the failure of flexible pavements is due to the development of fatigue cracking and rutting [10, 21, 30]. Hence, to overcome this problem, a gap-graded or discontinuous bituminous mix like Stone Matrix Asphalt (SMA) was developed in the 1960s in Germany to resist deformations caused by studded tyres.

R. K. Chinnabhandar (✉) · A. U. Ravi Shankar · V. Sai Ganesh · A. Cleetus · S. Chourasia
Department of Civil Engineering, National Institute of Technology Karnataka, Surathkal, India
e-mail: raghuramkchinnabhandar@gmail.com

© The Author(s), under exclusive license to Springer Nature Singapore Pte Ltd. 2023
M. V. L. R. Anjaneyulu et al. (eds.), *Recent Advances in Transportation Systems Engineering and Management*, Lecture Notes in Civil Engineering 261,
https://doi.org/10.1007/978-981-19-2273-2_18

261

Since SMA was found to be rut resistant, its use was continued even after the studded tyres were banned [22, 28, 32–34]. SMA is a gap-graded mixture consisting of a high coarse aggregate content (about 70-80%), high binder content (typically above 6%), a high filler content (about 10% by weight of the aggregates) [9] and a stabilising additive to control the draindown of the bitumen and bitumen mortar. The high coarse aggregate content provides the SMA mix with a stone-to-stone skeleton which not only imparts strength to the mix but also improves the rutting resistance while the high binder content mortar improves the durability of the mix [10]. Some of the advantages of SMA are high resistance to rutting [11, 31], high durability [36], improved resistance to reflective cracking and reduced noise pollution. However, drainage of the binder and high primary cost are some of the drawbacks of SMA.

2 Use of Natural Fibres in Asphalt Mixes

According to ASTM D 6390, the maximum allowable draindown in SMA mixes is 0.3% by weight of the mixture. To overcome the problem of draindown, stiffer asphalt binders such as Polymer-modified Bitumen can be used, but they are expensive and have a higher susceptibility to thermal cracking [12]. Hence, to control the draindown in an SMA mix, a stabilising additive is used, either natural or synthetic fibre and chemically inert to the bituminous binder. The fibres hold the binder in the mixture at high temperatures and prevent draindown during production, transportation and placement of the mixture [15]. The natural fibres show excellent tensile strength and high value of resilient modulus, in addition to the reduction in the draindown [29]. Instead of using expensive patented fibres such as Cellulose fibres, the by-products of different agricultural products can be used as stabilising additives which not only improve the mechanical properties of SMA but also eliminate the need for disposal of such wastes. Hence, to find economical alternatives to patented fibres, several studies have been carried out in the last two decades where natural fibres are used as stabilising additives in SMA mixes as follows: Kumar et al. [23] have used Jute fibres in SMA and observed that though the tensile strength was higher, the resilient modulus was slightly lower than cellulose fibres. Coconut fibres were used as an alternative to cellulose fibres by Vale et al. [15] and observed that the coconut fibres were effective in controlling the draindown and improving the indirect tensile strength and resistance to moisture damage such as Retained Marshall Stability and Tensile Strength Ratio. However, the fatigue life and workability of SMA mixes with Coconut fibre were reduced, which maybe because of the stiffening of the mixture due to the absorption of binder by the fibres and the higher lengths of the fibre tending to flock together while dry mixing the aggregates and the fibres. The use of Chicken Feather fibres in asphalt concrete mixes was studied by Dalhat et al. [13] and observed that the stability and rutting resistance were improved compared to the mixes without fibres. But they concluded that Chicken Feather fibres were prone to biodegradation when exposed to extreme moisture conditions. Banana Fibres were used in SMA mixtures and observed that the resistance to rutting, resistance to moisture-induced

damage and fatigue life were comparable to SMA mixes with pelletised fibres [22, 34]. Oda et al. [29] showed that Sisal fibres can provide similar performance in terms of mechanical properties such as indirect tensile strength, resilient modulus and fatigue life compared to cellulose and polyester fibres. Cotton straw fibres have been successfully used in asphalt mixtures as an alternative to cellulose fibres to improve the high-temperature stability, low-temperature properties and resistance to moisture-induced damage [24].

2.1 *Areca/Betel Nut Fibre*

Areca, also called Betel nut, being a species of Palm belonging to the family of Arecaceae/Palmae, is cultivated in about 12 Asian countries with an estimated cultivation of about 1.2 million tonnes. The Areca tree grows vertically to about 15–20 m with a solitary, slender and straight stem about 10–15 cm in diameter with annulated marks at regular intervals. After extracting kernels, the husk is dumped in the backyards of processing plants or burnt as firewood, and they do not have any industrial or commercial applications [14]. The total Areca fruit cultivation in 2019–2020 in India was 853,000 tonnes from an area of 518,000 hectares [27]. The fruit consists of about 40% of husk, which means an estimated 341,000 tonnes of husk biomass was generated in India alone. The husk does not rapidly decompose because of its lingo-cellulosic composition [14]. Hence, large heaps of husk biomass create environmental problems due to the lack of proper disposal methods and industrial and commercial applications [35]. Therefore, the areca husks can be utilised for other purposes. The areca fibres are extracted manually from the areca husk, though they can be obtained from leaf stalks and fronds [25]. The thermogravimetric analysis (TGA) conducted by Yusriah et al. [37] on ripe Areca fibre used in the present study revealed there was a mass loss of 7.26, 44.01 and 91.47% when the fibres were heated from 30–100 °C, 100–240 °C and 240–490 °C, respectively. However, for the present study, the fibres, along with the dry aggregates, were heated to a temperature not more than 170 °C while preparing the mixtures (Fig. 1).

3 Objective

The main objective of the present investigation is to evaluate the effect of Areca fibre in SMA mixes in the laboratory. To achieve the objective, SMA mixtures with Areca fibre were prepared using VG-30 (viscosity grade) bitumen which were then compared with SMA mixtures prepared with Polymer-modified Bitumen (PMB 64-10) prepared without stabilising additives.

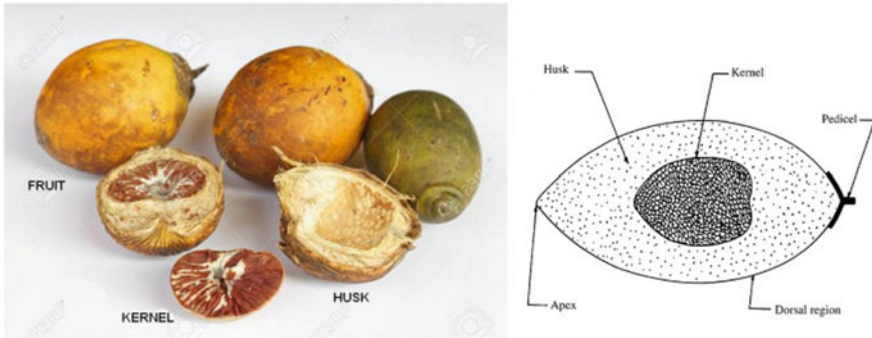


Fig. 1 Areca fruit, husk and kernel [19]

4 Materials Used

In the present study, crushed Granite stones were used as aggregates after evaluating their suitability for SMA mixes as per IRC SP 79 [16]. The basic properties of aggregates are tested as per IS:2386 Part IV and are shown in Table 1. Aggregate dust and hydrated lime, which improve the resistance of the mixture to moisture damage [26], were used as filler material. However, hydrated lime was limited to 2% by the mass of the aggregates in the mixture since the dynamic modulus of hot-mix asphalt is known to increase by 25% [8].

The aggregate gradation used is 13 mm Nominal Maximum Aggregate Size (NMAS) specified for wearing course in IRC SP 79 and is shown in Table 2. For the preparation of SMA mixes, either a modified bitumen or a bitumen with a stabilising additive is essential to reduce the draindown to the specified limits. Polymer-modified Bitumen (PMB), when carefully manufactured under controlled conditions using an additive such as an elastomer or polymer, improves its properties which makes it suitable for application as a wearing course under high rainfall and traffic conditions [12]. For this study, PMB 64-10 and VG-30 bitumen were used. When VG-30 was used, a stabilising additive, Areca fibre, was used in the SMA mix to control the drain down. Whereas the mixture with PMB was prepared without any stabilising

Table 1 Properties of aggregates

Test	Results	Requirements as per IRC SP 79 [16]
Combined flakiness and elongation index (%)	11.58	< 30
Specific gravity	2.69	–
Aggregate impact (%)	13.37	< 18
Los-Angeles abrasion (%)	15.24	< 25
Water absorption (%)	0.22	< 2

Table 2 Aggregate gradation

IS Sieve size (mm)	Cumulative % by weight of total aggregate passing	Adopted gradation
19.0	100	100
13.2	90–100	95
9.50	50–75	62.5
4.75	20–28	24
2.36	16–24	20
1.18	13–21	17
0.60	12–18	15
0.30	10–20	12
0.075	8–12	10

Table 3 Properties of VG-30 bitumen

Test	Results	Requirements as per IS:73 [18]
Penetration at 25 °C, 100 g, 5 s, 0.1 mm, Min	51	45
Absolute viscosity at 60 °C, Poises	2600	2400–3600
Flash point (Cleveland open cup), °C, Min	236	220 °C
Softening point (Ring and Ball), °C, Min	49	47 °C
Rolling thin film oven test, mass loss, % Max	0.61	1.0%
<i>Tests on residue from rolling thin film oven test</i>		
a. Viscosity ratio at 60 °C, Max	2.8	4.0
b. Ductility at 25 °C, cm, Min	47	40
Specific gravity	1.00	–

additives. Tables 3 and 4 show the results of basic tests conducted on both VG-30 and PMB 64-10 bitumen.

Table 5 presents the requirements of SMA as per IRC SP 79. Areca fibre was used as a stabilising additive when the SMA mixture was prepared using VG-30 bitumen. The SMA mixtures prepared using PMB 64-10 and VG-30 with Areca fibre are denoted as SMA-PMB and SMA-AF, respectively. Figure 2 shows the Areca fibre used for the study, and Tables 6 and 7 show the physical properties chemical composition of Areca fibre.

5 Experimental Design

The SMA mixtures were prepared using PMB 64-10 and VG-30 with 5.0, 5.5, 6.0, 6.5 and 7.0% bitumen by weight of dry aggregates. When VG-30 bitumen was used, Areca fibre was used as the stabilising additive to control the draindown. The asphalt

Table 4 Properties of PMB 64-10 bitumen

Test	Results	Requirements as per IS:15462 [17]
Softening point (R and B), °C, Min	64	45 °C
Viscosity at 150 °C, Pa.s, Max	0.9	1.2
Flash point (Cleveland open cup), °C, Min	241	230 °C
Elastic recovery of half thread in ductilometer at 15 °C, per cent, Min	77	70
Separation difference in softening point (R and B), °C, Max	1.8	3 °C
<i>Tests on residue from rolling thin film oven test</i>		
Loss in mass, per cent, Max	0.54	1.0
Specific gravity	1.01	–

Table 5 Requirements of SMA [16]

Mix design parameters	Requirements
Air voids, %	4.0
Bitumen content, %	5.8 min
Voids in mineral aggregate (VMA), %	17 min
Voids in the coarse aggregates mix (VCA _{MIX}), %	Less than VCA in the dry rodded condition, (VCA _{DRC})
Asphalt draindown, %	0.3 max
Tensile Strength Ratio (TSR), %	85 min

Fig. 2 Areca fibre

Table 6 Physical properties of Areca fibre [37]

Fibre properties	Values
Fibre diameter (mm)	0.45–0.55
Fibre length (mm)	55–70
Density (g/cm ³)	0.34
Tensile strength (MPa)	166.03
Young's modulus (MPa)	1381.31
Elongation at break (%)	23.21

Table 7 Chemical composition of Areca fibre [35]

Areca fibre	Lignin (%)	Hemi-cellulose (%)	Ash content (%)
	13–24.8	35–64.8	4.4

mixture properties were determined based on the Superpave mix design using the Superpave Gyrotory Compactor. The cylindrical specimens having a diameter of 100 mm were chosen based on the NMAS requirements mentioned in Superpave series No. 2 (SP-02) [2]. The number of gyrations selected for the present study ($N_{des} = 100$) is based on the criteria of Superpave mix design for medium to high traffic levels. For any SMA mixture, it is important to have VCA_{mix} (Voids in the coarse aggregate in the mixture) lesser than the VCA_{DRC} (Voids in the coarse aggregate in the dry rodded condition) to ensure proper stone-to-stone which confirms the presence of aggregate skeleton [10]. The voids in the coarse aggregates in the dry rodded condition and mixture were determined using ASTM C 29 [3]. The Optimum Bitumen Content (OBC) was determined corresponding to 4% air voids and a minimum void in the mineral aggregates (VMA) of 17% in accordance with IRC SP 79 [16]. All the specimens were then prepared at OBC. The specimens were then compacted at OBC in Superpave Gyrotory Compactor by providing 100 gyrations by maintaining the ram pressure, ram angle and the rate of gyrations at 600 kPa, 1.25° and 30 rpm, respectively. The volumetrics of the mixture such as air voids (V_a), voids in mineral aggregates (VMA), Voids filled with bitumen (VFB), bulk specific gravity (G_{mb}) and theoretical maximum density (G_{mm}) were determined. Then, the various mechanical properties of the mixture such as resistance to rutting using a laboratory wheel rut shaper, resistance to moisture-induced damage using the modified Lottman test, fatigue properties, and Marshall properties such as stability and flow were evaluated.

5.1 Draindown Test

The draindown test was conducted in accordance with ASTM D 6390 [5] for both SMA-PMB and SMA-AF mixtures. The test was conducted at a bitumen content of

7% and temperatures of 160 °C and 170 °C, respectively. The maximum allowable draindown as per IRC SP 79 [16] is 0.3%. The draindown observed for the mixture SMA-PMB was 0.16%. For the SMA-AF mixture, the fibre content was optimised based on the draindown values. The draindown test was conducted at 0.3, 0.2 and 0.15% fibre content by weight of the mixture. The draindown values obtained were 0.04%, 0.10% and 0.18%, respectively. There was a reduction in the draindown with an increase in the stabilising additive, which may be because higher OBC allows the binder to flow, and the addition of stabilising additive reduces the draindown characteristics of the SMA mixture [32]. It was also observed that the workability of the mixture reduced with an increase in fibre content. The fibres tended to flock together, and achieving a uniform distribution of fibre in the mixture was difficult. Hence, the optimum fibre content for SMA-AF mixtures was fixed as 0.15%, corresponding to an approximate draindown value of 0.20%.

5.2 Volumetric and Marshall Properties

To determine the volumetric properties of the prepared cylindrical specimens, their dimensions, mass in air and water were recorded. Table 8 gives the volumetrics of both the mixtures at OBC.

The G_{mm} values determined as per [4] using the asphalt mixture density tester in the loose state for SMA-PMB and SMA-AF mixtures were 2.431–2.508 g/cm³ and 2.405–2.476 g/cm³, respectively. The G_{mb} values for SMA-PMB and SMA-AF mixtures varied between 2.352–2.369 g/cm³ and 2.312–2.345 g/cm³, respectively. The Marshall stability test was conducted as per ASTM D 6927 [5] and the stability values obtained for SMA-PMB and SMA-AF which were 15.92–19.51 kN and 11.54–13.52 kN, respectively. The VMA values for both the mixes were above 17%, and the ratio of VCA_{mix} to VCA_{DRC} was less than one for all the bitumen contents. The OBC obtained at 4% air voids for SMA-PMB and SMA-AF are 6.05%

Table 8 Volumetrics and Marshall properties

Property of the mix	Mixture ID	
	SMA-PMB	SMA-AF
G_{mm} (g/cm ³)	2.469	2.447
G_{mb} (g/cm ³)	2.369	2.345
VMA (%)	18.12	18.10
VFB (%)	77.65	76.97
MS (kN)	19.51	13.52
VCA_{mix}	38.459	37.654
VCA_{mix}/VCA_{DRC}	0.93	0.91
OBC (%)	6.05	6.15

Table 9 Indirect tensile strength

SMA mix	IDT (MPa)		TSR (%)
	Unconditioned	Conditioned	
SMA-PMB	1.125	1.029	91.45
SMA-AF	0.676	0.601	88.90

and 6.15%, respectively, which were higher than 5.8% [16]. The higher OBC obtained for SMA-AF may be because of the absorption of bitumen by Areca fibres.

5.3 Indirect Tensile Strength

To determine the tensile strength ratio (TSR), indirect tensile strength (IDT) test was conducted as per ASTM D 6931 [7] on two sets of three cylindrical specimens each. One set of specimens called the unconditioned specimens was tested without any conditioning while the second set of samples called the conditioned specimens were subjected to a freeze–thaw cycle by placing them in a freezer maintained at -15 ± 3 °C for 16 h and then transferred to a hot water bath maintained at 60 °C for 24 h. Then, both sets of specimens were tested for their IDT at 25 °C. The ratio of the IDT values of the conditioned to unconditioned specimens cast at 7% air voids was computed to evaluate the TSR as per AASHTO T 283 [1], which is a measure of resistance to moisture-induced damage (Table 9).

5.4 Rutting Characteristics

Rutting or permanent deformation is the accumulation of unrecoverable strain in lesser magnitudes due to heavy wheel loads applied on pavements during their service life. The rutting characteristics of SMA mixtures were evaluated in the laboratory using Wheel Rut Tester (WRT). Slab specimens of $300 \times 300 \times 50$ mm were prepared at an air void of 7% (93% of G_{mm} , theoretical maximum density at OBC) in the Wheel Rut Shaper. The prepared slab was then conditioned at 60 °C in WRT for 6 h. WRT consists of a small wheel that moves back and forth on the slab specimen, which causes rutting. The wheel load, contact pressure and loading rate were 150 N, 700 kPa and 42 passes per minute. The test was conducted at 60 °C in dry condition, and the failure criteria for rutting is 6 mm [20]. The depth of rutting after 10,000 passes was noted. The permanent deformation noted for the SMA-PMB mixture was 4.0 mm compared to 4.9 mm for the mixture SMA-AF as shown in Fig. 3. It can be observed that though SMA-AF had higher rut depth than that of SMA-PMB, its performance was still satisfactory.

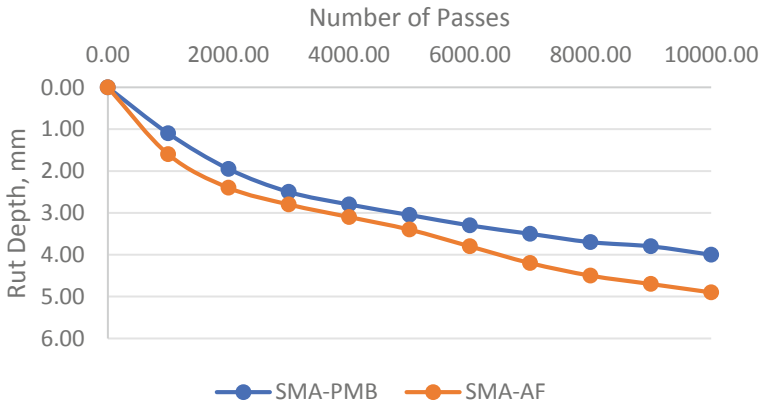


Fig. 3 Rutting characteristics of SMA mixtures

5.5 Fatigue Behaviour

One of the primary reasons for the failure of bituminous pavements is the repeated application of wheel loads during service life. The fatigue behaviour of SMA mixtures was determined in the laboratory using a Repeated Load Testing device by subjecting the prepared cylindrical samples to repeated loading. The load is applied through a hydraulic shaft in a half-sine wave pattern with a frequency of 1 Hz and a rest period of 0.9 s. The specimens were regarded to have failed when the deformation was 5 mm. The number of load repetitions required for the failure of specimens was considered as the fatigue life. The prepared cylindrical specimens were tested at three stress levels of 15, 33 and 50% of the lowest failure load obtained while determining the IDT of both the mixes. From Table 10 and Fig. 4, it can be seen that SMA-PMB performed better compared to SMA-AF. With an increase in stress levels, the fatigue life of both the mixes is reduced.

Table 10 Fatigue characteristics

SMA mix	Applied stress (%)	Applied load (Kg)	Fatigue life, No. of cycles
SMA-PMB	17.2	137.20	13,371
	36.1	287.96	7249
	53.2	424.36	3782
SMA-AF	13.2	105.29	10,623
	31.2	248.87	5232
	47.1	375.70	2129

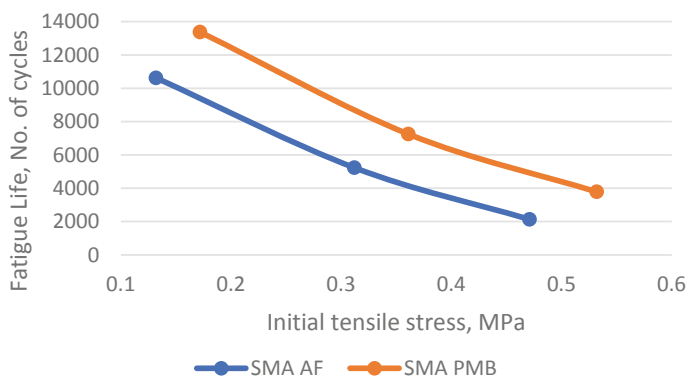


Fig. 4 Fatigue characteristics of SMA mixtures

6 Conclusions and Scope for Further Study

From the laboratory investigation, the following conclusions can be made after performing various mechanical tests on both the SMA mixes:

- The draindown values of the mixtures SMA-PMB and SMA-AF were 0.16 and 0.18% at an optimum fibre content of 0.15%, respectively. Hence, the Areca fibre used as stabilising additive was effective in controlling the draindown.
- The bulk densities obtained for SMA-PMB were slightly higher compared to the mix with stabilising additive.
- Though the IDT values of the SMA-AF mixture were lesser than the SMA-PMB mixture, the minimum requirement of Tensile Strength Ratio was satisfied in both cases. The lower IDT value for the SMA-AF mixture may be because of the ‘flocking’ of the fibres in the mixture which did not form a proper network in the mixture.
- Both the mixtures performed satisfactorily in the rutting test. The mixture SMA-PMB had better resistance to rutting with 4.0 mm compared to 4.9 mm deformation for SMA-AF mixture, respectively.
- The fatigue resistance of SMA-PMB was higher than the mixture with stabilising additive at all three stress levels.
- However, the workability of the SMA-AF mixture was lower, and the fibres tended to flock together while mixing with the aggregates, which may be because the Areca fibres used were not processed to a specific length.

To overcome the problem of workability of SMA-AF mixtures, the Areca fibres can be processed to specific lengths, and their effect on mechanical properties can be evaluated in the laboratory.

References

1. AASHTO T 283 (2014) Standard method of test for resistance of compacted asphalt mixtures to moisture-induced damage. Standard by American Association of State and Highway Transportation Officials, Washington DC, USA
2. Asphalt Institute (2001) Superpave mix design. Superpave Series No. 2 (SP-02). Asphalt Institute, Lexington
3. ASTM C29/C29M-17a (2017) Standard test method for bulk density (“unit weight”) and voids in aggregate. ASTM International, West Conshohocken, PA. https://doi.org/10.1520/C0029_C0029M-17A
4. ASTM D2041/D2041M-19 (2019) Standard test method for theoretical maximum specific gravity and density of asphalt mixtures. ASTM International, West Conshohocken, PA. https://doi.org/10.1520/D2041_D2041M-19
5. ASTM D6390-19 (2017) Standard test method for determination of draindown characteristics in uncompacted asphalt mixtures. ASTM International, West Conshohocken, PA. <https://doi.org/10.1520/D6930-19>
6. ASTM D6927-15 (2015) Standard test method for Marshall stability and flow of asphalt mixtures. ASTM International, West Conshohocken, PA. <https://doi.org/10.1520/D6927-15>
7. ASTM D6931-17 (2017) Standard test method for indirect tensile (IDT) strength of asphalt mixtures. ASTM International, West Conshohocken, PA. <https://doi.org/10.1520/D6931-17>
8. Bari J, Witczak MW (2005) Evaluation of the effect of lime modification on the dynamic modulus stiffness of hot-mix asphalt: use with the new mechanistic-empirical pavement design guide. *Transp Res Rec* 10–19. <https://doi.org/10.3141/1929-02>
9. Brown ER (1992) Experiences with stone matrix asphalt in the United States. US 4
10. Brown ER, Haddock JE (1997) Method to ensure stone-on-stone contact in stone matrix asphalt paving mixtures. *Transp Res Rec* 11–18. <https://doi.org/10.3141/1583-02>
11. Brown ER, Mallick R, Haddock J, Bukowski J (1997) Performance of stone matrix asphalt (SMA) mixtures in the United States. *J Assoc Asphalt Paving Technol* 66:426–457
12. Brulé B (1996) Polymer-modified asphalt cements used in the road construction industry: basic principles. *Transp Res Rec* 48–53. <https://doi.org/10.3141/1535-07>
13. Dalhat MA, Osman SA, Alhuraish AAA, Almarshad FK, Qarwan SA, Adesina AY (2020) Chicken feather fiber modified hot mix asphalt concrete: rutting performance, durability, mechanical and volumetric properties. *Constr Build Mater* 239:117849. <https://doi.org/10.1016/j.conbuildmat.2019.117849>
14. Deshmukh PS, Patil PG, Shahare PU, Bhanage GB, Dhekale JS, Dhande KG, Aware VV (2019) Effect of mechanical and chemical treatments of arecanut (areca catechu L.) fruit husk on husk and its fibre. *Waste Manage* 95:458–465. <https://doi.org/10.1016/j.wasman.2019.06.026>
15. do Vale AC, Casagrande MDT, Soares JB (2014) Behavior of natural fiber in stone matrix asphalt mixtures using two design methods. *J Mater Civ Eng* 26:457–465. [https://doi.org/10.1061/\(asce\)mt.1943-5533.0000815](https://doi.org/10.1061/(asce)mt.1943-5533.0000815)
16. IRC SP 79 (2008) Tentative specifications for stone matrix asphalt. Special Publication of Indian Roads Congress, IRC, New Delhi, India
17. IS 15462 (2019) Polymer modified specification (PMB)—specification, 1st Rev. Indian Standards Institution, New Delhi, India
18. IS 73 (2013) Paving bitumen specifications, 4th Rev. Indian Standards Institution, New Delhi, India
19. Kaleemullah S, Gunasekar JJ (2002) Moisture-dependent physical properties of arecanut kernels. *Biosys Eng* 82:331–338. <https://doi.org/10.1006/bioe.2002.0079>
20. Kandhal P, Cooley L (2003). Accelerated laboratory rutting tests: evaluation of the asphalt pavement analyser. National Cooperative Highway Research Program, NCHRP Report 508
21. Kar D, Giri JP, Panda M (2019) Performance evaluation of bituminous paving mixes containing sisal fiber as an additive. *Transp Infrastruct Geotechnol*. <https://doi.org/10.1007/s40515-019-00079-6>

22. Kumar GS, Shankar AUR, Teja BVSR (2019) Laboratory evaluation of SMA mixtures made with polymer-modified bitumen and stabilizing additives, 31, 1–9. [https://doi.org/10.1061/\(ASCE\)MT.1943-5533.0002652](https://doi.org/10.1061/(ASCE)MT.1943-5533.0002652)
23. Kumar P, Sikdar PK, Bose S, Chandra S (2004) Use of jute fibre in stone matrix asphalt. *Road Mater Pavement Des* 5:239–249. <https://doi.org/10.1080/14680629.2004.9689971>
24. Liu J, Li Z, Chen H, Guan B, Liu K (2020) Investigation of cotton straw fibers for asphalt mixtures. *J Mater Civ Eng* 32:1–9. [https://doi.org/10.1061/\(ASCE\)MT.1943-5533.0003181](https://doi.org/10.1061/(ASCE)MT.1943-5533.0003181)
25. Loganathan TM, Sultan MTH, Jawaid M, Md Shah AU, Ahsan Q, Mariapan M, bin Majid MSA (2020) Physical, thermal and mechanical properties of areca fibre reinforced polymer composites—an overview. *J Bionic Eng* 17:185–205. <https://doi.org/10.1007/s42235-020-0015-6>
26. Mohammad LN, Abadie C, Gokmen R, Puppala AJ (2000) Mechanistic evaluation of hydrated lime in hot-mix asphalt mixtures. *Transp Res Rec* 26–36
27. National Horticulture Board (2018) Area and production of horticulture crops: All India
28. Nejad FM, Aflaki E, Mohammadi MA (2010) Fatigue behavior of SMA and HMA mixtures. *Constr Build Mater* 24:1158–1165. <https://doi.org/10.1016/j.conbuildmat.2009.12.025>
29. Oda S, Leomar Fernandes J, Ildefonso JS (2012) Analysis of use of natural fibers and asphalt rubber binder in discontinuous asphalt mixtures. *Constr Build Mater* 26:13–20. <https://doi.org/10.1016/j.conbuildmat.2011.06.030>
30. Putman BJ, Amirkhanian SN (2004) Utilization of waste fibers in stone matrix asphalt mixtures. *Resour Conserv Recycl* 42:265–274. <https://doi.org/10.1016/j.resconrec.2004.04.005>
31. Richardson JTG (1999). Science lecture papers series stone mastic asphalt in the UK, pp 1–10
32. Sarang G, Lekha BM, Krishna G, Ravi Shankar AU (2016) Comparison of stone matrix asphalt mixtures with polymer-modified bitumen and shredded waste plastics. *Road Mater Pavement Des* 17:933–945. <https://doi.org/10.1080/14680629.2015.1124799>
33. Sheng Y, Li H, Guo P, Zhao G, Chen H, Xiong R (2017) Effect of fibers on mixture design of stone matrix asphalt. *Appl Sci (Switzerland)* 7. <https://doi.org/10.3390/APP7030297>
34. Shiva Kumar G, Shankar AURR, Ravi Teja BVS (2019) Laboratory evaluation of SMA mixtures made with polymer-modified Bitumen and stabilizing additives. *J Mater Civ Eng* 31:1–9. [https://doi.org/10.1061/\(ASCE\)MT.1943-5533.0002652](https://doi.org/10.1061/(ASCE)MT.1943-5533.0002652)
35. Swamy RP, Kumar GCM, Vrushabhendrapa Y, Joseph V (2004) Study of areca-reinforced phenol formaldehyde composites. *J Reinf Plast Compos* 23:1373–1382. <https://doi.org/10.1177/0731684404037049>
36. Xue Y, Hou H, Zhu S, Zha J (2009) Utilization of municipal solid waste incineration ash in stone mastic asphalt mixture: pavement performance and environmental impact. *Constr Build Mater* 23:989–996. <https://doi.org/10.1016/j.conbuildmat.2008.05.009>
37. Yusriah L, Sapuan SM, Zainudin ES, Mariatti M (2014) Characterization of physical, mechanical, thermal and morphological properties of agro-waste betel nut (Areca catechu) husk fibre. *J Clean Prod* 72:174–180. <https://doi.org/10.1016/j.jclepro.2014.02.025>

Linear Viscoelastic Limits for Aged and Unaged Bitumen



T. Srikanth and A. Padmarekha

Abstract The bitumen exhibits linear or nonlinear behavior, and the linear limit for loading is expected to vary with frequency, aging condition, and temperature of the material. The material characteristics such as dynamic modulus and phase lag can be meaningfully measured only when tested in a linear regime. This paper attempts to delineate the linear and nonlinear characteristics of the unaged and long-term aged bitumen under different test conditions. Two different binders of VG10 and VG30 grade as per IS73, 2018, were used to identify the linear and nonlinear behavior of bitumen material in the temperature range of 20–60 °C. Oscillatory shearing was applied to all the material using the dynamic shear rheometer. The strain amplitude during shear was linearly ramped from 0.01 to 15% at a rate of 0.01% s⁻¹, and the test was performed at 1, 5, and, 10 Hz frequency. The test was performed at different temperatures of 20, 30, 40, 50, and 60 °C. The linear and nonlinear limits were established based on dynamic modulus and torque. The linear viscoelastic limits were found to vary with the aging condition, frequency, and temperature of the test. The linear limit established from torque derivative was found to be on the lower side when compared with ASTM D7175, 2015 test protocol based on dynamic modulus.

Keywords Aging · Oscillatory shearing · Amplitude sweep · Linear viscoelastic behavior · Dynamic modulus

1 Introduction

The behavior of the binder is very sensitive with the temperature changes. In the pavement applications, the binder is subjected to different temperature ranges. The temperature of the pavement in India differs from -10 °C to 70 °C based on the location and the period time during the year [10]. The characteristic viscoelastic material functions that are commonly used are dynamic modulus (DM), phase lag (PA), loss modulus (LM), and storage modulus (SM). These functions are determined

T. Srikanth · A. Padmarekha (✉)
Department of Civil Engineering, SRM IST, Chennai, India
e-mail: padmarekha@srmist.edu.in

© The Author(s), under exclusive license to Springer Nature Singapore Pte Ltd. 2023
M. V. L. R. Anjaneyulu et al. (eds.), *Recent Advances in Transportation Systems Engineering and Management*, Lecture Notes in Civil Engineering 261,
https://doi.org/10.1007/978-981-19-2273-2_19

275

in linear viscoelastic (LVE) conditions. Hence, the rheological measurements must be made within the LVE response region. Among the LVE region, the connection between stress and strain is prompted simply through loading time and frequency and no longer through the significance of stress or strain [8].

The viscoelasticity of materials can be divided into two categories: linear viscoelasticity and nonlinear viscoelasticity. It can be distinguished by creep tests at different stress levels. If the creep compliance curve is independent of the applied creep stress, that is, the creep strain is proportional to the creep stress, and the material is linearly viscoelastic; otherwise, the material is nonlinearly viscoelastic [7]. The LVE strain limits against tests temperature reduced with modification of bitumen (a mineral filler was added to the conventional bitumen). Though, a second significance of modifying conventional bitumen on mixing filler is an increase in stiffness. The decrease in the LVE strain limit is actually somewhat by the reason of the higher stiffness of the modified bitumen instead of solely through the modification process [5]. The traditionally the nature of bitumen may be defined with respect to theoretical deformation throughout a wide variety of stress rates, stresses, and temperatures. By adopting a grouping of consistent stress change check at excessive temperatures and consistent strain (creep) at low temperatures, allowed then to discover the tensile, shear brief, and compressive nature of traditional bitumen. They identified that traditional bitumen of fifty penetration grade possessed linear viscous technique at decrease strain degrees and power-regulation creep behavior at better strain degrees [6]. The linearity consequences indicated that for moderately engineered modified binders (softer traditional bitumen having optimum modifier content), there is no primary narrowing of the linear variety. The manner of plastomeric, modified, and unmodified binders validated a stress established LVE requirements among 2 and 6% at lower temperatures (better stiffness and intermediate to decrease phase angles) in conjunction with a stress established LVE standards among 1.5 and 7 kPa at higher temperatures (decrease stiffness and better section angle). The thermoplastic rubbers (SBS and PMBs) indicated, moreover the lower temperature strain criteria, a higher temperature (decrease stiffness) polymeric primarily based totally strain established LVE standards among 50 and 200%. The strain established LVE standards for the SBS PMBs at higher temperatures did translate to a narrowing of the linear variety and a lower withinside the linearity restricts above the variety had been the elastomeric polymer turned into dominant [1]. The LVE limits of Bituminous Concrete Mixture in AMPT. The gathered information became studied and boundaries of linear viscoelastic have been decided for each specific temperature and frequency with the aid of using great to linear scaling and superposition. In comparison, it became pronounced that the pressure amplitude values calculated making use of the present AASHTO protocols have been determined to be better than the linear pressure amplitude values which were decided the usage of the pressure sweep information [11].

This paper reports an experimental investigation that was conducted to delineate linear and nonlinear response of the material. As this linear–nonlinear behavior transition is expected to vary with aging condition, the investigation was conducted on unaged (UA) and long-term aged (LTA) samples. ASTM D7175 [4], recommends

Table 1 Basic properties of bitumen

S. No.	Characteristic properties	Measured value	
		VG10	VG30
1	Penetration at 25 °C, 5 s, 0.1 mm, 100 g	98.8	60.5
2	Kinematic viscosity at 135 °C, cSt	364.51	510.11
3	Absolute viscosity at 60 °C, Poises	1142.83	2677.02
4	Tests on residue of rolling thin film oven test: Ductility at 25 °C, cm Viscosity ratio at 60 °C	> 100 2.29	> 100 2.54
5	Performance grade (high temperature)	PG 64	PG 70

using DM to delineate linear and nonlinear responses. In this study, in addition to ASTM D7175 approach, the linear limits were also identified using torque resistance during shearing. The influence of frequency and the temperature on the linear viscoelastic limits was captured.

2 Materials and Methods

Two conventional bitumens of viscosity grade VG10 and VG30 as per IS 73 [9], were adopted in the present study. Table 1 indicates the basic characteristics of the bitumen. The material was subjected to short-term aging in the laboratory following ASTM D2872 [2] and further too long-term aging as per ASTM D6521 [3], and used further for testing.

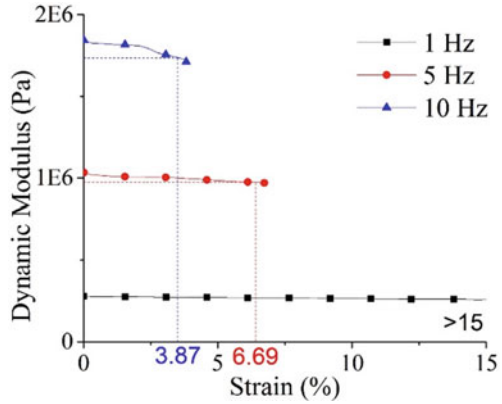
Oscillatory shearing was applied to all the material for a period of 1500 s using the DSR (Anton-Paar, MCR102 model). The strain amplitude during shearing was increased linearly from 0.01 to 15% at the rate of $0.01\% \text{ s}^{-1}$, and the test was conducted at frequencies of 1, 5, and 10 Hz. The tests were conducted at 20, 30, 40, 50, and 60 °C. Storage modulus, loss modulus, dynamic modulus, phase lag, and torque were collected from the conducted tests.

3 Results and Discussion

The 90% reduction of the initial dynamic modulus was identified as the linear viscoelastic limit [4]. Figure 1 shows to identify the LVE limit using DM for VG30 LTA at 40 °C, and from this figure, one can state that the LVE limit for 1, 5, and 10 Hz was > 15, 6.69, and 3.87% respectively. The same method was adopted to identify the LVE limit for all the temperatures, frequencies, and aging conditions.

The torque data was also collected, and it is well known that in amplitude sweep test, as strain increase linearly, the torque should also increase linearly, as binder

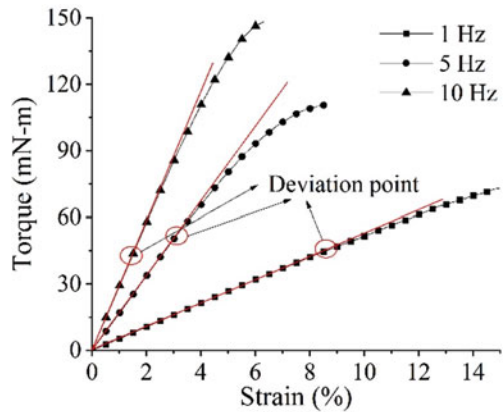
Fig. 1 LVE limits of VG30 LTA at 40 °C from DM



cannot withstand to higher strains at some point the linear increment of torque deviates, this indicates that the sample is about to fail, which can be seen in Fig. 2. One can say that the slope of torque for 1 Hz remains constant up to 9% strain and then deviates. Similarly, for 5 and 10 Hz, the slope remains constant till 3% and 2%, respectively. This deviation can easily identified by finding out the derivative of the torque as a function of strain. The derivative of torque was found for all the binders, temperatures, frequencies, and aging conditions, and from this data, the LVE limits were obtained.

Figures 3, 4, 5, and 6 show the variation in DM and derivative of torque concerning strain as a function of strain for UA and LTA aged of VG10 and VG30 binders respectively at 40 °C. Figure 6 shows the variation of SM, LM, and DM as a function of strain for VG30 LTA bitumen at 5 Hz of 20 and 60 °C, and from this figure, one can state that LM is more sensitive to strain at 20 °C and SM is more sensitive to strain at 60 °C.

Fig. 2 Torque of VG10 LTA at 40 °C



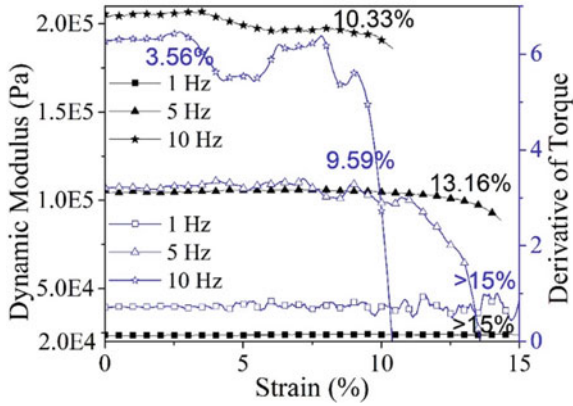


Fig. 3 LVE limits of VG10 UA at 40 °C

Fig. 4 LVE limits of VG30 UA at 40 °C

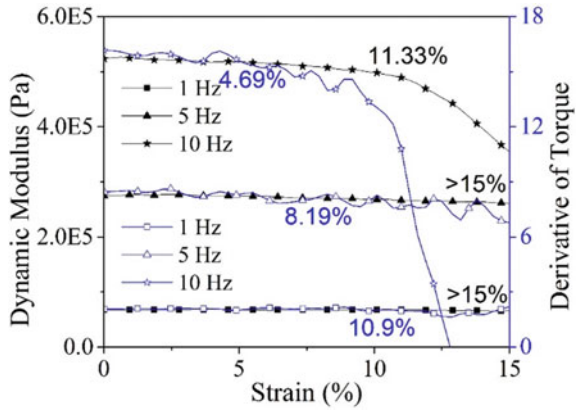


Fig. 5 LVE limits of VG10 LTA binder at 40 °C

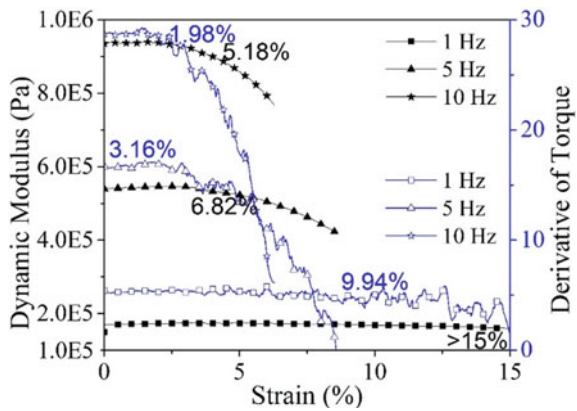


Fig. 6 LVE limits of VG30 LTA binder at 40 °C

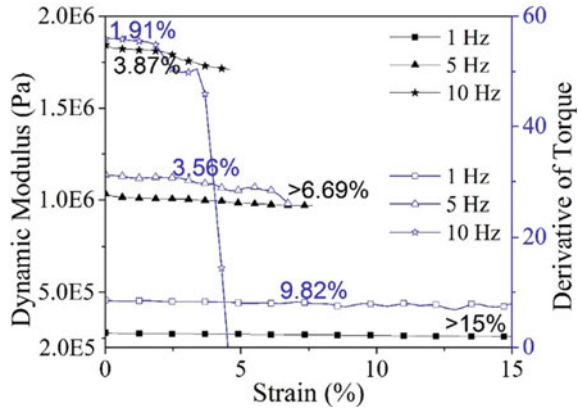


Figure 7 shows the variation of storage, loss, and dynamic modulus of VG30 LTA binder at 20 and 60 °C for 5 Hz frequency. From this figure, one can say that the DM is dependent on LM at intermediate temperatures, whereas as temperature increases, the DM is dependent on SM.

The LVE limit for UA and LTA aged of VG10 and VG30 binder at different temperatures and frequency is shown in Figs. 8, 9, 10, and 11, respectively, obtained from derivative of torque. It was also observed that the LVE limits were being decreased as the frequency is increased for both the binders and also for aging conditions. This indicates that LVE strain limits are dependent on frequency, the temperature of the test, and also the aging condition of the binder.

Table 2 gives the variation of linearity limits of VG10 and VG30 for the frequencies of 1, 5 and 10 Hz concerning torque and DM at different test temperatures.

The LVE limits obtained from DM show higher values when compared from limits obtained from torque. This variation was observed as in DM, the LVE limit was identified as the point where DM reduced to 90% of its first value as authorized by ASTM D7175 [4]. But, whereas from torque, the LVE limit was identified without any decrease in percentage.

Figure 12 shows the variation of DM as a function of strain and frequency. From this figure, one can say that as the frequency and the strain increase, the DM of the material increases, as expected. As the tests were performed for three frequencies, i.e. 1, 5 and 10 Hz, from this figure, one can predict the DM value other than the tested frequencies.

4 Conclusions

The linearity test was conducted for both VG10 and VG30 binders of UA and PAV at 20, 30, 40, 50, and 60 °C. It was observed that the linearity limit obtained from torque and dynamic modulus was not similar. The linear limit established from torque was

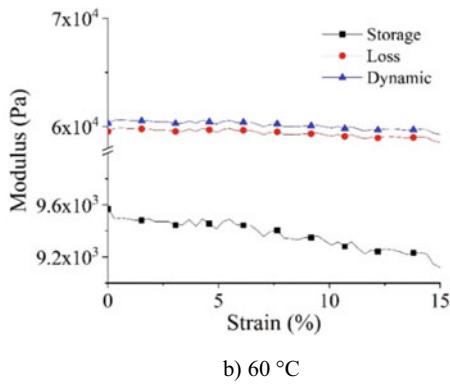
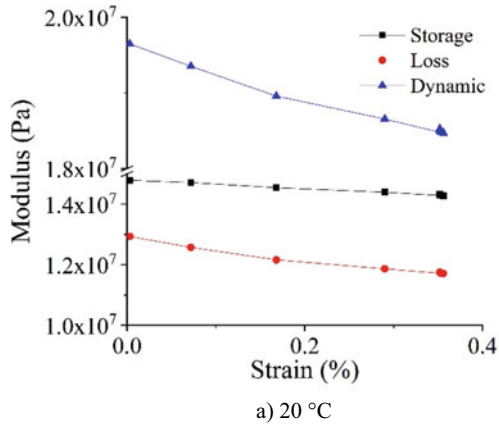
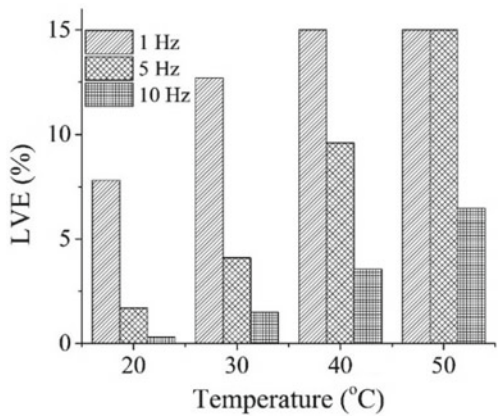


Fig. 7 Variation of modulus for VG30 LTA at 5 Hz **a** 20 °C, **b** 60 °C

Fig. 8 LVE limits of VG10 UA from derivative of torque



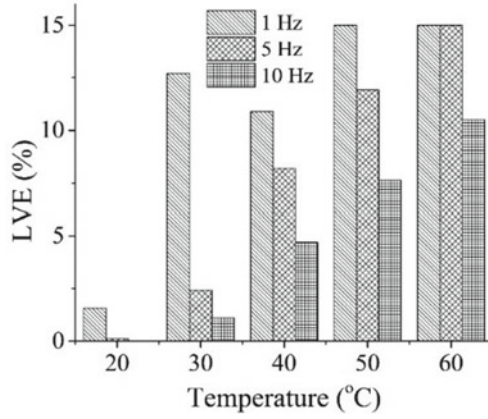


Fig. 9 LVE limits of VG30 UA from derivative of torque

Fig. 10 LVE limits of VG10 LTA binder from derivative of torque

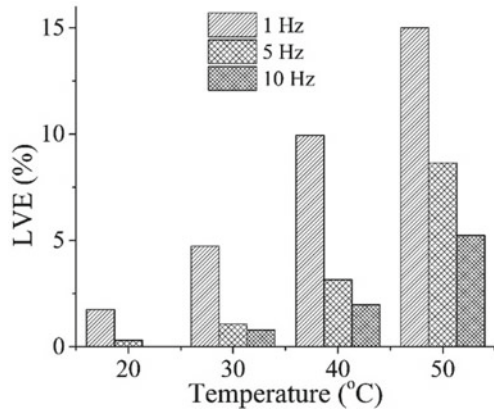


Fig. 11 LVE limits of VG30 LTA binder from derivative of torque

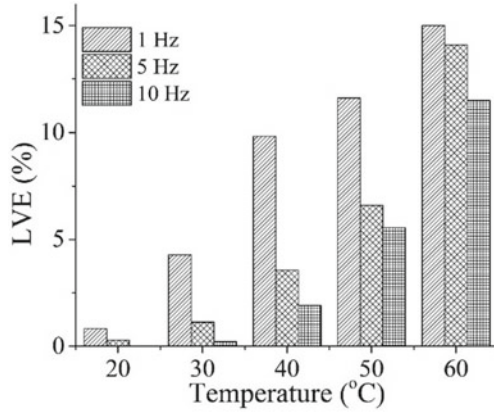
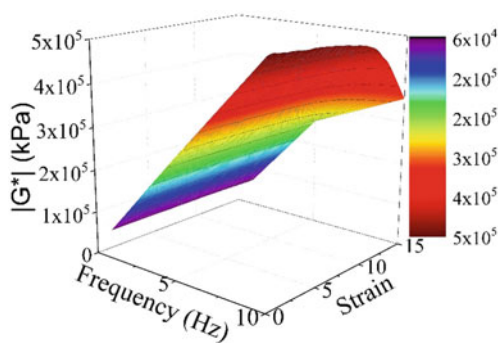


Table 2 Linear limit for different frequencies

Temperature (°C)	From torque			From dynamic modulus		
	Strain (%)					
	1 Hz	5 Hz	10 Hz	1 Hz	5 Hz	10 Hz
<i>VG10-Unaged binder</i>						
20	7.8	1.7	0.3	> 7.93	> 2.11	> 1.22
30	12.7	4.1	1.5	> 15	9.13	> 4.91
40	> 15	9.59	3.56	> 15	13.89	10.33
50	> 15	> 15	6.47	> 15	> 15	> 15
<i>VG10-Long-term aged binder (PAV)</i>						
20	1.75	0.31	0.02	> 1.78	0.56	0.34
30	4.73	1.07	0.79	8.59	3.71	1.92
40	9.94	3.16	1.98	> 15	6.82	5.18
50	> 15	8.65	5.24	> 15	11.04	7.91
<i>VG30-Unaged binder</i>						
20	1.57	0.11	0	2.0	0.41	0.15
30	12.7	2.42	1.11	> 15	> 4.34	2.21
40	10.9	8.19	4.69	> 15	> 15	11.33
50	> 15	11.91	7.62	> 15	> 15	> 15
60	> 15	> 15	10.5	> 15	> 15	> 15
<i>VG30-Long-term aged binder (PAV)</i>						
20	0.82	0.29	0	> 0.82	> 0.35	0.2
30	4.27	1.13	0.21	> 15	> 1.38	0.93
40	9.82	3.56	1.91	> 15	> 6.69	3.87
50	11.61	6.59	5.54	> 15	> 15	11.89
60	> 15	14.1	11.5	> 15	> 15	> 15

Note 1. Since the test was conducted until a 15% strain, the exact LVE limit could not be identified for a few temperatures
 2. At lower temperatures, the exact LVE limit could not be identified as the equipment torque capacity was reached

Fig. 12 Variation of DM for VG30 UA at 40 °C



found to be on the lower side when compared with dynamic modulus. The linear limit was found to vary with the aging of the binder, frequency, and temperature of the test. The LVE limits were found to be on the higher side for the lower frequency at a higher temperature. Hence, the critical condition for finding LVE has to be tested at low temperatures with higher frequency.

Acknowledgements The authors would really like to renowned the Science and Engineering Research Board (SERB) wing of Department of Science and Technology, New Delhi, India, for financial support (Project no: SERB/F/6157/2018-2019).

References

1. Airey GD, Rahimzadeh B, Collop AC (2002) Linear viscoelastic limits of bituminous binders. *Asphalt Paving Technol* 71:89–115
2. ASTM D2872 (2012) Standard test method for effect of heat and air on a moving film of asphalt (rolling thin-film oven test). American Society for Testing and Materials, West Conshohocken, PA, USA
3. ASTM D6521 (2019) Standard practice for accelerated aging of asphalt binder using a pressurized aging vessel (PAV). American Society for Testing and Materials, West Conshohocken, PA, USA
4. ASTM D7175 (2015) Standard test method for determining the rheological properties of asphalt binder using a dynamic shear rheometer. American Society for Testing and Materials, West Conshohocken, PA, USA
5. Bahia HU, Hislop WP, Zhai H, Rangel A (1998) Classification of asphalt binders into simple and complex binders. *J Assoc Asphalt Paving Technol* 67
6. Cheung CY, Cebon D (1997) Deformation mechanisms of pure bitumen. *J Mater Civ Eng* 9(3):117–129
7. Christensen R (2012) *Theory of viscoelasticity: an introduction*. Elsevier
8. Ferry JD (1980) *Viscoelastic properties of polymers*, 3rd ed. Wiley, New York
9. IS 73 (2018) *Paving bitumen-specification*, 4th Rev. Bureau of Indian Standards, New Delhi, India
10. Nivitha MR, Krishnan JM (2014) Development of pavement temperature contours for India. *J Inst Eng (India) Ser A* 95(2):83–90
11. Tejaswi P, Fatima J, Padmarekha A, Krishnan JM (2013) Linear viscoelastic limits for determination of dynamic modulus of bituminous concrete mixture in AMPT. In: *Airfield and highway pavement 2013: sustainable and efficient pavements*, pp 1100–1111

Evaluation of Mechanical Properties of Rigid Pavement with High RAP Content



M. K. Diptikanta Rout, Sabyasachi Biswas, and Abdhesh Kumar Sinha

Abstract In the recent period, major importance has been given for the development of concrete pavements rather than flexible pavements. These flexible pavements consist of more than 30–40% high quality aggregates which may be reused in the construction of new roads. Furthermore, due to the paucity of natural aggregates (NA) and environmentally friendly materials, reclaimed asphalt pavement (RAP) is frequently used as a substitute material for the construction of road. In this context, the aim of this study is also to define the optimum range of these RAPs as an alternative of the natural aggregate (NA) for sustainable pavement structures. In the present research, the different proportions of RAP content (coarse and fine) are about 25–50% of the natural aggregate that has been used in the concrete mix. Also, zirconia silica fume (ZSF) is used as an admixture that partially replaced the ordinary Portland cement (OPC) in the concrete mix. In this study, various proportions of ZSF (10, 20, 30 and 40%) were added for the improvement of the mechanical properties of rigid pavement. This experimental study investigated the performance of high RAP content and ZSF on compressive strength (CS), tensile strength (TS), flexural strength (FS), and water permeability of rigid pavement (RP). The experimental results indicate that the presence of ZSF improves the workability of the wet concrete mixes. However, excessive (more than 40% of the natural aggregate) use of RAP reduces the CS and TS of concrete. The overall result indicates that the performance of 30% fine RAP with admixtures (ZSF) is better as compared to the virgin aggregate in the concrete mixes. The final results were statistically evaluated by two-way factor variance analysis (ANOVA).

M. K. Diptikanta Rout (✉) · S. Biswas · A. K. Sinha
Department of Civil Engineering, NIT Jamshedpur, Jamshedpur, India
e-mail: deepucivil525@gmail.com

S. Biswas
e-mail: sbiswas.ce@nitjsr.ac.in

A. K. Sinha
e-mail: aksinha.ce@nitjsr.ac.in

Keywords RAP · Rigid pavement · Sustainable pavement · Strength of concrete · ZSF · ANOVA

1 Introduction

Nowadays, a new strategy for sustainable road development is the exploitation of recycled asphalt pavement (RAP). Usability of RAP for cement concrete pavements generally gives a number of benefits including minimizing RAP disposal issues, lowering greenhouse gas emissions, reducing natural aggregates usage, saving transportation costs, etc [1]. So, in Indian conditions, sustainable rigid pavements are substantially economical, eco-friendly along with prioritizing a greater durability. Thus, construction of rigid pavements requires a large amount of virgin aggregates and high-cost recycled materials. As a result, the purpose of this study is to discuss the application of zirconia silica fume (ZSF) which can be utilized as a cement substitute and mixed with various combinations of RAP aggregates.

Reclaimed asphalt pavements (RAPs) are a good potential highway construction material. RAP is a general term for the removal or reprocessing of asphalt and aggregates including pavement components. When asphalt pavements are scraped for resurfacing, recleaning, or rehabilitation operations, these materials are formed. Because of the reduced usage of virgin resources, reclaimed asphalt pavement has become the new approach for sustainable development [2], whereas RAP is the milled or dismantled bituminous pavement material that has been removed for various maintenance and rehabilitation purposes [3]. Shi et al. [4] stated that incorporating RAP seems to have become a realistic option for highway engineers, and consequently, RAP is not only cost-effective but also meets the needs of sustainability and green technology. Silva et al. [5] concluded that the RAP is generated from demolished process and has been applied in flexible pavements for granular and surface courses. In order to distinguish between coarse and finer RAP fraction, RAP is normally fractionated by 4.75 mm sieve while RAP passing across 2.36 mm sieve considered as finer RAP [6, 7]. Sahdeo et al. [8] characterized the RAP by different aggregate gradation types into various proportion of water-to-cement ratio for construction of pervious concrete pavements (PCPs). However, Brand et al. [9] classified the reclaimed asphalt pavement in the three different (T^3) cementitious mix and recommended that RAP be in the development of concrete pavements to replace the traditional virgin aggregates by 50%, while Singh et al. [10] suggested that coarse natural aggregates be replaced entirely with 100% RAP in pavement quality concrete (PQC). Abraham et al. [11] found the alternative method for determining the durability, porosity, and mechanical features of high RAP content by mercury intrusion porosimetry (MIP) technique of cement mortar specimen. Debbarma et al. [12] showed that the performance of roller compacted concrete pavement (RCCP) mixes was enhanced by use of 50% of RAP contaminated dust from various agricultural and industrial resources and they also developed the durability and the mechanical properties of RCCP mixes. Aghaeipour et al. [13] mentioned that the durability

properties of RCCP also improved by adding up to 60% of ground granulated blast furnace slag (GGBFS) as the substitute of cement content along with the porosity, concrete permeability, and water absorption are frequently reduced at 40% of slag level. Erdam et al. [14] also demonstrated that the strength properties significantly increase with the addition of RAP as replacement of 100% waste recycled aggregates.

Fakhri et al. [15] observed that using silica fume (SF) as a partial replacement of Portland cement strengthened the durability and mechanical aspects of conventional concrete while also producing the calcium-silicate-hydrated paste in RAP concrete. Moreover, Debbarma et al. [16] observed that the introduction of various mineral admixtures, i.e., SF, fly ash (FA) and bagasse ash (BG) as Portland cement substitute might be improved the RAP-RCCP strength. Sahdeo et al. [17] also developed the mechanical and durability properties of pervious concrete pavements (PCP) by substituting natural aggregates with different fractions of coarse RAP and fine RAP. According to Gupta et al. [18], upto 15% of jarosite (extraction of zinc ore concentrate) may develop the strength characteristics of concrete pavements which could further be used to build low volume roads or village roads. As per the report by Saride et al. [19], the long-term performance and durability characteristics of RAP are related to the age hardening of the asphalt layer which functionally covers on RAP aggregates. Thomas et al. [20] suggested that upto 50% replacement by volume with RAP gives the appropriate pavement strength as that of virgin natural coarse aggregates for flexible pavement construction, while Nandi et al. [21] suggested that 100% coarse RAP can be used for the production of concrete paver blocks (CPB). However, Singh et al. said that the incorporating of higher amount of silica fume in concrete mix results the economic issues as well as superior strength attributes, whereas Siddique et al. mentioned that silica fume (SF) has been replaced Portland cement for production of cement concrete mixes/mortar due to its pozzolanic action [10, 22]. Singh et al. [23] identified that addition of fine RAP might significantly reduce the compressive strength as compared to the coarse aggregates in cement concrete pavements. Abraham et al. [24] experimentally concluded that the strength parameters of cement mortar mixes decrease as the fine RAP content increases in different curing ages and similar to the porosity of cement mortar mixes increases as the RAP content increases. Singh et al. [25] also explored that 50% RAP dust is suitable for the mechanical characteristics of concrete pavements by various separation processes. Debbarma et al. [26] suggested 50% of RAP aggregates are suitable for roller compacted concrete pavements and enrich the strength benchmark for pavements.

Moreover, Ibrahim et al. [27] and Mohmoud et al. [28] also recommended 50% of RAP is acceptable for the self-consolidating concrete (SSC) in place of conventional virgin aggregates. Kumari et al. [29] aimed to optimize the long-term qualities of RAP within the dense bituminous macadam (DBM) mixes around the RAP material. The study concluded that adding of RAP to warm mix asphalt (WMA) improves the resistance of aging and longevity in road construction. Dubey et al. [30] found that the moisture content is less susceptible than the fine RAP percentages affecting the strength characteristics of dry lean concrete (DLC) mixes by two-way analysis of variance (ANOVA). Hence, the use of RAP materials as a structurally sound

and environmental safe material for construction of rigid pavement is significantly supported by researchers [31].

So, the RAP which is used as the substitute of recycled aggregates is extracted from quarrying of conventional virgin aggregates. Hence more, utilization of RAP materials for concrete pavement applications may be able to alleviate a number of issues in day-to-day life. From the previous researchers, no study is available on the effect of ZSF admixtures on the RAP concrete pavements and its strength behavior in high RAP content. This study brings the attention of the practical use of RAP in concrete pavements and the application of ZSF in highway construction.

2 Research Objectives

According to the earlier studies, RAP is the viable material for the road construction, whereas the application of ZSF for inclusive RAP concrete has never been recognized. Finding the optimal content of RAP materials as a replacement for traditional aggregates along with evaluation of the various mechanical characteristics of rigid pavement with high RAP content is the prime goal of this work. This is also an approach to gain a deeper understanding of the literature to enhance the effectiveness of RAP in order to minimize the expenses while also protecting the environment.

Moreover, it also shows a link between the RAP physical qualities and natural virgin aggregate in the rigid pavement design as well as the effect of zirconia silica fume (ZSF) on long-term road sustainability. The result of this study intended to assist researchers in better understanding the behavior of RAP mixes including different concentrations of ZSFs, which could be essential in enhancing the sustainability of rigid pavement.

3 Materials and Mix Design

This current research attempts to develop the sustainability of concrete pavements. The different materials like natural aggregate (NA), RAP aggregates, ordinary Portland cement (OPC) grade 53 and ZSF admixtures are used for preparing the specimen. The Mix design criteria of rigid pavements are governed by Indian Road Congress (IRC): 44-2017 specifications [32]. For mix design, the water-to-cement (w/c) ratio of 0.46 was used.

3.1 Natural Aggregates (NA)

Natural coarse and fine aggregates from a local supplier have been gathered and conforms to IS:383-1970 [33]. Table 1 includes the basic combined properties of

Table 1 Basic properties of NA and RAP

Properties	NA	Coarse RAP	Fine RAP	Requirements as per IS 383 (BIS 2016 and MoRTH 2013) specification
Sp. Gravity	2.68	2.31	2.6	–
Water absorption in %	0.61	0.74	0.68	< 2
Density in kg/m ³	1671	1390	1549	–
Los Angles abrasion Value in %	20	13	12	< 35
Impact value in %	19	14	17	< 45

aggregates with a maximum specified size of 10 mm and natural fine aggregates of size 4.75 mm.

3.2 RAP Aggregates

For the current study, the RAP was obtained from the bituminous pavement in the district of Sareikela, Jharkhand, with a design life of 20 years. The collected RAP was the product of unregulated milling to generate a nominal aggregate size of 13 mm from the national highway. The researchers report that unregulated milling adds to the intermixing of dust particles from the underlying pavement layers [34] and large portions of soft asphaltic layers covered with RAP aggregates. To use these materials in the best possible way, separation of the aggregates from the agglomerations is required [35]. Therefore, RAP aggregates were then uniformly heated at 1100 °C for 40–50 min and fragmented by centrifuge extractor in the laboratory into individual aggregate.

3.3 Cement

In this analysis, 53 grade of ordinary Portland cement (OPC) was used and purchased from local supplier at Jamshedpur circle. Table 2 shows the required test results of cements as per the IS: 12269-2013 specifications.

3.4 Zirconia Silica Fume (ZSF)

Zirconia silica fume (ZSF) is a by-product of silicon metal or ferrosilicon alloys and consists of zirconium dioxide and zirconium oxide. The zirconia silica fume is

Table 2 Physical characteristics of cement grade 53

S. No.	Physical characteristics of cement	Outcomes	IS 12269-2013 specification
I	Specific gravity	3.15	3.10–3.15
II	Consistency (%)	28	30–35
III	Initial setting time	35 min	30 minimum
IV	Final setting time	178 min	600 maximum
V	Compressive strength-7 days	38.5 MPa	43 MPa
VI	Compressive strength-28 days	52.31 MPa	53 MPa
VII	Fineness	7%	5–9

Table 3 Chemical properties of ZSF

Component	SiO ₂	LOI	Al ₂ O ₃	Fe ₂ O ₃	CaO	MgO	K ₂ O	Na ₂ O	Al ₂ O ₂
Amount (%)	94	1.73	1.04	0.80	0.35	0.21	0.5	1.3	0.04

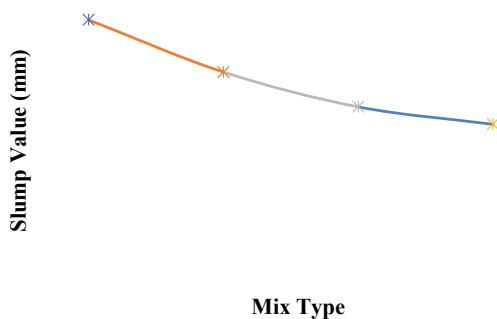
derived from zirconia compounds by fusion process in industry having fine granularity features. It is a powder form of white color in nature and characterized by a particle size less than 1 micron. Due to its high cementation qualities, filler properties, and environmental benefits, some industries in India have recently manufactured ZSF in a large scale. Table 3 shows the chemical properties of ZSF admixtures collected from the Chemical Enterprises Pvt. Ltd, Mumbai.

4 Experimental Program

The slump test cone method was used in laboratories to assess the workability of concrete mixes. On $15 \times 15 \times 15$ cm cubes, the compressive strength was examined for 7, 14, and 28 days of wet curing as per IS:516 [36]. At the very same stage of curing, the flexural intensity was estimated using a prism of $10 \times 10 \times 15$ cm specimen. The split tensile strength of cylindrical specimens, 10 cm in diameter and 20 cm in length were measured according to IS: 5816 [37]. The water permeability was checked after twenty-eight days of moist curing in comparison with a control mix by using ZSF as substitute admixtures.

Table 4 Various mix proportions of slump value

Mix	Sample	Slump value (mm)
Mix-1	25% RAP + 10% ZSF	32
Mix-2	25% RAP + 20% ZSF	26
Mix-3	50% RAP + 30% ZSF	22
Mix-4	50% RAP + 40% ZSF	20

Fig. 1 Fresh concrete properties of RAP-ZSF admixtures

5 Result and Discussions

5.1 Workability Test

The properties of a fresh concrete mix containing various combinations of RAP and ZSF admixtures are depicted in Table 4. The findings showed that the integration of RAP aggregate and ZSF reduced the initial workability of concrete. For contrast, the slump value of ZSF mix was 32 mm which was reduced slightly when 25% RAP aggregates were added where the slump value of 20 mm was seen as a further 50% of RAP aggregates. This result of the workability of fresh concrete is due to the combined influence of various shapes of RAP aggregates and water absorption present in sample. The water from the mixture was also absorbed due to hygroscopic nature of ZSF and the slump value was greatly reduced (Fig. 1).

5.2 Influence of ZSF Admixtures on Compressive Strength of RAP Base Concrete Pavement

Three cubes were tested at 7, 14, and 28 days of curing age to evaluate the CS of the different trial mix having 12 samples inclusive of ZSF admixtures.

Despite curing age, the compressive strength of concrete was found to decrease as the amount of RAP aggregates increased (Fig. 2). After 7 days of curing, the

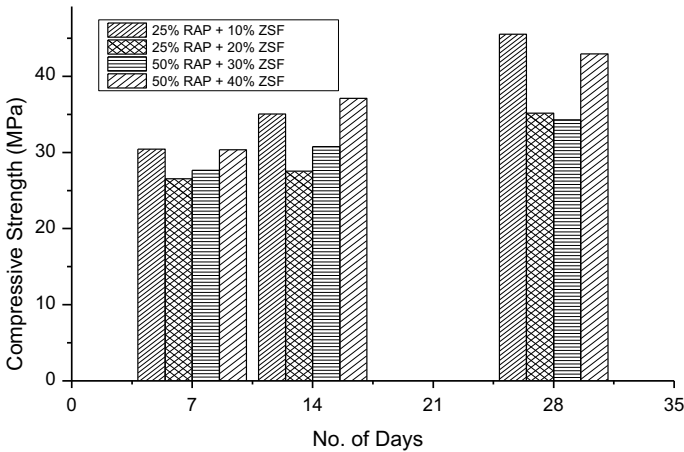


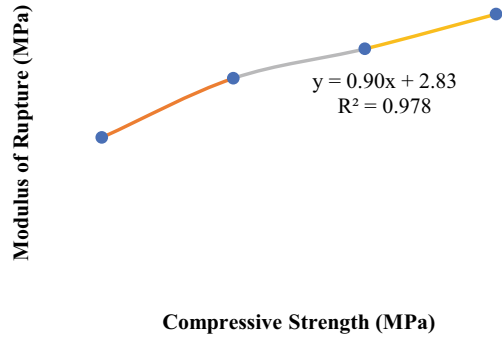
Fig. 2 Sensitivity of ZSF admixtures on compressive strength of RAP base RP

CS of various mixes is marginally reduced after incorporating the ZSF. Similarly, when 40% zirconia silica fume was replaced, the compressive strength of RAP was found as 37.11 Mpa at 14 days of curing period as compared to the control mix. At 28 days of curing, the additional incorporations were found to be around 43 Mpa. This reduction in CS values with various proportions of ZSF admixtures indicates the presence of asphalt coating on RAP.

5.3 Modulus of Rupture

There are many guidelines on the connection between CS and modulus of rupture of natural aggregates in concrete mix. The relation between the CS and modulus of rupture is represented as $f_r = 0.7 \times (f_{ck})^{0.5}$ by IS: 456-2000 specifications [38]. The RAP is performed in concrete pavements to predict a correlation among compressive strength, and rupture modulus has an equation of $f_r = P \times (f_{ck})^Q$ where the P and Q are the co-efficients obtained from the regression analysis [25, 39]. As it improved the strength performance, the rupture module values of various mix combinations are used to construct the concrete pavements. Figure 3 depicts a regression relationship involving the mechanical constraints like rupture modulus and compressive strength of reclaimed asphalt rigid pavements of curing time 28 days. The addition of RAP and ZSF admixtures results in a co-relation equation ($R^2 = 0.978$).

Fig. 3 Relationship between rupture modulus versus compressive strength of RAP base RP



5.4 Influence of ZSF Admixtures on Split Tensile Strength of RAP Base Concrete Pavement

Figure 4 depicts the impacts of splitting tensile strength at various curing days. The tensile strength of RAP tends to improve at 7 days of curing age. When 50% substitution rate of RAP drops to 25% of RAP, it reflected the lower strength compared to 14 and 28 days of curing time. These reductions of TS are due to the film bituminous material barrier around the RAP aggregate in the pavement. Therefore, this may be claimed that 30% RAP is a better result in the control mix and might greatly improve the concrete pavement.

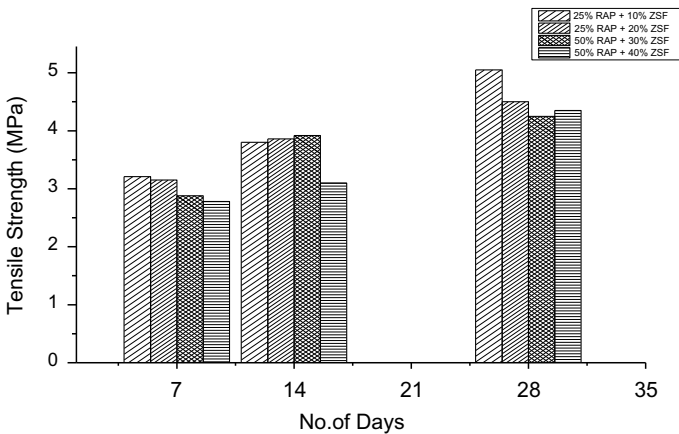


Fig. 4 Sensitivity of ZSF admixtures on tensile strength of RAP base concrete

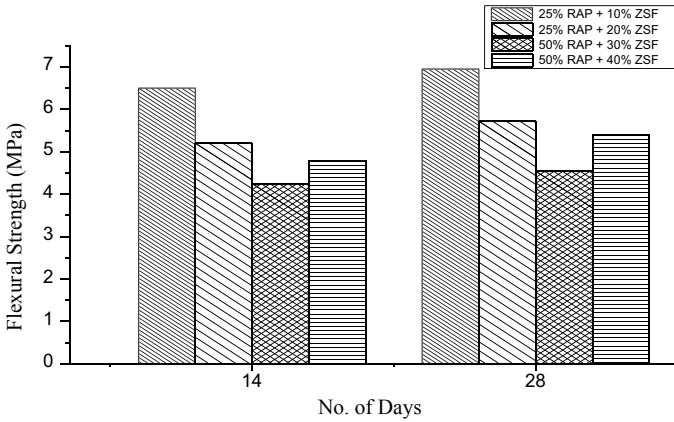


Fig. 5 Sensitivity of ZSF admixtures on flexural strength of RAP base RP

5.5 Influence of ZSF Admixtures on Flexural Strength of RAP Base Concrete Pavement

It can be a remark that from Fig. 5, the flexural intensity tends to reduce with increases in the fine RAP material. At 14 days of curing period, fine RAP replaced 20% of virgin aggregates resulting in a flexural strength of 5.2 Mpa, whereas 50% of replacement resulted in a slightly higher the flexural value of 5.4 Mpa. This 30% of fine control mix RAP is ideal for concrete pavements. Henceforth, the outcome is owing to optimize by using ZSF admixtures in the control mix.

5.6 Water Absorption

The effects of RAP aggregates and ZSF contribute to the toughened properties on the water absorption at 28 days of curing time. From Fig. 6, it has been observed that addition of RAP aggregates in concrete minimizes the water absorption. The permeable gaps in 30% of FRAP mix are responsible for this reduction. This is due to the formation of additional calcium silicate hydrate (C-S-H) gel by the reaction of hydrated substances with the reactive silica fume micropores.

6 Statistical Analysis

To examine the statistical detection of RAP percentages, ZSF proportions, and moisture content on different strength parameters of RAP profiles, a two-way analysis of

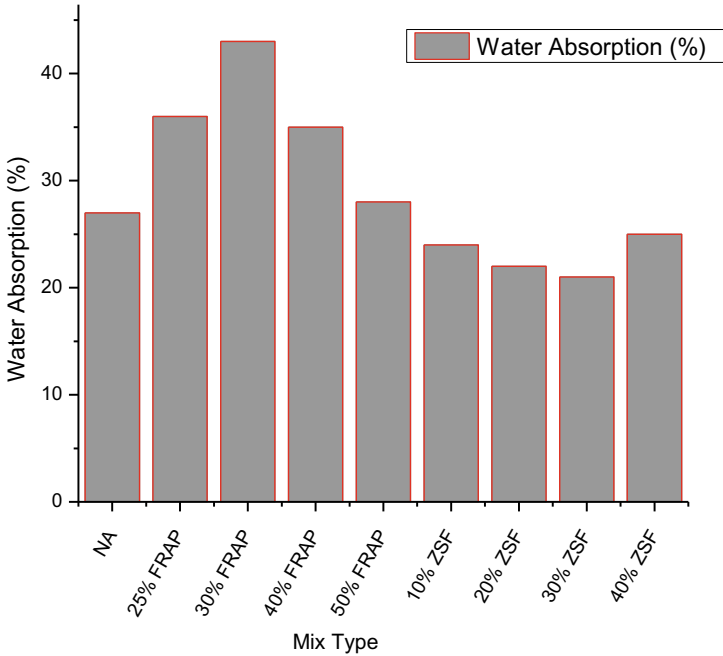


Fig. 6 Variation of water absorption properties in FRAP-ZSF mixes

variance (ANOVA) was used. Table 5 shows the summarized output of RAP fluctuation as compared to the ZSF proportions. It is clear that the F calculated $> F$ critical in case of RAP percentages while it comes to the similar results in case of ZSF mixes. So, the variation results show that the different parameters like moisture content, temperature, porosity, and strength criteria affected the RAP concrete pavements.

Table 5 Two-way analysis of variance (ANOVA) for statistical method

Property	Variation	SSq	Dof	MSq	F -calculated	P -value	F - critical
Compressive strength	RAP	1062.5	3	354.1667	17	0.021856	9.276628
	ZSF	312.5	1	312.5	15	0.030466	10.12796
	Error	62.5	3	20.8333	–	–	–
	Total	1437.5	7	–	–	–	–

Note SSq = Sum of Squares, Dof = Degrees of freedom, MSq = Mean square

7 Conclusions

The objective of this work is to check how the RAP aggregates affect the characteristics of concrete mixes. It is also improving the mechanical properties and sustainable solutions of RAP mix containing the different fractions of zirconia silica fume (ZSF). A total of 4 mixes were made and tested with various ratios of fine RAP along with ZSF. The workability of concrete paving can be decreased by substitution of virgin aggregates by RAP aggregates. Due to the presence of high dust and angular aggregates, the inclusion of fine RAP in concrete greatly decreased the original slump and density of fresh concrete. Moreover, it was noticed that upto 25% of fine NA could be substituted by fine RAP aggregates to achieve strength of 45.5 MPa with 10% ZSF admixtures, which is considered suitable for cement concrete pavement construction. There was a strong relationship ($R^2 > 0.978$) between modulus of rupture and estimated compressive strength values from the regression models. Similarly, over 40% of natural aggregates can diminish concrete pavement's tensile strength while increasing RAP's the flexural strength. So even though ZSF combines with RAP, the efficiency of concrete pavement improves when 30% of fine RAP is used. Thereby it can be inferred that the use of RAP in rigid pavement construction along with 30% of ZSF admixtures is ideal for sustainable approach. In addition to that, an ANOVA result also gives a better result for ZSF mixes for the construction of concrete pavements. However, moisture content was found to be less sensitive than RAP percentages imparting the strength properties. Henceforth, it remarked that RAP aggregate in rigid pavement construction with ZSF gives many technical benefits and environmentally friendly options at this current time.

References

1. Singh S, Ransinchung GDRN, Kumar P (2019) Feasibility study of RAP aggregates in cement concrete pavements. *Road Mater Pavement Des* 20:151–170. <https://doi.org/10.1080/14680629.2017.1380071>
2. Singh S, Ransinchung RNGD (2020) Laboratory and field evaluation of RAP for cement concrete pavements. *J Transp Eng Part B Pavements* 146:1–11. <https://doi.org/10.1061/JPEODX.0000162>
3. Taha R, Ali G, Basma A, Al-Turk O (1998) Evaluation of reclaimed asphalt pavement aggregate in road bases and subbases. *Transp Res Rec* 264–269
4. Shi X, Grasley Z, Hogancamp J, Brescia-Norambuena L, Mukhopadhyay A, Zollinger D (2020) Microstructural, mechanical, and shrinkage characteristics of cement mortar containing fine reclaimed asphalt pavement. *J Mater Civ Eng* 32:04020050. [https://doi.org/10.1061/\(asce\)mt.1943-5533.0003110](https://doi.org/10.1061/(asce)mt.1943-5533.0003110)
5. Silva RV, de Brito J, Dhir RK (2019) Use of recycled aggregates arising from construction and demolition waste in new construction applications. *J Clean Prod* 236:117629. <https://doi.org/10.1016/j.jclepro.2019.117629>
6. Shi X, Mukhopadhyay A, Liu KW (2017) Mix design formulation and evaluation of Portland cement concrete paving mixtures containing reclaimed asphalt pavement. *Constr Build Mater* 152:756–768. <https://doi.org/10.1016/j.conbuildmat.2017.06.174>

7. Papakonstantinou CG (2018) Resonant column testing on Portland cement concrete containing recycled asphalt pavement (RAP) aggregates. *Constr Build Mater* 173:419–428. <https://doi.org/10.1016/j.conbuildmat.2018.03.256>
8. Kant Sahdeo S, Ransinchung GD, Rahul KL, Debbarma S (2020) Effect of mix proportion on the structural and functional properties of pervious concrete paving mixtures. *Constr Build Mater* 255:119260. <https://doi.org/10.1016/j.conbuildmat.2020.119260>
9. Brand AS, Roesler JR (2016) Expansive and concrete properties of SFS–FRAP aggregates. *J Mater Civ Eng* 28:04015126. [https://doi.org/10.1061/\(asce\)mt.1943-5533.0001403](https://doi.org/10.1061/(asce)mt.1943-5533.0001403)
10. Singh S, Ransinchung GDRN, Monu K, Kumar P (2018) Laboratory investigation of RAP aggregates for dry lean concrete mixes. *Constr Build Mater* 166:808–816. <https://doi.org/10.1016/j.conbuildmat.2018.01.131>
11. Abraham SM, Ransinchung GD (2019) Effects of reclaimed asphalt pavement aggregates and mineral admixtures on pore structure, mechanical and durability properties of cement mortar. *Constr Build Mater* 216:202–213. <https://doi.org/10.1016/j.conbuildmat.2019.05.011>
12. Debbarma S, Ransinchung GD, Singh S, Sahdeo SK (2020) Utilization of industrial and agricultural wastes for productions of sustainable roller compacted concrete pavement mixes containing reclaimed asphalt pavement aggregates. *Resour Conserv Recycl* 152:104504. <https://doi.org/10.1016/j.resconrec.2019.104504>
13. Aghaeipour A, Madhkan M (2017) Effect of ground granulated blast furnace slag (GGBFS) on RCCP durability. *Constr Build Mater* 141:533–541. <https://doi.org/10.1016/j.conbuildmat.2017.03.019>
14. Erdem S, Blankson MA (2014) Environmental performance and mechanical analysis of concrete containing recycled asphalt pavement (RAP) and waste precast concrete as aggregate. *J Hazard Mater* 264:403–410. <https://doi.org/10.1016/j.jhazmat.2013.11.040>
15. Fakhri M, Saberik F (2016) The effect of waste rubber particles and silica fume on the mechanical properties of roller compacted concrete pavement. *J Clean Prod* 129:521–530. <https://doi.org/10.1016/j.jclepro.2016.04.017>
16. Debbarma S, Ransinchung G, Singh S (2020) Improving the properties of RAP–RCCP mixes by incorporating supplementary cementitious materials as part addition of Portland cement. *J Mater Civ Eng* 32:04020229. [https://doi.org/10.1061/\(asce\)mt.1943-5533.0003283](https://doi.org/10.1061/(asce)mt.1943-5533.0003283)
17. Sahdeo SK, Ransinchung G, Rahul KL, Debbarma S (2021) Reclaimed asphalt pavement as a substitution to natural coarse aggregate for the production of sustainable pervious concrete pavement mixes. *J Mater Civ Eng* 33:04020469. [https://doi.org/10.1061/\(asce\)mt.1943-5533.0003555](https://doi.org/10.1061/(asce)mt.1943-5533.0003555)
18. Gupta T, Sachdeva SN (2019) Investigations on Jarosite mixed cement concrete pavements. *Arab J Sci Eng* 44:8787–8797. <https://doi.org/10.1007/s13369-019-03801-1>
19. Avirmeni D, Peddinti PRT, Saride S (2016) Durability and long term performance of geopolymer stabilized reclaimed asphalt pavement base courses. *Constr Build Mater* 121:198–209. <https://doi.org/10.1016/j.conbuildmat.2016.05.162>
20. Thomas RJ, Fellows AJ, Sorensen AD (2018) Durability analysis of recycled asphalt pavement as partial coarse aggregate replacement in a high-strength concrete mixture. *J Mater Civ Eng* 30:04018061. [https://doi.org/10.1061/\(asce\)mt.1943-5533.0002262](https://doi.org/10.1061/(asce)mt.1943-5533.0002262)
21. Nandi S, Ransinchung GDRN (2021) Performance evaluation and sustainability assessment of precast concrete paver blocks containing coarse and fine RAP fractions: a comprehensive comparative study. *Constr Build Mater* 300
22. Siddique R, Chahal N (2011) Use of silicon and ferrosilicon industry by-products (silica fume) in cement paste and mortar. *Resour Conserv Recycl* 55:739–744. <https://doi.org/10.1016/j.resconrec.2011.03.004>
23. Singh S, Ransinchung GD, Debbarma S, Kumar P (2018) Utilization of reclaimed asphalt pavement aggregates containing waste from Sugarcane mill for production of concrete mixes. *J Clean Prod* 174:42–52. <https://doi.org/10.1016/j.jclepro.2017.10.179>
24. Abraham SM, Ransinchung GDRN (2018) Influence of RAP aggregates on strength, durability and porosity of cement mortar. *Constr Build Mater* 189:1105–1112. <https://doi.org/10.1016/j.conbuildmat.2018.09.069>

25. Singh S, Ransinchung GD, Kumar P (2017) Effect of mineral admixtures on fresh, mechanical and durability properties of RAP inclusive concrete. *Constr Build Mater* 156:19–27. <https://doi.org/10.1016/j.conbuildmat.2017.08.144>
26. Debbarma S, Ransinchung GDRN, Singh S (2019) Suitability of various supplementary cementitious admixtures for RAP inclusive RCCP mixes. *Int J Pavement Eng* 1–14. <https://doi.org/10.1080/10298436.2019.1703981>
27. Ibrahim A, Mahmoud E, Khodair Y, Patibandla VC (2014) Fresh, mechanical, and durability characteristics of self-consolidating concrete incorporating recycled asphalt pavements. *J Mater Civ Eng* 26:668–675. [https://doi.org/10.1061/\(asce\)mt.1943-5533.0000832](https://doi.org/10.1061/(asce)mt.1943-5533.0000832)
28. Mahmoud E, Ibrahim A, El-Chabib H, Patibandla VC (2013) Self-consolidating concrete incorporating high volume of fly ash, slag, and recycled asphalt pavement. *Int J Concr Struct Mater* 7:155–163. <https://doi.org/10.1007/s40069-013-0044-1>
29. Monu K, Ransinchung GD, Singh S (2019) Effect of long-term ageing on properties of RAP inclusive WMA mixes. *Constr Build Mater* 206:483–493. <https://doi.org/10.1016/j.conbuildmat.2019.02.087>
30. Dubey P, Paswan S, Sukhija M, Saboo N (2020) Assessing the effect of reclaimed asphalt pavement on mechanical properties of dry-lean concrete. *J Mater Civ Eng* 32:04020348. [https://doi.org/10.1061/\(asce\)mt.1943-5533.0003434](https://doi.org/10.1061/(asce)mt.1943-5533.0003434)
31. Park T (2003) Application of construction and building debris as base and subbase materials in rigid pavement. *J Transp Eng* 129:558–563. [https://doi.org/10.1061/\(ASCE\)0733-947X\(2003\)129:5\(558\)](https://doi.org/10.1061/(ASCE)0733-947X(2003)129:5(558))
32. IRC 44 (2017) Guidelines for cement concrete mix design for pavements. Indian Roads Congress, pp 1–60
33. B. of I.S. (BIS), IS 383 (1970) 1970 Specification for coarse and fine aggregates from natural sources for concrete. Indian Standards, pp 1–24
34. Kumari M, Ransinchung GDRN, Singh S (2018) A laboratory investigation on dense bituminous Macadam containing different fractions of coarse and fine RAP. *Constr Build Mater* 191:655–666. <https://doi.org/10.1016/j.conbuildmat.2018.10.017>
35. Singh S, Shintre D, Ransinchung GDRN, Kumar P (2018) Performance of fine RAP concrete containing flyash, silica fume, and bagasse ash. *J Mater Civ Eng* 30:04018233. [https://doi.org/10.1061/\(asce\)mt.1943-5533.0002408](https://doi.org/10.1061/(asce)mt.1943-5533.0002408)
36. IS 516:2014 (2004) Method of tests for strength of concrete. IS 516-1959, New Delhi, India
37. IS 5816 (1999) Indian standard splitting tensile strength of concrete-method of test (1st rev). Bureau of Indian Standards, New Delhi, pp 1–14
38. IS 456 (2000) Concrete, plain and reinforced. Bureau of Indian Standards, Delhi, pp 1–114
39. Rout MD, Biswas S, Sinha AK (2021) Mechanical and durability properties of alccofine used in reclaimed asphalt concrete pavements (RACP). In: *Advances in sustainable construction materials: select proceedings of ASCM 2020*, p 131

Public Transport

Analysis of Bus Stop Delay Variability Using Public Transit GPS Data



H. Ayana, Raviraj H. Mulangi, and M. M. Harsha

Abstract Travel time is considered as a direct measure of the efficiency and service reliability of a public transit system and increased travel time is contributed by delays at bus stops. Delay at bus stops affects the efficiency of bus operations and the level of service of public transportation. Day-to-day delay variability decreases passenger confidence in perceived reliability, causing uncertainty in making travel decisions. Many research works have been carried out to find delays at bus stops, but there are very few studies about the delay at bus stops in India using automatic vehicle location (AVL) data. In the present study, an attempt has been made to analyze delays at various bus stops in Mysore city using vehicle trajectory-based formulation based on AVL data collected from the Mysore Intelligent Transportation System (ITS). Delay variability has been analyzed using the coefficient of variation (COV) and also by fitting various probability distributions to the data, since distribution fitting helps in estimating the pattern of delay variability. The goodness of fit is tested by the Kolmogorov–Smirnov (KS) test. The results suggest that bus stops in the commercial area face more variability than the bus stops in residential areas. By fitting various distributions to delay data, it was observed that the performance of the generalized extreme value (GEV) distribution in fitting the data is better than other distributions.

Keywords Bus stop delay · Automatic vehicle location (AVL) · Delay variability · Intelligent transportation system

H. Ayana · R. H. Mulangi (✉)
Department of Civil Engineering, National Institute of Technology Karnataka, Surathkal, India
e-mail: ravirajmh@nitk.edu.in

H. Ayana
e-mail: ayanaharindran@gmail.com

M. M. Harsha
Department of Civil Engineering, Siddaganga Institute of Technology, Tumakuru, India
e-mail: harshammanjunath@gmail.com

1 Introduction

Urbanization is a process in which rural communities grow and form a city or the growth and extension of an existing city. The main reasons for urbanization include industrialization, commercialization, social benefits and services, and employment opportunities. Adequate transportation facilities are the need of the hour in urban areas. In cities, pollution, congestion on the roads, accidents, and higher vehicle population occur due to non-development and improper operation of public transportation systems. These days, private vehicles have become a sign of people's social status and most of the people use private vehicles for their convenience of travel. This trend leads to the rapid growth of vehicles on roads, which lead to traffic problems like congestion. Attracting more people to use public transit in the urban corridors is one way to tackle this specific problem. One of the best ways to encourage people to use public transit is to make it more attractive by improving the services offered. Intelligent transportation system (ITS) applications can help to relieve the congestion by attracting more people from personal vehicles to public transport by improving the efficiency of public transportation systems and providing a better level of service. Travel time is considered as a direct measure of the efficiency of a public transit operation. A large proportion of transit travel time is contributed by delays at bus stops. Delay at bus stops seriously affects the efficiency of bus operations and greatly influences the preferences of passengers to choose bus services. One of the major factors which affect the bus stop delay is the number of boarding and alighting passengers. Computation of bus stop delay based on the number of boarding and alighting passengers will be more accurate than any other method. In India, the conventional methods of data collection are manual and hence time-consuming. Automatic data collection methods such as automatic passenger count (APC) are a developing technology in India and hence are not available currently. However, it may be implemented in the near future. Technologies like BRT, ITS, etc. are implemented in metropolitan cities of India with the aim to improve the service reliability of the public transit system. These systems use GPS-mounted buses that give real-time vehicle location details at a certain frequency. Thus, computation of bus stop delay based on automatic vehicle location (AVL) data can be done since it is fairly accurate and is available from buses of ITS systems, which are now common in Indian cities.

The delay at bus stops can vary largely depending on the number of passengers, their age, luggage, payment methods, the performance of the bus, characteristics of bus stops, and surrounding traffic conditions. Thus, interpretation of delay variability at bus stops is critical. Day-to-day delay variability decreases passenger confidence in perceived reliability and causes uncertainty in making travel decisions.

In Indian conditions, since it is very difficult to obtain the number of boarding and alighting passengers through manual counts or videography methods and technologies like APC are not available throughout the country, there are only limited studies on bus stop delay. In the present study, the study area is Mysore city and the Mysore city bus transit system collects passenger details based on stage level only

(stages consist of two to three bus stops based on distance, fare, and other characteristics). Thus, it will be difficult to get passenger data of individual bus stops in Mysore city. The studies, which were based on the number of passengers, analyzed only dwell time and ignored delay caused due to deceleration and acceleration of bus when approaching and leaving the bus stop. Thus, the present study makes an attempt to analyze delays at various bus stops in Mysore city based on AVL data using GPS devices, so that the whole process of bus stop delay can be analyzed, that is, deceleration delay, dwell time at the bus stop, and acceleration delay. The analysis of variability in the delay is done using various statistical distributions. The goodness of fit is tested by the Kolmogorov–Smirnov (KS) test.

2 Literature Review

The conceptualization and implementation of intelligent transport systems (ITS) and bus rapid transit systems are the attempts being made to attract the commuters toward public transport systems and to solve the problem of traffic congestion. Understanding about the travel time distribution, which explains the variability in travel times, is necessary for analyzing the reliability of the system [1]. Advanced public transport systems (APTS), one of the most important ITS applications, provide accurate real-time bus arrival information to the passengers. This requires the prediction of travel time, which is the total elapsed time of travel, including stops and delays. A model-based prediction algorithm was developed in the study for the bus travel time prediction using Kalman filtering technique under heterogeneous traffic conditions taking into account the dwell time at bus stops explicitly [2].

Bus travel time is naturally unstable; small disturbances like delays in boarding or alighting can start a vicious cycle that results in bus unpunctuality [3]. The bus travel time on a route can be divided into dwell time and driving time [4, 5]. Bus delay at stops due to different cause factors leads to a distinct drop in bus travel efficiency [6]. Bus dwell time data collection typically involves labor-intensive ride checks [7]. Using automatic vehicle location (AVL) and automatic passenger count (APC) systems help in gathering transit data. The APC data comprises the passenger count information at the stop level and the actual arrival or departure information at the timepoint level [8]. AVL data collected from bus probe data can be used to analyze travel time [9, 10], control delay at intersections [11, 12], and delay at bus stops [13]. Numerous works have been done to analyze dwell time at bus stops using AVL/APC data. APC data has been used by various researchers to model delays at bus stops [7, 14]. Alhadidi and Rakha [15] introduced two multilinear models that compute bus passenger boarding/alighting times at bus stops using AVL and APC data. In Indian conditions, AVL data can be used for bus stop delay analysis. Low-frequency AVL data from transit buses was applied as probes to estimate link travel time and traffic delay caused by intersections or lighting and boarding at bus stops [13].

Analysis of delay variability is necessary to ensure reliable transport. Various methods have been used to study delay variability. The statistical modeling approach

using statistical software [16] has been used to model variability in bus stop dwell time, whereas analytic models [17, 18] have been used to investigate delay variability at signalized intersections. Various research works have been done to analyze delay variability using statistical distributions. Researchers have used generalized extreme value (GEV) [19], normal [20, 21], lognormal [22], logistic [8], gamma [16, 23], uniform [8], exponential [16, 24], log-logistic [25], Weibull [16, 26], Burr [27] and Erlang distributions [16, 28] for analysis of variability in intersection and bus stop delay.

In developing countries like India, presently, technologies like APC are not available everywhere; it is only an emerging technology in India, and hence, stop level data is not available for every bus stop for the analysis of delay. Thus, in the present study, an attempt has been made to analyze delay variability at bus stops using AVL data collected from transit buses operating in Mysore city, India. Vehicle trajectory-based formulation has been used to estimate delay from GPS data. Delay variability has been analyzed by fitting probability distribution to the data.

3 Data

The data from public transit buses operating in Mysore city was collected for the present study. The major form of public transit in the city is Mysore Intelligent Transport System operated by the Mysore City Division. The intelligent transport system (ITS) that Mysore implemented in 2012 in its entire city bus fleet has resulted in efficiency and safety in public transport service. The buses are enabled with Global Positioning System (GPS) and are continuously tracked at the control room in the ITS office placed at the city bus station. Mysore ITS operates GPS-mounted buses that provide real-time data at an update frequency of 10 s. GPS data collected from Mysore ITS consists of a large number of parameters. But only a few parameters that are significant for this study were considered. Those parameters are bus id, schedule date, longitude, latitude, GPS time, velocity, and trip number.

Data was collected for a period of two months (May and June, 2018) and extracted for a road stretch extending between Yelwala and Mysore City Bus Stand (CBS) and study sections were extracted using QGIS packages. Four bus stops have been considered for the present study. The details of the locations of bus stops are shown in Fig. 1. Premier Studio lies in the commercial area, whereas Hinkal, Daba, and SRS Hootagalli lie in the residential area.

4 Methodology

The detailed methodology used in the study is shown in Fig. 2. The GPS data collected from Mysore ITS was extracted after a series of pre-processing since it was in the form of sequential query language (SQL). The GPS database collected from ITS

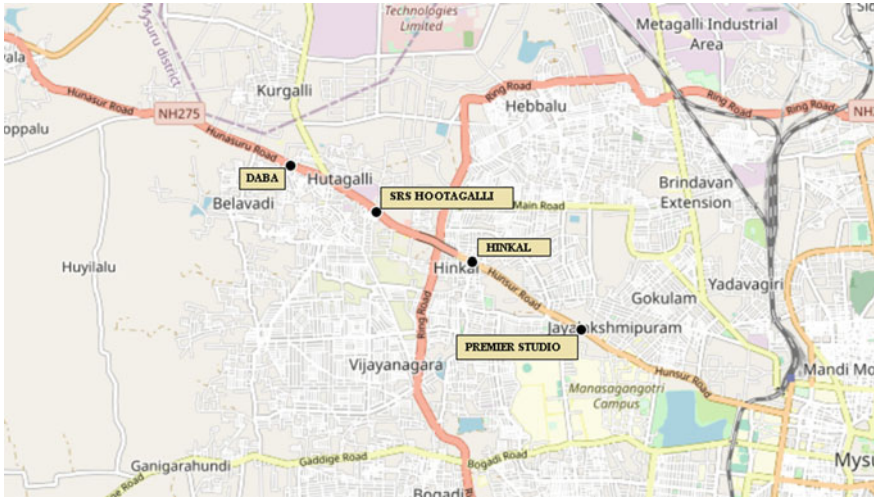


Fig. 1 Locations of study bus stops. Source OpenStreetMap

was extracted to local servers using SQL extract. Erroneous data was removed and only those updates with unique details have been used. The available GPS data provides details of the position in terms of geographic coordinates, that is, latitudes and longitudes.

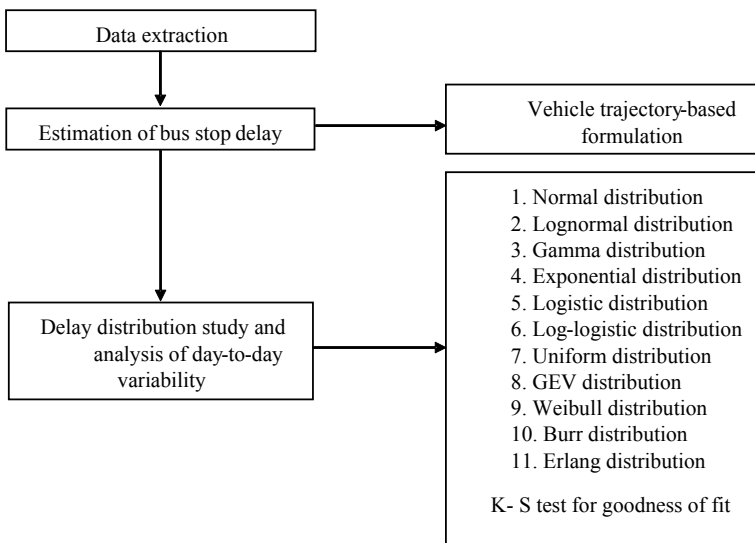


Fig. 2 Detailed methodology of the present study

Map matching has been done using the QGIS package to visualize the pre-processed data. Data related to selected bus stops has been extracted by considering a suitable distance on either side of the bus stop. For each trip, the vehicle trajectories have been developed. The instantaneous speed values obtained from GPS data have been used to plot speed profiles. The backward difference formula as given in Eq. (1) has been used to estimate acceleration at each data point.

$$a_i = \frac{V_i - V_{i-1}}{t_i - t_{i-1}} \quad (1)$$

where a_i = acceleration associated with GPS point i ; v_i = speed associated with GPS point i ; v_{i-1} = speed associated with GPS point $i - 1$; and t_i = time stamps associated with GPS point i ; and t_{i-1} = time stamps associated with GPS point $i - 1$.

The delay at bus stops occurs only when there will be a reduction in speed near bus stops. So, the trips which do not have a reduction in speed were not considered for delay computation. A speed threshold of 5 m/s (approximately 20 kmph) has been assumed based on the inventory studies carried out in the bus stops and also observations from trajectories of buses to filter out delay-causing trips.

Vehicle trajectory-based formulation has been used to estimate the delay of buses at bus stops. Bus stop delay consists of three components, deceleration delay, stopped delay, that is, dwell time, and acceleration delay. As illustrated in Fig. 2, Eqs. (2)–(6) have been developed based on vehicle trajectories.

$$\text{Decelerationdelay} = (t_2 - t_1) - \frac{d_2 - d_1}{v_f} \quad (2)$$

$$\text{stoppeddelay} = t_3 - t_2 \quad (3)$$

For non-stopping trajectories, as in Fig. 5, t_3 will be equal to t_2

$$\text{Accelerationdelay} = (t_4 - t_3) - \frac{d_3 - d_2}{v_f} \quad (4)$$

$$\text{Busstopdelay} = \text{decelerationdelay} + \text{stoppeddelay} + \text{accelerationdelay} \quad (5)$$

$$\text{Busstopdelay} = (t_4 - t_1) - \frac{d_3 - d_1}{v_f} \quad (6)$$

where t_1 , t_2 , t_3 , and t_4 are the critical points in delay estimation: t_1 = time at which bus traveling at desired speed start decelerating; t_2 = time when the bus comes to a stop in bus stop; t_3 = time at which bus starts accelerating; and t_4 = time of the end of acceleration and reaching desired speed or a speed reduction; $(d_2 - d_1)$ = distance covered in deceleration phase before vehicle come to a stop; and $(d_3 - d_2)$ = distance covered in the acceleration phase, to reach desired speed; v_f = free-flow

speed. From inventory analysis of transit buses operating in Mysore city, the free flow is observed as 60 kmph.

As seen in Eqs. (2)–(4), estimation of bus stop delay requires identification of critical points $t_1, t_2, t_3,$ and t_4 . The velocity profile is used for locating critical points associated with stopped delay, that is, t_2 to t_3 . The stopped delay is considered when speed is below the threshold value. Here in this study, the threshold velocity is taken as 5 kmph [29]. That is those buses that have a velocity less than 5 kmph are considered as stopped ones at the bus stop. Thus, t_2 and t_3 are GPS time stamps when velocity is less than 5 kmph, which can be obtained from the velocity profile and acceleration profile has been used for locating the deceleration beginning point and the ending acceleration point, that is, t_1 and t_4 . Given Figs. 3, 4, and 5 represents distance, speed, and acceleration profiles with and without stopping. Both these cases are considered because buses sometimes have a tendency to not stop at some bus stops when drivers see that no passengers are present.

In Fig. 4, it is seen that when a bus that is traveling at free-flow speed starts decelerating, the acceleration changes from positive or zero to negative and remains negative throughout the deceleration phase and changes from negative to positive when the bus starts accelerating. It remains positive in the acceleration phase and again changes from positive to negative or zero when the bus stops accelerating and reaches constant speed or experiences a reduction in speed. The time stamps at which acceleration becomes zero at the start of deceleration and at the end of acceleration are critical points t_1 and t_4 , respectively. t_1 is the time in the deceleration phase where acceleration is non-negative and t_4 is the time in the acceleration region where acceleration is non-positive. t_1 and t_4 are computed as the timestamps in deceleration and acceleration phases when the acceleration value changes from positive to negative. In some cases, in the acceleration phase, the vehicle may not reach the free-flow

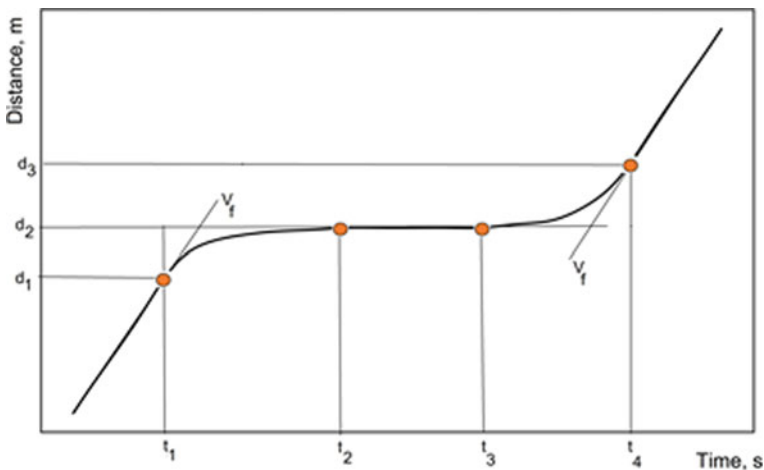


Fig. 3 Distance profile of bus stopped in a bus stop

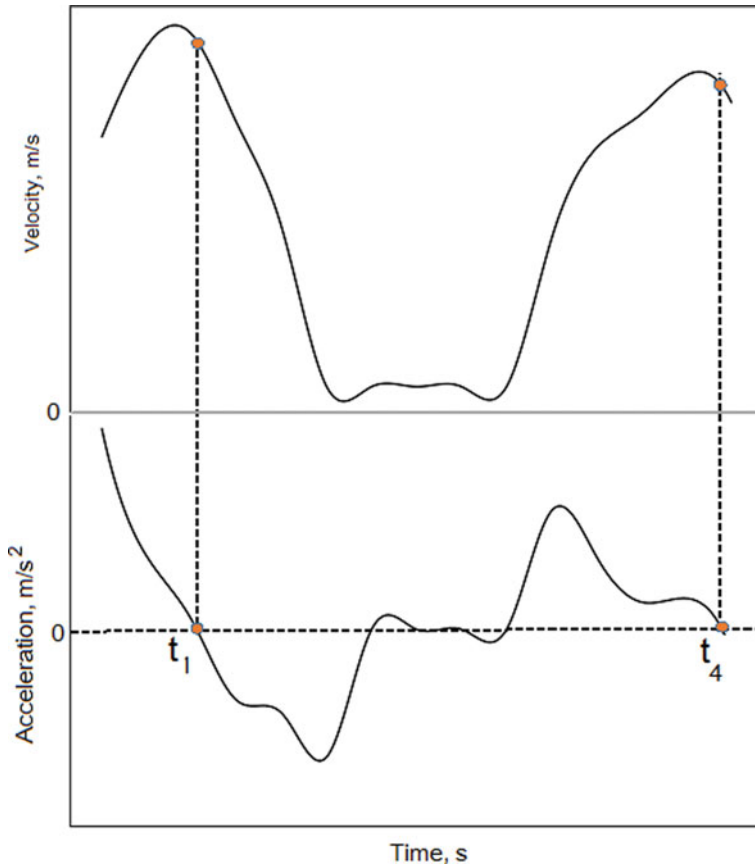


Fig. 4 Speed and acceleration profile with stopped delay

speed, instead keeps accelerating slowly. In such cases, the acceleration transition from positive to a negative value cannot be observed and a distance threshold has been used to estimate the approximate end of acceleration. The approximate distance at which most of the buses attain a uniform speed can be estimated by plotting the speed profile of all buses at a particular stop. The time update which is nearest to this distance is considered as the end of acceleration, t_4 .

5 Results and Discussion

Bus stop delay for a time period of 6:00 to 22:00 has been estimated using the proposed methodology. The coefficient of variation (COV) has been used as a measure for variability analysis of delay. Table 1 provides the average COV values

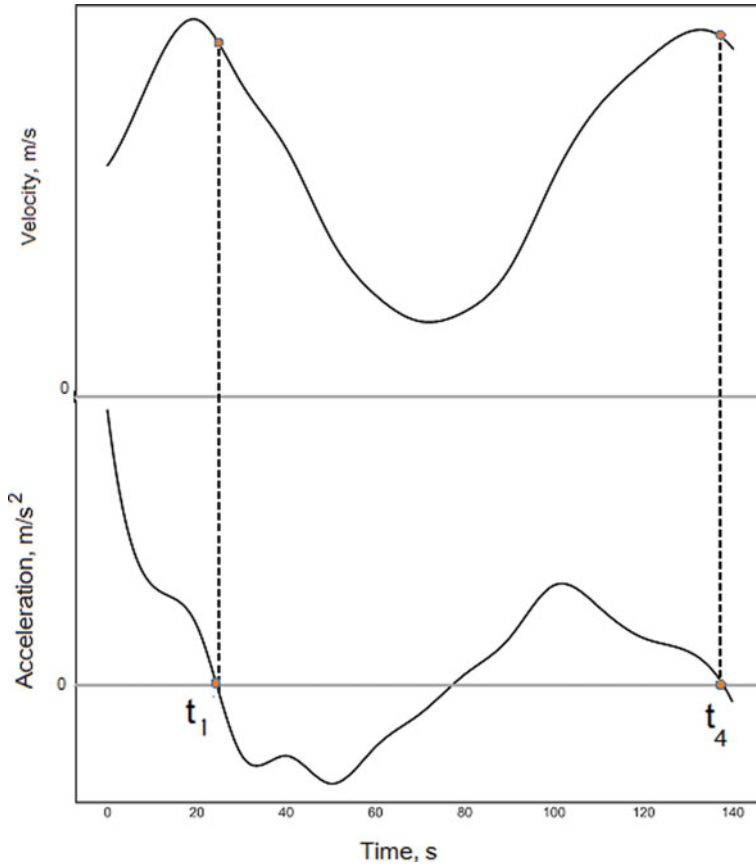


Fig. 5 Speed and acceleration profile without stopped delay

of study locations. From Table 1, it has been observed that Premier Studio, which lies in the commercial area has the highest average COV among all study locations and Daba stop has the lowest COV value. It is clearly seen that variability is more in commercial area bus stops and less in residential area bus stops.

For the purpose of a detailed study of variability, the delay at bus stops has been grouped as weekdays and weekends data and the hourly split has been done on this

Table 1 Average COV values of study locations

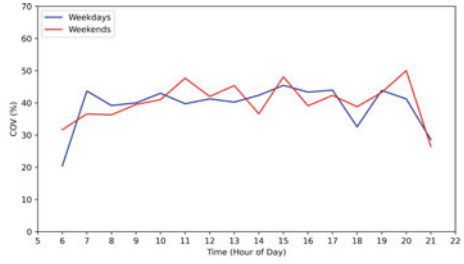
Locations	Number of trips	Average COV (%)
Premier Studio	2698	45.026
Hinkal	2923	32.208
SRS Hootagalli	2623	37.245
Daba	1717	28.701

data. The results are shown in Fig. 6. In most of the bus stops in the residential area, COV values have been observed more during morning hours. The COV values of the Premier Studio bus stop, which is in the commercial area, were reasonable and uniform between 7:00 to 20:00. During weekdays, COV is more in morning hours and evening hours whereas, on weekends, COV is more during morning hours 10:00 to 13:00 and during evening hours 19:00 to 21:00. This uniform and high variability are due to commercial activities during morning and evening hours. In Hinkal, a uniform COV value was observed on weekdays, whereas, on weekends, high variability was observed from 11:00 to 13:00 and during evening hours from 16:00 to 19:00. In SRS Hootagalli, during weekdays, high COV values were observed from 10:00 to 12:00, 13:00 to 15:00, and 17:00 to 20:00. High variability was observed during 8:00 to 10:00 and 15:00 to 17:00 during weekends. In Daba stop, during weekdays, variability was very high in morning hours, 7:00 to 9:00. The reason behind this can be the movement of people from the residential area to workplaces during morning hours. After 10:00 during weekdays, a uniform variability was observed. During weekends, more COV values were observed from 9:00 to 12:00. This is due to the movement of people for recreational purposes during weekends. Among the bus stop of residential area considered, Hinkal bus stop has more variability than the other two bus stops which is due to higher passenger demand and Daba bus stop has lower delay variation due to the lower passenger demand. The bus stop delay variation was found to be different for weekdays and weekends, and hence, the distribution study for bus stop delay has been conducted for weekdays and weekends separately.

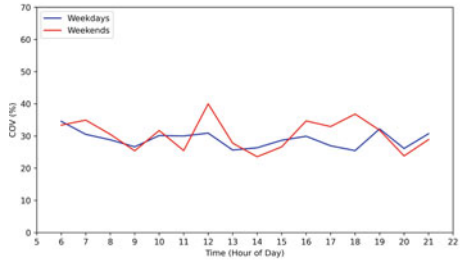
To estimate the best fit for the delay, eleven statistical distributions have been used as shown in Fig. 7. The results of distribution fitting for weekdays and weekends are shown in Tables 2 and 3, respectively. On weekdays, only GEV distribution has a 100% pass ratio in the K-S test, and it also has the highest cases in the top 3 and top 1, followed by normal and Weibull distribution with 93% cases passing ratio. Though Burr distribution has only a 91% pass ratio, it has cases top 3 ratios of 62%. Also, among all the distributions, GEV has the highest mean p -value of 0.788, followed by Burr (0.702). All other distributions have a lesser mean p -value compared with Burr and GEV distributions, even though some had a high percentage of cases passing ratio. It was observed that exponential distribution has the lowest mean, 0% cases passing, cases in top 3 and top 1, although it has the least standard deviation of p -value indicating that this distribution cannot be used for analyzing delay variability. Among all the distributions fitted, GEV has the minimum standard deviation value of 0.227, followed by normal (0.310), Burr (0.322), and Weibull (0.322).

On weekends, similar to weekdays, GEV distribution has 100% cases passing ratio and the highest cases in top 3 (81%) and top 1 (40%) ratios, followed by logistic and normal distributions with a case passing ratio of 97%. They are followed by 96% cases pass for log-logistic, lognormal, and gamma and 94% for Burr distributions. However, Burr distribution has a larger mean of 0.772 and has come in the top 3 for 65% of the time. GEV distribution has the highest mean p -value of 0.825. Similar to weekdays, on weekends also, exponential has the least mean, a standard deviation of p -value and 0%, cases passing ratio, cases in top 3 and top 1. This indicates that exponential distribution cannot be used for fitting weekend delay data. All other

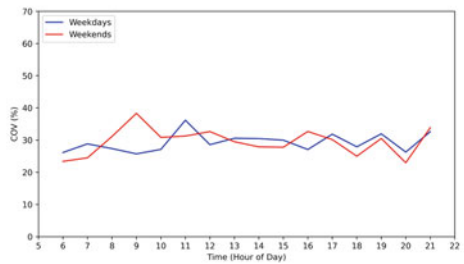
Fig. 6 Delay variability on weekdays and weekends at **a** Premier Studio, **b** Hinkal, **c** SRS Hootagalli, **d** Daba



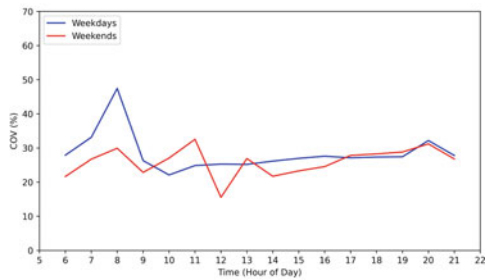
(a)



(b)



(c)



(d)

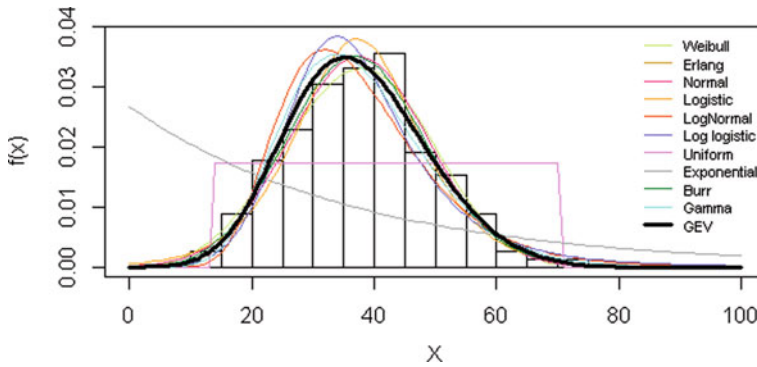


Fig. 7 Probability density functions of various statistical distributions

Table 2 Performance of distributions on weekdays

Distribution	Mean p -value	SD of p -value	Cases pass ratio (%)	Cases top 1 ratio (%)	Cases top 3 ratio (%)
Burr	0.702	0.322	91	22	62
Erlang	0.256	0.308	60	1	4
Exponential	0.00031	0.002	0	0	0
GEV	0.788	0.227	100	31	87
Gamma	0.587	0.325	90	10	34
Log-logistic	0.419	0.319	90	1	10
Lognormal	0.486	0.322	91	6	21
Logistic	0.480	0.306	88	7	19
Normal	0.544	0.310	93	3	25
Uniform	0.277	0.266	85	10	16
Weibull	0.551	0.322	93	7	22

distributions have lesser mean value compared to both the distributions, even though they had a high case passing ratio. Among the fitting distributions, GEV has a lesser standard deviation (0.186), followed by Burr (0.277). Although Weibull distribution has a comparable mean and pass ratio and less standard deviation, it has come in top 1 and top 3 for very few cases.

It is observed that the performance of GEV distribution in fitting the weekdays and weekends data is almost similar. GEV has the highest number of cases passing the K_S significance test, the highest ratio of top 3 and top 1, and the highest mean. However, Burr distribution is also capable of giving promising results. In either case, exponential distribution performed the worst, indicating that it cannot be used for fitting delay data.

Table 3 Performance of distributions on weekends

Distribution	Mean <i>p</i> -value	SD of <i>p</i> -value	Cases pass ratio (%)	Cases top 1 ratio (%)	Cases top 3 ratio (%)
Burr	0.772	0.277	94	22	65
Erlang	0.388	0.345	72	1	6
Exponential	0.003	0.012	3	0	0
GEV	0.825	0.186	100	40	81
Gamma	0.661	0.295	96	6	21
Log-logistic	0.561	0.302	96	1	24
Lognormal	0.617	0.304	96	4	26
Logistic	0.569	0.297	97	9	18
Normal	0.614	0.292	97	3	24
Uniform	0.481	0.304	91	7	16
Weibull	0.664	0.254	96	6	18

6 Conclusions

Congestion on roads as a result of urbanization and its after-effects can be reduced by attracting more people to use public transit. This can be done by improving the services offered. Travel time is a direct measure of the efficiency of a public transit operation and their prediction will make the public transport system more reliable. A large proportion of transit travel time is contributed by delays at bus stops and is dependent on the number of passengers, their age, luggage, payment methods, the performance of the bus, characteristics of bus stops, surrounding traffic conditions, etc. In Indian conditions, it is very difficult to obtain the number of boarding and alighting passengers through manual counts or videography methods and advanced techniques such as APC is not common. Thus, in the present study, an attempt had been made to analyze all the components of bus stop delay based on AVL data collected by the Mysore ITS and analyze the variability in delay using the descriptive performance of various statistical distributions.

The bus stops considered for the present study belong to the commercial area and residential area. It was observed that delay variability was more for the bus stop in commercial areas than bus stops in residential areas. Coefficient of variation (COV) was one of the measures used to analyze the variability. The COV value is more for the bus stop in the commercial area; this is due to the commercial activities occurring during the daytime. Delay variability was more during morning hours in residential area bus stops during weekdays; this may be due to the movement of people for work purposes. During weekends, it was more during morning hours and evening hours, which is due to people moving for recreational purposes on weekends.

Delay distribution helps in describing the pattern of delay variability. Statistical distributions have been used to estimate the best fitting distribution for bus stop delay. It is observed that the performance of the GEV distribution is better than other

distributions followed by Burr distributions in fitting the weekdays and weekends data. Whereas, in either case, exponential distribution has the worst performance in fitting the delay data. Hence, GEV distribution can be used by traffic and transit operators to model delay variability at bus stops.

References

1. Harsha MM, Mulangi RH, Kumar DHD (2019) Analysis of bus travel time variability using automatic vehicle location data. In: CONFERENCE 2019, world conference on transport research (WCTR), Mumbai, pp 1–16
2. Padmanaban RPS, Vanajakshi L, Subramanian SC (2009) Automated delay identification for bus travel time prediction towards APTS applications. In: CONFERENCE 2009, second international conference on emerging trends in engineering and technology (ICETET), IEEE, India, pp 564–569
3. Qu X, Jin S, Oh E, Weng J (2014) Bus travel time reliability analysis: a case study. *Proc Inst Civ Eng Transp* 167(3):178–184
4. Dorbritz R, Luthi M, Weidmann UA, Nash A (2009) Effects of onboard ticket sales on public transport reliability. *J Transp Res Board* 2110:112–119
5. Meng Q, Qu X (2013) Bus dwell time estimation at a bus bay: a probabilistic approach. *Transp Res Part C: Emerg Technol* 36:61–71
6. Chen S, Zhou R, Zhou Y, Mao B (2013) Computation on bus delay at stops in Beijing through statistical analysis. *Math Prob Eng* 2013
7. Dueker KJ, Kimpel TJ, Strathman JG (2004) Determination of bus dwell time. *J Public Transp* 7(1):21–40
8. Wong E, Khani A (2018) Transit delay estimation using stop-level automated passenger count data. *J Transp Eng, Part A: Syst* 144(3):04018005
9. Li Z, Kluger R, Hu XB, Wu YJ, Zhu XY (2018) Reconstructing vehicle trajectories to support travel time estimation. *Transp Res Rec* 2672(42):148–158
10. Wan N, Vahidi A (2014) Probabilistic estimation of travel times in arterial streets using sparse transit bus data. In: CONFERENCE 2014, IEEE 17th international conference on intelligent transportation systems (ITSC), IEEE, China, pp 1292–1297
11. Ko J, Hunter M, Guensler R (2008) Measuring control delay components using second by second GPS data. *J Transp Eng* 134(8):338–346
12. Wang H, Zhang G, Zhang Z, Wang Y (2015) Estimation of control delay at signalized intersections using low-resolution transit bus-based global positioning system data. *IET Intel Transport Syst* 10(2):73–78
13. Meng Z, Wang C, Peng L, Teng A, Qiu TZ (2017) Link travel time and delay estimation using transit AVL data. In: CONFERENCE 2017, 4th international conference on transportation information and safety (ICTIS), IEEE, Canada, pp. 67–72
14. Arhin S, Noel E, Anderson MF, Williams L, Ribisso A, Stinson R (2015) Optimization of transit total bus stop time models. *J Traffic Transp Eng* 3(2):146–153
15. Alhadidi TA, Rakha HA (2019) Modelling bus passenger boarding/alighting times: a stochastic approach. *Transp Res Interdisciplinary Perspect* 2(0):100027
16. Khoo HL (2013) Statistical modeling of bus dwell time at stops. *J Eastern Asia Soc Transp Stud* 10:1489–1500
17. Chen P, Liu H, Qi H, Wang F (2013) Analysis of delay variability at isolated signalized intersections. *J Zhejiang Univ-Sci A (Appl Phys Eng)* 14(10):691–704
18. Chen P, Sun J, Qi H (2017) Estimation of delay variability at signalized intersections for urban arterial performance evaluation. *J Intell Transp Syst* 21(2):94–110

19. Esfeh MA, Kattan L, Lam WHK, Esfe RA, Salari M (2020) Compound generalized extreme value distribution for modeling the effects of monthly and seasonal variation on the extreme travel delays for vulnerability analysis of road network. *Transp Res Part C: Emerg Technol* 120
20. Olszewski PS (1994) Modeling probability distribution of delay at signalized intersections. *J Adv Transp* 28:253–274
21. Gilani VNM, Ghasedi M, Ghorbanzadeh M, Samet MJ (2017) Estimation delay variation and probability of occurrence of different level of services based on random variations of vehicles entering signalized intersections. In: CONFERENCE 2017, IOP Conf Ser: Mater Sci Eng 245(4):042023
22. Bai S, Bai H, Pang H (2015) Statistical analysis of buses delay for signalized control intersection. In: CONFERENCE 2015, CICTP 2015, 15th COTA international conference of transportation professionals. ASCE, China, pp 1440–1450
23. Jeong J, Guo S, Gu Y, He T, Du DHC (2012) Trajectory-based statistical forwarding for multi-hop infrastructure-to-vehicle data delivery. *IEEE Trans Mob Comput* 11(10):1523–1537
24. Bergström A, Krüger N (2013) Modeling passenger train delay distributions: evidence and implications. Working papers in Transport Economics, CTS—Centre for Transport Studies Stockholm (KTH and VTI) 2013(3)
25. Li J, Zhang H, Zhang Y, Zhang X (2020) Modeling drivers' stopping behaviors during yellow intervals at intersections considering group heterogeneity. *J Adv Transp Hindawi* 2020
26. Yuan J (2006) Stochastic modelling of train delays and delay propagations in stations. Delft, The Netherlands: Netherlands TRAIL Research School
27. Susilawati Ramli MI, Yatmar H (2020) Delay distribution estimation at a signalized intersection. In: CONFERENCE 2020, IOP Conf Ser: Earth Environ Sci 419
28. Jiang X, Yang X (2014) Regression-Based Models for Bus Dwell Time. In: CONFERENCE 2014, 17th international conference on intelligent transportation systems (ITSC), IEEE, China, pp 2858–2863
29. Mousa MR (2002) Analysis and modeling of measured delays at isolated signalized intersections. *Int J Transp Eng* 128(4):347–354

Effectiveness of Passenger Attraction Policies: A Pre-COVID-19 and Post-lockdown Comparison



Sandra Kamar, S. Shaheem, B. Vinayaka, and Samson Mathew

Abstract The effectiveness of passenger attraction policies designed to induce a modal shift from private mode of transport to public mode of transport is tested frequently as a solution to the constantly dropping ridership rates in public transportation (PT). However, with COVID-19 pandemic in the picture, will the policies that were previously tested effective stand the test of time? Using the work-trip data collected from employees working in Thiruvananthapuram City, this study compares the effectiveness of six passenger attraction policies, aimed at decreasing the travel time and travel cost parameters, in a pre-COVID-19 and a post-lockdown scenario. Fuzzy logic-based mode choice models are developed to perform policy sensitivity analysis. The policies such as improving PT coverage and supply, introducing parking prohibition on major streets, operating non-stop bus services, reducing return-trip fares, early bird pre-peak hour discounts, and providing monthly PT season tickets are tested. The results show that, compared to the pre-COVID-19 model, the effectiveness of two out of the six policies reduces for the post-lockdown model, and the two policies being related to the travel cost parameter. The six policies are found to induce a private to public modal shift ranging from 5.8 to 7.9% for the pre-COVID-19 scenario, while the post-lockdown model gives a shift ranging from 5.8 to 7.1%.

Keywords Covid-19 · Fuzzy logic · Public transportation

S. Kamar (✉) · B. Vinayaka
REVA University, Bengaluru, India
e-mail: sandra.kamaruddin@gmail.com

B. Vinayaka
e-mail: vinayaknaikb@reva.edu.in

S. Shaheem · S. Mathew
KSCSTE-NATPAC, Thiruvananthapuram, India
e-mail: director.natpac@kerala.gov.in

1 Introduction

The public transportation (PT) system in India has been in a longstanding crisis with continually declining ridership rates over the past years. The sub-standard PT infrastructure and services, the appeal of private vehicle ownership and usage, and the psycho-socio-economic characteristics of users have contributed to this decline. Policy interventions are a viable solution to this problem as they can influence the decision-making of the public. Normally, PT passenger attraction policies are formulated with the objective of enhancing PT services and discouraging private vehicle ownership and usage. There have been several studies that tested and identified different policies for improving PT ridership. But the looming question is: How effective are these policies in the scenario of a worldwide pandemic?

COVID-19 was first reported in December 2019 in Wuhan, China. With more efficient and frequent transportation of people and goods, owing to globalisation, COVID-19 has turned into a worldwide pandemic, infecting about 170 million and claiming the lives of nearly 3.55 million as of May 2021. Every industry has taken a hit, but with conditions in the PT services facilitating contagion, the PT sector is easily one of the hardest hits. The COVID-19-induced lockdowns led to the suspension of operations of PT buses, only to be resumed with restrictions after the lockdowns were lifted. It is imperative to study the effects of the lockdown on the PT ridership rates, as well as on the response of users to previously effective policies aimed at improving PT patronage. A comparison of results between pre-COVID-19 and post-lockdown phases will help in identifying the shift in priorities of the users, thereby assisting the formulation of more effective policies for the future. The present study develops fuzzy logic mode choice models for both pre-COVID-19 and post-lockdown scenarios and employs policy sensitivity analysis to check the effectiveness of six passenger attraction policies.

2 Literature Review

There are several studies in the existing literature that assess the impact of policies that were introduced to attract PT ridership. By using the SimMobility agent-based simulation platform to create a synthetic population and evaluating 9 various pricing strategies, Adnan et al. [1] investigated the impact of changes in pricing strategies in Singapore. The findings advised that higher off-peak discount tactics be avoided, with a concentration on discount strategies in the AM peak's surrounding time periods. In addition, extending free pre-peak MRT/LRT to all stations may help to optimise system capacity. Using the extended convergent cross-mapping approach, Lee and Yeh [2] examined the causal relationship between bus ridership (BR) and bus revenue vehicle-kilometres (BK) in the context of a free fare bus policy, concluding that cities that want to promote public transit use should expand their route network or increase the number of scheduled runs, accompanied by the implementation of a free fare bus policy.

Liu et al. [3] compared the differences between two common licence-plate-number-based vehicle restriction strategies: One-Day-Per-Week (ODPW) and Odd-And-Even (OAE). ODPW reduces a tiny fraction of traffic volume and causes minor reactions in travellers, such as an increase in unlawful travel and travel intensity, but OAE causes a greater rise in illegal travel and travel intensity. ODPW can be in place for a long time since it creates a low incentive for unlawful travel, high travel intensity, and the purchase of a second vehicle. OAE, on the other hand, is suited for use as a contingency plan in the event of major events or excessive pollution control. However, relying only on OAE for a long time is not a good idea because the policy will produce other traffic issues, such as excessive second-car ownership. Continuing the research, Liu et al. [4] focused on noncompliance behaviour under ODPW and OAE, finding that non-local vehicles travelling in the city frequently are more likely to violate the two policies than local vehicles, vehicles that typically travel a long distance in the urban restriction area are prone to noncompliance behaviour, vehicles that emerge far from the city centre exhibit more noncompliance acts, and vehicles with a high unrestricted travel rate are more likely to exhibit noncompliance. Evangelinos [5] focuses on the issues that arise when businesses provide free or reduced parking, and experimentally evaluates the consequences of parking cash-out. Employers who provide parking subsidies must provide the financial equivalent of the parking service value to their employees under this policy. Parking cash-out has a negative and significant impact on private automobile choice probability, according to the findings. Rewarding the abandonment of on-site parking rather than penalising its use reduces the likelihood of car use.

Verma et al. [6] identified the effects of COVID-19 on transportation infrastructure and proposed a set of policy recommendations, strategies, and interventions to address transportation issues in a post-COVID-19 world. They concluded that agencies must reclaim public trust by ensuring that all safety protocols, such as social distancing, are followed in transit. The need of implementing staggered workhours and business schedules, as well as prioritising the migration of unskilled and low-skilled workgroups, was emphasised. Temporary bus-priority lanes, temporary bus stops, markings for passengers to keep a safe distance, and the adoption of smart-cards or QR-based ticketing, among other infrastructure adjustments, were suggested. Arellana et al. [7] investigated the short-term impacts on the transportation system caused by the various policies adopted by the Colombian government and local governments to contain the COVID-19 spread, finding lower demand for motorised trips, lower transit ridership, and lower transport externalities. Freight was found to be the most resilient mode of transportation, but it experienced a 38% decline, affecting mostly the supply chain for non-essential goods. According to the report, transportation service providers will confront a financial crisis exacerbated by the pandemic, requiring government support to recover.

Kumar et al. [8] focused on the application of fuzzy logic technique in which the mode choice model provides the estimated modal split at the specified work centres in Delhi, concluding that the fuzzy logic-based mode choice model offers significant flexibility in evaluating any kind of sensitive public transportation policy. With the use of a fuzzy rule-based mode choice model, Kedia et al. [9] investigated

the transit choice behaviour of urbanites in Surat, an Indian metropolitan city in the state of Gujarat. Travellers' views of accessibility features can be better articulated in linguistic form, hence, fuzzy-based models solve the inadequacies of Logit models, according to the study.

3 Methodology

The objective of the present study is to compare the effectiveness of a set of PT passenger attraction policies for a pre-COVID-19 and post-lockdown scenario. A review of the existing research helped in the formulation of the study methodology. Artificial intelligence techniques like fuzzy logic programming were found to be superior to conventional methods in developing mode choice models, especially with its flexibility in evaluating sensitive policies. The study area was selected, and a questionnaire survey was carried out. The survey included questions related to pre-COVID-19 work trips and post-lockdown work trips, among others. The data collected from the survey was analysed using descriptive statistical analysis and cross-tabulation analysis as a precursor to further analysis and to get an overall idea of the nature of the data, using the SPSS platform. A pre-COVID-19 mode choice model and a post-lockdown mode choice model were developed using fuzzy logic programming. To check the application of the models, a set of six policies that aimed at decreasing the travel time and travel cost parameters were tested using sensitivity analysis. Further, a comparison between the estimated modal split and the modal split induced by the selected policies were made to evaluate the effectiveness of these policies in the pre-COVID-19 and post-lockdown scenario.

3.1 Study Area

A review of the existing literature suggested that no studies have been made on how COVID-19 has affected the PT system of medium-sized cities. Since this study focuses on work trips, a medium-sized city with a high work participation rate had to be selected. Consequently, Thiruvananthapuram City, in the state capital of Kerala, India was selected. Thiruvananthapuram is the most populous city in Kerala with a population of 957,730, as per the 2011 census. The public bus services in the city are dominated by the state-run Kerala State Road Transport Corporation (KSRTC), while private bus services are also available. The 2011 census reports Thiruvananthapuram district to have a work participation rate of 37%. The survey questionnaire was designed to collect information regarding socio-economic characteristics of the respondents, pre-COVID-19, mid-lockdown and post-lockdown trip characteristics, data related to the pandemic situation, and Likert scale ratings on sustainable transport preferences.

3.2 Data Collection

For the current study, data was collected from employees at their respective workplaces in different parts of Thiruvananthapuram city. The main data collection points were Pattom, Palayam, Keshavadasapuram, Statue, Ulloor, and Nedumangad. The minimum sample size was calculated to be 385 samples using Cochran formula. After data entry and subsequent data cleaning, a total of 469 samples were taken for analysis. Descriptive statistical analysis shows that about 45.4% of the respondents are male and 54.6% are female. About 32.8% commuters belonged to the 31–40 age group, followed by 30.5% respondents in the 41 to 50 age group, and the respondents in the 21–30 age group were found to be 23.2%, among others. In case of marital status, 83.6% was married, 15.6% unmarried, and 0.9% responded as others. The data shows a majority response of 45.4% for the household size of four individuals, followed by 30.1% for more than four members, and 17.5% with three members, among others. The data shows that 49.7% has a graduate degree and 18.6% respondents hold a post-graduate degree. The monthly personal income of 30.1% respondents was between 20,000 and 30,000 rupees per month, followed by 23.5% earning 10,000 to 20,000, while 22.8% had between 30,000 and 40,000 per month. About 88.9% respondents were found to own at least one private vehicle.

The frequency of daily work/business trips was found to reduce from 95.9% pre-COVID-19 to 36.4% mid-lockdown but going back to 95.9% post-lockdown. The details of the mode of travel of the respondents in the pre-covid-19, mid-lockdown and post-lockdown time were also analysed to understand how the COVID-19-induced lockdown affected the mode choice of the people. The use of two-wheelers for work trips increased from 49.5% during pre-COVID-19 times to 57.9% mid-lockdown and decreased to 54.1% in the post-lockdown stage. A similar trend was seen for cars as well, increasing from 11.1% pre-COVID-19 to 19.1% mid-lockdown and then down to 15.6% post-lockdown. The PT mode, however, showed a steady decline from 23.7% pre-COVID-19 to 17.1% post-lockdown.

4 Fuzzy Logic

In 1965, with the ‘fuzzy set theory’, Lotfi Zadeh coined the term fuzzy logic. The concept behind this logic is that a value can range anywhere between completely true and completely false, hence the term ‘fuzzy’. Values in linguistic form are often an open, imprecise spectrum of data. Fuzzy logic can work with this data as input and give accurate results. This logic can be utilised for developing mode choice models as people make decisions based on imprecise and non-numerical information, and the human reasoning resembles the fuzzy logic method of reasoning. The MATLAB software, which provides a graphical user interface to carry out fuzzy logic programming with minimal coding, is used to develop the mode choice models in this study.

4.1 Membership Functions

In conventional mode choice models, the input values are in the form of crisp sets. For example, if 12 km distance is categorised as medium, 13 km, which is just one kilometre longer would not be included in the medium category. In the case of fuzzy logic, the crisp input data are fuzzified using membership functions (MF), which assigns a value ranging between 0 and 1, called ‘degree of membership’ or ‘membership value’ for each input within a certain category. In this example, 13 km will be assigned a certain degree of membership under the medium set, as illustrated in Fig. 1.

There are different shapes for MFs such as triangular, trapezoidal, Gaussian, and so forth, which can also be set to overlap as depicted in Fig. 2.

The fuzzified inputs are then fed into a fuzzy inference engine containing ‘if–then’ rules in which product-sum gravity technique is used to generate output in linguistic form. Since these outputs cannot be used directly, they are de-fuzzified to give a crisp output. In summary, the system takes crisp values as inputs, fuzzify them as per MFs,

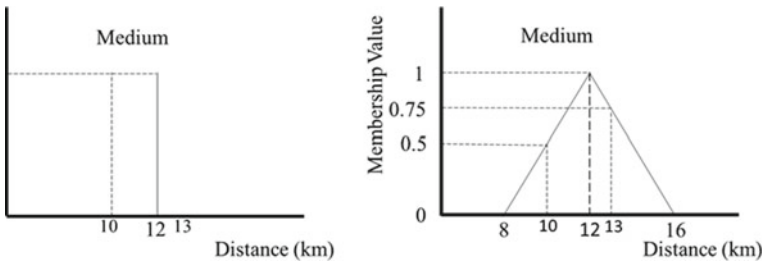


Fig. 1 Difference between crisp set and fuzzy set

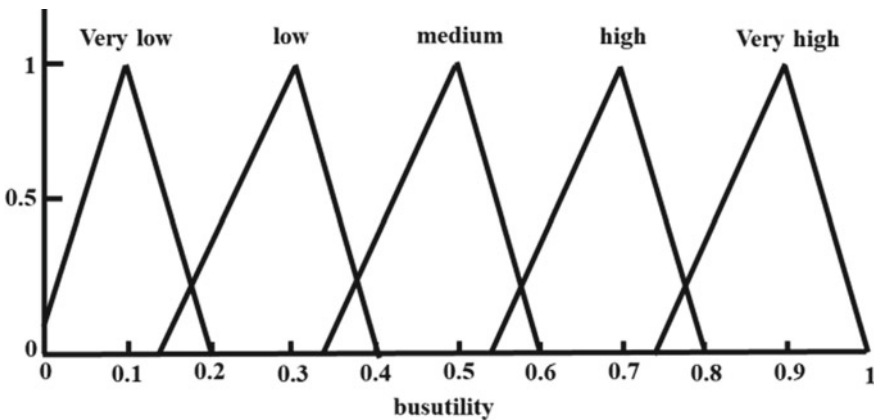


Fig. 2 Membership function plot for bus utility

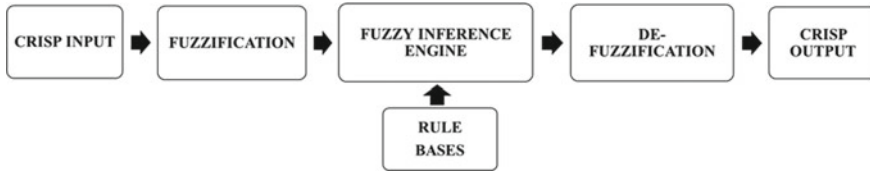


Fig. 3 Fuzzy logic system structure

and analyse based on fuzzy if–then rules in the fuzzy inference engine to generate output in the linguistic form, and then de-fuzzify to give crisp output (refer Fig. 3).

4.2 Rule Bases

The output given by the fuzzy logic model depends greatly on the rule bases fed into the model. The if–then rule bases specify the relationship between the input parameters and output parameters. The rule bases in fuzzy logic system are in the following format:

If (input 1) is (Level of MF) and/or (input 2) is (Level of MF), then (output A) is (Level of MF) and (output B) is (Level of MF)

The prediction accuracy of the fuzzy logic-based models can be improved by either modifying the rules or changing the MF levels. The rule bases are usually set based on the results from the descriptive statistical analysis carried out on the data that help reveal the nature of the respondents.

5 Mode Choice Model Using Fuzzy Logic Programming

For this study, pre-COVID-19 and post-lockdown fuzzy logic-based mode choice models were developed using six input parameters: time, travel cost, income, gender, percentage of working to total members in the household, and age. The shape of the MFs for all input and output parameters, except for the gender parameter, was set as triangular based on insights from the literature review, and gender variable was set as trapezoidal (gender does not require fuzzification). The membership levels set for the input and output variables are as given in Table 1.

The available alternatives were set as car, TW, bus, walk, and auto. The input variables were taken in a combination of two, and 300 rules were formulated for each mode for different groups of people according to their vehicle ownership, and a total of 4800 rule bases were set to make a single mode choice model. This way, two fuzzy logic-based mode choice models were developed for the comparison of policies: the pre-COVID-19 model and the post-lockdown model.

Table 1 Membership level ranges

Parameter	Level of MF	Range
Time (in minutes)	Very low	(0 15 30)
	Low	(10 30 50)
	Medium	(30 60 90)
	High	(60 80 100)
	Very high	(80 110 140)
Income group ^a	Very low	(0 0.8 1.5)
	Low	(0.5 1.5 2.5)
	Medium	(1.5 3 4.5)
	High	(3.5 4.5 5.5)
	Very high	(4.5 5.5 6.5)
Age	Very young	(15 20 25)
	Young	(20 30 35)
	Middle age	(30 40 50)
	Senior age	(45 55 60)
	Elder	(55 62 69)
Percentage of working members to total members in the household	Very low	(−20 0 20)
	Low	(6 25 45)
	Medium	(25 50 75)
	High	(55 75 95)
	Very high	(80 100 120)
Travel cost	Very low	(−20 0 20)
	Low	(5 30 60)
	Medium	(35 65 100)
	High	(75 100 130)
	Very high	(100 150 200)
^a Grouping of income—1— ≤ 10,000, 2—10,000 to 20,000, 3—20,000 to 30,000, 4—30,000 to 40,000, 5—50,000 to 100,000, 5— ≥ 100,000		
Bus utility/car utility/walk utility/TW utility/auto utility	Very low	(0 0.1 0.2)
	Low	(0.15 0.3 0.4)
	Medium	(0.35 0.5 0.6)
	High	(0.55 0.7 0.8)
	Very high	(0.75 0.9 1)

5.1 Pre-COVID-19 Fuzzy Logic Mode Choice Model

The prediction accuracy of the pre-COVID-19 fuzzy logic mode choice model is presented in Table 2. About 70% of the data was used for calibration and 30% was

used for validation. The prediction accuracy of the calibrated model was found to be around 70%.

To check its prediction accuracy, the calibrated model was validated using 141 samples, and the results of which are given in Table 3. A prediction accuracy of about 50% was observed for the validation model.

The prediction accuracy of the calibrated model with 70% data for the post-lockdown fuzzy logic mode choice model is illustrated in Table 4. The prediction accuracy of the calibrated model was found to be about 80%.

The calibrated model is further validated to check for prediction accuracy as presented in Table 5. The validated post-lockdown fuzzy logic model was found to have a prediction accuracy of about 57%.

Table 2 Calibrated prediction table for pre-COVID-19 fuzzy logic model

Pre-COVID-19 calibrated model							
	Observed			AUTO	CAR	BUS	Total estimated
		WALK	TW				
Estimated	WALK	0	0	1	0	0	1
	TW	1	169	5	12	43	230
	AUTO	2	0	0	0	0	2
	CAR	3	9	0	24	16	52
	BUS	5	1	0	0	35	41
Total observed		11	179	6	36	94	326
Prediction accuracy	$((0 + 169 + 0 + 24 + 35)/326) * 100 = 69.93\%$						

Table 3 Validated prediction table for pre-COVID-19 fuzzy logic model

Pre-COVID-19 validated model							
	Observed			AUTO	CAR	BUS	Total estimated
		WALK	TW				
Estimated	WALK	0	0	0	0	1	1
	TW	5	51	2	4	35	97
	AUTO	0	0	0	0	1	1
	CAR	1	3	4	9	5	22
	BUS	4	3	1	1	11	20
Total observed		10	57	7	14	53	141
Prediction accuracy	$((0 + 51 + 0 + 9 + 11)/141) * 100 = 50.35\%$						

Table 4 Calibrated prediction table for post-lockdown fuzzy logic model

Post-lockdown calibrated model							
	Observed				CAR	BUS	Total estimated
		WALK	TW	AUTO			
Estimated	WALK	0	0	1	0	0	1
	TW	1	189	4	17	16	227
	AUTO	1	0	0	0	0	1
	CAR	2	8	1	36	7	54
	BUS	5	1	2	0	35	43
Total observed		9	198	8	53	58	326
Prediction accuracy	$((0 + 189 + 0 + 36 + 35)/326) * 100 = 79.75\%$						

Table 5 Validated prediction table for post-lockdown fuzzy logic model

Post-lockdown validated model							
	Observed				CAR	BUS	Total estimated
		WALK	TW	AUTO			
Estimated	WALK	0	0	1	0	0	1
	TW	5	58	3	5	26	97
	AUTO	0	0	0	0	1	1
	CAR	2	5	1	11	3	22
	BUS	5	3	0	1	11	20
Total observed		12	66	5	17	41	141
Prediction accuracy	$((0 + 58 + 0 + 11 + 11)/141) * 100 = 56.73\%$						

6 Policy Sensitivity Analysis

The passenger attraction policies chosen for this study are aimed at reducing the travel time and travel cost parameters by 5%, 10%, and 15% each. An expert opinion survey was carried out to rate the reliability and feasibility of several policies and the following policies were chosen for sensitivity analysis:

- Policy 1: Improving PT coverage and supply, reducing travel time by 5%.
- Policy 2: Parking prohibition on major streets, reducing congestion, and PT travel time by 10%.
- Policy 3: Operating non-stop bus services, reducing PT travel time by 15%
- Policy 4: Early bird pre-peak hour discount of 5%.
- Policy 5: Reducing fare by 10% for return journey for passengers purchasing two-way tickets.
- Policy 6: Providing monthly PT season tickets at 15% subsidy.

Table 6 Pre-COVID-19 modal split after policy sensitivity analysis

MODE	Estimated	Policy1	Policy2	Policy3	Policy4	Policy5	Policy6
Private vehicles	86.7	80.5	80.9	80.9	80.5	79.2	78.8
Public transport	13.3	19.5	19.1	19.1	19.5	20.8	21.2
Shift to PT (%)		6.2	5.8	5.8	6.2	7.5	7.9

Table 7 Post-lockdown modal split after policy sensitivity analysis

MODE	Estimated	Policy1	Policy2	Policy3	Policy4	Policy5	Policy6
Private vehicles	85.9	79.7	80.1	79.9	79.7	79.0	78.8
Public transport	14.1	20.3	19.9	20.1	20.3	21.0	21.2
Shift to PT (%)		6.2	5.8	6.0	6.2	6.9	7.1

The six policies were applied to the pre-COVID-19 fuzzy logic mode choice model, as well as the post-lockdown fuzzy logic mode choice model, facilitating the comparison of how effective these policies will be for both scenarios. The results of the post-lockdown fuzzy logic mode choice model are especially important in formulating policies for a post-pandemic world.

The results of the policy sensitivity analysis for pre-COVID-19 fuzzy logic mode choice model as presented in Table 6 give that Policy 1 and 4 induce a shift to PT buses by 6.2%, Policy 2 and 3 show a shift of 5.8%, while Policy 5 shows a shift of 7.5%, followed by Policy 6 with a shift of 7.9%. It can also be seen that these policies effectively reduce private vehicle usage.

Table 7 contains the results of the policy sensitivity analysis applied on post-lockdown fuzzy logic mode choice model. The results suggest that Policy 1 and 4 will increase PT bus ridership by 6.2%, while Policy 2 will affect the shift by 5.8%. Policy 3 is found to induce a shift of 6.0%. Policy 5 and 6 are found to induce a shift of 6.9% and 7.1%, respectively. As in the pre-COVID-19 mode choice model, the post-lockdown model too predicts a decrease in private vehicle usage with these policies.

7 Results and Discussion

The fuzzy logic mode choice models have satisfactory percentages of prediction accuracy. This can be improved further by changing the level of MFs and/or rule bases. Changing MF levels were found to be more effective and comparatively less time-consuming than changing rule bases. Out of the 469 respondents, only 21 persons (4.4%) were found to use the mode walk, and only 13 persons (2.7%) were found to use auto for both pre-COVID-19 and post-lockdown data sets. The sample size constraints coupled with a prediction accuracy of about 70% for pre-COVID-19 model and about 80% for post-lockdown model explains why these modes were not

predicted. The results of the policy sensitivity analysis of both the pre-COVID-19 and post-lockdown fuzzy logic mode choice models suggest that all the policies considered may increase the PT ridership and reduce private vehicle usage. Comparing the sensitivity analysis results of both pre-COVID-19 and post-lockdown models, the policies induce a private to public modal shift ranging from 5.8 to 7.9% for the pre-COVID-19 scenario, while the post-lockdown model shows a shift ranging from 5.8 to 7.1%. The effectiveness of the PT passenger attraction policies is seen to have reduced for the post-lockdown model, especially for Policy 5 and Policy 6. Decreasing travel time and travel cost by 15%, each is found to induce a greater shift in the post-lockdown model as well as the pre-COVID-19 model. It must be noted that the PT services were not operating to their full capacity at the time of data collection, due to which all the PT users were not given the choice to use PT mode, and therefore, the results do not give a full picture of the pre-COVID-19 PT commuters returning to the PT mode. Another limitation is that the fuzzy logic mode choice model developed in this study does not consider the latent attributes that affect the PT ridership and consequently does not test the effect of policies in improving PT ridership as a consequence of enhancing them. Studies in future can address these limitations by including latent attributes in a fuzzy logic-based mode choice model for a post-pandemic scenario and comparing the findings with pre-COVID-19 results. The results, however, reinforces the importance of gaining back people's trust in PT, while discouraging the ownership and usage of private vehicles for a post-pandemic scenario.

8 Conclusion

The present study attempts to understand the change in the effectiveness of passenger attraction policies that may induce a modal shift from private mode of transport to public mode of transport due to the COVID-19 pandemic. The following are the conclusions drawn from this study:

- The fuzzy logic mode choice models proved to be significantly flexible in evaluating policy sensitivity analysis. However, the model development using trial and error method is a tedious and time-consuming process.
- The PT usage was found to decrease from pre-COVID-19 phase to post-lockdown phase for all trip purposes.
- Improving PT coverage and supply, thereby reducing travel time by 5% induces a modal shift of 6.2% in both the pre-COVID-19 and post-lockdown scenario.
- A modal shift of 5.8% in both pre-COVID-19 scenario and post-COVID-19 scenario is observed when parking prohibition on major streets is introduced, which reduces congestion and PT travel time by 10%.
- Operating non-stop bus services that reduce PT travel time by 15% is found to induce a shift of 5.8% in the pre-COVID-19 scenario and 6.0% for the post-lockdown scenario.

- Early bird pre-peak hour discount of 5% impacts the modal shift by 6.2% for both pre-COVID-19 and post-lockdown scenarios.
- Reducing fare by 10% for the return journey of passengers purchasing two-way tickets improves PT ridership by 7.5% pre-COVID-19 and by 6.9% post-lockdown.
- Providing monthly PT season tickets at 15% subsidy induces a major shift of 7.9% pre-COVID-19 and 7.1% post-lockdown.

References

1. Adnan et al (2020) Examining impacts of time-based pricing strategies in public transportation: a study of Singapore. *Transp Res Part A* 140:127–141
2. Lee and Yeh (2019) Causal effects between bus revenue vehicle-kilometres and bus ridership. *Transp Res Part A* 130:54–64
3. Liu et al (2018) Effects of vehicle restriction policies: analysis using license plate recognition data in Langfang, China. *Transp Res Part A* 118:89–103
4. Liu et al (2020) Noncompliance behaviour against vehicle restriction policy: a case study of Langfang, China. *Transp Res Part A* 132:1020–1033
5. Evangelinos (2018) Pricing workplace parking via cash-out: effects on modal choice and implications for transport policy. *Transp Res Part A* 113:369–380
6. Verma A (2020) Challenges in transportation planning for Asian cities. *J Urban Plan Dev* © ASCE
7. Arellana et al (2020) COVID-19 outbreak in Colombia: an analysis of its impacts on transport systems. *J Adv Transp*
8. Kumar M et al (2013) Development of fuzzy logic based mode choice model considering various public transport policy options. *Int J Traffic Transp Eng*
9. Kedia et al (2017) Transit shift response analysis through fuzzy rule based-choice model: a case study of Indian Metropolitan city. *Transp Dev Econ*

Evaluation of Transit Accessibility by Geoprocessing Techniques for Surat City



Rohit B. Rathod, Gaurang J. Joshi, and Shriniwas S. Arkatkar

Abstract In the journey using public transport, accessibility of transit becomes equally important as mobility. Available mobility modes become successful only when they perform well in accessibility too. The objectives of this study are, by means of geoprocessing techniques, to prepare an accessibility index and use it to evaluate the suitability of the public transport network offered to the various zones and economically active areas present in the municipal area of Surat city. The proposed accessibility index aims to assess the quality of the public transport structure offered regarding its connectivity to different locations and jobs as well as the ease (or difficulty) of access to different public transport modes. The results indicate that the public transport system is effective as an instrument for serving more than the average amount of accessibility to the population but does not show a better range of reachability to higher economically active areas. This tendency can be explained by the higher quality of public transport is experienced in the central and western regions and lower performance in the peripheral areas of the city.

Keywords Public transport · Accessibility · Reachability · Dynamicity · GDP contribution

1 Introduction

A developing country like India has a larger range of population with middle-income category engaged in manufacturing and agricultural activities. With the limited amount of resources, the working population tends to use the lesser amount on

R. B. Rathod (✉) · G. J. Joshi · S. S. Arkatkar
Sardar Vallabhbhai National Institute of Technology, Surat, India
e-mail: rohit.rathod2230@gmail.com

G. J. Joshi
e-mail: gjsvnit92@gmail.com

S. S. Arkatkar
e-mail: sarkatkar@gmail.com

transportation from their earnings. Public transport mode has become the essential mode of transport for the majority of the workforce. Public transport system provides economical as well environmental benefits to the society. In this sense, Rosa [1] emphasizes the importance of public transport as one of the tools to overcome problems, facilitating the access of segregated classes to a greater number of job offers and other services/activities present in the most central areas of urban space. Therefore, it is also necessary to develop tools that facilitate the assessment of the transportation network on offer and serve as a guideline for planning.

For the better performance of the transit system as a whole, equity in mobility and accessibility should be required. The initial step of the journey starts with access to public transport. Accessibility to transit shows how much easiness is available in the system to reach the origin stop. This stop level (local level) accessibility can be expressed by distance or time. The access distance depends on the type of the transit mode. The higher the capacity of the system, the more the ability to walk for access by the users. Ideally, 400 m of access distance is taken for city bus and BRTS system [2, 3] and a higher capacity mode like Metro is taken as 800 m ideally [4, 5]. These ideal distances are very much questionable and do not have strong evidence to justify them. El-Geneidy [6] had stated that the walking distance varies based on the characteristics of the local area and demographics.

Sony Sulaksono [7] explained the concept of equivalent walking distance by considering obstacles like road crossing, foot over bridge, etc. In stop level accessibility, the density of pedestrian streets in the buffer zone has equal importance for defining the accessibility [8, 9].

Network-level (accessibility of public transport) accessibility was explained by different researchers by accessibility index values. Reference [10] introduced the concept of accessibility level measurements with the use of GIS mapping tools. The Local Index of Transit Availability (LITA) [11] was developed to measure the transit accessibility in an area by considering the comfort and convenience aspect that makes this tool distinctive from the passengers' perspective. The Transit Capacity and Quality of Service Manual [12] provides a systematic approach to assessing transit quality and accessibility of service from both spatial and temporal dimensions.

Accessibility always shows the supply-side performance of the system and Gebeyehu [13] developed an index public transport coverage index (PTCI) for assessing the accessibility from the supply side of the system. Micro-level accessibility evaluation can be done by network geospatial-based accessibility index [14] and comprehensive public transport accessibility index [15].

Literature review strongly indicates that there is greater diversity in accessibility measurement by different approaches. The objective of this study is to consider the local level and network-level accessibility together and evaluate the performance of the transit system with the use of geoprocessing techniques for Surat city. The purpose of this index is to serve as a tool for public authorities in the planning of a collective transportation network to serve the transit service with average performance all over the area and connect higher economically active areas strongly.

2 Study Area

The Surat city is located in the eastern part of India, in Gujarat state. Surat city is located in the western part of India, in Gujarat state. The city is known as the ‘Diamond City’—‘Silk City.’ The study area has a population of about 44,66,826 inhabitants and an area of approximately 326 km² as per the Census 2011. According to the research institute of Oxford Economics, Surat will become the fastest growing city in the world by 2035.

At the beginning of the decade, it was observed that the vehicular traffic growth become exponential as the city could not have a well-established public transport system. In the direction of smart city development with the view of sustainable development consideration, the municipal corporation introduced the organized city bus system and Bus Rapid Transit System (BRTS) in 2013. In an integrated manner, both the systems are operated by SITILINK, a special purpose vehicle set up by the Surat municipal corporation. At present, total of 58 routes (46 city bus routes and 12 BRT routes) are in operation which has a network length of 457 km (355 km city bus and 102 km BRT) Fig. 1. With 741 (575 city buses and 166 BRT) fleet size, integrated system has an average daily ridership of 260,000 (before COVID-19 pandemic).

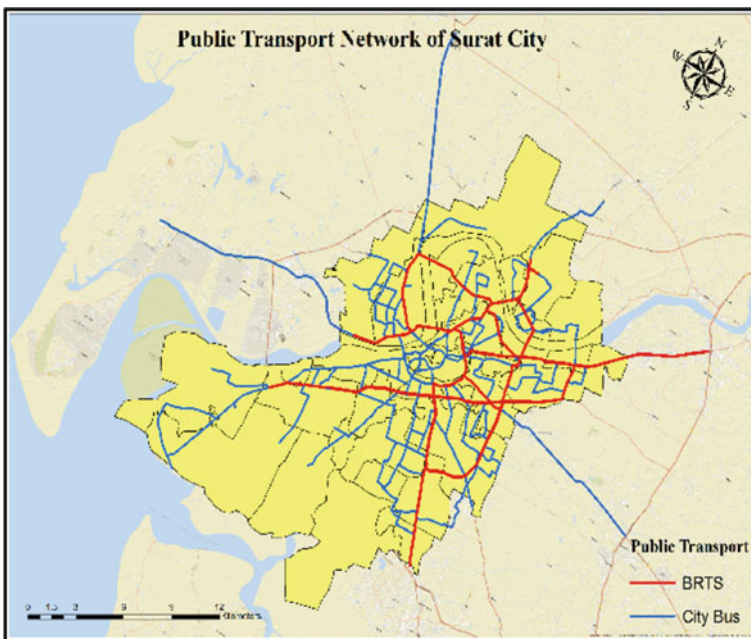


Fig. 1 Existing public transport network in Surat. *Source* Author’s creation

3 Methodology

3.1 Network Geospatial Analysis Based Accessibility Index

Based on the existing network, service, and operational characteristics of the public transportation system, the spatial coverage of the system, accessible amount of destination (reachable locations), and job posts could be estimated. The possibility of access from a given origin to the available number of destinations is dependent on the total travel time characteristics of the given O-D pairs.

Coverage, the reachable number of destinations, and job posts are the major representatives of accessibility through this approach [14]. These representatives are directly or indirectly affected by the maximum (and average) speed and capacity of the available transit modes in the overall public transportation system. An important premise in the elaboration of the accessibility index is that each mode of transit has a degree of importance in facilitating displacements according to their capacity and speed. The capacity of any transit route depends upon the seating capacity of a vehicle and the number of transits scheduled. The number of transits scheduled is varying with the time of the day. The speed of vehicles on each route depends on the traffic flow and the passenger flow, both the flow is varying with the time. During the peak hours, the speed of the vehicles gets reduced due to congestion on roads (or at crossings) and passenger flow increases due to higher demand in that hours. Capacity and speed both make the weight components dynamic over time. Final accessibility representative values have a direct effect of weight, which shows the temporal variation in accessibility.

Indicator 1—Spatial Offer and Coverage of the Various Modes of Public Transport Travel Offered

The first indicator selected to compose the proposed accessibility index aims to measure the spatial range of the available transit system. This indicator assumes that the greater the spatial range of the public transportation modes of travel being offered to a particular locality and how easy it is to reach these modes in that locality, the greater the accessibility.

$$I_1 = \sum_{i=1}^k \left(\frac{A_{\text{cob}_m}}{A_{\text{Tot}}} * W_m \right) \quad (1)$$

I_1 = Indicator 1.

A_{cob_m} = Area of coverage of each mode of transit in a TAZ.

A_{Tot} = Total area of TAZ.

W_m = Weight assigned to each transit mode.

k = Number of transit modes(1).

Indicator 2—Connectivity to Different Locations Through the Various Public Transport Modes Offered

The second indicator selected to compose the proposed accessibility index measures the connectivity of a given origin with the possible number of destinations with the use of public transportation, that is, the objective is to quantify the number of locations with which a specific location is connected by transit modes on a journey.

$$I_2 = \sum_{i=1}^k (N_{d_m} * W_m) \tag{2}$$

I_2 = Indicator 2.

N_{d_m} = Number of destinations reachable by each mode of transit from a given TAZ.

Indicator 3—Connectivity to Job Posts Through the Various Modes of Public Transport Travel Offered

The third indicator selected to compose the proposed accessibility index aims to measure the connectivity to job posts offered by the various modes of travel to a given location. This indicator assumes that the greater the number of job posts reachable by different modes of travel, from any location, the greater the possibility of the individuals from that locality occupying these positions, and the easier their locomotion to their jobs, the more accessibility increases.

$$I_3 = \sum_{i=1}^k (N_{e_m} * W_m) \tag{3}$$

I_3 = Indicator 3.

N_{e_m} = Number of jobs reachable by each mode of transit from a given TAZ.

Weight Assigned to Each Travel Mode

For the calculation of the weight for each mode of public transportation, the criteria used to assign greater or lesser weight refers to the capacity and speed of each modal, thus the following equation was used.

$$W_{m_{si}} = \left(\frac{C_m}{C_{max}} + \frac{V_m}{V_{max}} \right) \div 2 \tag{4}$$

$W_{m_{si}}$ = Weight assigned to the transit mode (without integration).

C_m = Transit mode’s average capacity.

C_{max} = Medium capacity of the largest capacity transit mode.

V_m = Average speed of the transit mode.

V_{max} = Average speed of the highest speed mode.

Each of the above indicators is calculated for each TAZs, out of which some of the TAZs have more than one transit mode at a time; to consider this condition in

the calculation, combine weights are estimated. The combined weights are based on the available route length of each mode of transit in TAZ. Share of a given mode of transit in a TAZ is calculated by the following equation.

$$\text{LPS} = \frac{L_{m_{si}}}{\sum_{i=1}^n (L_{m_{si}})_n} \quad (5)$$

LPS = Length percentage share.

$L_{m_{si}}$ = Route length of a transit mode in TAZ.

n = Number of modes.

Index Composition

The composition of the accessibility index took into account that accessibility can be divided into two complementary concepts, as already mentioned: accessibility to public transport and accessibility of public transport to the destinations. In the given methodology, the indicator 1 is referring accessibility to transit, while indicators 2 and 3 are referring accessibility of public transport as their calculation are based on accessibility as the maximum reachable location. Thus, the index composition was based on the sum of the product between each indicator and its weight.

In past studies, researchers used the arithmetic mean of their respective indicators to formulate the final index value. However, these indicators were calculated for different hours of operations and each given location in the study area. The considered indicators are dependent on frequency and show variations. To consider the effect of frequency variation in accessibility measurement, different weights were assigned to each indicator. In the present study, Analytic Hierarchy Process—Criteria Importance Through Intercriteria Correlation (AHP—CRITIC) method was used to assign weights. In this method, indicators involved in the corresponding level are compared in a pairwise manner, and a numeric scale is designed to calibrate the subsequent results.

$$\text{NGAI} = w_1 * I_1 + w_2 * I_2 + W_3 * I_3 \quad (6)$$

where w_1, w_2, w_3 are the weights for I_1, I_2 , and I_3 , respectively.

4 Accessibility Index Calculation

The methodology to calculate the proposed accessibility index can be divided into four main steps: data acquisition; treatment and processing of data; calculation of the indicators; accessibility index calculation as shown in Fig. 2. It is important to highlight that the standard spatial unit (traffic analysis zones—TAZs) used in this study was developed with the help of census tracts of the 2011 Census/Surat.

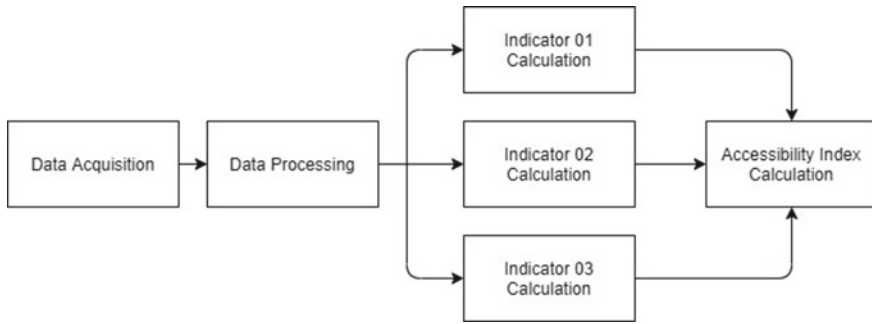


Fig. 2 Flow chart of accessibility index calculation

4.1 Data Acquisition

The present study proposes the use of easily acquired data so that the accessibility index calculation does not demand great resources. Thus, georeferenced public data (in the shapefile format) and alphanumeric data (in the xlsx format) available at the state and local municipal level levels were used as shown in Table 1.

To characterized the actual travel behavior of the passengers into accessibility measurement, a questionnaire survey was conducted. The survey locations were selected based on the higher demand and spatial coverage over the network. 1312 samples with complete information were collected. The collected information has travel characteristics, user’s demographics, and perception data about the transit system. Calculation of the total travel time between selected origin and destination pair was divided into four segments as shown in the following equation,

$$\text{Total travel Time} = \text{Access time} + \text{Total waiting time} + \text{In - vehicle time} + \text{Egress time}$$

Table 1 Data used in the present study

Data type	Information	Source
Georeferenced data	Ward boundary, land-use data	Surat Urban Development Authority
	Public transport network (city bus and BRTS)	Surat Municipal corporation, Surat SITILINK Pvt. Ltd.
	Road network	Open Street Map
Alphanumeric data	Population (census ward wise)	Census-2011 (forecast up to 2019) (SMC website)
	Employment (census ward wise)	Census-2011 (forecast up to 2019) (SMC website)

Access, egress, and waiting time were taken from primary survey data. The in-vehicle travel time has different characteristics on weekdays and off-week days. To take all possible variations of in-vehicle travel time, Google data were collected and considered in the calculation. Over the complete study area, 119 bus stops with higher demand were selected and in-vehicle time between them was noted from the Google data.

4.2 Treatment and Data Processing

The first step of the data treatment and processing was the conversion of the georeferenced data to the same geodetic reference and projection system to avoid compatibility errors in future spatial analysis. Thus, all the georeferenced data were converted to the GCS_WGS_1984 geodetic reference and to the UTM projection system.

Secondly, the census wards were converted into traffic analysis zones (TAZs) by considering homogeneous population density and adjacent boundaries. The proposed methodology was applied to these TAZs. Accessibility indicators and indices were calculated for each of the TAZs.

In the third step, the alphanumeric data were related to their respective georeferenced data through a geographic information system (GIS). Thus, the TAZs shapefile began to have as an attribute the population and number of employees in each of them. The demographic data were available from the 2011 Census data source. Surat city has a population growth rate of 4.5% each year. The census data of population and employment of 2011 were forecasted up to 2019. Finally, the road network and the public transport network were processed in the GIS to generate a single network. Finally, using survey data and Google travel time data total travel time matrix between all TAZs were generated.

Calculation of Indicators

(a) Public transport coverage area and the weights ($W_{m_{si}}$) for each mode used to calculate indicators

The public transport coverage area of given TAZ depends upon the available number of bus stops and their location in the zone. Around all the bus stops, a 400 m radius of buffer circle was constructed. Some of the bus stops have spacing less than twice their radius, which results in the overlapping of the buffer zone. To minimize the duplication of buffer areas, overlapped areas were merged. Figure 3 shows the public transport coverage area of Surat city with a 400 m buffer radius. The total coverage area for each TAZ was calculated in the GIS platform.

Weight for each mode was dependent upon the speed and capacity of vehicles. The GPS tracked data of vehicles gave the average speed of the vehicle on each route. The varying headway with the time of the day gave the total number of scheduled transit in each zone. By the use of Eq. (4), weights for each mode were calculated.

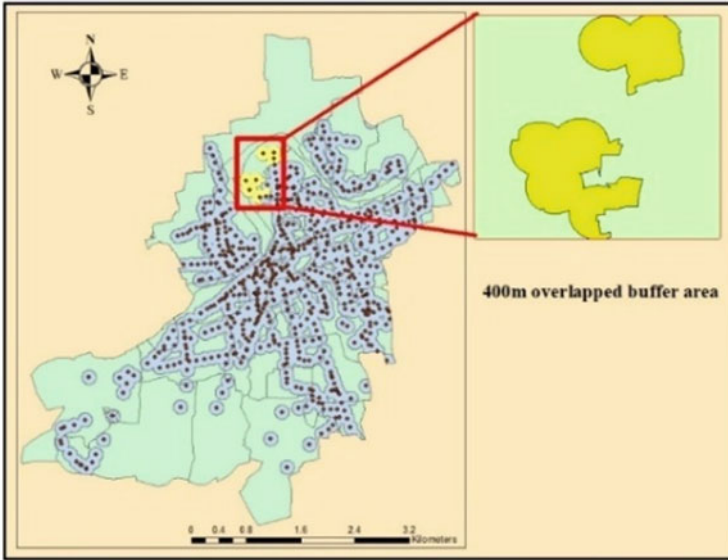


Fig. 3 Coverage area of transit system in Surat city (400 m buffer area)

For the zones with the integrated transit system, combined weights were calculated by the means of Eq. (5). For example, calculated weight values of five TAZs for different operation hours are shown in Table 2.

(b) Indicator 1 Calculation

The calculation of the spatial supply and coverage of the various transit modes of travel was performed through Eq. (1) so that it was considered the area of coverage of each mode of travel. Therefore, for a given TAZ, the ratio between the total coverage area of transit modes in that zone and the total area of the given zone was calculated; the resulting values were multiplied by the weight corresponding to each mode of travel and these results were summed. Finally, the value generated was normalized to produce indicator 1.

Table 2 Weights based on capacity and speed of the individual system

TAZ	Operational period				
	6-7	7-8	8-9	9-10	10-11
1	0.947	0.951	0.958	0.959	0.960
2	0.925	0.930	0.944	0.941	0.946
3	0.924	0.913	0.935	0.933	0.938
4	0.941	0.825	0.813	0.813	0.821
5	0.956	0.928	0.941	0.943	0.948

Table 3 Memory of indicator 1 calculation for seven TAZs

TAZ	TAZ area (km ²)	Buffer area (km ²)	Indicator 1 (normalized) for different time period		
			8–9	9–10	10–11
1	8.84	7.54	0.446	0.446	0.446
2	0.42	0.36	0.703	0.700	0.704
3	2.83	2.66	0.483	0.482	0.484
4	5.60	3.89	0.298	0.298	0.302
5	11.86	10.33	0.447	0.448	0.451

In this case, the calculation memory for three operation hours and five TAZs has shown in Table 3

The calculated value of indicator 1 represents the accessibility to public transport of a given zone. A higher value indicator indicates easier access to public transportation in that zone.

(c) Indicator 2 Calculation

The calculation of the connectivity to different locations by the different modes of travel in public transport was carried out using Eq. (2) so that it also considered the area covered by each mode of travel. To decide whether an origin zone is reachable to selected destination zones or not, the total travel time of the user survey data was used. 85th percentile [16] of the total travel time of the survey sample was taken as the threshold value for accessibility based on the time. The 85th percentile threshold value was taken from the literature study. For Surat city, the threshold value was calculated as 78 min from the transit users’ data. If from a given TAZ, the total travel time was less or equal to 78 min, which indicates that between this O-D pair, the transit system was accessible. The threshold value for the study area was calculated based on the actual field data after the survey which represents the ground scenario. The generated travel time matrix of 37 TAZs was used to calculate the number of reachable zones. The sum of the number of bus stops in reachable zones gave the reachable number of locations from the selected origin TAZ. These values were multiplied by the weight corresponding to each mode of travel, and these results were added together. Finally, the resulting values were normalized to produce indicator 2.

As an example, Table 4 demonstrates the calculation memory of indicator 2 for five TAZs and three operational hours.

(d) Indicator 3 Calculation

The calculation of the connectivity to job posts by the different modes of travel in public transport was carried out using Eq. (3). As with the other indicators, it considered the area of coverage of each travel mode. The calculation of the number of jobs connected by the transit mode and the employment data in each TAZ was considered. The 2011 census employment data for each ward was forecasted up to 2019 and then considered as evenly distributed over related TAZs. The coverage area

Table 4 Memory of indicator 2 calculation for seven TAZs

TAZ	Reachable number of destination	Indicator 2 (normalized) for different time period		
		8–9	9–10	10–11
1	482	0.887	0.888	0.889
2	204	0.298	0.296	0.298
3	224	0.334	0.333	0.336
4	242	0.306	0.306	0.310
5	167	0.220	0.220	0.222

Table 5 Memory of indicator 3 calculation for seven TAZs

TAZ	Reachable number of job posts	Indicator 3 (normalized) for different time period		
		8–9	9–10	10–11
1	482	0.684	0.684	0.685
2	204	0.066	0.065	0.066
3	224	0.072	0.071	0.072
4	242	0.023	0.023	0.023
5	167	0.145	0.145	0.146

of the transit system is less or equal to the actual area of the TAZ. Based on the ratio of these two areas, the covered number of job posts by transit system was calculated. By following the procedure mentioned in indicator 2, the reachable number of zones was calculated, and the sum of job posts of these reachable TAZs was taken as the reachable number of job posts from the given origin TAZ. These values were multiplied by the weight corresponding to each mode of travel, and these results were added together. Finally, the resulting values were normalized to give indicator 3.

As an example, Table 5 demonstrates the memory of indicator 3 calculation for five TAZs and three operational hours.

4.3 Accessibility Index Calculation

Finally, through Eq. (6), the accessibility index for each TAZ of the study area was calculated for different operational hours. To calculate the weights used in the final equation, AHP-CRITIC method was used. This AHP method calculates weights for different indicators based on the variation in their values. Table 6 shows the weights for all three indicators for five operation hours.

Table 6 Weights for three indicators for final index calculation

Operational time periods	Indicator 1	Indicator 2	Indicator 3
6–7	0.290	0.334	0.376
7–8	0.286	0.342	0.372
8–9	0.293	0.342	0.365
9–10	0.297	0.343	0.360
10–11	0.295	0.345	0.359

Table 7 Accessibility index calculation for seven TAZs

TAZ	Accessibility index values for different operational hours					
	6–7	7–8	8–9	9–10	10–11	11–12
1	0.674	0.679	0.683	0.683	0.685	0.681
2	0.320	0.322	0.332	0.333	0.335	0.355
3	0.275	0.271	0.282	0.283	0.285	0.302
4	0.237	0.202	0.200	0.202	0.205	0.209
5	0.262	0.253	0.259	0.261	0.262	0.272

As an example, Table 7 demonstrates the indexing calculation memory for five TAZs and six operational hours.

5 Results

The results obtained for indicator 1 show that the highest values are concentrated in highly dense areas with narrow streets and, mainly, in the central portion of Surat city. It should be noted that the old city area and the peripheral TAZ of the CBD also show results above 0.5 for indicator 1 (Fig. 4a). Surat city is known as the hub of textile and diamond business. A large number of the working force is also engaged with textile industries; with this point of view, the first phase of the transit system in the city was introduced near textile as well as diamond industrial areas. Regarding the results obtained for indicator 2, the highest values are concentrated in the areas of CBD and textile markets (Fig. 4b). The western part of the city where the first phase of the system was introduced performed well for indicator 3. These areas have better roadway connectivity by flyovers and have a perpendicular crossing network of the north to south direction. The well-connected network system in both the directions (west to CBD and north to south) reduces the overall travel time form and increases the number of reachable job posts from this region (Fig. 4d).

The accessibility index value for Surat city was varying from 0.05 to 0.78. The performance of the integrated transit system is very good in the CBD and the industrial activity areas. The denser and narrow street road network system in CBD increases the value of indicator 1 and reducing the access–egress travel time which results

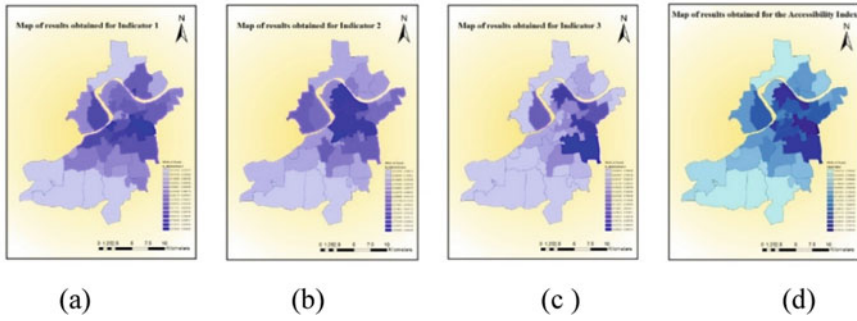


Fig. 4 a–c Are the map for indicators 1, 2, 3, respectively, and **d** is the map for accessibility index

in higher values for indicators 2 and 3. The south region of the city has a newly introduced city bus system with lower frequency. This region does not have BRTS routes. With overall lower capacity in terms of frequency, the outer peripheral TAZs did perform well in all four measurements.

Figure 5 shows the accessibility index values for all the TAZs for each operational hour (16 h of operation per day).

Weights of each mode in different TAZs depends upon the frequency and speed of the vehicle. Both the variables varied with the time of the day. As the system was run with higher frequency and has lower speed values in peak hours, in off-peak hours have higher speed and moderated frequency. This nature of frequency and speed has a direct impact on the overall accessibility of transit. With the time of the day, accessibility has dynamic values. Higher accessibility in peak hours and lower in off-peak hours shows the dynamic nature of accessibility over time. Figure 5 indicates that the higher the accessibility values in a given TAZ, the more the dynamic nature that TAZ has. The zones with poor performance in overall accessibility have less dynamicity in accessibility.

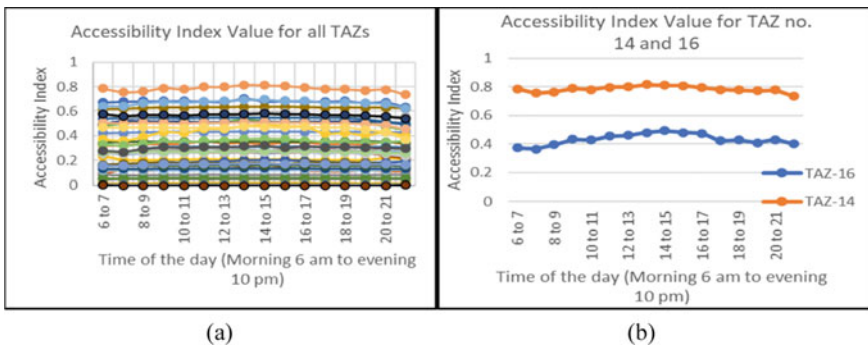
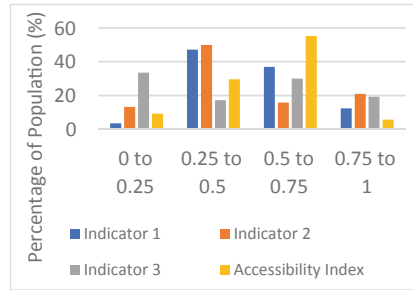


Fig. 5 a Accessibility index for all TAZ and b accessibility index for TAZ no. 14 and 16

Fig. 6 Percentage of population X range of the indicators value and the accessibility index



The zones with a well-established transit system in terms of network, infrastructure, and operation have better performance in the accessibility of transit. Accessibility of public transport is majorly affected by the frequency of the system which results in better performance of accessibility in peak hours. Final observations of the index indicate that accessibility has dynamic nature over time and space.

The majority of the population (47%) is located in areas with values between 0.25 and 0.50 for indicator 1, only 12% of the population is located in areas with values above 0.75. For indicator 2 (50%) and indicator 3 (34%), the majority of the population is located in the area with values between 0.25–0.50 and 0–0.25, respectively. While comparing the percentage share of the population obtain by three indicators, half of the population served very well by transit system for indicated 1 and 2. Indicator 1 is representative of the availability of the transit infrastructure and the calculated value shows the system performs more than average over the study area. Indicator 3 performed very poorly all over the area and population which indicates that the system could not connect all the regions with higher economically active areas. Concerning the accessibility index, more than half of the population (55%) is in areas that register values between 0.5 and 0.75; 30% of the population is in areas with values between 0.25 and 0.5; 9% of the population is in areas with values between 0 and 0.25, and only 9% of the population is in areas with values above 0.75 (Fig. 6).

Common practice says that whenever any new system will going to introduce should be connected and performed well in higher economically active areas. The availability of different sectors (agriculture, commercial, industrial) represents the contribution in GDP to the study area by given zone. The national-level GDP contribution of agriculture, commercial, and industrial is 17%, 29%, and 54%, respectively. Data collected from the Surat development authority include land-use data for the study area. From the land use, the percentage share in the area of each sector in different TAZ was calculated. Based on the percentage area, the percentage contribution in GDP of Surat city by each TAZ was calculated.

Figure 7 shows the TAZ-wise percentage contribution in the GDP of Surat. The dark color area indicates that the zone has a large amount of economically activity and has a higher contribution to GDP. However, lighter color zones have less contribution toward GDP. The transit system should perform well in high activity areas. The range of percentage contribution by different TAZs varies from 0.0005 to 10.5%.

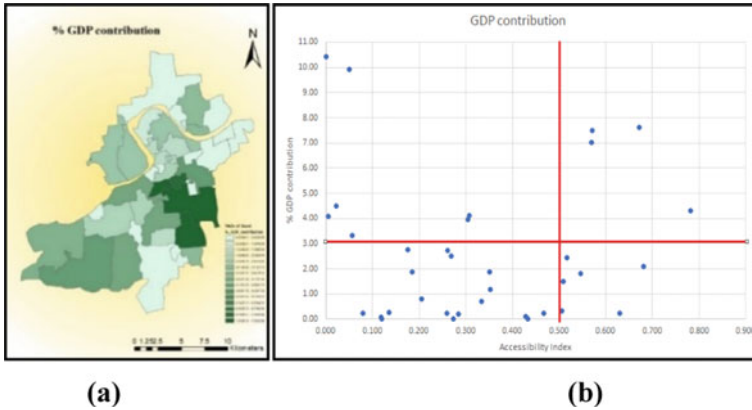


Fig. 7 a TAZ wise % contribution in GDP, **b** relation between % contribution in GDP and accessibility index

An accessibility value less than 0.5 indicates the performance of the transit system is below the average in the given zone. From the available land-use data, Surat city has a minimum of 3% contribution from each TAZs. If we make 3% as the threshold in measurements, the zones with more than 3% contribution value work as higher economically contributory zones. In these zones, the transit system should be performed above the average (0.5) value. But the observation said that some of the TAZ who worked as higher economically contributory zones have accessibility index values below the average. These zones were located in the southern part of the city and have agricultural and heavy industrial activities at most. The sum of the area of all these TAZ (whose GDP contribution was more than 3% and accessibility was less than 0.5) was calculated as 48%.

As indicator 3 indicates, there are very less amount of zones that have accessibility to the higher number of job posts, and analysis of GDP contribution also indicates that half of the highly economically active areas have poor accessibility.

6 Conclusion

The performance of public transportation is evaluated by the accessibility of the integrated transit system of Surat city. The present methodology used three different indicators with different aspects of public transport like availability of the system, ability to reach desire destination, and job posts. Taking all indicators separately, the existing system performs more than average on the availability of transit infrastructure and accessibility to transit stops. The system shows average performance on the ability to reach more numbers of destinations.

Working population with lower income group tend to use less amount of their earning on transportation due to which public transport becomes the most essential

civic service in urban areas. The area with higher economically activity should have better public transport infrastructure and connectivity to all other locations. The existing transport system performs below the average on accessibility aspect of the reachable number of job posts.

Dedicated lanes for the BRT system, availability of good infrastructure, and more number of bus stops per given area show better accessibility performance from the supply side of the system. On the other hand, the system performs average on the ability to reach the number of destinations and job posts which resulting in better performance of the existing system in Surat city at the aggregate level.

The proposed methodology used different weights to calculate the final index value which resulting in the dynamic accessibility over the operational periods per day. According to the characteristics of the given zone, different accessibility values were observed. Combined observations indicate that accessibility of a given study area has temporal and spatial dynamic nature.

The proposed accessibility index met the objective of the present study, but it does not presume to fully comprehend the broad meaning of accessibility, so other indicators can be considered for later studies with different objectives or aiming to improve this index. Another important point is that the accessibility index can gain greater practical usefulness when compared with data on the demand for journeys.

Finally, the geoprocessing techniques were fundamental to enable and streamline the analysis and processes demanded in this study, besides allowing the compatibility of a wide range of data from different sources.

References

1. Rosa SJ (2006) Transporte e Exclusão social: a Mobilidade da População de Baixa Renda da Região Metropolitana de São Paulo e Trem Metropolitano
2. O'Neill WA, Ramsey RD, Chou J (1992) Analysis of transit service areas using geographic information systems
3. García-Palomares JC, Gutiérrez J, Cardozo OD (2013) Walking accessibility to public transport: an analysis based on microdata and GIS," *Environ Plan B: Plan Des* 1087–1102(6):40
4. Kuby M, Barranda A, Upchurch C (2004) Factors influencing light-rail station boardings in the United States. *Transp Res Part A: Policy Pract* 38(3):223–247
5. Agrawal AW, Schlossberg M, Irvin K (2008) How far, by which route and why? A spatial analysis of pedestrian preference. *J Urban Des* 13(1):81–98
6. El-Geneidy AM, Tetreault P, Surprenant-Legault J (2010) Pedestrian access to transit: Identifying redundancies and gaps using a variable service area analysis. In: 89th Transportation research board annual meeting, no. July, pp 1–19
7. Wibowo S, Olszewski PS (2005) Modeling walking accessibility to public transport terminals: case study of Singapore mass rapid transit. *J Eastern Asia Soc Transp Stud* 6:147–156
8. Foda MOA (2010) Using GIS for measuring transit stop accessibility considering actual pedestrian road network. *J Public Transp* 13(4):23–40
9. Gahlot V, Swami BL, Parida M, Kalla P (2013) Availability and accessibility assessment of public transit system in Jaipur city. *Int J Transp Eng* 1(2):81–91
10. Shah J, Adhvaryu B (2016) Public transport accessibility levels for Ahmedabad, India. *J Public Transp* 19(3):19–35
11. Rood T (1999) Local index of transit availability (LITA). Cnu Vi P Anel Present a Tion

12. K. & A. I. P. B. I. K. G. I. T. A. T. Institute (2013) TCRP Report 165: transit capacity and quality of service manual, 3rd edn, Transportation Research Board of the National Academies
13. Gebeyehu MTS-E (2008) Demand responsive route design: GIS application to link downtowns with expansion areas. *J Public Transp* 11(1):43–62
14. R. e. S. P. W. A. d. A. Girão (2017) Accessibility index elaboration by network geospatial analysis. *Mercator* 16(4):1–20
15. Yang RLYLYLHGW Comprehensive public transport service accessibility index-a new approach based on degree centrality and gravity model. *Sustainability (Switzerland)* 11(20)
16. TCAM, SKR, Saptarshi Sen (2018) Assessing travel time reliability of public transport in Kolkata: a case study. In: *Advances in transportation engineering, select proceedings of TRACE, Kolkata, Springer Nature Singapore Pte. Ltd. 2019*, pp 21–34

Evaluation of Users Approbation Indicators of Delhi Metro



Salman Khursheed and Farhan Ahmed Kidwai

Abstract It is important to understand user's approbation indicators for the performance evaluation necessary for the successful operation and sustenance of the public transport system. BLUE line of Delhi Metro has been examined to identify and evaluate the user's approbation indicators. An on-board survey of metro commuters is conducted in December 2020. Some of the approbation indicators included in this paper are choice and captive ridership, access modes, access-egress time, main haul distance and time, interchange stations, metro fare, and comfort factors. The analysis of the data reveals that 57.9% of users are under 30 years and users above the age of 50 years do not prefer metro as primary PT mode. About 43.96% of the users are daily metro riders, whereas the 56.04% has different frequency of metro travel. The metro has 46.5% users as captive riders and remaining 53.5% owns at least one personal vehicle. It is noted that 50.8% of the users do not need parking facility and remaining 49.2% users have different opinions on the availability and affordability of parking facility. About 58.5% of user's report limited to insufficient seating capacity in coach and concourse. Significant users are satisfied with information, signages, and security system provided by Delhi metro. It is revealed that 90% trips have interconnectivity ratio between 0.082 and 0.424 for all access-metro-egress mode combinations. It is also observed that average main haul distance of users is (19.69 ± 11.19) km. To understand the user's approbation indicators and their inter-relationship, decision tree model is analysed and findings are presented.

Keywords Interconnectivity ratio · Decision tree model · Delhi metro fare

S. Khursheed (✉) · F. A. Kidwai
Department of Civil Engineering, Faculty of Engineering and Technology, Jamia Millia Islamia,
New Delhi, India
e-mail: salman.khursheed@spa.ac.in

F. A. Kidwai
e-mail: fkidwai@jmi.ac.in

© The Author(s), under exclusive license to Springer Nature Singapore Pte Ltd. 2023
M. V. L. R. Anjaneyulu et al. (eds.), *Recent Advances in Transportation Systems
Engineering and Management*, Lecture Notes in Civil Engineering 261,
https://doi.org/10.1007/978-981-19-2273-2_24

349

1 Introduction

The user's approbation of the quality of the services offered by the service provider is one of the important aspects for the successful and sustainable operations of any transportation system [1, 2]. The public transportation (PT) system is one of the important engineering intendants with high capital investment along with significant operational and maintenance cost. Depending on the size, extent, technology, economics, and several other factors, the life cycle costs of any public transportation system is a cost intensive decision [3]. Therefore, it is very important to identify the parameters influencing the user's approbation towards Delhi metro (DM) as mode choice, so that the services quality can be made more efficient and cost effective [4]. The periodic performance evaluation of a public transportation system is crucial to improve its efficiency and effectiveness.

Delhi metro (DM) is a popular PT mode for the users considering its route network. It is assumed to be affordable and time efficient with high passenger capacity [3, 5, 6]. The first section of Red line (Line 1) between Shahdara to Tees Hazari was commissioned on 25 December 2002. The "Blue line" (line 3 and 4) being the longest origin–destination route between Dwarka and Barakhamba road was commissioned in December 2005. The most recent expansion of Blue line was commissioned in March 2019 connecting NOIDA city centre to NOIDA electronics city. The entire route of 65.35 kms of Blue line is served through 56 stations including 5 underground, 51 elevated, and 1 at grade [3, 5].

2 Users Approbation Indicators Survey of Delhi Metro

The DM services and its operations of the entire metro network are managed by Delhi Metro Rail Corporation (DMRC) since 2002. The DM conduct periodical user's satisfaction surveys to assess the user's approbation level. The first ever customer satisfaction survey based on European standards–EN13816 is conducted at 22 stations in July 2013 [5]. DM conduct 7th such survey during March–April 2020. The main objective of the survey is to determine the user's perception and approbation level about various aspects of its services. The data of the survey helps DM to understand user's expectations so as to plan further improvement in services. The user's satisfaction survey through online/offline questionnaire includes information about availability, accessibility, reliability, information availability, safety and security, ease of use, and comfort [6].

3 Literature Review

Several researchers have explored different aspects of service quality. It is observed that service quality aspect includes reputation, functional, and technical parameters of the service provider. It is however, noted that functional aspects have more impact on the services quality than technical aspects [7]. It is further noted that physical, interactive, and corporate quality leads to process and output quality of any service provider [8]. In a study, the authors identified ten key factors of service quality as perceived by both the user's and service provider which includes competence, access, reliability, courtesy, responsiveness, security, communication, credibility, understanding/knowing the customer, and tangibility to formulate a service quality model (SERVQUAL) [9]. Based on the previous study, the service quality model (SERVQUAL) is further modified in 1988. The modified framework is based on five determinants including reliability, assurance, tangibles, empathy, and responsiveness and known as (RATER) model [10].

In a research, conducted to analyse the potential correlation between precursors, top events, injuries, and deaths based on CoMET and NOVA benchmarking, and the authors considered 27 precursors for breach in safety and security [11]. In a study, most of the user's approbation indicators reveal that the current patterns of urban travel are not sustainable. The author identifies several factors grouped into behavioural, economic, technological, planning, and management aspects to achieve transportation sustainability [12]. In other study, it is observed that user's satisfaction is very important aspect in the sustainable and successful operations of any PT system [13]. It is noted that for user's approbation, more numbers of ticket counters, more comfort, and reasonable cost are the key components [2]. The authors studied the impact of tangible and intangible factors of customer satisfaction towards DM and observed that operator's assurances, tangibles services, and prompt responsiveness have constructive impact towards customer satisfaction [1]. It is observed that comfort level offered by DM has a significant impact on the commuters, and up-gradation of the passenger's facilities has a positive impact on user's approbation [1]. In other study, the existing operational aspects of multimodalities with focus on functional, temporal, and service quality performance indicators are examined. The research reveals that the access and egress trips connectivity is another important issue to be addressed for improved performance and approbation of operator and users of DM, respectively [14].

In other studies, conducted to identify the various statistical techniques to determine the inter-relationship between the various approbation indicators, the authors have identified that decision tree (DT) is a method to solve classifier combination problem that make use of tree-structured base classifiers [15]. In a study, tree-structured nonparametric classification technique is used to propose an iterative partitioning for individual mode choice prediction [16]. In a study, conducted to compare the predictive performance results of decision trees, neural networks, and

multinomial logit models for mode choice reveals that that decision trees demonstrated higher estimation efficiency and better explicit interpretability among the three methods [17].

From the literature review, it is inferred that macro-level research is carried out in past studies, wherein the variability in the key approbation indicators is not considered across the demographics of a city. Furthermore, only few approbation factors as suggested in CoMET and NOVA standards are taken into consideration for research. Therefore, micro-level research is needed especially on the user's view of service quality considering the variability in the user's approbation perception, demographics, and other factors. Based on the limitations of previous studies and further scope of research, the objectives of this study are to identify the user's approbation indicators, their interdependent behaviours, and to establish qualitatively the factors involved in deciding second best PT system other than DM by proposing a decision tree model considering DT algorithm method. The aim of the model is an indirect assessment of the factors influencing DM as mode choice. Few other user's approbation factors suggested in CoMET and NOVA guidelines including parking facility offered by DM, seating and standing capacities in coaches and concourse, impact of metro fare on its suitability as mode choice, etc. are included in the present research. Further, transfer, waiting, access, egress, and main haul time components are considered to calculate TTT along with variation in main haul distance with respect to users is evaluated. The "BLUE" line serving a particular demography and longest in terms of route/network among all DM lines is chosen to evaluate and identify the variability in user's approbation indicators, so that necessary changes can be planned and implemented to improve the efficiency and ridership of DM.

4 Research Methodology

In the present research, to investigate approbation indicators of DM users, a sizeable and detailed commuter travel data is required. A small pilot study consisting of 60 respondents is conducted initially and based on the experience of non-response faced in the pilot survey owing to the long initial questionnaire, the proforma is modified and redesigned to get only the required information pertaining to the operational parameters of DM and user's perceptions of satisfaction level. A physical on-board survey is conducted to extract the following data.

1. Personal information of the passenger: Age, gender, vehicle ownership.
2. Functional services offered by DM: Preference of parking facilities, fare collection system, frequency of travelling, number of station interchanges, change in travelling time with respect to other PT modes, in vehicle travel time, out vehicle travel time, and main haul distance.
3. Comfort parameters: Standing and seating space in metro coaches and concourse, second best alternative other than DM, security arrangements, information signage's, and metro fare/trip.

A total of 630 random passengers comprising of 364 males and 266 female respondents are interviewed. The data based on the questionnaire is collected and tabulated in statistically standard format and scrutinized logically.

The analysis of survey data is performed using various statistical methods including descriptive statistics and cross-tabulation. Subsequently, random forest/tree decision model technique is performed to understand the inter-relationship among various factors related to approbation indicators of the users. In the present study, few inter-relationships of users including age, gender, second best PT alternative to DM, age, travel frequency in metro, age, ownership of vehicles along with approbation factors related to comfort and security are identified. One of user's approbation indicators in terms of travel time components known as interconnectivity ratio which is defined as ratio of access and egress time to total travel time (TTT) [18] and expressed as $(T_{\text{access}} + T_{\text{egress}})/TTT$ is evaluated. The results of the analysis are presented in the subsequent sections.

5 Data Analysis for Evaluation of User Approbation Indicators

Table 1 gives several inter-relationships among age of users, gender, and their preference of second best alternative of PT to DM. The data is analysed using cross-tabulation and reveals important travel behaviour. It is noted that 57.9% users are below the age of 30 years, 37.5% of users are between 30 and 50 years of age, and only 4.6% is above 50 years. These results are in variation as compared to the study conducted in 2008 [19]. The variation appears due to change in demographics, socio-economic conditions, as well as in access-egress modes over a period of time. It is also noted that males constitute a higher proportion comparing females up to 40 years of age, wherein this proportion changes for users with age more than 40 years. The results further reveal that 43% of commuters prefer cabs, 34.45% users prefer DTC bus, 16.7% prefers auto-rickshaw, 5.2% prefers e-rickshaw, and only 0.65% of commuters prefer feeder bus as second best alternative of PT to DM. These results are in small variation as compared to the study conducted in 2014 [20]. The variation appears due to change in demographics, socio-economic conditions, as well as in access-egress modes over a period of time. It is observed that 59% of commuters below the age of 30 years prefer DTC bus and 60.9% of users in the same age group prefer cab. It is further observed that 37.4% commuters prefer DTC bus and 33.5% prefers cab in the age group of 30–50 years. Only 3.6% and 5.6% of commuters above 50 years of age prefer DTC bus and cab, respectively. Quite importantly, 59.7% of commuters prefer cabs and auto-rickshaw with limited passenger's carrying capacity comparing 34.45% preferring DTC bus. It is revealed that male users in the age group up to 50 years constitute a higher ridership and across all age groups male commuters constitutes 57.8% and female 42.2%. The above results are important to understand the reasons of congestion on Delhi roads. The above noted

Table 1 Gender classifications and second best alternative

Age of respondents (years)	Number of responders (%)	Gender of respondents number (%)		Second best alternative of public transportation after Delhi metro number (%)				
		Male	Female	DTC bus	Cabs	Auto-rickshaw	E-rickshaw	Feeder bus
Less than 20	70 (11.1)	43 (61.4)	27 (38.6)	26 (12)	35 (12.9)	7 (6.7)	2 (6.1)	0 (0)
20–30	295 (46.8)	156 (52.9)	139 (47.1)	102 (47)	130 (48)	42 (40)	19 (57.6)	2 (50)
30–40	169 (26.9)	117 (69.2)	52 (30.8)	62 (28.6)	57 (21)	38 (36.2)	11 (33.3)	1 (25)
40–50	67 (10.6)	36 (53.7)	31 (46.3)	19 (8.8)	34 (12.5)	13 (12.4)	0 (0)	1 (25)
50–60	26 (4.1)	11 (42.3)	15 (57.7)	7 (3.2)	13 (4.8)	5 (4.8)	1 (3)	0 (0)
More than 60	3 (0.5)	1 (33.3)	2 (66.7)	1 (0.4)	2 (0.8)	0 (0)	0 (0)	0 (0)
Total	630 (100)	364 (57.8)	266 (42.2)	217 (34.45)	271 (43)	105 (16.7)	33 (5.2)	4 (0.65)

travelling behaviour may be attributed due to different socio-economic conditions of the different parts of Delhi. The results give an insight that user's approbation indicators include comfort and time effective travelling modes as important factors among others.

Table 2 shows the inter-relationship among age of users and frequency of travelling in DM. It is noted that commuters in the age group of 20–30 years constitutes the highest proportion (46.9%) and 30–40 years of users are next highest group (26%) among all users who travels daily in DM. It reveals that young commuters in 20–30 years of age constitute the group with highest proportion across all travel frequencies. The commuters 40 years of age and above constitute only 18.1% and 7.1% who travels daily or 2–3 times in a week, respectively. It is further noted that only 43.96% users travel daily in DM, whereas those travels 2–3 times in a week or 4–5 times in a month are only 17.78% and 15.26%, respectively.

The above result reveals that DM is a preferred mode for commuters in age group of 20–50 years with purpose of travelling to be either educational or working. This finding is in confirmation to the results obtained in studies conducted in 2008 and 2016, respectively [18, 19].

The middle age group commuters are not regular commuters and seem to use other modes of travelling. There is very small proportion of users above 50 years of age (4.6%) using DM and seems to prefer other modes. These results reveal important travelling and choice pattern of commuters. It is inferred that DM is preferred mode for young commuters, whereas due to age factor, accessibility, access-egress distance, waiting time, and other factors, the older commuters do not prefer DM and as such

Table 2 Age factor versus frequency of travelling in metro

Age of respondents (years)	Occasional (%)	1–2 times in a month (%)	4–5 times in a month (%)	2–3 times in a week (%)	Daily (%)	Total
	10 (11.4)	9 (15.8)	10 (10.4)	16 (14.3)	25 (9)	70 (11.1)
20–30	36 (40.9)	21 (36.9)	47 (48.9)	61 (54.5)	130 (46.9)	295 (46.8)
30–40	27 (30.6)	15 (26.3)	28 (29.2)	27 (24.1)	72 (26)	169 (26.9)
40–50	10 (11.4)	6 (10.5)	9 (9.3)	6 (5.3)	36 (13)	67 (10.6)
50–60	5 (5.7)	6 (10.5)	1 (1.1)	2 (1.8)	12(4.4)	26 (4.1)
More than 60	0 (0)	0 (0)	1 (1.1)	0 (0)	2 (0.7)	3 (0.5)
Total	88 (13.96)	57 (9.04)	96 (15.26)	112 (17.78)	277 (43.96)	630 (100)

enough scope of improvement in metro services are required to make it viable for all age group.

Table 3 shows the inter-relationship between age of commuters and ownership of private vehicles. It is noted that 46.5% of the respondents do not own any vehicle, whereas 30.33% owns two-wheeler and only 20.64% owns four-wheeler. It is observed that 63.1% users below 30 years of age do not own any vehicle, whereas 56.6% of the same age group owns two-wheeler. It is further noted that 73.1% users below 40 years of age own four-wheeler. The data reveals that 46.5% of users are captive riders (those who do not own any vehicles) and 50.97% of users are choice riders (those who own motorized vehicles). These results are in little variation as compared to the studies conducted in 2008 and 2016, respectively [19, 21]. The deviation appears due to change in socio-economic conditions, demographics, as well as in access-egress modes. These results reveal important travelling and choice pattern of commuters. It is inferred that still significant proportion of choice riders does not prefer DM as their travel mode and rely on their vehicles. These results seem to be another factor of congestion on Delhi roads.

Table 3 Age factor versus ownership of personal vehicles

Age of respondents (years)	No vehicle (%)	Number of bicycle (%)	Number of two-wheelers (%)	Number of four-wheelers (%)	Total
	32 (10.9)	4 (25)	28 (14.7)	6 (4.6)	70 (11.1)
20–30	153 (52.2)	9 (56.2)	80 (41.9)	53 (40.8)	295 (46.8)
30–40	68 (23.3)	2 (12.5)	63 (32.9)	36 (27.7)	169 (26.9)
40–50	27 (9.2)	1 (6.3)	16 (8.4)	23 (17.7)	67 (10.6)
50–60	10 (3.4)	0 (0)	4 (2.1)	12 (9.2)	26 (4.1)
More than 60	3 (1)	0 (0)	0 (0)	0 (0)	3 (0.5)
Total	293 (46.5)	16 (2.53)	191 (30.33)	130 (20.64)	630 (100)

Table 4 shows the result of the descriptive analysis of non-tangible user's approbation indicators. A significant proportion of users (50.8%) does not need parking facility. This number corroborates with proportion of captive riders. About 8.1% commuters feel parking facilities as insufficient and unaffordable, whereas 6.5% feels the parking facility as sufficient but unaffordable. Only 20.8% reports to be satisfied with parking facilities. These results corroborate the findings of the study conducted in 2014 [1]. It is noted that 24.2% of users feeling standing capacity in coaches as limited and insufficient, whereas 42.2% feels the same indicator to be enough and sufficient. It is noted that significantly high 58.5% of users report seating capacity in coaches as limited and insufficient, whereas only 23.2% feels the same indicator to have enough and sufficient capacity. These results are in little variation as compared to the studies conducted in 2014 and 2017, respectively [1, 22]. The variation in these findings may be due to the information sought separately for standing and seating capacities. A sizeable proportion of 65.5% reports seating capacity on concourse as insufficient and limited. A significant population (88.4%) reports high satisfaction with the security arrangements and rated as effective to very effective. These results corroborate the findings of the studies conducted in 2014 and 2017, respectively [1, 22]. A good proportion of commuters (77.6%) reports high satisfaction with the information system and signage's. These results also confirm the findings of the studies conducted in 2014 and 2017, respectively [1, 22]. A significant proportion of users (61.1%) reports satisfaction in terms of convenient and comfortable journey in DM. The above analysis suggests there are several aspects including parking facilities, seating spaces in coaches, and on concourse which needs improvement in order to enhance user's approbation level.

6 Data Analysis of Interconnectivity Ratio and Trip Length

Figure 1 shows the relationship between metro trips and interconnectivity ratio (IR). It is seen that IR varies from 0.082 to 0.647. The average IR is observed to be (0.312 ± 0.089) . It is noted that 40% (app.) trips have 0.342 as IR for all access-metro-egress mode combinations. It is further noted that 90% trips have IR between 0.082 and 0.424 for all access-metro-egress mode combinations. These results are in little variation as compared to the studies conducted in 2016 [14, 18]. The deviation appears due to change in demographics, sample size, different catchment zones, and due to change in travel pattern in access-egress modes over a period of time.

Figure 2 shows the inter-relationship between user's and their main haul distance (trip length). The trip length considered in the study corresponds to the metro fare scale. It is observed that the range of main haul distance varies from 0–2 km (6.1%) to 32–58 km. (10.8%). A sizeable user (38.7%) travel for a distance between 12 and 21 km. It is noted that 89.2% of users travel up to 32 km, and 10.8% users travel beyond 32 km. It is an important aspect of users travelling pattern which need attention of DM for performance optimization. It is revealed that the average main haul distance for given sample size is (19.69 ± 11.19) Km. According to a study

Table 4 Descriptive analysis of user's approbation indicators

Is sufficient and affordable parking facility offered by DM	Do not need parking facility No. (%)	Less parking space and unaffordable No. (%)	Less parking space but affordable No. (%)	Enough parking space but unaffordable (%)	Enough parking space and affordable
	320 (50.8)	51 (81)	87 (13.8)	41 (6.5)	131 (20.8)
Sufficient and user-friendly ticket vending machines	Do not use vending	Insufficient and difficult to use	Sufficient but difficult to use	Insufficient but difficult to use	Sufficient and easy to use
	168 (26.7)	38 (6.03)	44 (6.98)	131 (20.79)	249 (39.5)
Sufficient standing space in coaches	Insufficient	Limited	Just sufficient	Sufficient	Enough
	54 (8.6)	98 (15.6)	212 (33.6)	179 (28.4)	87 (13.8)
Sufficient seating space in coaches	Insufficient	Limited	Just sufficient	Sufficient	Enough
	152 (24.1)	217 (34.4)	115 (18.3)	92 (14.6)	54 (8.6)
Sufficient seating space on concourse	Insufficient	Limited	Just sufficient	Sufficient	Enough
	175 (27.8)	238 (37.7)	142 (22.6)	51 (8.1)	24 (3.8)
Adequate security at stations	Need improvement in security measures	Most ineffective	Ineffective	Effective	Very effective
	44 (7.0)	16 (2.5)	13 (2.1)	410 (65.1)	147 (23.3)
Information signages are helpful to locate directions and route	Never	Rarely	Sometimes	Mostly	Always
	34 (5.4)	43 (6.8)	64 (10.2)	243 (38.6)	246 (39)
Is it safe to travel in night	Never	Rarely	Sometimes	Mostly	Always
	69 (11)	41 (6.5)	97 (15.4)	237 (37.6)	186 (29.5)
Is it comfortable and convenient to travel in Delhi metro	Never	Rarely	Sometimes	Mostly	Always
	61 (9.7)	97 (15.4)	87 (13.8)	189 (30.0)	196 (31.1)

conducted in 2016 [18], the average main haul distance observed is (20.3 ± 0.5) Km, which confirm the present research findings. It is to be noted that only main haul distance of a metro trip is reported in this paper. Consequently, overall trip length, including access and egress will be much longer.

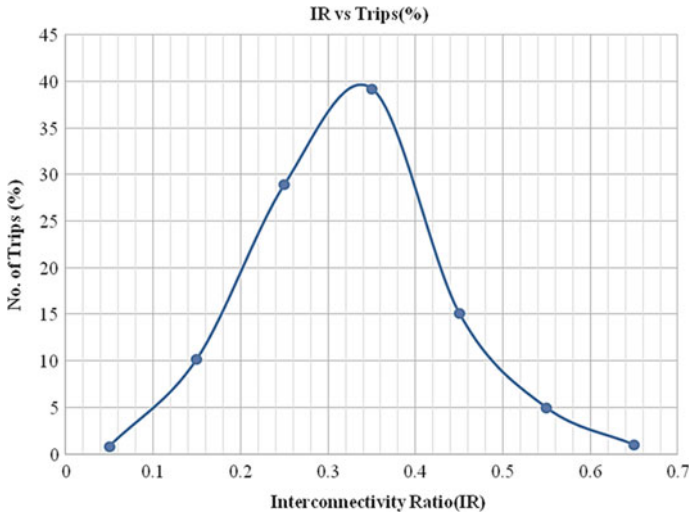


Fig. 1 Interconnectivity ratio versus number of trips (%)

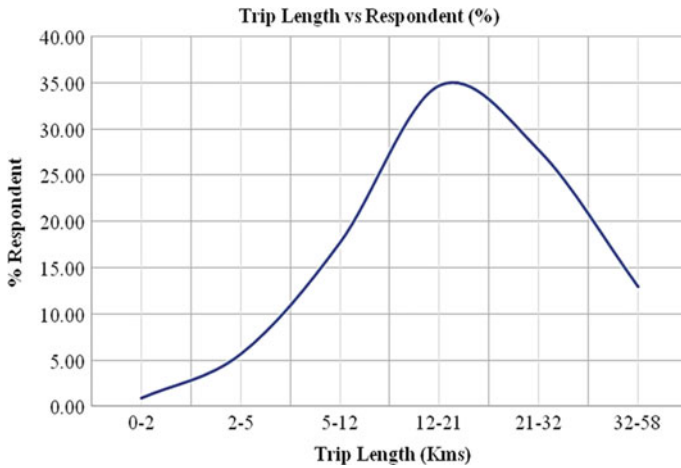


Fig. 2 Trip length versus % of respondents

7 Decision Tree Model

A Decision tree (DT) is a statistical model such that a tree is constructed randomly from a set of possible trees with random features at each node. “A random selection” implies that in the set of trees each tree has an equal chance of being sampled, i.e. trees have a “uniform” distribution. The DT can be generated efficiently and the combination of large sets of random trees generally leads to accurate models. A DT

starts from the root and moves downward. The first node of the tree structure is known as root node, while the last point of tree structure is known as the “leaf” node. Different branches can be extended from each internal node. A node represents a certain characteristic, while the branches represent a range of values [23]. The DTs are considered as a rule-based tool. The allurements of DT-based models lies on the fact that it represents instinctive rules. The tests are so chosen to best discriminate among target choices. Each path from the root to a leaf represents a decision rule [17].

The DT model helps in identifying characteristics of groups, while considering the relationships amidst independent variables in respect of the dependent variable and exhibits the statistics in a flow chart through nodes. This operation is used to understand categorization rules for future events, e.g. categorizing people who are expected to belong to a peculiar group. The most commonly used DT algorithms include chi-square (χ^2), automatic interaction detection (CHAID), classification and regression trees (CART), and the C4.5 algorithm [17]. The authors of a research conducted propose that DT model based on random forest is better with higher prediction precision (98.96%) than the Logit model with prediction precision of (77.31%) [24].

In the study, the authors have used chi-squared automatic interaction detection (CHAID)-based DT algorithm, wherein CHAID considers all discrete data within an independent variable as separate category. The CHAID method considers Pearson’s chi-squared to opt variable cleave.

The DT model as shown in Fig. 3 is developed considering second best alternative of PT other than DM as the dependent variable and non-tangible factors including age, gender, ownership of vehicles, parking facility, ease of ticket vending machines, seating/standing space in metro coach, metro fare is high comparing other PT systems in Delhi, etc. as independent variables.

Table 5 shows the DT model in which at each node, the dependent (category) variable is split into further nodes and predicted variable is identified at respective nodes. It is to be noted that from node 3 to node 9, all the predicted variables are statistically significant at <1% confidence level.

Table 6 shows the inference of the DT model as explained earlier. It is noted that all those commuters (younger and older than 28 years) who feels that the metro fare is “always” high comparing other PT prefers DTC bus as second best alternative to DM. It implies that metro fare is a critical factor for such commuters in their mode choice.

It is further noted that users older than 28 years and feel that metro fare is “never or sometimes” higher prefer cabs as second PT alternatives. It implies that travel comfort and total travel time (TTT) are the critical factors for such commuters in their mode choice. It is revealed that users younger than 28 years of age considering metro fare are “sometimes” higher, and seating space in metro coach as “limited to just OK” prefers cabs as second best alternative other than DM. It implies that comfort is a critical factor for such commuters in their mode choice. It is further revealed that the median and average age of metro users are 28 and (30.73 ± 9.64) years, respectively, for the given sample size.

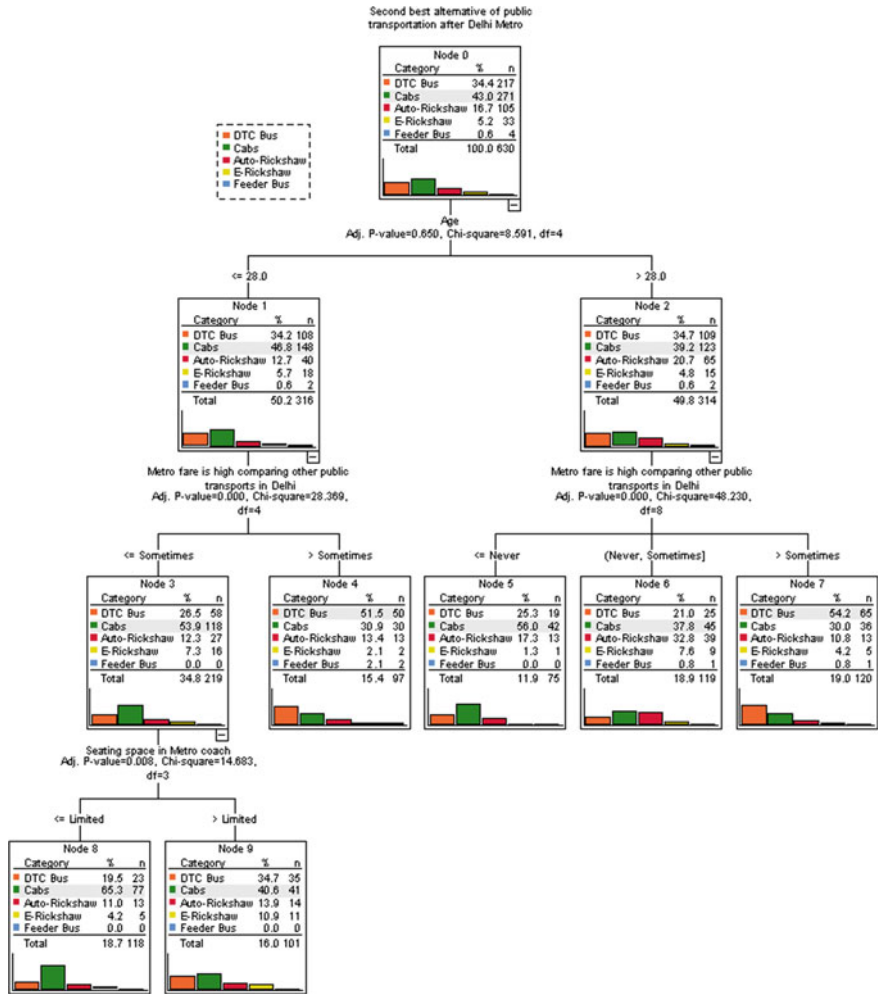


Fig. 3 Decision tree model of users approbation indicators

Table 5 Decision tree model

Node No	DTC bus	Cabs	Auto-rickshaw	E-rickshaw	Feeder bus	Total	Predicted category	Significance
	No. (%)	No. (%)	No. (%)	No. (%)	No. (%)	No. (%)		
0	217 (34.4)	271 (43)	105 (16.7)	33 (5.2)	4 (0.6)	630 (100)		
1	108 (34.2)	148 (46.8)	40 (12.7)	18 (5.7)	2 (0.6)	316 (50.2)	Age	0.65
2	109 (34.7)	123 (39.2)	65 (20.7)	15 (4.8)	2 (0.6)	314 (49.8)	Age	0.65
3	58 (26.5)	118 (53.9)	27 (12.3)	16 (7.3)	0 (0)	219 (34.8)	Metro fare is high comparing other PT in Delhi	0.000***
4	50 (51.5)	30 (30.9)	13 (13.4)	2 (2.1)	2 (2.1)	97 (15.4)	Metro fare is high comparing other PT in Delhi	0.000***
5	19 (25.3)	42 (56)	13 (17.3)	1 (1.3)	0 (0)	75 (11.9)	Metro fare is high comparing other PT in Delhi	0.000***
6	25 (21)	45 (37.8)	39 (32.8)	9 (7.6)	1 (0.8)	119 (18.9)	Metro fare is high comparing other PT in Delhi	0.000***
7	65 (54.2)	36 (30)	13 (10.8)	5 (4.2)	1 (0.8)	120 (19)	Metro fare is high comparing other PT in Delhi	0.000***
8	23 (19.5)	77 (65.3)	13 (11)	5 (4.2)	0 (0)	118 (18.7)	Metro fare is high comparing other PT in Delhi	0.008***
9	35 (34.7)	41 (40.6)	14 (13.9)	11 (10.9)	0 (0)	101 (16)	Metro fare is high comparing other PT in Delhi	0.008***

* $P < 0.1$, ** $P < 0.05$, *** $P < 0.01$

Table 6 Inference of decision tree model

Terminal node	Decision path	Classification group	Number correct	Number wrong
Node 4	Age less than 28 years > Metro fare is high comparing other public transport in Delhi (Always)	DTC buses	50	47
Node 5	Age less than 28 years > Metro fare is high comparing other public transport in Delhi (Never)	Cabs	42	33
Node 6	Age less than 28 years > Metro fare is high comparing other public transport in Delhi (Never or sometimes)	Cabs	45	74
Node 7	Age less than 28 years > Metro fare is high comparing other public transport in Delhi (Always)	DTC buses	65	55
Node 8	Age less than 28 years > Metro fare is high comparing other public transport in Delhi (Sometimes) > and seating space in metro coaches is (limited)	Cabs	77	41
Node 9	Age less than 28 years > Metro fare is high comparing other public transport in Delhi (Sometimes) > and seating space in metro coaches is (sufficient)	Cabs	41	60

8 Conclusion and Recommendations

The conclusions drawn from the above analysis are presented below.

It is revealed that the population less than 40 years of age constitutes 84.8% of the DM users. The result also substantiates the findings of other studies [1, 14]. A significant proportion of users (61.7%) travels either daily or 2–3 times in a week mostly for educational or work-related trips. This result confirms the findings of other studies [1, 14]. The population greater than 50 years of age which constitutes 16.2% of commuters do not prefer DM as their primary transport mode. This result confirms

the findings of other studies [1, 14]. This behaviour may be due to difficulties faced during access-egress trips, reaching, and disembarking from stations. It is observed that for the given sample size and age groups, users prefer “cabs” and “DTC bus” as second and third best alternatives to DM, respectively. These results are in little variation in comparison to the study conducted in 2014 [20]. This behaviour may be due to change in demographics, socio-economic factors, and access-egress modes over a period of time. It is further revealed that less than 44% of commuters use DM daily, whereas the remaining users have different frequencies of travel in DM. These findings are in agreement to the results drawn in studies conducted in 2008 and 2016, respectively [19, 21]. It is analysed that only 46.5% of users are captive riders, whereas the remaining are choice riders having at least one personal vehicle. The results further indicate that 50% of users do not need parking facility and remaining have mixed opinion about adequacy and affordability of parking, wherein a small proportion of users is satisfied with parking affordability and adequacy. These results are in confirmation with the findings of the study conducted in 2014 [1].

A significant number of users report that the seating arrangement in coaches and concourse is limited and insufficient which need improvement. Generally, users are satisfied with the information systems and signages provided by DM. A high proportion of users is satisfied in terms of convenience and comfortable journey in DM. These results are in confirmation with the findings of the studies conducted in 2014 and 2017, respectively [1, 22]. It is revealed that 90% trips have IR between 0.082 and 0.424 for all access-metro-egress mode combinations. These results are in little variations in respective of findings of other studies conducted in 2016 and 2004, respectively [14, 18, 25]. It is observed that 89.2% of users travel up to 32 km, and only 10.8% users travel beyond 32 km. It is further noted that the average main haul distance for given sample size is (19.69 ± 11.19) Km. These results are in confirmation with the findings of the study conducted in 2014 [20].

It is revealed in DT model that median age of users is 28 years for the given study. It is further noted that for users who feels that metro fare is always high prefer DTC as second PT alternative, whereas those users who feels that metro fare is sometimes higher prefer cabs as second PT alternative. The critical factors observed are metro fare, comfort, and TTT while deciding metro as mode choice.

From the outcomes of the study, following recommendations are proposed. The parking facilities offered by DM are important aspect for choice riders which have further scope of improvement in terms of parking fare and sufficient parking space. Seating capacity is another aspect which has scope of improvement. An optimized seating and standing arrangement may be explored to improve the comfort without compromising the total coach capacity. The feeder services are important for first and last mile connectivity which needs to be augmented.

9 Limitations and Future Scope of Research

The limitations of the study include sample size and survey of non-metro commuters. The study is limited to the on-board commuters. The comfort factors in reference to different weather conditions, intercity metro network, and metro fare impact are to be studied as future scope of research. A comparative analysis of DM with respect to DTC is also to be studied as future scope of research. The influence of above factors is needed to study on other cities of the country.

References

1. Singh B, Kumar D (2014) Customer satisfaction analysis on services of Delhi metro 1(5):124–131
2. Elangovan K, Kumar CB, Nallusamy S (2018) Study on effect of Chennai Metro Rail Limited routing system and its future growth. *Int J Mech Prod Eng Res Dev* 8(1):1079–1086. <https://doi.org/10.24247/ijmperdfeb2018128>
3. DMRC (2016) DMRC sustainability report. Pap Knowl Towar a Media Hist Doc 12–26
4. CSE (2019) The cost of urban commute: balancing: affordability and sustainability of public transport, p 64
5. DMRC (2015) Sustainability in motion (DMRC operations and maintenance)
6. DMRC (2020) DMRC
7. Christian G (1984) A service quality model and its marketing implications 18(4)
8. Lehtinen JR (1991) Two approaches to service quality dimensions. *Serv Ind J* 11(3):287–303. <https://doi.org/10.1080/02642069100000047>
9. Parasuraman A, Zeithaml VA, Berry LL (1985) A conceptual model of service quality and its implications for future research. *J Mark* 49(4):41. <https://doi.org/10.2307/1251430>
10. Berry LL, Parasuraman A, Zeithaml VA (1988) SERVQUAL: a multiple-item scale for measuring consumer perceptions of service quality. *J Retail* 64(1):12–40
11. Kyriakidis M, Hirsch R, Majumdar A (2012) Metro railway safety: an analysis of accident precursors. *Saf Sci* 50(7):1535–1548. <https://doi.org/10.1016/j.ssci.2012.03.004>
12. Wadhwa L (2000) Sustainable transport: key to sustainable cities 5–24
13. Bag S (2012) Kolkata metro railway and customer satisfaction: an empirical study 2(3)
14. Swami M, Parida M (2016) Diagnostic evaluation of multimodal urban transport system operation in Delhi. August
15. Breiman L (2001) Random forests. *Lect Notes Comput Sci (including Subser Lect Notes Artif Intell Lect Notes Bioinformatics)* 12343:503–515, LNCS. https://doi.org/10.1007/978-3-030-62008-0_35
16. Golias I, Karlaftis MG (2001) An international comparative study of self-reported driver behavior. *Transp Res Part F Traffic Psychol Behav* 4(4):243–256. [https://doi.org/10.1016/S1369-8478\(01\)00026-2](https://doi.org/10.1016/S1369-8478(01)00026-2)
17. Xie C, Lu J, Parkany E (2012) Work travel mode choice modeling with data mining: decision trees and neural networks. *Transp Res Rec* 1854:50–61. <https://doi.org/10.3141/1854-06>
18. Goel R, Tiwari G (2016) Access-egress and other travel characteristics of metro users in Delhi and its satellite cities. *IATSS Res* 39(2):164–172. <https://doi.org/10.1016/j.iatssr.2015.10.001>
19. Bhandari K, Kato H, Hayashi Y (2008) Mrts system in Delhi: increase in mode choice and its mobility and equity implications. *Int J Urban Sci* 12(2):158–172. <https://doi.org/10.1080/12265934.2008.9693638>
20. Goel R, Tiwari G (2014) promoting low carbon transport in India

21. Chauhan V, Suman HK, Bolia NB (2016) Binary logistic model for estimation of mode shift into Delhi metro. *Open Transp J* 10(1):124–136. <https://doi.org/10.2174/1874447801610010124>
22. Thanai D, Chugh N (2017) Customer satisfaction towards Delhi Metro Rail Corporation. XVIII Annu Int Conf Proc 978:264–276. [Online]. Available: http://www.internationalseminar.org/XVIII_AIC/TS5A/Dishathanai_264-276_pdf
23. Ali J, Khan R, Ahmad N, Maqsood I (2012) Random forests and decision trees. *Int J Comput Sci Issues* 9(5):272–278
24. C. R. Sekhar, Minal, and E. Madhu, “Mode Choice Analysis Using Random Forrest Decision Trees,” *Transp. Res. Procedia*, vol. 17, no. December 2014, pp. 644–652, 2016, doi: <https://doi.org/10.1016/j.trpro.2016.11.119>.
25. Krygsman S, Dijst M, Arentze T (2004) Multimodal public transport: An analysis of travel time elements and the interconnectivity ratio. *Transp Policy* 11(3):265–275. <https://doi.org/10.1016/j.tranpol.2003.12.001>

“Multi-criteria Approach for Identification of Suitable Land Parcels to Develop Intermodal Transit Hubs: A Case Study of Bengaluru, India”



Krishna Saw and Priyanka Kataria

Abstract Implementation of sustainable urban mobility solutions is key to address congestion challenges in India. To promote sustainable urban mobility, intermodal transit hubs (IMTHs) catering to various transit modes have emerged as one of the successful strategies, as it helps change the mobility pattern of the city and reduce traffic accidents and greenhouse gas emissions. Public and private transport operators, such as KSRTC and APRTC, cater to the intercity passenger demand in Bengaluru. Presently, the intercity buses travel all the way to the city centre, which operations result in duplication of services as well as traffic congestion within the city. The IMTHs need to be developed at the city’s periphery to avoid duplication of services and provide for seamless transfer of passengers to and from the city via intra-city modes available at IMTHs. The aim of the present study, therefore, is to identify suitable sites for the development of IMTHs at different locations on the periphery of Bengaluru. A multi-criteria approach has been adopted to evaluate various identified sites (land parcels). The evaluation parameters have been classified under several categories based on the site characteristics, such as area, transit operations, connectivity, economic development and constructability. Based on reconnaissance surveys and secondary data, the scores are assigned on a Likert scale to each potential site, and they are ranked based on the number of categories in which the site qualifies. This paper concludes with a recommendation of one most feasible site for each location based on evaluation results for implementation of the IMTH.

Keywords Intermodal transit · Multi-criteria · Urban mobility · Land parcel · Public transport

K. Saw (✉) · P. Kataria
RITES Limited, Gurgaon, India
e-mail: kriscivil_10@yahoo.com

P. Kataria
e-mail: priyanka.kataria@rites.com

1 Introduction

Until recently, the focus of most of the transport policies for Indian cities used to be on private vehicle-oriented transport. For instance, the Automotive Mission Plan's (2006–2016) aim was to make India the destination of choice in the world for the design and manufacture of automobiles [1]. This has resulted in rapid growth of private vehicles, such as two wheelers and cars, especially in metropolitan cities, where a huge demand for passenger and freight transport is observed due to their being centres of economic activities. For instance, private vehicle ownership in Bengaluru has increased from 284 vehicles per 1000 persons in 2001 to 419 vehicles per 1000 persons in 2011 [2]. The increased use of private vehicles has aggravated the adverse effects of transport. For illustration, the recent global report on congestion shows that Bengaluru is on top of the list of Indian cities with respect to traffic congestion levels, followed by Mumbai, Pune and Delhi [3].

In the wake of global paradigm shifts towards sustainable development, the focus of transport planners has now shifted towards sustainable urban mobility (SUM) measures to overcome the adverse effects of transportation, such as traffic congestion, road accidents and air pollution [4]. SUM refers to meeting the mobility needs of a society with minimum environmental damage and does not impair the mobility needs of future generations [5]. Bengaluru city has undertaken various initiatives in order to promote SUM. A few of the initiatives at the city level include upgradation of city bus services, implementation of an intelligent transport system such as vehicle tracking system, electronic ticketing machine, passenger information system, implementation of metro rail, revival of suburban rail, promoting electric vehicles, improving accessibility to transit stations [6]. One of the major elements of SUM is the accessibility to and seamless connectivity of the public transport system [7, 8]. A well-integrated public transport system facilitates door-to-door services that tempt commuters to change their travel mode and consequently, changes the mobility pattern of the city [9, 10]. The desired level of accessibility to public transport can be achieved only if there is an effective multimodal integration in terms of physical parameters (route structure, stops, stations, etc.), operational parameters (schedules), information parameters (trip planning, arrival and departure, etc.), fare parameters (common card mobility) and institutional parameters (policy and regulations) [11, 12]. Multimodal integration refers to the integration of two or more transit modes necessary to complete the journey from an origin to a destination [13–15]. IMTH is a facility that facilitates physical integration of multiple travel modes.

Karnataka State Road Transport Corporation's (KSRTC) services and privately owned buses cater to the intercity demand and connect to various parts of Karnataka and other neighbouring states. At present, all intercity buses move to the core of the city resulting in a duplication of services as well as traffic congestion on city roads. At the same time, intercity buses lose their commercial operation time due to slow speed in the core part of the city on account of traffic congestion. For instance, the travel speeds of buses in the core part of the city are in the range of 15–20 kmph [16, 17]. On the contrary, buses achieve speeds of 40 kmph or more on the

outside of the city [18]. Further, intercity commuters also access and egress intercity and interstate buses via the city centre, which add additional traffic to the city over and above the daily traffic. Therefore, the local authority has taken a sustainable initiative to develop eight intercity IMTHs at periphery of the city. This initiative will not only help to reduce congestion in the core part of the city, but will also help enhance the commercial operation distance of intercity and interstate buses. The locations (areas) of IMTHs are earmarked in such a way that they optimize travel time and travel distance for access and egress of commuters from other parts of the city. However, the actual site of IMTH is more important as it does not only improve the transport system, but also promote the development of urban regional economy significantly [19].

With an aim to promote seamless public transport, efficient management of public transport in the city and to ensure that public and private intercity and interstate buses do not enter the heart of the city, the main objectives of the present study are twofold. The first objective is the identification of the potential sites for development of the intercity IMTHs, and the second objective is the evaluation and selection of most the suitable sites for the development of IMTHs. A multi-criteria approach has been adopted to evaluate various identified sites. The scope of the present study is limited to only three IMTHs.

2 About Intermodal Transit Hubs

An IMTH is a transport node that caters to multiple modes of transport and provides a seamless transfer of passengers [20]. The primary objective of an effective IMTH is to provide an efficient and integrated transfer of passengers between various routes and modes of transport [21]. The modern transit hub in a city does not only serve the transfer of passengers within a mode and among modes but is increasingly becoming a hotspot for social, cultural and leisure purposes [22]. Intermodal terminals should provide the following in order to ensure their effectiveness [23]:

- Adequate level of facilities (integration with existing modes, such as metro bus) for passengers' transfer,
- Reliable and adequate operation of the terminal,
- Adequate accessibility to the site for all users (especially the disabled),
- Low-cost travel (i.e. the cost of travel involving transfers should be less than for travel without transfers),
- Shorter travel time compared to that needed for the same trip without transfers,
- Seamless integration within the terminal (movements of passengers from waiting area to boarding platforms).

IMTHs can be tailor made based on the characteristics including location, area, type of mode and passenger characteristics. Based on these characteristics, IMTH can be categorized into five types, i.e., intercity terminals, intra-city terminals,

interchanges, park and ride and on-street multimodal integration [24]. An intercity terminal mainly serves passengers travelling relatively long distances between cities or states. Considering the mode, intercity terminals may further be categorized into rail terminals, bus terminals, airports and port terminals. Intra-city terminal mainly provides travel to and from an urban centre from the surrounding areas. Interchanges are intermodal facilities developed at the connection points of different transport modes, services and routes [13]. Park and ride terminal facilities are provided on outskirts of a city where density is low [25]. On-street facilities are various public transport stops that serve different routes of bus or tram networks or transfers between different modes.

IMTH is a multipurpose tool of all avoid-shift-improve strategies [26]:

1. **Avoid and Planning:** Located in the optimal position, hubs help avoid unnecessary trips/long trips.
2. **Shift and Governance:** When implementing hubs, the government provides land, access, and finance.
3. **Improve and Technologies:** Effective design and smart technologies can greatly enhance an IMTH facility by providing physical, operational and institutional integration and make dwell times more pleasant and productive.

It is imperative that the design of IMTH considers sufficient infrastructure for all modes. Efficient use of information technology for dissemination of information to passengers is essential, and cooperation and coordination among the agencies are some of the key factors for a successful IMTH. A well-designed IMTH can result in better utilization of existing infrastructure, lower prices, reduction in the need for additional infrastructure, increased profitability and better customer service.

3 Literature Base: Evaluation Parameters

The planning of an IMTH requires consideration of several parameters. The main function of the IMTH is to accommodate the needs of all users while creating a user-friendly and attractive facility for them. The key planning parameters are physical location, design of the facility and potential for economic development. The physical location, i.e., the site location, of the IMTH, is most important from a coverage, connectivity and future development point of view. The selection of sites for IMTH involves various engineering, economical, institutional and social perspectives. Give some examples of these perspectives. The existing literature indicates that multiple criteria in these categories have been adopted to finalize the IMTH location [27–29].

Farkas [27] categorized site selection criteria into engineering, economic, institutional and social aspects. Major elements covered under engineering were construction and geology, public utilities and engineering characteristics, whereas economic factors include land acquisition, costs and revenue. Accessibility and connectivity were classified under institutional category, while mobility community disruption and

link to employment & education were included in the social category. Ecology, noise and energy consumption were clustered under environment category.

Zečević et al. [28] categorized the site selection criteria into six main groups, namely land use, connectivity, environmental impact, economic and social criteria, technical criteria and utilities. These criteria were selected based on interviews with experts and other relevant public and private entities. Liu et al. [29] used three main categories of criteria for site selection, i.e., topography, geology and socio-economics. The socio-economic criterion includes land use, proximity to roads and urban built-up areas and population density.

The key criteria for site selection for an IMTH adopted in the study “Newark Intermodal Hub Study, 2012” were ease of access for transit vehicles, available land, opportunity for the creation of nodes for pedestrian, cycle, transit and vehicle circulation and proximity of key destinations [30]. The road pattern is an important aspect for the mobility of the city, and it is also important from the planning aspect of IMTH. The intersection point of radial and orbital lines is one of the suitable locations for the IMTH [20].

The Transport for London’s interchange best practice guidelines (2009) fundamentally focus on improving the IMTH’s experience and expanding passenger choice by making transfers as smooth, seamless and stress free as possible [31]. One of the guiding principles in TfL’s guidelines is to create a sense of place that brings their major focus on the operation and maintenance of IMTH. The guidelines suggest a question-based approach for evaluation, which consists of four themes each consisting of four principles. The four themes are efficiency, usability, understanding and quality.

Transit Passenger Facility Design Guidelines [32] cover primarily design principles and design guidelines for IMTH. The main design guidelines suggested include surrounding pedestrian friendly land uses, accessibility for all users, intermodal integration, life cycle cost, revenue generation opportunities, site ecology and energy consumption. These parameters are also co-related to site selection criteria.

The literature review suggests that site characteristics, accessibility, connectivity, economy, land acquisition, social, environmental and future development are the main parameters that influence the site selection for the development of an IMTH. The present study has categorized these parameters into various categories based on their characteristics and employed them for the evaluation of identified sites.

4 Methodology

A multi-criteria approach has been adopted for the evaluation of potential sites for the development of IMTHs at the periphery of the city. The methodology in the present study is mainly framed based on evaluation parameters selected from a literature review and data collected from reconnaissance surveys and secondary sources. The sources for secondary data include master plan, development plan,

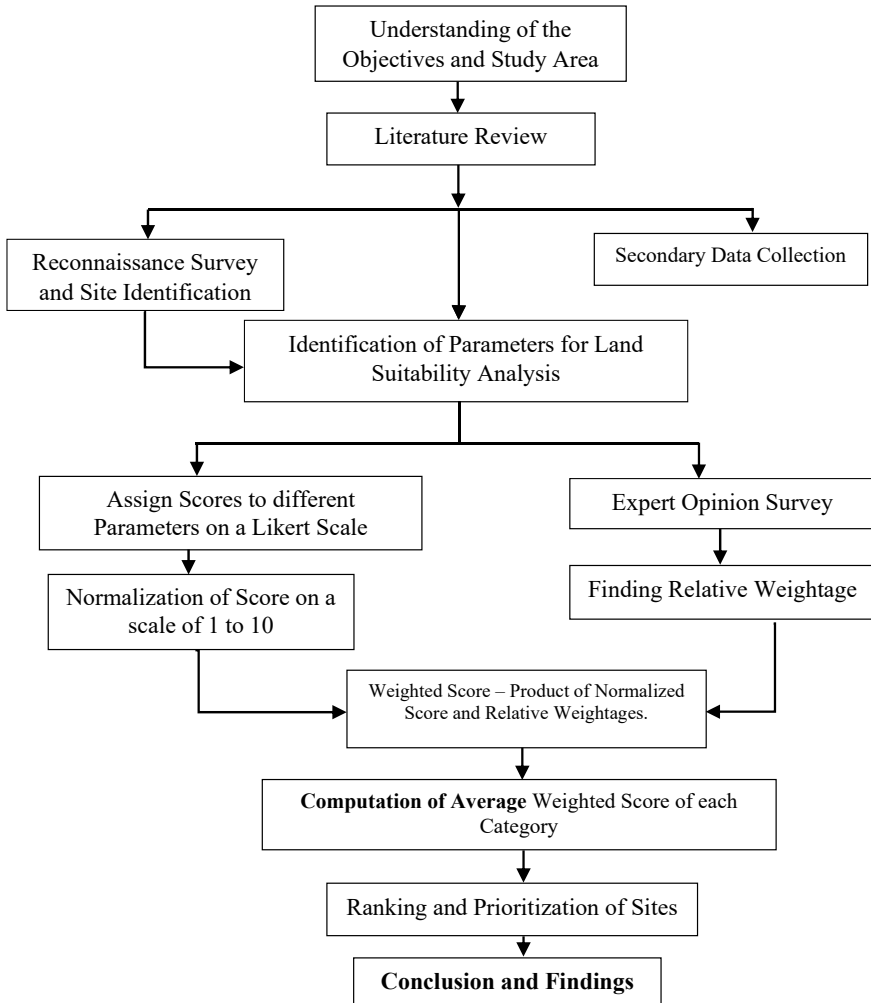


Fig. 1 Methodology—flow chart

comprehensive mobility plan, detailed project reports for metro and other source of information.

The methodology is shown in the flow chart (Fig. 1).

4.1 Study Area

Bengaluru is one of the fast-growing cities in Karnataka State in terms of area, population and vehicle ownership. As per Census 2011, the population of the Bengaluru

Urban Agglomeration was about 8.5 million, and various indicators suggest that 150,000 people move into the city every year as the city is the hub for education and employment. The city is well connected with other parts of state via road. The prominent entry and exit points to the city are Tumkur Road (NH 4), Hosur Road (NH 7), Bangalore Mysore Road, Doddaballapur Road, Bellary Road, Bangalore-Tirupati Highway, and Magadi Main Road (See the map in Fig. 2). In the first phase, locations earmarked for the IMTH development are along the entry/exit roads of Tumkur Road (NH 4), Hosur Road (NH 7) and Bangalore Mysore Road, i.e., Peenya, Bommasandra and Challaghatta, respectively. The salient features of Peenya, Bommasandra and Challaghatta are provided in Table 1.

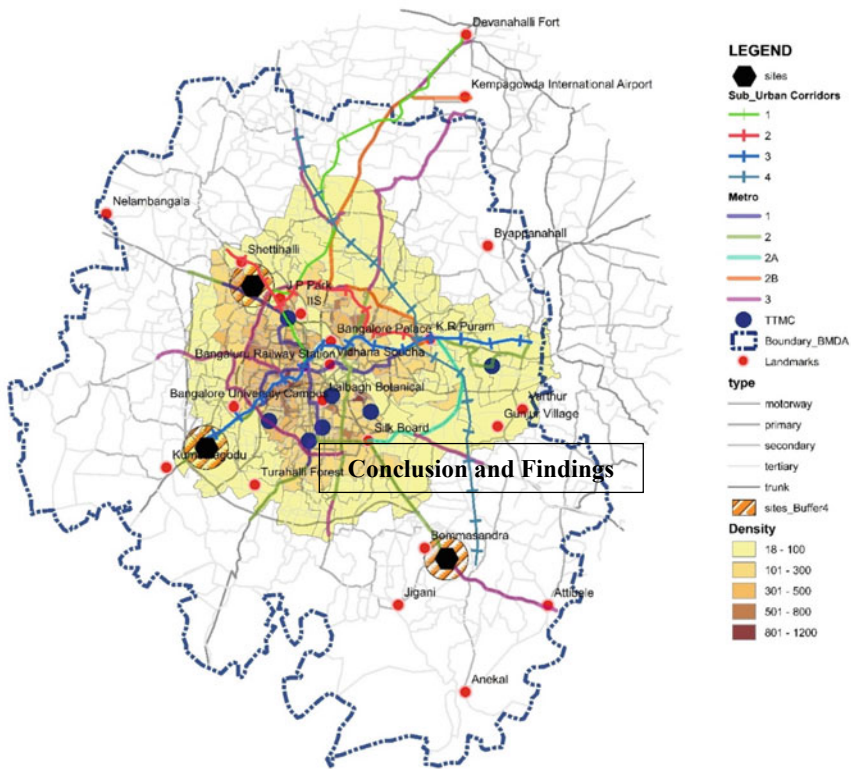


Fig. 2 Bengaluru city map

Table 1 Characteristics of location for IMTHs development

S. No.	Parameters	Area		
		Peenya	Bommasandra	Challaghatta
1	Jurisdiction	Within BBMC	Beyond BBMC	Within BBMC
2	Located along	NH 4 (Tumkur Road)	NH 7 (Hosur Road)	Bangalore–Mysore Road
3	Landmark	Peenya, Yeswanthpur	Electronic City	Kengeri, Mailsandra
4	Land use	Industrial, Residential and Institutional	Industrial	Residential and Commercial
5	Road connectivity	NH 4, Nice Ring Road, 100 ft Ring Road, SH 39	NH 7, NICE Ring Road, SH 35	Nice Ring Road, Bengaluru–Mysore Road
6	PT connectivity	Metro, City Bus	Metro, City Bus, Suburban Rail	Metro, City Bus, Suburban Rail

4.2 Reconnaissance Survey and Identification of Sites

The reconnaissance survey was conducted with twofold objectives in all three areas, i.e., Peenya, Bommasandra and Challaghatta. The first objective is to understand the characteristics of the area in terms of land use pattern, development scenario, road characteristics, public transport connectivity, pedestrian and cycling infrastructure, etc. The second objective is to identify the appropriate vacant land parcels for the development of IMTHs. During the survey, characteristics of identified vacant land such as size of land parcel and land ownership were also collected.

4.3 Site Evaluation Parameters

In view of the literature study, site visits and information collected pertaining to different sites, the parameters for evaluation have been identified. These identified parameters are grouped into five categories, i.e., site characteristics, transit operations, connectivity, revenue generation and future development and constructability as given in Table 2.

Table 2 Parameters identified for land suitability evaluation

S. No.	Parameters
1	<i>Site characteristics</i>
1.1	Site area
1.2	Site connectivity to local transit systems such as Intermediate Para Transit System (IPT), city bus, metro, suburban rail
2	<i>Transit operations</i>
2.1	Accessibility of buses to site from major roads
2.2	Travel time from site to connecting modes
3	<i>Connectivity</i>
3.1	Pedestrian accessibility
3.2	Access to residential/shopping areas/employment/educational centres
4	<i>Revenue generation and future development</i>
4.1	Revenue generation opportunity
4.2	Future expansion possibility
5	<i>Constructability</i>
5.1	Status of land ownership
5.2	Constructability including shape of identified sites
5.3	Demolition required or not
5.4	Minimum disturbance to community

4.4 Evaluation of Sites

Evaluation of sites process involves four steps: scoring, normalization, weighted score and ranking as discussed below:

Scoring

A score was assigned to each of the identified parameters on a Likert scale based on the subjective assessment, except for accessibility of buses and ownership of land. The criteria for assigning the score are detailed in Table 3. The score of accessibility of buses is to be assigned based on Yes and No, while land ownership is based on type of ownership such as government and private. The midpoint of a score is often a neutral point with a positive on one side and a negative on the other side.

Normalization of Scores

Since the scores to the parameters are proposed to be assigned on different scales, it is, therefore, necessary to normalize the assigned scores on a single scale to make them comparable. Therefore, all the parameters shall be normalized on a scale of 1–10. The normalization shall be arrived at by

$$\text{Normalized score} = \frac{(\text{Assigned Score} - \text{Min}_{AS})}{(\text{Max} - \text{Min})_{ASR}} \times (\text{Max} - \text{Min})_{NSR} + 1 \quad (1)$$

Table 3 Scoring criteria for identified parameters

S. No.	Parameters	Description	Measurement criteria	Score
1	<i>Site characteristics</i>			
1.1	Site area	The area extent of the site	>4 acres	3
			2–4 acres	2
			<2 acres	1
1.2	Site connectivity to local transit systems such as IPT, city bus, metro, suburban rail	Availability of number of transit modes (availability shall be considered if IPT and city bus within 200 m, metro within 500 m and suburban rail within 2 km)	4 modes	4
			3 modes	3
			2 modes	2
			1 mode	1
2	<i>Transit operations</i>			
2.1	Accessibility of buses to site from major roads	Direct connectivity or indirect connectivity to the sites from main roads	Yes	1
			No	0
2.2	Travel time from site to nearest transit station (metro)	Time taken for a passenger to reach the site from nearest transit station (metro)	<5 min	5
			5–10 min	4
			10–15 min	3
			15–20 min	2
			>20 min	1
3	<i>Connectivity</i>			
3.1	Pedestrian accessibility	The site must be accessible by walk to commuters around the IMTH and so ever wish to walk. This parameter measures the level of ease to access the site by walk	Very easy	5
3.2			Easy	4
			Moderate	3
			Difficult	2
			More difficult	1

(continued)

Table 3 (continued)

S. No.	Parameters	Description	Measurement criteria	Score
	Access to residential/shopping areas/employment/educational centres	Maximum distance one has to travel to reach nearest activity centres such as residential/shopping areas	Maximum	3
			Moderate	2
			Minimum	1
4	<i>Revenue generation and future development</i>			
4.1	Revenue generation possibility	Development of passenger facilities such as pay and use, property development opportunities such as mall, offices to enhance the revenue	Maximum	3
			Moderate	2
			Minimum	1
4.2	Future expansion possibility	Expansion of bus terminal and other facilities in future	Maximum	3
			Moderate	2
			Minimum	1
5	<i>Constructability</i>			
5.1	Status of land ownership	Ownership of the identified land parcel	Govt.	5
			Pvt.	0
5.2	Constructability including shape of identified sites	Complexity of design and construction and traffic manoeuvrability	Low	3
			Medium	2
			High	1
5.3	Demolition required or not	Requirement of demolition of any structure for developing the land parcel	Minimum	3
			Moderate	2
			Maximum	1
5.4	Disturbance to community	Level of discomfort during construction to the surrounding areas	Minimum	3
			Moderate	2
			Maximum	1

where

NSR—normalized score range

ASR—assigned scoring range

Min_{NS}—minimum value of assigned scale.

Weighted Score

Further, the weighted score shall be computed as a product of normalized score and weightages of each parameter. The weightages of different parameters shall be obtained from different experts of the relevant field using a designed questionnaire

based on the importance on scale of 1–10, where 1 is least important and 10 is highly important.

Ranking of Sites

Subsequently, the average weighted score of each category shall be worked out, and the site which scores equal or more than 0.6 (60%), weighted score shall be considered as qualified in respective category. The site that qualifies in maximum number of categories shall be considered as most suitable and accordingly ranked.

5 Site Identification and Assessment

In order to identify the potential sites for IMTH, extensive site visits and stakeholder consultations were undertaken for Peenya, Bommasandra and Challaghatta. The potential sites were identified and their characteristics such as size of plot, land ownership, road and public transport connectivity, adjoining land use and density were collected. The characteristics of the identified potential sites at Peenya, Bommasandra and Challaghatta are discussed in the subsequent sections.

5.1 Potential Sites at Peenya

Four potential sites have been identified at Peenya for development of IMTH facility as shown in Fig. 3.

Site 1

Site 1 is situated just beside NH 4 (Tumkur Road), and the area of the site is about 4 acres. The site is easily accessible by metro and city bus services. The metro station (Peenya) is just approx. 50 m away from the site, while city bus (BMTC) stops are located at 300–400 m on either side of the site. The site is connected with a major road on one side and a minor road on three sides. KSRTC buses can easily access the site. The ownership of the land is private. Mixed use dense development is observed around the site. Yeshwanthpur Junction Railway Station is located at 3 km.

Site 2

This site is located about 1 km from NH 4 and off Jalahalli Road (Subrato Mukherji Road). The site is adjacent to the existing traffic and transit management centre (TTMC) and the BMRCL metro rail depot. The vacant area is about 2.5 acres, and the ownership of the site is BMRCL. The area of the existing TTMC facility is about 5.5 acres, as the existing TTMC facility is not functioning and can be included in the development of the IMTH facility. The total area will increase to approx. 8 acres. There are three metro rail stations that are located within 1 km of the identified site. The site is accessible from all the major roads.



Fig. 3 Identified potential sites at Peenya location

Sites 3 and 4

Both the sites are located about 7 km away from the Peenya Metro Station and are located near the Bangalore International Exhibition Centre (BIEC). Site 3 is an area of about 14 acres, and Site 4 is an area of about 20 acres. BMRCL has proposed a metro rail station near the sites and it will be operational in the next phase. The sites are accessible from all the major roads. The ownership of the land belongs to BIEC which is private. The disadvantage to these sites is that they are located 7 km away from the Peenya area, it would be difficult for the passengers in terms of interchange with any other transport modes and the ownership of the land is private.

5.2 Potential Sites at Bommasandra

Three potential sites have been identified for the development of IMTH at Bommasandra as shown in Fig. 4.

Site 1 and Site 2

Both sites are located on NH 7 on the left side towards Bangalore. The sites are situated approximately 4 km from the Electronic City Expressway Toll and 13 km from Central Silk Board Junction. The plot size of Site 1 is about 1.63 acres and belongs to BMRCL which is a government organization. Site 2 is about 3.45 acres and belongs to a private agency. The proposed Bommasandra metro rail station is very close to the site and is easily accessible by walk. The city bus stop is also located within 50 m of the site. Heelalige railway station is situated about 2.5 km



Fig. 4 Identified potential sites at Bommasandra location

away from the sites. As these sites are situated on the service road, the disruption to the community is anticipated to be minimal during the construction of the IMTH.

Site 3

Site 3 is located on NH 7 on the left-hand side towards Hosur. The site is approximately 10 km away from the Central Silk Board Junction. The plot size of the site is about 2 acres and the ownership of the land is BMTC, which makes it one of the ideal sites. The existing land is about 10 ft. below with reference to the adjacent main road level, and this feature can be an added advantage for developing a multilevel bus terminal. The site is located at the corner of two sides of a road, making it easy to plan the traffic. The proposed metro station (Electronic City Phase-I Hub) is on the opposite side of the road that needs to be integrated. As the site is at the outside of the planning boundary of BBMP, the area adjoining the site is sparsely developed.

5.3 Potential Sites at Challaghatta

Seven potential sites have been identified at Challaghatta for the development of IMTH as shown in Fig. 5.

Site 1

The potential site is situated along the left side of the Bengaluru–Mysore Road while moving towards Bangalore. The site is in close proximity to the NICE Ring Road and the metro station. The Kengari suburban railway station is about 5 km from the site. The site area is approx. 50.78 acres. An elevated metro depot is proposed at the



Fig. 5 Identified potential sites at Challaghatta location

site. The depot is planned on this elevated deck with an approx. 1,64,000 m² area, and the space available at grade level is being considered for the IMTH. A proposed eight-lane highway passing through the land will subdivide the land parcel into two parts. The highway shall run across the site, sloping down to go beneath the railway tracks to the north-west.

Site 2 and 3

The potential sites 2 and 3 are also located at the intersection of Bengaluru–Mysore Road and NICE Ring Road. The sites are at a distance of about 8 km from the Outer Ring Road. The available area of Sites 2 and 3 is 4 acres and 5.5 acres, respectively. The proposed metro station (Kengeri) is within 1 km of the sites, and the proposed station for suburban rail (Kengeri) is around 2.5 km away. The city bus stop is also available nearby. The land parcels are located in the loops of the expressways which reduces their accessibility. The ownership of potential sites is with NICE.

Site 4

This site is also located next to Site 3 on Bengaluru–Mysore road while moving towards Bengaluru. The site is about 8 km away from the Outer Ring Road. The accessibility of the site is fairly good as it is abutting Bengaluru–Mysore Road and is also well connected with public transit systems. The proposed metro station (Kengeri) and bus stops are close to the site. The available site area is about 6.5 acres. The ownership of the land parcel is private.

Site 5

This site is located next to site number 4 on Bengaluru–Mysore Road. The distance of the site is about 7.5 km from the Outer Ring Road. The site has good accessibility from major roads and is well connected with public transit systems, i.e., city bus and

metro. The site has an area of about 22 acres. The ownership of the land parcel is multiple private parties.

Site 6

This site is located adjacent to the KSRTC depot along the Bengaluru–Mysore Road. The Outer Ring Road is about 8 km from the site. The site has good accessibility from major roads and is well connected with public transit systems. The site area is 12 acres. The ownership of the land parcel is private and is under litigation.

Site 7

The site is abutting Bengaluru–Mysore Road and is located adjacent to Kengeri TTMC. The land parcel has an area of about 3.7 acres. The site is well connected with the metro line and can be integrated with the Kengeri TTMC. The Mailasandra Metro Station is just 200 m from the site, and the proposed Kengeri suburban rail station is also within 1 km. The site belongs to KSRTC.

6 Evaluation of Potential Sites

6.1 Expert Opinion Survey

For the purpose of evaluation, anti-stereotyping is important. Therefore, the view of the industry experts is imperative for making decisions. The weightages of different parameters are important to evaluate the sites and rank them. The weightage given by the experts can be based on either subjective or objective criteria [33]. In the present study, the weightages of the parameters have been obtained from the experts of the relevant field based on subjective information and experience. The attribute weightage was obtained using a designed questionnaire on a scale of 1–10, where 1 is the least important and 10 is highly important. The questionnaire was distributed to ten experts, and the responses of six experts were received. The questionnaire was distributed highlighting the objective of the survey and instructions on how to provide the weightage to the parameters. The weightages provided by experts are summarized in Table 4. The average weightage has been worked out, and it varies from 5 to 9. The minimum weightage, i.e. 5, is given to demolition, whereas maximum is given to accessibility of buses to the site. Further relative weightages have been worked out as the ratio of weightage of individual parameters to the summation of weightages.

6.2 Scores and Ranking of the Sites

In view of the scoring criteria discussed in Sect. 4.4, scores have been assigned to each parameter of the sites based on their characteristics and information. The assigned

Table 4 Weightage of the parameters on scale of 1–10

S. No.	Parameter	E-01	E-02	E-03	E-04	E-05	E-06	Avg.	Relative weight	
1	<i>Site characteristics</i>									
1.1	Site area	6	9	7	10	10	7	8.2	0.09	
1.2	Connectivity to local transit systems such as IPT, city bus, metro, suburban rail	5	10	8	10	10	8	8.5	0.09	
2	<i>Transit operations</i>									
2.1	Accessibility of buses to site from major roads	8	10	10	8	10	8	9	0.09	
2.2	Travel time from site to nearest transit station (metro)	4	5	8	10	10	7	7.3	0.08	
3	<i>Connectivity</i>									
3.1	Pedestrian accessibility	9	8	8	10	10	7	8.7	0.09	
3.2	Access to residential/shopping areas/employment/educational centres	5	9	8	8	9	8	7.8	0.08	
4	<i>Revenue generation and future development</i>									
4.1	Revenue generation opportunity	10	6	10	10	9	8	8.8	0.09	
4.2	Future expansion possibility	–	–	7	10	9	7	8.3	0.09	
5	<i>Constructability</i>									
5.1	Status of land ownership	3	10	7	7	8	10	7.5	0.08	
5.2	Demolition required or not	8	3	2	5	8	4	5	0.05	
5.2	Constructability including shape of identified sites	10	10	5	6	9	5	7.5	0.08	
5.3	Minimum disruption to community	7	9	9	7	10	10	8.7	0.09	

^aE—expert, least important = 1, highest important = 10

scores are summarized in Table 5. Since the scores have been assigned on different scales, it is, therefore, necessary to normalize them on a single scale to make them comparable. Therefore, the assigned scores have been normalized on a scale of 1–10. Subsequently, the weighted score is computed as a product of the assigned score and relative weightage as summarized in Table 6. Based on the weighted score of each parameter, the average weighted score of each category has been worked out. Consequently, the ranking of sites for IMTH considering the average weighted score of each category is worked out. If the site, under a particular category, scores equal or more than 0.6 (60%), the site qualifies that particular category and the site that qualifies in maximum categories is the most suitable.

At Peenya, Site 1 qualifies in three categories, while Site 2 qualifies in four categories. Both Sites 3 and 4 qualify in only two categories. In view of this, Site 2 is most suitable for IMTH as it qualifies in the maximum number of categories followed by Site 1. However, the existing area of Site 2 is only 2.5 acres. Therefore, it must be developed with the existing TTMC, which has an area of about 5.5 acres. For pedestrian accessibility to the site from Peenya metro station, a controlled walkway or skywalk can be constructed. At Bommasandra, Sites 1 and 2 qualify in three categories, while Site 3 qualifies in only two categories. Based on this, Sites 1 and 2 have the potential for development of IMTH, followed by Site 3. It is preferable to combine the two sites to get sufficient land for IMTH. The ownership of Site 1 is BMRCL, whereas Site 2 belongs to a private entity. At Challaghatta, Sites 7 and 5 qualify in the maximum (four) categories, followed by Sites 4 and 6. All sites qualify in the category of site characteristics and transit operations, except Site 2 in site characteristics. Further, only Sites 5 and 7 qualify in the category of connectivity, whereas Sites 4, 5 and 6 qualify in revenue generation and future development, while only Site 7 qualifies in category of constructability. In view of this, Site 7 is the most suitable, followed by Sites 5 and 6.

6.3 Results

Table 7 provides the three most qualifying sites for each location based on sites evaluation outcomes. The table indicates that Sites 2, 1 and 7 are the most qualified sites for Peenya, Bommasandra and Challaghatta, respectively. Site 2 and Site 7 are most appropriate for the development of IMTH at Peenya and Challaghatta, respectively, as they qualified in four categories out of five. However, the area of Site 1 for Bommasandra is only 1.63 acres, which is not sufficient to develop the IMTH. This site can be combined with a second qualified site, i.e., Site 2, as these are adjacent to each other.

Numbers in parentheses are Number of Categories in which particular site qualifies.

Table 5 Assigned scoring to potential sites

S. No.	Parameter	Peenya sites							Bommasandra sites							Challaghatta sites						
		1	2	3	4	1	2	3	1	2	3	4	1	2	3	1	2	3	4	5	6	7
1	<i>Site characteristics</i>																					
1.1	Site area	2	3	3	3	1	2	1	2	1	3	2	3	3	3	3	3	3	3	3	3	2
1.2	Connectivity to local transit systems such as IPT, city bus, metro, suburban rail	4	3	2	2	4	4	3	3	3	3	3	3	3	3	3	3	3	3	3	3	4
2	<i>Transit operations</i>																					
2.1	Accessibility of buses to site from major roads	1	1	1	1	1	1	1	1	1	1	1	1	1	1	1	1	1	1	1	1	1
2.2	Travel time from site to metro station	4	3	1	1	5	5	5	5	5	5	5	5	5	5	5	5	5	5	5	5	5
3	<i>Connectivity</i>																					
3.1	Pedestrian accessibility	4	3	4	4	5	5	4	5	5	4	3	1	1	3	5	3	5	3	5	3	5
3.2	Access to residential/shopping areas/employment/educational centres	3	1	1	1	3	3	3	3	3	3	1	2	2	2	2	2	2	2	2	2	3
4	<i>Revenue generation and future development</i>																					
4.1	Revenue generation opportunity	2	3	3	3	2	2	2	2	2	2	1	1	1	1	3	3	3	2	3	2	3
4.2	Future expansion possibility	1	2	3	3	1	1	1	1	1	1	1	1	1	1	2	3	3	3	3	3	1
5	<i>Constructability</i>																					
5.1	Status of land ownership	0	5	0	0	5	0	5	0	5	0	5	0	5	0	0	0	0	0	0	0	5

(continued)

Table 6 Weighted score

Sr. No.	Parameter	Peenya Sites				Bommasandra Sites			Chalaghatta Sites							
		1	2	3	4	1	2	3	1	2	3	4	5	6	7	
1	Site Characteristics															
1.1	Site area	0.5	0.9	0.9	0.9	0.1	0.5	0.1	0.9	0.5	0.9	0.9	0.9	0.9	0.9	0.5
1.2	Connectivity to local transit systems such as IPT, City bus, Metro, Sub-Urban Rail	0.9	0.6	0.4	0.4	0.9	0.9	0.6	0.6	0.6	0.6	0.6	0.9	0.6	0.6	0.9
	Average	0.70	0.75	0.65	0.65	0.50	0.70	0.35	0.75	0.55	0.75	0.75	0.90	0.75	0.75	0.70
2	Transit Operations															
2.1	Accessibility of buses to site from major roads	0.9	0.9	0.9	0.9	0.9	0.9	0.9	0.9	0.9	0.9	0.9	0.9	0.9	0.9	0.9
2.2	Travel Time from site to Metro Station	0.6	0.4	0.1	0.1	0.8	0.8	0.8	0.8	0.8	0.4	0.6	0.8	0.4	0.4	0.8
	Average	0.75	0.65	0.50	0.50	0.85	0.85	0.85	0.85	0.85	0.65	0.75	0.85	0.65	0.65	0.85
3	Connectivity															
3.1	Pedestrian accessibility	0.7	0.5	0.7	0.7	0.9	0.9	0.7	0.5	0.1	0.1	0.5	0.9	0.5	0.5	0.9
3.2	Access to residential/shopping areas, employment/educational centres	0.8	0.1	0.1	0.1	0.8	0.8	0.8	0.1	0.5	0.5	0.5	0.5	0.5	0.5	0.8
	Average	0.75	0.30	0.40	0.40	0.85	0.85	0.75	0.30	0.30	0.30	0.50	0.70	0.50	0.50	0.85
4	Revenue Generation and Future Development															
4.1	Revenue Generation Opportunity	0.5	0.9	0.9	0.9	0.5	0.5	0.5	0.1	0.1	0.1	0.1	0.9	0.9	0.5	0.9
4.2	Future Expansion Possibility	0.1	0.5	0.9	0.9	0.1	0.1	0.1	0.1	0.1	0.1	0.1	0.5	0.9	0.9	0.1
	Average	0.30	0.70	0.90	0.90	0.30	0.30	0.30	0.10	0.10	0.10	0.10	0.70	0.90	0.70	0.50
5	Constructability															
5.1	Status of land ownership	0.1	0.8	0.1	0.1	0.8	0.1	0.8	0.8	0.1	0.1	0.1	0.1	0.1	0.1	0.8
5.2	Constructability including shape of identified sites	0.8	0.4	0.8	0.8	0.8	0.8	0.1	0.1	0.1	0.1	0.4	0.8	0.8	0.8	0.8
5.3	Demolition required or not	0.5	0.3	0.5	0.5	0.5	0.5	0.1	0.5	0.5	0.5	0.5	0.5	0.5	0.3	0.5
5.4	Minimum disturbance to community	0.1	0.9	0.9	0.9	0.5	0.5	0.1	0.9	0.9	0.9	0.9	0.9	0.9	0.9	0.9
	Average	0.45	0.60	0.58	0.58	0.65	0.48	0.28	0.45	0.10	0.10	0.48	0.58	0.53	0.75	0.75

— Qualified

— Not qualified

Table 7 Shortlisted sites

S. No.	IMTH location	Priority 1	Priority 2	Priority 3
01	Peenya	Site 2—8 acres (4)	Site 1—4 acres (3)	Site 4—20 acres (2)
02	Bommasandra	Site 1—1.63 acres (3)	Site 2—3.45 acres (3)	Site 3—2 acres (2)
03	Challaghatta	Site 7—3.7 acres (4)	Site 5—22 acres (4)	Site 6—12 acres (3)

7 Conclusions

In the present paper, a multi-criteria approach for determining suitable land parcels for the development of IMTHs considering intercity and interstate buses has been demonstrated. Past studies revealed that different studies adopted different parameters for evaluation of land parcels in order to develop IMTHs. Based on the literature review, twelve parameters, under five different categories, were adopted for site evaluation in the present study. These parameters are as follows: site area, connectivity to PT, bus accessibility, travel time to metro station, pedestrian accessibility access to different land use, revenue generation, future development, land ownership, shape of land parcels, demolition and disturbance to community. Expert opinions indicate that these parameters can be grouped into three levels based on their importance. The first level includes site area, connectivity to PT, bus accessibility, pedestrian connectivity, revenue generation and future expansion. The second level covers travel time to and from the metro station, access to different land use, land ownership and shape of the site, while the third level covers demolition. Further, the study suggests that the multi-criteria qualifying approach is more practical than the aggregation of scores of all parameters as the former approach provides results of each category at disaggregate level. Finally, it is important to mention that site area is one of the parameters that must be considered on the basis of the minimum land parcel area requirement in view of the facilities to be developed. Otherwise, a small site, insufficient to develop all facilities, can get selected due to better scoring in other parameters.

References

1. Kuriakose PN (2013) National transport policy of India: organization, issues, and bottlenecks for implementation. *Institute of Town Planners, India Journal*, vol 10×4, October–December, pp 51–70
2. Knight Rank (2020) Bengaluru urban infrastructure report–2020
3. https://www.tomtom.com/en_gb/traffic-index/ visited on 25/05/2021
4. Johansson H, Sandvik KO, Zsidákovits J, Lutczyk G (2016) A need for new methods in the paradigm shift from mobility to sustainable accessibility. *Transp Res Procedia* 14:412–421
5. Rodrigue JP, Comtois C, Slack B (2020) *The geography of transport systems*, 3rd edn. Routledge, New York
6. Bangalore Political Action Committee (2020) Sustainable mobility for Bengaluru

7. Costa MS, Silva ANR, Ramos RAR (2005) Sustainable urban mobility: a comparative study and the basis for a management system in Brazil and Portugal. *WIT Trans Built Environ* 77:323–332
8. United Nations Economic Commission for Europe (2020) A handbook on sustainable urban mobility and spatial planning—Promoting active mobility. United Nations Publication
9. Solecka K, Žak J (2014) Integration of the urban public transportation system with the application of traffic simulation. *Transp Res Procedia* 3:259–268
10. Kamargianni M, Li W, Matyas M, Schäfer A (2016) A critical review of new mobility services for urban transport. *Transp Res Procedia* 14:3294–3303
11. Zimmerman S, Fang K (2015) Public transport service optimization and system integration. *China Transport Topics No. 14*, World Bank Office, Washington
12. Litman T (2021) Introduction to multi-modal transportation planning: principles and practices. Victoria Transport Policy Institute
13. Monzon A, Hernandez S, Ciommo FD (2016) Efficient urban interchanges: the city-HUB model. *Transp Res Procedia* 14:1124–1133
14. Tadi S, Mladen K, Violeta R, Brnjac N (2019) Planning an intermodal terminal for the sustainable transport networks. *Sustainability* 11(4102):1–20
15. Roquel KD, Abad RP, Fillone A (2021) Proximity indexing of public transport terminals in metro Manila. *Sustainability* 13(4216):2–16
16. Alam MA, Ahmed F (2013) Urban transport systems and congestion: a case study of Indian cities. *Transp Commun Bull Asia Pac* 82:33–43
17. Harsha V, Karmarkar O, Verma A (2019) Sustainable urban transport policies to improve public transportation system: a case study of Bengaluru, India. *Transp Res Procedia* 3:3545–3561
18. Gota S, Bosu P, Anthapur K (2014) Improving fuel efficiency and reducing carbon emissions from buses in India. *J Public Transp* 17(3):39–50
19. Fan B, Yang Y, Li L (2018) Integrated optimization of urban agglomeration passenger transport hub location and network design. *EURASIP J Wirel Commun Netw* 2018(168):2–7
20. Margarita L, Bernal MD (2016) Basic parameters for the design of intermodal public transport infrastructures. *Transp Res Procedia* 14:499–508
21. Latinopoulou MP, Iordanopoulos P (2012) Intermodal passengers terminals: design standards for better level of service. *Procedia—Soc Behav Sci* 48:3297–3306
22. Bell D (2019) Intermodal mobility hubs and user needs. *Soc Sci* 8(2):1–9
23. Latinopoulou MP, Zacharakis E, Basbas S, Politis I (2008) Passenger intermodal terminal stations: role and infrastructure. *WIT Trans Built Environ* 101(XIV):233–242
24. Arup and Associated Consultants (2004) Sacramento Intermodal Transportation Facility. City of Sacramento, USA
25. Molan Y, Simićević J (2018) Park-and-ride system: urban parking management policy. *Int J Traffic Transp Eng* 8(4):426–445
26. <https://smmr.asia/topics/intermodal-mobility-hubs/> visited on 30/05/2021
27. Farkas A (2009) Route/site selection of urban transportation facilities: an integrated GIS/MCDM approach. In: *Proceedings-7th international conference on management, Enterprise and Benchmarking*, Budapest, pp 169–184
28. Zečević S, Tadić S, Krstić M (2017) Intermodal transport terminal location selection using a novel hybrid MCDM model Slobodan. *Int J Uncertainty Fuzziness Knowl-Based Syst* 25(6):853–876
29. Liu R, Zhang K, Zhang Z, Borthwick AGL (2014) Land-use suitability analysis for urban development in Beijing. *J Environ Manage* 145:170–179
30. Kinzelman Kline Gossman (2012) Front street analytics, ADR engineers: Newark intermodal hub planning study, Newark, Ohio
31. Transport for London (2009) Interchange best practice guidelines
32. Translinks (2011) Transit passenger facility design guidelines. Translink Infrastructure Planning, Kingsway, Burnaby
33. Zhang Q, Xiu H (2018) approach to determining attribute weights based on integrating preference information on attributes with decision matrix. *Comput Intell Neurosci* 2018:1–8

Identifying User Preference Criteria for Selecting Public Transportation System as a Mode of Transport: A State-of-the-Art Review



Kanika and Chetan R. Patel

Abstract The review paper aims to provide a comprehensive range of literature on the public transport system comprising all the factors which act as barriers and hinder the efficient movement of the PTS. It is observed that there are minimal articles available that cover the topic of public transportation systems using MCDM (multi-criteria decision-making) techniques to portray the findings and research directions. This compilation of review papers will bring together significant primary research published in presumed peer journals over 25 years regarding PTS. The research will discuss the predominant, hypothetical, conceptual, and theoretical suggestions underneath researching the field of PTS and give a brief review. According to user perception studies, the review result depicts six major indicators and criteria focusing on different researches and practices. These criteria underpin the significant barriers that hinder and affect the passenger's decision to opt for the private vehicle over public transport system. Therefore, the paper's primary objective is to review researches and identify and compile the crucial criteria and barriers.

Keywords Public transport · User perception · Hindrance/barrier

1 Introduction

The public transportation system is one of the most important modes of transportation, particularly in emerging cities. Despite the fact that the importance of public transportation is growing in lockstep with the world's population, the transportation infrastructure required to meet present demand is either lacking or inefficient. As a result, the pace of increase in private vehicles is considerably more significant than the growth rate in public transportation. Furthermore, high car ownership reduces demand for public transit in affluent countries, but demand is higher in developing countries with low vehicle ownership [9]. As a result, evaluating public transportation systems is a strategic decision-making problem that affects both the commercial and

Kanika (✉) · C. R. Patel

Department of Civil Engineering, National Institute of Technology, Surat, India
e-mail: kanu.rohilla2@gmail.com

public transportation sectors. Additionally, it has been observed [3] that when public transportation (light rail transit) lines are established, traffic congestion in several US cities is alleviated. Thus, public transportation is critical for economic growth, energy and resource conservation, congestion reduction, improved air quality, and critical assistance during emergencies and disasters. Additionally, it stimulates growth and boosts the value of real estate, improves mobility in small urban and rural communities, and reduces mobility-related health expenditures. All of this adds up to a better quality of life. But at the same time, it gets noticed by the users and users may not develop negative perception toward the public transportation system due to non-performance of the system. In order to improve public transportation as a mode of choice for urban commuters, it is critical to establish priorities for various criteria for attracting commuters to the public transportation system based on their preferences. Hence, the present study is conducted to compile all the barriers which hinder choosing public transport.

An exhaustive literature review is conducted by evaluating research papers from across the world to determine the criteria and barriers that hinder the effective movement of public transportation. The identified criteria are listed and grouped into sub-criteria. Barriers identified are classified in six major indicators: i.e., physical, operational, social, technical, economic, and environmental. This documented study on the barriers in choice of public transportation system considering the different parameters will help the researchers to explore new area of research.

2 Literature Review

Public transport services have an essential role in providing customers with effective and economical services, attracting future consumers, and efficient use of urban space. It is critical, however, to understand how consumers evaluate supplied services by examining both objective and subjective aspects of service quality assessment. The literature study aims to review the application of MCDM in public transportation. The articles are observed, and their significance is recognized as either the most relevant, relevant, less relevant, or not relevant after the research, as indicated in Table 1. As shown in Fig. 1, a total of 42 papers were reviewed from the last one decade from 2010–2020, and based on their relevance, 31 were finalised for the research.

This section provides a concise review of the literature, with an emphasis on MCDM and customer satisfaction in public transit.

2.1 Basis of Selection

See Fig. 1.

Table 1 List of relevant research papers based on the relevance

	Title	Author	Year	Relevant				Model
				Most	Very	Less	Not	
1	An Integrated Multi-Criteria Approach for Planning Railway Passenger Transport in the Case of Uncertainty	Stoilova [28]	2020		✓			AHP, SIMUS, decision tree model
2	A fuzzy Delphi analytic hierarchy model to rank factors influencing public transit mode choice: A case study	Ebrahimi and Bridgelall [9]	2020	✓				Fuzzy Delphi method, fuzzy AHP
3	State-of-the-art review on multi-criteria decision-making in the transport sector	Yannis et al. [30]	2020		✓			AHP
4	Determining the Importance of the Criteria of Traffic Accessibility using Fuzzy AHP and Rough AHP Method	Stanković [26]	2019	✓				Fuzzy AHP, rough AHP
5	Selection Criteria and Assessment of the Impact of Traffic Accessibility on the Development of Suburbs	Stanković et al. [27]	2018	✓				FAHP
6	An analysis of key factors of financial distress in airline companies in India using fuzzy AHP framework	Mahtani and Garg [22]	2018		✓			FAHP
7	Measuring the quality of PT systems and ranking the bus transit routes using multi-criteria decision-making techniques	Güner [12]	2018		✓			AHP-TOPSIS

(continued)

Table 1 (continued)

	Title	Author	Year	Relevant				Model
				Most	Very	Less	Not	
8	Combining the functional unit concept and the AHP method for performance assessment of public transport options	Pedroso et al. [25]	2018	✓				MCDAM AHP
9	Sustainability assessment of a transportation system under uncertainty: an integrated multi-criteria approach	Ngossaha et al. [24]	2017	✓				FAHP
10	Model for Selection of the Best Location Based on Fuzzy AHP and Hurwitz Methods	Arsovski et al. [1]	2017		✓			Fuzzy AHP, Hurwitz Method
11	A fuzzy-based multi-dimensional and multi-period service quality evaluation outline for rail transit systems	Aydin [2]	2017	✓				Fuzzy trapezoidal no., TOPSIS
12	An integrated MCDM approach to evaluate public transportation systems in Tehran	Nassereddine and Eskandari [23]	2017	✓				Delphi, PROMETHEE, GAHP
13	Sustainable decision making for joint distribution center location choice	He et al. [15]	2017		✓			Fuzzy EW-AHP, fuzzy TOPSIS
14	The importance of service quality attributes in PT: Narrowing the gap between scientific research and practitioners' needs	Guirao et al. [11]	2016		✓			MIMIC models

(continued)

Table 1 (continued)

	Title	Author	Year	Relevant				Model
				Most	Very	Less	Not	
15	Urban bus network of priority lanes: A combined multi-objective, multi-criteria and group decision-making approach	Hadas and Nahum [13]	2016		✓			TOPSIS, AHP, AHP-TOPSIS
16	Road safety analysis using multi criteria approach: A case study in India	Kanuganti et al. [18]	2016		✓			Fuzzy AHP, SAW, AHP
17	Evaluating transit operator efficiency: An enhanced DEA model with constrained fuzzy-AHP cones	Li et al. [20]	2016		✓			DEA Model, fuzzy AHP
18	Multi-criteria analysis model to evaluate transport systems: An application in Florianópolis, Brazil	Barbosa and Ferreira [4]	2016	✓				AHP
19	A hierarchical customer satisfaction framework for evaluating rail transit systems of Istanbul	Aydin et al. [3]	2015	✓				FAHP, fuzzy Choquet integral
20	The performance analysis of PT operators in Tunisia using AHP method	Boujelbene and Derbel [6]	2015	✓				

(continued)

2.2 Customer Satisfaction in Public Transportation

Transportation system quality assessment is the first step in enhancing customer satisfaction. It plays a significant role in elevating customer satisfaction by assessing different criteria related to service quality. Lot many studies have been carried out

Table 1 (continued)

	Title	Author	Year	Relevant				Model
				Most	Very	Less	Not	
21	Reviewing the use of MCDA for the evaluation of transport projects: Time for a multi-actor approach	Macharis and Bernardini [21]	2014		✓			MAMCA
22	Identifying public preferences using multi-criteria decision making for assessing the shift of urban commuters from private to PT: A case study of Delhi	Jain et al. [17]	2014	✓				AHP
23	A multi-dimensional framework for evaluating the transit service performance	Hassan et al. [14]	2013		✓			TOPSIS
24	A hybrid fuzzy methodology to evaluate customer satisfaction in a PTS for Istanbul	Bilişik et al. [5]	2013	✓				Delphi; AHP; TOPSIS
25	An integrated novel interval type-2 fuzzy MCDM method to improve customer satisfaction in PT for Istanbul	Celik et al. [7]	2013	✓				GRA, TOPSIS
26	A two-phased fuzzy multi criteria selection among PT investments for policy-making and risk governance	Kaya et al. [19]	2012		✓			Fuzzy sets, fuzzy AHP
27	Intelligent timetable evaluation using fuzzy AHP	Isaai et al. [16]	2010	✓				FAHP

(continued)

Table 1 (continued)

	Title	Author	Year	Relevant				Model
				Most	Very	Less	Not	
28	On the extent analysis method for fuzzy AHP and its applications	Ying-Ming Wang, Ying Luo	2008		✓			FAHP
29	Fuzzy multi criteria analysis for performance evaluation of bus companies	Yeh et al. [31]	1999		✓			FAHP
30	Fuzzy Multi criteria Ranking of Urban Transportation Investment Alternatives	Teng and Tzeng [29]	1996	✓				FAHP
31	Applications of the extent analysis method on fuzzy AHP	Chang [8]	1996		✓			FAHP

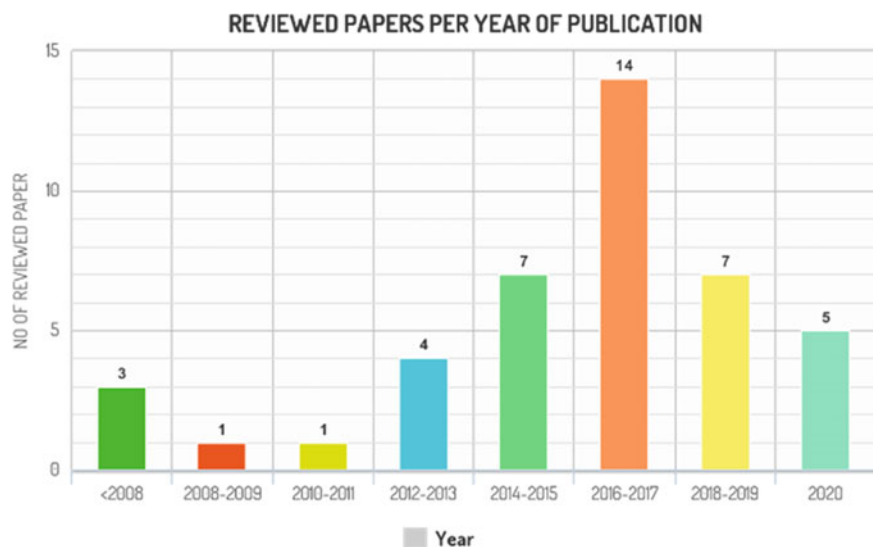


Fig. 1 Reviewed paper as per year of publication. The purpose of selection is based on few factors, such as publication types, year of publication, public transport sector (air transit, rail transit, and bus transit system), and as per the MCDM method, the main focus is given on FAHP and AHP component

which worked on customer satisfaction over 25 years [7], developed a methodology for evaluating Istanbul's five rail transport lines in 2012 [14], proposed a multi-level framework for assessing the performance of public transportation services. The paper has been evaluated based on user perception and various criteria. The perspectives of various stakeholders in public transit services regarding their willingness to participate in a multi-criteria evaluation procedure are weighed.

In terms of determining customer satisfaction in public transportation, several factors are used. Capacity, frequency, comfort, reliability, security, information, staff, cleanliness, ticketing, and pricing are among the most frequently mentioned factors.

Aydin et al. [3], proposes a hierarchical customer satisfaction framework that considers several data analyses (FAHP, fuzzy trapezoidal sets, and Choquet integral) in measuring the performance of the rail transport network in Istanbul. Bilisik et al. [5], used SERVQUAL method for classifying the public transportation service quality via evaluating criteria, evaluations of experts, weighting the criteria, and ranking the alternatives.

This paper provides a global synthesis of literature conducted over public transportation consisting of MCDM techniques and different criteria used as significant factors.

2.3 MCDM in Public Transportation

Multi-criteria decision-making (MCDM) is a concept that allows evaluating multiple criteria to choose the best option. It is a useful tool for solving decision-making issues because it compares alternatives based on multiple criteria. MCDM techniques are gaining popularity in the field of public transportation. Over the last few decades, MCDM techniques have aided decision-making initiatives in public transportation networks. As a result, MCDM has become one of the most important decision-making techniques used by academics, academicians, and government officials to assess customer satisfaction in public transportation systems [7].

A multi-attribute decision-making technique like the Analytical Hierarchy Process (AHP) was created by Saaty (1980) to offer an overall ordering of choices, from the most desired to the least liked [17]. In multi-criteria decision analysis, Analytic Hierarchy Process (AHP) is widely used. Hierarchy formation, priority analysis, and consistency verification are the three main components of AHP. AHP is a strategy for organizing and evaluating complicated decisions that use a pairwise comparison approach to allow for more precise priority ordering in decision-making [4, 6, 13, 18, 25, 28, 30].

In real-world challenges, observable values are frequently imprecise or vague. Unquantifiable, inadequate, and non-accessible data might result in imprecise or unclear information. Fuzzy numbers are integrated with AHP to successfully handle subjective impressions and imprecision, allowing the right expression of linguistic judgment.

Instead of a single value, a range of values is employed in fuzzy AHP to account for the decision maker's uncertainty. AHP can handle both quantitative and qualitative criteria of MCDM problems based on decision makers' judgments, whereas FAHP can reduce or even eliminate fuzziness and vagueness in many decision-making problems and can also contribute to decision makers' imprecise judgments in traditional AHP approaches [10]. The fuzzy AHP technique sets the AHP scale into the fuzzy triangle or trapezoidal scale to be access priority [22], used FAHP to prioritize and classify airline business financial distress. In order to explain fuzziness, [29] employed fuzzy triangular numbers. In this case, the fuzzy multi-criteria ranking approach is utilized to assess urban transportation investment alternatives to determine each option's relative relevance.

SIMUS is a hybrid method that incorporates linear programming, weighted sum, and outranking techniques [9].

TOPSIS (Technique for Order of Preference by Similarity to Ideal Solution) is a multi-criteria decision analysis technique developed by Ching-Lai Hwang and Yoon in 1981, with improvements made by Yoon in 1987 and Hwang et al. in 1993. The following publications referred to TOPSIS in the literature are as follows: Bilişik et al. [5], Celik et al. [7], Güner [12], Hadas and Nahum [13] and Hassan et al. [14].

PROMETHEE is an MCDM technique introduced by Brans. Compared to other MCA approaches, it is a very straightforward ranking method in terms of idea and application [23]. Aydin et al. [3]; used Choquet technique. AHP-Choquet and fuzzy Choquet are also taken into consideration in a few research studies. The literature review considers the significant contribution of the strategy based on customer satisfaction by employing survey study, statistical analysis, and MCDM approaches for accurate and dependable decision-making judgments.

FAHP will establish the weights of criteria used in the final ranking and sensitivity analysis in this article.

The research paper's relevance is determined, and the most relevant and relevant articles are evaluated, with less relevant and irrelevant publications being removed from the list of finding barriers. Other indicators related to the public transport system are listed down, and based on them, barriers are found out which hinder the usage of the public transport system.

3 Hindrance/Barriers

Measuring service quality is the first step in increasing customer satisfaction and attracting additional system users [3]. The assessment procedure involves the examination of many service-related criteria. Previous research has offered various qualities to assess the quality of public transport. Mahtani & Garg [22], classified influencing factors into six categories: operational, economic/government, performance-related, financial, market-related, and external. Each of these categories has a list

of influencing factors. The final list includes thirty-eight elements divided into six categories are listed in Fig. 2.

A complete literature analysis is done in this study to determine the most critical public transportation service quality attributes, and overlaps and redundancies are eliminated to provide a more manageable set of criteria/attributes, as shown in Table 2. Reference source not found (Table 2).

Barriers are identified based on six major indicators: i.e., physical, social, operational, technical, economic, and environmental. These indicators are classified based on service quality attributes/criteria and sub-criteria. These sections explain each service quality criteria and the hindrance caused by them as sub-criteria in detail (Fig. 2).

A. Physical Indicator

It consists of two criteria: frequency and vehicle performance.

Frequency: Reduced wait times result in increased use of public transportation services [17].

The barrier listed in frequency is lack of adequate buses in the fleet, inefficient bus route scheduling, and lack of timetable/inefficient timetable schedule.

Vehicular Performance: Performance measures forecast, assess, and monitor the extent to which the transportation system achieves/adopts public objectives [14].

It consists of barriers such as inefficient maintenance period of the buses, buses that already completed their life cycle, thus increasing the cost of operations, and regular cleaning of buses to protect users from airborne and unwanted harmful particles.

B. Operational Indicator

It consists of accessibility, information provision, responsiveness, infrastructure, technology acceptability, and speed.

Accessibility: According to Celik et al. [7], the use of public transportation is evaluated for accessibility depending on the distance that areas are willing to travel. The ease with which users will use public transportation services will be used to assess accessibility. According to Aydin et al. [3], accessibility is assessed using three sub-criteria: access to metro stations; condition of escalators, elevators, and belt conveyors; and the seamless operation of toll gates. Ebrahimi & Bridgelall [9], examine accessibility to determine how easily consumers will be able to use public transportation services.

It consists of the barrier as poor network performance due to inadequate road infrastructure to support buses on all routes, lack of bus shelters at an adequate distance for handling passengers impacting access, and multimodal integration.

Information Provision: Criteria for providing information may include the use of modern equipment to access services, such as screen displays to show schedules, vehicle departures, and routes; the use of modern equipment in public transit services; announcements in stations and vehicles during and after breakdowns; and timeliness. According to Stanković et al. [27], schedules provide the mode of operation of vehicles on a specific line during the day. Its primary objective is to meet the essential

Table 2 List of hindrance/barriers in the public transportation system

Indicators		Criteria	Hindrance/barrier	Literature support
1	Physical	Frequency	– More waiting time	Jain et al. [17], Hadas and Nahum [13], Aydin [2], Güner [12], Ebrahimi and Bridgelall [9], Stoilova [28]
2	Vehicle performance	<ul style="list-style-type: none"> – Lack of cleanliness in vehicle – System breakdown – Less maintenance – Lower performance 	Hassan et al. [14]	
3	Operational	Accessibility	<ul style="list-style-type: none"> – Demography – Inaccessible PT network lines – Inaccessible road network – Long distance walk – Inadequate route transferability – Remoteness – Bad condition of escalators elevators and belt conveyors – Elevators for wheelchairs not provided – Inadequate functioning of the tollgates 	Teng and Tzeng [29], Yeh et al. [31], Kaya et al. [19], Bilişik et al. [5], Celik et al. [7], Jain et al. [17], Boujelbene and Derbel [6], Aydin et al. [3], Hadas and Nahum [13], Guirao et al. [11], Arsovski et al. [1], Aydin [2], Barbosa and Ferreira [4], He et al. [15], Kanuganti et al. [18], Nassereddine and Eskandari [23], Ngossaha et al. [24], Pedroso et al. [25], Güner [12], Mahtani and Garg [22], Stanković et al. [27], Stanković [26], Ebrahimi and Bridgelall [9], Yannis et al. [30]
4	Responsiveness	<ul style="list-style-type: none"> – Users' needs – Willingness – Readiness – Promptness of service provider 	Bilişik et al. [5], Guirao et al. [11], Barbosa and Ferreira [4], Pedroso et al. [25], Ebrahimi and Bridgelall [9]	
5	Technology acceptability	– Lack of universal accessibility systems	Yeh et al. [31], Macharis and Bernardini [21], Guirao et al. [11], Ngossaha et al. [24]	

(continued)

Table 2 (continued)

Indicators		Criteria	Hindrance/barrier	Literature support
6	Information provision	<ul style="list-style-type: none"> - Poor timetable scheduling - Lack of modern equipment - Lack of screen display - Routes not properly defined - Timeliness - Inaccuracy of provided data 	Yeh et al. [31], Isaaï et al. [16], Celik et al. [7], Jain et al. [17], Aydin et al. [3], Guirao et al. [11], Ngossaha et al. [24], Stanković et al. [26], Ebrahimi and Bridgelall [9]	
7	Infrastructure	<ul style="list-style-type: none"> - Damaged infrastructure - Improper lighting system - Cleaning and low maintenance - Low quality of material used - Inadequate boarding - Less terminal space - Lack of parking space - No space for future expansion 	Teng and Tzeng [29], Yeh et al. [31], Hassan et al. [14], Macharis and Bernardini [21], Arsovski et al. [1], He et al. [15], Stanković et al. [26, 27]	
8	Speed	<ul style="list-style-type: none"> - Congestion - Lack of route modeling 	Hadas and Nahum [13], Kanuganti et al. [18], Stoilova [28]	
9	Social	Comfort	<ul style="list-style-type: none"> - Less seat availability - Lack of cleanliness - Lower vehicle illumination - Poor ventilation - Poor design and guidance system - Difficulty in vehicle movement - Higher noise level - Non-working AC - Crowding - Higher grade separation 	Yeh et al. [31], Celik et al. [7], Jain et al. [17], Aydin et al. [3], Guirao et al. [11], Barbosa and Ferreira [4], Pedroso et al. [25], Güner [12], Stanković et al. [26], Ebrahimi and Bridgelall [9]
10	Welcoming	<ul style="list-style-type: none"> - User satisfaction not considered - Inadequate staff behaviors - Bad service of the fare collector 	Celik et al. [7], Hassan et al. [14], Aydin et al. [3], Guirao et al. [11], Ebrahimi and Bridgelall [9]	
11	Technical	Capacity	<ul style="list-style-type: none"> - Insufficient sitting areas - Higher passenger capacity and low demand of vehicle - Higher load factor 	Kaya et al. [19], Hassan et al. [14], Guirao et al. [11], Li et al. [20], Mahtani and Garg [22], Stoilova [28], Yannis et al. [30]

(continued)

Table 2 (continued)

Indicators		Criteria	Hindrance/barrier	Literature support
12	Safety/security	<ul style="list-style-type: none"> - Lower travel safety - Higher risk of crashes - More accidents - Personal safety risk against robbery/assaults/muggings 	Yeh et al. [31], Kaya et al. [19], Celik et al. [7], Hassan et al. [14], Jain et al. [17], Aydin et al. [3], Guirao et al. [11], Barbosa and Ferreira [4], Nassereddine and Eskandari [23], Pedroso et al. [25], Güner [12], Ebrahimi and Bridgelall [9], Yannis et al. [30]	
13	Travel time reliability	<ul style="list-style-type: none"> - Higher departure time and arrival time - Long waiting time/transient time - Higher time taken to walk from stop to final destination - Less adherence to schedule (punctuality) - Less frequency 	Teng and Tzeng [29], Yeh et al. [31], Isaai et al. [16], Kaya et al. [19], Bilişik et al. [5], Celik et al. [7], Hassan et al. [14], Jain et al. [17], Aydin et al. [3], Hadas and Nahum [13], Guirao et al. [11], Li et al. [20], Aydin [2], Barbosa and Ferreira [4], He et al. [15], Mahtani and Garg [22], Stanković et al. [26, 27], Ebrahimi and Bridgelall [9], Stoilova [28], Yannis et al. [30]	
14	Economical	Ticketing	<ul style="list-style-type: none"> - Long queue exceed loading time - Smaller queuing area - Vending machine condition - Lack of multiple ticketing system 	Bilişik et al. [5], Aydin et al. [3], Guirao et al. [11], Barbosa and Ferreira [4], Ebrahimi and Bridgelall [9]
15	Cost	<ul style="list-style-type: none"> - Higher tariff system - Higher travel cost - Costliness of metro tickets and interchanges Mode of payment difficult for less educated people	Teng and Tzeng [29], Yeh et al. [31], Kaya et al. [19], Bilişik et al. [5], Hassan et al. [14], Jain et al. [17], Boujelbene and Derbel [6], Aydin et al. [3], Hadas and Nahum [13], Guirao et al. [11], Li et al. [20], Barbosa and Ferreira [4], Nassereddine and Eskandari [23], Ngossaha et al. [24], Güner [12], Mahtani and Garg [22], Stanković et al. [26, 27], Ebrahimi and Bridgelall [9], Stoilova [28], Yannis et al. [30]	

(continued)

Table 2 (continued)

Indicators		Criteria	Hindrance/barrier	Literature support
16	Ecological/environmental	GHG emissions	<ul style="list-style-type: none"> - Lack of green technology and ecological vehicles - Higher vehicular emission 	Teng and Tzeng [29], Bilişik et al. [5], Celik et al. [7], Ngossaha et al. [24], Pedroso et al. [25], Stanković et al. [27], Ebrahimi and Bridgelall [9]
17	Environmental impact	<ul style="list-style-type: none"> - Higher air and noise pollution - Higher ecological footprint - Less environmentally conscious vehicles - Negative effects on ecosystems 	Teng and Tzeng [29], Yeh et al. [31], Kaya et al. [19], Hassan et al. [14], He et al. [15], Ngossaha et al. [24], Stanković et al. [27], Güner [12], Yannis et al. [30]	

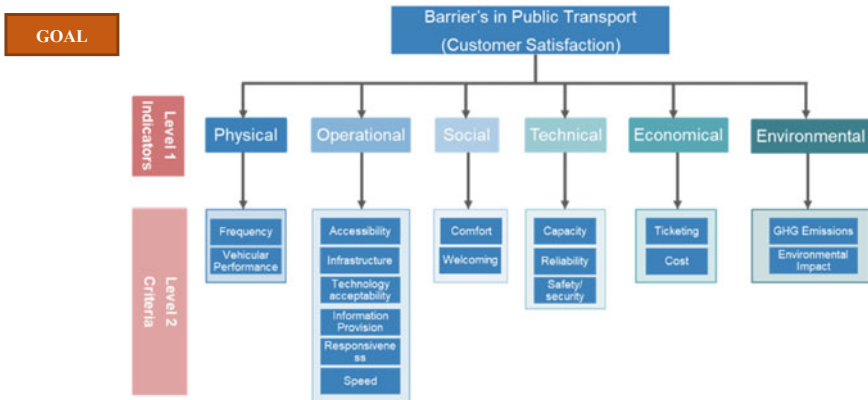


Fig. 2 Hierarchical structure

transportation demands of passengers during the day while maintaining a reasonable wait time.

The barrier listed in information provision is lack of control and command center, lack of system integration with the control center, lack of passenger information system in public buses, and inefficient route rationalization applications.

Responsiveness: Responsiveness reflects the level of service provided by personnel in responding to client demands. It may involve knowledge of users’ requirements and willingness, as well as the service provider’s readiness and rapid reaction to users’ concerns and needs. Barriers are lack of user’s needs, willingness, readiness, and promptness of service provider responses/concerns.

Infrastructure: The infrastructure might be shared with other private forms of transportation or dedicated to public transportation.

It consists of barriers like inefficient space design for the terminal building, lack of maintenance yard for buses/depot, poor/lack of engineering staff allocation, and inefficient planning for future expansion.

Technology acceptability: The gradual penetration of new transport modes or new technologies impacts the overall scenario of public transit. Barriers are the inability to accept or integrate technology to enhance the efficiency and accessibility of the system.

Speed: Speed is a vehicle's rate of motion. A vehicle's running speed is calculated by dividing the distance by the travel time and removing the delays [13, 18, 28].

Congestion and lack of route modeling impact the average travel speed of the vehicle, which reduces the reliability of the public transport system.

C. Social Indicator

It consists of the comfort and welcoming of the system for the user.

Comfort: According to Yeh et al. [31], comfort criteria are connected to the degree of service provided by the firm and the perceived quality of service by the passenger. Comfort is related to the cleanliness of the transit system, the level of noise, and the amount of vibration experienced during a travel, according to Jain et al. [17] and Aydin et al. [3]. Other elements that contribute to comfort include air conditioning in public transportation, congestion, and seating availability. According to Stanković et al. [27], comfort in a vehicle entails a lack of crowdedness, cleanliness, temperature, vehicle illumination, number of seats, and ease of mobility. Qualitative barriers also impact the choice of passengers traveling through the system, such as lack of cleanliness, poor ventilation, poor design, guidance system, congestion due to lack of poor or lack of infrastructure, type of seats, and availability of tickets.

Welcoming: Customer satisfaction relates to a user's comfort and acceptance of a public transport system, and welcoming is the attribute used to measure customer satisfaction in public transit service. Welcoming is one of the essential qualities of assessing client satisfaction in transportation service, according to Aydin et al. [3]. In addition, security and other crew members' attitudes and conduct toward passengers significantly impact the consumers' opinion of the service's quality.

Barriers listed are the user's satisfaction, attitudes, and harmful behaviors toward passengers and the service of the fare collector and driver.

D. Technical Indicator

It consists of capacity, safety/security, and travel time reliability.

Capacity: Capacity is the number of individuals, weight, or volume of the cargo transported under specified conditions through transportation. It is the average number of passengers per kilometer per day [19].

The barrier consists of lack of buses in the fleet; due to that, the loading factor increases in the buses and affects capacity adversely. The other barrier is the lack of route rationalization operating buses on low/lesser demand routes.

Safety/Security: Safety precautions for public transport services via access and indoor accessibility have an impact on overall performance of the system. It also

determines how safe and secure users feel about the system and other users in terms of criminality in public vehicles and the danger of collisions. According to Yeh et al. [31], the accident rate and average vehicle rate both impact vehicle performance. According to Aydin et al. [3], the technique for acquiring and entering public transportation services determines its safety. According to Güner [12], safety is also contingent on the prevention of criminality on the bus and at bus stops. Ebrahimi & Bridgelall [9], selected safety as the most critical quality attribute. Barriers listed are lower travel safety/security, risk of crashes, more accidents, and less personal safety against robbery/assaults/muggings.

Travel time reliability: Reliability describes how dependable public transportation systems are in getting customers to their destinations. According to Aydin et al. [3], reliability is described as a criterion based on passenger perception of the accuracy of planned and practiced departure, arrival, travel, and waiting times.

Travel time reliability is one of the significant barriers in public transport systems; with high travel time reliability or variability, passengers tend to opt for private transport to reduce generalized cost and eventually impact the public transport's overall performance and requirement.

E. Economic Indicator

It consists of ticketing and cost.

Ticketing: According to Hassan et al. [14], some passengers believe that a better ticketing system reduces loading time and, as a result, journey time. So, it is essential to improve the satisfaction of public transit users. Aydin et al. [3], assigned a value to ticket based on two sub-criteria: ticketing system and vending machines/services.

Barriers are in-efficiency in system operation which leads to high operating cost which affects ticket pricing and lack of technology integration such as vending machine and online mode of the ticket to save time and enhance the system's efficiency.

Cost: The term "travel cost" is frequently used to refer to the expense of using public transportation. Users compare the current rate to the expected reasonable cost, which is the perceived monetary worth of the service. According to Aydin et al. [3], criteria may be considered a price-quality ratio since they evaluate the service's quality by comparing the price to the passenger's perception. According to Güner [12], the cost of transit relies on the user and the ticket price's affordability. According to Stanković et al. [27], transportation costs are essentially a social category, and when a tariff system is used, the interests of the entire community are considered.

Lower accessibility and poor travel time reliability will impact the generalized cost and thus a significant barrier.

F. Ecological/Environmental Indicator

It consists of GHG emissions and environmental impact as significant criteria.

GHG Emissions: Greenhouse gas (GHG) emissions were utilized to assess the environmental impact of eco-friendly automobiles and green technologies [7], discovered that environmentally friendly vehicles are necessary components of public transportation systems.

Due to lack of advanced engine technology and higher cost, ecology has been dramatically impacted, thus increasing GHG values, but public transport systems still try to cut down emissions compared to private transport due to higher capacity per vehicle.

Environmental impact: According to Güner [12], the environmental effect of a service may be evaluated by examining the degree of air pollution, the level of noise, and the usage of environmentally friendly vehicles. Looking for the impact of transit service on the natural environment can reduce urban pollution.

Barriers are lack of technology adaptability like electrical buses/hybrid buses to keep a check on air pollution. Efficient use of public transport system will help in reducing carbon footprint and introduction of other green technology like solar power to generate power for transport infrastructure.

4 Conclusion

Present research paper provides insight of the barriers in uses of public transportation system and criteria of public satisfaction and perception in choice riding. The study also aimed to identify the use of MCDM techniques in ranking the factors to adopt public transportation as mode of travel. First, various criteria impacting the efficiency of the system and the significance of the public transport system are studied. These criteria are then sub-divided into various buckets. Bucketed criteria are defined further based on their sub-criteria and barriers in detail. This documented study provided the researchers and decision makers to get the insight of the research in the area of choice modeling. The most critical criteria for persuading urban commuters to switch from private automobiles to public transportation may be determined by ranking the criteria. Further, this research document will assist in how to revive the existing public transport system to compete with private vehicles and assist transportation planners in merging public preferences with available technology alternatives to ensure efficient resource allocation.

References

1. Arsovski S et al (2017) Model for selection of the best location based on fuzzy AHP and Hurwitz methods. *Math Prob Eng* 2017
2. Aydin N (2017) A fuzzy-based multi-dimensional and multi-period service quality evaluation outline for rail transit systems. *Transp Policy* 4, 55:87–98
3. Aydin N, Celik E, Gumus AT (2015) A hierarchical customer satisfaction framework for evaluating rail transit systems of Istanbul. *Transp Res Part A: Policy Pract* 7, 77:61–81
4. Barbosa SB, Ferreira MGG (2017) Multi-criteria analysis model to evaluate transport systems: an application in Florianópolis, Brazil. *Transp Res Part A: Policy Pract* 2, 96:1–13
5. Bilişik ÖN, Erdoğan M, Kaya I, Baraçlı H (2013) A hybrid fuzzy methodology to evaluate customer satisfaction in a public transportation system for Istanbul. *Total Qual Manag Bus Excell* 24(9–10):1141–1159
6. Boujelbene Y, Derbel A (2015) The performance analysis of public transport operators in Tunisia using AHP method. *Procedia Comput Sci* 73:498–508
7. Celik E et al (2013) An integrated novel interval type-2 fuzzy MCDM method to improve customer satisfaction in public transportation for Istanbul. *Transp Res Part E: Logist Transp Rev* 58:28–51
8. Chang D-Y (1996) Applications of the extent analysis method on fuzzy AHP, s.l.: s.n.
9. Ebrahimi S, Bridgelall R (2020) A fuzzy Delphi analytic hierarchy model to rank factors influencing public transit mode choice: a case study. *Res Transp Bus Manag*
10. Emrouznejad A, Ho W (2018) *Analytic hierarchy process and fuzzy set theory*. Taylor & Francis
11. Guirao B, García-Pastor A, López-Lambas ME (2016) The importance of service quality attributes in public transportation: narrowing the gap between scientific research and practitioners' needs. *Transp Policy* 7, 49:68–77
12. Güner S (2018) Measuring the quality of public transportation systems and ranking the bus transit routes using multi-criteria decision making techniques. *Case Stud Transp Policy* 6, 6(2):214–224
13. Hadas Y, Nahum OE (2016) Urban bus network of priority lanes: a combined multi-objective, multi-criteria and group decision-making approach. *Transp Policy* 11, 52:186–196
14. Hassan MN, Hawas YE, Ahmed K (2013) A multi-dimensional framework for evaluating the transit service performance. *Transp Res Part A: Policy Pract* 4, 50:47–61
15. He Y et al (2017) Sustainable decision making for joint distribution center location choice. *Transp Res Part D: Transp Environ* 8, 55:202–216
16. Isaai MT, Kanani A, Tootoonchi M, Afzali HR (2011) Intelligent timetable evaluation using fuzzy AHP. *Expert Syst Appl* 4, 38(4):3718–3723
17. Jain S et al (2014) Identifying public preferences using multi-criteria decision making for assessing the shift of urban commuters from private to public transport: a case study of Delhi. *Transport Res F: Traffic Psychol Behav* 24:60–70
18. Kanuganti S et al (2017) Road safety analysis using multi criteria approach: A case study in India. *Transportation Research Procedia* 25:4649–4661
19. Kaya H, Öztaysi B, Kahraman C (2012) A two-phased fuzzy multicriteria selection among public transportation investments for policy-making and risk governance. *Int J Uncertainty, Fuzziness Know-Based Syst* 6, 20(Suppl. 1):31–48
20. Li X, Liu Y, Wang Y, Gao Z (2016) Evaluating transit operator efficiency: an enhanced DEA model with constrained fuzzy-AHP cones. *J Traffic Transp Eng (English Edition)* 6, 3(3):215–225
21. Macharis C, Bernardini A (2015) Reviewing the use of multi-criteria decision analysis for the evaluation of transport projects: time for a multi-actor approach. *Transp Policy* 1, 37:177–186
22. Mahtani US, Garg CP (2018) An analysis of key factors of financial distress in airline companies in India using fuzzy AHP framework. *Transp Res Part A: Policy Pract* 11, 117:87–102
23. Nassereddine M, Eskandari H (2017) An integrated MCDM approach to evaluate public transportation systems in Tehran. *Transp Res Part A: Policy Pract* 12, 106:427–439

24. Ngossaha JM, Ngouna RH, Archimède B, Nlong JM (2017) Sustainability assessment of a transportation system under uncertainty: an integrated multicriteria approach. *IFAC-PapersOnLine* 7, 50(1):7481–7486
25. Pedroso G, Bermann C, Sanches-Pereira A (2018) Combining the functional unit concept and the analytic hierarchy process method for performance assessment of public transport options. *Case Stud Transp Policy* 12, 6(4):722–736
26. Stanković M, Gladović P, Popović V (2019) Determining the importance of the criteria of traffic accessibility using fuzzy AHP and rough AHP method. *Decis Mak: Appl Manag Eng*, 3, 2(1):86–104
27. Stanković M, Gladović P, Popović V, Lukovac V (2018) Selection criteria and assessment of the impact of traffic accessibility on the development of suburbs. *Sustainability (Switzerland)* 6, 10(6)
28. Stoilova S (2020) An integrated multi-criteria approach for planning railway passenger transport in the case of uncertainty. *Symmetry* 12(6)
29. Teng JY, Tzeng GH (1996) Fuzzy multicriteria ranking of urban transportation investment alternatives. *Transp Plan Technol* 20(1):15–31
30. Yannis G, Kopsacheili A, Dragomanovits A, Petraki V (2020) State-of-the-art review on multi-criteria decision-making in the transport sector. *J Traffic Transp Eng (English Edition)*, 8, 7(4):413–431
31. Yeh C-H, Deng H, Chang Y-H (1999) Perspectives for practice fuzzy multicriteria analysis for performance evaluation of bus companies, s.l.: s.n.

Urban Metrorail Funding and Financing in India: Empirical Analysis of Potential Innovative Options



Anjula Negi and Sanjay Gupta

Abstract Funding urban metros through limited public resources is well documented as inadequate and constrained, and post the pandemic, these challenges may have increased manifold for the government authorities. India's evolving economy poses a five-year investment task valued at around \$78.43 billion for the centrally governed urban metrorail sector. Financing needs for these 50 metrorails combined with 2021–22 budgetary announcements on Metrolite and MetroNeo in Tier II and Tier I periphery areas of cities are colossal and largely proposed from traditional monetary sources. Given the uncertainty around public sources, a sustained financial mechanism is required for funding this development in the country. Thereby, there is an emergent need to examine different funding and financing sources in the Indian metrorail sector and forms the baseline research gap for assessment in this paper. Authors in particular examine potential of innovative options within the transport infrastructure financing framework for metrorails. Analysis involves addressing innovation needs, measures, and approaches that can motivate innovative financing solutions and refer to key challenges. Using online variant of Delphi technique survey, experts' consenting views were collated over two rounds and analysed for building qualitative ex-ante options. Few challenges recorded were fiscal discipline improvements, funding options inadequacy, strengthening institutional capacities, absence of anchor leadership, non-availability of long-term finance, etc. Few funding tools such as raising bonds, optimum use of land value capture alongside structural reforms were identified. Assessment from surveys concluded a need for stakeholder wide innovations in the financing lifecycle for metrorails.

Keywords Urban metrorails · Innovative funding options · Transport infrastructure financing

A. Negi (✉) · S. Gupta
School of Planning and Architecture, New Delhi, India
e-mail: anjulanegi@gmail.com

© The Author(s), under exclusive license to Springer Nature Singapore Pte Ltd. 2023
M. V. L. R. Anjaneyulu et al. (eds.), *Recent Advances in Transportation Systems Engineering and Management*, Lecture Notes in Civil Engineering 261,
https://doi.org/10.1007/978-981-19-2273-2_27

411

1 Introduction

The urban metrorail or mass rapid transit system (MRTS) is globally being viewed as an answer to urban congestion, low carbon mobility, urban regeneration, and for opening up newer markets [15]. A drift away from cars in favor of urban metrorail is a trend observed worldwide and attributed to the peak in oil prices in 2008, which caused the global financial crisis [17]. Prominence was also revealed when a decline in car dependence was noted while urban rail showcased an increased ridership across many global cities [16]. Urban rail trips in Tokyo, New York, and Hong Kong are as high as 80–90% modal share. Beijing city chose urban rail owing to spatial constraints combined with high population densities and turned to the private sector for investment [2]. Transit planning is the primary concern rather than land development for value capture, which is a complimentary benefit, [15].

In India, mass-rapid transit gained momentum as envisioned in the National Urban Transport Policy (NUTP) of 2006, wherein the central theme is movement of people and not vehicles. In December 2019, government announced 50 new metro rails to be developed by the year 2025 under the National Infrastructure Pipeline (NIP). Total investment value estimated is massive around \$80 billion, and financing sources listed are budgetary provisions and sovereign guaranteed debt from multilateral banks. Use of public monetary sources accounts for 81% of the total, 3% from value capture, and unidentified sources for 16% funding. It is uncertain whether financing from these public sources is feasible and long-lasting for MRTSs' huge requirements, making innovation a critical aspect to study. Innovation is any 'newness' to a way, action, process till it is adapted, theory as defined by Schumpeter in 1939. Financing issues in contemporary literature were observed as ignored for innovation. Not only is innovation in finance needed, but it is for financial institutions too [12].

Funding urban mobility infrastructure (infra) only through conventional public sources has been a persistent issue for emerging economies. Developed countries too have faced treasury challenges on it owing to economic variability [21]. Striking a choice equilibrium between vital capital-intensive infra and developmental priorities is a paradox that discretionary forms of monetary resources can resolve. Beyond traditional financing, newer ways to sustain financing requirements have been reported world over to develop MRTS. For an uprising economy like India, potential of innovation in transport finance has not been comprehensively found in the literature. Besides, in application only a handful of non-traditional forms of finances have been witnessed for existing MRTS projects. Innovation potential in the design of financing and funding arrangements thereby becomes a critical aspect to be explored.

The underlying thought of this paper is whether financing these high-cost projects entirely from public sources is a feasible option or other sources of funding can be explored as sustainable preferences. ***The subject paper attempts to understand the potential of innovation to fund and finance mrts projects in India.*** Stakeholders such as government entities require to comprehend newer or alternative ways to meet funding gaps. Authors quest about methods and their adequacy, measures that can be

adopted to support innovations in funding options, and approaches that could motivate the use of innovative financing to develop metrorails? Further, to analyze what are the key challenges that can act as deterrents to the use of innovating financing? This paper attempts to add to the body of knowledge in transport finance on innovation and financing mechanisms for MRTS. To gain more understanding, a global review of literature pointing out key MRTS financing aspects is presented ahead.

2 Literature Review—Perspectives of Urban Rails and Urban Metrorail Funding and Financing Mechanisms

Financing is defined as a process leverage to future funds or revenue streams, has a return obligation, and does not reduce the infra funding gap. Funds are generated from payments for use of the service of a delivered asset. Sources of funds broadly are taxes (across the three governance levels), user fee (termed sustainable in long term as a supplement to tax sources provided users are incentivized to pay). Brown-field leveraging through monetisation of existing assets fills in for infra funding too. Broadly, four approaches to financing urban rails are noted. These forms are wherein; (a) entire Capex is invested by the public sector; (b) a larger share of capital by public sector alongside private partner's investments; (c) a larger share of capital by private sector supplemented by the public sector and lastly; (d) full capital risk assumed by private partner [15].

European countries have sourced from alternative financial schemes, concession grants, involving private sector funds, value capture reforms, etc. It was noted that the burden of social amenity development may fall on the beneficiaries rather than the taxpayers [25]. Private parties have borne construction and financial risks in many metro rail projects developed in the UK, France, and Greece. Urban rails were not considered favourable for self-finance, but, co-financed owing to limited recourse. In the short-run, bank loans were preferred and issuance of bonds (after implementation) for long-term as an approach towards arrangement of finances. Thereby, pooling together of finances from multiple sources was witnessed [4]. UK's City Deals gave few identified cities an unified investment fund covering access to tax increment finances (borrow against future revenue or tax receipts) [18]. Private sector consortia own and operate metro rails in Australian cities such as Sydney and Melbourne. Integration of private land has been observed and land has been used as a tool to fund [15]. London city in the pre-electrification era promoted housing estate along metro corridor. Later, Transport for London (TfL) chose an area-based integrated transit development approach and financing initiatives such as business rate supplements (BRS), a levy on commercial buildings and graduated tax for properties close to metro lines, stations redevelopment, mixed land-uses connecting purpose-based trips to key transit hubs. New York City noted a tax for transit movement. Hong Kong metro is the only non-subsidized and profitably run metro in the world. It has forms of property

development, commercial leases, sale of shares to a private investor and a systemized land value capture in the planning process as funding options [23].

A distinctive case of 'Speculative spatial fix' as a cost-recovery model by the private sector rail operator from its owned assets along the corridor, witnessed in Detroit city, USA. Federal reserves were not apprehended, municipalities had a weak tax base, and nil state resources to fall back on. Despite this capital was invested and linked to future returns riding on land-use zoning [7]. Indiana State, USA dealt with insufficient federal apportionment and state revenues by leveraging the Transportation Infra Finance and Innovation Act (TIFIA) program. It provided federal credit assistance in the form of direct loans, which helped build a new transit line ('Tran Urbano') in San Jaun, Peurto Rico [5]. Policymakers in Greece stated positive impacts on urban living and property values around metro corridors. Still, the majority surveyed negated the idea of fund payment for MRTS development [21]. Tokyo-Yokohama regions' private conglomerates have rail-based businesses in real estate, retail, tourism, etc., used to cross-subsidise low rail profits. Land value capture is through land readjustments and urban redevelopment schemes to finance urban transit [3]. China too owing to fiscal constraints was pressurized to raise funds for MRTS through diversified funding methods like social capital, business owner revenue, overseas capital, development of market economy, modification to financing system, land integration for rail development through property, commercial resources management, enhancing manager, and owners' abilities, government's boost to local enterprises [1]. Beijing Metro devised a public subsidy and revenue sharing scheme. Its contract used approaches like 'shadow price' (a technique used to isolate the private operator from social obligations) and 'shadow patronage' (compensate for demand risk by the private operator if lower ridership than projected) and guaranteed revenue per passenger not related to metro fares. It raised funds from fares and advertisements while investing in rolling stock through equity (30%) and bank debt (70%) [2].

For the European urban rail projects, projects were found socially desirable and less financially considerable and ones that could not be self-financed. Collaborations with the private sector were undertaken to achieve scale and to provide cost economies [6]. For the London underground case, the National Audit Office in 2009 attributed failure of Metronet consortia owing to issues in its governance, leadership, and corporate structure. Besides, it noted funding risked by Department for Transport (DfT) as they had underwritten Metronet's debt, and were ineffective in managing the grants that they provided [16]. Wu D. et al., summarised previous financing research in the MRTS sector as limited concerning providing selection options or comparisons in different financing approaches [21]. Other approaches were such as the creation of a dedicated fund for MRTS financing [17]. It was observed that innovative financial mechanisms and its tools can be a solution to shrinkage in public financial resources for urban transport [6, 22]. Implementation of land value capture mechanism is difficult, described as 'trial-error-transcend', and was not perceived as a cure to Urban Local Bodies (ULBs). On the other hand, Official Development Assistance (ODAs)

financing was indicated as insufficient [20]. Hale C. studied Public–Private Partnership (PPP) models in Asia Pacific and North America and concluded that development choices may lie either in being revenue-oriented or revenue-agnostic [6]. It was stated that focus on either the immediate financing horizon or the entire lifecycle transaction added clarity in the choice of funding options [10]. Necessity was to a wide range the financial instruments as requirements were huge [11]. Appropriate land values integrated within the land-use framework by planning agencies were gaining traction as a new revenue source. For India, country was found in a nascent stage of adoption of innovative financing [19].

From the above global urban rail cases it is inferred that innovation in financing is a '*fiscal constraint-driven approach*'. Measures adopted are multiple, unique and contextual, and many stakeholders partake in this development. Moreover, the private sector can help achieve the scale of development for MRTS. Varied approaches to funding are evidenced worldwide, which the emerging economies can benefit from. However, the potential of innovation in funding MRTS has not been comprehensively found in literature in an emerging economy like India.

3 Methodology

This paper is based on qualitative research designed to quantitatively apprehend views of experts through primary surveys. An online variant of Delphi technique survey was the approach adopted. Study's experts have sufficient knowledge on the domain, both by education and experience. Present study engaged to collect their opinion, ideas, experiences, etc. based on practical options obtained through literature review. Delphi survey scientific method for data collection was developed in the 1950s and has witnessed many variations, online type being one. For reliability, it relies on three factors; (a) selection of relevant experts, (b) size of the panel, (c) conducting an anonymous process, and the goal is to reach a consensus. To guarantee reliable results, a minimum size of 3–9 members in a panel has been prescribed to arrive at a consensus result. Heterogeneity amongst panel members is encouraged to negate the risk of axiomatic consensus. Delphi survey is iterative till consensus is achieved. Consensus considered is a geometric mean above fifty percent agreement to the majority choices in a given question [11]. Delphi surveys can also record views that are divergent from the majority [9]. Delphi survey has been an exploratory process as experts had divergent opinions/perspectives due to mixt experiences, uncertainties associated with implementation differed, etc. [24]. Figure 1 indicates the flow chart of Delphi technique for this paper.

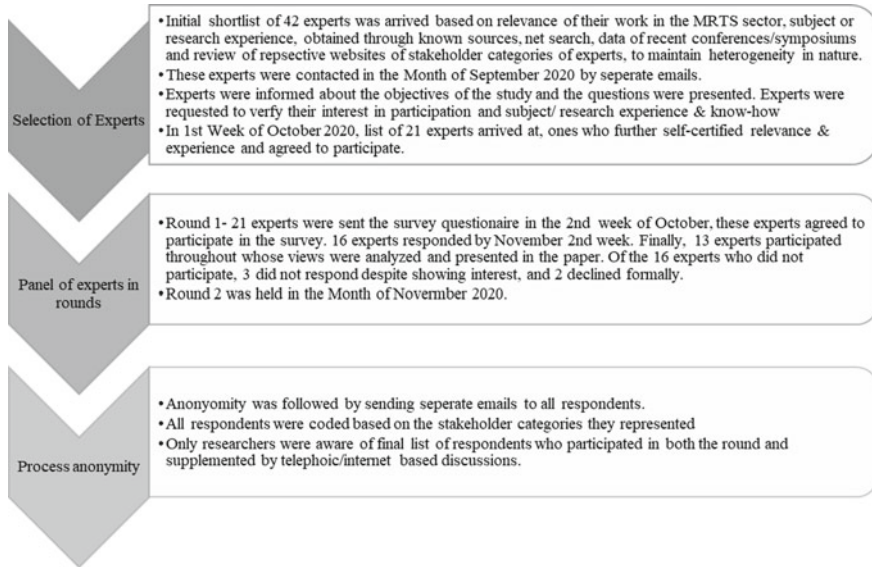


Fig. 1 Flow chart for the method adapted of the online Delphi technique variant in the study

3.1 Steps Considered for the Delphi Research Survey Based on Fig. 1.0 Above

As the First step, an initial shortlist of experts arrived based on relevance of their work in the MRTS sector/subject or research experience at national and international level. Further, a long list of varied stakeholders refined to 42 experts was as final experts detailed in Table 1 ahead. Final respondents’ profiles are provided at Table 2 ahead.

Study’s Delphi survey had heterogenous stakeholders: Multiple type of experts broadly following typology such as; *A = Government/Policy makers, B = Academia, C = Multilateral banks/Financial Institutions, D = Lawyer, E = Not for Profit NGO, F = International consultants, G = Indian consultants, H = Retired experts.* Experts are referred synonymously as ‘respondents’ in this study. Experts were informed about the objectives of the study, testing of questions and study’s context was presented, and feedback for improvements/clarity was considered to finalise questionnaires. Table 2 presents profiles of 13 final respondents, they self-certified as relevant and responded to both the rounds and supported in iterative discussions.

Based on the objective of the paper, five broad research questions were probed, each question comprised multiple choices with practical options adapted from literature reviewed. The questions, stated below, were aimed to understand the prevalence of innovation and capacity to adapt into the Indian scenario in the context of MRTS:

1. *Whether innovation is required in the financing process for upcoming MRTS projects & why?*

Table 1 Table for categories of expertise representative of stakeholder heterogeneity

Expert type	A	B	C	D	E	F	G	H	Total
No. of Experts	10	6	6	1	2	5	8	4	42
Experts who agreed	5	2	5	1	2	1	5	2	21
Final respondents	1	2	2	0	2	1	5	0	13
Remarks for Round 1 (R-1) and Round 2 (R-2)	5 experts gave NO response								
	1 declined-due to lack of knowhow on Indian scenario, 1 late to consider, 2 agreed, but, later NO response to questionnaire								
	1 NO response								
	1 Late response to consider though relevant								
					-				

(continued)

Table 1 (continued)

Expert type	A	B	C	D	E	F	G	H	Total
						1 declined-stated knowledge about Indian MRTS being limited, 3 NO response			
						1 each; as late response to consider, NO response & Decline			
						2 declined as know-how limited, 2 NO response after agreement			
						16 in R-1 13 in R-2			
NO response	Each expert with NO response was followed up, given 3 reminders, one in a week & called twice, at available office/ mobile numbers								

2. *What are the measures that could motivate the use of innovative financing?*
3. *What are the challenges/issues/deterrents in the use of innovative financing methods?*
4. *What are the innovative financing approaches that can encourage the use of newer or alternative financing sources/funding options across the life cycle of an MRTS asset?*
5. *What can be the decisive choices from various financing and funding options that can be used for new MRTS for Capex and revenue enhancements?*

Respondents' who had researched/worked on metrorail domain, had influenced decisions at national and global level and had sectoral knowledge with financing know-how were considered for this online Delphi study's research. Two rounds of structured questionnaires were undertaken with practical decision options for

Table 2 13 Final respondent's profile based on Table 1

Expert	Designation	Work-Ex	Qualification	Experience in MRTS or overall experience
A8	Managing Director of a leading Metrorail	30+	Post Graduate and M. Phil	Expert-Rail Transport, Finance, PPPs, Metro Implementation & Management
B2	Associate Professor at an international University, Australia	25+	B. Tech, MBA, Ph.D.	Urban-Infra & finance expert. Past in India: CEO-Infra advisory firm, founding Director-MBA, infra management
B6	Post doctorate scholar in transport planning	<5	Ph.D.	Researched & published widely on transport financing mechanisms
C1	Heads South Asia in transport & infra	25+	Ph.D.	Transport financing & lending to many metrorail projects, in India & abroad
C2	Heads South Asia in transport & infra	30+	B. Tech, M. Tech, MBA-finance	Project finance expert. India-worked in Govt. & Pvt. sector, Global-transaction structuring in multilateral bank for transport & metro rail
E1	CEO-Leading think tank	35+	B. Tech, M. Tech, Ph.D.	X-Executive Director-Leading business School, chaired transport committee's, Civil servant, an author of NUTP
E2	Director	28+	B. Tech, MBA, Ph.D.	Infra finance, metrorail bond financing, credit-rating, investment banking, advisory, development finance-India & Asia
F4	Team leader infra development/finance	30+	MBA	Skilled in finance, infra investment opportunities, shaped capital & operational finance structures in South Asia

(continued)

Table 2 (continued)

Expert	Designation	Work-Ex	Qualification	Experience in MRTS or overall experience
G2	Finance expert and team lead	30+	Ph.D.	Urban management and financial management expert
G4	Finance specialist, led team-metro project	30+	Chartered Accountant	Finance, PPP & infra development expert, worked in govt. & private sector
G6	Governance and Institutional development specialist	30+	B.Sc. and B. Commerce	Expertise in urban infra, metro projects, governance & institutional development, adjunct professor
G7	Director-firm dealing in research-based consultancy	20+	B-Arch, M. Plan (transport), MBA	Advisory in techno-commercial feasibility, metrorail project development, revenue modelling, valuations on UT
G8	Director-Consulting firm, Former MD of one of big fours	30+	MSc, MBA-Finance	Urban development specialist & infra transaction advisory, expert in various Govt. committees in India

quantification purposes. These were circulated through emails supplemented with telephonic/internet-based iterative discussions. Respondents were given two weeks for completion of each round and two weeks in between the two rounds. Telephonic/internet call interactions served as reprise to remove doubts like cases of high variance in views or for a low range of input in written responses during Round 1 or for further in-depth discussions on multiple choices, its options and reasons thereof. The process of identification of 42 experts was vetted by two external reviewers, one academic (international) and one policy think tank (national). Reviewers were senior professionals, with over 20 years of experience in areas of infra development, financing, and sustainability. Initial investigations led to 21 experts who agreed to participate, self-certified subject's knowledge, consequently were included in the round 1 process. However, of 21 only 16 responded in round 1, three dropped during round 2 with no response. Finally, 13 experts participated in both rounds throughout whose views were analyzed, quantified and are presented in the paper.

- In Round 1, each respondent filled the questionnaire, choose from given options along with articulating the reasons for the choices or stating any other views.
- 13 written responses once received were summarised, and Round 1 was completed with status on consensus and opinions thereof. Majority consensus (taken as a

geometric mean above 50% as noted in literature) of the choices in each question was analysed. Consensus was observed in questions 1, 4, and 5.

- Questions 2 and 3 emerged as consensus not achieved in round 1.
- Summary of views as provided by each expert, enumeration of questions that were with consensus or non-consensus was provided as written feedback to the all the 13 respondents in Round 2. The goal was consensus building of the majority. Respondents revisited each question to enable modification or updation of views based on Round 1 and iteration for improvements with rounds were made.
- In Round 2, all respondents again filled another structured questionnaire with summarised opinion and reasons thereof. It was noted that in Round 2, a clear consensus arrived for all five questions. It was observed that respondents built upon learnings from other respondents and updated the responses. Thereby, completing the iterative process of the Delphi survey in two rounds.
- Semi-structured telephonic conversations were held with few, 6 (A8, B2, E1, E2, G4, G6) of them during round 1, 3 (A8, G6, G7) of them during round 2, to discuss responses, further clarity enabling open questions based on practical options.

4 Survey Findings and Discussions

In the written responses and during discussions with respondents, many areas of interventions were highlighted. The study revealed new findings, such as a wider stakeholder perspective required to include innovative funding and financing mechanism for urban metrorails and that innovation is needed for its life cycle sustenance. Responses received generally corresponded to the literature from international examples, wherein the need for alternative finances was emphasised. This research corroborates with literature that innovation in financing for metrorails in India is also a '*fiscal constraint-driven approach*'. However, a variation in views of experts was observed when responding to its application to the Indian context. For example; few experts were unsure about land value capture being a sustained revenue source as real estate income was termed as highly volatile and cyclic in nature. Presented ahead are the survey results and discussions;

Whether innovation is required in the financing process for upcoming projects?

Majority respondents were in consensus that there is a potential for innovation in the financing process. However, various aspects were perceived to impact the innovation potential for financing. Farebox revenues were not expected beyond 50–60% of the total investment value. Thereby, this limitation could lead to innovations favouring other funding options. It was highlighted that greater attention was required to meet annual revenue gaps than merely filling capital cost gaps, to sustain asset's creation and debt servicing. These funding gaps when accumulated over time were regarded to be massive, highlighting a need for innovation. Innovations in operational finance too were deemed important. Respondents stated that users pay for operational revenue for services in the 'pay-as-you-go' model. While taxpayers too are paying for the development of metros rails though they may not users. The overall benefits go

to the user, such as the subsidised tariff regime in public projects for wider acceptability. Respondents felt that direct and indirect users need to be segregated, so that appropriate incentive can be worked out. Taxpayers can be incentivised for metro development as a part of the financing process and the user pay principle may be adopted. It was considered that delays in time and cost or implementation are likely to increase costs. Thereby, to mitigate this innovation in financing was termed as required. Experts emphasised life-cycle financing innovations.

What are the measures that could motivate the use of innovative financing?

Respondents felt multiple measures are required to motivate innovation in the financing cycle. *'Meeting market demand by adopting spatial planning techniques like Transit-oriented development (TOD)'* was the most cited measure by all experts. Other dominant choices stated by experts were measures concerning *'Governance and accountability'*, *'Leadership in the initial adoption of innovative mechanisms'*, *'Policy formulation capabilities and ability to articulate and analyse structures for new financial packages'*, *'Prioritisation of financial and economic skills in transit organisations and government entities for capability enhancement of employees and supported by improvements to organisational capabilities'*.

Other measures opined by experts were for structural reforms, which were perceived as enablers to this process, alongside governance reforms. It was highlighted that local government have jurisdictional control of land and they may view metro rails as another source of income only. However, their responsibility in the entire chain of development of metro rails is limited, thereby an enhanced role was sought at city levels. Measures such as policy reforms for market enabling environment alongside market discipline were needed, also noted in the literature. Experts felt that responsible capital spending was another measure of concern, besides the financial sustenance. Central government support during the O&M stage is suggested to meet working capital, debt servicing, or other short-term financial needs. Earmarking a clear responsibility for financing O&M through non-budgetary means will also create a positive impetus. Understanding key stakeholders' perspectives and their increased involvement especially at community levels was noted as desirable. Measures such as improvement in the capacity of professionals associated in the cycle of the financing were deemed essential.

What are the challenges/issues/deterrents in the use of innovative financing methods? Respondents viewed multiple challenges and deterrents that may impede the needed newness or in the use of innovation in the financing process. The most cited issues were *'liquidity crunch'*, *'improvements in fiscal discipline & financial management at local levels'*, *'over-leverage of debt'*, *'institutional capacity constraints'*, *'lack and delay in the release of funds from state govt. to local level govts.'* and *'absence of dedicated or anchor leadership'*.

Further views stated were that State govts. lack of funds to meet capital cost demands for such projects. Thereby, non-availability of funding often leads to ambiguity in the feasibility of financing options. State and Local government's role was considered crucial to bring about implementation efficiency with new ways in financing mechanisms. Besides, disputes were noted to increase owing to cost and time delays, issues in land acquisition, interdepartmental coordination being tedious

and time-consuming tasks, all of which add up as huge costs. Amidst this, dealing with administrative changes such as transfer of the administrator after short/intermittent periods leads to poor project ownership. It was expressed that the resultant impact of changed leadership may mean deferment or derailment of the overall implementation vision. MRTS in the current context was not perceived as the dominant public mode of transit, especially when compared to the large financial resources it will utilize on its development. Expert felt that the demand issues need to be addressed along with methods of financing and innovation thereof. It was felt that projects where even innovation cannot mobilise finance, have been taken up in the recent past thereby clouding the rationale behind demand analysis. It was also emphasised that innovations must be acceptable at local levels. Stakeholders' involvement was reported as limited in this sector besides not many who could participate in innovative financing. The need to develop a structure/product to encourage investor participation was stated. Further, even to take advantage of value capture, ULBs and its governance process was required to be strengthened from current levels. Multiplicity of institutions coupled with land-related challenges were indicated too; such as land being viewed as a speculative tool, sale of land was considered prone to corruption, and optimally addressing price increment benefits from value capture by public agencies required more analysis.

What are the innovative financing approaches to encourage the use of newer or alternative financing sources/funding options across the life cycle of the MRTS asset? Respondents cited the most preferred approaches as '*Creation of private and public sector capital investment opportunities that support the agreed strategic goals over time (such as mode share, ridership, system expansions)*', followed by '*The public interest*'. Other choices that were clearly identified were; '*Selecting a financing option in line with orderly ongoing capital investment programs*', '*optimising the value and impact of available subsidy and resources*' and '*effective land use integration and urban design outcomes*'.

Respondents opined that few significant factors that may help in the adoption of innovative financial approaches included: (a) laws or policies preventing their utilisation; (b) absence of necessary supporting infra (i.e. capital markets); and (c) skills, knowledge, and capability of designing and implementing the mechanisms. Experts stressed that metro projects should be pursued for their primary objective, i.e. as a mobility solution. It was expressed that these projects are long-term, thereby, any approach should consider longer goals along with effective integration with the transportation system and spatial plans. Financing approach was directed towards having a sustainable transit system, that is not solely dependent on passenger traffic, and providing a superior level of service to its users.

What can be the decisive choices from various financing and funding options that can be used for new MRTS for Capex and revenue enhancements? Respondents expressed that in general financing should follow after the funding options clarity has been obtained. The most cited option was '*Private financing initiatives through multilateral funding agencies*'. Other preferred funding choices that emerged in the survey were '*Land bonds by State entity*', '*Metro rail bond by Central Government*', '*Dedicated metro fund vide cess and pool finance activities*', '*PPPs*', '*TOD*'

and joint development revenue taking a cue from Honk Kong metro model, and 'Land endowment or land value capture'.

Few respondents felt that from a mix of financing instruments, namely, 'equity, debt, taxes, transfer and tariffs' choices can be unbundled for funding options for meeting MRTS Capex and operating costs. Generally, it was opined that innovation in funding options can come in the timing of cash flow, rates (interest/returns—stepped up, structured), tenor, and risk. Thereby, the scope of innovation is necessary to be identified. Other views expressed by experts were that sources of funds are required to be distinct and ring-fenced to lend certainty in funding flows. There is potential for innovation in the entire financing process as analysed from above. It is understood that multiple areas required integration, like fiscal integration with the spatial planning processes, funding options integration with the financing processes, institutional capacity building integration with lasting leadership, long-term financing integration to meet MRTS Capex and operating costs gaps.

Few noteworthy views provided by respondents that were divergent or ones with non-consensus view in round 1 are stated ahead. Experts noted that fundamentally MRTS projects are financially non-viable and maybe unjustified investments in terms of demand. Therefore, raising finances for unviable projects is a start-up challenge. Experts opined that mass service-oriented and capital-intensive projects are more suited for the public finance route; wherein socio-economic returns are more important than financial returns. It was expressed that both PPPs and land-based financing mechanisms have limitations for being truly innovative. To begin with, a greater scope of improvement was identified in the management of public finances, more than mobilising them. Experts highlighted that there are procedural delays in urban areas for MRTS implementation. Thereby, placing commercial financing obligations or financing linked to time default is quite difficult. Respondents observed a global trend for value capture finances (VCF) from development cess, transaction fees, etc. Cash flows from these were termed like equity returns (delayed, lumpy) and not dependable for debt service. Besides, these returns would accrue to the ULB, which are distinct from the urban rail agencies. Measures of VCF do not directly make the project reliant upon such income. Further, raising long-tenure finances for expensive projects ranging from \$2 to \$15bn against innovative methods may not be feasible. In addition to Capex, most projects will barely break-even against operating revenue. Summarised review is provided at Table 3 ahead.

5 Conclusions

The literature review identifies an increased preference for urban rail globally owing to its inherent advantages [15]. However, fiscal constraints were faced by developed and emerging countries that required them to explore and adapt to alternative methods of financing MRTS with varying degrees of success. It has been observed that innovative financing is not "one-size-fits-all", but, multiple policy scenarios are to be pursued to close financing gaps [14] This research study also supports

Table 3 Summary table of key observations based on main findings of Delphi survey rounds 1 (R1) & 2 (R2)

R-1	Few respondent views in round 1	R-2	Overall remarks
<p>Q 1–50% above consensus achieved</p>	<p>A8, E1 & G4 highlighted need for capital more during O&M stages C2 disagreed with innovation requirements; <i>“innovation in solutions for financing are more problematic than helpful. (i) Urban rail projects are inherently very expensive. Raising long tenure finances for these volumes, against innovative methods, is simply infeasible. (ii) In addition to capex, most projects will barely break-even against operating costs. Inherent ability to service debt is very low, let alone any equity returns. (iii) Since these are in urban areas, there are many delays in land, approvals, jurisdiction disputes, utilities, etc.”</i></p>	<p>Q 1–50% above consensus achieved</p>	<p>Majority respondents agreed to the need for more research on innovative funding and financing approaches for metro/rail development in the country, especially as these are capital intensive projects and each needs a customised financing solution</p>

(continued)

Table 3 (continued)

R-1	Few respondent views in round 1	R-2	Overall remarks
Q 2-Non consensus	<p>A8 & G6 opined that municipal bodies are not much involved in MRTS development, whereas it is their public responsibility first. Laws/Policies need to be strengthened. Planned approach to commercial activities is required, & realisation is an issue from commercial/land-based income sources</p> <p>B2 & G8 stated that fiscal constraints most project proponents have, coupled with adequate revenue model (B2 view "<i>fare box just not sufficient to meet the expenses</i>", innovative financing mechanisms are needed. Capital costs will likely increase in future, making finance more challenging</p> <p>C1 opined Indian urban mobility finance is a metropolitan governance challenge, it can be solved by rationalizing spend</p>	<p>Q 2-50% above consensus achieved</p>	<p>Two most important measures stated by majority respondent was improvement in governance frameworks and enhancement of awareness at local levels including at leadership/anchor levels to effectuate the innovative measures. To exemplify, these measures could application of TOD with local bodies and community support</p>

(continued)

Table 3 (continued)

R-1	Few respondent views in round 1	R-2	Overall remarks
<p>Q 3-Non consensus</p>	<p>C1 & C2 opined that metro rail projects are fundamentally not viable and are not investments that are justified. C1 considered it good “that it is difficult to raise funds for them”, and should be backed up by a plan for public transport mode integration. C2 stated that “urban rail projects will be justifiable on economic returns, and not financial.” G4 stated the biggest challenge as non-availability of funds at State government level for a huge investment with no return & limited expertise on innovative methods</p>	<p>Q 3-50% above consensus achieved</p>	<p>Few of multiple issues Alternative finance methods not considered Supporting strategic long-term goals of cities & effective transport integration are vital to long term financing Public funds are limited in extent and hence the underlying need to explore new resources</p>
<p>Q 4-50% above consensus achieved</p>	<p>G4 opined that “there is no much surplus revenue during the O&M period, the funding options should be self-sufficient to pay for itself e.g. toll-operate-transfer (TOT), dedicated cess fund”</p>	<p>Q 4-50% above consensus achieved</p>	<p>Expert agreed that adequate funding model is to be clearly developed for subject MRTS, financing can follow. Real estate income is cyclic and volatile to support overall development of metro rail</p>

(continued)

Table 3 (continued)

R-1	Few respondent views in round 1	R-2	Overall remarks
<p>Q 5–50% above consensus achieved</p>	<p>A8 & C2 opined that long-term finance not available, bonds do not have a fully developed market in India, for PPPs in infra; <i>“long-term is needed as interests rate very high around 11% for 15 years tenor; and cash out is front-ended, but, revenue is not”</i>. This hampers financial flows to metrorails sustenance C1 stated that an adequate funding model is required that is tailored to suit respective metrorail, generalised approach will fail. It needs to be investigated from <i>“where the funding coming from: users or tax payers? In the case of metro projects users rarely pay more than operational costs. Tax payers then—is it tax payers benefiting from an enhanced access?”</i></p>	<p>Q 5–50% above consensus achieved</p>	<p>Experts opined that regular taxes or funding options does not have much of “innovation” angle. The innovation can come in timing of cashflow, rates (interest/returns—stepped up, structured), tenor, and risk</p>

the idea that no one size fits all in its answers to question 1. Experts view that each metro rail requires exclusive solution to funding options at first, financing can follow. Researchers opined that innovative financial mechanisms and its tools can be a solution to shrinkage in public financial resources for urban transport [6]. This research supports the aforementioned literature reviewed in its questions 1 and 5 as experts answered that innovation is required, can come in at various times and processes and is necessary to sustain the overall development of metrorails. Financial institutions also require innovation [12]. This paper supports this view in responses received to question 2, where experts have pointed out need for improvements in governance frameworks and enhancement of leadership skills to effectuate the innovation in funding options. Developed countries too have faced treasury challenges on mass transit projects owing to economic variability [21]. This study analysed emerging economies like India too face funding issues and financing inadequacy, observed in responses of 1, 3 & 5 questions.

From an empirical standpoint, study identified that innovation is necessary for the new 50 metro rails. Innovation was analysed as required across life-cycle of the financing process for sustainable development in the country. Meeting annual revenue gaps were equally important as is Capex needs. Significant emphasis was given to meeting the market demand by adopting spatial planning techniques like TOD. Other important measures that came across dominantly were improvements in governance and accountability aspects, having a dedicated leader from the start towards early adoption of innovative mechanisms, enhancement of professional capabilities to address policy formulations, and to articulate and analyse structures for new financial packages. Challenges that require attention were improvements in fiscal discipline & financial management at local levels, checking the over-leverage of debt, addressing institutional capacity constraints, and tracking delays in the release of funds from state govt. to local levels apart from addressing liquidity crunch. Outcomes also showcase need for creation of private/public sector capital investment opportunities. Optimising value and impacts of available subsidies and resources was another learning. Evidenced from this study that value capture mechanism is viewed as a complex framework, which requires effective land-use integration within the planning process for sustained development. Raising bonds and private financing initiatives through multilateral funding agencies was preferred as funding options. Funding options required clarity upfront on case-to-case basis as each project is unique. Stakeholders' participation was cross-cutting and across finance processes.

As MRTS is centrally driven, proposed and implemented by the State. Whether a unified body at the central level could play a pivotal role to raise finances, for implementation and fund consolidation of a transport infra assets, a supplementary study may be required. Effects of pandemic is another area of research that can be linked to the underlined objective of this research.

Acknowledgements Authors are grateful to experts who painstakingly participated in the Delphi survey, unnamed due to anonymity in the process, and Prof. DTV Raghu Rama Swamy, Univ. of Melbourne and Mr. Rajneesh Sareen, CSE-New Delhi as the reviewers of this study.

References

1. Bao X (2018) Urban rail transit present situation and future development trends in China: overall analysis based on national policies and strategic plans in 2016–2020. *Urban Rail Transit* 4(1):1–12
2. Chang Z (2013) Public-private partnerships in China: a case of the Beijing No. 4 Metro line. *Transp Policy* 30(4):153–160
3. Chang Z, Phang SY (2017) Urban rail transit PPPs: lessons from East Asian cities. *Transp Res Part A: Policy Pract* 105(April):106–122
4. Deloukas A, Apostolou E (2003) Innovative financing techniques: European urban rail projects & the case of Athens metro extensions. In: *European transport conference*
5. Drike K, Genetti AV, Sinha KC (2002) An evaluation of innovative transportation financing techniques for Indiana. FHWA/IN/JTRP-2002/11
6. Hale C (2013) Mass transit project financing—new & alternative approaches. In: *13th WCTR, July 2013*, pp 1–17
7. Hall S, Jonas AEG (2014) Urban fiscal austerity, infra provision, and the struggle for regional transit in “Motor City.” *Camb J Reg Econ Soc* 7(1):189–206
8. Hickman R, Hall P, Banister D (2013) Planning more for sustainable mobility. *J Transp Geogr* 33:210–219
9. Jittrapirom P, Marchau V, van der Heijden R, Meurs H (2020) Future implementation of mobility as a service (MaaS): results of an international Delphi study. *Travel Behav Soc* 21(May):281–294
10. Kumar Jillella SS, Newman P (2016) Innovative value capture based rail transit financing: an opportunity for emerging transit cities of India. *J Sustain Urbanization, Plan Prog* 1(1)
11. Lilja KK, Laakso K, Palomki J (2011) Using the Delphi method. In: *PICMET: Portland International Center for Management of Engineering & Technology, proceedings*
12. Mikheeva O (2019) Financing of innovation: national development banks in newly industrialized countries of East Asia. *J Post Keynesian Econ* 42(4):590–619
13. Mostafavi A, Abraham D, Sullivan C (2011) Drivers of innovation in financing transportation infra: a systemic investigation
14. Mostafavi A, Abraham D, Sullivan C (2014) Assessment of policies for innovative financing in infra systems. *Policy Brief*. 2013
15. Newman P, Davies-Slate S, Jones E (2018) The entrepreneur rail model: funding urban rail through majority private investment in urban regeneration. *Res Transp Econ* 67:19–28. <https://doi.org/10.1016/j.retrec.2017.04.005>
16. Newman P, Kenworthy J, Glazebrook G (2013) Peak car use and the rise of global rail: why this is happening and what it means for large and small cities. *J Transp Technol* 03(04):272–287
17. Nguyen TB, Krabben E van der Musil C, Le DA (2018) Land for infra in Ho Chi Minh city: land-based financing of transportation improvement. 3475(May)
18. O’Brien Peter PA (2014) Deal or no deal? UK city deals as infra funding and financing mechanisms. *IBUILD, Centre for Urban and Regional Development Studies, Newcastle University, UK*, 44(8):1689–1699
19. Okoli C, Pawlowski SD (2004) The Delphi method as a research tool: an example, design considerations and applications. *Inf Manag* 42(1):15–29
20. Ramakrishnan TS (2014) Financing infra projects through public-private partnerships in India. *Transp Res Rec* 2450:118–126
21. Roukouni A, Macharis C, Basbas S, Stephanis B, Mintsis G (2018) Financing urban transportation infra in a multi-actors environment: the role of value capture. *Eur Transp Res Rev* 10(1)
22. Shaoul J, Stafford A, SP (2012) The fantasy world of private finance for transport via PPPs. In: *Paper, working transport, international discussion forum*. www.econstor.eu
23. Sharma R, Newman P (2017) Urban rail and sustainable development key lessons from Hong Kong, New York, London and India for emerging cities. *Transp Res Procedia* 26(2016):92–105

24. Steinert M (2009) A dissensus based online Delphi approach: an explorative research tool. *Technol Forecast Soc Chang* 76(3):291–300
25. Tether BS (2003) The sources and aims of innovation in services: variety between and within sectors. *Econ Innov New Technol* 12(6):481–505

Visualisation of Transit Passenger's Mobility from Automatic Fare Collection Data (AFC): Case Study of Hubli–Dharwad BRTS



Shivaraj Halyal, Raviraj H. Mulangi, and M. M. Harsha

Abstract The automatic fare collection system is an essential part of many public transportation systems and adopting more and more by public transit agencies. Even though the primary purpose is to collect revenue, they also produce large quantities of transaction data. The produced data is much needed for many transit planners for the long-term planning of transit network requirements. This paper aims to evaluate the application of automatic fare collection data, focusing on the visualisation of the aggregate pattern of passenger characteristics in terms of boarding and alighting values. Hubli–Dharwad Bus Rapid Transit System (HDBRTS) was used as a case study. The passenger flow characteristics are recognized by the spatial distribution of six months boarding and alighting data of all the network stations. The interactive plots were developed and analysed to understand passenger mobility variations between network stations concerning different days of the week. Thus, ultimately, the paper gives a complete and inclusive view of the passenger's flow characteristics. It helps transit agencies take decisions on the utility-based priority for improving strategies on various available routes of the network.

Keywords Visualisation · HDBRTS · AFC system · Boarding · Alighting

1 Introduction

Before the advent of automatic fare collection (AFC) systems, manual method of data gathering was adopted by many transit operators to check the overall performance of the system. Because of the more cost involved and colossal sample size, data was collected only whenever it is essentially in need by the system. Therefore, it was very challenging for any researcher to acquire the required data for the required purpose.

S. Halyal (✉) · R. H. Mulangi · M. M. Harsha
Department of Civil Engineering, National Institute of Technology, Surathkal, India
e-mail: shivaraj.halyal@kletech.ac.in

R. H. Mulangi
e-mail: ravirajmh@nitk.edu.in

The automatic fare collection system offers a one-stop integrated system that provides vast amounts of operational data, which are widely recognized as having the potential to serve functions beyond the designated purpose of revenue management. With the aid of available source of data, trend in the passenger's movement will be assessed temporally and spatially and finally to monitor the system performance [1]. These systems provide enormous range in the data spatially and temporally with higher quality control measures been adopted during processing the data [2]. Hence, transit operators and researchers find this type of data very vital for planning strategies and carrying out research.

Combining various Web applications with AFC data helps in assessing the overall performance of the system by the operators as well as users. In this process, various metrics will be used which systematically estimate the performance in various spatiotemporal levels. Various matrices used are such as passengers waiting time, bunching, bus trips that skip stops due to heavy loads, crowding level, and crowding level passengers travel time and on-time performance [2].

Many previous studies used the application of AFC data. Even though they have utilized the potential of data appropriately, very few studies have given attention to data visualisation in understanding the inclusive view of passenger flow characteristics spatially and temporally through various routes of the system network level. So, these characteristics can be used in deciding utility-based priorities while making necessary decisions on the improvement strategies. It also reveals the actual experience of transit riders and demand.

The objective of the current study is to evaluate the application of automatic fare collection data, focusing on the visualisation of the aggregate pattern of passenger characteristics in terms of average boarding and alighting values. Hubli–Dharwad Bus Rapid Transit System (HDBRTS) was used as a case study. Using visualisation techniques, characteristics of passenger's flow are recognized by the spatial distribution of six months average boarding and alighting data of all the stations of the system network and observations summarized in terms of plots on the variations in the passenger's demand from all the stations of the network.

Overall sequence of the current paper is as follows, firstly the application of AFC-based data in many previous studies has been viewed comprehensively as a literature review. We then consider HDBRTS as a case study and discuss salient features of the system such as network details, details of bus stations, data collection system adopted, and route details. Then, with the help of AFC data, passengers flow characteristics have been analysed spatially by visualisation methods and plotting variations in the alighting and boarding demands from various bus stations. Finally, conclusions are drawn.

2 Literature Review

Several researchers and planners have made considerable efforts in analysing AFC data of different types of public transit systems such as rail, metro, and Bus Rapid

Transit Systems in implementing strategies related to advanced technologies capable of improving transit service operations in terms of passengers'-oriented reliabilities. Blythe et al. [3] used the AFC data of route load profiles to manage the demand through the transit network. Chu and Chapleau [4] in National Capital Region of Canada studied automatic fare collection data applications in various transit agencies in pattern of vehicle load demands.

AFC data applications were worked out with entry and exit validation by Jang [5]. Gong et al. [6] worked on the spatial and temporal pattern of travel times to explain intra-urban trips during peak hours over a day and found that they are different between weekday and weekend using 5 million smart card records for six days in Shenzhen. Application of AFC data was investigated, focusing on the analysis of travel time reliability and estimation of the Beijing metro's route choice behaviour by Sun and Xu [7]. Gallia et al. [8] visualised the passenger flow of the London Underground Network by considering 5% sample data of journey data. Tao et al. [9] have used geo visualisation-based methods to spatiotemporal dynamics of passenger data of Brisbane BRT. Maa et al. [10] have worked on a visualisation technique to maintain transit system performance using passengers as well as travel time data from Beijing. Robinson et al. [11] have mentioned that AFC data will help in great extent to estimate the OD pairs, with no or very less efforts because of readily availability of required information pertaining to the complete trip origin and destination. Even though that data cleaning becomes essential in many cases. Sun [1] has given a comprehensive and holistic view of passenger's travel experience in the Shanghai metro. By spatially and temporally distributing the passenger's demand data at the route level and individual bus stations demand and performing station inflow and outflow imbalances, the author has also analysed the travel time reliability from the user's perspective. Pi et al. [2] worked out new method to analyse the transit data for the purpose of systematic planning of public transit system, and method was used for the case of Pittsburgh region transit systems to check the service quality in different spatiotemporal ranges.

As a summary of the literature, many previous studies have utilized the potential of passenger flow-related data from different types of transit systems. Most of the studies are based on data calculation or analysis using models developed or clustering of the data. Minimal importance has been given to systematic assessment of passenger flow data by distributing spatially and temporally with the help of visualisation techniques available. Hence, the authors conducted a case study considered a very recently started Bus Rapid Transit System in Hubli-Dharwad, the twin city of the northern part of Karnataka. So, it is essential to visualise the pattern of passenger's flow throughout the network at the early stage itself to understand the requirement and demand of the passengers and take necessary decisions on the system expansion and system improvement strategies.

3 Need for the Study

HDBRTS has started its operation on all the routes very recently. Within such a short duration, the project has won many accolades from the general public. Also, it has shown excellent ridership data in increasing trend in last two years from the day of commencing its operation. Meanwhile, it has also won the award for “Excellence in Urban Mass Transit Project” at the National Level from the Ministry of Housing and Urban Affairs during the year 2019. However, any transit system expansion or improvement strategies will depend majorly on passengers’ demand for particular routes or network and land use patterns. So that agencies can make the decision correctly as the existing HDBRTS network is a single straight corridor. And also, it is still developing a system, where it has many plans to expand its network and routes in further days coming along with designing and integrating feeder systems for making ease in the operation. So, it is vital for the systematic analysis of aggregate patterns of passenger’s flows considering boarding and alighting data and distributing them spatially and understanding the variations in the flow demands along all the stages and routes of the system.

4 Hubli–Dharwad Bus Rapid Transit System

The Hubli–Dharwad BRTS is registered as company on 7 May 2012, it is Government of Karnataka Undertaking, and responsibility of company is operation and maintenance of HDBRT on continuous basis. The Government of Karnataka has established the company for the specific purpose of implementing the BRTS project in the twin cities of Hubli and Dharwad.

The HDBRTS is having single network corridor having total length of 22.25 km which stretches between twin cities Hubli and Dharwad, and the corridor Right of Way (ROW) width of the cross sections ranges from 44 to 35 m. HDBRTS is a hybrid-based system, where buses ply on dedicated as well as non-dedicated lanes for short length. Dedicated corridor from the Hosur circle in Hubli to the Jubilee circle in Dharwad. Beyond Hosur circle up to CBT, Hubli and beyond Jubilee circle up to CBT, Dharwad, the BRT buses ply on non-dedicated lane along with heterogenous traffic mode. The system has 35 stations, out of which one station is yet to start the operation (Station 25) effectively, including both side terminals where the AFC system has been adopted. Fig. 1 shows the transit corridor map of HDBRTS along with route details. BRTS corridor ROW also includes mixed traffic lanes, footpaths, etc. Details are given as follows

- Stretches from Hosur circle to Naveen Hotel, Hubli—Total length 35 m
- Stretches from Naveen Hotel, Hubli to Gandhinagar, Dharwad—Total length 44 m
- Stretches from Gandhinagar to Jubilee circle, Dharwad: Total length 35 m.

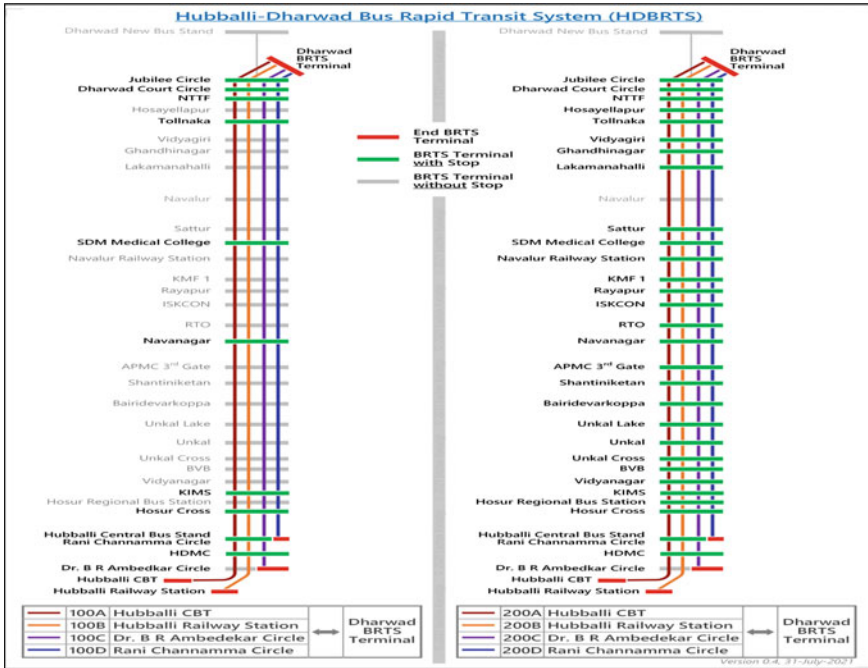


Fig. 1 Corridor and bus route detail

HDBRTS corridor is equipped with many features such as dedicated lanes, controlled bus stations, physical and fare integrated with BRT feeder, tickets issued by off-board facility, off-boarding through smart cards and tokens, and with all these high-quality buses. The corridor is designed for operating regular and express services. The BRT corridor consists of two lanes for BRTS buses on either side of the median bus station facilitating overtaking lanes for express services. Salient features of HDBRTS characteristics are listed in Table 1 as follow,

Table 1 Features of HDBRTS

Features	Details
Began operation	2 October 2018
Type of system	Closed BRTS
Number and type of corridor	Single and straight corridor
Length of network	22.25 kms
Number of stations	31 (3 bay stations 7, 2 bay station 24)

(continued)

Table 1 (continued)

Features	Details
Total routes	6 all operational (as per march 2020 data)
Service time	6 am to 11 pm midnight
Fleet size	100 (70 regular buses which stops all the stations & 30 express buses stops at 7 stations)
Daily ridership	More than 60,000
Average headway	Regular buses 3.0 min & Express buses 4.0 min
Bus capacity	Total 54 in numbers
Type of bus station	Median type

5 Data

The automatic fare collection system is being one of the features of HDBRTS. The data considered for the study purpose covers six months period starting from 1 January to 31 June 2019. The system works on weekdays with rarely slight variation in the number of schedules during weekends and weekdays. HDBRTS works on ticket bases where passengers stand in the queue and collect the tickets from the onboard ticket collecting system for the journey they planned. Tickets will be provided with QR codes and scanned on the fare gate at the entry and exit. So, this data captures all bus transit passengers in each station or bus stop separately. Considered data filed includes the date of journey, operators ID, device ID, boarding stop, and alighting stop, and other information is not considered in the current study.

6 Visualisation of Passengers Flow Characteristics

In the current study, visualisation of passenger's flow data of HDBRTS is performed by using chord plots and heat maps. Chord plots will provide clear picture on how boarding and alighting activities are happening by distributing collected data spatially on different days of the week. Heat maps are the significant visualisation tool to understand the variations in the collected data. Here, in this study, heat maps are used to understand variations in the demand of passengers boarding and alighting activity at all bus stations on the different days of the week.

6.1 Spatial Distribution

For the spatial distribution of passenger flow data, passenger boarding and alighting from each station and terminals have been calculated for all the week and week-ends separately. According to the first arrival on the corridor from the Hubli sides, numbering has been given for each station and terminals. The numbering system has shown in Table 2.

With the help of data visualisation techniques, we can plot chord diagrams for average boarding and alighting data of all the weekdays and weekends separately. So that we can represent actual flows or connections between every bus station throughout the network or corridor. Each station on the corridor is represented by a fragment on the outer part of the radial plot. Then, arcs are drawn between each station, and these arcs represent all the trips between those two stations. Darker arcs represent higher average passengers boarding and alighting between those sets of stations. These radial chords for passenger’s flow data allow visualizing the weighted relationship between each station and demand in the trips on those particular stations. Figure 2 represents for data boarding and alighting data for Monday; similarly, Fig. 3 for Tuesday, Fig. 4 for Wednesday, Fig. 5 for Thursday, Fig. 6 for Friday, Fig. 7 for Saturday, and finally Fig. 8 for the weekend, i.e. Sunday data, respectively. Along with this, to comprehend the overall spatial distribution of average passenger’s demand separately for weekdays and weekends, chords have been plotted considering six

Table 2 Numbering of bus stations

Station	Number	Station	Number	Station	Number
Hubli CBT	1	Unakal lake	13	Navalur (not operating yet)	25
Railway Station	2	Bairridevarkoppa	14	Lakamanahalli	26
DR.B.R. Ambedkar circle	3	Shantinikethan	15	Gandhinagar	27
HDMC	4	APMC 3rd gate	16	Vidyagiri	28
Hubballi central bus terminal	5	Navanagar	17	Toll naka	29
Hosur circle	6	RTO office	18	Hosa yellapur cross	30
Hosur regional terminal	7	Iskon temple	19	NTTF	31
KIMS	8	Rayapur	20	Court circle	32
Vidyanagar	9	KMF 1	21	Jubliee circle	33
BVB college	10	Navalur railway station	22	Dharwad BRTS terminal	34
Unakal cross	11	SDM medical college	23	Dharwad new bus stand	35
Unakal	12	Sattur	24		

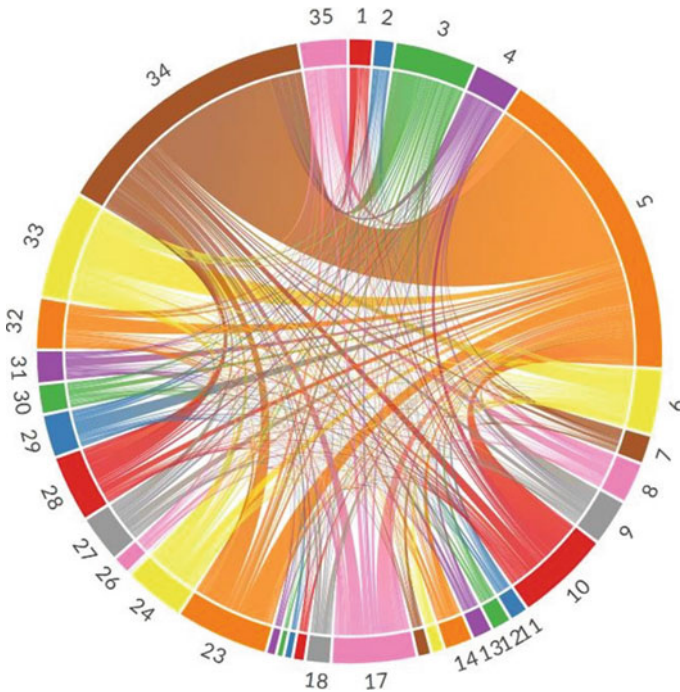


Fig.2 Spatial distribution of Monday average boarding and alighting

months of data as shown in Figs. 9 and 10, respectively. So that overall trend of weekdays and weekends demand can also be easily understandable.

As per spatial distribution of passenger flow from Figs. 2, 3, 4, 5, 6, 7 and 8, it has been observed that all the weeks except Wednesday follow a similar trend in the averaging boarding and alighting between all 35 stations. Even weekend follows weekday trend of passenger’s flow. The CBD area in Hubli is closed on every Wednesday instead of any other weekend. Hubli is being second largest city in the Karnataka and first place taken by Bangalore. Hubli is mainly serving as the corporate and commercial hub of Northern Karnataka. Most of the business centres, shopping centres, and commercial streets are located in the CBD area of Hubli. Even many people from Dharwad, which is at other side of the HDBRTS terminal, travel daily to run their business setup there in the Hubli city itself.

So, it is evident that, on Wednesday, most regular passengers will not travel between Hubli and Dharwad. This may be one of the solid reasons for getting dissimilar spatial distribution trends of average passengers boarding and alighting values associated with other weekdays. It is also astonishing that weekdays and weekends follow almost the same pattern, i.e. spatial distribution of passenger trips. It can also infer from this spatial distribution that stations 35, 34, and 5 are significant stations with the highest passenger demand in terms of the board and alight. Whereas at stations 1 and 2, passenger demand is average based on visualisation plots.

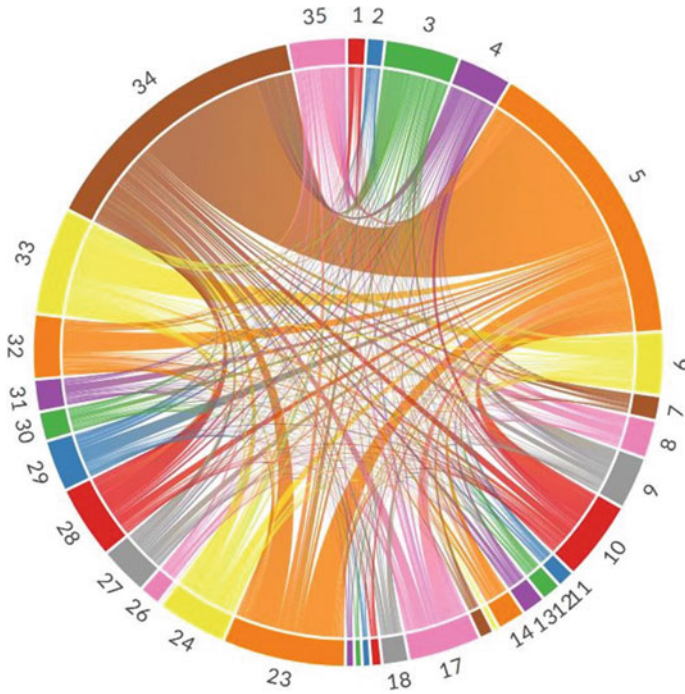


Fig. 3 Spatial distribution of Tuesday average boarding and alighting

Generally, terminals of any public transit system will have higher demand in terms of boarding and alighting. Here, in the case of HDBRTS, a similar trend follows with stations 5 and 34. Meanwhile, it has to be noted here that one more significant reason for higher demand is that both terminals in Hubli and Dharwad are located in the CBD areas of both the cities. Most passengers alight and board at both terminals as final destinations for their workplace, shopping place, or recreational activities. So, this trend at both the terminals of Hubli and Dharwad is observed on all weekends and weekdays except on Wednesdays.

Spatial distribution chords have also been plotted separately for average weekdays and weekends passenger's demand as shown in Figs. 9 and 10. It has been comprehended from respective plots that weekdays and weekends follow almost the same trend. Mainly due to Hubli being named for many commercial activities in Karnataka, and also Hubli Junction Railway Station is located in the South Western Railway district. It has excellent connections to cities in Karnataka and cities such as Mumbai, Hyderabad, Goa, and others. So, continuous passenger demand is observed in between twin cities that depend much on the public transit system itself.

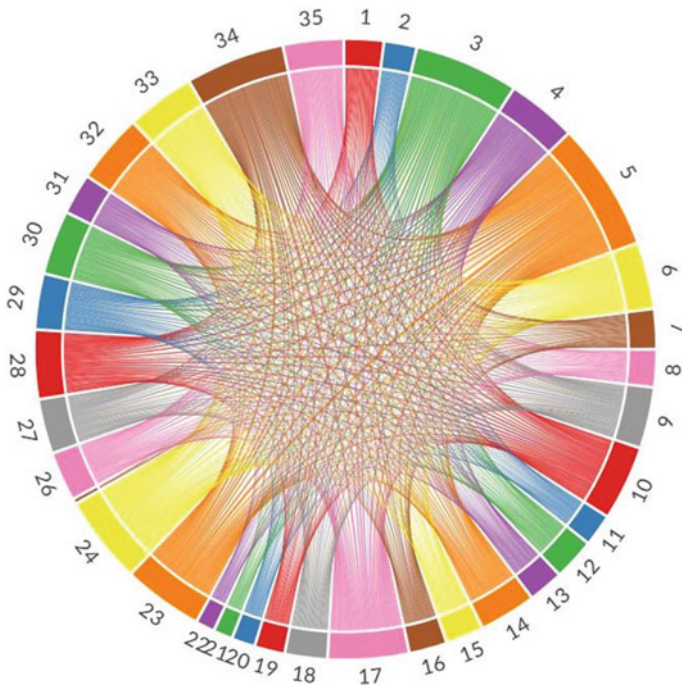


Fig. 4 Spatial distribution of Wednesday average boarding and alighting

6.2 Boarding and Alighting Variations

Variation in the passenger's demand at some stations is a common phenomenon in the public transit system operation. Variation may be observed due to different days of the week or maybe due to some influencing events at any hour of the day or day of the week. Perceptibly, these variations in the passenger's demand will alert optimal transit operation and result in different passenger travel times and operation costs of selected trips. So, in the current study, to understand this variation in the passenger's demand, the coefficient of variation (COV) has been considered. COV is the measure that states the ratio of standard deviation to mean for the data selected in the study. Here in this study, COV is defined as variations in the passengers boarding and alighting demand at each station, considering all the days of the week, respectively. For this purpose, whole six-month AFC data has been considered. Prepared data for the COV analysis is then visualised by plotting the coefficient of variation (COV) of the board and alight data throughout the six months with the aid of a heat map. Heat maps are one of the effective visualisation tools that utilise colour-coded systems. Colours in the heat maps communicate the values and display a more generalised view of numerical values. For the data considered, the uses COV data for six months have been previously clustered, according to the total number of boarding and alighting on each day of the week separately for each station. Maps have been plotted to board

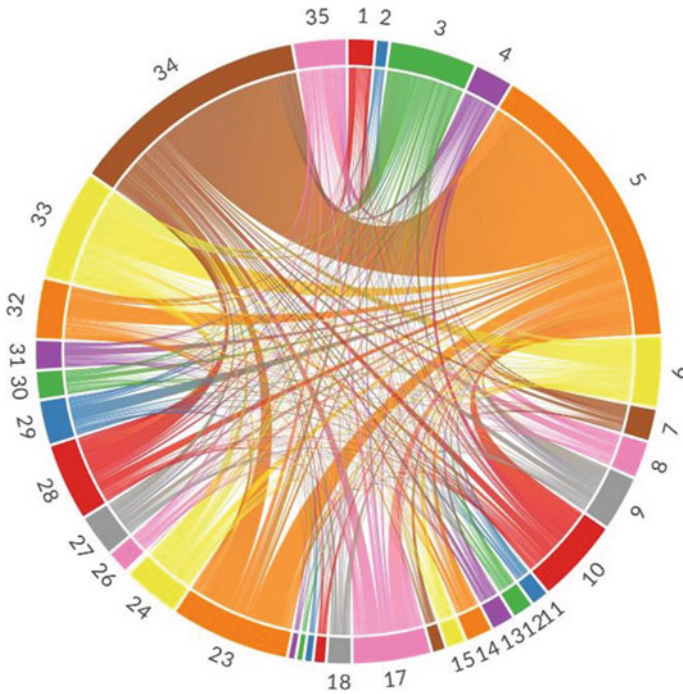


Fig. 5 Spatial distribution of Thursday average boarding and alighting

and alight data individually, as shown in Figs. 11 and 12, respectively. Here, in the study, the colour in the heat map represents the variation in the board and alight demand at the station. If darker the box's colour, then it will be considered more variation in the demand in terms of the board or alight at that particular station.

As per Fig. 11 boarding COV plot, it has been observed that significant bus stations in terms of highest passenger's demand like no 5 and 34 are meanwhile having significant COV in their passenger's demand. This trend follows throughout the week, mainly because stations 5 and 34 belong to the Hubli and Dharwad side terminals, respectively. In general, public transit terminals will have higher demand concerning both boarding and alighting activities. This trend is ideally driven by the different days of the week and the hour of the day, and HDBRTS will follow the same trend. So, with this, it can be said that, even in such complex situations, visualisation of existing boarding and alighting data helps to observe the variation trend and accordingly work for schedule adjustments by transit agencies. Station no. 17, which even has good demand in the passenger's flow, variation can be observed for weekdays to weekends. This is mainly due to station no. 17 is existed in the planned residential town between Hubli–Dharwad. It can be understood that demand is constant during weekdays as passengers more specifically need to travel CBD areas of both the cities for the activities like business, work, education, etc. But this demand may vary during weekends for shopping, recreational activities with increased values.

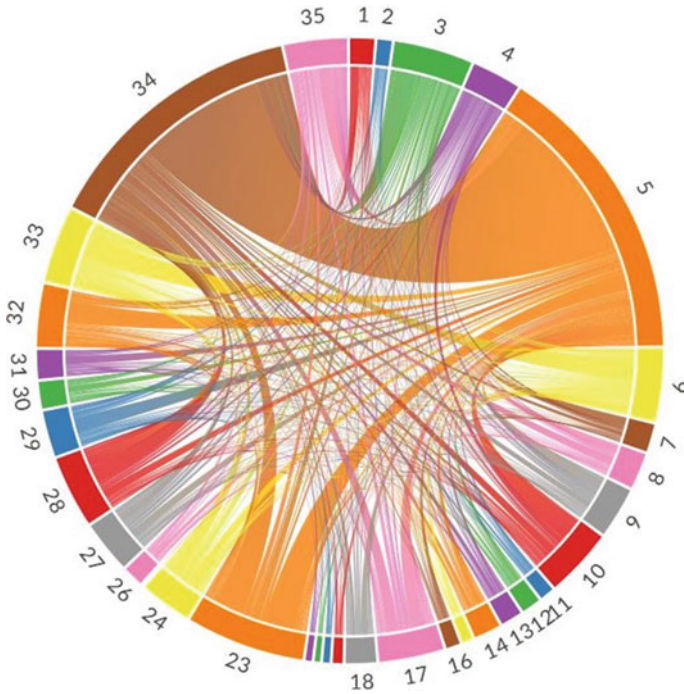


Fig.6 Spatial distribution of Friday average boarding and alighting

It can also observe from Fig. 11 that station no. 3 has higher variations in the boarding demand. This is prevalent because this particular station is located near Hubli junction railway station, and it is busiest railway station next to Bangalore in Karnataka. Due to this, demand will vary throughout the day and week.

As similar to the COV of boarding demand data, Fig. 12 shows COV plots for alight data. Here, variations in the alighting demand can be observed very clearly, considering all the stations mentioned in the previous sections. From the plot, it shows that all the stations considered are not having significant variation alighting demand. Wednesday's trend shows a significantly less variations compared to all other weekdays and weekends. Mainly due to the CBD area in the Hubli city typically closed every Wednesday instead of on weekends.

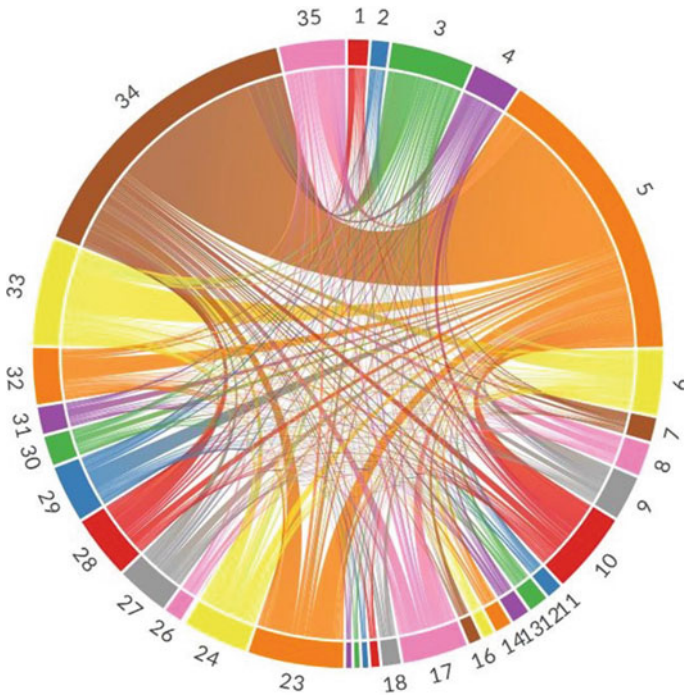


Fig. 7 Spatial distribution of Saturday average boarding and alighting

7 Discussions

- Smart data like automatic fare collection (AFC), automated passenger count (APC), automatic vehicle location (AVL), etc., from different transit operations, provides data for good understanding of the fundamental patterns and characteristics of the systems where agencies can make necessary decisions on the various strategies related to maintenance and further improvement system.
- However, organised manner of data arrangements and analysing them comprehensively will help understanding a potential data value.
- The visualisation technique is an efficient method, where it is possible to evaluate the system operations from various perspectives. The visualisation method adopted for HDBRTS AFC data in the current study is the satisfied requirement to reveal the aggregate characteristics of passenger trips in terms of passenger perspective.
- For the visualisation of passenger data, two major aspects are considered in the current study. Such as spatial distribution of average passenger's board and alight data from all the corridor stations and understanding the variations in the demand of passenger's board and alight on different days of the week, through plotting heat maps of the board and alight COV.

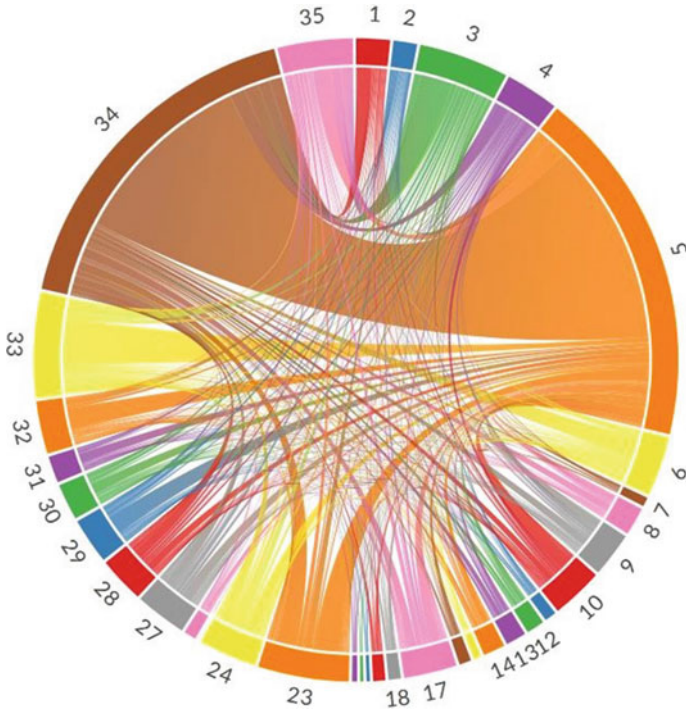
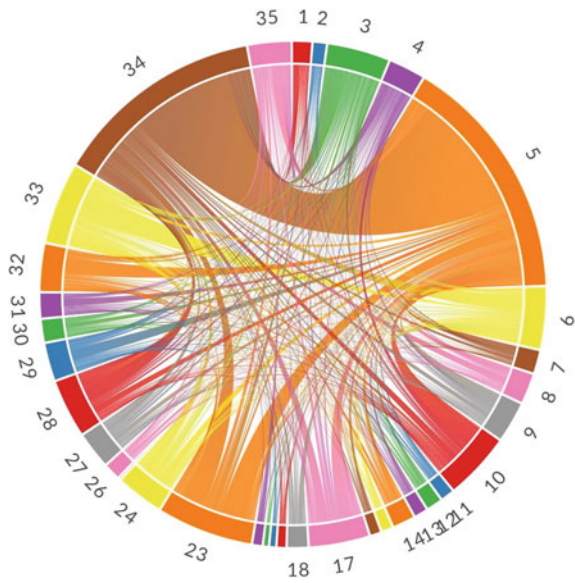


Fig. 8 Spatial distribution of Sunday average boarding and alighting

Fig. 9 Spatial distribution of weekdays average boarding and alighting



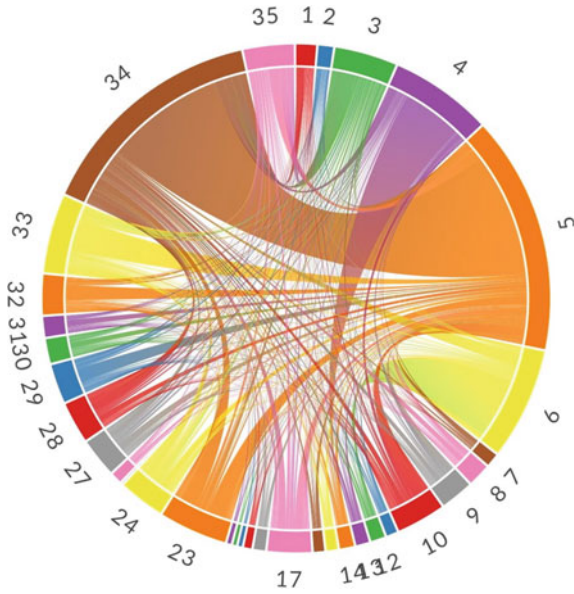


Fig. 10 Spatial distribution of weekend average boarding and alighting

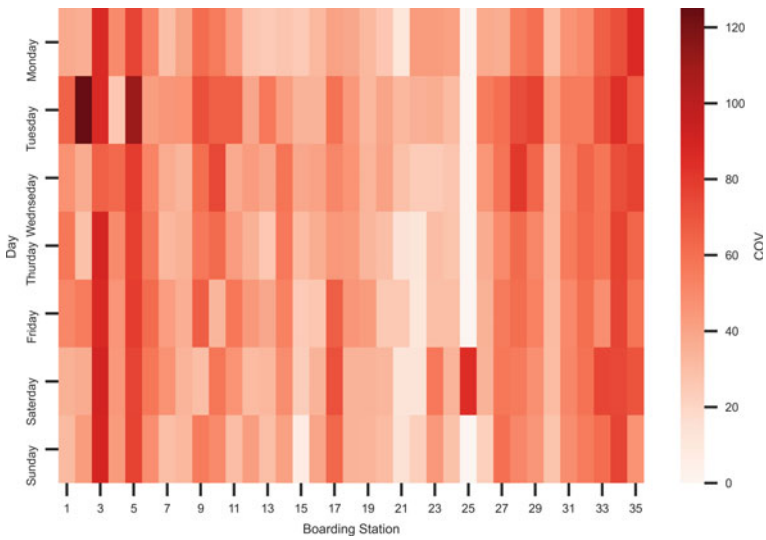


Fig. 11 Coefficient of variation (COV) of weekend and weekdays boarding data

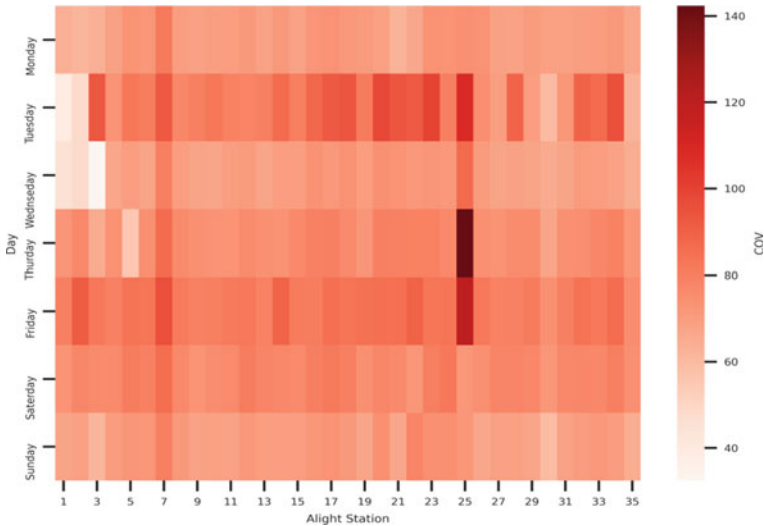


Fig. 12 Coefficient of variation (COV) of weekend and weekday alighting data

8 Conclusion

- In the current study, the application of AFCS data has been evaluated, focusing on the visualisation of the aggregate pattern of passenger characteristics in terms of average boarding and alighting values. HDBRTS was used as a case study.
- Study proposes how proper visualisation methods can help to get valuable patterns and trends from big data, particularly in this study characteristics of passenger's flow are recognized by the spatial distribution of six months average boarding and alighting data of all the stations of the system network and observations summarized in terms of plots on the variations in the passenger's demand from all the stations of the network.
- Spatial distributions of passenger flow characteristics will help in identifying critical stations with the highest boarding as well as alighting are happening. So that adjustments in the route schedules plans on day-wise can be made to handle such high demand stations.
- Plotting COV of all the day's board and alight will help to understand how demand varies on weekdays and weekends, along with the importance of each station. So that while making strategic decisions, utility-based priorities can be given to the station's improvements.
- Dissimilar patterns can be easily understood by common person by visualisation kind of techniques such as from spatial distribution plots of current case study, as Wednesday's plot follows dissimilar trend in the passenger's flow pattern in compares to other days in the week, it is due to CBD area in Hubli is closed on every Wednesday instead of any other weekend.

- Besides all these advantages, such visualisation methods are easy to understand the situation by the general public. The paper is also recommended to utilize the potential application of research efforts in taking strategic decisions on further development or improvisation of transit systems from transit agencies.

Acknowledgements The authors acknowledge the Hubli–Dharwad Bus Rapid Transit System Company Limited for their kind help in providing the data used in the current research.

References

1. Sun Y, Shi J, Schonfeld PM (2016) Identifying passenger flow characteristics and evaluating travel time reliability by visualizing AFC data: a case study of Shanghai metro. *Public Transp* 8(3):341–363
2. Pi X, Egge M, Whitmore J, Silbermann A, Qian ZS (2018) Understanding transit system performance using AVL-APC data: an analytics platform with case studies for the Pittsburgh Region. *J Public Transp* 21(2):2
3. Blythe PT (2004) Improving public transport ticketing through smart cards. In: Proceedings of the institution of civil engineers-municipal engineer, vol 157. Thomas Telford Ltd., Scotland, pp 47–54
4. Chu A, Chapleau R (2008) Enriching archived smart card transaction data for transit demand modelling. *Transp Res Rec* 2063(1):63–72
5. Jang W (2010) Travel time and transfer analysis using transit smart card data. *Transp Res Rec* 2144(1):142–149
6. Gong Y, Liu Y, Lin Y, Yang J, Duan Z, Li G (2012) Exploring spatiotemporal characteristics of intra-urban trips using metro smartcard records. In: 20th International conference on geoinformatics. IEEE, Hong Kong, pp 1–7
7. Sun Y, Xu R (2012) Rail transit travel time reliability and estimation of passenger route choice behaviour: analysis using automatic fare collection data. *Transp Res Rec* 2275(1):58–67
8. Gallia W (2021) A day on the London underground. <http://wgallia.com/#!/underground> 2021/05/26
9. Tao S, Corcoran J, Mateo-Babiano I, Rohde D (2014) Exploring bus rapid transit passenger travel behaviour using big data. *Appl Geogr* 53:90–104
10. Ma X, Wu YJ, Wang Y, Chen F, Liu J (2013) Mining smart card data for transit riders' travel patterns. *Transp Res Part C: Emerg Technol* 36:1–12
11. Robinson S, Narayanan B, Toh N, Pereira F (2014) Methods for pre-processing smartcard data to improve data quality. *Transp Res Part C: Emerg Technol* 49:43–58

Stabilisation

Chemically Stabilized Laterite Soil Using Rice Husk Ash



Somnath Paul  and Dipankar Sarkar 

Abstract This research focuses on optimum usage of industrial waste in soil stabilization. Shear strength alteration happens in subsoil due to environmental fluctuations or seismic events that are generally observed in hilly areas with unsupported backfills. This problem becomes worst in the case of problematic soil that causes collapse or swelling followed by shrinkage in contact with water due to the high anisotropic nature of the subsoil. The cyclic behavior of various problematic soils under transient loading directly incorporates the economic loss and human lives. The present experimental work has briefly described the suitability of using rice husk ash (RHA) in soil stabilization and reducing the dumping of toxic waste responsible for environmental pollution. In place of common stabilizer units such as fly ash and pond ash, we use a cheap stabilizing agent which has no use in soil improvement in past as single unit. RHA is used as a chemical stabilizer as it contains high percentage of silica. If the soil has a larger fraction of clay mineral, then RHA (produced by controlled incineration ~400–500 °C) mixed soil in different proportion (4 and 6% by weight of soil sample) performed differently in serviceability and workability tests on soil sample like UCS, modified proctor test, CBR, Atterberg's limit, permeability, consolidation test, etc. Excellent results were obtained at 6% optimum dosage of RHA in locally available laterite soil (inside NIT Agartala campus) from NE part of India.

Keywords Rice husk ash · Soil strength · Serviceability

S. Paul (✉)
Graduate Engineer, NIT Agartala, Agartala, India
e-mail: somnathpaul.iitgn@gmail.com

D. Sarkar
Assistant Professor, NIT Agartala, Agartala, India
e-mail: dipankarnita@gmail.com

1 Introduction

Soil stabilization is primary concern for geotechnical and transportation aspects in recent time. Many of new techniques like mixing and curing of soil with bitumen, tar emulsions [13], fly ash [4, 6], bagasse ash [2], cement [13], lime [13] and pond ash [9] can be used as binding agents for producing durable soil matrix in pavement construction. But, environmental safety and health issues should kept in mind during their usage. Because, each material can create detrimental effects on nature by erosion and release CO_2 in open atmosphere during their manufacturing. Among the top seven states with the highest rate in land degradation in last 10 years, six states are from NE, India. Weathering erosion and water logging on pavement cause poor performance of subgrade which is frequently observed in hilly area of NE, India, during monsoon. Central investigation [15] reports find that the most common cause of land degradation is acidification in soil. About 7.5 lakh hectares of land in Nagaland and 6.3 lakh hectare of land in Manipur are acidic in nature found by GSI [5]. Soil acidity increases when metallic ions like calcium, magnesium, potassium and sodium are lost from the soil and only hydrogen ions present. This hydration of soil minerals causes sudden disintegration of soil block from sides of hill cuts during heavy rainfall and causes devastating landslides. Those weaken the subgrade properties due to rearrangement of particle in pavements during course time. In recent investigations, some landslides were taken place at NE, India. One of those are landslide reportedly occurred at Lokchao area, Tengnoupal District, Manipur, heading as “Landslide hits NH-102” at August 3, 2018 (Fig. 1). The main causes of slide includes extensive slope cutting result in increase of gravity load, sparse vegetation above the crown, poor drainage along the faults, development of widening in cracks that covered the slope from top to bottom.

Another example of landslide took place at Lumding-Badarpur Railway Line that collapsed during heavy rainfall at July 2018. It caused a huge mass slide near Bandarkhal Railway Station in the midnight of July 14 (Fig. 2). Heavy rainfall, fluvial

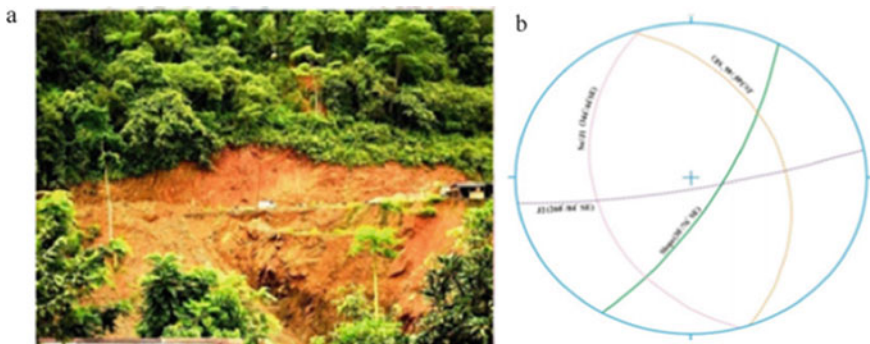


Fig. 1 **a** Plane view of Lokchao slide along NH-102 along Imphal-Morch road, **b** stereographic projection of joint planes



Fig. 2 Slope fails and causes sliding failure on railway embankment of Lumding-Badarpur Line

action, soil comprising of small and large fragments of sandstone, undrained surface run-off and seepage of water along the pre-existing cracks were identified as some of the contributing factors.

From the given examples, it is clear that in most of the places the soil is dispersive in nature and forms flocks in the presence of water which supports gravitational forces and causes landslides. The failure plane crosses toe of the slope and passes below the earth structures which causes global failure of soil slope system. Constructors are mainly focused on local stabilization of slope by installing gabion wall, retaining structure. But it is hard to identify the long term stability behavior of soil [10]. Different uncertainties like sudden drawdown of water table and the seismic shakes due to earthquake cause huge damage in form of sliding, overturning and topple of earth retaining structures. In highway embankment, fatigue crack and potholes appeared (Fig. 3) due to differential settlement which gradually split on surface of road pavement and frequently reduce serviceability of it. NH-208A also suffers from tremendous cracks during monsoon in every year due to heavy rainfall and water logging.

Therefore, soil stabilization is prime concern in NE part of India. The main objective of soil stabilization is to increase mechanical strength of soil, stability of soil slope and reduce construction cost with best use of locally available stabilizers. Cement and

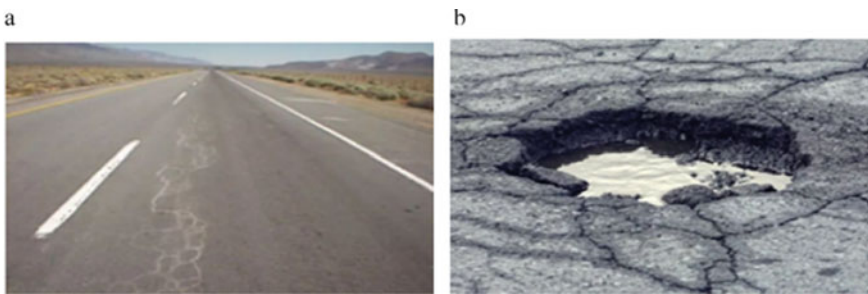


Fig. 3 a Fatigue cracking, b potholes

lime are two common materials used for soil stabilization [3, 7, 12]. These materials have rapidly increased in price due to sharp increase in production cost. Use of agricultural waste (e.g., RHA) will considerably reduce the cost of construction [8] and release less CO₂ in open atmosphere compared to other chemical stabilizers such as lime and fly ash. Rich husk is generally produced by using incineration process [14]. Rice husk is an agricultural waste obtained from milling of rice. About 20 million tons of husks are produced worldwide in every year [11]. The husk is not suitable as animal feed because of its abrasive character and almost negligible digestive protein content. Its high ash and lignin contents make it unsuitable as a raw material for paper manufacturing.

In present investigation, we use different dosage of rice husk ash (manufactured at control temperature burning of 400–500 °C called incineration process) in the proportion of 4 and 6% weight of tested soil specimen to investigate the effects on index and engineering characteristics of problematic soil. The effect of soil stabilization on soil properties like compaction property, California bearing ratio, settlement characteristics, unconfined compressive strength and permeability is observed. The self-potential of optimum usage for rich husk ash still left to be unexplored on ground improvement and controlling soil migration in a heavy rainfall area (specifically hilly area) with improvement in local available laterite soil properties used for highway constructions.

2 Experimental Work

2.1 Materials

The tested soil sample was collected from west district of Tripura, India at a depth of 1 to 1.5 m using disturbed sampling process. The classification of soil is silty sandy (SM) type, and other geotechnical index properties are explained in Table 1.

Table 1 Geotechnical properties of the natural soil collected from Institute Campus

Geotechnical characteristics	Experimental values
Natural moisture content (%)	19.81
Specific gravity, G_s	2.59
Liquid limit (%)	34
Plastic limit (%)	25.5
Maximum dry density (gm/cc)	1.71
Optimum moisture content (%)	14
UCS (%) and CBR (kN/m ²)	6.34 and 57.98

2.2 Methods of Testing

The laboratory tests carried out mostly on RHA mixed soil in different dosage which includes particle size distribution, Atterberg's limits, compaction test, CBR and UCS test, Oedometer test and permeability test. The geotechnical properties of the soil are determined in accordance with Indian Standard Code.

3 Results and Discussion

3.1 Grain Size Distribution

About 99.6% of soil is finer than 4.75 mm aperture sieve size and 0.4% of soil is finer than 75 μ aperture sieve size has been shown in Table 2. Hence, major percentage of specimen contains silt which is generated by weathering of quartz mineral.

For particle size less than 75 μ m is analyzed by hydrometer analysis which is based on the principle of Stoke's law that allows the particle to set in an infinite fluid under free boundary condition.

From Fig. 4, it is clearly noticed that more than 50% of fine fraction of soil is retained on 2 μ sieve size and about 90% of soil is finer than 75 μ aperture size.

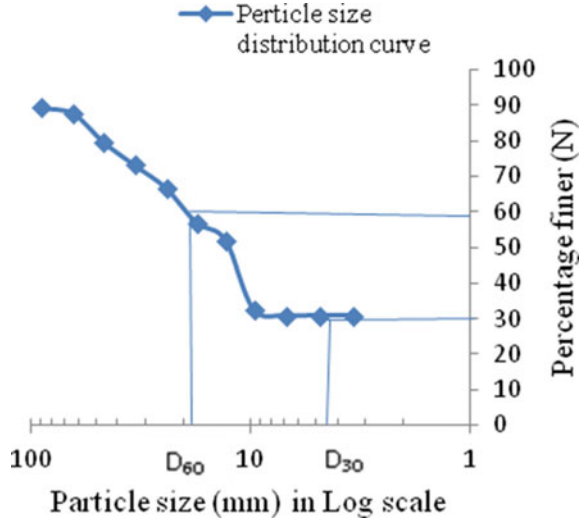
3.2 Atterberg's Limit

The Atterberg's limits are tested according to the code of IS: 2720-Part V. The liquid limit comes to 23.78% (Fig. 5), and plastic limit comes to 14.58% on Institute soil. Plasticity index (I_p) comes to 9.21% which determines the range of water content in plastic state of soil. From plasticity chart, I_p obtained as 2.77. Therefore, soil

Table 2 Particle size distribution data of natural soil collected from Institute Campus

IS Sieve size in mm	Percentage finer (%)
4.75	99.6
2.36	99.2
1.18	97.2
0.6	95.6
0.425	60.8
0.3	40.8
0.15	3.6
0.075	0.4

Fig. 4 Particle size distribution curve of NIT Agartala soil



ranges above the A-Line. But from hydrometer analysis, it proves that there is minor percentage of clay in current soil. So, it is obvious that silt is predominant in soil matrix.

The liquidity index of soil indicates the nearness of sample in-situ water content to its liquid limit

$$I_p = \frac{w - w_p}{I_p} \times 100 \tag{1}$$

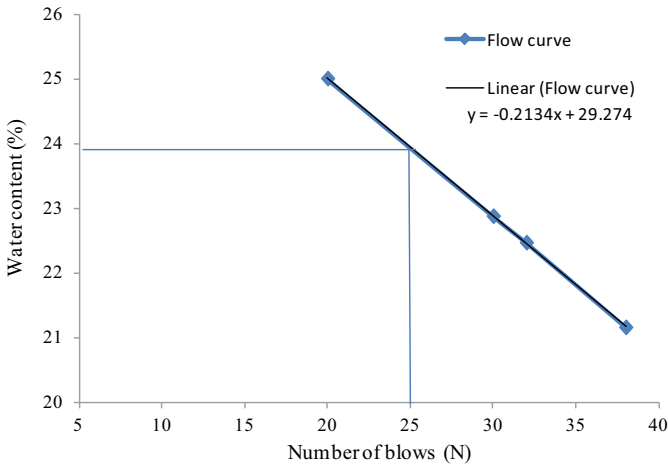


Fig. 5 Flow curve for liquid limit testing

Liquidity index calculated from the test is 0.56 means that the soil lies intermediate between plastic and semi-solid state.

Consistency index indicates the water content of soil nearness to its plastic limit.

$$I_c = \frac{w_1 - w}{I_p} \times 100 \quad (2)$$

Consistency index obtained from the test is 0.43, means that the soil has significant strength even at the intermediate stage of plastic and semi-solid stage.

Toughness index (I_t) can be measured as following,

$$I_t = \frac{I_p}{I_f} \quad (3)$$

where I_p = Plasticity index,

I_f = Flow index, slope of the flow curve obtained from liquid limit test.
= 12.05%.

I_t comes out 1.31, shows higher shear strength at plastic limit by the given Eq. (4),

$$\text{Log}_{10}(S_p) = I_t + C, C = \text{correction factor} = 0.431 \quad (4)$$

3.3 Modified Proctor Test

Using modified proctor test (IS 2720, Part-VIII), the optimum moisture content and maximum dry density are obtained as 15% and 1.85 gm/cc by using 6% of RHA (Fig. 6). Dry density decreases due to the presence of RHA which increased fine content and water retention capacity, respectively, using current available laterite soil.

3.4 California Bearing Ratio

California bearing ratio test is generally used to predict the bearing capacity and strength of subgrade with base soil.

It is observed from Fig. 7 that CBR value increases from 16.11 to 19.43% at 2.5 mm penetration due to stabilization of soil in between 4 and 6% RHA content with soil. Similar trend can be observed for the values of CBR at 5 mm penetration which rise from 14.86 to 16.82%. The increase in CBR values can be attributed to the fact that as percentage (%) of RHA content increases from 4 to 6%, there is an increase in the formation of cementations compound as the RHA forms bonds with other inorganic compounds present in the soil. If we further increase RHA content,

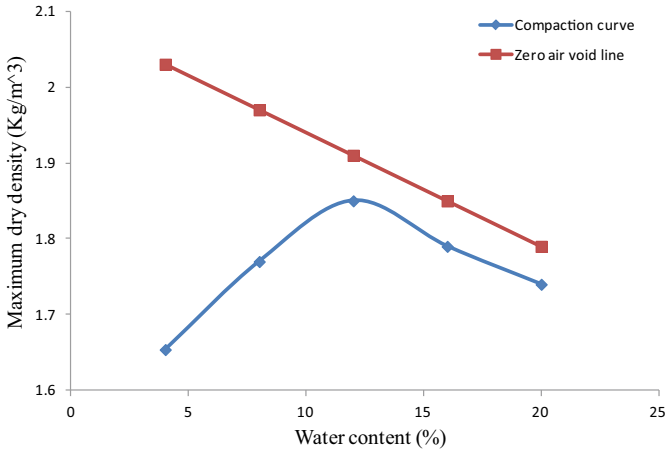
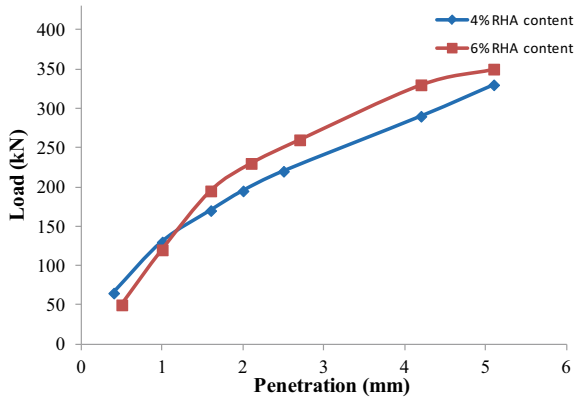


Fig. 6 Graphical representation of modified proctor test

Fig. 7 Graphical representation of CBR value of soil with 4 and 6% RHA mixture

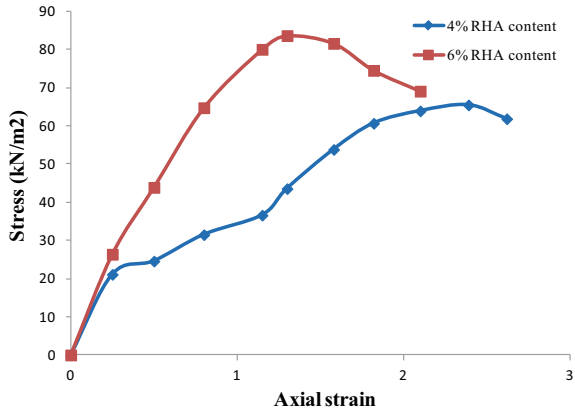


there might be a gradual decrease in the value of CBR due to replacement of soil by finer fraction of RHA.

3.5 Unconfined Compressive Strength

UCS test helps to find different parameters like compressive strength and shear strength of soil. It helps to determine the strain rate at which a given specimen fails along with the maximum bearable compressive stress that a soil specimen can endure. The value of UCS at 4 and 6% use of RHA in soil was found to be 65.46 and 83.62 kN/m² as observed from Fig. 8. The specimen used for testing was remolded at OMC and MDD. An important change that can be observed was that the specimen

Fig. 8 Graphical representation of UCS value of soil at 4 and 6% RHA mixture



used for determining UCS was predominantly cohesion-less soil specimen having negligible compressive strength in natural state. However the compressive strength substantially increased on stabilizing with RHA. Curing technique also increases the confining strength of specimen. If UCS value of stabilized soil is compared with that of natural soil which has UCS value of 57.98 kN/m², in both cases, UCS values have shown an increasing trend. However, it should be kept in mind that the specimen is remolded at OMC and still remains in cohesion-less state, but adding RHA in soil helps to overcome disintegration by acting as a binder.

3.6 Permeability Characteristics

Subsequent increase in the percentage of RHA in soil, Permeability decreases in the power of 10 (Fig. 9). At 4% RHA content in soil specimen, permeability obtained from falling head permeability apparatus is 4.1×10^{-4} mm/s. However at 6% RHA content, permeability obtained as 1.49×10^{-5} mm/s (Table 3). This logarithmic decrease happens due to gradual migration of natural soil and subsequent occupation of RHA which has almost 70% of silica present in it. Thus it reduced the void spaces between two consecutive molecules. The metric suction of soil changes, and there will be less possibility of water infiltration in the subgrade of pavement system. Thus reduces crack formation and disintegration of soil specimen.

3.7 Oedometer Test

In consolidation test, the void ratio for each incremental load is calculated using height of solids method. Here, soil type is SM (silty sand), and hence, secondary or creep consolidation will not predominant. Primary consolidation is main concern.

Fig. 9 Permeability of soil at 4% and 6% RHA content

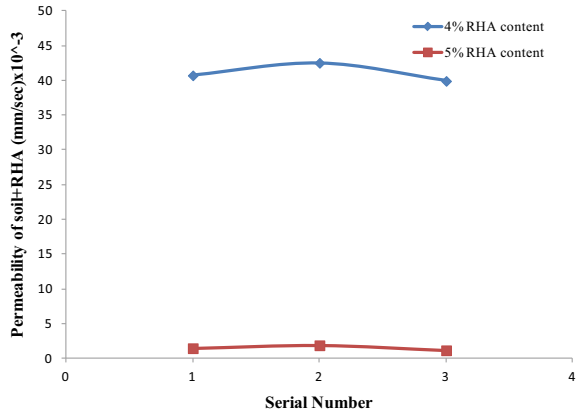


Table 3 Differences between the permeability values for soil at 4 and 6% RHA content

Serial number	K ₂₇ °C at 4% RHA content (mm/s)	K ₂₇ °C at 6% RHA content (mm/s)
1	0.000407839	1.45138E-05
2	0.000425028	1.87679E-05
3	0.000399337	1.1554E-05
Average K	0.000410735	1.49452E-05

The C_c and C_r values obtained from the test as 0.29 and 0.004, respectively. As per AASTHO [1], effective overburden pressure of one storey building is 20 kPa on the foundation soil, and consolidation test uses 800 kPa which is equivalent to 40 storey building. From test, it can observe that soil is safe for load up to 200 kPa (~10 storey building). It also can be used in the subgrade of highway carrying transient traffic loading because the residual strain will not affect the strength of subgrade as particle-to-particle interlocking is good due to mixing of optimum percentage in RHA (Figs. 10 and 11).

Fig. 10 e (Void ratio) versus $\log \sigma$ curve

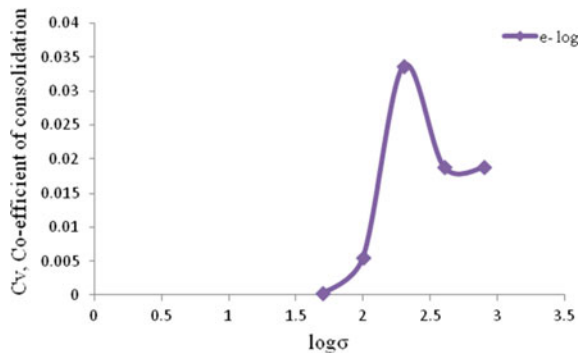


Fig. 11 Semi-log plot between void ratio versus pressure

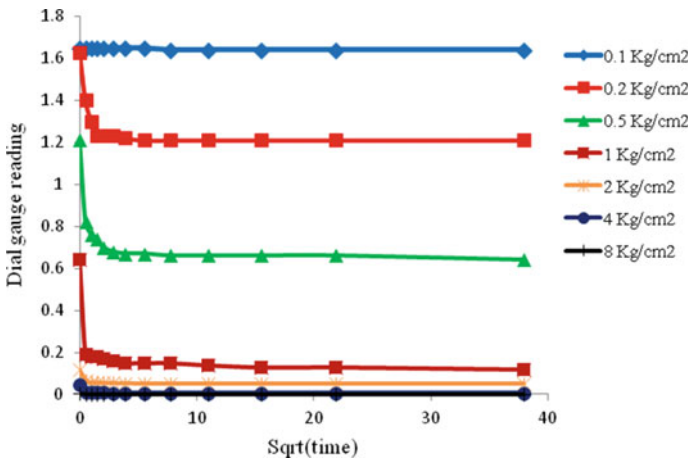
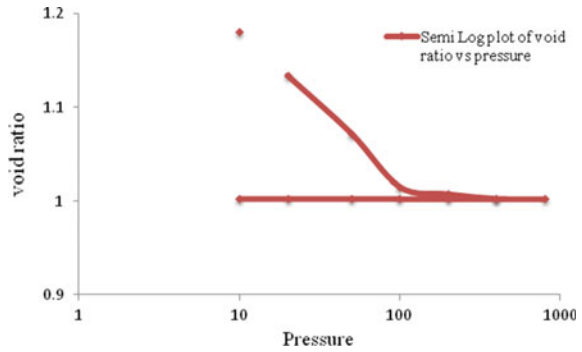


Fig. 12 Dial gauge reading versus sqrt(t) graph from oedometer test

The dial gauge reading for each load increment is measured using graphical representation (Fig. 4.9) by applying Taylor method (\sqrt{t} method) (Fig. 12).

3.8 XRD Pattern of Sample

The XRD pattern of the sample is shown in Fig. 13.

XRD analysis of RHA from laboratory-controlled incineration (RHA500, RHA650, RHA800, and RHA900) is given in Fig. 3.10. Peaks in the diffraction angles (2θ) such as 21.96, 31.42 and 36.35 degrees ($^\circ$) are observed in the XRD of the RHA which are characteristics of cristobalite (a crystalline form of silica generated at high temperature).

The chemical composition of rich husk ash is mentioned in Table 4.

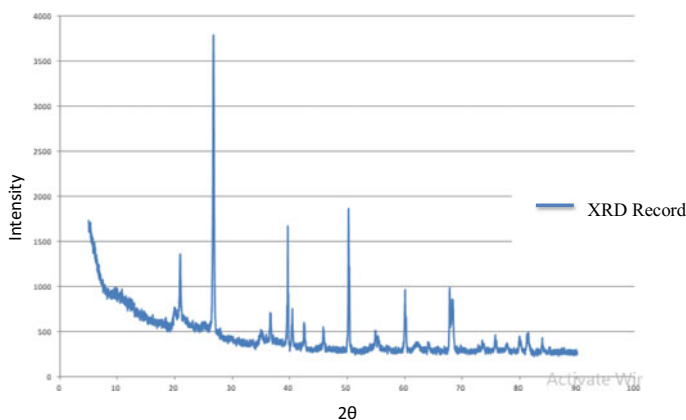


Fig. 13 XRD pattern of 6% RHA mixed soil

Table 4 Chemical component of rice husk ash (collected from Agartala city) experimentally found based on XRD record

Compound	Percentage (%)
SiO ₂	86
Al ₂ O ₃	2.6
Fe ₂ O ₃	1.8
CaO	3.6
MgO	0.3
Loss of ignition	4.2

4 Conclusion

Dispersive nature of soil causes major landslide, failure of road embankment and cracks on pavement during heavy rainfall in north-eastern part of India. The Atterberg's limit indicates that with addition of RHA to soil, the swelling potential (potential to volume change) reduces linearly in case of seasonal variation. Standard proctor test, permeability test and consolidation test have shown that mechanical as well as index properties of soil improves by using 6% RHA (optimum dosage) mixing with the natural soil sample (SM type) collected from institute campus. Soil skeleton got modified, interlocking has improved, and void sizes decreased which caused reduction in differential settlement at major overburden load on soil. However, the improvement got reduced when dosage of RHA increased beyond 6%. It is because of less Pozzolanic reaction happens in deficiency of water. Whereas, dosage less than 6% causes less formation in CSH gel which is not sufficient to hold discrete laterite soil particles during partially and fully submerged condition. Dumping of RHA is also harmful, as it reacts with soil and changes natural mineral composition. That's why RHA is used in soil improvement; less construction cost and provides more reliability in strength and stability of soil.

References

1. AASTHO (2011) https://www.academia.edu/31863807/AASHTO_2011_pdf
2. Ahmed B, Rahman A, Das J (2015) Improvement of subgrade CBR value by using Bagasse ash and Eggshell powder. *Int J Adv Struct Geotech Eng* 4(2):86–91
3. Alhassan M, Alhaji MM (2017) Utilisation of rice husk ash for improvement of deficient soils in Nigeria: a review. *Niger J Technol* 36(2):386–394
4. Andavan S, Pagadala VK (2020) A study on soil stabilization by addition of fly ash and lime. *Mater Today: Proc* 22:1125–1129
5. GSI(2018) <https://employee.gsi.gov.in/cs/groups/public/documents/document/b3zp/mtyx/~edisp/dcport1gsigovi161646.pdf>
6. Gupta G, Sood H, Gupta P (2020) Performance evaluation of pavement geomaterials stabilized with pond ash and brick kiln dust using advanced cyclic triaxial testing. *Materials* 13(3):553
7. Jamsawang P, Yoobanpot N, Thanasisathit N, Voottipruex P, Jongpradist P (2016) Three-dimensional numerical analysis of a DCM column-supported highway embankment. *Comput Geotech* 72:42–56
8. Jongpradist P, Homtragoon W, Sukkarak R, Kongkitkul W, Jamsawang P (2018) Efficiency of rice husk ash as cementitious material in high-strength cement-admixed clay. *Adv Civ Eng* 2018
9. Jiang X, Huang Z, Ma F, Luo X (2019) Analysis of strength development and soil-water characteristics of rice husk ash-lime stabilized soft soil. *Materials* 12(23):3873
10. Jha AK, Sivapullaiah PV (2020) Lime stabilization of soil: a physico-chemical and micro-mechanistic perspective. *Indian Geotech J* 50(3):339–347
11. Karatai TR, Kaluli JW, Kabubo C, Thiong'o G (2017) Soil stabilization using rice husk ash and natural lime as an alternative to cutting and filling in road construction. *J Constr Eng Manag* 143(5):04016127
12. Khan AN, Ansari Y, Mahvi S, Junaid M, Iqbal K (2020) Different soil stabilization techniques
13. Lu N, Wayllace A, Oh S (2013) Infiltration-induced seasonally reactivated instability of a highway embankment near the Eisenhower Tunnel, Colorado, USA. *Eng Geol* 162:22–32
14. Liu Y, Chang CW, Namdar A, She Y, Lin CH, Yuan X, Yang Q (2019) Stabilization of expansive soil using cementing material from rice husk ash and calcium carbide residue. *Constr Build Mater* 221:1–11
15. NECRP (2017) <https://employee.gsi.gov.in/cs/groups/public/documents/document/b3zp/mtyx/~edisp/dcport1gsigovi161649.pdf>

Effect of Stabilized Subgrade on Rutting Resistance of Asphalt Concrete Pavement



Polukonda Gopalam, Barnali Debnath, and Partha Pratim Sarkar

Abstract Pavement distress has become a common issue nowadays due to the increased traffic growth, overloading, inferior pavement materials, etc. Rutting is one such major pavement distress that reduces the long-life performance of flexible pavements. This study aims to a systematic study and analysis of the rutting behaviour of conventional asphalt concrete (AC) pavements on stabilized subgrades by using the finite element method. In this study, subgrade stabilization is done using different percentages of nano-silica and cement. Initially, the focus is paid to check the effect of nano-silica in subgrade stabilization, and then to check the effect of these stabilized subgrade materials on the rutting resistance of flexible pavement under the action of both static and repeated traffic loading conditions. Different pavement models are created in finite element-based software having stabilized subgrade. From the test results, it is found that the strain and rutting generated in AC pavement on stabilized subgrade are much lower than the AC pavements with the natural subgrade. From the static loading and dynamic loading test results, it is found that the vertical strain in the subgrade and rutting in asphalt layer can be reduced up to 60–69% and 18–22%, respectively, after adding 2% nano-silica with 6% cement.

Keywords Subgrade · Soil stabilization · Nano-silica · Resilient modulus · Repeated loading

1 Introduction

Asphalt concrete pavements or flexible pavements are the most commonly used pavements in India, but the current infrastructure development has been leading to the high growth traffic loading and overloading issues, which causes various types of structural distress of pavement. Pavement rutting is a serious pavement distress, which develops as a form of longitudinal surface deflection along the wheel paths in the bituminous concrete layer [1]. The assessment of asphalt pavement for its

P. Gopalam · B. Debnath (✉) · P. P. Sarkar
National Institute of Technology Agartala, Agartala, India
e-mail: brnali540@gmail.com

© The Author(s), under exclusive license to Springer Nature Singapore Pte Ltd. 2023
M. V. L. R. Anjaneyulu et al. (eds.), *Recent Advances in Transportation Systems Engineering and Management*, Lecture Notes in Civil Engineering 261,
https://doi.org/10.1007/978-981-19-2273-2_30

465

tendency to rutting has been a significant research topic across the globe. The capability of predicting the amount of rutting in flexible pavements is a vital feature of pavement design. Rutting is the main distressing factor in flexible pavement design, which may be caused due to heavy commercial vehicles, the strength of existing soil as well as a severe environmental condition. It was observed that 80–90% of rutting mostly occurs at the surface due to either plastic deformation of the surface layer (instability rutting) or due to the lower layer's permanent settlement (structural rutting) [2, 3]. The present study focuses on the latter aspect, i.e. the settlement of lower pavement layers, and tries to improve the subgrade layer by means of soil stabilization. Indian Road Congress (IRC) has also mentioned that the rutting might be a part of weak subgrade or subgrade deformation [4]. Several researchers have suggested the usage of soil improvement techniques, where soil improvements are generally categorized into two processes: (a) soil modification and (b) soil stabilization [5]. The drastic changes in population growth and urbanization rate are leading to the dearth of good quality foundation soil. Suitable properties of soil for civil engineering constructions especially for pavement construction are not available, and in most cases, existing natural subgrade soil may not give satisfactory performance for supporting the structures with desired facilities [6]. Soil stabilization is one of the widely used methods for the improvement of problematic soils with locally available customary cementitious additives such as fly ash, lime, cement, etc. [7]. In recent years, researchers are increasing interest in finding alternative materials with low energy consumption, and environmentally friendly alternative materials. The application of industrial by-products in the form of nano-scaled dimensions (i.e. nanomaterial) reduces the cost and saves energy in addition to satisfy the requirement of environmental awareness [8]. Because of its nano-size property, it has a high specific surface area, so it can easily interact with soft soils, and it has been proved to be an effective method in reducing the overall thickness of the pavement [8, 9]. The previous literature mentioned that the addition of nanomaterials in soil improves the engineering properties as well as the strength of the soil. Therefore, in the present study, a nanomaterial (nano-silica) has been taken under consideration for the stabilization of soil. Along with the nano-silica, a certain amount of cement is also added to improve the strength. The addition of cement in soil stabilization is already an established method, and many studies have also been conducted to check the effect of cement in soil/subgrade stabilization. However, the addition of nano-silica along with cement is relatively a new concept. Moreover, there is a scarcity of literature related to the effect of this subgrade stabilization in the rutting behaviour of asphalt concrete pavement, and in this respect, the present work holds great importance. The basic objectives of this study are

1. To improve the strength of subgrade by the addition of nano-silica and cement, and
2. To check the effect of subgrade stabilization in the rutting behaviour of asphalt concrete pavement.

The rutting resistance of flexible pavement on different subgrade conditions can be determined by means of computer-developed finite element-based software [10]. In

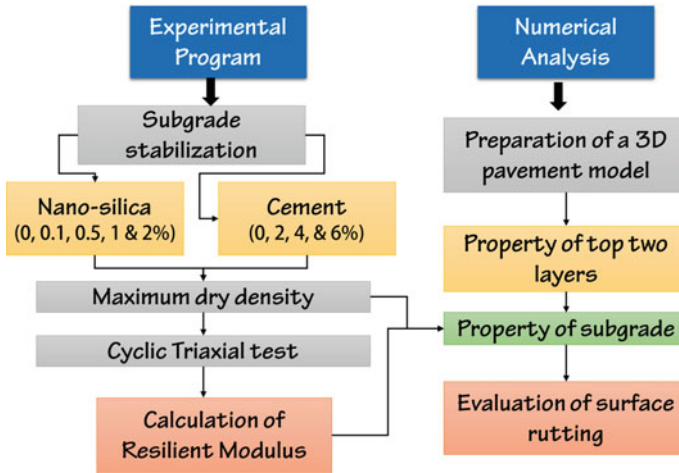


Fig. 1 Methodology followed in the present study

this research, the response of the pavement system is investigated and modelled using the ABAQUS program (ver. 6.12-1). Initially, laboratory experiments are conducted to find the resilient modulus of subgrade stabilized with nano-silica and cement. Later on, numerical models are prepared in ABAQUS using the subgrade properties evaluated in the laboratory. The numerical models are performed under static loading condition as well as repeated loading conditions. The detailed methodology used in the present study is explained through a flow chart in Fig. 1.

2 Experimental Details

2.1 Types of Materials

Locally available natural soil is collected as subgrade soil. The sieve analysis of soil is carried out to check the particle size distribution, and from the size distribution, the soil is classified as silty-sand. The sieve analysis is shown in Fig. 2. The maximum dry density of soil is evaluated through the standard proctor test. The other properties of subgrade soil are mentioned in Table 1. Nano-silica and cement are collected from a vendor having the properties mentioned in Tables 2 and 3. Here, nano-silica is mixed with soil at various percentages such as 0.1, 0.5, 1 and 2% by the weight of the soil. Similarly, cement is also added at a percentage of 2, 4 and 6% by the weight of total soil. Several researchers have used nano-silica for strengthening the soil, and proposed the dosage of nano-silica and cement. In the present study, the dosage of nano-silica was selected from those literature.

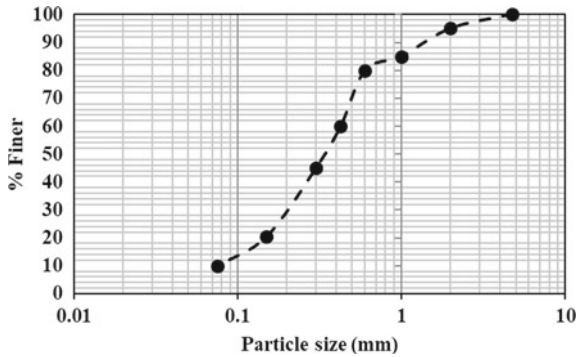


Fig. 2 Sieve analysis of subgrade soil

Table 1 Physical properties of subgrade soil

Particulars	Value
Specific gravity	2.816
Maximum dry density (g/cm ³)	1.83
Optimum moisture content (%)	20

Table 2 Properties of nano-silica

Property	Result	Property	Result
Specific surface area (m ² /g)	202	Chloride content (%)	0.009
p ^H value	4.12	Al ₂ O ₃ (%)	0.005
Loss on drying @ 105 °C (%)	0.47	TiO ₂ (%)	0.004
Loss on ignition @ 1000 °C (%)	0.66	Fe ₂ O ₃ (%)	0.001
Sieve residue	0.02	Specific gravity	2.3
Sio ₂ content (%)	99.88	Particle size	17 nano
Carbon content (%)	0.06		

Table 3 Properties of cement

Property	Result
Specific gravity	3.15
Compressive strength (MPa)	25
3 days	38
7 days	47
28 days	
Fineness (m ² /kg)	225

2.2 Resilient Modulus Test

Resilient modulus (M_R) describes the mechanical behaviour of all pavement layers including subgrade soil to the applied traffic load, and hence, it is considered as an important property for pavement design [11]. Resilient modulus of subgrade soil is a deciding factor for the overall performance of the pavement. In the present study, a cyclic triaxial apparatus is used for determining the resilient modulus of the subgrade. Recoverable deformation of soil samples is obtained by conducting the repeated triaxial load tests under constant confining pressure and standard temperature of 25 °C [12]. AASHTO T307-99 procedure is used to follow the preparation of the testing specimen. The suitably prepared and conditioned cylindrical specimens (100 mm × 200 mm) are used to conduct the resilient modulus test under the repeated triaxial stress of required magnitude, time and frequency at a predefined cell pressure. According to AASHTO T307-99, duration of each cycle is 1 s consisting of 0.1 s loading time followed by 0.9 s resting time. The average value of the last five cycles of each sequence from the cyclic axial stress yields the value resilient modulus of all tested samples [13, 14].

3 Numerical Modelling

The finite element methods are one of the versatile methods for the determination of pavement performance under different loading conditions. ABAQUS™ V6.13 (2013) is one of the most accurate, useful and user-friendly software for pavement engineers developed by Dassault systems (Rhode Island, RI, USA). ABAQUS is one of the most powerful numerical simulation tool, and it can simulate the pavement behaviour under different material properties and loading conditions.

3.1 Selection of Model Geometry

Model geometry includes the preparation of the model with appropriate dimensions. In this study, the pavement is chosen as a square slab section with a dimension of 3.5 m. The total depth of the pavement is taken as 0.75 m, where thickness of asphalt concrete layer is 10 cm, thickness of granular base layer is 15 cm and the subgrade thickness is 50 cm. The model preparation along with the dimensions is shown in Fig. 3. The ground contact area of the tyre is taken as an equivalent loading area which is 0.3 m × 0.15 m with the contact pressure of 0.8 MPa in static as well as dynamic loading condition. The parameters such as M_R and unit weight of soil are used as input parameters in the pavement modelling, and the other properties are kept constant. The properties of the materials are mentioned in Table 4.

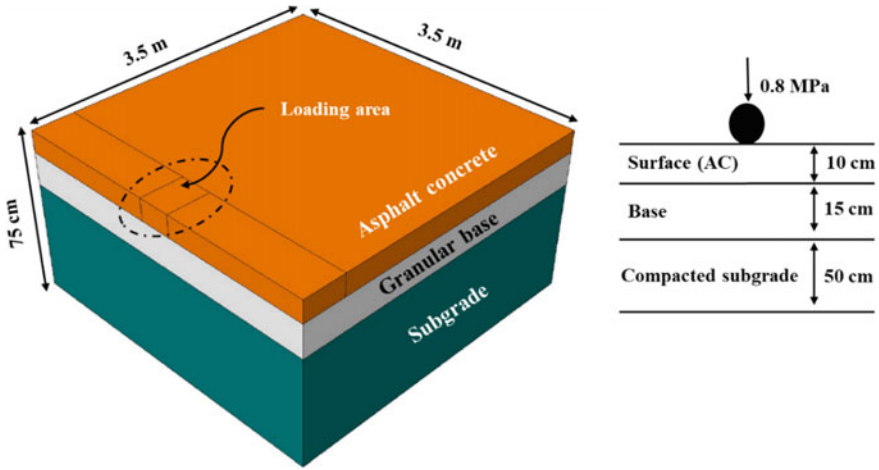


Fig. 3 Model geometry and dimensions

Table 4 Properties used in finite element modelling

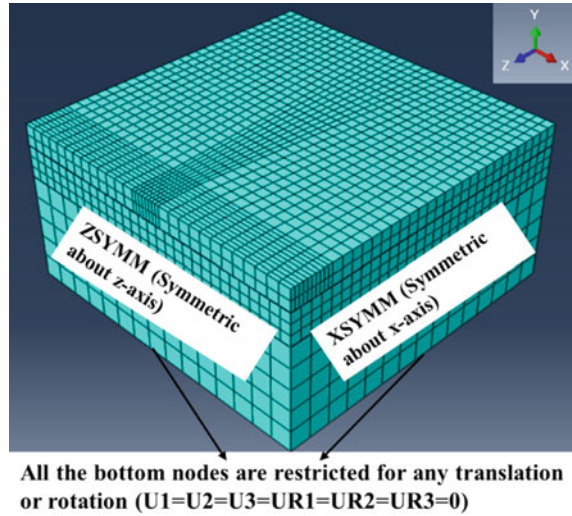
Layer name	Density (kg/m ³)	Poisson's ratio	Resilient modulus (MPa)
Surface layer (AC)	2200	0.35	240
Granular base layer	1800	0.35	138
Subgrade layer	From experimental test	0.35	From experimental test

3.2 Contact Surface, Meshing Pattern and Boundary Conditions

In the present study, frictional interaction is considered between two pavement layers based on the “Coulomb Friction Law”. For meshing of the given model, eight-nodded hexahedral brick element (C3D8R) was used in the process. The pavement model was meshed in all three global directions as well as mesh size is very small near the loading zone, and it will be increasing gradually away from the loading area as shown in Fig. 4. The following boundary conditions were used in pavement model:

- The bottom of the pavement structure (subgrade) was fixed by using a fully fixed constraint option.
- Any kind of displacement of the sides of the numerical model was restricted.
- Symmetrical planes in the model were constrained by symmetrical constraints.

Fig. 4 Meshing pattern and boundary



4 Results Obtained from Experimental Tests

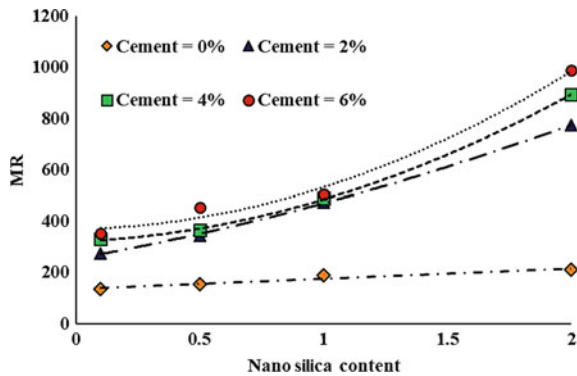
4.1 Resilient Modulus Test

The values of resilient modulus of treated and untreated soils at different percentages of cement and nano-silica are shown in Table 5. It is observed that the unmodified mix, i.e. the mix prepared without any cementing additives or nano-silica, has shown the minimum value of resilient modulus and the resilient modulus of subgrade continues to increase with the addition of nano-silica as well as with the addition of cement. The increase in the resilient modulus may be attributed to the formation of C–S–H clusters due to the chemical reactions among the nano-silica particles and cement. Previous literature mentioned that the nano-silica particles have high pozzolanic activity, which helps in developing a stronger bond. From Fig. 5, it can also be understood that the resilient modulus increases linearly for the mixes which are modified only by adding nano-silica (without cement). However, when cement is also added with the nano-silica, there exist an exponential increase in the resilient modulus. This may be the presence of C–S–H bond in the cementitious mix, which gets stronger with the addition of nano-silica. Moreover, nano-silica helps in the hydration process of cement due to which imparts in the strength improvement. The soil sample with 1% of nano-silica and 6% of cement yields the value of M_R is 505 MPa, and the sample with 2% of nanomaterial and 6% of cement yields the value M_R is 990 MPa.

Table 5 Resilient modulus for various mixes

% of nano-silica	% of cement	M _R (MPa)
0	0	70
0.1	0	135
0.5	0	155
1	0	190
2	0	210
0.1	2	275
0.1	4	330
0.1	6	355
0.5	2	345
0.5	4	365
0.5	6	456
1	2	475
1	4	490
1	6	505
2	2	775
2	4	895
2	6	990

Fig. 5 Changes of resilient modulus with nano-silica content



4.2 Numerical Results

4.2.1 Static Loading Condition

In this case, the load is applied in the form of pressure (0.8 MPa) in static condition, i.e. the load is applied once and the deformations are noted. For the numerical analysis, three models are prepared, (a) unmodified mix, (b) modified mix with 1% nano-silica and 6% cement, (c) modified mix with 2% nano-silica and 6% cement. The

vertical strain at the top of the subgrade and the rutting in the surface layer are shown in Fig. 6. It is found that the vertical strain produced at the top of subgrade soil reduced by 10% and 69% by adding 1% of nano-silica with 6% of cement and 2% of nano-silica with 6% cement, respectively, in subgrade soil stabilization. As the vertical strain the subgrade has a major role in the rutting of the asphalt concrete pavement (IRC 37-2018), it can be confirmed that the reduction in strain values after subgrade stabilization might be helpful in controlling the rutting of the pavement. From Fig. 7 it is also found that the surface rutting is decreased by 4.5%, 18.5% due to the addition of 1% of nano-silica with 6% of cement and 2% of nano-silica with 6% cement, respectively. The deformation of pavement observed from the numerical modelling is displayed in Fig. 8.

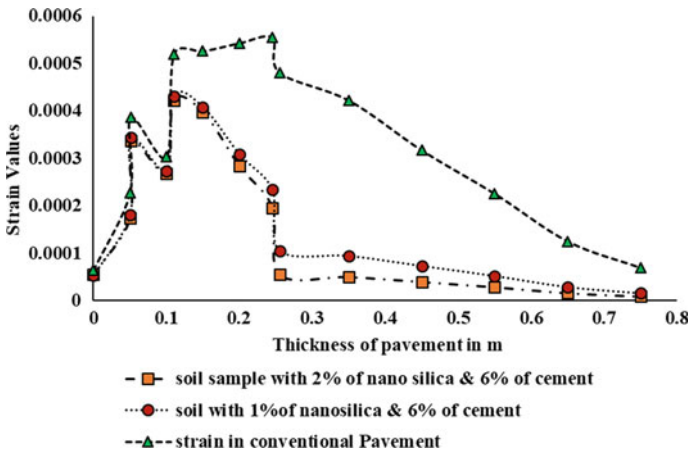


Fig. 6 Variation vertical strain on subgrade under static loading

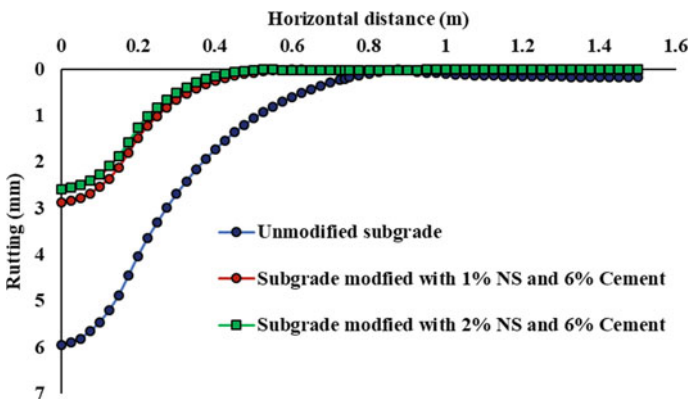


Fig. 7 Variation of surface rutting with the horizontal distance

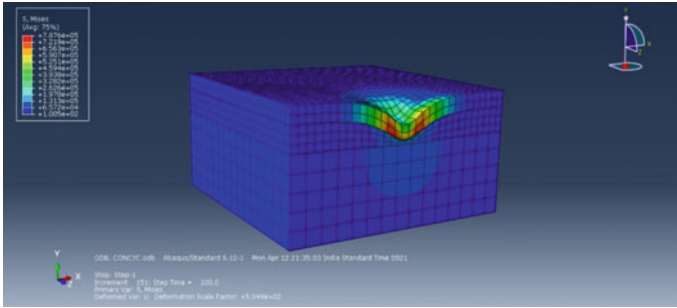
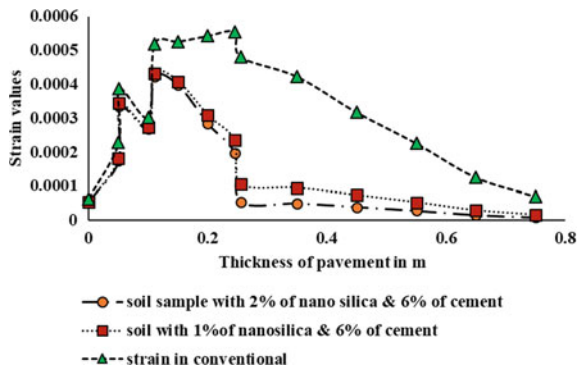


Fig. 8 Deformation occurred in the model pavement

4.2.2 Repeated Loading Condition

In repeated loading condition, the load is applied for 1000 cycles, where each cycle is 1 s with 0.1 s loading time and 0.9 s of resting time. Similar variations of strain and rutting are also observed for repeated loading case. The vertical strain at the top of the subgrade and the rutting in the surface layer under repeated loading are shown in Figs. 9 and 10. It is found that the strain values produced at the top of subgrade soil are reduced by 11% and 60% after adding 1% of nano-silica with 6% of cement and 2% of nano-silica with 6% of cement, respectively. The rutting produced at surface layer is decreased by about 11.5% and 22% by adding 1% of nano-silica with 6% of cement and 2% of nano-silica with 6% of cement, respectively. From the static and repeated loading, it is also observed that the rutting in static loading case is slightly higher than the rutting caused during the repeated loading case. The reason may be attributed to the elastic recovery of the asphalt concrete layer. In repeated loading case, there is a recovery of the pavement during the rest period, and hence, the rutting is lesser in this case.

Fig. 9 Variation vertical strain on subgrade under repeated loading



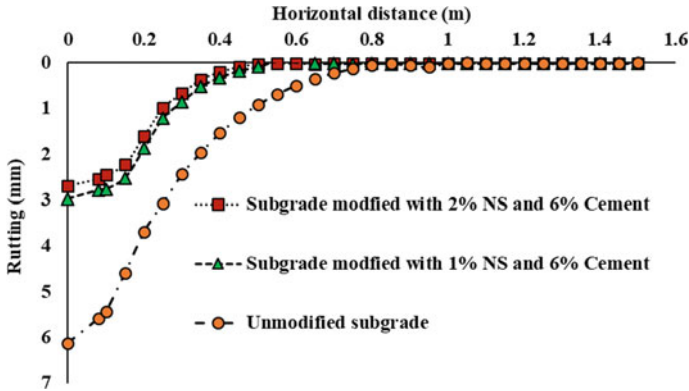


Fig. 10 Variation of surface rutting with the horizontal distance under repeated loading

5 Conclusion

The purpose of this study was to investigate the effect of the adding of nano-silica on the strength of the subgrade and also to check the effect of subgrade stabilization in the rutting behaviour of asphalt concrete pavement. The conclusions drawn from the above study can be summarized as

1. The strength of the subgrade can effective be increased by adding nano-silica and cement. There is a substantial increase in the resilient modulus of the subgrade after the addition of nano-silica with the cementitious material.
2. Vertical strain in the subgrade can be reduced up to 60–69% after adding 2% nano-silica with 6% cement.
3. Similar to the vertical strain, the rutting in the asphalt concrete pavement can also be reduced by using a stabilized subgrade. The rutting can be reduced by about 18–22% by adding 2% nano-silica with 6% cement.
4. A higher rut depth is achieved in static loading conditions as compared to that of the repeated loading case because the static loading has no rest period to recover.
5. From the overall results, it can be said that the subgrade stabilization has a positive impact on the rutting behaviour as the rutting of asphalt concrete pavement can be reduced by using a stabilized subgrade. The improved rutting resistance indicates that the pavement can allow more number of load repetition in during the life span.

References

1. Du Y, Dai M, Deng H, Deng D, Wei T, Li W (2020) Evaluation of thermal and anti-rutting behaviors of thermal resistance asphalt pavement with glass microsphere. *Constr Build Mater* 263:120609

2. Du Y, Chen J, Han Z, Liu W (2018) A review on solutions for improving rutting resistance of asphalt pavement and test methods. *Constr Build Mater* 168:893–905
3. Ali B, Sadek M, Shahroui I (2009) Finite-element model for urban pavement rutting analysis of pavement rehabilitation methods. *J Transp Eng* 135(4):235–239
4. IRC-37 (2018) Guidelines for the design of flexible pavements. Indian Road Congress (Fourth Revision)
5. Choobbasti AJ, Kutanaei SS (2017) Microstructure characteristics of cement-stabilized sandy soil using nano-silica. *J Rock Mech Geotech Eng* 9(5):981–988
6. Linear Choobbasti AJ, Vafaei A, Soleimani Kutanaei S (2018) Static and cyclic triaxial behavior of cemented sand with nano-silica. *J Mater Civ Eng* 30(10):04018269
7. Ghasabkolaei N, Janalizadeh A, Jahanshahi M, Roshan N, Ghasemi SE (2016) Physical and geotechnical properties of cement-treated clayey soil using silica nanoparticles: an experimental study. *Eur Phys J Plus* 131(5):1–11
8. Kulanthaivel P, Soundara B, Velmurugan S, Naveenraj V (2020) Experimental investigation on stabilization of clay soil using nano-materials and white cement. *Mater Today: Proc*
9. Bahmani SH, Huat BB, Asadi A, Farzadnia N (2014) Stabilization of residual soil using SiO₂ nanoparticles and cement. *Constr Build Mater* 64:350–359
10. Si C, Cao H, Chen E, You Z, Tian R, Zhang R, Gao J (2018) Dynamic response analysis of rutting resistance performance of high modulus asphalt concrete pavement. *Appl Sci* 8(12):2701
11. Changizi F, Haddad A (2015) Strength properties of soft clay treated with mixture of nano-SiO₂ and recycled polyester fiber. *J Rock Mech Geotech Eng* 7(4):367–378
12. Rahman MM, Islam KM, Gassman S (2019) Estimation of resilient modulus for coarse-grained subgrade soils from quick shear tests for mechanistic-empirical pavement designs. *Designs* 3(4):48
13. Prabhu SS, Suku L, Babu GL (2018) Evaluation of resilient modulus of geosynthetic reinforced layers using repeated load triaxial tests. *Indian J Geosynthetics Gr Improv* 7(1):9–16
14. Dong Q, Huang B (2014) Laboratory evaluation on resilient modulus and rate dependencies of RAP used as unbound base material. *J Mater Civ Eng* 26(2):379–383

Modal Studies on the Performance of Geosynthetic Reinforced Soil Walls Under Static Local Loading



M. K. Hudha and Renjitha Mary Varghese

Abstract Geosynthetic Reinforced Soil (GRS) wall is a composite structure consisting of fill material and closely spaced reinforcement that gives stability to the walls. These are economical and are widely used nowadays over conventional retaining walls. This study focuses mainly on the performance of the GRS walls under static loading. The position of static load application is mainly studied. Parametric studies are carried out to understand the effects of reinforcement strength, reinforcement spacing, facing stiffness, length of reinforcement and backfill soil type on the minimum offset distance of the footing. It was found that the bearing capacity of the wall increases as the offset distance increases from the facing of the wall and an optimum offset distance was found between $0.2H$ and $0.4H$ in most of the cases. The increase in stiffness of facing increases the bearing capacity by nearly five times at an optimum offset distance. When strength of reinforcement was increased it improves the performance of GRS walls and reduces the displacements by 40% at optimum offset distance. Decrease in spacing increases the performance of GRS wall, but 0.2 m spacing increases the number of reinforcement to double the value and for 0.6 m spacing, the displacements were very high compared to 0.4 m spacing. Increase in length of reinforcement increases the performance of GRS walls. In this study, the performance of GRS walls was studied by conducting numerical analysis using finite element software Plaxis 2D.

Keywords Offset distance · Geosynthetic reinforced soil wall · Displacement · Backfill soil · Plaxis 2D

M. K. Hudha (✉) · R. M. Varghese
Department of Civil Engineering, NIT Calicut, Calicut 673601, India
e-mail: hudhakunhoth65@gmail.com

R. M. Varghese
e-mail: renjitha@nitc.ac.in

© The Author(s), under exclusive license to Springer Nature Singapore Pte Ltd. 2023
M. V. L. R. Anjaneyulu et al. (eds.), *Recent Advances in Transportation Systems Engineering and Management*, Lecture Notes in Civil Engineering 261,
https://doi.org/10.1007/978-981-19-2273-2_31

477

1 Introduction

Geosynthetic Reinforced Soil (GRS) walls are commonly used nowadays than conventional retaining structures as they are more tolerant of differential movements because of the excellent flexibility and uniformity of geosynthetic materials. Moreover, GRS retaining structures are found to be resistant to corrosion and other chemical reactions. GRS structures are cost-effective as their construction is quicker and less weather dependent and the volume of earthwork required is very less. Geosynthetic Reinforced Soil (GRS) Walls have horizontal layers of closely spaced tensile inclusions (geosynthetics) in the fill material to achieve stability of the soil mass. The reinforcement is embedded in the soil which takes tension and hence the wall is stable for larger heights also. The shear strength developed between the soil and reinforcement increases the shear strength of the backfill soil.

The reinforcements that are commonly used are geotextiles, geogrids, metallic strips, etc. the backfill soil used nowadays is free draining granular soils, as in case of cohesive soils there will be effect of pore water which reduces the shear strength of soil. The GRS walls are designed for both internal as well as external stability. Internal stability mainly focuses on tension and pull-out resistance in reinforcing elements. Whereas the external stability includes determining overturning, sliding and bearing capacity failure.

Several factors control the behaviour of GRS walls including wall height, reinforcement stiffness, facing types, toe resistance [5], surcharge loading, reinforcement spacing, backfill soil characteristics [2, 3], backfill soil compaction-induced stress [7] and GRS walls have been successfully used for many applications under static and dynamic loading. Nowadays GRS walls with shallow footings are increasingly used to support bridge abutments. In case of abutment walls, large footing loads are often applied close to the wall facing and this is different from typical and traditional applications of GRS walls [8]. GRS abutment walls with shallow footings help to eliminate the use of pile foundations which are heavy and costly.

When performance of GRS walls under static loading is considered the location of placement of footing is very important [1, 9]. Hence the minimum offset distance of the footing from the GRS wall facing need to be studied. Also, the variations in different parameters like facing stiffness, reinforcement strength, length of reinforcement, spacing of reinforcement will also affect the minimum required offset distance.

The objectives of the study are:

1. To determine the minimum offset distance of the footing from the wall face.
2. Parametric studies by considering strength of reinforcement, length of reinforcement, spacing of reinforcement and facing stiffness.

2 Numerical Validation

The two-dimensional finite element programme PLAXIS 2D was used for the numerical evaluation of reinforced soil walls. Full-scale reinforced soil walls modelling, performed at the Geotechnical Laboratory of COPPE/UFRJ, was used for validation of the performed analyzes.

Figure 1 shows the geometry of the numerical model used in the analysis [4]. The geosynthetic retaining wall 6.8 m high with a batter angle of 1:10 was considered for the analysis. The length of the geosynthetic reinforcement was 0.7 times the height of the wall as per FHWA standard and the vertical spacing of the reinforcement was 0.4 m. The wrapped facing was modelled with inclination of 6° to the vertical. Table 1 shows the material properties used for the model validation.

The bottom of the wall was considered to be fixed in both vertical and horizontal directions and the extreme right side of the wall was allowed to move only in the vertical direction (Fig. 1). Staged construction was considered; soil layers were placed every 0.2 m and compacted until the final wall height was achieved. The constitutive model in this study was hardening soil model, which is a hyperbolic soil model. 15-node triangular elements were used.

Figure 2 shows the validation of the model by comparing the lateral displacements along the height of the wall and it was found that results are converging with the observations by Mirmoradi [6]. Results show that the maximum horizontal displacements were 42 mm which was comparable to the present study where displacement obtained was 40.75 mm. The further studies were also conducted with this model.

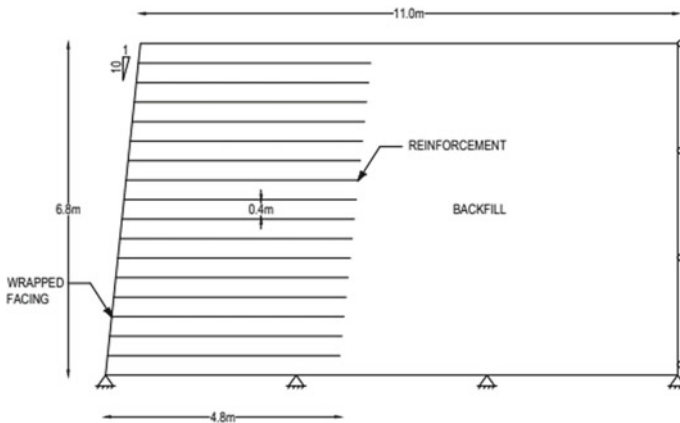
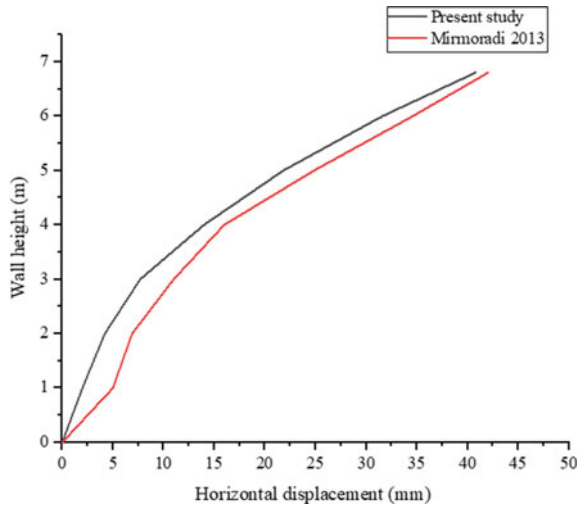


Fig. 1 Model geometry adopted for validation (Mirmoradi and Ehrlich [4])

Table 1 Material properties used for validation [6]

Parameter	Value
<i>Backfill</i>	
Peak plane strain friction angle, φ ($^{\circ}$)	50
Cohesion, C (kPa)	1
Dilation angle, Ψ ($^{\circ}$)	0
Unit weight, γ (kN/m ³)	21
E_{ref50}	42,500
$E_{ref_{oed}}$	31,800
$E_{ref_{ur}}$	127,500
Stress dependence exponent. m	0.5
Failure ratio R_f	0.7
Poisson's ratio, ν	0.25
<i>Reinforcement</i>	
Elastic axial stiffness (kN/m)	600
<i>Facing</i>	
Elastic axial stiffness (kN/m)	60
Elastic bending stiffness (kNm ² /m)	1

Fig. 2 The horizontal displacement of wall with respect to wall height



3 Results and Discussions

The parametric studies were conducted using the input parameters of the validation model. The geometry of the model for the parametric study is given in Fig. 1. The model geometry was same as that adopted for numerical validation. However, a

footing of width ‘b’ was placed at the top surface. The offset distance of the footing from the facing wall is denoted as ‘D’. In the entire analysis, the width of footing considered in this study is 2 m. Different parameters like facing type, strength of geogrid, spacing of reinforcement and length of reinforcement are considered. The variations in horizontal and vertical displacements under different conditions were monitored.

3.1 Effect of Offset Distances from Wall Facing to the Applied Footing Pressure

The effect of offset distances from the wall facing to the footing pressure was studied by varying the offset distance from very small offset (0.15H) to the pressure beyond the reinforcement length which is 0.7 times the height of the wall (0.8H). The parametric studies were carried out in between distances such as 0.2H, 0.3H, 0.4H, 0.6H. The maximum lateral, as well as vertical displacements for different offset distances and footing pressures, were noted and for different applied footing pressure, the variations in the maximum horizontal and vertical displacements at different offsets are plotted Fig. 3. The vertical and lateral displacements are denoted as ‘h’ and ‘x’, respectively. The deformations are normalized with respect to the height of the wall (H).

From Fig. 3 it was clear that at initial offset distance of 0.15H, the wall gets collapsed when the maximum lateral deformation was 55 mm. It was observed that the load-bearing capacity increased with increase in offset distance of the footing from the facing. However, an increase in horizontal and vertical displacements was also noted at higher footing pressure. In case of 0.2H, the maximum load-bearing value was near to 75kN/m², for 0.3H it was near to 100 kN/m² and when it comes to

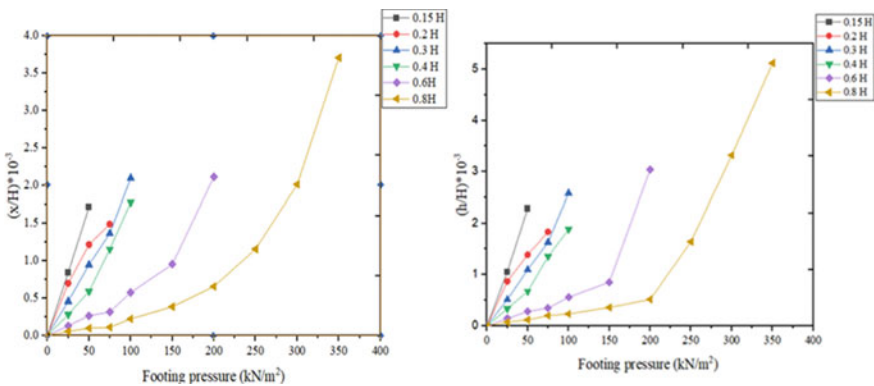


Fig. 3 Variation of normalized horizontal and vertical displacement of model GRS wall under footing load

0.4H the maximum load-bearing before failure of the wall was 120 kN/m^2 . In this case when the displacements are considered it was found the horizontal and vertical displacements are lower at a higher pressure of 120 kN/m^2 for an offset distance of 0.4H. When 0.2H and 0.3H have considered the displacements decreased by 5% at a load of 75 kN/m^2 . When 0.3H and 0.4H offset distances were considered, the displacement gets decreased by nearly 25% when the load was 100 kN/m^2 .

When 0.6H and 0.8H are considered the horizontal and vertical displacements are having higher values and increase to a value of more than 50% when compared to 0.4H offset distance. The settlement of the footing increases, when the location of the footing goes beyond the influence of the reinforcement zone, due to the uneven distribution of the reinforcing members. In case of 0.8H, the footing is completely in unreinforced zone and here the bearing capacity value depends on the strength of the unreinforced soil.

Hence the safe offset distance to be considered can be 0.3H to 0.4H, where there is no high displacements and also enough bearing capacity is achieved. While considering the horizontal displacements it was found that the max displacements occur towards the top end of the wall facing and it decreases towards the bottom.

3.2 Effect of Facing Stiffness at Different Offset Distance Under Footing Pressure

The GRS wall modal used for the study was having a wrapped facing and it was given as plate element in plaxis 2D software during analysis. Here the wrapped facing used in the base model was replaced by concrete panel facing or a rigid facing having a very high stiffness value ($EA = 3.55 \times 10^6$ and $EI = 5800$) than that of wrapped facing.

The facing panels were modelled as beam (plate) elements in both the cases. The increases in the stiffness of facing decreases displacements in the case of GRS walls. Hence for structures having high footing load acting it is better to go for rigid facing than that of flexible one.

The footing experiences maximum displacement when the offset distance is least, i.e., 0.15H (Fig. 4a). This can be attributed to the fact that when $D = 0.15H$, on one side of the footing there exists a rigid wall facing while on the other side there is a presence of extended reinforcement member, causing uneven reinforcement, leading to the failure of the wall and excessive settlement. When the offset distance was between 0.2H and 0.4H it is seen that the displacements were low when compared to the initial offset distance. When it comes to 0.4H the displacements were almost same as that of 0.2H and were nearly 10% change.

When the horizontal displacements are considered (Fig. 4b), it was observed that in case of rigid facing the greater lateral deformation occurs at the mid-section of the wall rather than at the top as in the case of wrapped faced GRS wall.

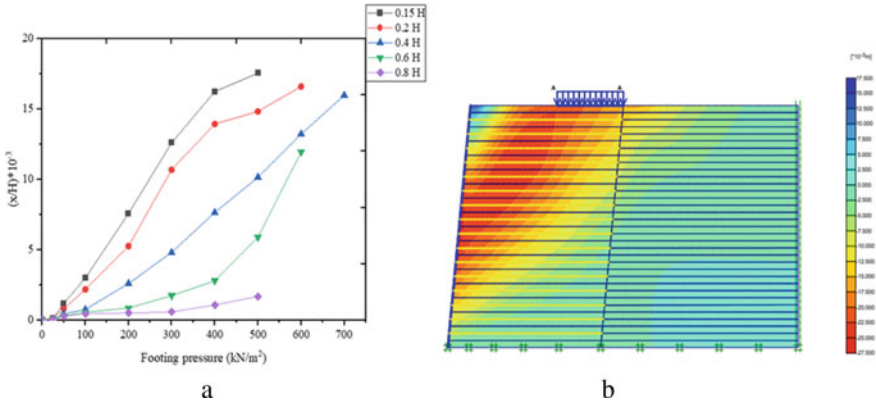


Fig. 4 Normalized Horizontal displacement of rigid-faced GRS walls under footing load

Considering vertical settlements, (Fig. 5a, b) its value was very high than lateral displacements. When vertical settlements are considered, it was more at the bottom of the footing and it also extended to the top left portion of the GRS wall.

But when the offset distance is further increased to 0.6H the load-bearing gets reduced. When it comes to unreinforced zone the load carrying capacity decreased. Hence the type of facing has important role in load-bearing capacity. Here their values mainly depend on the properties of the backfill soil than that of reinforcement and facing.

So it can be concluded that when the wrapped facing was replaced by block facing the load-bearing capacity got increased at initial offsets and safe offset distance found was 0.2–0.4H and 0.6H also gives safer values but it is much far away from the facing of the GRS walls which is not practical.

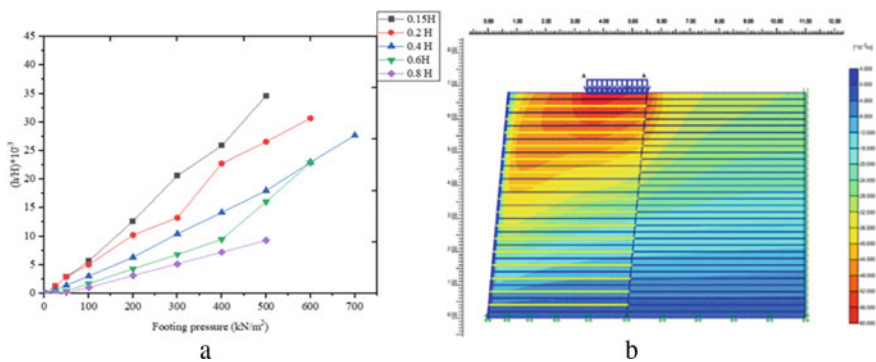


Fig. 5 Normalized vertical displacement of rigid-faced GRS walls under footing load

3.3 Effect of Increase in Strength of Reinforcement

The strength of reinforcement is one of the important factors that affect the performance of GRS walls under footing pressure. When the strength is increased or decreased, the effect on performance is more. Initially, the strength of base model GRS wall was taken as 600 kN/m. When the strength is doubled, i.e., 1200 kN/m, the performance of GRS walls at different offset distances under applied footing pressure are studied as in Fig. 6a and b.

When the strength of reinforcement was doubled, it was found that the load-bearing capacity got increased. While considering the case of geogrid strength of 600 kN/m, within the optimum offset distance (i.e., 0.3–0.4H) the maximum load carried before failure was 120 kN/m². But when the geogrid strength is increased, it was found that the load carrying capacity in this safe offset distance also increased by 75% (400 kN/m²). Hence it can be concluded that the increase in strength of geogrid increases the load carrying capacity of GRS walls under applied footing load. The lateral displacement in this case was also found more towards the top end (Fig. 6) of the wall but the value of displacement was less compared to that of the flexible wall facing with 600 kN/m² strength.

Similarly, the vertical displacement also shows a similar trend and the settlement value, in this case, increased when the applied load increased. Here it was found the settlements are maxed towards the top end and also at the bottom of the footing. Hence even though 0.15H has a higher load-bearing value the settlements in these cases is very high and hence the structure won't be practical. But when it comes to offset distance of 0.3–0.4H it shows a lesser displacement and also, they have a higher load carrying capacity. When 0.6 and 0.8H are considered, the load-bearing got reduced even though the settlements are less. And also, in practical sense, this offset distance is not suitable since it is far away from the facing of the wall.

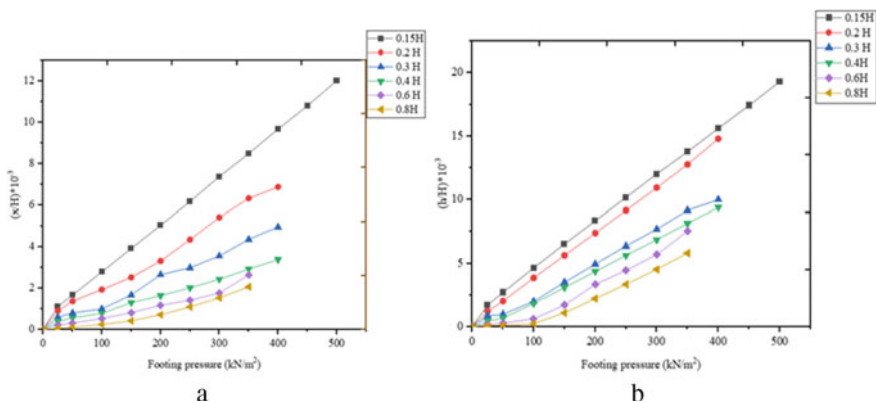


Fig. 6 Variation of normalized horizontal and vertical displacement when strength is doubled to 1200 kN/m

3.4 Effect of spacing of reinforcement on performance of GRS wall under applied footing pressure

To study the effect of spacing of reinforcement on the performance of GRS walls under footing loading, 0.2 m, 0.4 m and 0.6 m spacing are considered. It was found that as the spacing increases the displacements increase to a higher value.

Consider Fig. 7a, here variation of lateral displacements at an offset distance of 0.2H is considered for different cases of spacing of reinforcement. It was found that for a spacing of 0.6 m the displacements are very high and is more than 30% of that of 0.4 m spacing for a footing pressure of 50kN/m². It was observed that sudden increase in displacement occurs in case of 0.6 m spacing when load changes from 50 to 75 kN/m². When considering 0.2 m spacing, the displacements are less and have larger load-bearing compared to 0.4 m spacing. But the main problem with 0.2 m spacing was that the number of reinforcements required will be doubled than that of 0.4 m spacing and hence it is not economical.

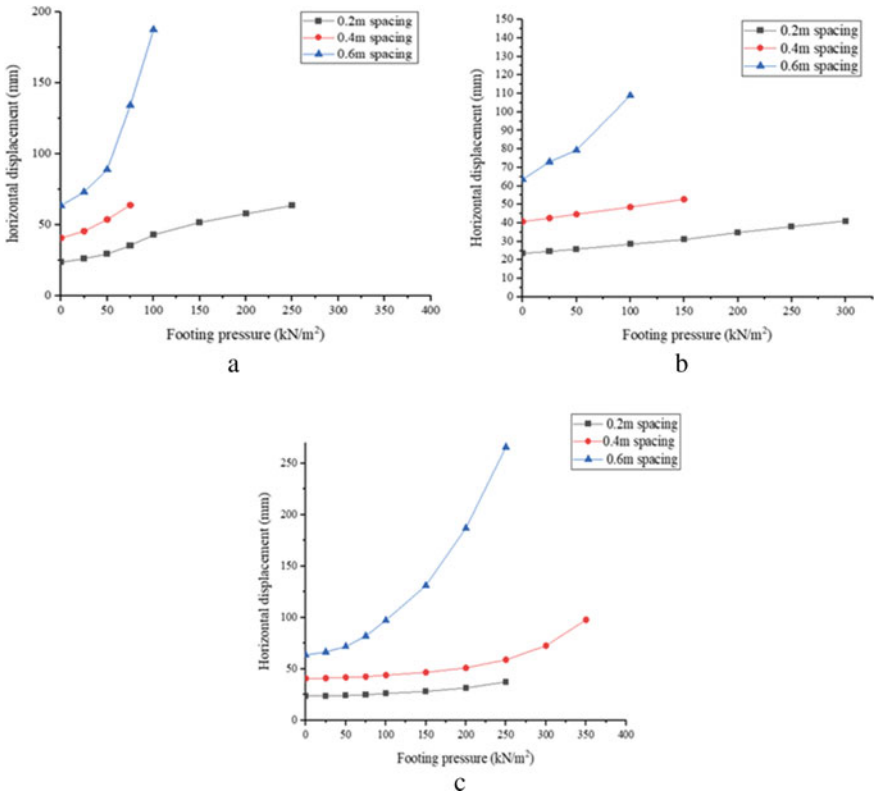


Fig. 7 Variation of horizontal displacement at an offset distance of 0.2H (a), 0.4H (b) and 0.8H (c) with different values of spacing between the reinforcement

Similar is the case for 0.4H offset distance (Fig. 7b), here the load-bearing capacity of 0.4 m spacing got increased, since the offset distance increased. And 0.2 m spacing of reinforcement was also having more bearing capacity and less displacement. But in case of 0.6 m spacing, the behavior is similar to that of 0.2H offset distance but the increase in displacement decreased for higher loads.

When an offset distance of 0.8H is considered (Fig. 7c), which is completely in an unreinforced zone it is found that 0.4 m spacing was having more load-bearing capacity while compared to 0.2 m spacing. The lateral displacements were almost same for both cases and there was only 10% difference. And considering 0.6 m spacing the load-bearing capacity increased compared to 0.4H offset distance but displacements are more.

3.5 Effect of Length of Reinforcement on Performance of GRS Wall Under Applied Footing Pressure

The length of reinforcement considered in the base model was 0.7H (H is the height of the wall) which is the minimum length of reinforcement as per FHWA. Here in the model study, three lengths of reinforcement are considered, 0.6H, 0.7H and 0.8H. It is generally found that as the length of reinforcement increases, the performance of the GRS walls increases.

The variation in horizontal displacement and bearing capacity are studied at different lengths of reinforcement at a particular offset distance of 0.2H as in Fig. 8a. When a footing pressure of 50 KN/m² is considered the horizontal displacement of 0.6H length was 12% more than that of 0.7H length of reinforcement. And when 0.8H length of reinforcement was considered, it was found that the displacements were nearly 15% less than that of 0.7H. When a load increment from 50 to 75 KN/m² is considered the percentage increase in displacement was only 15%. When load increased from 75 to 100KN/m² the increase in displacement was nearly 30%.

When offset distance of 0.4H (Fig. 8b) was considered, the load-bearing capacity for all the lengths of reinforcement increased compared to that of 0.2H offset distance. When a footing load of 75kN/m² was considered the 0.6H length of reinforcement has 11% increase in displacement when compared to 0.7H length. But when 0.8H length of reinforcement is considered, it was found that 15% decrease in displacement than that of 0.7H length. Up to 100KN/m² the increase in displacement at each load increment was at a rate of 30% for all the cases of length of reinforcement.

When offset distance of 0.8H was considered (Fig. 8c), the bearing capacity got increased in case of all lengths of reinforcement. In this case, it was found that 0.7H length of reinforcement was having a higher displacement value at a footing pressure of 350KN/m² and the increase in displacement was almost 50% more than that of 0.8H length of reinforcement. For 0.6H and 0.7H length, the rate of increase in displacement was almost same for each load increment and was nearly 11%.

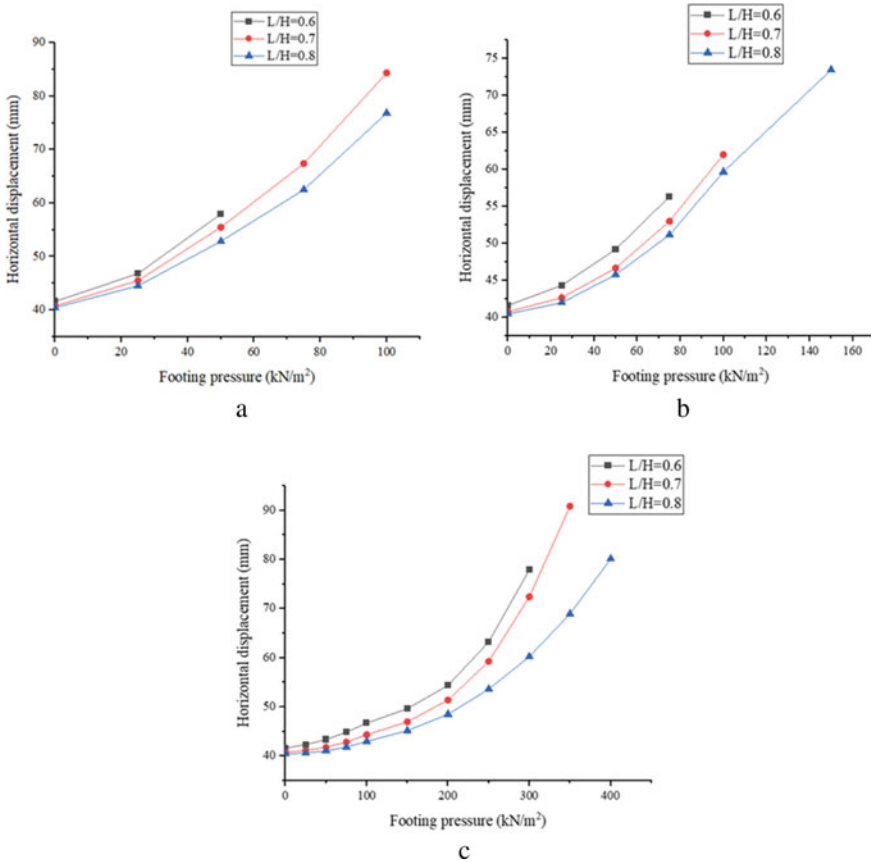


Fig. 8 Variation of horizontal displacement at an offset distance of 0.2H (a), 0.4H (b) and 0.8H (c) with different values of length of the reinforcement

4 Conclusions

Geosynthetic Reinforced Soil (GRS) walls are commonly used nowadays as they are more tolerant of differential movements because of the excellent flexibility and uniformity of geosynthetic materials. GRS walls have been successfully used for many applications under static and dynamic loading. When performance of GRS walls under static loading is considered the location of placement of footing is very important. Hence the minimum offset distance of the footing from the GRS wall facing need to be studied. Also, the variations in different parameters like facing stiffness, reinforcement strength, length of reinforcement, spacing of reinforcement will also affect the minimum required offset distance.

From the parametric studies conducted it can be concluded that the minimum offset distance of footing lies between 0.3H to 0.4H meters from the wall facing,

where H is the height of the wall. Also when the facing of the GRS wall was replaced from wrapped to rigid facing there was huge difference found in the displacement as well as the load-bearing capacity. Here the load-bearing capacity got increased at initial offsets and safe offset distance found was $0.2\text{--}0.4H$ and $0.6H$ also gives safer values but it is much far away from the facing of the GRS walls which is not practical. When strength of reinforcement was doubled or geogrid strength is increased, it was found that the load carrying capacity in the safe offset distance of $0.3\text{--}0.4H$ also increased by 75% (400 kN/m^2) and the displacement got decreased by 40%. When spacing of reinforcement was considered, decrease in spacing increases the performance of GRS wall, but 0.2 m spacing increases the number of reinforcements to double the value and 0.6 m spacing the displacements were very high compared to 0.4 m spacing. Increase in length of reinforcement increases the stability and performance of the GRS walls.

References

1. Ahmadi H, Bezuijen A (2018) Full-scale mechanically stabilized earth (MSE) walls under strip footing load. *Geotext Geomembr* 46(3):297–311
2. Choudhary AK, Jha JN, Gill KS (2010) Laboratory investigation of bearing capacity behaviour of strip footing on reinforced fly ash slope. *Geotext Geomembr* 28(4):393–402
3. Guler E, Hamderi M, Demirkan MM (2007) Numerical analysis of reinforced soil-retaining wall structures with cohesive and granular backfills. *Geosynthetics Int* 14(6):330–345
4. Mirmoradi SH, Ehrlich M (2013) Numerical evaluation of the behaviour of reinforced soil retaining walls. In: 18th international conference on soil mechanics and geotechnical engineering
5. Mirmoradi SH, Ehrlich M (2016) Evaluation of the combined effect of toe resistance and facing inclination on the behaviour of GRS walls. *Geotext Geomembr* 44(3):287–294
6. Mirmoradi SH, Ehrlich M (2013) Modelling of the compaction induced stresses in numerical analyses of GRS walls. *Int J Comput Methods* 11(2):1342002 (14 pages).
7. Mirmoradi SH, Ehrlich M (2018) Numerical simulation of compaction-induced stress for the analysis of RS walls under working conditions. *Geotext Geomembr* 46(3):354–365
8. Rahmaninezhad SM, Han J, Al-Naddaf M (2020) Limit equilibrium analysis of geosynthetic-reinforced retaining walls subjected to footing loading. *Geo-Congress 2020 GSP 316 464:464–471*
9. Xiao C, Han J, Zhang Z (2016) Experimental study on performance of geosynthetic-reinforced soil model walls on rigid foundations subjected to static footing loading. *Geotext Geomembr* 44(1):81–94

Performance Evaluation of Cement-Treated Recycled Concrete Aggregate Bases



Sarella Chakravarthi, Matta Devendra Vara Prasad, and S. Shankar

Abstract Recycled Concrete Aggregates (RCA) are replaced with natural aggregates in pavement bases in the present study. The blended mixes are stabilized with cement at 2, 4, and 6% of the dry weight of aggregates. The compaction characteristics, Indirect Tensile Strength (ITS), Unconfined Compressive Strength (UCS), durability, and Resilient Modulus (M_R) were evaluated. The results show that with the increase in the proportion of RCA, no proper trend is observed in the OMC due to the gradation differences and heterogeneity of the RCA. Further, there is a decline in the engineering properties with RCA percentage. In spite, their mechanical properties were improved with cement stabilization. The maximum ITS and UCS are found at 50% RCA. There is no significant difference found in the modulus values of RCA blends. However, the modulus values from the empirical equations are near to the specifications. Further, a relationship was established between UCS and M_R . Overall, the stabilized bases of RCA blends can be used as bases and sub-bases.

Keywords Cement-treated bases · Recycled concrete aggregate · UCS · ITS · M_R

1 Introduction

Conventional aggregates which are currently used in road construction are limited and may get depleted in the near future. In addition, quarrying, lifting, and hauling these natural aggregates consume vast amounts of fuel, result in emissions, and consequently damage the environment. Given all these problems in acquiring natural aggregate, there is a significant need to look for non-conventional materials and methods. Recycled Concrete Aggregate (RCA) is one such material that is generated continuously from the building and other reinforced concrete structures. The production

S. Chakravarthi (✉) · M. Devendra Vara Prasad · S. Shankar
NIT Warangal, Warangal, India
e-mail: chakravarthi.sarella@student.nitw.ac.in

S. Shankar
e-mail: ss@nitw.ac.in

of the RCA is a continuous process as long as there are construction activities. So, the RCA production cannot be prevented nor restricted. Despite the utilization of the RCA for parking lots and shoulders, a considerable amount of RCA is remaining used for landfills which is not an eco-friendly process. The most effective alternatives are to reutilize these RCA in different structures like buildings and roads.

The engineering properties of RCA are not up to the mark as that of the Virgin Aggregates (VA) due to their deterioration during their service life and due to the contamination with other materials while crushing and processing. So, stabilization is preferred to enhance the mechanical and structural properties of the RCA. Among several stabilization methods, cement stabilization is considered adequate as it is readily available in the markets. As the RCA already has some self-cementing properties [1], the addition of little cement can impart further cohesion properties and rejuvenate the structural functionality of the RCA as a pavement base. Several studies reported improved strength and stiffness properties with cement to the RCA [2, 3]. A study reported a substantial increase in the strength and stiffness of the cement-treated bases. However, the stiffness is in the range of 40–70 MPa for different RCA and limestone aggregate blends obtained from plate load testing at 5% cement content. The maximum stiffness is observed at 75% of RCA content in the mix [2]. Another study found no significant variation in the stiffness of the blend with the RCA content. However, the stiffness is increased with the curing periods. The M_R values reported are in the range of 800–1600 MPa at 4–5% cement contents tested under compression resilient modulus testing using UCS samples [4]. One study reported maximum strength and stiffness at 30% RCA replacement in the blend. The M_R values were found to be 1100–1500 MPa when tested under compression resilient modulus testing machine stabilized at 10% cement content [5]. Another study evaluated cement-treated RCA-Fine Recycled Glass (FRG) combinations in the pavement bases. Maximum stiffness is obtained at 90% RCA and 10% FRG at 3% cement content. The modulus values from the RLT test are reported below 1000 MPa. At the same time, the modulus values from the flexural beam test are reported higher, which range between 9000 and 23,000 MPa [6].

From the studies, there is variability in the modulus with the test setup. Further, the stiffness is influenced by the cement content and curing period. The RCA influence on the mechanical properties in the mix is uncertain. Because of these drawbacks, there is a necessity in evaluating the treated RCA-VA blends in terms of physical characteristics, strength, and stiffness.

Further, the M_R values are calculated using an Indirect Tensile resilient modulus testing machine which is generally used for bituminous mixes. The obtained M_R results are compared using empirical equations and with other research results using different test setups. In addition to the stiffness/ M_R , the study presents the various physical properties, UCS, and ITS of the RCA-VA blends at various stabilization levels using cement. As the development of the strength is mainly influenced by the cement content than other factors, the analysis is carried out at different cement contents (2, 4, 6%) [7].

2 Experimental Program

2.1 Raw Materials

Cement. Ordinary Portland cement of Grade 53 is selected as a stabilizer and evaluated for the basic properties presented in Table 1.

Aggregate. Virgin aggregates are collected from the local quarry. RCA is collected from in and around the city and then processed manually and crushed using a jaw crusher to obtain the required gradation. The processing of the RCA is shown in Fig. 1.

RCA is processed in three stages to eliminate any foreign matter presence and provide homogeneous material. In the first stage of the process, the demolished RCA is crushed into the size range of 50–100 mm, and any visible clayey and metal substances are removed. The RCA is further crushed into 30–40 mm size in the second stage to feed easily into the Jaw crusher. At this stage, further screening is done to remove loose particles and dust. After, the processed RCA is fed into the jaw crusher in two stages to eliminate flaky and elongated particles followed by washing and drying. The obtained Recycled concrete from crushing is subjected to physical characterization using Ministry of Road Transport and Highways (MoRTH), 2013 specifications [9].

The physical properties of the RCA and VA blends were studied to understand their variation with the percentage of RCA which is presented in Fig. 2. The percentage of RCA in the blend is shown on the *x*-axis, and the corresponding property is shown on the *y*-axis. The red line indicates the specification limits. There is an increase in abrasion, water absorption, aggregate impact value, and a decrease in specific gravity. An increase in the Flakiness and Elongation Index of the blends was observed with an increase in RCA share in the mix. RCA was found inferior to VA in terms of Los Angeles abrasion and water absorption. Depending on the quality of RCA, the adhered mortar loss depends on the strength of RCA. During the testing process, this adhered mortar might be subjected to abrasion.

Table 1 Physical properties of cement

Test	Result	Specifications [8]
Fineness (%)	95	–
Normal consistency (%)	35	–
Initial setting time (minutes)	68	30
Final setting time(minutes)	435	600
Specific gravity	3.20	–

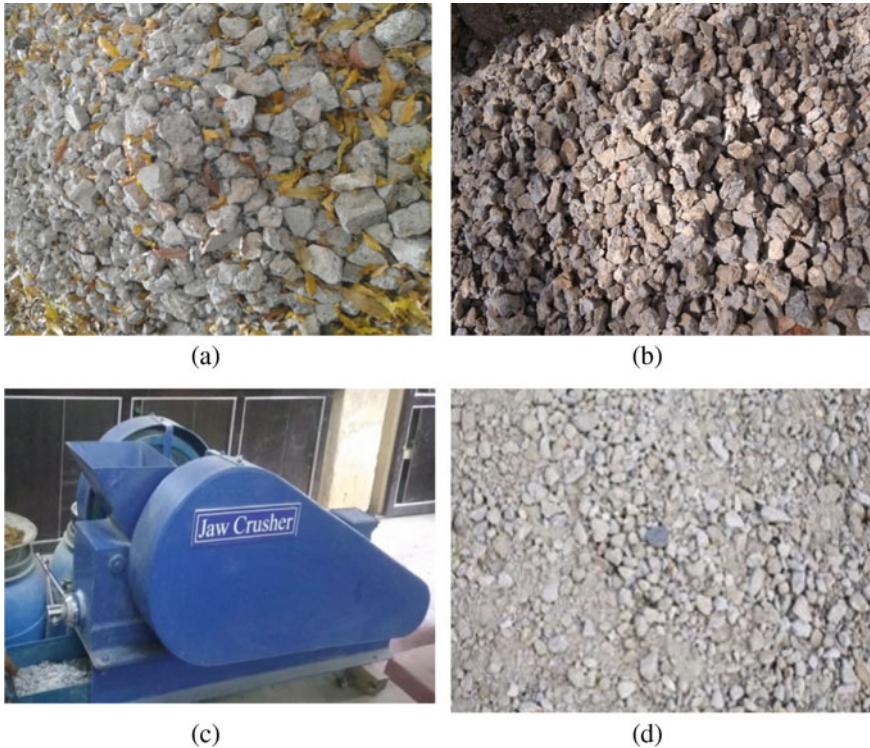


Fig. 1 **a** First stage of manual crushing of RCA in the range of 50–100 mm size, **b** Screening and crushing of RCA into the size range of 30–40 mm, **c** Final Crushing using Jaw crusher in two stages, **d** Final product of RCA after processing

2.2 Specimen Preparation

To evaluate the cement-treated RCA as a base material, characterization related to strength, stiffness, and durability is carried out at ambient temperature. Three specimens in number were prepared at different percentages of RCA (25, 50, 75, and 100%) at cement content 2, 4, and 6%, and all the specimens are compacted at Optimum Moisture Content (OMC) and Maximum Dry Density (MDD). Specimens of 100 mm diameter and 200 mm height for durability and UCS, 100 mm diameter, and 63 mm height for ITS and M_R are adopted. The gradation of different blends of RCA with VA is presented in Fig. 3. All the RCA blends fall within the specification limits.

Compaction characteristics of each mixture are presented in Fig. 4 with mix id, RCA content, cement content, MDD, and OMC. All the mixes are compacted using modified proctor compaction [10]. It is observed that the OMC of the mixes increases with the increase in the cement content as the demand for water increases to counter the hydration reactions. There is no significant variation in the dry density with

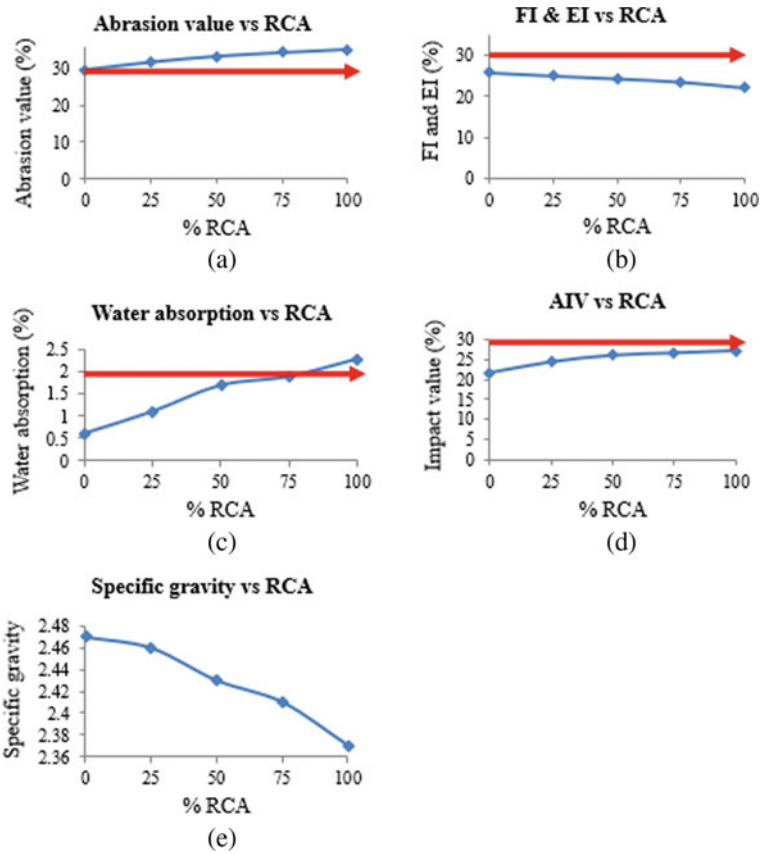


Fig. 2 Variation of physical properties with RCA content in the blends

the addition of the RCA and cement content. From Fig. 3, the mixes' gradations are not the same; they tend to vary and are almost close to the mid-gradation. The OMC variation concerning the RCA content might not follow a specific trend. As the gradation of the RCA blends is not the same and due to the heterogeneity properties of RCA, differences in the OMC and MDD are observed.

3 Experimental Program

3.1 Unconfined Compressive Strength (UCS)

UCS is used to measure the bound materials' cohesive nature and to optimize the mix's stabilizer. It is the ratio of the maximum failure load to the area of the contact of

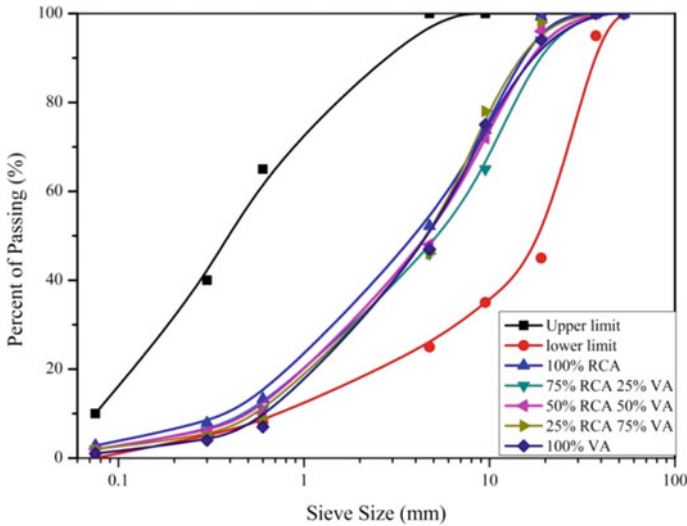
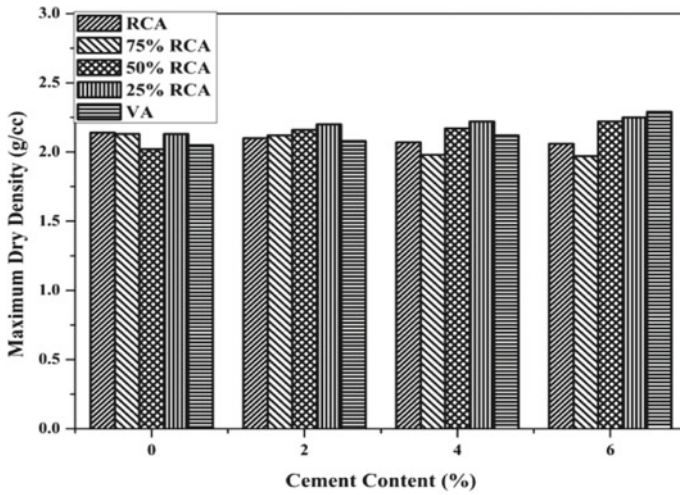


Fig. 3 Gradation curve for different blends of aggregates

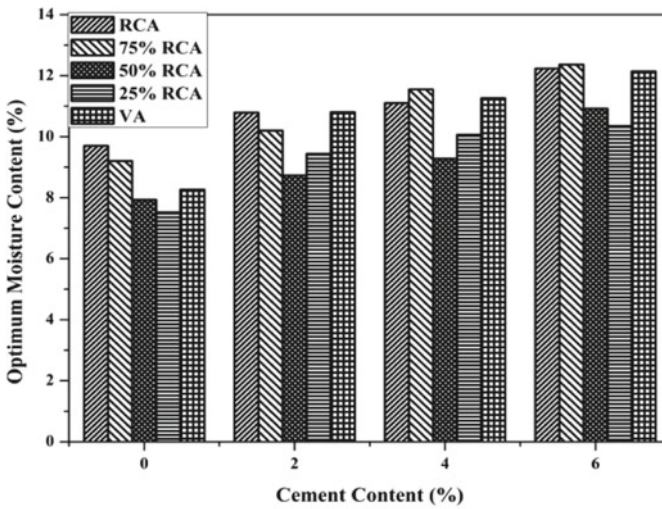
the load with the specimen. The test is performed on specimens of 100 mm diameter and 200 mm height [11]. All the blends were tested at the 7 and 28 days of curing period at various cement contents, and the average values are presented in Fig. 5. There is an obvious increase in the UCS with the curing period and the cement content from the obtained results. Further, the maximum UCS is obtained at the 50% RCA replacement. The 7-day UCS values range from 0.5 to 1 MPa, 1 to 2 MPa, and 1.7 to 3.5 MPa at 2, 4, and 6% cement contents. The UCS values after 28 days range from 1 to 2 MPa, 1.7 to 3 MPa, and 4.5 to 5 MPa at 2, 4, and 6% cement content. According to the MoRTH, 2013, the requirements of UCS for low volume roads are 1.70 MPa for sub-base and 2.76 MPa for base course. For high-volume roads, the UCS requirement is 1.5–3.0 MPa for sub-base and 4.5–7.0 MPa for base applications [9]. According to Portland Cement Association, the acceptable range is 2.1 to 5.5 MPa [12]. From the results, the RCA mixes satisfied the requirements of the specifications as sub-bases and bases at 4% and 6% cement content at 28 days of curing period. The lower value of UCS at 7 days is influenced by many factors like aggregate gradation, packing density, and the reaction between the binder and the aggregates. When RCA compared with VA, their UCS is typically more due to the presence of the mortar around the RCA and due to their self-cementing properties.

3.2 Durability

Durability studies are carried on the cement-treated RCA blends to know the loss of fines from the base. For this test, three mix types, namely RCA, VA, and 50



(a)



(b)

Fig. 4 Variation of **a** MDD and **b** OMC with RCA and cement content

RCA, are considered at 4% and 6%, respectively. The commonly used test method for durability studies follows alternate Wet and Dry (W-D) cycles [13]. The test is generally performed for 14 W-D cycles in which 48 h of soaking in water followed by 5 h oven-dried at 70 °C. The specimen’s size of 100 mm diameter and 200 mm height is used for the durability evaluation. After each drying phase, the initial weight and final weight are measured, and dimensions are recorded at the end of the cycle. In the current study, samples are cured at 7 days before subjecting to the alternate

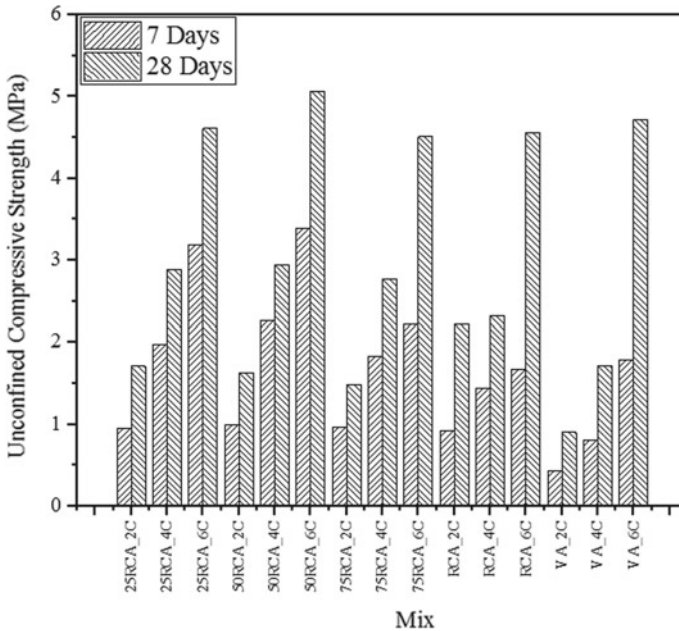


Fig. 5 UCS of RCA-VA blends at various curing periods

wet and dry cycles. The conditioned and unconditioned samples are tested for UCS at the end of 7 cycles, and the average values are shown in Fig. 6. The results show no significant strength decline of conditioned samples, emphasizing that the cement-treated recycled bases are durable in terms of strength. Moreover, the specimens with 6% cement content expressed more strength than 4% cement before and after the W-D cycles.

Another aspect of measuring durability is determining the amount of material loss with W-D cycles. To understand this phenomenon, 7 wet and dry cycles are conducted for the specimens, and the amount of weight loss is measured for each W-D cycle. The values of weight loss with the progress of a number of W-D cycles are indicated in Fig. 7. It is observed that the RCA has more loss of material compared with VA at 4 and 6% cement content. Inter-transition zones in RCA and the binder might not have bonded properly at 7 days of curing period. Furthermore, the percentage of cumulative weight loss is less than 2.5% for all the cycles.

3.3 Indirect Tensile Strength

ITS is identified as a pre-test for the determination of M_R . The tensile strength of a stabilized base can be evaluated from the ITS test. It is the ratio of the applied load to the area of the diametric plane on which the load is applied and calculated using

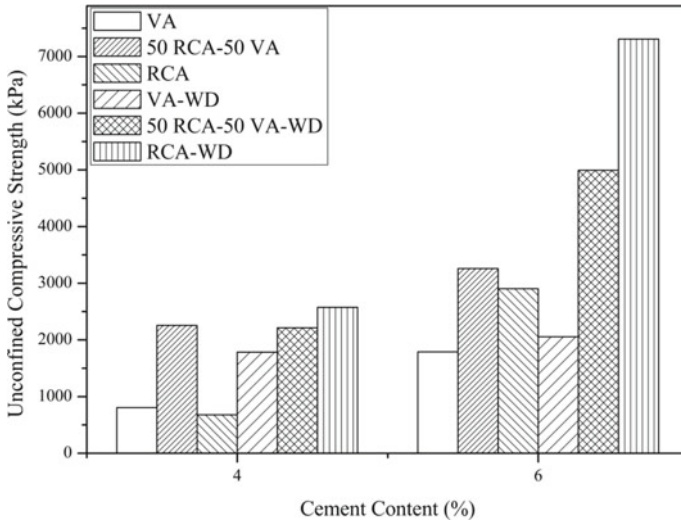


Fig. 6 Comparison of UCS for specimens with and without W-D cycles

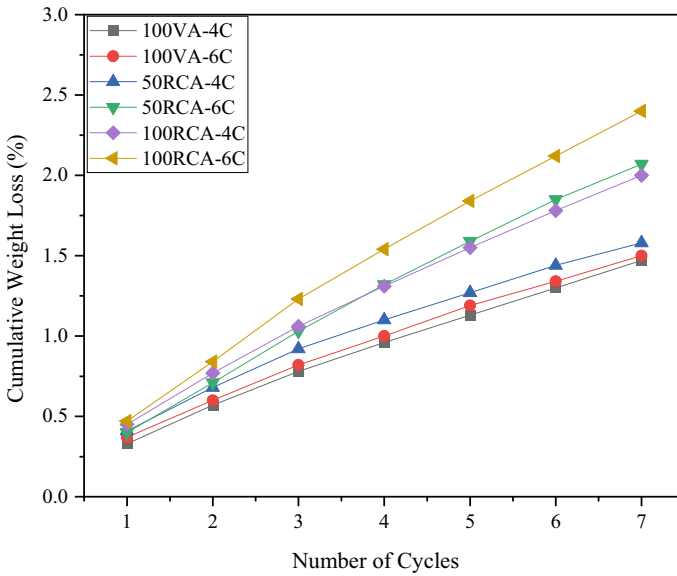


Fig. 7 Comparison of cumulative mass loss with respect to the number of W-D cycles

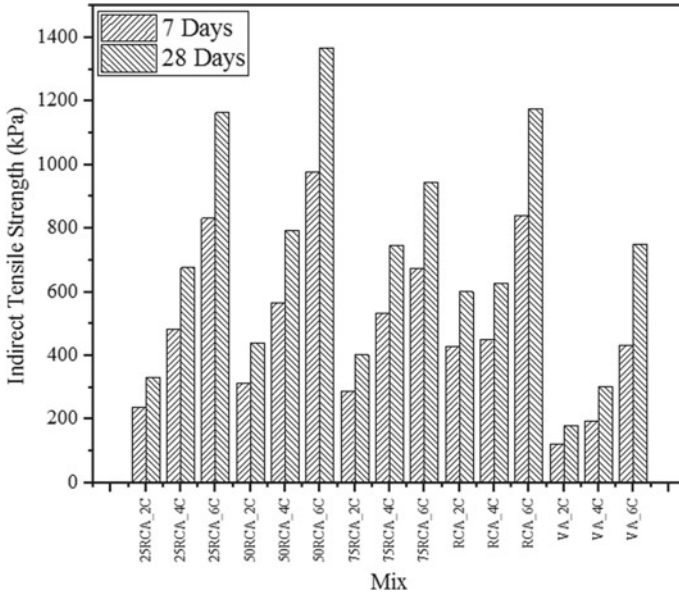


Fig. 8 Variation of ITS at various curing periods

the Eq. (1). The specimens of size 100 mm diameter and 63 mm height are used for testing after curing for 7 days and 28 days, and the average values are shown in Fig. 8. The maximum ITS values are obtained at 50% RCA specimen at all cement contents from the results, and the ITS values of RCA blends are comparatively more than that of the VA.

$$ITS = \frac{2000P}{\pi Dt} \tag{1}$$

Here, D the specimen’s diameter, t is the thickness of the specimen, and P is the applied load.

4 Resilient Modulus (M_R)

The resilient modulus test is used to characterize different pavement materials which are used in the pavement design and analysis. This test can be performed at different temperatures and loading rates to simulate the field conditions. Cylindrical samples with an internal diameter of 101.60 mm and 63.5 ± 2.5 mm in height are prepared and cured [11]. The test was conducted according to ASTM D 7369 by applying repeated load with a haversine waveform at 25 °C and 1.0 Hz of loading frequency [14]. The Poisson’s ratio for the calculation of M_R is taken as 0.25 and calculated

using Eq. (2). The obtained values of M_R are shown in Fig. 10. The graph includes the M_R values calculated using the empirical equation from UCS, M_R values from 7 and 28 days of the curing period of the experiment. The empirical equation from IRC 37: 2018 is shown in Eq. (3) [15].

$$M_R = \frac{P(\mu + 0.27)}{\Delta H \times t} \quad (2)$$

Here, μ is the Poisson's ratio and ΔH is the horizontal resilient deformation.

$$E = 1000 \times \text{UCS} \quad (3)$$

Here, E is the modulus values in MPa, and UCS values are at 28-day curing period in MPa.

From Fig. 9, the average modulus values from the empirical equation are quite higher than that of the calculated from the experimental values. There is a noticeable increase in the modulus values with the curing period. However, no significant variation in Modulus with RCA content is found from the test. The modulus values from the Indirect Tensile resilient modulus test are higher than the plate load test, compression modulus testing, and RLT testing [2, 4–6]. Further, the M_R testing from the Indirect Tensile mode is more straightforward and measures the stiffness of the cylindrical cores obtained from the field. Further, it is challenging to extract beam cores from the field.

The modulus values at 6% cement content are 3500 MPa from the laboratory testing. According to the specification limitations, the recommended modulus value is 5000 MPa after 28 days of curing [15]. Nevertheless, the obtained values did not reach the specified limits. The test method and techniques might differ in the modulus values. In contrast, the modulus values from the empirical equations are close to 5000 MPa. A linear relationship is established between UCS and M_R from the obtained results of various blends, as shown in Fig. 10. It is found that the two parameters are well correlated, and the following equation is obtained (Table 2).

$$M_R = 658.17\text{UCS} \pm 105.27 \quad (4)$$

5 Conclusions

RCA is a significant demolition waste from the construction industry that increases over time due to the new infrastructure and construction activities. Utilizing these recycled aggregates in the pavement bases by stabilizing with cement creates a clean and eco-friendly environment that will decrease landfilling and dumping activities. A detailed study is carried out on the properties of the RCA blends, strength, durability,

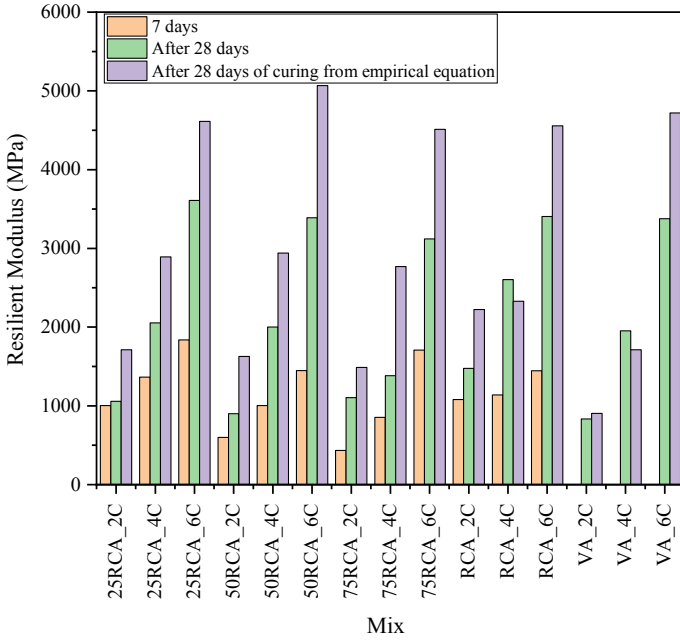


Fig. 9 Resilient Modulus of the mixes at various curing periods

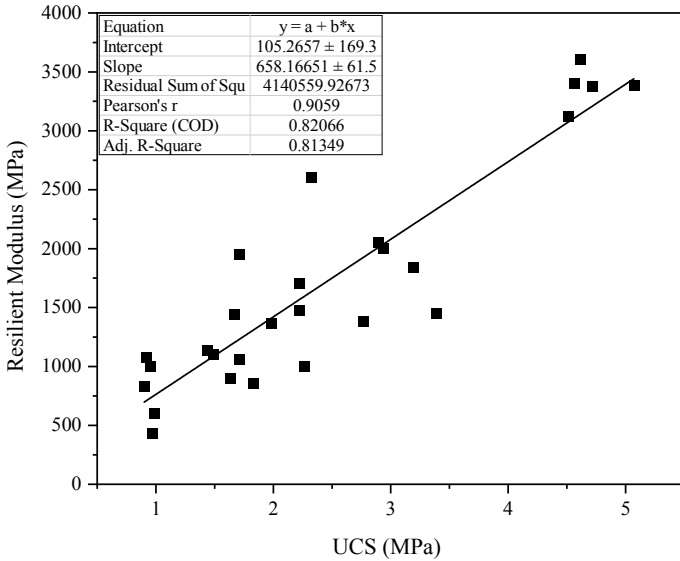


Fig. 10 Relation between resilient modulus and UCS

Table 2 Summary of the results for 7 days of curing period

Mix type	UCS (MPa)		ITS (MPa)		M_R (MPa)	
	μ	σ	μ	σ	μ	σ
25RCA-2C	0.95	0.03	0.24	0.01	1002	105
25RCA-4C	1.98	0.03	0.48	0.03	1366	79
25RCA-6C	3.19	0.02	0.83	0.01	1837	156
50RCA-2C	0.99	0.02	0.31	0.05	600	57
50RCA-4C	2.26	0.03	0.57	0.07	1004	101
50RCA-6C	3.39	0.03	0.98	0.03	1447	135
75RCA-2C	0.97	0.04	0.29	0.02	434	27
75RCA-4C	1.83	0.02	0.53	0.05	854	73
75RCA-6C	2.22	0.06	0.68	0.07	1708	133
RCA-2C	0.92	0.07	0.43	0.10	1081	93
RCA-4C	1.44	0.02	0.45	0.11	1139	67
RCA-6C	1.67	0.12	0.84	0.09	1446	171
VA-2C	0.43	0.05	0.12	0.01		
VA-4C	0.81	0.01	0.19	0.01		
VA-6C	1.79	0.06	0.43	0.02		

and M_R . The following are the conclusions that are drawn from the experimental results.

- There is a decline in engineering properties with the addition of the RCA to the blend, leading to increased water absorption, abrasion value, and impact value. However, the mechanical properties of the stabilized bases are unaffected by the RCA content.
- Differences in the OMC and MDD are observed due to the mortar presence and heterogeneity of the RCA.
- With the increase in cement content, the value of ITS and UCS increases, and the maximum is found at 50% RCA. The RCA content does not influence the modulus values at both curing periods. Moreover, the laboratory values are quite lower than that of the modulus values from the empirical equations.
- The material loss with the number of W-D cycles is increased, but the material loss rate concerning the number of w-d cycles is decreased. There is no significant loss in strength of the conditioned samples and considered durable.
- The performance of the stabilized RCA is almost equivalent to that of the VA despite the poor engineering properties.

Acknowledgements We wish to place on record our heartfelt gratitude and indebtedness to the Department of Science and Technology (DST), Government of India, for sponsoring this prestigious research project entitled “Performance Evaluation of Emulsified Asphalt Treated Bases and Cement Treated Bases” carried out at the National Institute of Technology Warangal, Telangana, India.

References

1. Poon CS, Qiao XC, Chan D (2006) The cause and influence of self-cementing properties of fine recycled concrete aggregates on the properties of unbound sub-base. *Waste Manag* 26:1166–1172
2. Behiry AEAEM (2013) Utilization of cement treated recycled concrete aggregates as base or subbase layer in Egypt. *Ain Shams Eng J* 661–673
3. Faysal M, Mahedi M, Aramoon A, Thian B, Hossain MS, Khan MA, Khan MS (2016) Determination of the structural coefficient of different combinations cement-treated/untreated recycled base materials. *Geotech Struct Eng Congr* 2016:1198–1208
4. Hou Y, Ji X, Su X (2019) Mechanical properties and strength criteria of cement-stabilized recycled concrete aggregate. *Int J Pavement Eng* 20:339–348
5. Yan K, Li G, You L, Zhou Y, Wu S (2020) Performance assessments of open-graded cement stabilized macadam containing recycled aggregate. *Constr Build Mater* 233:117326
6. Arulrajah A, Disfani MM, Haghghi H, Mohammadinia A, Horpibulsuk S (2015) Modulus of rupture evaluation of cement stabilized recycled glass/recycled concrete aggregate blends. *Constr Build Mater* 84:146–155
7. Lim S, Zollinger DG (2003) Estimation of the compressive strength and modulus of elasticity of cement-treated aggregate base materials. *Transp Res Rec* 30–38
8. IS 12269—ordinary Portland cement-53 Grade specification (2013)
9. Ministry of Road Transport and Highways, Specifications for Road and Bridgeworks, Fifth Revision, Ministry of Road Transport and Highways, New Delhi, India (2013)
10. Indian Standard, Methods of tests for soils (Part 8), determination of water content, dry density relation of soil using heavy compaction (second revision). IS 2720. Bureau of Indian Standards, New Delhi, India (1983)
11. American Society for Testing and Materials, Standard practice for making and curing soil-cement compression and flexure test specimens in the laboratory. ASTM, D. 1632. ASTM International, West Conshohocken, PA, USA (2007)
12. <https://www.cement.org/docs/default-source/th-paving-pdfs/ctb-cement-treatedpuppala-base/cement-treated-base-pca-logo.pdf?sfvrsn=2>. Last accessed 17 Oct 2019
13. ASTM, D 559–03 (2003) Standard test methods for wetting and drying compacted soil-cement mixtures. American Society for Testing and Materials, West Conshohocken, Pennsylvania, USA
14. ASTM, D 7369–09 (2009) Standard test method for determining the resilient modulus of bituminous mixtures by indirect tension test
15. Congress IR (2018) Guidelines for the design of flexible pavements. Indian code of practice, IRC, 37

Performance Evaluation of Low-Volume Road Sections Consisting of Enzyme Stabilized Inverted Base



Kakara Srikanth, Attada Haresh, B. Raj Kumar, Mahammad Sameer, Matta Devendra Vara Prasad, Satyaveer Singh, Shubham Ghosh, S. Shankar, Venkaiah Chowdary, C. S. R. K. Prasad, and Apoorva Modi

Abstract Inverted base pavements are becoming more popular due to its strong base and lower cost of construction compared to conventional pavements. The purpose of the present study is to evaluate the performance of bitumen-surfaced low-volume road sections consisting of conventional and enzyme stabilized inverted base sections. An enzyme-based stabilizer was used to stabilize the lower base of the inverted base pavement section. Performance evaluation studies were carried on four roads located in two districts of Andhra Pradesh. The present study is initiated by hypothesizing that the performance of inverted base pavement sections is same as the performance of the corresponding control sections. The relative performance of inverted base pavement sections is compared with control sections for four roads in terms of roughness, Benkelman beam deflection, rutting, and dynamic cone penetration. The performance in terms of roughness for pavement sections consisting of inverted base is relatively better than the control sections for one road, even though the difference is not significant. However, for the remaining three roads, the performance of control sections is relatively better than the inverted base sections. Based on the Benkelman beam deflection and the rutting data, it is observed that the control sections are performing better than the inverted base sections even though the difference is not significant. The difference in performance between inverted base sections and control sections

K. Srikanth (✉) · A. Haresh · B. Raj Kumar · M. Sameer · M. Devendra Vara Prasad · S. Singh · S. Ghosh · S. Shankar · V. Chowdary · C. S. R. K. Prasad
Civil Engineering Department, Transportation Division, National Institute of Technology Warangal, Warangal, India
e-mail: sri717004@student.nitw.ac.in

S. Shankar
e-mail: ss@nitw.ac.in

V. Chowdary
e-mail: vc@nitw.ac.in

C. S. R. K. Prasad
e-mail: csrk@nitw.ac.in

A. Modi
Avijeet Agencies (P) Ltd, Chennai, India
e-mail: apoorva@avijeetagencies.com

for different roads is attributed to the prevailing local conditions. Considering the fact that the cost of inverted base sections is lower compared to the conventional pavement sections, the comparable performance of both the pavement types justifies the use of inverted pavement sections for low-volume roads.

Keywords Conventional pavement · Enzyme-based stabilization · Functional evaluation · Inverted base pavement · Structural evaluation

1 Introduction

Low-volume roads (LVRs) or local roads are usually constructed to connect farms with markets and provide access to inhabitants of rural areas. LVRs are designed to cater to a low volume of traffic, and thus, it is desirable to construct those using locally available materials like gravels. However, a few local materials used in various pavement layers may fail to meet the required engineering properties. For granular layers, these inferior materials are usually stabilized using chemical stabilizers. Cement and lime are predominantly used chemical stabilizers to improve the engineering properties of the inferior materials in the granular layers and produce a durable material. However, in practice, the use of cement and lime is unsustainable, and their application is energy-intensive [1]. To address this, enzyme-based stabilizers are a feasible alternative because of their ease in the method of application and efficiency in stabilization [2–5]. Enzyme stabilizers are liquid-based organic stabilizers, and thus, they are inherently non-toxic and eco-friendly. Enzymes are observed to produce an effect of catalytic stabilization after applying them to the granular materials, and a very minimum quantity of stabilizer is required to be applied [6]. TerraZyme is one such enzyme-based stabilizer, which catalyzes soil particles less than 0.01 mm [4]. TerraZyme imparts a microscopical crosslinking in soil particles by linking the opposite group ions. Due to crosslinking, the soil group reaches an orderly movement from Brownian movement, and a grid structure would be formed. Orderly grid structure eliminates the free negative ions and groups, and thereby, the hydrophobic property is induced in the soil structure [4]. Thus, an addition of TerraZyme imparts an enhancement in engineering properties like shear strength, abrasion resistance, water stability, and the structural strength in the granular layers of pavement. TerraZyme and other enzyme-based stabilizers are usually composed of a proprietary formulation, and usually, their chemical composition is not disclosed [7]. As the composition of the enzyme stabilizers depends on the preference of manufacturers, it is of pivotal importance to test the materials in the laboratory and evaluate in-field performance.

Several researchers have tried to study the mechanism of enzyme-based stabilizers based on laboratory and field studies. Based on the stabilization of several soils, it was observed that this stabilization technique is ineffective in soils without organic matter [8, 9]. In another study on clayey soils with Optimum Moisture Content (OMC) lying between 15 to 30%, it was observed that enzyme stabilization reduced

the compaction effort required to reach the 95% maximum dry density (MDD) determined in the laboratory [8]. However, it is also observed that the performance of enzyme stabilized clayey soil is poor when subjected to wet and dry cycles. The Unconfined Compressive Strength (UCS) of enzyme stabilized soil samples reduced by 38% to 50% due to leaching [10]. In a field study on the performance of unpaved roads with enzyme stabilized soil, the soil stabilized with cement or cement combined with enzyme showed higher California Bearing Ratio (CBR) and modulus than soil treated with enzyme alone [11]. Various studies carried out in the past have reported contradicting results in the performance of pavements with enzyme stabilized soils. On the other side, studies reporting the performance of bitumen-paved roads with enzyme stabilized roads are scant. Thus, it is imperative to perform appropriate laboratory tests, field tests, or both before employing enzyme stabilization on a wide scale [11]. The present study is intended to study the performance of bitumen-paved low-volume road sections consisting of enzyme stabilized inverted base and compare it with control sections of bitumen-paved low-volume roads consisting of unstabilized granular layers.

Structural evaluation and functional evaluation are the two main methods of evaluating the performance of flexible pavements. The structural evaluation deals with the assessment of the structural adequacy of the pavement for rehabilitation. It is a quantitative evaluation and is of vital importance to the highway engineers. Structural adequacy is the primary response of pavement to transient loads and consists of deformation, deflection, stresses, strain, and permanent deformation at critical points in pavement layers. Deflection criteria are widely used as a tool for structural evaluation. The maintenance practices in developing countries require structural evaluation using Benkelman Beam Deflectometer (BBD) or Falling Weight Deflectometer (FWD). The permanent deformation on roads is also considered for structural evaluation. Functional evaluation is primarily concerned with the ride quality or surface texture of a road section. Everyone who drives a vehicle or travels in a vehicle over the surface of a pavement can subjectively judge the smoothness of the ride. Pavement roughness is defined as an expression of irregularities in the longitudinal profile of its surface that adversely affects the ride quality, thus causing discomfort to the road user. The functional evaluation includes the manual distress data collection to identify various distresses present in the pavement section as per the guidelines given in IRC: 82–2015 [12].

2 Site Description

For the present study, field performance evaluation was carried out on low-volume roads constructed under the program, Pradhan Mantri Gram Sadak Yojana (PMGSY). The data was collected from four roads constructed using TerraZyme stabilized inverted base sections consisting of one each in the Chennur block (AP04131405) and Pendlimarri block (AP04131406) of YSR Kadapa district, Andhra Pradesh, and Chillakur block (AP141402) and Doravarisatram block (AP141403) of Sri Potti

Sriramulu Nellore district, Andhra Pradesh. The road located in YSR Kadapa district with package no. AP 04,131,405 in the Chennur block is hereafter referred as Kadapa road-1. The total length of the road is 5.2 km with average daily traffic (ADT) of 214 with 51 Commercial Vehicles Per Day (CVPD). The total width of road is 7.5 m including shoulders and 3.75 m of carriageway. For performance evaluation, the test sections were selected from the following chainages: 3/1–4/2 (TerraZyme sections) and 5/840–6/8 (control sections). The road located in YSR Kadapa district with package no. AP04131406 in the Pendlimarri block is hereafter referred as Kadapa road-2. The total length of road is 4.1 km with average daily traffic of 206 with 47 CVPD. The total width of road is 7.5 m including shoulders and 3.75 m of carriageway. For performance evaluation, the test sections were selected from the following chainages: 3/4–5/2 (TerraZyme sections) and 12/080–12/840 (control sections). The road located in Chillakur mandal of Sri Potti Sriramulu Nellore district with package no. AP141402 is hereafter referred as Nellore road-1. The total length of road is 7.46 km. For performance evaluation, the test sections were selected from the following chainages: 0/0–1/0, 5/4–6/4 (TerraZyme sections) and 4/640–5/4, 6/4–7/4 (control sections). The average daily traffic is 185 with 38 CVPD. The road located in Sri Potti Sriramulu Nellore district with package no. AP 141,403 in the Doravarisatram block is hereafter referred as Nellore road-2. The total length of road is 8.23 km with average daily traffic of 110 and 37 CVPD. The total width of road is 7.5 m including shoulders and 3.75 m of carriageway. For performance evaluation, the test sections were selected from the following chainages: 2/4–3/4, 4/6–5/6 (TerraZyme sections) and 5/6–6/0, 4/2–4/6, 2/0–2/4 (control sections).

Figure 1a–g shows the cross-sections of all the roads considered in this study. In all the roads with TerraZyme stabilized layers, the original layers of Wet-Mix Macadam (WMM), Water Bound Macadam (WBM), and Gravel Sub-Base (GSB) of control sections were replaced fully or partially with TerraZyme stabilized gravel layer. The TerraZyme stabilized gravel layer is economical when compared to WMM and WBM layers, because gravel is a locally available material and in situ stabilization is possible with TerraZyme. Thus, the present study is initiated hypothesizing that the performance of TerraZyme stabilized inverted base pavements is as same as the performance of the corresponding control sections. In all the four road stretches, TerraZyme stabilized inverted base sections and the control sections are on the same stretch of road and no connecting roads are found in between them. Thus, both the sections experience the same traffic, and a relative comparison of performance is justified.

3 Study Methodology

The methodology of the study includes field evaluation of the selected low-volume roads. Field performance evaluation includes structural performance evaluation and functional performance evaluation. Figure 2 shows the methodology flowchart adopted for the current study. The structural capacity evaluation of a pavement

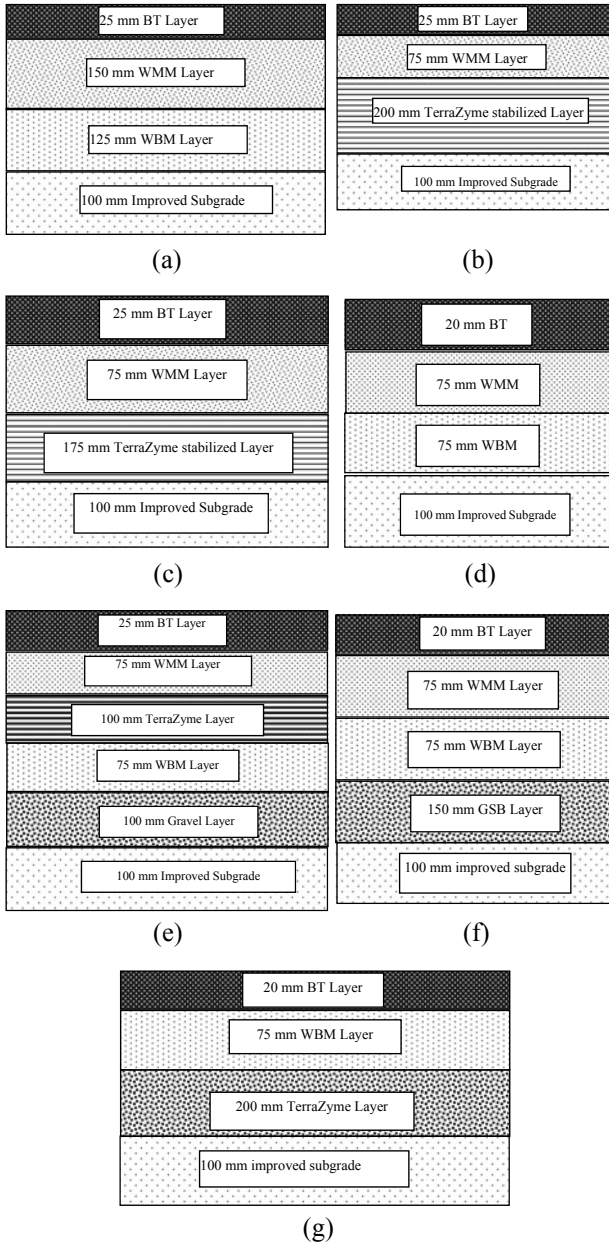


Fig. 1 **a** Cross-section of control section on Nellore road-1 (4/640 – 5/4, 6/4 – 7/4) and Nellore road-2 (5/6 – 6/0, 4/2 – 4/6, 2/0 – 2/4); **b** cross-section of TerraZyme section on Nellore road-1 (0/0 – 1/0); **c** cross-section of TerraZyme section on Nellore road-1 (5/4 – 6/4) and Nellore road-2 (2/4 – 3/4, 4/6 – 5/6); **d** cross-section of control section on Kadapa road-1 (5/840 – 6/8); **e** cross-section of TerraZyme section on Kadapa road-1 (3/1 – 4/2); **f** cross-section of control section on Kadapa road-2 (12/080 – 12/840); and **g** cross-section of TerraZyme section on Kadapa road-2 (3/4 – 5/2)

comprises of the assessment of structural adequacy of the pavement, i.e., the load transfer capacity of the pavement. The present study compares the structural capacity of bitumen-surfaced low-volume road sections consisting of conventional and enzyme stabilized inverted base sections. As shown in Fig. 2, the structural capacity is evaluated in terms of deflection, penetration in granular layers, and total rut depth. On the other hand, functional evaluation includes the rideability of the pavement, and it is quantified in terms of roughness and visible distresses on the pavement.

The in situ strength of the pavement is represented by the deflection of the pavement, measured using Benkelman Beam Deflectometer (BBD) as per guidelines of IRC: 81-1997 [13]. The principle of BBD is to measure the elastic recovery of the pavement after the removal of the load. The deflection in a flexible pavement depends on the modulus of various layers, and thus, elastic recovery on removal of this load is considered as a measure of the structural strength of the pavement. Dynamic Cone Penetrometer (DCP) is used to measure the in situ strength of compacted soils in the base and sub-base layers. In situ strength is determined in terms of CBR. There are several empirical equations available to determine the in situ CBR depending on the type of soil. However, all the equations are a function of average depth of penetration per each blow. In the present study, average depth of penetration per each blow in TerraZyme layer and the corresponding layer in the control section is used for the comparison. The other structural evaluation parameter is the permanent deformation, which is represented as rutting in both the wheel paths. Rutting is measured using

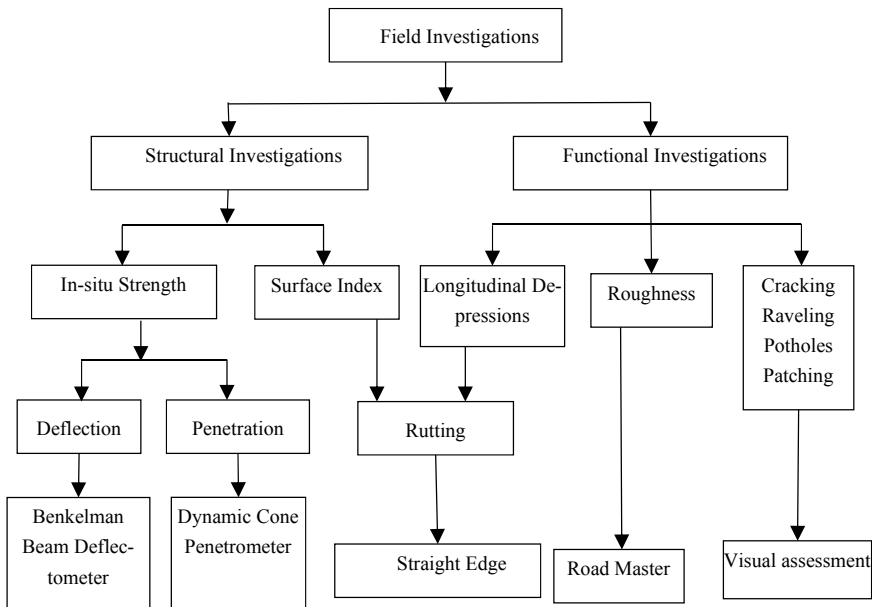


Fig. 2 Flowchart representing the experimental program of the study

Table 1 Performance criteria for low-volume roads [16]

S. No.	Riding quality	Roughness IRI (m/km)	Average rut depth (mm)	Average longitudinal depression (mm)
1	Very good	<4	< 2	< 3
2	Good	4–5.5	2–5	3–4
3	Fair	5.5–6.7	5–13	4–5.5
4	Poor	6.7–8.5	13–25	5.5–7.3
5	Very Poor	>8.5	>25	>7.3

a straight edge of length 50 cm at an interval of 20 m throughout the length of the test sections. The average rutting in both wheel paths is used as a parameter for comparing the performance of the test sections.

Functional performance of the pavement is quantified in terms of distress observed on the pavement and roughness of pavement. “*The deviations of a surface from a true planar surface with characteristic dimensions that affect vehicle dynamics, ride quality, dynamic loads and drainage, for example, longitudinal profile, transverse profile and cross slope*” is defined as the roughness [14]. In the present study, roughness of the pavement is measured in terms of International Roughness Index (IRI). A vehicle mounted roughness measuring instrument “Road Master” is used in the study, and the average IRI of both wheel paths of a pavement section is used for comparison. The various types of distresses including raveling, potholes, edge cracks, edge failures, and patching were measured manually through a distress survey. The percentage area of each distress in each section of the pavement is quantified according to guidelines of IRC: 82–2015 [15]. Based on the roughness and average rutting observed in the low-volume roads, the performance of the road is classified. Table 1 shows the performance criteria adopted for the low-volume roads [16].

4 Roughness

The roughness of the selected test sections is measured using Road Master [17]. The observed roughness is represented in International Roughness Index (m/km). The TerraZyme stabilized inverted base pavement section roughness over 1 km length is compared with control section roughness over the same reference length. Figure 3 shows the roughness data collected from all four road sections in both the TerraZyme stabilized inverted base pavement sections and the control sections. The TerraZyme stabilized inverted base pavement sections hereafter are termed as TerraZyme sections.

From Fig. 3a, b, it is observed that the performance of control section is relatively better than the TerraZyme section with a difference in IRI of 1 m/km. It is worth to note here that the roughness of the control section is within a range of 4 to 5.5 m/km indicating that the riding quality is good as per the threshold limits given in Table 1.

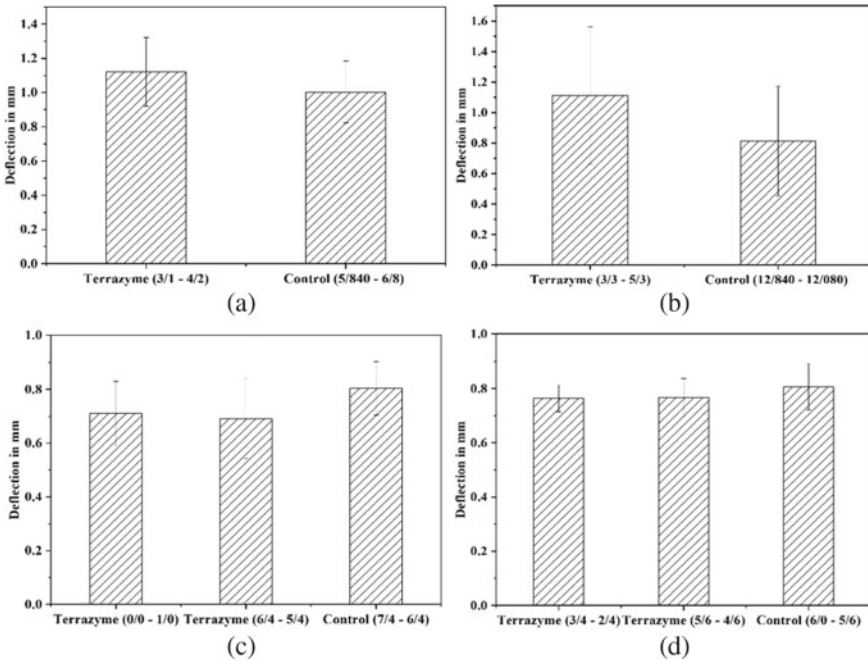


Fig. 3 Roughness of all the test sections on: **a** Kadapa road-1, **b** Kadapa road-2, **c** Nellore road-1, and **c** Nellore road-2

Similarly, the roughness of the TerraZyme section is within a range of 5.5–6.7 m/km indicating that the riding quality is fair as per the threshold limits given in Table 1. From Fig. 3c, it is observed that the performance of TerraZyme sections is relatively better than the control sections. However, the difference in terms of roughness is not significant. It is worth to note here that the roughness of both the TerraZyme and control sections is less than 4 m/km indicating that the riding quality is very good as per the threshold limits given in Table 1. From Fig. 3d, it is observed that the performance of control Sects. (5/6–6/0, 4/2–4/6) is relatively better than the TerraZyme Section (4/6–5/6). However, the difference in terms of roughness is not significant. The roughness of both the TerraZyme and control sections is less than 4 m/km indicating that the riding quality is very good as per the threshold limits given in Table 1. Further, the performance of TerraZyme Section (2/4–3/4) is equal to the control Section (2/0–2/4). The roughness of both the TerraZyme and control sections is within a range of 4.0–4.5 m/km, i.e., slightly more than 4 m/km indicating that the riding quality is good as per the threshold limits given in Table 1.

5 Benkelman Beam Deflection (BBD) Survey

The structural evaluation was carried out using BBD on the selected test sections. The truck with rear axle load of 8 tons and tire pressure of 5.6 kg/cm² is used for the BBD survey. The deflection measurements were taken at 50 m intervals on alternate wheel paths of the road, and the average of 10 location deflections is reported in mm. The temperature of pavement and moisture content of soil were measured, and corrections are applied as per IRC: 81-1997 [13]. Figure 4 shows the characteristic deflection data collected from all four road sections in both TerraZyme and control sections.

The characteristic deflection is a measure of structural strength of the pavement, and it depends on the subgrade soil properties, subgrade moisture content, pavement thickness and composition, temperature, and loading parameters. From Fig. 4a, b, it is observed that the performance of control section is relatively better than the TerraZyme section even though the difference in terms of deflection is not significant. From Fig. 4c,d, it is observed that the performance of TerraZyme sections is relatively better than the control sections. However, the difference in terms of deflection is not significant.

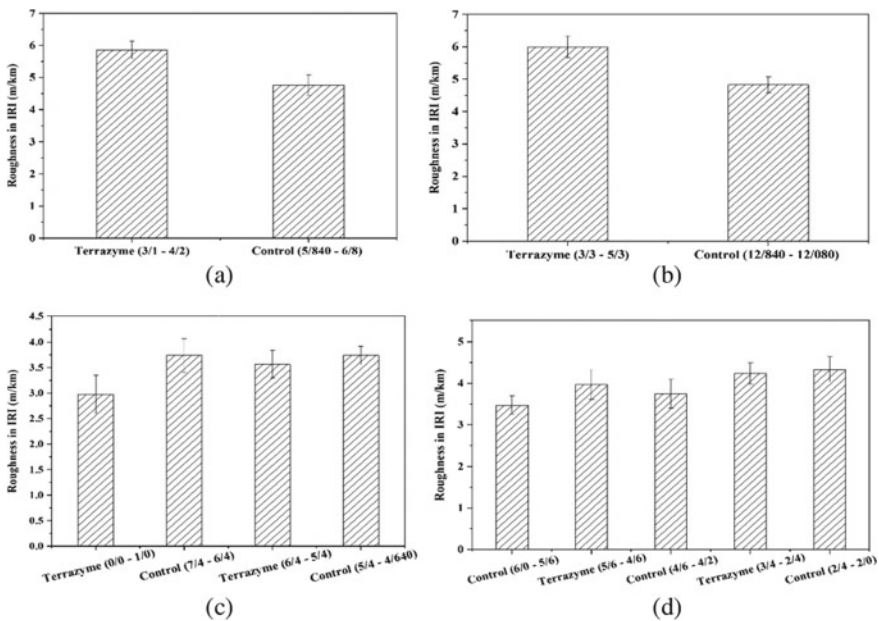


Fig. 4 Characteristic deflection of all the test sections on: **a** Kadapa road-1, **b** Kadapa road-2, **c** Nellore road-1, and **d** Nellore road-2

6 Dynamic Cone Penetrometer (DCP) Survey

The DCP results are shown in Fig. 5a–d, where the cumulative average depth of penetration of DCP cone in TerraZyme section layers is compared with the cumulative average depth of penetration of corresponding layers at the same depth in the control section. The cumulative average depth of penetration shown is the average of 10 locations in each stretch. In Fig. 5a, the cumulative average depth of penetration in TerraZyme section layer-1 is found to be equal to the corresponding layer in the control section. This is because 20/25 mm BT is used in both the TerraZyme and control sections. For the cumulative average depth of penetration from 25 to 100 mm, 75 mm WMM layer is used in TerraZyme section, whereas 75 mm WBM layer is used in control section resulting in equal cumulative average depth of penetration. For the cumulative average depth of penetration from 100 mm to 175/200 mm, one layer of 100 mm thick TerraZyme is used, whereas, for the control section, 75 mm WBM layer is used. The cumulative average depth of penetration from 100 mm to 175/200 mm is relatively higher for the TerraZyme section compared to the control section. It is important to note here that the applicability of the DCP should be limited to fine-grained soils and the variability in DCP penetration will be much higher for coarse-grained soils as location of a coarser aggregate particle below the DCP cone can significantly affect its penetration. Considering these constraints with the DCP, no significant conclusions can be drawn even though the cumulative average depth of penetration is more in the TerraZyme section compared to the control section.

In the Fig. 5b, the cumulative average depth of penetration in TerraZyme section layer-1 is found to be equal to the corresponding layer in the control section. This is because 20 mm BT is used in both the TerraZyme and control sections. For the cumulative average depth of penetration from 20 to 100 mm, 75 mm WBM layer is used in both the TerraZyme section and the control section resulting in equal cumulative average depth of penetration. For the cumulative average depth of penetration from 100 mm to 300/325 mm, one layer of 200 mm thick TerraZyme is used, whereas, for the control section, 75 mm WBM layer is used followed by 150 mm GSB. The cumulative average depth of penetration from 100 mm to 300/325 mm is relatively higher for the TerraZyme section compared to the control section.

In Fig. 5c, the cumulative average depth of penetration in TerraZyme section layer-1 is found to be equal to the corresponding layer in the control section. This is because 25 mm BT is used in both the TerraZyme and control sections. For the cumulative average depth of penetration from 25 to 100 mm, 75 mm WMM layer is used in both TerraZyme and control section resulting in equal cumulative average depth of penetration. For the cumulative average depth of penetration from 100 to 300 mm, two layers of TerraZyme are used where the thickness of each TerraZyme layer is 100 mm, whereas, for the control section, the top 75 mm consists of WMM layer and the remaining 125 mm consists of the GSB layer. Even though the cumulative average depth of penetration from 100 to 200 mm is equal for both the TerraZyme and control sections, the cumulative average depth of penetration from 200 to 300 mm in TerraZyme section reached in a smaller number of blows compared to the control

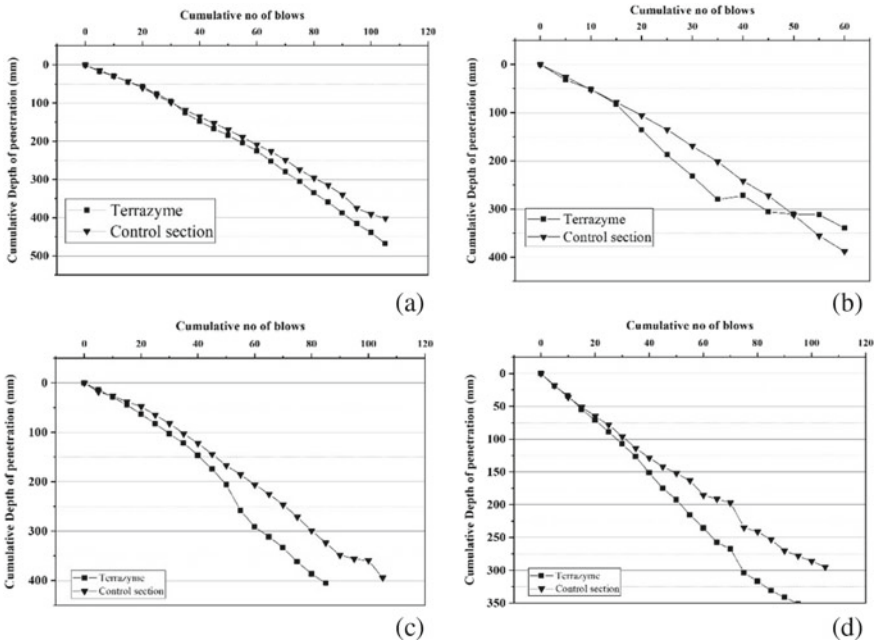


Fig. 5 Cumulative average depth of penetration of all test sections on: **a** Kadapa road-1, **b** Kadapa road-2, **c** Nellore road-1, and **d** Nellore road-2

section. This shows that the second layer of 100 mm thick TerraZyme is likely to be less stiffer than the corresponding GSB material used in the control section. In Fig. 5d, for the cumulative average depth of penetration from 25 to 100 mm, 75 mm WMM layer is used in both TerraZyme and control section resulting in equal cumulative average depth of penetration. For the cumulative average depth of penetration from 100 to 275 mm, one layer of 175 mm thick TerraZyme is used, whereas, for the control section, the top 75 mm consists of WMM layer, and the remaining 100 mm + 25 mm consists of the GSB layer. The cumulative average depth of penetration from 100 to 275 mm is equal for both the TerraZyme and control sections.

7 Rutting Survey

Rutting was measured using a straight edge on both the wheel paths at 20 m intervals and represented as average rut depth of lane in mm. Figure 6 shows the average rutting observed in all the pavement sections considered in the study.

From Fig. 6a, it is observed that the performance of control section is better than the TerraZyme section with a difference in average rutting of 3 mm. Similarly, from Fig. 6b, it is observed that the performance of control section is much better than the

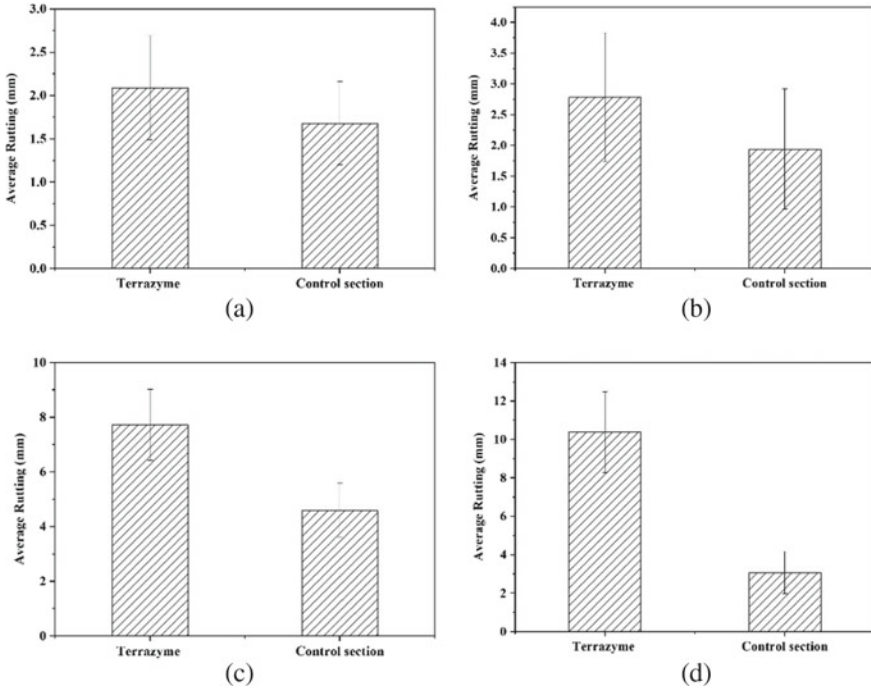


Fig. 6 Average rutting of all test sections on: **a** Kadapa road-1, **b** Kadapa road-2, **c** Nellore road-1, and **d** Nellore road-2

TerraZyme section with a difference in average rutting of 7 mm. It is worth to note here that, in both Kadapa road- and Kadapa road-2, the average rutting of the control section is within a range of 2–5 mm indicating that the riding quality is good as per the threshold limits given in Table 1. Similarly, the average rutting in the TerraZyme section is within a range of 5–13 mm indicating that the riding quality is fair as per the threshold limits given in Table 1. From Fig. 6c, d, the average rutting of Nellore road-1 and Nellore road-2, is slightly less on the control sections compared to the TerraZyme sections. That is, the performance of control sections is relatively better than the TerraZyme sections. However, the difference in terms of average rutting is not significant. As per low-volume road threshold limits given in Table 1, in the two roads both the control and TerraZyme sections offer good riding quality as the average rut depth is close to 2 mm for both the control and TerraZyme sections.

8 Other Significant Distresses Observed

All the distresses observed in the selected chainage are negligible except patching. The patching is represented as percentage of area of pavement surface. The observed

percentage of patching on all the TerraZyme sections and control section are shown in Fig. 7. In Kadapa road-1 and Kadapa road-2, as shown in Fig. 7a, b, considerable patchwork is observed on TerraZyme section which significantly affects the ride quality, whereas patchwork is not observed on the control section. The patchworks observed in the TerraZyme section might have been laid due to formation of fatigue cracking/potholes/shear rutting. In Nellore road-2, as shown in Fig. 7c there is considerable patchwork in control and TerraZyme sections which significantly affect the ride quality. It is observed that more patchwork was done in the TerraZyme stretch compared to the control section. The patchworks observed in these sections might have been applied due to formation of fatigue cracking/potholes/shear rutting. This is mainly due to presence of tank bund on one side of this road within 2/0–3/4 stretch resulting in poor drainage conditions. The stagnated rainwater might have triggered the initiation and subsequent propagation of distresses within 2/0–3/4 stretch of the road. Further, man-made distresses in terms of cutting across the road were observed in this stretch where water pipelines were laid across the road from the tank to the adjacent paddy fields. To cover-up these transverse cuts across the road, patchwork was applied.

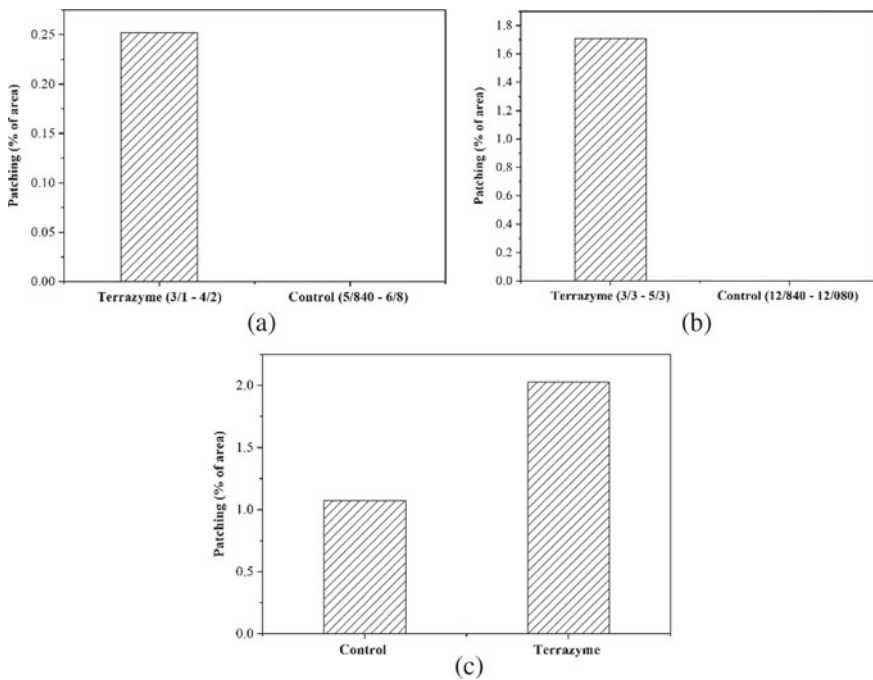


Fig. 7 Percentage of patching of all test sections on: **a** Kadapa road-1, **b** Kadapa road-2, and **c** Nellore road-2

9 Conclusions

The purpose of the present study is to evaluate the performance of bitumen-surfaced low-volume road consisting of enzyme stabilized inverted base pavement sections and conventional pavement sections. The present study is initiated by hypothesizing that the performance of TerraZyme stabilized inverted base pavement sections is same as the performance of the corresponding control sections. The relative performance of TerraZyme stabilized inverted base pavement sections is compared with control sections for four roads in terms of roughness, Benkelman beam deflection, rutting, and dynamic cone penetration. Based on the roughness survey, in Nellore road-1, it is observed that the performance of TerraZyme stabilized inverted base pavement sections is relatively better than the control sections even though the difference is not significant. However, in all the other three roads, the performance of control sections is relatively better than the TerraZyme stabilized inverted base pavement sections. Further, the roughness on both the TerraZyme stabilized inverted base pavement and control sections lies between 4 m/km and 6 m/km, which indicates that the riding quality of all the roads ranges from very good to fair.

Based on the Benkelman beam deflection survey, it is observed that the performance of control sections is relatively better than the TerraZyme stabilized inverted base pavement sections even though the difference is not significant. Based on the distress survey, it is observed that the performance of control sections is relatively better than the TerraZyme stabilized inverted base pavement sections as the average rut depth is slightly less on the control sections compared to the TerraZyme stabilized inverted base pavement sections. Even though the difference in terms of average rutting is not significant, both the control and TerraZyme stabilized inverted base pavement sections offer good riding quality as the average rut depth is close to 2 mm for both the control and TerraZyme stabilized inverted base pavement sections. Based on the DCP survey, the cumulative average depth of penetration in the corresponding layers of the TerraZyme and control sections is more or less same up to a cumulative average depth of penetration of 200 mm. However, the cumulative average depth of penetration is observed to be relatively higher for TerraZyme second layer in Nellore road-1 compared to the corresponding GSB layer in the control section. Considering the obvious limitations of the DCP in terms of strength evaluation of the layers for coarse-grained soils, no significant conclusion could be drawn from the DCP survey. Overall, based on the roughness, Benkelman beam deflection, and rutting survey, it is observed that the performance of TerraZyme stabilized inverted base pavement sections is comparable to that of the performance of the control sections for Nellore road-1 and road-2. In Kadapa road-1 and road-2, the performance of control section is relatively better than the performance of the TerraZyme stabilized inverted base pavement section. However, the riding quality on TerraZyme section is in fair condition as could be observed from roughness and rut depth measurements. It is important to note here that there is significant effect of local conditions like movement of caged-wheel tractors on these roads as could be observed from its imprints on the entire stretch of this road and thin wearing courses of bituminous mixtures are expected to

deteriorate at a much faster rate due to movement of cage-wheeled tractors. Overall, the performance of TerraZyme stabilized inverted base pavement sections is comparable to the conventional pavement sections with the added advantage that the cost of TerraZyme stabilized inverted base pavement is less than that of the conventional pavement. This shows that the TerraZyme stabilized inverted base pavement sections prove to be a successful alternative for low-volume roads. However, additional road sections constructed over various subgrades need to be evaluated on a long-term basis under varied loading and climatic conditions to evaluate the life cycle cost of the TerraZyme stabilized inverted base sections.

References

1. Lax C (2010) Life cycle assessment of rammed earth. University of Bath, United Kingdom
2. Brazetti R (1998) Considerations about the influence of different additives in organic micro-morphological, mineralogical, physical, mechanical and hydraulics characteristics of a lateritic soil. Escola Politecnica de Sao Paulo, Sao Paulo
3. Brazetti R, Murphy SR (2001) Objective performance measurement of actual road sites treated with an organic soil stabilizer. In: First road transportation technology transfer conference in Africa, Dar Es Salaam, Tanzania
4. Li YJ, Li L, Dan HC (2011) Study on application of TerraZyme in road base course of road. *Appl Mech Mater* 97:1098–1108
5. Moloisane RJ, Visser AT (2014) Evaluation of the strength behaviour of unpaved road material treated with electrochemical-based non-traditional soil stabilisation additives. *J S Afr Inst Civ Eng* 56:28–39
6. Muguda S, Nagaraj HB (2019) Effect of enzymes on plasticity and strength characteristics of an earthen construction material. *Int J Geo-Eng* 10:2
7. Rauch AF, Harmon JS, Katz LE, Liljestrang HM (2002) Measured effects of liquid soil stabilizers on engineering properties of clay. *Transp Res Rec: J Transp Res Board* 1787:33–41
8. Velasquez RA, Marasteanu M, Hozalski R (2006) Investigation of the effectiveness and mechanisms of enzyme products for subgrade stabilization. *Int J Pavement Eng* 7(3):213–220
9. Tingle JS, Santoni RL (2003) Stabilization of clay soils with nontraditional additives. *Transp Res Rec: J Transp Res Board* No.1819, pp 72–84
10. Parsons RL, Milburn JP (2003) Engineering behavior of stabilized soils. *Transp Res Rec: J Transp Res Board* No. 1837, pp 20–29
11. Guthrie WS, Simmons DO, Eggett DL (2015) Enzyme stabilization of low-volume gravel roads. *Transp Res Rec* 2511(1):112–120
12. IRC:82—2015 (2015) Code of practice for maintenance of bituminous road surfaces. Indian Road Congress, New Delhi, India
13. IRC: 81—(1997) Guidelines for strengthening of flexible road pavements using Benkelman beam deflection technique, Indian Roads Congress, New Delhi, India
14. ASTM E867—(2002) Terminology relating to vehicle-pavement systems, American society for testing of materials, Pennsylvania, United states
15. IRC: 82 (2015) Code of practice for maintenance of bituminous road surfaces, Indian Road Congress, New Delhi, India
16. Sahoo UC, Reddy KS (2011) Performance criterion for thin surfaced low-volume roads. *Transp Res Rec: J Transp Res Board* No. 2203, pp 178–185
17. Roadmaster, <https://www.al-engineering.fi/en/roadmaster.html>. Last accessed 04 Jun 2021

Performance Evaluation of Scrap Rubber-Sand Mixture Reinforced with Geogrids



K. P. Anjali and Renjitha Mary Varghese

Abstract The disposal of scrap tires is one of the major environmental issues in recent years. Several experimental studies proved that scrap rubber-sand mixture can be effectively used as reinforced backfill material in retaining structures which is common in transportation projects. However, studies on interaction properties between rubber-sand mixture and geosynthetics are needed for effective backfill designing. Hence, this study is mainly focused to evaluate the shear behavior of rubber-sand mixture with various rubber contents and also estimates the interface shear strength properties of rubber-sand mixture with geogrid reinforcement when this material is used in mechanically stabilized retaining walls. The large direct shear tests were conducted on the rubber-sand mixture for rubber contents varied from 10 to 50% by volume. The influence of the different sizes of scrap tires and normal stresses on the strength characteristics was also studied. It was observed that the maximum peak strength was obtained for a rubber content of 30%, and there is a significant increase in shear strength with an increase in the size of rubber. The interface shear strength responses of the rubber-sand mixture and geogrid showed that there is no significant difference in the interfacial frictional strength when the rubber-sand mixture is reinforced with geogrids and it is independent of the size of the rubber particles in the mixture which enhances the usage of bigger rubber shreds. The findings lead to a sustainable as well as the cost-effective design of retaining structures.

Keywords Rubber-sand mixture · Large-scale direct shear test · Interface shear properties

K. P. Anjali (✉) · R. M. Varghese
Department of Civil Engineering, NIT Calicut, Kerala 673601, India
e-mail: anjalikp.1995@gmail.com

R. M. Varghese
e-mail: renjitha@nitc.ac.in

1 Introduction

The waste tire rubber has many applications in construction and geotechnical fields like replacement material for bitumen and asphalt in roadways, a replacement for railway sub-ballast layers, soil stabilization, seismic isolation of buildings, lightweight backfill material for retaining wall backfills, and embankments [1]. These effective incorporations of waste tire rubbers in various civil engineering works can reduce the tire disposal problem in an economically and environmentally beneficial way.

Some previous studies showed that scrap tire can be used as a lightweight backfill material for embankments and retaining walls [2, 3]. Certain field and laboratory studies also indicated that the use of tire chip-soil mixture, which is defined as a blend of scrap tire chips and soil mixed in various proportions, can potentially enhance the stability of the foundation and reduce settlements in problematic areas. Many experimental studies proved that the use of tire rubber-sand mixture mixed in various proportions can effectively improve the backfill stability by increasing its shear strength properties [4].

In this study, a series of large-scale direct shear tests are done to understand the variation of shear strength on varying rubber content in the sand, the mean grain size ratio of sand and rubber, and applied normal stresses.

2 Materials

The locally available sand was used in the present study (see Fig. 1). Table 1 represents the properties of sand. According to IS.1498–1970, sand is classified as poorly graded (SP).

As per ASTM D6270-12, the shredded tire can be classified into different groups according to their sizes. The products of rubber tires are usually referred to as tire



Fig. 1 Sand and rubber samples, *R1* and *R2* used in the present study

Table 1 Properties of sand

Property	Value
Specific gravity, G	2.62
D_{10}	0.21 mm
D_{30}	0.33 mm
D_{60}	0.5 mm
Coefficient of uniformity, C_u	2.381
Coefficient of curvature, C_c	1.037
Maximum unit weight, γ_{dmax}	14.61 kN/m ³
Minimum unit weight, γ_{dmin}	13.24 kN/m ³
Maximum void ratio, e_{max}	0.94
Minimum void ratio, e_{min}	0.758

Table 2 Size of granulated rubber

Sample name	Size of granulated rubber
$R1$	<4.75 mm
$R2$	<12 mm

shreds between 50 and 305 mm in size, tire chips between 12 and 50 mm in size, granulated rubber from 0.425 mm to 12 mm in size, and ground rubber from <0.425 mm to 2 mm in size. Two sets of granulated rubber ($R1$ and $R2$) have been used in the present study (see Fig. 1) with different size specifications shown in Table 2.

Specific gravity for both the sets of rubber particles was found according to ASTM D854-02 as 1.023 and 1.061 for $R1$ and $R2$, respectively, which is within the range of 0.88–1.27 as mentioned in the previous literature [5].

Other preliminary properties such as grain size distribution, coefficient of curvature, and uniformity coefficient for sand and two sets of rubber were also determined. Figure 2 shows the particle size distribution of $R1$ and $R2$ compared to pure sand. $R1$ is found to be poorly graded as compared to $R2$.

2.1 Reinforcing Material

Commercially available geogrids made of high-density polyethylene (HDPE) were used as the planar reinforcement (see Fig. 3). The uniaxial physical and mechanical properties of the geogrid material used for the experiment are listed in Table 3.

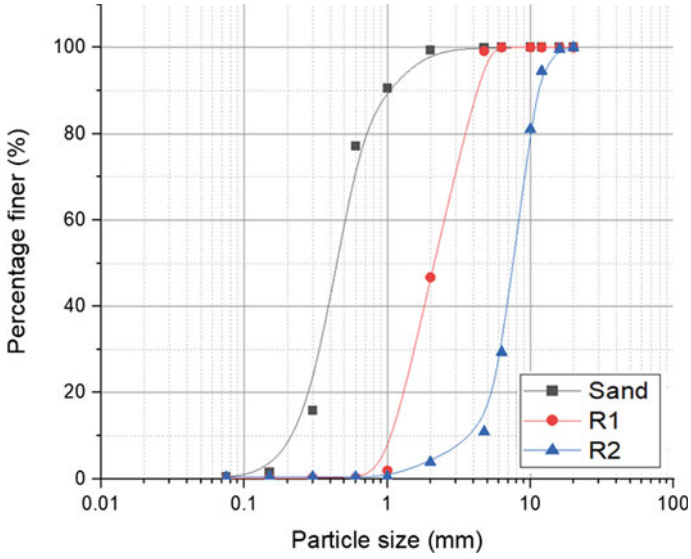


Fig. 2 Particle size distribution of sand, R1, and R2

Fig. 3 Geogrid used in the present study

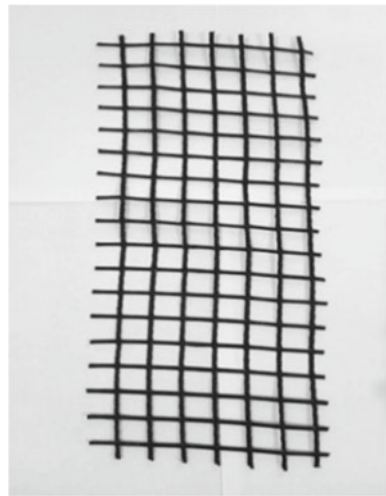


Table 3 Properties of geogrid used for the present study

Property	Value
Opening size	2 mm × 2 mm
Rib thickness (mm)	0.1 mm
Mass per unit area (g/m ²)	68
Ultimate tensile strength (kN/m)	40
Axial tensile strain at failure (%)	11

3 Experimental Program

The stress–strain behavior and interfacial friction angle of the rubber-sand mixture reinforced with geogrids were found out by conducting a series of large size direct shear tests. The length, breadth, and height of the test box were of dimension 300 mm × 300 mm and 150 mm, respectively. The effects of rubber size, normal stress, and rubber percentage on shear strength of rubber-sand mixture were also studied from direct shear tests, and altogether 81 large-scale direct shear tests were performed. Table 4 represents the experiment details of the present study. RxSy in Table 4 represents the rubber-sand mixture with x % of rubber mixed with y % of sand by volume.

The rubber-sand mixtures have been prepared at ratios 0:100, 10:90, 30:70, and 50:50 by volume. The volume of particles in the rubber-sand mixture is calculated as per Eq. (1):

$$V_p(\chi) = \frac{m_S(\chi)}{G_{sS}} \left(\frac{g}{\gamma_w} \right) + \frac{m_R(\chi)}{G_{sR}} \left(\frac{g}{\gamma_w} \right) \tag{1}$$

where m_S and m_R are masses of sand and rubber, respectively. G_{sS} and G_{sR} are the specific gravities of sand and rubber, respectively [5].

The amount of sand and rubber required to achieve the relative density of 70% for each percentage composition was estimated for both the rubber sizes. The rubber-sand mixtures were thoroughly mixed by hand and transferred to the shear box in different layers for getting uniformity. The prepared specimen was filled in the box in four different layers, and proper compaction was given to obtain the prescribed related density.

Geogrid samples of length 300 mm and breadth 250 mm were taken and placed in between the upper and lower halves of the direct shear test box with rubber-sand mixtures for obtaining the interface shear properties. The test specimens were prepared by the same procedure similar to that adopted for the rubber-sand mixture

Table 4 List of experiments

Unreinforced			Geogrid reinforced		
Test code (R_xS_y)	Normal stress (kPa)	No of tests	Test code (R_xS_y)	Normal stress (kPa)	No of tests
R_0S_{100}	50,100,150	9	–	–	–
$R1-R_{10}S_{90}$	50,100,150	9	–	–	–
$R1-R_{30}S_{70}$	50,100,150	9	$R1-R_{30}S_{70}$	50,100,150	9
$R1-R_{50}S_{50}$	50,100,150	9	–	–	–
$R2-R_{10}S_{90}$	50,100,150	9	–	–	–
$R2-R_{30}S_{70}$	50,100,150	9	$R2-R_{30}S_{70}$	50,100,150	9
$R2-R_{50}S_{50}$	50,100,150	9	–	–	–

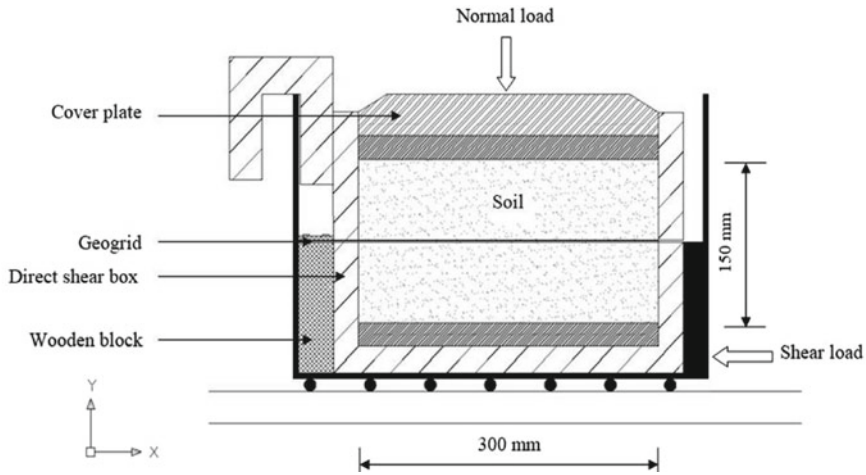


Fig. 4 Schematic diagram of the direct shear test box

without the geogrid case and were transferred to the shear box. The geogrid was placed in the shear box by clamping one end to the wooden clamping block using bolts and cover plates.

The tests were conducted for three normal stresses of 50, 100, and 150 kPa to cover the stress range in field applications of lightweight fill used in embankment construction [6], and the shear strain was applied at a constant rate of 1.25 mm/min, and Fig. 4 shows the shear box filled with rubber-sand mixture sample with the placement of geogrid. From previous studies [2] and [7], they pointed out the lack of definition of the failure point for the sand-tire mixtures and adopted a failure point at 25 mm horizontal displacement for a 305 mm direct shear box. In case of lack of definite failure point for the rubber-sand mixture, the shear stress corresponding to 9% of the maximum horizontal displacement is taken as peak stress value [7]. Hence, the experiments are conducted for a maximum horizontal displacement of 25 mm.

3.1 Results and Discussions

The shear strength parameters for rubber-sand mixtures were obtained from the large-scale direct shear tests for both geogrids reinforced and unreinforced cases. The interface shear parameters between geogrid and rubber-sand mixtures such as adhesion, (ca) and interface friction angle between rubber-sand mixture and geogrid, (δ) were also determined.

Effect of rubber content on shear strain behavior: Initially, the stress–strain behavior of rubber-sand mixtures for various percentages of rubber content was studied. Figure 5 shows the stress–strain behavior at different rubber content for R1 and R2 under normal stress of 150 kPa. An increase in the shear stress was observed

with an increase in the percentage of rubber, up to 30%, and then decreases. The initial increase is contributed by the filling of voids with rubber but after reaching a specific rubber content, segregation occurs, and thus the rubber-sand mixture behaves less like reinforced soil and more like a rubber mass with sand inclusions. This is similar to the results obtained in [8], where for different applied normal stresses, shear resistance of rubber-sand mixture was higher than that of pure sand, but the increasing trend is maintained only up to 30% of rubber, beyond which the shear resistance decreases.

It is noted that the addition of rubber has increased the axial strain at which the maximum stress was observed. Shear stress of the sand only case is higher than the rubber-sand mixtures at low shear displacement. This could be the effect of the higher deformability of rubber mixtures in the rubber-sand mixed samples. When the percentage of rubber content is 50%, the maximum stress which is equal to the maximum shear stress of normal sand was obtained at higher strain levels. The peak shear strength of pure sand reaches at an axial strain of 1.3–1.7%, whereas for $R_{50}S_{50}$ mixture, it reaches an axial strain of 5–8.4%. This indicates the additional flexibility obtained by sand by introducing rubber content. Similar observations were reported in [9, 10] and [11]. The experimental results showed that $R_{30}S_{70}$ mixture has the highest shear strength values.

It is also observed that rubber-sand mixtures exhibit a lower initial stiffness than the corresponding sands without rubber granules. A reduction in initial stiffness with increasing rubber content can be seen. This is due to the lower stiffness of rubber particles compared to sand particles and higher rubber–rubber interaction in samples with higher rubber fractions. The presence of highly deformable rubber particles changes the brittle behavior of the specimens to more ductile behavior [12]. It is evident from [13] that the shear modulus reduces with increasing rubber content. At any given axial strain level, pure sand and pure rubber are found to have the highest and least shear stiffness, respectively. The triaxial compression tests result from [11] that initial tangent modulus decreases with an increase in chip content. Thus, it is evident that tire chip content should not normally exceed about 30%. Beyond this rubber content, large deformations may occur, which may not be permissible.

The variation of the internal friction angle of rubber-sand mixtures with varying rubber contents for $R1$ and $R2$ rubber types shows that the internal friction angle increases with increasing rubber content and reaches a maximum value when the rubber content is 30% and then decreases for rubber contents beyond this value (see Fig. 6). A similar trend was observed in [14]. The decrease in friction angle at higher rubber contents may attribute more rubber in the failure plane which increases rubber-to-rubber interaction and reduces rubber-sand and sand-sand interactions. This mechanism ultimately resulting in a reduction in friction angle and shear strength [8].

Effect of rubber size on shear strength: The variation of peak shear stress for both $R1$ and $R2$ mixtures at 30% rubber content shows that with an increase in rubber size from $R1$ to $R2$, the peak shear strength increases (see Fig. 7). A similar pattern is observed for other rubber-sand mixtures of various proportions. These results are similar to those obtained in [8].

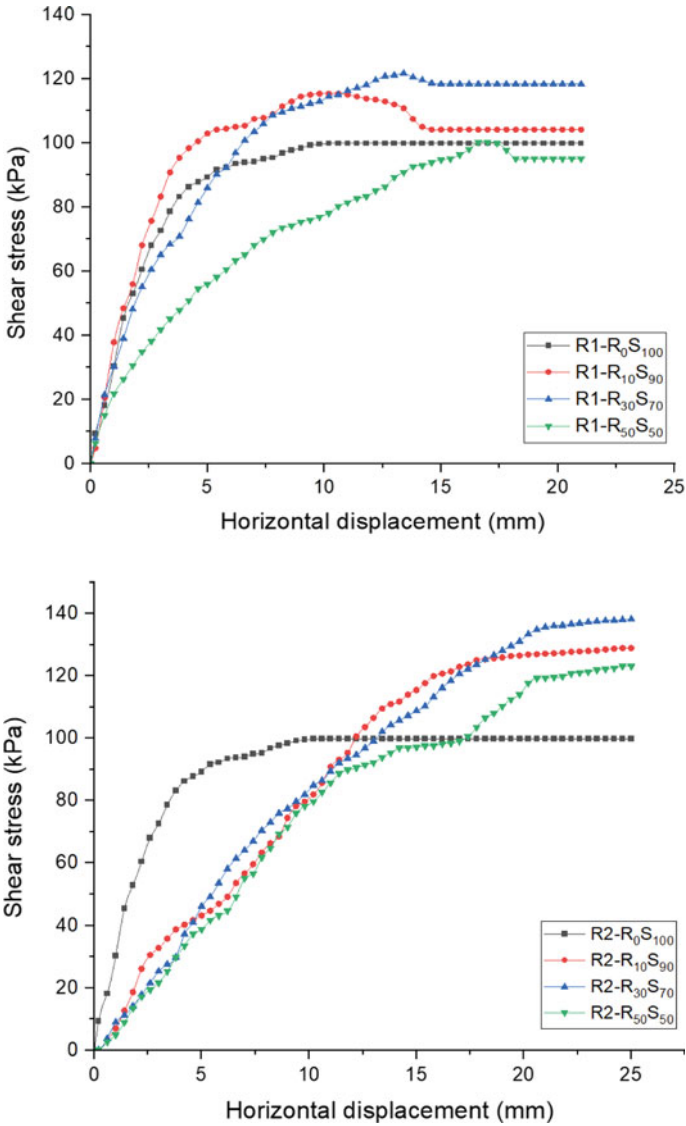


Fig. 5 Shear stress versus horizontal displacement curve for R1-sand mixture and R2- sand mixture at 150 kPa normal stress

This variation in shear strength with the size of rubber particles can be due to the more interlocking capacity of bigger particles than the smaller particles. In the case of R1, the average percentage increase peak shear stress is 31.2%, and for R2, it is 45%. The comparison of axial strain indicates that 30% of R2 sized rubber provides 12% more maximum peak. It is found that when the size of the rubber is increased,

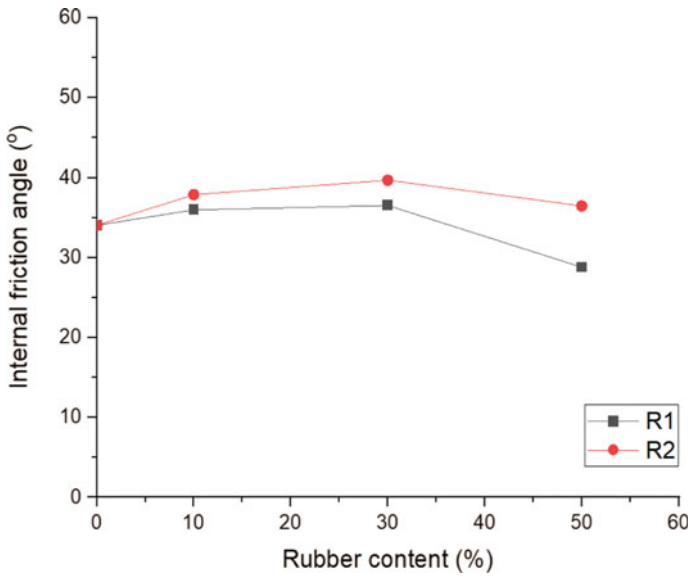


Fig. 6 Variation of internal friction angle with rubber content

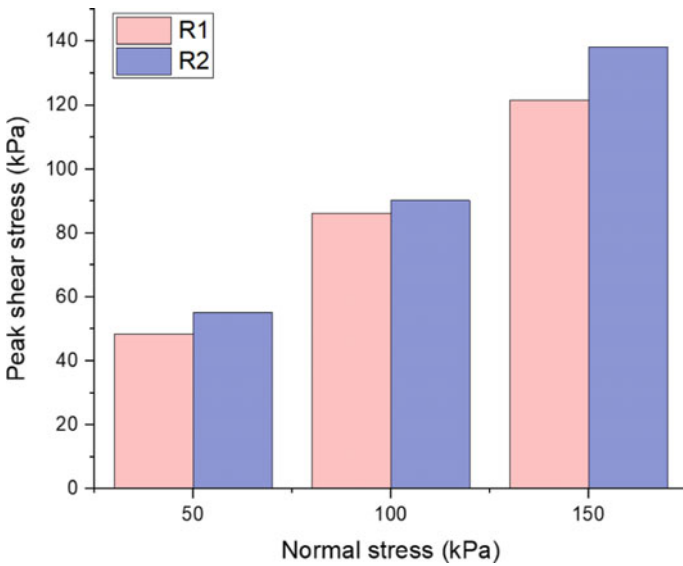


Fig. 7 Variation of peak shear stress with normal stress for R1 and R2 mixtures at 30% rubber content

the shear strength and flexibility for all percentages of rubber content are increased which enables in reducing the cost of shredding by using bigger tire shreds.

It is observed that the friction angle for bigger-sized *R2* is higher at all rubber contents compared to smaller-sized *R1* (see Fig. 6). This increase can be due to the more interlocking capacity of larger rubber particles with sand thus giving rise to higher internal friction in the shearing zone.

Influence of normal stress: The peak shear stress versus normal stress characteristics at different rubber contents for *R1* and *R2* mixtures in the sand at normal stresses of 50, 100, and 150 kPa shows that the shear parameters for all rubber-sand mixtures were higher when compared to sand only case (*R0S100*) (see Fig. 8).

Also at all normal stresses, the maximum shear strength was obtained for *R30S70* combination. At *R50S50*, the peak strength reduction is found higher. The increase in shear strength with an increase in normal stress occurs due to a reduction in the voids when overburden pressure is increased. This ultimately increases the interlocking capacity of rubber-sand granules with each other [15]. The peak stress is found to decrease at higher rubber contents due to the presence of more voids compared to lesser rubber content cases.

Interfacial shear strength coefficient: The interfacial shear properties between the rubber-sand mixture and the geogrids were studied for two sets of rubber sizes at varying normal stress at 30:70 by volume mixture ratio of sample for which the maximum shear stress was observed. The interface shear parameters between geogrid and rubber-sand mixtures such as adhesion, (c_a) and interface friction angle between rubber-sand mixture and geogrid, (δ) were also determined from large direct shear tests. For comparing the interface shear strength of soil against any geosynthetic, the shear strength values were normalized using a non-dimensional parameter called interface shear strength coefficient (α). Interfacial friction strength coefficient can be calculated by using the formula [16],

$$\alpha = \tau_{\text{sand-geosynthetic}} / \tau_{\text{sand}} \quad (2)$$

where $\tau_{\text{sand-geosynthetic}}$ is the peak shear stress at sand-geosynthetic interface and τ_{sand} is the peak shear stress of unreinforced sand. Using Eq. (2), the shear strength coefficient for the rubber-sand mixture with geogrid reinforcement can be determined. Table 5 gives the values obtained from the tests for shear strength parameters for two sets of rubber types mixed at various proportions. The shear parameters were found to be higher at *R30S70* proportion in both *R1* and *R2* cases. The interface friction angle between the rubber-sand mixture and geogrid (δ) was found to be 36.5 and 40.0 for *R1* and *R2* cases, respectively, which is found to be slightly greater than the unreinforced case. The shear strength variation of the geogrid reinforced case with varying rubber size is similar to that of the unreinforced case.

The peak shear strength for *R1* sand geogrid combination was found to be 124.2 kPa, and *R2* sand geogrid combination was found to be 141.6 kPa. Consequently, the interfacial shear strength coefficient values for *R1* and *R2* combination were found to be 1.0191 and 1.0277, respectively, i.e., it provides only 2 and 2.8% improvement in interface shear strength compared to unreinforced sand. Thus, the

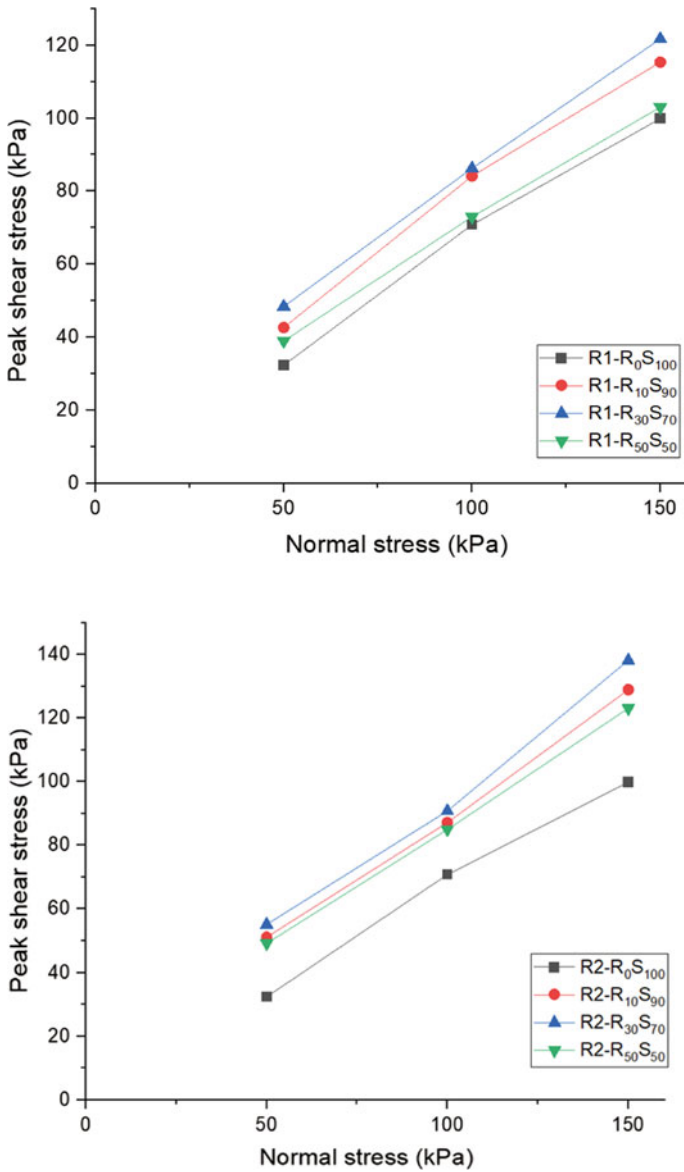


Fig. 8 Peak shear stress versus normal stress characteristics at different rubber contents for R1 and R2

Table 5 Shear parameters for geogrid reinforced and unreinforced rubber-sand mixtures

Rubber set	Unreinforced case		Geogrid reinforced case		
	φ	c	δ	ca	α
<i>R1-R₁₀S₉₀</i>	35.9	8.0			
<i>R1-R₃₀S₇₀</i>	36.2	12.3	36.5	13.3	1.0191
<i>R1-R₅₀S₅₀</i>	28.8	6.7			
<i>R2-R₁₀S₉₀</i>	37.8	11.2			
<i>R2-R₃₀S₇₀</i>	39.6	12.6	40.0	13.6	1.0277
<i>R2-R₅₀S₅₀</i>	36.4	10.5			

interface shear strength responses of the rubber-sand mixture and geogrid showed that there is no significant difference in the interfacial frictional strength when the rubber-sand mixture is reinforced with geogrids and it is independent of the size of the rubber particles in the mixture which enhances the usage of bigger rubber shreds. The findings from the experimental studies lead to a sustainable as well as a cost-effective design of retaining structures.

4 Conclusions

The shear strength properties of different percentages of rubber-sand mixtures (0:100, 10:90, 30:70, 50:50 by volume) were studied by large-scale direct shear tests. The interaction between rubber-sand mixtures with geogrid reinforcement was also studied. It has been found that rubber content, rubber granule size, and normal stresses are the influencing factors on the shear strength of the mixtures.

The conclusions that can be drawn from the results are:

- The incorporation of tire rubber shreds into the sand increases the shear strength of the sand in both unreinforced and geogrid reinforced cases.
- With an increase in the percentage of rubber content, the shear stress has increased initially up to 30% and then decreases beyond this value. This explains the sand-like and rubber-like behavior shown at different rubber percentages.
- As the size of the rubber granules increases, shear strength and flexibility increased for all percentages of rubber content. This reduces the cost of shredding by using bigger tire shreds.
- Normal stress is also an important factor that affects the increase in the strength of rubber-sand mixtures. As normal stress increases, shear strength of the mixture increases for both R1 and R2 combinations at all percentage contents.
- The shear strength parameters were also found to increase initially with increasing percentage rubber content and later found to decrease.
- The interface friction strength coefficient for the R1-sand combination was found to be 1.0191, and the R2-sand mixture was found to be 1.0277. This shows an

interface shear strength improvement of 2% and 2.8%, respectively, in comparison with unreinforced sand. Also, it is independent of the size of the rubber particles in the mixture which enhances the usage of bigger rubber shreds.

- The findings from experimental studies lead to a sustainable as well as the cost-effective design of retaining structures.

References

1. Mohajerani A, Burnett L, Smith JV, Markovski S, Rodwell G (2020) Resources, conservation and recycling recycling waste rubber tyres in construction materials and associated environmental considerations: a review. *Resour Conserv Recycl* 155(January):104679
2. Pincus H, Edil T, Bosscher P (1994) Engineering properties of tire chips and soil mixtures. *Geotech Test J* 17(4):453. <https://doi.org/10.1520/gtj10306j>
3. Lee JH, Salgado (1999) Shredded tires and rubber-sand as lightweight backfill. *J Geotech Eng* 125(February):132–141
4. Tanchaisawat T, Bergado DT, Voottipruex P, Shehzad K (2010) Geotextiles and geomembranes interaction between geogrid reinforcement and tire chip—sand lightweight backfill. *Geotext Geomembr* 28(1):119–127. <https://doi.org/10.1016/j.geotextmem.2009.07.002>
5. Mashiri MS (2014) Monotonic and cyclic behaviour of sand-tyre chip (STCh) mixtures, 290. <http://ro.uow.edu.au/theses/4267>
6. Youwai S, Bergado DT (2003) Strength and deformation characteristics of shredded rubber tire—Sand mixtures. *Can Geotech J* 40(2):254–264. <https://doi.org/10.1139/t02-104>
7. Foose GJ, Benson CH, Bosscher PJ (1996) Sand reinforced with shredded waste tires. *J Geotech Eng* 122(9):760–767. [https://doi.org/10.1061/\(asce\)0733-9410\(1996\)122:9\(760\)](https://doi.org/10.1061/(asce)0733-9410(1996)122:9(760))
8. Anbazhagan P, Manohar DR, Rohit D (2017) Influence of size of granulated rubber and tyre chips on the shear strength characteristics of sand—rubber mix. *Geomech Geoeng* 12(4):266–278. <https://doi.org/10.1080/17486025.2016.1222454>
9. Masad E, Taha R, Ho C, Papagiannakis T (1996) Engineering properties of tire/soil mixtures as a lightweight fill material. *Geotech Test J* 19(3):297–304. <https://doi.org/10.1520/gtj10355j>
10. Zornberg JG, Cabral AR, Viratjandr C (2004) Behaviour of tire shred—sand mixtures. *Can Geotech J* 241:227–241. <https://doi.org/10.1139/T03-086>
11. Rao GV, Dutta RK (2006) Compressibility and strength behaviour of sand—tyre chip mixtures. *Geotech Geol Eng* 711–724. <https://doi.org/10.1007/s10706-004-4006-x>
12. Rouhanifar S, Afrazi M, Fakhimi A, Yazdani M (2020) Strength and deformation behaviour of sand–rubber mixture. *Int J Geotech Eng* 00(00):1–15. <https://doi.org/10.1080/19386362.2020.1812193>
13. Madhusudhan B, Boominathan A, Banerjee S (2019) Engineering properties of sand–rubber tire shred mixtures. *Int J Geotech Eng* 00(00):1–17. <https://doi.org/10.1080/19386362.2019.1617479>
14. Ghazavi M (2011) Experimental determination of waste tire chip-sand-geogrid interface parameters using large direct shear tests. no. December 2015
15. Marto A, Latifi N, Moradi R, Oghabi M, Zolfeghari SY (2013) Shear properties of sand-tire chips mixtures. *Electron J Geotech Eng* 18B(March 2015):325–334
16. Makkar FM (2017) Performance of 3-D geogrid-reinforced sand under direct shear mode. *Int J Geotech Eng* 6362(June):1–9. <https://doi.org/10.1080/19386362.2017.1336297>

Traffic Flow Modelling

A Review of Real-Time Traffic Data Extraction Based on Spatio-Temporal Inference for Traffic Analysis Using UAV



K. Prathibaa and K. Gunasekaran

Abstract The growing demand for Unmanned Aerial Vehicles (UAVs) in the field of computer vision applications leads the researcher into UAV video analysis for extracting real-time traffic data. This paper systematically reviews studies that apply vehicle detection and extraction methods of Spatio-temporal traffic parameters from UAVs for efficacious traffic analysis. A synthesis of bibliographic sources clarifies the advantages and limitations of different methods of vehicle detection, Spatio-temporal data extraction, and discovers recent trends in the applications of UAVs in real-time traffic analysis. This paper reviews various studies that analytically handle Spatio-temporal data in traffic flow analysis, and paying special attention to infer the effective application of UAVs to extract microscopic traffic data. Thus, the three main questions for this review are:

- How to detect vehicles from UAV videos?
- How is the application of UAV performing to estimate traffic flow parameters in the context of present traffic research?
- What are recent approaches available for Spatio-temporal data extraction from UAV video data?

This paper concludes that there is a clear need for the development of comprehensive techniques for selecting suitable Spatio-temporal data extraction methods for analyzing non-lane-based heterogeneous traffic conditions.

Keywords Vehicle detection · Spatio-temporal · Extraction · UAV

K. Prathibaa (✉)

Research Scholar, Division of Transportation Engineering, College of Engineering Guindy, Anna University, Chennai 600025, India

e-mail: prathibaak@gmail.com

K. Gunasekaran

Professor, Division of Transportation Engineering, College of Engineering Guindy, Anna University, Chennai 600025, India

e-mail: kgunasekaran@annauniv.edu

© The Author(s), under exclusive license to Springer Nature Singapore Pte Ltd. 2023

535

M. V. L. R. Anjaneyulu et al. (eds.), *Recent Advances in Transportation Systems*

Engineering and Management, Lecture Notes in Civil Engineering 261,

https://doi.org/10.1007/978-981-19-2273-2_35

1 Introduction

The continual growth of motorized vehicles in developing countries leads to high travel demands, which promotes the effective and innovative measures consider to handle the issues of high traffic volumes and levels of congestion. The basic requirement of traffic studies is the collection of high-quality traffic data. The accuracy, expenses, and purpose of the survey are the three important factors that should consider for the selection of the right method of data collection. In recent years, traffic data acquirement can be carried out using technologies based on infrastructure and non-infrastructure-based techniques. There is much infrastructure-based traffic data collection such as induction loop, pneumatic road tubes, and piezoelectric sensors. These methods can help to collect traffic flow but cannot record the speed and location of vehicles. Unmanned Aerial Vehicles (UAV) also known as drones are taken into consideration the best dynamic and multi-dimensional technology of recent time traffic studies [1]. The main advantages of deploying UAV above ground-level infrastructure-based techniques also include possibility of recording naturalistic behavior of road users who are unaware of the measurement taking place, maneuverability, mobility, and broad field of view. [2]. The UAV equipped with high-definition cameras and sensors, which induces high installation and operation cost of video capturing and challenges involve in image processing to extract data causes difficulties to implement UAV in traffic research. Despite these, the reduced cost of UAV products, and extensive application of video analytics using computer vision techniques, UAVs are becoming the foremost tool in transportation safety, planning, engineering, and operations [3]. Real-time traffic data extraction is a difficult process for a UAV to accomplish not only due to the high complexity of Aerial images by flight height, distortion due to motion, angle, etc. Recent research studies exploring these problems, it can be addressed by the researchers with the advanced approaches of deep learning (DL) [4] and computer vision (CV) techniques. The following framework guides the organization of this paper: The vehicle detection from UAV recordings is discussed in Sect. 2. The assessment of traffic flow parameters from UAV video is described in Sect. 3. Spatio-temporal data extraction from UAV video data is detailed in Sect. 4. Conclusions are summarized in Sect. 5.

2 Vehicle Detection from UAV Videos

Vehicle detection is one of the most essential tasks for UAV-based traffic extraction. Various research being conducted in the field of vehicle detection, and different methods put forward to explore the most constructive way of imparting and analyzing traffic data acquired from UAV. Vehicle detection, vehicle reidentification, and effective vehicle classifications are the relative field of research attention on vehicle detection from UAV video [5]. This section organized about the existing studies involving UAV flight execution to capture video data, the current emerging trend

of Unmanned Aerial Vehicle (UAV)-based traffic analysis and various deep learning (DL) and computer vision (CV) technologies involved to detect vehicles from UAV videos.

2.1 UAV Flight Execution

UAV flight execution consists of detailed UAV flight preparation and implementation to acquire traffic data. Based on the literature, the intense and detailed flight planning should require base on the scope and the parameters involved in the project. The three major factors considered in UAV flight execution are safety (Fly zone, Safety Threshold, and Permit), environment (Weather, Wind, Location Characteristics, and Time), and flight path planning (Waypoints and Parameter Assignment). Evaluation of the flying zone of the study area through local flying zone map. The safe distance should maintain from sensitive installments and active airfields. Spatial and temporal planning of UAV flight is also important for flight execution [1]. The captured video should not be shaky during the flight implementation. To avoid the shaky and wobbly issue, UAV holds a gimbal which allows camera rotation in all the axis about single axis only. Ground control points [6] should visible in all the frames and to ensure accurate orientation and reduce inaccuracies in the picture geometry of each frame, the region of analysis was collected uniformly. Drones features like the material of the body, type of rotors, weight of the payload, battery power, maximum flight without payload, flight time, wind speed, operative temperature, GPS, drive mode (Manual/flight planning), and video quality (resolution, optical zoom, and frame rate) should be considered for the recording. Figure 1 shows the Sample Road Section Captured by UAV. Table 1 represents the summary of the features of the UAV Experimental process such as type of UAV, flying altitude, image resolution, frame rate, and road user class detection.

From the past studies, it is observed that DJI Phantom 4 Pro (4 K) is a widely used UAV product for video capturing. It is observed that the selection of UAVs flying altitude varies between a minimum of 50 m to a maximum of 150 m, and most of the studies preferred the flying altitude of UAVs about 100 m. Flight time varies between a minimum of 10 min to a maximum of 25 min depends on the battery capacity, flying altitude, and configuration of the drone capacity. Challenges involved in UAV-based traffic analysis are.

- Varying illumination condition (Weather condition, air pollution, and solar radiation) and background motion due to UAV movement (Wind, altitude, high mobility, etc.)
- Difficult to handle complicated scene (complex building layout, infrastructural alignment, etc.) and different traffic condition (free and congested)
- Multi-category vehicle detection and flying time restricted based on battery power
- Rules and regulations maintained by the government and automation installation to overcome crash happening due to loss of communication

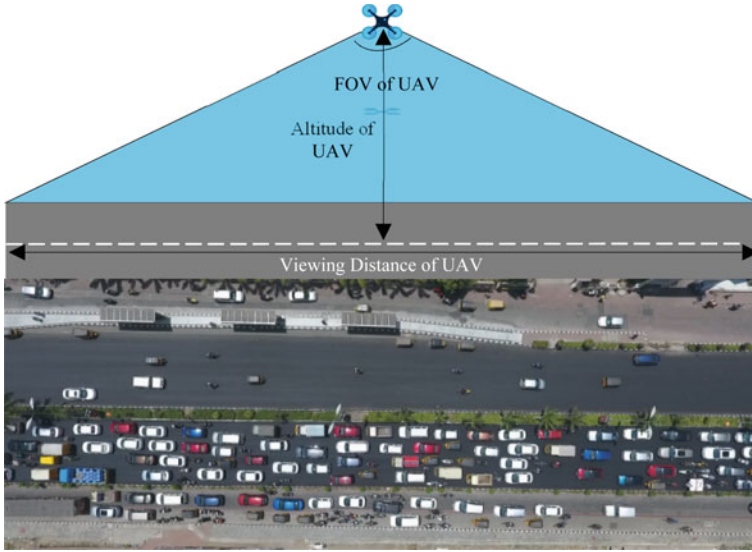


Fig. 1 Sample road section captured by UAV

- Real-time communication, location setup, high bandwidth, power consumption, mobility management, quality of service, and data security are all issues that need to be addressed.

2.2 DL and CV Technology in Vehicle Detection from UAV

Recently, deep learning (DL) and computer vision (CV) has been extensively researched in the area of vehicle detection for extracting traffic characteristics and road user behavior. Vehicle detection becomes the essential tools for solving complex vision related tasks for traffic scene understanding, vehicle identification, classification, and tracking. The static vehicle can be identified as the background wrongly due to the condition of fast-moving UAV camera, to avoid this the road detection is considered as a foundational step of static vehicle detection is road detection [23]. Hough transform is applied to identify the geometric shape of the road line in current frame. The number of training sample should arrange by Haar Cascade [24] training process. Region proposal effect consider for reducing the bounding box region. Convolutional neural network (CNN) with Haar Cascade proposed as the ensemble classifier for vehicle detection. Region-based convolutional neural network (RCNN) [12] helps to eliminate several regions in selective search methods. SVM classifier forecasts the vehicle presence within the region and identifies its class. Spatial pyramid pooling network (SPPNet) performs feature maps calculate only once from the image and avoid complex computation of its convolutional features. Faster region convolutional neural network (Faster RCNN) [3] performs simultaneously as detector and bounding

Table 1 Summary of UAV experimental process

Year	Reference	Type of UAV	Flying altitude	Image resolution (pixels)	Frame rate (frames per second)	Road user class of detection
2021	[7]	DJI Phantom 3 and 4 UAV	50 m	3269 × 720	20	Car and Bicycle
2020	[8]	MOR-UAV dataset	Different altitudes	1280 × 720 to 1920 × 1080	25	Cars and heavy vehicles
2019	[9]	DJI Phantom 2 quadcopter	100 m	1920 × 1080	30	Car, bus, truck, tanker, motor, and bicycle
2019	[5]	DJI Phantom 4 Pro (4 K)	100 m	4096 × 2160	25	Pedestrian, bicycle, car, truck, and bus
2019	[10]	Canon Eos 1Ds Mark III camera	60 m	5616 × 3744	25	Cars and Van
2019	[11]	DJI Matrice 100	100 m	1920 × 1080	50	Sedans, Jeeps, taxis, sport utility vehicles, and compact cars
2019	[12]	UAV drone with eight propellers	Different Altitude	1000 × 300	25	Cars
2019	[13]	DJI-MATRICE 100	80 m	1280 × 960	60	Cars
2019	[14]	DJI Phantom 4 Pro	60 to 150 m	2720 × 1530	30	Cars
2018	[15]	Phantom 4 Advanced	92 m	4096 × 2160	30	Cars
2018	[2]	Custom-built octocopter UAV with Panasonic Lumix GH4 DSLM camera	80 m	4 K	25	Cars
2017	[16]	DJI Phantom 2 quadcopter	100 m to 150 m	1920 × 1080	24	Cars
2017	[17]	UAV drone with eight propellers	-	4 K	23	Cars
2016	[18]	UAV drone with eight propellers	60 m (8 min)	1920 × 1080	23	Cars

(continued)

Table 1 (continued)

Year	Reference	Type of UAV	Flying altitude	Image resolution (pixels)	Frame rate (frames per second)	Road user class of detection
2016	[19]	Quadcopter, a camera mount,	100 m, 120 m & 150 m	1920 × 1080	30	Cars and Trucks
2015	[20]	GoPro Hero3 Black Edition mounted on a UAV	100 m	1920 × 980	30	Cars
2014	[21]	Cessna T210L Centurion II aircraft	2800 m	7216 × 5412	-	Cars
2012	[22]	Quad rotor helicopter equipped with a camera	100 m to 150 m	720 × 576	25	Cars

box regressor. Feature pyramid networks (FPN) follows top-down approach and has good improvement in detecting small objects. Mask R-CNN [4] is the extension of faster RCNN and it solve segmentation problem instantly. You Only Look Once (YOLO) [25–27]. It performs by splitting the entire images into small region, and it predicts the bounding box for each region and class probability. Single Shot Multi-Box Detector (SSD) [5, 19, 27]: It uses a single slot to detect multiple features from a single image. Table 2 represents summary of related works for recent methods for vehicle detection from UAV. Figure 2 represents the comparison of accuracy value of different vehicle detection algorithm.

The following Fig. 2 represents the visualization of the accuracy of various vehicle detection algorithms from the reviewed studies depends on number of training and testing datasets and UAV's flying altitude. From this visualization, it is observed that the YOLOv3 algorithm is outperforming other methods with more than 90 percentage accuracy with a smaller number of training and testing datasets as well as with the UAV's flying altitude of more than 60 and 100 m.

2.3 Vehicle Detection Using YOLOv3

According to the past studies, You Only Look Once (YOLOv3) third version is the foremost applied algorithm in the real-time vehicle detection. The convolution neural network [27] using only once in the complete image, and it predicts the bounding box of the class of vehicle ex, car, bus, two-wheeler, etc., depends the context of

Table 2 Summary of related works for recent methods for vehicle detection from UAV

Year	Reference	Datasets	Methods	Adaptation	Pros	Cons
2021	[26]	2288 training, 654 validation, and 327 test samples	YOLOv4	Detection, tracking and speed estimation with different flight height	Good performance under cars moving at high speed and in varying lighting conditions	Limited battery endurance and legislative restrictions
2020	[12]	MOR-UAV dataset (Training 3749 frames Testing 679 frames)	MOR-UAVnetv1 to MOR-UAVnetv4	Performance of diverse objects and camera movement	Moving object recognition (MOR) of large scaled dataset	Motion and rotation of vehicles and variable speed
2019	[5]	VOC dataset with 4344 images	SSD, RefineDet, and proposed ACM	Congested and non-congested conditions, intersections, and scenes, including vehicles with occluded, multi-angle, and illuminated	Effective performance of small-sized vehicles	Detection accuracy needs improvements to address vehicle occlusion
2019	[19]	18,450 samples	SSD	Detection model with light weight CN and GAN	Reduction of computational cost and accuracy improvement	Detection in short time and degree of distortion
2019	[27]	1000 samples	YOLOv3, Faster RCNN, and SSD	Long-time occlusion considered	Cost effective and high performance	Errors in geolocation
2019	[25]	–	YOLOv3	Multivehicle tracking approach	The reidentification method is resistant to occlusions that last fewer than 30 frames	Proposed tracking sensitive to vehicle colors, different lighting and different vehicle models

(continued)

Table 2 (continued)

Year	Reference	Datasets	Methods	Adaptation	Pros	Cons
2018	[28]	289 samples	Kalman filtering	Adjust the sampling time to build a more efficient system in computational resources	False alarm detection	Large number of targets with high maneuvering
2017	[3]	12,240 samples	Faster RCNN	Robust to illumination changing and cars in-plane rotation	Vehicle detection from both static and moving UAV platform	Lack of training sample for modes like buses, trucks, TW and bicycles

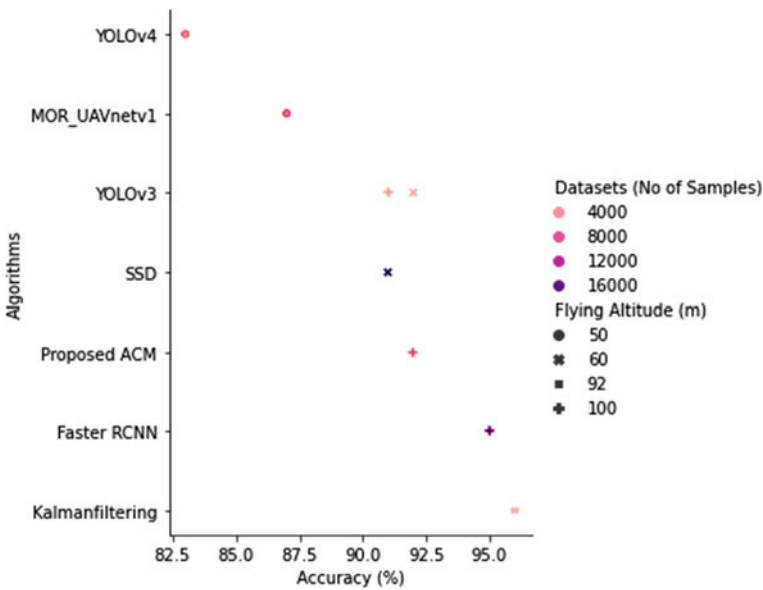


Fig. 2 Comparison of accuracy of different vehicle detection algorithm

each frame. Figure 3 shows the architecture of YOLOv3. Only one bounding box is applied in YOLOv3 in each ground truth vehicle class. YOLOv3[25] performs three time faster due to the adaptation of spatial features. To improve the accuracy of smaller vehicle detection scale variant is applied in the feature.

Figure 4 represents the road map of vehicle detection. The vehicle detection framework consists of two phases. The first phase involves the training before the model experiment and the second phase performs vehicle detection on board. The



Fig. 3 YOLOv3 architecture

compilation of aerial image data is the first step in vehicle detection. Before the experiment, these photos are preprocessed and trained, and they are all labeled. The labeled images are segregated for training, validation, and testing process. To train the model, YOLOv3 [25] is applied before the experiment. The second phase involves the detection of vehicles, initially the testing datasets are given as the input for initiating the testing process. From the input video, each frame is extracted. The automatic numbering performed in order to improve the confidence of detecting various vehicles from the video frame. The vehicle with highest confidence value is consider as the target of interest.

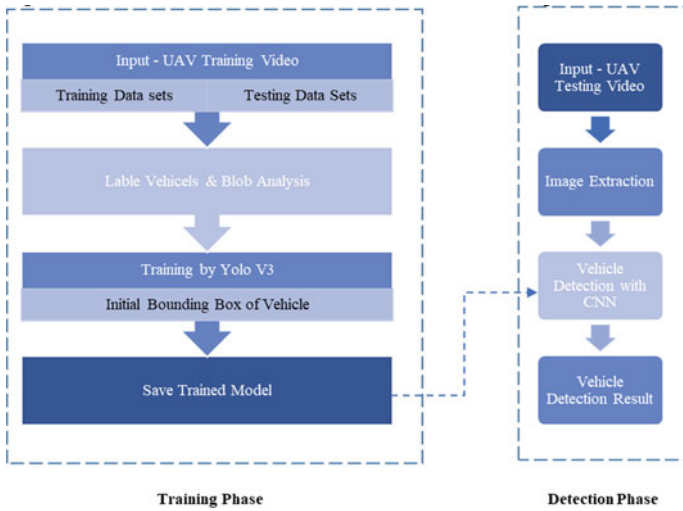


Fig. 4 Vehicle detection from UAV road map

3 Traffic Parameter Estimation from UAV Videos

UAV video data has been gathered, and traffic parameters such as speed, acceleration, flow, density, and population have been determined and updated based on the information. The development of traffic and road user features encourages the duplication of the traffic model, which will make it much easier to illustrate traffic conditions later. The proportion of vehicles turning proportions through crossing points, queue, and delay parameters can be determined by detecting successive vehicles. At the distinctive sites of the observed area, location-based characteristics such as traffic flow rate, time mean speed, and time headways and gaps can be estimated. Table 3 represents the summary of related works of estimation of traffic flow parameters using UAVs.

Challenges of UAV-based vehicle tracking in mixed traffic conditions.

- Challenges in preparation of dataset attributes contains object density variability, small size of objects, various classification of vehicles, complicated background, and field of view (FOV) variation. Due to the distance between UAV and vehicles, the size of the target vehicles is small.
- Variation in appearance of objects is multi-scale due to variation of UAV's flying altitude
- Vehicle path detection among all moving objects and vehicles for similar types of vehicles is difficult.
- Probability of errors in detection due to vehicle intensities are close to the road intensities especially at intersection, roundabouts, etc.
- Vehicle position transformation in UAV frames creates incorrect identity switches of vehicle detection as well as develop lack of efficient tracking of same vehicle throughout the video frame.
- Appearance changes of same vehicles in the UAV video will be severe depend on the different maneuvering behavior in non-lane-based condition
- Reidentification of tracking same vehicles along the consecutive video frames, multiple videos captured from different cameras.

Advantages of UAV-based vehicle tracking in mixed traffic conditions.

- The preservation of naturalistic driver behavior for heterogeneous of traffic condition
- The availability, response time, and cost of UAV promotes the real-time extraction of information
- Identification of real-time non-lane-based vehicle maneuvering behavior and potential conflicts
- Possibility of high-quality datasets can be developed and applied for real-time dynamic simulation models for traffic analysis and forecasting.

Table 3 Summary of related works of estimation of traffic flow parameters using UAVs

Year	Reference	Methods	Traffic flow parameters	Traffic condition	Accuracy	Constraints
2021	[11]	Shi-Tomasi features, Motion vector clustering algorithm, and Kanade-Lucas optical flow algorithm	Traffic Count, Speed, Density and Volume Bi-Directional Traffic Flow	Free and moderately congested	96% Speed 87% Count	Investigate to improve accuracy for estimation of large vehicles
2019	[16]	Haar Cascade Classifier for Region Proposal, Convolutional Neural Network for Vehicle Detection and KLT-Based Motion Estimation	Traffic Count, Speed, Density and Volume	Free flow and congested	97% Speed 95.8% Count	Multi Group Vehicle Classification, Longer Monitoring with low Quality Video, Different Heights
2019	[15]	YOLOv3, Motion compensation by Homograph Matrix, speed estimation algorithm	Traffic speed	Free	measurement speed was about 0.5 m/s	Using statistical information about the bounding box size to estimate the pixel scale isn't particularly precise
2018	[1]	Vehicle Detection and Tracking, Trajectories Management, Pre-processing, Video stabilization and Geo-Registration, Vehicle Detection and Tracking	Traffic Count, Speed, Density and Volume, TS-Diagram, Shockwave Characteristics, Signal Cycle Length and Queue Length	Free	94.15%	Trajectory Noise from partial occlusions, shadows, close proximity objects, and erroneous detections
2017	[29]	Removal of fish-eye effect, Frames Extraction and Georeferencing (Quantum GIS)	Hourly OD Matrix, Driving Style—Aggressive, neutral and cautious	Free flow	-	Climate factors, physical obstructions instrumental factors and legal factors

4 Spatio-Temporal Data Extractions from UAV Video

Preparing a vehicle trajectory dataset using a UAV entail utilizing a computer vision system to accurately detect, track, and classify all road users. Requirement of trajectory datasets protect the naturalistic behavior of road user, adequate size, multiple recording locations and times, identification and tracking all type of road users, high accuracy of road user tracking, and inclusion of different infrastructure layout. The overlapping of each UAV based on the area of visibility allow to properly synchronize the videos and reidentifying vehicles from one drone to other depends on the vehicle type, color, time stamp, spatial information, etc. [30]. Vehicle detection and track association generated based on strong and weak vehicle classifiers from geocoded frames. Track updates carried based on infra independent Bayesian bootstrap particle filter, and it performs based on transition density. Track termination employed based on target leaves the area, time steps and overlapping with another target [20].

Feature-based tracking method is applied in the practice to solve the problem of motion, stereo, and tracking. These features gathered based on spatial proximity or similar motion pattern [21]. Contour-based approaches performing better on detection and produce more consistent results in tracking of vehicles rely on its contour and motion. This approach dynamically updates to fit the targeted vehicle outline. OpenCV background extraction, contour detection algorithm used to train the model by Mask RCNN with the datasets. Lane identification algorithm help to generate the lane numbers. Vehicle trajectories with lane numbers are developed and vehicle tracked based in kinematic constraints using Mask RCNN [4]. The objective of motion-based tracker is to extract the trajectories over time by locating their positions. This method associated with assigning identification ID for extracting trajectories using Kalmen filter [17] and detect vehicles across the frames to reduce assignment problem. Two consecutive frames were matched based on their distance, following that postprocessing have done to smooth the vehicle positions, speed, and acceleration using Bayesian smoothing [2] and constant acceleration model. Optical track flow algorithms involve with direction and speed of moving pixels and Lucas-Kanade optical flow algorithm [1] tracked the corner points of the features throughout the video. Computer vision algorithms applied to trajectory extraction of multiple vehicles and time space diagrams of platoons fabricated.

Trajectory classification based on the location of vehicles in each frame and speed judgements [24] works to estimate the true trajectory movement. Trajectory compensation applied to correlate the broken trajectories and created the complete trajectories. Empirical mode functions used to correct the nonlinear and non-stable trajectories. Yolov2 [31] performs high for vehicle detection and tracking and Kalman filter applied to remove the tracking errors. Optimal bounding box determination employed to reduce the positional error and geometric displacement of the camera. Levenberg–Marquardt optimization method [32] used by OpenCV is about 500 times faster in detection. Kernelized correlation filter (KCF) [33] implemented to track the vehicle fast and accurately and Wavelet transformation denoising algorithm performed at

the end on outliers position removal and abnormal oscillations in raw vehicle trajectories. Predefined scale line used to generate Spatial–temporal map [34], this can be achieved by frame by frame stacking of the pixel value, illustrate the time progression of groups of pixels from moving vehicles. Pixel trajectories generated using these groups of moving strands. Table 4 represents the summary of existing road user trajectory datasets comparison.

Advantages of existing road user trajectory datasets.

- The datasets are spread open and freely available to the research community
- Helps to develop new behavioral algorithm and encouraging for the improvisation of existing algorithm
- Time and cost saving and large multiclass datasets availability
- The trajectories data are fully annotated with their target ID
- High quality naturalistic behavior of different road users preserved in static and dynamic conditions.

Disadvantages of existing road user trajectory datasets.

- Few datasets are required hand annotation requires script writing to convert the annotated.
- Required coding tools to handle and to create the visualization and extract maneuvers provided
- High dimensional datasets tend to be unstructured may contains with noise and uncertainties
- Raw datasets consist of false positive trajectory values and illogical speed of vehicles and accelerations in this case manual re-extraction required for improvising trajectories.

5 Conclusions

In this paper, the substantial systematic review of versatile application of UAV in the area of traffic studies for real-time data extraction. This review provides the wide selection of implemented prototype with a UAV, an onboard camera aided by the video and different data processing algorithms and its own applications. The video processing includes different stages of vehicle detection and tracking by using various deep learning and computer vision algorithms. The detailed and accurate Spatio-temporal details can be collected beyond the range of sensors by combining the UAV and video processing technology. The researchers accumulating high-resolution trajectory data for investigating fundamental laws influencing traffic flow which involves immense quantity and quality of traffic flow studies. Deep learning and computer vision-based vehicle detection technology is developing extensively day by day in the field of traffic engineering due to evolving computational power. The deployment of DL-based detectors is urgently needed for the implementation of self-driving cars, high precision, real-time adaptive traffic management systems. Finally, the promising future direction in this research filed are not limited to before mentioned

Table 4 Summary of existing road user trajectory datasets comparison

Title of data set	Location	No. of trajectories	No of locations	Road user type	Method of annotation	Flying and recording details	Coding tools and methods used
NGSIM [35] (2009)	Highways	-	5	Cars	Cameras installed on Multi-story Building	97 m and 154 m (45 min)	Customized software application developed for the NGSIM program
Ko-PEP [8] (2014)	Urban intersection	350	1	Pedestrian, bicycle car, and Truck	Sensor	Laser scanners and eight monochrome CCD cameras	MATLAB
KITTI - 360 [36] (2013)	Mid-size city of Karlsruhe, in rural areas and on highways	-	-	Car, Van, Truck, Cyclist, Pedestrian, Tram and Misc	Velodyne laser scanner & a GPS localization system	Dataset consists of 320 k images and 100 k laser scans in a driving distance of 73.7 km	C++/MATLAB code
Stanford Drone [37] (2016)	Stanford Campus	10,240	8	Bicyclists, Skateboarders, Cars, Buses, and Golf Carts	Drone	Approx. 80 m	Deep learning algorithms (MTT)
HighD [9] (2018)	German highways around Cologne	110 000	6	Cars and Trucks	Drone	60 recordings with an average length of 17 min covering a road segment of 420 m length	MATLAB and Python

(continued)

Table 4 (continued)

Title of data set	Location	No. of trajectories	No of locations	Road user type	Method of annotation	Flying and recording details	Coding tools and methods used
inD [14] (2019)	Urban intersection	11,500	4	Pedestrian, Bicycle, Car, Truck bus	Drone	100 m 20–22 min	Faster- RCNN
DUT [38] (2019)	DUT campus	1793	2	Pedestrian, Vehicle	Drone	–	SIFT, RANSAC, k-NN
p-NEUMA [39] (2020)	Road network low, medium, and high-volume arterials	More than 0.5 million trajectories	total of 1.3 km ² area a 100 km lanes of road network,	Cars, Powered two wheelers, Taxis, Buses, Medium and heavy vehicles	Drone	Five flight sessions for 2.5 h per day each flight approx. 25 min	Deep learning algorithms

aspects, and also the research when it comes to application of UAV in the field of traffic engineering data extraction is still definitely not complete.

References

1. Khan MA et al (2018) Unmanned aerial vehicle-based traffic analysis: a case study for shock-wave identification and flow parameters estimation at signalized intersections. *J Remote Sens* 1–16
2. Bock J et al (2019) The inD Dataset: a drone dataset of naturalistic road user trajectories at German intersections, computer vision and pattern recognition, Cornell University
3. Xu Y et al (2017) Car detection from low-altitude UAV imagery with the faster R-CNN. *Hindawi J Adv Transp* 1–10
4. Murthy CB et al (2020) Investigations of object detection in images/videos using various deep learning techniques and embedded platforms—a comprehensive review. *Appl Sci MDPI*, 1–46
5. Yang J et al (2019) Effective contexts for UAV vehicle detection. *IEEE Access Special Sect AI-driven Big Data Process: Theory Methodol Appl* 7:85042–85054
6. Khan MA et al (2017) Unmanned aerial vehicle-based traffic analysis methodological framework for automated multivehicle trajectory extraction, transportation research record. *J Transp Res Board* 25–33
7. Wang L et al (2016) Detecting and tracking vehicles in traffic by unmanned aerial vehicles. *Autom Construct* 1–15
8. Ko-PER Intersection Dataset <https://www.uni-ulm.de/in/mrm/forschung/%20datensaeetze.html>. Last accessed 22 May 2021
9. High-D Datasets <https://www.highd-dataset.com/format>. Last accessed 02 Jun 2021
10. Yu H et al (2019) The unmanned aerial vehicle benchmark: object detection, tracking and baseline. *Int J Comput Vision*, Springer, 1–19
11. Ke R et al (2020) Advanced framework for microscopic and lane-level macroscopic traffic parameters estimation from UAV video. *J Inst Eng Technol IET Intell Transp Syst* 14:724–734
12. Mandal M et al (2020) MOR-UAV: a benchmark dataset and baselines for moving object recognition in UAV videos. *Proceedings of the 28th ACM international conference on multimedia*, pp 2626–2635
13. Brkić I et al (2020) An analytical framework for accurate traffic flow parameter calculation from UAV aerial videos. *J Remote Sens* 1–20
14. inD Datasets <https://github.com/ika-rwthachen/inD-dataset>. Last accessed 22 May 2021
15. Li J et al (2019) An adaptive framework for multi-vehicle ground speed estimation in airborne videos. *J Remote Sens* 1–28
16. Ke R et al (2019) Real-time traffic flow parameter estimation from UAV video based on ensemble classifier and optical flow. *IEEE Trans Intell Transp Syst* 20:54–64
17. Kim EJ et al (2019) Extracting vehicle trajectories using unmanned aerial vehicles in congested traffic conditions. *Hindawi. J Adv Transp* 1–16
18. Eplex Homepage, <https://eplex.cs.ucf.edu/toyota/trajectory-data-dictionary.html>. Last accessed 21 May 2021
19. Shen J et al (2019) Vehicle detection in aerial images based on lightweight deep convolutional network and generative adversarial network. *IEEE Access* 7:148119–148130
20. Babinec A (2015) Automatic vehicle trajectory extraction from aerial video data, excel FIT, student conference of innovation, technology and science in IT, Brno University of Technology, pp 1–8
21. Azevedo CL et al (2014) Automatic vehicle trajectory extraction by aerial remote sensing. *Procedia—Soc Behav Sci Sci Direct*, 849–858
22. Ke R et al (2017) Real-time bidirectional traffic flow parameter estimation from aerial videos. *IEEE Trans Intell Transp Syst* 18:890–901

23. Yang Y et al (2012) Vehicle detection methods from an unmanned aerial vehicle platform. *IEEE international conference on vehicular electronics and safety* 411–415
24. Feng R et al (2020) Mixed road user trajectory extraction from moving aerial videos based on convolution neural network detection. *IEEE Access* 8:43508–43519
25. Wang J et al (2019) Orientation- and scale-invariant multi-vehicle detection and tracking from unmanned aerial videos. *J Remote Sens* 1–23
26. Balamuralidhar N et al (2021) MultEYE: monitoring system for real-time vehicle detection, tracking and speed estimation from UAV imagery on edge-computing platforms. *Remote Sens* 1–2
27. Zhao X et al (2019) Detection, tracking, and geolocation of moving vehicle from UAV using monocular camera. *IEEE Access* 7:101160–101170
28. Lee M-H et al (2018) Detection and tracking of multiple moving vehicles with a UAV. *Int J Fuzzy Logic Intell Syst* 18:182–189
29. Salvo G et al (2017) Traffic data acquirement by unmanned aerial vehicle. *Euro J Remote Sens Taylor and Francis* 50:343–351
30. Barmponakis E et al (2019) On the new era of urban traffic monitoring with massive drone data: the pNEUMA large-scale field experiment. *Transp Res Part C*, 50–71
31. Seong S et al (2019) Determination of vehicle trajectory through optimization of vehicle bounding boxes using a convolutional neural network. *J Sens* 1–18
32. Kaufmann S et al (2017) Aerial observations of moving synchronized flow patterns in over-saturated city traffic. *Transp Res Part C Sci Direct*, 393–406
33. Chen X et al (2020) High-resolution vehicle trajectory extraction and denoising from aerial videos. *IEEE Trans Intell Transp Syst* 1–13
34. Zhang T et al (2019) A longitudinal scanline-based vehicle trajectory reconstruction method for high-angle traffic video. *Transp Res Part C Sci Direct* 104–128
35. NGSIM Dataset <https://catalog.data.gov/th/dataset/next-generation-simulation-ngsim-vehicle-trajectories>. Last accessed 20 May 2021
36. KITTI Data set http://www.cvlibs.net/datasets/kitti/raw_data.php. Last accessed 22 May 2021
37. Stanford Drone Datasets https://cvgl.stanford.edu/projects/uav_data/. Last accessed 22 May 2021
38. DUT Dataset <https://github.com/dongfang-steven-yang/vci-dataset-dut>. Last accessed 02 Jun 2021
39. pNEUMA Dataset <https://open-traffic.epfl.ch/index.php/downloads/>. Last accessed 02 Jun 2021
40. Zhao D et al (2019) Real-world trajectory extraction from aerial videos—a comprehensive and effective solution. *IEEE intelligent transportation systems conference (ITSC)*, pp 2854–2859
41. Guido G et al (2016) Evaluating the accuracy of vehicle tracking data obtained from Unmanned Aerial Vehicles. *Int J Transp Sci Technol* 5:136–151
42. Niu H et al (2018) A UAV-based traffic monitoring system. *IEEE Access* 1–5
43. Hossain M et al (2019) A UAV-based traffic monitoring system for smart cities. *International conference on sustainable technologies for industry 4.0 (STI)*, IEEE
44. Wan Q et al (2020) Spatiotemporal trajectory characteristic analysis for traffic state transition prediction near expressway merge bottleneck. *Transp Res Part C, Sci Direct*, 1–24
45. Ke R et al (2015) Motion-vector clustering for traffic speed detection from UAV video. *IEEE Access*

Analysis of Effect of Crossing Pedestrians on Traffic Characteristics at Urban Midblock Sections Using Support Vector Regression



Sreechitra, Yogeshwar V. Navandar, Hareshkumar D. Golakiya,
and M. V. L. R. Anjaneyulu

Abstract Walking is a commonly used movement mode, and the transport mode is denoted by the term pedestrian. Walking is an unavoidable part of almost all kind of trips especially when using public transport services such as trains and buses. Usually, pedestrians need to cross the road in order to access various residential and commercial lands for many purposes. However, many developing countries, such as India, lack suitable pedestrian crossing infrastructure. As a result, pedestrians must coexist with motor activity on the roadway. These facilities are available at a few areas, however, pedestrians are unwilling to utilize them and prefer to cross the road at their own convenience. These crossings are illegal. As previously mentioned, unlawful pedestrian crossings are fairly widespread in many nations. This study is looking into the analysis of the impact of such undesignated crossings on the speed and other traffic characteristics at various urban midblock sections in India with the use of an effective machine learning algorithm, support vector regression (SVR). When there is a large amount of data available and the variability in the data is significantly high, conventional modeling techniques fail to handle them. In that case, data-driven approaches show superior performance over other techniques. So, the prediction of speeds using SVR by considering the effects of pedestrian crossing is considered in this study, and the results are compared with results from traditional techniques. Results show that SVR outperforms the traditional models.

Keywords Pedestrian crossing · Urban midblock sections · Speed and capacity · Support vector regression

Sreechitra · Y. V. Navandar (✉)
National Institute of Technology Calicut, Calicut, India
e-mail: navandar@nitc.ac.in

H. D. Golakiya
Dr. S. and S. S. Gandhi Government College of Engineering, Surat, India

M. V. L. R. Anjaneyulu
Department of Civil Engineering, National Institute of Technology Calicut, Calicut, India
e-mail: mvlr@nitc.ac.in

1 Introduction

Vehicular traffic is highly heterogeneous in nature, especially in countries where traffic is increasing on a daily basis, with a diverse spectrum of static and dynamic traffic characteristics. Furthermore, automobiles are not lane-disciplined and may occupy any available road area. In many developing countries, such a complex scenario is a major concern. There are also numerous friction elements like as vehicles that are not motorized, bus shelters, pedestrians who uses the carriageway, stopped vehicles, parked vehicles, various commercial and business activities, bays for buses, and so on, all of these add to the complexity. Pedestrian on the road is an unavoidable component of the urban and rural transportation system and will continue to be one of the most important modes of mobility in the cities. As a result, numerous pedestrian facilities are required. However, as previously indicated, in many countries, pedestrian facilities are insufficient. Pedestrians cross the road for a variety of purposes, including access to residential and commercial land uses in areas where there are no crossing signs or markings provided. Pedestrians, on the other hand, interact with traffic flow during such crossings, prompting vehicle drivers to change their courses or slowdown in order to avoid colliding with pedestrians, resulting in a reduction in vehicle speed. As a result, it is critical to examine such portions. Such sections are called non-base sections, and the sections which are not affected by any friction factors including pedestrian crossings are termed as base sections. Technology advancements have recently impacted every field throughout the world, and data-driven approaches, one of the most efficient and rising technologies, have shown various uses in the transportation field as well. The application of various data-driven algorithms to the previously stated traffic scenario could be a potential study topic for predicting and analyzing traffic speeds and capacity.

2 Literature Review

Speed has been modeled using traditional modeling methodologies that take into account density-speed relationships. The composition and flow of vehicles determine the speed of urban arterials. At non-base sections, pedestrian crossflow is a critical parameter that may be defined as the pedestrian-vehicle interaction factor, along with the vehicular flow and composition.

Pedestrian safety can be assessed using variety of ways, and the interaction between vehicles and pedestrians is studied using a variety of methodologies such as by considering time-to-collision and post encroachment time [1]. When employing a latent variable approach to analyze pedestrian crossing behavior in metropolitan roads, it was discovered that the greater distance reduces the likelihood of the individual choosing safer choices [2]. The previous studies on crossing pedestrians have also determined that pedestrian crossings have an impact on speed and capacity of traffic flow using conventional mathematical models [3]. There are also studies

which considered age and gender effect of pedestrians on the activity of crossing at midblock sections in India and they conclude that male waiting times are around half that of females, and males are involved in nearly twice as many automobile collisions as females [4]. The results of the study for finding out the safe distance (SD) for pedestrians at urban midblock sections using trajectory plots show that when SD is 1.75 m for VPF and 19 m for PPF, where VPF and PPF stand for vehicle-pass-first criteria and pedestrians-pass-first criteria, respectively, the pedestrian will be at higher risk [5]. Some researchers have also developed models for the crossing behavior and accident risk of pedestrians along urban trips by developing an algorithm [6]. Some authors conducted research on the impact of pedestrians while crossing a road on the capacity of that urban road using three different pedestrian crossing approaches to effectively relieve conflict between pedestrians and motor vehicles, make sure persons crossing the street are safe, and improve the capacity of urban roads: Freely crossing, uncontrolled crossing, and regulated crossing are all examples of how to cross the street. It produces the empirical mathematical model after establishing the basic formula for road capacity during pedestrians crossing, based on some pre assumptions and survey data [7]. A study looked into the influence of pedestrian crossing designs and various other features on accident circumstances at signalized intersections on major public transport routes of urban regions. To identify factors that impact accidents and compare accident numbers at those junctions to reference locations, various statistical and analytical tests were performed, and stepwise regression models were developed [8].

Today's technology advancements have greatly improved the ability to collect traffic statistics. Most of the traditional models are based on mathematical formulas and traffic flow theories, which makes them often more restricted. Nevertheless, data-driven approaches are more versatile, and they can incorporate additional data also; but, sometimes, traditional models may provide more insight into traffic flow theory, but they may not. Data-driven techniques have a wide range of applications in transportation field, and numerous studies have been conducted in this area. The application of data-driven techniques into the car following models is one among them [9]. In their study, they provide a novel methodological framework for estimating car following models that is suitable for the inclusion into microscopic traffic simulation models, based on a data-driven technique. A comprehensive framework for data-driven model estimation is provided by some researchers. In a novel fashion, computational procedures including clustering, classification, and regression techniques are used, and model components are also investigated as part of their studies [10]. In urban signaled traffic flow forecasting, studies of the potentialities of data-driven techniques such as data-driven nonparametric regression are conducted [11]. In addition, the simulation procedure was carried out utilizing both theoretical models and data-driven methodologies [12]. There are studies done regarding the application of support vector machines such as for evaluation of snowplow truck performance and relevance of features [13].

The in-depth literature review demonstrates that only a small number of pedestrian studies have been conducted, as well as the use of data-driven techniques in pedestrian research field. The main goal of this research is to examine if support

vector regression, a promising data-driven technique, can be used to study the influence of pedestrian crossings and vehicular volume on vehicle speed, as well as to predict vehicle speed by adding these variables.

3 Research Methodology

The speed, density, and flow of a traffic stream are all key factors in traffic management. Traffic safety, comfort, service level, road geometry, and other environmental elements are all influenced by speed. All of these parameters, however, remain unchanged at the time of data collection. Depending on vehicle and driver attributes, each vehicle can normally go at its preferred speed smoothly when traffic volume and density are low. This is the free flow speed of each type of vehicle. Because of the relative interaction between vehicles, as the number of automobiles on the road grows, the vehicle's speed tends to slow down. When pedestrian crossflow aggravates such situations, the speed of each vehicle category diminishes as a result of the interaction between vehicles and pedestrians. The goal of this research is to examine this circumstance using a popular data-driven approach called support vector regression (SVR). Python, a high-level interpreted general-purpose programming language, is used for the study. Python is useful for dealing with large amounts of data and has a fast-computing speed. The results of this research are then compared to traditional mathematical models constructed using the linear regression methodology [3], using various goodness-of-fit criteria including mean absolute percentage error (MAPE) and root mean square error (RMSE). Furthermore, the speed of each category of vehicle at each of the non-base sections is compared to the speed of the same type of vehicle at the selected base section to investigate the influence of crossing pedestrians on vehicle speed using statistical measures such as mean speed.

4 Selection of Site

The videographic technique is used to collect the data. The data for this study came from a variety of six-lane divided highways with 3.5 m lane width each, three of which were non-base sections with pedestrian crossing effects and one of which was a base section with no friction factors, all of which had identical geometric and environmental characteristics. Surat, Baroda, and Noida are the three non-base sections considered in this study, whereas the base section is the section from Udhana. Figure 1 represents the approximate location of all the study locations in India.

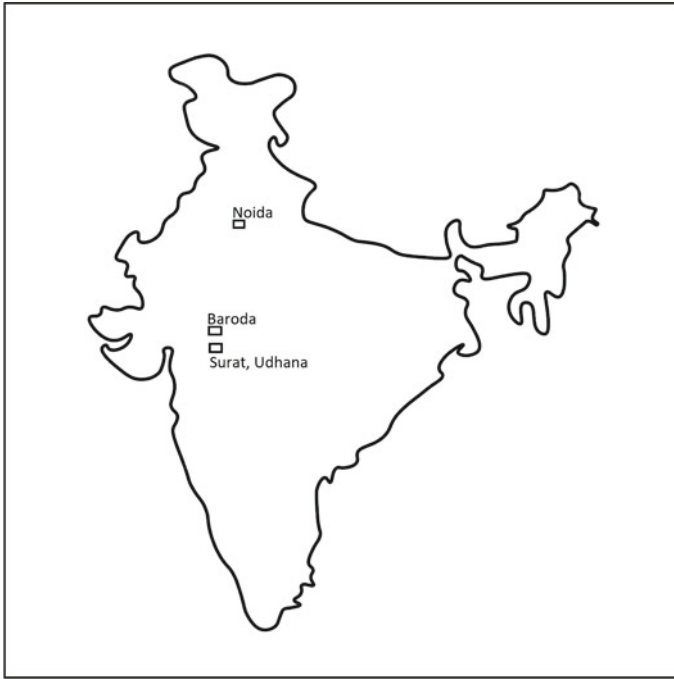


Fig. 1 Location of study sections

5 Data Collection and Extraction

Video cameras set on stands and placed at observation locations throughout the whole length of the traps were used to collect data (From 6:00 AM to 6:00 PM). In the midst of the chosen 500 m stretch of midblock section, a 60 m longitudinal trap is designated to obtain traffic characteristics such as speed and flow. Using the Avidemux 2.6 software, the extracted video is presented on a large monitor. Figure 2 depicts a screen shot of the Avidemux 2.6 working interface. This software allows the video to play in 25 frames with 40 ms of accuracy. The entry and exit times are recorded when the vehicle enters the 60 m stretch, and the difference between them gives the total time taken by each vehicle to cross the 60 m section. Each vehicle's speed is calculated using this value. Figure 2 shows an example of the selected location from Surat (non-base section). The section marked between the blue lines in the figure represents the selected 60 m stretch of road considered for the study. The total number of vehicles passing through the segment is divided into five groups: two-wheelers (2 W), three-wheelers (3 W), small cars (SC), big cars (BC), and heavy vehicles (HV). Table 1 displays the vehicle categorization criterion, as well as the average dimensions and plan area of various vehicle classifications.

The speed of every vehicle category is calculated over a one-minute timeframe. For these 1 min intervals, the number of each category of vehicle is also determined.



Fig. 2 Example of non-base section (Surat)

Table 1 Types of vehicles with physical dimensions

Vehicle type	Vehicles included	Dimensions		Plan area (m ²)
		Breadth (m)	Length (m)	
Two-wheeler	Motorcycle, scooter	1.87	0.64	1.19
Three-wheeler	Auto-rikshaw	3.20	1.40	4.48
Small car	Standard car (<1400 cc)	3.72	1.44	5.35
Big car	Big utility vehicle (>1400 cc, <2500 cc)	4.58	1.77	8.10
Heavy vehicle	Standard bus, heavy goods vehicle	10.10	2.43	24.54

To avoid large data fluctuation, these values are subsequently transformed to 5 min intervals. Similarly, for each 1 min interval, the total number of pedestrian crossings is recorded. The weighted average of the available observations was used to convert this value to a 5 min period. The average breakdown of traffic at the selected locations is shown in Table 2. The 5 min flow rate varies greatly depending on the vehicle composition. The average pedestrian crossflow per hour (PPH) and traffic volume (veh/hr), on the other hand, are also seen in Table 2.

Table 2 Composition of vehicles and other characteristics

Section number	Section type	2 W (%)	3 W (%)	SC (%)	BC (%)	HV (%)	PPH	Traffic volume (pph)
Udhana	base	32	28	26	8	6	–	4182
Surat	Non-base	53	35	9	1	2	408	2028
Baroda	Non-base	46	11	36	6	1	300	4104
Noida	Non-base	34	21	33	8	4	840	2544

6 Support Vector Regression

In transportation studies, data has become increasingly crucial. Unfortunately, conventional traffic models are not data driven and hence fundamentally incapable of assessing modern traffic data from many sources with varying time resolution and spatial coverage, despite having been developed and used for decades. To acquire fresh insights into traffic dynamics, accurate traffic forecasts, and effective traffic control, a new paradigm based on data-driven theories that can fully exploit and harness traffic data is required. In this study, SVR, a promising data-driven approach, is utilized to estimate speeds. Support vector machines (SVMs) are a machine learning approach that is still relatively young. SVMs were created to handle classification problems, and they offer appealing theoretical and practical qualities for this purpose. After that, the SVM technology was applied to problems like regression (function approximation) and density estimation. There are various flexible regression algorithms for use in the data-driven techniques available for speed estimates, including locally weighted regression (LOESS), support vector regression (SVR), Gaussian processes (GP), and others. The basic principle behind support vector regression is to draw a tube around the fitted regression curve of a specified radius and assume that the error is zero if the observations are contained within this tube (Fig. 3). X and Y axes in Fig. 3 correspond to datasets (X, Y) used for regression. Other observations could be penalized by an inaccuracy equal to their distance from the tube, or its square. The boundary curves in Fig. 3 are called decision boundaries. The central curve which is the best fit line also called hyperplane in higher dimensions has maximum number of points. So, the decision boundaries are drawn at a distance of ϵ from the hyperplane.

Consider the equation of the hyperplane is as follows:

$$Y = WX + b \tag{1}$$

Then, the equation of decision boundaries becomes:

$$WX + b = +\epsilon \tag{2}$$

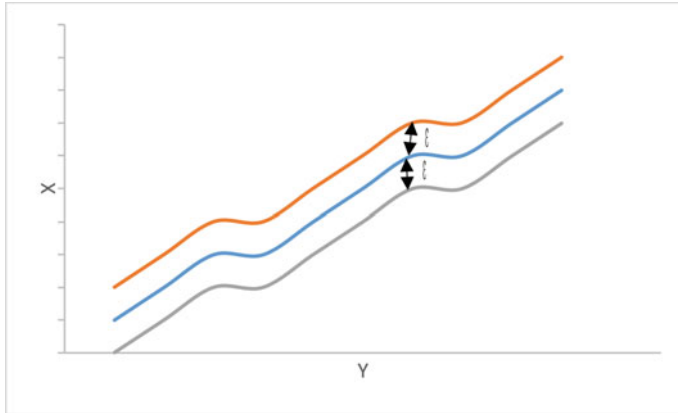


Fig. 3 Support vector regression

$$WX + b = -\varepsilon \tag{3}$$

As a result, every hyperplane that fulfills the SVR must satisfy the following conditions:

$$-\varepsilon < Y - (WX + b) < +\varepsilon$$

The main goal is to select a decision boundary that is ε distance from the original hyperplane and contains data points or support vectors that are closest to the hyperplane. As a result, points that fall within the decision boundary and have the lowest error rate, or those that fall within the margin of tolerance only are considered. This results in a more accurate model. Support vectors are points outside the tube that help support the tube’s structure or creation. These feature vectors were given the label support vectors because they intuitively support the separating hyperplane, or because they serve the same function for the separating hyperplane as pillars do for a building.

The decision boundaries must be found or placed correctly in support vector regression. There are some kernel functions that can help with this. In summary, the kernel method allows us to translate data into higher dimensions in a more efficient and less expensive manner. To establish the decision boundary, the kernel function is used to split the dataset. Without computing the coordinates of the data in a higher dimensional space, it is possible to build decision boundaries without traveling into higher dimensional space. Because they compute the dot product of two vectors x and y in a high-dimensional feature space, kernel functions are often referred to as generalized dot products. The optimization function for SVR is as follows:

$$\begin{aligned}
 & \text{Maximize, } \sum_{i=1}^n \alpha_i - \frac{1}{2} \sum_{i=1}^n \sum_{j=1}^n \alpha_i \alpha_j y_i y_j K(x_i^T \cdot x_j) \\
 & \text{Subject to } 0 \leq \alpha_i \leq C \text{ for all } i = 1, 2, \dots, n \text{ and} \\
 & \sum_{i=1}^n \alpha_i y_i = 0
 \end{aligned} \tag{4}$$

α_i is the vector of n variables, where n is the number of training samples. Each component α_i is a training sample (x_i, y_i) . $K(x_i, x_j)$ is the kernel function which is used as a measure of similarity between objects x_i and x_j , and C is an upper restriction on α_i .

Using the kernel function simply means using the it to replace the dot product of two vectors. There are various types of kernels available to use in SVR, but radial basis function (RBF) kernel is used in this study because it is a general-purpose kernel that can be utilized in situations when no prior data knowledge is required. The RBF kernel format is seen in the equation below.

$$K(x_i - x_j) = \exp\left(-\gamma \|x_i - x_j\|^2\right) \tag{5}$$

The parameter γ specifies how much a single training example has. The greater it is, the closer other examples must be to be affected.

7 Results and Discussion

The dataset was subjected to support vector regression in order to determine the effects of vehicle volume and crossflow of pedestrians on the speed of all categories of vehicle. SVR is used to predict vehicle category speeds at three different non-base sections: Surat, Baroda, and Noida by incorporating density of vehicles and pedestrian crossflow as explanatory variables. The results are compared to the findings obtained from the mathematical models developed by Golakiya and Dhamania, 2019, using RMSE and MAPE values against field data. The mathematical models developed by Golakiya and Dhamania are written by Eqs. 6–10.

$$\begin{aligned}
 V_{2W} = & 16.35 - 68.54 \left(\frac{n_{2W}}{V_{2W}}\right) - 28.36 \left(\frac{n_{3W}}{V_{3W}}\right) - 24.53 \left(\frac{n_{SC}}{V_{SC}}\right) \\
 & - 49.42 \left(\frac{n_{BC}}{V_{BC}}\right) - 38.56 \left(\frac{n_{HV}}{V_{HV}}\right) - 28.24 \left(\frac{n_{ped}}{V_{2W}}\right)
 \end{aligned} \tag{6}$$

$$\begin{aligned}
 V_{3W} = & 13.92 - 45.61 \left(\frac{n_{2W}}{V_{2W}}\right) - 59.11 \left(\frac{n_{3W}}{V_{3W}}\right) - 28.48 \left(\frac{n_{SC}}{V_{SC}}\right) \\
 & - 16.92 \left(\frac{n_{BC}}{V_{BC}}\right) - 41.39 \left(\frac{n_{HV}}{V_{HV}}\right) - 28.72 \left(\frac{n_{ped}}{V_{2W}}\right)
 \end{aligned} \tag{7}$$

$$V_{SC} = 16.96 - 60.73\left(\frac{n_{2W}}{V_{2W}}\right) - 33.30\left(\frac{n_{3W}}{V_{3W}}\right) - 40.43\left(\frac{n_{SC}}{V_{SC}}\right) - 61.96\left(\frac{n_{BC}}{V_{BC}}\right) - 70.52\left(\frac{n_{HV}}{V_{HV}}\right) - 30.87\left(\frac{n_{ped}}{V_{2W}}\right) \tag{8}$$

$$V_{BC} = 17.36 - 72.16\left(\frac{n_{2W}}{V_{2W}}\right) - 40.40\left(\frac{n_{3W}}{V_{3W}}\right) - 33.71\left(\frac{n_{SC}}{V_{SC}}\right) - 79.43\left(\frac{n_{BC}}{V_{BC}}\right) - 85.39\left(\frac{n_{HV}}{V_{HV}}\right) - 31.17\left(\frac{n_{ped}}{V_{2W}}\right) \tag{9}$$

$$V_{HV} = 13.50 - 50.91\left(\frac{n_{2W}}{V_{2W}}\right) - 47.70\left(\frac{n_{3W}}{V_{3W}}\right) - 23.80\left(\frac{n_{SC}}{V_{SC}}\right) - 53.40\left(\frac{n_{BC}}{V_{BC}}\right) - 141.52\left(\frac{n_{HV}}{V_{HV}}\right) - 4.55\left(\frac{n_{ped}}{V_{2W}}\right) \tag{10}$$

As can be seen from the tables, the error obtained when forecasting speeds using SVR and mathematical models differs greatly. The results show that when speed prediction is done using a data-driven approach (SVR), all error values are lower, demonstrating the superiority of data-driven strategies over traditional methods with more accurate results. Tables 2, 3, and 4 show the comparative results obtained while predicting speeds using SVR for data from Surat, Baroda, and Noida, respectively.

Table 3 Comparison of SVR and mathematical model at Surat

Vehicle type	SVR		Mathematical model	
	RMSE	MAPE(%)	RMSE	MAPE (%)
Two-wheeler	0.39	3.31	0.62	5.353
Three-wheeler	0.364	3.43	1.63	9.97
Small car	0.64	5.31	0.92	7.814
Big car	0.975	7.924	1.11	9.254
Heavy vehicle	0.854	7.79	2.40	9.967

Table 4 Comparison of SVR and mathematical model at Baroda

Vehicle type	SVR		Mathematical model	
	RMSE	MAPE (%)	RMSE	MAPE (%)
Two-wheeler	0.479	3.53	2.599	25.720
Three-wheeler	0.63	5.67	1.871	20.646
Small car	0.395	2.96	2.793	27.975
Big car	0.762	5.97	2.935	28.996
Heavy vehicle	1.53	15.34	2.590	35.274

Table 5 Comparison of SVR and mathematical model at Noida

Vehicle type	SVR		Mathematical model	
	RMSE	MAPE (%)	RMSE	MAPE (%)
Two-wheeler	1.005	10.685	1.223	12.838
Three-wheeler	0.931	10.823	1.138	11.0446
Small car	0.501	5.01	1.402	15.4626
Big car	1.24	18.66	1.996	30.7814
Heavy vehicle	6.433	15.34	7.072	35.274

Table 6 Comparison of speeds at non-base and base sections

Location	Two-wheeler		Three-wheeler		Small car		Big car		Heavy vehicle	
	MS	SD	MS	SD	MS	SD	MS	SD	MS	SD
Udhana	56.13	3.16	52.94	3.42	51.04	2.29	49.51	2.16	48.13	2.64
Surat	34.97	0.73	30.58	0.69	34.34	0.93	34.82	1.13	32.29	1.16
Baroda	35.94	0.80	31.77	0.79	36.19	1.00	36.10	1.14	29.16	1.97
Noida	29.65	1.54	26.58	1.07	27.86	0.79	24.18	1.49	32.61	6.67

The speeds at both non-base sections and base sections are compared to each other using various statistical measures such as mean speed (MS), standard deviation (SD), 85th percentile speed, and so on to check the influence of undesignated pedestrian crossing on to the speed of all vehicles variants. The results obtained from this comparison are shown in Table 5. All the speed values in the table are given in kmph (Table 6).

The table shows the values of mean speed and standard deviation of speeds at all the four study locations. Because Udhana is the basic section and has no pedestrian crossflow, the average speed of all vehicle categories is substantially higher than in other non-base sections. Similarly, the standard deviation of speeds is having a bigger value for base section as compared to non-base sections which can be interpreted as the freedom of choice of drivers to drive at any desired speed is higher at base sections due to the lack of any inhibiting factors such as pedestrian crossflow while the drivers will have to maintain a low-constant speed in order to avoid the collision with pedestrians.

These results are also explained in graphical format as shown in Figs. 4a–e where 1 on Y-axis stands for base section and 2, 3, 4 correspond to non-base sections. It is seen in the graphs that the average speed at non-base sections is very less as compared to base sections.

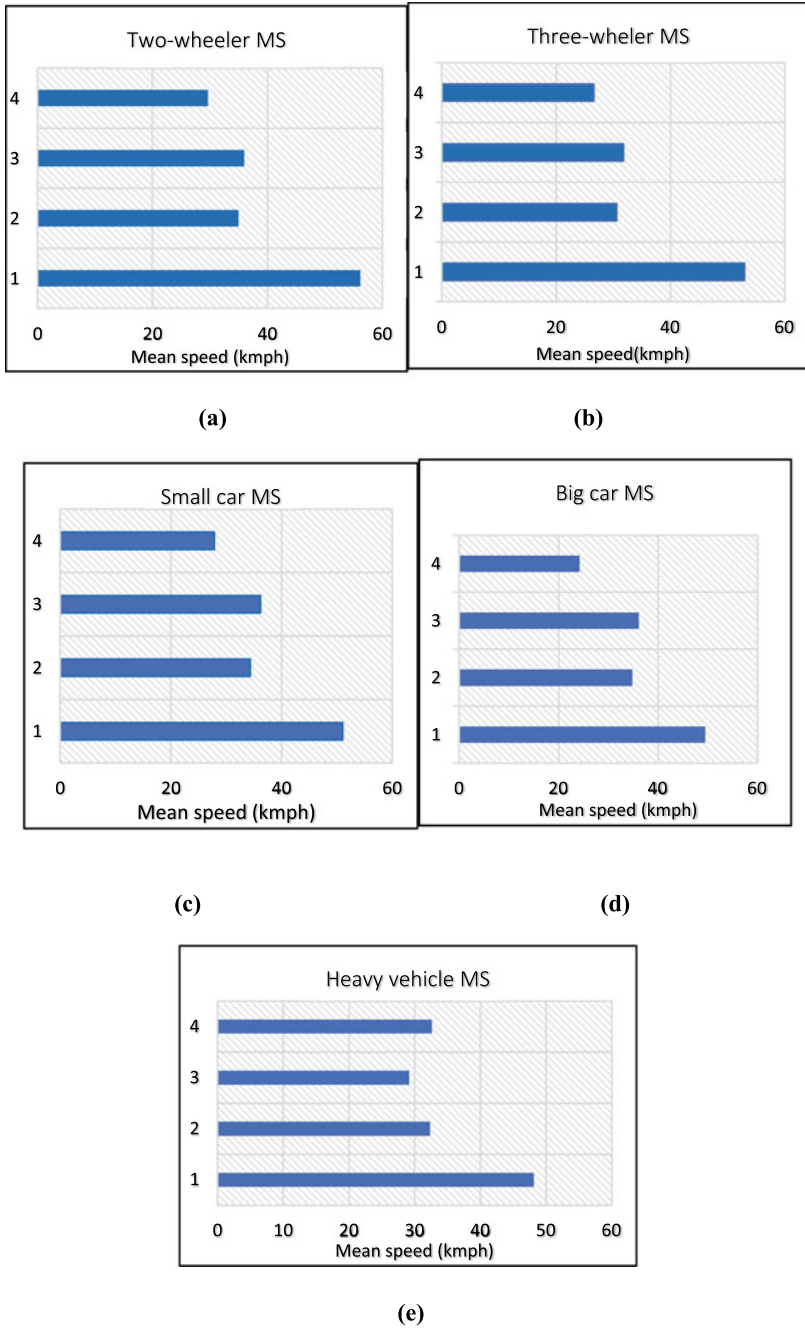


Fig. 4 a, b, c, d, and e Graphical comparison of speed

8 Validation of Results

Figure 5 shows the predicted speed values versus the observed speeds of individual vehicle categories such as two-wheeler, three-wheeler, small car, big car, and heavy vehicles. It can be observed that the speed values of various vehicle categories fall on a 45 degree line, indicating that the two sets of speed data are in good agreement.

9 Conclusion

Because of the absence of particular facilities for them in a developing country like India, metropolitan roadways are frequently shared by not just motorized cars, but also non-motorized vehicles and walkers. In order to reach multiple land uses, pedestrians use roadways and cross undesignated segments that are more convenient to them. This will have a detrimental impact on smoothness of vehicle movement, both in terms of speed and capacity. There are some traditional strategies for estimating vehicle speed that involve using vehicle density as an explanatory variable. Some researchers have used linear regression approaches to incorporate pedestrian crossing into speed estimate in terms of number of pedestrians. Data-driven speed prediction algorithms promise to be a powerful tool, with model results that are more accurate and reliable. Furthermore, adding more explanatory factors is much simpler. The primary objective of this study is to employ support vector regression, a potentially efficient data-driven technique to forecast the speed of all types of vehicles by taking into account the effect of pedestrian crossflow as well as vehicle density. The speed of each category of vehicle is determined to be dependent on the number of each category of vehicle on the roadway, as well as the number of crossing pedestrians in the particular time interval investigated, according to the analysis of the data. The predicted results represent that the data-driven technique outperforms the traditional method for all vehicle types. While comparing the predicted speeds and observed speeds, it is found that there is no much difference between the values which further indicate usefulness of SVR for predicting speeds when unknown input conditions occurred. By comparing the field values of speed at the base and non-base sections, the effect of crossing pedestrians on the speed of each category of vehicle is evaluated. Due to the negative impact of pedestrian crossings, the speed of vehicles at base sections appears to be substantially higher than that of vehicles at non-base portions, according to the data. When MAPE and RMSE values were used to compare the findings provided by SVR and mathematical models with field data, SVR was found to be a very accurate and less time-consuming methodology for speed prediction. Since several advanced data collection systems have gained popularity in recent years, a vast amount of data is now available for modeling, particularly when real-time speed forecasts are required. As a result, data-driven techniques like SVR seem to be quite effective in dealing with them. It also has a strong generalization capacity and a good

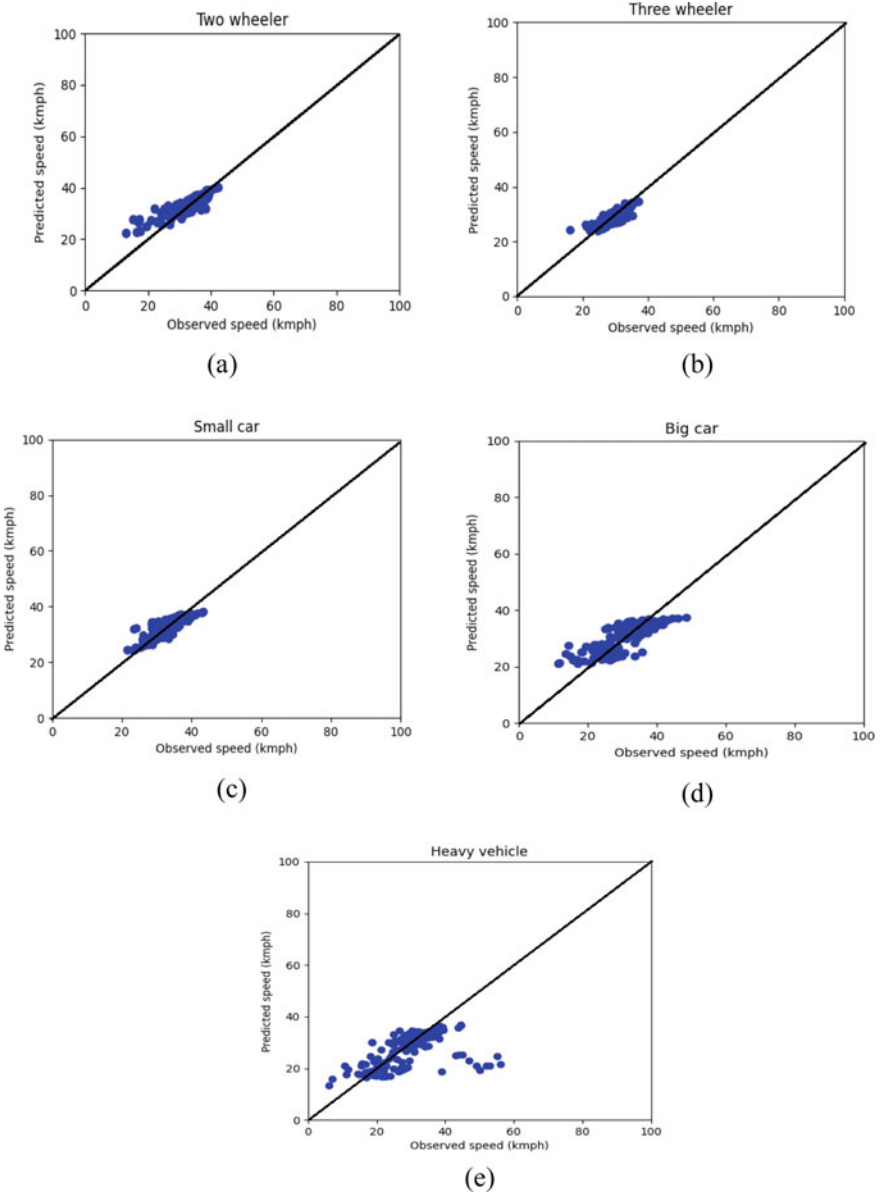


Fig. 5 Comparison between observed speed and predicted speeds

prediction accuracy. In comparison with many other strategies, it is also quite simple to implement.

It is possible to create traffic flow models with greater accuracy using pure self-learning and data-driven methodologies. A data-driven strategy can be a complete technical system that may be applied to socioeconomic issues that are fundamental to transportation policymaking. Data-driven models, of course, have their limitations. In contrast, whereas traditional models are derived from theory and are more transparent and beneficial for teaching and gaining insights into the features of the problem, data-driven techniques are less visible and take more effort to ensure that the results are compatible with expectations. Future works can rely on these aspects.

References

1. Patel MR, Shukla PRN, Golakiya HD (2018) Study of interaction between pedestrian and vehicle at undesignated urban mid-block section. *Int Res J Eng Technol* 5(2):56–72
2. Cantillo V, Arellana J, Rolong M (2015) Modelling pedestrian crossing behaviour in urban roads: A latent variable approach. *Transport Res F: Traffic Psychol Behav* 32:56–67
3. Golakiya HD, Dhamaniya A, Ph D (2019) Modeling speed and capacity estimation at urban midblock sections under the influence of crossing pedestrians. *J Transp Eng Part A: Syst* 145(9):04019036
4. Ferenchak NN (2016) Pedestrian age and gender in relation to crossing behavior at midblock crossings in India. *J Traffic Transp Eng* 3(4):345–351
5. Golakiya HD, Chauhan R (2020) Evaluating safe distance for pedestrians on urban midblock sections using trajectory plots. *Euro Transport* 75:1825–3997
6. Yannis G, Golias J, Papadimitriou E (2007) Modeling crossing behavior and accident risk of pedestrians. *J Transp Eng* 133(11):634–644
7. Zheng CJ, He R, Wan X, Wang C (2016) The study on in-city capacity affected by pedestrian crossing. *Math Probl Eng* 2016:1–8
8. Gitelman V, Carmel R, Pesahov F, Hakkert S (2017) Exploring safety impacts of pedestrian crossing configurations at signalized junctions on urban roads with public transport routes. *Int J Inj Contr Saf Promot* 25(1):31–40
9. Papathanasopoulou V, Antoniou C (2015) Towards data-driven car-following models. *Transp Res Part C: Emerg Technol* 55:496–509
10. Papathanasopoulou V, Antoniou C, Koutsopoulos HN (2019) Data-driven traffic simulation models: mobility patterns using machine learning techniques. *Mobility Patterns, Big Data and Transport Analytics*, pp 263–295
11. Yoon B, Chang H (2014) Potentialities of data-driven nonparametric regression in urban signalized traffic flow forecasting. *J Transp Eng* 140(7):04014027
12. Kouskoulis G, Spyropoulou I, Antoniou C (2018) Theoretical models versus data driven techniques. *Int J Transp Sci Technol* 7(4):241–253
13. Yi Z, Liu XC, Wei R, Grubestic TH (2021) Snowplow truck performance assessment and feature importance analysis using machine-learning techniques. *J Transp Eng Part A: Syst* 147(2)

Analysis of the Impact of Pedestrian Crossing Activity on the Traffic Characteristics at Urban Midblock Sections Using Simulation Technique



C. M. Prakash, Yogeshwar V. Navandar, Hareshkumar D. Golakiya, and Ashish Dhamaniya

Abstract In India, pedestrians in urban area, mostly, cross the road at midblock sections to save time and to access the nearby residential and commercial places. These midblock locations are undesignated; pedestrian crossing operations at these locations will cause interruption to the vehicular movement because of using force gaps to cross the road. So, it is necessary to focus on such undesignated locations of urban midblock, and studies need to be conducted to find the effect of these vulnerable crossing pedestrians on traffic characteristics like vehicular speed. Hence, this study aims to analyze the impact of pedestrian crossing on speed characteristics of vehicles and to quantify percentage reduction in speeds for different vehicle categories at undesignated urban midblock section using microscopic simulation software VISSIM. Traffic data were collected at three locations from two distinct cities in India using high-resolution video cameras, and data were extracted using Avidemux software. This extracted data were used to develop simulation model and to define model parameters. The developed simulation models were calibrated and validated using GEH and t-statistics to replicate the actual site conditions. Using the validated simulation models, percentage reduction in speeds for different vehicle categories was quantified. The present study revealed that there is a significant reduction in average speed of different vehicle categories. The overall speed of the traffic stream is reduced by 58.33% due to crossing pedestrians.

Keywords Urban midblock section · Crossing pedestrians · Undesignated locations · Simulation

C. M. Prakash
NIT Calicut, Calicut, Kerala, India

Y. V. Navandar (✉)
Department of Civil Engineering, NIT Calicut, Calicut, Kerala, India
e-mail: navandar@nitc.ac.in

H. D. Golakiya
Dr. S and S.S Gandhi Government College of Engineering, Surat, Gujarat, India

A. Dhamaniya
Department of Civil Engineering, SVNIT Surat, Surat, India

1 Introduction

In India, where heterogeneous traffic conditions exist, each vehicle category has different static and dynamic characteristics. As there is no lane-discipline behavior, vehicles occupy the entire road space for traffic movement. In addition to this, side frictions like bus stops and parked vehicles again increase the complexity of vehicular movement. Pedestrians are considered as basic elements and integral part of urban transportation system. Pedestrian walking and crossing facilities like sidewalks, footpaths, foot over bridges are required in urban transportation system for efficient pedestrian movement. As there are no adequate pedestrian facilities in India, pedestrians share the carriageway for their movement along with the traffic. Even such facilities are available at some locations, pedestrians avoid to use them in order to save the time and to access nearby residential and commercial places. Figure 1 shows the pedestrian crossing at urban midblock sections in Indian scenario. This behavior of pedestrians usually occurs at midblock sections, and pedestrians are at greater risk particularly at multilane roads due to high speed of vehicles and large crossing distances. The decision of crossing the road depends upon several factors along with pedestrian characteristics like age, gender, and the traffic flow [1]. Generally, while crossing the roads, pedestrians observe the approaching traffic in the stream, analyze them, and select appropriate gaps to cross the road. Pedestrians will use force gaps for crossing and force the approaching vehicles to apply the brakes to avoid the conflicts.

These interruptions of crossing pedestrians at unmarked urban midblock section affect speeds of approaching vehicles which results in increase in delay, travel times,



Fig. 1 Indian scenario of pedestrian crossing at urban midblock section

and ultimately reduction in capacity [2]. As it is difficult to study the vehicle–pedestrian interactions in the field and to conduct field experiments by considering the large variations in roadway and traffic conditions, alternative modeling tools like computer simulation software are used to study these complex characteristics [3]. VISSIM is one of the most widely used modeling tool in which model can be studied over time. In the present study, VISSIM software is used to build the simulation models and to estimate the effect of crossing pedestrians on vehicular speeds.

2 Literature Review

In the present study, attempt is made to quantify the effect of crossing pedestrians on vehicular speeds at undesignated urban midblock using simulation. Hence, the literature is reviewed separately for the effect of pedestrian crossing on vehicular speeds at urban midblock and the simulation software (VISSIM) applied for modeling the Indian traffic scenario.

Donell et al. [4] attempted to model the speed of trucks on 2-lane rural roads and developed the models for predicting the speed. Perco et al. [5] compared the free flow speeds of motorized two-wheelers and passenger cars in urban areas. Speed modeling has been attempted by many other researchers for homogeneous and mixed traffic conditions. Most of the previous researches are conducted with homogeneous traffic conditions in developed countries, but very less researches are reported on mixed traffic conditions without lane discipline. Golakiya and Dhamaniya [2] developed speed prediction models to find the variation in speeds of different vehicle categories due to pedestrian crossing at urban midblock sections. Khaled shaaban et al. [6] studied the pedestrian crossing behavior at unmarked sections and found that the crossings at these locations are unsafe, risky, especially in case of multi-lanes. Multiple regression models were developed and model suggested that waiting time, critical distance, vehicle speed, and its position of vehicle have strong influence on size of gap. Most of the studies concentrated on evolving pedestrian flow parameters and their interrelationships at a pedestrian facility. However, studies dealing with effect of pedestrian crossflow are limited in number. Mahendrakumar Metakari and Akhilkesh Kumar [7] developed traffic simulation model for heterogeneous traffic with no lane discipline, and traffic stream was simulated using this model; preliminary results like speed were obtained from the developed model. Siddarth and Gitakrishnan [8] presented a procedure for calibrating VISSIM models for Indian traffic conditions. PTV VISSIM user manual [9] used for building a simulation model and giving model inputs.

The intensive literature review reveals that very few numbers of studies happened regarding pedestrian crossing at undesignated urban midblock sections and also the application of simulation techniques in the field of pedestrian studies.

3 Research Objectives

The present study mainly focuses on analyzing the impact of crossing pedestrians on the average speeds of different vehicle categories and quantifying the percentage reduction in average speeds of each vehicle category due to pedestrian crossing using simulation approach.

4 Research Methodology

Traffic speed is the important parameter which needs to be considered for safe traffic operations, traffic safety ultimately toward capacity and level of service. At any given location, speed is also affected by road geometry and environmental factors. But, road geometry and environmental factors are unchanged during the observation period. Vehicular movement and their interaction play important role in traffic operations. Interaction of vehicles in traffic stream depends on static and dynamic characteristics and driver's skill and experience. Speeds of vehicles further affected by pedestrians sharing the carriage way. Crossing pedestrian volume is the main parameter to be considered for evaluating the speed characteristics of vehicles. In this study, simulation models were developed for both the base section (no crossing pedestrians) and non-base section (with crossing pedestrians) and are calibrated and validated using GEH statistic and t-statistic.

Speeds values obtained from the validated simulation models for both base and non-base sections are compared to get percentage reduction in average speed of each vehicle category.

5 Data Collection

5.1 Identification of Study Site

To achieve framed research objectives, three study locations are selected on 6-lane divided urban midblock sections with and without pedestrian crossing. All the selected non-base sections have the similar geometric characteristics but with varying pedestrian crossflow. The section spanning 500-m-length midblock section with uniform traffic flow conditions is selected [2]. The criteria used for selecting the base section are that it should be free from any other side frictions like bus stops, parked vehicles, and well away from intersections to have minimum effects. Non-base sections were selected if the section has only crossing pedestrians with no other side frictions. Both base and non-base sections were identified, selected on midblock sections. Figure 2 shows the identified study locations for base and friction (non-base) sections.



Fig. 2 Identified study locations, base, and friction sections

5.2 Data Collection

Traffic data were collected on 6-lane divided urban arterial roadway sections from three locations in two distinct cities in India, namely Noida, Surat. The selected cities are densely populated, cultural, and behavioral differences of people can be taken into account due to the presence of migrated people from different parts of the country. Data were collected using videographic survey with high-resolution cameras. The survey was conducted on six-lane urban roadway sections from morning 6 AM to 6 PM. For collecting the traffic data, a 500-m midblock study stretch with restricted access on to the lanes is selected. In the middle of selected midblock, a longitudinal trap of 60 m was marked to obtain the traffic characteristics like speed. Cameras are fixed to stands and placed at a point such that it covers the selected trap length. Different vehicle types observed in the study site are categorized into five vehicle classes, namely two-wheelers (2 W), three-wheelers (3 W), small cars (SC), big cars (BC), and heavy goods vehicles (HGV), based on physical dimensions, as described in Table 1.

Cars are again splitted into two groups, namely small cars (SC) and big cars (BC) because of large variation in static and dynamic characteristics of cars. Cars with

Table 1 Vehicle categories based on physical dimensions

Vehicle class	Vehicle type	Length (m)	Width (m)	Rectangular plan area (m ²)
2 W	Motorcycles, scooters	1.87	0.64	1.2
3 W	Auto-rickshaw	3.2	1.4	4.48
SC	Standard car	3.72	1.44	5.36
BC	Big utility vehicles	4.58	1.77	8.11
HGV	Standard bus, heavy trucks	10.10	2.43	24.54

average length of 3.72 m, average width of 1.44 m, and engine power upto 1400 cc were designated as SC, cars with average length and width of 4.58 and 1.77 m, respectively, and engine power around 2500 cc was designated as BC. The average dimensions are considered if more than one vehicle type included in particular vehicle class.

5.3 Data Extraction

The recorded video was replayed to extract the data which is collected through video cameras. Avidemux 2.6 software was used for extraction, which is capable of converting 1 s video into 25 frames. By taking front wheel of vehicle as reference, entry time and exit times of vehicles into the study stretch were noted using Avidemux software. When the vehicle enters into the 60-m study stretch, the entry time and exit time is noted for each vehicle, and the difference between the times gives the total time taken by the vehicle to cross 60-m trap length. Obtained time is used for computing vehicular speeds.

Along with the speed data, classified vehicular volume and the pedestrian data per minute was extracted. The speed values of each category of vehicles were later converted into 5 min interval by taking weighted average of obtained observations, to avoid large variability in the data. Similarly, vehicular volumes and pedestrian data also converted into 5 min interval.

6 Data Analysis

Classified vehicular volume and average speeds of each vehicle category were extracted from the recorded video and converted to 5 min data as explained in the previous section. Then, data were further analyzed to obtain the average traffic composition, peak, and non-peak hour traffic data in both base and non-base sections. The ranges of traffic volumes and average vehicular composition of the traffic stream at all the study locations are shown in Table 2.

The speed characteristics such as mean speed, 15th, 50th, and 85th percentile speeds observed at these study locations are as given below in Table 3.

7 Simulation Model

Simulation modeling is the mimicking (replicating) the road conditions in actual traffic scenario in a simplified manner over time [10]. Simulation modeling is the popular technique used to study traffic flow and its characteristics, in which created models can be studied over a period or after certain span of time. In the present study,

Table 2 Average vehicular composition

Section number	Name of the city	No. of lanes	Type of section	Traffic volume range (vph)	Average traffic composition (%)				
					2 W	3 W	SC	BC	HGV
1	Noida	6	Non-base	3400-4900	34	21	33	8	4
2	Surat	6	Non-base	3000-5400	53	36	8	1	2
3	Surat	6	Base	2200-4800	37	26	24	8	5

Table 3 Observed speed characteristics at base section and non-base section

Type of section	Location	Speed characteristic	2 W	3 W	SC	BC	HGV
Non-base	Noida	Mean speed, Kmph	29.65	26.58	27.84	24.03	20.50
		V15	23.91	23.05	24.75	18.90	16.53
		V50	30.57	26.85	28.09	24.97	20.32
		V85	34.85	30.55	30.61	28.83	24.76
Non-base	Surat	Mean speed, Kmph	34.99	30.58	34.35	34.82	32.29
		V15	31.83	27.84	30.75	31.08	28.23
		V50	35.20	30.75	34.45	34.68	32.33
		V85	37.64	33.31	37.53	38.80	36.35
Base	Udhana, Surat	Mean speed, Kmph	51.45	39.59	49.52	48.99	49.23
		V15	46.90	33.35	46.93	44.14	42.22
		V50	49.24	38.34	49.28	48.70	48.47
		V85	57.25	45.15	51.91	53.32	54.55

simulation models were created for both base (with pedestrians) and non-base (with pedestrians) as a bidirectional traffic to replicate the actual site conditions (Traffic composition was assigned same for both the directions). PTV VISSIM software is used, which is effective and handy tool for studying mixed traffic conditions with non-lane discipline driving behavior. It has the advantage of easy understanding and comprehensive documentation. In this study, the development of model of simulation model follows the flowchart shown in Fig. 3.

The analyzed information like vehicular composition, vehicular input, average vehicle speeds, and pedestrian composition (for friction section) is used for building the base and non-base models in VISSIM software. Then, the developed models were calibrated with average speeds of each category of vehicles and validated using

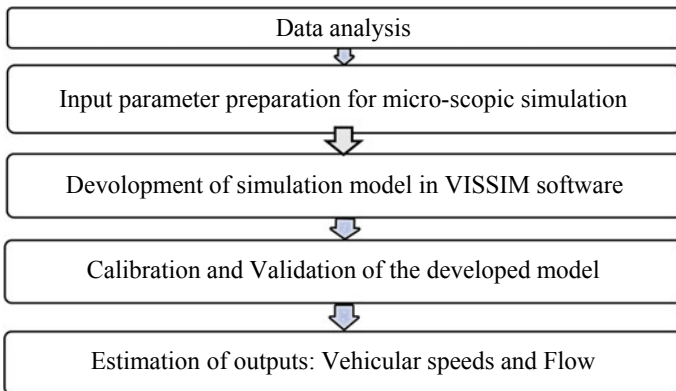


Fig. 3 Flowchart for simulation modeling

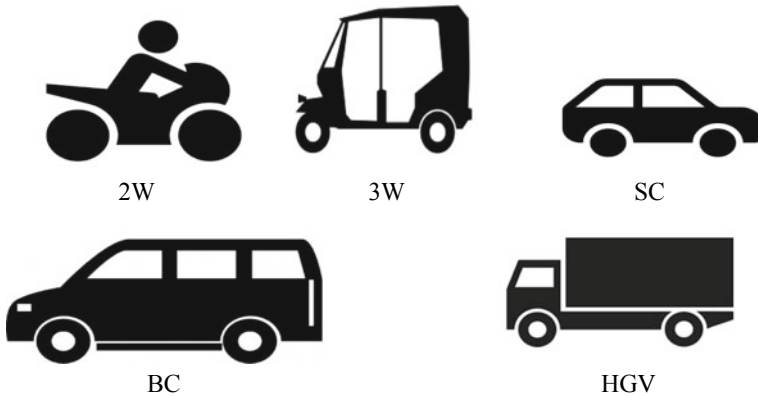


Fig. 4 Vehicle categories considered for the study

GEH statistic and t- statistic, to make the developed model suitable to represent the actual site conditions. After calibrating and validating the models, these models are used to study the behavior and to estimate the traffic characteristics.

7.1 Development of Simulation Model

Six-lane divided urban arterial link of span 500 m was created and another 200 m, each 100 m at the starting and ending of the link as a buffer zone using links and connectors, with a median of 2 m width. Links and connectors are considered as the basic network building components in the VISSIM software. Models representing the physical dimensions of each vehicle type plying on the study site were defined in the simulation software. Model parameters like vehicular inputs observed at the peak hour of each section of base and friction sections, vehicular compositions and their proportions, desired speed distribution of vehicles and pedestrian volumes were given input to the simulation model. The following Fig. 4 shows the different vehicular models considered in the simulation modeling.

Desired speed distribution curves were defined for each category of vehicles plying on both base and non-base sections taking minimum, maximum, 15th, 50th, and 85th percentile speeds of vehicles defined in S-shaped curve. Figure 5 shows the desired speed distribution curves defined for two-wheelers and small cars.

7.2 Calibration and Validation of Simulation Model

Calibration is the iterative process in which model is adjusted to reproduce the field conditions to a sufficient level to achieve the framed research objectives. Calibration

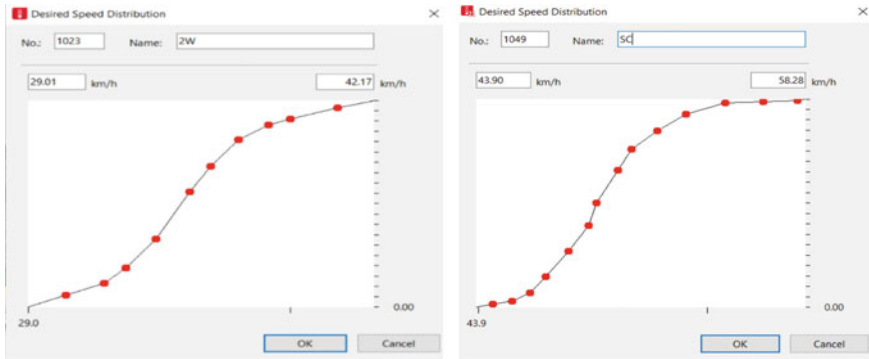


Fig. 5 Desired speed distribution curves for 2 W and SC

enables the modeler to modify the model parameters so that developed model produce filed measured and observed traffic.

Then, the results are reviewed and compared with the data collected in the field. Calibration process involves adjusting the driver behavior and walking behavior. Driving behavior adjustment involves modifying the following, lane change, and lateral behaviors. Urban motorized driving behavior, Wiedemann 74 car following model was used to represent the urban conditions, which PTV recommends for arterials. Pedestrian behavior in the network is adjusted using the walking characteristics to replicate the site conditions. As there is no lane discipline behavior observed from the actual site conditions, vehicles in the simulation model are allowed free to choose any lateral position and overtake from any side during the simulation. All these parameters are given as input to the simulation model, simulation is performed to estimate the output. Each time, 10 simulation runs were made for a total simulation time of 4200 s which includes a warmup period of 600 s to have accurate simulation output.

Absolute percentage error was computed by comparing the simulated values and observed values. If the computed error was within 10–15%, then the model considered as well calibrated; otherwise, process will be repeated till the error lies within the limit [11]. Table 4 shows default and calibrated values after trial-and-error procedure of driving behavior.

For calibrating the pedestrian behavior, sensitivity analysis for walking characteristics was done to identify the influencing parameters, and these parameters were adjusted to replicate the ground conditions. It was observed that the default values in the software replicate the pedestrian behavior. Table 5 shows the sensitive walking parameters and their default values.

Validation is the process of checking the simulated values from calibrated model with field values like traffic volume and average speeds of each category of vehicles using some goodness of fit measures. Traffic volumes are validated using GEH statistic which is calculated using Eq. 1. Model is said to be validated when GEH statistic value is less than 5.

Table 4 Calibration of driving behavior

Behaviors	Parameters	Default values	After trail and error
Following behavior	Average standstill safety distance (in m.)	2.00	0.5
	Additive part of safety distance (bx_add)	2.00	1.1
	Multiplicative part of safety distance (bx_mult)	3.00	1.4
Lateral behavior	Desired position at free flow	Middle	Any
	Keep lateral distance to vehicles on next lane (s)	Not active	Active
	Distance standing at 0 kmph	1.0	0.1
	Distance driving at 50 kmph	1.0	0.7

Table 5 Walking behavior parameters and their defaults values

Parameter	Default values
Tau	0.4
Lambda	0.176
A social (isotropic)	2.72
VD	3

$$GEH = \sqrt{\frac{2(Y_s - Y_o)^2}{Y_s + Y_o}} \tag{1}$$

where

Y_s = Output traffic volume from the simulated volume (vph).

Y_o = Input traffic volume from the field (vph).

GEH statistic is obtained as 0.286, which is very less than 5, shows that the model is validated. Average speeds of vehicles were validated using t-statistic at 95% confidence level. The calculated and critical value of t-statistic (tabulated value) is obtained as 0.415, 1.796, respectively. As calculated value is less than tabulated value, it can be said that the model is validated. A snap of running simulation in VISSIM is shown in Fig. 6.

8 Results and Discussions

The validated simulation model is applied to evaluate framed research objectives. A comparison was made for observed, simulated traffic volumes, and average speeds. It shown in Fig. 7a, b, it was observed that the simulation values are almost near to

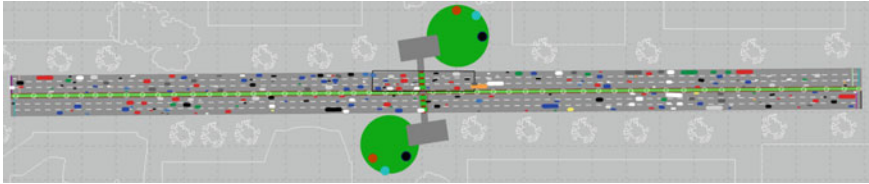


Fig. 6 Snap of running simulation in VISSIM

the filed observed values, and software is capable of effectively replicating the actual ground conditions.

8.1 Reduction in Average Speeds Due to Pedestrian Crossing

Average speeds for each category of vehicles at the undesignated pedestrian crossing were found from the validated non-base model and are compared with the average speeds of each vehicle category from the base model; percentage reduction in speeds is computed. Table 6 shows the percentage reduction in average speeds of each vehicle categories.

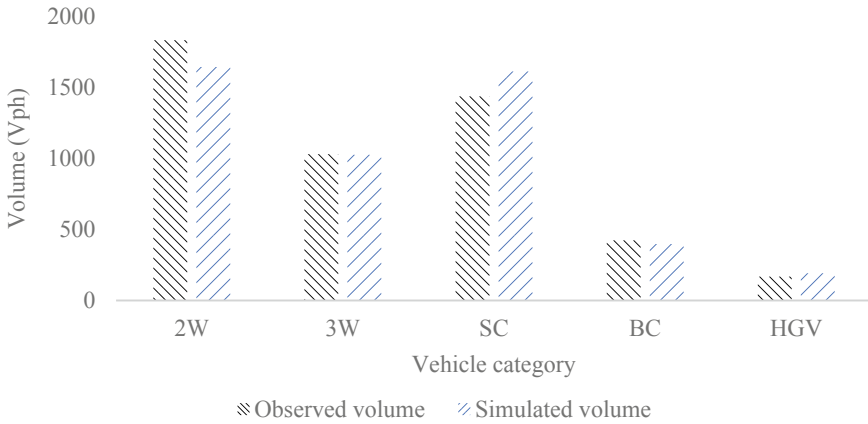
From the above table, it is observed that speed reduction is highest for heavy vehicles and lowest for two-wheelers. The reason includes, two-wheelers require lesser area and have higher maneuverability leads to higher speeds than heavy vehicles. The overall speed of the traffic stream is reduced by 58.33% due to pedestrian crossing.

8.2 Sensitivity Analysis

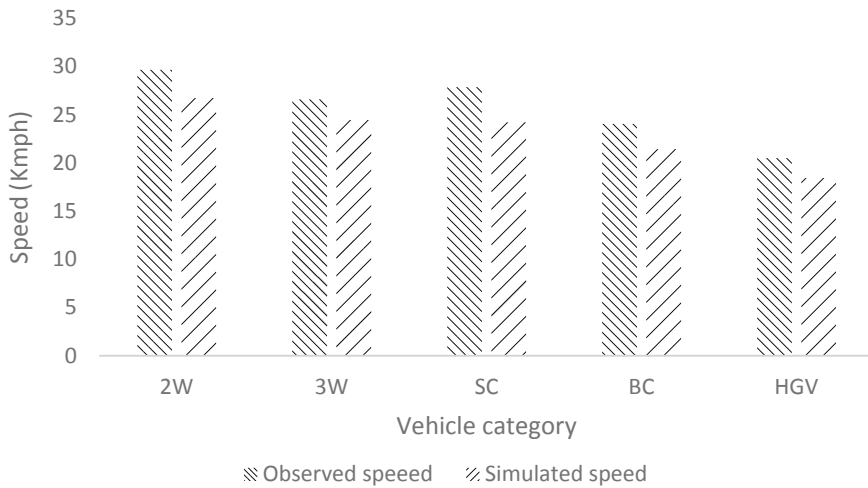
Vehicular speed in the traffic stream depends up on traffic composition and traffic flow at any point of time. With increase in traffic flow and density, interaction between vehicles increases and reduces the freedom to select desired speed in vehicular speed. In the non-base section, speed of any category of vehicles is affected by pedestrian crossflow, along with traffic flow and composition. Sensitivity analysis was done to identify differences in vehicular speed due to pedestrian crossflow. Figure 8 shows variation in speed for different vehicle categories with traffic flow at non-base section.

Traffic composition (Average proportion of vehicles observed in the field) and pedestrian crossflow of 454 pedestrians per hour (ped/hr) were kept constant for evaluating speed of different vehicle categories. Traffic flow was altered from 500 to 5000 veh/hr in steps of 500 veh/hr.

The average speed of different vehicles was decreased with increase in the traffic flow, but it is observed the diverse variation of speeds of different vehicles. Variation of speed for 2 W, 3 W is small than for SC, BC, HGV. Figure 9 depicts the variation in average speed of different vehicles with varying pedestrian crossflow.



(a)



(b)

Fig. 7 **a** Comparison of observed and simulated volumes. **b** Comparison of observed and simulated average speeds

Table 6 Reduction in average speed due to pedestrian crossing

Vehicle category	Distance traveled, (m)	Average speed (Kmph)		
		Base section	Non-base section	% Reduction
Two-wheelers	60	38	18.50	51.32
Three-wheelers	60	36.87	17.24	53.24
Small cars	60	44.39	16.82	62.11
Big cars	60	43.11	16.51	61.7
Heavy goods vehicles	60	40.40	14.82	63.32

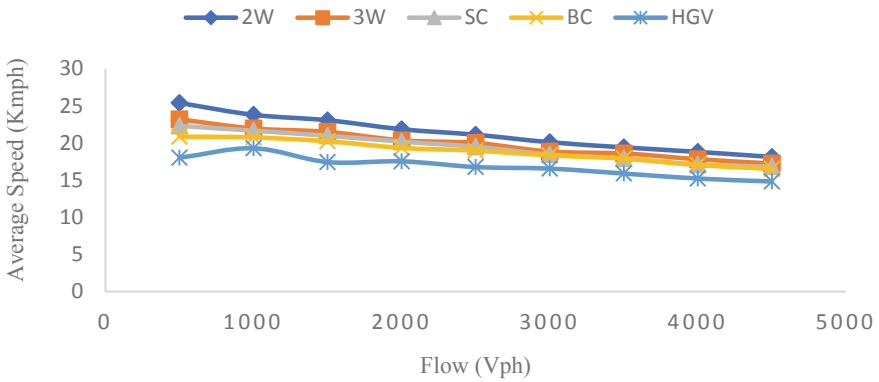


Fig. 8 Variation in average speed of different vehicles at non-base section

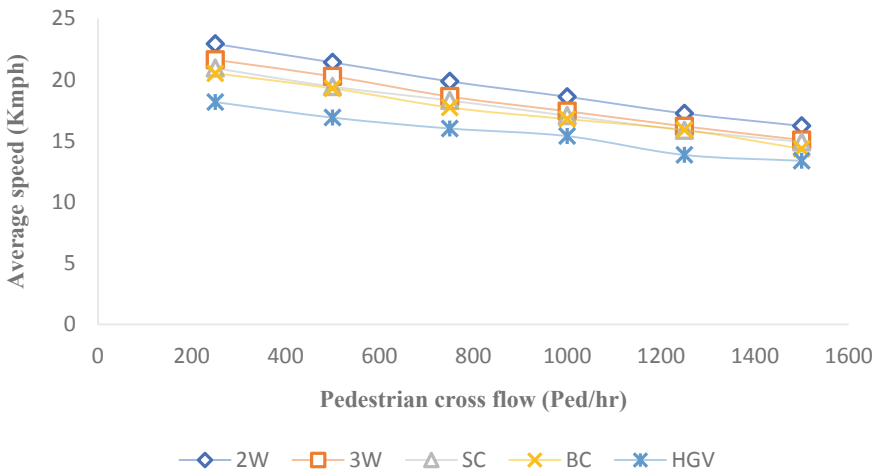


Fig. 9 Variation in speed with varying pedestrian crossflow

Above figure shows the effect of pedestrian crossing on average speeds of different vehicle categories at constant vehicular flow. The average speed of all vehicle categories decreases with increase in pedestrian crossflow, and considerable speed reduction is observed for 2 W, 3 W, SC and BC, and very less for HGV. The reason includes pedestrians may not cross the road in presence of HGV.

9 Conclusions

In India, urban roads are usually shared not only by motorized vehicles but also non-motorized vehicles and pedestrian because of lack of specific pedestrian facilities to walk and cross the urban roads. In order to access various land uses, pedestrians make use of the road ways and crosses undesignated sections which are more convenient to them. This will negatively affect the smooth movement of vehicles in terms of speed of vehicles. There are some conventional techniques available for predicting the speed of vehicles by considering the density of vehicles. Incorporation of pedestrian crossing into the speed estimation in terms of number of pedestrians also has been done by some studies using linear regression techniques. In India, side frictions like pedestrian crossings are very common. Traffic characteristics on urban roads are described in the Highway Capacity Manual (CSIR-CRRI 2017), but the impact of pedestrian crossing on speed characteristics was not mentioned. Therefore, the present study is more related for present Indian traffic situations. Present study is attempted to analyze the impact of crossing pedestrians on average speed of different vehicle categories due to pedestrian crossflow at undesignated urban midblock section. From the analysis results, it is seen that the speed of each category of vehicles significantly affected by crossing pedestrians, and it is depending upon number of each category of vehicles and number of pedestrians crossing the road section. Result of the present study shows that the microscopic simulation modeling provides more accurate results as compared to conventional analytical methods. Pedestrian warrants can be developed by using the results of the present study.

References

1. Dhamaniya A, Chandra S (2014) Influence of undesignated pedestrian crossings on midblock capacity of urban roads. *Transp Res Rec* 2461:137–144
2. Golakiya, Patkar M, Dhamaniya (2019) Impact of midblock pedestrian crossing on speed characteristics and capacity of urban arterial. *Arabian J Sci Eng*
3. Dhikhale P (2019) Study of the impact of roadside bus stop on speed using simulation software. Academic Thesis. National Institute of Technology Surathkal
4. Donell E, Adolini M (2001) Speed prediction models for two-lane rural highways. *Transp Res Rec*
5. Perco P (2008) Comparison between powered two-wheeler and passenger car free-flow speeds in urban areas. *Transp Res Rec*
6. Khaled S, Deepti M, Abdulla M (2019) Modeling pedestrian gap acceptance behaviour at a six-lane urban road. *J Transp Saf Secur*
7. Mahendrakumar M, Budhkar A, Akhileshkumar M (2013) Development of simulation model for heterogeneous traffic with no lane discipline. *Procedia Soc Behav Sci*
8. Siddarth SMP, Gitakrishnan R (2013) Calibration of VISSIM for Indian heterogeneous traffic conditions. *Procedia Soc Behav Sci*
9. Bak R, Kiec M (2012) Influence of midblock pedestrian crossings on urban street capacity. *Transp Res Rec* 2316:76–83

10. Manraj Singh B, Balaji P, Arkatkar S. (2012) Modeling of traffic flow on indian expressways using simulation technique. *Procedia Soc Behav Sci* 43
11. Kadali and Vedagiri: Gap acceptance behaviour of crossing pedestrians at urban midblock section. *Transportation Research Record* (2013)

Analysis of Vehicle Time Headway Distributions for Passenger Car and Commercial Vehicles Interaction



Sandeep Singh and S. Moses Santhakumar

Abstract Time headway is a fundamental and crucial aspect of any traffic system. Time headway is inextricably linked to the performance and safety analysis of traffic operations of the highways. To deal effectively with any given traffic system, a precise time headway measurement is imperative. The research aims to analyze the time headway distribution functions for Passenger Car (PC) and Commercial Vehicles (CVs) interaction for different leader–follower vehicle conditions. An Infra-Red (IR) traffic detector system was used to collect the vehicle class and time headway data from the four National Highway (NH) sections in India. The maximum-likelihood estimation, Kolmogorov–Smirnov (K–S) test, was used to determine the best-fit distribution function. This aided in characterizing and discerning the driver behavior in maintaining different headway distributions under diverse PC–CV interaction conditions. The detailed statistical findings show that the mean headway and the corresponding headway distributions under various vehicular interaction conditions vary from one another. Thus, implying that the interaction between the vehicles influences the pattern of time headway distributions under different traffic conditions. The reported time headway distributions can be used in the generation of vehicles using the microscopic traffic simulation software.

Keywords Passenger car · Commercial vehicle · Time headway · Probability distribution · Rural highway · Mixed traffic

1 Introduction

Having a thorough understanding of how drivers respond to interacting vehicles and the variables that influence their actions helps in the understanding of drivers’

S. Singh (✉) · S. M. Santhakumar
Transportation Engineering and Management, Department of Civil Engineering, National Institute of Technology Tiruchirappalli, Tiruchirappalli, India
e-mail: sandeepsingh.nitt@gmail.com

S. M. Santhakumar
e-mail: moses@nitt.edu

© The Author(s), under exclusive license to Springer Nature Singapore Pte Ltd. 2023
M. V. L. R. Anjaneyulu et al. (eds.), *Recent Advances in Transportation Systems Engineering and Management*, Lecture Notes in Civil Engineering 261,
https://doi.org/10.1007/978-981-19-2273-2_38

585

behavior [1]. The time elapsed from bumper to bumper of successive arrivals of vehicles at a reference point of measurement on a road segment in a lane is known as time headway [2]. The time headway impacts the driving safety, capacity, and Level of Service (LoS) [3]. The time headway is influenced by the vehicular characteristics during interaction in the highway section [4]. The headway maintained by the vehicles varies with respect to the traffic conditions. For example, the higher the traffic flow, the lower is the time headway and vice-versa [5]. Additionally, the modeling of headway is the base for the creation of vehicles for simulation models [6, 7].

Precise metrics such as time headway are necessary to solve any traffic issues [8]. The conventional use of single headway distribution may not measure the variability while developing microscopic traffic simulation models [9]. The selection of the suitable probability distribution function for a specific leader–follower condition of traffic remained an open question. This study examines and analyses the theoretical time headway distributions for Passenger Car (PC) and Commercial Vehicle (CVs) interaction considering the leader–follower driving nature. The PC includes the light motorized vehicle, while the CVs consists of the Light Commercial Vehicle (LCV) and Heavy Commercial Vehicle (HCV). PC–PC, PC–LCV, PC–HCV, LCV–PC, and HCV–PC are the most diverse vehicle leader–follow patterns. The best-fit distribution model for these vehicle-specific pairs is evaluated using a non-parametric fitness test.

2 Review of Literature

Several theoretical headway distributions have been formulated over the last few decades. Jang [2] modeled the headway characteristics of suburban traffic at different traffic flow levels using many distributions. Zhang et al. [3] measured the headway from urban freeways and described the double displaced negative exponential distribution to better match the urban freeways. Jang et al. [4] found that the Gamma distribution and Pearson VI distribution suited well, at low to moderate flow rates and at all flow rates, respectively. Nevertheless, these studies were conducted on homogeneous traffic under different traffic conditions. In the Indian context, Maurya et al. [8] analyzed the speed and time headway characteristics at varying flow and density conditions for mixed traffic. The studies emphasized the consideration of different traffic conditions for any traffic simulation modeling.

Kong and Guo [5] found that the lognormal model is appropriate for the car–car and truck–truck interactions, and the inverse Gaussian model is ideal for the car/truck interactions. Peeta et al. [10] suggested a level of discomfort based on behavior analysis of car-truck interactions. The study concluded that the more significant the impact of the truck, the greater is the discomfort. Moridpour et al. [11] investigated the car-truck relationship and discovered that cars and trucks had substantially different characteristics. Finally, Ye and Zhang [12] explored and formulated headway distribution models based on various vehicle leader–follower pairs.

Nonetheless, there are several limitations of using these distribution models since a variety of variables influence them. The amount of research focusing on the time

headway characteristics considering the influence of PC and CVs interaction on multilane highways is limited. A deeper statistical analysis of headway on the divided highways at different PC–CVs is needed. The present research investigates and analyzes the time headway variations using probability distribution functions for different PC and CVs interaction conditions.

3 Study Locations

Four National Highway (NH) sections were chosen as the study locations. The NH-32 connects Chennai city with Villupuram city, and the NH-38 connects Tiruchirappalli city with Villupuram city. Both the highways are located in the southern state of Tamil Nadu, India. The NHs are level terrain with minimal disturbance from external factors such as intersections, toll plazas, etc. It has two lanes per direction. Each lane's width is 3.5 m, and a paved shoulder lane with 1.5 m in width. The median width is 5.0 m for both the NHs. The Infra-Red (IR) sensor instrument setup across the study locations and the geometric layout of the NH-32 and NH-38 are depicted in Fig. 1a, b, respectively.

The bi-directional traffic data from the four NHs is collected using the IR sensor instrument for 6 h each, between 06:00 PM–12:00 AM, covering peak hours and off-peak hours. The traffic data was recorded on weekdays (typically on Friday) in one direction and on weekends (typically on Sunday) in the other direction. This was done so to ensure that the complete traffic behavior of PC and CVs interaction is captured. The CVs include two types viz. Light Commercial Vehicle (LCV) and Heavy Commercial Vehicle (HCV). The NHs constituted the following composition of traffic (in percentage), as shown in Table 1.

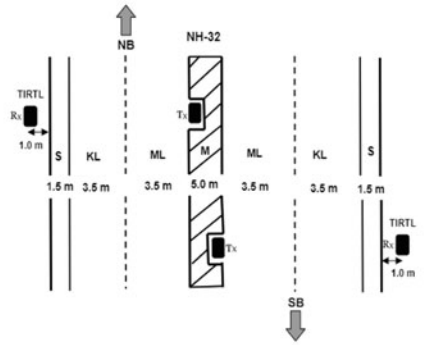
4 Data Acquisition

An IR sensor instrument named Transportable Infra-Red Traffic Logger (TIRTL) collects the traffic data from the highways. It includes a transmitter (Tx) and receiver (Rx). Both are kept opposite to each other across the highway. It can record various traffic variables like volume, vehicle dimensions, speed, and time headway. The Tx serves as the foundation for the IR beam generation. The Rx detects the disturbance in the IR beams due to the passing by vehicles. Two diagonal and two parallel beams transmit between Tx and Rx, as illustrated in Fig. 2.

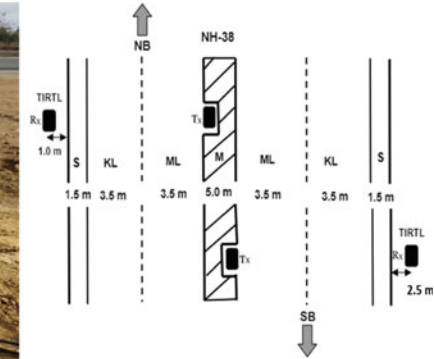
A comparison of the IR sensor data from the NH-38-NB with that of videotaped data from the same site for an hour revealed 97% accuracy in vehicle classification, 95% accuracy in vehicle speed, and 96% accuracy in time headway. Another study by Minge et al. [13], which used the same TIRTL instrument, reported that the vehicle speed accuracy was up to 98%, and vehicle volume accuracy was up to 98%.



(a) NH-32



(b) NH-38



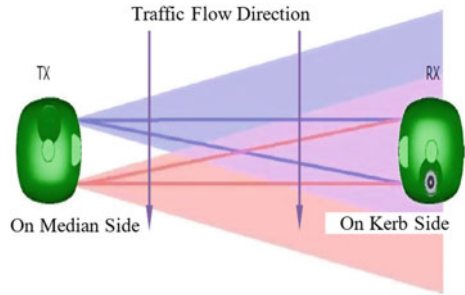
Note: M-Median, ML-Median lane, KL-Kerb lane, S-Shoulder lane, NB-North Bound, and SB-South Bound.

Fig. 1 Study location and geometric features

Table 1 Composition of traffic at the study locations

Vehicle class	NH-32-NB (%)	NH-32-SB (%)	NH-38-NB (%)	NH-38-SB (%)
Two-wheeler (2 W)	16.8	17.7	15.6	15.5
Three-wheeler (3 W)	1.5	1.2	3.6	2.7
Passenger car (PC)	52.6	54.3	48.7	50.2
Light commercial vehicle (LCV)	7.2	9.2	8.9	10.6
Heavy commercial vehicle (HCV)	18.7	14.0	18.4	16.6
Multi-axle vehicle (MAV)	3.2	3.6	4.8	4.4

Fig. 2 Tx and Rx placement for vehicle detection



Additionally, the research by Singh et al. [14] may be referred to for a more detailed description of the working and efficiency of the IR sensor instrument.

5 Time Headway Analysis and Results

The descriptive statistics were used to investigate the variation in the statistical characteristics of the time headway for the various leader–follower conditions. In addition, the study explored the time headway distribution of heterogeneous traffic at different PC–CV interactions. This includes the different leader–follower combinations of five vehicle types: PC–PC, PC–LCV, PC–HCV, LCV–PC, and HCV–PC.

5.1 Descriptive Statistical Analysis

The descriptive statistics on time headway data explain the quality of service of traffic. The fundamental descriptive statistics of the gathered data logically matched the general features of time headway for all five types of leader–follower vehicle combinations. The summary of descriptive statistics is shown in Table 2.

Table 2 Summary of descriptive statistics of time headway data

Statistical Variable	Leader–follower pair				
	PC–PC	PC–LCV	PC–HCV	LCV–PC	HCV–PC
Sample size	938	257	638	361	442
Mean	1.52	2.27	3.33	4.01	5.08
Median	1.38	2.05	3.17	3.94	4.86
Std. deviation	0.42	1.56	1.21	1.77	1.91

The descriptive statistics show that the time headway range from a minimum of 1.52 s for PC–PC to a maximum of 5.08 s for HCV–PC. The comparison between the mean and median values confirms the unsymmetrical existence of the distributions. When the PC is a leader vehicle, the time headway is shorter than when the PC is a follower vehicle. Therefore, the time headway sustained by the PC (as a leader) is lower when interacting with the PC, LCV, and HCV. However, when the PC is in a follower condition, the time headway increase. This increase in the time headway can be attributed to being due to the safe driving culture by the PC as the large-size vehicle drivers in the leader conditions exhibit risky behavior. To maintain a safe distance from the larger-sized vehicles, the PC tends to keep a higher time difference leading to higher time headway. Furthermore, the vehicle length is responsible for the PC maintaining a higher time headway. The variation in the mean headway values indicates that the driver behavior in the traffic gets impacted due to the varying leader–follower combinations.

5.2 Time Headway Distributions of Vehicle Pairs

The time headway data is useful in many aspects such as driver behavior analysis, traffic flow modeling, capacity assessment, and LoS evaluation [15]. The distribution analysis provides more insights into the driver behavior characteristics with respect to diverse vehicle-type combinations. Further, to determine the best-fit distribution for the time headway data, the Easy-fit software was used. The time headway distributions are ranked on the basis of the best-fitted probability distribution functions based on the goodness-of-fit test called the Kolmogorov–Smirnov (K–S) test. The various probability distribution functions of the different vehicle-type leader–follower pairs, namely, PC–PC, PC–LCV, PC–HCV, LCV–PC, and HCV–PC, are shown in Figs. 3, 4, 5, 6, and 7, respectively.

Figure 3 shows that the best-fitted distribution pattern in the case of PC–PC vehicle pair is Gamma distribution. The distribution pattern is skewed to the right due to the vehicular interaction of PC with PC. Lower time headway is maintained by the PC when it is interacting with another PC. The interference of a PC with a PC is less due to their physical and operational characteristics. This distribution pattern perceived by the following vehicle shows that the following vehicle characteristics are also dependent on the dimensions of the leading vehicle. Smaller size vehicles following a smaller size vehicle tend to have lower time headway. The reason is that the following smaller vehicle can quickly encounter the forward view, avoid encumbrance of the lead vehicle by shifting laterally to another lane, and pass by. This avoids the congestion of the vehicles.

The goodness-of-fit test showed that the Gumbel Max is the best-fit distribution for the PC–LCV case, which is depicted in Fig. 4. When considering the PC–LCV interaction, it showed that the distributions are not as skewed as those in the case of PC–PC. This may be due to the interaction of the LCV with the PC for the reason of overtaking and trying to lead the PC. The LCV constantly evaluates possible

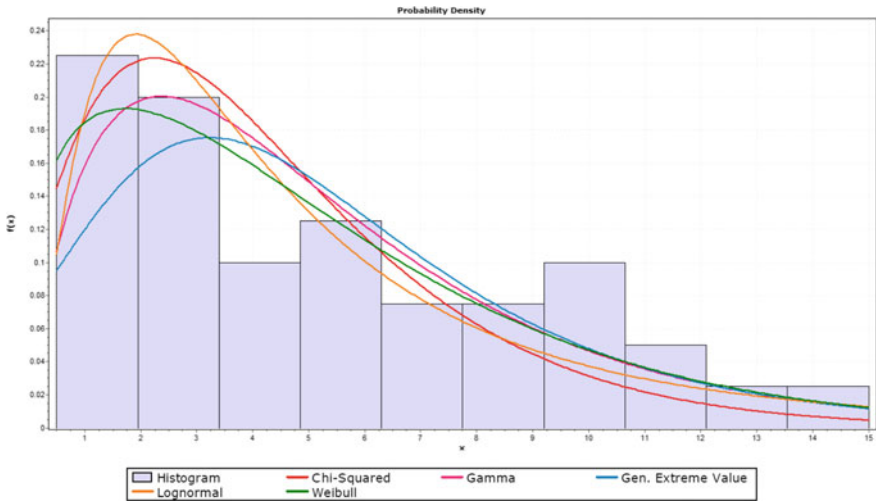


Fig. 3 Probability distribution patterns for PC-PC

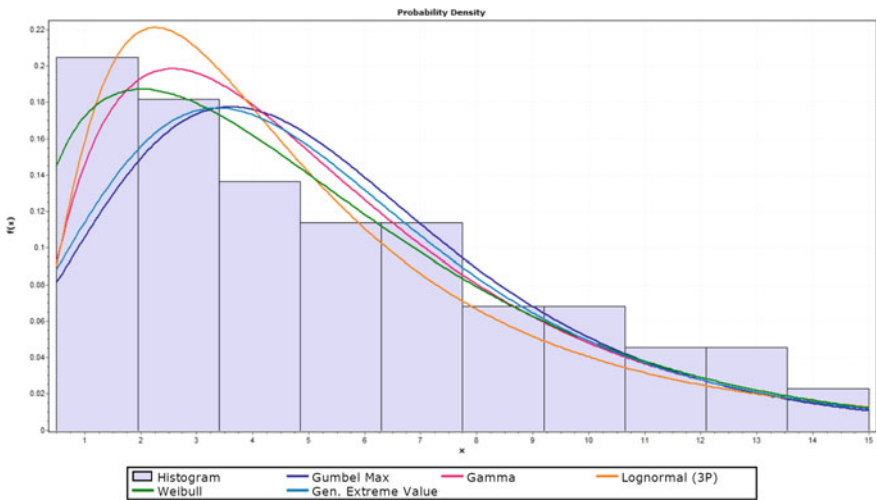


Fig. 4 Probability distribution patterns for PC-LCV

opportunities to perform a lateral movement and overtake the leading PC. As a result, the LCV keeps a smaller headway with its leader PC, resulting in reduced vehicle headways. However, due to the PC’s superior operational capabilities, the LCV may occasionally catch up with the PC, resulting in slightly higher headway values for the PC-LCV than the PC-PC.

Based on the goodness-of-fit test, Weibull distribution was selected as the best-fit model for the PC-HCV vehicle pair, which is depicted in Fig. 5. Because the leading

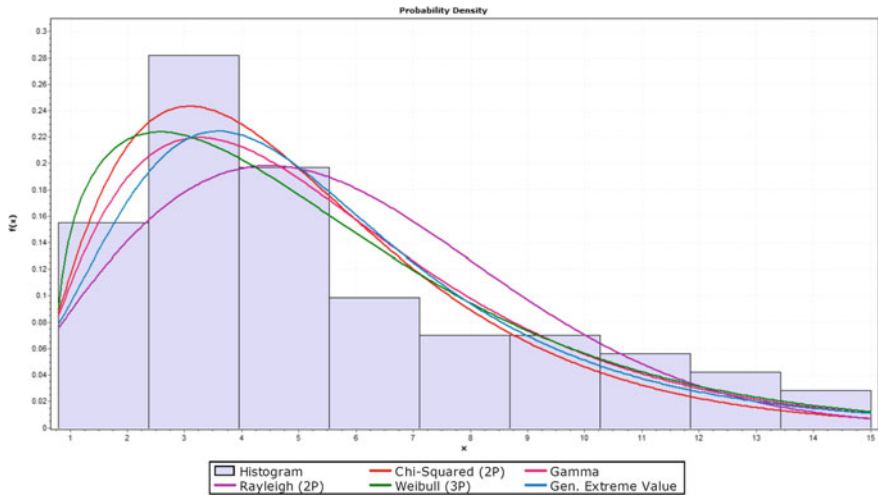


Fig. 5 Probability distribution patterns for PC-HCV

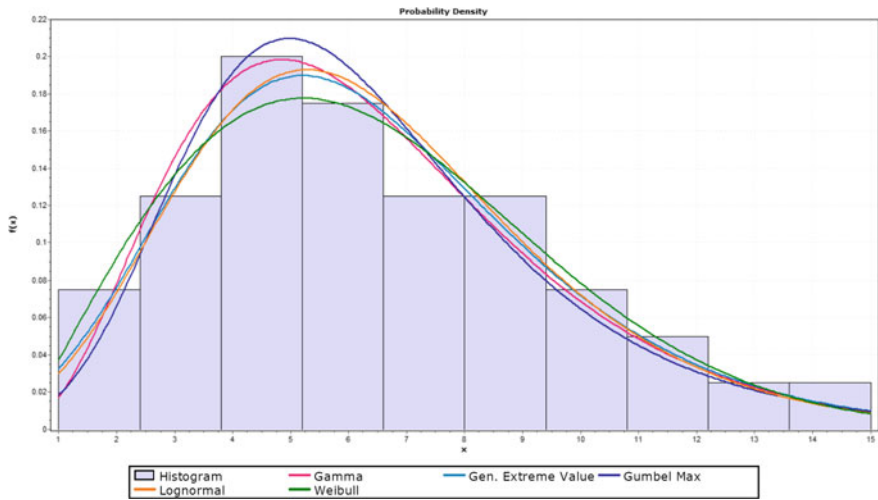


Fig. 6 Probability distribution patterns for LCV-PC

vehicle (PC) (with smaller dimensions) does not impede the following drivers of the HCV and does not limit their ability to look beyond the leading vehicle, the HCVs maintain lower separation. This results in lower headway values. However, the headway values are slightly higher than in the PC-LCV case due to the differences in vehicle dimensions.

The best-fitted time headway distribution for the LCV-PC is the General Extreme Value (GEV) distribution, shown in Fig. 6. The GEV distribution patterns clearly

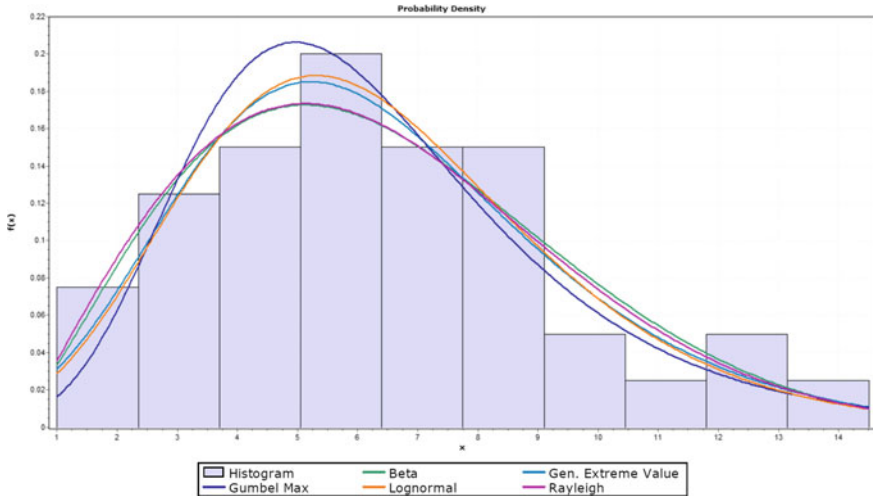


Fig. 7 Probability distribution patterns for HCV-PC

depict the effect of PC (follower) interaction with an LCV (leader). The LCV disrupts the PC movement due to its lower operational capabilities (poor intuitive steering). Furthermore, because of their relatively large size and poor lane behavior, LCVs frequently make the PC follow them [16]. Thus, the PC does not exhibit any lateral movement and hence affects the following headways of PCs.

The best-fitted time headway distribution for the HCV-PC is the beta distribution, shown in Fig. 7. When the PC interacts with a larger vehicle, such as an HCV, whose dimensions are greater than those of the LCV, the time headway maintained by the PC increases. The time headway distribution demonstrates that when the PC (follower) interacts with the HCV (leader), the distribution shifts to the right. However, the skewness of the distribution is less compared to the skewness of the distribution when the PC is interacting with another PC. The underlying reason is that the trailing PC experience higher impedance while interacting with the HCV or following an HCV. Due to its longer length and taller height, the following PC fails to anticipate the lead vehicle’s behavior, causing the follower PC to maintain higher headways with the leading HCV vehicle [17]. Another reason being the poor dynamic characteristics of the HCV does not allow the PC to change the lane and overtake, thereby restricting the lateral and longitudinal control process in disorderly traffic environments [18].

Despite the fact that PCs have faster speeds and excellent maneuverability than LCVs and HCVs [19], they must maintain longer headways with LCVs and HCVs to avoid danger and crashes. On the other hand, the LCV and HCV have inferior dynamic characteristics [20] and thus travel at lower speeds while maintaining larger headways. Because of these variable characteristics of vehicles to maintain differential headways, the headway distributions considerably vary. This indicates that the changing leader-follower combinations have an impact on the driver actions of vehicles in traffic. These findings demonstrate that the prevailing vehicle-to-vehicle

interaction characteristics determine the behavior of the traffic in maintaining a time headway. Furthermore, the probability distribution functions are interpreted to differ as the traffic condition comprising different vehicle pairs varied.

6 Conclusions

This study aimed to identify the different time headway distributions of mixed vehicular pairs during their interaction in heterogeneous traffic. The best-fit distributions are estimated based on the K-S test. The critical observations of the study are discussed below.

- This study showed that the time headway distributions vary with the nature of the vehicle-type specific leader–follower pair.
- The vehicle-type-specific analysis provided unique insights into the behavioral characteristics of various vehicle pairings.
- Subsequently, the time headway distributions tend to change in accordance with the traffic interaction conditions, thus proving the assumption of using the identical time headway distributions for varying traffic interaction conditions as probably erroneous.
- The results of the study imply that most of the commercial vehicles with weak dynamic characteristics maintain longer time headways and impose higher impedance to the following vehicles.
- The distributions aid in interpreting the riders' risky driver behavior or belligerence, directly impacting traffic safety.

The current study's findings may not be generalized as the traffic data pertains to Indian NHs. However, the methodology is generic and can be utilized to investigate vehicular driving behavior. The developed distribution models open the possibility for transportation practitioners, planners, and agencies to identify driver characteristics. Also, the study outcomes can be used to create microsimulation systems for analyzing car-following and lane-changing behavior in highway traffic. However, like any other study, this study has certain limitations, which paves the way for further research. The study is limited to analyzing time headway distributions on highway sections, which can be extended to other road sections in the future. Further, more research could be conducted to determine the time headway distributions for different vehicle combinations.

References

1. Singh S, Rajesh V, Santhakumar SM (2022) Effect of mixed traffic platooning by commercial vehicle types on traffic flow characteristics of highways. *Periodica Polytech Transp Eng* 50(4):344–356. <https://doi.org/10.3311/PPtr.18200>

2. Jang J (2012) Analysis of time headway distribution on suburban arterial. *KSCE J Civ Eng* 16:644
3. Zhang G, Wang Y, Wei H, Chen Y (2007) Examining headway distribution models with urban freeway loop event data. *Transp Res Rec* 1999:141–149
4. Jang J, Kim B, Choi N, Biak N (2011) Analysis of time headway distribution on Korean multilane highway using loop event data. *J Eastern Asian Soc Transp Stud* 9:1447–1457
5. Kong D, Guo X (2016) Analysis of vehicle headway distribution on multilane freeway considering car–truck interaction. *Adv Mech Eng* 8(4):1–12
6. Arasan V, Koshy R (2003) Headway distribution of heterogeneous traffic on urban arterials. *J Inst Eng* 84:210–215
7. Al-Ghamdi S (2001) Analysis of time headways on urban roads: case study from Riyadh. *J Transp Eng* 127:289–294
8. Maurya AK, Das S, Dey S, Nama S (2016) Study on speed and time-headway distributions on two-lane bidirectional road in heterogeneous traffic condition. *Transp Res Procedia* 17:428–437
9. Singh S, Santhakumar SM (2022) Assessing the impacts of heavy vehicles on traffic characteristics of highways under mixed traffic platooning conditions. *European Transport \ Trasporti Europei*. <https://doi.org/10.48295/ET.2022.86.3>
10. Peeta S, Zhang P, Zhou W (2004) Behavior-based analysis of freeway car–truck interactions and related mitigation strategies. *Transp Res Part B: Methodol* 39(5):417–451
11. Moridpour S, Rose G, Sarvi M (2010) Effect of surrounding traffic characteristics on lane changing behaviour. *J Transp Eng: ASCE* 136:973–985
12. Ye F, Zhang Y (2009) Vehicle type-specific headway analysis using freeway traffic data. *Transp Res Rec J Transp Res Board* 2124:222–230
13. Minge E, Kotzenmacher J, Peterson S (2010) Evaluation of non-intrusive technologies for traffic detection. Minnesota department of transportation, research services, Office of the Policy Analysis Research and Innovation, Roseville, USA. MN/RC 2010–36. <http://www.lrrb.org/PDF/201036.pdf> Accessed in Jan 2021
14. Singh S, Santhakumar SM (2021) Evaluation of lane-based traffic characteristics of highways under mixed traffic conditions by different methods. *J Inst Eng (India): Series A* 102(3):719–735. <https://doi.org/10.1007/s40030-021-00549-6>
15. Singh S, Barhmaiah B, Kodavanji A, Santhakumar SM (2020) Analysis of two-wheeler characteristics at signalised intersection under mixed traffic conditions: a case study of tiruchirappalli city, resilience and sustainable transportation systems. In: 13th Asia Pacific transportation development conference. American Society of Civil Engineers (ASCE), Shanghai, China, pp 35–43. <https://doi.org/10.1061/9780784482902.005>
16. Das S, Maurya AK (2018) Bivariate modeling of time headways in mixed traffic streams: a copula approach. *Transp Lett* 1–11. <https://doi.org/10.1080/19427867.2018.1537209>
17. Singh S, Santhakumar SM (2022) Modeling traffic parameters accounting for platoon characteristics on multilane highways. *Transp Dev Econ* 8, 30. <https://doi.org/10.1007/s40890-022-00166-3>
18. Mahapatra G, Das S, Maurya AK (2021) Joint distribution modelling of vehicle dynamic parameters using copula. *Transp Lett*. <https://doi.org/10.1080/19427867.2021.1897936>
19. Singh S, Vidya R, Shukla BK, Santhakumar SM (2021) Analysis of traffic flow characteristics based on area-occupancy concept on urban arterial roads under heterogeneous traffic scenario—a case study of Tiruchirappalli city. In: Mehta YA et al (eds) *Trends and recent advances in civil engineering (TRACE) 2020, advances in water resources and transportation engineering, lecture notes in civil engineering*. Springer Nature, Singapore, vol 149, pp 69–84. https://doi.org/10.1007/978-981-16-1303-6_6
20. Singh S, Santhakumar SM (2021) Empirical analysis of impact of multi-class commercial vehicles on multilane highway traffic characteristics under mixed traffic conditions. *Int J Transp Sci Technol* 11(3):545–562. <https://doi.org/10.1016/j.ijst.2021.07.005>

Deep Bi-LSTM Neural Network for Short-Term Traffic Flow Prediction Under Heterogeneous Traffic Conditions



Kranti Kumar  and Bharti 

Abstract Continuous expansion of cities has resulted in the growing traffic network to cater the demand of increasing number of vehicles. The rapid growth in population, unplanned development, and inadequate infrastructure have led to several problems like pollution and traffic congestion. Traffic congestion is one such issue with which not only metropolitan cities but also medium and small cities are dealing on day-to-day basis. Intelligent transportation system (ITS) helps in providing relief to the traffic congestion-related problems. Accurate prediction of short-term traffic flow is an important pillar of ITS. Several researchers have tried to model and predict traffic flow using different methods/techniques. Heterogeneous traffic flow makes traffic studies often more critical and challenging. This study aims to find the optimal deep bidirectional long short-term memory (LSTM) neural network to predict the short-term traffic flow under heterogeneous traffic conditions. Real data from an urban location in Delhi was collected using video cameras. Deep learning techniques like LSTM neural network and bidirectional long short-term memory (Bi-LSTM) neural network (NN) were used in this study to predict the traffic flow for the next 5 min using collected data. It was found that Bi-LSTM neural network with 2 layers gives better results as compared to LSTM NN, single-layer Bi-LSTM NN, and three-layered Bi-LSTM NN.

Keywords Road traffic flow · Heterogeneous traffic · Bi-LSTM neural network · Deep learning

1 Introduction

In a developing country, its major as well as medium and small cities constantly undergo many changes due to rising population and travel demands. This results in soaring number of vehicles especially in peak hours due to more travel demand of people working in diverse areas and results in heterogeneous traffic flow. These traffic

K. Kumar (✉) · Bharti

School of Liberal Studies, Dr. B. R. Ambedkar University Delhi, Delhi, India

e-mail: kranti@aud.ac.in

conditions can include heavy trucks, buses, fast-moving bikes, cars to lightweight and slow-going e-rickshaws, and bicycles, all commuting on the same road at the same time with different moving style and speed, and without proper lane discipline. This makes driving in the city more difficult and time consuming than on highways. One can clearly observe this phenomenon from Fig. 1 taken during data collection for this study where in (a) bicycle is in between of the road with heavy traffic and in (b) heavy vehicles like trucks are moving in the same lane as cars and bikes without any discipline. Not just these elements but also rising vehicles create a situation of chaos. Such a diverse range of vehicles of different proportions and speed results in slowing down the traffic flow and leads to congestion [2]. These conditions give rise to more variables which result in more complex nonlinear problems for modeling. This makes it very tough to use usual macroscopic and microscopic models of traffic flow prediction. Also, it becomes necessary to use parameters of different vehicles separately for short-term prediction which is a critical component of ITS.

ITS plays a very important role in the development of new and efficient type of transportation network that is observed in many developed countries. With some planning and modifications, these systems can be implemented in Indian traffic network as well. Its applications focus on many aspects including safety of passengers and vehicles, traffic congestion reduction, public transportation systems, optimal traffic flow, and routing of vehicles.

Many fundamental properties of traffic like sources and dynamics of overcrowding of vehicles can be explained by traffic flow. With the given conditions of traffic in India, it becomes difficult to predict the traffic flow and other parameters by applying simple mathematical or statistical models. The literature shows that various statistical techniques were used for short-term traffic flow prediction including auto-regressive integrated moving average (ARIMA) [23], SARIMA [21, 24], Kalman filter method [3, 17], and support vector machines (SVM) [28]. However, these methods cannot describe the complicated nonlinearity, heterogeneity, and uncertainty of the traffic flow precisely. Also, they cannot express small changes in parameters as they are free from dependency on short-term data. Mathematical models cannot capture the



Fig. 1 Heterogeneous traffic at a location in Delhi, India, during peak hours

randomness and uncertainty of traffic behavior accurately. Neural networks and deep learning methods like LSTM NN and hybrid models have significantly boosted the prediction accuracy as compared to traditional methods with the use of big data. These methods have been used in various fields of computer science, but they also improved accuracy in prediction of various parameters in road traffic theory. Most of the studies reported in the literature use data collected from lane disciplined traffic under homogeneous conditions for traffic flow prediction. Models based on these assumptions do not work well under Indian traffic conditions where most of the traffic is heterogeneous in nature. It becomes necessary to find the methods/techniques which are suitable for Indian traffic conditions. This study attempts to model and predict the traffic flow under heterogeneous conditions and to find optimal deep bidirectional LSTM neural network architecture for this purpose. Prior traffic flow information obtained through the proposed model will be helpful for traffic planners to take suitable actions on the spot like traffic diversion to tackle the possible traffic congestion formation.

2 Literature Survey

In the beginning, Bi-LSTM neural network was mainly used for the natural language processing, image processing, and speech recognition [4, 8, 14, 19]. It has been used less extensively for road traffic flow prediction [7, 12, 34, 36]. LSTM and Bi-LSTM neural networks in past have been used in traffic networks for trajectory prediction [19], traffic speed prediction [13, 31], and accident prediction [1]. To the best of author's knowledge, this method has not been used for short-term traffic prediction in heterogeneous traffic conditions.

Vlahogianni et al. [29] have done an analysis of traffic flow prediction for statistical, hybrid, and neural network-based methods. They described the challenges faced in traffic flow prediction including freeway and arterial networks, type of data associated with traffic management, quality of data, and use of new technology for prediction. Do et al. [11] and Li et al. [18] reviewed different models related to neural networks for short-term road traffic prediction and outlined the importance and dominance of deep learning models including LSTM and Bi-LSTM neural network. Kumar et al. [15, 16] have done short-term traffic flow prediction for non-urban highway in 2013 and included the perspective of heterogeneous traffic situation in their study conducted in 2015. They used multi-layer perceptron (MLP) neural networks for traffic flow prediction using historical data.

Since basic NN structure fails to apprehend the deep characteristics of traffic flow, Wang et al. [32] proposed a deep bidirectional LSTM (DBL) neural network. They used residual connections in between the subsequent layers followed by a layer of average pooling. To solve the problem of overfitting, a dropout method was used. This method was proved to be more accurate as compared to other statistical models. The same authors later took influence of precipitation factor and tourist destination into consideration [33]. They took additional data as input using one-hot encoding

due to which this method is called P-DBL. Addition of extra factors has enhanced the results from DBL.

A technique namely deep urban traffic flow prediction framework (DST) was used by Wang et al. [30]. Convolutional neural network (CNN) along with LSTM neural network was used to extract both spatial and temporal features. This method gives better results than normal single-layer Bi-LSTM, HA (historical average), ARIMA, and support vector regression (SVR).

Cui et al. [10] used a stacked bidirectional and unidirectional LSTM (SBU-LSTM). This method tackles the problem of missing values by masking mechanism which can predict freeway traffic networks. It was shown that appending more layers of LSTM/Bi-LSTM neural network, adding more spatial features like volume and occupancy of vehicles, the dimension of weight matrices improves the results significantly. In 2020, Cui et al. [9] used the same method with missing values, added an imputation unit, and proposed a data imputation mechanism in LSTM (LSTM-I) neural network. This network was then consolidated in the structure of SBU-LSTM. It was shown that Bi-LSTM neural network outperforms the time series forecasting by Siami et al. [27]. It was observed that the extra number of training layers that can be appended to tune the variables resulted in better performance by Bi-LSTM neural network.

An approach to consider spatial factors and correlation between the chosen and surrounding road was proposed by Liu et al. [20]. Hierarchical attention was used to emphasize the variables at each step. The spatial-temporal attention was applied, after which the temporal attention was used in the decoder using two different Bi-LSTM networks. The proposed method performs better than LSTM, gated recurrent neural network (GRU), and SVR. Park et al. [25] used Bi-LSTM neural network and K-NN to discover the major time zones of overloaded vehicles to reduce accidents. A path-based deep learning approach using Bi-LSTM neural network to forecast the traffic speed was given by Wang et al. [31]. They used multiple layers of Bi-LSTM NN to include spatial and temporal characteristics of various paths of the network, and then, the results were amalgamated for the prediction.

Bi-LSTM network for the prediction of traffic flow on expressway was used by Xue et al. [35]. A hybrid deep learning model with attention-based Conv-LSTM neural network to bring out intrinsic properties of the short-term traffic flow was investigated by Zheng et al. [37]. This method considers both daily and weekly periods. Attention mechanism allocates the different amounts of attention to the traffic flow at a separate time. The proposed method outperforms all other methods even for extended predictions. Pearson Correlation Coefficient (PCC) and Bi-LSTM neural network were combined by Zou et al. [38] to forecast short-term traffic flow. PCC measures the degree of correlation between two time series and hence was used to extract the spatial features and Bi-LSTM NN for the temporal characteristics. The performance of PCC-Bi-LSTM was better than Bi-LSTM and LSTM alone. Ma et al. [22] used time series analysis and combined LSTM NN with Bi-LSTM neural network after standardizing the data. This method has given better results than single LSTM NN, Bi-LSTM NN, and RNN.

3 Methodology

The idea of Bi-LSTM came from bidirectional RNN (BRNN) which was first introduced by Schuster and Paliwal [26]. This network processes sequential data in both forward and backward directions with two separate hidden layers. It connects two hidden layers to the same output layer. During the training process, BRNN is trained in both forward and backward directions. In practice, this structure requires to duplicate the first recurrent layer in the network so that there are two adjacent layers, and then, in the first layer, an input is provided in a sequence after which a reversed copy of the input sequence is sent to the second layer [5].

Figure 2 shows the working of one LSTM unit with different gates, and Fig. 3 represents the architecture of a Bi-LSTM network. In Bi-LSTM neural network, the forward layer output sequence, \vec{h} , is iteratively calculated using inputs in a positive sequence from time $T - n$ to time $T - 1$, while the backward layer output sequence, \overleftarrow{h} , is calculated using the reversed inputs from time $T - n$ to $T - 1$. In a unit cell of LSTM network, the sequence has to pass through three gates. These gates help in reducing the error of backpropagation created by vanishing gradient. It does so by these sigmoid layers by deciding which data is redundant and which one is important.

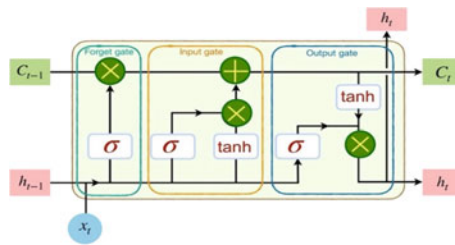


Fig. 2 Internal mechanism of a single LSTM cell

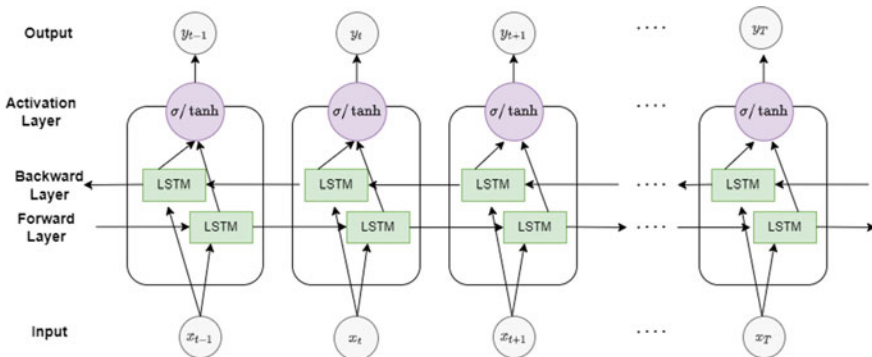


Fig. 3 Structure of one Bi-LSTM unit

Now using the working equations of one LSTM cell, the network processes input sequence $x = (x_1, x_2, \dots, x_N)$ by iteration from $n = 1$ to N in following steps described by Eqs. 1–4:

$$f_t = \sigma(W_f x_t + U_f h_{t-1} + b_f) \quad (1)$$

$$i_t = \sigma(W_i x_t + U_i h_{t-1} + b_i) \quad (2)$$

$$g_t = \tanh(W_g x_t + U_g h_{t-1} + b_g) \quad (3)$$

$$o_t = \sigma(W_o x_t + U_o h_{t-1} + b_o) \quad (4)$$

where W 's and U 's are weights of input and recurring connections, f , i , g , o , are the forget, input, part of the input, and output gates, respectively, defined by Eqs. 1–4, b 's are the biases, and σ and \tanh are the activation functions used. Along with these gates, the current internal cell state C_t and current hidden state h_t are defined by Eqs. 5 and 6, respectively:

$$C_t = i_t \cdot g_t + f_t \cdot C_{t-1} \quad (5)$$

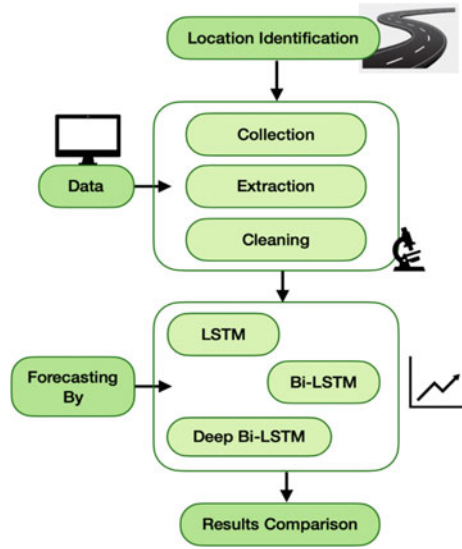
$$h_t = o_t \cdot \tanh(C_t) \quad (6)$$

Additionally, in Bi-LSTM a final output Y_t is generated. Here, each element is calculated by $y_t = \sigma(\vec{h}_t, \overleftarrow{h}_t)$ and the final output is written as $Y_T = [y_{T-n}, \dots, y_{T-1}]$. Figure 4 describes the overall methodology adopted in this study for short-term traffic flow prediction. The study began with identifying location based on the number of intersections, traffic lights, and presence of foot over bridge to collect the data. Next, the collected data was processed, followed by application of different methods for the prediction. Present study utilizes different features of heterogeneous traffic in the stacked Bi-LSTM neural network for short-term traffic prediction to get the desired results.

3.1 Evaluation Metrics

To evaluate the performance of the given models, mean absolute error (MAE), root mean squared error (RMSE), coefficient of correlation (r), and mean absolute percentage error (MAPE) were used. These metrics are defined by Eqs. 7–10. MAE and RMSE are the loss functions that are used to update weights in order to minimize the loss. A smaller error value indicates a more effective model, and the value of r closer to 1 indicates good prediction results.

Fig. 4 Overview of steps involved in the traffic flow prediction



$$MAE = \frac{1}{N} \sum_{i=1}^N |\hat{y} - y_i| \tag{7}$$

$$RMSE = \sqrt{\frac{1}{N} \sum_{i=1}^N (\hat{y} - y_i)^2} \tag{8}$$

$$r = \frac{\sum (\hat{y} - \bar{y})(y_i - \bar{y})}{\sqrt{\sum (\hat{y} - \bar{y})^2 (y_i - \bar{y})^2}} \tag{9}$$

$$MAPE = \frac{1}{N} \sum_{i=1}^N \left| \frac{\hat{y} - y_i}{y_i} \right| * 100 \tag{10}$$

where \hat{y} , and \bar{y} are predicted and mean values of y_i , the observed target vectors; N is the number of samples.

4 Data Collection and Extraction

The primary data used for this study has been collected at the Inner Ring Road, South Extension-II (28°34' 7.41'', 77°13' 3.38''), Delhi, India, from the foot over bridge (Fig. 5). The highway chosen was of three lanes on both sides where a trap of 15 m was marked to collect the necessary data. This location was chosen since it represents

an urban road, and the volume of traffic was in masses. During peak hours, it leads to congestion as well, not just this but the mixed nature of traffic was appealing.

Data was collected from both sides of the road during the peak hours, i.e., 8–11 am and 4:30–7 pm for the five days in February 2020. Moreover, it has been observed that the volume of traffic at each peak hour on both sides was different, i.e., high on one side and low on other side in the morning and vice-versa in the evening, which can be seen in the Fig. 6. To obtain variables for heterogeneous traffic, all the vehicles were divided into 7 categories: C/V/J (car/van/jeeep), 2 W (two-wheelers), 3 W (three-wheelers), bus, LCV (light commercial vehicles, i.e., minibus/ambulance, etc.), truck, and B/R (bicycles/rickshaw). For each of these categories, the volume and average speed have been calculated manually from the video in the intervals of 5 min and stored in excel sheets. This in total gave 660 data points for each category including both sides. However, if we choose the data only from one side, that will give 330 data points, which are quite less for training and testing in deep learning, and may result in giving poor predictions.

Under heterogeneous traffic conditions, it becomes very important to include passenger car units (PCUs) [6] to give proper weightage to dimensions of different vehicle categories. Since dimension of vehicles varies significantly from one category to another, PCU acts as a factor to adjust vehicles with different dimension other than cars. There are various methods to calculate PCU depending on the traffic parameters that are taken into consideration. Since this study contains both speed and volume as primary variables, PCU has been calculated using the Eq. 11, which was proposed by Chandra and Sikdar [6]:

$$PCU_i = Q_i \frac{V_c/V_i}{A_c/A_i} \quad (11)$$

where i denotes the category of vehicles, Q_i , V_i , and A_i are speed, volume, and area for each category, and c denotes the category of cars.



Fig. 5 Handycam setup at foot over bridge for data collection

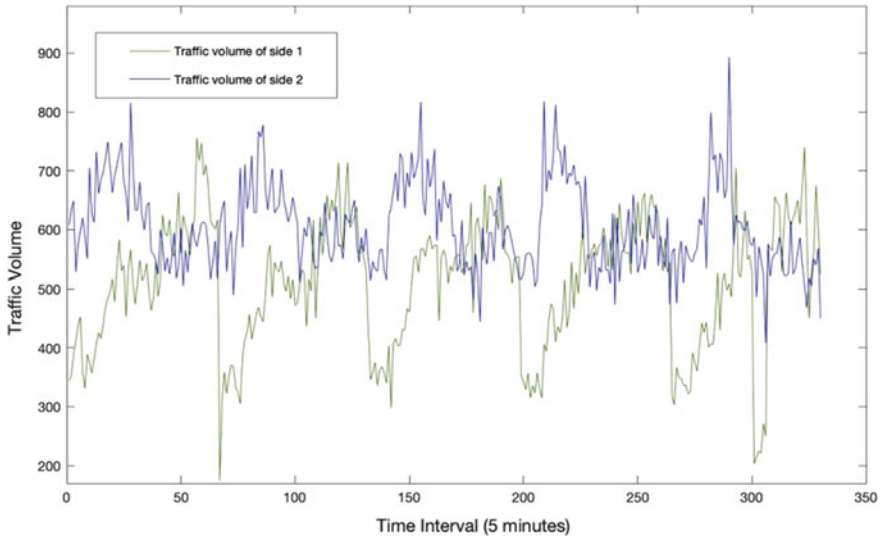


Fig. 6 Traffic volume of both sides of the location for fifth day

5 Results and Discussion

The extracted dataset contains 17 parameters including day, time of the day, categorized volume (7 categories of vehicles), and corresponding speed of vehicles, and one parameter to be predicted is the traffic flow. Total 660 datasets were used in this study. Out of 660 datasets, 462 datasets were used for training and 198 datasets were used for testing purpose. All considered models were trained and tested using the same amount of datasets. Deep learning methods used in this study were implemented in MATLAB R2020a. In the LSTM and Bi-LSTM networks, first layer consists of an input sequence where all 16 input variables were taken in the array; then, in the second layer LSTM/Bi-LSTM network has been implemented with features described in the Table 1. Table 2 describes hyperparameters, which were common throughout the training and testing of all the models. Hit and trial approach was used to obtain the optimum values for these hyperparameters. Outputs of second layer are then passed through fully connected layer leading to regression output layer creating sequence-to-sequence. In the case of a stacked Bi-LSTM network, two layers of Bi-LSTM NN have been added simultaneously with other layers being the same. However, when more than two layers have been added, effectiveness, i.e., time consumption of the program, increased a lot with increased errors. Framework of layers in deep Bi-LSTM network is shown in the Fig. 7.

The number of neurons for each category has been taken as 100, 150, and 200, and the numbers of epochs were gradually increased from 200 up to 500 in the steps of 100. These numbers were chosen by hit and trial method to obtain the optimized results. Stopping criterion was the threshold where either the error started increasing

Table 1 Structure of deep neural network models

Network name	Input variables	Output variable	Activation function	Number of layers
LSTM	Speed, volume, time	Traffic flow	Sigmoid, hyperbolic tangent	1
Bi-LSTM	Speed, volume, time	Traffic flow	Sigmoid, hyperbolic tangent	1
Deep Bi-LSTM	Speed, volume, time	Traffic flow	Sigmoid, hyperbolic tangent	2
Deep Bi-LSTM	Speed, volume, time	Traffic flow	Sigmoid, hyperbolic tangent	3

Table 2 Model hyperparameters for LSTM/Bi-LSTM neural network

Gradient threshold	0.001
Initial learning rate	0.11
Minimum batch size	22
Solver for training	adam
Learning rate schedule	piecewise
Learning rate drop period	20
Learning rate drop factor	0.4

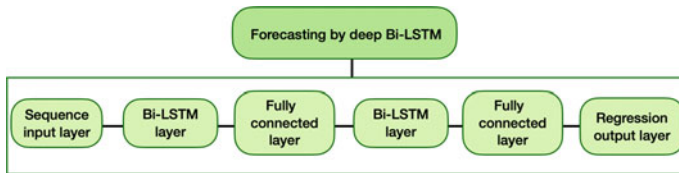


Fig. 7 Framework of layers in deep Bi-LSTM network

or the time taken by network for training was more than the previous architecture. Hence, when the values of these features were increased more than the shown values in the Table 3, it resulted in poor prediction. It can be observed from Table 3 that the stacked Bi-LSTM with two layers gave significantly better results for multi-variate conditions as compared to LSTM, Bi-LSTM, and stacked Bi-LSTM NN with three layers. Two-layered Bi-LSTM was able to minimize the MAPE by less than 1.3% and RMSE less than 10.9 and obtained r as 0.9996 which is closer to 1.

Figures 8 and 9 represent the observed and predicted traffic flow during the training and testing stage obtained from 2-layer Bi-LSTM neural network. It can be clearly noticed that the difference between observed and predicted values is much less during the testing stage in Fig. 9. Prediction performance of best architecture of LSTM

Table 3 Performance comparison of different deep neural network models

Model	Training	NHL	NHN	NOE	MAE	RMSE	r	MAPE
LSTM	1	1	100	500	13.6079	19.0601	0.9988	2.4505
	2			400	13.5284	18.9612	0.9988	2.4361
	3			300	13.8975	19.4252	0.9988	2.5030
	4			200	14.3019	19.9456	0.9987	2.5761
	5	1	150	500	11.0355	15.9713	0.9992	1.9855
	6			400	10.6621	15.5409	0.9992	1.9195
	7			300	11.2245	16.1927	0.9991	2.0191
	8			200	11.6673	16.7073	0.9991	2.0990
	9	1	200	500	9.6198	14.3868	0.9993	1.7361
	10			400	9.7025	14.4747	0.9993	1.7507
	11			300	9.9747	14.7666	0.9993	1.7987
	12			200	10.3555	15.1873	0.9992	1.8657
Bi-LSTM	1	1	100	500	9.9371	14.7262	0.9993	1.7920
	2			400	10.0118	14.8065	0.9993	1.8052
	3			300	10.1895	15.0009	0.9993	1.8365
	4			200	10.5124	15.3670	0.9992	1.8932
	5	1	150	500	9.0615	13.8035	0.9994	1.6376
	6			400	8.7904	13.5216	0.9994	1.5897
	7			300	9.4008	14.1568	0.9993	1.6974
	8			200	9.8988	14.6854	0.9993	1.7853
	9	1	200	500	7.3916	11.9640	0.9995	1.3460
	10			400	7.3054	11.8644	0.9995	1.3310
	11			300	7.7987	12.4364	0.9995	1.4168
	12			200	8.3060	12.9982	0.9994	1.5051
Stacked Bi-LSTM	1	2	100	500	8.1690	12.8491	0.9995	1.4813
	2			400	8.0226	12.6913	0.9995	1.4558
	3			300	8.4350	13.1392	0.9994	1.5275
	4			200	8.6756	13.4002	0.9994	1.5694
	5	2	150	500	7.6432	12.2541	0.9995	1.3898
	6			400	7.7227	12.3465	0.9995	1.4036
	7			300	7.9460	12.6088	0.9995	1.4424
	8			200	8.3716	13.0696	0.9994	1.5165
	9	2	200	500	6.6401	10.8469	0.9996	1.2951
	10			400	6.8066	10.9946	0.9996	1.3286
	11			300	7.0292	11.1835	0.9996	1.3728
	12			200	7.0539	11.5681	0.9996	1.2875

(continued)

Table 3 (continued)

Model	Training	NHL	NHN	NOE	MAE	RMSE	r	MAPE
Stacked Bi-LSTM	1	3	100	500	8.4598	13.1665	0.9995	1.5318
	2			400	8.4966	13.2069	0.9994	1.5382
	3			300	8.4350	13.1392	0.9994	1.5275
	4			200	8.8127	13.5453	0.9994	1.5936
	5	3	150	500	7.8284	12.4717	0.9995	1.4219
	6			400	8.0526	12.7236	0.9995	1.4610
	7			300	8.2658	12.9543	0.9995	1.4981
	8			200	8.5212	13.2335	0.9994	1.5425
	9	3	200	500	6.9068	11.0805	0.9996	1.3487
	10			400	6.7030	10.9038	0.9996	1.3078
	11			300	7.0975	11.2411	0.9996	1.3862
	12			200	7.3166	11.4315	0.9996	1.4286

NHL number of hidden layers; *NHN* number of hidden neurons; *NOE* number of epochs

NN, Bi-LSTM NN, 2-layer Bi-LSTM, and 3-layer Bi-LSTM has been shown in the Fig. 10. It is apparent from Fig. 10 that 2-layer Bi-LSTM neural network has less prediction error as compared to other models which proves its better prediction performance under heterogeneous traffic conditions.

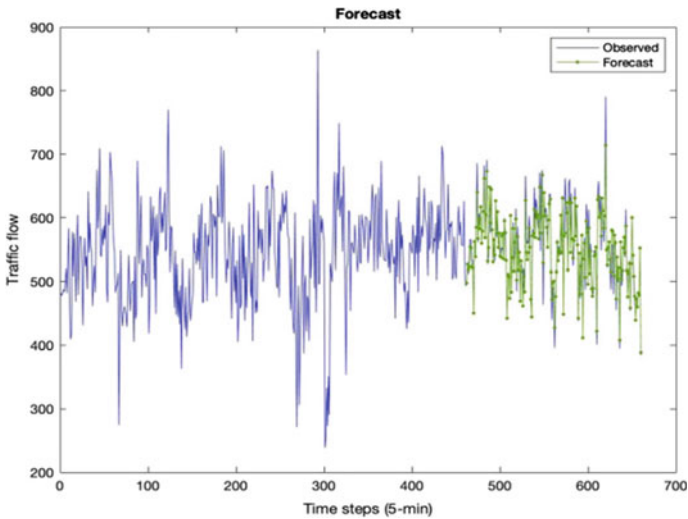


Fig. 8 Observed and predicted traffic flow during training stage (2-layer Bi-LSTM NN)

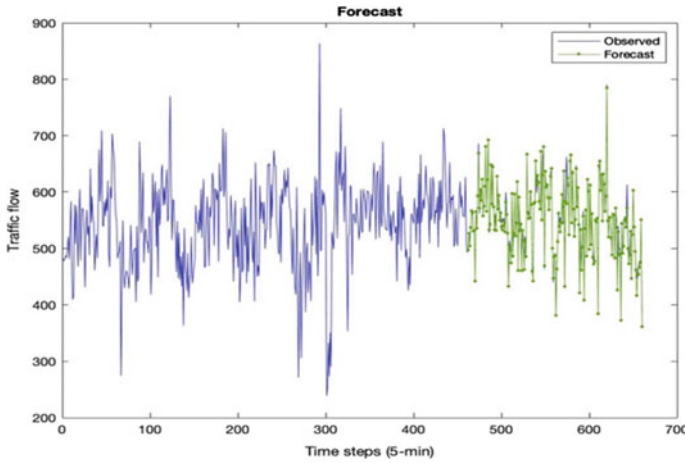


Fig. 9 Observed and predicted traffic flow during the testing stage (2-layer Bi-LSTM NN)

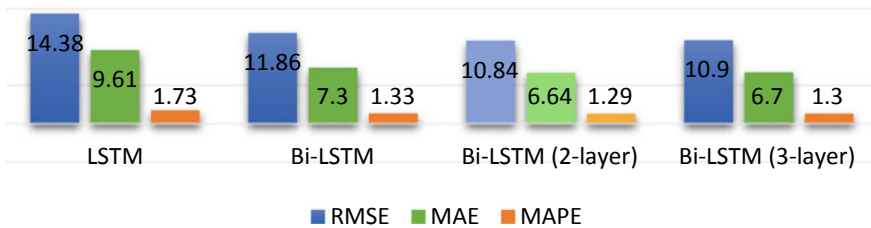


Fig. 10 Prediction performance of used models

6 Conclusions

This study applied LSTM, Bi-LSTM, and deep Bi-LSTM neural networks to predict the short-term traffic flow for next 5-min interval. These models were successful to capture the features of heterogeneous traffic. The result and effectiveness of these models were compared on the basis of error functions like MAE, MAPE, RMSE, and the coefficient of correlation (r). Weights in the models were updated according to these error layers to optimize the loss. It was also observed that when the numbers of layers in Bi-LSTM were increased from one to two, the results significantly improved but upon further increasing the number of layers from two to three, the performance of model dropped. It was found that deep Bi-LSTM neural network with two layers produced results with best accuracy as compared to its counterparts. In future, the model can be extended using attention mechanism focusing on particular variables affecting the traffic flow like buses or trucks. Also, the robustness of the models can be increased by collecting more data for better training and testing.

Acknowledgements “Authors are thankful to the University Grants Commission (UGC), New Delhi, India, for providing financial support to carry out this study through the start-up grant project *Modeling and simulation of vehicular traffic flow problems* via the grant No. F.30-403/2017(BSR). Authors also convey their gratitude to anonymous reviewers for their valuable suggestions which significantly improved this article.”

References

1. Ali F, Ali A, Imran M, Naqvi RA, Siddiqi MH, Kwak KS (2021) Traffic accident detection and condition analysis based on social networking data. *Accid Anal Prev* 151:105973
2. Arasan VT, Divya G (2008) Measuring heterogeneous traffic density. *World Acad Sci Eng Technol* 46:342–346
3. Emami A, Sarvi M, Bagloee SA (2019) Short-term traffic flow prediction based on faded memory Kalman Filter fusing data from connected vehicles and Bluetooth sensors. *Simul Model Pract Theory* 102025
4. Bin Y, Yang Y, Shen F, Xu X, Shen HT (2016) Bidirectional long-short term memory for video description. In: *Proceedings of the 24th ACM international conference on Multimedia*, pp 436–440
5. Brownlee J (2017) Long short-term memory networks with python: develop sequence prediction models with deep learning. *Mach Learn Mastery*
6. Chandra S, Sikdar PK (2000) Factors affecting PCU in mixed traffic situations on urban roads. *Road Transp Res* 9(3):40–50
7. Chen YY, Lv Y, Li Z, Wang FY (2016) Long short-term memory model for traffic congestion prediction with online open data. In: *19th international conference on intelligent transportation systems (ITSC)*, IEEE, pp 132–137
8. Cornegruta S, Bakewell R, Withey S, Montana G (2016) Modelling radiological language with bidirectional long short-term memory networks. *arXiv preprint [arXiv:1609.08409](https://arxiv.org/abs/1609.08409)*
9. Cui Z, Ke R, Pu Z, Wang Y (2020) Stacked bidirectional and unidirectional LSTM recurrent neural network for forecasting network-wide traffic state with missing values. *Transp Res Part C: Emerg Technol* 118:102674
10. Cui Z, Ke R, Pu Z, Wang Y (2018) Deep bidirectional and unidirectional LSTM recurrent neural network for network-wide traffic speed prediction. *arXiv preprint [arXiv: 1801.02143](https://arxiv.org/abs/1801.02143)*
11. Do LN, Taherifar N, Vu HL (2019) Survey of neural network-based models for short-term traffic state prediction. *Wiley Interdisc Rev: Data Min Knowl Discovery* 9(1):e1285
12. Duan Y, Yisheng LV, Wang FY (2016) Travel time prediction with LSTM neural network. In: *19th international conference on intelligent transportation systems (ITSC)*, IEEE, pp 1053–1058
13. Elmi S (2020) Deeo stacked residual neural network and bidirectional LSTM for speed prediction on real-life traffic data. In: *Proceedings of the 24th European conference on artificial intelligence*
14. Graves A, Jaitly N (2014) Towards end-to-end speech recognition with recurrent neural networks. In: *International conference on machine learning*, pp 1764–1772
15. Kumar K, Parida M, Katiyar VK (2013) Short term traffic flow prediction for a non urban highway using artificial neural network. *Procedia Soc Behav Sci* 104:755–764
16. Kumar K, Parida M, Katiyar VK (2015) Short term traffic flow prediction in heterogeneous condition using artificial neural network. *Transport* 30(4):397–405
17. Kumar SV (2017) Traffic flow prediction using kalman filtering technique. *Procedia Eng. The Author(s)*, 187:582–587
18. Li W, Wang J, Fan R, Zhang Y, Guo Q, Siddique C, Ban XJ (2020) Short-term traffic state prediction from latent structures: accuracy versus efficiency. *Transp Res Part C: Emerg Technol* 111:72–90

19. Liu H, Lee I (2017) End-to-end trajectory transportation mode classification using Bi-LSTM recurrent neural network. In: 12th international conference on intelligent systems and knowledge engineering (ISKE), IEEE, pp 1–5
20. Liu D, Tang L, Shen G, Han X (2019) Traffic speed prediction: an attention-based method. *Sensors* 19(18):3836
21. Tan MC, Wong SC, Xu JM, Guan ZR, Zhang P (2009) An aggregation approach to short-term traffic flow prediction. *IEEE Trans Intell Transp Syst* 10(1):60–69
22. Ma C, Dai G, Zhou J (2022) Short-term traffic flow prediction for urban road sections based on time series analysis and LSTM_BiLSTM method. *IEEE Trans Intell Transp Syst* 23(6): 5615–5624
23. Hamed MM, Al-Masaeid HR, Said ZMB (1995) Short-term prediction of traffic volume in urban arterials. *J Transp Eng* 121(3):249–254
24. Omkar G, Vasantha Kumar S (2017) Time series decomposition model for traffic flow forecasting in urban midblock sections. In: International conference on smart technologies for smart Nation, pp 720–723
25. Park S, On BW, Lee R, Park MW, Lee SH (2019) A BiLSTM and k-NN based method for detecting major time zones of overloaded vehicles. *Symmetry* 11(9):1160
26. Schuster M, Paliwal KK (1997) Bidirectional recurrent neural networks. *IEEE Trans Signal Process* 45(11):2673–2681
27. Siami-Namini S, Tavakoli N, Namin AS (2019) The performance of LSTM and BiLSTM in forecasting time series. In: 2019 international conference on big data, IEEE, pp 3285–3292
28. Theja PVVK, Vanajakshi L (2010) Short term prediction of traffic parameters using support vector machines technique. In: 3rd International conference on emerging trends in engineering and technology, pp 70–75
29. Vlahogianni EI, Karlaftis MG, Golias JC (2014) Short-term traffic forecasting: Where we are and where we're going. *Transp Res Part C: Emerg Technol*, pp 3–19
30. Wang J, Cao Y, Du Y, Li L (2019) DST: a deep urban traffic flow prediction framework based on spatial-temporal features. In: International conference on knowledge science, engineering and management, Springer, pp. 417–427
31. Wang J, Chen R, He Z (2019) Traffic speed prediction for urban transportation network: a path based deep learning approach. *Transp Res Part C: Emerg Technol* 100:372–385
32. Wang J, Hu F, Li L (2017) Deep bi-directional long short-term memory model for short-term traffic flow prediction. In: International conference on neural information processing. Springer, Cham, pp. 306–316
33. Wang J, Hu F, Xu X, Wang D, Li L (2018) A deep prediction model of traffic flow considering precipitation impact. In: International joint conference on neural networks (IJCNN), IEEE, pp 1–7
34. Wu Y, Tan H (2016) Short-term traffic flow forecasting with spatial-temporal correlation in a hybrid deep learning framework. arXiv preprint [arXiv:1612.01022](https://arxiv.org/abs/1612.01022)
35. Xue X, Jia Y, Wang S (2020) Expressway traffic flow prediction model based on Bi-LSTM neural networks. In: IOP conference series: Earth and environmental science 587(1): 012007. IOP Publishing
36. Yu R, Li Y, Shahabi C, Demiryurek U, Liu Y (2017) Deeo learning: a generic approach for extreme condition traffic forecasting. In: SIAM international Conference on Data Mining. Society for Industrial and Applied Mathematics, pp 777–785
37. Zheng H, Lin F, Feng X, Chen Y (2020) A hybrid deep learning model with attention-based conv-LSTM networks for short-term traffic flow prediction. *IEEE Trans Intell Transp Syst* 22(11): 6910–6920
38. Zou H, Wu Y, Zhang H, Zhan Y (2020) Short-term traffic flow prediction based on PCC-Bi-LSTM. In: International conference on computer engineering and application (ICCEA), IEEE, pp 489–493

Delay Variability Analysis at Intersections Using Public Transit GPS Data



Arathy Lal, Raviraj H. Mulangi, and M. M. Harsha

Abstract India is competing with the fastest-growing countries in the world in terms of urbanization and development. Rapid urbanization and motorization have led to congestion in urban roads in India. Delay forms a significant part of congestion. It is necessary to analyze variability in delay for mitigation of traffic congestion. In recent years, GPS data has emerged as a novel data source for traffic state monitoring and analysis due to its better accuracy, coverage, and accessibility. However, little work has been done for control delay estimation especially in Indian traffic condition. In this paper, an attempt has been made to estimate control delay at selected intersections in Mysore city using GPS data from transit buses. A vehicle trajectory-based formulation is adopted for the estimation of delay. The results are fitted to statistical distributions to analyze variability in delay. Kolmogorov- Smirnov (K-S) test for goodness of fit is used to estimate best fitting distribution. Generalized extreme value (GEV) distribution is found to best-fit delay in terms of fitting performance, robustness, and accuracy. The performance analysis indicates greater variability in delay during morning and evening peak hours. Successful estimation of delay variability allows for the analysis of traffic state at various intersections, thus paving the way for effective congestion mitigation.

Keywords Control delay · Vehicle trajectory · Delay variability · Public transport system · Intelligent transport system

A. Lal · R. H. Mulangi (✉)

Department of Civil Engineering, National Institute of Technology Karnataka, Surathkal, India
e-mail: ravirajmh@nitk.edu.in

M. M. Harsha

Department of Civil Engineering, Siddaganga Institute of Technology, Tumakuru, India

1 Introduction

Developing countries like India are undergoing rapid urbanization and motorization. Urbanization in India is occurring at a very rapid rate compared to developed countries like the U.S. or U.K. Urbanization often results in gridlocks and congestion. India has experienced this trend in the recent period. According to the 2011 census, the urban population in India increased from 290 million in 2001 to 377 million in 2011, accounting for about 30% of the country's population. With an increase in urban population has come increased mobility and an associated increase in vehicle ownership. The annual vehicle growth rate in India is expected to grow at a rate higher than the population growth rate. With the tremendous increase in vehicle population has come problems of traffic congestion, accidents and deteriorating air quality.

Traffic congestion results in loss of productive time of motorists and passengers, energy loss, and increased pollution. Traffic congestion results in a decrease in employment hours and negatively impacts the country's economy. It is nearly impossible to experience congestion-free mobility in metropolitan cities, especially during peak hours. Problems of congestion need to be addressed to ensure a smooth flow of traffic. Traffic congestion may be recurring congestion or non-recurring congestion [1]. Recurring congestion occurs periodically or routinely, which makes it predictable. Non-recurring congestion occurs due to unpredictable causes such as a vehicle accident, breakdown, or weather conditions. Signalized intersections are one of the hotspots of recurring urban traffic congestion. A major component of this congestion is delay. Congestion is the delay a vehicle causes to another vehicle. As the number of vehicles increases, delay increases which in turn causes increased congestion. Traffic congestion has always been a key issue in metropolitan and urban cities. It is, therefore, necessary to study and quantify delay to address the issue of traffic congestion. A large amount of data is required to study delay at signalized intersections.

Developed countries use automatic traffic data collection systems such as loop detectors, acoustic sensors, radars, image processing, or even artificial intelligence-based sensors. However, the data collection methods commonly adopted in India are manual, which makes the studies time-consuming and tedious. Automatic vehicle monitoring (AVM) systems of the public transit system, which have become an integral part of intelligent transport system (ITS) provide automatic vehicle location (AVL) data. Implementation of ITS in many metropolitan cities of India has made the availability of AVL data easier. This bus-based data may be used to estimate control delay at signalized intersections. AVL data comprises location data collected from GPS receivers installed in advanced transit vehicles. The data provides spatio-temporal information such as position, velocity, and timestamp describing the behavior of a vehicle. Applications of AVL data include identification of congestion and bottlenecks, analysis of driver behavior, estimation of control delay at signalized intersections, etc. Thus, AVL data from transit buses proves appropriate as probe data for delay studies.

Delay experienced at the signalized intersection often depends on arrival and departure of vehicles, signal timings, queue length, land use pattern of the area, time of day, etc. A longer delay is experienced at peak hours compared to the non-peak hours. Traffic engineers who desire to tackle the problems of congestions need to analyze this variability in the delay before suggesting recommendations or improvements. Delay variability analysis is critical in the evaluation of the performance of intersections under various traffic conditions. However, modeling delay variability is complex because of the non-uniform arrival and departure of vehicles at intersections. Various studies have been conducted to understand delay variability. The most common method of analysis of delay variability is by the use of statistical distributions. In the present study, an attempt has been made to estimate control delay at various signalized intersections in Mysore city and analyze variability in the delay using statistical distributions.

2 Literature Review

Traffic congestion is a major issue in many cities in India. Modeling traffic congestion on urban roads has always been a key area of interest [2, 3]. Analysis of congestion involves the collection and analysis of a large amount of traffic data. Researchers have used numerous techniques to obtain the required data. Videography techniques have been used by some researchers to collect, extract, and visualize traffic state data [4]. Loop detectors [5] and inductive detectors [6] have also been used for collecting traffic data. However, these techniques involve labor cost, installation charges, and maintenance cost of equipment. In recent years, advanced techniques such as radar sensor [7] and Wi-Fi sensor [8]-based techniques have been used though they are expensive. Hence, attempts have been made to collect less expensive and accurate traffic data from probe vehicles that represent the traffic stream.

Probe vehicles fitted with communication devices such as GPS can be used to collect real-time traffic data. Attempts had been made to collect data from probe vehicles such as taxis for the analysis of traffic conditions [9]. Smartphone sensors equipped with GPS receivers were also used for the purpose [10]. Recently, in many developing countries, intelligent transport system (ITS) equipped with GPS devices have been implemented. These devices provide real-time automatic vehicle location (AVL) data at a certain frequency. The AVL databases are often handled by public transit agencies. With ITS becoming popular in many metropolitan cities of India, a huge amount of real-time and accurate AVL data can be obtained from these buses. Public transit buses act as probe vehicles that can represent the traffic stream. AVL data collected from bus probe data can be used for various studies such as travel time estimation [11], estimation of control delay at intersections [12], vehicle trajectory reconstruction [13], signal analysis and design [14], and congestion estimation [15].

Various studies have been conducted to estimate control delay at signalized intersections. HCM delay model [16] and Webster's delay model are often used to model delay at signalized intersections. These methods are based on traffic conditions in

U.S. and U.K., respectively, which are mostly homogeneous and involves strict lane discipline. In developing countries like India with highly heterogeneous traffic conditions, the Equations cannot be used directly to estimate delay. In such cases, modified HCM model [4] and modified Webster's model [17, 18] have been used. Vehicle trajectory-based models [12, 19] and simulation-based methods [20, 21] have also been developed for the estimation of control delay at signalized intersections.

Most of the researches consider average delay at signalized intersections for study and analysis of traffic state, although it varies depending on various factors such as arrival and departure of vehicles, queue length, land use pattern of the area, and time of day. Analysis of this variability in the delay is necessary for implementing appropriate corrective measures and tackle congestion. Numerical methods [16] and analytical methods which use empirical curves have been used to study delay variability under highly over-saturated and highly under-saturated traffic conditions [22]. However, these curves cannot model delay variability at conditions in between the two. In such cases, statistical models have been used to analyze the variability in delay [23]. Another most common method that has been used to analyze delay variability is by using statistical distributions [24, 25]. Researches have been done to use Normal [26, 27], Lognormal [28, 29], Gamma [30], Exponential [29, 31], Logistic [29], Log-logistic [32], Uniform [27, 33], Generalized Extreme Value (GEV) [34], Weibull [35], Burr [36], and Erlang distributions [37] for analyzing delay variability.

In the present study, control delay at signalized intersections has been estimated using GPS-based data collected from transit buses operating in Mysore city, India. Vehicle trajectory-based formulation has been used to estimate delay from bus feed data. Delay variability has been analyzed by fitting probability distributions to the estimated delay.

3 Methodology

The GPS data collected from Mysore ITS was in the form of sequential query language (SQL) format. The data required various stages of pre-processing before using for delay estimation and variability analysis. The detailed methodology used in the study is as shown in Fig. 1.

The GPS database collected from ITS was extracted to local servers using SQL extract. The raw data could contain erroneous information due to improper communication between servers. Those data were eliminated and only data points with unique timestamps and trip details have been used in the study. The available GPS data provides details of the position in terms of geographic coordinates, i.e., latitudes and longitudes only. In order to visualize the pre-processed data, map matching has been done using the QGIS package. Data pertaining to selected intersections has been extracted considering suitable distances on either side of the intersection. Vehicle trajectories—distance, speed and acceleration profiles have been developed for each trip. Backward difference formula as given in Eq. (1) has been used to estimate acceleration at each data point.

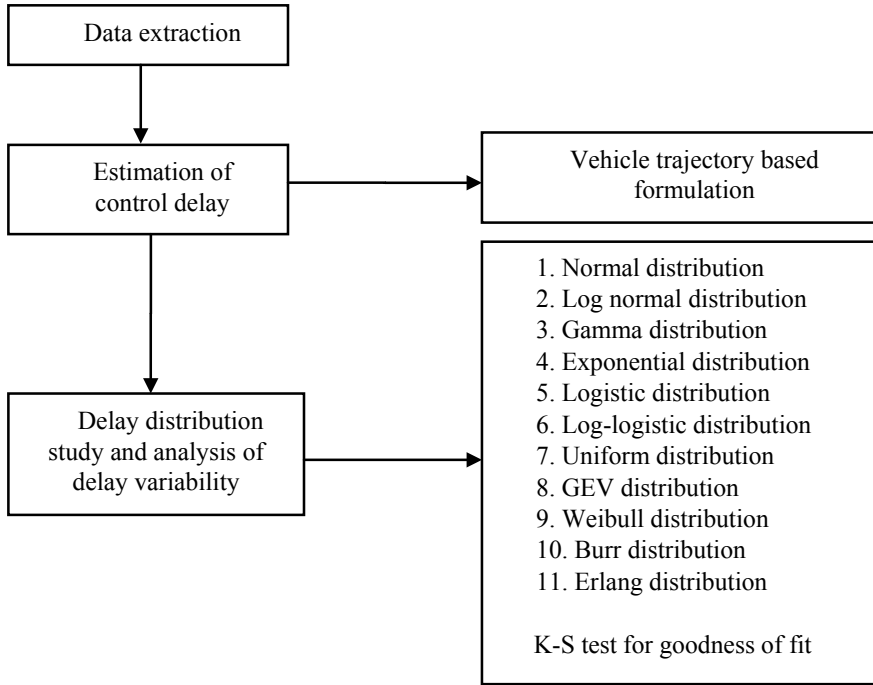


Fig. 1 Flow chart for methodology

$$a_i = \frac{V_i - V_{i-1}}{t_i - t_{i-1}} \tag{1}$$

where

- a_i Acceleration associated with GPS point i
- V_i and V_{i-1} Speeds associated with GPS points i and $i - 1$, respectively
- t_i and t_{i-1} Timestamps associated with GPS points i and $i - 1$, respectively

For effective analysis of congestion, the delay experienced by both stopped and non-stopped vehicles need to be studied. Previous studies show that the delay of non-stopped vehicles is very less compared to stopped vehicles and hence can be neglected [38]. Instantaneous speed values obtained from GPS data have been used to identify stop time. The maximum queue length observed during inventory studies has been used as a distance threshold for identification of stopped vehicles. If at least one GPS update had a speed less than 5 kmph [38] within this limit, the vehicle was considered to have stopped at the intersection. Vehicle trajectory-based formulation has been used to estimate the delay of stopped vehicles. Control delay consists of three components—deceleration delay, stopped delay and acceleration delay. As illustrated in Fig. 2, Eqs. (2)–(5) have been developed based on vehicle trajectories.

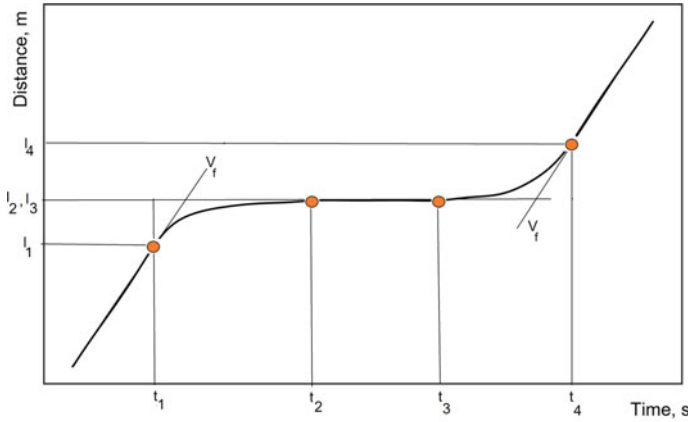


Fig. 2 Intersection delay components

$$d_d = (t_2 - t_1) - \frac{(l_2 - l_1)}{V_f} \tag{2}$$

$$d_s = t_3 - t_2 \tag{3}$$

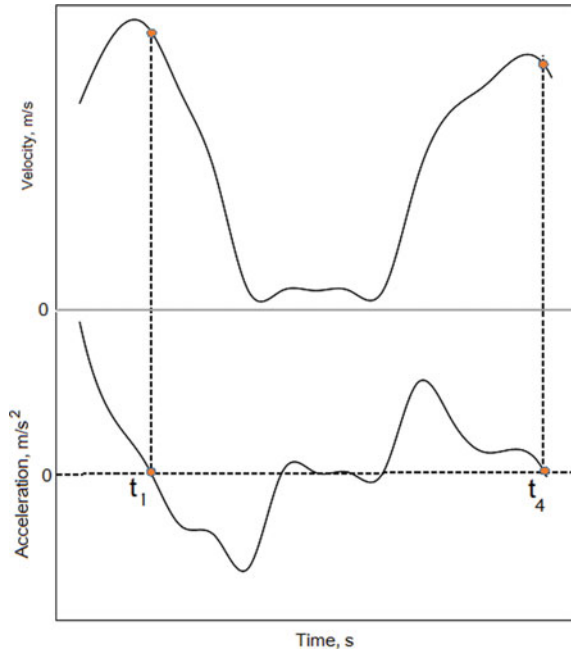
$$d_a = (t_4 - t_3) - \frac{l_4 - l_3}{V_f} \tag{4}$$

$$\text{Control delay, } d = d_d + d_s + d_a = (t_4 - t_1) - \frac{(l_4 - l_1)}{V_f} \tag{5}$$

Where, t_1 , t_2 , t_3 and t_4 are the critical points in delay estimation. t_1 is the time of beginning of deceleration; t_2 is the time of stop; t_3 is the time of beginning of acceleration and t_4 is the time of end of acceleration. $(l_2 - l_1)$ is the distance covered in deceleration before the vehicle comes to a stop and $(l_4 - l_3)$ is the distance covered in acceleration. V_f is the free-flow speed. From inventory analysis of transit buses operating in Mysore city, it has been observed that the free flow speed is 60 kmph, and the same has been assumed in the delay estimation.

As evident from Eq. (5), estimation of control delay requires the identification of critical points in deceleration (t_1) and acceleration (t_4). The effective detection of these critical points can be done by using acceleration profiles. It is seen that acceleration remains negative during deceleration and positive during acceleration, as shown in Fig. 3. This concept is adopted to estimate critical points t_1 and t_4 . t_1 is the time in the deceleration phase where acceleration is non-negative and t_4 is the time in the acceleration region where acceleration is non-positive. The t_1 and t_4 are computed as the respective times in deceleration and acceleration phases when the acceleration value changes from positive to negative. However, in the acceleration phase, the vehicle may not reach free-flow speed. Instead, it keeps on accelerating

Fig. 3 Critical points for delay estimation



slowly and hence, the transition of acceleration value from positive to negative cannot be obtained. In such conditions, the distance threshold has been used to estimate the approximate end of acceleration. From the examination of the speed profiles of all vehicles at an intersection, the approximate distance at which most of the vehicles attain free-flow speed can be estimated. The time update nearest to this distance is considered as the end of acceleration, t_4 .

The variability in delay has been studied using descriptive statistics and statistical distributions. As mentioned in literature, Normal, Log-normal, Gamma, Exponential, Logistic, Log-logistic, Uniform, Erlang, Weibull, Burr, and GEV distributions have been used. Delays experienced by vehicles on weekdays and weekends have been analyzed separately. Parameters of each of the probability distribution functions have been estimated using the maximum likelihood estimation method. Goodness of fit has been analyzed using Kolmogorov-Smirnov (K-S) test [5, 39]. For fitted distributions, K-S test has been performed to test if the statistical distribution passes the null hypothesis H_0 that the observations come from the same statistical distribution at 95% confidence. A larger p-value of K-S test indicates better fitting performance of the model. The distribution fitting model is rejected if the p-value is less than 0.05. The distributions passing the test have then been arranged in increasing order of p-value. Goodness of fit is analyzed on the basis of ranking. Descriptive statistics and rank of the distribution indicate the accuracy of the distribution model in fitting delay. The robustness of statistical distributions is measured using the number of cases passing

K-S test. It highlights the probability that distribution can give promising results in fitting data at a specified level of significance.

4 Data and Study Area

The data for the work has been collected from public transit buses operating in Mysore city. Mysore intelligent transport (MITRA) operated by Mysore city transport division (MCTD), is the major form of public transit in Mysore city. Mysore intelligent transport (MITRA) System operates transit buses equipped with GPS devices that provide real-time AVL data at an update frequency of 10 s. The GPS data contains information such as timestamp, date stamp, position, velocity, trip details, and several other attributes.

GPS data has been collected for a period of two months and extracted using QGIS package. Data has been extracted for a road stretch extending between Yelwala and Mysore city bus stand (CBS). Three signalized intersections have been selected for the present study. The intersections that are not affected by nearby bus stops are considered in this study. The locations of the intersections are as shown in Fig. 4. The land use pattern varies as we move from CBS to Yelwala. Gopala Setty Circle lies in the central business district (CBD) area, whereas Premier Studio and Hutagalli Junction lies in commercial and residential areas, respectively.

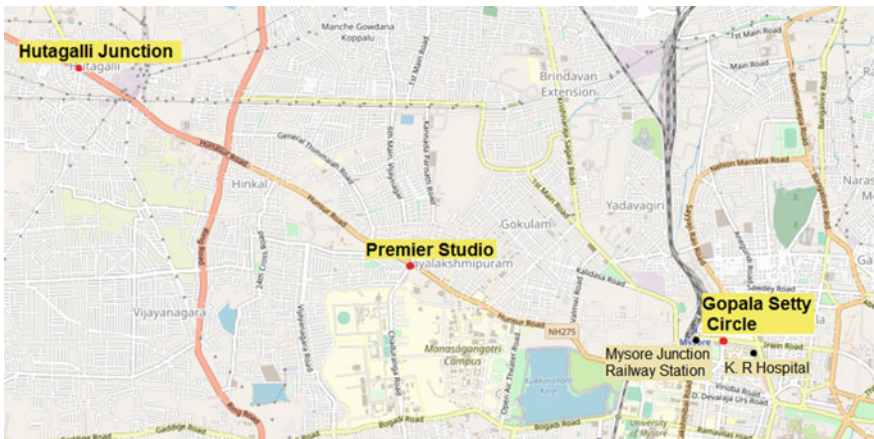


Fig. 4 Locations of intersections under study. (Source OpenStreetMap)

5 Results and Discussion

Control delay for the intersections has been estimated from 8:00 to 20:00 using the proposed approach. The average coefficient of variation (COV) of delay at selected intersections is tabulated in Table 1. It has been found that the COV is fairly decreasing as we move from CBS to Yelwala. The variability in the delay is higher in CBD area, followed by commercial and residential areas. The greater COV in CBD area may be due to high traffic movement in the area and lower COV in residential areas maybe because of the routine activities occurring in the area.

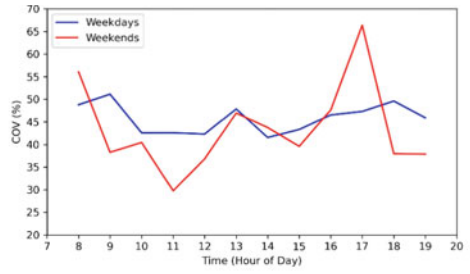
For a detailed analysis, the data has been grouped as weekdays and weekends. The results are as shown in Fig. 5. It can be seen that maximum COV on weekdays is mostly during morning hours, which may be due to a large number of trips originating. At 8–9, in most locations, greater COV is observed on weekdays. This may be due to randomness in the arrival of vehicles at intersections. On weekends, maximum delay variability is observed in evening hours. At 15–17 h, higher COV is observed on weekends, which is due to the trips for recreational purposes. At 18–19 h, there is no much difference in COV on weekdays and weekends. This is because of trips reaching back to destinations is a routine phenomenon. In Gopala Setty Circle (toward railway station), COV on weekdays is greater than on weekends in the morning. However, at 8–9, a greater COV is observed on weekends. In afternoon hours, COV is almost the same on both weekdays and weekends. During evening hours, weekends show greater variability in delay compared to weekdays. In Premier studio, on weekdays, COV is higher in the morning hours, whereas on weekends, it is higher in evening hours. At 8–9, weekends show greater variability in delay whereas in the afternoon, at 13–15 h, a greater COV is observed on weekdays. In Hutagalli Junction, there is no much difference in COV on weekdays and weekends. Although a higher COV is observed on weekends than weekdays for most of the hours, a greater variability is observed on weekdays in evening hours. At 8–9 and 12–13 h, COV on weekends is significantly higher than that observed on weekdays. In Gopala Setty Circle (toward K.R Hospital), for most of the time, greater variability of delay is observed on weekdays. However, at 13–15 h, COV is higher on weekends. In afternoon hours, the variability in the delay is the same on weekdays and weekends.

In order to estimate the best fitting distribution for delay, various statistical distributions have been used (Fig. 6). The distribution performance on weekdays and weekends are shown in Tables 2 and 3, respectively.

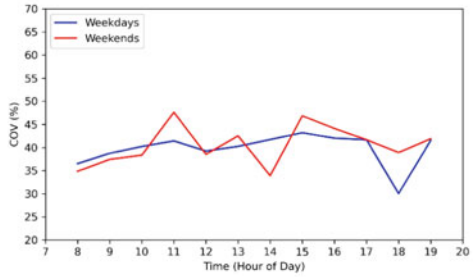
Table 1 Average COV in delay at intersections

Intersection	Average COV (%)
Gopala Setty Circle (towards railway station)	45.57
Premier studio	40.59
Hutagalli Junction	35.71
Gopala Setty Circle (towards K.R Hospital)	44.91

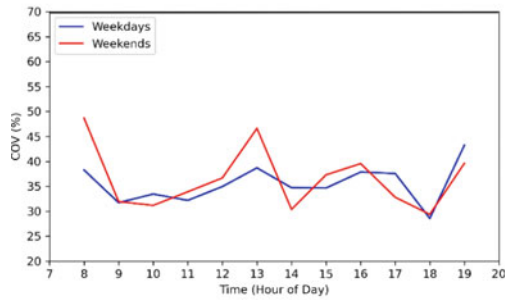
Fig. 5 Delay variability on weekdays and weekends at **a** Gopala Setty Circle (toward railway station) **b** Premier studio **c** Hutagalli Junction **d** Gopala Setty Circle (toward K.R Hospital)



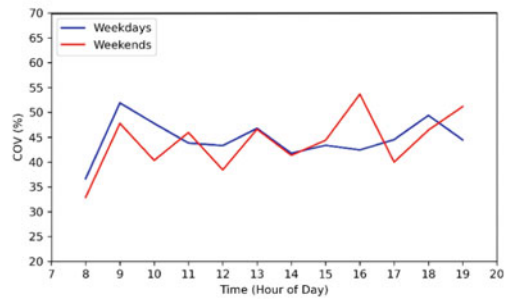
(a)



(b)



(c)



(d)

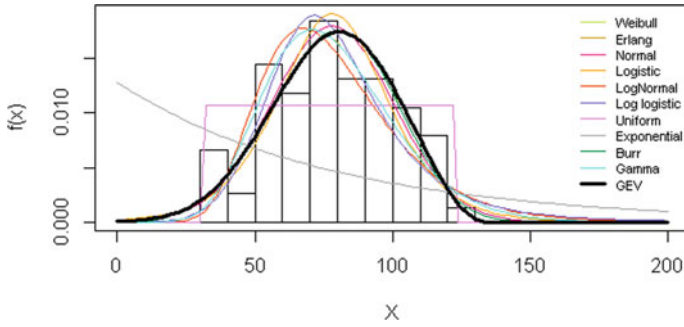


Fig. 6 Probability density function for various distributions plotted for sample data

Table 2 Distribution performance of weekdays

Distribution	Mean <i>p</i> -value	S.D of <i>p</i> -value	Cases pass ratio (%)	Cases top 3 ratio (%)	Cases top 1 ratio (%)
Burr	0.588	0.229	100	67	8
Erlang	0.121	0.219	33	0	0
Exponential	0.000	0.001	0	0	0
GEV	0.673	0.209	100	88	29
Gamma	0.473	0.287	98	29	19
Log-logistic	0.195	0.184	75	2	0
Log-normal	0.302	0.231	85	10	2
Logistic	0.282	0.223	90	8	2
Normal	0.427	0.210	100	21	8
Uniform	0.354	0.269	90	25	15
Weibull	0.561	0.252	100	50	17

Table 3 Distribution performance of weekends

Distribution	Mean <i>p</i> -value	S.D of <i>p</i> -value	Cases pass ratio (%)	Cases top 3 ratio (%)	Cases top1 ratio (%)
Burr	0.612	0.314	88	40	10
Erlang	0.254	0.231	75	0	0
Exponential	0.010	0.035	6	0	0
GEV	0.814	0.162	100	90	29
Gamma	0.620	0.270	98	31	13
Log-Logistic	0.420	0.285	96	4	2
Log-normal	0.532	0.301	96	19	6
Logistic	0.571	0.242	98	15	4
Normal	0.660	0.248	100	40	8
Uniform	0.557	0.296	98	33	19
Weibull	0.656	0.230	100	29	8

On weekdays, Burr, GEV, Normal and Weibull distributions have a 100% pass ratio in the K-S test. These distributions also have the highest cases top 3 ratios. Though Gamma and Uniform distribution has better top three ratios than normal distribution, they have cases pass ratios of only 98% and 90%, respectively. However, Gamma distribution has a higher mean than normal distribution. GEV distribution has the highest average p-value of 0.673, followed by Burr (0.588), Weibull (0.561), Gamma (0.473), and Normal (0.427) distributions. GEV has the least standard deviation of the p-value. The results indicate that these distributions can be used to model weekday delay at the intersections as they have better fitting performance and robustness.

On weekends, GEV, Normal, and Weibull distributions have a 100% pass ratio in K-S test. These distributions also have the highest cases top three ratios. Although Gamma and Uniform distributions have 98% cases pass ratio, they have more cases in the top 3 compared to the Weibull distribution. However, the mean p-value of Uniform distribution is less compared to other performing distributions. GEV distribution has the highest average p-value of 0.673, followed by Normal (0.660), Weibull (0.656), Gamma (0.620), and Burr (0.612) distributions. Burr distribution has only 88% cases pass ratio, although it has come in top three cases as much as normal distribution. Among the performing distributions, GEV has the least standard deviation of *p*-value.

It is observed that GEV distribution performs better in the case of both weekdays and weekends with the highest mean value among its alternatives. The robustness of the distribution is high as it has the maximum number of cases passing K-S significance test and is listed in the top three best-fitting distributions in either case. It also has the least standard deviation of *p*-value among the performing distributions indicating the accuracy of the model. GEV distribution can model the data for both negatively and positively skewed data [34, 40]. The probability distribution function for GEV distribution given in Eqs. 6 and 7 can be used to model the delay variability at intersections. Burr, Weibull, Normal, and Gamma distributions are also suitable for fitting delay on weekdays. However, in the case of weekends, Normal, Weibull, and Gamma distributions follow GEV in fitting delay data.

$$GEV (\mu, \sigma, \xi) = f(x) = \frac{1}{\sigma} t(x)^{\xi+1} e^{-t(x)} \tag{6}$$

$$f(x) = \begin{cases} \left(1 + \xi \left(\frac{x-\mu}{\sigma}\right)\right)^{-\frac{1}{\xi}} & \text{if } \xi = 0 \\ e^{\frac{x-\mu}{\sigma}} & \text{if } \xi \neq 0 \end{cases} \tag{7}$$

where, $\mu \in R$ is the location factor, $\sigma > 0$ is the scale factor and $\xi \in R$ is the shape factor.

6 Conclusion

Increasing motor vehicle growth in urban cities of India often results in congestion and delay. Signalized intersections are one of the major hotspots of congestion. Though various techniques have been used for data collection, it is often tedious, cost-intensive and time-consuming. In recent years, GPS data has emerged as a potential data source for traffic studies. Moreover, it is relatively accurate and easily accessible. In the present study, an attempt has been made to estimate delay at selected signalized intersections in Mysore city and analyze delay variability using descriptive statistics and statistical distributions.

It is observed that delay variability is higher in the CBD area and least in residential areas. In the CBD area, heavy traffic movements result in a higher COV, whereas the least COV in residential area may be due to routine movements in this area. Weekday-weekend analysis of delay variability indicates that COV is higher in morning and evening peak hours. Generally, on morning hours, weekdays show greater variability in delay compared to weekends. However, the trend is reversed in evening hours as greater COV is observed on weekends. In noon hours, delay variability is almost the same in most of the locations.

Statistical distributions have been used to estimate the best fitting distribution for delay at the intersections. Distribution fitting has been done separately for weekdays and weekends. The performance of Burr, Normal, Weibull, and Gamma distributions are similar in either case. But, GEV distribution performs better compared to alternate distributions in both the cases. This study shows that GEV distribution can be used for the analysis of delay variability at signalized intersections and to adopt effective and efficient measures for congestion mitigation.

This way of measuring delay variability gives an idea of variability in delay at signalized intersections. In the absence of availability of signal timings, traffic flow, and composition data, this method can be used to analyze the variability in delay at signalized intersections.

References

1. Afrin T, Yodo N (2020) Survey of road traffic congestion measures towards a sustainable and resilient transportation system. *Sustainability* 12
2. Maitra B, Sikdar PK, Dhingra SL (1999) Modeling congestion on urban roads and assessing level of service. *J Transp Eng* 125(6)
3. Jabari SE (2016) Node modeling for congested urban road networks. *Transp Res Part B* 91:229–249
4. Saha A, Chandra S, Ghosh I (2017) Delay at signalized intersections under mixed traffic conditions. *J Transp Eng Part A Syst* 143(8), (2017).
5. Hellinga B, Abdy Z (2008) signalized intersection analysis and design: implications of day to day variability in peak hour volume on delay. *J Transp Eng* 134(7):307–318
6. Lu XY, Varaiya P, Horowitz R (2012) Estimating traffic speed with single inductive loop event data. *Transp Res Rec J Transp Res Board* 2308(1):157–166

7. Lu C, Dong G (2018) Estimating freeway travel time and its reliability using radar sensor data. *Transportmetrica B Transp Dyn* 6(3):97–114
8. Khadir A, Bindu MH, Sreedhar S, Chilukuri BR, Vanajakshi L (2018) A comparative study of delay estimation methods at signalized Intersections. Researchgate
9. Song L, Zhang D, Chen J (2008) Analysis of Taxi operation characteristics with traffic control. *J Transp Syst Eng Inf Technol* 8(6):127–131
10. Tao S, Manolopoulos V, Rodríguez Duenas S, Rusu A (2012) Real-time urban traffic state estimation with A-GPS mobile phones as probes. *Journal of Transportation Technologies* 2(1):22–31
11. Li Z, Kluger R, Hu XB, Wu YJ, Zhu XY (2018) Reconstructing vehicle trajectories to support travel time estimation. *Transp Res Rec* 2672(42):148–158
12. Ko J, Hunter M, Guensler R (2008) Measuring control delay components using second by second GPS data. *J Transp Eng* 134(8):338–346
13. Wan N, Vahidi A, Luckow A (2016) Reconstructing maximum likelihood trajectory of probe vehicles between sparse updates. *J Transp Res Part C Emerg Technol* 65:16–30
14. Fayazi SA, Vahidi A, Mahler G, Andreas W (2015) Traffic signal phase and timing estimation from low-frequency transit bus data. *IEEE Trans Intell Transp Syst* 16(1):19–28
15. Ma Q, Zou Z, Ullah S (2017) An approach to urban traffic condition estimation by aggregating GPS data. *Cluster Comput J Netw Softw Tools Appl* 3
16. Noroozi R, Hellenga B (2012) Distribution of delay in signalized intersections: day to day variability in peak hour volume. *J Transp Eng* 138(9):1123–1132
17. Sharma R, Patel P, Umrigar N, Zala LB (2018) Delay estimation at signalized intersections under heterogeneous traffic conditions. *Int Res J Eng Technol* 5(5)
18. Preeti P, Varghese A, Ashalatha R (2016) Modelling delay at signalized intersections under heterogeneous traffic conditions. *Transp Res Procedia* 17:529–538
19. Wang H, Zhang G, Zhang Z, Wang Y (2015) Estimation of control delay at signalized intersections using low-resolution transit bus-based global positioning system data. *IET Intel Transp Syst* 10(2):73–78
20. Mousa RM (2003) Simulation modeling and variability assessment of delays at traffic signals. *J Transp Eng* 129(2)
21. Wu M, Xue L, Yan H, Yu C (2010) Simulation of a signalized intersection delay model. In: *International Conference on Intelligent Computing and Information Science* pp 630–635
22. Fu L, Hellenga B (2000) Delay variability at signalized intersections. *Transp Res Rec J Transp Res Board* 1710(1):215–221
23. Gu X, Lan C (2009) Estimation of delay and its variability at signalized intersections. *Transp Res Board 88th Annual Meeting No. 09–3612*
24. Chen P, Liu H, Qi H, Wang F (2013) Analysis of delay variability at isolated signalized intersections. *J Zhejiang Univ Sci A (Appl Phys Eng)* 14(10):691–704
25. Chen P, Liu H, Qi H, Wang F (2014) Incorporating non-uniform arrivals in delay variability modeling at signalized intersections. *J Central South Univ* 21:4021–4032
26. Olszewski PS (1994) Modeling probability distribution of delay at signalized intersections. *J Adv Transp* 28:253–274
27. Gilani VNM, Ghasedi M, Ghorbanzadeh M, Samet MJ (2017) Estimation delay variation and probability of occurrence of different level of services based on random variations of vehicles entering signalized intersections. In: *IOP conference series: materials science and engineering*, vol 245, issue no 4
28. Bai S, Bai H, Pang H (2015) Statistical analysis of buses delay for signalized control intersection. In: *CICTP 2015, 15th COTA international conference of transportation professionals*, pp 1440–1450. ASCE, China (2015)
29. Wong E, Khani A (2018) Transit delay estimation using stop-level automated passenger count data. *J Transp Eng Part A Syst* 144(3)
30. Jeong J, Guo S, Gu Y, He T, Du DHC (2012) Trajectory-based statistical forwarding for multi-hop infrastructure-to-vehicle data delivery. *IEEE Trans Mob Comput* 11(10):1523–1537

31. Bergström A, Krüger N (2013) Modeling passenger train delay distributions: evidence and implications. Working papers in transport economics, CTS—centre for transport studies Stockholm (KTH and VTI) 2013(3)
32. Li J, Zhang H, Zhang Y, Zhang X (2020) Modeling drivers' stopping behaviors during yellow intervals at intersections considering group heterogeneity. *J Adv Transp* Article ID 8818496
33. Yang Y, Huang P, Peng Q, Li J, Wen C (2019) Statistical delay distribution analysis on high-speed railway trains. *J Mod Transp* 27:188–197
34. Esfeh MA, Kattan L, Lam WHK, Esfe RA, Salari M (2020) Compound generalized extreme value distribution for modeling the effects of monthly and seasonal variation on the extreme travel delays for vulnerability analysis of road network. *Transp Res Part C Emerg Technol* 120
35. Yuan J (2006) Stochastic modelling of train delays and delay propagations in stations. Netherlands TRAIL Research School, Delft
36. Susilawati, Ramli MI, Yatmar H (2020) Delay distribution estimation at a signalized intersection. In: IOP conference series: earth and environmental science, vol 419
37. Jiang X, Yang X (2014) Regression-based models for bus dwell time. In: 17th international conference on intelligent transportation systems (ITSC). IEEE, China, pp 2858–2863
38. Mousa RM (2002) Analysis and modeling of measured delays at isolated signalized intersections. *Int J Transp Eng* 128(4):347–354
39. Rahman MM, Wirasinghe SS, Kattan L (2020) Analysis of bus travel time distributions for varying horizons and real-time applications. *Transp Res Part C Emerg Technol* 86:453–466
40. Zheng L, Sayed T, Tangelin A (2018) Before-after safety analysis using extreme value theory: a case of left-turn bay extension. *Accid Anal Prev* 121:258–267

Influence of Roadside Friction on Speed and Lateral Clearance for Different Types of Vehicles



S. K. Santosh, S. Geethanjali, M. R. Archana, and V. Anjaneyappa

Abstract Mobility on roads is influenced by many factors like pavement surface condition, shoulder, driver skills, width of carriageway, roadside activities and type of terrain. Lateral clearance is the distance maintained by moving vehicle from the friction. Frictional activities along the road significantly influence speed and lateral clearance. In this study the influence of friction types on travel speed and lateral clearance for State highways (SH) and Major district roads (MDR) has been explored. The reduction in speed was found to be lowest for all the types of friction for two-wheelers and high for buses and trucks. The reduction in speed is found to be lesser on MDR compared to SH for cars, buses and trucks with respect to friction types of parking and roadside marketing. The lateral clearances maintained by trucks and buses are lesser compared to two-wheelers, three-wheelers, tractors and cars on SH. Reductions in lateral clearance distances on MDR are observed for different types of vehicles with respect to types of friction compared to SH.

Keywords Lateral clearance · Roadside friction · Travel speed

1 Introduction

Mobility on roads is influenced by many factors like pavement surface condition, shoulder, driver skills, width of carriageway, roadside activities and type of terrain. Roadside friction includes bus stops, fuel stations, on-street parking, roadside trading

S. K. Santosh (✉) · S. Geethanjali · M. R. Archana · V. Anjaneyappa
R.V. College of Engineering, Bengaluru, India
e-mail: santoshsk.cht18@rvce.edu.in

S. Geethanjali
e-mail: geethanjalis.cht18@rvce.edu.in

M. R. Archana
e-mail: archanamr@rvce.edu.in

V. Anjaneyappa
e-mail: anjaneyappa@rvce.edu.in

and physical features like trees and electric poles. Lateral clearance is the distance maintained by moving vehicle from the friction. Frictional activities along the road significantly influence speed and lateral clearance of moving vehicles. In this study the effect of friction type on travel speed and lateral clearance for State Highway (SH) and Major District Road (MDR) is determined.

The roadside frictions compel the vehicles to reduce the speeds [1]. Pedestrians, vehicles stopping on shoulder and carriageway and parking are identified as roadside friction factors [2]. The combined and individual effects of these factors would vary for facilities and terrains [3]. Difference between the actual speed/capacity and the predicted speed/capacity is found when friction is high for urban roads [4].

The quality of traffic stream, in terms of average speed, decreases rapidly beyond certain flow levels, in case of kerbside stops [5]. The capacity of six-lane urban road is reduced to almost half when pedestrian crossing volume is 1360 pedestrians/hour. The pedestrian crossing of about 100 pedestrians/hour would reduce the capacity by 3.5% [6]. Buses stopped at bus stops, pedestrian walking along the sides of carriageways and street parking influencing speed reduction is related by the multi-linear regression. It was found that speed reduction is maximum at bus stops followed by parking and then by pedestrian dense sections. For combined sections, the reduction was found to be 50% in case of traffic volume higher than 3000 PCU/hour [7]. Bus bays and kerb side bus stops on urban roads showed the reduction in capacity and more for kerbside bus stops compared to bus bays [8]. Reduction in the capacity was observed to be 57% due to side parking and reduction in effective utilization of carriageway width. Presence of the non-motorized mode reduced the speed by 14% in Patna city compared to Pune city in India [9].

Roadside friction index (RSFI) has been developed and capacity reduces from 1950 to 800 PCU/hour as the friction level increases from insignificant (RSFI <50) to severe level (RSFI >130). Limits for LOS have been suggested based on speed and opportunity of overtaking [10]. Different threshold values for urban street speeds are observed compared to the values specified in the Highway Capacity Manual [11].

Several studies were carried out to find the influence of roadside features on the lateral placement of vehicles. The average number of accidents was halved and the number of fatal accidents was reduced by a factor of four after trees had been cut down. It is recommended that no obstacles should be in the safety zone which is at least 4.5 m from the lane edge for 80 km/hour [12]. Effect of kerbs on driver behaviour in four-lane rural highways was analyzed and found that speed is not affected by driver ability to see distances, but rather by the heterogeneity of surrounding areas. It is suggested that placing of guard rail at the beginning on left curves should be avoided [13–15]. Presence of trees on two-lane rural roads do not present an immediate threat [16]. In the presence of a guardrail, drivers increased the speed when shoulder width was equal to 1.2 and 3.0 m and decreased for narrow shoulder width of 0.5 m [17]. Roadside parking is found as the significant factor in speed reduction [18, 19]. It is observed that speed is reduced by 15–34% and capacity by 18–26% on road stretches with side friction [20].

The capacity of urban arterials is reduced by 6.6–28.3% when frequency of stopping varies from 20 to 120 bus/h [21]. The urban road capacity reduces with the

increase in pedestrian crossflow, although no reduction in capacity was noticed when the pedestrian flow increased up to 200 pedestrians per hour [22]. With the increase in parking manoeuvres, the capacity and effective carriageway width decrease. With 2.95–21.81% reduction in effective width, the capacity reduction is 3.37%–26.08%, respectively. [23]. The capacity of a section reduces by 3.60–35.82% as the percentage of non-motorized vehicles increase from as low as 5% to as high as 25% [24].

Limited studies were carried out on the effect of roadside friction on speed and lateral clearance of different classes of vehicles under heterogeneous traffic conditions. Hence there is a need to study these parameters for conditions prevailing in a country like India.

2 Objectives

Studies are carried out with following objectives.

- i. To study the influence of different types of frictions on speed of different types of vehicles plying on SH and MDR
- ii. To study the influence of speed of different types of vehicles plying SH and MDR on the lateral clearance from friction.

3 Field Studies

The field studies were carried out on a two-lane State Highway and Major District Road in Vijayapura district, Karnataka state, India. The SH has good pavement surface condition with paved shoulder of 1.5 m and about 2 m earthen shoulders with good sight distance. Similarly, the pavement surface condition of MDR of 5.5 m width carriageway is also good and having good visibility is passing through plain gradient and has 0.5 m of earthen shoulders. The types of frictions considered include street parking, pedestrian walking, roadside marketing, trees and electrical pole. The speed and lateral clearance data with respect to different roadside frictions and different types of vehicles were collected. The various factors affecting the speed and lateral clearance are presented in Figs. 1, 2 and 3.

4 Influence of Type of Side Friction on Speed of Different Types of Vehicles

Analysis was carried out to find out the influence of particular type of roadside friction on speed reduction for different classes of vehicles and the clearance distance that vehicles maintain due to the friction type on SH and MDR.



Fig. 1 Ideal and frictional zone for one and both side parking conditions



Fig.2 Pedestrian walk and roadside marking along the roads



Fig. 3 Presence of trees and electrical poles along the roads

The reduction in speed was found to be lowest for two-wheelers and high for buses and trucks which may be attributed to the size of vehicle. The reduction in speed of two-wheelers found to be in the range of 1–26.8%. The trees, electric poles and pedestrian walk were found to influence less on reduction of speed compared to roadside parking and market. The reduction was found to be in the range of 4.3–38.2% for trucks due to friction. Light commercial vehicles (LCV) are less influenced by the friction compared to cars which may be attributed to lower speeds of LCV compared to cars.

The reduction in speed is found to be lesser on MDR for cars, buses and trucks with respect to friction types of parking and roadside marketing compared to SH. The reduction in speed of trucks is 14.8, 20 and 16.4% for parking, pedestrian and roadside marketing, respectively. Similar reductions were found to be 19.2, 24.6 and 6.4% for buses. The reduction was found to be 27.6 and 27% for friction type of parking and roadside marketing on MDR compared to SH. This may be due to lower speeds on MDR and lower level of service of MDR. The reduction in speed is generally high for vehicles moving at higher speeds. The tractors are found to travel at lower speeds as compared to other vehicles and hence the speed reduction is lower as compared to other vehicles.

The reduction in speed of different types of vehicles due to different types of friction is presented in Tables 1 and 2 for SH and MDR, respectively.

5 Influence of Type of Side Friction on Lateral Clearance Maintained by Different Types of Vehicles

Vehicles maintain certain clearance from an object/road friction that drivers perceive as an obstacle. The lateral placement of vehicles in the friction zone was recorded manually by considering the average clearance distance for each type of vehicle both on SH and MDR. The lateral clearance distance was measured at different friction zones and non-friction zone of the same stretches.

The lateral clearances maintained by trucks and buses are lesser compared to two-wheelers, three-wheelers, tractors and cars on SH. Two-wheelers maintained a lateral clearance of 1.68, 1.83, 1.9, 2.0, 1.35 and 0.58 m for the friction types of both side parking, one side parking, pedestrian walk, roadside marketing, trees and electric poles, respectively on SH. Similarly 1.26, 1.45, 1.32, 1.24, 0.56 and 0.15 m for trucks on SH. An increase of 500 and 660% in lateral clearance is found on SH for both side parking and roadside marketing compared to non-friction zones for two-wheelers on SH. Similarly 260 and 169% for friction types of both side parking and roadside marketing, respectively for trucks on SH. Clearance for friction types of trees and electric poles was found to be lower compared to other friction types.

Reductions in lateral clearance distances on MDR are observed for different types of vehicles with respect to types of friction compared to SH. The reduction on MDR was found to be 58.3, 89.5 and 109.5% for two-wheelers, cars and trucks for friction

Table 1 Speed of different vehicles types and speed reduction due to different friction on SH

Friction type	Friction length, m	Distance from carriageway, m	Speed, kmph					
			2w	3w	Car	LCV	Bus	Truck
Both side parking Friction zone	30	0	41.6	38.9	49.2	40	39.5	38.2
Non-friction zone			56.8	52.6	85.5	56	58.5	51.6
Reduction in speed, %			26.8	26.1	42.5	28.6	32.5	25.9
One side parking Friction zone	150	0	55.2	46.9	70.9	52.7	53.6	47.9
Non-friction zone			63.5	54.6	86.5	60.8	65.1	58.3
Reduction in speed, %			13.1	14.1	18	13.3	17.7	17.8
Pedestrian walk Friction zone	–	1	57.9	46.9	73.5	52.6	52.6	45.6
Non-friction zone			63.5	54	86.5	60.8	65.1	58.3
Reduction in speed, %			8.8	13.2	15	13.5	19.2	21.8
Roadside market Friction zone	120	0	32.6	25.7	28.5	24.5	20.9	19.9
Non-friction zone			63.5	54	86.5	60.8	65.1	58.3
Reduction in speed, %			48.7	52.4	67.1	59.7	67.9	65.9
Presence of trees Friction zone	–	1	54.2	49.7	62.7	52.7	52.5	50.3
Non-friction zone			56.9	51.7	66.6	55.1	57.7	53.8
Reduction in speed, %			4.8	3.9	5.8	4.3	9.01	6.5
Electrical poles Friction zone	–	1.5	56.3	49.3	65.6	53.3	55.8	51.5
Non-friction zone			56.9	51.7	66.6	55.1	57.7	53.8
Reduction in speed, %			1.05	4.6	1.5	3.2	3.3	4.3

Table 2 Speed of different vehicles types and speed reduction due to different friction on MDR

Friction type	Friction length, m	Distance from carriage way, m	Speed, kmph					
			2w	3w	Car	LCV	Bus	Truck
One side parking Friction zone	20	0	48.3	39.6	54.7	42.1	41.4	37.7
Non-friction zone			53.3	45.3	63.7	47.5	50.4	44.6
Reduction in speed, %			9.38	12.6	14.1	11.4	17.9	15.5
Pedestrian walk Friction zone	–	1	51.5	37.4	53.7	39.6	42.8	37.6
Non-friction zone			56.5	41.8	64.5	46.9	50.6	45.9
Reduction in speed, %			8.85	10.5	16.7	15.6	15.4	18.1
Roadside market Friction zone	50	0	27.8	21.3	25.1	23.1	18.3	19.9
Non-friction zone			56.5	41.8	53.7	46.9	50.6	45.9
Reduction in speed, %			50.8	49	53.3	50.7	63.8	56.6
Presence of trees Friction zone	–	1.2	50.6	42.4	56.7	43.2	43.3	39.7
Non-friction zone			53.3	45.3	63.7	47.5	50.4	53.8
Reduction in speed, %			5.07	6.4	11	9.05	14.1	26.2
Electrical poles Friction zone	–	1.5	55.1	40.1	62.4	45.8	48.9	43.2
Non-friction zone			56.5	41.8	64.5	46.9	50.6	45.9
Reduction in speed, %			2.48	4.0	3.2	2.35	3.3	5.8

type of pedestrian walk. Similarly 77.6, 24.1 and 36.8% for trees. The reduction in lateral clearance on MDR was found to be least for electric poles compared to SH. Lateral clearances for different types of vehicles and increase in lateral clearance due to roadside frictions on SH and MDR is presented in Tables 3 and 4, respectively. Generally, the speeds of heavy vehicles like buses and trucks are lower and hence the lateral clearance for these vehicles are lower.

Table 3 Lateral clearances for different types of vehicles and increase in lateral clearance due to roadside frictions on SH

Friction type	Lateral clearance, m						
	2w	3w	Tractor	Car	LCV	Bus	Truck
Both side parking Friction zone	1.7	1.6	1.4	1.7	1.6	1.3	1.3
Non-friction zone	0.3	0.4	0.4	0.4	0.3	0.3	0.4
Increase in lateral clearance, %	500	290.5	237.5	307.1	403.1	309.7	260
One side parking Friction zone	1.8	1.8	1.4	1.8	1.6	1.5	1.5
Non-friction zone	0.3	0.4	0.5	0.4	0.5	0.4	0.4
Increase in lateral clearance, %	471.9	309.3	180	337.5	255.6	317.1	245.2
Pedestrian walk Friction zone	1.9	1.8	1.5	1.8	1.7	1.6	1.3
Non-friction zone	0.3	0.5	0.3	0.5	0.5	0.5	0.5
Increase in lateral clearance, %	660	256	360.6	304.4	225	243.5	153.8
Roadside market Friction zone	2.1	1.8	1.6	1.9	1.7	1.4	1.2
Non-friction zone	0.2	0.4	0.5	0.4	0.5	0.4	0.5
Increase in lateral clearance, %	1033	311.6	212	392.5	280	294.3	169.5
Presence of trees Friction zone	1.4	0.8	0.7	0.8	1.7	0.5	0.6
Non-friction zone	0.3	0.4	0.4	0.3	0.5	0.4	0.4
Increase in lateral clearance, %	382.1	83.7	73.6	140.6	280	42.1	36.5
Electrical poles Friction zone	0.6	0.5	0.5	0.4	0.5	0.5	0.5
Non-friction zone	0.3	0.4	0.4	0.4	0.4	0.4	0.4
Increase in lateral clearance, %	107.1	18.1	12.5	19.4	16.6	28.5	21.9

6 Influence of Type of Side Friction on Capacity

Capacity of a traffic lane is the ability of the traffic lane to allow maximum traffic volume or flow. Practical capacity of roadway is affected by lane width, lateral clearance, width of shoulders, alignment, road geometrics, commercial vehicles and speed. Roadside friction increases the lateral clearance which results in reduction of effective width of the lane and thus reducing the capacity of roadway. Roadside friction also results in reduction in speed of vehicles and which in turn reduces the roadway capacity. The theoretical capacity of roadway depends on speed (V) and space headway (S) of vehicles and it is given by formula shown in Eq. (1).

$$q = 1000 * \frac{V}{S} \quad (1)$$

Table 4 Lateral clearances for different types of vehicles and increase in lateral clearance due to roadside frictions on MDR

Friction type	Lateral clearance, m						
	2w	3w	Tractor	Car	LCV	Bus	Truck
One side parking Friction zone	1.0	0.8	0.7	0.9	0.8	0.6	0.6
Non-friction zone	0.3	0.3	0.3	0.4	0.3	0.3	0.3
Increase in lateral clearance, %	264.3	150	106.1	136.1	153.3	132.1	138.5
Pedestrian walk Friction zone	1.2	0.7	0.7	0.9	0.8	0.8	0.6
Non-friction zone	0.2	0.4	0.4	0.3	0.3	0.3	0.3
Increase in lateral clearance, %	445.5	142.9	91.7	182.4	159.4	188.5	152
Roadside market Friction zone	2.03	1.4	1.4	1.5	1.4	1.1	0.8
Non-friction zone	0.2	0.4	0.5	0.4	0.5	0.4	0.5
Increase in lateral clearance, %	91.1	225.6	180	265	208.9	202.9	80.4
Presence of trees Friction zone	0.8	0.6	0.4	0.6	0.5	0.5	0.4
Non-friction zone	0.3	0.3	0.3	0.4	0.3	0.3	0.3
Increase in lateral clearance, %	67.1	41.8	26.7	41.9	41.2	41.7	36.6
Electrical poles Friction zone	0.6	0.4	0.3	0.4	0.4	0.3	0.3
Non-friction zone	0.2	0.4	0.3	0.3	0.3	0.3	0.3
Increase in lateral clearance, %	60.7	25.7	13.8	11.7	18.8	11.5	12

where

q = capacity of traffic lane, vehicles per hour per lane.

V = speed of vehicles, kmph.

S = average centre to centre spacing of vehicles or space headway, m and it is given in Eq. (2).

$$S = 0.278Vt + L \tag{2}$$

where

t = average reaction time, seconds (0.7–0.75 s).

L = length of vehicles, metres.

Capacity of SH and MDR were calculated using above equations. Length of vehicles was considered by referring to Indian Road Congress IRC:SP:41. Reduction in capacity of SH and MDR due to roadside friction were shown in Tables 5 and 6, respectively. The reduction in capacity, considering different types of vehicles varies from as low as 0.2% to 53.5% due to various types of frictions.

Table 5 Capacity for different types of vehicles and decrease in capacity due to roadside frictions on SH

Friction type	Two wheeler			Three wheeler			Tractor			Car			LCV			Bus			Truck			
	L	S	C	L	S	C	L	S	C	L	S	C	L	S	C	L	S	C	L	S	C	
	m	veh/hr/lane	m	veh/hr/lane	m	veh/hr/lane	m	veh/hr/lane	m	veh/hr/lane	m	veh/hr/lane	m	veh/hr/lane	m	veh/hr/lane	m	veh/hr/lane	m	veh/hr/lane	m	veh/hr/lane
<i>Both side parking</i>																						
Friction zone	4	12	3439	4	12	3362	9	15	2098	5.7	15	3213	6	14	2902	15	23	1741	16.7	24	1583	
Non-friction zone	4	15	3773	4	14	3695	9	16	2318	5.7	22	3821	6	17	3314	15	26	2217	16.7	27	1930	
Reduction in capacity, %			8.8			9.0			9.5			15.9			12.4			21.5			18	
<i>One side parking</i>																						
Friction zone	4	15	3744	4	13	3573	9	16	2270	5.7	20	3629	6	16	3242	15	25	2108	16.7	26	1841	
Non-friction zone	4	16	3882	4	15	3733	9	17	2427	5.7	23	3832	6	18	3410	15	28	2353	16.7	28	2079	
Reduction in capacity, %			3.5			4.2			6.4			5.3			4.92			10.4			11.5	
<i>Pedestrian walk</i>																						
Friction zone	4	15	3792	4	13	3573	9	16	2232	5.7	20	3667	6	16	3240	15	25	2084	16.7	26	1783	
Non-friction zone	4	16	3882	4	15	3722	9	17	2424	5.7	23	3832	6	18	3410	15	28	2353	16.7	28	2079	
Reduction in capacity, %			2.3			4.0			7.9			4.3			4.9			11.4			14.2	

(continued)

Table 5 (continued)

Friction type	Two wheeler			Three wheeler			Tractor			Car			LCV			Bus			Truck				
	L	S	C	L	S	C	L	S	C	L	S	C	L	S	C	L	S	C	L	S	C		
m	m	veh/hr/lane	m	m	veh/hr/lane	m	m	veh/hr/lane	m	m	veh/hr/lane	m	m	veh/hr/lane	m	m	veh/hr/lane	m	m	veh/hr/lane	m	m	veh/hr/lane
<i>Roadside marker</i>																							
Friction zone	4	10	3152	4	9	2855	9	13	1599	5.7	11	2525	6	11	2275	15	19	1096	16.7	21	967		
Non-friction zone	4	16	3882	4	15	3722	9	17	2424	5.7	23	3832	6	18	3410	15	28	2353	16.7	28	2079		
Reduction in capacity, %			18.8			23.2			34			34.1			33.3			53.4			53.5		
<i>Presence of trees</i>																							
Friction zone	4	15	3726	4	14	3635	9	17	2338	5.7	18	3495	6	16	3242	15	25	2082	16.7	27	1899		
Non-friction zone	4	15	3775	4	14	3677	9	17	2440	5.7	19	3561	6	17	3295	15	26	2200	16.7	27	1980		
Reduction in capacity, %			1.3			1.13			4.1			1.8			1.6			5.3			4.1		
<i>Electrical poles</i>																							
Friction zone	4	15	3764	4	14	3627	9	17	2380	5.7	51	1278	6	16	3256	15	26	2158	16.7	27	1927		
Non-friction zone	4	15	3775	4	14	3677	9	17	2440	5.7	52	1280	6	17	3295	15	26	2200	16.7	27	1980		
Reduction in capacity, %			0.2			1.3			2.4			0.17			1.2			1.9			2.6		

Table 6 Capacity for different types of vehicles and decrease in capacity due to roadside frictions on MDR

Friction type	Two wheeler		Three wheeler		Tractor		Car		LCV		Bus		Truck					
	L	S	L	S	L	S	L	S	L	S	L	S	L	S				
	m	veh/hr/lane	m	veh/hr/lane	m	veh/hr/lane	m	veh/hr/lane	m	veh/hr/lane	m	veh/hr/lane	m	veh/hr/lane				
<i>One side parking</i>																		
Friction zone	4	13	3605	4	12	3383	9	15	2010	6	14	2966	15	23	1796	16.7	24	1568
Non-friction zone	4	14	3709	4	13	3535	9	16	2228	6	15	3116	15	25	2032	16.7	25	1757
Reduction in speed, %			2.8			4.3			9.81			1.85			11.6			10.8
<i>Pedestrian walk</i>																		
Friction zone	4	14	3673	4	11	3316	9	15	2046	6	14	2889	15	23	1835	16.7	24	1566
Non-friction zone	4	15	3768	4	12	3445	9	16	2314	6	15	3100	15	25	2036	16.7	26	1791
Reduction in speed, %			2.5			3.7			11.6			2.2			9.9			12.6
<i>Roadside market</i>																		
Friction zone	4	9	2954	4	8	2615	9	13	1434	6	11	2201	15	19	986	16.7	21	967
Non-friction zone	4	15	3768	4	12	3445	9	16	2314	6	15	3100	15	25	2036	16.7	26	1791
Reduction in speed, %			21.6			24.1			38.1			29			51.6			46
<i>Presence of trees</i>																		
Friction zone	4	14	3654	4	12	3461	9	15	2086	6	14	2999	15	23	1848	16.7	24	1625

(continued)

Table 6 (continued)

Friction type	Two wheeler			Three wheeler			Tractor			Car			LCV			Bus			Truck		
	L	S	C	L	S	C	L	S	C	L	S	C	L	S	C	L	S	C	L	S	C
Non-friction zone	4	14	3709	4	13	3535	9	16	2228	5.7	50	1274	6	15	3116	15	25	2032	16.7	27	1980
Reduction in speed, %			1.4			2.0			6.3			1.4			3.7			9.0			17.9
<i>Electrical poles</i>																					
Friction zone	4	15	3743	4	12	3397	9	16	2246	5.7	49	1271	6	15	3071	15	25	1995	16.7	25	1721
Non-friction zone	4	15	3768	4	12	3445	9	16	2314	5.7	51	1276	6	15	3100	15	25	2036	16.7	26	1791
Reduction in speed, %			0.6			1.3			2.9			0.3			0.9			2.0			3.9

The capacity reduction is more due to roadside marketing and is reduced by 53.4 and 51.6% for bus on SH and MDR, respectively. Electric poles were found to be the least influencing friction type on capacity (Table 5).

7 Conclusions

The reduction in speed was found to be lowest for all the types of frictions for two-wheelers and high for buses and trucks which may be attributed to the size of vehicle. The trees, electric poles and pedestrian walk were found to influence less on reduction of speed compared to other friction factors like parking and roadside marketing. The reduction in speed is found to be lesser on MDR compared to SH for cars, buses and trucks with respect to friction types of parking and roadside marketing. This may be due to lower speeds on MDR and lower level of service of MDR. The lateral clearances maintained by trucks and buses are lesser compared to two-wheelers, three-wheelers, tractors and cars on SH. Reduction in lateral clearance distances on MDR are observed for different types of vehicles with respect to types of friction compared to SH. The reduction in capacity was found to be 53.4 and 51.6% for the buses due to the friction of roadside marketing on SH and MDR, respectively.

References

1. Das AK, Bhuyan PK (2017) Hardcl method for defining LOS criteria of urban streets. *Int J Civ Eng* 15(7):1077–1086
2. Bang KL, Carlsson A, Palgunadi (1995) Development of speed flow relationship for Indonesian rural roads using empirical data and simulation. *Transp Res Rec*, Washington DC, pp 24–32
3. Chiguma MLM (2007) Analysis of side friction impacts on urban road links. KTH School of Architecture and the Built Environment, Stockholm, Sweden
4. Munawar A (2011) Speed and capacity for urban roads, Indonesian experience. *Procedia Soc Behav Sci* 382–387
5. Koshy RZ, Arasan VT (2005) Influence of bus stops on flow characteristics of mixed traffic. *J Transp Eng* 131(8):640–643
6. Chandra S, Rao GS, Dhamaniya A (2014) Effect of pedestrian cross-flow on capacity of urban arterials. *Indian Highways* 42(1):51–58
7. Salini S, George S, Ashalatha R (2016) Effect of side frictions on traffic characteristics of urban arterials. *Transp Res Procedia* 17:636–643. <https://doi.org/10.1016/j.trpro.2016.11.118>
8. Ashalatha R, Shalini S, Prakash N (2013) Capacity reduction of urban roads due to bus stops. *Transp Res Board*
9. Patel CR, Joshi GJ (2014) Mixed traffic speed–flow behavior under influence of road side friction and non-motorized vehicles: a comparative study of arterial roads in India. *Int J Civ Environ Struct Construct Architect Eng* 8(11):1198–1204
10. Pal S, Roy SK (2019) Impact of side friction on performance of rural highways in India. *J Infrastruct Syst* 25(2):04019006. [https://doi.org/10.1061/\(asce\)is.1943-555x.0000476](https://doi.org/10.1061/(asce)is.1943-555x.0000476)
11. Bhuyan PK, Krishna Rao KV (2011) Defining level of service criteria of urban streets in Indian context. *Euro Transp* 38–52

12. Van der Horst R, de Ridder S (2007) Influence of roadside infrastructure on driving behavior. *Transp Res Rec: J Transp Res Board* 2018(1):36–44. <https://doi.org/10.3141/2018-06>
13. Antonson H, Mardh S, Wiklund M, Blomqvist G (2009) Effect of surrounding landscape on driving behavior: a driving simulator study. *J Environ Psychol* 29(4):403–502. <https://doi.org/10.1016/j.jenvp.2009.03.005>
14. Peng Y, Geedipally S, Lord D (2012) Effect of roadside features on single-vehicle roadway departure crashes on rural two-lane roads. *Transp Res Rec: J Transp Res Board* 2309(1):21–29. <https://doi.org/10.3141/2309-03>
15. Bella F (2013) Driver perception of road side configurations on two-lane rural roads: effects on speed and Lateral placement. *Accid Anal Prev* 50:251–262. <https://doi.org/10.1016/j.aap.2012.04.015>
16. Jamson S, Lai F, Jamson H (2010) Driving simulators for robust comparisons: a case study evaluating road safety engineering treatments. *Accid Anal Prev* 42(3):961–971. <https://doi.org/10.1016/j.aap.2009.04.014>
17. Ben-Bassat T, Shinar D (2011) Effect of shoulder width, guardrail and roadway geometry on driver perception and behavior. *Accid Anal Prev* 43:2142–2152
18. Dhamaniya A, Chandra S (2017) Influence of operating speed on capacity of urban arterial midblock sections. *Int J Civ Eng* 15(7):1053–1062. <https://doi.org/10.1007/s40999-017-0206-7>
19. Yang Q, Overton R, Han L, Yan X, Richards S (2013) The influence of curbs on driver behaviors in four-lane rural highways: a driving simulator based study. *Accid Anal Prev* 50:1289–1297. <https://doi.org/10.1016/j.aap.2012.09.031>
20. Salini S, Ashalatha R (2018) Analysis of traffic characteristics of urban roads under the influence of roadside frictions. *Case Stud Transp Policy*. <https://doi.org/10.1016/j.cstp.2018.06.008>
21. Parkar M, Dhamaniya A (2020) Developing capacity reduction factors for curbside bus stops under heterogeneous traffic conditions. *Arab J Sci Eng* 45:3921–3935
22. Golakiya HD, Patkar M, Dhamaniya A (2019) Impact of midblock pedestrian crossing on speed characteristics and capacity of urban arterials. *Arab J Sci Eng* 44:8675–8689
23. Parkar M, Dhamaniya A (2019) Effect of on-street parking on effective carriageway width and capacity of urban arterial roads in India. *Euro Transp\Trasporti Europei* 73, ISSN 1825–3997
24. Parkar M, Dhamaniya A (2020) Influence of Nonmotorized Vehicles on Speed Characteristics and Capacity of Mixed Motorized Traffic of Urban Arterial Midblock Sections. *J Transp Eng Part—A* 146(4):04020013

Study of Lane Adherence of Heterogeneous Traffic on Intercity Roads



S. Satheesh, V. Guruprasath, and K. Gunasekaran

Abstract Heterogeneity in traffic poses challenges in the analysis of traffic data for future forecast planning and design of highway facilities. Of the various parameters that are essential for the data analysis, lane adherence is an important parameter that plays a vital role in mapping traffic characteristics of a stream, in terms of capacity, safety, etc. There is a common perception that lane adherence of mixed traffic is poor. It is learnt from studies that the speed range of motorized vehicles is becoming narrower and attempt to stick to a lane is on the rise. Lane adherence needs to be promoted for better discharge at intersections in urban areas and safe travel. The improved design and construction of roads to standards are encouraging drivers to follow lane discipline. There seems to be pattern in selection of lane according to the speed of travel and size of vehicles. Automatic classified counting sensors have facilitated recording the position of vehicles with respect to cross section of the road. Precise information of vehicle position recording helps in study of lane adherence at a section. Daylong continuous data recording was carried out with infra-red-based sensor, TIRTL on three intercity roads. Apart from information about vehicle position from the edges of road, data such as speed, flow, headway and vehicle category was obtained. The traffic flow characteristics on the three intercity roads (two-lane undivided, four-lane and six-lane divided highways) and lane adherence observed are reported in this paper. The results indicate lane adherence of heterogeneous traffic flow is observed. The results could help planners and engineers to decide deployment of sensors for data collection and to plan optimal traffic management.

Keywords Lane adherence · Intercity roads · TIRTL · Heterogeneous traffic

S. Satheesh (✉) · V. Guruprasath · K. Gunasekaran
Division of Transportation Engineering, Anna University, Kotturpuram, Chennai, India
e-mail: satheesh.subramaniam@gmail.com

K. Gunasekaran
e-mail: kgunasekaran@annauniv.edu

© The Author(s), under exclusive license to Springer Nature Singapore Pte Ltd. 2023
M. V. L. R. Anjaneyulu et al. (eds.), *Recent Advances in Transportation Systems
Engineering and Management*, Lecture Notes in Civil Engineering 261,
https://doi.org/10.1007/978-981-19-2273-2_42

645

1 Introduction

Building intercity roads to standards with good quality carriageway, mountable and motorable shoulders and with all features is the desire of governments, duty of highway engineers and expectation of the public. Traffic is expected to choose lanes according to speed, possible if multi-lanes are available per direction. Frequent lane changing by a vehicle is considered to be a risky driving practice and a prime reason for accidents and capacity reduction. In heterogeneous traffic condition, the prevalence of smaller size vehicles in large proportion and vehicles with high variation in acceleration and driving speed has led to frequent lane changing. Heterogeneous traffic flow in developing countries is often characterized as that of not following lane discipline and termed as haphazard. The intercity roads have been built to higher standards with an objective of safe and quick travel to destination. It is essential to promote lane discipline and monitor the level of lane adherence.

The lane adherence on Indian expressways has been said to be quasi-lane disciplined, with some vehicles following a lane-based driving and many others not [1]. Lane discipline is difficult to observe and enforce in urban roads as the flow is high most of the time and worst at sections near intersection. Reduction in overall speed and large following of slow-moving heavy vehicle in front with low possibility of overtaking warrants creation of additional lanes to reduce traffic congestion.

Development of sensors to measure the lateral position of vehicles with respect to the highway and observe lane adherence on highways was contemplated. On rural roads, flow is uninterrupted and measure of lane discipline would depict the driver's overall willingness to practise the same. So, an attempt was made to study driving practices on three different National Highway road stretches in Tamil Nadu. In all the three stretches, 24-h traffic data was recorded using The Infra-Red Traffic Logger (TIRTL) which is an automatic traffic data recorder that can provide a number of useful data from the field. The recorded traffic data contains information of vehicles which traversed every minute. The data was analysed to determine the vehicles' lane adherence study, and the findings are reported.

2 Literature Review

Arkatkar et al. [1] studied the lane usage characteristics on Delhi–Gurgaon expressway which is an urban multi-lane road. It was observed that there are significant number of cars, three wheelers and heavy vehicles which do not follow perfect lane discipline. But, this observed degree of lane-based vehicle movement was relatively different as compared to the other multi-lane roads (National Highways, urban arterial roads, etc.) in India. Geetimukta and Akhilesh [2] studied the relation between the dynamic parameters (speed and lateral/longitudinal acceleration) that can exhibit the flow characteristics of vehicles with weak or no lane discipline. It was found that the lateral acceleration increases linearly with the increase in the longitudinal

acceleration for all vehicles which indicates that higher manoeuvrability exists at lower speeds as longitudinal acceleration is higher at such speeds.

Adherence to a particular lane causes delay and consequent changes in approach speed, lateral movement, lateral acceleration and lateral gap at major city road network. For safe and capable movement of large volumes of traffic on city road network, intersections and crossings, the lane discipline is important [3]. According to Asaithambi et al. [4], staggered following between two vehicles, passing and lateral shifts were driving behaviours that are specific to mixed traffic streams. The paper outlines an integrated model (car following, longitudinal and lateral movement gap acceptance) framework for the two-dimensional movement of vehicles that has the potential to capture interdependencies in the movements. Knoop et al. [5] studied that lane changing behaviour conducted an online survey among Dutch and Swiss drivers in which they responded for video clips showing various scenario. The results show that most people have a strategy to choose a speed first and stick to that, which is the first strategy. A second, less often chosen, strategy is to choose a desired lane and adapt the speed based on the chosen lane. A third strategy, slightly less frequently chosen, is that drivers have a desired speed, but contrary to the first strategy, they increase this speed when they are in a different lane overtaking another driver.

3 Methodology

The traffic flow data is recorded with the TIRTL equipment. The TIRTL has the capability to record classified count, wheelbase, speed, headway, lateral position of vehicle and direction of traffic flow. While setting the equipment, the distance between receiver and transmitter is configured with the lane widths on field. The equipment detects the innermost (minimum distance) and outermost edges of vehicle from the receiver. The lateral position of vehicle with respect to lane edges helps to identify whether the vehicle is traversing exactly within edges of each lane or sharing the lanes. The deployment of receiver, transmitter and measurement of distances to edges of vehicle is shown in Fig. 1.

If the minimum and maximum distances measured from the receiver, i.e., if the distance of both edges of vehicle from receiver falls within the lane (L1 or L2) boundaries, the vehicle has to follow lane discipline and if partly in both the lanes, then it is said to share the lanes. Out of the total vehicle count, the number of vehicles traversing in the lane, speed of vehicles in the lane, per cent of vehicles traversing within the lane or sharing lanes are computed.

3.1 Study Area

Three rural road stretches, viz. six-lane divided, four-lane divided and two-lane undivided intercity roads, were considered for the study. All the sections were rural road

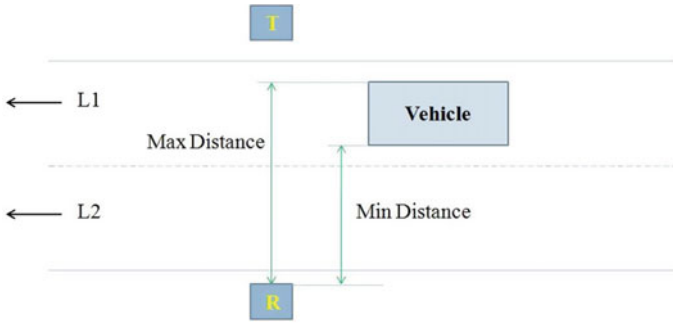


Fig. 1 Method of lane adherence detection

Table 1 Characteristics of study stretches

Section	NH 45—Km.56/8	NH 32—Km5/0	NH 209—Km21/1
Location	Chengalpet 12°47'46" N 79°57'47" E	Thiruneermalai 12°57'14" N 80°06'42" E	Puduchathiram 10°28'14" N 77°47' 59" E
Direction	Towards North (i.e. Chennai)	Towards North (i.e. Maduravoyal)	East–West, bidirectional Dindigul–Palani
Type of carriageway	4-lane divided	6-lane divided	2-lane undivided
Lane width	3.5 m/lane	3.5 m/lane	3.5 m/lane
Shoulder width	1.25 m	1.00 m	1.4 m
End of Carriageway	Gravel shoulders	W-beam crash barrier	Gravel shoulders

sections without any control for speed restrictions or curvature, the terrain being flat. The basic characteristics of the study locations are given in Table 1 and also shown in Fig. 2.

3.2 Collection of Field Data

For the collection of traffic data which is primary input for the study, an automatic traffic detecting equipment called The Infra-Red Traffic Logger (TIRTL) is used, from which a traffic flow data was obtained in Excel spreadsheet on logging the equipment to a computing system. The data was collected for a direction on divided roads and for both directions on an undivided road for 24 h continuously. The vehicles were classified into six categories, namely two wheelers (2 W), three wheelers (3 W), cars, light commercial vehicles (LCV), heavy commercial vehicles (HCV, i.e., bus and truck) and multi-axle and articulated vehicles (MAV).

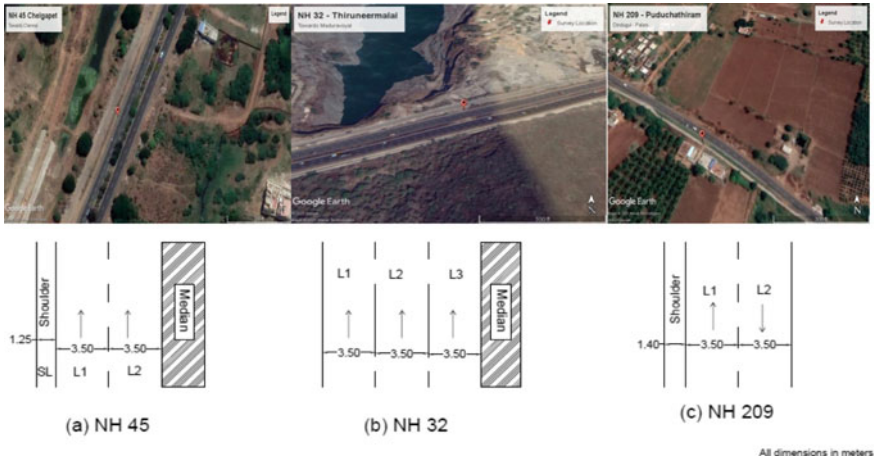


Fig. 2 Aerial view and cross-sectional details of study sections

4 Traffic Characteristics

Traffic flow characteristic at the three study sections with the data extracted from TIRTL was analysed and expressed as composition, flow and stream speed.

4.1 Traffic Composition

Buses, trucks and three-axle vehicles were indicated as HCV, while all other multi-axle vehicles were indicated as MAV. The composition of the vehicular flow on the three study stretches for 24 h duration is shown in Fig. 3. The three study stretches were part of three National Highways. Cars were the major share of total flow, followed by commercial vehicles (light, heavy and MAV) and two wheelers.

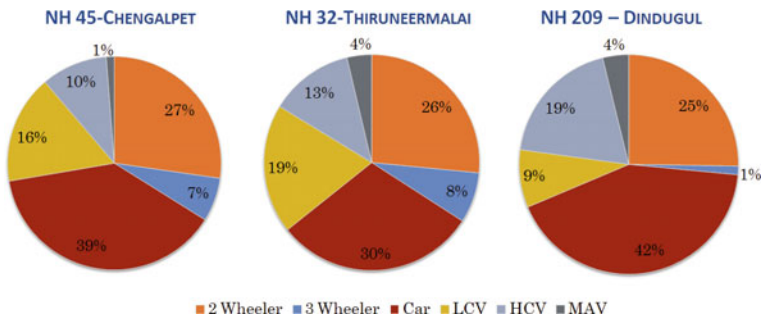


Fig. 3 Vehicle composition

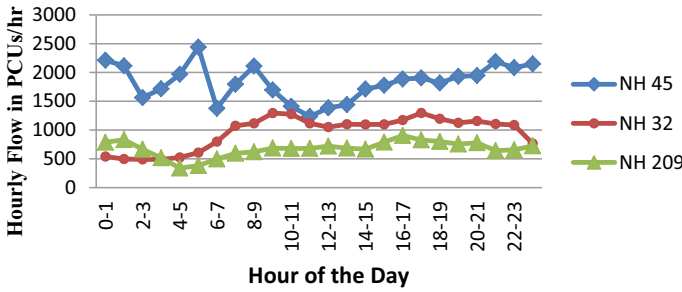


Fig. 4 Hourly traffic observed at the study sections

4.2 Traffic Flow

The flow data was aggregated for every 5 min and expressed in vehicles/hour and PCUs/hour. During the entire period, i.e., 24 h duration of survey, the total number of vehicles recorded was 43,232, 22,045 and 17,831 on NH 45, NH 32 and NH 209, respectively. The mixed traffic flow was converted into equivalent number of passenger car units (PCU) by calculating the PCU factors for each type of vehicle in the five-minute count using the equation proposed by Chandra and Kumar [6] which is given below.

$$PCU_i = (V_c/V_i)/(A_c/A_i)$$

PCU_i = Passenger car unit of vehicle type i .

V_c, V_i = Average speed of small car and vehicle type i , respectively.

A_c, A_i = Projected area of small car and vehicle type i , respectively.

The hourly flow in terms of PCUs/hr at the three study sections is represented in Fig. 4. Maximum flow is observed on the selected NH 45 section, and minimum flow was observed on the NH 209 section. Two wheelers were less during nighttime, whereas trucks and more buses were observed. Maximum hourly flow was observed at 5–6 h, whereas on NH 32 it was during 9–10 h and on NH 209 it was during 16–17 h.

4.3 Traffic Stream Speed

Speed of the vehicles along the stretch is represented as stream speed which is the average speed of all vehicles within the duration under consideration. Figure 5 shows the hourly variation of the speed over entire study duration with respect to flow. It can be observed that the speed of the vehicles does not show appreciable variation

on NH 45. Speed variation was also not significant on NH 32. The speed was more than 60 kmph for NH32 and NH 45.

The stream speed on NH 209 section was around 50 kmph. The stream speed on NH 209 was less as it was an undivided road.

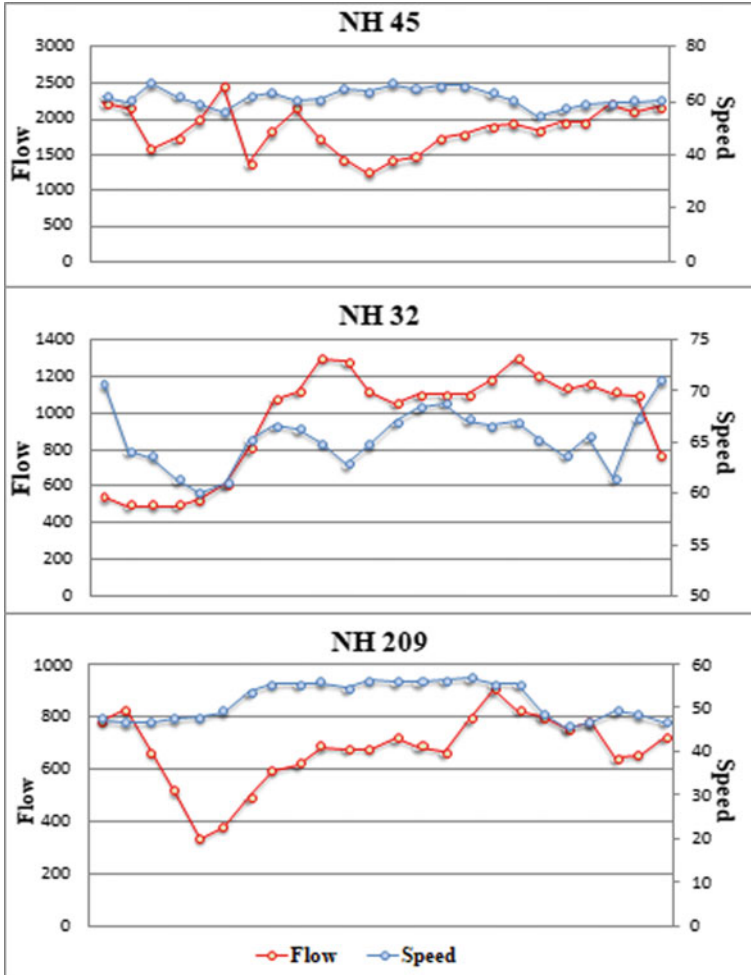


Fig. 5 Observed hour wise flow per lane and stream speed at study sections

Table 2 Percentage flow on each lane

Section	Percentage of flow out of total flow			
	Shoulder	L1	L2	L3
NH 45	19.56	48.73	31.71	–
NH 32	–	22.30	42.56	35.14
NH 209	7.32	43.58	49.10	–

Table 3 Average stream speed on each lane

Section	Average speed (kmph)			
	Shoulder	L1	L2	L3
NH 45	58.25	61.25	60.98	–
NH 32	–	60.62	67.21	66.51
NH 209	39.07	50.29	53.04	–

4.4 Lane Usage

The road space and the speed at which it was used were considered as the lane usage parameters. Here the lane in which more than 50% of width of a vehicle lies is said to the lane of travel of that particular vehicle. The lane usage of each lane in terms of percentage of flow per lane and the average stream speed were given Tables 2 and 3.

5 Lane Adherence

Lane adherence was examined by measurement of the exact position of each vehicle traversing with the aid of TIRTL. The lateral position of vehicle edges from the receiver was compared to ascertain whether the vehicle is completely in a lane or sharing two lanes. Percentage of lane adherence of the vehicles with respect to total flow and percent of vehicles sharing lanes, i.e., level of non-adherence by the vehicles, was also established.

From data analysis, it was found that the lane adherence was practised by majority of vehicles though it was heterogeneous traffic condition. Lane adherence was around 81, 85 and 91% on NH45, NH 32 and NH 209, respectively.

The non-adherence of lane of vehicles category-wise as percent of the total flow is given in Table 2. Cars were the vehicles which were violating the lane adherence to the maximum (Table 4). It could also be due to higher speed and frequent overtaking by cars when compared to other vehicles.

Two wheelers preferred the paved shoulders. The level of non-adherence was computed by the portion of vehicle width in the other lane. If 10% of a vehicle width was in another lane, then it is reported 10% lane non-adherence. The level of lane

Table 4 Share of non-adherence of lanes by vehicles

Vehicle class	% of Non-adherence of lane discipline		
	NH 45	NH 32	NH 209
2 W	4.73	2.75	0.44
3 W	1.28	1.04	0.20
CAR	8.13	4.89	5.08
LCV	1.92	2.23	0.70
HCV	2.69	3.08	2.12
MAV	0.16	1.05	0.31
Total	18.91	15.04	8.84

observed on the three study sections is given in Tables 5, 6 and 7. Major portion of lane non-adherence was within 20%.

Lane adherence was found to be higher at low volume flow and at maximum flow. A decline in the lane adherence was observed at moderate flow; this may be due to higher rate of overtaking practices to maintain higher speeds by vehicles (Fig. 6). However at low volumes, the need for overtaking does not arise and at higher volumes the chances for overtaking are restricted, so lane adherence is higher at low volume flow and at higher flow. Only low to moderate flow was observed on the six-lane

Table 5 Level of non-adherence on NH 45

Percentage of area of vehicle in adjacent lane (%)	Number of vehicles in the lane considered				Percentage out of total volume
	Shoulder	L1	L2	Total	
0–10	254	837	737	1828	4.23
10–20	217	889	667	1773	4.10
20–30	189	845	498	1532	3.54
30–40	137	856	403	1396	3.23
40–50	88	663	460	1211	2.80

Table 6 Level of Non-adherence on NH 32

Percentage of area of vehicle in adjacent lane (%)	Number of vehicles in the lane considered				Percentage out of total volume
	L1	L2	L3	Total	
0–10	105	333	813	1251	5.67
10–20	76	217	468	761	3.45
20–30	80	194	250	524	2.38
30–40	90	218	180	488	2.21
40–50	65	178	138	381	1.73

Table 7 Level of Non-adherence on NH 209

Percentage of area of vehicle in adjacent lane (%)	Number of vehicles in the lane considered				Percentage out of total volume
	Shoulder	L1	L2	Total	
0–10	6	238	157	401	2.25
10–20	12	164	178	354	1.99
20–30	11	119	222	352	1.97
30–40	10	93	178	281	1.58
40–50	20	102	118	240	1.35

divided road, NH32, and the trend observed on four-lane divided road (NH45) and on undivided road (NH209) is not observed on NH32.

6 Results and Discussion

Deployment of sensors has enabled precise data collection. The classified count, speed, headway and lateral position of vehicles could be precisely measured with infra-red sensors like TITRL. Figure 7 shows the lane adherence percentage of vehicles in three study stretches. Higher lane adherence was observed on undivided roads. On divided roads, 80–85% lane adherence was observed on divided roads. The low lane adherence was due to overtaking manoeuvre by cars.

Heterogeneous traffic flow had lane discipline by 81–85% on divided roads and 90% on undivided roads. There seems to be good percentage of lane discipline adherence habits among the drivers on intercity roads. Only 20% of vehicle's width share the adjacent lane, which is an indication of lesser tendency for lane sharing behavior among drivers. Practice of discipline would promote safe flow at higher speed. From the results, it is evident that drivers of motorized vehicle are gradually willing to adopt driving with lane adherence. Monitoring lane-based driving and educating violators would further increase the share of lane-based driving. It is suggested to measure the lane discipline level on intercity roads initially and then promote the practice on urban roads and at intersections.

Lane adherence was found to be higher at low flow levels and at higher flow levels. A decline in the lane adherence was observed at moderate flow, and this may be due to higher rate of overtaking practices to maintain higher speeds by vehicles.

The scope of this study for future works and limitations to be considered is as follows:

- Methodology and data collection is suitable for any kind of road section as it does not produce hindrance or influence in the traffic behavior.
- Suitable for roads with or without lane marking and also for comparative study between them.

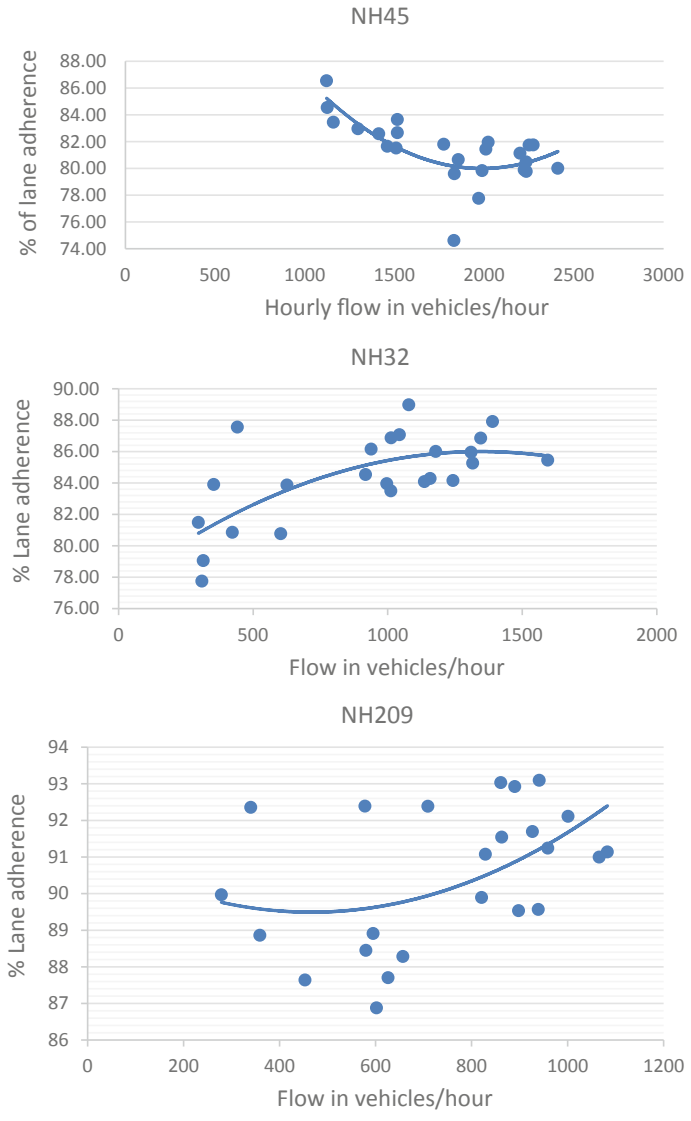


Fig. 6 Observed lane adherence with respect to hourly flow at study sections

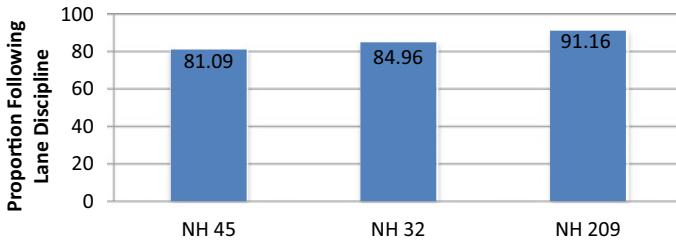


Fig. 7 Lane adherence in study stretches

- For more accurate prediction of the traffic behaviour, a section of road stretch up to 100 m or more would be appropriate than a single point for the study. Data collection has to be done with help of videographic recording from elevated points.

References

1. Arkatkar S et al (2014) Study of lane utilization on delhi-gurgaon expressway. In: 11th transportation planning and implementation methodologies for developing countries TPMDC 2014, Mumbai, India
2. Mahapatra G, Maurya AK (2018) Dynamic parameters of vehicles under heterogeneous traffic stream with non-lane discipline: An experimental study. *J Traffic Transp Eng* 5(5):386–405
3. Trivedi MM, Gor VR Study of lane discipline and its effects. *Int J Eng Develop Res* 5(2) | ISSN: 2321–9939
4. Asaithambi G et al (2016) Driving behaviors: models and challenges for non-lane based mixed traffic. Springer International, *Transp. in Dev. Econ.* (2016)
5. Knoop VL, Keyvan-Ekbatani M et al (2018) Lane change behavior on freeways: an online survey using video clips. *J Adv Transp*
6. Chandra S, Kumar U (2003) Effect of lane width on capacity under mixed traffic conditions in India. *J Transp Eng ASCE* 129(2):155–160

Traffic Analysis and Forecast for Meghalaya Road Network



Manmeet Singh and Ravindra Kumar

Abstract The growth of traffic is significant to the planning and development of the transportation system, as it aids in the identification of future investments. Traffic forecasting is defined as an evaluation of traffic capacity and the number of vehicles that will use a specific type of transportation facility in the future. This method uses appropriate assumptions to estimate overall average traffic, giving adequate weight to traffic growth in figures, considering the volume of design services as recommended by IRC: 64 for various road types, for the following three decades, this model is used to forecast future traffic volumes in PCU/day. After analyzing several research publications, a methodology based on the elasticity method is adopted to determine the overall traffic growth rate. To develop the future traffic prediction model, the vehicle registration figures are collected from the RTO-Shillong, correlated with the help of GDP, per-capita income, and population of the Meghalaya to generate the growth rates as per IRC recommendations. The model of traffic forecasting might be quite subjective and approximate due to the lack of adequate data and the volatility of the expanding economy. Thus, proposing lanes required after ten, twenty, and thirty years for smooth serviceability of different roads classified based on location and function as per IRC recommendations will be obliging.

Keywords Traffic forecast · Elasticity forecast model · Traffic growth rates

1 Introduction

Transportation is required to transfer goods and services from their supply locations to demand destinations. Trades at all levels, from local to global, have enhanced the economy's vibrancy. Road transport in India is a vast system that includes a wide range of vehicles, both motorized and non-powered, but also human- and animal-driven vehicles. Road transport is India's most popular mode of transportation due to benefits such as maneuverability, door-to-door delivery, and quick access to remote

M. Singh · R. Kumar (✉)
TPE Division, CSIR-CRRI, ACSIR, New Delhi, India
e-mail: ravinder.crrri@nic.in; ravindra261274@gmail.com

© The Author(s), under exclusive license to Springer Nature Singapore Pte Ltd. 2023
M. V. L. R. Anjaneyulu et al. (eds.), *Recent Advances in Transportation Systems Engineering and Management*, Lecture Notes in Civil Engineering 261,
https://doi.org/10.1007/978-981-19-2273-2_43

657

habitations. Any road transportation-related planning requires an assessment of travel demand, as well as forecasting travel demand, that further involves identifying the previous trend and using it to predict the future trend using a combination of well-defined assumptions, experiments, and models built using explanatory variables.

India currently has 159.5 million automobiles, with 16.7 million added each year, the volume of traffic on Indian roads is rising at a CAGR of 10.5% per year [1]. With the recent emphasis on upgrading highways to strengthen the national economy, the significance of traffic forecasts has grown significantly. As projected traffic volume plays an essential role in engineering design, economics, and financial commitments of highway improvement projects [2]. To provide a healthier level of service to long-distance traveling vehicular traffic along the National Highways as well as to increase their capacity, it is crucial to evaluate traffic over a significant period [3]. The world's second-largest road network is in India, long-term traffic flow is an influential factor when planning and developing transportation infrastructure, and even when evaluating the required investments, hence forecasting future traffic flow is required to deliver the optimum level of service over extended periods [4]. Meghalaya has less road density compared to the rest of India. The state, meanwhile, has a strategic border with Assam on the north and east, and Bangladesh on the south and west. In 2019–20, Meghalaya's GSDP was US\$4.79 billion at current prices. Between 2015–16 and 2020–21, the state's GSDP (in Rs.) rose at a CAGR of 6.74%. Meghalaya had a total installed power production capacity of 616.03 MW as of February 2021. During the 2019–20 fiscal year, Barapani Airport received 30,552 passengers. During the same period, there were 691 aircraft movements at the airport [5]. The state's natural resources, policy incentives, and infrastructure encourage investment in the tourism, hydropower, manufacturing, and mining sectors. The key sectors for industrialization have been identified as minerals and mining, agriculture and horticulture, and tourism; as a result, there will be an increase in travel demand. The road capacity is quite diverse, and capacity guides have been created in several industrialized nations; based on limited research, The Indian Roads Congress (IRC) has proposed service volume for different kinds of urban roads (IRC 106, 1990) and a guideline for traffic projection on highways [6]. In this study, an attempt is made to anticipate traffic volume in PCU/day using an elasticity demand model and correlating it with single, intermediate, and multilane roads to suggest economical and sustainable approaches for future decades for better transportation maneuverability.

The study proposes a model for estimating travel demand by predicting traffic growth rates based on the transportation demand elasticity method with the assistance of a correlation between vehicle registration, GDP, per-capita income, and population using Meghalaya as a case study.

2 Gap in Research

Prior research has revealed that routes with the highest traffic and those link multiple states receive the most attention. Several studies have also presented an assessment of

various methods for estimating future traffic. Different methods could be correlated to justify the results, and studies could be conducted across a broad spectrum, with weightage given to various sectors in terms of future development, and even studies could be conducted for the entire road network, which could help in diluting traffic evenly across all roads, thus minimizing the impact of heavy traffic on a specific route. Traffic forecasting can also be done on a wider scale, taking into consideration the entire state or country instead of just a specific stretch of road. For affordable and sustainable development, transportation estimations must also be correlated with a different category of road based on location, functionality, utility, economic, and strategic relevance, as well as recommending greener ways to address the anticipated issues in the coming decades. Meghalaya, as one of the country's most important north-eastern states, has a large complex road network consisting of intermediate lanes, double lanes, and 0.0024% of the four-lane road. As a result, predicting based on road width becomes essential in such states.

3 Need of Traffic Forecast

Anticipating and predicting vehicle population growth is a must for every major transportation engineering development, and it necessitates collecting the previous trend and employing it to anticipate the future trend based on qualifying assumptions, simulations, and models developed using significant variables [7]. Determining road capacity is a critical issue for transportation planners. The two most prevalent types of estimation are direct empirical methods and indirect empirical (simulation) approaches. Because of the complexities of variable, heavy mobility on Indian metropolitan roadways, it is important to model flow characteristics and estimate them using direct empirical approaches [8]. The vast majority of India's national and state highways have two-lane, undivided carriageways. These two-lane highways reach their maximum capacity relatively quickly and require upgradation from two-lane to four or six-lane. To facilitate such growth in traffic flow, existing roadways must be modernized, and additional highways should be designed and built. As a consequence, traffic forecasts and capacity assessments for highways are crucial for transportation projects while also strengthening the Indian economy [2]. In India, national highways are built with a 15-year lifespan in consideration. The magnitude of average daily traffic has a significant impact on traffic forecasting accuracy. The larger the forecasting inaccuracy implies lower the average daily traffic is. The future traffic patterns, particularly the induced traffic effect [9], assert that upgrades in transportation infrastructure frequently result in the generation of new traffic demand as a result of new users who did not utilize these facilities before the new developments, i.e., a rise in highway capacity. Infrastructure-related traffic impacts, primarily owing to changes in land-use patterns, could have a substantial impact on future traffic demand predictions. Unexpected and unaccounted socioeconomic changes, as well as the development of new roadways, diversions, and many other infrastructures, may result in undervaluation or overestimation [10].

4 Literature Review

This research's literature review included a review of relevant literature on older traffic prediction models, their problems, and development opportunities, as well as a review of more recent, current forecasting systems.

Raj and others [1], their research focuses on traffic forecasting on an Indian multi-lane highway, as well as the development of a simulation model to study the speed-flow relationship. On a 50-m stretch of National Highway-06, a strip-based approach method is deployed. This research stretch was video recorded regularly on weekdays both mornings and evenings. Among other things, the footage was utilized to calculate traffic volume, space mean speed, vehicle category, and vehicle frequency. A speedflow relationship was constructed to predict capacity.

Kamplimath et al. [2], a case study was used to estimate traffic growth using the transport demand elasticity method. Due to a lack of suitable data and the volatility of the developing economy, the traffic growth estimation is exceptionally subjective and ambiguous.

Thabassum [3] in her research work considered a stretch of NH-2, the road runs from kilometers 398.240 to kilometers 521.120 in the Indian states of Jharkhand and West Bengal and is 122.880 km long. The major part of the vehicles on the stretch are registered in Bihar, Rajasthan, Haryana, and Nagaland. For estimating future traffic growth rates, the growth rates of these states are taken into account. This research looks at past trends in state traffic growth as well as their rise in socioeconomic aspects.

Praveen Tapashetti and others [4], in their study, the complete procedure of traffic forecasting of two segments of State Highway-41 using the elasticity methodology is presented. To determine future traffic growth, PWD Vijayapur City traffic volume data is collected; however, these data do not show a definite trend, so Vehicular Registry Data collected from the RTO Vijayapur District, together with GDP, per-capita income, and population of Vijayapur District is used to determine future growth rate as per IRC guidelines.

KartikeyaJha and others [7], time series analysis methodology was developed. The accuracy of three fundamentally distinct techniques in predicting vehicle population for the same year was compared. Within the scope of this study and estimation, the results of TS Analysis were shown to be much more accurate than those of trend line analysis and significantly better than those of econometric analysis. To verify these findings, the second set of analyses was conducted on more recent data using AADT data from PeMS, California. Across all data types and locations examined, the time series analysis approach was consistently found to be a powerful tool for predicting.

Suresh [8] in their research work investigated the fundamentals of traffic flow to assess the capacity of an urban midblock section, particularly for a two-lane divided cross-section. A videographic survey was used to collect traffic statistics in ten places in Chennai. For every 5-min timeframe, detailed extractions of traffic headway (inter-arrival time), volume, and speed were made, encompassing both peak and non-peak periods. Three approaches were used to evaluate section capacities

using the fundamental parameters: the headway technique, the observed volume method, and the fundamental diagram technique.

As per IRC: 108-1996 [11], the width of the pavement is determined by the amount of traffic it can efficiently handle. The pavement needs to be widened when the traffic flow exceeds its capacity. Pavements are designed based on the volume of commercial vehicles using the facility, and more importantly the number of repetitions of standard axle loads during the design period. How pavements perform and deteriorate is governed by the volume of commercial vehicles and the repetitions of standards axles; however, the present guidelines are intended for predicting traffic on rural sections of highways, including intersections. They cannot be used for urban situations, where the prediction is more complicated.

5 Methodology

There are several techniques for calculating capacity values. Procedures are categorized as direct empirical or indirect empirical methods based on the data collected and the technique applied. Roadway width, headway, volume, speed, and density are the fundamental statistics needed to evaluate capacity. The observed data are effectively used to predict the capacity of indirect empirical methods. Indirect approaches, on the other side, need the calibration of observed data and the development of models to estimate capacity.

In this study, an economic model for Meghalaya’s road network is created using historical data to forecast future traffic growth.

The previous 10 years of vehicle registration data were obtained from the Meghalaya Department of Regional Transport, Government of Meghalaya, along with related data on socioeconomic indicators such as NSDP, per-capita income, and population obtained from the Department of Economic Planning and Statistics, Government of Meghalaya were used to develop an economic model to forecast future traffic as given in equation

$$\text{Log}_e P = A_0 + A_1 \text{Log}_e (\text{E.I}) \tag{1}$$

where

- P = number of vehicles of any particular category.
- E.I = Economic indicators such as GDP, per-capita income, or population.
- A_0 = Constant.
- A_1 = Regression coefficient (elasticity value).

The value of A_1 is known as the elasticity coefficient. The elasticity coefficient is the factor by which the economic indicator (EI) growth rate has to be multiplied to arrive at the growth rate of traffic.

The key steps employed in this study are as follows:

- i. Considering the entire Meghalaya road network is divided into (single, intermediate, and multilane roads).
- ii. Time series of registered vehicles in Meghalaya correlated with economic indicators were used to estimate the elasticity of traffic growth.
- iii. The traffic growth rate for various vehicle categories is calculated using the appropriate economic indicator.
- iv. The aggregate growth rate of automobiles for the next three decades is calculated using a weighted average.
- v. Taking into account the growth rates derived from the elasticity demand model, the recommended design service volume for single, intermediate, and multilane roads, as defined by IRC-64, is used to anticipate traffic flow in PCU/day over the following three decades.

6 Data Analysis

Various statistical data have been collected to arrive at a realistic and sensible assessment of growth factors. The elasticity demand model is estimated using vehicle registration data and economic indicators which are further cross-checked to validate the significance level. The whole road network considered in this study is presented in Fig. 1, it consists of 28,391.70 km and is categorized as:

- i. Four-Lane road—65.64 km
- ii. Two-Lane road—3135.21 km
- iii. Intermediate and Single Lane road—25,190.84 km.

Though it was difficult to inspect and gather accurate data on single and intermediate lane roads owing to inaccessibility and time constraints, they have been grouped.

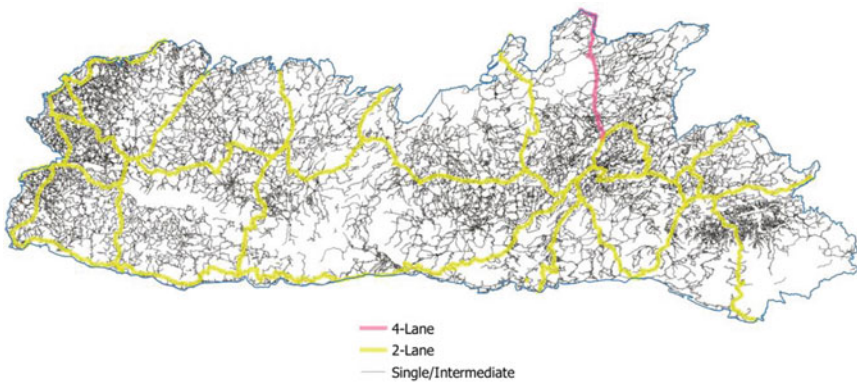


Fig. 1 Road Network of Meghalaya

6.1 Regression Analysis

The equation for a simple regression line is given in Eqs. (2)–(4).

$$Y = a + bX, \tag{2}$$

with X as the explanatory variable and Y as the dependent variable. The intercept (the value of y when $x = 0$) is ‘ a ’, while the slope of the line is ‘ b ’ and ‘ n ’ is the number of observations.

The value of ‘ a ’ and ‘ b ’ can be determined by the following equation:

$$Y = a + bx$$

$$a = \frac{(\sum y \sum x^2 - \sum x \sum xy)}{(\sum x^2) - (\sum x)^2} \tag{3}$$

$$b = \frac{(n \sum xy - (\sum x)(\sum y))}{n \sum x^2 - 2(\sum x)^2} \tag{4}$$

6.2 Econometric Model for Vehicles

Table 1 shows the vehicle registration along with the logarithmic value of Meghalaya with the current growth rate.

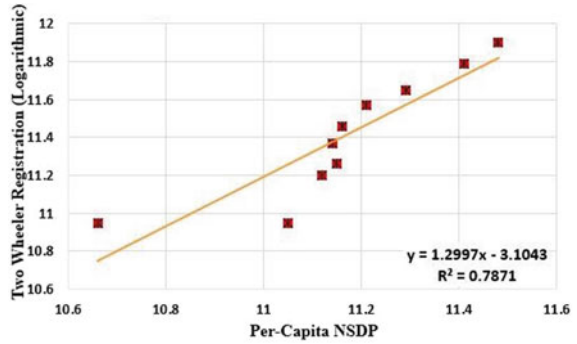
The current average growth is found to be 11.404%, 9.519%, 4.74%, 6.744%, 14.559% for two-wheeler, cars, buses, commercial vehicles, and other vehicles, respectively.

Figures from 1, 2, 3, 4, 5 to 6 shows the simple regression econometric model for the two-wheeler, bus, truck, car, and others class of vehicles, respectively. To select an economic indicator for a certain vehicle type, a correlation between vehicle type and economic indicator was established, followed by a significance test (F -test) to ensure that the variable was significant. For two-wheelers along with per-capita NSDP, the value obtained is $r(8) = 0.7871$ and $p < 0.001$, and for cars along with per-capita NSDP, the value obtained is $r(8) = 0.781$ and $p < 0.001$ which indicates a significant positive relationship among the vehicle type and economic indicator. However, the trend of growth for two-wheelers and cars is found to be similar; moreover, an inference can be drawn that as per-capita NSDP rises, so does the number of private or personal vehicles. For buses along with per-capita NSDP, the value obtained is $r(8) = 0.7632$ and $p < 0.001$, for Commercial vehicles along with NSDP, the value obtained is $r(8) = 0.8598$ and $p < 0.001$, and for other classes of vehicles along with per-capita NSDP, the value obtained is $r(8) = 0.7158$ and p

Table 1 Vehicle registration and current growth rate

Year	Two-wheeler registered (log value)	Two-wheeler growth rate	Car registered & (log value)	Car growth rate	Bus registered & (log value)	Bus growth rate	Commercial vehicle registered & (log value)	Commercial vehicle growth rate	Other vehicle registered & (log value)	other vehicle growth rate	Per Capita NSDP & (log value)	NSDP & (log value)
2011	56,791 (10.95)	-	59,442 (10.99)	-	4071 (8.31)	-	37,355 (10.53)	-	9556 (9.16)	-	42,509 (10.66)	1,249,929 (14.04)
2012	56,791 (10.95)	0%	59,442 (10.99)	0%	4071 (8.31)	0%	37,357 (10.53)	0%	8064 (9)	15.61%	62,989 (11.05)	1,862,182 (14.44)
2013	73,093 (11.2)	28.71%	74,975 (11.22)	26.13%	4902 (8.5)	20.41%	44,509 (10.7)	19.15%	12,784 (9.46)	58.53%	67,575 (11.12)	2,073,867 (14.54)
2014	78,022 (11.26)	6.74%	81,923 (11.31)	9.27%	4981 (8.51)	1.61%	47,696 (10.77)	7.16%	14,243 (9.56)	11.41%	69,679 (11.15)	2,184,428 (14.6)
2015	86,303 (11.37)	10.61%	89,134 (11.4)	8.8%	5256 (8.57)	5.52%	49,662 (10.81)	4.12%	14,568 (9.59)	2.28%	68,794 (11.14)	2,202,768 (14.61)
2016	95,127 (11.46)	10.22%	96,437 (11.48)	8.19%	5478 (8.61)	4.22%	52,978 (10.88)	6.68%	14,965 (9.61)	2.73%	69,924 (11.16)	2,287,227 (14.64)
2017	106,391 (11.57)	11.84%	104,752 (11.56)	8.62%	5671 (8.64)	3.52%	56,170 (10.94)	6.03%	15,454 (9.65)	3.27%	73,844 (11.21)	2,467,113 (14.72)
2018	115,239 (11.65)	8.32%	114,355 (11.65)	9.17%	5826 (8.67)	2.73%	57,910 (10.97)	3.1%	24,324 (10.1)	57.4%	80,315 (11.29)	2,741,162 (14.82)
2019	132,338 (11.79)	14.84%	124,036 (11.73)	8.47%	5921 (8.69)	1.63%	60,917 (11.02)	5.19%	26,651 (10.19)	9.57%	89,879 (11.41)	3,134,071 (14.96)
2020	147,372 (11.90)	11.36%	132,738 (11.8)	7.02%	6100 (8.72)	3.02%	66,559 (11.11)	9.26%	27,037 (10.2)	1.45%	96,766 (11.48)	3,446,818 (15.05)

Fig. 2 Regression for two wheeler



< 0.001 which indicates a significant positive relationship among vehicle type and economic indicator; an inference can be drawn that for commercial vehicles including trucks is highly correlated with NSDP, and for buses, it is highly influenced by both NSDP and population of the state.

Fig. 3 Regression for bus

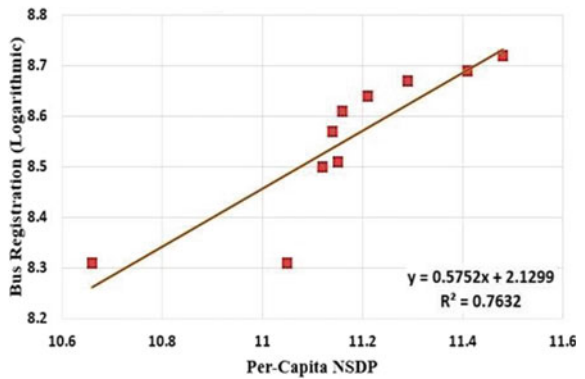


Fig. 4 Regression for truck

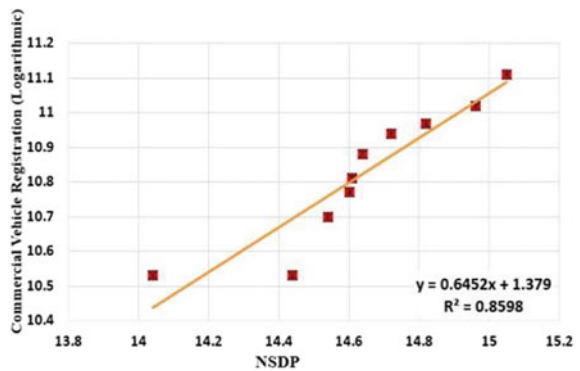


Fig. 5 Regression for car

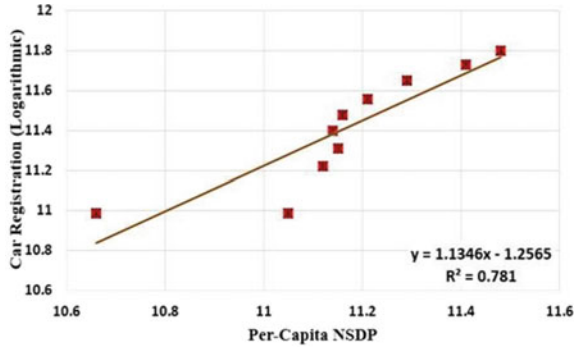
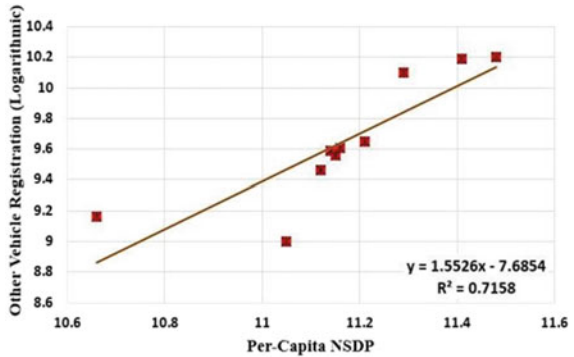


Fig. 6 Regression for others



6.3 Econometric Model for Different Vehicles

Table 2 shows the outcomes of the simple regression econometric model for various vehicle classifications, along with elasticity and R^2 values.

6.4 Projected Traffic Growth for Next Three Decades

To forecast the elasticity constant, and economic indicators for the next three decades, the following assumptions are made:

- i. Elasticity constant is assumed to decline at the rate of 10% for every five years.
- ii. Per-capita NSDP is assumed to increase at the rate of 4%.
- iii. NSDP is assumed to increase at the rate of 10% every five years.
- iv. GDP is assumed to increase at the rate of 5% every five years.

The assumptions are made to generate a realistic model, and time series regression analysis is used to validate the assumptions and findings obtained.

Table 2 Econometric models

Vehicle type	Elasticity constant	Econometric model equation ($Y = a + bx$)	a	b	R^2
Two-wheeler	1.2997	$\text{Ln } P = -3.1043 + 1.2997 \text{ Ln PCI}$	-3.1043	1.2997	0.7871
Car	1.346	$\text{Ln } P = -1.2565 + 1.1346 \text{ Ln PCI}$	-1.2565	1.1346	0.781
Bus	0.5752	$\text{Ln } P = 2.1299 + 0.5752 \text{ Ln PCI}$	2.1299	0.5752	0.7632
Commercial Vehicle	0.6452	$\text{Ln } P = 1.379 + 0.6452 \text{ Ln NSDP}$	1.379	0.6452	0.8598
Truck	0.6452	$\text{Ln } P = 1.379 + 0.6452 \text{ Ln NSDP}$	1.379	0.6452	0.8598
Others	1.5526	$\text{Ln } P = -7.6854 + 1.5526 \text{ Ln PCI}$	-7.6854	1.5526	0.7158

Table 3 illustrates the elasticity values for several vehicle types for a period of up to three decades, based on the assumption mentioned above.

Table 4 illustrates the econometric indicators (PCI, NSDP, GDP) values for a period of up to three decades, based on the assumption mentioned above.

Table 3 Projected elasticity constant for three decades

Vehicle type	Before 2020	2021–2025	2026–2030	2031–2035	2036–2040	2041–2045	2046–2050
Two-wheeler	1.30	1.17	1.05	0.95	0.85	0.77	0.69
Car	1.35	1.21	1.09	0.98	0.88	0.79	0.72
Bus	0.58	0.52	0.47	0.42	0.38	0.34	0.31
Commercial vehicle	0.65	0.58	0.52	0.47	0.42	0.38	0.34
Others	1.55	1.40	1.26	1.13	1.02	0.92	0.83
Trucks	0.65	0.58	0.52	0.47	0.42	0.38	0.34

Table 4 Projected economic indicator for next three decades

Economic indicator	Before 2020	2021–2025	2026–2030	2031–2035	2036–2040	2041–2045	2046–2050
PCI	10	10.73	11.16	11.61	12.07	12.56	13.06
NSDP	12.6	13.89	15.28	16.80	18.49	20.33	21.15
GDP	6.61	6.94	7.29	7.65	8.03	8.44	8.77

Table 5 Corresponding economic indicator

Vehicle type	Economic indicator (EI)
Two-wheeler	Per-capita NSDP
Car	Per-capita NSDP
Bus	Per-capita NSDP
Commercial vehicle	NSDP
Trucks	GDP

Table 6 Forecasted traffic growth rates

Vehicle type	2021–2025	2026–2030	2031–2035	2036–2040	2041–2045	2045–2050
Two-wheeler	12.55	11.75	11.00	10.29	9.64	9.02
Car	13.00	12.17	11.39	10.66	9.98	9.34
Bus	5.56	5.20	4.87	4.56	4.26	3.99
Commercial vehicle	8.06	7.98	7.90	7.83	7.75	7.25
Others	15.00	14.04	13.14	12.30	11.51	10.77
Trucks	4.03	3.81	3.60	3.40	3.21	3.01

6.5 Traffic Growth Projection for Next Three Decades

The elasticity constant is multiplied by the appropriate economic indicator to calculate the traffic growth rate for each vehicle type. Table 5 shows the corresponding economic indicator for different categories of vehicles.

Table 6 gives the forecasted traffic growth rates for different category of vehicle which is obtained by the product of elasticity constant and its respective econometric indicator as obtained in Tables 4 and 5.

Table 7 gives the average growth rates for 10-year intervals for up to three decades, computed from the growth rates (Table 6) and the growth in figures obtained from vehicle registration (Table 1).

The data in Table 7 is utilized to calculate the overall average growth rate, with the growth in figures given sufficient weightage.

6.6 Traffic Projection in Volume (PCU/Day) Based on Carriage Width of the Road

Assuming that, as recommended by IRC-64, hill roads are constructed for service traffic. The suggested traffic volume as per IRC-64 is compounded by the total projected average growth rate (Table 8) to produce the anticipated traffic volume over the next three decades.

Table 7 Average projected traffic growth

Vehicle type	Average growth rates of 10 years (%)	Growth in figures	Average growth rates of 20 years (%)	Growth in figures	Average growth rates of 25 years (%)	Growth in figures	Average growth rates of 30 years (%)	Growth in figures
Two-wheeler	12.15	365,089	11.40	696,993	11.05	961,851	10.71	1,320,336
Car	12.59	339,443	11.81	664,930	11.44	929,699	11.09	1,292,767
Bus	5.38	9147	5.05	11,920	4.89	13,559	4.74	15,376
Commercial vehicle	8.02	121,054	7.94	189,957	7.9	241,143	7.8	306,411
Others	14.52	79,621	13.62	175,208	13.2	259,892	12.79	382,996
Trucks	3.92	48,530	3.71	58,801	3.61	64,573	3.51	70,755

Table 8 Weighted average of overall traffic growth rates

Weighted average for (years)	Figures
10	11.50253506
20	11.10746842
25	10.88646503
30	10.6493892

Table 9 Recommended design service volumes for hill roads (IRC-64)

S. No.	Types of road	Design service volume in PCU/day		
		Carriage width (m)	For low curvature (0–200 degrees per km)	For high curvature (above 0–200 degrees per km)
1	Single lane	3.75	1600	1400
2	Intermediate lane	5.5	5200	4500
3	Two-lane	7.0	7000	5000

Tables 9, and 10 show the recommended design service volumes for hill roads (IRC-64), projected service volume after 10, 20, 30 years, respectively.

7 Results and Discussion

Table 11 displays the forecasted traffic volume for low curvature and high curvature roads for up to three decades, respectively.

With each passing year, the state's economy has been growing at a higher rate, as Meghalaya is a tourist hotspot attracting more tourists from all over the world, as well as a national strategic corridor between India and Bangladesh, which contributes to

Table 10 Projected service volume after 10, 20, and 30 years

Projected service volume	S. No.	Types of road	Design service volume in PCU/day				
			Carriage width (m)	For low curvature (0–200°)	Projected traffic for low curvature (0–200)	For high curvature (above 200°)	Projected traffic for high curvature (above 200)
After 10 years	1	Single lane	3.75	1600	4753	1400	4159
	2	Intermediate lane	5.5	5200	15,447	4500	13,368
	3	Two-lane	7.0	7000	20,794	5000	14,853
After 20 years	4	Single lane	3.75	1600	13,152	1400	11,508
	5	Intermediate lane	5.5	5200	42,743	4500	36,989
	6	Two-lane	7.0	7000	57,539	5000	41,099
After 30 years	7	Single lane	3.75	1600	33,311	1400	29,147
	8	Intermediate lane	5.5	5200	108,261	4500	93,688
	9	Two-lane	7.0	7000	145,737	5000	104,098

Table 11 Projected service volume for low curvature roads for up to three decades

S. No.	Types of road	Projected service volume in PCU/day			IRC recommended design values
		10 years	20 years	30 years	
1	Single lane (low curvature)	4753	13,152	33,311	1600
2	Single lane (high curvature)	4159	11,508	29,147	1600
3	Intermediate lane (low curvature)	15,447	42,743	108,261	5200
4	Intermediate lane (high curvature)	13,368	36,989	93,688	5200
5	Two-lane (low curvature)	20,794	57,539	145,737	7000
6	Two-lane (high curvature)	14,853	41,099	104,098	7000

the Asian Highway. All of these reasons have contributed to rapid growth in traffic as time goes on.

Although single and intermediate roads make up the vast majority of Meghalaya’s road network in both rural and urban regions, it is high time to consider upgrading them as soon as possible to prevent traffic congestion and improve

mobility. According to the statistics provided in the compressed form in the above table following interpretations are done:

Within 10 years, both higher and lower curvature single and intermediate lane roads would qualify for double lane roads.

Within 20 years, all roads will be eligible for upgradation to double lanes, with priority given to multi lanes (minimum four lanes) for road connection essential locations, accounting for more important characteristics such as agricultural, industry, border areas, and tourism.

Various alternative transportation modes must be researched and planned for up to 30 years to minimize traffic loads on the road, and this data may be utilized to develop a more precise model for metropolitan regions where traffic congestion is quite high throughout. In terms of the study's limitations, the findings do not indicate directly any particular stretch of road across Meghalaya for upgradation; rather, they can be used in conjunction with field studies (such as AADT, O-D survey, and videographic survey) to consider a particular road for up-gradation; additionally, they can be used in conjunction with other parameters such as tourism, industries, and agricultural centers, network analysis, environmental impact analysis to prioritize the upgradation of the road in the future. Furthermore, vehicle influx from other states is not taken into account in this study, and traffic corridors that encompass the majority of other states' vehicle traffic could be integrated into this study to establish the route's relevance and future transportation upgrades.

8 Conclusion

For the next ten years, the weighted average anticipated growth percentage of Meghalaya traffic is 11.50%, which is quite high. If current trends continue, traffic volumes will double in 6.4 years and triple in 10 years. According to IRC guidelines, maximum capacity for roads with distinct carriageways will be reached within 10 years of operation by assessing current and prior traffic volumes.

Single and intermediate lane roads will be eligible for upgradation to double lanes, with priority given to major thoroughfares with higher traffic volumes and services. This study might serve as a blueprint for prioritizing road network development based on necessary functions and applications, which could then be carried out in due course of time.

Using appropriate assumptions, this method estimates overall average traffic, giving adequate weight to traffic growth in figures. The weighted average growth obtained is used to project future traffic volume in PCU/day for up to the next three decades, taking into account design service volume as per IRC: 64 recommendations for different road types.

By the end of the next thirty years, Meghalaya's present road network will be overburdened. It is essential to investigate various modes of transportation and prioritize them depending on local needs to alleviate traffic congestion on the roads. To reroute the significant traffic of metropolitan regions, a major route must be suggested.

References

1. Raj P Forecasting of traffic simulation model under heterogeneous traffic condition. *Int Res J Eng Technol (IRJET)*, eISSN: 2395-0056
2. Kamplimath HM Traffic growth rate estimation using transport demand elasticity method: a case study for National Highway-63. *Ijret: Int J Res Eng Technol*, eISSN: 2319-1163, pISSN: 2321-7308
3. Thabassum S (2013) Impact of state-wise vehicle contribution on traffic growth rates for national highways. *Int J Eng Res Technol (IJERT)* 2(10), IJERT ISSN: 2278-018
4. Tapashetti P (2018) A study of traffic volume and traffic forecasting on State Highway-41. *Int Res J Eng Technol (IRJET)*, e-ISSN: 2395-0056
5. The Department for Promotion of Industry and Internal Trade (DPIIT)
6. IRC-64 Guidelines for capacity of roads in rural areas. IRC-108 (2015) Guideline for traffic forecast on highways
7. Kartikeya J (2013) Modeling growth trend and forecasting techniques for vehicular population in India. *Int J Traffic Transp Eng* 3(2):139–158
8. Suresh V, Empirical methods of capacity estimation of urban roads. Global Journals Inc. (USA) Online ISSN: 2249-4596 & Print ISSN: 0975-5861
9. Cervero R (2002) Induced travel demand and induced road investment: a simultaneous equation analysis. *JTEP* 36(3):469–490
10. Clark C (2006) Exposure-effect relations between aircraft and road traffic noise exposure at school and reading comprehension the RANCH project. *Am J Epidemiol* 163(1):27–37
11. IRC-108 2015 Guideline for traffic forecast on highways
12. Moeinaddini M (2014) The relationship between urban street networks and the number of transport fatalities at the city level. *Saf Sci* 62:114–120
13. IRC-108 (1996) Guideline for traffic forecast on rural highways

Traffic Impact Assessment of a Proposed Shopping Mall in a Medium-Sized Town



Neelu Mammen, K. C. Wilson, and Vincy Verghese

Abstract Urbanization rapidly causes new construction and other developmental activities, and that has its own traffic impact which affects the surrounding road network. One such developmental activity is proposed for a town center in the form of a three-story shopping mall. The objective of this study is to assess the impact of the proposed shopping mall in the town center on the existing road network and review the future transportation infrastructure requirements to accommodate additional trips that would be generated by the developmental activity. Impact assessment is done by comparing the volume of vehicles at different time periods with the theoretical capacities of the road network. After the impact assessment, traffic management plan was developed to reduce the negative impacts on the road network due to land use change. The strategy for the traffic management was also analyzed using PTV VISSIM software and found that the mitigation measures suggested could manage the traffic conditions at the town center.

Keywords Trip rate analysis · Traffic impact analysis · Traffic management · VISSIM · Etc.

1 Introduction

Urbanization has led to a rapid increase in new construction and land use developments. Interactions between land use and transportation are directly related to each other and their balance is much required in urban planning. Land use developments produce and attract traffic around the road network, i.e., new improvements

N. Mammen (✉) · V. Verghese
Jyothi Engineering College, Thrissur, India
e-mail: neelumammen123@gmail.com

V. Verghese
e-mail: vincyverghese@jecc.ac.in

K. C. Wilson
KSCSTE-NATPAC, Trivandrum, India

generate new or additional traffic. This generated traffic causes negative impacts like congestion, accidents, waste of time and fuel, pollution, etc. on the current urban transportation system. Traffic Impact Analysis (TIA) will help planners to understand the negative impact of land use changes [1]. TIA analyses the current and integrated newly developed traffic conditions on the road network and possible mitigation measures in transportation planning to minimize these causes. This paper focuses on the impact of the transportation planning system due to the upcoming shopping mall in a town center named Pathanapuram in Kerala, India. Pathanapuram is situated in the middle of surrounding towns, such as Konni, Adoor, Kottarakara, Punalur, and several villages, and is already a heavily congested area. A new shopping mall named “Town Center Mall” has been proposed to be constructed in the middle of this town area. The upcoming shopping mall is located adjacent to the KSRTC bus station and nearly 100 m away from the private bus station. The proposed mall has three floors for shops/theaters; ground, first and second floors; and two levels of basements (Basements 1 and 2) for parking, constituting a total floor area of 1.5 lakh sqft. The mall is expected to open in 2022. The new shopping mall in the town center will generate additional trips and will affect the operational capacity of the road network, which is already congested. Therefore, TIA study is important in this medium-sized town to understand the present and future traffic conditions due to the new shopping mall. This study helps planners and authorities to understand the issues and the possible solutions to the similar development that could happen in similar towns in the nearby areas.

1.1 Objectives

The major objectives of the study are,

- To estimate the expected traffic volume that will be generated by the proposed shopping mall.
- To determine the impact of the generated traffic on the operational capacity of the road network in the town area.
- To develop a traffic management strategy to minimize the impact.
- To check the feasibility of traffic management measures using PTV Vissim software.

2 Study Area

The Town center mall is proposed at the heart of Pathanapuram town in Kerala, India. It is a triangle-shaped mall with one side facing State Highway (SH) 08, Pathanapuram—Kottarakara road (MDR) on another side and the rear side facing the KSRTC bus station. The mall has two accesses, one from the junction and the other from the KSRTC bus station. The surrounding road network within a 1 km

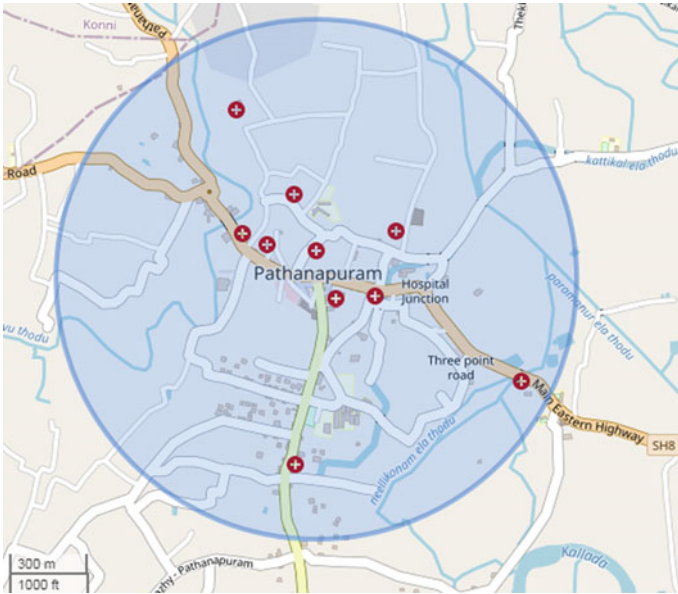


Fig. 1 Location map of the study area

radius of the proposed site, as shown in Fig. 1, is taken as the study area, because the CBD area is enclosed within it.

3 Literature Review and Research Gap

Omkar et al. [2] used a regression method for the evaluation of traffic growth rate according to past traffic data and trip generation was analyzed by considering the number of people working and the number of vehicles owned as independent variables [2]. Omkar et al. [2] stated that Traffic Impact Analysis is a study carried out to determine the significance and effects of proposed developments on the road network. The TIA study would help to decrease traffic problems after the completion of the land use development [2]. Ponnurangam and Umadevi [1] conducted a traffic volume study, speed and delay study to determine the traffic scenario, and trip generation was analyzed by collecting average inbound and outbound vehicles per hour. As per the study conducted by Ponnurangam and Umadevi [1], Traffic impact analysis is a vital prerequisite for allowing the development of any land use activities, thus recognizing the characteristics of the generated trips and their impacts on traffic. Gazder et al. [3] used average travel time and average travel speed as the validation criteria and evaluated queue length (m), delay (s), and gaseous emissions. Any solution planned to solve traffic problems can be evaluated from many aspects using a traffic simulation model [3]. Previous studies have explored the traffic impact analysis and studied the

effects of the proposed developments in a major town area. Only limited studies are conducted on traffic impact analysis in a medium-sized town and simulation using PTV VISSIM software.

4 Methodology

In order to assess the traffic impact assessment, primary and secondary data were collected. Primary data was collected by conducting a traffic volume count survey, a road inventory survey, and a questionnaire survey. Secondary data includes the current and future land use activities of the town and the detailed characteristics of the proposed mall. Based on the collected data, four stage processes (Trip generation, Trip distribution, Mode choice, and Trip assignment) have been evaluated for understanding the traffic behavior of the shopping mall. With this analyzed data, future traffic conditions and network performance based on LOS and the delay of the intersection in the vicinity of the developing shopping mall were evaluated. The traffic management plan has been developed to overcome the worst scenario and its feasibility has also been checked using the VISSIM software.

5 Data Collection and Analysis

5.1 Traffic Volume Survey

To determine the current traffic scenario, a traffic volume survey was conducted by videography method at four junctions, shown in Fig. 2. The surveys were done for 12 h from 7 AM to 7 PM on a normal working day and found that evening peak hour traffic is higher. Therefore, for the remaining junctions, the volume count surveys were done for 3 h from 3 to 6 PM. The classified turning movement of vehicles every 15 min was taken to assess the mode-wise traffic distribution. Observed morning peak hour traffic is 3133 PCU/hr between 9:15 AM and 10:15 AM and observed evening peak hour traffic is 4092 PCU/hr between 4:15 PM and 5:15 PM at the town junction. Observed peak hour traffic was 2026pcu/hr between 4:30 PM and 5:30 PM at Kallumkadavu, 2540 pcu/hr between 4:30 PM and 5:30 PM at Janatha Junction, and 1574pcu/hr between 4:15 PM and 5:15 PM at Nedumparamb. The majority of the mode share was contributed by two-wheelers and cars.



Fig. 2 Locations of traffic volume survey

5.2 Road Inventory Survey

A road inventory survey was carried out on the major roads in every 100 m of the study area based on IRC-SP: 19-2001 and details like carriageway type, presence of shoulders, formation width, type of terrain, land use type, surface conditions, intersections, etc. were collected. The carriageway is of good quality. The formation width for SH 08 and MDR ranges from 9 to 12 m and 7.7 m to 16.6 m, respectively.

5.3 Trip Rate Analysis

A questionnaire survey has been adopted. A survey has been conducted in 19 retail shops and other services outside the nearby developing mall, which has somewhat similar facilities to the upcoming mall. Surveys of customers, employees, and owners of each shop were carried out for 3 weeks. From each facility, 115 samples have been collected, i.e., a total of 2185 samples have been collected. The customer survey considered origin, travel mode, vehicle occupancy, frequency of trip, and trip purpose. The owner’s survey considered the area of the shop, the number of employees and their trip behavior, and the minimum and maximum per-day customers on a typical day. From the collected data, analysis of vehicular trips/day and mode share of minimum and maximum trips per day has been estimated. From the earlier studies, it is estimated that peak hour trips range from one-twelfth to one-tenth of total trips per day and the latter was taken for the study. Trip rates are calculated, as shown in Table 1, by evaluating the trips generated based on the Gross Floor Area (GFA) of

nearby existing facilities. The following Eq. (1) was used to determine the trip rates to each shop.

$$\text{Trip rates (pcu per hour per 100 ft}^2\text{)} = \frac{\text{Peak hour trips (pcu/hr)} \times 100}{\text{Gross floor area (sqft)}} \quad (1)$$

The home appliance store has the least trip rate of 0.77 pcu/100 ft²/hr and the ATM has the highest trip rate of 42.2 pcu/100 ft²/hr followed by the medical store with a trip rate of 16.38 pcu/100 ft²/hr.

Table 1 Trip rates in pcu trips per hour per 100 ft²

Land use description	Existing shop area (sqft)	Peak hour trips (pcu/hr)	Peak hour trip rate per 100 ft ²
Supermarket	3778.13	61	1.60
Textiles	720.00	11	1.56
Foot ware and bag shop	393.32	6	1.40
Bakery	1087.32	39	3.62
Fancy store	181.16	9	5.02
Medical store	416.30	68	16.38
Home appliances store	1398.45	11	0.76
Mobile shop	146.39	12	8.31
Bookstall	780.39	21	2.67
Restaurant	1693.21	44	2.60
Electrical & lighting store	348.59	8	2.29
Theater	13,200.00	284	2.15
Jewelry	482.60	6	1.32
Gift shop	216.36	5	2.25
ATM	113.08	48	42.20
Watch & clock shop	222.01	8	3.39
Optical shop	196.39	7	3.44
Pet shop	183.10	3	1.44
Computer & accessories	677.99	8	1.14

Table 2 Peak Hour Trip generation from the Shopping Mall after completion

Shop category in the mall	Shop area	Peak hour trip rate per 100 ft ²	Peak Hr trips (pcu/hr)
Supermarket	8390.53	1.60	134
Textiles	6983.81	1.56	109
Foot ware and bag shop	2132.55	1.40	30
Bakery	2610.94	3.62	94
Fancy store	1434.08	5.02	72
Medical store	823.50	16.38	135
Home appliances store	4122.06	0.76	31
Mobile shop	534.09	8.31	44
Book stall	989.52	2.67	26
Restaurant	4048.84	2.60	105
Electrical & lighting store	1117.88	2.29	26
Theater	10,696.62	2.15	230
Jewelry	1871.00	1.32	25
Gift shop	747.44	2.25	17
ATM	165.22	42.20	70
Watch & clock shop	1132.46	3.39	38
Optical shop	871.87	3.44	30
Pet shop	196.65	1.44	3
Computer & accessories	1494.36	1.14	17

5.4 Trip Generation

At this stage, it is estimated the number of trips generated by the proposed shopping mall. With the obtained trip rates, peak hour trips generated in the proposed shopping mall have been calculated, as shown in Table 2. From the analysis, traffic generated at peak hours in the opening year was obtained as 1237 pcu/hr.

Peak hour trips to each facility were calculated from the analysis of the survey. To check its accuracy, peak hour trips to these facilities have been compared with the peak hour trips calculated using the ITE Trip Rate Manual. It is found that the obtained peak hour trips in malls from survey analysis and the ITE manual have only slight variation.

5.5 Trip Distribution and Mode Choice

From the collected samples of the questionnaire survey, the obtained trip distributions are 44.21% from Kallumkadavu (western part), 28.92% from Punalur (eastern part), and 26.86% from Kottarakara (South side). It is expected that the same trend will

Table 3 Trip distribution of mall

Direction	Kallumkadavu		Punalur		Kottarakara	
	To	From	To	From	To	From
% Distribution	44.21		28.92		26.86	
Trip distribution (pcu/hr)	547		358		332	
	274	274	179	179	166	166

Table 4 Maximum per-day traffic estimated in terms of vehicles and PCU

Types of vehicle	Mode share (%)	Predicted per-day vehicular trips in the shopping mall	Adopted PCU values	Predicted per-day traffic (PCU)
Car/Jeep	33.19	2872	1.00	2872
Two wheeler	36.88	3191	0.3	957
Three wheeler	9.69	838	1.2	1006
Bus	17.69	1531	4.5	6890
LCV	1.73	150	3	449
HCV	0.41	35	5	176
Cycle	0.42	36	0.4	14
Total		8654		12,365

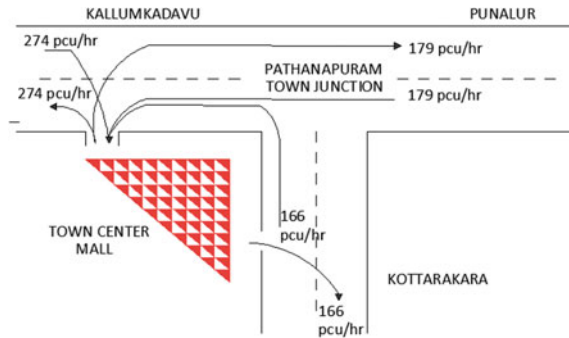
follow in the proposed shopping mall. Both inbound and outbound trips to the mall are assumed to be 50% during peak hours. Table 3 shows the distribution of trips generated in the shopping mall.

From the analysis of the questionnaire survey, the existing proportions of various types of vehicles and the vehicle occupancy for each category of the shop have been determined. The same mode share contribution is adopted for mall-bound traffic. Table 4 shows the maximum per-day traffic estimated in terms of vehicles and PCU.

5.6 Traffic Assignment

The Town Center Junction is a critical junction from the traffic point of view. The shopping mall has one entry gate and two exit gates. The entry gate opens in the Kallumkadavu direction and the exit gates face the Kallumkadavu and Kottarakara directions. The traffic toward Kallumkadavu direction will not use the Town Center Junction, because its entry and exit gates are far beyond the junction. Trips were assigned to the road network based on the position of entry and exit gates of the shopping mall and the direction of traffic. Figure 3 shows the entering and exiting of peak hour trips onto the road network after opening the mall.

Fig. 3 Predicted peak hour trips generated in the mall



5.7 Traffic Forecasting

Since the mall will be completed in 2022, the peak hour traffic was forecasted for 2022, 2025, 2030, and 2035. Based on the earlier studies conducted on similar towns, a growth rate of 4% is adopted for traffic forecasting. Equation (2) used for forecasting traffic is,

$$P_n = P_o(1 + r)^n \tag{2}$$

where

- P_n —peak hour traffic in the n th year
- P_o —peak hour traffic flow in the base year
- n —no. of years
- r —annual growth rate of traffic.

Table 5 shows the forecasted traffic volume affecting the Town Center Junction at the peak hour using Eq. (2). From the volume survey conducted, it is found out that the peak hour traffic volume is higher at the Town Center Junction and also in the direct vicinity of the proposed shopping mall. Therefore, traffic forecasting is done in the town center only to assess the traffic impact. Forecasted traffic volume at the Town Center Junction considered the traffic generated in the mall in addition to the road network traffic.

Table 5 Peak hour forecasted traffic volume at Town Center Junction

Year	2021	2022	2025	2030	2035
Projected peak hour traffic volume at Town Center Junction (pcu/hr) without the mall-bound traffic	4092	4256	4787	5824	7086
Peak hour traffic generated from the shopping mall (pcu/hr)	–	1237	1391	1692	2059
Forecasted peak hour traffic volume at Town Center Junction (pcu/hr)	4092	5492	6178	7516	9145

Table 6 Existing road network performance

Road segment	Direction of traffic flow	Existing		
		Peak hour volume (pcu/h)	V/C ratio	LOS
Kallumkadavu—Pathanapuram Town Section	East Bound	1428	1.19	F
	West Bound	1430	1.19	F
Punalur—Pathanapuram Town Section	East Bound	1323	1.10	F
	West Bound	1471	1.23	F
Kottarakara—Pathanapuram Town Section	South Bound	1338	1.12	F
	North Bound	1193	0.99	E

6 Impact Assessment

The impact assessment compares the existing and forecasted traffic volume with the theoretical capacity of the road network, i.e., v/c ratio, and evaluates the Level of Service (LOS) of the road network. The theoretical capacity of the road network and parameters of LOS are taken from Indo HCM. As per Indo HCM, the capacity of the two-lane undivided road is 2400 pcu/hr and the lane capacity is 1200 pcu/hr. Also, the condition of the road network is poor when the v/c ratio exceeds 1. Tables 6 and 7 shows the performance of the road network in the existing and forecasted years, respectively. From the assessment of traffic impact on the road network, it is evident that even though the current operating condition is poor, LOS F is obtained on the majority of the links and needs to be managed.

7 Traffic Management Measures

The road network shows poor operating condition; hence it requires serious management measures. The widening of the road network is suggested, but due to the immediate action needed to overcome the existing negative impact, alternative routes for different directions for some classes of vehicles to traverse without passing through the Town Center Junction are suggested. They are:

- (a) Alternative Route 1: Light traffic from Kallumkadavu to Punalur has not been allowed to travel from Kallumkadavu to Punalur through Town Center Junction. Light traffic from Kallumkadavu takes a left turn from Janatha Junction (which is between Kallumkadavu and Town Center Junction) and rejoins the SH 08 at a point after the town center, as shown in Fig. 4. This rerouting has a carriageway width that ranges from 5.4 to 6.2 m, imposing an additional 400 m of travel on light vehicles and taking around 2 min in normal traffic, but considering the delays during peak hours, this alternate route will be useful.

Table 7 Forecasted road network performance

Road segment	Direction of traffic flow	Peak hour volume (pcu/h)						V/C ratio		
		2022	2025	2030	2035	2022	2025	2030	2035	
Kallumkadavu-Pathanapuram Town Section	East Bound	1759	1978	2407	2928	1.47	1.65	2.01	2.44	
	West Bound	2106	2369	2882	3506	1.75	1.97	2.40	2.92	
Punalur—Pathanapuram Town Section	East Bound	1555	1750	2129	2590	1.30	1.46	1.77	2.16	
	West Bound	1709	1922	2338	2845	1.42	1.60	1.95	2.37	
Kottarakara—Pathanapuram Town Section	South Bound	1558	1752	2132	2593	1.30	1.46	1.78	2.16	
	North Bound	1586	1783	2170	2640	1.32	1.49	1.81	2.20	

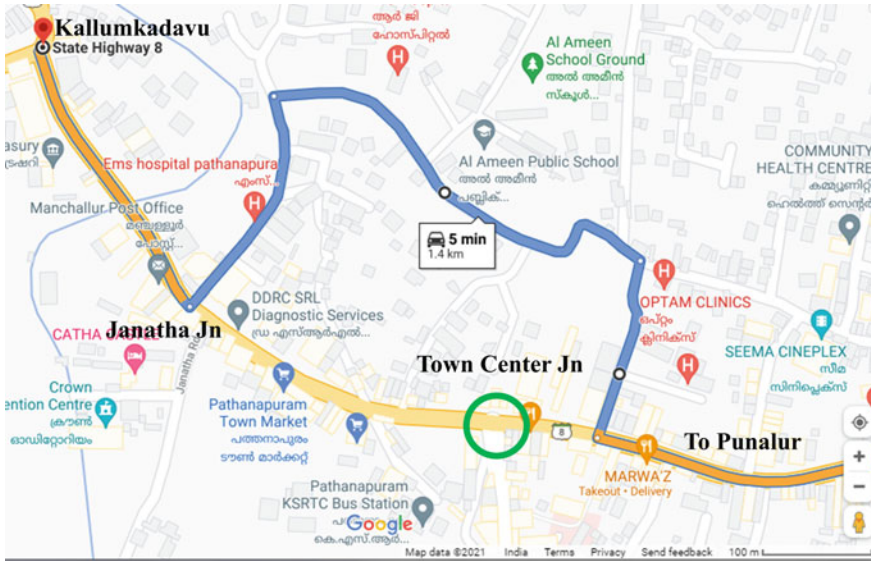


Fig. 4 Alternate route 1

- (b) Alternative Route 2: Light traffic from Punalur to Kottarakara has not been allowed to travel through Town Center Junction. These vehicular classes are diverted through a route between Nedumparamb and Town Center Junction and end at a point after the Town Center Junction, as shown in Fig. 5. This rerouting has a carriageway width that ranges from 3.75 to 4.7 m.
- (c) Alternative Route 3: The next measure is that buses from Kottarakara to Kallumkadavu and Kallumkadavu to Kottarakara are not allowed to traverse through the Town Center Junction. An alternative route, as shown in Fig. 6, is suggested for the same.

8 Traffic Network Modeling Using PTV VISSIM

The network performance with and without the traffic management plan was simulated using the PTV VISSIM 11 software. The vehicle delay and queue length at the junction before and after the implementation of traffic management were compared to analyze its feasibility. Study stretch has been created using links and connectors. The existing condition of the road network was replicated by inputting vehicle volumes, vehicle classes, speed, types, and composition, vehicle routing decisions, data collection points, and configuration are given according to the collected data. After inputting, calibration and validation were done. Calibration and validation are done in VISSIM to simulate the field conditions. Calibration was done by adjusting various parameters of the driving behaviors of the simulation model till the model

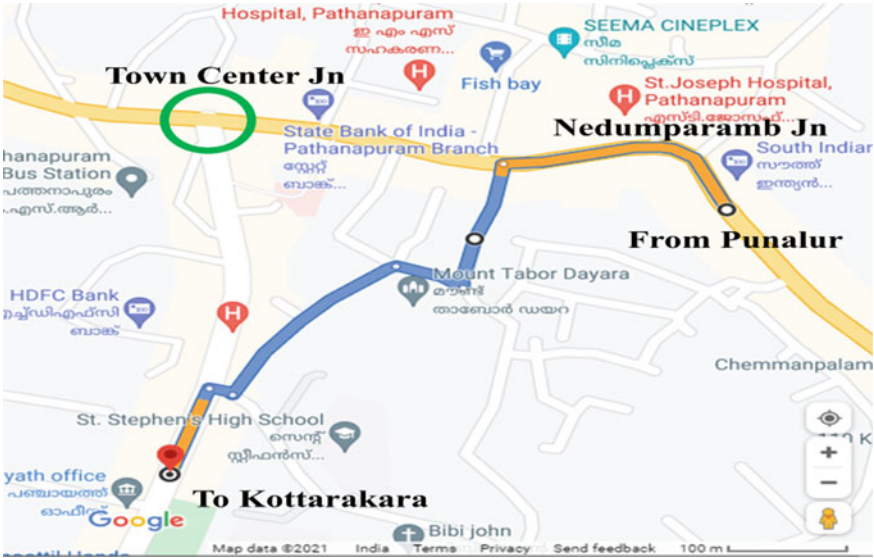


Fig. 5 Alternate route 2



Fig. 6 Alternative route 3

characterizes field conditions. By checking the error between the observed and simulated midblock traffic volume in each run, the validation was performed. Then, different scenarios mentioned below were analyzed.

8.1 Simulation Scenarios

For traffic simulation, two scenarios are considered. In each case, evaluation of the road network based on delay in percentage, comparison of travel time in seconds and queue length in meters has been estimated. In scenario 1, the performance of the road network with the shopping mall-bound traffic devoid of traffic management measures was evaluated. In scenario 2, traffic management measures have been adopted along with scenario 1. In both cases, performance of the Town Center Junction is considered critical since it is located in the direct vicinity of the proposed shopping mall.

8.2 Evaluation and Results

After achieving the field condition in the simulation model by calibration and validation, evaluation of network performance based on links and queue evaluation were done. Table 8 shows the comparison of link segment results of scenarios 1 and 2. The link segment results analyze the relative delay and average speed of vehicles in each scenario. It is obtained that after the implementation of traffic management measures in the model, the average speed of vehicles increased and the relative delay at the Town Center Junction has decreased. Adoption of traffic diversion reduced relative delays of vehicles by approximately 31%, 41%, and 54% in Punalur-Town Center, Kottarakara-Town Center, and Kallumkadavu-Town Center directions, respectively.

Table 9 shows the comparison of queue evaluation results of scenarios 1 and 2. In queue evaluation, it measures the maximum queue length and queue delay of vehicles. It is observed that after the implementation of traffic management measures

Table 8 Link segment results of scenarios 1 and 2

Direction	Scenario 1		Scenario 2	
	Relative delay (%)	Average speed (km/hr)	Relative delay (%)	Average speed (km/hr)
Punalur—Town Center	84.09	5.11	52.65	15.01
Town Center—Punalur	2.32	31.03	1.82	31.20
Kottarakara—Town Center	69.17	9.79	28.10	22.73
Town Center – Kottarakara	3.04	30.82	1.53	31.18
Kallumkadavu—Town Center	88.22	3.78	34.48	20.74
Town Center—Kallumkadavu	2.94	30.63	4.61	30.16
Alternative route 1	–	–	1.50	31.49
Alternative route 2	–	–	2.88	31.16

Table 9 Results of queue evaluation of scenarios 1 and 2

Direction	Scenario 1		Scenario 2	
	Max. queue length (m)	Queue delay (s)	Max. queue length (m)	Queue delay (s)
Kallumkadavu—Town Center	520.89	260.73	112.72	19.36
Punalur—Town Center	512.39	243.47	144.44	27.05
Kottarakara—Town Center	512.38	160.81	133.72	19.08

in the model, the maximum queue length and queue delay of vehicles has decreased. Adoption of traffic diversion reduced the maximum queue length of vehicles by approximately 78%, 72%, and 74% in Kallumkadavu-Town Center, Punalur-Town Center, and Kottarakara-Town Center and directions, respectively.

From the analysis, it is found that with the adoption of suggested traffic management measures, the performance of the road network has been enhanced.

9 Summary and Conclusion

Changes in land use have a considerable impact on traffic and transport operations in an urban area. Both land use and transportation planning help to curtail the negative impacts of these changes. Traffic impact analysis is an effective tool to analyze the future traffic conditions of the area with or without new activities. In this study, the future traffic was predicted and distributed to all the road corridors and the critical locations/stretches were identified. From the traffic impact analysis, it is found that the network performance within the CBD area is worse than in the present condition. For the majority of road segments, the level of service obtained was LOS F. To improve the network performance, it is required to apply traffic management measures such as widening of existing roads, rerouting of vehicles, one-way regulations, etc. Since the widening of the road network consumes time and requires financial aid, it is suggested to use the possible alternative routes available in the CBD area as an immediate solution. The feasibility of the suggested management measures was also analyzed using simulation software, VISSIM. From the analysis, it is found that the suggested traffic management measures improve the network performance. The alternative routes can reduce the relative delays of vehicles by 31%, 41%, and 54% in Punalur-Town Center, Kottarakara-Town Center, and Kallumkadavu-Town Center directions, respectively. Thus, the use of alternative routes will enhance the mobility of the area at the commencement of the mall and the capacity augmentations of existing roads will be considered in the near future.

Acknowledgements The authors are gratefully acknowledged for the support provided by Ms. Amrutha Nair, Project Engineer, and other staff of KSCSTE-NATPAC during the study.

References

1. Ponnurangam P, Umadevi G (2016) Traffic impact analysis (TIA) for Chennai IT Corridor. *Transp Res Procedia* 17
2. Khade OS, Khode BV, Bhakhtyapuri VK (2017) Evaluation of traffic impact on road network due to new commercial development. *IJSTE—Int J Sci Technol Eng* 3(09)
3. Gazder U, Saleh MHM, Al Zoubi YM, Mohammed O, Alhalabi KAN (2019) Calibrating traffic microsimulation model for Bahrain and estimating traffic impacts of a mall on road network. *Int J Comput Digit Syst*, ISSN (2210-142X)
4. Dey AC, Roy S, Uddin MA (2018) Calibration and validation at Vissim model of an intersection with modified driving behavior parameters. *Int J Adv Res (IJAR)*, ISSN: 2320-5407
5. Minhans A, Zaki NH, Belwal R (2013) Impact assessment: a case of proposed hypermarket in Skudai Town of Malaysia. *JournalTeknologi, Sci Eng*, eISSN 2180-3722 | ISSN 0127-9696
6. Indian Highway Capacity Manual (Indo-HCM), Council of Scientific and Industrial Research (CSIR), New Delhi (2012–2017)
7. IRC: 108-1996—Traffic prediction on rural highways
8. IRC: SP 19 2001 Manual for road DRP prefeasibility study
9. Errampalli M, Kayitha R (2016) Traffic management plan for Port Blair city, India. *Transp Res Procedia* 17:548–557
10. Sangaradasse P, Eswari S (2019) Importance of traffic and transportation plan in the context of land use planning for cities—a review. *Int J Appl Eng Res* 14(9), ISSN 0973-4562
11. Salim R, Samuel L, Francis L, Muhzina MI, Haris PH (2019) Microscopic traffic simulation using VISSIM and traffic management measures at Kalady. *IJESC* 9(7), ISSN 2321 3361
12. Muniruzzaman S, Orvin M, Hadiuzzaman M, Wasif S, Nasrin S (2019) Investigating network efficiency improvement measures using simulation technique in Mirpur Area. *Int J Traffic Transp Eng* 8(1):8–17
13. Traffic Operations and Safety Analysis Manual (TOSAM)—Version 2.0, VDOT Governance Document (2020)
14. Wilson KC, Salini PN, Sanjay Kumar VS, Sreedevi BG (2017) Transportation system planning for a work centre campus with direct access to national highway. *Indian Highw* 47(7)

Traffic Management

Effectiveness of Speed Calming Measures Along Arterial Roads



Akshata Badiger, Kuldeep, M. R. Archana, and V. Anjaneyappa

Abstract Excessive speed is one of the main factors in road traffic safety problem, increasing accident probability and affecting accident severity. To elevate the level of road safety, traffic calming measures like speed bumps, speed humps, raised crosswalks, rumble strips need to be implemented. This aids to reduce vehicle speeds at locations where low speed is essential, especially at accident-prone locations. The analysis based on the study carried out on outer ring road, Bengaluru city, India. The effectiveness of three types of traffic calming interventions viz., circular humps, trapezoidal humps and rumble strips is considered. Studies have been carried out to know the effect of different types of speed calming measures on speed of the vehicles. The performance of traffic calming measures in reducing vehicle speed is analysed, and the effect of speed calming measures on different categories of vehicles is presented. Trapezoidal humps are found to be more effective in reducing speeds of cars, motor bikes, auto-rickshaws, LCV, HCV and buses by 33.9, 22.8, 31.8, 29.5, 34.9 and 29.5%, respectively compared to rumble strips. The highest speed reduction is observed in buses followed by HCV compared to other class of vehicles. Regression analysis showed high correlation greater than 0.8 for speed of all class of vehicles.

Keywords Rumble strips · Circular humps · Trapezoidal humps · Vehicular speed

1 Introduction

Vehicle speed is one of the most important risk factors for road traffic safety, as it influences both the probability and severity of accidents [1–3]. Use of traffic calming measures is one of the most effective ways to reduce road accidents and improve

A. Badiger (✉) · Kuldeep · M. R. Archana · V. Anjaneyappa
R.V. College of Engineering, Bengaluru, India
e-mail: akshatab.cht19@rvce.edu.in

M. R. Archana
e-mail: archanamr@rvce.edu.in

safety. The speed calming measures aid in ensuring road safety for all users including non-motorised vehicle users and reduce crash occurrence and severity. They are enforcing measures that produce greater benefits. Speed calming techniques used in urban areas are classified into four categories viz., vertically deflected, horizontally deflected, narrowed road and central islands. The most efficient and reliable speed mitigation steps are the vertical deflected in the carriageway such as circular humps, parabolic humps, trapezoidal humps and rumble strips. Speed breakers used along urban roads may vary in terms of their height, base width and shape. Adaptability of speed breakers mainly depend on type vehicle using the carriageway, geometry of carriageway and category of road.

Setting up vertical calming measures would influence road safety by reduction in accidents [4–6]. The vertical interventions on urban roads have significant influence in speed reduction of all types of vehicles [7, 8]. The impact of vertical deflections in road alignment on traffic performance in terms of speed profile is dependent on physical and geometric properties [9]. Traffic calming devices, such as speed humps, should be located at appropriate distances from one other to establish a balance of speed and road safety advantages against capacity [10]. The height of speed calming measure is positively correlated with percentage of speed reduction, and width of the hump is negatively correlated [11, 12]. The speed breaker should be 17 m wide and 0.1 m in height, according to IRC guidelines for speed of the vehicle measured at 25 km/hr is as shown in Fig. 1 [13]. The different types of speed calming measures are represented in Figs. 2 and 3.

The shape of traffic calming measure has the influence on traffic flow parameters; the decrease in speed for flats was 71.6%, 66% for double bumps and 60% for

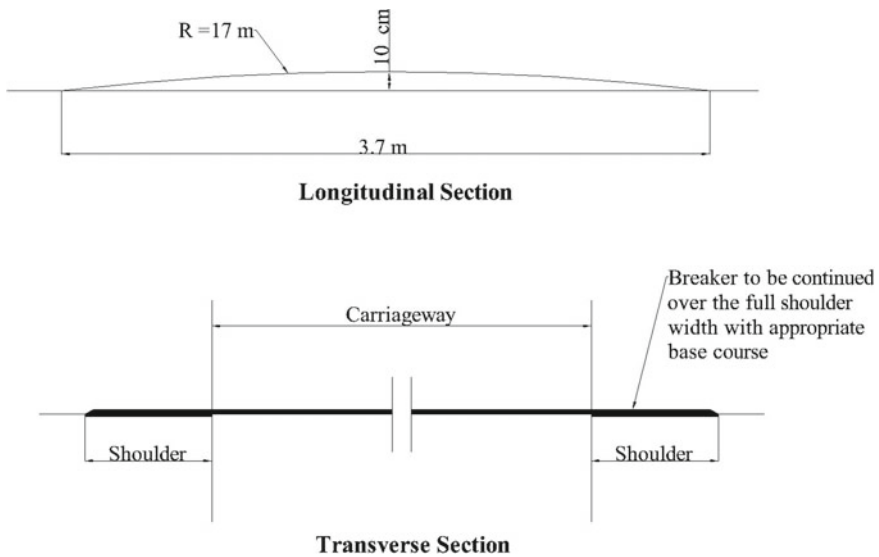


Fig. 1 Recommended specification for rounded hump type [13]



Fig. 2 Rumble strips and transverse markings



Fig. 3 Circular and trapezoidal humps

single humps [14]. The effect on heterogeneous traffic from the implementation of speed humps results in a drop of level of service [15–17]. The drivers reduce speeds, accelerate immediately after passing the humps and recover their original speeds around 30 m from the humps [18]. The driver deceleration and acceleration patterns near speed humps are consistent with those in previous observational studies [19–21]. This indicated that the installation of speed humps is effective in reducing speed variation and shows their potential to control drivers having more extreme speeds.

Mixed land uses involve a variety of environments and road user behaviour, which is commonly found in most Indian cities. Limited information exists on traffic calming measures used in India and their effectiveness in reducing speeds. Hence, this work has been taken up to study the effectiveness of different speed calming measures for different types of vehicles for urban roads.

2 Methodology

The urban road stretch is selected, and reconnaissance survey is carried out for the selected road. Field data are collected including traffic volume, geometric features of speed calming measures, spot speed of heterogeneous traffic. Different types of speed calming measures of circular humps, trapezoidal humps and rumble strips are selected for studies. The sequence of adopted methodology is shown in Fig. 4.

The multi-linear regression analysis with average speed as dependent variable and geometry, speed calming measure type as independent parameters is developed. The regression models for all the vehicular class are obtained.

2.1 Study Area

An arterial road of 62 km was chosen for the study of effectiveness of speed calming measures on different type of traffic in Bengaluru city. The geometry of the road consists of either four-lane divided or 2-lane undivided carriageway. The study road consists of bituminous and concrete overlay pavement. The total of 55 speed calming

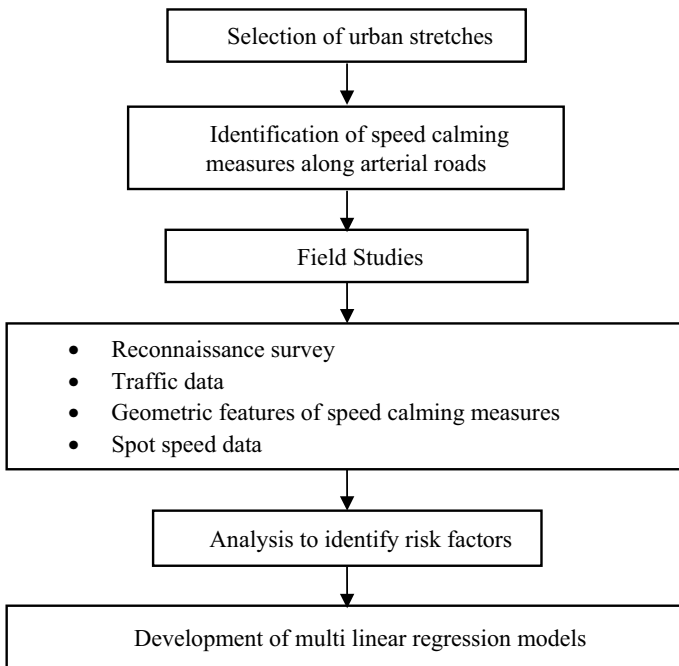


Fig. 4 Flowchart of methodology

Table 1 Traffic volume count of different vehicles

Class of vehicle	Average annual daily traffic (AADT)
Motorbikes	4697
Auto-rickshaws	684
Cars/jeeps	5574
LCV	425
HCV	250
Buses	240

measures is studied. Based on field studies, the effectiveness of speed calming measures viz., circular, trapezoidal humps and rumble strips is analysed.

3 Data Collection

Speed data were measured at 55 locations along arterial, sub-arterial and collector streets. Out of the 55 speed calming measures, there were 30 rumble strips, 9 circular humps and 16 humps with trapezoidal humps.

3.1 *Traffic Along the Selected Stretch*

The traffic volume count was carried out to know the heterogeneity of traffic and traffic distribution along the carriageway. Different classes of vehicles viz., motorbikes, cars, jeeps, trucks, LCV, HCV and buses were calculated along the road. The average annual daily traffic is shown in Table 1.

3.2 *Geometric Features of Speed Calming Measures*

Types of speed calming measures were mainly transverse rumble strips, circular humps and trapezoidal humps. The variation in terms of height, width, length of speed calming measure is shown Table 2.

Table 2 Geometric features of speed calming measures

Height/thickness (m)	Width (m)	Length (m)	Type of SCM
0.01	5.90	10.6	Rumble strip
0.01	7.14	9.75	Rumble strip
0.015	5.85	9.75	Rumble strip
0.015	6.30	9.75	Rumble strip
0.01	3.80	10.5	Rumble strip
0.01	1.11	10.5	Rumble strip
0.01	4.80	7.0	Rumble strip
0.01	3.21	10.5	Rumble strip
0.005	3.10	7.0	Rumble strip
0.005	4.00	7.0	Rumble strip
0.015	3.25	7.0	Rumble strip
0.1	3.66	7.0	Circular hump
0.1	1.10	7.0	Circular hump
0.1	3.78	7.0	Circular hump
0.08	1.50	7.0	Circular hump
0.05	3.00	5.5	Circular hump
0.05	2.20	5.5	Circular hump
0.05	3.00	5.5	Circular hump
0.05	3.90	7.0	Trapezoidal hump
0.1	3.00	5.5	Trapezoidal hump
0.1	3.00	5.5	Trapezoidal hump
0.05	6.10	5.5	Trapezoidal hump
0.1	3.78	7.0	Trapezoidal hump
0.15	3.78	7.0	Trapezoidal hump
0.1	3.78	7.0	Trapezoidal hump

3.3 Speed Data

Radar gun is used to measure spot speed of different vehicle classes at various SCMs. Speed profile assessment was done by measuring spot speed at 55 different locations on either side of the vertical deflection type SCMs, i.e. at a distance of 30 m before and 30 m after SCM.

4 Results and Discussion

The speed data were collected 30 m before, on the spot of SCM and 30 m after SCM. The speed data were also measured in between two consecutive SCMs which are placed 20 m apart. The speed profile obtained for the two rumble strips exhibited reduction in vehicle speed for all categories of vehicles at SCM. The lowest speed was measured in between the rumble strips. Speed reduction compared to HCV for two wheelers, auto-rickshaws, cars, LCV and buses is 31.3%, 33.4%, 41.2%, 28.6% and 25.9%, respectively, as shown in Fig. 5.

The effectiveness of circular and trapezoidal humps placed at 20 m distance was studied and was observed that average speed of two wheelers, auto-rickshaws, cars, LCV increased between the two speed calming measures, but the speed reduced in HCV and buses. The speed reduction on traffic calming measure compared to 30 m before was 25.9% for two wheelers, 14.8% for auto rickshaws, 24.2% for cars and LCV, 3.85% for HCV and 33.3% for buses as shown in Fig. 6.

At the approach of speed calming measure, trapezoidal humps are more effective in reducing speed compared to rumble strips by 30.8, 27.9, 39.2, 35.7, 25.6, 14.36% for cars, two wheelers, auto-rickshaws, LCVs, HCVs, buses, respectively. Compared to circular humps, the speed reduction is 10.4, 5.9, 17.3, 17.6, 3.2% for cars, two wheelers, auto-rickshaws, LCVs, HCVs, respectively, as shown in Fig. 7.

The speed obtained at the location of speed calming measure for different class of vehicle and speed calming measure is presented in Fig. 8. Speed reduction at trapezoidal humps compared to rumble strips is 33.9% for cars, 22.8% for two wheelers, 31.8% for auto-rickshaws, 29.5% for LCVs, 34.9% for HCVs and 29.5% for buses. In comparison with circular humps, the speed reduction in trapezoidal humps is 5.9%

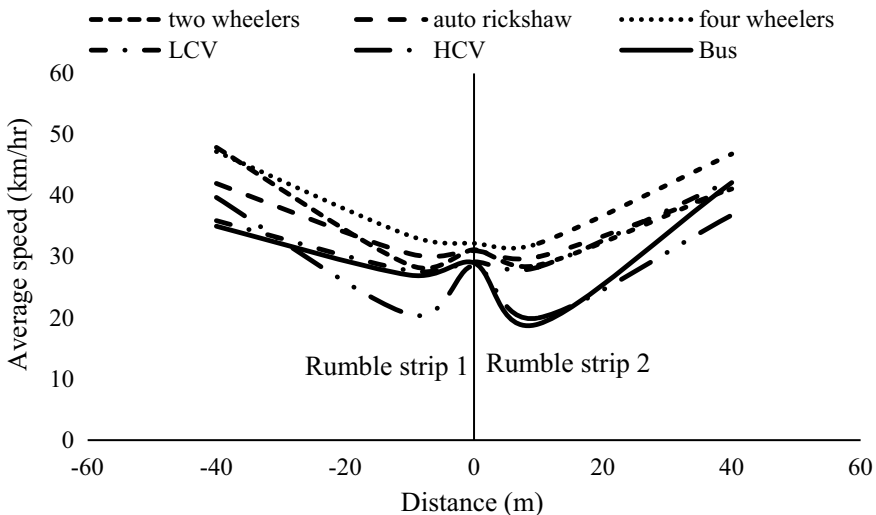


Fig. 5 Effectiveness of rumble strips placed 20 m apart

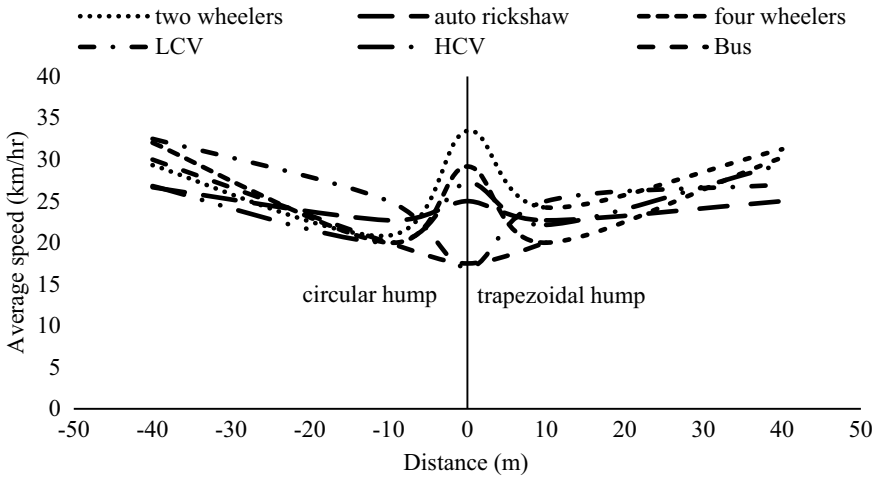


Fig. 6 Effectiveness of circular and trapezoidal humps placed 20 m apart

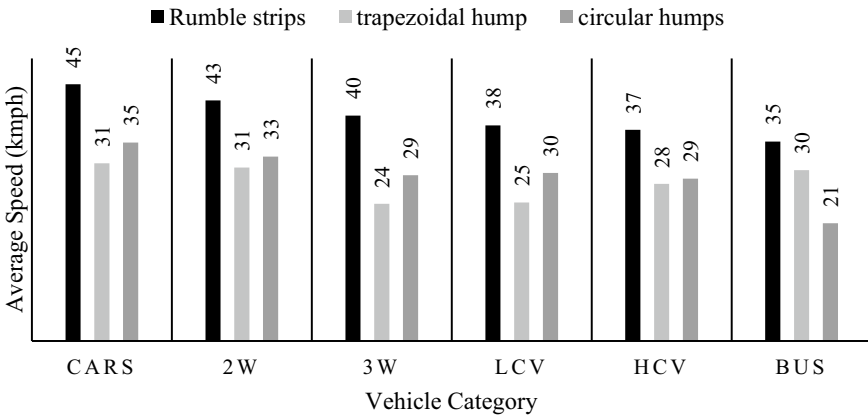


Fig. 7 Speed variation before the speed calming measures

for cars, 10.3% for two wheelers, 17.8% for auto-rickshaws, 25.7% for LCVs, 4.7% for HCVs and increase in speed by 15.8% for buses.

The average speed of vehicles after passing the SCM, as shown in Fig. 9, the speed reduction in circular humps compared to rumble strips is 8.4% for cars, 14.8% for two wheelers, 25% for auto-rickshaws, 23.8% for LCVs, 23.5% for HCVs and 23.9% for buses. In comparison with trapezoidal humps, the speed reduction in circular humps is 2.4% for cars, 9.2% for two wheelers, 1.2% for LCVs, 28.8% for buses, but there was increase in speed by 4.3% for auto-rickshaws and 0.2% for HCVs.

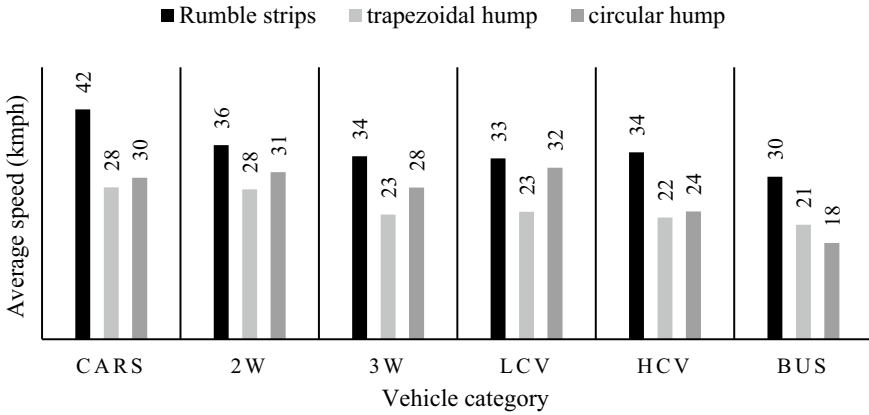


Fig. 8 Speed variation on the speed calming measures

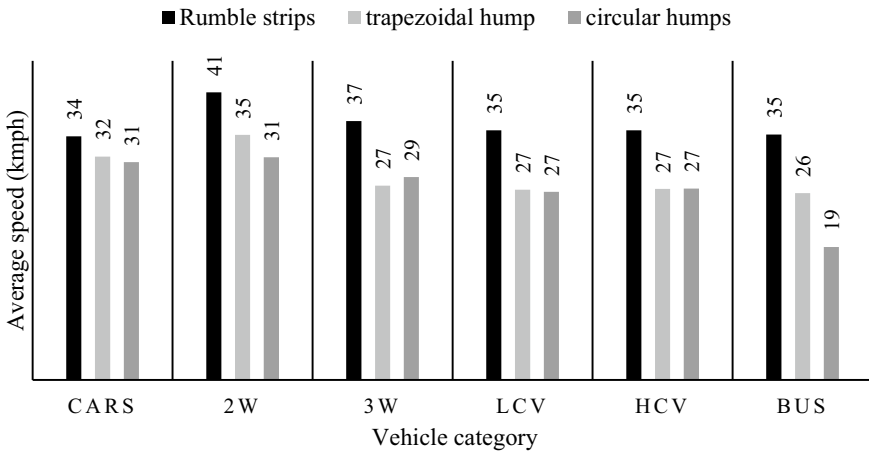


Fig. 9 Speed variation after the speed calming measures

4.1 Regression Analysis

The multi-linear regression analysis with average speed as dependent variable; speed calming measure type, type of vehicle, geometry, etc. as independent parameters are developed. The developed equations are presented in Eq. 1–6.

$$V_{\text{motorbikes}} = 18.934 - 3.98 \log(H) - 0.0009W^3 + 6.18 \log(L) - 8.84 \log(S) \tag{1}$$

$$R^2 = 0.92$$

$$V_{\text{autorickshaws}} = 10.56 - 7.80 \log(H) - 0.0095W^3 + 6.73 \log(L) - 5.16 \log(S) \quad (2)$$

$$R^2 = 0.87$$

$$V_{\text{cars}} = 14.24 - 9.36 \log(H) - 0.0016W^3 + 5.12 \log(L) - 0.45 \log(S) \quad (3)$$

$$R^2 = 0.82$$

$$V_{\text{LCV}} = 13.35 - 15.648 \log(H) - 0.0018W^3 + 13.9 \log(L) - 24.0 \log(S) \quad (4)$$

$$R^2 = 0.89$$

$$V_{\text{HCV}} = 4.98 - 8.5189 \log(H) - 0.0009W^3 + 16.6 \log(L) - 5.79 \log(S) \quad (5)$$

$$R^2 = 0.93$$

$$V_{\text{buses}} = 15.11 - 10.40 \log(H) - 0.0014W^3 + 6.78 \log(L) - 1.43 \log(S) \quad (6)$$

$$R^2 = 0.84$$

where

- V average speed of vehicle, kmph
- H height/thickness of speed calming measure, m
- W width of SCM, m
- L length of speed hump, m
- S type of speed calming measures

5 Conclusion

Following conclusions are drawn from the studies carried out. The three types of traffic calming measures viz., rumble strips, circular humps and trapezoidal humps

are analysed for their effect on speed of different vehicle class for heterogeneous traffic along selected urban roads.

- i. The speed variation along the speed calming measures indicated that there is gradual decrease in speed from the approach to speed calming measure.
- ii. There is speed reduction in between the 2 sets of rumble strips. However, in between circular and trapezoidal humps, there is slight increase in speed compared to the average speed of vehicles at the two speed calming measures.
- iii. Trapezoidal humps are more effective in reducing speeds of cars, motor bikes, auto rickshaws, LCV, HCV and buses by 33.9, 22.8, 31.8, 29.5, 34.9 and 29.5%, respectively, compared to rumble strips. Compared with circular humps, the speed reduction in trapezoidal humps is 6.0% for cars, 10.3% for two wheelers, 17.8% for auto rickshaws, 25.7% for LCVs, 4.7% for HCVs and increase in speed by 15.9% for buses on the speed calming measure.
- iv. Speed calming measures affect vehicle speed cars, motorbikes, auto, trucks and buses differently. The highest speed reduction is observed in buses followed by HCV compared to other class of vehicles.
- v. The strong correlation of greater than 0.8 was found between the average speed all vehicles and geometric characteristics of speed calming measures.

References

1. Aljanahi AA, Rhodes AH, Metcalfe AV (1999) Speed, speed limits and road traffic accidents under free flow conditions. *Accid Anal Prev* 31:161–168
2. Gitelmana V, Doveh E, Bekhor S (2017) The relationship between free-flow travel speeds, infrastructure characteristics and accidents, on single-carriageway roads. *Transp Res Procedia* 25:2026–2043
3. De Pauwa E, Daniels S, Franckx L, Mayeres I (2018) Safety effects of dynamic speed limits on motorways. *Accid Anal Prev* 114:83–89
4. Jateikienė L, Andriejauskas T, Lingytė I, Jasiūnienė V (2016) Impact assessment of speed calming measures on road safety. *Transp Res Procedia* 14:4228–4236
5. Chen L, Chen C, Ewing R, McKnight EM, Srinivasan R, Roe M (2013) Safety countermeasures and crash reduction in New York City-Experience and lessons learned. *Accid Anal Prev* 50:312–322
6. Distefano N, Leonardi S (2015) Experimental investigation of the effect of speed bumps in sequence on noise emission level from motor vehicles. *Noise Control Eng J* 63(6):582–597
7. Yang Y, Sun X, He Y (2010) Effectiveness of rumble strips on freeways. In: Proceedings of the 10th international conference of Chinese transportation professionals, pp 425–433. American Society of Civil Engineers, Beijing, China
8. Zhang Y, Hu Z, Chen A (2015) Urban road speed humps setting technology. In: Fifth international conference on transportation engineering. American Society of Civil Engineers, Dalian, China, pp 1092–1101
9. Mahdy H (2012) Speed calming using vertical deflections in road alignment. In: 12th COTA international conference of transportation professional. American Society of Civil Engineers, Beijing, China, pp 2085–2094
10. Abdi A, Bigdeli Rad H, Azimi E (2017) Simulation and analysis of traffic flow for traffic calming. *Proc Inst of Civ Eng Municipal Eng* 170(1):16–28

11. Korra RK, Kumar M, Abhinay B (2019) Critical analysis of speed hump and speed bump and geometric design of curved speed hump. In: World conference on transport research—WCTR, transportation research Procedia 48. Mumbai, India, pp 1211–1226
12. Al-Omari BH, Al-Masaeid HR (2010) Effect of speed humps on traffic delay in Jordan. *Road Transp Res* 11(4)
13. IRC-99–2018. Guidelines for traffic calming measures in urban and rural areas. Indian Road Congress (2018)
14. Abdulmawjoud AA, Jamel MG, Al-Taei AA (2020) Traffic flow parameters development modelling at traffic calming measures located on arterial roads. *Ain Shams Eng J* 12(1):437–444
15. Hao Y, Pan L, Jia H, Xu Z (2011) Developing the simulation module of traffic operations in vicinity of speed bumps on highways in VISSIM, In: 11th international conference of chinese transportation professionals (ICCTP). American Society of Civil Engineers, Nanjing, China, pp 2375–2384
16. Cheng L, Hongwei G, Yujie Z, Wuhong W (2016) Simulation for the impacts of speed bumps on traffic flow considering driving behaviors. In: 16th COTA international conference of transportation professionals. American Society of Civil Engineers, Shanghai, China, pp 1134–45
17. Korra RK, Molugaram K, Manthirikul S (2020) Analysis of speed profile at speed hump under various dimensions and simulating their LOS using VISSIM. *Transp Res Procedia* 48:1200–1210, Elsevier B.V.
18. Yeo J, Lee J, Cho J, Kim DK, Jang K (2020) Effects of speed humps on vehicle speed and pedestrian crashes in South Korea. *J Safety Res* 75:78–86. <https://doi.org/10.1016/j.jsr.2020.08.003>
19. Barbosa H, Tight MR, May AD (2000) A model of speed profiles for traffic calmed roads. *Transp Res Part A* 34:103–123
20. Moreno AT, Garcia A, Romero MA (2011) Speed Table evaluation and speed modeling for low-volume crosstown roads. *Transp Res Rec* 2203(1):85–93. <https://doi.org/10.3141/2203-11>
21. Pau M, Angius S (2001) Do speed bumps really decrease traffic speed? An Italian experience. *Accid Anal Prev* 33(5):585–597. [https://doi.org/10.1016/s0001-4575\(00\)00070-1](https://doi.org/10.1016/s0001-4575(00)00070-1)

Traffic Management in Forest and Ecosystem Conservation. A Study on NH 766 Through Bandipore National Park and Proposing a Traffic Management Plan with Alternate Route Consideration



Arun Baby M. Wilson  and M. A. Naseer 

Abstract Transportation network is inevitable in the developing world. In India where we have a rich forest cover, many of the roads are passing through eco-sensitive areas such as national parks and wildlife sanctuaries. There are issues being reported due to these roads passing through the eco-sensitive areas such as animal deaths due to road accidents, loss of habitats, fragmentation of ecosystems, and loss of forest cover. The Calicut–Kollegal national highway, NH766 is passing through Bandipore national park on the stretch which connects Sultan Bathery and Gundelpette. Recently, a conflict had risen between environmental activists and the public for imposing a complete traffic ban along the NH766 passing through the Bandipore NP. A baseline study had conducted on the NH766, and the impact of the same on the ecosystem existing is analyzed through the data collected. A network analysis is performed on the alternate route available for bypassing the traffic. Traffic management plan and policies are derived out of the analysis on the baseline data collected and the inferences drawn from the network analysis performed on the alternate routes.

Keywords Traffic management plan · Forest conservation · Sustainable transportation

A. B. M. Wilson (✉)

School of Architecture, Christ (Deemed to be University), Kengeri, Bangalore, India

e-mail: arunbaby.wilson@christuniversity.in

M. A. Naseer

Department of Architecture and Planning, National Institute of Technology-Calicut, Kozhikode, India

e-mail: naseer@nitc.ac.in

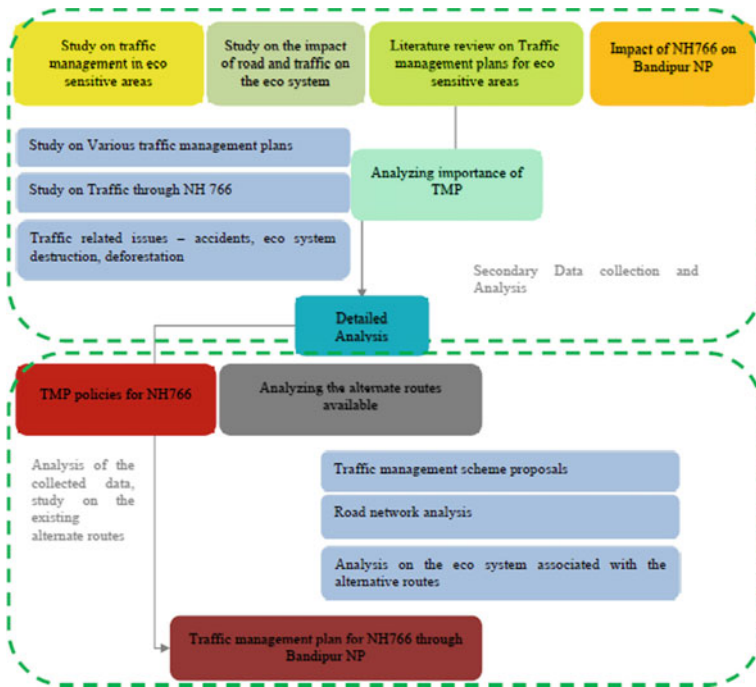
1 Introduction

In the present scenario of rapidly increasing vehicular volume and road transport dependency, the concern should be about the environmental impacts that the transportation network causes. It is already a hot topic of discussion among the environmental activists, transportation planners, urban planners, and all the people. The irreparable damages that the environment is subjected to are need to be addressed for a sustainable way of living. Very well-prepared traffic management plans and policies can serve as the most efficient tool in ensuring an environment friendly transportation system.

Recently, issues are being reported on the conflict between environmental activists and people upon the traffic regulations and proposal of traffic ban along the NH766 stretch passing through Wayanad wildlife sanctuary and Bandipore National Park which connects Calicut in Kerala and Kollegal in Karnataka. The route is already imposed with traffic regulations as night traffic is completely banned as the gates are open only from 6 am to 9 pm. This strategy had implemented after witnessing high rate of human animal conflicts and loss of wildlife in road accidents during night time. But, at present, the environmental activists are requesting for the permanent closure of the NH766 through the reserved forest area for the betterment of the ecosystem. The common people of Kerala, particularly the people residing in Sultan Bathery in Wayanad district are protesting against the call for complete traffic ban as the road being major transportation and commercial spine on that area. This study is focused on the present situation of traffic along NH766 through the reserved forest area and identifying the impact of traffic upon the ecosystem to analyze the need for a well-derived traffic management plan to regulate and manage the traffic flow than imposing a complete traffic ban considering the alternate routes present to bypass the night traffic and the effectiveness of the present traffic management strategies also analyzed. The expected outcome of this study is a well-defined traffic management plan strategy for the NH766 through the reserve forest area to preserve the ecosystem and biodiversity.

2 Materials and Methodology

For conducting the study and analysis, there are not enough secondary data available and thus needed to collect primary data. On field, survey and personal interviews are adopted as data collection tools and the data collected. The methodology flowchart is shown below;



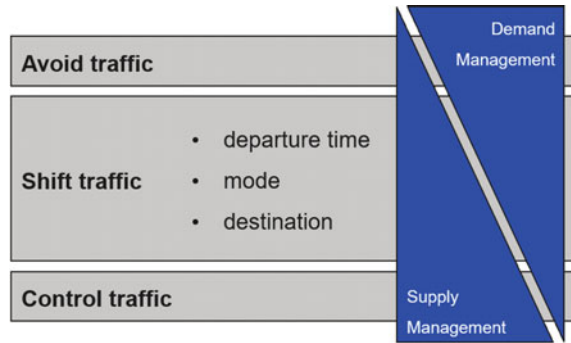
The importance of traffic management in forest and ecosystem conservation is studied and analyzed based on the study reports available on traffic management policies and ecosystem and environment protection or conservation. A baseline study had conducted on the NH766, and the impact of the same on the ecosystem existing in Bandipore NP is analyzed through the data collected. A network analysis is performed on the existing roads available which can be proposed as the alternate route bypassing the traffic. Traffic management plan and policies are derived out of the analysis on the baseline data collected and the inferences drawn from the network analysis performed on the alternate routes.

3 Importance of Traffic Management Plan

Traffic management plans are prepared to reduce and mitigate the negative impacts of traffic on the safety, environment, traffic flow, and the economic efficiency. These measures intended to reduce the demand of traffic through the region and to maximize the capacity. The term capacity doesn't only mean the carrying capacity of the road but of any quality including the purity of air and water and the green cover efficiency.

For ecosystem conservation, traffic management plan is very effective as it efficiently controls and reduces the demand for traffic and thus emphasizing the natural environment. While bringing the traffic demand lower, the air quality, atmospheric

Fig. 1 Levels of traffic management



conditions, wildlife safety, temperature, foliage are all get refreshed, and the serenity would be bringing back to the nature. Three different types of measures enable traffic management as shown in Fig. 1 [1].

Traffic management can be separated into two main categories [1];

- i. Static traffic management: These are long-term measures which are mostly restricting or controlling traffic for a longer span of time.
- ii. Dynamic traffic management: Dynamic management measures are short-term measures and more effective than static measures as it addresses specific traffic situations. These measures are issue specific and well defined such as diversion of traffic according to time period and restriction of heavy-duty vehicles in narrow broadsheet.

Table 1 enumerates different dynamic traffic management measures for different modes of transportation. Since these measures are issue specific, they are highly effective and efficient in managing the traffic rather than long-term static measures as it completely imposing restrictions rather than managing the traffic.

3.1 Preparation of Eco-Sensitive Traffic Management Plan

Eco-sensitive traffic management plans are dynamic measures since it is defined for specific purpose. It focuses on the environmental protection by managing the demand for traffic through eco-sensitive regions. The preparation of traffic management plan for eco-sensitive regions consists of following steps;

- i. Assessing the effect of traffic on the ecosystem
- ii. Identifying the problems and critical parameters posing the issues
- iii. Projection of identified issues and impacts
- iv. Identifying and proposing measures to mitigate the issues
- v. Assessing the effectiveness of the measures proposed

Table 1 Possible measures for dynamic traffic management [1]

Private transport measures	Public transport measures	Multi-modal and inter-modal measures	Non-motorized transport measures
i. Rerouting of traffic streams ii. Increase of capacity (through, e.g., traffic signal control) iii. Allow temporary special lanes iv. Dynamic adjustment of available parking spaces v. Dynamic toll system vi. Pre-emption of emergency vehicles vii. Variable speed limits viii. Ramp metering ix. Restriction of overtaking	i. Redistributing passenger inside public transport ii. Rerouting public transport vehicles iii. Public transport prioritization increase of capacity of a line iv. Introduce special lines, lanes, and stops v. Secure (inter-) connections between lines vi. Increase of accessibility and attractiveness vii. Adjust ticket prices	i. Information about all modes and diverting measures ii. Influencing the mode choice iii. Shifting the start of the trip iv. Changing the use of transport areas v. Mobility pricing vi. Information about available car-sharing vehicles	i. Prioritization of cyclists at intersections ii. Prioritization of pedestrians at intersections iii. Temporary special lanes for cyclists iv. Temporary pedestrian areas v. Information about available bike-sharing systems

4 Eco-Link @BKE

The Eco-Link@BKE (Fig. 2) is an intervention with an ecological bridge that runs over the Bukit Timah Expressway, connecting Bukit Timah Nature Reserve and Central Catchment Nature Reserve. The one of its kind in Southeast Asia, this overpass serves the purpose of restoring the ecological connection between two nature reserves, allowing wildlife to expand their habitat, genetic pool, and survival chances.

Once the BKE has started functioning, instances of roadkill got increased near the two nature reserves. They recorded even the death of species listed in IUCN red list like Sunda pangolins (*Manis javanica*), large forest gecko (*Gekko smithii*), and cream-colored giant squirrel (*Ratufa affinis*). So, as to mitigate these problems, the Eco-Link@BKE—an ecological corridor over the BKE—was built in 2013 [2].

Wildlife bridges help animals safely pass through their corridors, across heavy traffic bearing roads without being affected. The 62 m-long Eco-Link@BKE is the best example of a wildlife bridge.

The ability to move between one forest areas to another is important for animals as most of the wild animals are territorial in nature, and they need large spaces. The hunt for food and search for water is also demands the animals to move in between forest regions. The change in whether creates movement of animal groups from one region to another through spaces called wildlife corridors. Wildlife bridges reinvent the lost wildlife corridors due to the introduction of road transportation through forest areas.

Animals could be directed through the wildlife bridges with the use of native plants and vegetation over the bridge to make it merges with the existing forest region and



Fig. 2 Ariel view of Eco-Link @BKE [2]

appears to be a regular wildlife corridor to the animals. There are no study results have been posted till now regarding the effectiveness of these wildlife bridges, but there are incidents recorded which clearly shows the wildlife using these bridges. Thermal cameras set up on these wildlife bridges had recorded images of wildlife crossing the BKE through the Eco-Link bridges.

These types of wildlife bridges which are integrated with the existing forest region can be a very effective solution for the loss of wildlife corridors and habitat fragmentation. It needs a lot of monetary support as it requires a very solid and strong bridge construction, but in turn, it can be the greatest solution for these issues faced by wildlife due to the road transportation infrastructure.

5 Traffic Study on NH766 Through Wayanad Wildlife Sanctuary and Bandipore National Park

The present situation of NH766 and the effect of the traffic flow through the reserved forest area are documented to assess the impact of traffic upon the ecosystem present. Personal interviews are conducted, and location mapping also had done through primary surveys to record and analyze the data (Fig. 3). The major criteria considered are the wildlife accidents due to the road traffic as it is raised as the prominent issue by the environmental activists for the permanent closure of the road. The locations of the wildlife accidents are marked in the map to analyze the spatial relationship between the accident locations and road traffic.

The NH 766—Calicut—Kollegal highway is having a 19.7-km-long stretch passing through the reserved forest region in which 7.2 km is through Wayanad wildlife

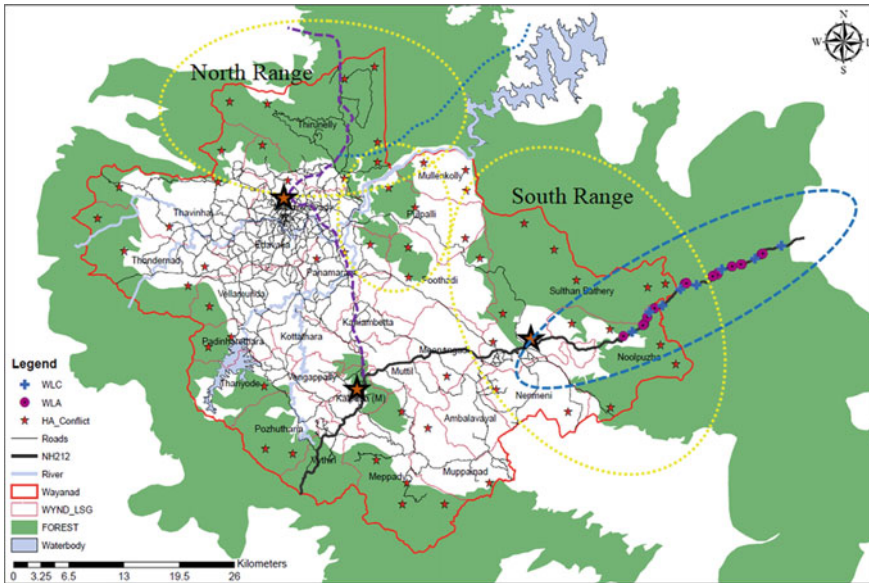


Fig. 3 Map of Wayanad showing reserved forest area and traffic routes

sanctuary and 12.5 km is passing through Bandipore national park as represented in Fig. 4. This stretch of road is imposed with night traffic ban on notice of the increasing rate of wildlife accidents.

After recording the locations of wildlife accidents and deaths on road (Fig. 5), it is found that the locations are mostly away from the demarcated wildlife crossing points. Another important factor is that the accident locations lie just near the bends, turns, and speed reducers as the vehicles speed up after these locations. The already marked wildlife crossings have trenches and fences nearby restricting the volume of wildlife crossing which in result making the wildlife to cross the road wherever possible. The over speeding and carelessness of drivers in areas other than notified wild crossings causes most of the accidents. The stretch of NH766 marked in blue ellipse in Fig. 2 is passing through the reserved forest area. The same is blown up in Fig. 4 with location of wildlife crossing and wildlife accidents marked.

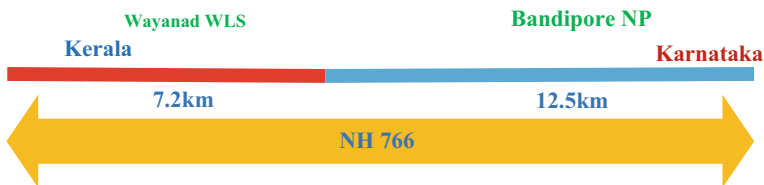


Fig. 4 Length of NH766 passing through reserved forest region

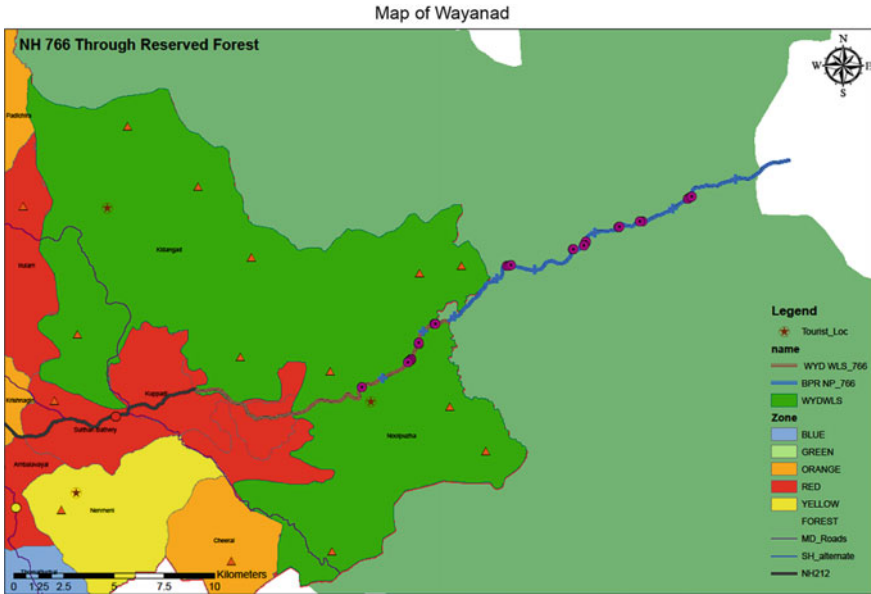


Fig. 5 Location of wildlife crossing and wildlife accidents along NH766 through reserved forest

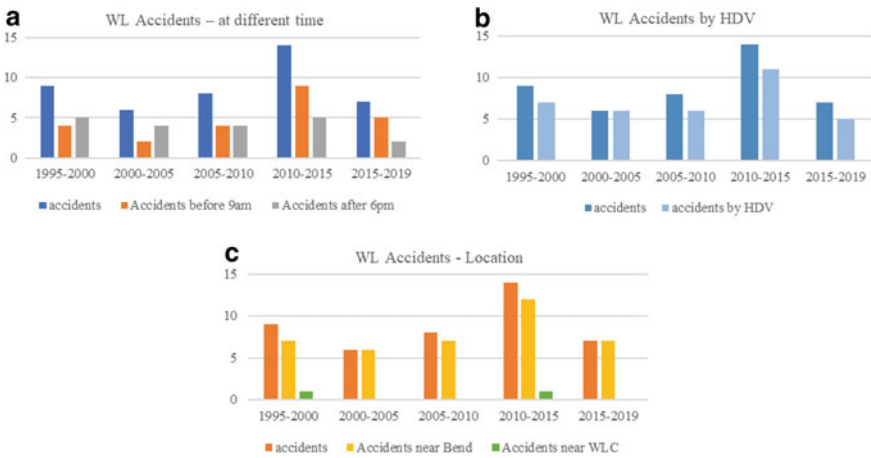


Fig. 6 a Wildlife accidents based on time intervals, b wildlife accidents caused by heavy-duty vehicles, c wildlife accidents based on location

While assessing the data on accidents, it is very clear that the greater number of accidents caused are by heavy-duty vehicles, and interestingly, they are mostly happened in the time period of 6:00 am–9:00 am in the morning the 3 h gap just after opening the gates and 6:00 pm–9:00 pm in the evening the three-hour gap just before the closing of the gate (Table 2). This is because of the atmospheric conditions

Table 2 Data on wildlife accidents along NH766 through reserved forest

Year	Accidents	Accidents by HDV	Accidents before 9am	Accidents after 6 pm
1995–2000	9	7	4	5
2000–2005	6	6	2	4
2005–2010	8	6	4	4
2010–2015	14	11	9	5
2015–2019	7	5	5	2

during these time periods are very comfortable for the wildlife to move for different purposes.

The NH766 is passing through the reserved forest area as along Wayanad WLS human inhabited land is also present within the reserved forest area where in Bandipore NP the road passes completely through forest area. The inhabited lands in Wayanad lie in red zone which is the most critical region in the ESZ. Thus, highly imposed restrictions and regulations have to be deployed considering the fact that traffic management plan would affect the daily life of people living in the area.

5.1 Traffic Data on NH766

There are three entry points from Karnataka to Wayanad, namely Muthanga, Bavali, and Tholpetty forest check points (Fig. 7). All these entry points are led to roads passing through reserved forest area consists of national parks and wildlife sanctuaries. Among this, the road through Muthanga gate connecting to Mysore via Gundalpet is national highway (NH766), and other two are state highways (Fig. 7).

The following map (Fig. 9) shows the network of main roads bearing the maximum traffic flow. All the traffic moving to Karnataka (Mysore or Bangalore) through Wayanad and vice versa have to run through any of these roads. Among these, the most taken road is NH766 which is passing through Muthanga Range of Wayanad WLS and Bandipore NP since it is the most known route and having better connectivity of towns and commercial centers in between. Considering the fact that NH766 is the most chosen route, complete ban of traffic is not possible and has to be provided with proper traffic management plan strategies.

5.2 Alternate Routes for NH766

There are two alternative roads present to bypass the traffic (Fig. 10). Each road has three different route combinations considering the origin as Calicut and destination as Mysore. Consider the alternate roads as Road 1 and Road 2 with three route combinations as a, b, and c as in Table 3. These combinations are listed below in

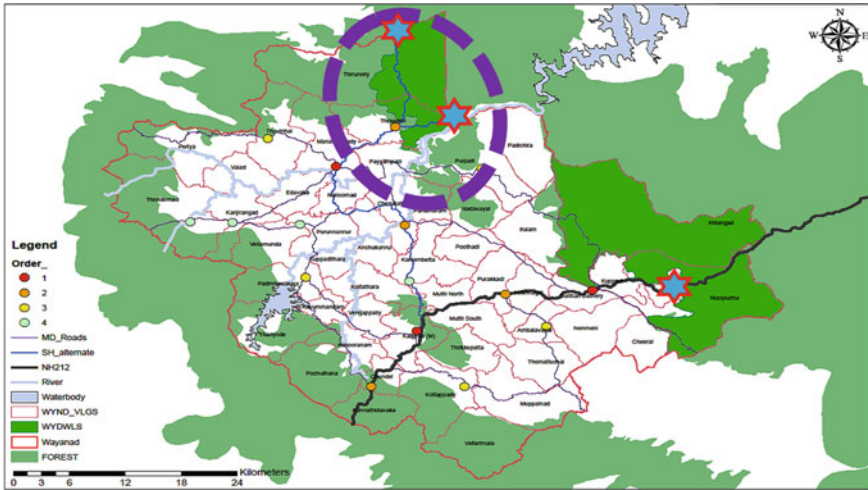


Fig. 7 Map showing locations of alternate route entry points to Kerala

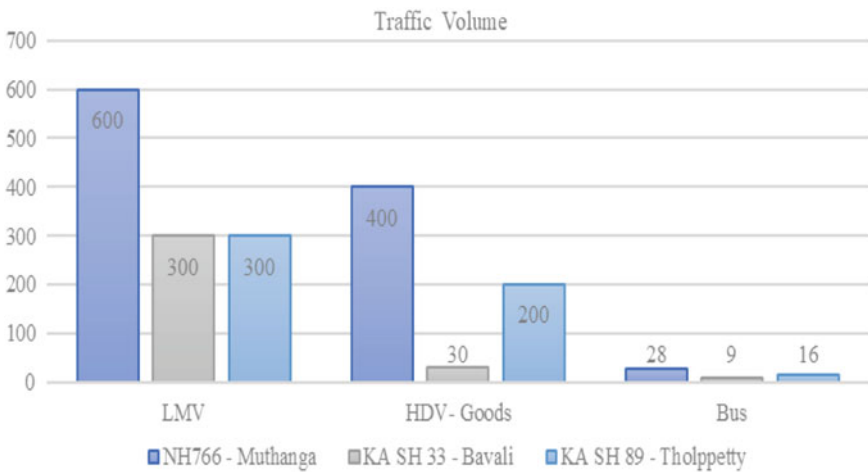


Fig. 8 Traffic data on alternate route entry points to Kerala

the table with their length in kilo meters. Road 1 is through Nagarhole NP which is having a controlled traffic flow with traffic ban from 6 pm–6am.

Since Road 1 is closed from 6 pm–6am, it can only be used as a day time alternate route. Road 2 is not having any traffic restrictions or regulations and been used by long-route vehicles traveling in the night. The roads are in good condition which are well maintained and more activity nodes being developed along this route. Road 2 is longer by 47 km than Road 1 which increases the travel time by 1–2 h which makes the road least preferred. (Table 4).

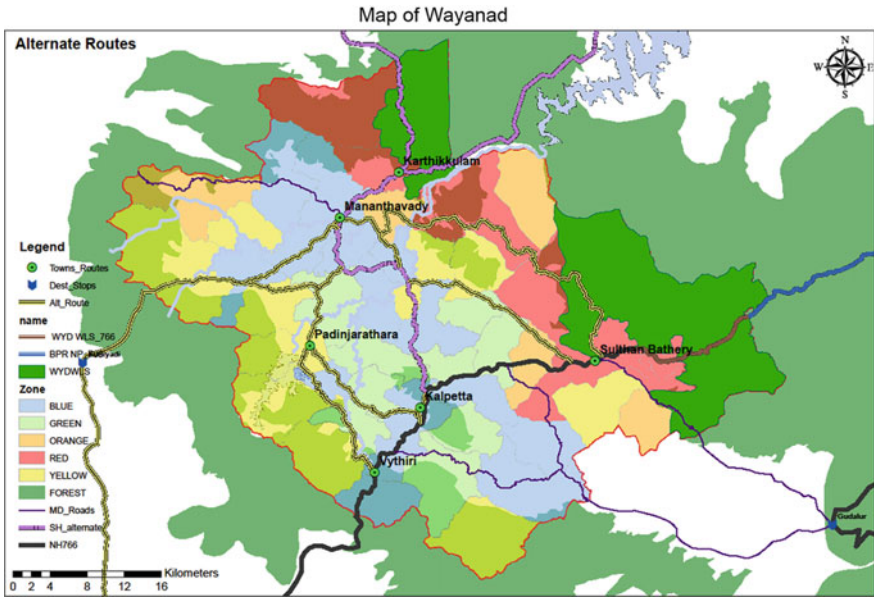


Fig. 9 Major road network through Wayanad

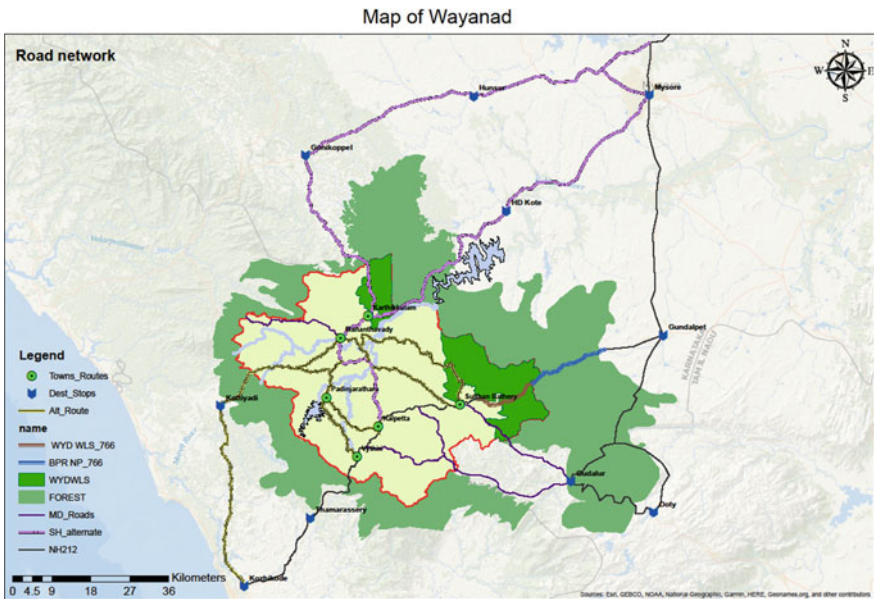


Fig. 10 Alternate routes for NH766 through Wayanad

Table 3 NH766 and alternate routes—length in kilometers

Road	Route	Origin	Destination	Via	Distance (km)
NH 766	Main	Calicut	Mysuru	Kalpetta—Sultan Bathery—Gundalpet	213
1	a	Calicut	Mysuru	Kalpetta—Mananthavady—HD Kote	215
	b	Calicut	Mysuru	Vythiri—Panjarathara—Mananthavady—HD Kote	210
	c	Calicut	Mysuru	Kuttiyadi—Mananthavady—HD Kote	201
2	a	Calicut	Mysuru	Kalpetta—Mananthavady—Hunsur	252
	b	Calicut	Mysuru	Vythiri—Panjarathara—Mananthavady—Hunsur	257
	c	Calicut	Mysuru	Kuttiyadi—Mananthavady—Hunsur	248

Table 4 NH766 and alternate routes—comparison of condition





Road	Route	Type of Road	Traffic volume	Condition of road	Reserved forest area	Traffic regulations
NH 766	Main	NH	Highest	Very good	WYD WLS, Bandipore NP	9 pm – 6am traffic ban
1	a	SH	High	Nagarhole NP—narrow road with restrictions, speed breakers	Nagarhole National Park—20 km through reserved Forest	6 pm–6am traffic ban
	b	SH	Low			
	c	SH	Low			
2	a	SH	High	Wide, well-maintained road—newly constructed	Kattikkulam to Tholpetty—16-km road runs through periphery of North Range of WYD WLS	NA
	b	SH	Low			
	c	SH	Low			

5.3 Traffic Management Plan for Nagarhole Tiger Reserve

Nagarhole tiger reserve is a portion of Bandipore national park lies along the road connecting Mananthavady in Kerala to Mysore in Karnataka. The traffic through this road already subjected to some traffic management strategies as in Table 5 which are very much effective in protecting the ecosystem and wildlife from the negative impacts of road traffic.

The various traffic management strategies adopted for Nagarhole tiger reserve and the results are listed in Table 3;

Table 5 Traffic management strategies for Nagarhole tiger reserve

Strategy		Results
Timing—6am to 6 pm		Reduced traffic—WL accidents reduced to almost 15%
Road width—reduced to 3.8 m		Reduced HDV traffic—less congestion in traffic
Road length—increased by 14 km by diverting through human inhabited area		Long route bus services dropped to 50%—undisturbed WL area
Ticketing to control speed and timing		Reduced level of illegal activities—stopping in forest, disturbing wildlife, anti-social activities

6 Results and Interpretations

The study conducted led to the following results regarding the traffic management for eco system conservation;




- i. A well-defined traffic management plan is required for NH766 through the reserved forest area
- ii. The time period of the day and type of vehicles passing have very evident role in the reported wildlife accidents
- iii. Most of the accidents are caused by heavy-duty vehicles, and the time period of most accident is 6:00 am–9:00 am in the morning and 6:00 pm–9:00 pm in the evening
- iv. The location of the accident shows that they are not near to the marked wildlife crossing areas
- v. The dynamic short-term measures implemented on the road passing through Nagarhole tiger reserve are very effective in managing the traffic and achieving the desired goals.
- vi. With the present traffic management policies on the two roads among the three roads available for the transportation between Wayanad and Karnataka, the one road which has no traffic regulations or restrictions receiving higher traffic at present.

6.1 Traffic Management Plan Strategies

The traffic management plan for NH766 through Wayanad WLS and Bandipore NP can be laid out as strategies derived based on dynamic measures as it is a major inter-state national highway and most importantly supports all kind of traffic movements between Karnataka and Kerala (mainly Wayanad and Kozhikode districts). Thus, to ensure the wildlife safety and controlled and regulated flow of vehicular traffic, the TMP could be formulated based on the observations made and inferences drawn. With the results observed, strategies for preparation of traffic management plan for NH766 are found as follows;

- i. Complete closure of the road is not a viable solution as it totally bring down the economic growth of Wayanad and Kerala
- ii. The most important area to look upon is the movement of heavy-duty vehicles according to the time periods.
- iii. HDV has to be restricted in traffic through the reserved forest area in the first three hours after opening gates and last three hours before closing the gate to reduce the risk of wildlife accidents
- iv. More speed-reducing measures have to be introduced to limit the speed of vehicles through the reserved forest.
- v. Ticketing and monitoring of time of vehicles have to be implemented to avoid the chance of vehicles stopping in between within the forest area
- vi. Dune crossings for wildlife can be introduced which will ensure wildlife safety and uninterrupted traffic flow
- vii. The width of the road should not be subjected to expansion from the present situation
- viii. More signages and warning boards have to be installed.
- ix. Full-time surveillance has to be introduced and periodic patrolling to ensure wildlife safety (Table 6)

Table 6 Traffic management strategies for NH766 through Wayanad WLS and Bandipore NP

Strategy		Focused outcome
<p>Timing—6am to 9 pm</p> <ol style="list-style-type: none"> 1. Retaining the existing time restrictions 2. Truck timing: 9am–6 pm 3. Noon time (12 pm–2 pm) <p>Controlled traffic flow</p> <ol style="list-style-type: none"> 4. Passenger carrier services: 7am–7 pm 		<ul style="list-style-type: none"> • Bringing down accident rates due to vehicular traffic, mainly heavy-duty vehicle accidents • Reduce the risk of human animal conflict
<p>Speed controlling measures</p> <ol style="list-style-type: none"> 1. Introducing speed breakers near to the accident spots 2. Scrapping and roughening bends 3. Heat camera surveillance to detect animal crossing 		<ul style="list-style-type: none"> • Minimizing the speed along the road • Ensuring lower speed and higher safety during rainy season • Ensure wildlife crossing is not affected by vehicular movement
<p>Wildlife safety measures</p> <ol style="list-style-type: none"> 1. Animal Bridges to reinvent wildlife corridors 2. Real-time surveillance to monitor all the human activities along the road 3. More signages to be introduced 		<ul style="list-style-type: none"> • Rejoining the wildlife habitat on both sides of the road • Eliminate illegal stopping of vehicles in between the WLS • More traffic controlling and informative signages

(continued)

7 Conclusion

Traffic management plan is a very important tool in ecosystem conservation when it comes to the case of roads passing through reserved forests and eco-sensitive regions. Dynamic measures which are more of regulating than restricting found to be the most efficient method of traffic management. Results and interpretations of the study reveal that with a defined set of traffic management strategies the traffic management plan

Table 6 (continued)

Strategy		Focused outcome
Monitoring the traffic 1. Ticketing to record the traffic flow 2. Regular patrolling and check posts at certain intervals		<ul style="list-style-type: none"> • Recording the traffic flow • Avoid unnecessary traffic flow • Monitor and control the speed of traffic within the WLS

could be the best tool to protect the ecosystem and thus bringing back the serenity of the reserved forest areas. The achieved goals are as follows: reducing the risk of wildlife accidents, increasing the capacity of the road, enhancing the atmospheric and environmental qualities, and protecting the ecosystem and biodiversity.

References

1. Horn B (2000) Traffic safety and environment, Conflict or Integration. IATSS Research 24
2. “National Parks Board (NParks) (2021) Singapore Government, [Online]. <https://www.nparks.gov.sg/>. Accessed 23 Sept 2021

Traffic Safety

Accident Blackspot Ranking: An Alternative Approach in the Presence of Limited Data



Sivakumar Balakrishnan and Krishnamurthy Karuppanagounder

Abstract Ranking of accident blackspots for safety improvement works is always a challenging task for traffic professionals. A suitable ranking criterion is very essential to reduce the false positive (a site included in the list when it is not needed) and false negative (a site not included in the list when it is needed) in prioritising the promised sites. Many of the existing blackspot ranking methodologies being used in developed countries require too much of sophisticated and detailed information containing volume, details of geometric design, spot speed details, control measures, etc. that are hardly recorded or accessible in developing countries like India. Hence methods based on the counts/rates of accidents are being widely accepted in these countries, even though they have deficiencies. In this context, a new concept based on the cost of accidents is proposed here. Cost of fatality and injury accidents have arrived through SP choice experiment. These costs are aggregated according to the actual severity distribution at each site and cost of different categories of accidents are calculated for each site. Based on the total economic impact, the blackspots are ranked for improvement. This method involving the evaluation of the real economic burden created by the road accidents at each location may be considered as a better option over traditional blackspot ranking criteria. This study expects that it will rectify shortcomings of the conventional procedures for ranking of hazardous sites.

Keywords Accident blackspots ranking · Cost of accidents · Willingness to pay (WTP)

S. Balakrishnan (✉)

Research Scholar, Department of Civil Engineering, NIT Calicut, Calicut, India
e-mail: bsivakumar007@gmail.com

K. Karuppanagounder

Department of Civil Engineering, NIT Calicut, Calicut, India
e-mail: kk@nitc.ac.in

1 Introduction

Blackspots can be defined as sites that experience significantly higher accident frequency or death rates in contrast to other similar locations [1]. Spotting such sites is the initial step of highway safety improvement projects leading to prioritising these locations for a rapid treatment. Such a ranking criterion is imperative to guarantee an optimal utilisation of the limited resources. Inaccuracies in the blackspot ranking criteria due to faulty negative (considering dangerous spots as safe) and faulty positive (safe spots mistakenly identified as hazardous spots) information will lead to unproductive utilisation of the finite economic wealth, especially in growing nations. Therefore, precise blackspot ranking criteria is unavoidable for effective safety improvement projects.

Many of the effective blackspot identification and ranking methods currently in use in developing countries are more scientific and sophisticated such as Safety Performance Functions (SPF), Empirical Bayes (EB), etc. They need huge data like traffic volume, details of the geometric parameters, information on traffic control measures, detailed accident data, etc. which are rarely available or recorded in developing countries like India. There is hardly any administrative effort to collect the whole accident-related data and in most of the cases, accident counts and casualty counts and its nature may only be available for future analysis. In such a situation, even though the reliability of a decision to infer whether a certain spot is safe or not is doubtful, simple methods like Accident Frequency (AF), Equivalent Property Damage Only (EPDO), etc. are based only on frequency or severity rate are being widely used in developing countries like India.

Such blackspots identification methods that are in use in developing countries fail in conveying the actual severity of the site. Locations with high frequency of accidents may have experienced low fatality rate and on the contrary, sites with a handful accidents will have reported elevated death rates. So, to generate a better ranking norm, it will be beneficial to look upon the economic implication that these accidents create to the society. We have to identify those blackspots for immediate treatment in which place the corrective measures are further economical. Taking this into account, a method is developed in this study to rank the dangerous spots for improvement based on financial implications.

The consequences of accidents to the victim or his dependents and ultimately to the society will differ based on the accident type (minor, major or fatal). Each accident type results in unlike economic burdens to the sufferer and his/her family. Similarly, each blackspot will be dissimilar with regards to the accident classification and accident count at that spot and so the aggregate economic burden to the society will vary from spot to spot. In this scenario, it will be more appropriate to pinpoint and rank the blackspots based on the total economic losses involved, for an effective resource administration.

In developed countries road accident costs used to be quantified over the past several years but such attempts are not generally reported in developing countries. Out of the various methods listed by Transport Research Laboratory (TRL), Stated Choice

(SC) experiments is being extensively accepted in developed countries as a better procedure to evaluate the cost of accidents to the society [2]. In advanced economic practices, the willingness to pay (WTP) for an avoided death or injury derived from SC study is used to evaluate the safety improvement measures. It specifies the cost that an individual is prepared to spend for a lower possibility of engaging in a road mishap.

In this study, individual WTP for a reduced probability of involving in a road accident is found out through a Stated Choice Method (SCM). The WTP values, which can be explained as an absolute value for own life, can be averaged over the whole population travelling on a particular route to obtain value of avoiding one fatality termed as Value of Statistical Casualty (VSC). As the respondents will find it tough to differentiate between the death and grievous injury in assessing the risk, the factor VSC is estimated which contains both casualties and grievous injuries. Employing death risk equivalency (DRE) indicating comparative value of averting a grievous injury (Value of Statistical Injury, VSI) regard to avoiding a death (Value of Statistical Life, VSL) value of grievous injury reduction are derived; $DRE = VSI/VSL$ (DRE value is decided based on earlier works and medical records). Aggregating costs of different accident severities based on the distribution of the severity, value of various accident categories can be calculated. Gross economic burden of a blackspot can then be obtained by aggregating categorised cost values according to the classified accidents count at that spot. In that way, economic impact of various blackspots can be calculated and thus they can be ranked for safety improvement works weighing the financial burden.

This study makes an attempt to the assess road accident costs and then rank hazardous zones for safety upgradation based on economic criteria in Indian scenario. Next section describes some literature reviews related to this topic, followed by methodologies and data analysis and the paper ends with discussion and conclusion.

2 Literature Review

Many blackspot identification methods are available in the literature. Locations are sorted out based on accident count or repetition or a combination of both [3]. Models are there which are based on accident rates and also statistical models which are formed on estimates. Some methods weigh accidents based on the severity. Literatures show that methodologies based on elementary ranking of accident numbers or rates will produce false positives and false negatives on account of yearly random fluctuation of accidents and thus resulting in an ineffective use of national resources [4–6].

Many of the effective hot spot identification methods being used in developed countries require detailed data like volume, spatial design details, traffic regulatory details, etc. Meanwhile, many studies have demonstrated that the underreporting of road accident data is a universally accepted fact [7, 8]. This lack of reporting is mainly limited to the slight injuries and the property damage only categories in

developed countries whereas in developing countries like India it is beyond this level [9, 10]. It can be observed in India that only accident count and the number of deaths is available with the police records in most of the cases. So, in Indian scenario, a methodology using the frequency and/or severities may only be effective to prioritise the accident blackspots.

Literature shows that many studies are concentrated on modelling accident frequencies and purifying the procedures with little significance to severity [11, 12]. It is obvious that ignoring frequency or the severity emanates only a casual analysis of safety whereas accuracy or additional insights would be acquired otherwise. Contrarily, there are studies that weigh severity into the analysis, where the weights are casually decided and are rarely explained. But there are works in which financial consequences created by various accident severities have also been examined [13, 14]. Literatures also show that exposure is an important factor in deciding the risk of a location. So, it is very important to include, directly or indirectly, the traffic volume count indicating the exposure, into the decision-making process.

Thus, it is important to devise a method that takes into account the various components in each category of accidents and also the traffic volume of the spot. Here the authors propose a new criterion to index the blackspots, taking these factors into consideration. In the proposed method, the costs of accidents are calculated through WTP values of the public which they are ready to pay so that their probability of being a victim of a traffic accident is reduced.

Transport Research Laboratory (TRL) specifies various methodologies which can be employed to find the cost of road accidents [15]. Hills and Jones-Lee suggested that among these options, only methodologies that seem to be straight away appropriate are the WTP approach and Human Capital (HC) approach [16]. According to them the HC approach (Gross Output) is appropriate when a nation's wealth is considered and the WTP approach is suitable when social welfare is planned.

Since ancient days the WTP analysis has been used to evaluate the lost quality of life. New practices try to take into account the discrete WTP for a prevented casualty or trauma to evaluate safety upgradation programmes. WTP specifies the money that individuals are ready to spend for a better-quality life or for reduced risk of being involved in accidents. Studies indicate that WTP analysis is an effectual method to value intangible variables of casualties like misfortune, suffering, lost standard of living, etc. [17, 18]. For the past several years Stated Choice exercises have come out as a superior substitute to assess casualty risk variations [2].

For effective implementation of road safety upgradation projects, it is advisable to consider users' perspectives on safety and their readiness to spend for a reduction in their chances of participation as a sufferer. The summation of the personal WTP values will represent an apprehension of the society regarding safety improvisation works. This process assists in calculating the amount that the individual allocates to the struggle and hardship by analysing the payment they actually make (Revealed Preference (RP) approach) or what amount the individuals are prepared to spend (Stated Preference (SP) approach) for reducing their chance of being a victim of an accident.

Very few studies have been administered in developing nations to evaluate cost of accidents [19]. Only very few studies were conducted in India to evaluate accident costs and many of them used elementary economic frameworks. Mohan reports that the studies done at Delhi in 1968 and the one for Chennai in 1978 were constructed on insurance details [20]. In 1982, Road User Cost Study had taken road accidents as an element of road user cost. All these experiments took unrealistic values for life expectancy and death–injury ratio. The costs of damage of vehicles were also underrated as most of the slight and damage only mishaps weren't been documented correctly. Also in all these studies, indirect effects like cost of life, enduring disability cost, emotional harm, pain and social effects were not taken into consideration. At the same time Bhattacharya et al. used Contingent Valuation (CV) method to calculate pedestrians' and two-wheeler drivers' willingness to pay for a risk change in Delhi, India [19]. In their study, a payment card was given to respondents to pick an amount or to state a bid. At the same time, Whittington pointed out some trouble in CV method in developing nations [21]. He observed that the survey respondents found it difficult to appreciate the economic concept in terms of willingness to pay and payment to avert risk. Despite these issues, many researches carry on with the willingness to pay concept for costing of financial implications of road accidents.

3 Methodology

The methodology used in this study contains two parts: calculation of the costs of accidents and then using these cost values to rank the accident blackspots for safety improvement works. Since this paper is aimed at discussing the effectiveness of the new ranking criteria based on cost of accidents and also due to space restrictions, detailed explanation on the procedure for the costing of accidents is not included in this paper. A brief idea regarding the costing is given in the following paragraph and analysis of the ranking criteria is followed thereafter.

A route choice experiment with binary choices through a questionnaire survey was employed for the evaluation of accident costs. Different levels of time of travel, cost of travel and yearly accident count were used as the attributes. The experiment is designed based on the fractional factorial setup on different attribute levels [2, 22]. Different choices for route were formulated varying the levels of time and cost of travel and yearly accident numbers pivoting about the actual values of a recent/regular trip. Twenty-seven combinations were formed with two alternatives and three levels of the three attributes. As the persons may get exhausted, these twenty-seven sets were grouped into three blocks and each individual was introduced with an arbitrarily selected block [2, 23]. After a detailed description of the recent or regular trip of the respondent, various hazardous scenarios compared to their recent trips were explained to the individuals and were asked to make a selection from the given hypothetical choices. As the respondents cannot apprehend the real meaning of the various attribute levels it was explained by attaching to their recent trips. A detailed description on this method and analysis can be found elsewhere [24].

To evaluate the effectiveness of the present method under the limited information scenario, suggested by the authors, the performance is compared with other three blackspot prioritisation methods; Accident Severity Index (ASI), Equivalent Property Damage Only (EPDO) and Accident Frequency (AF).

AF method ranks blackspots depending on accident numbers. This process identifies spots having high density of crashes, but severity of accidents is not considered. So, the probability of identifying a site with high frequency of minor accidents as blackspot will be high whereas locations with fewer accidents with higher number of casualties may be ranked low.

In EPDO concept, various levels of accident severity are taken into consideration to determine if the site is dangerous or not. Here, the total incidents at a spot are indicated in terms of an EPDO index which is derived as the weighted sum of fatal accidents, PDO, major injury and minor injury utilising costs of different accidents. Then ranking is done based on these EPDO indexes. Even if various severity levels are taken into consideration, the extent of severity in each category of accidents is omitted. As an example, casualty accidents may contain death, major and minor injuries and also damages to properties and this composition will be different for each fatal accident and also from location to location; and these variations are not taken into account while deciding a standard weight to all fatal occurrences. The same situation repeats for the other accident categories. The exposure level (traffic volume) at a spot is also not taken into account, which leads to erroneous conclusions as collisions may increase with increased traffic volume. Also, chances are there for a bias for rural areas where the severity will be high due to high speed under low volume [25]. Over-emphasising of spots with fewer severe accidents may also lead to biases. Studies show existence of various weighting values for EPDO calculation [25–27]. This study refers a weigh of 33.05 for fatality, 14.98 for major accidents, 1.16 for minor accidents and 1 for PDO [28].

ASI criteria, evaluate dangerous locations based on the ASI values of the locations which are obtained through weighing factors to casualties and severe accidents related to property damage only accidents. In this paper, the values proposed by National Highways Authority of India (NHAI) are used to calculate the ASI values [29]. Fatal accident is given a weightage of 7 and a value of 3 is given to grievous accident referring to the PDO.

Very few tools are available in literature to compare the performance of different ranking methods. Judgemental capacity of these available tools is also doubtful as they are mainly based on simple historical count of accidents. Yet we use some of these tools such as site consistency test, method consistency test and total rank difference test as put forth by Cheng and Washington to compare the output of these ranking methods [30]. The tests are based on consistent identification of a site as blackspot during two study periods with a condition that no safety improvement works has been undertaken at these sites.

The site consistency test measures the ability of a ranking method to consistently identify a site as blackspot over subsequent years if no safety improvements are undertaken. It compares the sum of observed accident frequency in the top n blackspots in two study periods. The method which yields the highest sum in the

second time period is taken as the best one. The method consistency test measures a method’s performance by comparing the number of same sites being identified as black spots in both the subsequent time period. A method showing greater numbers of same sites as blackspots in the subsequent observation periods is considered to be more reliable and consistent. The total rank differences take into account the difference in the rankings of blackspots in the consecutive observation periods. The method which gives the sum of the rank differences a smaller value is considered as a better method.

Performance of the various ranking methods are compared based on these tests. The efficiency of these tests is also discussed as these tests are simply based on the number of events and so findings of these tests are also arguable.

3.1 Data and Analysis

From the SP data, the WTP values were calculated using a binary logit model. Suppose a person n makes m trips in a period, resulting mn dummy respondents, aggregating to an overall sample size equivalent to number of data points [23]. This population indicates the flow over a specified duration (year) on a route. WTP values are expressed in ‘per individual per trip’. Multiplying this value with the total trip generated along a route gives the value of risk reduction.

Then, the performance testing is done using accident data obtained from FIR reports for three years (2016, 2017 and 2018) all over the state of Kerala [29]. For each location, the severity levels (PDO, minor injury accident, grievous injury accident and fatality accidents) and the number of persons suffering from minor injury, major injury and the number of deaths were collected from FIR reports.

3.2 Value of Accidents

WTP values indicate an absolute value for one’s life; aggregating it for the entire trips generated along a highway road gives cost of averting a single casualty per time unit [31]. This value, termed as Value of Statistical Casualty (VSC) is equivalent to

$$VSC = \sum_{j=1}^N WTP_j \tag{1}$$

whereas N indicates the passenger count moving enroute per year.

As the respondents will find it tough to differentiate between the death and grievous injury in assessing the risk, the factor VSC is estimated which contains both casualties and grievous injuries. Employing death risk equivalency (DRE) indicating comparative value of averting a grievous injury (Value of Statistical Injury, VSI) regard to

avoiding a death (Value of Statistical Life, VSL) value of grievous injury reduction are derived; $DRE = VSI/VSL$ [32]. Jones-Lee et al. calculated DRE value about 0.10–0.15, whereas in a Swedish study it was about 0.15–0.20 [31, 33]. Based on these studies and based on various data in the country, we considered DRE equal to 0.2 in this study. Calculation of VSL and VSI is as explained below:

$$VSL = \frac{VSC}{DRE \times \delta_{si} + \delta_f} \quad (2)$$

$$VSI = DRE \times VSL \quad (3)$$

where δ_{si} indicates shares of serious injuries and δ_f indicates that of fatalities [34]. Values of shares of injuries and fatalities can be assessed as 0.85 and 0.15 from Kerala Police Records from 2009 to 2019.

Costs of various accident categories can be calculated by aggregating costs of various severity levels corresponding to the severity distribution. Total economic implication of a hazardous spot can be calculated by summing up the product of respective accident count and its cost. Once, economic implication of all the dangerous spots is estimated, these blackspots can be prioritised for safety upgradation on an economic criterion comparing the total accident costs.

3.3 Comparison of Blackspot Ranking Methods

The ranking methods are evaluated for consistency in identification of a site as hotspot during two periods [30]. For evaluation, data for the three years is divided into two time periods; 2016 as period 1 and 2017 and 2018 as period 2. Top ten spots listed in various blackspot ranking criteria for both the time periods were evaluated to check the effectiveness of various methods using method consistency test, site consistency test and total rank difference test.

4 Results and Discussion

Costing of accidents and ranking strategy are explained in detail in the remaining portion of the paper.

4.1 Cost of Accidents

The binary logit model gives the amount of money that an individual is prepared to offer to bring down his/her probability of becoming a victim killed or harmed

Table 1 Category-wise costs of accident and severity spread

	Death (individual)	Serious injury (individual)	Minor injury (individual)	Vehicle (count)
Fatal RTA	1.08	1.28	1.65	1.4
Major RTA		1.06	1.7	1.6
Minor RTA			1.41	1.6
PDO				1.03

in highway accidents. Statistically insignificant variables were removed and the model was finalised. The WTP value of averting a road accident is calculated as 0.2356/person/trip (due to space restrictions detailed WTP analysis is not included in this paper). The value of averting a traffic accident can be estimated from the Average Daily Traffic (ADT) and count of individuals moved per day. A value of 215,000 is observed as average urban daily personal trips based on vehicle occupancy and ADT in an urban corridor [35]. According to this, the VSC, VSL and VSI are calculated as

$$VSC = 0.2356 \times 365 \times 215,000 = \text{Rs. } 18,488,710 \tag{4}$$

$$VSL = \frac{18,488,710}{0.2 \times 0.85 + 0.15} = \text{Rs. } 57,777,220 \tag{5}$$

and

$$VSI = 18,488,710 \times 0.2 = \text{Rs. } 3,697,742 \tag{6}$$

Cost of vehicle damage and cost of minor injuries are collected from hospital records, various annual reports, data from insurance agencies, repair workshops, etc. Cost of minor injury is obtained as Rs. 42,197 and property damage cost is observed as Rs. 59,225 for fatal and major injuries and Rs. 25,180 for PDO accidents. Table 1 shows severity distribution and composition of accidents as per the records of Kerala Police. Using the classified count of accidents from the blackspot identification list and the costs of various types of accidents, comprehensive financial burden for each of the blackspots are calculated and sites are ranked based on this (Table 2).

4.2 Comparative Analysis of the Various Ranking Methodologies

The blackspots are ranked using AF method, EPDO method, ASI and the accident costs conceived by the authors (Cost method) and are listed in Table 2. Evaluation results are given in Table 3.

Table 2 Accident information of the sites

Rank	Period 1					Period 2										
	site	AF	Site	EPDO	Site	Cost (Cr)	Site	ASI	Site	AF	Site	EPDO	Site	Cost (Cr)	Site	ASI
1	B	206	B	2096	B	153	B	404	B	168	A	1869	A	188	A	366
2	E	175	E	1813	E	121	E	350	A	166	B	1830	B	185	B	357
3	A	102	A	973	A	112	A	188	C	153	C	1616	I	159	C	314
4	C	94	C	921	H	84.9	C	177	F	148	D	1572	D	155	D	306
5	D	86	D	798	D	77.4	D	153	D	146	E	1547	H	155	E	300
6	F	83	F	686	G	72.9	H	132	E	146	F	1532	G	154	F	297
7	G	73	H	679	C	70.9	F	129	M	137	G	1396	F	152	G	275
8	L	72	G	649	R	67.6	G	124	L	136	H	1351	C	138	H	264
9	J	70	O	537	P	66.7	O	101	N	132	I	1325	K	136	I	262
10	H	68	I	522	K	56.4	I	98	Q	127	L	1291	M	135	J	250
11	Q	68	N	494	F	55.7	N	92	H	126	J	1279	J	127	K	249
12	K	67	K	470	I	55.2	K	87	K	120	K	1276	O	127	L	248
13	N	67	J	437	N	53.2	J	79	S	119	M	1268	N	125	M	243
14	I	66	Q	424	M	48.5	R	78	G	118	N	1254	E	124	N	241
15	P	66	M	422	J	44.4	M	77	J	117	O	1212	L	117	O	236
16	M	65	R	419	O	42.1	Q	76	O	116	P	1177	P	117	P	234
17	O	64	P	410	L	40.5	P	75	R	111	Q	1153	R	113	Q	220
18	R	61	L	383	S	33.6	L	67	I	110	S	1140	S	113	R	219
19	S	61	S	340	Q	29.3	S	60	T	105	R	1130	T	113	S	219
20	T	61	T	231	T	11.8	T	36	P	91	T	1124	Q	89	T	219

Table 3 Evaluation test results of various methods

Method	Site consistency	Method consistency	Total rank difference
AF	1063 (76%)	7 (70%)	23
EPDO	1281 (92%)	9 (90%)	17
Cost	997 (71%)	7 (70%)	29
ASI	1281 (92%)	9 (90%)	19

As per the rules of these testing tools, the results (Table 3) indicate that EPDO index performs relatively better in all the tests than all other ranking methods. In site consistency test, the EPDO method and ASI method perform best with total accident count in period 2 of the top ten selected sites in period 1 being the maximum (1281). In method consistency test, the EPDO and ASI methods identify nine common locations in the two test periods whereas AF and Cost methods identify only seven common locations in the reference periods. In the total rank difference test, EPDO method shows a better performance with minimum rank difference of 17 and the cost method shows the worst performance with a total rank difference of 29.

Now, we may discuss the reliability of these test results. All these tests are formulated on the number of accidents. Accident locations may come across variations in yearly accident counts as accidents are supposed to be occurring rarely and randomly, even if safety improvisation measures have not been implemented [36–40]. Similarly, the number of injuries and death will change from incident to incident and it may be happening by chance [41, 42]. Sites may experience accidents with a high death toll in one single incident during a period just by chance, but may not be repeating in next years and will be with lesser number of accidents and death in the successive years. Such variations should be attributed to the unpredictability before finalising a spot as hazardous and it may not be taken as a norm for the appraisal of the prioritisation processes.

The evaluation methods being suggested for evaluating the various ranking processes by comparing the sites identified during two different periods based on the counts of the accidents only as explained in the previous section do not seem to fulfil the task satisfactorily. These performance measures obtained from the various consistency tests are not fully reliable. So, to have a better evaluation, we may look into a detailed investigation of the accidents.

For this purpose, ten top-listed blackspots by various methods in the second period are compared and detailed investigation is done to judge the performance of the ranking procedure (Tables 4 and 5).

We can see site J is positioned at rank 10 in the AF approach and positioned at 9 in ASI and EPDO criterion but has moved down to rank 3 in the proposed method. It specifies the economic burden created by this site. Even though the count of fatal accidents at site J is less, it experienced higher count of serious accidents as opposed to other spots and so resulted into a higher economic impact. Similarly, for site B, even if it has a lower count with respect to location A, site B results in an elevated economic burden and therefore is positioned at a higher level in the method proposed

Table 4 Category-wise count of accidents in period 2

Sites	Fatal accidents	Grievous accidents	Minor injury accidents	Vehicle damage only
A	15	87	38	26
B	15	84	44	25
C	8	86	30	29
D	12	74	41	19
E	6	86	39	15
F	12	71	42	23
G	14	59	30	15
H	15	53	23	35
I	16	50	17	27
J	10	60	14	33

Table 5 Ranking comparison

Rank	Accident frequency	EPDO	Cost method	Accident severity index
1	A	B	B	B
2	B	A	A	A
3	C	C	J	C
4	D	E	G	E
5	E	F	E	F
6	F	D	H	D
7	G	H	D	H
8	H	G	C	G
9	I	J	I	J
10	J	I	F	I

in this study. It is possible to state similar explanation for the location G too. The above-mentioned observations eliminate the possibilities of exaggerating the number of casualty accidents in the ranking of locations for safety upgradation. Number of fatal accidents are low at sites A and B with respect to site J but they fall to a higher order ranking with respect to site J. Here we can see the economic criteria of ranking proposed in this study performs in a better way and so can be recommended as a superior criterion when accident information is limited.

The cost method developed here identifies the locations with higher economic implications as opposed to other approaches that are centred on incident counts or weighing the entire incident. This method also considers the composition of the individual accident category and the economic burden of various elements are aggregated jointly to evaluate the real economic burden as a result of accidents at a spot.

5 Conclusion

It is high time that the true financial burden of road accidents to the society has to be taken care of seriously in decision-making processes. The hazardous sites resulting into huge financial losses are to be identified and prioritised and limited financial resources are to be allocated efficiently for safety improvement works at these locations.

This study discusses the ranking of hazardous locations based on accident costs. It is expected that findings in this study will overcome the shortcomings of the traditional methods of blackspot ranking, which are generally pivoted on over-representation of specific types of accidents. High weights allocated in the traditional methods are misleading in a way that a spot reporting a single incident of five fatalities may be taken as blackspot whereas five accidents each with single serious injury may be listed as comparatively safe. Also, sites having fewer fatal accidents than a site identified as blackspot but experienced very high frequency of grievous and minor injury accidents are often overlooked by the traditional methods.

The framework explained in this study to rank the accident blackspots for safety improvement works based on the cost of traffic accidents will help to identify the critical locations which result in higher financial loss to the society and thus to channelise the limited financial resources effectively. This method of prioritisation is not simply based on the overall count of accidents but considers the various elements of the accidents thus represent the real economic burden that each accident and each site create to the society.

In this paper, the potency of the available ranking appraisal tests is also discussed. Comparison on the consistency in the ranks which are generated based on number of accidents is not enough to describe the effectiveness of a ranking criterion. Alternatively, a detailed investigation into the various components of the accidents and history of incidents at each spot will only give a representation of the true impact as accidents may be a coincidence.

The method devised in this study is from a particular location of the country and so it may be tried with care in other locations. In future studies, procedures can be formulated for calculating the WTP values to prevent different injury levels.

References

1. Elvik R (2007) State-of-the-art approaches to road accident black spot management and safety analysis of road networks. Report 883. Institute of Transport Economics, Oslo
2. Rizzi LI, Ortúzar JDD (2003) Stated preference in the valuation of interurban road safety. *Accid Anal Prev* 35:9–22
3. Hauer E (1996) Identification of sites with promise. *Transp Res Rec J Transp Res Board* 1542:54–60
4. Hauer E (1997) Observational before–after studies in road safety. Pergamon Elsevier Science Inc., Tarrytown, NY

5. Persaud BN (1986) Safety migration, the influence of traffic volumes, and other issues in evaluating safety effectiveness. *Transp Res Rec J Transp Res Board* 1086:33–41
6. Persaud BN, Hauer E (1984) Comparison of two methods for de-biasing before and-after accident studies. *Transp Res Rec J Transp Res Board* 975:43–49
7. James HF (1991) Under-reporting of road accidents. *Traffic Eng Control* 32(12):574–583
8. Naji JA, Djebarni R (2000) Shortcomings in road accident data in developing countries, identification and correction: a case study. *IATSS Res* 24(2):66–74
9. IRTAD (2011) Reporting on serious road traffic casualties. International Traffic Safety Data and Analysis Group, International Transport Forum, Geneva
10. Mohan D, Tiwari G, Bhalla K (2016) Road safety in India: status report. Transportation Research and Injury Prevention Program, Indian Institute of Technology, Delhi
11. Anastasopoulos A, Tarko A, Mannering F (2008) Tobit analysis of vehicle accident rates on interstate highways. *Accid Anal Prev* 40(2):768–775
12. Li W, Carriquiry A, Pawlovich M, Welch T (2008) The choice of statistical models in road safety countermeasure effectiveness studies in Iowa. *Accid Anal Prev* 40(4):1531–1542
13. FHWA (2008) Five percent report, exhibit 1. U S Department of Transportation
14. Tarko AP, Sinha KC, Eranky S, Brown H, Roberts E, Scinteie R, Islam S (2000) Crash reduction factors for improvement activities in Indiana. Joint Highway Research Project, Final Report. Purdue University, West Lafayette, Indiana
15. Jacobs G (1995) Costing of road accidents in developing countries. Overseas Road Note 10. Overseas Centre, TRL
16. Hills PJ, Jones-Lee MW (1983) The costs of traffic accidents and the valuation of accident-prevention in developing countries. In: Proceedings OF Highway Investment in Developing Countries, ICE conference, London
17. Ainy E, Soori H, Ganjali M, Le H, Baghfalaki T (2014) Estimating cost of road traffic injuries in Iran using willingness to pay (WTP) method. *PLoS One* 9
18. Andersson H, Lundborg P (2007) Perception of own death risk, an analysis of road-traffic and overall mortality risks. *J Risk Uncertainty* 34:67–84
19. Bhattacharya S, Alberini A, Cropper ML (2007) The value of mortality risk reductions in Delhi, India. *J Risk Uncertainty* 34:21–47
20. Mohan D (2002) Social cost of road traffic crashes in India. In: First safe community conference on cost of injuries proceedings. Viborg, Denmark, pp 33–38
21. Whittington D (1998) Administering contingent valuation surveys in developing countries. *World Dev* 26(1):21–30
22. Hensher DA, Barnard PO (1990) The orthogonality issue in stated choice design. In: Fischer MM, Nijkamp P, Papageorgiou YY (eds) Spatial choices and processes. Elsevier Science Publishers, B.V., North-Holland, pp 183–202
23. Hensher DA, Rose JM, Ortúzar JDD, Rizzi LI (2009) Estimating the willingness to pay and value of risk reduction for car occupants in the road environment. *Transp Res Part A Policy Pract* 43:692–707
24. Balakrishnan S, Karuppanagounder K (2020) Estimating the cost of two-wheeler road accident injuries in India using the willingness to pay method. *Aust J Civ Eng* 18(1):65–72
25. Millen RD (1999) Statistical evaluation in traffic safety studies. Institute of Transportation Engineers (ITE)
26. TAC (Transportation Association of Canada) (2004) The Canadian guide to in service road safety reviews. Ottawa, Ontario, Canada
27. TAC (Transportation Association of Canada) (2010) National guidelines for the network screening of collision-prone locations. Ottawa, Ontario, Canada
28. Sen AK, Tiwari G, Upadhyay V (2010) Estimating marginal external costs of transport in Delhi. *Transp Policy* 17:27–37
29. NATPAC (2019) Identification and short term improvement of crash black-spots in Kerala state, Stage I: identification and prioritisation of crash black-spots in Kerala state, Final Report, Trivandrum

30. Cheng W, Washington SP (2008) New criteria for evaluating methods of identifying hot spots. *Transp Res Rec (TRB)* 2083:76–85
31. Jones-Lee MW (1974) The value of changes in the probability of death or injury. *J Polit Econ* 82(4):835–849
32. Jones-Lee MW, Loomes G, Philips PR (1995) Valuing the prevention of nonfatal road injuries: contingent valuation vs. standard gamble. *Oxford Economic Papers* 47(4):676–695
33. Svensson M (2009) The value of a statistical life in Sweden: estimates from two studies using the ‘certainty approach’ calibration. *Accid Anal Prev* 41(3):430–437
34. Hultkrantz L, Lindberg G, Andersson C (2006) The value of improved road safety. *J Risk Uncertainty* 32:151–170
35. NATPAC (2016) Annual report 2014–15. Trivandrum
36. Hauer E (1978) Traffic conflict surveys: some study design considerations. *TRRL Supplementary Report* 352
37. Hutchison TP, Mayne AJ (1977) The year-to-year variability in the number of road accidents. *Traffic Eng Control* 18
38. Nicholson AJ (1983) Road safety: the interpretation and use of accident data. In: *NZ Road Symposium*, National Roads Board, Road Research Unit, Wellington, August
39. Nicholson AJ (1985) The variability of accident counts. *Accid Anal Prev* 17(1):47–56
40. Theofilatos A, Yannis G, Kopelias P, Papadimitrion F (2016) Predicting road accidents: a rare-events modeling approach. *Transp Res Procedia* 14:3399–3405
41. MacLean AS, Teale G (1982) Probability distributions for traffic accidents, injuries and deaths. *Aust Road Res* 12(1)
42. Transport Scotland (2016) Reported Road Casualties Scotland, The Scottish Government

Accident Prediction Modeling for Collision Types Using Machine Learning Tools



T. C. Harsha Jasni , S. Moses Santhakumar , and S. Ebin Sam 

Abstract Road accidents are one of the most significant concerns being addressed by developing countries. It is highly imperative to scientifically analyze road accidents to reduce the increasing number of accidents and victims. This study aimed to develop accident prediction models for the predominant collision types on a selected road stretch in Calicut City of a length of 7 km. The main objectives of the project were to identify predominant collision types of accidents and develop prediction models using machine learning algorithms. Rear-end collisions and pedestrian hit collisions were the most predominant types of collision on the study stretch. The developed artificial neural network gave a satisfactory prediction for rear-end collisions, and the major influencing factors were maximum gradient and traffic volume. The random forest model showed promising results for predicting pedestrian hit collisions, and the significant factors that contributed were pedestrian volume, traffic volume, presence of bus stop, and maximum gradient.

Keywords Accident prediction model · Collision Type · Machine learning · Artificial neural network · Random Forest

1 Introduction

An accident is defined as a series of events that resulting in injury or property damage resulting from a collision between at least one motorized vehicle and another motorized vehicle, a bicyclist, a pedestrian, or an object. Accidents are rare and random

T. C. Harsha Jasni (✉) · S. Moses Santhakumar
NIT Tiruchirappalli, Tiruchirappalli, India
e-mail: harshajasni06@gmail.com

S. Moses Santhakumar
e-mail: moses@nitt.edu

T. C. Harsha Jasni · S. Ebin Sam
KSCSTE-National Transportation Planning and Research Centre, Thiruvananthapuram, India
e-mail: ebin.natpac@gmail.com

events. Different characteristics of drivers, vehicles, roadway, and traffic will impact whether or not an accident occurs. In India, road transport is still the most used means of freight and passenger transportation. People have become more vulnerable to frequent road accidents due to the fast-growing population, remarkable pace of motorization, and ever-increasing urbanization. India is responsible for over 11% of all accident-related deaths worldwide (MORTH 2018). Despite a 4.4% increase in accidents in 2018, Kerala maintains its fifth-place ranking in 2018 in Indian states.

The high fatality rates on Indian roads are mainly caused due to heterogeneous traffic mix, overspeeding, unsafe road infrastructure, and poor automobiles condition. In order to continue to improve road safety in India, safety assessment tools are essential. Because the social costs of accidents are so high, it is critical to reducing them as much as possible. Engineers and transportation planners have used accident prediction models to investigate and enhance road safety. Several studies on the development of accident prediction models for predicting possible accidents on a road network have been undertaken over the years. Modeling accident frequencies by collision type can help to understand better the impact of numerous factors on different types of accidents, which can lead to the development of more effective countermeasures. According to accident occurrence configuration and pre-crash conditions, traffic accidents occur in various collision types. Based on the literature, multi-vehicle collisions, such as head-on, rear-end, and angle collisions, are more persistent than single-vehicle accidents and often result in severe consequences. So there is a need to develop specific collision type models for analyzing factors influencing crashes, which can produce more accurate results than aggregate accident modeling.

2 Literature Review

The extensive literature reveals that several studies have been conducted to develop models for predicting future road network accidents and the factors that cause them. It is very crucial to examine the factors that influence the occurrence of accidents and injuries. The relationships between accidents, the severity of injuries, and possible risk factors could vary depending on the type of collision. There is a need to model the expected frequency of accidents by collision type to detect problems and implement effective design strategies and countermeasures. Spatial zero-inflated negative binomial models between rear-end accident and road physical characteristics are developed. The factors influencing accident occurrence were segment length, traffic volume or travel, truck proportion, urban area, and physical road characteristics [1].

While conducting an intersection-related safety analysis, the speed limit, number of legs, entering lanes, exiting lanes, median islands, traffic control system, etc., are the main parameters that must be considered [2]. Superior nature of disaggregated model by accident type over overall accident modeling is studied. As a result, road safety performance is heavily influenced by speed. Rainfall and several geometric parameters are also strongly linked to the occurrence or severity of accidents [3].

According to factor analysis and logit model, speed, rainy weather, and driver age play significant factors in the severity of accidents. Rainy climate and lighting conditions are the significant contributing factors in the severity of pedestrian accidents. The machine learning model has superior predictive power, particularly in the forecast of major accidents, enhanced by 41.6%. Thus, the artificial neural network model has been identified as the best choice in predicting the number of accidents and severity of crashes [4].

Response time and road adhesion are two critical factors influencing rear-end accidents. Also, we can study the importance of minimum car-following distance by an artificial neural network [5]. The non-linear association between accident frequency by severity and risk factors can be accurately explained using neural network models [6]. The Deep Forests algorithm was used in a novel way to forecast the severity of traffic accidents. Under various levels of training data amount, the Deep Forests method exhibits good stability, fewer hyper-parameters, and maximum accuracy [7]. Using machine learning algorithms, hybrid K-means and random forest, researchers identified driving experience, light condition of the time, driver's age, and vehicle service as the main factor causing accidents [8].

Traffic accident data can separate into three clusters using a K-means approach to increase the ANN classifier's prediction accuracy [9]. The high performance and practicability of the random forest algorithm revealed the model developed by this algorithm for accident prediction having 87.5% accuracy. Furthermore, the calculating speed is quick; therefore, it is more suited to predicting congested conditions [10].

Nevertheless, very few studies were carried out in the case of collision type modeling and application of machine learning algorithms to predict accidents was found to be very rare in the safety analysis. The survey conducted by the KSCSTE—National Transportation Planning and Research Centre (NATPAC) in 2019 resulted that the selected road segment has many black spots indicating the reliability of the study. Reliable predictive models are required to identify the hidden and non-linear relationship between accidents and factors. So, the authors attempt to apply the machine learning algorithms to explore the relationship between predominant collision types and factors associated with them.

3 Objectives

The main objectives of the study are as follows:

- To develop prediction models for predominant collision types of accidents on the study stretch.
- To identify factors causing predominant collision types on selected stretch and analyze the relationships.
- To analyze the effect of traffic, roadway, and vehicle characteristics on accidents.

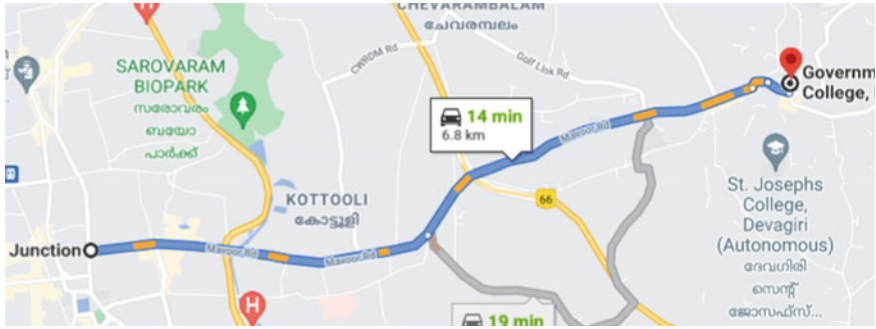


Fig. 1 Mavoor road

4 Study Area

The selected study stretch, starting from IG junction to Medical College, on Mavoor Road, has a length of 7 km (Fig. 1). Mavoor Road is the busiest high stretch of Kozhikode city in Kerala, India. This study stretch comes under the Major District Road category and is characterized by commercial establishments on either side. According to a study conducted by NATPAC in 2019, there are six black spots on the study stretch in Mavoor Road. The road stretch carries a heavy volume of traffic, and the intersections along the study stretch are severely congested.

5 Methodology

The literature review reveals that more in-depth study should be required in accident analysis by collision type in Indian mixed traffic conditions. The study stretch was segmented into 34 road segments of length 200 m for the conduct of the study.

Crash data for the years 2016–2020 were collected from the local police stations in Kozhikode City. Determination of predominant collision types was carried out from the analysis of crash data. The data include date and time of the accident, location, type of collision (Overturning, head-on collision, rear-end collision, skidding, right turn collision), classification of accident (fatal, grievous injured, minor injured), cause of the accident (rash driving, negligent driving, rash and negligent driving), road type (straight road, intersection), and details of road users.

Primary surveys were conducted to collect traffic data and road geometric data. Traffic surveys were conducted using videographic and manual methods. The percentage distribution of each mode in the entire traffic stream and the classified count of vehicles done for peak hours were analyzed. The road inventory data such as lane width, median width, number of median openings, shoulder and footpath width, number of access points, presence of street lights, presence of illegal parking were collected by conducting field surveys. Data from the past studies conducted by

KSCSTE—National Transportation Planning and Research Centre (NATPAC) on the study stretch were also collected.

Models for accident frequencies were determined for predominant collision types. The developed model was validated using an appropriate dataset, and a sensitivity analysis was done to examine the effect of various factors, both qualitative and quantitative.

6 Descriptive Analysis

Accurate data collection and extraction are essential to maintain the integrity of research. In this study, the variables required for the analysis are extracted from collected data and subjected to further analysis. The variables were defined, coded, and split into various ranges for ease of analysis performed using both SPSS and Microsoft Excel software.

6.1 Accident Data Analysis

The accidents that occurred on the study stretch were collected from the Kozhikode city police station from 2016 to 2020. A total of 406 accidents occurred on the selected stretch from 2016 to 2020. In the year 2020, the number of accidents showed a considerable decrease in numbers due to the COVID-19 pandemic.

The predominant accident type is rear-ended collision, which is about 29% of total accidents on selected road stretches followed by pedestrian collisions (27%) and Right angled collisions (18%) (Fig. 2).

Driver distraction, trailing, sudden stops, frictional characteristics due to wet weather, worn-out pavement, etc., are common factors resulting in the occurrence of rear-end collisions. The total distribution of accidents indicated that more accidents occurred on Thondayad junction followed by Arayidathupalam junction. Many of the segments showing zero accidents and mainly concentrated on intersections. According to the police, both rash and negligent driving caused a high proportion of accidents. The most vulnerable road users identified were motorized two-wheelers followed by cars, jeeps, and trucks for rear-end collisions. Time of collision is an important factor depending on accident occurrence. A higher percentage of rear-end collisions on Mavoor road occurred at 11:00–15:00 h, about 34%, and the second higher percentage is 24.5% from 7:00 to 11:00 h. Only less rate of rear-end collisions happens in the early morning on Mavoor road. Due rear-end collisions, 52% of the victims are grievously injured, and 6% resulted in loss of life.

The distribution of pedestrian accidents shows that pedestrian collision is more vulnerable at medical college junction followed by new stand region, Kovoov, Thondayad, and Arayidathupalam. Pedestrian crashes are caused by two-wheelers and

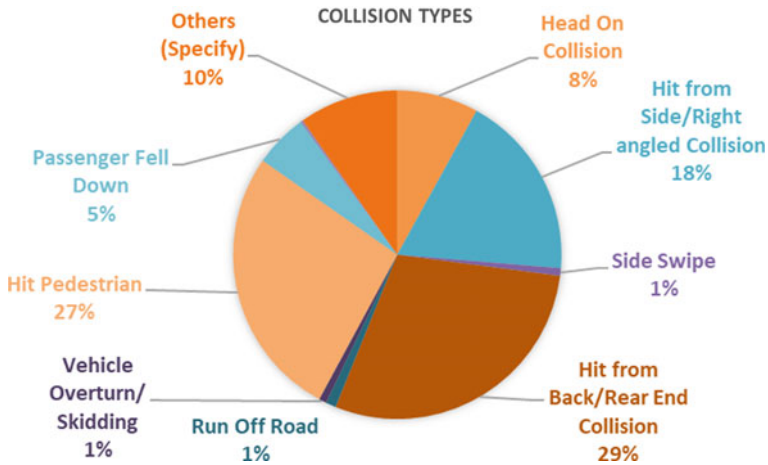


Fig. 2 Distribution of collision types

car/jeep drivers in large proportion. It may be due to the negligence of both pedestrians and drivers. So, analysis of two predominant types of collision shows that a detailed study must analyze causing factors and provide countermeasures.

6.2 Road Inventory Data Analysis

The collected data include lane width, median width, no of median openings, paved shoulder width, unpaved shoulder width, the width of the footpath, the presence of signalized intersection, no of the access point, presence of bus stops, presence of on-street parking, posted speed limit, etc. The 34 segments were surveyed for these parameters, and descriptive statistics are explained (Table 1).

Some attributes are encoded like presence of signalized intersection (Yes = 1/No = 0), presence of bus stop (Yes = 1/No = 0), illegal parking (Yes = 1/No = 0), type of land use (commercial = 1/residential = 2), road surface condition (Good = 1/Bad = 0), and street light (centered = 1, staggered = 0). The road segments have uniform width, but there is a considerable increase in lane width when coming to intersection areas. Another important thing is the non-uniformity of footpath and shoulder geometry and types along study stretch. Access points were taken as all side roads that connecting to stretch and some legs of the intersection. The speed limit is 40kmph throughout the roadway. Land use is commercial, and street light is centered. Surface condition is almost good, and some regions consist of construction.

Table 1 Descriptive statistics of parameters in road inventory survey

Attribute	Range	Minimum	Maximum	Mean	Standard deviation
LL width (m)	4.00	6.00	10.00	7.99	1.05
RL width (m)	4.00	6.00	10.00	7.86	0.95
Median width (m)	0.35	1.25	1.60	1.43	0.093
Median opening (numbers)	5.00	1.00	6.00	2.28	1.41
LF width (m)	2.50	1.2	3.70	1.96	0.66
RF width (m)	2.20	1.30	3.50	2.17	0.68
Presence of signalized intersection	1.00	0.00	1.00	0.12	0.33
Number of access points	6.00	0.00	6.00	2.41	1.23
Presence of bus stop	1.00	0.00	1.00	0.38	0.49
Illegal parking	1.00	0.00	1.00	0.41	0.50
Speed limit (kmph)	0.00	40.00	40.00	40.00	0.00
Type of land use	1.00	1.00	2.00	1.79	0.41
Surface condition	1.00	0.00	1.00	0.91	0.28
Street light	0.00	1.00	1.00	1.00	0.00
Traffic volume (pcu/h)	2437	3218	5655	4239	961
Pedestrian volume (pedestrian/h)	1942	265	2207	649	423

LL Left lane, RL Right lane, LF Left footpath, RF Right footpath, m Meter

6.3 Traffic Survey Data Analysis

Accident study required traffic data for the proper prediction of its occurrence. Data about traffic volume and its composition were collected for all major roads through a link volume survey. The surveys were carried out during peak hours between 8:00 and 12:00 h and between 15:00 and 19:00 h. The study revealed that peak hour traffic volume passing through major links in the study area varied from 3218 PCU to the maximum of 5655 PCU. The highest peak hour traffic volume of 5655 PCU was observed between Pottammal Jn and Thodayad, followed by a road stretch between Thodayad and Medical college junction carrying 5645 PCU. Peak hour pedestrian cross-flow is taken, and high volume is found at Mofussil Stand and Medical College Junction.

7 Accident Prediction Modeling

Road authorities, road designers, and road safety practitioners require Accident Prediction Models to understand potential safety issues, identify the root cause of

accidents, and estimate the potential improvements in terms of accident reduction. Even though a single accident is nearly impossible to predict due to its rare and random nature, studies have discovered that aggregating many accidents over a sufficiently large area and long period tends to improve a level of predictability that can be described using mathematical/statistical relationships. Multivariate accident prediction models have commonly adopted methods to represent a relationship between accident frequency and a set of causing factors. These are derived empirically, and their format varies based on the explanatory factors utilized. Unfortunately, accident data are not a continuous type, and in some cases, it became zero. Therefore, it is tough to choose a prediction model because of the randomness. The traditional statistical models for accident predictions are Poisson, Negative binomial, Zero-inflated negative binomial, Linear regression, etc. However, sometimes, the minimal number of accidents causes the dispersion, and sometimes data could be a reason for overfitting. For rectifying such problems, advanced studies revealed the usage of Machine learning Algorithms to predict accident frequency.

The software explored in this study is called Orange, a software package for data visualization, machine learning, data mining, and data analysis that uses component-based visual programming. Widgets are the components that span from simple data presentation to subset selection and preprocessing and empirical evaluation of learning methods and predictive modeling. Orange consists of a file, data table, data sampling, rank, test and score, prediction, etc., which are used for modeling. Explain widget can be used to get feature effect on model prediction. It explains which features contribute the most and how they contribute toward the prediction for a specific class. Explain Model widget presents classification and regression models with SHAP library.

7.1 Rear-End Collision Modeling

The predominant collision type on Mavoor road, about 29%, is rear-ended type of collisions. The main objective is to get a model that accurately predicts accident frequency and determine major factors causing rear-end accidents for providing countermeasures to reduce accidents. For getting proper model and validation, we can divide data into a training set and testing set. The training set is used for preparing the model. The working interface of Orange is illustrated (Fig. 3).

Here, six intersections are taken for modeling because there are very much smaller accident occurrences on-road sections. Validation has been done by the leave one out method due to the little data available on the intersection. We have a correlation widget that explains the positive or negative correlation between parameters. It computes Pearson or Spearman correlation scores for all features in a dataset to detect the monotonic relationship. Based on the applicable internal score, the rank widget score the variables according to their correlation with the discrete or numeric target variable. Here, univariate regression and RReliefF are used to find features

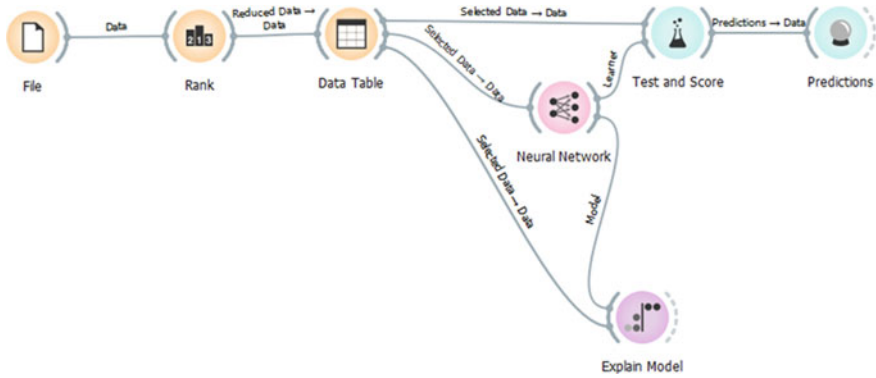


Fig. 3 Schematic of rear-end collision

contributing to prediction. Traffic volume and maximum gradient are the two critical parameters that predict rear-end accidents.

After analyzing machine learning algorithms, the neural network showed satisfactory predictive nature compared to other algorithms. The neural network is a multilayer perceptron algorithm working with backpropagation. The neural network widgets can learn linear and non-linear models by using sklearn’s Multi-layer Perceptron algorithm. The neurons in the hidden layer were 100, and the activation function used for the hidden layer is ReLu in this analysis. It is a rectified linear unit function. The solver used for weight optimization is Adam, which is a stochastic gradient-based optimizer (Fig. 4).

Both traffic volume and gradient have a high impact on model prediction, and the increase in value of these two parameters is responsible for the rise in the possibility of rear-end accidents. Validation is done by using 20% of the sample using the orange widget. The obtained R^2 value is 0.571, which is satisfactory, and the Root Mean Square Error (RMSE) is 8.88% and found to be less than 10%. Other statistical parameters Mean Square Error (MSE) and Mean Absolute Error (MAE) are 25.514 and 4.325, respectively.

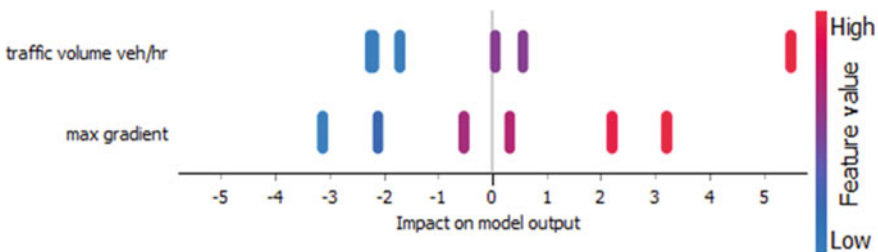


Fig. 4 Output from model explains widget

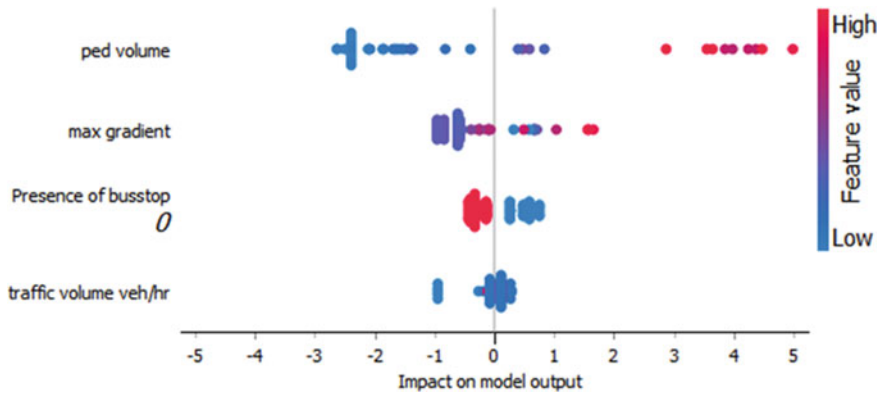


Fig. 5 Output from model explain widget

7.2 Pedestrian Accident Modeling

Pedestrian collision is the second-highest accident that occurred on the stretch of about 27% of total collisions on the study stretch. For the analysis of pedestrian collisions, a total of thirty-four segments were taken and analyzed. A ranking widget is used to finding the parameters that causing pedestrian Collision. RReliefF is used as scoring methods in which bus stop presence, pedestrian volume, and traffic volume are the first three parameters that significantly impact accident prediction. Here, random forest shows good results than other machine learning algorithms. The number of trees incorporated in this model is ten (Fig. 5).

SHAP library is used to analyze the effect of features on model output. The pedestrian volume and traffic volume are significant parameters. The segments having bus stop show more correlation to the occurrence of pedestrian collision. The gradient is also affecting because most of the gradients are associated with the intersection. In the case of pedestrian modeling, the obtained R^2 value is 0.610, and this value is satisfactory, and the Root Mean Square Error (RMSE) is 7.67% and found to be less than 10%. Other statistical parameters Mean Square Error (MSE) and Mean Absolute Error (MAE) are 11.917 and 2.242, respectively.

8 Sensitivity Analysis

Sensitivity analysis is a technique to evaluate the effect of different values of an independent variable (causing factors) on a dependent variable under consideration with some set of assumptions. In other words, sensitivity analyses look at how the sources of uncertainty in a mathematical model could affect the performance of the model. Here, the sensitivity analysis was conducted to quantify the variation of the number of collisions with the change in causing factors.

The total rear-end collisions can be reduced by 2%, when the maximum gradient decreases by 5%. In the case of pedestrian hit collisions, the crashes can be reduced by 2%, when bus stops decrease by 5%.

9 Conclusions

The limitation of traditional statistical models in predicting rare events (accidents) can be solved by using machine learning algorithms called random forest and neural network. Factors that cause accidents differ depending on the type of collision. So, the countermeasures should be taken according to the predominant collision type and factors at the location under consideration.

Random forest model predicting pedestrian accident with *R* square value of 0.610 and percentage Root Mean Square Error (PRMSE) of 7.67. Similarly, we can use a neural network algorithm for predicting rear-end accidents with a satisfactory *R* square of 0.571 and a Root Mean Square Error (PRMSE) of 8.88%. The factors responsible for rear-end collision are traffic volume and maximum gradient. In the case of a pedestrian collision, pedestrian volume and traffic volume have a crucial role and segment having bus stop is a vulnerable spot.

Traffic volume and pedestrian volume are two major uncontrollable factors to reduce accidents. So, traffic calming measures including speed management and improvement in physical measures are the possible solutions applicable to required segments. Several segments in the stretch have non-uniformity of shoulders and footpaths. Lack of control at the access points should be properly addressed. The reduction of gradient percentage and proper speed management can help to reduce rear-end collision. Future scopes of these study including models will be more accurate if we collect data from more intersections, we can develop models for other collision types and application of Surrogate Safety Assessment Model (SSAM) to explore collision types modeling.

References

1. Champahom T, Jomnonkwo S, Karoonsoontawong A, Ratanavaraha V (2020) Spatial zero-inflated negative binomial regression models: application for estimating frequencies of rear-end crashes on Thai highways. *J Transp Saf Secur* 14(3):1–18
2. Al-Marafi MN, Somasundaraswaran K, Bullen F (2020) Development of crash modification factors for intersections in Toowoomba city. *Int J Urban Sci* 1–20
3. Pei X, Sze NN, Wong SC, Huang L, Yao D (2013) Disaggregated crash prediction models for different crash types using joint probability model. In: Proceedings of 2nd international conference on improving multimodal transportation systems-information, safety, and integration (ICTIS 2013), pp 1298–1305
4. Ghasedi M, Sarfjoo Kasmaei M, Bargegol I (2021) Prediction and analysis of the severity and number of suburban accidents using logit model, factor analysis and machine learning: a case study in a developing country. *SN Appl Sci* Vol 3. <https://doi.org/10.1007/s42452-020-04081-3>

5. Luo Q, Chen X, Yuan J, Zang X, Yang J, Chen J (2020) Study and simulation analysis of vehicle rear-end collision model considering driver types. *J Adv Transp* 2020
6. Zeng Q, Huang H, Pei X, Wong SC (2016) Modeling nonlinear relationship between crash frequency by severity and contributing factors by neural networks. *Anal Methods Accid Res* 10:12–25. <https://doi.org/10.1016/j.amar.2016.03.002>
7. Gan J, Li L, Zhang D, Yi Z, Xiang Q (2020) An alternative method for traffic accident severity prediction: using deep forests algorithm. *J Adv Transp* 2020
8. Yassin S, Pooja (2020) Road accident prediction and model interpretation using a hybrid K-means and random forest algorithm approach. *SN Appl Sci* 2(9): 1–13
9. Alkheder S, Taamneh M, Taamneh S (2017) Severity prediction of traffic accident using an artificial neural network. *J Forecast* 36:100–108. <https://doi.org/10.1002/for.2425>
10. Liu Y, Wu H (2017) Prediction of road traffic congestion based on random forest. In: 10th International Symposium on Computational Intelligence and Design (ISCID) 2:361–364
11. Farid A, Ksaibati K (2020) Modeling two-lane highway passing-related crashes using mixed ordinal probit. *Regression* 146(9): 1–9
12. Iranitalab A, Khattak A (2017) Comparison of four statistical and machine learning methods for crash severity prediction. *Accid Anal Prev* 108:27–36
13. Kardar A, Davoodi SR (2020) A generalised ordered probit model for analysing driver injury severity of head-on crashes on two-lane rural highways in Malaysia. *J Transp Saf Secur* 12(8):1067–1082
14. Jonathan AV, Wu KF, Donnell ET (2016) A multivariate spatial crash frequency model for identifying sites with promise based on crash types. *Accid Anal Prev* 87:8–16
15. Report of crash scenario of Kozhikode district (2020) National Transportation Planning and Research Centre, Kerala
16. E. Faculty and P. Communication (2015) An artificial neural network model for highway accident prediction: a case study of Erzurum, Turkey. *PROMET-Traffic Transp* 27(3), pp 217–225
17. Prieto F, Gómez-Deniz E, María J (2014) Modelling road accident blackspots data with the discrete generalised pareto distribution. *Accid Anal Prev* 71:38–49
18. IRC: SP:88-2019 Manual on road safety audit, Indian Road Congress
19. IRC:99-2018 Guidelines for traffic calming measures in urban & rural Areas, Indian Road Congress
20. Park J, Asce AM, Abdel-aty M, Asce F (2020) Application of random effects non-linear model for analysing motorised and nonmotorised traffic safety performance. *J Transp Eng Part A Syst* 2(1):1–8
21. Essa M, Sayed T (2020) Comparison between surrogate safety assessment model and real-time safety models in predicting field-measured conflicts at signalized intersections. *Transp Res Rec* 2674(3):100–112. <https://doi.org/10.1177/0361198120907874>
22. Hosseinpour M, Sahebi S, Hasanah Z, Shukri A (2018) Predicting crash frequency for multi-vehicle collision types using multivariate Poisson-lognormal spatial model: a comparative analysis. *Accid Anal Prev* 118:277–288
23. Luo Q, Zang X, Yuan J, Chen X, Yang J, Wu S (2020) Research of vehicle rear-end collision model considering multiple factors. *Math Prob Eng* 2020
24. Wu Q, Chen F, Zhang G, Liu XC, Wang H, Bogus SM (2014) Mixed logit model-based driver injury severity investigations in single- and multi-vehicle crashes on rural two-lane highways. *Accid Anal Prev* 72:105–115
25. Jonsson T, Ivan JN, Zhang C (2007) Crash prediction models for intersections on rural multilane highways: differences by collision type. *Transp Res Rec* 2019:91–98
26. Zhou X et al (2020) Accident prediction accuracy assessment for highway-rail grade Crossings using random forest algorithm compared with decision tree. *Reliab Eng Syst Saf* 200:106931
27. Lao Y, Zhang G, Wang Y, Milton J (2014) Generalised non-linear models for rear-end crash risk analysis. *Accid Anal Prev* 62:9–16

28. Zhou Y, Li S, Zhou C, Luo H (2019) Intelligent approach based on random forest for safety risk prediction of deep foundation pit in subway stations. *J Comput Civ Eng* 33(1):1–14
29. Xi J, Guo H, Tian J, Liu L, Sun W (2019) Analysis of influencing factors for rear-end collision on the freeway. *Adv Mech Eng* 11(7):1–10

Operating Speed Prediction of Vehicles at Combined Curves Using Mixed Effect Modeling Approach



Neena M. Joseph, M. Harikrishna, M. V. L. R. Anjaneyulu,
and IceyElzen Mathew

Abstract An increase in traffic crashes can be attributed to inconsistencies in roadway geometry. The operating speed model is a statistical tool to evaluate geometric design consistency. This paper explores the relationship between radius, gradient, sight distance parameters, extra widening, and operating speeds at two-lane two-way non-urban roads in India. Data of 107 curves and 107 tangents with horizontal within crest curve combinations were selected. Correlation analysis was done to find the significant geometric variable affecting the operating speed of vehicles. Using these significant variables, operating speed models were developed using a mixed effect modeling approach for different classes of vehicles.

Keywords Operating speed · Combined curves · Mixed effect models · Geometrics of the curve

1 Introduction

A consistent road design assures that consecutive aspects are coordinated, resulting in coordinated driver behavior and no unexpected events. Since design consistency is necessary for safe driving. Operating speed is the most common and simple measure of design consistency. The vertical grades or curvature of combined curves of the roadways are also related to road safety. When a vehicle traverses from a long straight

N. M. Joseph (✉)

Viswajyothi College of Engineering and Technology, Vazhakulam, India
e-mail: neenajoseph.m@gmail.com

M. Harikrishna · M. V. L. R. Anjaneyulu

Department of Civil Engineering, National Institute of Technology Calicut, Calicut, India
e-mail: Harikrishna@nitc.ac.in

M. V. L. R. Anjaneyulu

e-mail: mvlr@nitc.ac.in

I. Mathew

WSP Consultants, Bengaluru, India

to a vertical curve, there is a reduction in operating speed. In such cases, the driver has to take more effort to maneuver the vehicle along the road. These complex maneuvering tasks can cause speed variations that deviate from safety limits, resulting in crashes. Vertical alignment's primary goal is to provide a transition between two roadway grades using a vertical curve. As a result, a change in vehicle speed is an apparent evidence of geometric design inconsistencies [1]. This study focuses on combined curves. A combined curve is a combination of horizontal and vertical curves introducing a complex geometry such that the drivers find it difficult to judge and maneuver. This complexity in geometry obviates the need for study from a safety point of view. The various combinations include horizontal curve within crest vertical curve, horizontal curve within sag vertical curve, vertical curve within the horizontal curve, horizontal curve preceding vertical curve, and vertical curve preceding horizontal curve. The study deals with horizontal within crest vertical curve combination. The objectives of the study are to identify the factors affecting the speed of combined curves and to develop operating speed models on combined curves on non-urban roads.

2 Previous Researches

There are various studies related to road safety evaluation that gives an insight into different factors affecting safety on curves. Numerous studies also presented models to predict speed in terms of road geometry and volume. There are only a few works that considered the three-dimensional alignment of roads. A combined curve is a combination of horizontal and vertical curves. Hence the factors which are affecting horizontal and vertical curves should be considered for the three-dimensional alignment of the road. The important studies on horizontal curves are shown that radius and degree of curvature are strong measures of crash severity [2, 3, 4, 5]. Sight distance at horizontal curve is another main aspect of the roadway that affects crash rates [3, 6, 7]. Extra widening, curve length, and approach tangent length are all considered to affect the safety of curves [2, 8]. Hence in the case of combined curves, the geometric factors which are affecting the safety of vertical curves also have to be considered.

The basic design criterion for vertical alignment is the grade of percent. A road segment with a constant percentage gradient is commonly referred to as a straight grade, regardless of its horizontal alignment. The grades of the curve, the degree of the curve, and sight distance are the main concerns in the design of vertical curves [9, 10, 11]. Since the horizontal and vertical curves are vulnerable to crashes, when the horizontal curves are combined with gradients are more dangerous Srinivasan [4].

The combination of horizontal and vertical crest curves may increase the driver's workload. This is due to reduced sight distance and the other has to navigate the vehicle in a three-dimensional field. Since the unusual or extreme function involves the combination of horizontal and vertical features, the workload of the driver is

increased even further. Such inconsistencies can lead to road crashes and fatalities. Several studies have found out that the probability of a crash increases as the complexity of the alignment increases and that the erroneous perception of horizontal curves interfering with crest vertical curves could be significantly important [12, 13, 14]. It has been shown that combined curves that are poorly constructed can raise the driving risk by drivers leading to excessive speed changes through the curve [15].

Geometry parameters of the road or curve of the road will have to decide the consistency of the entire road system. Moreover the geometry of the curve, the driver speed changes are also good indicators of roadway safety in the case of combined curves [12, 15].

Very few studies are conducted on methods for developing operating speed prediction models for combined curves. The types of vehicle, speed, and types of models are very important for developing speed prediction models. In India, there are very few works are done safety of combined curves on the road. Jacob [16], mainly focuses on the speed variation of different points at vertical curves and they developed operating speed prediction models. However, the safety effect of extra widening and sight distance is not considered in this work.

Most of the researchers used regression models for speed prediction. In this study mixed effect modeling approach is proposed for the prediction of speed on combined curves. The aforementioned models also take into account the effect of clustering in data. In the linear mixed-effects models, the between-subject variance is omitted from random errors. However, the ordinary regression model is found to be related to error variance. Regression implies that when one variable varies, all other variables remain the same. If we do an experiment where all variables are set up such that they vary completely independently, the regression concept works perfectly well. However, in the real world, variables have many other variables and several subtle interrelationships. Regression does not capture these. The linear mixed model segregates into within-subject variance and between-subject variance [17].

3 Data Requirements

A reconnaissance study was conducted to identify the road stretches having combined curves from seven districts of Kerala. The study is limited to horizontal within crest vertical curves on two-lane two-way non-urban roads. Figure 1 shows the plan and profile of this combination. The curves were selected based on the following criteria: The approach tangent length should be at least 100 m, and it should not be positioned near towns or developed regions that could have a substantial impact on curve speed patterns. The plan and profile of the combined curves are shown in Fig. 1.

107 curves were chosen from various stretches in the above-mentioned districts based on the speed data. Speed data, geometry data, and traffic volume are all needed for the study. To get the geometric specifics of these curves, a Total Station survey

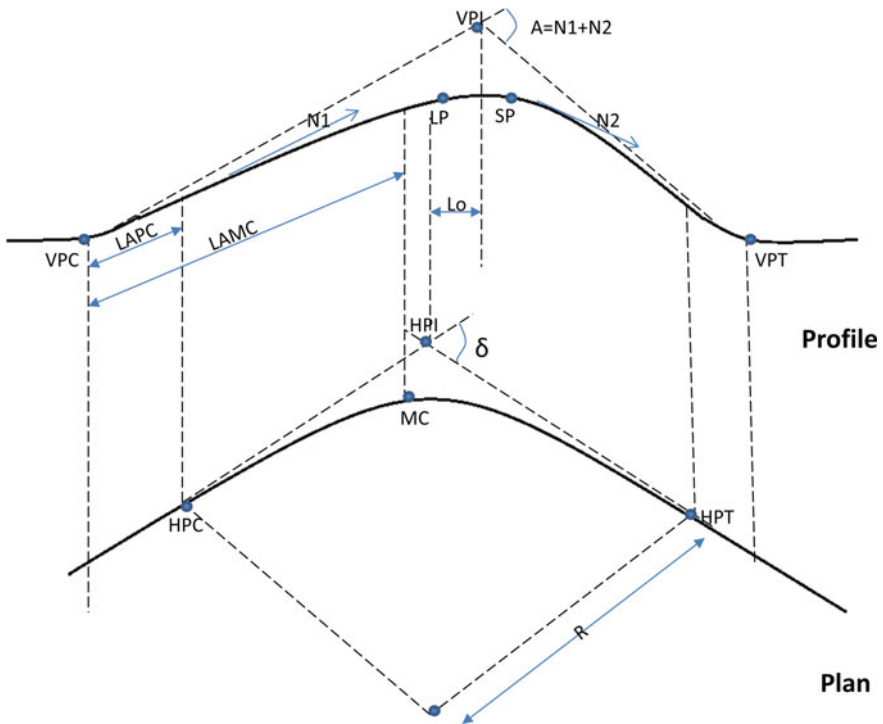


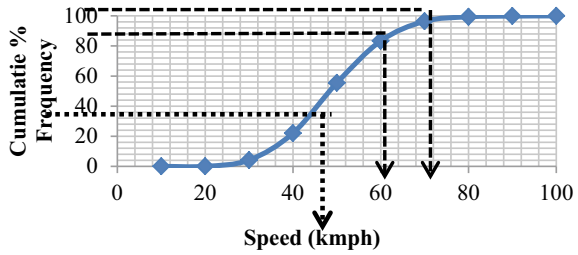
Fig. 1 Plan and profile of combined curve. *PT* Point of Tangency, *MC* Mid Curve, *LAPC* Length of ascending grade up to HPC, *LAMC* Length of ascending grade up to MC, *LP* Limiting Point, *HPI* Horizontal point of Intersection, *SP* Crest Point, *A* Change in Grade, δ Deflection Angle, *R* Radius of Horizontal Curve

was done. A sight distance survey was also carried out. Traffic data that included speed and volume data were collected using a portable infrared traffic data logger (TIRTL).

4 Preliminary Analysis

The preliminary analysis of collected data was done using correlation analysis and scatter plot analysis. These analyses were done to identify the candidate variables for modeling speed. Some of the important scatter plots are shown and explained here. Speed data is collected at two locations: one at a point on the tangent section and the other at a point on the curve section. Cumulative percentage frequency plots were prepared for all free-flowing vehicles. The 50th, 85th, and 98th percentile speeds for various vehicle classes were determined using the cumulative frequency plot. This process was carried out for all vehicles at the curve as well as at the tangent section.

Fig. 2 Cumulative Frequency plot for all vehicles at midcurve at one site



Figures 2 show the cumulative frequency charts for speeds of all vehicles at the mid curve. Percentile speeds at all locations were found out from respective cumulative frequency plots. 85th percentile speed is considered as the operating speed. Values of percentile speeds at tangent and at curve reveal that the speed of vehicles reduces on approaching the curve.

Analysis of variance (ANOVA) is a set of statistical methods for analyzing variations in group averages, as well as procedures like “variation” within and between groups. The ANOVA test was used to see if there were any significant differences in the speeds of different vehicle classes. Two-wheelers, Light Motor Vehicles (LMV), Medium Commercial Vehicles (MCV), Light Commercial Vehicles (LCV), and Small Commercial Vehicles (SCV) were among the vehicles evaluated (SCV).

The findings show that there is no substantial difference in speeds between two-wheelers and SCVs. Hence these can be grouped under one category. All other combinations showed significant differences in speed. So while developing models separate models are to be developed for other categories. Scatter plot analysis was carried out to identify the relationship between geometric variables and operating speed. Figure 3 shows the relationship between operating speed for all vehicle categories and geometric variables.

From the scatter plots it can be inferred that sight distance has a positive relation with speed. Higher the radius, wider the curve, and hence driver finds it easy to negotiate the curve even at a higher speed. Also if sufficient sight distance is available speed will increase. As the ascending grade increases the speed reduces because of the tractive effort required to move up the grade. Preceding tangent length and extra widening are also showing a positive trend with operating speed.

The correlation statistics of the variable confirm the above-said relation with the operating speed (Table 1). Operating speed is highly correlated with (R), sight distance (SD), ascending grade (G1), change in grade (A), carriageway width (CWM), Degree of curvature (K), and extra widening. Two-wheelers, Passenger cars, and HCV show high correlation with these variables. Gradient, Degree of curvature showed a negative relation with operating speed and other variables gave positive correlation with operating speed. Traffic volume is also one of the important variables which directly affect the speed variation of the vehicle on the road. However, since the multi-collinearity of these variables with traffic volume, traffic volume is omitted for the further operative speed model development in this paper.

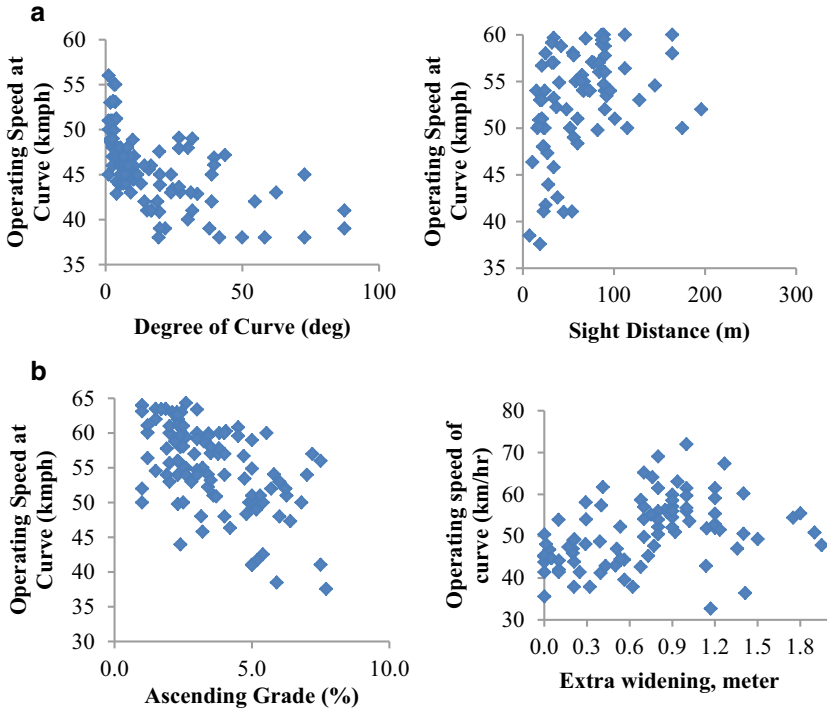


Fig. 3 Operating speed versus geometric variable. **a** Operating speed versus degree of curvatures and sight distance. **b** Operating speed versus ascending grade and extra widening

5 Model Development

A preliminary analysis is performed initially to define the trend and pattern of the collected data. From the results of the preliminary analysis, the variables which affect the operating speed at curves are identified. These variables are used in modeling and predicting the operating speed. Out of 107 curves, data 77 curves are used to develop models, and remaining 30 curves data are used for the validation.

5.1 Linear Mixed-Effects Models

A mixed effect model is a statistical model, which includes both fixed and random effects. Such models are useful where calculations are made on related statistical unit clusters. Mixed effect models are often favored over more traditional approaches because of their benefit in handling missing values. As mentioned in Eric et al. [17], “A linear model with mixed effects is the generalization of a linear model in which data will show correlation and non-constant variability”. The general form of a linear

Table 1 Correlation matrix for speed at mid curve

Variables	Speed (all vehicles)	Speed (two-wheeler)	Speed (HCV)	Speed (LMV)	Speed (MCV)
Preceding tangent length (m)	0.442	0.441	0.487	0.414	0.597
Carriageway width (m)	0.421	0.215	0.457	0.389	0.374
Shoulder width (m)	0.412	0.485	0.512	0.367	0.354
Sight Distance (m)	0.574	0.612	0.502	0.587	0.484
Extra widening (m)	0.471	0.387	0.657	0.622	0.420
Gradient (%)	-0.487	-0.687	-0.678	-0.710	-0.675
Rate of curvature	0.415	0.474	0.471	0.397	0.345
Radius	0.480	0.436	0.565	0.468	0.444
Degree of curvature	-0.644	-0.645	-0.557	-0.610	-0.654
Deflection angle	0.284	0.312	0.3210	0.287	0.294
Superelevation	-0.389	-0.367	-0.400	-0.394	-0.334

mixed effect model is shown below in Eq. 1:

$$Y = X.\beta + Z.\gamma\varepsilon \tag{1}$$

where “Y” is the matrix of response vectors, “X” is the fixed-effects coefficient matrix, “Z” is the random effects coefficients matrix, “β” is the vector of fixed-effects slopes, “γ” is a random vector with mean zero and “ε” is the error variance. According to Simon et al. (2003), “Mixed models are mathematical models containing parameters for fixed effects as well as random effects. Because of the way the random effects are interpreted, there is always at least one fixed-effect parameter in a model of random effects. So any random-effect model is a mixed model”. The proposed models use operating speed as the dependent variable and geometric variables as the explanatory variables. Using scatter plots, correlation matrices, and information from the literature review, a list of tentative variables to be included in the models is identified. Many trials are performed using the software “R” and only the most significant and logical models are presented here.

Here different combinations of variables were studied and the models with the highest R² are presented here. The mixed effect models for predicting the operating speed considering vehicle type having better R² values are found to have better prediction capability compared to multiple linear regression models. This can be

attributed to the clustering of the variables which is found to improve the prediction accuracy of the model. Hence the mixed effect model is the best choice for the fixed and random-effect data sets with clustering. Table 2 shows the models developed and the goodness of fit statistics.

Table 2 **a** Operating speed model for LMV at mid curve, **b** Operating speed model for TW at mid curve, **c** Operating speed model for MCV at mid curve, **d** Operating speed model for HCV at mid curve, **e** Operating speed model for all vehicles at mid curve

	Estimate	Std. error	<i>t</i> value	R^2	AIC	BIC
<i>(a)</i>						
Intercept	59.4078	4.9501	12.001	0.742	421	436
SD	0.0413	0.0191	2.158			
DC	-0.3320	0.0439	-7.554			
G1	-0.6806	0.2117	-3.212			
EW	0.0094	0.0056	1.678			
<i>(b)</i>						
Intercept	46.8464	1.8413	25.441	0.873	349	360
SD	0.0304	0.0124	2.453			
DC	-0.0639	0.0302	-2.113			
G1	-0.6691	0.3314	-2.019			
EW	0.0084	0.0021	3.84			
<i>(c)</i>						
Intercept	53.9479	4.1186	13.098	0.788	396	411
SD	0.0428	0.0159	2.690			
DC	-0.2984	0.0365	-8.160			
G1	-0.7171	0.3991	-1.797			
EW	0.081	0.0350	2.31			
<i>(d)</i>						
Intercept	47.9872	4.5747	10.490	0.691	458	470
SD	0.0153	0.0049	3.120			
DC	-0.2679	0.0442	-6.065			
G1	-0.1079	0.0523	-2.063			
EW	0.7155	0.3620	1.976			
<i>(e)</i>						
Intercept	54.9546	2.9557	18.593	0.782	350	366
SD	0.020	0.0114	1.754			
DC	-0.2782	0.0262	-10.604			
G1	-0.3798	0.2863	-1.326			
EW	0.0131	0.0033	3.916			

From the different trials performed the models that gave highest R^2 value were selected. AIC and BIC values also confirm the significance of the selected models. The signs of coefficients of variables are logical. Degree of curvature shows a negative relation with operating speed. Since DC and radius are inversely related, this negative relation can also be justified. Also, degree of curvature is a measure of sharpness of the curve. Speed of vehicles will reduce on a sharp curve. Sight distance also gave a positive relation indicating that if the road ahead is visible to the driver, he increases the speed. It is also found that the speed of vehicle decreases on higher grades because of the tractive effort required. The extra widening also gave a positive relation. As the mid curve width increases the drivers will approach the curve at a high speed. Thus the signs of the variables in the models are logical.

5.2 Model Validation

The calibrated models were applied on the one-third dataset for validation. Operating speeds on these sites were calculated using these models and a comparison is made between observed and predicted values of operating speed. The comparison is done by calculating RMSE (Root Mean Square Error) values and also by observed Vs predicted graphs. RMSE represents the square root of mean of errors and is shown in Table 3.

RMSE values of all models are less showing that the models are good. Elasticity Analysis.

Elasticity is calculated to evaluate the independent variables’ marginal effects, which provides insight into the consequences of parameter estimation results.

It can be concluded that for all vehicle categories one percent change in degree of curvature and approach grade causes a decrease in operating speed by about 4.79 and 1.34%, respectively and for one percent increase in extra widening, the percentage increase in operating speed is 4.18%. For two-wheelers and passenger cars, one percent increase in sight distance increases the operating speed by 2.23 and 3.02%, respectively. Similarly, other relationships can also be inferred from the table.

As per the above models and result obtained, the recommended speed of each type of vehicle based on the sight distance variation from 50 to 250 m and keep

Table 3 RMSE Statistic for operating speed models

Vehicle type	At curve	
	Calibration	Validation
All Vehicles	2.98	3.01
TW	3.25	3.25
LMV	8.57	8.31
MCV	9.44	9.00
HCV	4.79	4.93

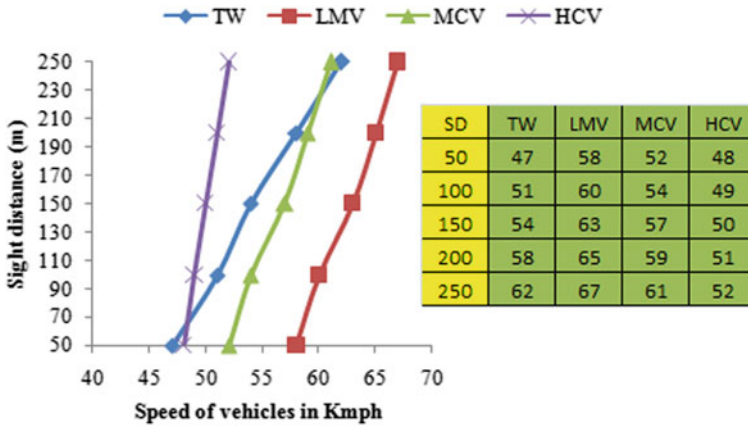


Fig. 4 Variation of the speed of vehicles versus sight distance

corresponding extra widening is 2.5 m, degree of curvature is 5, gradient is 5% and carriageway width is taken as 7 m are shown in Fig. 4.

6 Conclusions

This study presents the development of operating speed models for vehicles at combined curves. The operating speed at the curves is related to the geometric features of the curve. The ANOVA test showed that there is a significant difference between speeds of different categories of vehicles and hence separate models for each category of vehicles were developed. Analysis was done to identify the variables that significantly influence the speeds of the vehicles at combined curves. Correlation and scatter plot analysis showed that degree of curvature, ascending grade, sight distance, and extra widening are the variables that affect the operating speed at the mid curve of the combined curve. Grade, degree of curvature, and sight distance are the most important variables for predicting the operating speed of all categories of vehicles at the curve. The degree of curvature is negatively related to operating speed. Sight distance also provides a positive correlation, indicating that if the driver sees the road ahead, they will increase speed. The vehicle speed was also found to be reduced to a higher grade due to the required traction. The additional widening also gives a positive correlation. As the width of the middle curve increases, the driver will approach the curve at high speed. The operating speed model can be used in the design of the combined curve. It can also be used to check design consistency and improve safety by improving road characteristics.

References

1. Nicholas J, Phillip R (2010) Development of safety performance functions for two-lane roads maintained by the Virginia Department of Transportation
2. Aram A (2010) Effective safety factors on horizontal curves of two-lane highways. *J Appl Sci (Faisalabad)* 10(22):2814–2822
3. Glennon JC (1987) Effect of alignment on highway safety, state of the art report. Transportation Research Board, National Research Council, Washington, DC
4. Srinivasan S (1982) Effect of roadway elements and environment on road safety. Institution of Engineers, p 63
5. Voigt AP, Krammes RA (1996) An operational and safety evaluation of alternative horizontal curve design approaches on rural two-lane highways. Texas Transportation Institute Research Report 04690-3, Texas A and M University, College Station
6. Easa SM (1991) Sight distance model for unsymmetrical sag curves. *Transp Res Rec.* 51–62, Journal of Transportation Research Board, No. 1303, Washington, DC
7. Garber NJ, Ehrhart AA (2000) Effect of speed, flow, and geometric characteristics on crash frequency for two-lane highways. *Transp Res Rec (Journal of Transportation Research Board No. 1717, Washington, DC)*
8. The Indian Road Congress (IRC)-73 (1980) Geometric design standards for rural (non-urban) highways
9. Hassan Y (2003), Improved design of vertical curves with sight distance profiles, in transportation research record, vol 1851. TRB, National Research Council, Washington, DC, pp 13–24
10. Labi S (2005) Effects of geometric characteristics of rural two-lane roads on safety, report. FHWA/IN/JTRP-2005/2, Federal Highway Administration
11. Thomas U, Hinshaw W, Fambro DB (1989) Safety effects of limited sight distance on crest vertical curves. *Transp Res Rec* 1208
12. Francesco B (2014) Effects of combined curves on driver's speed behavior: driving simulator study. *Transp Res Procedia* 3:100–108. In: 17th Meeting of the EURO working group on transportation, EWGT2014, 2–4 July, Sevilla, Spain
13. Wooldridge CMD, Fitzpatrick KPJ, Brewer MA (2000) design factors that affect driver speed on suburban arterials, FHWA/tx-00/1769-3. Texas Transportation Institute
14. Morris CM, Donnell ET (2014) Passenger car and truck operating speed models on multilane highways with combinations of horizontal curves and steep grades. *J Transp Eng. ASCE.* ISSN 0733-947X/04014058
15. AASHTO (2011) A policy on geometric design of highways and streets
16. Jacob A and Anjaneyulu MVLR (2003) Operating speed of different classes of vehicles at horizontal curves on two-lane rural highways. *J Transp Eng* 139(3):287–294 (ASCE)
17. Fitzsimmons EJ, Kvam V, Souleyrette RR, Nambisan SS, Bonet DG (2013) Determining vehicle operating speed and lateral position along horizontal curves using linear mixed effects models. *Traffic Injury Prevent* 14(3):309–321 (Taylor & Francis)
18. Lamm R, Psarianos B, Mailaender T (1999) Highway design and traffic safety engineering handbook. McGraw Hill, TRID, Transportation Research Board, Washington, DC

Pedestrians Safety Analysis at Uncontrolled Midblock Crosswalks



Siddharth Jain, Mukti Advani, and Lalit Kumar Yadav

Abstract Road accidents are major but neglected worldwide problem, requiring collaborative efforts for effective prevention. Pedestrians are the most vulnerable victims in fatal road accidents. Pedestrian's perceived time of crossing and actual time of crossing at uncontrolled midblock crosswalks play an important role in preventing accidents at uncontrolled midblock crosswalks. It provides critical information regarding individual's crossing time and its variation with actual crossing time at uncontrolled midblock crosswalk. For this purpose, a field survey was carried out on uncontrolled midblock crosswalks at two locations of Ahmedabad. The data was collected with the help of designed questionnaire and stopwatch. The data collected included the pedestrian's individual characteristics like gender, age, etc., with their perceived time and actual time of crossing at uncontrolled midblock crosswalks. Accidents on uncontrolled midblock crosswalks happen due to difference in perceived and actual traffic flow. Pedestrians do not perceive the traffic conditions correctly. 68% of people overestimated and 32% underestimated the crossing time w.r.t actual crossing time on four-lane midblock crosswalk. 82% of people overestimated and 18% underestimated crossing time w.r.t actual crossing time on six-lane midblock crosswalk. The level of risk increases with increase in crossing width from four-lane midblock crosswalks to six-lane midblock crosswalks as the difference between average perceived time and average actual time of crossing increases. Female pedestrians had better evaluation of traffic conditions at four-lane uncontrolled midblock crosswalks, whereas at six-lane uncontrolled midblock crosswalks, male pedestrians had better evaluation of traffic conditions.

S. Jain (✉)

Department of Civil Engineering, Amity University, Noida, India

e-mail: jsiddharth4444@gmail.com

M. Advani

Transport Planning Division, Central Road Research Institute, New Delhi, India

L. K. Yadav

UITP India, Gurgaon, India

Keywords Uncontrolled · Midblock · Crosswalk · Accidents · Pedestrians · Crossing time

1 Introduction

1.1 *Importance of Pedestrians Safety Analysis on Uncontrolled Midblock Crosswalks*

The most vulnerable road users' categories in India are the pedestrians, two wheelers, non-motorized transport, bicycles, and auto-rickshaw. They are highly prone to accidents and comprise approximately 50–60% of accidents taking place in India. Pedestrians are the most vulnerable victims in fatal road accidents. Pedestrian's safety is a very important issue that is mostly neglected as in most of the cities incidents are underreported. The pedestrians themselves have to make crossing time estimation on uncontrolled midblock crosswalks, as they do not get any kind of assistance from anyone, i.e., not from the signals nor from any traffic personnel, etc. In addition, they cannot control the traffic coming toward them. Therefore, it becomes very difficult for them to consider environment factors, geometrical factors, distance of vehicle approaching toward crosswalks, and time required to cross the midblock crosswalks simultaneously. Due to all these, they have to perceive the time required to cross the uncontrolled midblock crosswalks. Now, this perceived time could be less than the actual time required to cross the uncontrolled midblock crosswalks, which means they have underestimated the crossing time on uncontrolled midblock crosswalk. If this perceived time is more than the actual crossing time, it means that they have overestimated the crossing time on uncontrolled midblock crosswalk. In both the cases, there is risk involved as if the pedestrian while crossing the uncontrolled midblock crosswalks underestimates, it means that they assumed that they would cover more distance on midblock crosswalk in time 't' but in actual covered less distance w.r.t the perceived. Due to this error in perception, the pedestrian might end up standing in between points of crosswalk. If the pedestrian while crossing the uncontrolled midblock crosswalks overestimates, it means that he assumed that he would cover less distance on midblock crosswalk, but in actual he covered more distance w.r.t the perceived. Due to this error in perception, there are chances of conflict with the vehicles approaching if the width of uncontrolled midblock crosswalk is large (Figs. 1 and 2).

1.2 *Objectives of the Study*

The primary purpose of the study is to determine the actual and perceived time required by pedestrian for crossing the uncontrolled midblock road section. The secondary objective is to determine the level of risk for the pedestrian.



Fig. 1 Pedestrians halting in between of uncontrolled midblock crosswalk

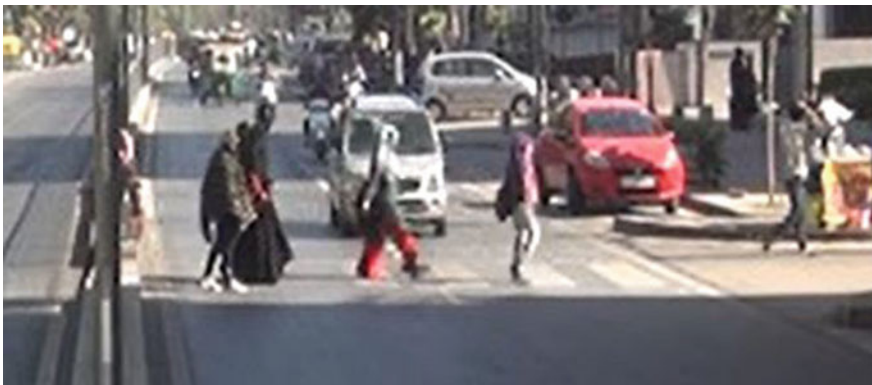


Fig. 2 Pedestrians crossing on uncontrolled midblock crosswalk

2 Literature Review

2.1 Past Studies

Pedestrian velocity is an important parameter in transportation planning and layout of pedestrian facilities [17]. The pedestrians have greater exposure to vehicular traffic at crosswalk locations (Morth 2017). In India, respectable facts in 2017 confirmed that 134,796 human beings were killed in street traffic crashes [11]. Despite the fact that pedestrians frequently have the option of crossing a avenue the usage of an underpass or overpass, most often they do not use it [4]. Time saving is the principle element for crossing the street at grade [16]. Pedestrians visitors hole reputation for midblock avenue crossing in city areas. In specific, elements of pedestrians crossing conduct at midblock places are tested, namely the dimensions of site visitors gaps regular by using pedestrians [2]. Pedestrians at two-lane one manner road section show off higher crossing pace compared with four-lane divided roadway conditions.

The results, additionally, concluded that crossing pace of pedestrians is higher as compared to theirs on foot pace [8]. Pedestrian behavioral characteristics just like the rolling gap, driving force yielding conduct, and frequency of try perform a crucial role in pedestrian uncontrolled avenue crossing [5]. Pedestrian crossing speed is quite different compared with pedestrian speed at sidewalks. However, there has been no significant impact of lighting on pedestrian crossing speed [13]. The average crossing speeds on crosswalks are decreased close to educational and bus terminus areas and greater at tourist and buying places. Rastogi et al. [13] observed that crossing speed will increase with road width, traffic volume, and length of the city vicinity as with the increase in width of avenue; they should cross a larger distance retaining surroundings and different factors into consideration [3]. The perceived safety for any area also increasingly plays an essential function in proactive protection planning. Räsänen et al. [12] located that relatively greater regularly; they opt to move the roads on the floor in preference to the usage of foot over bridge or underpass, which might alternatively increase their standard safety. Hatfield and Murphy [7] observed that the use of cell phones all through crossing reduces the velocity of pedestrians as their cognizance gets shifted and that they forget to present precedence to road crossing [9]. Actual crash information evaluation explains the crash frequency and presents a severity contrast; however, it does not now offer any information related to the character of the protection problem itself. Simpson et al. [14] studied crossing behavior of kids and young adults at midblocks. Younger kids (elderly 5–9 years) made the finest number of dangerous street crossings and the oldest members (elderly >19 years) the fewest [15]. The pedestrians' options also are very important for planning a safer environment for pedestrians [6]. Safety of pedestrian depends on how pedestrians reply to the traits of the environment as they choose their routes [1]. The built surroundings may also have a substantial effect on pedestrian crash charges. A huge number of research have checked out the relationship between real crash quotes of pedestrians and built surroundings capabilities, to identify interventions to reduce crashes. Lam and Cheung [10] completed a study in Hong Kong to look at the pedestrian float characteristics at numerous walking facilities. The results show that the pedestrians on crosswalks with midblock generally stroll slower than the ones on crosswalks without midblock.

2.2 Research Gap

Lack of research studies in perception crossing time and its comparison with their actual crossing time. Pedestrian on uncontrolled midblock crosswalk has to take decision of crossing the uncontrolled crosswalk. They have to estimate their crossing time and speed themselves. Pedestrian crossing perception time is an important factor on uncontrolled midblock crosswalks as if it is underestimated or overestimated, it leads to high amount of risk of conflict with approaching vehicles. As a result, this is marked as a gap that deserves more attention because most of the fatal accidents involving pedestrians take place on uncontrolled midblock crosswalks.

3 Study Methodology

3.1 Site Selection

Two different types of uncontrolled midblock crosswalks were selected from Ahmedabad. One was four-lane divided uncontrolled midblock crosswalk having width of 12.8 m ($23^{\circ}01'36.7''N$ $72^{\circ}33'25.1''E$), and the other was six-lane divided uncontrolled midblock crosswalk with width of 21 m ($23^{\circ}00'49.9''N$ $72^{\circ}33'56.0''E$) (Figs. 3 and 4).



Fig. 3 Four-lane midblock crossing with total width = 12.8 m



Fig. 4 Six-lane midblock crossing with total width = 21 m

3.2 Traffic Characteristics

The traffic composition on four-lane midblock crossing site of study consists of 57% cars, 29% two wheelers, 9% buses, and 5% three wheelers. On the other hand, the traffic composition on six-lane midblock crossing site of study was involving 61% cars, 26% cars, 10% buses, and 3% three wheelers.

3.3 Questionnaire Design and Data Sampling

The questionnaire was designed to collect data of pedestrians crossing at uncontrolled midblock crosswalks at two different types of midblock crosswalks of Ahmedabad. The data consisting of gender, age, perception time of crossing, and actual time of crossing was collected at both the study sites. During sampling 100 pedestrians, each at random was chosen for questionnaire survey at both the locations. They were asked about the time they would take to cross the midblock crosswalk. Then with the help of stopwatch, actual time of crossing of pedestrians was calculated. The total of 200 pedestrian's samples were collected at random from both the locations. The pedestrians were asked about their perceived time of crossing. The actual time of crossing was calculated with the help of stopwatch.

4 Data Analysis

4.1 Analysis of Perceived and Actual Crossing Time from Different Sites

The first location for survey was GLS entry gate, Ahmedabad; the type of uncontrolled midblock crosswalk was four-lane divided with the width = 12.8 m. The samples collected on GLS entry gate were of 100 pedestrians. Out of which, 83 were males and 17 were females. The data such as gender, age, perceived, and actual time was collected. The calculated perceived average time by males is 17.59 s and for females is 15.23 s. The overall average perceived time by males and females combined is 17.19 s. The minimum time perceived by pedestrians was 5 s, and the maximum time perceived by pedestrians was 60 s. The calculated average actual time by males was 11.85 s and for females was 12.05 s (Fig. 5).

The overall average actual time by males and females combined is 11.89 s. The minimum actual time by pedestrians was 7 s, and the maximum actual time by pedestrians was 21 s. The second location for survey was Paldi, Ahmedabad; the type of uncontrolled midblock crosswalk was six-lane divided with the width = 21 m. The samples collected on Paldi were of 100 pedestrians with the help of questionnaire. Out of which, 61 were males and 39 were females. The data such as gender, age, and

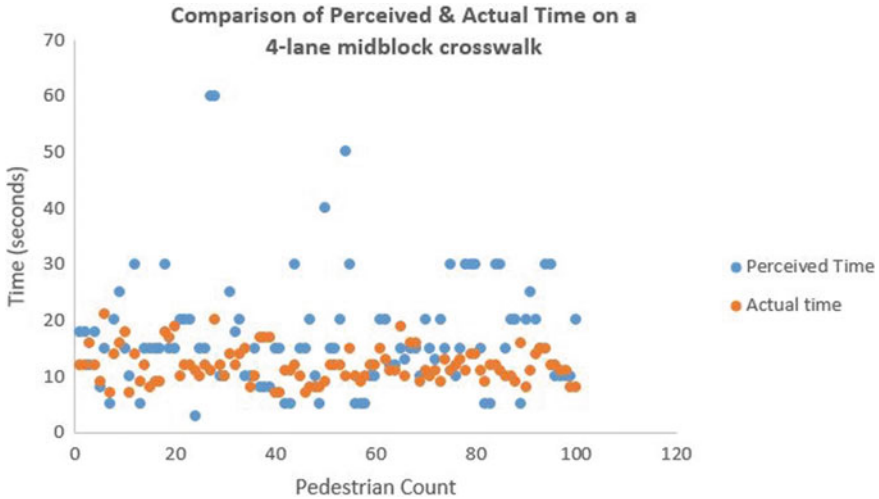


Fig. 5 Pedestrian’s perceived and actual crossing time at four-lane midblock crosswalk

perceived and actual time was collected with the help of questionnaire and stopwatch. The calculated perceived average time by males is 31.22 s and for females is 39.48 s. The overall average perceived time by males and females combined is 34.45 s (Fig. 6).

The minimum time perceived by pedestrians was 5 s, and the maximum time perceived by pedestrians was 120 s. The calculated actual average time by males is 20.08 s and for females is 20.64 s. The overall average actual time by males and females combined is 20.3 s. The minimum actual time by pedestrians was 10 s, and the maximum actual time by pedestrians was 40 s.

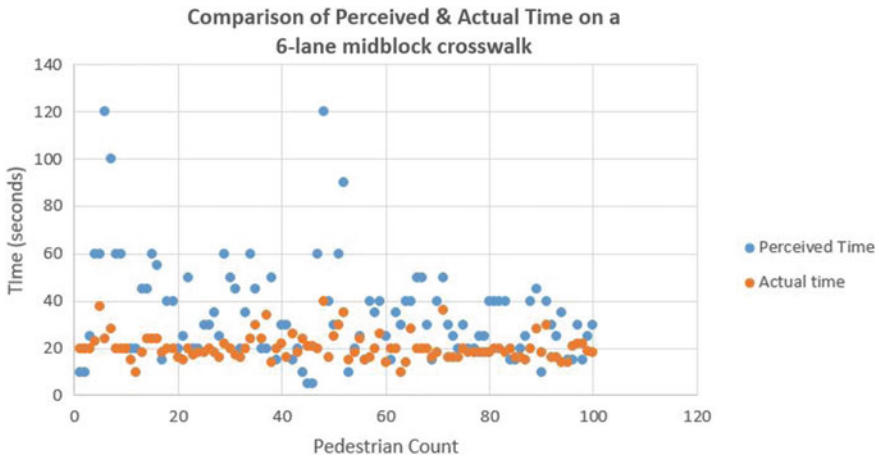


Fig. 6 Pedestrian’s perceived and actual crossing time at six-lane midblock crosswalk

Table 1 Results of paired *T*-test

<i>T</i> test	GLS entry gate Ahmedabad (1) <i>T</i> values	Paldi Ahmedabad (1) <i>T</i> values
1. Perceived and actual time	0.000	0.000
2. Perceived and actual time by males	0.000	0.000
3. Perceived and actual time by females	0.0370	0.000

4.2 The *T*-Test

A paired *T*-test was done between perceived time and actual time of crossing at uncontrolled midblock crosswalks of both the sites. In that test, we found out that there is a significant difference between perceived and actual time of both males and females (Table 1).

5 Results and Discussions

5.1 Overestimation and Underestimation by the Pedestrians

The estimation of crossing time on uncontrolled midblock crosswalks is very important for pedestrian’s safety as if the pedestrian underestimates, they might end up standing in between crosswalk, and in case, they overestimate that means his speed was more than perceived. In both the cases, risk of conflict with the approaching vehicles is very high. As this estimation is very important, to improve the safety of pedestrians, we analyzed overestimation and underestimation of pedestrians.

Estimation of time (%) = ((Perceive time – Actual time)/Actual time) * 100.

If estimation of time (%) = +ve, then it is an overestimate w.r.t actual time.

If estimation of time (%) = –ve, then it is an underestimate w.r.t actual time.

Study Location 1: GLS Entry gate

Out of 100 pedestrians, 68 pedestrians overestimated, while 32 pedestrians underestimated the crossing time at uncontrolled midblock crosswalk at GLS entry gate, Ahmedabad. Sixty-eight on an average overestimated the value of crossing time (seconds) by 88.20% w.r.t actual time. Thirty-two pedestrians on an average underestimated the value of crossing time (seconds) by 32.80% w.r.t actual time (Fig. 7).

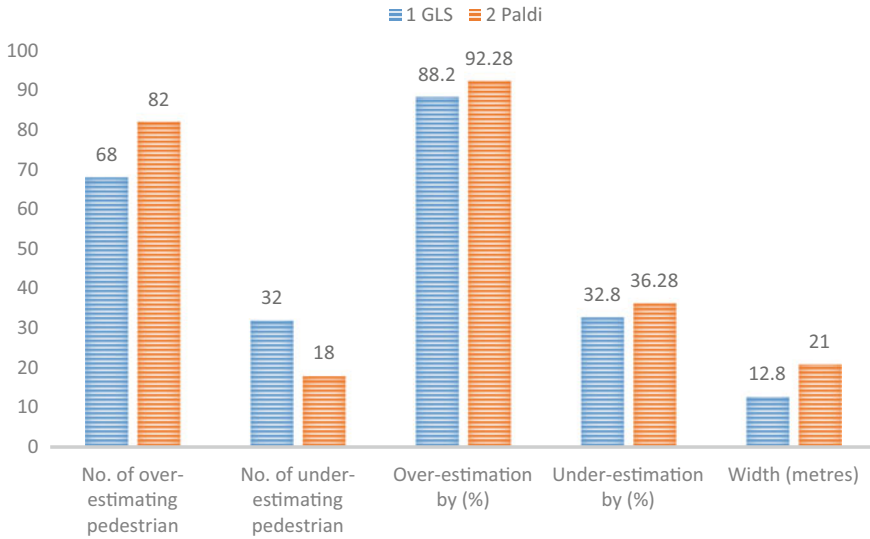


Fig. 7 Summary of the location and pedestrian characteristics

Study Location 2: Paldi.

Out of 100 pedestrians, 82 pedestrians overestimated, while 18 pedestrians underestimated the crossing time at uncontrolled midblock crosswalk at Paldi, Ahmedabad. Eighty-two on an average overestimated the value of crossing time (seconds) by 92.28 w.r.t actual time. Eighteen on an average underestimated the value of crossing time (seconds) by 36.28% w.r.t actual time (Fig. 8).

Therefore, we can also conclude that, as we move from four-lane divided midblock crosswalk to six-lane divided midblock crosswalk, the overestimation of crossing time by the pedestrians increases as the width of crosswalks increases. The underestimation of crossing time by the pedestrians also increases as the width of crosswalks increases.

5.2 Level of Risk of Accidents for the Pedestrians

In our study, we found out that level of risk of occurrence of accidents increases from four-lane midblock crosswalks to six-lane midblock crosswalks for the pedestrians as the difference between average perceived time and average actual time of total pedestrians also increases. Female pedestrians were at lower level of risk of accidents as compared to male pedestrians on four-lane divided uncontrolled midblock crosswalks, whereas on six-lane midblock crosswalk, female pedestrians were at high risk of accidents as compared to male pedestrians (Fig. 9).

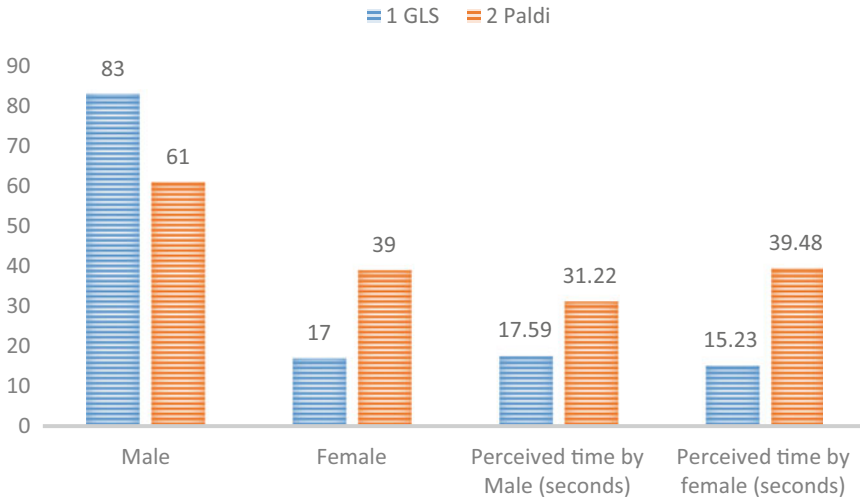


Fig. 8 Perceived time detail—Gender wise

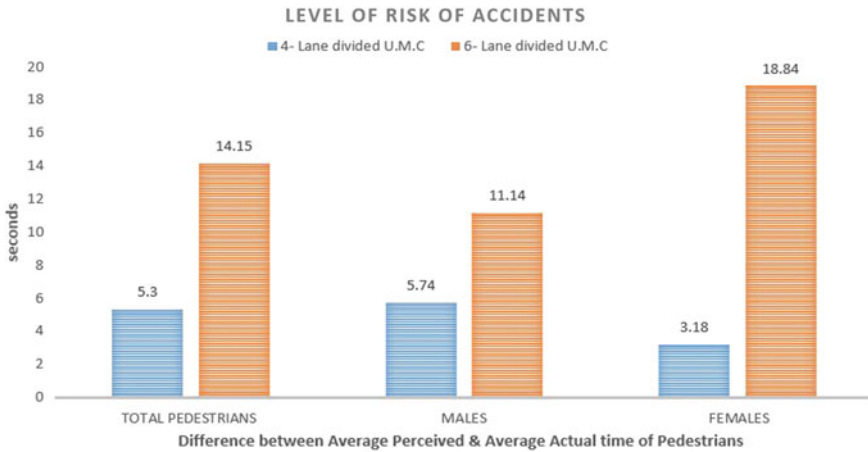


Fig. 9 Level of risk of accidents comparison between males and females

From a four-lane to six-lane midblock crosswalk, difference between average perceived time and average actual time of total pedestrians increased from 5.3 s to 14.15 s.

Difference between average perceived time and average actual time of male pedestrians increased from 5.74 to 11.14 s. Difference between average perceived time and average actual time of female pedestrians increased from 3.18 to 18.84 s.

6 Summary and Conclusions

According to Morth report 2019, India ranks third in number of accidents and ranks first in number of persons killed in road accidents all over the world. The most vulnerable road users' categories in India are the two wheelers, pedestrians, non-motorized transport, bicycles, and auto-rickshaw. They are highly prone to accidents and comprise approximately 50–60% of accidents taking place in India. In India, around 50% of persons are killed or injured on uncontrolled intersections, and pedestrians are the most vulnerable victims in fatal road accidents. Pedestrian's perceived time of crossing and its comparison with actual time of crossing at uncontrolled midblock crosswalks also increasingly play an important role in proactive safety planning, because it provides critical information regarding individual's crossing time and identifies overestimation and underestimation of their crossing time with respect to actual crossing time at uncontrolled midblock crosswalks. The pedestrian accidents are high because of their underestimation or overestimation of crossing time at uncontrolled midblock crosswalks. The underestimation and overestimation of perceived crossing time w.r.t actual crossing time by pedestrians increase with increase in width of midblock crosswalk.

Accidents on uncontrolled midblock crosswalks happen due to misevaluation of traffic conditions. Pedestrians do not perceive the traffic conditions correctly. Level of risk of accidents also increases as the width of midblock crosswalk increases. In our study, we found that female pedestrians were at low level of risk as compared to male pedestrians at four-lane midblock crosswalks as the difference of perceived time and actual time was less than that of male pedestrians. Male pedestrians were at low level of risk as compared to male pedestrians at six-lane midblock crosswalks as the difference of perceived time and actual time was less than that of female pedestrians.

Limitation: More data is required in terms of sample size, variability in number of lanes, and city, to arrive at certain guidelines for provision of pedestrian crossing.

References

1. Brude U, Larsson J (2000) What roundabout design provides the highest possible safety? *Nordic Road Trans Res* 12:17–21
2. Chandra S, Bharti AK (2013) Speed distribution curves for pedestrians during walking and crossing. *Procedia e Soc Behav Sci* 104(660):e667
3. Cho G, Rodríguez DA, Khattak AJ (2009) The role of the built environment in explaining relationships between perceived and actual pedestrian and bicyclist safety. *Accid Anal Prev* 41:692–702
4. Demiroz YI, Onelcin P, Alver Y (2015) Illegal road crossing behavior of pedestrians at overpass locations: factors affecting gap acceptance, crossing times and overpass use. *Accid Anal Prev* 80:220–228
5. Goh BH, Subramaniam K, Wai YT et al (2012) Pedestrian crossing speed: the case of Malaysia. *Int J Traffic Transp Eng* 2(4):323–332.
6. Hamed MM (2001) Analysis of pedestrians' behaviour at pedestrian crossings. *Safety Sci*

7. Hatfield J, Murphy S (2007) The effects of mobile phone use on pedestrian crossing behaviour at signalized and unsignalized intersections. *Accid Anal Prev* 39(1):197–205
8. Kadali BR, Vedagiri P (2013) Effect of vehicular lanes on pedestrian gap acceptance behaviour” *Procedia e Soc Behav Sci* 104:678e687
9. Kononov J, Allery B, Znamenacek Z (2007). “Safety planning study of urban freeways”: proposed methodology and review of case history. *Transp Res Rec* 146–155
10. Lam WHK, Cheung C-Y (2000) Pedestrian speed/flow relationships for walking facilities in Hong Kong. *J Transp Eng* 126(4):343–349
11. Rankavat S, Tiwari G (2016) Pedestrians perceptions for utilization of pedestrian facilities—Delhi, India. *Transp Res Part F* 42(3):495–499
12. Räsänen M, Lajunen T, Alticafarbay F, Aydin C (2007) Pedestrian self-reports of factors influencing the use of pedestrian bridges. *Accid Anal Prevent* 39(5):969–973
13. Rastogi R, Chandra S, Vamsheedhar J et al (2011) Parametric study of pedestrian speeds at midblock crossings. *J Urban Plan Dev* 137(4):381–389
14. Simpson G, Johnston L, Richardson M (2003) An investigation of road crossing in a virtual environment. *Accid Anal Prev* 35:787–796
15. Sisiopiku VP, Akin D (2003) Pedestrian behaviour and perceptions towards various pedestrian facilities: an examination based on observation and survey data. *Transp Res Part F* 6:249–274
16. Yannis G, Papadimitriou E, Theofilatos A (2013) Pedestrian gap acceptance for mid-block street crossing. *Transp Plan Technol* 36(5):450–462
17. Zhang C, Zhou B, Chen GJ et al (2018) Pedestrian crossing behaviour at uncontrolled multi-lane mid-block crosswalks in developing world. *J Safety Res* 64:145–154

Two Wheeler Rider Support System



Gunendra Mahore , Sonam Solanki , Ritik Barua ,
and Rupesh Mahore 

Abstract A two wheeler rider support system is developed as a smart helmet. With capabilities to detect drowsiness of two wheeler rider and traffic sign detection, it would enhance the driving experience as well as safety. Traffic Sign detection and traffic sign recognition algorithm are trained with YOLO v3. Rider is notified through a warning signal in the form of vibration and voice command preventing road accidents and injuries caused due to rider's ignorance and physiological factors like drowsiness or tiredness.

Keywords Smart helmet · Traffic sign detection · Traffic sign recognition · YOLO v3 · IOT · Drowsiness detection · Road accident prevention · Two wheeler safety

1 Introduction

In-depth research of powered two wheelers (PTW) accidents from the Motorcycle Accident In-Depth Study (MAIDS) database is done with 921 PTW accidents. Out of these accidents total of 245 was due to human error only [1]. Another study of 316 victims of road accidents shows the unsafe act of drivers in the list of causes. In the unsafe act of driver inappropriate speed, improper turning, improper overtaking, wrong side driving, distraction, etc., are considered which rises by the ignorance of road signs and in some cases drowsiness [2]. A study of 474 accidents in which 90% of cases were due to human error shows the importance of a driver assist. Due to overloading of information in the driver's mind, sight obstruction, sun glare, distraction, and drowsiness causes avoidance of road signs which can be corrected by a driving assist [3].

G. Mahore (✉) · S. Solanki · R. Barua
Madhav Institute of Technology and Science, Gwalior, India
e-mail: 29gulshanmahore@gmail.com

R. Mahore
National Institute of Technology, Rourkela, India

For assisting the driver many “driver support systems” or “ADAS Advanced Driver Assistance Systems” have been developed for cars. These support systems assist driver with blind-spot detection, intelligent cruise control, automatic emergency braking, and lane-keeping assist. The main purpose of these systems is to reduce driver error and improving driver safety [4].

Our main focus area is developing a “Rider Support System (RSS)” for two wheeler riders. This system will assist the rider by providing the road traffic sign information on a real-time basis reducing the chances of human error. RSS will also be featured with drowsiness detection which will alert the rider to take rest during the stressed condition. The whole system will be embedded in the riders’ helmets for enhancing safety.

2 Indian Road Sign Orientation

In India road signs are normally placed on the left side of the road. In hilly areas signs are mounted on valley side of road. The extreme edge of signboards mounted adjacent to roadway are at distance between 6 and 3 m from carriageway. The bottom most point of road signs are at a distance between 2 and 2.5 m above the ground. Gantry mounted signs are placed more at a distance more than 7 m from roadways. Basic dimensions of sign boards are given in Figs. 1 and 2 [5].

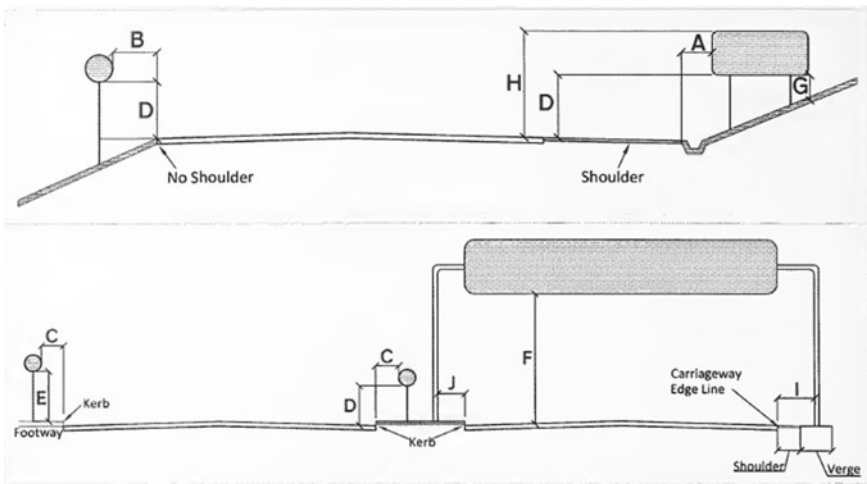


Fig. 1 Siting of signs with respect to carriageway (height and clearance) [5]

	Minimum (mm)	Desirable (mm)	Maximum (mm)
A	600	1000	2500
B	1000	2000	3000
C	300	600	1000
D	2000	2000	2500
E	2100	2100	2500
F	5500	6000	6500
G	750		
H			5000
I	5000	7000	9000
J	1800	2000	2500

Fig. 2 Height and clearance required for sign placement [5]

3 Traffic Sign Detection and Recognition

ADAS provides the traffic sign recognition system in the car which alerts the driver with any traffic sign on road. This system is based on image processing and computer vision [6]. Traffic sign detection (TSD) and traffic sign recognition (TSR) are the two main components of ADAS in finding and alerting the driver regarding restrictions and information about the road. Currently, TSD and TSR are use deep learning techniques like convolutional neural network (CNN). For real-time situations like self-driving cars, a highly tuned version of faster R-CNN is used. It is a double-stage object detection network consisting of bounding box regressor, classifier networks, and region proposal network. You Look Only Once (YOLO) is a single-stage object detector that gives real-time speed in object detection but does not come with the required accuracy and encounter difficulties with small objects in the image. This problem is solved in the V3 version of YOLO which we will be considered in our research [7] (Fig. 3).

4 Drowsiness Detection

Currently, there are two popular ways of detecting drowsiness. The first way deals with physiological factors analysis such as eyelid closer, electroencephalogram [8], and electrooculogram [9]. Another way is based on the driving behavior and reaction time of driver and steering movement [10, 11].

Detecting drowsiness with eyelid closer is based on image processing and computer vision. First, the state of the eye in real time is detected. In real-time



Fig. 3 Traffic sign detection and recognition

eye state detection ‘state-of-art’ landmark detector is used for capturing characteristic points on the face in which eye corners and eyelids are also available. From the landmark, available eye aspect ratio (EAR) is derived which gives us the scalar value for opening and closing of eyes in real time [12] (Fig. 4).

For detecting drowsiness, the opening and closing time of eyelids is compared with threshold values. The average time for eye blinking lies between 75 and 400 ms. So, time for detecting drowsiness is considered to be 400 ms. It is based on the fact that if a car is at speed of 90 kmph then we will get a distance of about 10 m which is sufficient time for alerting the driver [13].



Fig. 4 Drowsiness detection model

5 Proposition

The main goal of our project is to increase the safety of two wheeler riders. This is done by supporting the rider with an assist that can alert him while riding. For supporting the rider with such an assist a helmet is designed. This helmet will be embedded with a device that will keep monitoring the road for traffic signs and driver for drowsiness in real time and warn the driver with voice command. The device embedded in helmet rather than in bike as it will improve the accuracy of drowsiness detection and provide a better view for TSD and TSR.

6 Helmet Design

The helmet is designed in such a way that it can provide a support system without compromising the safety parameters of the helmet in case of an accident. First, its support system is designed with all the electronic parts. After finishing the electronic parts helmet is modified so that it can fit with all the electronic parts and could be analyzed under impact conditions for ensuring rider's safety.

6.1 *Electronic Parts*

The main control unit of the support system is Raspberry pi-zero. For providing the road view to raspberry pi for TSD and TSR a camera is attached on the top of the helmet. The two other cameras are attached near the eye of the rider without blocking its view inside the helmet which can provide the state of the eye in real time. The system is powered with the 3.7 V Li-ion battery which will be charged wirelessly when placed on the bike with the help of a wireless charger in the bike. Two mini speakers are attached near the ear position inside the helmet which can provide voice feedback to the rider along with a vibration created by a vibrator motor fitted in the helmet (Fig. 5).

6.2 *Helmet Structure Design*

The structure of the helmet is redesigned for holding cameras, speakers, and providing room for all electronic items. Electronic items are fitted such that no item is in direct contact with the head when rider wears the helmet. All items are outside the solid boundary around the head so that items cannot penetrate the head during an accident. The helmet is 3D-modeled and redesigned in SolidWorks for virtual simulation in ANSYS (Fig. 6).

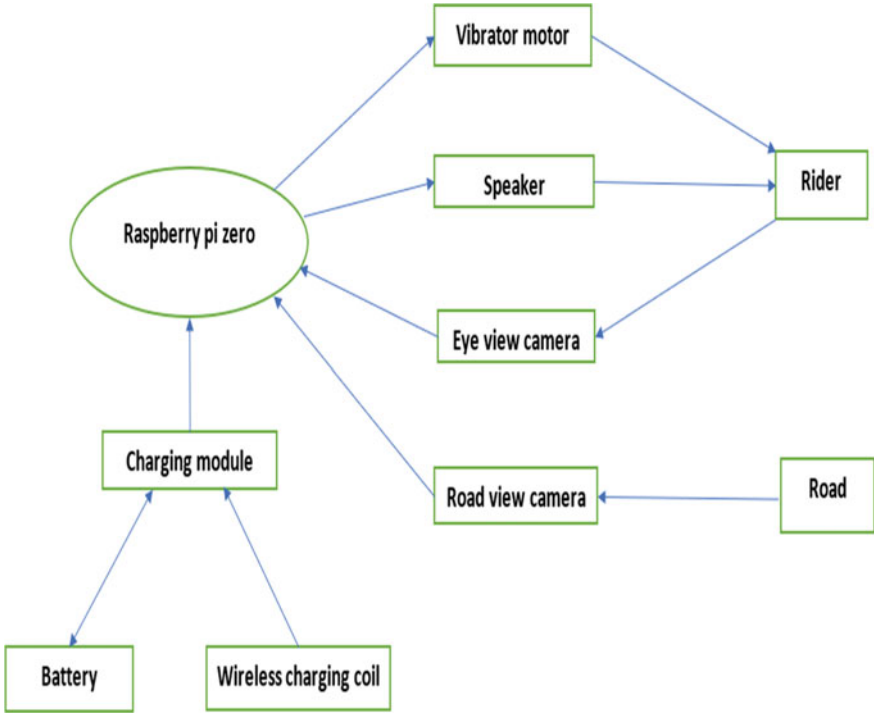


Fig. 5 Helmet electronic design

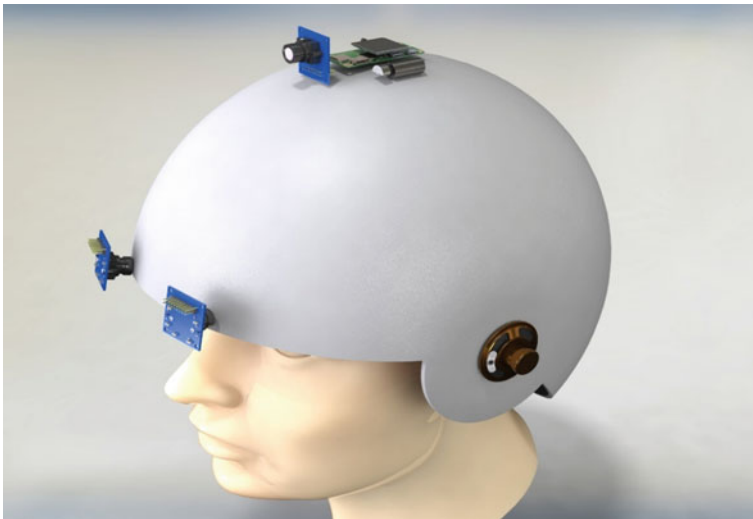


Fig. 6 Helmet interior boundary with components

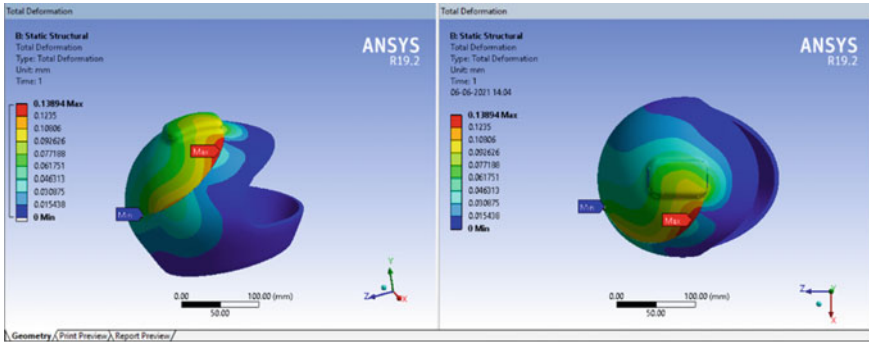


Fig. 7 ANSYS static structural analyses

6.3 Helmet Simulation

The 3D-modeled helmet is simulated in ANSYS for ensuring safety parameters. In ANSYS static structural analyses is performed on the helmet and deformation is recorded and design is further altered for any failure during the impact test. Once the required safety parameter is achieved the simulation process of the helmet is finished.

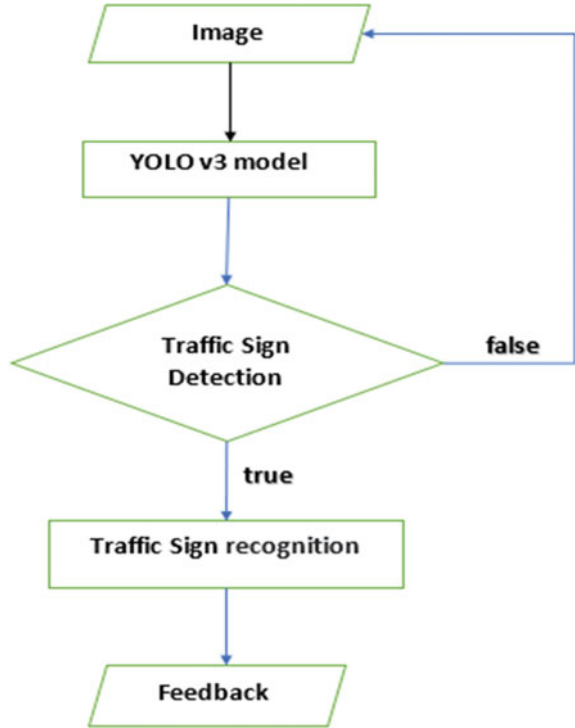
Static structural analyses have been performed in ANSYS. A 5 mm carbon fiber material is used to make helmet structure for analyses. A 2000 N external force is applied keeping the inner shell of helmet structure fixed. A maximum deformation of 0.138 mm is observed (Fig. 7).

7 Operation

The operation of the helmet is based upon two parameters, rider’s road view capture for TSD and TSR and rider’s eyes capture for drowsiness detection. First image is captured from the road view camera and passed through trained model for TSD in raspberry pi zero. The trained model uses YOLO weight file for TSD. This weight file is created from the Google Collaboratory with the help of YOLO v3 model and 10,000 custom image dataset. The model is iterated up to 1000 times for more accuracy. The image is tested for any traffic sign available in the class list of model. Once any traffic sign is detected it is tested for 43 available classes of traffic sign under which this will fall under. After recognition of the sign, the corresponding feedback is passed to the rider with the help of saved voice command and vibration through speakers and vibrator motor respectively (Fig. 8).

Second pair of cameras is installed in front of helmet, outside the proximity of shell facing the eyes and providing image of the eyes to the raspberry pi without blocking the vision or hindering the structural safety of helmet. This image is passed

Fig. 8 TSD and TSR operation

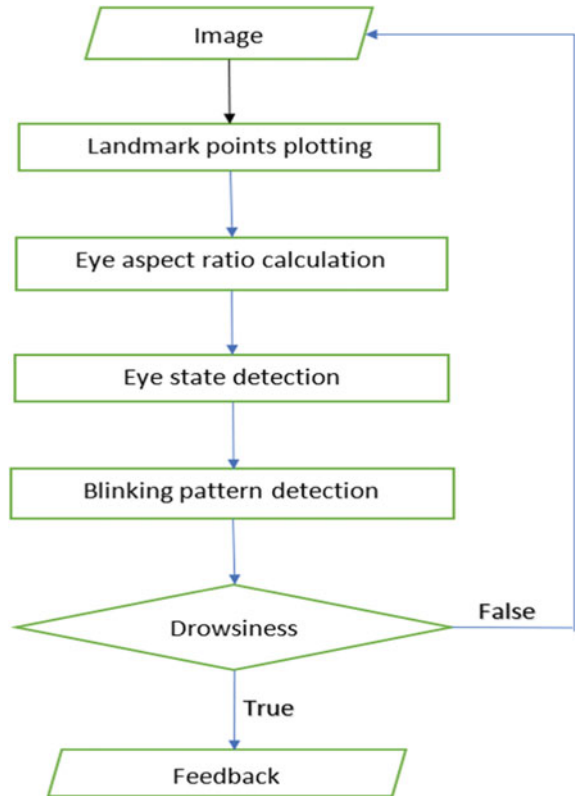


to the eye detection model in which landmark points are plotted on eyes and aspect ratio is calculated. As an output it gives the status of eyes in specified interval of time. This status is passed to the algorithm which detects the pattern of eye blinking and checking the condition of drowsiness. Once a condition is satisfied for drowsiness the feedback is given to the rider in the form of voice command and vibration (Fig. 9).

8 Result and Discussion

Two wheeler rider support system is recent advancement in technology as the technology used in building helmet like TSD and TSR are currently being used in cars for sign board detection. With Indian context, some primary design of smart helmets are already available in market with limited features. Our work is advancement and addition to the former technology. Our work includes choosing an appropriate ML model, and training the model with a myriad of dataset. Classifying the dataset in 42 standard classes of road signs. It also includes optimization of the helmet –architecture including the electronic components and impact analyses of the proposed architecture. The cost of the helmet has not been discussed under the scope of this paper. A rough estimate of the prototype would be around Rs. 3000. The intrinsic

Fig. 9 Drowsiness detection operation



factors like driver’s skill, age, gender can’t be quantitatively incorporated within our simulation.

The accuracy of model would depend on how the dataset is trained (quantity/quality of data and no of iteration). The accuracy of our model is around 79% (as shown in Fig. 1). The accuracy of detection would depend the quality of the traffic road sign [14]. The model changes the colored image into greyscale image before processing so there is no issue associated with specific colors. The model has been trained with standard road signs, so it would detect all the signs of standard size (as approved by authority). The distance would again depend upon the resolution of the camera. In our design, it is about 40 ft range. The dataset is based on the Indian road signs. TSD threshold has been set 0.6 so any sign having accuracy below 60% will not be detected as a road sign, so the driver won’t get any false alarm.

TSD and TSR is based on dataset provided during model training so every sign available in trained dataset can be detected. A number of traffic signs with the same meaning can be put in a same class in the trained dataset. Advised speed at which the model would work is below 80 kmph, for anything above this threshold the precision would be a function of frame rate of camera and processing power of microprocessor used. At the speed of 50-70kmph driver has reaction time of about 3–4 s [15].

The camera (IR camera) for drowsiness detection will work in all weather and light condition as it is embedded inside the helmet, where it is not affected by the external weather. The drowsiness detection camera is positioned in such a way that it covers both the eyes within the field of view (FOV) of camera.

9 Conclusion

A helmet is designed with TDS and TSR capabilities to optimize driving experience and safety. Model is trained with YOLO, using weight file the operation is carried out. A Raspberry pi is used as microcontroller. A Li-ion 3.7 V battery to run the system is installed which can be wirelessly charged from bike itself. All that being done without compromising the structural safety of helmet and without hindering the vision of motorbike rider.

Drowsiness and unawareness of traffic signals are the major causes of accident and on road casualties. Helmet would enhance driver safety in cases where important road signs are missed like speed limit, school ahead, narrow bridge, no left turn, etc. Model is trained with 41 different types of traffic sign images and a signal is sent to driver when those are detected by camera. It would also prevent drunk driving.

References

1. Penumaka AP et al (2014) In-depth investigations of PTW-car accidents caused by human errors. *Safety Sci* 68:212–221
2. Singh J et al (2016) Reasons for road traffic accidents—Victims' perspective. *Int J Med Sci Public Health* 5:814–818
3. Staubach M (2009) Factors correlated with traffic accidents as a basis for evaluating advanced driver assistance systems. *Accid Anal Prev* 41(5):1025–1033
4. Brookhuis KA., De Waard D, Janssen WH (2001) Behavioural impacts of advanced driver assistance systems—An overview. *Eur J Transp Infrastruct Res* 1(3)
5. IRC 067. Code of practice for road signs, 3rd rev.
6. Avramović A, Tabernik D, Skočaj D (2018) Real-time large scale traffic sign detection. In: 2018 14th symposium on neural networks and applications (NEUREL). IEEE
7. Rajendran SP et al (2019) Real-time traffic sign recognition using YOLOv3 based detector. In: 2019 10th international conference on computing, communication and networking technologies (ICCCNT). IEEE
8. Santamaria J, Chiappa K (1987) The EEG of drowsiness in normal adults. *J Clin Neurophysiol* 4(4):327–382
9. James B, Sharabaty H, Esteve D (2008) Automatic EOG analysis: a first step toward automatic drowsiness scoring during wake-sleep transitions. *Somnologie* 12:227–232
10. Liu CC, Hosking SG, Lenné MG (2009) Predicting driver drowsiness using vehicle measures: recent insights and future challenges. *J Safety Res* 40(4):239–245
11. Dinges D (1998) PERCLOS: a valid psychophysiological measure of alertness as assessed by psychomotor vigilance Indianapolis. Technical report, MCRT-98-006. Federal 232 Highway Administration, Office of Motor Carriers

12. Cech J, Soukupova T (2016) Real-time eye blink detection using facial landmarks. Center for Machine Perception, Department of Cybernetics, Faculty of Electrical Engineering, Czech Technical University, Prague, pp 1–8
13. Danisman T et al (2010) Drowsy driver detection system using eye blink patterns. In:2010 International conference on machine and web intelligence. IEEE
14. Babić D, Babić D, Fiolić M, Šarić Ž (2021) Analysis of market-ready traffic sign recognition systems in cars: a test field study. *Energies* 14(12):3697
15. Aliane N, Fernandez J, Mata M, Bemposta S (2014) A system for traffic violation detection. *Sensors* 14(11):22113–22127

User Preferences and Behaviour

Determinants of Mobile Phone Use and Seat Belt Non-compliance Among Vehicle Drivers in Nigeria: An Observational Study



Yingigba Chioma Akinyemi

Abstract The use of mobile phone and non-use of seat belt by drivers while driving is associated with the risk of crashes, injuries, and fatalities. Annual road traffic fatalities in Nigeria were over 5000 during the period 2000–2017. This study examined the rate and factors influencing mobile phone use and non-compliance to use of seat belt in Ibadan metropolis, Nigeria. A total of 6056 drivers were observed at 10 intersections. Overall, 611 (10.1%) drivers were found using a mobile phone while 1903 (31.4%) did not wear seat belt. Results of multiple logistic regression indicated that male drivers were more likely than females to use phones and not wear seat belt. Young drivers were more likely to use phones while driving than older drivers. Commercial vehicle drivers had higher odds of not wearing seat belt compared to other vehicles. No association was found between phone use and seat belt non-compliance. Educational campaigns and improved enforcement strategies need to be implemented.

Keywords Mobile phone · Seat belt · Road crashes

1 Introduction

According to reports of the Federal Road Safety Corps (FRSC), over 5000 persons died yearly due to road traffic injuries on Nigerian roads between 2000 and 2017 [1]. Given the economic, social, and health impacts of road injuries on children, young adults, elderly, families, and the society, road traffic crashes (RTC) are a major health problem in Nigeria. Hence, road safety is an important health priority that requires specific and appropriate intervention.

Human behaviors that increase the risk and severity of crashes include inappropriate or excessive speed, non-use of seat belt, child restraint and helmet, drink-driving, and driver distraction [2]. In 2017, 71% of road crashes in Nigeria were due

Y. C. Akinyemi (✉)

Department of Geography, University of Ibadan, Ibadan, Nigeria

e-mail: chiomajaja@yahoo.com

to human factors, specifically, speed violation, loss of control, dangerous driving, wrongful overtaking, and use of phone while driving [1].

Studies have shown that seat belt use is an effective way of preventing and reducing injury severity among vehicle occupants during road crashes [3]. Seat belt hold down vehicle occupants in their seats and prevent them from colliding with objects or being thrown out from the vehicle [4]. Use of seat belt reduces the risk of death by 45–50% among drivers and front seat occupants and 25% among rear seat occupants [5]. Fatal and non-fatal injuries in front and rear seat occupants can be reduced by 60% and 44%, respectively [6]. Also, risk of sustaining fatal and serious injury is 8.3 times and 5.2 times higher among drivers without seat belt compared to drivers who wear seat belt [7].

Driver distraction is a major cause of road crashes as it accounts for 1–50% of road crashes [8]. Driver distraction involves the driver attending to other activities rather than paying attention to activities critical for safe driving [9]. Distraction occurs when the driver shifts attention to some event, activity, object, or person within or outside the vehicle, causing delay in recognition of information needed to accomplish driving task [10]. Mobile phone use while driving is a very risky source of distraction compared with other sources. Mobile phone activities while driving involve mainly answering and making calls, replying, sending, and reading text messages [11].

Studies in the literature indicate that use of mobile phone while driving escalates the risk of road crashes, injuries, and fatalities as well as impair driver's performance and behavior. Redelmeier and Tisbshirani [12] noted that the use of mobile phones while driving increased crash risk four times compared with non-use of a phone. Violanti [13] noted that drivers using a phone when collision occurred had a nine-fold risk of a fatality. Mobile phone conversation of more than 50 min in a month resulted in a 5.59 increased risk of having a RTC [14], and risk of a road crash by 2–9% [2]. Texting increased the risk of a RTC by six fold [15]. Drivers who text message and dial a mobile phone while driving were 23.2 and 5.9 times likely to be involved in a road crash [16].

Further, mobile phone use while driving results in increase or decrease in reaction time [17], impaired detection and reaction to changes in speed of front vehicles [18], lane deviation [19], increase mental workload [20], influence vehicle speed [21], affect response to unexpected brake and cause more frequent braking [22], reduce glances to the mirror, roadway, and speedometer [23], impair perception and decision-taking, and causes delay in recognition and response to traffic events [24].

Enforcement of laws mandating the use of seat belt and prohibiting mobile phone use by drivers has been shown to be effective in changing driver behavior. Although Nigeria has national seat belt and mobile phone use laws which are enforced by the FRSC, compliance to these laws is not optimal. According to the national child restraint law in Nigeria, child passengers are required to use child restraints until seven years of age while those above seven should wear a seat belt [5]. However, child occupants are rarely protected using appropriate restraints. Non-use of child restraint by children increases crash risk and fatalities. Available data from FRSC indicate that a total of 149,857 seat belt violation offenders and 7243 drivers using mobile phones while driving was arrested in 2010 [25]. Analysis of the prevalence

and factors associated with seat belt and mobile phone use among drivers is important for the implementation of public health interventions that will reduce injuries and fatalities associated with road crashes. Observational and self-reported studies on the use of seat belt and mobile phone by drivers are replete in the literature. However, studies on the rate of compliance and factors related to the non-use of seat belt and mobile phone use among drivers in Nigeria are sparse.

Most of the studies on the use of seat belt and mobile phone while driving focus on high-income countries with low(7%)-road traffic deaths compared with low- and middle-income countries which account for 13% and 80% of road deaths, respectively [5]. Very few studies have examined the use of seat belt and mobile phone by drivers on roads in sub-Saharan African countries [26–28] and Nigeria [29–31] in particular. With the exception of studies by Sangowawa et al. [32] and Popoola et al. [33], most of the previous researches conducted in Nigeria utilized self-reported rates which are influenced by social–desirability bias as participants increase the rate of their seat belt use and reduce their mobile phone use rate, thereby making the data unreliable [34]. Given the increasing rate of phone subscription and high rate of non-use of seat belt in Nigeria, regular roadside observations surveys are required to determine the level of seat belt and phone use among drivers.

The study objectives are to (1) assess the level of mobile phone use and of seat belt non-compliance by drivers on roads in Ibadan metropolis, Nigeria using a direct observation approach, (2) examine the relationship between use of mobile phone and seat belt non-compliance, and driver’s gender, estimated age, time of day, vehicle type, and vehicle usage using binary logistic regression analysis, and (3) investigate the association between seat belt non-compliance and mobile phone use. Results from the study will aid the identification of high-risk groups and guide the development of educational campaigns and enforcement of traffic safety regulations.

2 Material and Methods

2.1 Research Design

A fixed observational methodology was adopted in this study since the goal was to examine drivers’ use of seat belt and mobile phone while driving in Ibadan Metropolis, Nigeria.

2.2 Sample Size

Following Sangowawa et al. [32], the sample size was determined using the formula for estimating population proportion: $n = z_{1-\alpha/2}^2 [0.25]/d^2$ where n is the sample

size, z is confidence level, and d represents precision. We assumed confidence level of 95%, estimated population proportion of 20%, and precision of 0.01. A sample size of 6147 was determined. Hence, 615 vehicles were observed at each of the 10 selected sites.

2.3 Site Selection

Vehicle drivers were observed at intersections controlled by traffic light where vehicles are stationary or slowed down. Selected sites are located in both the rural and urban parts of the metropolis. The research assistants were stationed at a raised median so that only vehicles on the kerb lanes were observed. This was to enable the field assistants observe the interior of vehicles. In order to avoid observing a driver more than once, only one site was selected along roads with several intersections. Due to limited budget and resources, ten sites were selected for the study.

2.4 Observer Training and Pilot Testing

The research assistants were trained on safety measures to be adopted, data collection procedure and observation protocols. A supervised pilot survey was conducted at one of the selected sites to identify problems related to the observational procedure and data collection. After the pilot survey, issues identified were discussed so as to avoid observer bias.

2.5 Observational Checklist

Information on the driver's gender and estimated age, vehicle type, vehicle usage, presence of a child aged less than eight years, number of vehicle occupants, the use of seat belt and mobile phone was collected. Driver's age was classified into three age groups: 18–24 years, 25–59 years, and 60 years and older. Vehicles observed were restricted to sport utility vehicle (SUV), car, taxi, van, and pick-up. Vehicles used as taxi are painted in a specific color to distinguish them from other vehicles. Trucks, buses, and service vehicles such as police cars, ambulance, and fire vehicles were excluded. Observed indicators of mobile phone use were driver holding a phone to the ear, using a headset or Bluetooth while talking, manipulating a handheld device, texting and reading a message. An observational form was used to record the information collected.

2.6 Data Collection

The observational survey was conducted on weekdays by trained field assistants. The survey was conducted from 7 to 11 am and 3 to 6 pm at each site on weekdays (Monday–Friday) for a period of one week. Traffic is usually heavy during these periods. Two observers were assigned to each site for observation. A total of 20 research assistants conducted the survey. The observers were positioned at the driver’s side of the road. When vehicles were stationary at a red light, one observer recorded information on mobile phone use by the driver, while the other observer recorded information on drivers’ seat belt use. Observation forms with inconsistent and incomplete information were excluded. Overall, observations for 6056 vehicles were used for the analysis.

2.7 Data Analysis

Descriptive statistics were presented in frequency and percentages. Pearson chi-square tests were performed to determine the association between mobile phone, seat belt use, and the explanatory variables. Further, multivariate logistic regression analysis was used to assess the factors associated with seat belt non-compliance and use of mobile phone by drivers. Seat belt was coded as 1 = Yes, if the driver used seat belt while driving and 0 = No, if otherwise. Similarly, mobile phone use was coded as either 1 or 0. Correlation analysis and variance inflation factor (VIF) were used to test for multicollinearity. In the model for seat belt non-compliance and mobile phone use, the VIF for all the variables were less than 2.0, and the correlation coefficients between the variables were less than 0.6 indicating absence of multicollinearity problems. The statistical package for the social sciences (version 25.0) was used for bivariate and logistic regression analyzes at statistical significance levels of $p < 0.05$.

3 Results

3.1 Sample Characteristics

The analysis was based on information obtained on 6056 drivers. The sample characteristics are presented in Table 1. There were 5045 (83.3%) male and 1011 (16.7%) female drivers. A high proportion (93.9%) of the drivers was aged 25–59 years (93.9%). This was followed by drivers aged 60 years and above (3.6%) and 18–24 years (2.5%). Vehicles observed were mostly cars (54.9%), followed by SUV (22.5%) and taxi (16.6%). A total of 3716 vehicles (61.4%) had multiple occupants,

while drivers were the only occupant in 2340 vehicles (38.6%). Vehicles observed were used mainly for private (75.0%) and commercial (20.5%) purposes.

Table 1 Driver and vehicle characteristics

Variable	Category	Frequency	Percentage
Gender	Male	5045	83.3
	Female	1011	16.7
Age	18–24 years	154	2.5
	25–59 years	5685	93.9
	60 years and above	217	3.6
Vehicle type	SUV	1361	22.5
	Car	3325	54.9
	Taxi	1003	16.6
	Van	238	3.9
	Pick-up	129	2.1
Vehicle usage	Private	4544	75.0
	Commercial	1243	20.5
	Government	57	0.9
	Company	212	3.5
Vehicle occupant	Single	2340	38.6
	Multiple	3716	61.4
Child passenger < 8 years	Yes	445	7.3
	No	5611	92.7
Mobile phone use behavior	Holding phone to the ear	248	4.1
	Talking using a headset or hands-free	140	2.3
	Texting or reading a message	107	1.8
	Talking on handheld	80	1.3
	Manipulating handheld phone	234	3.9
Mobile phone use	No	5445	89.9
	Yes	611	10.1
Seat belt use	Yes	4153	68.6
	No	1903	31.4
Vehicle occupant	Single	2340	38.6
	Multiple	3716	61.4
Time of day	7–11 am	3749	61.9
	3–6 pm	2307	38.1

3.2 Mobile Phone and Seat Belt Use by Drivers

Table 1 indicates that out of the 6056 vehicles observed during the survey, 611 (10.1%) drivers used a mobile phone while driving while 5445 (89.9%) did not use a phone. Drivers who used a mobile phone held the phone to the ear (4.1%), manipulated a handheld phone (3.9%), and talked with a headset or hands-free device (2.3%). Some of the drivers used their mobile phone for dual purposes, for example, talking with a hands-free device and manipulating a handheld phone. Further, 4153 (68.6%) drivers were observed wearing seat belt while 1903 (31.4%) did not wear seat belt.

Results of bivariate analysis of seat belt and mobile phone use, driver and vehicle characteristics are presented in Table 2. A higher (10.4%) proportion of male drivers used a mobile phone compared with female drivers (8.7%). Seat belt use compliance was higher among female (86.9%) than male (64.9%) drivers. Table 2 reveals that mobile phone use is not related to gender of the driver, however, seat belt non-compliance was significantly associated with gender ($\chi^2 = 189.98, p = 0.00$). Drivers' age was significantly associated with mobile phone use ($\chi^2 = 6.904, p = 0.03$) but not associated with non-use of seat belt. The analysis of prevalence rates by age group indicates that drivers aged 18–24 years had a significantly higher rate (15.6%) of mobile phone use compared with persons aged above 25 years. In terms of vehicle type, majority of drivers who used a mobile phone drove cars (10.6%) and taxis (10.5%), while the least usage of mobile phone was among pick-up (7.8%) drivers.

The rate of seat belt non-compliance was higher among drivers who drove taxis (94.8%) while most SUV (85.7%) drivers used seat belt. The type of vehicle is significantly associated with the use of seat belt but not related to mobile phone use. The greatest usage of mobile phone was among private vehicle drivers (10.2%), followed by government (10.5%), company (9.9%), and commercial vehicle (9.8%) drivers. A higher proportion of commercial drivers (90.3%) did not wear seat belt. Seat belt compliance was higher (84.4%) among private vehicle drivers. The association between vehicle usage and phone use was not significant, but seat belt use was significantly related to vehicle usage ($\chi^2 = 2527.04, p = 0.00$).

The results in Table 2 further indicate that there was a highly statistically significant relationship between number of vehicle occupant, mobile phone ($p = 0.00$), and seat belt ($p = 0.00$) non-compliance. The prevalence of mobile phone use was higher (11.1%) among drivers who were the only occupants in the vehicles compared with multiple occupant vehicles (9.4%). Non-use of seat belt was higher among drivers with other vehicle occupants (38.5%) compared with drivers that were alone in the vehicle (20.2%). Drivers who had children aged less than eight years in the vehicle had a higher rate of mobile phone use (17.1%) and non-use of seat belt (34.4%). The proportion of drivers who used a phone while driving was high (10.5%) between 3 and 6 pm while 32% of drivers did not wear seat belt between 7 and 11 am. Time of day was not significantly associated with phone and seat belt use.

Table 2 Characteristics of seat belt and phone users and non-users

Variable	Mobile phone use				Seat belt use				p-value	
	Yes	%	No	%	Yes	%	No	%		
Gender										
Male	523	10.4	4522	89.6	3274	64.9	1771	35.1	189.9	0.00*
Female	88	8.7	923	91.3	879	86.9	132	13.1		
Age										
18-24 years	24	15.6	130	84.4	116	75.3	38	24.7	5.373	0.07
25-59 years	571	10.0	5114	90.0	3879	68.2	1806	31.8		
60 years and above	16	7.4	201	92.6	158	72.8	59	27.2		
Vehicle type										
SUV	123	9.0	1238	91.0	1166	85.7	196	14.3	2311.7	0.00*
Car	353	10.6	2972	89.4	2700	81.2	625	18.8		
Taxi	105	10.5	898	89.5	52	5.2	951	94.8		
Van	20	8.4	218	91.6	141	59.2	97	40.8		
Pick-up	10	7.8	119	92.2	94	72.9	35	27.1		
Vehicle usage										
Private	462	10.2	4082	89.8	3834	84.4	710	15.6	2527.0	0.00*
Commercial	122	9.8	1121	90.2	121	9.7	1122	90.3		
Government	6	10.5	51	89.5	40	70.2	17	29.8		
Company	21	9.9	191	90.1	158	74.5	54	25.5		
Vehicle occupant										
Single	260	11.1	2080	88.9	1867	79.8	473	20.2	222.4	0.00*

(continued)

Table 2 (continued)

Variable	Mobile phone use				Seat belt use							
	Yes	%	No	%	χ^2	p-value	Yes	%	No	%	χ^2	p-value
Multiple	351	9.4	3365	90.6			2286	61.5	1430	38.5		
Child passenger					25.866	0.00*					1.95	0.16
Yes	76	17.1	369	82.9			292	65.6	153	34.4		
No	535	9.5	5076	90.5			3861	68.8	1750	31.2		
Time of day					0.66	0.42					1.710	0.19
7-11 am	369	9.8	3380	90.2			2548	68.0	1201	32.0		
3-6 pm	242	10.5	2065	89.5			1605	69.6	702	30.4		
Phone use											0.414	0.52
Yes							426	69.7	185	30.3		
No							3727	68.4	1718	31.6		
Total	611	10.1	5445	89.9			4153	68.6	1903	31.4		

* Significant at $p < 0.05$

Generally, the result shows that 3727 drivers obeyed the law relating to non-use of mobile phone and use of seat belt while driving. This represents 68.4% of the drivers observed during the survey. Of the 611 drivers who used their phone while driving, 426 (69.7%) wore seat belt, while 185 (30.3%) did not wear seat belt. There was no significant relationship between seat belt and phone use.

3.3 Factors Associated with Mobile Phone and Seat Belt Use Among Drivers

Results of the multivariate logistic regression analyzes assessing the association between mobile phone and seat belt use by drivers and explanatory variables are presented in Table 3. Hosmer Lemeshow test indicated that goodness of fit of the model for mobile phone (Chi-square = 7.971, $df = 8$, $p = 0.436$) and seat belt non-compliance (Chi-square = 7.037, $df = 8$, $p = 0.533$) was good.

The odds of male drivers using mobile phones were significant and 34% higher relative to female drivers (Adjusted odds ratio-AOR = 1.338, 95% confidence interval-CI: 1.047–1.709). The variable, age of drivers, was significantly associated with mobile phone use ($p < 0.03$). Drivers aged 18–24 years had a significantly higher odd of using mobile phone compared to drivers aged 60 years and above (AOR = 2.332, 95% CI: 1.189–4.577). Although vehicle type had no statistically significant association with mobile phone use, but the odds of mobile phone use among taxi drivers were two times the odds among pick-up drivers (AOR = 2.085, 95% CI: 0.900–4.828). Number of vehicle occupant was another variable that had significant odds ratio of driver's mobile phone use. Compared to drivers who had other occupants in the vehicle, those who were alone in the vehicle had significantly higher odds of using a mobile phone (AOR = 1.374, 95% CI: 1.143–1.653). Presence of children aged less than eight years in the vehicle was significantly associated with use of mobile phone by drivers. Drivers who had children in their vehicles were two times more likely to use a mobile phone (AOR = 2.266, 95% CI: 1.722–2.982).

As shown in Table 3, the odds of non-use of seat belt by male drivers were 61% higher than females ($p < 0.000$). Although the age group variable had no statistically significant association with seat belt non-compliance, the odds of non-use of seat belt among drivers aged 18–24 years (AOR = 1.072, 95% CI: 0.98–1.924) and 25–29 years (AOR = 1.078, 95% CI: 0.731–1.589) were higher than for those aged 60 years and above. For the variable vehicle type, the odds ratio for non-use of seat belt by taxi drivers was 7.7 times higher than pick-up drivers. Compared with drivers of company vehicles, drivers of commercial (AOR = 7.157, 95% CI: 4.612–11.109) vehicles had significantly higher odds of not wearing a seat belt, while private vehicle drivers had a lower odd (AOR = 0.609, 95% CI: 0.400–0.926). The variables vehicle occupant, presence of child passenger aged less than eight years and time of day had no statistically significant association with driver's non-use of seat belt. However, drivers, who were alone in the vehicle, had a child passenger and those observed in

Table 3 Results of multivariate logistic regression analysis of factors associated with mobile phone and seat belt non-compliance by drivers

Variable	Mobile phone use			Seat belt non-compliance		
	Adjusted odds ratio	p-value	95% CI	Adjusted odds ratio	p-value	95% CI
<i>Gender</i>						
Male	1.338	0.020*	1.047–1.709	1.615	0.000*	1.302–2.002
Female	Ref.	Ref.	Ref.	Ref.	Ref.	Ref.
<i>Age</i>						
18–24	2.332	0.014*	1.189–4.577	1.082	0.791	0.603–1.943
25–59	1.431	0.176	0.851–2.407	1.080	0.705	0.733–1.593
>60	Ref.	Ref.	Ref.	Ref.	Ref.	Ref.
<i>Vehicle type</i>						
SUV	1.318	0.469	0.624–2.784	0.766	0.292	0.466–1.258
Car	1.548	0.243	0.743–3.227	0.997	0.990	0.616–1.614
Taxi	2.085	0.086	0.900–4.828	7.746	0.000*	4.347–13.804
Van	1.148	0.737	0.513–2.570	0.990	0.969	0.593–1.654
Pick-up	Ref.	Ref.	Ref.	Ref.	Ref.	Ref.
<i>Vehicle usage</i>						
Private	0.804	0.483	0.438–1.477	0.608	0.020*	0.400–0.925
Commercial	0.614	0.164	0.308–1.221	7.134	0.000*	4.596–11.073
Government	1.103	0.845	0.413–2.944	1.150	0.681	0.590–2.244
Company	Ref.	Ref.	Ref.	Ref.	Ref.	Ref.
<i>Vehicle occupant</i>						
Single	1.374	0.001*	1.143–1.653	0.983	0.825	0.843–1.145
Multiple	Ref.	Ref.	Ref.	Ref.	Ref.	Ref.
<i>Child passenger less than 8 years</i>						
Yes	2.266	0.000*	1.722–2.982	0.965	0.811	0.722–1.291
No	Ref.	Ref.	Ref.	Ref.	Ref.	Ref.
<i>Time of day</i>						
7–11 am	0.935	0.447	0.786–1.112	1.073	0.360	0.922–1.249
3–6 pm	Ref.	Ref.	Ref.	Ref.	Ref.	Ref.
<i>Phone use</i>						
No				1.111	0.401	0.869–1.420
Yes				Ref.	Ref.	Ref.

CI Confidence interval, *Significant at $p < 0.05$

the morning had lower odd of not wearing a seat belt compared with drivers who had other occupants and had no child passenger and those observed in the afternoon. Although use of seat belt is not significantly associated with phone use, drivers who did use their phone while driving are more likely not to use a seat belt.

4 Discussion

This observational study examined the use of seat belt and mobile phones while driving among drivers in Ibadan metropolis, Nigeria. The factors associated with seat belt non-compliance and mobile phone use by drivers have not been thoroughly studied in Nigeria despite the fact that the country had the highest (39,802) modeled number of road traffic deaths in Africa in 2016, and most of these deaths were due to human factors [1, 5].

In this study, of the 6056 vehicles observed, 68.6% of the drivers wore seat belt. This indicates improvement in seat belt use rates compared with the previous observational studies that reported a rate of 18.7% [32]. The increase in seat belt wearing rates among drivers could be attributed to improved enforcement by FRSC. However, prevalence of seat belt use was lower than the rate reported in South Africa –81% [35].

The results indicated a strong association between use of seat belt and gender. Male drivers were significantly more likely not to wear seat belt while driving compared to female drivers. This is consistent with findings by Shaaban and Abdelwarith [36], Mohammadi [37], Mahfoud et al. [38]. High rate of compliance to seat belt use by women could be related to their low risk-taking behavior. Young drivers accounted for the least of number of drivers observed (2.5%), but most of them (75.3%) used a seat belt compared with drivers aged 25–59 years (68.2%) and >60 years (72.8%). Similar high rate of seat belt use by young drivers was reported by Ojo and Agyemang in Ghana [39]. The use of seat belt by young drivers is particularly important due to their risky driving behavior [40]. There was no significant association between driver's age and seat belt non-compliance in this study. This is similar to the result of the bivariate analysis which showed that there was no significant difference in non-compliance to seat belt use by drivers in the different age groups. This is because both young and old aged drivers did not wear seat belts. Vehicle type and usage were significantly associated with seat belt use.

Non-compliance to seat belt use was highest among taxi drivers. The adjusted OR shows that taxi drivers had high odds of non-use of seat belt compared with drivers of other vehicle types. Similarly, commercial vehicle drivers were significantly more likely not to wear seat belt compared to company vehicle drivers. Further, drivers of private vehicles were significantly less likely not to wear a seat belt. This result corroborates findings by Ojo and Agyemang [39]. Non-use of seat belt by commercial vehicle drivers has been shown to be due to inconvenience associated with frequent stops and poor safety concerns [41]. Another possible reason is that the FRSC officials

enforce the use of seat belt among private vehicle drivers on urban roads while neglecting commercial drivers.

Of the 6056 drivers observed, 10.1% used mobile phone while driving. Phone usage rate is higher than the rate obtained in the previous studies in Ibadan –4.6% [31]. The high prevalence of mobile phone use by drivers could be due to their persistent daily use of phones and inefficient enforcement of the law prohibiting mobile phone use by drivers. It was found that the association between age, number of vehicle occupants, number of child passengers, and mobile phone use by drivers was significant in the bivariate analysis, while gender, vehicle type, vehicle usage, and time of day were not significant. Further, the result of logistic regression analysis indicated that gender was significantly associated with mobile phone use. Male drivers were significantly more likely to use mobile phone while driving compared to female drivers. This result is similar to findings obtained by Cooper et al. [42], Grøndahl and Sagberg [43] but contrary to results obtained by Shaaban and Abdelwarith [36]. The high prevalence of mobile phone use by male drivers is probably due to work-related reasons and frequent phone use in everyday life [44].

This observational survey revealed strong association between driver's age and mobile phone use. In addition, the prevalence of mobile phone use was high among lower age group categories. Drivers aged 18–24 years had significantly higher odds of using mobile phone while driving more than older drivers. This result corroborates the previous findings [36, 42]. Young persons are heavy users of mobile phones in day-to-day life and are likely to use it while driving. Young drivers spend more time talking, texting, downloading games, music, and sending e-mails via a mobile phone [45].

There was no significant association between vehicle type, vehicle usage, and mobile phone use. As shown in Table 2, the proportion of drivers observed using a mobile phone varied between 7.8% for pick-up to 10.6% for car and from 9.8% for commercial vehicles to 10.5% for government vehicles. This suggests that there is no significant difference in mobile phone use among the various types of vehicles observed. This result is similar to those obtained from the previous studies [42].

The number of occupants in the vehicle was significantly associated with the use of mobile phone by drivers. The adjusted odds ratio shows that drivers who were alone in the vehicle were more likely to use a mobile phone compared to those with passengers. Possibly, the presence of passengers in the vehicle discourage driver's use of phone. Drivers with a child aged less than eight in the vehicle had significantly higher odds of using a mobile phone compared with drivers without a child in the vehicle. The use of mobile phone by drivers with child passengers exposes such passengers to great risk when a crash occurs.

5 Conclusion

Using observational approach, this study examined the rate of seat belt and mobile phone use by vehicle drivers in Ibadan metropolitan area, Nigeria. In addition, the

association between these behaviors, vehicle, and driver's socio-demographic characteristics was analyzed using multivariate logistic regression. The results showed that out of 6056 vehicles observed, 10.1% of drivers were observed using a mobile phone while 31.4% did not wear seat belt. These rates are high considering the impact of mobile phone use on road crashes, injuries, drivers' behavior, and performance. Use of mobile phone was significantly associated with age, gender, number of vehicle occupants, and number of children younger than age eight. Seat belt use was significantly related to gender, vehicle type, and usage.

A major contribution of this study is that it has determined the rate and factors associated with seat belt non-compliance and mobile phone use by drivers based on on-road observation. Findings indicate that a high proportion of drivers is distracted through the use of mobile phone while driving and non-compliance to regulations relating to seat belt use is high. One limitation of the study is that the results represent seat belt and phone use at the times and places where observations were conducted. Hence, the results cannot be generalized to the whole country. However, it provides an insight into the use of mobile phone and seat belt by drivers in a developing country with high-road crashes, injuries, and fatalities.

Findings in this study have important policy implications. Given the high rate of mobile phone use and non-compliance to seat belt use, the road safety agencies need to strengthen enforcement of the law relating to seat belt and mobile phone use while driving through the adoption of automated approach. This will ensure that offenders are arrested and penalized adequately. In addition, strategies that will motivate behavior change are necessary. These include educational campaign in schools and commercial vehicles motor parks, advertisement on mass media, stricter enforcement, and installation of road side cameras. Policymakers should increase the fine drivers pay for violating the rules. Vehicle inspection officers should check the availability of seat belts in vehicles before they are registered.

References

1. Federal Road Safety Corps (2017) 2017 Annual report. Abuja, Nigeria
2. World Health Organisation. Mobile phone use: a growing problem of driver distraction. Geneva, Switzerland. http://www.who.int/violence_injury_prevention/publications/road_traec/en/index.html. Last assessed 12 May 2021
3. Carpenter CS, Stehr M (2008) The effects of mandatory seatbelt laws on seatbelt use, motor vehicle fatalities, and crash-related injuries among youths. *J Health Econ* 27(3):642–662
4. Abbas AK, Hefny AF, Abu-Zidan FM (2011) Seatbelts and road traffic collision injuries. *World J Emergency Surgery* 6:18
5. World Health Organization (2018) Global status report on road safety 2018. Geneva, Licence: CC BYNC-SA 3.0 IGO
6. Hoye A (2016) How would increasing seat belt use affect the number of killed or seriously injured light vehicle occupants? *Accid Anal Prev* 88:175–186
7. Febres JD, García-herrero S, Herrera S, Gutiérrez JM, Mariscal M (2020) A: Influence of seat-belt use on the severity of injury in traffic accidents. *Eur Transp Res Rev* 12:9
8. Lee JD (2005) Driving safety. *Rev Hum Factors Ergon*

9. Lee JD, Young KL, Regan MA (2008) Defining driver distraction. In Regan MA, Lee JD, Young K (eds) *Driver distraction: theory, effect, and mitigation*. CRC Press, Boca Raton, pp 31–40
10. Stutts JC, Reinfurt DW, Staplin L, Rodgman EA. The role of driver distraction in traffic crashes. www.aaafoundation.org Assessed last on 23 Mar 2021
11. Shi J, Xiao Y, Atchley P (2016) Analysis of factors affecting drivers' choice to engage with a mobile phone while driving in Beijing. *Transp Res Part F* 37:1–9
12. Redelmeier DA, Tibshirani RJ (1997) Association between cellular-telephone calls and motor vehicle collisions. *New England J Med* 336(7):453–458
13. Violanti JM (1999) Cellular phones and fatal traffic collisions. *Accid Anal Prev* 30(4):519–524
14. Violanti JM, Marshall JR (1996) Cellular phones and traffic accidents: an epidemiological approach. *Accid Anal Prev* 28(2):265–270
15. Drews FA, Yazdani H, Godfrey CN, Cooper JM, Strayer DL (2009) Text messaging during simulated driving. *J Hum Factors Ergon Soc* 51(5):762–770
16. Olson R, Hanowski R, Hickman J, Bocanegra J (2009) *Driver distraction in commercial vehicle operations (Report No. FMCSA-RRR-09-042)*. Federal Motor Carrier Safety Administration, Washington, DC
17. Charlton SG (2009) Driving while conversing: cell phones that distract and passengers who react. *Accid Anal Prev* 41:160–173
18. Törnros J, Bolling A (2006) Mobile phone use-effects of conversation on mental workload and driving speed in rural and urban environments. *Transp Res Part F* 9:298–306
19. Spyropoulou I, Linardou M (2019) Modelling the effect of mobile phone use on driving behaviour considering different use modes. *J Adv Transp* 26:1–10
20. Alm H, Nilsson L (1994) Changes in driver behaviour as a function of hands-free mobile phones—A simulator study. *Accid Anal Prev* 26(4):441–451
21. Crisler MC, Brooks JO, Ogle JH, Guirl CD, Alluri P, Dixon KK (2008) Effect of wireless communication and entertainment devices on simulated driving performance. *Transp Res Rec* 2069:48–54
22. Hancock PA, Lesch M, Simmons L (2003) The distraction effects of phone use during a crucial driving maneuver. *Accid Anal Prev* 35:501–514
23. Nunes L, Recarte MA (2002) Cognitive demands of hands-free-phone conversation while driving. *Transp Res Part F* 5:133–144
24. Caird JK, Willness CR, Steel P, Scialfa C (2008) A meta-analysis of cell phone use on driver performance. *Accid Anal Prev* 40:1282–1293
25. Federal Road Safety Corps (2010) 2010 Annual report. Abuja, Nigeria
26. Peltzer K, Pengpid S (2016) Seatbelt use among university students from 26 low-, middle- and high-income. *Afr Saf Promot J* 14(1):26–41
27. Woldegebriel MK, Aregawi BG, Gebru HT (2019) Assessment of seat belt use and its associated factors among public transport drivers in North Gondar, Ethiopia: a cross-sectional study. *BMC Research Notes*, pp 1–6
28. Donkor I, Gyedu A, Edusei AK, Ebel BE, Donkor P (2018) Mobile phone use among commercial drivers in Ghana : an important threat to road safety. *Ghana Med J* 52(3):122–126
29. Akande TM, Ajao MS (2006) Awareness of hazards and use of GSM mobile phone among non-commercial drivers in Ilorin, Nigeria. *Ann Afr Med* 5(4):166–169
30. Olubiyi SK, Jibril UN, Hauwa UG, Balarabe F (2016) Relationship between use of mobile phone and road traffic accident amongst motorists in Zaria. *Res J Health Sci* 4(4):285–295
31. Olumami HO, Ojo TK (2014) Rate of mobile phone usage by automobile drivers in Ibadan Metropolis, Nigeria. *Eur J Bus Manage* 6(31)
32. Sangowawa AO, Alagh BT, Ekanem SEU, Ebong IP, Faseru B, Adekunle BJ, Uchendu OC (2010) An observational study of seatbelt uses among vehicle occupants in Nigeria. *Inj Prev* 16:85–89
33. Popoola SO, Oluwadiya KS1., Kortor JN, Denen-Akaa P, Onyemaechi NOC (2013) Compliance with seat belt use in Makurdi, Nigeria: an observational study. *Ann Med Health Sci Res* 3(3):427–432

34. Grimm P (2010) Social desirability bias in Wiley International Encyclopedia of Marketing
35. Olukoga A, Noah M (2005) The use of seat belt by motor vehicle occupants in South Africa. *Traffic Inj Prev* 6(4):398–400
36. Shaaban K, Abdelwarith K (2018) Understanding the association between cell phone use while driving and seat belt noncompliance in Qatar using logit models. *J Transp Safety Secur.* <https://doi.org/10.1080/19439962.2018.1477895>
37. Mohammadi G (2009) Mobile phone and seat belt usage and its impact on road accident fatalities and injuries in southeast Iran. *Int J Crashworth* 14(4):309–314
38. Mahfoud ZR, Cheema S, Alrouh H, Al-thani MH, Al-thani AAM, Mamtani R (2015) Seat belt and mobile phone use among vehicle drivers in the city of Doha, Qatar: an observational study. *BMC Public Health* 15(937):1–6
39. Ojo TK, Agyemang W (2018) Occupants' seatbelt use are related to vehicle type and usage on a Ghanaian university campus. *Int J Inj Contr Saf Promot* 26(2):1–6
40. Fergusson DM, Swain-Campbell NR, Horwood LJ (2003) Risky driving behaviour in young people: prevalence, personal characteristics and traffic accidents. *Aust N Z J Public Health* 27(3):337–342
41. Kim K, Yamashita EY (2007) Attitudes of commercial motor vehicle drivers towards safety belts. *Accid Anal Prev* 39(6):1097–1106. <https://doi.org/10.1016/j.aap.2007.02.007>
42. Cooper JF, Ragland DR, Ewald K, Wasserman L, Murphy CJ (2013) Observational study of use of cell phone and texting among drivers in California comparison of data from 2011 and 2012. *Transp Res Rec* 2365:66–72
43. Grøndahl AB, Sagberg F (2011) Driving and telephoning: Relative accident risk when using hand-held and hands-free mobile phones. *Saf Sci* 49:324–330
44. Brusque C, Alauzet A (2008) Analysis of the individual factors affecting mobile phone use while driving in France: socio-demographic characteristics, car and phone use in professional and private contexts. *Accid Anal Prev* 40:35–44
45. Dragutinovic N, Twisk D (2005) Use of mobile phones while driving – effects on road safety (Report No. R-2005–12). SWOV Institute for Road Safety Research, Leidschendam, The Netherlands

Determinants of Ride-Hailing Applications Adoption: How Travelers' Characteristics and Attitudes Affect the Adoption of New Online Mobility Platforms in Bangkok?



Wattana Laosinwattana, Phathinan Thaitatkul, and Saksith Chalermpong

Abstract As Bangkok expanded and urbanized over the past decades, the population and travel demand have increased rapidly. Urban mobility such as ride-hailing applications (RHAs) has become a popular alternative travel mode in Bangkok. Knowledge of these services, therefore, becomes more important for a sustainable development of an urban mobility system. In this paper, the factors affecting the adoption of ride-hailing services were investigated by observing the use of RHAs through the questionnaire survey in Bangkok. Binary logistic regression was used to analyze the influence of socio-demographic variables, socioeconomic variables, and attitudes toward RHAs adoption. This study revealed that RHAs users are young adults, have high income, and are using a smartphone for a long time. RHAs were mostly used for personal business and meeting friends. This study also showed that RHAs users are the same pool of demand for taxis. In other words, RHAs were likely to substitute taxis. Therefore, RHAs regulations are required in order to keep the fair competition between RHAs and taxis.

Keywords Ride-hailing applications · Ride-sourcing services · Urban mobility · Individual mobility

1 Introduction

The rapidly advancing digital technology has become more influential in people's lives. It has improved the quality of life, helped managing the environmental

W. Laosinwattana · S. Chalermpong (✉)
Department of Civil Engineering, Chulalongkorn University, Bangkok, Thailand
e-mail: Saksith.C@chula.ac.th

W. Laosinwattana
e-mail: 6170268121@student.chula.ac.th

P. Thaitatkul · S. Chalermpong
Transportation Institute, Chulalongkorn University, Bangkok, Thailand
e-mail: Phathinan.T@chula.ac.th

resources, and responded to infinite human needs. Technology has become a part of many activities in people's lives, such as communication, marketing, entertainment, and daily travel. However, the use of technology requires knowledge and experience. Otherwise, it may lead to harmful results rather than being beneficial to the society.

In transportation, ride-hailing applications (RHAs) platform is one of the technology-enabled platforms which enhances the effectiveness of ride-hailing and vehicle-dispatching processes. This platform can therefore promptly serve previously unmet demand in urban areas [1] with a higher utilization rate than conventional taxi service operated without RHAs platform [2], especially in terms of driver-passenger matching, percentage of miles driven with a passenger, and fare calculation. However, the use of RHAs has been debated in many cities around the world on various issues including regulations, safety and security, impacts on travel behavior, and preferable role of RHAs in sustainable mobility system [3]. In Thailand, even though RHAs services in the form of car-based and motorcycle-based are available, ride-hailing services have been waiting for a legal status which is still under consideration [4]. Even though the regulations of RHAs have been discussed, there was no discussion in terms of transport and urban planning. Therefore, the knowledge of RHAs becomes a necessity to solve the conflict of benefits of stakeholder and be important for transportation planning to achieve sustainable society in the future.

The objective of this study is to investigate the characteristics of travelers who use RHAs to hail a car (car-based RHAs users). Binary logistic regression model is used to analyze the impacts of socio-demographic variables, socioeconomic variables, and attitudes on car-based RHAs adoption.

2 Literature Review

2.1 *Ride-Hailing Applications*

RHA is a platform to allow passengers and drivers to connect to each other. Firstly, this service is commonly referred to as 'ridesharing' or 'peer-to-peer mobility' services. Many experts initially argued that a label of ridesharing for this service was a misnomer because drivers and passengers did not share the same destination, but rather, the drivers provided services analogous to limousines or taxis for a fee [5]. RHAs can provide a ridesharing service by matching at least two passengers who have similar travel itineraries to share the same ride. In 2009, RHA was first launched by Garrett Camp, known as 'UberCab' [6]. Initially, Uber only provided an on-demand limousine service. It later involved professional taxi drivers and non-professional drivers with their private vehicles to provide a taxi-like service on its platform. In the present, RHA has become a popular platform in many countries around the world and has many service providers in each country, such as Uber and Lyft in United States of America, DiDi in China, and Grab and Gojek in Southeast Asia.

Regarding the impact of an emergence of RHAs, RHAs can affect both positively and negatively the overall transportation system. For example, motorcycle-based RHAs acted as a complement to the public transport network in Jakarta as it provided a first/last mile service [7]. The positive effect of congestion reduction in the long term can also be expected as some groups of travelers are more likely to stop using their personal cars or replacing their own cars by RHAs [1, 5, 8]. Nevertheless, according to some studies, some groups of travelers decide to use RHAs instead public transportation [9, 10]. This may induce more cars and result in more traffic congestion. The reduction of public transportation users can diminish the transportation system's efficiency.

2.2 Ride-Hailing Applications in Thailand

In 2011, the first RHA launched in Thailand was 'Easy Taxi', a RHA operated by a Brazilian company. In the same year, Grab has entered the ride-hailing application market in Thailand. Both Easy Taxi and Grab by that time only allowed professional taxi drivers to provide taxi-like services on their platforms. In the following year, Grab expanded its service by also allowing non-professional drivers to provide the service by using their own personal vehicles, so-called GrabCar. This service has significantly induced more supply (i.e., drivers) and demand (i.e., passengers). In 2016, Easy Taxi was officially retired from Thailand's RHAs market. However, many RHAs service providers (e.g., Uber, GET (or Gojek), LINE TAXI, Bolt) have successively come to compete in the RHAs market with the extended services. In the present, there are four main RHA providers: Grab, Gojek, LINE TAXI, and Bolt. Grab provides the most extended services including car based and motorcycle based driven by both professional and non-professional drivers RHA services, food and parcel delivery services, and other personal assistance services. Gojek provides RHA service for hailing only professional motorcycle driver and food and parcel delivery. LINE TAXI provides a taxi-based RHA service together with food and parcel delivery services and other personal assistance services. Bolt is the only RHA that does not provide other services, but only car-based and motorcycle-based RHA.

To date, ride-hailing services are still not legally permitted in Thailand [4]. Since, there are also claims of competitive inequality among transport operators in the public transportation service market, such as incumbent taxi drivers, motorcycle taxi drivers, non-professional private car/motorcycle drivers and other public transport operators [11].

2.3 Socio-Demographic Characteristics of RHAs User

Travel mode choices often vary with socio-demographic characteristics. The findings from studies in Western countries indicated that RHAs users tended to be younger,

well-educated, and live-in urban area [1, 5, 8–10]. However, the study from China found that RHAs users were low-educated individuals [12]. Similarly, Indonesian high-educated individuals were less likely to use motorcycle-based RHAs for travel [7]. This means that socioeconomic of RHAs users may differ over the country. In addition, Rayle's study [1] found that gender also affected the adoption of RHAs, where male individuals were more likely to adopt RHAs than female individuals. Hence, based on the same logic, the following hypotheses are proposed:

- H1: Males are more likely to use car-based RHAs than females.
- H2: Car-based RHAs users are the younger individuals.
- H3: Car-based RHAs users are the individuals with high educated.

The attitudes toward environment and technology savviness also influenced the RHAs adoption, where environmental concern and smartphone-savvy individuals were more likely to adopt RHAs than another group [8, 13]. Based on the same logic, in this study, it is hypothesized that:

- H4: Environmental concern is positively associated with car-based RHAs adoption.
- H5: Smartphone savviness is positively associated with car-based RHAs adoption.

In terms of socioeconomic characteristics, previous studies found that individuals who lived in the urban area were more likely to use RHAs than individuals who lived in the suburb [5, 13] and RHAs users tended to be the high-income individuals [1, 5, 8–10]. The effect of number of vehicles in household on RHAs adoption could not yet be concluded. Rayle et al. (2014), found that the number of vehicles in the household has a negative effect on RHAs adoption in San Francisco [1]. On the other hand, there was no statistical evidence that the number of vehicles in household affected the RHAs adoption in other states of USA nor other countries [5, 10]. Moreover, general travel behavior also found to affect the RHAs adoption. A report surveying over 3000 adults in California found that RHAs users tended to be the high frequent taxi users [8] and those who frequently traveled by airplane [8, 13]. Based on these arguments, the following hypotheses are proposed:

- H6: Car-based RHAs users are individuals with high income.
- H7: The number of cars in household is negatively related to car-based RHAs adoption.
- H8: Taxis usage is positively associated with car-based RHAs adoption.

3 Methodology

3.1 Study Area

The study area of this study is Bangkok, a capital of Thailand. Bangkok has 1600 km² of total land areas with 5.59 million registered population [14]. Bangkok consists of both urban and suburban areas. Many public transportation systems are provided such

as urban rail systems, public buses, public vans, ferries, taxis, motorcycle taxis, and converted pickup truck (Songthaew). However, they are not integrated, not covered, and insufficient capacity for existing travel demand. Since 2013, many of RHAs companies have come to compete in the on-demand transport service market such as Grab, LINEMAN, Gojek, Muvmi, and Bolt. Even though RHAs have not been legalized, these services have attracted substantial travelers resulting in large RHAs and taxis market size at US\$1654 million in 2020 [15]. Although RHAs are more expensive than taxis in Bangkok, door-to-door trips using RHAs are cheaper than multimodal trips as the fare systems of existing public transport systems are not yet integrated. This argument makes Bangkok an interesting area to study ride-hailing services.

3.2 Data Collection

Data was collected from a sample of individuals aged between 18 and 75 years old and resided in Bangkok area since July 2019 or before. A quota sampling approach was used to represent the actual age distribution of population in Bangkok. The sample sizes by age group were determined according to the population statistics provided by The Bureau of Registration Administration [14]. The participants were recruited by offline and online channels during September–December 2020 in Bangkok. For the former, the participants were recruited by intercepting travelers on the street in the areas with high traffic density such as shopping areas, train stations, and parks. The data was collected either by on-site interview or online survey which participants can response to a questionnaire later. For the latter, the online questionnaire link was distributed via social networking system. As a result, there were 483 complete responses from a total of 491 responses.

The questionnaire contains four sections: (1) socio-demographic information: general information of responder, (2) general travel mode and RHAs usage: the frequency of each travel mode usage in December 2019 to February 2020 and car-based RHAs usage experience, (3) smartphone usage and technology savviness: the frequency of application on smartphone usage and the number of years of smartphone usage, and (4) attitudes toward environment and car ownership: attitudinal statements on a five-point Likert-type scale from ‘Strongly disagree’ to ‘Strongly agree’.

3.3 Data Analysis

A binary logistic regression model was employed to examine the effects of socio-demographics factors and personal attitudes on the adoption of ride-hailing services. In this study, the model can be formulated as follows:

$$\text{logit}(P) = \ln[P(y = 1)/(1 - P(y = 1))] = \beta_0 + X\beta + Z\alpha, \quad (1)$$

where y is a binary variable representing an adoption (i.e., 1 if a respondent has (already) used car-based RHAs, and 0 otherwise), P represents the probability of the occurrence of car-based RHAs adoption, X is a vector of socio-demographic and socioeconomic variables, β is a vector of coefficients corresponding to X , Z is a vector of latent variables (i.e., attitudes and smartphone savviness) that obtained from exploratory factor analysis, and α is a vector of coefficients corresponding to Z .

An exploratory factor analysis (EFA) was used to reduce the number of technology savviness and attitude variables. The number of extracted factors is determined by eigenvalue (more than 1.00) [16]. The measurement items must have factor loading higher than 0.40 [17] and KMO value higher than 0.60 [18]. Binary logistic regression and EFA analyses were performed by using the ‘glm’ function and ‘psych’ packages in *R*, respectively.

4 Results and Analysis

4.1 Descriptive Statistics

Table 1 provides descriptive statistics of socio-demographic characteristics. There were 483 complete responses. The samples had a very similar proportion of male and female, which was close to gender distribution of Bangkok population: 2.56 million of male population (0.47%) and 2.90 million of female population (0.53%). Most of the respondents were younger adult (54.45% of respondents aged between 18 and 39 years old) and were relatively well educated (61.70% of respondents were bachelor’s or higher degree holders). Most respondents had an average monthly income between THB15001 and THB30000¹ (47.20%) which were a middle-income group of people in Bangkok and following by low-income group (41.61%).

In this dataset, 178 respondents (36.85%) have used application for hailing a car. This group of people is called ‘RHAs users’ onwards. Most of the users were young adult (18–39 years old), well-educated, and middle-income individuals as shown in Figs. 2, 3, and 4, respectively. RHAs users were not found in the elder group (60–75 years old) nor graduated primary school or below. Moreover, users were not different between male and female (Fig. 1).

Table 2 shows the descriptive statistics of respondent’s travel behaviors. Half of respondents were non-personal car users (50.72%). More than half of respondents used mass transit at least once a month, e.g., bus (60.04%) and rail (69.56%). Almost all respondents have never traveled by van or minibus (79.09%) nor airplane (77.22%), while 70% of the samples used a taxi at least once a month.

¹ The official currency of Thailand (THB 1 = USD 0.032 as of May 27, 2021).

Table 1 Key demographic characteristics of respondents ($N = 483$)

		<i>N</i>	%
Respondents		483	100
Gender	Male	243	50.31
	Female	240	49.69
Age	18–29	104	21.53
	30–39	159	32.92
	40–49	73	15.11
	50–59	61	12.63
	60–75	86	17.81
Education level	None educated	6	1.24
	Primary school	60	12.42
	High school	79	16.36
	Vocational school or associate degree	40	8.28
	Bachelor’s degree	263	54.45
	Master’s degree or higher	35	7.25
Average monthly income	Less than THB15001	201	41.61
	THB15001–THB30000	228	47.20
	More than THB30000	54	11.18

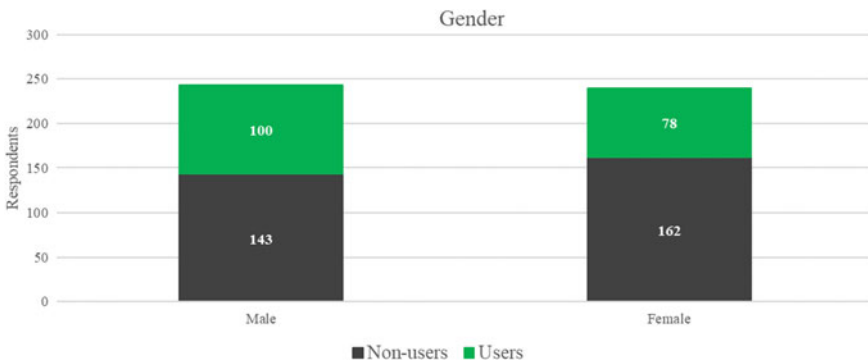


Fig. 1 Adoption of use of car-based RHAs by gender cohort ($N = 483$)

4.2 Exploratory Factor Analysis

EFA was used to define the structure of the potential underlying the following variables: technology savviness (five levels of smartphone’s applications usage frequency) and the attitudes toward environment and car ownership (five-point Likert scale) and to reduce the number of these variables to a manageable size.

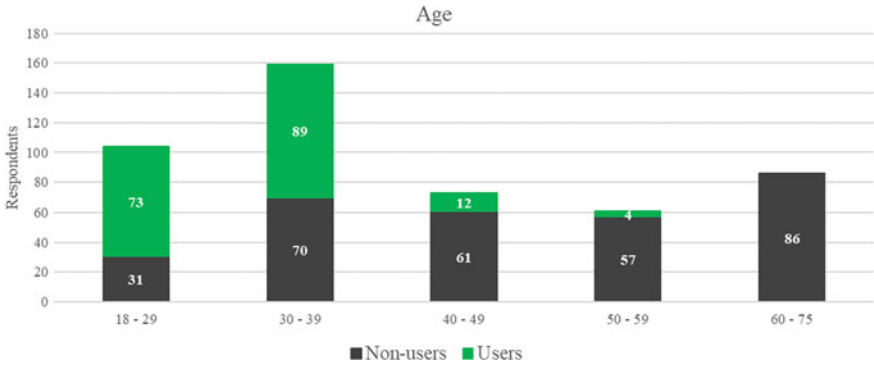


Fig. 2 Adoption of use of car-based RHAs by age cohort ($N = 483$)

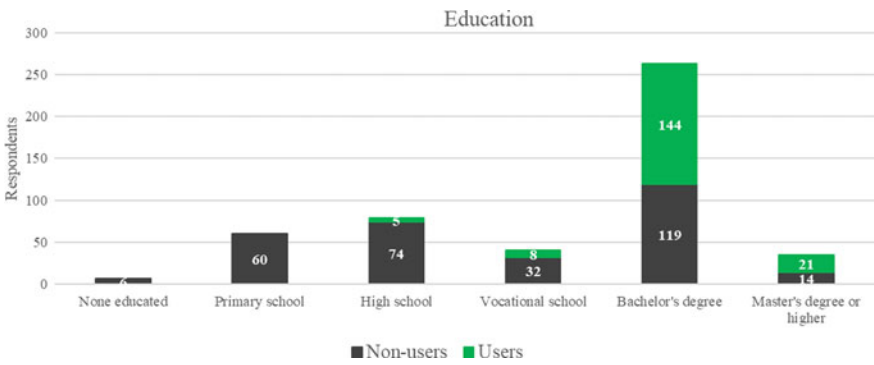


Fig. 3 Adoption of use of car-based RHAs by education cohort ($N = 483$)

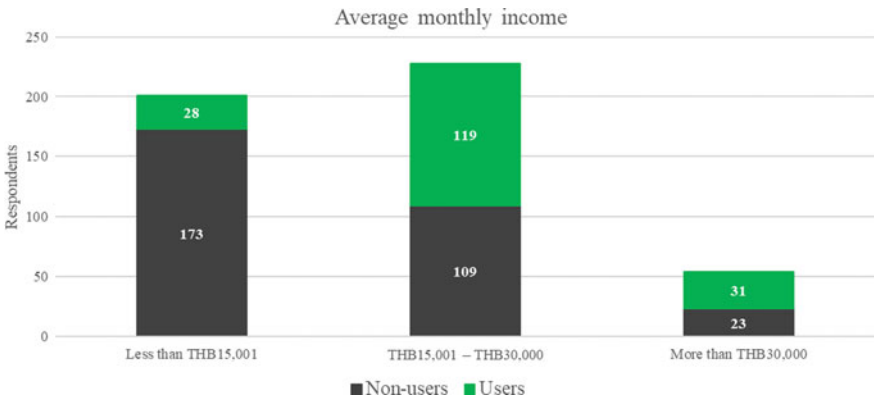


Fig. 4 Adoption of use of car-based RHAs by the average monthly income cohort ($N = 483$)

Table 2 Travel mode and usage frequency of respondents (*N* = 483)

Number of respondent (%)	Travel Frequency (time/month)				
	Mode	Never	<1	1–3	4–12
Personal car	245 (50.72%)	16 (3.31%)	52 (10.77%)	40 (8.28%)	130 (26.92%)
Personal motorcycle	174 (36.02%)	67 (13.87%)	65 (13.46%)	54 (11.18%)	123 (25.47%)
Bus	193 (39.96%)	170 (35.20%)	64 (13.25%)	28 (5.80%)	28 (5.80%)
Rail	147 (30.43%)	128 (26.50%)	89 (18.43%)	30 (6.21%)	89 (18.43%)
Van and Minibus	382 (79.09%)	62 (12.84%)	24 (4.97%)	12 (2.48%)	3 (0.62%)
Taxi	142 (29.40%)	210 (43.48%)	106 (21.95%)	19 (3.93%)	6 (1.24%)
Airplane	373 (77.23%)	103 (21.33%)	7 (1.45%)	0 (0.00%)	0 (0.00%)

From the original eighteen measurement items, there were six excluded items consisted of three items regarding attitudes toward the environmental responsibility: “You think the problem of pollution on the road. It is something that should not be overlooked”, “You think you should help reduce road pollution”, “Do you think that reducing pollution on the road have to start with yourself” and three items regarding attitudes toward car ownership: “Cars allow one to distinguish oneself from others”, “Cars allow one to be independent”, and “You feel good when you have your own car”.

The results of EFA based on twelve remaining measurement items are shown given in Table 3. The Oblimin rotation method was chosen for EFA procedure as these variables might be correlated with each other [16]. Three factors were extracted with eigenvalues > 1 [16], which could explain 75.57% of the total variance. These three factors were labeled as follows: travel application usage (five items), general application usage (four items), and attitudes toward environment (three items). The overall KMO value of 0.83 showed that the sample size was adequate for factor analysis, and Bartlett’s test ($\chi^2 = 6907.13, p < 0.00$) was significant. The factor loadings of twelve measurement items were higher than 0.4. Therefore, all the items were retained. The Cronbach’s alpha values ranged from 0.90 to 0.95, indicating the high reliability of all five extracted factors.

4.3 Binary Logistic Regression

Table 4 presents the factors effecting the car-based RHAs adoption analyzed by binary logistic regression. The dependent variable is binary, where a value of 1 denotes an

Table 3 Results of exploratory factor analysis

	Exploratory factor analysis (<i>N</i> = 483)			
	Factor loadings	Eigen-values	Explained variance	Cronbach's alpha
<i>Travel application usage</i>		5.70	43.30	0.95
E-Commerce	0.54			
GPS navigation	0.91			
Route finding	0.94			
Place finding	0.86			
Traffic planning	0.85			
<i>General application usage</i>		1.61	18.61	0.92
Communication	1.00			
Entertainment	1.00			
Utility applications	0.76			
E-banking	0.62			
<i>Attitudes toward environment</i>		1.18	13.66	0.90
More cars on the road causing more pollution to the environment	0.90			
More cars on the road causing more resource usage	0.92			
Road pollution adversely affect your lifestyle	0.79			
	KMO = 0.83, $\chi^2 = 6907.13, p < 0.00$			
	Total variance explained = 75.57%			

Note KMO Kaiser–Meyer–Olkin
 χ^2 Barlett's test of sphericity

individual who has ever used application to hail a car and 0 otherwise. The results showed that a negatively intercept value (−9.82) represents the unobserved variables that have a negative effect on car-based RHAs adoption. Socio-demographic variables significantly impacted the RHAs adoption. Young adult better educated individuals (bachelor's degree or higher) and individuals who had the middle–high monthly income were more likely to adopt RHAs than elder, lower educated individuals and individuals who had low income. This could imply that elders and low-educated individuals could not access to this service, while low-income people could not afford RHAs. These results are consistent with the findings from previous studies [1, 5, 8–10], which means that H2, H3, and H6 are supported. However, an evidence to

support H1 could not be found as the effect of gender variable was not significant. This result is contrast with Rayle's study [1], which found that men were more likely to adopt this service than women. The number of cars in household had negative effect on the car-based RHAs adoption, which means that individuals who owned a greater number of cars in household were less likely to use RHAs, consistent with the findings of the effect of vehicle ownership in previous studies [1], then H7 are accepted. Moreover, this study also found individuals who were merchants or had their own businesses were more likely to use RHAs than civil servants or private company employees. This result could suggest that car-based RHAs were less likely to be used for routine travel.

A location of residence was found to influence the adoption of RHAs. Individuals who lived near bus stop (less than 500 m) were less likely to use RHAs than individuals who lived farther than 1 km away from bus stop. In contrast, individuals who lived near taxi stand (less than 500 m) were more likely to adopt RHAs. This could imply that RHAs are not a substitution of the bus, but conventional taxi. However, the effects of distance from residence to rail station and types of residence could not be found for car-based RHAs adoption.

This analysis also showed the impact of the use of other transportation mode on the adoption of car-based RHAs. Personal car and personal motorcycle users were more likely to adopt RHAs than those who never used these modes. The higher the frequency of taxi use, the more likely to adopt car-based RHAs, consistent with the findings in Alemi's study that frequent taxi users were more likely to use Uber and Lyft [13], indicating the acceptance of H8. This again indicates that RHAs substitute the conventional street-hailing taxis. Additionally, individuals who often used rail (more than 4 time/month) and individuals who had traveled by airplane were more likely to adopt car-based RHAs, consistent with the result of previous study [13]. The frequency of bus usage has a negative effect on car-based RHAs adoption. This could be because most of the frequent bus users were low-income people who could not afford usage of RHAs and people who lived near the bus stop were less likely to use this service as mentioned earlier.

Regarding the smartphone savviness, the rate of adoption of RHAs was significantly higher among individuals with a higher number of years of smartphone usage. Although we could not find the main effects of general applications usage and travel-related applications usage, we found their interaction affect where individuals who frequently used both general and travel-related application were likely to adopt RHAs. These results are consistent with Alemi et al. [13] which found that the individuals who were familiar with transportation-related applications (e.g., navigation, maps, and traffic checker) were more likely to adopt this service, H5 is supported. However, in this study, there was no significant effect of the attitudes toward environment on RHAs adoption (rejected H4).

Table 4 Results of binary logistic regression

Variables	Estimates (<i>p</i> -values)	OR
Intercept	-9.82 (0.00)***	
Socio-demographic variables and socioeconomic variables		
Gender [Reference = Male]		
Female	0.38 (0.51)	1.46
Age	-0.22 (0.00)****	0.80
Education level [Reference = Bachelor's degree or higher]		
Vocational school or associate degree	-2.24 (0.02)**	0.11
High school or lower	-6.51 (0.00)****	0.00
Average monthly income [Reference = Less than THB15001]		
THB15001-THB30000	1.78 (0.09)*	5.94
More than THB30000	4.03 (0.00)***	56.37
Occupation [Reference = Civil servant and Private company employee]		
Student	1.54 (0.26)	4.65
Employee or freelance	0.39 (0.49)	1.48
Personal business or merchant	2.66 (0.02)**	14.36
Unemployed	2.53 (0.20)	12.53
Retirement	1.55 (0.53)	4.71
Household characteristics		
The number of household member	0.59 (0.06)*	1.80
The number of cars in household	-0.99 (0.02)**	0.37
Residence [Reference = Detached house]		
Townhouse	-1.24 (0.18)	0.29
Commercial buildings	1.23 (0.29)	3.43
Apartment or condominium	1.36 (0.14)	3.89
Distance from residence to		
Rail station [Reference = Less than 0.5 km]		
0.5-1 km	-1.22 (0.48)	0.29
1-2 km	-1.62 (0.37)	0.20
2-5 km	-1.37 (0.45)	0.25
More than 5 km	0.41 (0.82)	1.51
Bus stop [Reference = Less than 0.5 km]		
0.5-1 km	1.26 (0.32)	3.53
1-2 km	5.18 (0.00)****	177.53
2-5 km	3.92 (0.01)**	50.56
More than 5 km	3.79 (0.10)	44.14
Taxi stand [Reference = Less than 0.5 km]		

(continued)

Table 4 (continued)

Variables	Estimates (<i>p</i> -values)	OR
0.5–1 km	–4.18 (0.00)****	0.02
1–2 km	–6.04 (0.00)****	0.00
2–5 km	–6.18 (0.00)****	0.00
More than 5 km	–13.18 (0.99)	0.00
<i>Frequency of use of the transport</i>		
<i>Personal car [Reference = Never]</i>		
Less than 1 time/month	–0.97 (0.40)	0.38
1–3 time/month	4.05 (0.01)**	57.66
4–12 time/month	–1.36 (0.35)	0.26
More than 12 time/month	0.97 (0.37)	2.63
<i>Personal motorcycle [Reference = Never]</i>		
Less than 1 time/month	3.65 (0.00)***	38.38
1–3 time/month	2.27 (0.04)**	9.73
4–12 time/month	2.04 (0.16)	7.70
More than 12 time/month	3.94 (0.00)****	51.19
<i>Bus [Reference = Never]</i>		
Less than 1 time/month	–0.7 (0.32)	0.50
1–3 time/month	–2.12 (0.03)**	0.12
4–12 time/month	–2.47 (0.07)*	0.08
More than 12 time/month	–1.36 (0.39)	0.26
<i>Rail [Reference = Never]</i>		
Less than 1 time/month	0.38 (0.76)	1.46
1–3 time/month	–0.5 (0.70)	0.61
4–12 time/month	4.64 (0.01)***	104.00
More than 12 time/month	3.69 (0.02)**	40.13
<i>Van and Minibus [Reference = Never]</i>		
Less than 1 time/month	–0.96 (0.25)	0.38
1–3 time/month	–1.37 (0.41)	0.25
4–12 time/month	–2.53 (0.15)	0.08
More than 12 time/month	2.91 (0.95)	18.42
<i>Taxi [Reference = Never]</i>		
Less than 1 time/month	3.09 (0.00)***	21.91
1–3 time/month	4.55 (0.00)****	94.73
4–12 time/month	6.66 (0.00)****	777.74
More than 12 time/month	3.52 (0.14)	33.92
<i>Airplane [Reference = Never]</i>		

(continued)

Table 4 (continued)

Variables	Estimates (<i>p</i> -values)	OR
Less than 1 time/month	1.53 (0.04)**	4.60
1–3 time/month	−0.6 (0.73)	0.55
<i>Technology savviness and individual attitudes</i>		
<i>The number of years of smartphone usage</i>	0.99 (0.00)****	2.69
<i>Smartphone savviness and Attitudes (Factor Scores)</i>		
General applications usage	−2.36 (0.02)**	0.09
Travel-related applications usage	−0.89 (0.14)	0.41
Attitudes toward environment	−0.24 (0.33)	0.79
General applications usage: travel-related applications usage	2.17 (0.01)**	8.79
Model log-likelihood	−86.08 (<i>df</i> = 60)	
McFadden's pseudo- <i>R</i> ²	0.54	

Note *p*-values **** = 0.001, *** = 0.01, ** = 0.05, * = 0.10

5 Conclusions

In this study, descriptive and binary logistic regression analyses have been performed to investigate factors affecting the adoption of car-based ride-hailing applications (RHAs) in Bangkok, Thailand. This study found that socio-demographic variables are good predictors of the adoption of car-based RHAs. The young, well-educated, and middle–high-income individuals were more likely to adopt car-based RHAs. The results also show that smartphone savviness positively affected the RHAs adoption. These findings suggested the inequality in accessing the RHAs services, especially for low-income and elderly people. The location of residence also affected the RHAs adoption. Individuals who lived near the bus stop were less likely to adopt RHAs, while individuals who lived near the taxi stands were more likely to use RHAs. Moreover, this study also found that frequent taxi and rail users were more likely to adopt car-based RHAs. This indicates the substitution of RHAs for conventional street-hailing taxis. However, it is unclear whether RHAs complement public transport system.

The results of inaccessibility of elderly, low educational attainment, and low-income individuals to this service suggested the need of appropriate regulations and transport policies on RHAs to provide thoroughly inclusive mobility services. In particular, this service should be designed to be a service that increases the quality of life for people, such as increasing travel options for the elders who are currently experiencing travel-related problems.

Moreover, the analysis in this study was limited to only car-based RHAs adoption. The study can be extended to incorporate the motorcycle-based RHAs, another popular travel choice in Bangkok, into the analysis. In addition, this study suggested

that the future study on the RHAs usage behavior is required for determining the present role of RHAs in Bangkok, which will be useful for transportation planning.


Acknowledgements This study is financially supported by Graduate School Thesis Grant, Chulalongkorn University.

References

1. Rayle L et al (2014) App-based, on-demand ride services: comparing taxi and ridesourcing trips and user characteristics in San Francisco. *Citeseer*
2. Cramer J, Krueger AB (2016) Disruptive change in the taxi business: the case of Uber. *Am Econ Rev* 106(5):177–182
3. Craggs R (2017) Where Uber is banned around the world. *Conde Nast Traveler*, Apr 2017, vol 20, p 2017
4. Suthikoen K et al (2019) The role of supporting the Thai economy and the necessity of developing legal regulations to meet sustainable development in Ride-hailing service industry
5. Clewlow RR, Mishra GS (2017) Disruptive transportation: the adoption, utilization, and impacts of ride-hailing in the United States
6. Movmi (2018) The ridehailing trend: past, present, and future overview of ridehailing
7. Irawan MZ et al (2019) To compete or not compete: exploring the relationships between motorcycle-based ride-sourcing, motorcycle taxis, and public transport in the Jakarta metropolitan area. *Transportation* 1–23
8. Alemi F et al (2018) What influences travelers to use Uber? Exploring the factors affecting the adoption of on-demand ride services in California. *Travel Behav Soc* 13:88–104
9. Henao A, Marshall WE (2019) The impact of ride-hailing on vehicle miles traveled. *Transportation* 46(6):2173–2194
10. Tirachini A, del Río M (2019) Ride-hailing in Santiago de Chile: users' characterisation and effects on travel behaviour. *Transp Policy* 82:46–57
11. Phun VK, Kato H, Chalermpong S (2019) Paratransit as a connective mode for mass transit systems in Asian developing cities: case of Bangkok in the era of ride-hailing services. *Transp Policy* 75:27–35
12. Tang B-J et al (2020) How app-based ride-hailing services influence travel behavior: an empirical study from China. *Int J Sustain Transp* 14(7):554–568
13. Alemi F et al (2019) What drives the use of ridehailing in California? Ordered probit models of the usage frequency of Uber and Lyft. *Transport Res Part C: Emerg Technol* 102:233–248
14. Distribution of population by age in Bangkok, December 2019. Department of Provincial Administration, The Bureau of Registration Administration
15. Statista (2021) Mobility services: ride-hailing & taxi
16. Kaiser HF (1960) The application of electronic computers to factor analysis. *Educ Psychol Measur* 20(1):141–151
17. Hair JF (2009) *Multivariate data analysis*
18. Tabachnik B, Fidell L (2001) *Using multivariate statistics*. Allyn & Bacon Needham Heights, Massachusetts

Genealogy of Shared Mobility in India



Nidhi Kathait  and Amit Agarwal 

Abstract With the increasing urbanization and recent advancements in information and communication technology (ICT), Indian cities are witnessing faster growth of shared mobility services over the last few years. This paper presents a historical development of common shared mobility services in India to bring better clarity to the emerging mobility services and discusses the opportunities and challenges to their implementation and operation. As most of the Indian cities still have compact designs and have high population density and high share of shorter trips, they foster an ideal precondition for shared mobility services as substantial form of sustainable mobility. Shared mobility services such as carpooling or vanpooling can effectively reduce the usage of private cars in India and can provide various transportation, environmental, and social benefits. Additionally, shared mobility can increase the popularity of low-carbon transportation mode with the help of bicycle sharing and electric shared vehicle. It was concluded that having a strategic policy framework is only way through in developing a sustainable shared mobility ecosystem to meet the requirement of an urban city over time.

Keywords Shared mobility · Car-sharing · Ride-sharing · On-demand ride services · Micro-mobility · Bicycle sharing

1 Introduction

Urban mobility has evolved significantly over the last few decades and is still changing dramatically. The share of urban population in the world has crossed 55% mark [15]. Increase in urbanization, population growth, and economic development have resulted in increasing growth of vehicles on the urban roads. Over the last two

N. Kathait (✉) · A. Agarwal
Indian Institute of Technology Roorkee, Roorkee, India
e-mail: nkathait@ce.iitr.ac.in

A. Agarwal
e-mail: amitfce@iitr.ac.in

decades, India is witnessing rapid growth of private vehicle ownership and decreasing ridership of public transit and non-motorized transport [19]. Growth of private vehicles has led to myriad of problems such as traffic congestion, accidents, and pollution and, thus, directly impacts the India's energy consumption and carbon emission [2]. As a fact, emissions from passenger road transport have increased four times since 2000 [10].

As the Indian economy continues to grow, the demand of vehicles will grow in a business-as-usual case, which will escalate the pressure on the transportation infrastructure. To cope up with the increasing demand of urban mobility, mobility needs are evolving and mobility options are expanding. Technological advancements and new transportation services are making movement of people in the cities more efficient and safe and have proven to be a great aid in case of over/fully saturated road infrastructure and public transit services [4]. Transition to shared mobility offers an innovative transport mode choice, which allows travelers to access mobility as a service [11]. It is based on advanced digital technologies to improve the efficiency of vehicle use and to provide personalized and diversified services to the travelers [11, 13]. Shared mobility has gained momentum in the last decade across the country and is considered to be the future of urban mobility. Widespread availability within the cities' boundaries and ease of use have made such services appealing to the users. The fact that shared mobility relies on the development of smartphone provides a huge potential market for shared mobility in India. Smartphones have become quite affordable in India and in reach of almost everyone. At the end of 2019, more than 0.5 billion people were connected to internet, primarily through their smartphones. The smartphone user base is expected to rise to 0.82 billion by 2022 [9]. Development of digital technologies and growth of smartphones foster a perfect environment for development of shared mobility services in India.

Although shared mobility services are expected to reduce the vehicular ownership, improve public transit ridership by providing first- and last-mile connectivity to public transport, and positively impact the environment altogether, the effects of the same are seen to be varying in many cases. Even after the widespread adoption of shared mobility services in India, there is a lack of an up-to-date and well-structured review of such services. So in this study, a historical overview of the evolution of shared mobility in India is presented to bring better clarity to the emerging mobility services. The present study helps in developing preliminary insights into the important aspects of shared mobility services such as their background, operational models, strengths, weakness, opportunities, and challenges to their implementation and proposed solutions.

The objectives of this work are (a) to list and differentiate the different types of shared mobility services in India (b) to present the historical development of the most common shared mobility models in India (c) to draw policy lessons from the perspective of users/operators/policymakers.

2 Shared Mobility and Modalities

The main and common idea behind shared mobility services is “using instead of owning.” Shared mobility is a strategy that enables short/ midterm access to various transportation modes on a “pay-per-use” or an “as-needed” basis [2, 13]. It includes shared use of car, bicycle, motorcycle or any other transport mode or service according to the diverse need of the users. It enables user to plan and book their trip based on real-time information and digital fare payment into a personal-user interface. These innovative transportation services and re-sources are shared consecutively or concurrently among users, resulting in higher utilization of assets that a society or user can afford, reducing the vehicle ownership [13]. Shared mobility services are primarily categorized into five groups: car-sharing, on-demand ride services (commonly known as ride-hailing), ride-sharing, micro-mobility services, and micro-transit services.

Car-Sharing It is a type of Internet-based car-rental service, which provide access to a vehicle for a short period of time in self-driving mode [13]. The service is offered by an organization that maintains and deploys a fleet of vehicles located within neighborhoods, near or at the transit stations, commercial centers, etc. Based on the returning location of the vehicle-after-use, car-sharing service model are differentiated into fixed station-based (round-trip and one-way) and free-floating car-sharing models. In station-based round-trip car-sharing, vehicle is picked up from a designated station and returned to the same car-sharing station after use; whereas in station-based one-way car-sharing, vehicle can be returned to any other designated station. In free-floating car-sharing model, vehicle can be picked up and returned anywhere within a pre-specified geo-fenced area.

On-Demand Ride Services The transportation services where the driver and passengers connect through an online platform or application by transport network companies (TNCs) [5]. Operation of these services is mostly based on information and communication technologies (ICT) to request and dispatch vehicles upon users’ requests. On-demand ride services are broadly classified into three groups: ridesourcing, ride splitting, and e-hail (radio cabs) services. Ridesourcing (also known as TNCs, ride-hailing, or cab aggregators) is the major segment of the on-demand ride services, which uses a smartphone app to connect the drivers and passengers provided by the TNCs (e.g., Uber, Ola, Lyft). TNCs aggregate the fleet of vehicles owned by people, operator or micro-entrepreneur without owning a single vehicle. Ridesplitting allows sharing of a TNC-provided ride and splitting of fare with another passenger having a similar route. E-hail services, earlier known as radio cabs, allow booking of a taxi with the help of Internet/smartphone application/ telephone maintained by a taxi company.

Ride-Sharing It refers to formal or informal sharing of vehicle (generally a car or a van) between the drivers and passenger with similar or overlapping path. Carpooling refers to the informal ride-sharing among three to six commuters not belonging to

same family or group [13, 17]. Vanpooling refers to the sharing of van among seven to fifteen people who commute on a regular basis and share the operating expenses [13].

Micro-mobility It refers to the shared use of small transportation modes such as bicycles, e-bikes, scooters, or other any other low-speed modes. It mostly covers short-distance trips including first- and last-mile connecting trips to public transit stations. There are different service models available to meet the diverse need of the users: docked (dedicated pickup/ drop-off stations) bicycle sharing and dock-less (free-floating) bicycle sharing, e-bikes, and scooter sharing.

Micro-transit Privately or public operated shared transport system, providing services either with fixed route and schedules or flexible routes and on-demand [2, 17]. It includes vehicles such as shuttles, vans, multi-passenger vehicle, or mini-buses, where drivers and passengers are linked through IT-enabled applications as per their mobility needs.

Shared mobility services offer competitive environment to taxi and transport organizations to provide user-friendly services. Figure 1 provides comparison among shared mobility services with respect to private (owned) vehicle and public bus, based on travel time, trip cost, and privacy. Shared mobility services fill the gap between public and private transportations. In urban areas, shared mobility services help in relieving the stress on public transit services during peak hours and can also supplement them in off-peak hours. In shared mobility services, ICT enables disruptive forms of market interaction that provides improved efficiency in resource utilization.

3 Development of Shared Mobility in India

Shared mobility landscape is rapidly evolving in India, owing to its appealing convenience and affordability. Development of Internet services and GPS technology has fueled the growth of different shared mobility service models in India (illustrated in Fig. 2). The shift away from “asset ownership” lifestyle is predominant in major Indian cities, which drives the demand for shared mobility services.

Despite gaining popularity in the last decade, the concept of shared mobility is relatively old in India. The shared vehicle market has been dominated by city taxis and auto-rickshaws for the greater part of the twentieth century. However, the launch of Radio Cabs at the onset of the new millennium revolutionized the transportation industry in India. They allowed users to pre-book a vehicle using phones or websites. By the mid-2000s, large fleets of such shared taxis were operating in major cities. Advancement in mobile technology in the late-2000s paved way for “aggregator” or “on-demand” model which allowed companies to aggregate vehicles under single brand, without having to own a fleet. During the same time, a new concept of vehicle sharing was introduced in the Indian market. In the context of vehicle sharing, a

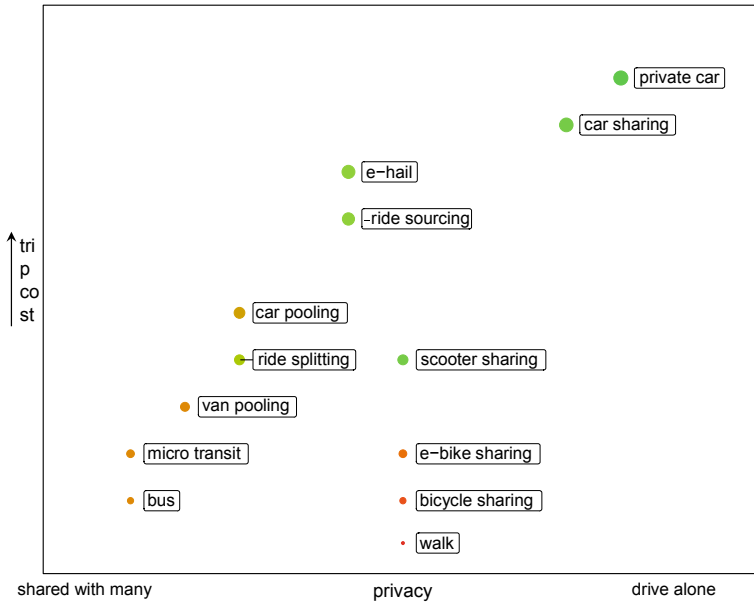


Fig. 1 Comparison of various shared mobility services based on typical travel time, cost, and privacy. Color denotes travel time (green is low, red is high) and size represents trip cost

person can have temporary access to car, scooter, or bicycle which are made available by the vehicle-sharing facilitator. Figure 2 shows the evolution of shared mobility services in India. Many service operators, following their positive growth curve, expanded their operation to include different service types. However, there are many companies who could not sustain and had to shut down their operations. Development of each shared mobility service type is explained in the subsequent sections.

3.1 Car-Sharing

In India, car-sharing is still an emerging concept, which is based on Internet and smartphone application. The first self-driving, car-sharing service of India was launched in 2010; however, the car-sharing market saw significant growth after company called “ZoomCar” launched its service in 2013 in Bangalore [18]. Various car-sharing companies entered the shared mobility market especially from 2013 to 2017 (See Fig. 2). During the starting year, many of the car-sharing services were operated manually, i.e., a person used to be present at each station to check the documents, to issue the cars to customers, to refuel the vehicles and to provide assistance to the customers. Later on, with the technological advancement pickup and drop-off of vehicle from station became more convenient. Over the past 7 years, car-sharing system has brought in major changes. Nowadays, one can also have a car delivered

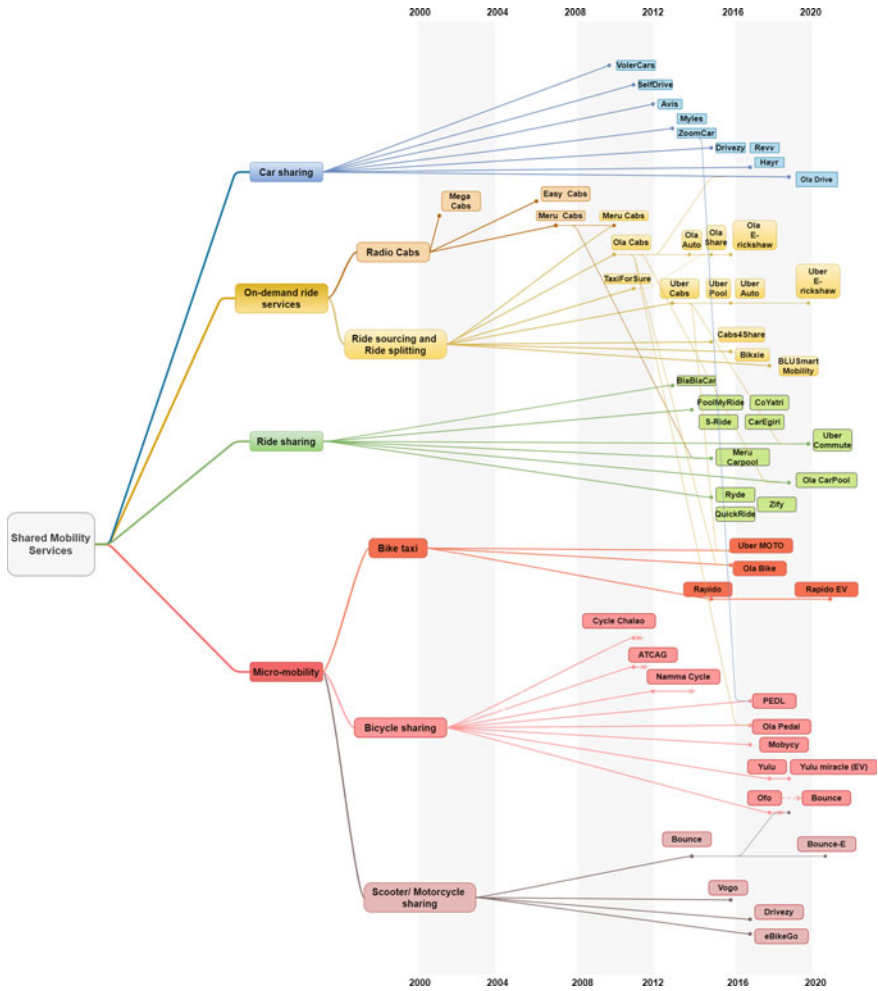


Fig. 2 Evolution of shared mobility services in India

at their doorsteps. Most of the car-share services in India work on the station-based model, where the user has to return the car to the designated stations. The first free-floating car-sharing service model was launched by “Hayr” in Chandigarh in 2017.

In 2018, India’s first peer-to-peer (P2P)-based car-sharing was launched, under which privately owned cars can also be temporarily made available in self-driving mode for use by an individual or P2P sharing company. In case of India, operation of shared mobility and vehicle is institutionalized under the Motor Vehicle Act, 1988, which does not allow sub-rental of vehicles having private number plate. However, popularity of shared mobility service providers such as Ola, Uber, and ZoomCar is compelling the government to reform the regulation policy for highly promising P2P

car-sharing segment. In addition, TNCs like “Ola” entered the car-sharing market in 2019 with slightly advanced features. It enables users to personalize their own packages such as deciding number of km, hours, fuel inclusion, etc.

P2P car-sharing programs offer more direct manifestation of asset utilization than traditional car-sharing. It allows a car owner to earn extra money by renting his car when he is not using it. However, the majority of car owners to use P2P car-sharing services in India are either tour operators or individuals having vehicles with commercial license plate, instead of regular car owners. This is one of the biggest bottlenecks in achieving the real purpose of P2P car-sharing services, i.e., utilization of idle personal vehicles. Hence, radical ideas are needed to avoid conversion of sharing economy business model (personal vehicles for rent) to servitization model (travel agencies vehicles for rent) [7].

Various car-sharing operators have also started offering car subscription service, which allows users to rent a car for a longer duration (number of days or months). Demand for a monthly subscription has witnessed significant rise amid COVID-19 pandemic. Subscription-based access to vehicles has proven to be in favor of the growth of car-sharing companies.

As Indian government is pushing toward zero emission transportation agenda¹ post Paris Climate Change agreement, many car-sharing operators in India introduced electric vehicles in their fleet. Sustainable transport modes such as car-sharing and carpooling play a vital role in boosting adoption electric vehicles [3].

3.2 *On-Demand Ride Services*

On-demand ride services have been growing notably in the last few years. It includes services such as ride-sourcing, ride splitting, and e-hail taxis (see Sect. 3) On-demand ride service market in India is composed of number of TNCs. Some of the TNCs operating in Indian market are shown in Fig. 2.

The advent of ride-sourcing in 2010 revolutionized the commuter experience in India by providing them vehicle on-demand. In the early stage, to attract a reliable customer base and to manage a good starting point, companies offered low-fare rides and high subsidies to passengers and drivers. From the perspective of industry development, TNCs like Ola, Meru Cabs, Uber, and Cabs4Share have successively set up their ride-sourcing operation from 2010 to 2017. Most of the companies are in Tier-I and Tier-II cities with high mobility demands, better Internet connectivity and more limitation to private cars. Several distinct features that make TNCs different from taxi or radio-cab operators are price transparency, technological platform to connect driver and customer, real-time fleet optimization, etc.

Various TNCs, such as Ola and Uber, have always been in a price war among themselves and also with other cab services. The competition for increased ridership has resulted in discounted rides, more demand for vehicles and increased pressure

¹ India currently has a target to have 30% of vehicles as electric vehicles by 2030.

of maintaining adequate driver incentives. There were many companies that could not survive in the competitive business environment. TaxiForSure, a small company, launched in 2011, was acquired by Ola in 2015 and later on was shut-down to cut operational cost and save the cash reserves that were deployed elsewhere. Soon after, Ola launched India's first ride-splitting service, Ola Share, where a user can share a cab with other users traveling along the same route. Keeping the need of Indian public in view, companies also introduced auto-rickshaws in their fleets. Getting an auto service on the online platform has increased the reach and appeal of ride-sourcing services. Following sustainable transport strategy, Ola and Uber introduced E-rickshaws in their fleets as a ride-sourcing service. Another TNC, "BLUSmart mobility" became the first company to launch all-electric shared-cab services. It currently operates a fleet of 320 + EVs in Delhi and Mumbai. It is using an in-house driver and traveler matching algorithm to balance the supply and demand, keeping the factors like battery state and nearest charging station location into consideration to overcome challenges related to insufficient charging stations.

Despite widespread popularity in the metro cities, TNCs faced various issues related to surge pricing, longer wait times, wrong drop-off location, canceling rides by the drivers, behavioral issues of the drivers, women safety, etc., were reported by the users. Companies have introduced many in-app features to resolve most of the operational issues and improve their service quality. Recently, Ministry of Road Transport and Highway (MoRTH) has addressed many of these problems and released first ever Motor Vehicle Aggregator guidelines. The new regulatory guidelines outline rules for both aggregators and drivers. It lays down rule for maximum surge pricing, eligibility of drivers, base fare, cancellation penalties, responsibilities of aggregators with respect to safety and customer data privacy.

3.3 Ride-Sharing

Ride-sharing happens when people from different household share a private vehicle together while traveling to the same destination. Passengers share the ride cost and driving responsibilities, making the travel cost significantly lower than ride-hailing and private taxis. Ride-sharing includes carpooling and vanpooling services. In India, ride-sharing has witnessed notable growth over the last decade. The first carpool service was launched in 2013. Over more than 85 carpooling platforms were launched between 2015 and 2017 across various Indian cities. Seeing growing popularity of carpool model in India, travel agencies, taxi companies, and TNCs also started introducing their own carpool services.

In order to reduce the number of vehicles on the roads, the Government of India has indulged in promoting carpooling as a lifestyle and spreading awareness of its benefits. During 2016, odd-even scheme was rolled out in Delhi as an anti-pollution measure. According to [8], during the first phase the scheme led to 20% reduction in PM_{2.5} and around 5% increase in average vehicle speed on road indicating reduction in congestion. Significant rise in carpool trips was reported during the scheme. In

Kolkata, police department and IIT Kharagpur worked on a pilot project of introducing carpool/ vanpool service for transportation of school students. Seeing the positive response, state transport department launched a carpool application with tracking system also. Karnataka government has banned ride-sharing operations by TNCs such as Ola and Uber and has urged the central government to amend the Motor Vehicle Act. This is because TNCs are only allowed to operate the vehicles as contract carriages (door-to-door pickup and drop-off), whereas carpooling and vanpooling fall under the category of stage carriages (pickup at intermediate points). Thus, the state government suggests that ride-sharing services should be allowed only for private vehicles, which will help in reducing the number of private vehicles on road. However, MoRTH is yet to issue guidelines on carpooling services. The formal framework is expected to bring uniformity in rules across India to encourage carpooling and thus reduce regulatory challenges.

For Indian cities, the impact of technology-enabled ride-sharing services continues to evolve. In a study, it is shown that after entry of carpool service, congestion on city roads considerably reduced [6]. The concern related to comfort, privacy, safety, and security remains to be a barrier [16].

3.4 *Micro-mobility*

Shared micro-mobility refers to shared use of bicycle, scooter, electric bike, and any other low-speed modes. All of these are promising transport mode to replace or reduce short private vehicle trips in urban agglomerations. In India, various micro-mobility start-ups have emerged over the last decade. There are primarily three business models: bicycle sharing, scooter sharing, and motorbike/bike-taxis. Example of various micro-mobility operators is shown in Fig. 2.

Bicycle Sharing In India, bicycles are still looked upon as a “poor man’s travel mode” [14]. However, the concept of public bicycle sharing (PBS) system is changing people’s perception. PBS provides citizens the flexibility of renting bicycles for short trips at nominal rates. Traditional station-based (docked) bicycle sharing model has been successfully launched in many cities across India. It encourages people to cycle more and promotes healthy and active travel. While cycling clearly has environmental and health benefits [1], high infrastructure and operation costs continue to be a barrier in PBS adoption by other cities. In wake of this, smart dock-less bicycle system is introduced in many cities. It allows dock-less operation and involves lighter infrastructure.

Various PBS programs have been tested and successfully introduced in India (see Fig. 2). “Cycle Chalao” was India’s first organized system to rent out cycles to provide last-mile connectivity in the city of Mumbai. In the same year, another innovative pilot project Automated Tracking and Control of Green Assets (ATCAG) was launched in Bangalore under which bicycles are automatically issued and accepted. The system

helps in reducing human interventions and cutting the waiting time to make its usage easier. Many other PBS projects are also being implemented in cities under the smart city mission by Government of India. In 2017, Bhopal became the first Indian city to introduce fully automated bicycle sharing system that provides dedicated lanes and helps in connecting to public transportation. A similar type of project is being tested in Bangalore and Mysore. In recent years, following the growing demand of bicycle sharing in India, private companies like Ola, Uber, and Mobyicy have also started operating PBS services through public–private partnership (PPP) model. However, there are several big start-up companies that were not able to sustain, one very famous example is of Chinese bike-share company, Ofo's. The rapid expansion of the service without monitoring the situation led to the huge losses for the company. Ofo followed “park-anywhere” model, which is not feasible, presently, for a country like India. Vogo and Yulu considered this issue and set up designated zones for parking before deploying their “park-anywhere” model.

In a country like India, bicycle sharing start-ups to address the first- and last-mile connectivity issue have a rich opportunity. However, most of the Indian cities do not have a long-term vision for PBS or cycling, in general. The major reason is high investment to setup stations and overall lower return on investment. Operators are taking up various measures to improve their operation and prevent theft and vandalism such as the installation of robust tracking devices and sensor. It was noticed that start-ups that focused on improving safety processes and poor-infrastructure facilities have proven to be more successful. Also, the gradual and user-centric expansion of the services worked better in case of India thus can be considered to create an efficient end-to-end PBS system.

Scooter Sharing It is comparatively new entrant into India's shared mobility market. It has been experiencing highs and lows since its entry into the market. The first scooter rental service was launched in Bangalore in 2014 as a docked scooter sharing model, which later on was converted to completely dock-less model to avoid the investments in infrastructure. In 2016, metro scooter service was also initiated, to provide a first- and last-mile connection to public transport. Scooter sharing companies such as Vogo, partnered with Ola to have 100,000 scooters made available to Ola's customer base of more than 150 million from the Ola application. The partnership between VOGO and Ola has turned into a beneficial strategy for both companies. Transitioning toward green mobility, big player such as Bounce, Vogo started adding electric scooters to its fleet. Many companies launched with all-electric scooter fleet.

Motorbike-Taxis Online motorbike-taxi aggregator is gradually gaining user's confidence in India. A motorbike-taxi service is an on-demand bike aggregator service, where a bike-rider will provide the service to the customers. Currently, Rapido, Ola Bike and Uber Moto are the only player in India's bike-taxi market. Motorbike-taxi service was first launched in 2015 and has faced legal troubles in various cities in the starting year of its operation. As per Motor Vehicle Act, it is considered illegal to use private motorbikes for commercial purposes, so the service was suspended in many cities. Later on, an approval was given to the companies under which the vehicle used for motorbike-taxi service should have commercial number plate. However, it

is still considered illegal in 14 states across India. Because bike-taxis are more affordable than cab services and can seep through congested roads, these are getting more popular among millennials. Following the rising popularity of bike-taxi service, the central government appealed to all state governments to legalize the operation of such bike-taxi services.

4 Policy Recommendations for Shared Mobility

Shared mobility models in India have to meet several challenges because of lack of a clear profit model, insufficient infrastructure and inadequate policies and regulations. Policymakers play an important role in the development of shared mobility services with the help of range of initiatives-for example enabling access to on-street or odd-street parking space. While deciding to launch new shared mobility services, policymakers need to understand that these services are in development phase and therefore imperfect, so the policies should be designed to support them during their establishment phase [12]. These policies should aim at achieving integrated and sustainable urban mobility environment while controlling the negative impact of motorized transport. Integration of service operations and transportation infrastructure would help in achieving seamless mobility and integration of a user interface would allow the users to make better travel decisions. Indian cities foster an ideal environment for embracing shared mobility services [2]. So, in the subsequent section we discuss policy framework related to implementation and operation of shared mobility schemes.

Policy Framework for Car-Sharing There is very little information on how to introduce, expand, and promote self-driving car-sharing in a sustainable manner in developing countries. Therefore, an efficient policy framework is required to encourage the growth of car-sharing into urban transport and planning. To reduce the car-ownership, self-driving car-sharing can be expanded to include carpooling services in association with carpooling operators. Further, integrating and promoting self-driving car-sharing services with public transit network has a great potential to reduce the negative externalities of personal car-travel. Some of the key policy recommendations are shown in Table 1.

Policy Framework for On-Demand Ride Services Seeing the surge in popularity of on-demand ride services/ TNCs, India is trying to bring them under dedicated regulation that might produce mixed results for users, drivers and operators. The guidelines were instituted recently and deals with the concerns related to the regulation of fares, TNCs licensing, cancelation fee, surge pricing, safety standards, etc. The government should also consider policies that enable PPP model to fill public transport service gaps, examples are shown in Table 2.

Table 1 Car-sharing policy recommendations

Policy	Advantage	Disadvantage
Development of legal framework with clearly defined indicators	Ensure use of car-sharing services as a valuable alternative to personal car-travel	
Integrating and promoting car-sharing services with public transit (PT) network	Demand-oriented transit outlook, minimize negative externalities of personal car travel	Integrating of service need technological, operational, fare and infrastructure integration, lack of any can affect the appeal of car-sharing service
Dedicated parking policies for shared cars	Improve integration with PT services if provided near PT stations, reduces number of parking zones in an area, financial profit	Car-sharing operators may be charged in return of providing parking spaces by city officials
Zoning policies such as incentive zoning	Encourage car-sharing in a defined zone, ease zoning regulation, mitigate parking costs	Complex administration
Equity policies	Make service accessible to older adults, disabled people, low-income households, and minorities	Complex to plan and implement
Sharing and monitoring car sharing user data between city authorities and operators	Better configuration of services, identification of areas suitable for expansion of the service in a sustainable way	Users' privacy-related issues
Providing incentives to the car-sharing users ending their trips near PT stops	Attract more people to car sharing, increases PT ridership and multimodality	High operational cost
Ticketing and fare integration with PT	Provide seamless transfer and discounted ride options	Complications due to multiple operators in the market, cost-intensive

Policy Framework for Ride-Sharing Indian cities are slowly recognizing the benefits of ride-sharing services such as carpooling or vanpooling. While Motor Vehicle Act does not specifically restrict ride-sharing services, no formal framework has been issued yet to regulate these services and thus create a barrier in their expansion. Different states have different policies for operation of ride-sharing services, therefore a national level policy intervention will bring uniformity across different states and will reduce regulatory hurdles. Key policy considerations for improving the carpooling service and integrating it with urban ecosystem are shown in Table 3.

Policy Framework for Bicycle Sharing Although bicycle sharing, being a low-cost mode, showed high level of acceptance among users in Indian cities, it is not being

Table 2 On-demand ride services policy recommendations

Policy	Advantage	Disadvantage
Safety of passenger	Ensure better service, safety of passenger and drivers too, increase profit	Better technological need
Kerb space management	Safe pickup and drop-off of ridesourcing passengers	Additional infrastructure cost, may increase user’s walking distance
Enabling public–private partnership (PPPs)	Support existing public transportation network and improve first- and last-mile connection, providing service during off-peak hour and to low-density areas where public transport are operating in lower frequency, integration with transit apps	Need strategic allocation of revenue/demand risk between public and private operators, complex regulation
Spatial quotas or systematic pricing of ride-sourcing trips	Minimize the substitution rate of public transit trips (in city centers)	May not be beneficial to operators
Equity policies	Make service accessible to disadvantaged communities	Complex to plan and implement

Table 3 Ride-sharing policy recommendations

Policy	Advantage	Disadvantage
Parking policies	Encourage vehicle pooling, shift to public transit	Need proper infrastructure
Kerb space management	Encourage high occupancy modes	Additional infrastructure cost may increase user’s walking distance
Associating with companies to promote carpool	Reduce single-occupant vehicle work trips	May shift people using PT to carpool
Incentive zoning	Encourage vehicle pooling, ease zoning regulation, reduce parking costs	Complex administration
Developing carpooling as a complementary service within city’s public transport network	Reduce single-occupant vehicles on road	May reduce PT ridership if not planned strategically

implemented by many cities due to multiple barriers [14]. Because of the lack of proper policy framework, it is very difficult to deal with these barriers altogether. Some of the key policy recommendations for operators and cities to successfully implement PBS schemes are described in Table 4.

Table 4 Bicycle sharing policy recommendations

Policy	Advantage	Disadvantage
Upscaling and transferability	Target new population group	Requires a high capital investment and city-specific plans
Registration/Licensing of bicycle sharing operator	Quantify the bicycles or users, monitor the fleet efficiency	Need separate management authority
User-centric approach	Long-term success and easy profit	Less revenue generation for operators
Dedicated cycling infrastructure integrated with public transport network	Make cycling more comfortable and safe for riders, provide first- and last-mile connectivity, promotes multimodality	Cost-intensive
Rider data sharing with city government	Identify service impacts and gaps, monitor service standards, offer real-time transportation information	Privacy issues
Regulating responsible bicycle usage	Deal with theft and vandalism, beneficial for operators	Cost-intensive
Diversifying the provision of bicycles	Ensure the widespread adoption, introduction of electric bikes, pedal-assisted electric bikes, tricycles, etc., make the service more attractive	May create confusion among users
Providing end-of-trip facilities such as locker and shower facilities at bicycle station or transit stations, etc	Encourage people to adopt cycling	Man-power needed at such facilities
Re-balancing/Redistribution	Maintain proper demand and supply	Cost-intensive

5 Conclusion

The ecosystem of shared mobility services in India evolved over past few years with emerging technologies. Despite being a popular cost-efficient transport mode, there are very few published studies on shared mobility in Indian context. So, this paper presented the historical review of shared mobility services while discussing their development trends, barriers to their implementation, governance policies, and influencing factors. It also provides various future dedicated research directions. The study mainly emphasizes the importance of clear distinction among existing and emerging shared mobility services. As shared mobility services continue to expand alongside existing mobility services, a clear distinction between different service models can aid the growth of these service by providing policymaker and government with greater understanding of various forms of shared mobility and their impacts.

Furthermore, government can continue to support shared mobility services in terms of infrastructure and providing access to public rights-of-way.

Unlike developed countries, developing countries like India mostly struggle with the implementation of new and innovative strategies. Indian government has introduced several policies to make the operation and regulation of shared mobility services easier such as providing dedicated parking space for car-sharing and bicycle sharing services, putting caps on fare prices and surge prices of ridesourcing services, regulating type of vehicles for carpooling, etc. But there is almost no quantitative evaluation of the impact of such policies, obstructing the continued policy advancement. So, the government and policymakers need to understand how a particular shared mobility model impacts on the urban transport. In the wake of COVID-19 pandemic, it is important to pay more attention to consumer travel preferences and to understand the underlying mechanism driving shared mobility usage.

Author Contribution The authors confirm contribution to the paper as follows: Conceptualization: NK, AA; Resources, Data Curation: NK; Writing—Original manuscript: NK; Supervision: AA. All authors read and approved the final manuscript.

References

1. Agarwal A (2021) Quantifying health & economic benefits of bicycle superhighway: evidence from Patna. *Procedia Comput Science* 184C:692–697. <https://doi.org/10.1016/j.procs.2021.03.087>
2. Bhandari A, Juyal S, Maini H, Saxena A, Srivastava A (2018) Moving forward together: enabling shared mobility in India. Technical report. NITI Aayog, Rocky Mountain Institute, and Observer Research Foundation. <https://niti.gov.in/node/251>
3. Burghard U, Du`tschke E (2019) Who wants shared mobility? Lessons from early adopters and mainstream drivers on electric carsharing in Germany. *Transp Res Part D: Transp Environ* 71:96–109. <https://doi.org/10.1016/j.trd.2018.11.011>
4. Calderón F, Miller EJ (2019) A literature review of mobility services: definitions, modelling state-of-the-art, and key considerations for a conceptual modelling framework. *Transp Rev* 0(0):1–21. <https://doi.org/10.1080/01441647.2019.1704916>
5. Chakraborty J, Pandit D, Chan F, Xia JC (2020) A review of ride-matching strategies for ridesourcing and other similar services. *Transp Rev* 0(0):1–22. <https://doi.org/10.1080/01441647.2020.1866096>
6. Dewan KK, Ahmad I (2006) Carpooling: a step to reduce congestion (a case study of Delhi). *Eng Lett* 14:61–66
7. Govindan K, Shankar KM, Kannan D (2020) Achieving sustainable development goals through identifying and analyzing barriers to industrial sharing economy: a framework development. *Int J Prod Econ* 227:107575. <https://doi.org/10.1016/j.ijpe.2019.107575>
8. Greenstone M, Harish S, Pande R, Sudarshan A (2017) The solvable challenge of air pollution in India. In: India policy forum. National Council of Applied Economic Research (NCAER), New Delhi
9. ICEA (2020) Contribution of smartphones to digital governance in India. Technical report. India Cellular & Electronics Association (2020). <https://icea.org.in/wp-content/uploads/2020/07/Contribution-of-Smartphones-to-Digital-Governance-in-India-09072020.pdf>
10. IEA (2021) India energy outlook 2021. Technical report International Energy Agency. <https://www.iea.org/reports/india-energy-outlook-2021>

11. Jittrapirom P, Caiati V, Feneri AM, Ebrahimigharehbaghi S, Gonzalez MJA, Narayan J (2017) Mobility as a service: a critical review of definitions, assessments of schemes, and key challenges. *Urban Plan 2*. <https://doi.org/10.17645/up.v2i2.931>
12. Kent JL, Dowling R (2018) Commercial car sharing, complaints and coping: does sharing need willingness? *Urban Policy Res* 36(4):464–475. <https://doi.org/10.1080/08111146.2018.1486297>
13. Machado C, Hue N, Berssaneti F, Quintanilha J (2018) An overview of shared mobility. *Sustainability* 10:4342. <https://doi.org/10.3390/su10124342>
14. Patel SJ, Patel CR (2020) A stakeholder's perspective on improving barriers in implementation of public bicycle sharing system (PBSS). *Transp Res Part A* 138:353–366. <https://doi.org/10.1016/j.tra.2020.06.007>
15. Ritchie, H, Roser, M (2020) Urbanization. OurWorld in Data. <https://ourworldindata.org/urbanization#citation>, <https://ourworldindata.org/urbanization>
16. Shah P, Varghese V, Jana A, Mathew T (2020) Analysing the ride sharing behaviour in ICT based cab services: A case of Mumbai, India. *Transp Res Procedia* 48:233–246. <https://doi.org/10.1016/j.trpro.2020.08.018>
17. Shaheen S, Cohen A (2018) Shared ride services in North America: definitions, impacts, and the future of pooling. *Transp Rev* 1–16. <https://doi.org/10.1080/01441647.2018.1497728>
18. Shalender K (2021) Building effective social media strategy: case-based learning and recommendations. In: *Digital entertainment*, pp 233–244. https://doi.org/10.1007/978-981-15-9724-4_12
19. Vasudevan V, Agarwala R, Dash S (2021) Is vehicle ownership in urban India influenced by the availability of high quality dedicated public transit systems? *IATSS Res*. <https://doi.org/10.1016/j.iatssr.2020.12.005>

Investigating the Barriers for Electric Vehicle Adoption Using Analytical Hierarchy Process Approach



Manivel Murugan, Sankaran Marisamynathan, and Preetha Nair

Abstract To mitigate environmental problems and develop sustainable modes of transport in India, the government is trying to boost the electric vehicle (EV) market by introducing policies and subsidies. However, despite all the efforts, the share of EVs on Indian roads is quite negligible. Understanding the potential barrier and potential area to improve will significantly help to overcome the issues and increase EV sales in India. Therefore, this study aims to investigate the most influential barriers to adopt EV. For this purpose, questionnaire survey was conducted to the experts having rich experience related to EV works. Analytical hierarchy process (AHP) approach was used to prioritize the most influential barriers for EV adoption. This study finds that the higher initial purchase price. Many EV manufacturers being new companies, less mileage (in km) on a full charge of battery, non-reliable battery technology, limited availability of public charging stations, higher charging time in of vehicle using slow charging, safety concern among high-speed vehicle flow on the highway, and lack of understanding of subsidy policies are the major barriers to adopt EV in India. Unknown resale value of EV, limited availability of EV dealerships, overall maneuvering difficulties, lesser competitiveness with ICE technology development, limited availability of local technician, higher installation cost for fast charging facility, safety concern while charging, non-availability of charging facility on long trip, and lack of awareness of long-run cost benefits are the minor significant factor that influences EV adoption.

Keywords Electric vehicle · Analytical hierarchy process · Transport planning · Electric vehicle adoption · Sustainable transport

M. Murugan · S. Marisamynathan (✉)
Department of Civil Engineering, National Institute of Technology, Tiruchirappalli, Tamil Nadu, India

e-mail: marisamy@nitt.edu

M. Murugan

e-mail: er.veldpi92@gmail.com

M. Murugan · P. Nair

Department of Civil Engineering, Pandit Deendayal Energy University, Gandhinagar, India

1 Introduction

Being a developing country, India is witnessing a rapid change in the boundaries of rural–urban fringes. The rise in carbon emissions over recent years and deteriorating air quality in million-plus cities have been seen as an effect of this urban sprawl. The road transport sector alone consumed 2.9 Million Tera Joule of energy in 2017–18 and emitted 213 million tons of carbon-di-oxide [1]. It is obligatory to transition energy sources, especially in the road transport sector, to have sustainable resources for the coming generations. Electric vehicles (EV) contribute to low carbon emission transport up to a considerable extent even if the emissions from power generated to propel EV are considered. Globally, EV technologies have a decent improvement over the recent years. Various advancements in technology are brought into play in EVs, for example, advanced induction motors, Li-ion battery technology, ultra-capacitors, light body technology but rigid material, advanced charging, and power steering to improve driving range [2].

India's auto industry is the largest producer of two-wheelers and the fourth-largest producer of cars globally. Two-wheelers are the most popular mode of commute among Indian road users, especially for work trips [1]. A mass transition of users from internal combustion engine vehicles (ICEVs) to EVs will drastically reduce the tailpipe emissions. The Government of India (GoI) has taken several initiatives to diffuse EV in the Indian market. A goal of 6–7 million EVs was set up to achieve by 2020 under NEMMP in 2013. FAME India scheme was started with the aim of promoting research, development, and demonstration projects on EVs, and 11 cities in India are selected for the pilot project to monitor the development of EVs in the Indian scenario. The scheme is planned in two phases: Phase I (2015–2018) and Phase II (2018–2023). Unfortunately, Phase I has not achieved the target because of the user dilemma in adopting the EV. Various states in India are coming up with subsidy schemes apart from central government policies to encourage EV adoption. Karnataka and Maharashtra have successfully diffused EVs into Indian roads in terms of electrified public transport or intermediate public transport [3]. The Government is focusing on electrifying public transportation, and the option available for EVs as personal vehicles is relatively smaller [4].

India, being in its nascent stage of EV development, has fewer EVs on roads. At present, the EV market in India is not impressive, and the EV sales number is negligible compared to the ICE vehicle sales. So, there is a need to identify all the possible barriers to EV adoption and identify the critical improvement areas as per the expert perspective. This research intends to bridge the gap between EV buyers' requirements and EV manufacturers, transport planners, and policymakers to better understand the buyer's intention. This study makes a novel contribution by identifying all the possible EV adoption barriers based on expert view. The following are the research objectives for this study:

1. To identify the potential barriers to EV adoption through literature survey and expert opinion.

2. To prioritize the most influential barriers for EV adoption using analytical hierarchy process (AHP) approach.

This study employs an analytical hierarchy process (AHP) method to analyze and prioritize the critical barriers for adopting EVs.

2 Review of Literature

2.1 Consumer Characteristics and EV Adoption

Consumer attitudes on accepting EVs resulted the dynamic progress, depending on their previous experience with EVs. When given a choice between fuel-powered vehicles, hybrid electric vehicles (HEVs), and battery electric vehicles (BEVs), it is more likely that users prefer to have HEVs, probably due to range anxiety in BEVs. Road users feel confident to have a vehicle that utilizes more than one type of fuel [5]. People in Norway, who had an experience of driving both petrol cars and battery-operated electric cars, were happier and more comfortable to have electric cars in their day-to-day lives. Users termed it as “fun to drive” at extreme acceleration [6]. Also, the convenience of charging an EV at home was considered as an experiential advantage [7]. The combined effect of socio-demographic characteristics and psychological profiles on EV acceptance has been explored in various studies [8–11].

2.2 Charging Infrastructures and Range Anxiety

The dilemma between the precedence of charging infrastructure and EV uptake has become a problem in recent times. Experts have been trying to figure out this issue and have concluded that the availability and accessibility of charging infrastructure precede EV diffusion for a sustainable EV uptake [3]. According to a study in the UK, many users feel that it is convenient to charge BEV at home overnight but reluctant to make huge investments for faster-charging facilities at home [12]. The main reason for the non-adaptability of EVs is range anxiety because the number of charging stations is comparatively less than gasoline vehicles. The introduction of more charging stations provides an ease to range anxiety up to an extent [13].

2.3 Studies Related to AHP

AHP approach was developed by Saaty as a multi-criteria decision-making tool [14]. AHP uses the ratio scale measurements based on pairwise comparisons to indicate the strength of preference [15]. A wide variety of applications of AHP are identified

in various literature because it is easy to use and adjust in any size to accommodate decision-making problems [16]. For example, the selection of monorail projects planned for Istanbul was evaluated and selected based on AHP and goal programming methods [17]. AHP was used to develop software for selecting and evaluating project proposals [15]. Because of its flexibility, the AHP method is combined with various other methods to achieve the targets of the problem as per the requirements [18].

2.4 EV Studies in India

The Government of India encourages EV adoption by setting up policies and schemes at both national and state levels [19]. The order of priority for electrifying vehicles is fleet cars, E-buses, three-wheelers, and two-wheelers [4]. Though Government is trying to increase the number of EVs by providing benefits to the users, the lack of awareness acts an important unrecognized barrier for EV market development [20]. EVs have started to occupy spaces on the road slowly, especially in cities. E-Rickshaws are quite a common type of EV in few cities in India. A study in Patna surprisingly revealed that E-Rickshaws are the main mode of travel for about 77% of the users [21]. One of the concerns of potential adopters for EVs as personal vehicle was battery life. Consumers have negative comments on charging of battery as they feel that it is cumbersome compared to refueling gasoline vehicles and the absence of well-distributed public charging stations [22]. Few studies discussed the problem of generating electricity to power EVs. If the electricity generated is not sufficient to charge EVs, then more diesel generators are required to meet the demand. In the long run, the above-mentioned solution contradicts the concept of sustainable transportation [23]. According to experts, the three most significant barriers of EV adoption are identified in India: the high cost of batteries, which automatically increases the purchase cost, lack of public charging infrastructures, and range anxiety. The priority of the barriers varies according to the incentives and policies in a given state [24].

Most of the studies based on EVs are concentrated in China as it is the key player in the EV market and have many of the early adopters of EVs. In India, limited studies have been conducted on EVs, which are focused on electricity demand and supply for EV charging, environmental concern in EV adoption, vehicle usage pattern and safety perspective, vehicle ownership cost, and economic viability. None of the Indian studies focused on identifying the barriers to adopt the EV. So, this study aims to understand the various barriers to EV adoption. Because the customer requirement varies in different countries, understanding the customer need and taking necessary measures to satisfy the same is the only way to improve EV adoption in Indian in the near future.

3 Methodology

The detailed flow of the study methodology is shown in Fig. 1. A two-phase methodology is adopted in this study for evaluating the barriers to adopt EVs. In the first phase, the barriers to EV adoption are identified through an extensive literature review and conducting two rounds of a brainstorming session with experts. The internal expert group for the barrier selection includes academicians, industry personnel, and end-user. In the first brainstorming session, the authors have presented this study's aim and explained the authors' view on the present Indian EV market scenario and barriers identified in the outcome of literature review. Further, all the possible barriers with a different aspect like EV manufacturing, technology, cost, available policy options, user awareness, etc., are discussed during this session. In the second session, the major EV barriers are discussed, and the important barriers are grouped under the selected category. Finally, 32 barriers under nine groups are considered for further analysis as shown in Table 1. In the second phase, a group of external experts has been identified from a different field but has relevance and enough experience in the field of EVs. The external expert panel consists of ten members: three senior-level professors with research expertise in EV-related studies, four managers from the automotive industry, and then, the empty data sheet containing the pairwise barrier was shared with experts.

The experts evaluated one barrier over another with respect to their direct relationship using a linguistic scale, and hence, nine matrices were formed for modeling. AHP was used to assess the importance of EV barriers based on an expert pairwise comparison matrix. Further, the barriers are ranked, and the most important barrier in each group is adopted for further analysis in consultation with the experts. Finally, the practical implication of this study and suggestions to the policymakers to overcome the EV barriers are discussed along with the future scope of this study.

4 Model Formulation

4.1 Analytical Hierarchy Process (AHP)

Nowadays, multi-criteria decision-making (MCDM) strategies are used in transportation-related decision-making studies because of their ability to make justifiable, explainable, and transparent decisions. The most commonly used MCDM method in transport sector problems is AHP [18]. The AHP approach is distinguished by its use of pairwise comparisons, which are used to compare options against different criteria and estimate criteria weights. In this study, the AHP approach was used to prioritize the most significant barriers to adopt EV in India. It is best suitable to assign a priority or ranking of the factors for the decision-making process. AHP assists researchers and decision-makers in finding the best suitable solution for a complex problem by decomposing, organizing, and analyzing the various factors.

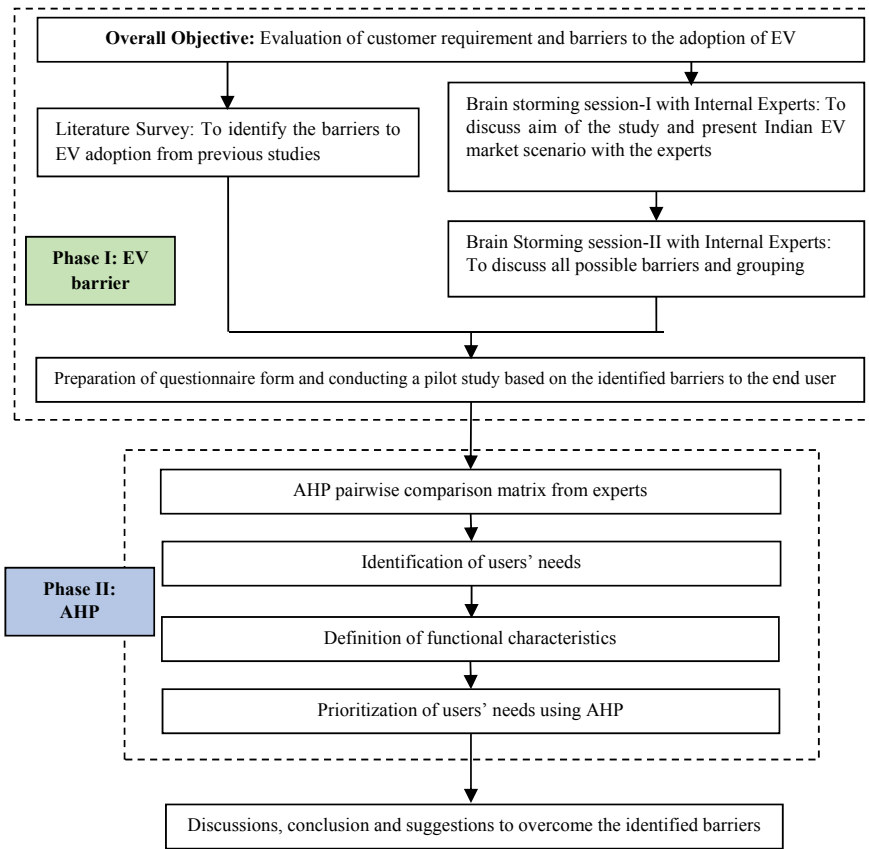


Fig. 1 Flowchart of overall study methodology

This method converts the problem into a hierarchical structure consisting of various levels like the goal, criterion, and alternative. Existing studies prioritized various transportation policies by adopting the various weighted average method and AHP [25, 26].

The various steps involved in the AHP are described as below:

Step 1—Formulation of the aim of work and identification of barriers: Identify the list of barriers related to EV study with the assistance of the literature survey, managerial interviews, and experts’ opinion.

Step 2—Formulation of pairwise comparisons: Constructing the questionnaire form to collect the data for pairwise comparison with EV experts’ assistance on the basis of the Saaty scale for pairwise comparison as shown in Table 2.

Let $F = \{F_j; j = 1, 2, \dots, n\}$ be the set of “ n ” factors responsible for EV adoption or non-adoption. The pairwise comparisons of n factors are summarized into an $n \times n$ matrix named A . The elements of the matrix say a_{ij} are the quotient of weights of

Table 1 Barriers with notations in bracket

Group	Barriers with notations in bracket
EV cost related	Higher initial purchase cost of vehicle (C1)
	Cost of battery (C2)
	Higher maintenance cost (C3)
	Unknown resale value of EV (C4)
EV manufacturer related	Many EV manufacturers are new companies (M1)
	A limited number of model on EV (M2)
	Limited availability of EV dealerships (M3)
EV vehicle factor related	Less Mileage (in km) on a full charge of battery (V1)
	Technical specification of the vehicle (power, acceleration, etc.) (V2)
	Load carrying capacity (V3)
	Lesser speed of the vehicle (V4)
	Comfort during ride (V5)
	The efficiency of vehicle performance in hilly and undulated terrain (V6)
	Overall maneuvering difficulties (V7)
EV technology related	Non-reliable battery technology (T1)
	Lesser adaptive competitive vehicle design (T2)
	Lesser competitiveness with ICE technology development (T3)
Maintenance and service related	Limited availability of local technician (MS1)
	Less spare parts available in local markets (MS2)
	Limited availability of local EV service centers (MS3)
Charging facility related	Limited availability of public charging stations (CH1)
	Limited-service provider to install fast charging station for home-based charging (CH2)
	Higher installation cost for fast charging facility (CH3)
Psychological barriers related	Higher waiting time at charging station if many vehicles are there (P1)
	Higher charging time in of vehicle using slow charging (P2)
	Safety concern while charging (P3)
Driving safety and reliability related	Safety concern among high-speed vehicle flow on the highway (DR1)
	Non-reliability of the vehicle on long trip travel (DR2)

(continued)

Table 1 (continued)

Group	Barriers with notations in bracket
	Non-availability of charging facility on long trip (DR3)
User awareness and reliability related	Lack of understanding of subsidy policies (vehicle purchase subsidy and other EV incentives by government) (A1)
	Lack of awareness of available EV companies and models in the market (A2)
	Lack of awareness of long run cost benefits (A3)

Table 2 Scales used in pairwise comparisons [27]

Importance intensity	Preference judgments
1	Equally important
3	Moderately important
5	Strongly important
7	Extremely important
9	Extremely more important
2, 4, 6, 8	Intermediate values between adjacent scale values

the factors.

$$A = \begin{bmatrix} a_{11} & \cdots & a_{1n} \\ \vdots & \ddots & \vdots \\ a_{n1} & \cdots & a_{nn} \end{bmatrix}$$

where $a_{ij} = 1$ when $i = j$ and $a_{ji} = 1/a_{ij}$ when $i \neq j$, $a_{ij} \neq 0$.

Step 3—Computation of maximum eigenvalues: The formulated pairwise comparison matrices are operated to calculate the maximum eigenvalues, which are further used to estimate the relative importance weights of the factors. The weights (w) for the factors are provided by the eigenvector of the largest eigenvalue (λ_{\max}) as $Aw = \lambda_{\max}w$.

Step 4—Evaluation of the consistency ratio: The consistency ratio is calculated to ensure the pairwise comparison’s consistency.

The consistency index for the pairwise comparison matrix is calculated using Eq. (1).

$$CI = \frac{(\lambda_{\max} - n)}{(n - 1)} \tag{1}$$

The consistency ratio is calculated using Eq. (2).

Table 3 Average random consistency index (RI) based on matrix size (*n*) [28]

<i>n</i>	1	2	3	4	5	6	7	8	9	10
RI	0	0	0.58	0.9	1.12	1.24	1.32	1.41	1.45	1.49

$$\text{Consistency ratio (CR)} = \frac{\text{CI}}{\text{RI}} \tag{2}$$

where RI is the average random consistency index as shown in Table 3.

If the consistency ratio value is less than 0.1, the decision is acceptable. Otherwise, the pairwise comparison matrix should be modified to remove the inconsistency [17].

5 Analysis and Results

5.1 Results from the AHP Approach

A total of 32 factors were considered barriers to EV adoption, and the list was sent to the experts to provide the pairwise comparison ratings. Each barrier under the same category was compared with one another, and hence, nine matrices were formulated. The expert reviews were checked for estimating the consistency index and consistency ratio of all the matrices using Eqs. (1) and (2), respectively. The consistency ratio results were reported within the limit, i.e., less than 0.1. The data was analyzed using AHP to rank the barriers and find the most critical factors from each category. The results and ranking of the AHP barrier analysis are shown in Tables 4, 5, 6, 7, 8, 9, 10, 11 and 12.

From the outcome of AHP analysis, it is interesting to note that most of the rankings are observed in order. During the brainstorming session, the authors discussed the most critical factors which are identified through literature surveys from different EV adoption studies. Further, based on the experts’ opinion, the factors were finalized, and order was arranged in each group like most important factor was considered first (e.g., in the cost-related factors, the purchase price of the vehicle is the most important factor in most of the studies followed by maintenance cost of the vehicle, cost of a battery, and resale value).

Table 4 Pairwise assessment matrix for cost-related factors

Barriers	C1	C2	C3	C4	Relative weight
C1	1	5	7	9	0.646
C2	0.200	1	4	7	0.230
C3	0.143	0.250	1	3	0.084
C4	0.111	0.143	0.333	1	0.041

Maximum eigenvalue = 4.254; CI = 0.085; CR = 0.094

Table 5 Pairwise assessment matrix for EV manufacturer-related factors

Barriers	M1	M2	M3	Relative weight
M1	1	5	9	0.743
M2	0.200	1	4	0.194
M3	0.111	0.250	1	0.063

Maximum eigenvalue = 3.071; CI = 0.036; CR = 0.062

Table 6 Pairwise assessment matrix for EV-related factors

Barriers	V1	V2	V3	V4	V5	V6	V7	Relative weight
V1	1	3	3	5	6	9	9	0.374
V2	0.333	1	3	6	8	6	7	0.254
V3	0.333	0.333	1	4	6	5	6	0.158
V4	0.200	0.167	0.250	1	3	3	5	0.108
V5	0.167	0.125	0.167	0.333	1	3	4	0.050
V6	0.111	0.167	0.200	0.333	0.333	1	3	0.034
V7	0.111	0.143	0.167	0.200	0.250	0.333	1	0.022

Maximum eigenvalue = 7.751; CI = 0.125; CR = 0.094

Table 7 Pairwise assessment matrix for EV technology-related factors

Barriers	T1	T2	T3	Relative weight
T1	1	5	9	0.743
T2	0.200	1	4	0.194
T3	0.111	0.250	1	0.063

Maximum eigenvalue = 3.071; CI = 0.036; CR = 0.062

Table 8 Pairwise assessment matrix for maintenance and service facility-related factors

Barriers	MS1	MS2	MS3	Relative weight
MS1	1	4	9	0.717
MS2	0.250	1	4	0.217
MS3	0.111	0.250	1	0.066

Maximum eigenvalue = 3.037; CI = 0.018; CR = 0.031

Table 9 Pairwise assessment matrix for charging facility-related factors

Barriers	CH1	CH2	CH3	Relative weight
CH1	1	6	8	0.761
CH2	0.167	1	3	0.166
CH3	0.125	0.333	1	0.073

Maximum eigenvalue = 3.074; CI = 0.037; CR = 0.063

Table 10 Pairwise assessment matrix for psychological factor related to charging of vehicle

Barriers	P1	P2	P3	Relative weight
P1	1	3	6	0.635
P2	0.333	1	5	0.287
P3	0.167	0.200	1	0.078

Maximum eigenvalue = 3.094; CI = 0.047; CR = 0.081

Table 11 Pairwise assessment matrix for driving safety and reliability-related factors

Barriers	DR1	DR2	DR3	Relative weight
DR1	1	3	6	0.644
DR2	0.333	1	4	0.271
DR3	0.167	0.250	1	0.085

Maximum eigenvalue = 3.054; CI = 0.027; CR = 0.046

Table 12 Pairwise assessment matrix for awareness-related factors

Barriers	A1	A2	A3	Relative weight
A1	1	6	9	0.770
A2	0.167	1	3	0.162
A3	0.111	0.333	1	0.068

Maximum eigenvalue = 3.054; CI = 0.027; CR = 0.046

6 Discussion and Conclusion

This study aimed to identify the factors related to EV adoption based on expert’s opinions on the present Indian EV market. The lists of influential factors were identified, and AHP approach was applied to identify the most important factors which were significant to EV adoption. The CR values of all the selected factors are within the limit, i.e., CR less than 0.1. From the AHP results, Table 4 shows that for cost related the higher purchase cost of EV (RW = 0.646) compared to conventional is the major barrier followed by vehicle and maintenance cost of EV (RW = 0.230). The cost of battery and resale value of EV are minor significant factor for EV adoption. This shows that at initial stage the purchase price matters than the resale value. The higher purchase price of EV has significant negative impact in the EV adoption. From Table 5, many EV manufacturers in the Indian EV market are new companies (RW = 0.743), especially in two-wheeler category which is a major barrier related to the EV manufacturer. Also, very limited number of model availability in each segments (RW = 0.194) plays a key role in EV adoption. Limited availability of dealership comes as a minor significant factor in this category with RW = 0.063. Related to the vehicle factors, the less mileage on full charge and technical specification of the vehicle like power, acceleration, etc., are the major significant factors with RW

of 0.347 and 0.254, respectively. The efficiency of vehicle on hilly and undulated terrain and overall maneuvering are the minor significant factors. This results show that users prefer EV for regular usage in city or highway where the overall cost savings will be advantageous, but the mileage and technical specification acts major barrier to consider the EV purchase decision. Related to EV Technology, Table 7 shows that the present non-reliable battery technology is the major barrier for the EV adoption. The lesser competitiveness with ICE technology is a minor significant barrier with $RW = 0.063$. Similarly, Table 8 shows that limited availability of local technician and service centers are the major significant factor related to maintenance and service with $RW = 0.717$ and $RW = 0.217$, respectively. Related to charging facility, limited availability of public charging facility is the major barrier with $RW = 0.761$. Similarly, higher charging time using slow charger and more waiting time at public charging stations are the significant barriers in user psychological related factors. Safety concern among high-speed vehicle flow on the highway and lack of understanding of subsidy policies are the major influential barrier related to driving safety and user awareness, respectively.

It is found that cost-related concerns are most significant among the road users, which is similar to the studies conducted by Bhosale et al. [29], Kumar et al. [30]. The availability of various models and inadequate public charging stations remains the concern of customers, which is in line with a number of studies conducted in India [29–31]. An increase in the number of local service centers for EVs, ease of availability of spare parts in the nearby market areas and increasing the number of public charging stations prove to be a confidence booster among the customers as they are bothered about the reliability of long trip travel using EVs. Also, a higher waiting time during charging of the EV is not desired by the users, which has to be rectified by encouraging turbocharging stations and other methods like battery swapping. The technical specifications of the EVs, such as speed, power, and acceleration, are unsatisfactory compared to fuel-based vehicles, which calls for the need for improvement in technology with the help of research and development. The sub-barriers are grouped under a category based on the expert's opinion. Explanatory factor analysis can be adopted for the grouping of sub-barriers in the future study. This study does not include users' socio-demographic and attitudinal factors, which is a limitation of this study. Further, the present study can be extended by incorporating user socio-demographic and attitudinal characteristics to find the EV adoption from customer perspective. Also, a policy framework study can be conducted to overcome a few of the identified barriers in this study. Further, more advanced methods like structural equation model can be used by considering the socio-economic factors of user and policy options to check the variation in the barriers. The outcome of this study will be helpful to the researcher, policymakers, and automotive key players who can incorporate the customer requirements at the time of decision making.

References

1. Teri (2019) Faster adoption of electric vehicles in India: perspective of consumers and industry. New Delhi
2. Chan CC, Wong YS (2004) Electric vehicles charge forward. *IEEE Power Energy Mag.* 2:24–33
3. Ernst and Young LLP (2019) Technical study of electric vehicles and charging infrastructure. *Bur Energy Effic* 455
4. Innovation Norway (2018) India EV story, emerging opportunities. <https://www.Innovasjon Norge.No/Contentassets/815Ebd0568D4490Aa91D0B2D5505Abe4/India-Ev-Story.Pdf> 1–74
5. Wu J, Liao H, Wang JW (2020) Analysis of consumer attitudes towards autonomous, connected, and electric vehicles: a survey in China. *Res Transp Econ* 80:100828. <https://doi.org/10.1016/j.retrec.2020.100828>
6. Ingeborgrud L, Ryghaug M (2016) User perceptions of EVs and the role of EVs in the transition to low-carbon mobility. *ECEEE Summer Study Proc* 1985:893–900
7. Bühler F, Cocron P, Neumann I et al (2014) Is EV experience related to EV acceptance? Results from a German field study. *Transp Res Part F Traffic Psychol Behav* 25:34–49. <https://doi.org/10.1016/j.trf.2014.05.002>
8. Zieffle M, Beul-Leusmann S, Kasugai K, Schwalm M (2014) Public perception and acceptance of electric vehicles: Exploring users' perceived benefits and drawbacks. In: *Lecture notes in computer science (including subseries lecture notes in artificial intelligence and lecture notes in bioinformatics)*, pp 628–639
9. Priessner A, Sposato R, Hampl N (2018) Predictors of electric vehicle adoption: an analysis of potential electric vehicle drivers in Austria. *Energy Policy* 122:701–714. <https://doi.org/10.1016/j.enpol.2018.07.058>
10. Weinert JX, Chaktan M, Yang X, Cherry CR (2007) Electric two-wheelers in China: Effect on travel behavior, mode shift, and user safety perceptions in a medium-sized city. *Transp Res Rec* 62–68. <https://doi.org/10.3141/2038-08>
11. Peters A, Dütschke E (2014) How do consumers perceive electric vehicles? A comparison of German consumer groups. *J Environ Policy Plan* 16:359–377. <https://doi.org/10.1080/1523908X.2013.879037>
12. Skippon S, Garwood M (2011) Responses to battery electric vehicles : UK consumer attitudes and attributions of symbolic meaning following direct experience to reduce psychological distance. *Transp Res Part D* 16:525–531. <https://doi.org/10.1016/j.trd.2011.05.005>
13. Egbue O, Long S, Samaranyake VA (2017) Mass deployment of sustainable transportation: evaluation of factors that influence electric vehicle adoption. *Clean Technol Environ Policy* 19:1927–1939. <https://doi.org/10.1007/s10098-017-1375-4>
14. Saaty TL (1999) Fundamentals of the analytic network process. *Proc ISAHP* 1999:1–14
15. Palcic I, Lalic B (2009) Analytical hierarchy process as a tool for selecting and evaluating projects. *Int J Simul Model* 8:16–26. [https://doi.org/10.2507/IJSIMM08\(1\)2.112](https://doi.org/10.2507/IJSIMM08(1)2.112)
16. Velasquez M, Hester PT (2013) An Analysis of multi-criteria decision-making methods. *Int J Oper Res* 10:56–66
17. Hamurcu M, Eren T (2018) Transportation planning with analytic hierarchy process and goal programming. *Int Adv Res Eng J* 02:92–97
18. Yannis G, Kopsacheili A, Dragomanovits A, Petraki V (2020) State-of-the-art review on multi-criteria decision-making in the transport sector. *J Traffic Transp Eng (English Ed)* 7:413–431. <https://doi.org/10.1016/j.jtte.2020.05.005>
19. Mohanty P, Kotak Y (2017) Electric vehicles: status and roadmap for India. In: *Electric vehicles: prospects and challenges*. Elsevier Inc., pp 387–414
20. Digalwar AK, Giridhar G (2015) Interpretive Structural modeling approach for development of electric vehicle market in India. In: *Procedia CIRP*. Elsevier B.V., pp 40–45
21. Priye S, Manoj M (2020) Exploring usage patterns and safety perceptions of the users of electric three-wheeled paratransit in Patna, India. *Case Stud Transp Policy* 8:39–48. <https://doi.org/10.1016/j.cstp.2020.01.001>

22. Jena R (2020) An empirical case study on Indian consumers' sentiment towards electric vehicles: a big data analytics approach. *Ind Mark Manag* 0–1. <https://doi.org/10.1016/j.indmarman.2019.12.012>
23. Saxena S, Gopal A, Phadke A (2014) Electrical consumption of two-, three- and four-wheel light-duty electric vehicles in India. *Appl Energy* 115:582–590. <https://doi.org/10.1016/j.apenergy.2013.10.043>
24. Tarei PK, Chand P, Gupta H (2021) Barriers to the adoption of electric vehicles: evidence from India. *J Clean Prod* 291:125847. <https://doi.org/10.1016/j.jclepro.2021.125847>
25. Möser G, Bamberg S (2008) The effectiveness of soft transport policy measures: a critical assessment and meta-analysis of empirical evidence. *J Environ Psychol* 28:10–26. <https://doi.org/10.1016/j.jenvp.2007.09.001>
26. Rabello Quadros SG, Nassi CD (2015) An evaluation on the criteria to prioritize transportation infrastructure investments in Brazil. *Transp Policy* 40:8–16. <https://doi.org/10.1016/j.tranpol.2015.02.002>
27. Saaty TL (1986) Axiomatization of the analytic hierarchy process. 91–108
28. Saaty TL (2000) Fundamentals of decision making and priority theory with the analytic hierarchy process. RWS Publications
29. Bhosale AP, Gholap A, Mastud SA, Bhosale DG (2019) A research on market status and purchasing decision influencing parameters for electric vehicles: Indian context. *Int J Recent Technol Eng* 8:2700–2706. <https://doi.org/10.35940/ijrte.B1331.0982S1119>
30. Kumar R, Jha A, Damodaran A et al (2020) Addressing the challenges to electric vehicle adoption via sharing economy: an Indian perspective. *Manag Environ Qual Int J* 32:82–99. <https://doi.org/10.1108/MEQ-03-2020-0058>
31. Alamelu R, Sivasundaram Anushan C, Selvabaskar SG (2015) Preference of E-bike by women in India—A niche market for auto manufacturers. *Bus Theory Pract* 16:25–30. <https://doi.org/10.3846/btp.2015.431>

Investigating the Influencing Factors to Adopt Public Electric Vehicle Charging Facility at Existing Fueling Station: A Study Based on Users Perceptive



Manivel Murugan, Sankaran Marisamynathan, and Tejas Panjwani

Abstract This study aims to identify the influencing factors that affect users' acceptance of plug-in charging stations or battery swapping stations (BSSs) facilities to charge their electric vehicles. After conducting a detailed literature review, the authors identified the motivating and demotivating factors affecting road users using the charging method at the existing fueling station. Further, a questionnaire survey was conducted to the visitors at the selected fueling station in Ahmedabad city, India. A total of 592 samples were collected and used for the analysis. This study used partial least square-structural equation modeling (PLS-SEM) to determine the relationship between motivating factors and demotivating with users' willingness to use the charging method at the existing fueling station. The study result shows that if charging facilities are available on existing fuel pump people shows their willingness to purchase EV; the step taken by the government of India to install charging facilities at existing fueling stations increases electric mobility in the country. The study further indicates that very large numbers of respondents are willing to select plug-in charging methods compared to the battery swapping method though more charging time will be required to charge a battery of EV. This study outcome would help the service provider establish EV charging stations with either a plug-in charging method or battery swapping method at their existing fueling station. Also, this study would help the transport planner to identify the feasible charging facility for public EV charging.

Keywords Electric vehicle · Plug-in charging station · Battery swapping station · Structural equation modeling · Charging facility

M. Murugan · S. Marisamynathan (✉)
Department of Civil Engineering, National Institute of Technology Tiruchirappalli,
Tiruchirappalli, Tamil Nadu, India
e-mail: marisamy@nitt.edu

T. Panjwani
Department of Civil Engineering, Pandit Deendayal Energy University, Gandhinagar, Gujarat,
India

1 Introduction

After China, India has the second-highest populated country in the world. The population density of India has been increasing for the last decade consequently. The rate of vehicles on the road is also jumped. The transport sector is the fastest-growing infrastructure in India. India is the 4th largest transportation sector in the world. This continued growth in the transportation sector leads to greenhouse gas (GHG) emissions, creating great concern for the environment and humans. One of the significant reasons to create GHG emission issues occurs due to the existence of a large number of ICE vehicles in the automobile industry. Electric vehicles are a significant alternative to achieve a completely eco-friendly transportation system by reducing GHG. Moreover, India imports crude oil from overseas countries so that EVs can reduce this dependency of oil on the automobile sector. Along with the reduction of greenhouse gas emission, EV has other advantages also like the running cost of EV is very less compare to ICE vehicle; maintenance costs are also less; performance parameters such as speed, acceleration of the vehicle are also powerful enough as the ICE vehicles, and it is also helping in reducing local air pollution. Majorly, two types of EV are available in the market: plug-in hybrid electric vehicle and battery electric vehicle. Plug-in hybrid electric vehicle (PHEV) has an electric battery and an IC engine. The electric battery is charged by an external source (plug). An electric battery fully powers a battery electric vehicle (BEV). They have no engine in vehicles. Also, they need an external power point to charge the battery. EV is a new technology in the Indian automobile market. To increase the sale of EVs, the government's support is a must to the EV industry. In this regard, government of India has launched so many initiatives to push for electric mobility in India. The government of India has launched the Faster Adoption and Manufacturing of (Hybrid) and Electric Vehicles (FAME-1) scheme in 2015, whose objective is to encourage the use of electric vehicles by providing subsidies. India has also launched Phase-II of the FAME Scheme in the year 2019, whose main aim is to establish 2700 charging stations across India in upcoming years. Till now, a total of 970 charging stations are installed in India up to March 2021. India is still struggling to get more number of EV on roads. Less than 1% EV is sales of the total vehicle sales. The major barrier to the adoption of EVs in India is lack of charging infrastructure, charging time, driving range, lack of awareness, and lack of EV manufacturers. The barriers like charging time and driving range can be minimized by improving charging infrastructure installed on a large scale in the existing road network at a regular interval. Presently, there are most commonly two ways of charging EVs, plug-in charging method and battery swapping method. The time-span electric vehicle takes to recharge in plug-in charging is about 30–50 min which is higher than fueling the current ICE vehicles. To overcome this situation, battery swapping is the ideal alternative. Replace discharge battery with charged one within about 5–10 min at battery store, which is highly recommendable than plug-in charging method. The battery swapping system also provides an advantage while purchasing a vehicle, like consumers don't need to buy a battery which also decreases the primary cost of the vehicle. It also secures customers questions

regarding battery span, as it solves the apprehensiveness of users about battery run for a long period. If a charging station is installed over the existing fueling station, service providers (fueling station owners) can install it because ready infrastructure is available with a service provider. They do not have to purchase land to install it, and also, it can spread awareness about EVs to regular users visiting fueling stations. This can motivate the ICE users to use EV and thus directly affect increasing the EV adoption rate.

Most of the existing research is about finding the charging station's location or its operation and management problem. But, these studies not considered the willingness of road users to select the charging facility of an electric vehicle. As the author discussed above, the government has to install at least one kiosk at the existing fueling station. So, before it applies, it is necessary to determine and understand the influence factors and effects on charging facilities to purchase electric vehicles rather than ICE vehicles among the Indian road users; by keeping in view the necessity author prompt to carry out this research. The following are the specific objective of this study.

1. To understand the user's willingness to shift on EV if the charging station is installed at the existing fueling station near their residential area or work area.
2. To identify road users' willingness to use the battery swapping method or plug-in charging method at the existing fueling station.
3. To identify the influence factor that affects users' acceptance to use plug-in charging method or battery swapping method facilities to charge their vehicle if charging facilities are available at the existing fueling station.

SEM method was adopted for the analysis to achieve the above objective. SEM is not only the statistical method but a framework of many different multivariable techniques. Many researchers used SEM to find out the relationship between the observed variable and unobserved variables in recent years. SEM can help us assess the measurement properties and test the proposed theoretical relationships using a single technique. The SEM purpose is to establish complex relationships which are not possible while using multiple regressions in SPSS. This study uses partial least square-structural equation modeling (PLS-SEM) to determine the relationship between motivating factors and demotivating with users willing to use the charging method at exiting fueling stations.

2 Review of Literature

A detailed literature review was conducted to find the influence factor affecting users selecting or using the charging method. At the initial stage, the government is planning to set the charging station on existing petrol stations. So, it is essential to identify the factors that affect the road users' perception to select a particular fueling station. In the second phase, the factor was found related to the user's perspective, which affects adopting EV. Further, the advantages and disadvantages of battery

swapping technology are identified. Finally, the hypothesis was developed at the end of this chapter based on literature for further analysis.

2.1 Users' Perception of the Choice of Fueling Stations

Fuel stations are the service industry, which deals with a person's day-to-day life [1]. As the demand for vehicles is rising, the fuel urging has also increased. However, as the low number of EVs is on-road, investors are not willing to install charging stations because the government is planning to install a charging station on fueling stations. So, there is a need first to find the factors affecting the user's perception to choose a fueling station. The main factor that affects people's perception is the location of the fueling station, whether it is near to residents, near to their workplace or destination, on the way to work location. The second most important factor is comfort and convenience, such as congestion at a station, service speed, waiting time, air service, water, and parking facilities. Other factors are also affecting for selection of fueling stations, such as type and price of fuel [2], company brand, quantity and quality of fuel, time taken to reach the station, and service speed [3, 4].

2.2 Factors Affecting EV Adoption-Users' Perspective

The major factors affecting EV adoption are classified in four main groups: lack of infrastructure, performance and operational, financial factors, and government policy. Charging infrastructure is the main key factor for developing a market of EVs [5]. Several authors have suggested that the lack of charging infrastructure is the main demotivating factor for consumers to buy EVs. Because of insufficient charging infrastructure, consumers tend to go toward other options than EV [6]. Barriers such as high time to refueling vehicle, lower range of EV and battery technology is coming under operation and performance category. Users are using a personal vehicle for the city and use it for a longer trip purpose [6]. The driving range of EVs is one of the main barriers affecting purchasing decisions [5, 7]. The range of EVs is almost five times low compared to conventional diesel or petrol vehicles, making users think again about going forward to the EV option for their use [8]. Because of the low range of vehicles, people use EVs only as a secondary option. Also, the charging time of EVs is very high compared to ICE vehicles [5, 6, 8, 9]. Although charging behavior is dependent on the vehicle battery size, type of charger [10]. ICE vehicles take only 2–3 min for fully refueling a vehicle, while current EV models take a minimum of 30 min to charge a vehicle which makes more conjunction at stations and making users unsure about shifting to EV [6]. Because of the low range and high time for refueling, EV sellers are trying to make changes in their battery technology, which is confusing the users to buy EVs now or wait for new technology [11]. The company is trying or experimenting with making or changing its battery technology to increase

the vehicle range. From an economic perspective, high-cost EV, the maintenance cost of EV, battery replacement cost are the barriers in the adopt EV. One of the biggest challenges in the EV adoption path is that the vehicle's initial cost is very high [5, 9, 12–14]. Two-thirds of cars purchased in India are between 5 and 7 lakhs in 2018. At the same time, the prices of the EV segment in India are starting from about 10 lakh to 12 lakh, which is more compere to the ICE vehicles segment [6]. Because of the high price and low range of vehicles, most people are unwilling to buy EVs. The other financial factor is the high maintenance cost of EV [9, 15]. EV technology is new for the automobile market, and as it is not much popular, servicing and repairing are a prime concern. And to resolve this issue, trained technicians are required [8]. However, there will be a lack of local service stations in the starting phase because of the non-availability of EV parts in the market. Fewer trained people will present, so consumers will have very few options available to service their EV due to the lower availability of technicians and fewer parts of the vehicle that could lead to high maintenance [9].

2.3 Battery Swapping Method

The battery swapping method is very beneficial compares to other EV charging methods. First, this method permits customers to continue their journey without spending more time charging EVs [16]. Secondly, slow charging speed at the charging station is a great concern. The battery swapping method consumes less waiting time than other available vehicle charging methods [16–18]. To add on, customers have no tension of battery life and warranty [17]. Because vehicle owners do not need to purchase a battery, they can pay only rent of battery, reducing the vehicle's initial cost [19, 20]. People know that BSM takes less time, but this method is not primarily used because users use it only as an alternative method for charge a vehicle [19]. The reason behind this mindset is customers' doubts about the quality of the exchange battery due to compatibility issues with vehicles [16, 19]. In addition, the battery design is a major barrier (hurdle) felt by customers for the battery swapping method because every manufacturer has its own design and battery size [16]. And if different manufacturers will agree to keep the common and universal design of the battery, this leads to limited innovation and effects on production development [16]. Consequently, charging batteries will affect battery life and lead to poor performance in the long run [21].

2.4 Smart PLS Approach in Transportation Research Work

Many researchers used smart PLS in recent years widely for their research purpose in the transportation field. For example, Youcef used a smart PLS approach to find out workers' job satisfaction with the transport department [22]. Also, this approach

was used by Nguyen to find the most impacting factors which affect smart city development. The author considers smart governance, smart economy, smart people, and environmental conditions of near that area [23]. The main objective of the Ammd study was to find out challenges regarding the construction safety field. The author uses a smart PLS approach to find out the most influential factors that affect workers' safety at construction work [24]. Abdul-kahar adam used the smart PLS approach to determine how work culture impacts job satisfaction of good governance in the transportation industry [25]. To find out the performance of the urban freight transport, Mourad and his team friend use the smart PLS approach for their research work [26]. The detailed methodology along with the data collection process is explained in the following section.

3 Methodology

The research was carried out in three phases. The first phase found out the factors using the literature survey and divided into groups under relevant constructs. The second phase comprises developing a questionnaire form and a pilot survey. The pilot survey aimed to notice the time taken to fill the survey form by participants and to check users' understanding of the questionnaire. After the preparation of questioners form, data were collected through offline surveys. In the third phase, the data were analyzed by using the PLS-SEM technique.

3.1 *Conceptual Framework of the Research*

This research aimed to find out influencing factors that affect willingness to prefer EV charging methods, including plug-in charging or battery swapping. After a detailed literature review study, the author predicts the hypotheses that can affect road users choosing the charging method. While preparing questionnaires, questions related to motivating road users for selection of charging method and questions related to demotivate the road users for selection of charging method either plug-in charging method or battery swapping method were incorporated. Based on the detailed literature study, the authors have formulated the following hypotheses. The conceptual PLS-SEM framework is shown in Fig. 1.

Hypothesis H1: The motivating factors to prefer plug-in charging facilities impacts positively on the user's willingness.

Hypothesis H2: The demotivating factors to prefer plug-in charging facilities negatively impact on user's willingness.

Hypothesis H3: The motivating factors to prefer battery swapping facilities positively impact on user's willingness.

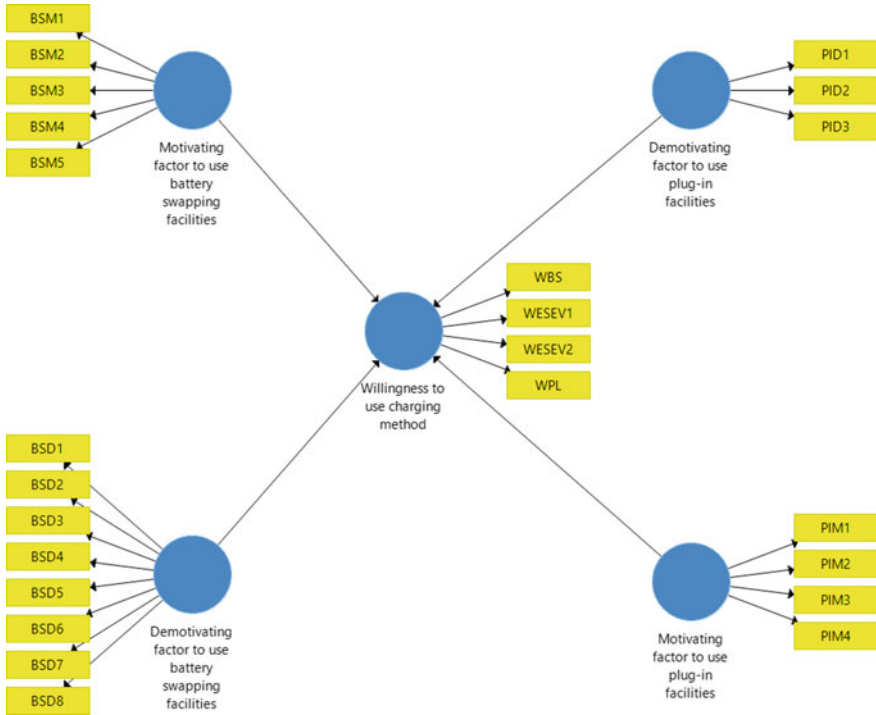


Fig. 1 Conceptual PLS-SEM framework

Hypothesis H4: The demotivating factors to prefer battery swapping facilities negatively impact on user’s willingness.

3.2 Preparations of Questionnaire and Data Collection

A well-designed questionnaire form was formulated, and the survey was conducted using the direct interview method. The list of factors considered for the survey and its notations is shown in Table 2. The survey was conducted by visiting the existing fueling stations at Ahmedabad, Gujarat. To avoid misinterpretation and make it easy for customers, the purpose of the study was explained. Customers who give consent for participating in survey work were requested to fill a questionnaire form. Customers who are not aware of electric vehicle technology were explained about EV, plug-in charging, and battery swapping methods. Total 21 numbers existing fueling stations were selected from Ahmedabad city were visited during offline survey work. The data were stored using Likert scale (5 = strongly agree, 4 = agree, 3 = neutral, 2 = disagree, 1 = strongly disagree). A total of 592 responses were received, and the same was used for the analysis. The details of the participants are shown in Table 1.

Table 1 Details of the participants

Profile of respondents		Responses	Percentage
Gender	Male	410	69
	Female	182	31
Age	<20	16	3
	20–30	315	53
	31–40	105	18
	41–50	67	11
	51–60	67	11
	>60	22	4
Members are in the household	1	2	0
	2	29	5
	3	131	22
	4	205	35
	5	107	18
	6	118	20
	More than 6	62	10
Education background	No schooling	3	1
	High school or lower	39	7
	Diploma/Undergraduate	97	16
	Graduate	328	55
	Postgraduate	117	20
	Ph.D. and higher	8	1
Occupation	Student	172	29
	Government employee	110	19
	Private employee	172	29
	Business/Freelancer	71	12
	Not working	67	11
Annual family Income	Up to 2.5lakh	89	15
	2.5–5 lakhs	140	24
	5–7.5 lakhs	143	24
	7.5–10 lakhs	93	16
	10–12.5 lakhs	67	11
	12.5–15 lakhs	23	4
	Above 15 lakhs	37	6
The number of Electric vehicle	0	551	93
	1	33	6
	2	3	1

(continued)

Table 1 (continued)

Profile of respondents		Responses	Percentage
	More than 2	0	0
Are you aware about battery replacement method?	Very well aware	96	15
	Aware	199	34
	Natural	92	16
	Not aware	161	27
	Not aware at all	45	8

Analysis indicates that 69% of respondents are male, and 31% are female participated in survey work. 53% of participants belong to age 20–30 years, and 18% are between ages 31–40 years; 11% are between 41 and 50 years; 11% are between 51 and 60 years, and 4% are above 60 years. Considering the educational point of view, 55% of participants have a graduate degree, and 20% have postgraduate degrees. This indicates that major persuasion received from well-educated participants indicates that the feedback received seems realistic and truthful. It is also noticed from the above table that 7% of participants have EVs. This proves that the development of the EV market in India is limited. Further, in point of awareness of battery swapping method, 33% of responders are aware that 16% are very well aware, and 51% are not aware and give neutral opinions.

4 Data Analysis and Results

4.1 Structure Equation Modeling

In second generation, structure equation modeling (SEM) was used by many researchers to find relationships between a dependent variable and an indented variable. This study aims to find the influence factor that affects the willingness of users to use the charging method at the existing fueling station. SEM has been applied by two approaches covariance-based approach and variance-based approach. In this study, partial least square SEM was used for analysis. The main advantage of using PLS is that it can be applied in small sample size, and also, no need to have normalized data while using PLS [27]. Smart PLS 3 software was used for analysis. PLS is an approach, and smart PLS is software to carry out this approach. PLS path model consists of two elements (1) structural model displays the relationship between the construct; (2) measurement model displays the relationship between construct and variables. A measurement model is used to check the consistency and validity of our dataset. And structure model is used to check the hypothesis.

Table 2 Constructs with outer loading

Construct	Indicators	Description	Outer loading
Motivating factor to use plug-in facilities	PIM1	EV can be used for long-distance travel because of the availability of charging facilities at existing fueling stations	0.830
	PIM2	Flexibility to charge the vehicle in nearby refuel station with fast charging facility	0.840
	PIM3	Higher confidence to use EV for regular purpose	0.824
Demotivating factor to use plug-in facilities	PID1	Higher waiting time at charging station	0.736
	PID2	Non-availability cost standards for charging the vehicle	0.746
	PID3	Nonstandard battery design in terms of type, size, capacity, and brand	0.846
Motivating factor to use battery swapping facilities	BSM1	The initial purchase cost of an electric vehicle will reduce drastically if battery cost is excluded (as user only need to rent and not own battery)	0.684
	BSM2	Waiting time of battery swapping is very less compared to charging vehicle	0.695
	BSM3	A highly convenient method to adopt which reduce range anxiety	0.783
	BSM4	Overall maintenance cost of the vehicle will be less	0.747
	BSM5	No tension about battery life and warranty	0.690
Demotivating factor to use battery swapping facilities	BSD1	Compatibility issue with the vehicle for the different manufacturer which will be very difficult to standardize	0.783
	BSD2	Changes of damaging components of the vehicle due to variation in power supply	0.764
	BSD3	Addition cost for lease on the battery	0.767
	BSD4	Life of battery might be different: non-reliable range of the swapped battery accurately	0.795

(continued)

Table 2 (continued)

Construct	Indicators	Description	Outer loading
	BSD5	I feel the battery swapping method is a temporary solution	0.659
	BSD6	Non-availability of proper business models about battery swapping in rural/remote location	0.774
	BSD7	The EV batteries might be replaced with fake battery	0.707
	BSD8	Handling/swapping issue of battery to female and elder user because of higher weight	0.666
Willingness to use a charging method	WBS	Would you prefer to adopt a battery swapping facility at the existing fueling station	0.603
	WESEV1	Are you willing to shift from conventional vehicle to Electric vehicle	0.679
	WESEV2	If public charging facility for EV will be provided in the fuel station, will you shift to EV?	0.754
	WPL	Would you prefer to adopt a plug-in charging facility at the existing fueling station	0.703

4.2 Evaluation of Measurement Model

Smart PLS 3 was used to assess the model. A measurement model is assessed by calculating internal consistency reliability, indicator reliability, convergent validity, and discriminant validity. By using indicator reliability, the relationship between latent variables to measure variables can be identified. The relationship was found by using factor loading. The threshold reliability should be at least 0.5–0.6 [28]. During the analysis, PIM4 was found less than 0.6, and it was removed to improve the reliability. The constructs and their outer loadings are shown in Table 2.

The purpose of internal consistency is to understand whether our measurement items represent the construct. The internal reliability of our construct was tested by using Cronbach’s alpha and composite reliability (CR). The threshold value of CR is higher than 0.708 [29]. The average variance extracted (AVE) was used to evaluate the convergent validity. To obtain ample convergent validity, the AVE value should be at least required 0.5 [28]. The value of AVE and CR is represented in below Table 3.

Discriminant validity is used to find the uniqueness of the construct. The cross-loading and Fornell–Larcker’s criterion is the two types of discriminant validity that exist. Applying Fornell–Larcker’s criterion needs a latent variable that should have

Table 3 Results of measurement model

Construct	Composite reliability (CR)	AVE
Motivating factor to use plug-in facilities	0.870	0.691
Demotivating factor to use plug-in facilities	0.820	0.604
Motivating factor to use battery swapping facilities	0.844	0.520
Demotivating factor to use battery swapping facilities	0.907	0.549
Willingness to use a charging method	0.764	0.503

more variance with its assigned indicator than other latent variables. The square root of the AVE of each construct should be higher than its highest correlation with their construct. The latent construct is shown in off-diagonal elements in Table 4.

Table 4 Correlations among the constructs

Constructs	Demotivating factor to use battery swapping facilities	Demotivating factor to use plug-in facilities	Motivating factor to use battery swapping facilities	Motivating factor to use plug-in facilities	Willingness to use a charging method
Demotivating factor to use battery swapping facilities	0.741				
Demotivating factor to use plug-in facilities	0.673	0.777			
Motivating factor to use battery swapping facilities	-0.362	-0.349	0.721		
Motivating factor to use plug-in facilities	-0.207	-0.236	0.429	0.831	
Willingness to use charging method	-0.301	-0.228	0.560	0.511	0.670

4.3 Evaluation of Structural Model

The structural model reflects the paths hypothesized in the research framework. The model's goodness is determined by the strength of each structural path determined by the R^2 value for the dependent variable [30]. The value for R^2 should be equal to or over 0.1 [31]. The result of R^2 in this model is 0.416. Applying the bootstrapping procedure (5000 bootstrap samples) provides the p -values (Table 4). In structural models, connected paths to latent variables represent the hypothesis. Path coefficients are used to determine how strong the relationship between dependent and independent variables. Bootstrapping technique used to calculate path coefficients, along with t -statistics. Author had considered 5000 sub-sample for bootstrapping, and the results are shown below Table 5.

H1 evaluates whether the motivating factor for plug-in charging facilities positively impacts users' willingness. The result shows that the motivating factor for plug-in charging facilities positively impacts on user's willingness ($\beta = 0.332$, $t = 7.899$, $p = 0.000$). Hence, H1 was supported. H2 evaluates whether demotivating factors prefer plug-in charging facilities, which will negatively impact users' willingness. The result shows that the demotivating factor for plug-in facilities does not negatively impact user willingness ($\beta = 0.088$, $t = 1.834$, $p = 0.067$). Hence, H2 was not supported. H3 evaluates whether motivating factors to prefer battery swapping facilities which positively impact on user's willingness. The result shows that the motivating factor for battery swapping facilities positively impacted user willingness ($\beta = 0.395$, $t = 9.052$, $p = 0.000$) H3 was supported. H4 evaluates whether demotivating factors to prefer battery swapping facilities which negatively impact user's willingness. The result shows that demotivating factors for swapping facilities negatively impact users' willingness ($\beta = -0.148$, $t = 3.218$, $p = 0.001$). Hence, H4 was supported.

Table 5 Path coefficients and T -values

Hypothesis	T Statistics	P values	Inference
Motivating factor to use plug-in facilities -> willingness to use charging method (H1)	7.899	0.000	Significant
Demotivating factor to use plug-in facilities -> willingness to use charging method (H2)	1.834	0.067	Not significant
Motivating factor to use battery swapping facilities -> willingness to use charging method (H3)	9.052	0.000	Significant
Demotivating factor to use battery swapping facilities -> willingness to use charging method (H4)	3.218	0.001	Significant

4.4 Global Fit Index of the Model

For PLS path modeling, global fit measure (GOF) is obtained by the geometric mean of average communality and average R^2 shown in Eq. (1). GOF is useful to evaluate model fitness and explaining the power of the model. The cutoff value of GOF small, medium, and large is 0.1, 0.25, and 0.36, respectively [32].

$$\text{Goodness of Fit (GOF) Index} = \sqrt{\text{Average } R^2 \times \text{Average communality}} \quad (1)$$

The GOF for this model is 0.484, which shows that data fit the model satisfactory and have substantial (48.40%) predictive power in comparison with the baseline values. All the above results confirm that the measurement model and structural model are good and valid.

5 Discussion

From the results in Table 5, hypothesis H1 supports the hypothesis that the motivating factor in selecting plug-in charging method has had a significant positive effect on the willingness of participants to choose the plug-in method for charging their electric vehicle. It shows that people have high confidence to adopt EVs long distances, while charging facilities are available on the existing fueling station. Also, it creates more comfort and confidence in the customer. It is proved that the factor predicted/anticipated in the study in connection with motivating factors to adopt the plug-in charging method is correct. Also, the non-requirement of home-based charging facilities got a minimum factor loading in motivating factor. So, it was concluded by the author that users want both home-based charging facilities and charging facilities at the fueling station for them high confidantes and use EV as a primary method over ICE vehicle. Table 5 shows that hypothesis H2 developed in this study is not supported; it means that factors presume in hypothesis H2 negatively affect participants; however, loading factors show a very little positive effect on participants. It shows that though the factors considered conveying negative effects, participants are not ignoring the factors. The main reason to convey a negative effect on participants in the higher waiting time to charge the vehicle. It is a fact that higher waiting time requires people to be ready to go with the plug-in charging method by keeping other advantages like less running cost and low maintenance cost compared to conventional vehicles. It is necessary to highlight that when gasoline vehicles were introduced in the market, people hesitated to go with gasoline vehicles due to the higher waiting time for filling the gas tank. But nowadays, people are adjusted with compressed natural gas (CNG) vehicles by keeping in mind that CNG vehicles' running cost is much less than ICE. Currently, users observed that many gasoline pumps are established across India, and the waiting time for filling the tank is considerably reduced compared with the initial stage. It is assumed that the same theory

will be applicable in the case of electric vehicles. It shows that higher waiting time to charge EV having a negative effect on hypothesis is not extremely affected to participants as the EV market is in the developing stage. Further, it is obvious that the price of petrol and diesel is very high because of this running cost of an ICE vehicle is very much higher. In view of this, people are ready to consume more time to charge their vehicle if there will be less running cost. In concern of hypothesis in H3, Table 5 indicated that hypothesis is supported means factor considered as motivating factor to use battery swapping method have made a significant effect on the willingness of participants. People are attracted to go with the battery swapping method as very little time was spent by customers exchanging discharged batteries with fully charged batteries. In battery swapping, range and anxiety are very much reduced, and customers do not bother regarding battery life and warranty. Because they have to replace swapped battery again with another battery in the future during the swapping procedure. Customers also think that the vehicle's initial cost will be less and no need to purchase a new battery, and they have to pay a lease amount and only rent of battery. Table 5 shows that hypothesis H4 in this study is supported. SEM diagram path shows that factors considered for a hypothesis to demotivate the people to use the battery swapping method negatively affect willingness. It shows that the author's predictions considered before the study are true. The result shows that people are very much conscious regarding compatibility issues with vehicle manufacture. People were also thinking about the life of the swapped battery and worried regarding the replacement of the original battery with a fake battery. People are also not willing to use battery swapping methods because EV technology is new, and they are not sure whether battery swapping points will be available in rural/remote areas. These factors are majorly influenced by willingness, and participants are not ready to adopt the battery swapping method as the primary method. Study shows people are willing to adopt battery swapping method as a secondary method over plug-in charging method.

6 Conclusion

This study conducted by direct interview survey of 592 participants to explore willingness of road users to shift from ICE vehicle to EV and further to know willingness for adoption of plug-in charging method or battery swapping method to charge the vehicle. Smart PLS software is used for analysis. The collected data were used for structural equation modeling (SEM) to test the influence of different motivated and demotivated factors affecting the willingness of adoption of EV and select the method for EV charging at the existing fueling station. The study indicates that many respondents are showing their willingness to the adoption of EV. Results show that more people are attracted to show their willingness to adopt EV when public charging facilities are available at the nearby existing fuel stations. The study further indicates that very large numbers of respondents are willing to select plug-in charging methods compared to battery swapping methods to charge EV. More respondents are

selecting a plug-in charging method instead of the battery swapping method though there is a higher waiting time to charge the vehicle in the plug-in charging method. A larger number of respondents select plug-in charging method due to factors like increasing their confidence, flexibility to charge the vehicle in nearby fueling station, and maybe feeling the anxiety to adopt battery swapping method in connection to the battery like, possibilities to exchange with fake battery, nonstandard battery design in terms of type, size, capacity, and brand. It shows that people are ready to wait for their vehicle in the plug-in method because they don't want to replace their battery at the station. This study helps the service provider decide to install either a plug-in charging method or battery swapping method.

This study has evaluated the viewpoints of road users on EV charging stations and as they show reluctance toward purchasing electric vehicles due to several reasons. The majority of studies confirm that people are willing to adopt charging facilities if available on existing pumps. The government plans to set up a charging facility on current fuel stations to resolve this issue. According to the public's opinions, this research is proposed, but similarly, the fueling station owner's perspective also equally matters. So, there is a scope for studies in this field in the future, such as owner's expectations regarding government policies and subsidies and barriers and requirements to install efficient infrastructure for the EV charging station. Therefore, all these norms have to be considered for the completion of a successful EV business. Few studies have highlighted that the socioeconomic factors have influence on the use of charging facility. Socioeconomic factors were not considered in this study during the analysis which is the limitation. The influence of socioeconomic factors on users charging facility adoption is the future scope of this study.

References

1. Galankashi MR, Fallahiarezoudar E, Moazzami A et al (2018) An efficient integrated simulation—Taguchi approach for sales rate evaluation of a petrol station. *Neural Comput Appl* 29:1073–1085. <https://doi.org/10.1007/s00521-016-2491-5>
2. Brey JJ, Brey R, Carazo AF et al (2016) Incorporating refuelling behaviour and drivers' preferences in the design of alternative fuels infrastructure in a city. *Transp Res Part C Emerg Technol* 65:144–155. <https://doi.org/10.1016/j.trc.2016.01.004>
3. Kelley S (2018) Driver use and perceptions of refueling stations near freeways in a developing infrastructure for alternative fuel vehicles. *Soc Sci* 7. <https://doi.org/10.3390/socsci7110242>
4. Srinivasan T (2015) A study on consumer preferences of petroleum retail outlets. *IOSR J Bus Manag II* 17:2319–7668. <https://doi.org/10.9790/487X-17223540>
5. Nair S, Rao N, Mishra S, Patil A (2018) India's charging infrastructure—Biggest single point impediment in EV adaptation in India. In: 2017 IEEE transportation electrification conference ITEC-India 2017, 1–6 Jan 2018. <https://doi.org/10.1109/ITEC-India.2017.8333884>
6. Kumar R, Jha A, Damodaran A et al (2020) Addressing the challenges to electric vehicle adoption via sharing economy: an Indian perspective. *Manag Environ Qual An Int J* 32:82–99. <https://doi.org/10.1108/MEQ-03-2020-0058>
7. Noel L, Zarazua de Rubens G, Kester J, Sovacool BK (2020) Understanding the socio-technical nexus of Nordic electric vehicle (EV) barriers: a qualitative discussion of range, price, charging and knowledge. *Energy Policy* 138:111292. <https://doi.org/10.1016/j.enpol.2020.111292>

8. Aswani G, Singh J (2020) Electric vehicles in India: opportunities and challenges. *Int Conf Autom Comput Eng* 2018:65–71
9. Verma M, Verma A, Khan M (2020) Factors influencing the adoption of electric vehicles in Bengaluru. *Transp Dev Econ* 6:1–10. <https://doi.org/10.1007/s40890-020-0100-x>
10. Goel S, Sharma R, Rathore AK (2021) A review on barrier and challenges of electric vehicle in India and vehicle to grid optimisation. *Transp Eng* 4:100057. <https://doi.org/10.1016/j.treng.2021.100057>
11. Digalwar AK, Giridhar G (2015) Interpretive structural modeling approach for development of electric vehicle market in India. In: *Procedia CIRP*. Elsevier B.V., pp 40–45
12. Roma TIS, De LS, Di PR et al (2020) ScienceDirect accounting for attitudes and perceptions influencing users' willingness accounting for electric attitudes and perceptions users' willingness to purchase vehicles through influencing a hybrid choice modeling to p. *Transp Res Procedia* 45:467–474. <https://doi.org/10.1016/j.trpro.2020.03.040>
13. Adhikari M, Ghimire LP, Kim Y et al (2020) Identification and analysis of barriers against electric vehicle use. *Sustain* 12:1–20. <https://doi.org/10.3390/SU12124850>
14. Bireselioglu ME, Demirbag Kaplan M, Yilmaz BK (2018) Electric mobility in Europe: a comprehensive review of motivators and barriers in decision making processes. *Transp Res Part A Policy Pract* 109:1–13. <https://doi.org/10.1016/j.tra.2018.01.017>
15. Goel P, Sharma N, Mathiyazhagan K, Vimal KEK (2021) Government is trying but consumers are not buying: a barrier analysis for electric vehicle sales in India. *Sustain Prod Consum* 28:71–90. <https://doi.org/10.1016/j.spc.2021.03.029>
16. Ahmad F, Alam MS, Alsaidan IS, Shariff SM (2020) Battery swapping station for electric vehicles: opportunities and challenges. *IET Smart Grid* 3:280–286. <https://doi.org/10.1049/iet-stg.2019.0059>
17. Huang FH (2020) Understanding user acceptance of battery swapping service of sustainable transport: an empirical study of a battery swap station for electric scooters, Taiwan. *Int J Sustain Transp* 14:294–307. <https://doi.org/10.1080/15568318.2018.1547464>
18. Save B, Sheikh A, Goswami P (2019) Recent developments, challenges, and possible action plans for electric vehicle charging infrastructure in India. In: 2019 9th International conference on power and energy systems ICPES 2019. <https://doi.org/10.1109/ICPES47639.2019.9105530>
19. Bobanac V, Pandzic H, Capuder T (2018) Survey on electric vehicles and battery swapping stations: expectations of existing and future EV owners. In: 2018 IEEE international energy conference, ENERGYCON 2018, pp 1–6
20. Cheah L, Heywood J (2010) The cost of vehicle electrification : a literature review. *Fuel* 2–6
21. Sarker MR, Dvorkin Y, Ortega-Vazquez MA (2016) Optimal participation of an electric vehicle aggregator in day-ahead energy and reserve markets. *IEEE Trans Power Syst* 31:3506–3515. <https://doi.org/10.1109/TPWRS.2015.2496551>
22. Youcef S, Ahmed SS, Ahmed B (2016) The impact of job satisfaction on turnover intention by the existence of organizational commitment, and intent to stay as intermediates variables using approach PLS in sample worker department of transport Saida. *Management* 6:198–202. <https://doi.org/10.5923/j.mm.20160606.03>
23. Bui HK, Nguyen TN (2019) Factors impacting to smart city in Vietnam with SMARTPLS 3.0 software application. *Iioab* 10:1–8
24. Ammad S, Alaloul WS, Saad S, Qureshi AH (2021) Personal protective equipment (PPE) usage in construction projects: a systematic review and smart PLS approach. *Ain Shams Eng J*. <https://doi.org/10.1016/j.asej.2021.04.001>
25. Adam A-K, Salim N, Saadi A et al (2020) Asia Proceedings of social sciences (APSS) the importance of work culture on job satisfaction and good governance in the transportation industry. *Asia Proc Soc Sci* 6:20–24
26. Moufad I, Jawab F (2018) The determinants of the performance of the urban freight transport—An empirical analysis. In: 2018 International colloquium on logistics and supply chain management. *Logistiqua* 2018 0021266798, pp 99–104. <https://doi.org/10.1109/LOGISTIQUA.2018.8428296>

27. Hamdollah R, Baghaei P (2016) Partial least squares structural equation modeling with R. *Pract Assessment Res Eval* 21:1–16
28. Gefen D, Straub D (2005) A practical guide to factorial validity using PLS-graph: tutorial and annotated example. *Commun Assoc Inf Syst* 16. <https://doi.org/10.17705/1cais.01605>
29. Wasko MML, Faraj S (2005) Why should I share? Examining social capital and knowledge contribution in electronic networks of practice. *MIS Q Manag Inf Syst* 29:35–57. <https://doi.org/10.2307/25148667>
30. Briones Peñalver AJ, Bernal Conesa JA, de Nieves NC (2018) Analysis of corporate social responsibility in Spanish agribusiness and its influence on innovation and performance. *Corp Soc Responsib Environ Manag* 25:182–193. <https://doi.org/10.1002/csr.1448>
31. Falk RF, Miller NB (1992) A primer for soft modeling. University of Akron Press, p 80
32. Akter S, D'Ambra J, Ray P (2011) Trustworthiness in mHealth information services: an assessment of a hierarchical model with mediating and moderating effects using partial least squares (PLS). *J Am Soc Inf Sci Technol* 62:100–116. <https://doi.org/10.1002/asi.21442>

Public Bicycle Sharing System: A Global Synthesis of Literature and Future Research Directions



Samir J. Patel and Chetan R. Patel

Abstract The aim of this review paper is to portray inclusive and up-to-date material on the wide range of topics on PBSS research. It is observed that very limited articles are available that cover a broad literature review on the topic of PBSS and portray the findings and future research directions for the same. This compendium of research brings together some of the research articles published in the reputed peer-reviewed journals over the time horizon of the last 15 years about PBSS. The paper deliberates the leading conceptual and theoretical propositions beneath research in the field of PBSS and gave a brief review limited to barriers, solutions, and enablers of PBSS. The review result depicts that the topics such as barriers, solutions, and enablers are major focused area by researchers and practitioners. It is also observed that the burgeoning of PBSS research articles and PBSS programs both are noticeably increasing after 2005, however, very few articles are available that conduct a comprehensive review on the barriers, solutions, enablers of PBSS. Therefore, the primary objective of this paper is to provide a review of the studies on above mention topics for PBSS globally and identify their limitations and provide guidelines for future research directions in the area of PBSS to the researchers and practitioners.

Keywords Sustainable transport · Non-motorized transport · Public Bicycle sharing

1 Introduction

Public Bicycle Sharing programs have existed for almost 50 years and within this period it has been increased in both their popularity and acceptance in almost all continents of the world. Bike sharing has numbers of benefits and for this reason

S. J. Patel (✉)

Department of Civil Engineering, IITE, Indus University, Rancharda, Ahmedabad,
Gujarat 382115, India
e-mail: patelsamir141@gmail.com

C. R. Patel

SVNIT, Surat, India

© The Author(s), under exclusive license to Springer Nature Singapore Pte Ltd. 2023
M. V. L. R. Anjaneyulu et al. (eds.), *Recent Advances in Transportation Systems Engineering and Management*, Lecture Notes in Civil Engineering 261,
https://doi.org/10.1007/978-981-19-2273-2_57

869

city planners prefer to implement bike share programs in their cities for improving livability, environment, personnel savings, last mile connectivity, and health benefits [30]. Globally bike share programs are increasing rapidly and expanded from 05 numbers in 2000 to 1963 numbers in 2019. According to bike share world map of April 2019, 1963 programs around the world operating either small, medium or large scale PBSS programs with fleet size of nearly 14.85 million. Before year 2000 the PBSS was limited to few European countries. However, after year 2000 enthusiastic spurred was found to implement new PBSS in various other continents. Currently, the largest PBSS systems in terms of bicycle fleet size are in two Chinese cities, i.e., Hangzhou, Shanghai followed by Washington D.C, London, and Paris. However, European programs are very popular due to its effective utilization. The Institute for transportation and development policy (ITDP) provides two measurements for assessing performance of bike share programs [17]. An average number of daily trips per bicycle was considered as a first measurement and average bicycle trips per thousand residents per day within the system coverage area were considered as a second measurement for assessing reliability of bicycle sharing [30]. The global growth of PBSS has encouraged an vigorous response from transport researchers, which has resulting in burgeoning of PBSS research [11]. The topics such as docking station location, users' perceptions, redistribution system, system performance, route choice, safety analysis, accident analysis, motivators for PBSS, barriers for PBSS, etc. are the focused area in PBSS research. Out of that, topics like docking station location, redistribution systems, user perception, and factors influencing of PBSS are the majorly focused research area among researchers. However, very few articles were available which offer a comprehensive literature review on various PBSS topics. The available review articles by Shaheen et al. [35], Shaheen and Guzman [34], Mateo-Babiano [24], Si et al. [36] largely focused on the topic related to history of PBSS, users' perception to adopt PBSS and effectiveness of various bike share system and scientometric review of PBSS. The review articles by Shaheen et al. [35], Fishman et al. [12], Fishman [11, 10] mainly encompasses the PBSS literature and research which conducted recently from North America, Asia, Europe, and Australia. The article by Fishman [11] covers the literature review across a variety of PBSS parameters, including its documented history and growth, user preferences, usage patterns, trip purpose, rebalancing, demographics of users, barriers for PBSS, impacts of PBSS, etc. The article by Mateo-Babiano [24] focuses on evaluation of bike share program and comparison of different program in Asian cities. The attempt made by Si et al. [36] encompasses the scientometric review of PBSS research from 2010 to 2018. In the scientometric review the network analysis of country, authors, articles, co-citation, journals, topics, top keywords used, cluster analysis, etc. are analyzed using citation data in the Citespace software. However, all the above literature articles are failed to discuss on the critical topics such as barriers, solutions, enablers of PBSS and its methodology, research findings as well as critical research gaps. Therefore, it is very important to fill this gap and to redress this limited research. To attain this, present paper discusses available academic literature on numerous topics of PBSS such as PBSS systematic and bibliographical analysis in Sect. 2, Identification of barriers, solutions, and enablers in Sect. 3, and finally portrays the findings, research

gaps, and future scope of work in Sect. 4 which will help the planners and researchers to open the new opportunities in the PBSS research. In conclusion, this compendium of literature will provide wide range of documented research articles from reputed journals on variety of topics. This approach would help practitioners and researchers to select the specific theme for PBSS research and those articles further help to shortlist the articles related to respective theme of the research.

2 PBSS Systematic Review and Bibliographical Analysis

For any study and to identify the research gap a systematic review process is must. A process of conducting systematic review is an explicit, reproducing, and comprehensive method for synthesizing, evaluating, and identifying the recorded work which is explored by practitioners and researchers [28]. The flow diagram for systematic review carried out in this study is presented in Fig. 1.

The literature search is carried out with the help of Scopus database search engines using keywords “Public bicycle sharing” and “Public bike sharing”. The result found 829 articles initially. Later, 293 articles are shortlisted based on articles published in last 15 years from 2004 to 2019. Finally, 132 articles are reviewed and analyzed for further discussion. Figure 2 represents the results of literature search and analysis about the rapid rise of PBS Programs and growing academic articles on similar topics from January 1995 to December 2019.

Figure 2 clearly shows that trends of PBSS program implementation and research conducted on PBSS burgeoning consistently after 2005.

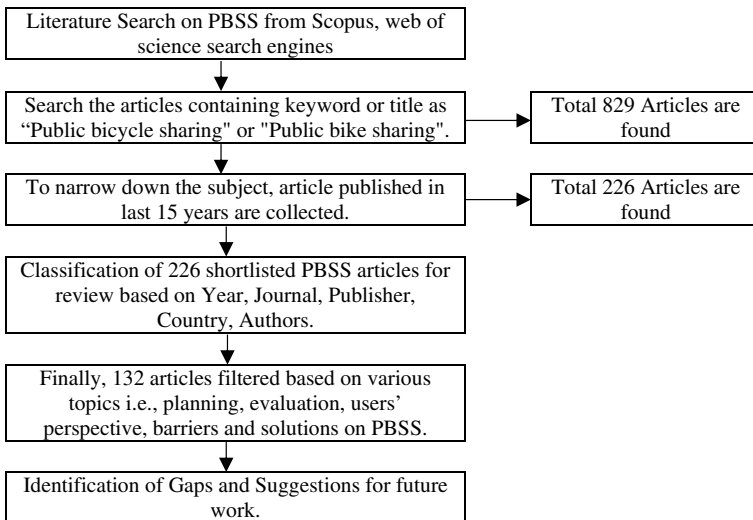


Fig. 1 Flow diagram for systematic review

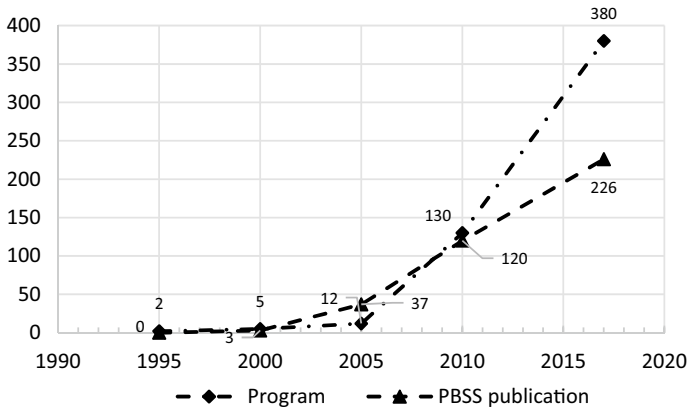


Fig. 2 Year-wise list of PBSS programs and publications

Further, the Distribution of PBSS research articles according to journal is analyzed and presented in Table 1.

Among the all reputed journals, the PBSS research articles are majority published in Transportation Research Record (TRR) followed by International Journal of Sustainable Transportation, Transportation Research Part A: Policy and Practice, Journal of Transport Geography, and Transport Reviews. The PBSS literature has been conducted in and around 28 countries across the globe. Table 2 provides the distribution of top ten countries that contributed in PBSS research.

Table 1 Distribution of PBSS research articles according to journal

Name of Journal	Article (%)	Name of Journal	Article (%)
Transportation Research Record	9.735	Sustainability	1.77
International Journal of Sustainable Transportation	7.08	Transportation Research Part F: Traffic Psychology and Behavior	1.77
Transportation Research Part A: Policy and Practice	6.637	Accident Analysis and Prevention	1.327
Journal of Transport Geography	5.31	American Journal of Public Health	1.327
Transport Reviews	2.655	Applied Geography	1.327
Journal of Urban Planning and Development	2.212	Journal of Physical Activity Health	1.327
Preventive Medicine	2.212	Journal of Transport Health	1.327
Transportation Research Part D: Transport and Environment	2.212	Transportation Research Part C: Emerging Technologies	1.327
American Journal of Preventive Medicine	1.77	Other journals	47
PLOS One	1.77		

Table 2 Distribution of PBSS articles according to countries

Country	Articles (%)
USA	25.60
Canada	11.95
Peoples R. China	11.26
Australia	7.85
England	7.51
Spain	7.17
Netherlands	6.14
Taiwan	3.41
France	2.39
Japan	1.71

The USA contributes the highest percentage of articles around 33%. The other countries such as Canada, China, Australia, and England are major countries and having substantial number of research articles and hold the second, third, fourth, and fifth positions, respectively. The PBSS articles are found significantly low in other countries which indicates that there are ample opportunities to conduct research on PBSS. The USA, Canada, and China alone contributed almost 50 percent of the total research articles.

3 Identification of Barriers, Solutions, and Enablers of PBSS

The PBSS is a non-motorized public transport mode that is commonly used for short-distance trips in university campuses, central business districts, and neighborhoods of city. It also serves as a feeder link between public transit stations to a destination of commuters [2]. Bicycle sharing system may offer additional benefits to the users than the apparent ones. The apparent benefits such as improved air quality [14], ecological impacts [14], personal financial savings, health [3, 14], convenience, space savings, reduction in investments, high catchment areas with low cost, last mile are the major contribution by PBSS. Apart from that several indirect or additional benefits such as improved business sales [3], Time savings [3], reduction in accident [14], political advantages [7], social advances [7] are also viewed as important contributors.

However, some of the study conducted by Parkin et al. [29], Handy and Xing [13], Zhao et al. [46] reveals that certain barriers like absence of cycle-friendly policy, habits of individual, safety, unavailability of empty docks, insufficient docking stations, insufficient bicycles, lack of accessibility and longer trip distance are significantly affecting the adoption of bicycle as transport mode. Hence, it is very important to identify such barriers and exploring factors before PBSS implementation. Therefore, to explore the studies related to barriers, influencing factors, and solutions for

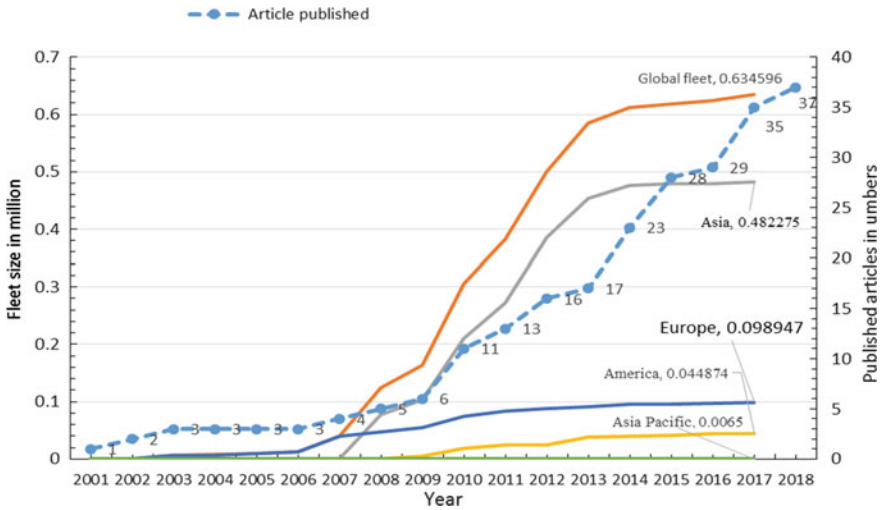


Fig. 3 Year-wise published articles (as on May 2018) and Global fleet size of PBSS (as on Dec-2017)

bicycle sharing systems further literature search is led using certain keywords such as “factor influencing bicycling”, “barriers of PBSS” and “deterrent to public bicycle sharing system”, etc. in Scopus database search engine which were published during 2001–2019. Figure 3 shows year-wise publication of articles published on barriers, solutions, and deterrents to public bicycle sharing systems.

Majority of articles are focused on personnel bicycling and very limited articles are found that concentrates on public bicycle sharing. Numerous studies are found on factors affecting bicycles as commuting mode [6, 13, 16, 43]. Based on the available literature it is further delineated into three categories, identification of barriers for bicycling, identification of solutions, and enablers for PBSS which are in detail discussed in following sections.

3.1 PBSS Barriers

PBSS is serving as a complementary mode for public transport still acceptance of PBSS by peer groups is questionable [4, 37]. Therefore, to implement PBSS successfully, it is very important for transport planners to identify the barriers prior to implementation. The numerous researchers conducted their studies investigating factors affecting the use of bicycle as commuting modes [6, 16, 43]. These investigations demonstrated that personal factors, social-economic factors, and physical factors are the major factors influencing cycling behavior in cities. Table 3 shows the list of barriers identified and reported by various researches.

Table 3 List of barriers reported by the various researches

S. No	List of barriers	Literature support
1	Risk perceptions and aberrant riding behaviors	Alexandros [26], Velasco [41]
2	Habit of Private mode of travel	FHWA [8], Moro et al. [25]
3	Number of signalize junctions	Verma et al. [42]
4	Negative Perception toward cycling	FHWA [8], Fishman et al. [12], Majumdar et al. [23]
5	Cost and value of time	FHWA [8], Stinson and Bhat [40]
6	Wealthy social status of citizen	FHWA [8], Majumdar et al. [23], Moro et al. [25]
7	Unsuitable demographic pattern of users	Majumdar et al. [23], Rastogi [33]
8	Lack of awareness for adopt NMT	Moro et al. [25], Winters et al. [44]
9	Poor tech-savvy level of citizen	Patel and [31]
10	Lack of priority and vision toward future plan for NMT development	Dhingra and Kodukula [5], Fishman et al. [12]
11	Poor enforcement policy regarding Traffic rules	Majumdar et al. [23], Velasco [41], Winters et al. [44]
12	Lack of provision of laws and regulations	Moro et al. [25]
13	Unsuitable dressing culture	Stinson and Bhat [39]
14	Lack of marketing strategy to promote NMT	Dhingra and Kodukula [5]
15	Lack of finance for NMT infrastructure development	Dhingra and Kodukula [5]
16	Lack of team involvement for implementation	Moro et al. [25]
17	Lack of finance for operation	Dhingra and Kodukula [5]
18	Unsuitable city structure	Rastogi [33], Majumdar et al. [23]
19	Need for high initial investment	Moro et al. [25]
20	Bad physical condition of road	Majumdar et al. [23], Wardman et al. [43], Winters et al. [44]
21	Unavailability of space for exclusive bicycle lane	Majumdar et al. [23], Rastogi [33]
22	Lack of simplicity and length of contract with the service provider	Moro et al. [25]
23	Poor intersection management	Winters et al. [44]
24	Absence of hierarchy of road network	FHWA [8]
25	Congested street	Majumdar et al. [23], Stinson and Bhat [39], Wardman et al. [43]
26	Higher land use density	Rastogi [33], Stinson and Bhat [40]
27	High travel time	FHWA [8]

(continued)

Table 3 (continued)

S. No	List of barriers	Literature support
28	Longer trip length	FHWA [8]
29	Multi-destination long trips	Stinson and Bhat [40]
30	Lack of continuity of bicycle lane	Wardman et al. [43]
31	A trip with more than one person or with cargo	Rastogi [32], Winters et al. [44]
32	Lack of last and first-mile connectivity for PT, IPT facilities	FHWA [8], Winters et al. [44],
33	Lack of know-how for planning NMT	Dhingra and Kodukula [5]
34	Steep terrain	FHWA [9], Wardman et al. [43]
35	Lack of IT infrastructure system	Patel and Patel [31]
36	The lack of readily availability of NMT components	Dhingra and Kodukula [5]
37	Unavailability for real-time big data	Patel and Patel [31]
38	High level of pollution	Patel and Patel [31]
39	No CCTV surveillance	Patel and Patel [31]
40	Unfavorable climatic conditions	FHWA [8], Majumdar et al. [23], Rastogi [33], Stinson and Bhat [39], Wardman et al. [43], Winters et al. [44]
41	Lack of traffic cell	Dhingra and Kodukula [5]

3.2 PBSS Solutions to Overcome PBSS Barriers

The solution approaches play a key role to overcome the influence of barriers. Therefore, the study related to motivators and solutions is extremely essential to highlight the aspects for successful implementation of PBSS. Various authors are exploring encouraging factors for cycling [45]. Heinen et al. [16] examined the work-related aspects on the choice of bicycle as a mode of commute in the four Dutch cities. The outcome of the study reveals that availability of bicycle parking nearer to the work area, positive attitude, a cloth changing amenities are the vital factors that upsurge the adoption of cycling. Dill and Carr [6] conclude that by developing infrastructure for bicycling is not sufficient to increase bicycle tradition but the network for the same should be connected at important locations [8]. Bicycle networks, paths, and lanes may also encourage commuters to adopt bicycle as mode of travel [8, 16, 36, 40].

The technical document published by FHWA [9] proposed to create complete and safe non-motorized transport infrastructure. FHWA adopted six principles namely Cohesion, Directness, Accessibility, Alternatives, comfort, Safety, and security from the Dutch CROW (Center for Research and Contract Standardization in Civil and Traffic Engineering) manual to evaluate pedestrian and bicyclist network facilities [9].

Verma et al. [42] recommended about providing dedicated bike lanes, separate parking infrastructure, separate signals, easy access around important locations, and integrating cycling with PT services would inspire commuters to use bicycles as regular mode. The awareness-raising activities such as awareness-raising campaigns, endorsing a bicycle through sportspersons or most followed celebrities, advertisements might encourage bicycle usage. Majumdar et al. [23] find the eighteen factors of urban characteristics like socio-economic analysis, city populations, a demographic pattern of users, a city structure, users' perception of bicycle mode choice which influence the use of bicycle in two cities Kharagpur and Asansol in India. According to Li et al. [20], people are more willing to choose cycle if the bicycle path is wider and the rental station is closer from their origin. The study by Heesch et al. [15] showed that motivators like quality of bicycle, subsidy on bicycle price, direct cycling routes, and cycling training helps in increasing bicycle commuting. The summary of the solutions identified by various researchers is presented in Table 4.

Table 4 List of solutions reported by various researchers

S. No	Solutions	Literature support
1	Spatial structure of PBSS	Dill and Carr [6], Li et al. [20]
2	Awareness raising	Winters et al. [44], Verma et al. [42]
3	Promotional schemes for users	Dhingra and Kodukula [5], Yang et al. [45]
4	Promotional schemes for manufactures	Yang et al. [45]
5	Government policies	Winters et al. [44], Verma et al. [42]
6	PBSS operation, maintenance, and redistribution of system (services)	Dhingra and Kodukula [5], Yang et al. [45]
7	Finance	Dhingra and Kodukula [5], Yang et al. [45], Karki and Tao [19]
8	Access and linkage	FHWA [8], Winters et al. [44]
9	Public space/personal amenities/refreshing aids	FHWA [8], Dhingra and Kodukula [5], Sirkis (2010), Heinen et al. [16]
10	Presence of bicycle facilities and bicycle infrastructure	Winters et al. [44], Heinen et al. [16], FHWA [9], Verma et al. [42]
11	Internet of things and big data	Patel and Patel [31]
12	Simplified approach	Heinen et al. [16]
13	Safety gadgets	Karki and Tao [19]
14	Provision of high-end E-bicycle	Nkurunziza et al. [27]

3.3 Enablers to Achieve Environmental Sustainability Through PBSS Implementation

The numerous researchers have documented the environmental sustainability through PBSS implementation in urban areas which include reduced fuel consumption; greenhouse gas (GHG) emissions; traffic congestion and noise; increased public transport use; enhanced accessibility; lower travel cost; improved cities livability; improved health and increased physical activity [21]. Therefore, it is very important to identify the enablers, which can reduce the effect of barriers as well as helps to implement solution approaches. The article by Karki and Tao [19] posted that community acceptance and customer satisfaction is the most important criteria in the success of any PBSS. In their study, the awareness-raising campaign, promotional schemes for users, traffic calming measures, effective implementation strategy are the key enablers identified to achieve customer satisfaction. The PBSS acceptance by peer group mainly depends upon the three basic criteria that are easy access and linkage to PBSS [36], equitable and affordable to all [19], and how safe and fast [16]. To achieve the access and linkage three parameters are essential, i.e., spatial planning of docking station, integration of PBSS with PT, and providing safe bicycle infrastructure with dedicate bicycle lane. The equitable and affordability can be achieved by various encouraging factors for the stakeholders, which invariably increases the ridership of PBSS. The users change their perception if promotional schemes such as free or concessional services, easily accessible payment option, and E-bicycle can be made available to them [27]. However, to support this promotional scheme, the government should exempt the taxes or provide subsidies or grants to the service providers and bicycle industries [19, 22]. Safety is the major concerning issue for the riders under heterogeneous traffic conditions which is majorly seen in developing countries. Undisciplined lane-changing the behavior of motorist vehicles in developing countries discourages the uses of bicycle as a mode of travel even in the case of a shorter ride. Therefore, conducting awareness-raising campaigns, education, and bicycle training program can improve the safety of bicyclists in urban traffic [6, 15, 19, 42, 44]. The reported enablers identified by numerous researchers are summarized and listed in Table 5, which supports the implementation of PBSS in developed and developing countries.

4 Way Forward and Conclusions

The aim of this study is to make comprehensive review on various topics of PBSS research carried out worldwide. Additionally, research topics on PBSS is highly varied depending upon the development of system county-wide. Therefore, to narrow down the study area, this study focuses to explore various topics that help in developing PBSS. Finally, The study results show that PBSS research is mainly dominated

Table 5 List of enablers for PBSS implementation

S. No.	Solutions	Literature support
1	Seamless transport	Jäppinen et al. [18]
2	Community acceptance by changing –ve perception	Karki and Tao [19], Patel and Patel [31]
3	Enforcement and enactment of legislation	Wardman et al. [43]
4	Spatial Structure	Dill and Carr [6]
5	Awareness-raising campaign and bicycle training program	Dill and Carr [6], Stinson and Bhat [39], Winters et al. [44], Heesch et al. [15], Nkurunziza et al. [27], Karki and Tao [19], Verma et al. [42]
6	Institute vision and policy	Sirkis [37], Verma et al. [42]
7	Encouraging factors for stakeholder	Karki and Tao [19], Maioli et al. [22]
8	Budget allocation	Dhingra and Kodukula [5]
9	Improve health, quality of life and air quality	Maioli et al. [22]
10	Customer satisfaction	Karki and Tao [19], Maioli et al. [22]
11	Traffic calming measures	Karki and Tao [19]
12	Access and linkage with PT	Stinson and Bhat [40], Winters et al. [44], Abolhassani et al. (2019)
13	Planning strategy for successful implementation of PBSS	Karki and Tao [19], Verma et al. [42]
14	Provide equity and safety	Karki and Tao [19]
15	Environmental sustainability	Lu et al. [21]
16	For operators subsidies, start-ups, technology transfer	Patel and Patel [31]
17	For users—E-bikes, Free services, simplified approach	Heinen et al. [16]
18	PBSS infrastructure and amenities	Heinen et al. [16]
19	Improve Ridership	Maioli et al. [22]
20	PBSS cell	Moro et al. [25]

among various broad themes that include planning of PBSS, redistribution of bicycles, people's perception toward bicycling and PBS, barriers, motivation, enablers in PBSS implementation. The analysis provides the current status of the research in terms of their findings, methodology adopted and issues investigated on different topics related to PBSS. The database for literature search are gathered from Scopus database search engines using keyword “Public Bicycle Sharing”, “Public Bike Sharing” and “Bicycle Sharing” and to narrow down the study area further, articles are shortlisted that were published between 2004 to 2019. It is also found that studies were reported with the uses of most advanced research tools and techniques in mathematical programming, and hypothesis testing along with the use of various software such as ArcGIS, SPSS, MATLAB, VISSUM, CUBE, Lingo, etc. Previously, very few

attempts have been made by Shaheen et al. [12, 35], Mateo-Babiano [24], Fishman [11], Si et al. [36] to encompass PBSS literature in single article. However, the critical review on findings, methodologies, and research gap pertaining to barriers and facilitators in implementing PBS system is missing. User's perception and hidden barriers play a major role in success of the PBS project and also affect the ridership in long run, if barriers are not addressed with appropriate solution approaches then chances of failure of PBSS may increase. Hence, this categorized PBSS literature review will facilitate practitioners and researchers to understand existing state of research including barriers and solutions in PBSS implementation. It also provides opportunities for future research directions.

This approach of systematic review will provide information regarding existing status of PBSS program worldwide, sequential growth of the same, research outcome by various studies, methods adopted, and challenging themes of PBSS research. This type of systematic review will help the budding researchers to ponder in to the PBSS research in depth.

The outcome of this study shows that PBSS program and its research both are growing rapidly after 2005 and significant rise is observed after the year 2010. Within last decade, it is observed that the developed countries are dominating in conducting PBSS-related researches whereas researches like planning of docking station location, optimum number of fleet size for PBS operation, effective redistribution strategies, and users/non-users perceptions are major one in developing nations. This is due to the introduction of new PBSS which has just taken a pace in these countries. Out of all reported studies majority are found with review of mathematical programming and conceptual analysis and very few studies are reported that show the statistics on bike share, status of bike share program, usage charges, user motivation, preference, and purpose of use, demographics of bike share users, scientometric review of PBSS, etc. Based on the reviewing the current literature and knowledge gain during the same, following are some of the avenues for future research directions in PBSS.

From the documented literature, it has been found that no study reported or attempted the systematic review on PBSS research and portrays findings, status of research work carryout in similar domain, critical research gaps, and future research directions in single article which can be an oasis for budding researchers.

Additionally, it is found that majority of work has been carried out considering only limited number of barriers and that to they are falling under the same classification or characteristics. Further, it is also important to understand the multiple effects of each barrier and cumulative effect of one or more barriers. If the study considering the classified barriers with cumulative or multiple effects is conducted, then it may provide better insight to the problem. Prioritization of such barriers or ranking of barriers and their solutions from perspective of different stakeholders using decision theories is hardly reported. The perceptive view of different stakeholders on PBSS implementation and PBSS acceptance or factors affecting PBSS ridership from user point of view in developed or developing countries is altogether missing which can be the best research in current climate-intensive research to motivate the users in adopting low carbon mobility.

Very few studies are found which discuss quantitative and qualitative assessment of barriers with limited number of the samples or data. In line with this, various articles have identified barriers and motivators to use PBSS. But how to overcome these using probable solution strategies to tackle the barriers and how logically they are linked is still a gray area in research.

References

1. Abolhassani L, Afghari AP, Borzadaran HM (2019) Public preferences towards bicycle sharing system in developing countries: the case of Mashhad, Iran. *Sustain Cities Soc* 44:763–773. <https://doi.org/10.1016/j.scs.2018.10.032>
2. Akar G, Clifton K (2009) Influence of individual perceptions and bicycle infrastructure on decision to bike. *Transp Res Rec: J Transp Res Board* 2140(2140):165–172. <https://doi.org/10.3141/2140-18>
3. Bullock C, Brereton F, Bailey S (2017) The economic contribution of public bike-share to the sustainability and efficient functioning of cities. *Sustain Cities Soc* 28:76–87 (Elsevier B.V). <https://doi.org/10.1016/j.scs.2016.08.024>
4. Campbell AA et al (2016) Factors influencing the choice of shared bicycles and shared electric bikes in Beijing. *Transp Res Part C: Emerging Technol* 67:399–414 <https://doi.org/10.1016/j.trc.2016.03.004> (Elsevier Ltd.)
5. Dhingra C, Kodukula SC (2010) Public bicycle schemes: applying the concept in developing cities
6. Dill J, Carr T (2003) Bicycle commuting and facilities in major U.S. cities: if you build them, commuters will use them. *Transp Res Rec: J Transp Res Board* 1828:116–123. <https://doi.org/10.3141/1828-14>
7. European Commission (1999) Cycling: the way ahead for towns and cities. <https://doi.org/10.2767/458972>
8. FHWA (1992) Case study No. 9: linking bicycle/pedestrian facilities with transit, national bicycling and walking study. Available at http://safety.fhwa.dot.gov/ped_bike/docs/case9.pdf
9. FHWA (2016) Noteworthy local policies that support safe and complete pedestrian and bicycle networks. Available at https://safety.fhwa.dot.gov/ped_bike/tools_solve/docs/fhwasa17006.pdf%0A, <https://trid.trb.org/view/1464800>
10. Fishman E (2016) Cycling as transport. Taylor and Francis 1647:1–8. <https://doi.org/10.1080/01441647.2015.1114271>
11. Fishman E (2016) Bikeshare: a review of recent literature. *Transp Rev* 36(1):92–113. <https://doi.org/10.1080/01441647.2015.1033036>
12. Fishman E, Washington S, Haworth N (2013) Bike share: a synthesis of the literature. *Transp Rev* 33(2):148–165. <https://doi.org/10.1080/01441647.2013.775612>
13. Handy SL, Xing Y (2011) Factors correlated with bicycle commuting: a study in six small U.S. cities. *Int J Sustain Transp* 5(2):91–110. <https://doi.org/10.1080/15568310903514789>
14. Hartog JJ De et al (2010) Review do the health benefits of cycling outweigh the risks ? *118(8):1109–1116*. <https://doi.org/10.1289/ehp.0901747>
15. Heesch KC, Sahlqvist S, Garrard J (2012) Gender differences in recreational and transport cycling: a cross-sectional mixed-methods comparison of cycling patterns, motivators, and constraints. *Int J Behav Nutr Phys Act* 9:1–12. <https://doi.org/10.1186/1479-5868-9-106>
16. Heinen E, Maat K, van Wee B (2013) The effect of work-related factors on the bicycle commute mode choice in the Netherlands. *Transportation* 40(1):23–43. <https://doi.org/10.1007/s11116-012-9399-4>
17. ITDP (2013) The bike-sharing planning guide. Institute for Transportation and Development Policy, p 152. Available at www.itpd.org

18. Jäppinen S, Toivonen T, Salonen M (2013) Modelling the potential effect of shared bicycles on public transport travel times in Greater Helsinki: an open data approach. *Appl Geogr* 43:13–24. <https://doi.org/10.1016/j.apgeog.2013.05.010> (Elsevier Ltd.)
19. Karki TK, Tao L (2016) How accessible and convenient are the public bicycle sharing programs in China? Experiences from Suzhou city. *Habitat Int* 53:188–194. <https://doi.org/10.1016/j.habitatint.2015.11.007> (Elsevier Ltd.)
20. Li M et al (2015) Identification of prior factors influencing the mode choice of short distance travel. *Discret Dyn Nat Soc*. <https://doi.org/10.1155/2015/795176>
21. Lu M et al (2018) Improving the sustainability of integrated transportation system with bike-sharing: a spatial agent-based approach. *Sustain Cities Soc* 41(March):44–51. <https://doi.org/10.1016/j.scs.2018.05.023> (Elsevier)
22. Maioli HC, de Carvalho RC, de Medeiros DD (2019) SERVBike: riding customer satisfaction of bicycle sharing service. *Sustain Cities Soc* 101680. <https://doi.org/10.1016/j.scs.2019.101680>
23. Majumdar BB, Mitra S, Pareek P (2015) Methodological framework to obtain key factors influencing choice of bicycle as a mode. *Transp Res Rec: J Transp Res Board* 2512:110–124. <https://doi.org/10.3141/2512-13>
24. Mateo-Babiano I (2015) Public bicycle sharing in Asian cities. In: Eastern Asia society for transportation studies conference (11th, EASTS, 2015), vol 11, p 15. <https://doi.org/10.11175/easts.11.60>
25. Moro SR et al. (2018) Barriers to bicycle sharing systems implementation: analysis of two unsuccessful PSS. In: *Procedia CIRP*, vol 73. Elsevier B.V., pp 191–196. <https://doi.org/10.1016/j.procir.2018.03.312>
26. Alexandros N (2016) The paradox of public acceptance of bike sharing in Gothenburg. *Proc Inst Civ Eng Eng Sustain* 169:101–113. <https://doi.org/10.1680/jensu.14.00070>
27. Nkurunziza A et al (2012) Examining the potential for modal change: motivators and barriers for bicycle commuting in Dar-es-salaam. *Transport Policy* 24:249–259. <https://doi.org/10.1016/j.tranpol.2012.09.002> (Elsevier)
28. Okoli C (2015) A guide to conducting a standalone systematic literature review. *Commun Assoc Inf Syst* 37(1):879–910. <https://doi.org/10.17705/1cais.03743>
29. Parkin J, Ryley T, Jones T (2007) Barriers to cycling : an exploration of quantitative analyses. In: *Cycling and society*, 67–82
30. Patel S, Patel C (2018) An Infrastructure review of public bicycle sharing system (PBSS) Global and Indian scenario. In: *Innovative research in transportation infrastructure*. Springer, Ahmedabad, pp 111–120. <https://doi.org/10.1007/978-981-13-2032-3>
31. Patel S, Patel C (2019) Prioritizing barriers for successful implementation of public bicycle sharing system. In: *Proceedings of the institution of civil engineers. Municipal Engineer*, pp 1–25. <https://doi.org/10.1680/jmuen.18.00068>
32. Rastogi R (2010) Willingness to shift to walking or bicycling to access suburban rail: case study of Mumbai, India. *J Urban Plan Dev* 136:3–10. [https://doi.org/10.1061/\(ASCE\)0733-9488\(2010\)136:1\(3\)](https://doi.org/10.1061/(ASCE)0733-9488(2010)136:1(3))
33. Rastogi R (2011) Promotion of non-motorized modes as a sustainable transportation option: policy and planning issues. *Curr Sci* 100(9):1340–1348
34. Shaheen SA, Guzman S (2011) Worldwide bikesharing. *Access* 39:22–27
35. Shaheen S, Guzman S, Zhang H (2010) Bikesharing in Europe, the Americas, and Asia. *Transp Res Rec: J Transp Res Board* 2143:159–167. <https://doi.org/10.3141/2143-20>
36. Si H et al (2019) Mapping the bike sharing research published from 2010 to 2018: A scientometric review. *J Clean Prod* 213:415–427. <https://doi.org/10.1016/j.jclepro.2018.12.157> (Elsevier Ltd.)
37. Sirkis A (2000) Bike networking in Rio: the challenges for non-motorised transport in an automobile-dominated government culture. *Local Environ* 5(1):83–95. <https://doi.org/10.1080/135498300113282>
38. Sirkis A (2010) The international journal of justice and sustainability bike networking in Rio: the challenges for non-motorised transport in an automobile- dominated government culture. *Local Environ* 37–41. <https://doi.org/10.1080/135498300113282>

39. Stinson MA, Bhat CR (2003) Analysis using a stated preference survey. *Transp Res Rec* 1828:107–115. <https://doi.org/10.3141%2F1828-13>
40. Stinson M, Bhat C (2004) Frequency of bicycle commuting: internet-based survey analysis. *Transp Res Rec: J Transp Res Board* 1878(512):122–130. <https://doi.org/10.3141/1878-15>
41. Velasco L (2015) Safety issues with elderly cyclists and barriers to cycling. *Proc Inst Civ Eng Munic Eng* 168(ME2):87–95. <https://doi.org/10.1680/muen.14.00003>
42. Verma M et al (2016) The factors influencing bicycling in the Bangalore city. *Transp Res Part A Policy Practice* 89:29–40. <https://doi.org/10.1016/j.tra.2016.04.006> (Elsevier Ltd.).
43. Wardman M, Tight M, Page M (2007) Factors influencing the propensity to cycle to work. *Transp Res Part A: Policy Practice* 41(4):339–350. <https://doi.org/10.1016/j.tra.2006.09.011>
44. Winters M et al (2011) Motivators and deterrents of bicycling: Comparing influences on decisions to ride. *Transportation* 38(1):153–168. <https://doi.org/10.1007/s11116-010-9284-y>
45. Yang J et al (2015) Major issues for biking revival in urban China. *Habitat Int* 47:176–182. <https://doi.org/10.1016/j.habitatint.2015.01.022> (Elsevier Ltd.)
46. Zhao C et al (2018) Cycling environmental perception in Beijing—A study of residents' attitudes towards future cycling and car purchasing. *Transport Policy*. 66:96–106. <https://doi.org/10.1016/j.tranpol.2018.02.004>

Travelers' Response to Network Disruptions in Ernakulam City



Navitha Valsalan, P. C. Haritha, and M. V. L. R. Anjaneyulu

Abstract The study aimed to investigate the travelers' response to network disruptions, considering Ernakulam city as the study area. Ernakulam city is one of the most congested cities in Kerala with growing travel demands and insufficient infrastructure. The entire study area was divided into 13 blocks, and analysis was done for each block separately. The concept of resilience is used as a connotation for measuring performance of road network. Resilience metrics used are classified into three categories which include connectivity-based metrics, centrality-based metrics, and performance-based metrics. Programs were written in Python programming language to compute the resilience metrics. Betweenness centrality and disruption details collected from past were used to identify the critical blocks: Edappally, Paravur, Palluruthy, and Vypeen. From the network analysis, it was observed that among the four critical blocks identified Paravur had the least loss of resilience value which makes it as the most resilient block within the city. To know the responses of people to a disruption, a Revealed-Stated preference (RP-SP) survey was organized. It was observed that the responses varied depending on the type of activity. Multinomial logistic regression analysis was conducted to identify the variables which significantly influence the travel decision-making process in the event of a disruption. The model results showed that personal and household characteristics and trip purpose significantly influence the response of individual to a network disruption.

Keywords Network analysis · Resilience · Traffic assignment

N. Valsalan (✉) · P. C. Haritha · M. V. L. R. Anjaneyulu
Department of Civil Engineering, National Institute of Technology Calicut, NITC PO,
Calicut 673601, India
e-mail: navithavalsalan@gmail.com

P. C. Haritha
e-mail: Haritha_p180099ce@nitc.ac.in

M. V. L. R. Anjaneyulu
e-mail: mvlr@nitc.ac.in

1 Introduction

1.1 General

One of the major issues our cities facing is the increase of travel demand with insufficient infrastructure. Transportation/road networks experience various disruptions which significantly affect their performance. The disruptions vary from day-to-day disruptions to rare natural disasters. To study the performance of road networks in case of disruption, the concept of resilience has been used in the recent years and is found promising. The ability of the system to reduce both the duration and magnitude of effects and bring it back to the desired level is the connotation of resilience. The resilience measurement of a facility is based on four attributes: robustness, redundancy, resourcefulness, and rapidity. So, here comes a need where the definition of the resilience has to be considered, on which the analysis can be done. Hence, it is better to understand resilience, so that a resilient network can be designed, which will be helpful in building better infrastructure.

1.2 Aim and Objectives

Aim of the study is to assess the performance of a road network, before, at, and after disruption incorporating the concept of free mobility. The objectives of the study are to develop a set of indicators for measurement of resilience of road network, identify the most resilient part within the study area, and to study the travel behavioral effects on shopping activity during a disruption.

2 Review of the Literature

Kattan et al. [1] investigated travel behavioral responses and responses to real-time information by conducting a survey for the road users. Data collection was done through survey for the road users. Findings on en-route information showed that driving experience, employment, and purpose of trip have significant effect on traveler's en-route decisions.

Marsden et al. [2] studied the travel behavior response to major transport systems' resilience by adopting engineering resilience-oriented approaches, which focus on returning assets to good workable order as soon as possible. Surveys were conducted to relate the impact of disruption on travelers, how society might implement better smarter disruption management plans. A questionnaire survey on overview of public perceptions of disruption and how they are experienced and managed was also done.

A study on passenger' travel behavior in response to unplanned transit disruptions was done by Golshani et al. [3]. An RP-SP survey was conducted to analyze the

willingness to wait during disruption. Also, various influencing factors were obtained through the study.

A study by Zhou et al. [4] on resilience of transportation systems reviewed various metrics and mathematical models used to measure resilience. The identified resilience metrics were classified into three which include topological metrics, attribute-based metrics, and performance-based metrics. Also, the various measurement techniques that were listed are optimization model, topological model, simulation model, probability theory model, fuzzy logic model, and data-driven model. Both the advantages and disadvantages of these measurement techniques were discussed briefly.

A study on resilience thinking in transport planning was done by Wang [5] to study the importance of resilience in transport planning. Four characteristics of resilience and their importance were studied in detail. Also, the importance of incorporating transformability in comprehensive resilience in transportation was studied.

A study on resilience and efficiency in transportation network was done by Ganin et al. [6] to study the interconnection between resilience and efficiency for road transportation networks. It was concluded from the study that resilience and efficiency are found to be uncorrelated for transportation system. And there is a characteristic difference in resilience for different urban areas.

Resilience modeling concept in transportation systems: a comprehensive review based on mode and modeling techniques was studied by Ahmed et al. [7] to quantify resilience and to identify improvement strategies. The various metrics identified were travel time reliability, vulnerability, travel demand, shortest path, restoration time, cost or budget, capacity, and resilience triangle. And the quantification techniques identified were optimization and simulation techniques.

A study on road network resilience: how to identify critical links subjected to day-to-day disruptions was done by Gauthier et al. [8]. Ranking of the links was done based on the various metrics considered. And merging static and topological metrics and demand-based metrics were done for the identification of the critical links.

An operational indicator for network mobility using fuzzy logic-based study was performed by Rashidy and Muller [9] to assess mobility of road transport network from network's perspective. Two types of attributes were considered in this study which include physical connectivity and traffic condition attribute. Two case studies were done. One is to assess the correlation between the proposed mobility indicator and geo distance per minute. The other one is to illustrate the ability of proposed mobility indicator to reflect the variation in travel demand. It was found that the proposed indicator was a better tool for understanding the dynamic nature of mobility under various disruptions.

Resilience in transportation system was studied by Martinson [10] to develop a value-based approach to deliver on resilience. The various metrics used include system resilience indicators, negative resilience indicators, process indicators, output indicators, and proxy impact indicators. Study was done through questionnaire survey to identify a resilient system, and indicators of resiliency were suggested as guidance for the measurement of resiliency.

A study on incorporating public transport in a methodology for assessing resilience in urban mobility performed by Azolin et al. [11] classified urban commuting trips as persistent, adaptive, and transformable trips based on maximum possible distance (MPD). It was concluded from the study that for shortest MPD walking and cycling is the preferred mode and for longer distances public transport routes will increase mobility options. Also, the spatial distribution of trips shows the relative importance of resilient trips and the cities' spatial structure. And incorporation of public transport routes has an impact on the level of accessibility of lower income users.

Most of the earlier works focused on the topological aspects of networks. Dynamic aspects like change in flow were not taken into consideration. Addition of a new link to improve network performance was also less studied. In most of the studies related to resilience measurement, capacity of the network elements was ignored during traffic assignment. Performance of the network with change in travel demand during disruptions is less studied. Recovery speed and time were not considered. Role of human beings in immediate response was not studied.

3 Indicators of Network Resilience

Twelve resilience metrics are identified for the present study from the review of the literature and are categorized into connectivity-based resilience metrics, centrality-based resilience metrics, and performance-based resilience metrics. The connectivity-based resilience metrics include cyclomatic number, alpha index, beta index, gamma index, eta index, and average degree. The centrality-based resilience metrics include closeness centrality, link betweenness centrality, degree centrality, and Eigen vector centrality. Performance-based resilience metrics include resilience triangle and network mobility index.

4 Methodology

Selection of Network

The first step of the study was the selection of the study area. Ernakulam city in Kerala state was chosen for the study.

Network Analysis

Second step is to perform the analysis of the selected road network. Adjacency and OD matrix for the network were prepared. Then, critical link identification was carried out based on link betweenness centrality. As part of this stage, the network was disrupted by sequential removal of links. Traffic assignment was done after each link removal. Resilience metrics were also calculated. Once the disruption was completed, revival of the network was carried out by restoring removed links back

to the original network. Resilience metrics were calculated at each revival phase. Based on the metrics, calculated inferences were drawn.

Revealed-Stated Preference Survey

Conduct RP-SP survey for understanding the behavior of people during disruption depending on the type of activity.

Model Development

Develop Multinomial logistic regression model for identifying the significant variables that affect the decision-making process.

5 Study Area and Context

Ernakulam district in Kerala is one of the most congested cities with insufficient road infrastructure. The district is located at the central part of the state, covering an area of 3000 square kilometers. Ernakulam district has well-connected road network with three National highways, State highways, and other roads. District has got maximum number of vehicles in the state. The city is susceptible to frequent disruptions due to the growing demand. During the floods in 2018, the district was intensely affected.

Digitization of Real Road Network

All the roads including National highways, State highways, and other roads were considered for the study. Digitization of the road network was performed in GIS software. Boundaries, roads, and junctions were converted into polygon, polyline, and point features. From the shape file attribute table, the link node details were obtained (Fig. 1).

The entire district was divided into 13 blocks which include Angamaly, Edappally, Pampakuda, Parakkadavu, Muvattupuzha, Palluruthy, Paravur, Vadavucode, Alangad, Vazhakulam, Vypeen, Kothamangalam, and Mulanthuruthy. Table 1 gives the number of links and nodes of the blocks.

6 Network Analysis

The first and foremost stage of network analysis begins with the identification of the critical blocks. For this purpose, two criteria were adopted which are based on the link betweenness centrality and collecting the disruption details which occurred in the city in past years. Adjacency metrics connecting the blocks were prepared in spreadsheets. Link betweenness centrality is basically the number of shortest paths traversing through the node pairs. Links were arranged based on their betweenness centrality in rank order. Also, from the past disruption collected within the district 13 blocks were arranged in its rank order. Based on above two criteria, four blocks,

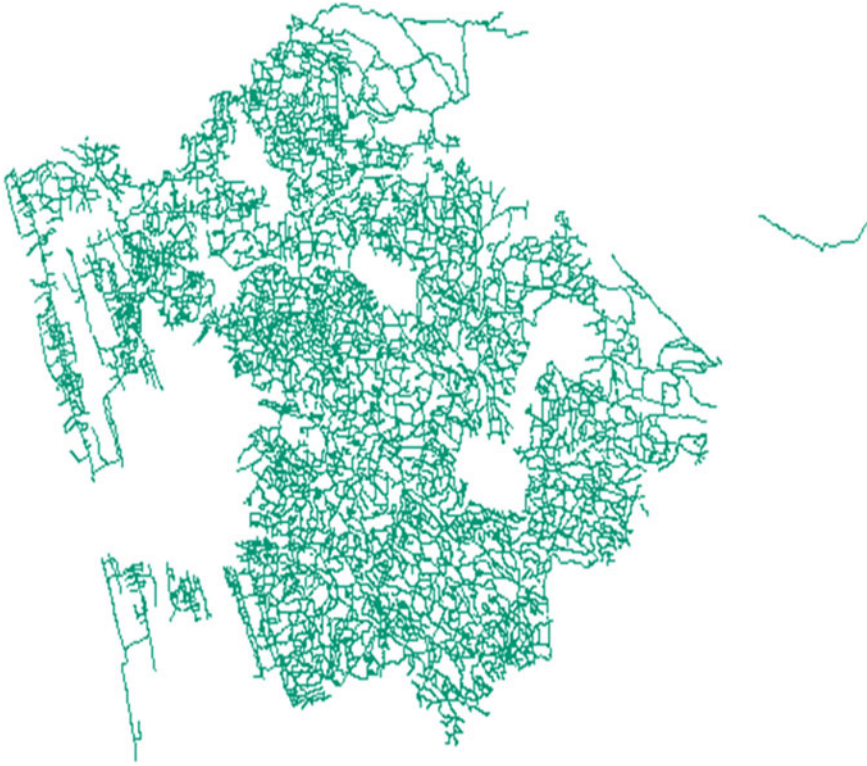


Fig. 1 Digitized road map of Ernakulam city

Table 1 Link-node details of blocks in Ernakulam

S. No.	Name of Block	Nodes	Links
1	Angamaly	530	322
2	Edappally	104	60
3	Pampakuda	522	327
4	Parakkadavu	204	204
5	Muvattupuzha	508	312
6	Palluruthy	121	69
7	Paravur	112	65
8	Vadavucode	548	327
9	Alangad	364	215
10	Vazhakulam	671	382
11	Vypeen	178	98
12	Kothamangalam	515	296
13	Mulanthuruthy	479	303

Edappally, Palluruthy, Vypeen, and Paravur, were identified as critical. For each of the blocks, analyses were then carried out separately. Adjacency matrix and origin–destination matrix were prepared in spreadsheets format. These were used as the inputs to prewritten programs for calculating the metrics considered for the study. Once the pre-disruption analysis was done, the networks were subjected to triggered disruption by the sequential removal of the links based on betweenness centrality. Metrics were calculated for each disruption phase.

In order to forecast future demand for existing routes, incremental assignment technique was used. For a network, the shortest path changes with the degree of traffic congestion. In this technique, demand is allotted to the shortest path having minimum travel time. Demand is assigned without considering capacity, and link time was revised in consideration of both volume and capacity.

After the removal of all the top rank-ordered links, the revival for the network was performed by restoring the removed links based on rank order. Metrics were calculated after restoring each link. Table 2 shows the percentage change in the resilience metrics when the links are disrupted.

As the links are removed simultaneously from the network, the connectivity between node/link pair is lost which makes the network vulnerable. Due to the reduction in the connectivity, the number of cycles present in the network also decreases; hence, cyclomatic number and alpha index have decreased. Also, with the decrease in number of links, the possible paths in the network get reduced which results in low beta and gamma indices. When disruption happens, criticality of the links changes making some links more important, and hence, more traffic is assigned to those links which makes them congested. Once the congested link crosses the assumed threshold value, trips become impossible through that link, which leads to lesser assignment of trips. Hence, satisfied demand decreases when the links are disrupted. Similarly,

Table 2 Percentage change in resilience metrics when links are disrupted for Ernakulam road network patterns

Metric	Edappally	Paravur	Vypeen	Palluruthy
Cyclomatic number	6.67	6.25	6.173	5.66
Alpha index	6.76	3.392	6.06	5.803
Beta index	5.025	4.483	5.263	4.388
Gamma index	5.102	4.568	5.376	4.145
Eta index	0.802	0.24	1.839	0.752
Average degree	5.025	4.823	5.26	4.388
Average closeness centrality	13.85	49.46	26.104	57.18
Average link betweenness centrality	19.976	31.37	19.687	20.631
Degree centrality	11.11	4.673	4.854	3.57
Eigen value centrality	55.89	15.467	61.61	10.54
Satisfied demand	13.41	11.559	24.847	7.686
Network mobility index	5.102	4.568	5.376	4.145

Table 3 Loss of resilience for Ernakulam road network

S. No.	Network	Loss of resilience
1	Edappally	1,193,760
2	Paravur	539,425
3	Vypeen	2,759,970
4	Palluruthy	593,690

when the links are restored, travel demand increases and reaches original state when revived completely.

As the satisfied demand is the indicator of system quality, it is being plotted against the time, to find the loss of resilience in transportation network. The area of the resilience triangle gives the resilience loss (RL) due to an event as given in Eq. 1.

$$\text{Loss of resilience, RL} = \int_{t_0}^{t_1} (100 - Q(t))dt \tag{1}$$

where

- t_0 Time of disruption
- t_1 Time of final revival
- $Q(t)$ Quality of the system.

Using shoelace formula, the area of the polygon formed from the time of disruption to final revival was found. Table 3 shows the loss of resilience value calculated for the four blocks in Ernakulam. It is evident that Paravur is the most resilient among the four critical blocks. Vypeen has the least resilience.

7 Revealed-Stated Preference Survey

7.1 Data Collection

The questionnaire consisted of six sections and 23 questions in total. The questionnaire included (1) Personal details, (2) Household details, (3) Travel details, (4) Past disruption details, and (5) Hypothetical disruption details.

The survey was conducted through online mode via Google forms and also offline mode by direct interview. A total of 400 samples were collected. Survey covered 42 major areas within the district. The activities considered for analyzing the response of individual are work, shopping, education, recreation, medical, drop/pick up, religious, bill payment and other offices, and social visits. The respondents were asked to indicate what they did in case of disruption due to floods in 2018. The nine options given are (1) Will continue as planned before, (2) Will cancel the travel, (3) Will reschedule to some other time on the same day, (4) Will reschedule to some other

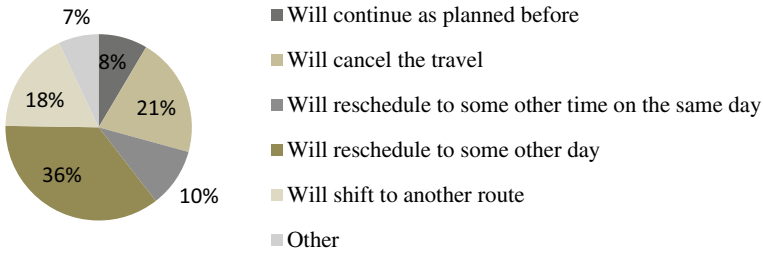


Fig. 2 Response of individual for shopping trip due to disruptions

day, (5) Will wait for the situation to clear, (6) Will shift to another route, (7) Will shift to other mode of private transport in the same route, (8) Will shift to other mode of public transport in the same route, and (9) Will change destination of travel.

7.2 Descriptive Statistics

The proportion of male and female respondents is 46% and 54%, respectively. According to the last census data (2011), the district is composed of 49% male and 51% female. Hence, the collected data of male and female respondents represents the population. 68% of the respondents belonged to the age group of 18–25 years. This is because major portion of the samples was obtained by online survey. 45% of the respondents are graduates. Nearly 32% of the survey participants are private employees who make trips regularly. 38% of the respondents have monthly income in the range of INR 10,000–25,000. 48% of the respondents are having driving license.

61% of the respondents belong to household size of 4, which influences the number of trips. 39% of the respondents had an income in the range of INR 25,000 to 50,000. Around 36% of the respondents have faced disruption some weeks back followed by 28% in last month. 38% of the respondents have faced disruption to travel due to road closure due to repair/maintenance. 28% have faced service disruption due to construction on roads.

For shopping trips, 30% of the people opted to reschedule to some other time on the same day and 22% people chose to cancel the trip. Figure 2 shows the responses of the surveyed persons with respect to shopping trips.

7.3 Modeling Travelers' Response to Travel Disruptions

Multinomial logistic regression (MNL) technique was used to understand the behavioral response of individual to disruption to travel in Ernakulam. Statistical tool was used for analysis of the collected data. The probability of choosing an alternative i

from a set of j alternatives is given in Eq. 2.

$$P(i) = \frac{\exp(V_i)}{\sum_{j=1}^j \exp(V_j)} \quad (2)$$

where

$P(i)$ probability of the decision maker choosing alternative i

V_j systematic component of the utility of alternative j .

The following were considered as alternatives available to the respondents for different travel purposes in case of disruption to network:

1. Will continue as planned before
2. Will cancel the travel
3. Will reschedule to some other time on the same day
4. Will reschedule to some other day
5. Will wait for the situation to clear
6. Will shift to another route
7. Will shift to other mode of private transport in the same route
8. Will shift to other mode of public transport in the same route
9. Will change destination of travel.

From the preliminary analysis of survey data for shopping activity, it was observed that least number of responses was marked against will wait for the situation to clear, will shift to other private mode of transport in the same route, will shift to other public mode of transport in the same route, and will change destination of travel. Hence, all these responses were grouped into other. Table 4 shows the significant variables chosen for modeling.

Table 5 shows the model fitting information for the travelers' response for shopping trips. Null hypothesis, that there is no significant relationship between the dependent variable and the independent variables, is rejected. There is a significant relationship between the dependent variable and the independent variables.

Table 6 shows the Pseudo R-square values obtained for the model. The R-square values indicate that the model is a reasonably good model.

Table 7 shows the parameter estimates for travelers' response to shopping trip disruptions. B value represents the estimated MNL regression coefficients for the various estimated parameters. $\text{Exp}(B)$ is the odds ratio, which indicates the change in odds resulting from a unit change in the predictor. It indicates the odds of the response being in the comparison category compared with respect to being in the reference category, which is not opting the particular response. If the value is greater than 1, then it indicates that as the predictor value increases, odd of the outcome occurring increases.

Coefficients were estimated for all the variables. Variables having p value ≤ 0.05 were considered as significant and included in the final model. A positive coefficient denotes positive relation between that independent and the dependent variable.

Table 4 Summary of the variables and coding

Variable	Level	Coding
Gender	Male	0
	Female	1
Occupation	Student	0
	Seeking employment	1
	Part-time employed	2
	Government employee	3
	Private employee	4
	Self-employed	5
	Retired	6
	Homemaker	7
Type of driving license	Two-wheeler	0
	Four-wheeler	1
	Heavy vehicle	2
	Do not have driving license	3
Household size	1	0
	2	1
	3	2
	4	3
	5	4
	6	5
	7	6
	8	7
	9	8
	10	9
	More than 10	10
Monthly household income	Less than 25,000	0
	25,001–50,000	1
	50,001–1,00,000	2
	1,00,001–2,00,000	3
	2,00,001–5,00,000	4
	Above 5,00,000	5
Number of vehicles in the household (car)	0	0
	1	1
	2	2
	More than 2	3
Elderly in the household	0	0

(continued)

Table 4 (continued)

Variable	Level	Coding
	1	1
	2	2
	More than 2	3
Route selection criteria (purpose of travel)	No	0
	Yes	1
Type of disruption	Road closure due to repair/maintenance	0
	Construction	1
	Processions on road	2
	Road accident	3
	Heavy rainfall	4
	Natural disaster (e.g., flood)	5
Response to shopping trip due to disruptions	Will continue as planned before	1
	Will cancel the travel	2
	Will reschedule to some other time on the same day	3
	Will reschedule to some other day	4
	Will shift to another route	5
	Other	6

Table 5 MNL model fitting information for shopping trips

Model	Model fitting criteria-2 log Likelihood	Chi-square	df	Sig.
Intercept only	282.409			
Final	863.644	418.765	250	0.000

Table 6 Pseudo *R*-square value

Cox and snell	0.652
Nagelkerke	0.677
McFadden	0.323

Multinomial logistic regression analysis performed above shows the influence of various parameters on the travelers’ decision-making procedure. Male respondents with positive coefficient and having odd ratio greater than one imply that males had the greater tendency to continue the trip/shifting to another route than canceling or rescheduling it. This indicates that males have greater risk-taking behavior as compared to females. Similarly, private and Government employees have the tendency to continue the trip, shift to another route, or wait for the situation to clear. This is because working people are daily trip makers, and they will be familiar with all the routes in case a route is non-functional. On the other hand,

Table 7 Parameter estimates for travelers' response to shopping trip disruption

Response	Intercept	<i>B</i>	Sig.	Exp(<i>B</i>)
Will continue as planned before	Gender (male)	-0.267	0.003	
	Occupation (private employee)	0.253	0.025	1.288
	Driving license (two-wheeler)	0.831	0.003	2.296
	Household size (4)	0.719	0.002	0.002
	Number of cars in the household (2)	-2.363	0.002	0.094
	Elderly in the household (2)	-0.380	0.008	0.684
	Type of disruption (Heavy rainfall)	4.331	0.006	76.053
Will cancel the travel	Intercept	4.721	0.008	
	Gender (male)	-0.308	0.017	0.738
	Occupation (retired)	0.511	0.044	1.667
	Household size (6)	1.663	0.001	5.274
	Elderly in the household (2)	0.055	0.003	1.057
	Type of disruption (road construction)	2.391	0.000	10.92
Will reschedule to some other time on the same day	Intercept	-6.605	0.012	
	Occupation (govt. employee)	5.539	0.019	254.393
	Driving license (two-wheeler)	0.527	0.016	1.694
	Household size (6)	3.399	0.032	29.934
	Route selection criteria (purpose of travel)	0.359	0.020	1.432
	Type of disruption (heavy rainfall)	1.317	0.006	3.73
Will reschedule to some other day	Intercept	13.567	0.089	
	Gender (male)	-1.412	0.038	0.244
	Occupation (retired)	2.610	0.009	13.599
	Driving license (two-wheeler)	-1.96	0.044	0.822
	Household size (6)	5.028	0.012	152.57
	Household monthly income (25,000-50,000)	6.857	0.001	950.51
	Number of vehicles in the household (car = 1)	1.685	0.038	5.390
	Elderly in the household (2)	0.392	0.026	1.480

(continued)

Table 7 (continued)

Response	Intercept	<i>B</i>	Sig.	Exp(<i>B</i>)
	Type of disruption (heavy rainfall)	3.803	0.022	44.84
Will Shift To other route	Intercept	0.647	0.000	
	Gender (male)	1.571	0.027	4.811
	Occupation (private employee)	3.194	0.012	24.393
	Household size (6)	1.371	0.000	3.938
	Elderly in the household (2)	-0.273	0.019	0.761
	Type of disruption (accident)	4.106	0.000	60.680
Other (will wait for the situation to clear, mode shift, change destination)	Intercept	1.07	0.000	
	Gender (male)	-1.571	0.002	0.208
	Occupation (govt. employee)	4.174	0.02	64.97
	Household size (6)	-0.212	0.000	0.468
	Elderly in the household (2)	-0.293	0.009	0.746
	Type of disruption (construction)	2.913	0.02	18.44

retired persons opt to either cancel the trip or reschedule the trip. It was also observed that individuals with two-wheeler license tend to continue the trip or shift to other route rather than canceling the trip/rescheduling.

Persons with elderly people in the house tend to cancel the trip/reschedule it to some other time/day as evident from the positive coefficients and greater odd ratio. This shows that elderly people have less risk-taking behavior as compared to other age group people. Also, with the increase in the household size, persons choose to cancel the trip/reschedule the trip. Persons from household with higher income have the tendency to reschedule the trip rather than waiting for the situation to clear which they might result in loss of time. Higher the household car ownership, higher the chances of rescheduling the trips. Type of disruption also had significant effect on the decision-making purpose. In case of accident/road construction/maintenance, the respondents were ready to shift to another route. While in case of heavy rainfall, people tend to cancel their trip or reschedule the trip to some other day/time.

8 Conclusions

Twelve metrics were identified from the literature review, and they were grouped into centrality-related resilience metrics, connectivity-based resilience metrics, and performance-based resilience metrics. Analysis of the whole district network

revealed that four blocks as critical blocks. Among the four critical blocks, Vypeen is the least resilient block with greater loss of resilience in case of disruption. Thus, in case of disruption or any natural disaster greater precautions has to be taken in recovering these critical blocks. Also, improvement to the present network can be also done based on the results of the study.

RP-SP Survey indicated that respondents choose to reschedule shopping trips to some other day or cancel the trip, which means that shopping trips get significantly affected due to disruptions to road network.

MNL models developed for shopping trips showed that variables like gender, occupation, driving license type, number of vehicles in the household, household size, household monthly income, type of disruption, and purpose of travel significantly influence the travelers' response to disruptions for shopping trips.

The procedure opted for the study can be extended to other road networks to assess its resilience comparing it with the study.

References

1. Kattan I, Barros AG, Saleemi H (2013) Travel behavior changes and response to advanced traveller information in prolonged and large-scale network disruptions: a case study of west LRT line construction in the city of Calgary. *Transp Res Part F* 21:90–102.
2. Marsden G, Anable J, Shires J (2016) Travel behavior response to major transport systems resilience. *International Transport Forum*
3. Golshani N, Rashmi E, Shabanpour R, Mohammadian K (2020) Passenger' travel behavior in response to unplanned transit disruptions. An thesis report submitted to Department of Civil & Materials Engineering, University of Illinois at Chicago
4. Zhou Y, Wang J, Yang H (2018) Resilience of transportation systems. *IEEE Trans Intell Transp System* 20(12)
5. Wang JYT (2015) Resilience thinking' in transport planning. In: *Civil engineering and environmental systems*, vol 32, no 1–2, pp 180–191
6. Ganin AA, Kitsak M, Marchese D, Keisler JM, Seager T, Linkov I (2020) Resilience and efficiency in transportation network. *Sci Adv*
7. Ahmed S, Dey K (2020) Resilience modeling concept in transportation systems—A comprehensive review based on mode and modeling techniques. *J Infrastruct Preserv Resil*
8. Gauthier P, Furno A, Faousi NE (2018) Road network resilience: how to identify critical links subject to day to day disruptions. *Transp Res Rec*
9. Rashidy RA, Muller SM (2014) An operational indicator for network mobility using fuzzy logic. A thesis report submitted to Institute of transport studies
10. Martinson R (2017) Resilience in a transportation system. *Transp Res Circ*
11. Azolin LG, Silva AN, Pinto N (2020) Incorporating public transport in a methodology for assessing resilience in urban mobility. *Transp Res Part D* 85

User Perceived Service Quality of Indian Railway Platform Using Structural Equation Modeling and Importance-Performance Map Analysis: A Case Study of Tiruchirappalli Railway Junction



Rameshwar Metage and Darshana Othayoth 

Abstract The Indian Railway (IR) is one of the oldest public transport systems in India. Over the period, many changes have happened in railway services. In this study, user perceived service quality of the Tiruchirappalli railway junction platform is carried out, which is the second-largest railway station in Tamil Nadu. Three hundred samples have been collected through a web-based survey using Google Forms and an on-board data collection survey. The satisfaction of users toward various services is measured using 22 different indicators of five constructs. All ratings are taken on Likert's five-point scale. Structural equation modeling (SEM) results show that all the five constructs have positive and significant effect on the overall service quality of the platform. Based on importance-performance map analysis (IPMA) results, facilities like waiting area, refreshment, and behavior of ticket inspector require more attention when compared to other factors. This study provides insight to planners and experts to understand which is the most important attributes for improving the user perceived service quality of railway platforms.

Keywords User perception · Structural equation model · Importance-performance map analysis

1 Introduction

The Indian Railway (IR), more than 150 years old, is among one of the largest and oldest systems in the world, fondly called by people as the 'Lifeline of the Nation' [1]. To handle passengers, proper and sufficient services must be provided. Services provided at platforms are equally important as the services provided inside the vehicle. The IR services can be divided into three broad categories, namely online services, on-board services, and facilities at platforms. There are many studies which

R. Metage · D. Othayoth (✉)
NIT Tiruchirappalli, Tiruchirappalli, India
e-mail: darshana@nitt.edu

focus on quality of railway service, but very less studies can be found on railway platform service quality.

Waiting at platforms may range from 10 min to several hours under some emergent conditions, especially in India where probability of train getting late is quite normal. So, in such cases, poor services at platform will just add to overall bad experience of passenger's journey. Evaluation of service quality is important to efficiently allocate resources for improvement of service quality.

Satisfaction from service quality is usually evaluated in terms of technical quality and functional quality [2]. Transit Cooperative Research Plan (TCRP) Report 100 (Chap. "Analyzing Traffic Performance of Toll Plazas Using Performance Box: A Case Study") defines transit quality as 'the overall measured or perceived performance of transit service from the passenger's point of view'. Service quality can be evaluated from different perspectives, operators' perspective, in which we identify the gap between the targeted and delivered service quality, passengers' perspective, in which we identify the gap between the expected and perceived service quality and integrated perspective, where we combine both perspectives. In this study, user's perspective has been incorporated, which is in growing interest in the view of researchers and policy makers.

2 Objectives

The study was carried out with the following objectives:

- To identify the attributes that influence the user's perception of service quality of Indian railway platforms.
- To perform bivariate analysis to understand the effects of demographical indicators on the satisfaction of overall service quality.
- To check the validation of proposed path relationships in the study, using confirmatory factor analysis and path analysis.
- To identify indicators to be concentrated on to improve the service quality of platforms.

3 Literature Review

According to the study conducted by Geetika and Nandan [3], availability and quality of refreshments, effectiveness of information systems, behavior of railway staff, basic amenities provided on platforms, and safety and security are important determinants of the service quality of railway platforms. Service characteristics like punctuality, regularity and frequency of runs, and cleanliness have the highest positive effect on service quality [4]. RAILQUAL is a comprehensive instrument developed based on SERVQUAL attributes specially for the evaluation service quality of railway passenger services. In RAILQUAL, the service quality dimensions considered are

tangibles, reliability, responsiveness, assurance, empathy, comfort, and connection [5]. Mandhani et al. [6] considered service availability, passenger information, ease of accessing various amenities, safety and security, seamless connectivity, and environment impact as the service quality constructs for the Delhi metro service quality study.

Different approaches have been used in service quality studies. Starting from basic factor analysis on SPSS platform [3] to the latest machine learning algorithms like artificial neural network [7]. Structural equation modeling (SEM) is used in quite many studies [4, 6, 8, 9], even some used hybrid approach of SEM–NN for service quality study [10–14]. From the literature, it has been found that very less studies have been carried out on the service quality of railway platforms. Combination of SEM and importance-performance map analysis (IPMA) analysis is not done in any transportation service quality studies.

4 Data Collection and Preliminary Analysis

4.1 Data Collection

The study area selected is platform no. 1 of Tiruchirappalli railway junction. Out of eight platforms in the station, platform no.1 is chosen as most of the services are available. A user perception survey has been conducted to collect the data regarding the users' perception of service quality of platforms. From the literature review, various factors influencing the users' perception of service quality of platforms have been identified and incorporated in the questionnaire. A total of 22 service quality indicators were incorporated.

Initially, a pilot survey was conducted, and based on the comments and suggestions from the respondents, the questionnaire was modified. The modified questionnaire is organized into two sections. The first section includes socioeconomic information like age, gender, annual income, and travel characteristics such as frequency of using the Tiruchirappalli junction. Table 1 shows the categorization of variables included in Sect. 1 of the questionnaire. The second section collects data related to users' perception of service quality. Respondents were requested to rate their level of importance and satisfaction toward each of the service quality indicators on a Likert's five-point scale. Table 2 gives the list of attributes used in this study.

Data was collected by two different methods. Initially, it was decided to conduct an on-field survey. But due to pandemic, it was difficult to conduct field survey. Hence, only few samples were collected from the field and remaining were collected through an online survey. Even though data is collected by two different methods, the consistency and authenticity of the data are maintained. Sample size required for the survey was calculated based on Cochran's formula for infinite population and is given by Eq. 1.

Table 1 Variable description

Variable	Categorization of variable
Age (in years)	18–25, 25–40, 41–60, >60
Gender	Male, female
Annual income (in INR)	Not earning; less than 1 Lakh; 1 Lakh–3 Lakhs; 3 Lakhs–8 Lakhs; more than 8 Lakhs
Frequency to station in last 3 years	Less than 5 times; 5–15 times; more than 15 times

$$n_s = \frac{z^2 pq}{e^2} \tag{1}$$

where n_s : minimum number of samples, z : z-score, p : proportion of attributes, q : $1 - p$, and e : precision

For this study, 95% confidence interval with 80% proportion of attributes in population and 5% precision is considered. By this assumption, required sample size came as 245. Totally, 317 samples were collected, out of which 159 samples were collected from Google Form and 158 from on-board data collection. Out of 158 on-board data samples, 17 were scrapped. So, totally 300 samples were used for this study.

5 Data Analysis

For primary analysis, Microsoft Excel and SPSS are used. Descriptive analysis and data reliability test are also performed. Figure 1 shows the statistics of socioeconomic and travel data.

Most of the respondents are male (62%), and age distribution shows that most respondents belong to 18–25 age group (50%). Annual income analysis shows that most of the respondents belong to 3–8 lakhs (34%) income group, and analysis of frequency to the junction shows that 67% respondents at least visited the junction platform for 5 times in last 3 years. Data validity and reliability test was conducted on the dataset using SPSS package. According to the test results, the collected data is adequate and homogenous as the Kaiser–Meyer–Olkin (KMO) measure of sampling adequacy value came above 0.8 (obtained value = 0.884) and Bartlett’s test got significant value (p -value = 0.000).

6 Bivariate Analysis

To ascertain the relationship between service quality attributes and demographic characteristics of users, bivariate analysis using Chi-square test was carried out using

Table 2 List of attributes

Latent constructs	Measurable indicators	Symbol
Information system efficiency (INFS)	Clarity and frequency of announcements	Ann
	Reservation chart display	Res_disp
	Train schedule display	Scd_disp
	Sign boards	Sign_board
	Overall information system efficiency	O_infs
Basic facilities (BF)	Sufficient seating facility	Seat
	Lighting fans charging ports	Electric
	Ticket counters	Counter
	Availability of drinking water	Water
	Toilets and washrooms	Toilet
	Refreshment	Refreshment
	Availability of dustbins	Dustbin
	Overall basic facilities	O_bf
Staff behavior (BEHAVIOR)	Behavior of staff at ticket counters	Bh_counter
	Behavior of staff for doubt clarification	Bh_doubt
	Behavior of ticket inspector	Bh_tickinsp
	Overall staff behavior	Os_behavior
Additional facilities (AF)	Wi-Fi availability	Wi-Fi
	Waiting rooms	Coach_disp
	Train coach position display	Cross
	Platform crossover facility	Disabled_access
	Facilities for disabled	Waiting_room
	Overall additional facilities	O_af
Safety and security (SAFETY)	Security of self	P_saf
	Security of luggage	L_saf
	Floor quality	Floor_qual
	Overall safety and security	O_safety
Overall service quality		OSAF

SPSS software, and the cross-table of significant relation is presented. The results of bivariate analysis are given in Table 3.

Results show that gender has significant effect on the overall service quality of the platform. Male and female have different perception toward the overall service quality. Other socio-demographic variables like age, annual income, and frequency

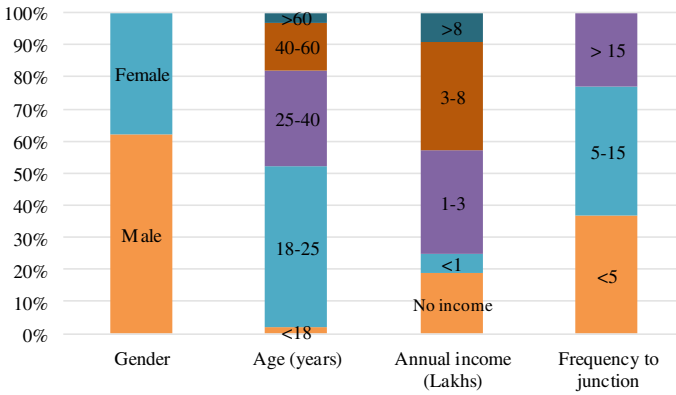


Fig. 1 Statistics of socioeconomic and travel data

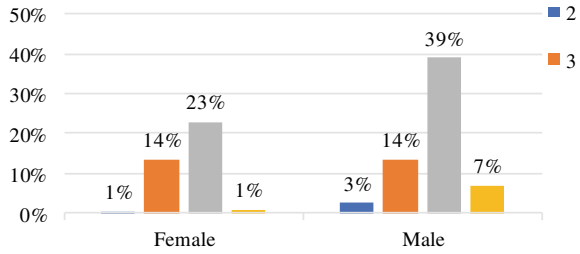
Table 3 Bivariate analysis

Variables	Service quality attributes	Chi-square value	p-value	Cramer’s V value
Gender	Overall service quality	8.918	0.03*	0.211
Age	Overall service quality	7.1	0.85	–
Annual income	Overall service quality	10.543	0.568	–
Frequency to station in last 3 years	Overall service quality	3.930	0.686	–

*Significant at 5% significance level

to station do not affect the user perceived overall service quality of the platform. Generally, it is expected that increase in income level increases the aspiration of better service, but in this study, results do not support that. Cross-table between gender and overall service quality is shown in Fig. 2. It can be seen that no respondents rated the overall service quality as ‘highly dissatisfied’. 30% of the male respondents rated 4 point to overall service quality.

Fig. 2 Relation between gender and overall service quality



7 Structural Equation Modeling of User Perceived Service Quality of Indian Railway Platform

7.1 Model Development

Based on the conceptual framework, the model is developed on SmartPLS platform. The model is developed in two stages; first, the outer model or the measurement model is developed in which the relation between individual constructs and their measurable indicators is considered. As the measurement model is formative, for redundancy analysis, each latent construct is related to their global latent construct. After that, the inner model or structural model is developed. All the latent constructs in measurement model are connected to overall service quality (OSAF). Figure 3 shows the SEM model. The blue circles are latent constructs, orange color circle is global indicator constructs of corresponding latent constructs, and the black color circle is overall service quality constructs.

7.2 Model Estimation Results

After the development of the model based on the conceptual framework, consistent PLS algorithm is run on the model to find out the path coefficient and other results. After that, bootstrapping is done to check the significance of individual values based on t-statistics values. The results are analyzed separately for measurement model and structural model. The results of measurement model are given in Table 4. Constructs in measurement model are formative, so there is no need to report indicator reliability, internal consistency reliability, and discriminant validity. For path loading, consider their outer weights for formative constructs. But outer weights of some indicators are not showing significant effect based on the *p*-values, in that case, the *p*-value of their outer loading is checked and that is significant, so there is no need to remove those indicators from the model [15].

In a formative measurement model, the problem of indicator collinearity may occur if the indicators are highly correlated with each other. Here, collinearity is checked using variance inflation factors (VIF) values. Table 5 gives the collinearity

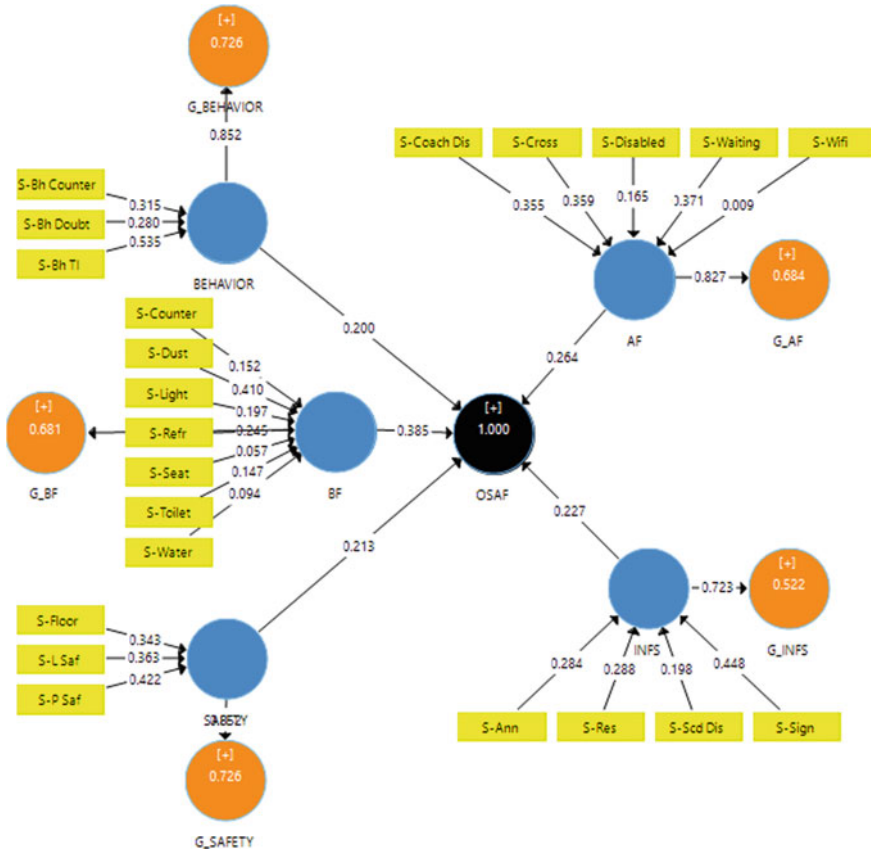


Fig. 3 Structural equation model of perceived service quality

statistics, as all the VIF values are less than 5, it can conclude that there is no collinearity in the indicators [15].

As the measurement model is formative, convergent validity and collinearity of indicators have been analyzed to establish convergent validity. Redundancy analysis is carried out for each latent construct separately, and results are given in Table 6. All the path coefficient values are above 0.80; hence, the convergent validity is established [16].

Results of structural model are given in Table 7. All the latent constructs are having significant impact on the overall service quality. With path coefficient value of 0.385, basic facilities (BF) are having the strongest effect on the overall service quality followed by information system efficiency and additional facilities.

Table 4 Measurement model results

Indicators		Latent constructs	Outer weights	p-values	Outer loadings	p-values
Coach_disp	→	AF	0.355	***	0.764	***
Cross	→	AF	0.359	***	0.835	***
Disabled_access	→	AF	0.165	***	0.797	***
Waiting_room	→	AF	0.371	***	0.788	***
Wi-Fi	→	AF	0.009	0.857 ^a	0.532	***
Bh_counter	→	BEHAVIOR	0.315	***	0.861	***
Bh_doubt	→	BEHAVIOR	0.280	***	0.854	***
Bh_ticksinp	→	BEHAVIOR	0.535	***	0.916	***
Counter	→	BF	0.152	**	0.670	***
Dustbin	→	BF	0.410	***	0.864	***
Electricity	→	BF	0.197	***	0.750	***
Refreshment	→	BF	0.245	***	0.750	***
Seat	→	BF	0.057	0.415 ^a	0.708	***
Toilet	→	BF	0.147	**	0.741	***
Water	→	BF	0.094	0.179 ^a	0.674	***
Floor_qual	→	SAFETY	0.284	*	0.837	***
L_saf	→	SAFETY	0.288	**	0.766	***
P_saf	→	SAFETY	0.198	*	0.830	***
Ann	→	INFS	0.448	***	0.843	***
Res_disp	→	INFS	0.343	***	0.837	***
Scd_disp	→	INFS	0.363	***	0.910	***
Sign_board	→	INFS	0.422	***	0.906	***

*** Significant at 1% significance level, **Significant at 5% significance level

*Significant at 10% significance level, ^aNot significant

8 Importance-Performance Map Analysis

IPMA analysis is performed to identify the indicators and constructs having relatively high importance for the target constructs (overall service quality) but also have a relatively low performance. The performance value is calculated by rescaling indicators score on a range between 0 and 100 using the Eq. (2) given below [17].

$$x_{ij}^{\text{rescaled}} = \frac{E[x_{ij}] - \min[x_i]}{\max[x_i] - \min[x_i]} \times 100 \tag{2}$$

The study used Likert’s five scale with minimum rating as 1 and maximum as 5. $E[.]$ is the value rated by user. After the calculation of all responses, mean value of individual indicators is taken as performance value. Importance value is derived from the total effect of the relationship between indicator and target construct [17].

Table 5 Collinearity statistics

Indicators	VIF
Clarity and frequency of announcements	2.28
Behavior of staff at ticket counters	2.38
Behavior of staff for doubt clarification	2.40
Behavior of ticket inspector	1.90
Train coach position display	1.57
Ticket counters	1.66
Platform crossover facility	1.95
Facilities for disabled	2.18
Availability of dustbins	2.13
Lighting, fans, and charging ports	2.06
Floor quality	1.84
Security of luggage	2.79
Security of self	2.48
Refreshment	1.64
Reservation chart display	1.82
Train schedule display	2.31
Sufficient seating facility	2.05
Sign boards	1.77
Toilets and washrooms	1.87
Waiting rooms	1.62
Availability of drinking water	1.79
Wi-Fi availability	1.42

Table 6 Redundancy analysis

Latent constructs		Global latent constructs	Path coefficient	t-statistics	p-value
AF	→	G_AF	0.827	29.11	***
BEHAVIOR	→	G_BEHAVIOR	0.852	34.18	***
BF	→	G_BF	0.825	29.37	***
INFS	→	G_INFS	0.723	17.05	***
SAFETY	→	G_SAFETY	0.852	39.79	***

***Significant at 1% significance level

All these calculations are done in SmartPLS software under IPMA algorithm. The result values of unstandardized effects from analysis are presented in Table 8.

Importance-performance map is shown in Fig. 4. On X-axis, importance values are reported, and performance values are reported on Y-axis. The graph is divided into four quadrants using mean values of overall mean of importance and performance of

Table 7 Structural model results

Latent constructs		Overall service quality	Path coefficient	<i>t</i> -statistics	<i>p</i> -value
AF	→	OSAF	0.264	13.73	***
BEHAVIOR	→	OSAF	0.200	14.33	***
BF	→	OSAF	0.385	26.79	***
INFS	→	OSAF	0.227	15.04	***
SAFETY	→	OSAF	0.213	15.05	***

***Significant at 1% significance level

Table 8
Importance-performance values

Indicator	Importance	Performances
Clarity and frequency of announcements	0.037	66.5
Behavior of staff at ticket counters	0.043	60.6
Behavior of staff for doubt clarification	0.034	60.3
Behavior of ticket inspector	0.071	60.3
Train coach position display	0.059	62.9
Ticket counters	0.039	60.3
Platform crossover facility	0.060	62.6
Facilities for disabled	0.028	62.8
Availability of dustbins	0.102	65.1
Lighting, fans, and charging ports	0.048	65.4
Floor quality	0.051	62.0
Security of luggage	0.046	59.3
Security of self	0.068	66.0
Refreshment	0.057	60.5
Reservation chart display	0.039	57.1
Train schedule display	0.027	68.5
Sufficient seating facility	0.014	66.0
Sign boards	0.064	66.0
Toilets and washrooms	0.035	52.9
Waiting rooms	0.057	59.5
Availability of drinking water	0.021	55.5
Wi-Fi availability	0.001	42.1
Mean	0.048	61.90

Bold numbers indicate the mean value for importance and performance ratings

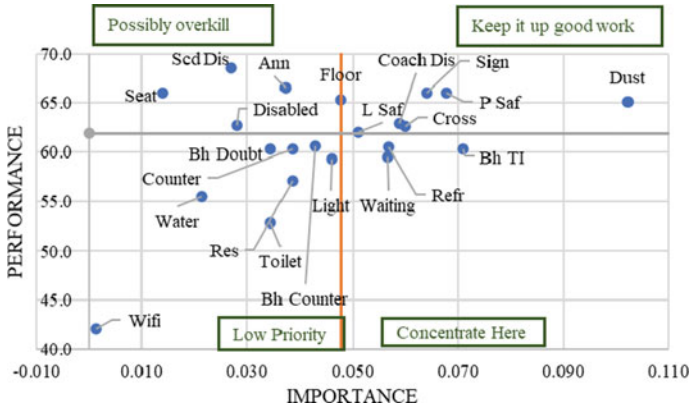


Fig. 4 Importance-performance map of indicators

all indicators as divider. To start from bottom right corner, the fourth quadrant contains indicators, which should be concentrated on priority as they are of more importance but have low performance. So, the indicators to be concentrated are waiting room, refreshment facility, and behavior of ticket inspector. After that, priority should be given low priority quadrant importance and as well as performance is low. While concentrating on improving the quality of facilities from bottom quadrants, we have to maintain quality of facilities from top right corner quadrant, keep it up good work quadrant as they are performing as per the level importance they got. Improvements in facilities from possibly overkill quadrant can hold for some duration in as they are performing better than the level of importance they got.

9 Conclusions

In this study, various analyses are performed on the collected dataset, and based on the results, conclusions are made. Based on bivariate analysis results, gender has significant effect on overall service quality of platform which implies that male and female have significantly different perception on overall service quality of platform, whereas other user characteristics like age, annual income, and their frequency to visiting station are not showing any significant effect on overall service quality.

Based on the results from measurement model (confirmatory factor analysis), supporting to the hypothesis of the study, all the 22 indicators are having positive and significant influence on their corresponding latent variables information system, basic facilities, additional facilities, staff behavior, and safety and security, respectively. Based on the results from structural model, supporting to the hypothesis of the study, all the five latent variables are having positive and significant on the overall satisfaction of the service. Basic facilities (0.385) are having the most significant

effect on the overall service quality followed by additional facilities (0.264), information system (0.227), safety and security (0.213), and staff behavior (0.200) has least significant effect.

IPMA analysis gave priority levels to implement improvements in specific facilities starting from facilities from 'concentrate here' quadrant. This includes waiting room, refreshment, and ticket inspector behavior. Facilities from 'keep it up good work' quadrants, passenger safety, luggage safety, crossing facilities, sign boards, coach position display, and dustbins are performing quite well considering their importance level. These facilities quality should be maintained as it is in the future. This study provides insight to planners and experts to understand, which is the most important attributes for improving the user perceived service quality of railway platforms. The present study looked at the user's perception of service quality of platform but has not taken into consideration the perspective or the threshold values which have been decided by the operators or railway station authorities while deciding to provide the facilities. Considering these aspects can be the future scope of the study.

References

1. Maruvada DP, Bellamkonda RS (2010) Analyzing the passenger service quality of the Indian Railways using railqual: examining the applicability of fuzzy logic. *Int J Innov Manage Technol* 1(5):478–482
2. Gronroos C (1984) A service quality model and its marketing implications. *Eur J Mark* 18:36–44
3. Geetika, Nandan S (2010) Determinants of customer satisfaction on service quality: a study of railway platforms in India. *J Public Transp* 13(1):97–113
4. Eболи L, Mazzulla G (2012) Structural equation modelling for analysing passengers' perceptions about railway services. *Procedia Soc Behav Sci* 54:96–106
5. Prasad MD, Shekhar BR (2010) Development of railqual. *Manage Sci Eng* 4(3):87–94
6. Mandhani J, Nayak JK, Parida M (2020) Interrelationships among service quality factors of Metro Rail Transit System: an integrated Bayesian networks and PLS-SEM approach. *Transp Res Part A* 140(September):320–336
7. Garrido C, De Oña R, De Oña J (2014) Neural networks for analyzing service quality in public transportation. *Expert Syst Appl* 41(15):6830–6838
8. Shen W, Xiao W, Wang X (2016) Passenger satisfaction evaluation model for Urban rail transit: a structural equation modeling based on partial least squares. *Transp Policy* 46:20–31
9. Soltanpour A, Mesbah M, Habibian M (2020) Customer satisfaction in urban rail: a study on transferability of structural equation models. *Public Transp* 12(1):123–146
10. Sharma SK, Gaur A, Saddikuti V, Rastogi A (2017) Structural equation model (SEM)-neural network (NN) model for predicting quality determinants of e-learning management systems. *Behav Inf Technol* 36(10):1053–1066
11. Priyadarshinee P, Raut RD, Jha MK, Gardas BB (2017) Understanding and predicting the determinants of cloud computing adoption: a two staged hybrid SEM—Neural networks approach. *Comput Hum Behav* 76:341–362
12. Golob TF (2003) Structural equation modeling for travel behavior research. *Transp Res Part B Methodol* 37(1):1–25
13. Henseler J, Hubona G, Ray PA (2016) Using PLS path modeling in new technology research: updated guidelines. *Ind Manage Data Syst* 116(1):2–20
14. Hair JF, Ringle CM, Sarstedt M (2011) PLS-SEM: indeed a silver bullet. *J Mark Theory Practice* 19(2):139–151

15. Wong KKK-K (2013) 28/05—Partial least squares structural equation modeling (PLS-SEM) techniques using SmartPLS. *Mark Bull* 24(1):1–32
16. Hair JF, Hult GTM, Ringle CM, Sarstedt M (2013) *A primer on partial least squares structural equation modeling (PLS-SEM)*. Sage, Thousand Oaks
17. Ringle CM, Sarstedt M (2016) Gain more insight from your PLS-SEM results. *Ind Manage Data Syst*

Which Factors Affect Lane Choice Behavior at Toll Plaza? An Analytical Hierarchical Process (AHP) Approach



Rohit Chopade, Chintaman Bari, and Ashish Dhamaniya

Abstract In developing countries like India, mostly barrier toll plazas are present, where the approaching vehicle driver has to choose a particular toll lane for the transaction, whether it is a Manual Toll Collection (MTC) or Electronic Toll Collection (ETC) system. Further, mixed traffic conditions prevail on the roadways in developing nations, and the same has been observed at the toll lanes. Dedicated lanes are present for different vehicle classes at toll plazas for a seamless transaction. The approaching vehicle driver chooses the lane, which causes the minimum delay to him/her and thus causes mixed traffic conditions at toll plazas, i.e., the presence of different vehicle classes in the dedicated lanes. Due to these mixed traffic conditions, the operations at toll plazas get hampered, leading to bottleneck formation, causing delays to users. Hence, it is necessary to monitor the lane choice behavior of the drivers' at toll plazas to minimize his/her own delay. The present study evaluates the factors affecting the lane choice behavior using the Analytical Hierarchical Process (AHP) and thus computes the most affecting factor for lane choice behavior at toll plazas under mixed traffic conditions. The factors are modeled using the user perception data collected in the pairwise comparison matrix as per the AHP scale. The factors considered for the present study are queue length, lane changes, Proportion of heavy vehicles, Proportion of trailers, and approach lane. It is also found that the queue length affects lane choice the most, carrying a weight of 0.32, followed by Proportion of HCV (0.28), while the lane changes (0.09) were the least affecting factor. These factors are helpful to monitor the traffic at the toll plaza to avoid the situation of congestion. Further, the AHP weights can be used with any Multi-Criteria Decision-Making (MCDM) method to form an algorithm of lane choice for connected autonomous vehicles.

Keywords Analytical hierarchical process · Queue length · Lane choice

R. Chopade · C. Bari · A. Dhamaniya (✉)
Sardar Vallabhbhai National Institute of Technology, Surat, India
e-mail: adhmaniya@gmail.com

© The Author(s), under exclusive license to Springer Nature Singapore Pte Ltd. 2023
M. V. L. R. Anjaneyulu et al. (eds.), *Recent Advances in Transportation Systems Engineering and Management*, Lecture Notes in Civil Engineering 261,
https://doi.org/10.1007/978-981-19-2273-2_60

915

1 Introduction

To curtail the congestion levels at toll plazas, the Government of India (GOI) has started the flagship program of implementing 100% Electronic Toll Collection (ETC), commonly called FASTag, but still, congestion prevails, maybe due to the under design of toll plazas [1]. For the effective design of toll plazas, one must have a significant understanding of the queuing process at a toll plaza. The most significant factors affecting the queuing process at a toll plaza depend upon the approaching driver’s toll lane choice behavior [1]. Instead of knowing the importance of lane choice behavior, limited efforts were made in the past. Dedicated lanes are present for different vehicle classes at toll plazas for a seamless transaction. The approaching vehicle driver chooses the lane, which causes the minimum delay to him/her and thus causes mixed traffic conditions at toll plazas, i.e., presence of different vehicle classes in the dedicated lanes [2, 3] (Fig. 1).

Due to these mixed traffic conditions, the operations at toll plazas get hampered, leading to bottleneck formation, causing delays to users [4]. Very few studies are attempted to check the drivers’ lane choice behavior under heterogeneous traffic conditions (having more than seven classes of vehicles in the traffic stream [5]) as in developing countries like India. This paper attempts to study the factors affecting lane choice behavior at toll plazas using Analytical Hierarchical Process (AHP). Various factors are reported in the literature as the queue length [1], vehicle composition, number of lane changes required, approach lane [3], etc. that are important for the study of lane choice behavior at toll plazas.

The AHP is a system of hierarchy of objective/goal, attributes, and finally, alternatives. The AHP is used to decide how decision-makers think using the weights obtained from the pairwise comparative matrix. It takes into consideration both the qualitative and quantitative factors of decision-making [6]. AHP is the process mostly used for the ranking of the factors and thus the selection of the alternatives. It is easy to understand and use for decision-making problems [7]. The AHP is used in the



Fig. 1 Mixed traffic condition at Kamrej and Karjan toll plaza

present study because it can handle the consistency [8] and the inconsistency [9] in the pairwise comparison matrix given by the individual decision-maker with the help of proper analytical procedure for finding the consistency index [10]. Further, when there are constraints about the physical or statistical measures, the AHP is a tool for developing measures in physical or social environments. It is used to convert subjective assessments into relative weights. Firstly, deciding the goals, attributes, and alternatives. In the present study, the goal is to study the factors affecting the lane choice behavior at toll plaza under mixed traffic conditions, and the attributes are number of vehicles in the queue, number of lane changes, Proportion of heavy vehicles, and Proportion of trailer.

2 Literature Review

The Analytical Hierarchical Process (AHP) is a better way of finding the weights of the factors using the pairwise comparison matrix filled by the decision-maker. It was founded by Saaty, in which the intangible factors are measured on a scale to make them tangible [11] as the relation between two factors is judged by the experts and is then scaled to formulate the weights. AHP is used in decision-making in the field of personal decision-making, social selection, and engineering selection. It is mostly used in the evaluation and selection. Holguín-Veras [12] compared the AHP, and multi-attribute value (MAV) functions for highway planning. The author concluded that AHP is a better one than the MAV method in terms of hierarchy. Ye et al. [13] evaluated congestion levels at intersections using AHP and TOPSIS methods. He et al. [14] developed the evaluation index with safety, economic, technical, and time factors for highway projects using AHP and Gray Correlation Analysis. Taherdoost [15] suggested that AHP is a step-by-step approach that also works on combining qualitative and quantitative attributes. Lidinska and Jablonsky [16] addressed AHP as a structuring and analysis tool for complicated decision-making problems and is ideal for such tasks. They also used AHP for the performance evaluation of the employee at a consulting company. Darani et al. [17] used the Fuzzy-AHP method to locate the parking site to avoid the extra-economic and environmental costs as it is a complex decision-making problem. Mudigonda et al. [18] studied lane choice at the toll plaza and stated that it depends on the position of entry and exit ramps and also on the queue length in each toll lane. They also assigned weights to the parameters depending on the site and developed utility equations. Vehicle chooses the toll lane with the highest utility [18]. The selection of toll lanes depends on the direction of entry or exit from the freeway along with the shortest queue [19]. Driver prefers to choose the toll lane with minimum queue length with the minimum number of lane changes [20]. Correa et al. [21] proposed that the driver try to choose the shortest queue length other than the dedicated vehicle class even if not allowed. This causes the condition of mixed traffic at the toll plaza. The lane choice is dependent on the equivalent queue length of a toll lane which is equal to the actual queue length plus the number of lane changes required to select the targeted lane [22]. Lane choice

model for autonomous vehicles was shown based on two parameters, the rod speed SR_i and the decision-making parameter D_{SR_i} [23]. Higher the value of both the parameters more favorable the lane to choose. An equation was formed based on the factors of service rate, lateral distance traversed, vehicle length and width, lane width, and proportion of vehicle. Combination of toll collection systems for the increasing percentage of autonomous vehicles was proposed.

The most significant factors affecting the queuing process at a toll plaza depends upon the arriving volume and approaching driver’s toll lane choice behavior. However, studies have explored the effect of arriving vehicle volume on toll plaza performance. The highly heterogeneous and quasi-lane disciplined traffic observed in developing countries like India is still not well explored. Hence, the present study aims to study the factors affecting on field’s lane choice behavior of different vehicle drivers at toll plazas operating under mixed traffic conditions observed in India.

3 Data Collection and Methodology

Data required for the study is collected using expert advice. The Google form was prepared to get the data from the drivers and the telephonic survey was carried out due to Covid-19 pandemic. Data from 25 experts having driving experience of more than 4 years were inquired in person, and their responses were recorded in the matrix of relative importance. Out of total data collected 80 percent were male drivers and 20 percent were female drivers.

AHP is used to find the weightage of the factors. It is a threefold system with goals/objectives at the top, followed by attributes, and finally, the alternatives. It deals with the decision-making of both the qualitative and quantitative factors. AHP uses the user input to find the weights. The methodology for computing weights through AHP includes:

1. Identify the goals, criteria, and sub-criteria.
2. Then the relative importance matrix is found out by inquiring the experts/decision-makers (DM) (here experienced drivers) having experience in that field.

$$A_{M \times M} = E_1 \ E_2 \ E_3 \ \dots \ E_M$$

$$\begin{matrix}
 E_1 \\
 E_2 \\
 E_3 \\
 \vdots \\
 E_M
 \end{matrix}
 \begin{bmatrix}
 1 & e_{12} & e_{13} & \dots & e_{1M} \\
 e_{21} & 1 & e_{23} & \dots & e_{2M} \\
 e_{31} & e_{32} & 1 & \dots & e_{3M} \\
 \vdots & \vdots & \vdots & \ddots & \vdots \\
 e_{M1} & e_{M2} & e_{M3} & \dots & 1
 \end{bmatrix}
 \tag{1}$$

$A_{M \times M}$ = relative importance matrix (say A_1); M = number of attributes.

Table 1 Scale for AHP

Intensity of importance	Definition	Explanation
1	Equal importance	Two activities contribute equally to the objective
3	Moderate importance	Experience and judgments slightly favor one activity over another
5	Strong importance	Experience and judgments strongly favor one activity over another
7	Very strong	An activity is favored very strongly over another, its dominance demonstrated in practice
9	Extreme importance	An evidence favoring one activity over another is of the highest possible order of affirmation
Reciprocals of above	If activity <i>i</i> has one of the above non-zero numbers assigned to it when compared to activity <i>j</i>	
1.1–1.9	If the activities are very close	Difficult to assign the best value bur when compared with other contrasting activities, the size of the small numbers will not be too noticeable

Source [8]

The importance for each pair of factors is recorded in the respective box, say a_{ij} by using scale given in Table 1. Now for vice versa $a_{ji} = 1/a_{ij}$. For $i = j$ $a_{ij} = a_{ji}$. For example: if, according to the experts, the number of vehicles in the queue is extremely important than the number of lane changes, then in the matric $a_{ij} = 9$, at the same time $a_{ji} = 1/9$.

3. The relative normalized weight (w_j) of each attribute is found out by taking the geometric mean (GM) as shown in Eq. (2).

$$GM_j \left[\prod_{j=1}^m a_{ij} \right]^{1/M} \tag{2}$$

$$w_j \frac{GM_j}{\sum_{j=1}^m GM_j} \tag{3}$$

The weighted matrix is taken as A_2

$$A_2 = [w_1, w_2, w_3, \dots, w_M] \tag{4}$$

4. Now, the matrices A_3 and A_4 are calculated using Eqs. (5) and (6), respectively.

$$A_3 = A_1 \times A_2 \tag{5}$$

$$A_4 = \frac{A_3}{A_2} \tag{6}$$

- 5. The maximum eigenvalue (λ_{max}) is calculated by taking the average of matrix A_4 .
- 6. Consistency index CI is calculated using the Eq. (7).

$$CI = \frac{(\lambda_{max} - M)}{(M - 1)} \tag{7}$$

- 7. The consistency ratio is used to check the consistency of the pairwise comparison matrix given by a particular individual and is calculated as per Eq. (8).

$$CR = \frac{CI}{RI} \tag{8}$$

where RI is the Random index which is given by Saaty [11]. The value of CR should be less than 0.1 then only the weights are said to be consistent. If not, then a combined matrix is to be formed as suggested by Wakchaure and Jha [9].

- 8. If CR is more than 0.1, then the combined matrix is to be developed. The procedure of finding the combined matrix suggested by Wakchaure and Jha [9] is adopted in the present study. Suppose the values given by “ n ” respondents for a_{12} are $\times 1, \times 2, \dots, x_n$, and priority weights given by “ n ” respondents are $w_1, w_2 \dots w_n$, where the priority weight is obtained by subtracting the consistency ratio from 1, then for the combined matrix, the value of a_{12} is calculated by using Eq. (9). Similarly, for other factors, the final weights are calculated.

$$a_{12} = [x_1^{w_1} * x_2^{w_2} * \dots * x_n^{w_n}]^{\frac{1}{[w_1+w_2+\dots+w_n]}} \tag{9}$$

The steps from (1)–(7) are carried out on the combined matrix, and thus the final weights are obtained, which can cumulate the users’ perception of different decision-makers.

4 Data Analysis

The stepwise AHP methodology is given below, with the solution, for a pairwise comparison matrix filled by one respondent.

- 1. Now the matrix of relative importance is found out by inquiring the experts or decision-makers. As the study is for lane choice behavior, the decision-makers are drivers who have experience driving through the toll road. The relative importance was recorded on a scale shown in Table 2. For example: if, according to the experts the number of vehicles in queue is extremely important than the number of lane changes then in the matrix, $a_{ij} = 9$ (as per AHP scale), on the same time a_{ji}

Table 2 Matrix of relative importance

	QL	LC	P (HCV)	P (Trailer)	AL
QL	1.00	9.00	5.00	5.00	6.00
LC	0.11	1.00	0.20	0.20	0.17
P (HCV)	0.20	5.00	1.00	7.00	6.00
P (Trailer)	0.20	5.00	0.14	1.00	0.17
AL	0.17	6.00	0.17	6.00	1.00

= 1/9 (i.e., inverse of a_{ij}). The relative importance matrix (A_1) for one of the decision-makers (DM) is shown in Table 2.

Where

QL = (Queue length) Number of vehicles in queue.

LC = Number of lane changes.

P (HCV) = Proportion of HCV in the queue.

P (Trailer) = Proportion of trailers in the queue.

AL = Approach Lane.

2. Matrix A_2 is calculated using Eqs. (2) for the sample values of DM1 from Table 3.

$$GM_{(QL)} = [1 \times 9 \times 5 \times 5 \times 6]^{1/5} = 4.277$$

Similarly, GM for other attributes is also calculated and their summation is done. Now, the weight is founded using Eq. (3)

$$w_j = \frac{4.277}{\sum_{j=1}^m GM_j} = \frac{4.277}{8.049} = 0.53$$

Table 3 Final combined matrix

	QL	LC	P (HCV)	P (Trailer)	AL	GM	A_2 (Weights)	A_3	A_4
QL	1	4.00	1.27	0.94	3.34	1.74	0.32	1.63	5.18
LC	0.25	1	0.41	0.44	0.76	0.51	0.09	0.46	5.04
P (HCV)	0.79	2.43	1	2.00	2.16	1.52	0.28	1.40	5.09
P (Trailer)	1.06	2.26	0.50	1	1.21	1.07	0.19	1.02	5.26
AL	0.30	1.32	0.46	0.82	1	0.68	0.12	0.63	5.07
						5.540		λ_{max}	5.13
								CI	0.03
								CR	0.03

Hence using Eq. (4)

$$A_2 = [0.53, 0.03, 0.26, 0.06, 0.12]$$

- The matrix A_2 obtained from Eq. (4) is the weightage matrix. The summation of weights of all the attributes should be equal to one, i.e., $\sum_{j=1}^m w_j = 1$. Also, the consistency of the weights obtained is to be checked. To check the consistency, matrix A_3 and A_4 is estimated using the Eqs. (5) and (6), respectively.

$$A_3 = A_1 \times A_2$$

$$A_3 = [3.14, 0.17, 1.67, 0.37, 0.78]$$

$$A_4 = \frac{[3.14, 0.17, 1.67, 0.37, 0.78]}{[0.53, 0.03, 0.26, 0.06, 0.12]}$$

$$= [5.98, 5.88, 6.37, 6.27, 6.32]$$

- The maximum eigenvalue (λ_{max}) is calculated by taking the average of matrix A_4 .

$$\lambda_{max} = \frac{5.98 + 5.88 + 6.37 + 6.27 + 6.32}{5} = 4.64$$

- Consistency index (CI) is calculated using Eq. (7)

$$CI = \frac{(6.16 - 5)}{(5 - 1)}$$

$$= 0.29$$

- Consistency ratio (CR) is calculated with Eq. (8).

$$CR = \frac{CI}{RI} = \frac{0.29}{1.11} = 0.32$$

where RI is the Random index which is given by Wakchaure and Jha [9] is equal to 1.11 in the present case. The value of $CR > 0.1$, hence the weights obtained are inconsistent. Now, the consistent weights are obtained using the Eq. (9). A total of 25 respondents were inquired about their perception of having a minimum of 4 years of driving experience. For the combined matrix, the priority weights of all the respondents are determined and the new cell value of a_{ij} , using Eq. (9). Combined matrix showing the consistent weights with $CI = 0.03$ and $CR = 0.03$ which is < 0.1 is shown in Table 3.

From Table 3, it is clearly seen that the highest weight of 0.32 is allocated to queue length followed by Proportion of heavy vehicles with weight of 0.28, Proportion of trailers with weight of 0.19, approach lane with the weight of 0.12, and lowest is assigned to lane changes having a weightage of 0.09. This shows that the people

prefer to choose the toll lane with the shortest queue mostly. Lane change being the last shows that it is given the least priority. Queue length is the factor that affects the people most in selecting the toll lane. The least effect of lane changes is because it can be looked at as a dependent parameter as if the condition in the toll lane ahead is appropriate to choose there is no need to change lane, but in the case where the toll lane ahead is having longest queue or inappropriate causing more delay then the driver will then only prefer to change lane.

5 Conclusions

In the present study, the factors affecting the operation of lane choice at toll plaza are studied. The share of each factor contributing to the lane choice operation is found using the analytical hierarchical process (AHP). It is found out that the queue length is the most influencing factor with a weight of 0.32, i.e., if we consider a share of 100%, then 32% of the time, factor queue length affects the lane choice decision of the people, which is highest followed by proportion of heavy vehicles with a weight share of 0.28. The proportion of trailer and approach lane has a weight of 0.19 and 0.12, respectively. And the factor which affects the lane choice least is the number of lane changes with a weight of 0.09, which means only 9% of the time, the people consider lane change as a significant factor in choosing a lane. This is because lane choice can be a secondary parameter depending on the queue length and vehicle proportion. The factors like safety and speed of vehicle also have a significant effect on the lane choice, but as this is a user perception-based weight, it is difficult to incorporate the effect of safety and speed, and it cannot be predicted or experienced unless and until the drive is on the field.

In future studies, more datasets can be collected from different parts of country, and comparison of weights can be done with the present study. This study can help to model the lane choice behavior at the toll plaza and avoid the formation of a bottleneck as the weights are obtained using user perception. It can be a better way to model the behavior according to the user. Also, an algorithm predicting the lane to be chosen can be developed, which will help people to choose the best lane at the toll plaza, which can minimize their delay. Same studies can also be done for parking lots or multilevel parking, which informs the user about the best and convenient parking space.

Acknowledgements The authors would like to thank TEQIP-III, a Government of India initiative, for sponsoring this project. The project is entitled “Development of Warrants for Automation of Toll Plazas in India.” (Project number SVNIT/CED/AD/TEQIPIII/144/2019). The present study is a part of the project.

References

1. Dubedi A, Chakroborty P, Kundu D, Reddy KH (2012) Modeling Automobile drivers' toll-lane choice behavior at a toll plaza. *J Transp Eng* 138:1350–1357. [https://doi.org/10.1061/\(ASCE\)TE.1943-5436.0000440](https://doi.org/10.1061/(ASCE)TE.1943-5436.0000440)
2. Navandar YV, Bari CS, Dhamaniya A, Arkatkar S, Patel DA (2021) Investigation on the determinants of service headway variability at tollbooths under mixed traffic scenario in emerging countries. *Curr Sci* 1–39
3. Bari CS, Navandar YV, Dhamaniya A (2020) Vehicular emission modeling at toll plaza using performance box data. *J Hazardous Toxic Radioact Waste* 24:1–19. [https://doi.org/10.1061/\(ASCE\)HZ.2153-5515.0000550](https://doi.org/10.1061/(ASCE)HZ.2153-5515.0000550)
4. Bari CS, Chandra S, Dhamaniya A, Arkatkar S, Navandar YV (2021) Service time variability at manual operated tollbooths under mixed traffic environment: towards level-of-service thresholds. *Transp Policy* 106:11–24. <https://doi.org/10.1016/j.tranpol.2021.03.018>
5. Bari CS, Navandar YV, Dhamaniya A (2020) Delay modelling at the manually operated toll plazas under mixed traffic conditions. *Int J Transp Sci Technol* 1–120. <https://doi.org/10.1016/j.ijst.2020.10.001>
6. Li H, Zhu X, Huo Y (2009) Uncertain type of AHP method in layout of expressway service areas. In: *International conference on transportation engineering*, pp 747–752
7. Velasquez M, Hester PT (2016) A comparative analysis of multi-criteria decision-making methods. *Prog Artif Intell* 5:315–322. <https://doi.org/10.1007/s13748-016-0093-1>
8. Saaty TL (2008) Decision making with the analytic hierarchy process. *Int J Serv Sci* 1:83–98. [https://doi.org/10.1016/0305-0483\(87\)90016-8](https://doi.org/10.1016/0305-0483(87)90016-8)
9. Wakchaure SS, Jha KN (2012) Determination of bridge health index using analytical hierarchy process. *Constr Manage Econ* 30:133–149. <https://doi.org/10.1080/01446193.2012.658075>
10. Topcu YI (2004) A decision model proposal for construction contractor selection in Turkey. *Build Environ* 39:469–481. <https://doi.org/10.1016/j.buildenv.2003.09.009>
11. Saaty RW (1987) The analytic hierarchy process—What it is and how it is used. *Math Model* 9:161–176
12. Holguín-Veras J (1995) Comparative assessment of AHP and MAV in highway planning: Case study. *J Transp Eng* 121:191–200. [https://doi.org/10.1061/\(ASCE\)0733-947X\(1995\)121:2\(191\)](https://doi.org/10.1061/(ASCE)0733-947X(1995)121:2(191))
13. Yu J, Wang L, Gong X (2013) Study on the status evaluation of urban road intersections traffic congestion base on AHP-TOPSIS Modal. *Procedia Soc Behav Sci* 96:609–616. <https://doi.org/10.1016/j.sbspro.2013.08.071>
14. He H, Li Y, Zhang Z (2016) Scheme optimization of large-scale highway transport based on AHP-grey correlation degree. *J Highw Transportation Res Dev* 10:98–102
15. Taherdoost H (2017) Decision making using the analytic hierarchy process (AHP); a step by step approach. *Int J Econ Manage Syst* 2:244–246
16. Lidinska L, Jablonsky J (2018) AHP model for performance evaluation of employees in a Czech management consulting company. *Cent Eur J Oper Res* 26:239–258. <https://doi.org/10.1007/s10100-017-0486-7>
17. Darani SK, Eslami AA, Jabbari M, Asefi H (2018) Parking lot site selection using a fuzzy AHP-TOPSIS framework in Tuyserkan. *Iran J Urban Plan Dev* 144:1–10. [https://doi.org/10.1061/\(ASCE\)UP.1943-5444.0000456](https://doi.org/10.1061/(ASCE)UP.1943-5444.0000456)
18. Mudigonda S, Bartin B, Ozbay K (2008) Microscopic modeling of lane selection and lane-changing at toll plazas. In: *88th Annual meeting*, vol 855, pp 1–18. Transportation Research Board, Washington, DC
19. Ozbay K, Mudigonda S, Bartin B (2005) Development and calibration of an integrated freeway and toll plaza model for New Jersey Turnpike using Paramics microscopic simulation tool. *IEEE conference on intelligent transportation systems. Proceedings, ITSC, 2005*, pp 1165–1170. <https://doi.org/10.1109/ITSC.2005.1520216>

20. Gulewicz V, Danko J (1995) Simulation-based approach to evaluating optimal lane staffing requirements for toll plazas. *Transp Res Rec* 1484:33–39 (Journal of Transportation Research Board)
21. Correa E, Metzner C, Niño N (2004) Tollsims: simulation and evaluation of toll stations. *Int Trans Oper Res* 11:121–138. <https://doi.org/10.1111/j.1475-3995.2004.00446.x>
22. Lin F-B, Su C-W (1994) Level-of-service analysis of toll plaza on freeway mainlines. *J Transp Eng* 120:246–263
23. Yu B, Mwaba D (2020) Toll plaza lane choice and lane configuration strategy for autonomous vehicles in mixed traffic. *J Transp Eng Part A Syst* 146:1–11. <https://doi.org/10.1061/JTEPBS.0000457> (ASCE)